# The nature, extent and age of the lower crust and underlying subcontinental lithospheric mantle (SCLM) beneath the Siberian Craton (Russia)

Irina G. Tretiakova

Australian Research Council Centre of Excellence for Core and Crust Fluid Systems (CCFS) and GEMOC

Department of Earth and Planetary Sciences

Macquarie University

Sydney, Australia

A thesis submitted for the degree of Doctor of Philosophy,

October, 2016

# Table of contents

**Abstract** ..... **5**

**Acknowledgements** ..... **7**

**Declaration** ..... **9**

**List of figures** ..... **11**

**List of tables** ..... **18**

**Chapter 1. Introduction** ..... **19**

**Chapter 2. The Siberian Craton: literature overview** ..... **21**

*2.1 Geological and tectonic structure* ..... *21*

*2.2 Kimberlites of the Siberian craton.* ..... *34*

Types of kimberlite ..... 36

Ages of kimberlitic magmatism ..... 37

*2.3 Subcontinental lithospheric mantle of the Siberian craton* ..... *41*

Composition of the lithospheric mantle based on xenoliths study ..... 41

Re-Os and platinum-group elements data ..... 43

Thickness of the lithosphere ..... 46

Thermal state of the lithosphere ..... 47

**Chapter 3. Samples, analytical methods and techniques.** ..... **49**

*3.1. Samples: location, types, and preparation* ..... *49*

*3.2. Analytical methods used for zircon studies* ..... *53*

Quantitative crystallographic orientation analysis ..... 53

Cathodoluminescence (CL) imaging ..... 53

LAM-ICPMS trace-element analysis and U-Pb dating ..... 53

SHRIMP U-Pb dating ..... 56

Zircon Hf-isotope analyses ..... 56

Zircon O-isotope analysis ..... 57

*3.3. Analytical methods used for sulfide inclusion studies in-situ Re-Os dating* ..... *57*

**Chapter 4. The Magan terrane** ..... **59**

*4.1. The Malo-Botuobia kimberlite field* ..... *60*

Zircon U-Pb data ..... 61

Rutile U-Pb data ..... 68

Zircon trace-element data ..... 69

Oxygen isotopes data ..... 78

Hafnium-isotope data ..... 79

*4.2. The Kharamai kimberlite field* ..... *81*

Zircon U-Pb data ..... 81

**Chapter 5. The Markha terrane ..... 85**

*5.1. The Upper Muna kimberlite field ..... 87*
Zircon U-Pb data ..... 87
Zircon trace-element data ..... 96
Oxygen isotope data ..... 101
Hafnium-isotope data ..... 102

*5.2. The Daldyn kimberlite field ..... 106*
Zircon U-Pb data ..... 106
Zircon trace-element data ..... 119
Oxygen isotopic data ..... 136
Hafnium-isotope data ..... 136
Sulfide Re-Os and PGE data ..... 142

*5.3 The Alakit-Markha kimberlite field ..... 144*
Zircon U-Pb data ..... 144
Zircon trace-element data ..... 151
Oxygen isotopic data ..... 168
Hafnium-isotope data ..... 169

*5.4. The Nakyn kimberlite field ..... 175*
Zircon U-Pb data ..... 175
Trace-element data ..... 181
Hafnium-isotope data ..... 185
Oxygen isotopic data ..... 187

**Chapter 6. The Daldyn terrane. ..... 189**

*6.1. The Chomurdakh kimberlite field ..... 191*
Zircon U-Pb data ..... 191
Zircon trace-element data ..... 194

*6.2. The Kuranakh kimberlite field ..... 197*
Zircon U-Pb data ..... 198
Zircon trace-element data ..... 199

**Chapter 7. The Khapchan terrane ..... 203**

*7.1 The Ukukit kimberlite field ..... 205*
Zircon U-Pb data ..... 205

*7.2 The Ogoner-Yuryakh kimberlite field ..... 207*
Zircon U-Pb data ..... 207
Zircon trace-element data ..... 211
Hafnium-isotope data ..... 217

**Chapter 8. The Birekta terrane ..... 219**

*8.1. The Merchemden kimberlite field ..... 220*
Zircon U-Pb data ..... 220
Zircon trace-element data ..... 223
Hafnium-isotope data ..... 226

*8.2. The Kuoika kimberlite field ..... 227*
Zircon U-Pb data ..... 227

Zircon trace-element data ..... 236
Oxygen-isotopes data ..... 244
Hafnium-isotopes data ..... 246

**Chapter 9. Discussion ..... 251**

*9.1. Zircons from kimberlites: what are we dating? ..... 251*

*9.2. The Magan terrane: lithospheric structure, age and evolution. ..... 252*
Zircon U-Pb data ..... 252
Zircon trace-element data ..... 256
Oxygen-isotope data ..... 257
Hafnium-isotopic composition ..... 258

*9.3. The Markha terrane: lithosphere structure, age and evolution. ..... 261*
Zircon U-Pb data ..... 261
Zircon trace-element data ..... 264
Oxygen isotopic data ..... 265
Hafnium-isotopic data ..... 266
Sulfide Re-Os data ..... 269

*9.4. The Daldyn terrane ..... 272*
Zircon U-Pb and trace-element data ..... 272

*9.5. The Khapchan terrane ..... 274*
Zircon U-Pb and trace-element data ..... 274
Hafnium-isotopic data ..... 276

*9.6. The Birekta terrane ..... 279*
Zircon U-Pb data ..... 279
Zircon trace-element data ..... 281
Oxygen isotopic data ..... 283
Hafnium isotopic composition ..... 283

*9.7. The Siberian Craton Lithosphere ..... 286*
U-Pb age data ..... 286
Trace-element data ..... 289
Hf-isotopes data ..... 290

**Chapter 10. Conclusions ..... 293**

**References ..... 295**

**Appendices ..... 317**

*Appendix 1.1. Zircon U-Pb age data for 91500 and MudTank standards ..... 317*
*Appendix 1.2. Compilation for Hf standards MudTank and Temora-II ..... 323*
*Appendix 2.1. Zircon U-Pb age data for samples from the Magan terrane ..... 325*
*Appendix 2.2. Zircon trace-element data for samples from the Magan terrane ..... 331*
*Appendix 2.3. Zircon Hf and O isotopes data for samples from the Magan terrane ..... 335*
*Appendix 3.1. Zircon U-Pb age data for samples from the Markha terrane ..... 337*
*Appendix 3.2. Zircon trace-element data for samples from the Markha terrane ..... 353*
*Appendix 3.3. Zircon Hf and O isotopes data for samples from the Markha terrane ..... 363*
*Appendix 3.4. Re-Os data for samples from the Markha terrane ..... 373*
*Apeendix 3.5. Sulfide platinum-group element data for samples from the Markha terrane ..... 374*

*Appendix 3A.1. Zircon U-Pb age data for samples from the Nurbinskaya pipe.....375*
*Appendix 3A.2. Zircon U-Pb SHRIMP age data for mosaic zircons from the Nurbinskaya pipe.....377*
*Appendix 3A.3. Zircon trace-element data for samples from the Nurbinskaya pipe.....379*
*Appendix 3A.4. Zircon O-isotopes data for mosaic zircons from the Nurbinskaya pipe.. .381*
*Appendix 3A.5. Zircon Hf-isotopes data for samples from the Nurbinskaya pipe..... ..383*
*Appendix 3A.6. Calculated temperature of zircon crystallization using Ti-in Zirc termometer, Nurbinskaya pipe..... .386*
*Appendix 4.1. Zircon U-Pb age data for samples from the Daldyn terrane..... 387*
*Appendix 4.2. Zircon trace-element data for samples from the Daldyn terrane.....389*
*Appendix 5.1. Zircon U-Pb age data for samples from the Khapchan terrane.....391*
*Appendix 5.2. Zircon trace-element data for samples from the Khapchan terrane.....393*
*Appendix 5.3. Zircon Hf and O isotopes data for samples from the Khapchan terrane....395*
*Appendix 6.1. Zircon U-Pb age data for samples from the Birekta terrane.....397*
*Appendix 6.2. Zircon trace-element data for samples from the Birekta terrane.....401*
*Appendix 6.3. Zircon Hf and O isotopes data for samples from the Birekta terrane.....403*

# Abstract

The lower continental crust and subcontinental lithospheric mantle (SCLM) are very interesting and important part of the Earth planet that has influenced significantly processes, which are continually altering surface of the Earth. Knowledge of the nature, structure and evolution of these layers may lead to understanding of the deep Earth's processes.

The Siberian craton is one of a few regions where samples of lower crust and underlying subcontinental lithospheric mantle can be found. Many geological and geophysical studies were carried out in this region but the role of crust and SCLM in the Earth's evolution is not completely understood yet. Modern analytical techniques allow solving problems that were outstanding up to now. For example, isotopic and trace-element studies on zircon can specify not only the age of rock but also the source of melts and thus identify different stages in the craton evolution.

The Siberian craton has experienced widespread Phanerozoic kimberlite magmatism. Besides diamonds, kimberlites also carry up a unique set of xenogenic material (xenoliths and xenocrysts) derived from depths of the lithosphere-asthenosphere transition zone (230-250 km) to the upper crust. Thus, kimberlitic pipes are natural drill holes, supplying with upper-mantle and crustal xenoliths and allowing us to investigate and reconstruct the structure of the deeper sections of the lithosphere.

More than 1000 zircon grains from five terranes (Magan, Markha, Daldyn, Khapchan and Birekta) of the Siberian craton were analysed for U-Pb ages, trace-element characteristics, hafnium and oxygen isotopes composition. These data were supplemented by Re-Os isotope information collected on sulphide inclusion in silicate minerals from the mantle xenoliths. This combined isotopic information show that there were several events that involved both reworking of older crust and some addition of mantle-derived material. Moreover, integration of U-Pb age and Hf-isotopic data for zircons from different terranes indicates that the main magmatic-tectonic events are coeval for all studied terranes. For kimberlitic fields located within the Magan and Markha terranes the results of U-Pb and model ages show a good agreement with previous data. However, the ages from the eastern part of the craton (Khapchan and Birekta terranes) are much older than those reported previously. This implies that the amalgamation of the Siberian craton happened much earlier than it was previously suggested, which might have a significant impact on the diamond-bearing potential of the eastern part of the craton.

# Acknowledgements

This thesis could never have been completed without a support of many people. First of all, I would like to thank my supervisors Elena Belousova, Bill Griffin, Norman Pearson and Vlad Malkovets for their time, knowledge, experience and thoughts they shared with me. I cannot stress enough how I am grateful to learn from all of them. I also would like to especially thank Sue O'Reilly for all her support and help during my candidature.

This research project would be impossible without help from technical and academic staff of the CCFS/GEMOC centre and EPS Department. Thank you, Will Powel and Steve Craven, Rosanna, Yoann and Nicole for hours in the lab, for help in data processing and interpretation, and for a great experience to work in such a knowledgeable, powerful and fun team. I also much appreciate all talks and discussions with Jose Maria Gonzalez Himenez, Sandra Piazolo, Olivier Alard, and other members.

I would like to thank people who have kept me going and helped a lot with the hard moments: the best flatmate ever Nurman Noor; my adventure buddy Mathijs van Gerwen; Captain John, his boat "Finesse" and the crew (Larisa, Trevor and Roger), who sailed with me through the rough sea of candidature. I am especially thankful to Sophia, Daria and Cait for a great time in and out of the office and to all people from the Department, who I have not mentioned yet, but they know who they are.

I also would like to thank Macquarie University and the Australian Government for the scholarship and opportunity to come to this beautiful country and do my study. For the financial, technical and analytical support I am also thankful to the CCFS/GEMOC centre of excellence.

Thanks to my parents, siblings and all my family and friends in Russia, who not only understood why I moved to another side of the world, but also supported me, encouraged, and believed in my abilities and power.

And the final thanks are to Misha, who is the wizard and Ironman, because only Ironman could go through all he has gone and only wizard could make all those magic he has done for me.

## Declaration

I hereby declare that this thesis has not been submitted for any higher degree to any university or institution. The thesis is based on work carried out at Macquarie University over a period between April, 2013 and October, 2016. All data and interpretations presented in this study are my own, except otherwise stated in the text.

IrinaTretiakova,

October, 2016

# List of figures

Figure 2.1.1. Main structural elements of the basement of the Siberian Craton. .....23
Figure 2.2.1. Modified terrane map of the Siberian Platform, showing the locations of kimberlite fields and major tectonic elements. .....35
Figure 2.3.1 Detailed distribution of harzburgitic garnets within each field along the Olenek trend ....42
Figure 2.3.2. $T_{MA}$, $T_{RD}$, and $^{187}Re/^{188}Os$ of sulfides from silicate minerals. .....44
Figure 2.3.3. Variation in lithosphere structure, composition and thermal state along the Olenek trend.. .....48
Figure 3.1.1. Map of the Siberian Craton showing sample locations.. .....50
Figure 3.2.1. The weighted mean age of the 91500 zircon standard. .....55
Figure 3.2.2 The weighted mean age of the MudTank zircon standard. .....55
Figure 4. The location of the Magan terrane and studied kimberlite fields. .....59
Figure 4.1.1. Probability plot of zircon U-Pb ages, Mir pipe, Magan terrane. .....62
Figure 4.1.2. The weighted mean age of the youngest major population, for zircons, Mir pipe .....62
Figure 4.1.3. The weighted mean age of the second major peak for zircons from the Mir pipe. .....63
Figure 4.1.4. Probability plot of zircon U-Pb ages, Sputnik pipe, Magan terrane. .....64
Figure 4.1.5. The weighted mean age of the youngest major population of zircons, Sputnik pipe. .....64
Figure 4.1.6. The weighted mean age of the main population of zircons, Sputnik pipe. .....65
Figure 4.1.7. The weighted mean U-Pb age for zircons from the Amakinskaya pipe, Magan terrane ..66
Figure 4.1.8. Probability plot of zircon U-Pb ages, Internationalnaya pipe, Magan terrane. .....66
Figure 4.1.9. The weighted mean age of the major peak, Internationalnaya pipe, Magan terrane .....67
Figure 4.1.10. The weighted mean age of the second major peak, Internationalnaya pipe .....67
Figure 4.1.11. U-Pb age of rutile inclusions from Internationalnaya pipe, Magan terrane .....68
Figure 4.1.12 Trace-element and rare-earth-element patterns of zircons from the Mir pipe. .....70
Figure 4.1.13. Total REE and U contents *vs* U-Pb age for zircons from the Mir pipe. .....71
Figure 4.1.14. Hf *vs* Y discrimination diagram for zircons from the Mir pipe. .....71
Figure. 4.1.15. Trace-element and rare-earth-element patterns of zircons from the Sputnik pipe. .....73
Figure 4.1.16. Total REE and Lu contents *vs* U-Pb age for zircons from the Sputnik pipe. .....74
Figure 4.1.17. Y *vs* Yb/Sm discriminant diagram for zircons from the Sputnik pipe. .....74
Figure. 4.1.18. Trace-element and rare-earth-element patterns of zircons,Internationalnaya pipe. .....76
Figure 4.1.19. Total REE and Lu contents *vs* U-Pb age for zircons from the Internationalnaya pipe. ..77
Figure. 4.1.20. Y *vs* Yb/Sm discrimination plot for zircons from the Internationalnaya pipe. .....77
Figure 4.1.21. $\delta^{18}O$ *vs* U-Pb age for zircons from the Sputnik pipe. .....78
Figure 4.1.22. εHf *vs* U-Pb age plot for zircons from the Sputnik pipe. .....80
Figure 4.2.1. The Concordia diagram: U-Pb age of zircons from the Eclogit pipe, Magan terrane. .....82
Figure 4.2.2. The U-Pb age of zircons from the Evenkiya pipe, Magan terrane. .....83
Figure 5. The location of the Markha terrane and studied kimberlite fields. .....85
Figure 5.1.1. Probability plot of zircon U-Pb ages, Zimnyaya pipe, Markha terrane. .....88

Figure 5.1.2. U-Pb age of young zircons from the Zimnyaya pipe, Markha terrane. ..... 89
Figure. 5.1.3. U-Pb age of the old zircon population from the Zimnyaya pipe, Markha terrane. ..... 89
Figure 5.1.4. U-Pb age of zircons from the kimberlite pipe “325 years of Yakutia”, Markha terrane. . 90
Figure 5.1.5. U-Pb age of zircons from the sample ZP-10-04, Zapolyarnaya pipe, Markha terrane..... 91
Figure 5.1.6. The weighted mean age of the oldest zircons, sample ZP-10-04, Zapolyarnaya pipe. .... 91
Figure 5.1.7. Concordia age for oldest zircons from the sample ZP-11-04, Zapolyarnaya pipe. ..... 93
Figure 5.1.8. U-Pb concordia for zircons from the sample ZP-11-04, Zapolyarnaya pipe..... 93
Figure 5.1.9. Probability plot of zircon U-Pb ages, sample ZP-16-04, Zapolyarnaya pipe. ..... 94
Figure. 5.1.10. The weighted mean age of the main population, sample ZP-16-04, Zapolyarnaya pipe. ..... 94
Figure 5.1.11. The weighted mean age of the second main population, sample ZP-16-04, Zapolyarnaya pipe. ..... 95
Figure 5.1.12. U-Pb concordia for zircons from the sample ZP-201-04, Zapolyarnaya pipe..... 95
Figure 5.1.13. U-Pb age of oldest zircons from the sample ZP-201-04, Zapolyarnaya pipe..... 96
Figure 5.1.14. Trace-element and rare-earth element patterns of zircons from the Zimnyaya pipe. ..... 97
Figure 5.1.15. Total REE and U contents *vs* U-Pb age for zircons from the Zimnyaya pipe. ..... 98
Figure 5.1.16. Y *vs* Yb/Sm discrimination diagram for zircons from the Zimnyaya pipe. ..... 98
Figure 5.1.17. Trace-element and rare-earth element patterns of zircons, 325 years of Yakutia pipe. . 99
Figure 5.1.18. Y *vs* U discrimination diagram for zircons from the 325 years of Yakutia pipe..... 100
Figure 5.1.19. $\delta^{18}O$ *vs* U-Pb age for zircons from the Zimnyaya pipe. ..... 101
Figure 5.1.20. εHf *vs* U-Pb age plot for zircons from the Zimnyaya pipe..... 103
Figure 5.1.21. εHf *vs* U-Pb age plot for zircons from the 325 years of Yakutia pipe. ..... 104
Figure 5.1.22. εHf *vs* U-Pb age plot for zircons from the Zapolyarnaya pipe. ..... 105
Figure 5.2.1. U-Pb concordia for zircons from the Udachnaya Eastern pipe. ..... 108
Figure 5.2.2. U-Pb age of oldest zircons from the Udachnaya Eastern pipe. ..... 108
Figure 5.2.3. U-Pb ages for the different domains as revealed on CL images for zircon grains from the Udachnaya Eastern pipe. ..... 109
Figure 5.2.4. U-Pb concordia for zircons from the Zarnitsa pipe. ..... 109
Figure 5.2.5. The weighted mean age of the main age population, Zarnitsa pipe. ..... 110
Figure 5.2.6. U-Pb ages of zircons from the Popugaeva pipe. ..... 111
Figure 5.2.7. U-Pb concordia for zircons from the main age peak, Popugaeva pipe. ..... 111
Figure 5.2.8. U-Pb ages of different domains recognised on CL images of zircon grains from the Popugaeva pipe. ..... 112
Figure 5.2.9. U-Pb ages of zircons from the Zagadochnaya pipe. ..... 113
Figure 5.2.10. The weighted mean age of the main age population, Zagadochnaya pipe. ..... 113
Figure 5.2.11. The weighted mean ages of the minor age populations, Zagadochnaya pipe. ..... 114
Figure 5.2.12. U-Pb ages of zircons from the Kusova pipe. ..... 115
Figure 5.2.13. The weighted mean age of the main age population, Kusova pipe. ..... 116
Figure 5.2.14. The weighted mean age of the minor age population, Kusova pipe. ..... 116

Figure 5.2.15. The weighted mean age of zircons from the xenolith OCYB-2, Udachnaya pipe.....117
Figure 5.2.16. The weighted mean age of the main age population, sample OCYB-5, Udachnaya pipe. .....118
Figure 5.2.17. U-Pb concordia for zircons from the sample OCYB-5, Udachnaya pipe.....118
Figure 5.2.18. Trace-element and rare-earth element patterns of zircons, Udachnaya Eastern pipe. ..120
Figure 5.2.19. Y *vs* Yb/Sm discrimination diagram for zircons from the Udachnaya Eastern pipe. ...121
Figure 5.2.20. Trace-element and rare-earth element patterns of zircons from the Zarnitsa pipe. .....122
Figure 5.2.21. Total REE and Yb concentrations *vs* U-Pb age of zircons from the Zarnitsa pipe.....123
Figure 5.2.22. Y *vs* U discrimination diagram for zircons from the Zarnitsa pipe .....123
Figure 5.2.23. Trace-element and rare-earth element patterns of zircons from the Popugaeva pipe...125
Figure 5.2.24. Total REE and Lu concentrations *vs* U-Pb age of zircons from the Popugaeva pipe...126
Figure 5.2.25. Rare-earth element patterns of zoned zircons from the Popugaeva pipe.....126
Figure 5.2.26. Trace-element and rare-earth element patterns of zircons, Zagadochnaya pipe.....128
Figure 5.2.27. Total REE and Lu concentrations *vs* U-Pb age of zircons, Zagadochnaya pipe.....129
Figure 5.2.28. Hf *vs* Y discrimination diagram for zircons from the Zagadochnaya pipe.....129
Figure 5.2.29. Rare-earth element patterns of zoned zircons, Zagadochnaya and Kusova pipes. .....130
Figure 5.2.30. Trace-element and rare-earth element patterns of zircons from the Kusova pipe. .....131
Figure 5.2.31. Total REE and Lu concentrations *vs* U-Pb age for zircons from the Kusova pipe.....132
Figure 5.2.32. Hf *vs* Y discrimination diagram for zircons from the Kusova pipe.....132
Figure 5.2.33. Trace-element and rare-earth element patterns of zircons from xenoliths, Udachnaya pipe.....134
Figure 5.2.34. Total REE and Lu concentrations *vs* U-Pb age of zircons from the Udachnaya pipe. .135
Figure 5.2.35. Y *vs* U discrimination diagram for zircons from the Udachnaya pipe.....135
Figure 5.2.36. $\delta^{18}O$ *vs* U-Pb age for zircons from xenoliths, Udachnaya pipe.....136
Figure 5.2.37. εHf *vs* U-Pb age plot for zircons from the Udachnaya Eastern pipe. .....137
Figure 5.2.38. εHf *vs* U-Pb age plot for zircons from the Zarnitsa pipe. .....138
Figure 5.2.39. εHf *vs* U-Pb age plot for zircons from the Popugaeva pipe.....139
Figure 5.2.40. εHf *vs* U-Pb age plot for zircons from the Zagadochnaya pipe. .....139
Figure 5.2.41. εHf *vs* U-Pb age plot for zircons from the Kusova pipe. .....140
Figure 5.2.42. εHf *vs* U-Pb age plot for zircons from xenoliths, Udachnaya pipe.....141
Figure 5.2.43. $T_{RD}$ model age and PGE patterns of the Group 1 sulfide inclusion. .....143
Figure 5.2.44. $T_{RD}$ model age and PGE patterns of the Group 2 sulfide inclusion. .....143
Figure 5.3.1. The weighted mean age of zircons from the Kismet pipe. .....145
Figure 5.3.2. The weighted mean age of zircons from the Geochemical pipe.....145
Figure 5.3.3. The U-Pb ages of zircons from the Vostok pipe.....147
Figure 5.3.4. The weighted mean age of the main age peak, Vostok pipe.....147
Figure 5.3.5. U-Pb concordia for zircons from the Krasnopresnenskaya pipe. .....148
Figure 5.3.6. The U-Pb ages of zircons from the Markha pipe.....149
Figure 5.3.7. The weighted mean age of the main age peak, Markha pipe.....149

Figure 5.3.8. The U-Pb ages of zircons from the Aikhal pipe. ..... 150
Figure 5.3.9. The weighted mean age of the main age peak, Aikhal pipe. ..... 151
Figure 5.3.10. Trace-element and rare-earth element patterns of zircons from the Kismet pipe. ..... 152
Figure 5.3.11. Y *vs* Nb/Ta discrimination diagram for zircons from the Kismet pipe. ..... 153
Figure 5.3.12. Trace-element and rare-earth element patterns of zircons, Geochemical pipe..... 154
Figure 5.3.13. Hf *vs* Y discrimination diagram for zircons from the Geochemical pipe..... 155
Figure 5.3.14. Trace-element and rare-earth element patterns of zircons from the Vostok pipe. ..... 157
Figure 5.3.15. Total REE and U concentrations *vs* U-Pb age of zircons from the Vostok pipe..... 158
Figure 5.3.16. Hf *vs* Y discrimination diagram for zircons from the Vostok pipe. ..... 158
Figure 5.3.17. Trace-element and rare-earth element patterns of zircons from the Veselaya pipe. .... 160
Figure 5.3.18. Total REE and Hf concentrations *vs* U-Pb age of zircons from the Veselaya pipe. .... 161
Figure 5.3.19. Hf *vs* Y discrimination diagram for zircons from the Veselaya pipe. ..... 161
Figure 5.3.20. Trace-element and rare-earth element patterns of zircons, Krasnopresnenskaya pipe. 162
Figure 5.3.21. Y *vs* U discrimination diagram for zircons from the Krasnopresnenskaya pipe. ..... 163
Figure 5.3.22. Trace-element and rare-earth element patterns of zircons from the Markha pipe..... 164
Figure 5.3.23. Total REE and Lu concentrations *vs* U-Pb age of zircons from the Markha pipe. ..... 165
Figure 5.3.24. Y *vs* Yb/Sm discrimination diagram for zircons from the Markha pipe. ..... 165
Figure 5.3.25. Trace-element and rare-earth element patterns of zircons from the Aikhal pipe. ..... 167
Figure 5.3.26. Hf *vs* Y discrimination diagram for zircons from the Aikhal pipe..... 168
Figure 5.3.27. $\delta^{18}O$ *vs* U-Pb age for zircons from the Aikhal pipe. ..... 169
Figure 5.3.28. εHf *vs* U-Pb age plot for zircons from the Kismet pipe. ..... 171
Figure 5.3.29. εHf *vs* U-Pb age plot for zircons from the Geochemical pipe..... 172
Figure 5.3.30. εHf *vs* U-Pb age plot for zircons from the Vostok pipe. ..... 172
Figure 5.3.31. εHf *vs* U-Pb age plot for zircons from the Veselaya pipe. ..... 173
Figure 5.3.32. εHf *vs* U-Pb age plot for zircons from the Krasnopresnenskaya pipe..... 174
Figure 5.3.33. εHf *vs* U-Pb age plot for zircons from the Aikhal pipe..... 174
Figure 5.4.1. Mosaic structure by cathodoluminescenceimaging and EBSD mapping..... 177
Figure 5.4.2. U-Pb ages of zircons from the Nurbinskaya pipe..... 177
Figure 5.4.3. The weighted mean age of the youngest age peak, Nurbinskaya pipe..... 178
Figure 5.4.4. The weighted mean age of the oldest age peak, Nurbinskaya pipe..... 178
Figure 5.4.5. U-Pb ages of zircons from xenolith BT-07-03, Botuobinskaya pipe. ..... 179
Figure 5.4.6. The weighted mean age of the major age peak, sample BT-07-03, Botuobinskaya pipe. ..... 180
Figure 5.4.7. U-Pb concordia for zircons from sample BT-39-03, Botuobinskaya pipe..... 180
Figure 5.4.8. The weighted mean age of the major age peak, sample BT-39-03, Botuobinskaya pipe. ..... 181
Figure 5.4.9. Trace-element and rare-earth element patterns of undeformed zircons from the Nurbinskaya pipe..... 182

Figure 5.4.10. Total REE and Lu concentrations *vs* U-Pb age of undeformed zircons from the Nurbinskaya pipe. ....183
Figure 5.4.11. Trace-element and rare-earth element patterns of zircons, Nurbinskaya pipe.....184
Figure 5.4.12. Y *vs* Yb/Sm discrimination diagram for zircons from the Nurbinskaya pipe.....185
Figure 5.4.13. εHf *vs* U-Pb age plot for undeformed and mosaic zircons, Nurbinskaya pipe. .....186
Figure 5.4.14. εHf *vs* U-Pb age plot for zircons from xenoliths, Botuobinskaya pipe.....187
Figure 5.4.15. $\delta^{18}O$ plot for zircons from the Nurbinskaya pipe. .....188
Figure 6. The location of the Daldyn terrane and studied kimberlite fields.....189
Figure 6.1.1. U-Pb concordia for zircons from the Druzhba pipe.....192
Figure 6.1.2. The weighted mean age of zircons from the Druzhba pipe. .....192
Figure 6.1.3. U-Pb concordia for zircons from the Rassvet pipe. .....193
Figure 6.1.4. U-Pb concordia for zircons from the Khairgastakh pipe. .....194
Figure 6.1.5. Trace-element and rare-earth element patterns of zircons from the Rassvet pipe. .....195
Figure 6.1.6. Hf *vs* Y discrimination diagram for zircons from the Rassvet pipe.....196
Figure 6.1.7. Y *vs* Nb/Ta discrimination diagram for zircons from the Rassvet pipe.....197
Figure 6.2.1. U-Pb concordia for zircons from the Malokuonapka pipe.....198
Figure 6.2.2. Trace-element and rare-earth element patterns of zircons, Malokuonapka pipe. .....200
Figure 6.2.3. Y *vs* Nb/Ta discrimination plot for zircons from the Malokuonapka pipe. .....201
Figure 7. The location of the Khapchan terrane and studied kimberlite fields: .....203
Figure 7.1.1. The weighted mean age of zircons from the Babie Leto pipe. .....206
Figure 7.2.1. Probability plot of zircon U-Pb ages, Baltiiskaya pipe.....208
Figure 7.2.2. The weighted mean age of the major peak, Baltiiskaya pipe. .....208
Figure 7.2.3. The weighted mean age of the second peak, Baltiiskaya pipe.....209
Figure 7.2.4. Probability plot of zircon U-Pb ages, Aerogeological pipe. .....210
Figure 7.2.5. U-Pb concordia for zircons from the main age group, Aerogeological pipe. .....210
Figure 7.2.6. Trace-element and rare-earth element patterns of zircons from the Baltiiskaya pipe.....211
Figure 7.2.7 Total REE concentration vs U-Pb age of zircons from the Baltiiskaya pipe.....212
Figure 7.2.8. Hf vs Y discrimination diagram for zircons from the Baltiiskaya pipe. .....213
Figure 7.2.9. Trace-element and rare-earth element patterns of zircons, Aerogeological pipe. .....215
Figure 7.2.10. Total REE and Lu concentrations vs U-Pb age of zircons, Aerogeological pipe. .....216
Figure 7.2.11. Hf vs Y discrimination diagram for zircons from the Aerogeological pipe. .....216
Figure 7.2.12. εHf vs U-Pb age plot for zircons from the Baltiiskaya pipe. .....217
Figure 7.2.13. εHf vs U-Pb age plot for zircons from the Aerogeological pipe. .....218
Figure 8. The location of the Birekta terrane and studied kimberlite fields.....219
Figure 8.1.1. The U-Pb concordia for zircons from the Vostok-6 pipe. .....221
Figure 8.1.2. Probability plot of zircon U-Pb ages, Operatorskaya pipe. .....222
Figure 8.1.3. The U-Pb concordia for zircons from the main age population, Operatorskaya pipe.....222
Figure 8.1.4 Weighted mean age of the second main peak, Operatorskaya pipe.....223
Figure 8.1.5. Trace-element and rare-earth element patterns of zircons, Operatorskaya pipe.....224

Figure 8.1.6. Total REE and Lu concentrations vs U-Pb age of zircons, Operatorskaya pipe. ..... 225
Figure 8.1.7. Y vs Yb/Sm discrimination diagram for zircons from the Operatorskaya pipe. ..... 225
Figure 8.1.8. εHf *vs* age plot for zircons from the Operatorskaya pipe.. ..... 226
Figure 8.2.1. The U-Pb concordia for zircons from the Khrizolit pipe. ..... 228
Figure 8.2.2. The U-Pb concordia for zircons from the Pyatnitsa pipe. ..... 229
Figure 8.2.3. Probability plot of the U-Pb ages of zircons from the Ruslovaya pipe. ..... 229
Figure 8.2.4. U-Pb concordia of zircons from the youngest age population, Ruslovaya pipe..... 230
Figure 8.2.5. The weighted mean age of zircons of the major age population, Ruslovaya pipe. ..... 231
Figure 8.2.6. The weighted mean age of zircons of the oldest age population, Ruslovaya pipe. ..... 231
Figure 8.2.7. Probability plot of the U-Pb ages of zircons from the Olivinovaya pipe. ..... 232
Figure 8.2.8. Probability plot of the U-Pb ages of young zircons from the Olivinovaya pipe. ..... 233
Figure 8.2.9. The weighted mean age of zircons of the oldest age population, Olivinovaya pipe. ..... 233
Figure 8.2.10. Probability plot of the U-Pb ages of zircons from the Vtorogodnitsa pipe. ..... 234
Figure 8.2.11. Probability plot of the U-Pb ages of young zircons from the Vtorogodnitsa pipe. ..... 235
Figure 8.2.12. The weighted mean age of zircons of the oldest age population, Vtorogodnitsa pipe. 235
Figure 8.2.13. Trace-element and rare-earth element patterns of zircons, Ruslovaya pipe. ..... 237
Figure 8.2.14. Total REE and U concentrations *vs* U-Pb age of zircons from the Ruslovaya pipe..... 238
Figure 8.2.15. Hf *vs* Y discrimination diagram for zircons from the Ruslovaya pipe. ..... 238
Figure 8.2.16. Trace-element and rare-earth element patterns of zircons, Olivinovaya pipe. ..... 239
Figure 8.2.17. Total REE and U concentrations *vs* U-Pb age of zircons from the Olivinovaya pipe.. 240
Figure 8.2.18. Y vs Yb/Sm discrimination diagram for zircons from the Olivinovaya pipe. ..... 240
Figure 8.2.19. Trace-element and rare-earth element patterns of zircons, Vtorogodnitsa pipe. ..... 242
Figure 8.2.20. Total REE and Lu concentrations vs U-Pb age of zircons, Vtorogodnitsa pipe. ..... 243
Figure 8.2.21. Hf vs Y discrimination diagram for zircons from the Vtorogodnitsa pipe. ..... 243
Figure 8.2.22. $\delta^{18}O$ vs U-Pb age for zircons from the Ruslovaya pipe. ..... 244
Figure 8.2.23. $\delta^{18}O$ vs U-Pb age for zircons from the Olivinovaya pipe. ..... 245
Figure 8.2.24. $\delta^{18}O$ vs U-Pb age for zircons from the Vtorogodnitsa pipe. ..... 246
Figure 8.2.25. εHf *vs* age plot for zircons from the Ruslovaya pipe. ..... 247
Figure 8.2.26. εHf *vs* age plot for zircons from the Olivinovaya pipe. ..... 248
Figure 8.2.27. εHf *vs* age plot for zircons from the Vtorogodnitsa pipe. ..... 249
Figure 9.2.1. Probability plot of U-Pb ages of zircons from the Magan terrane. ..... 252
Figure 9.2.2. Probability plot of zircon U-Pb ages (<1000 Ma), Magan terrane. ..... 253
Figure 9.2.3. Probability plot of zircon U-Pb ages (>1500 Ma), Magan terrane. ..... 254
Figure 9.2.4. Lu vs U-Pb age plot for zircons from the Magan terrane. ..... 257
Figure 9.2.5. εHf vs U-Pb age plot for zircons classified by their oxygen-isotopic composition, Sputnik pipe, Magan terrane. ..... 258
Figure 9.2.6. Initial $^{176}Hf/^{177}Hf$ *vs* U-Pb age plot for zircons from the Sputnik pipe, Magan terrane. 259
Figure 9.3.1. Probability plot of zircon U-Pb ages from the Markha terrane. ..... 261
Figure 9.3.2. Probability plot of zircon with U-Pb ages <1500 Ma, Markha terrane. ..... 262

Figure 9.3.3. Probability plot of zircon U-Pb ages (>1500 Ma) from the Markha terrane. .....263
Figure 9.3.4. Lu (ppm) *vs* U-Pb age plot for zircons from different kimberlite fields. .....265
Figure 9.3.5. Oxygen composition of zircons from the Markha terrane. .....266
Figure 9.3.6. εHf vs U-Pb age plot for zircons from the Markha terrane. .....267
Figure 9.3.7. Initial Hf *vs* U-Pb age plot for zircons from the Markha terrane. .....268
Figure 9.3.8. εHf vs U-Pb age plot for zircons analysed for their oxygen-isotopic composition, Markha terrane .....269
Figure 9.4.1. Probability plot of zircon U-Pb ages, Daldyn terrane. .....272
Figure 9.4.2. Lu *vs* U-Pb age of zircons from the Daldyn terrane. .....273
Figure 9.5.1. Probability plot of zircon U-Pb ages, Khapchan terrane. .....274
Figure 9.5.2. Probability plot of young zircon U-Pb ages, Khapchan terrane. .....275
Figure 9.5.3. Probability plot of old zircon U-Pb ages, Khapchan terrane. .....275
Figure 9.5.4. Lu vs U-Pb age of zircons from the Khapchan terrane. .....276
Figure 9.5.5. Initial Hf *vs* U-Pb age plot for zircons from the Khapchan terrane. .....277
Figure 9.6.1. Relative-probability plot of zircon U-Pb ages, Birekta terrane. .....279
Figure 9.6.2. Relative-probability plot of zircon U-Pb ages (<1000 Ma), Birekta terrane. .....280
Figure 9.6.3. Relative probability plot of zircon U-Pb ages (>1500 Ma), Birekta terrane .....281
Figure 9.6.4. Lu *vs* U-Pb age of zircons from the Birekta terrane. .....282
Figure 9.6.5. $\delta^{18}O$ *vs* U-Pb age of zircons from the Birekta terrane. .....283
Figure 9.6.6. εHf vs U-Pb age of zircons from the Birekta terrane. .....284
Figure 9.6.7. Initial Hf *vs* U-Pb age plot for zircons from the Birekta terrane .....285
Figure 9.7.1. U-Pb ages of zircons from the Siberian Craton. .....286
Figure 9.7.2. U-Pb ages (>1.5 Ga) of zircons from the Siberian Craton. .....287
Figure 9.7.3. U-Pb ages (<1 Ga) of zircons from the Siberian Craton. .....288
Figure 9.7.4. Lu and U *vs* age of zircons from the Siberian Craton. .....289
Figure 9.7.5. Hf crustal model ages of zircons from the Siberian Craton. .....290

# List of tables

Table 2.1. Summary of the terrane ages available in the literature. ..... 30
Table 2.2. Comparison of the isotopic data for kimberlites..... 38
Table 3.1. Samples location, types and analytical work performed. ..... 51
Table 4. Analytical work done for samples from the Magan terrane. ..... 60
Table 4.1.1. A summary of U-Pb age data for zircons from the Malo-Botuobia kimberlite field, Magan terrane. ..... 61
Table. 4.1.2. Summary table of Hf-isotopic data for zircons from Sputnik pipe..... 79
Table 5. Analytical work done for samples from the Markha terrane. ..... 86
Table 5.1.1. U-Pb ages of zircons from heavy-mineral concentrates from the Upper-Muna kimberlite field. ..... 87
Table 5.1.2. A summary of U-Pb ages of zircons from xenoliths from the Zapolyarnaya kimberlite pipe ..... 92
Table. 5.1.3. A summary table of Hf-isotope data for zircons from the Zimnyaya pipe ..... 102
Table. 5.1.4. A summary table of Hf-isotope data for zircons from the Zapolyarnaya pipe ..... 105
Table 5.2.1. U-Pb ages of zircons from heavy-mineral concentrates, Daldyn kimberlite field..... 107
Table 5.3.1. U-Pb ages of zircons from heavy-mineral concentrate, Alakit-Markha kimberlite field 146
Table. 5.3.2. Summary table of Hf-isotopic data for zircons from the Alakit-Markha kimberlite field. ..... 170
Table 5.4.1. U-Pb ages of zircons from the Nurbinskaya kimberlite field ..... 176
Table 6. Analytical work done for samples from the Daldyn terrane..... 190
Table 6.1.1. A summary of U-Pb age results for zircons from the Chomurdakh kimberlite field, Daldyn terrane. ..... 191
Table 7. Analytical work done for samples from the Khapchan terrane. ..... 204
Table 8. Analytical work done for samples from the Birekta terrane..... 220

# Chapter 1. Introduction

The lower crust and subcontinental lithospheric mantle, while very challenging to sample, are important parts of the Earth that influence many processes, which are continually altering the planet's surface. Studies of the nature, structure and evolution of these layers may lead to better understanding of processes in the Earth's core and mantle.

The Siberian Craton is one of a few regions where samples of the lower crust and underlying subcontinental lithospheric mantle (SCLM) can be found. During widespread kimberlitic magmatism, xenoliths and xenocrysts from the lithospheric mantle and all layers of the crust have been entrained and transported to the surface. Many geological and geophysical studies have been carried out in this region, but the structure, age and evolution of the lithosphere are still not fully understood.

This research project is dedicated to a detailed study of the crust and subcontinental lithospheric mantle of the Siberian craton, mainly using zircon xenocrysts from kimberlitic pipes. Zircon is a robust mineral, which retains information about the timing and conditions of its crystallization through time and despite the high pressure and temperature of the Earth's lithosphere. An integrated study of zircons utilising a range of modern analytical techniques has provided information about the crystallization age, origin and compositional type of the parental melts, as well as estimated ages of the primary protoliths.

Another important part of the project is the study of sulfide inclusions in silicate minerals from kimberlitic pipes. *In situ* Re-Os analytic technique is a unique approach to obtain age information on an individual sulfide grains, and is the only meaningful tactic to study sulfides from multicomponent rocks such as kimberlite. Together with detailed investigation on platinum-group-element composition of those sulfide inclusions, the Re-Os systematics allow derivation not only the age of primary melt but also ages of subsequent re-mobilization during melting processes and metasomatic events.

The application of these two research approaches to the same area (or even the same kimberlitic pipe) results in an extended dataset that provides information about the entire mantle-crust system, the processes, sources and timing of magmatic activity, and global tectonic and geodynamic events as well as kimberlite magmatism itself.

A significant number of studies have been done on kimberlites of the Siberian craton, but most of them were focused on the finding regularities in, and possible reasons for, their diamond-bearing potential. As a result, very little is known about the non-diamondiferous kimberlite fields of the eastern part of the craton - only limited and controversial data about the

age of those kimberlites have been reported. In addition, most dating was performed long ago and by techniques which may not be always suitable for kimberlite dating. The current study involves a set of samples from the eastern part of the area. The results of those investigations may clarify the significance of the eastern kimberlite fields in the history of the Siberian craton.

The economic importance of this project is based on the paradigm long known as "Clifford's rule" (Clifford, 1966). This empirical classification dictates that economically important diamond-bearing kimberlitic pipes are located only within cratonic areas with an Archean crust. This has been confirmed for most of the primary diamond deposits of the world. There are very few exceptions to this rule, and the only significant one is the Argyle Mine in Australia. Based on this rule, some terranes within the Siberian craton have been considered as non-prospective because of the proposed younger age of their crust. This study delivers new insights on the cratonic nature of some of these terranes, forcing a re-assessment of their diamond potential.

To summarize, this research project aims to provide a better understanding of the "lithospheric mantle – crust system", its role in the evolution of terranes, processes happening at the different stages of the terrane history, and links and interaction between the mantle and the crust. Despite the primary focus on the Siberian craton, the methodology and results of this study can be applicable to any areas with similar geological structure and history, including Australian Archean –Proterozoic cratons.

# Chapter 2. The Siberian Craton: literature overview

## 2.1 Geological and tectonic structure

The Siberian Craton represents a relatively stable platform area about $4x10^9$ $km^2$, mostly buried beneath the Late Proterozoic-Phanerozoic sedimentary cover 1–8 km thick (average *ca* 4 km). To the north and east, it is framed by essentially sedimentary belts of the Phanerozoic foreland (Taimyr and Verkhoyansk belts). Volcanic orogenic belts (Paleozoic Central Asian and Mesozoic Mongolo-Okhotsk) occur in the south and in the west (Fig. 2.1.1) (Rosen *et al.*, 2002).

Most of the tectonic maps of the Siberian Craton were based on the analysis of mainly geological and/or geophysical data (for example, a summary in Yanshin and Borukaev (1988)). Later, the use of isotopic data resulted in historic-geological models for the craton's evolution (Dobretsov, 1986, Frost *et al.*, 1998, Popov & Smelov, 1996, Rosen *et al.*, 1994, Rosen *et al.*, 2000, 1988, Smelov *et al.*, 1998) and others). A view was put forward that the terranes of different types and ages, the main structural elements of the craton, had originated and evolved initially independently of one another, as isolated microcontinents and later, as a result of collision, had been amalgamated into one craton. That is supported by the fact that the faults separating the terranes show indications of tectonic compression and overthrusting and are classified as the zones of collision (sutures). Another necessary indication of collision boundaries between the terranes is the synchroneity between local metamorphism and granitic magmatism in the collision zones (sutures) with areal metamorphism in the adjacent terranes. This synchroneity might have originated as the result of thermal relaxation (spontaneous heating) in the thickened crust of the collision prism, as suggested by theoretical modeling (England & Thompson, 1984) and geological observations (Rosen & Fedorovskii, 2001).

Thus, the present-day structure of the craton is generally interpreted as the result of the collision and accretion of microcontinents of different ages, which now make up the different tectonic blocks (terranes) (Brakhfogel, 1984, Rosen *et al.*, 1994, Rosen *et al.*, 2000, Smelov *et al.*, 1998). This process coincided in age with the amalgamation of other cratons and indicates that a supercontinent existed at that time.

It has been long accepted that the basement of the craton consists of two major elements of first rank, namely granulite-gneiss and granite-greenstone areas (Petrov *et al.*, 1985). Subsequent studies have shown that in most cases they differ distinctly in the texture and composition of the initial complexes as well as in the age of their formation. It appeared that, in essence, these elements were produced during the Early Proterozoic amalgamation of the craton and are of different genesis and varying age. Therefore, they were categorized as terranes

(Rosen *et al.*, 1994). They are subdivided into two types depending on which rocks are predominant: granulite complexes (granulite-gneiss terranes) or granitoids associated with volcanogenic, essentially basaltoid, synforms of greenschist or amphibolite grade (granite-greenstone terranes). However, across the craton, these structural elements can have different characteristics; some terranes cannot be assigned unambiguously to one of these types. One should bear in mind that the granulite-gneiss associations are lower-crust formations, whereas the granite-greenstone complexes originate in the upper crust. In addition to metamorphic grade, a crucial factor is the different conditions of origin. Therefore, to recognize the terranes as historical units, geological comparison and isotope dating are essential. We do not rule out that these two types could coexist within the erosional surface of one terrane. To a first approximation, recognition of two types of terranes in the cratonic basement seems to be a useful simplification and a tool for historical study, until new geological and geochronological data are obtained.

The granulite-gneiss terranes consist chiefly of two-pyroxene plagiogneisses, enderbites, mafic granulites (supposedly island-arc metavolcanic assemblage (Rosen, 1992)) as well as of granulite-grade metacarbonates and quartzites. They are traceable beneath the cover due to positive linear magnetic ($\Delta$Ta) anomalies and increases in the gravity field (Genshaft, 1996). The granite-greenstone terranes include vast areas of granitoids, among which linear volcanic greenstone belts occur, distinguished by the presence of ultramafic lavas (komatiites (Popov *et al.*, 1990)). This association can be quite distinctly outlined owing to slightly negative nonlinear mosaic magnetic signatures and decreased gravitational fields, outlining large buried granite massifs (Khorev, 1987) and linear, differently oriented greenstone belts and/or mafic-ultramafic intrusions (Gafarov *et al.*, 1978). The collisional zones are made up of blastomylonites and tectonites, migmatites, and autochthonous granitoids and contain large outliers of the rocks from adjacent terranes (Lutz & Oksman, 1990, Rosen, 1995). These are hundreds of meters to 30 km wide, and are easily followed beneath the cover for over 1000 km because of an intense variable polarity of linear magnetic fields. The accretion of microcontinents seems to have occurred in several stages, and generally larger units (superterranes) or tectonic provinces had appeared before they consolidated to form the craton structure. The surface geology and interpretation of geophysical data on the buried territory of the Siberian Craton has allowed recognition of the following tectonic provinces: Tungus, Anabar, Olenek, Aldan, and Stanovoi (Rosen *et al.*, 1991, Rosen *et al.*, 1994, Yanshin & Borukaev, 1988). These are in turn composed of diverse tectonic blocks (terranes) and include Early Proterozoic orogenic fold belts (Fig. 2.1.1).

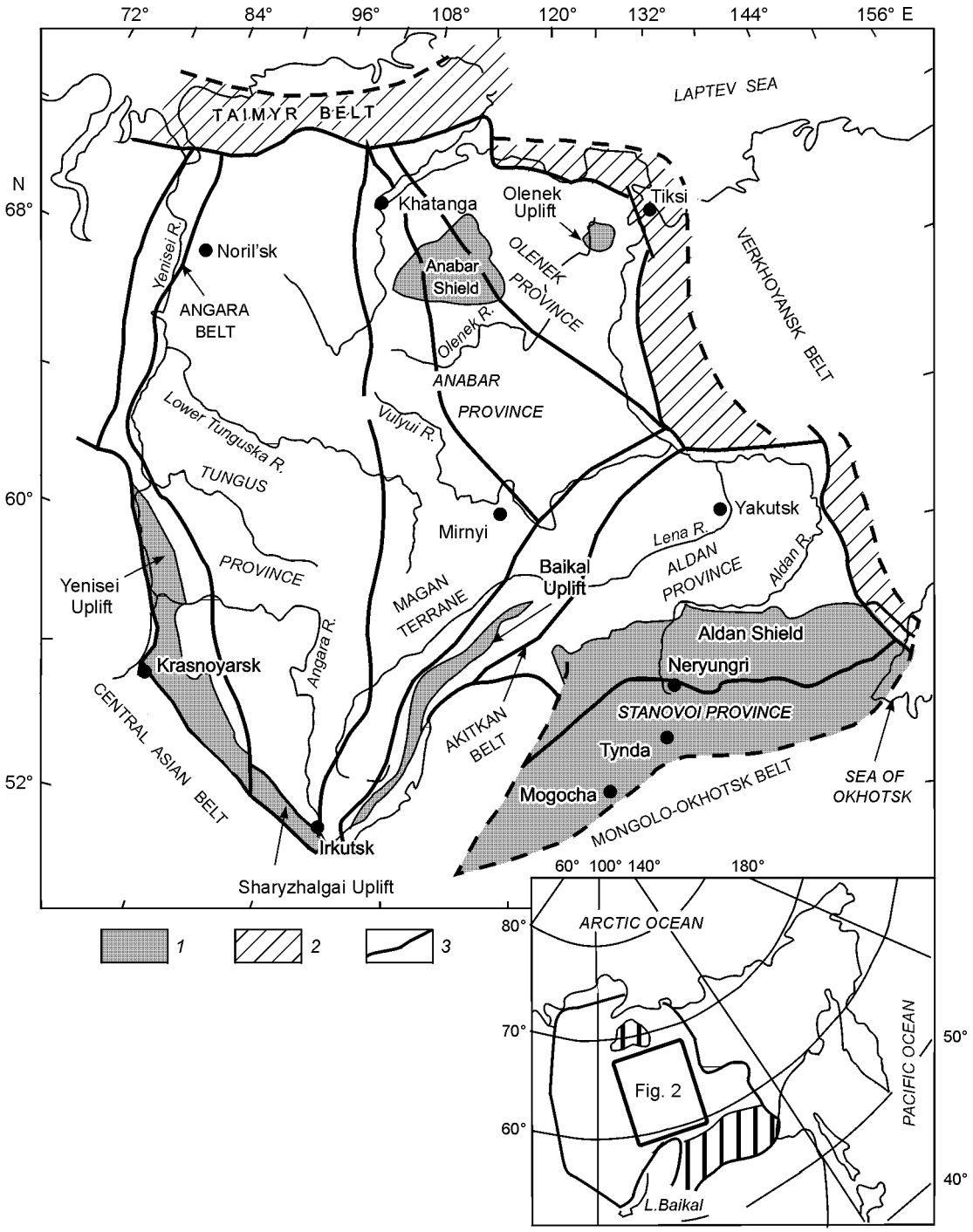



Figure 2.1.1. Main structural elements of the basement of the Siberian Craton (Rosen et al., 2002). 1 — denuded areas of the basement; 2 — Paleozoic-Mesozoic fold belts of foreland; 3 — main shear zones (within the craton, suture).

In general, it was thought that there is a trend of decreasing age of the crust from south-west to north-east (Fig. 2.1.1): Archean crust is recognized in the Tunguss province which is located in the western part of Siberian Platform (3.3 - 2.6 Ga by different techniques (Smelov & Timofeev, 2007)), while the eastern Olenek province consists of Proterozoic crust (Birekta,

Khapchan terranes, 2.4 - 1.8 Ga by different techniques (Griffin *et al.*, 1999a, Rosen *et al.*, 1991)). The Anabar and Aldan blocks in the central part of the craton provinces have yielded both Archean and Proterozoic ages. The summary of available ages of different terrane is presented in Table 2.1.

The largest **Tungus province (Fig. 2.1.1)** in the western half of the craton, consists mostly of the Tungus granite-greenstone terrane. It is overlain by the platform cover and only comes to the surface in the southern part, in the Sharyzhalgai Uplift. There, volcanic and sedimentary rocks of the Onot greenstone belt are intruded by tonalites 3.25 Ga in age, and weakly metamorphosed at 2.8–2.7 Ga (Rosen *et al.*, 1994). The belt is surrounded by granulites that were subjected to metamorphism at 2.5–2.4 Ga (Aftalion *et al.*, 1991), and the whole complex was intruded by collision-related granites at 1.96–1.95 and 1.87–1.82 Ga (Mekhonoshin, 1999). At that time, deeply metamorphosed mafic-ultramafic rocks, interpreted as fragments of subducted oceanic crust (Sklyarov *et al.*, 1998) and, possibly, lower crust and lithospheric mantle (Sharkov *et al.*, 1995), were moved through faults to the zone of collision.

The Angara fold belt frames the Tungus terrane to the west and southwest; it is exposed in the Yenisei Ridge and in the Sayan region (Nozhkin, 1999, Rosen *et al.*, 1993). This fold belt can be traced beneath the cover northward to the Taimyr Peninsula owing to negative linear magnetic anomalies and a weaker gravitational field. Its granulite basement was formed at 2.73 Ga and contains charnockites with ages of 1.83 Ga. Metavolcanic rocks (biotite-hornblende gneisses) were formed simultaneously with granite gneiss domes at 2.2–1.9 Ga (Nozhkin, 1999), and giant linear massifs of granites (Sayan and Tarak) intruded along the southern and western boundaries of the terrane at 1.90–1.78 Ga. This association of the Archean basement, Early Proterozoic volcanism, and giant craton-framing granitoid plutons indicates that an active continental margin existed there in the late Early Proterozoic (Nozhkin, 1999, Rosen *et al.*, 1993). Most likely, this regime continued into Riphean time, when volcanic rocks (0.87 Ga) accumulated and granite-gneissic domes formed (Nozhkin, 1999). Later, Riphean-Vendian ophiolites and island-arc volcanic rocks of the Isakovka (Vernikovsky, 1996) and Predivino terranes dated at 0.64 Ga (Chernykh, 2000, Vernikovsky *et al.*, 1999) were thrust over the Paleoproterozoic basement.

The Kan granite-greenstone terrane, which is separated from the southwestern margin of the Tungus province by the Sayan fault, was once considered to be part of this province (Rosen *et al.*, 1994). However the magmatic rocks have been dated at 2.3 Ga, with a $T_{(DM)}$ Nd model age of 2.4–2.5 Ga (Nozhkin *et al.*, 2001). In addition to these granite-greenstone associations of Proterozoic age, the Riphean island-arc complexes have been recognized, with associated plagiogranites (Sm-Nd isochron age of 1017 Ma), and granitoids (dated at 606 and 686 Ma, the

upper intercept of a discordia for zircon), and late superimposed processes at 540–550 Ma (Ar-Ar (Rumyantsev, 2001, Rumyantsev *et al.*, 2000)). This region is evidently a part of the Central Asian Fold Belt.

To the east, the Tungus province is limited by the submeridional Sayan-Taimyr fault (collision) zone, which in essence divides the whole Siberian Craton into eastern and western parts. It is traceable beneath the deposits of the platform cover, where the mosaic geophysical fields inherited from the Tungus terrane are abruptly replaced by the linear fields typical of the Magan terrane. This zone is exposed only in the south, west of Lake Baikal, where the late metamorphism of the Sharyzhalgai series is ascribed to the collision processes (Aftalion *et al.*, 1991, Zonenshain *et al.*, 1989).

The central and northeastern parts of the craton are occupied by the Anabar and Olenek tectonic provinces. **The Anabar province (Fig. 2.1.1)** includes the Magan and Daldyn granulite-gneiss terranes exposed within the Anabar Shield. The rocks were formed at 3.1 Ga; granulite-facies metamorphism and melting of granitoids took place at 1.9 and 1.8 Ga, respectively. The Anabar Province also includes the Markha granite-greenstone terrane buried beneath the cover sequences in the Markha River basin. The cores from deep boreholes in this area contain granitoids (see below). The age of the substrate is estimated at 2.5 Ga, and metamorphism at 1.76 Ga (Rosen *et al.*, 2000).

The Daldyn terrane, as exposed in the Anabar Shield, consists of high-grade metamorphic rocks, thrust to the southwest over the Tungus Province along the Kotuykan Shear Zone. Its northern boundary is the Billyakh Shear Zone, a major suture marked by a shear belt 10–20 km wide and traceable for ca 1500 km to the southeast by magnetic and gravity anomalies. The exposed rocks are felsic to mafic granulites with both supracrustal and igneous protoliths, reflecting metamorphism at lower-crustal conditions (8–12 kbar). Similar rocks are found as xenoliths in the Udachnaya kimberlite pipe of the Daldyn field, which lies within this terrane. Zircon ages indicate crustal formation at *ca* 3.0 Ga, with (minor?) metamorphic events down to *ca* 1.9 Ga. The Markha terrane is not exposed at the surface; an irregular SW–NE boundary separating it from the Daldyn terrane is based on changes in the style and orientation of gravity and magnetic anomalies, accompanied by minor faulting in the overlying sediments. Crustal xenoliths in the kimberlites of the Alakit and Upper Muna fields also are different from those in the Daldyn field; they are mainly mafic to intermediate volcanic rocks, metamorphosed to amphibolite- to granulite facies. The few reliable geochronological data are interpreted by Rosen *et al.* (1994) to indicate ages similar to those of the Daldyn terrane. To the south, the Tungus and Anabar provinces are separated by the Akitkan Fold Belt. This belt strikes northeast from Prebaikalia up to the Lena River, where it is overlain by the volcanics and sediments of

the Paleozoic Vilyui Rift with the same strike. The belt nearly orthogonally truncates the southeastern strikes of the Anabar and Olenek provinces along the Vilyui fault zone; the Lena zone separates it from the Aldan province. Diverse volcanic and sedimentary units (or sequences), supposedly of island-arc origin are accompanied by granitoids mostly dated at 1.91–1.86 Ga (the most ancient is 2.18–2.03 Ga) and in places these were metamorphosed to the granulite facies at 1.88 Ga. That assemblage characterizes the belt as an isolated island-arc system of Late Paleoproterozoic age (Rosen *et al.*, 1994). At that time it was a marginal magmatic arc (Nozhkin, 1999), with considerable amounts of anorogenic granites intruded at 1.87–1.82 Ga (Neymark *et al.*, 1998). The latest granitoids intruded at 0.73–0.32 Ga, and superimposed thermal events are dated at 0.5–0.45 Ga. These are interpreted as due to influence tectonic events in the Paleoasian ocean near the Barguzin terrane, situated east of the southern Akitkan belt.

**The Olenek province (Fig. 2.1.1)** includes tectonic features of varying origin and a poorly explored region of the Ust'-Lena raised portion of the basement on the northeastern margin of the craton. In the west of the province (within the Anabar Shield), granulite-facies metagraywackes (garnet gneisses) and metacarbonates (calc-silicate rocks and calciphyres) of the Khapchan fold belt are exposed. The age of the metasediments is 2.5 Ga and granulite metamorphism occurred 1.97 Ga (Rosen *et al.*, 2000). These rocks appear to be the basement of the Birekte granite-greenstone terrane and the sediments of the Khapchan belt accumulated on its passive margin (western margin in the modern structure). The Birekte terrane is distinguished from the Khapchan belt entirely on geophysical grounds, as the basement is overlain by up to 10 km of Riphean and Phanerozoic sedimentary sequences.

The SW margin of the terrane is defined by a series of major curvilinear magnetic anomalies, which may represent a shear zone with associated intrusive rocks. A similar but less pronounced anomaly in the middle of the terrane, between the Merchimden and Toluopka–Upper Molodo kimberlite fields, may represent another large shear zone. The geophysical anomaly pattern beneath the Birekte terrane is interpreted by Rosen *et al.* (1994) as a greenstone–granite basement.

The Aekit orogenic belt is exposed In the Olenek uplift. The belt consists of felsic volcanics and carbonaceous-siliceous rocks, which were metamorphosed to greenschist facies and intruded by granitoids at about 1.8 Ga.

The Billyakh collisional (shear) zone separates the Olenek province from the Anabar province. The age of the associated metamorphic rocks of the Khapchan belt is 1.97 Ga, and

the collisional migmatites and granitoids formed at 1.9 and 1.8 Ga, respectively (Rosen *et al.*, 2000). Geochronological data on rocks within the Kotuykan and Billyakh shear zones, and on some syntectonic intrusive rocks, suggest that the assembly of at least the northern part of the Siberian Craton started with a collision between the different terranes at 2.0 - 1.9 Ga. A single age datum on zircon from a basement xenolith in the Chomurdakh field may suggest a slightly younger age (1.78 Ga) (Griffin *et al.*, 1999a). This assembly may have involved remobilisation of the Archean basement, at least in the northern parts of the area.

In the southeast part of the craton, the Aldan and Stanovoi provinces are recognized; these are separated by the Kalar (Stanovoi) zone of overthrusting (Rosen *et al.*, 1994). Analyses of geochronology and petrological features by Popov, Smelov, and other authors(Popov & Smelov, 1996, Smelov *et al.*, 1998), suggest that the Aldan (Aldan-Stanovoi) Shield was formed as a result of the successive accretion of fragments of different orogenic belts and cratonic blocks to the Aldan and Tynda terranes during the period from 2.1 to 1.7 Ga.

**The Aldan province** includes two terranes: the Olekma to the west and Batomga to the east, which are divided by the Aldan and Uchur granulite-gneiss terranes. The Olekma terrane is composed mainly of basalts and komatiites at lower stratigraphic levels, with andesites, felsic volcanics, and volcaniclastic sediments at higher levels. The age defined by SHRIMP zircon dating of tonalitic gneisses and by Sm-Nd isochrons is about 3.2 Ga; however, there are several zircons and Sm-Nd isochron ages of 3.0 - 2.9 Ga (Rosen *et al.*, 1994).

The Aldan terrane is a small high-grade block bounded on both the east and west by east-dipping thrust faults, and it is composed chiefly of tonalite-trondhjemite-granodiorite (TTG) complexes including charnockites, granites, and metasediments. Geological mapping has revealed two stages of deformation and plutonism in the Aldan terrane, both under granulite-facies conditions. The granulite plagiogneisses of the Aldan terrane (Frost *et al.*, 1998) yield $T_{(DM)}$ Nd model ages of 3.25 and 2.74 Ga, and the metapelites give $T_{(DM)}$ Nd model ages of 2.18–2.21 Ga, close to the time of intrusion of mafic rocks in the Ungra Block with $T_{(DM)}$ Nd of 2.22 Ga. The Early Proterozoic igneous rocks seem to be the source of some metasedimentary granulite-facies metamorphic rocks of the Aldan terrane. The Sm-Nd model ages of granulite –facies metagraywackes of the Olekma, Aldan, and Uchur terranes (Kovach *et al.*, 1999) give average ages for the eroded source rocks of 3.5, 3.0, and 2.6 Ga, respectively.

The Uchur terrane consists of a charnockite-mafic granulite association, which probably represents a TTG-greenstone association that experienced granulite facies metamorphism. Geochemical studies of metavolcanics from the Uchur terrane reveal a complete suite from

mafic to felsic compositions, with mafic components dominating in most successions. However, plutonic components in the central structure of the terrane are bimodal in composition, with the felsic end member (charnockite) dominating.

Exposures of the Batomga terrane in the eastern Aldan shield indicate that it is a TTG-greenstone terrane of presumably Archean age. The terrane generally comprises a TTG association with supracrustal enclaves composed of mafic igneous rocks, pelites, quartzites, and carbonates. Locally, all rocks are metamorphosed to granulite grade.

Moreover, the Aldan Province also contains the Udokan and Ulkan orogenic belts, which consist of metasediments, volcanoclastic and post-tectonic granite complexes directly overlying the granite-greenstone basement of the Olekma and Batomga terranes, respectively. The Udokan belt probably accumulated 2.2 b.y. ago inside the mountain foretrough that appeared at the front of the Stanovoi superterrane as it began to move northward (in the modern structure) along the Kalar overthrust. The Ulkan belt filled an intermontane trough 1.7 b.y. ago within the collisional orogen of the Aldan tectonic province, which formed at that time.

The collision between the Aldan and Uchur terranes along the Timpton and Tyrkanda fault zones dates from the time of melting of charnockites out of the Izhek complex at 1.92 Ga (Bibikova *et al.*, 1986, Frost *et al.*, 1998) and of orthopyroxene diorites in the Timpton basin at 1.95 Ga (with $T_{(DM)}$Nd protolith model ages of 2.8–3.0 Ga) (Kovach, 1994).

**The Stanovoi province** is situated on the southeastern margin of the Siberian Craton and includes the Mogocha, Tynda, and Sutam terranes, which are separated by the Dzheltulak orogenic belt.

The Mogocha terrane comprises chiefly an Archean TTG-greenstone complex, with major greenstone belts in the southern part. Rocks are metamorphosed to amphibolite grade, reaching granulite grade in the central part of the terrane. Geochemical characteristics of both the TTG and greenstone components are similar to those of Archean TTG-greenstone associations. However, Archean zircons ages have not yet been reported from the Mogocha terrane. Zircons from amphibolites in the Archean basement give SHRIMP ages of 1.87 Ga (Nutman *et al.*, 1992a) which may be related to metamorphic events.

The Tynda terrane combines both granulite-grade and amphibolite-grade domains. Moreover, numerous large anorthosite bodies are exposed in the terrane. The granulite-facies domains are mainly composed of enderbite and hornblende-gneisses, ultramafic schists with interlayered felsic pyroxene gneisses, calc-silicates and quartzites. The amphibolite-grade

doimains contain diorite-tonalite-tronhjemite, basalt, gabbro, and paragneisses. Zircons from tonalitic gneisses have been dated by SHRIMP and show different ages of cores and rims. Zircon cores, which are thought to provide the time of tonalite intrusion, yielded an age of 2785 ± 9 Ma, while the zircon overgrowths gave an age of 1960 ± 25 Ma, probably related to granulite-facies metamorphism (Rosen *et al.*, 1994).

The Sutam terrane is placed between the Aldan province and Stanovoi province. The terrane is composed chiefly of an enderbite-mafic granulite association known as the Zverev Group, and includes large intrusions of anorthosite (e.g. Kalar massif), as well as major shear zones with extensive mylonites. As indicated by previous thermobarometric studies (Kitsul, 1986), the Sutam terrane appears to represent a slice of the middle- to lower crust. A few available isotopic ages are from U-Pb studies of zircons and Sm-Nd mineral isochrons. Zircon xenocrysts from a metagabbro in the western part of the terrane yielded an upper intercept U-Pb discordia age of 3460±16 Ma and lower intercept age of 2200±20 Ma (Bibikova *et al.*, 1989b). The later age is generally related to granulite-facies metamorphism. Zircons from the Kalar anorthosite yielded an upper intercept discordia age of 2660±60 Ma with a lower intercept age of 1800 Ma (Levchenkov *et al.*, 1987). A Sm-Nd mineral isochron age of 1950 Ma for the Zverev Group, and a 2150 Ma age for a low-grade mafic volcanic rock (Dook, 1989), are both interpreted as metamorphic ages. These results indicate that both Early and Late Archean rocks occur in the Sutam terrane and several stages of high-grade metamorphism are recorded in the terrane.

Table 2.1. Summary of the terrane ages available in the literature.

| Province | Terrane | Location and rock type | Event dated | Age, method | Reference |
|---|---|---|---|---|---|
| Stanovoi | Tynda | Tonalitic gneisses, Gilyuy River | | 2785 ± 9 Ma (zircon core, SHRIMP)<br>1960 ± 25 Ma (zircon rim, SHRIMP) | (Nutman *et al.*, 1992b) |
| | | Granulites, Larba Complex | | 2585 ± 20 Ma (zircons) | (Bibikova *et al.*, 1984)<br>(Shuldiner & Panchenko, 1985) |
| | | Ultramafic and mafic dikes | | 1929 ± 13 Ma (zircons)<br>1924 ± 24 Ma (zircons) | (Nutman *et al.*, 1992b) |
| | | Anorthosite, Gheran intrusion, Zhugzhur massif | | 1734 ± 12 Ma (zircons) | (Neymark *et al.*, 1992) |
| | Sutam | Metagabbro, Kurulta group | Granulite-facies metamorphism | 3460 ± 16 Ma (zircons, U-Pb)<br>2200 ± 20 Ma (zircons, U-Pb) | (Bibikova *et al.*, 1989b) |
| | | Enderbite/charnockite, Kalar anorthosite | | 2660 ± 60 Ma (zircons)<br>1800 Ma (zircons) | (Levchenkov *et al.*, 1987) |
| | | Zverev group | | 1950 Ma (Sm-Nd mineral isochrone) | (Dook, 1989) |
| | | Mafic volcanic rock | | 2150 Ma (Sm-Nd mineral isochrone) | (Dook, 1989) |
| | Mogocha | Amphibolite, sequence near Mogocha town | metamorphic | 1873 ± 6 Ma (zircons) | (Nutman *et al.*, 1992b) |
| | | Paragneisses, sequence near Mogocha town | metamorphic | 1950 | (Bibikova *et al.*, 1989b) |
| | | Migmatitic granite gneisses, southeastern part of Mogocha terrane | metamorphic | 1930 | (Iskanderova *et al.*, 1980) |

| Province | Terrane | Location and rock type | Event dated | Age, method | Reference |
|---|---|---|---|---|---|
| Aldan | Olekma | Tonalitic gneisses, Tungurcha domain | | 3212 ± 8 Ma (zircon, SHRIMP)<br>3235 ± 144 Ma (Sm-Nd isochrone) | (Nutman *et al.*, 1992a)<br>(Puchtel *et al.*, 1989) |
| | | Greenstone volcanism, Olondo domain | | 3018-3000 (SHRIMP, Sm-Nd) | (Bibikova *et al.*, 1989a)<br>(Baadsgaard *et al.*, 1990) |
| | | TTG plutonism, Olondo domain | | 2860 | (Bibikova *et al.*, 1989a)<br>(Baadsgaard *et al.*, 1990) |
| | | Syntectonic granitoid plutons | | 2984 ± 22 (zircons)<br>2999 ± 51 (zircons) | (Neymark *et al.*, 1993) |
| | | Eastern border of terrane | Euhedral zircon, granulite-grade metamorphism | 1895 ± 4 Ma (zircon, SHRIMP) | (Nutman *et al.*, 1992a) |
| | Aldan | Biotite granite and trondhjemite, Aldan River | | 3386 ± 100 Ma (zircons) | (Morozova *et al.*, 1989) |
| | | Nebulitic felsic granulites, Aldan River | | 3335 ± 3 Ma (zircons, SHRIMP)<br>1929 ± 9 Ma (zircons, SHRIMP) | (Nutman *et al.*, 1992a) |
| | | TTG, Iengra Group, Aldan River | | 3570 ± 50 Ma (zircons) | (Glebovitsky & Drugova, 1993) |
| | | Migmatite, Aldan River | Aldan-Kilier thrust age | 3328 Ma (zircon core, SHRIMP)<br>1947 ± 5 Ma (zircon rim, SHRIMP) | (Nutman *et al.*, 1992a) |
| | | Phlogopite, Central Aldan | | 1840 (K-Ar) | (Shepel, 1980) |
| | | Leucogabbro, Ungra complex, southwestern part of Aldan terrane | Aldan-Kilier thrust age | 2037 ± 20 Ma (zircon) | (Bibikova *et al.*, 1984) |

| Province | Terrane | Location and rock type | Event dated | Age, method | Reference |
|---|---|---|---|---|---|
| Aldan | Aldan | Charnockite massif, Izhek zone | Collision of Aldan and Uchur terranes | 1916 ± 10 Ma (zircon)<br>1770 ± 130 Ma (whole rock, Rb-Sr) | (Bibikova *et al.*, 1986, Dook, 1989) |
| | Udokan orogenic belt | Tuffaceous sandstone, Udokan Group | | 2180 ± 50 Ma (zircon) | (Berezhnaya *et al.*, 1988) |
| | | Mudstone | Metamorphic age | 1950 ± 110 Ma (Rb-Sr, whole rock) | (Gorokhov *et al.*, 1989) |
| | | Granite, Udokan Group | Post-tectonic | 1800 Ma (Rb-Sr, whole rock) | (Tauson *et al.*, 1983) |
| | | Granite, Kodar massif | Post-tectonic | 1780 ± 50 Ma (zircon, Pb-Pb) | (Rublev *et al.*, 1981) |
| | Ulkan orogenic belt | Granite | | 1703 ± 18 Ma (zircon) | (Neymark *et al.*, 1992) |
| | | Hornblende syenite | | 1727 ± 6 Ma (zircon) | (Neymark *et al.*, 1992) |
| | | Rhyolite, Ulkan | | 1727 ± 18 Ma (zircon) | (Neymark *et al.*, 1992) |
| | | Granite, Ulkan | | 755 ± 31 Ma (K-Ar)<br>453 ± 16 Ma (K-Ar) | (Gamaleya, 1968) |
| | Hapschan | Paragneisses | | 2400 Ma ($T_{DM}$ model age, Sm-Nd) | (Rosen *et al.*, 1991) |
| | | Garnet paragneiss | Granulite-facies metamorphism | 1970 ± 20 Ma (U-Pb) | (Rosen *et al.*, 1991) |
| Olenek | Daldyn | Crustal xenolith in the Chomur pipe (Chomurdakh field) | | 1780 ± 45 Ma (U-Pb SHRIMP) | (Griffin *et al.*, 1999a) |
| | | Enderbites, Anabar shield | | 3164 ± 32 Ma (zircon, U-Pb SHRIMP) | (Rosen *et al.*, 1991) |
| | | Mafic granulites, Anabar shield | | 3063 ± 80 Ma (Sm-Nd, whole rock) | (Spiridonov *et al.*, 1991) |
| | | Daldyn enderbite | Granulite-facies metamorphism | 2760 ± 10 Ma (zircon, U-Pb) | (Rosen *et al.*, 1991) |
| | | Mafic granulite xenolith, Udachnaya pipe | Metamorphism | 1884 ± 5 (Sm-Nd, mineral isochrone) | (Neymark *et al.*, 1993) |

| Province | Terrane | Location and rock type | Event dated | Age, method | Reference |
|---|---|---|---|---|---|
| Anabar | Markha | Sulfide inclusions, olivine-macrocryst, Udachnaya pipe | | 3 Ga (Re-Os)<br>3.5 Ga (Re-Os) | (Pearson *et al.*, 2002) |
| | | Sulfide inclusions, olivine-macrocryst, Udachnaya pipe | | 2.9-3.5 (Re-Os) | (Griffin *et al.*, 2002a) |
| | | Garnet-amphibolite xenolith, Novinka pipe, Muna field | | 1756 ± 6 Ma (Sm-Nd, whole rock isochrone)<br>2920 Ma (Sm-Nd, $T_{DM}$ model age) | (Neymark *et al.*, 1993) |
| | Onot greenstone belt | Tonalitic gneisses | | 3250 ± 50 Ma (zircon, U-Pb) | (Bibikova *et al.*, 1982) |
| | Sharyzhalgay uplift | Gneisses and charnockites, Sharyzhalgay Complex | | 2778-2710 Ma (zircons, U-Pb) | (Bibikova *et al.*, 1990b)<br>(Aftalion *et al.*, 1991) |
| | | Kinzigite and high-Al gneisses | Granulite facies metamorphism | 2568-2560 Ma (zircon, U-Pb) | (Aftalion *et al.*, 1991, Bibikova *et al.*, 1990a) |
| | | High grade granitoids | | 2540-2530 Ma (Rb-Sr, isochrone) | (Krylov *et al.*, 1980) |
| Tunguss | Magan | Granites and charnockites | Collision of the Tunguss and Magan provinces | 1965 ± 4 Ma (zircon, U-Pb)<br>1950 ± 5 Ma (zircon, U-Pb)<br>2.4 - 2.3 Ga (Sm-Nd, $T_{DM}$) | (Bibikova *et al.*, 1990a)<br>(Aftalion *et al.*, 1991) |
| | | Granitoids | | 1873 ± 4 Ma<br>1817 ± 30 Ma (zircon, U-Pb)<br>1862 ± 4 Ma (monazite, U-Pb) | (Aftalion *et al.*, 1991) |
| | | Cpx-Amph xenolith, Mir pipe | | 3000 Ma (Sm-Nd, $T_{DM}$ model age) | (Neymark *et al.*, 1993) |
| | | Anorthosite, Kotuykan shear zone | | 2 Ga (zircon, U-Pb) | (Sukhanov & Rachkov, 1988) |
| | | Monzodiorite, Kotuykan shear zone | | 2.7 Ga (zircon, U-Pb)<br>2180 ± 20 Ma (Sm-Nd, mineral isochrone) | (Sukhanov & Rachkov, 1988, Sukhanov *et al.*, 1990) |
| | | Migmatite, Kotuykan shear zone | syntectonic | 1925 ± 100 Ma (monazite, U-Pb)<br>2000-1900 Ma (uraninite, Pb-Pb) | (Stepanov, 1974) |
| | | Biotite granite, Kotuykan zone | | 1870-1840 Ma (zircon, U-Pb) | (Stepanov, 1974) |

## 2.2 Kimberlites of the Siberian craton.

Most occurrences of kimberlite volcanism within the Siberian Platform are confined (Kharkiv *et al.*, 1998) to the Yakutian Kimberlite Province (YKP). Beyond the province, kimberlites have been found in the Krasnoyarsk Territory (Kharamai and Kotui fields) and in the East Sayan region (Ingashi field) (Kostrovitsky *et al.*, 2007).

The YKP is divided into two subprovinces: the southern Vilyui subprovince (fields #1-5, Fig. 2.2.1) in the center of the Siberian platform and the northern Anabar-Olenek subprovince (fields #6-20, Fig. 2.2.1) in the northeastern margin of the platform (Smelov & Zaitsev, 2013). The kimberlites of those two subprovinces differ in a number of features. Kimberlites from the Vilyui subprovince are mainly of explosive type. Northward, there is an increase in the number of intrusive bodies unevenly distributed amongst the explosive ones. The overall number of kimberlite bodies in the Anabar-Olenek subprovince is 4.5 times higher than in the Vilyui one, but their diamond tenor is 90 % lower. The diamond morphology and size also differ in the two subprovinces. For both subprovinces, excluding Anabar shield, it is typical that Upper and Middle Paleozoic sediments have been almost completely removed by erosion. Sediments of Carboniferous and Permian age preserved only in the areas of the Siberian traps (Kharkiv *et al.*, 1998). The main fields of diamondiferous and non-diamondiferous kimberlites are located within the limits of several kimberlite-controlling zones; the Vilyui-Markha and Daldyn-Olenek zones have northeast strikes, and the Anabar zone a north–northwest strike. It has been proposed that the existence of the Arga-Sala zone of nearly west-east strike controls the locations of kimberlite fields on the western slope of the Anabar shield (Brakhfogel, 1984, Ilupin *et al.*, 1990, Kharkiv *et al.*, 1998).

Because of the significant variations in terrane drawing from different map in some cases it is hard to tell within which terrane the kimberlite field is located. Following description of fields and terrane reference is based on the map given by (Griffin *et al.*, 1999a) which is the modification of the tectonic scheme of the Siberian Craton published by (Rosen *et al.*, 1994). A chain of Paleozoic to Mesozoic kimberlite fields (called the ‘Olenek trend’) stretches nearly 1000 km SW–NE across the north-central part of the platform, and a trail of Mesozoic kimberlites (the ‘Anabar trend’) extends 320 km to the northwest from the middle part of the Olenek trend, along the eastern boundary of the Anabar Shield (Fig. 2.2.1).

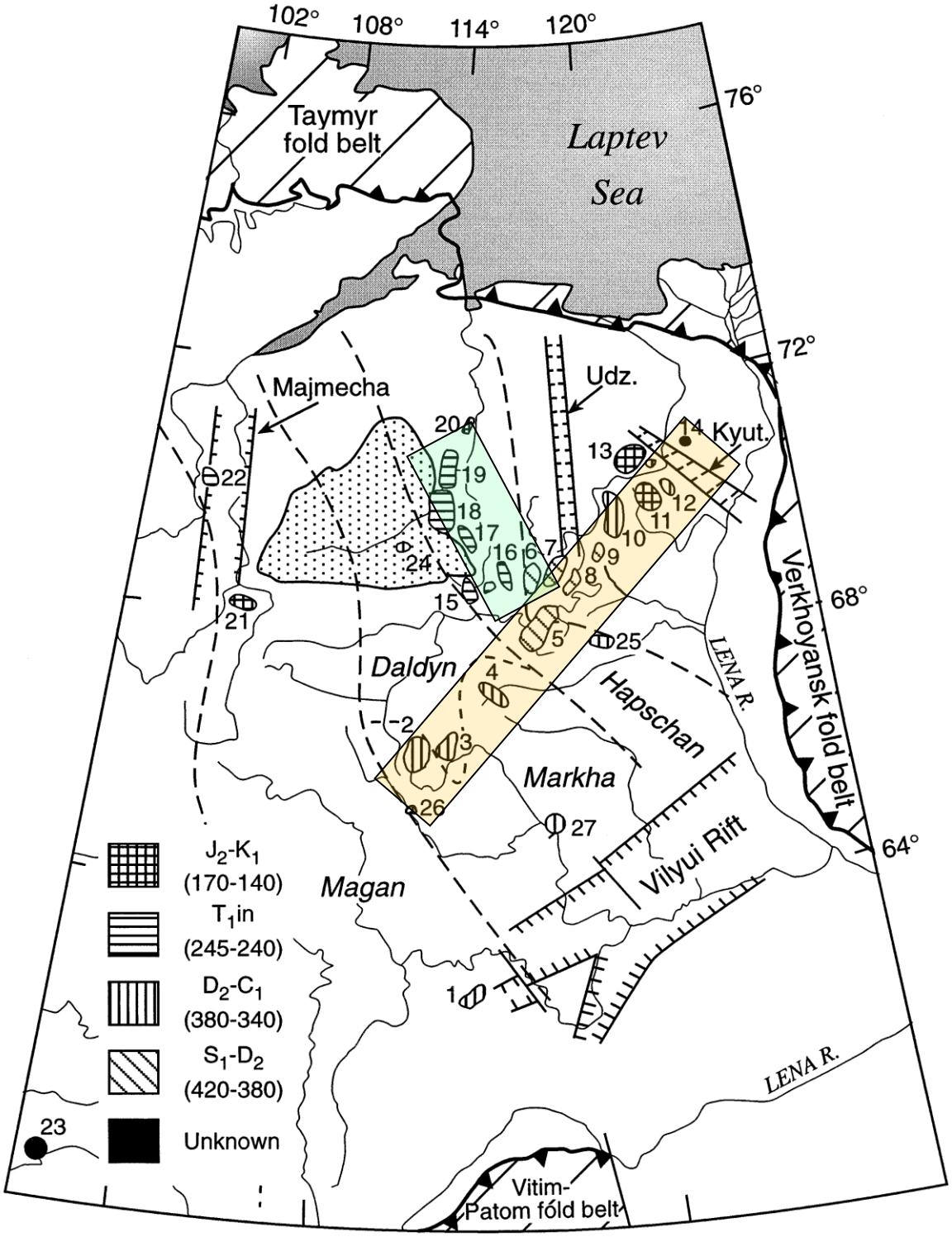



Figure 2.2.1. Modified terrane map of the Siberian Platform, showing the locations of kimberlite fields and major tectonic elements. Anabar trend is shown in green, the Olenek trend in yellow. Kimberlitic fields: 1 – Malo-Botuobinskoe, 2 – Alakhit_Markha, 3 – Daldyn, 4 - Upper Muna, 5 – Chomurdakh, 6 – West-Ukukit, 7 – East-Ukukit, 8 – Ogoner-Yuryakh, 9 – Merchemden, 10 – Molodo, 11 – Kuoika, 12 – Toluopka, 13 – Kuranakh, 14 - Lower Lena; 15 – Biriginda, 16 – Luchakan, 17 – Duken, 18 – Ary-Mastakh, 19 - Lower Kuonamka; 20 - Orto Irigakh; 21 - Kharamai; 22 - Dalbicha; 23 - Chadobez; 24 - Central Anabar; 25 - Severnei; 26 - Morkoka; 27 - Markha

***Types of kimberlite***

Most kimberlite-related studies utilize the classification proposed by Craig Smith (1983). Using samples selected on a petrographic basis by E. Michael W. Skinner (De Beers), Smith demonstrated that monticellite-calcite-serpentine kimberlites and phlogopite kimberlites from the Kaapvaal craton (South Africa) possess distinctive Sr and Nd isotopic compositions. On the basis of these data, Smith (1983) suggested that monticellite serpentine calcite kimberlites, termed group I kimberlites, and phlogopite kimberlites, termed group II kimberlites, were derived from asthenospheric and lithospheric mantle sources respectively. It should be particularly noted that Smith (1983) introduced the terms group I and group II as a means of classifying kimberlites primarily on an isotopic basis and not upon their petrographic character. As a consequence of these isotopic studies, Smith *et al.* (1985) and Skinner (1986) proposed that kimberlites can be divided into two distinct groups, I and II, on the basis of differences in their distribution patterns, age, petrography, content of mantle-derived xenocrysts, xenoliths and megacrysts, isotopic characteristics and whole-rock geochemistry. Mitchell (1995) later proposed that these group I and II kimberlites display such distinct differences, that they may not be as closely related as once thought. He showed that Group II kimberlites actually show closer affinities to lamproites than to Group I kimberlites. Hence, he renamed Group II kimberlites as orangeites to prevent confusion. However, the term Group II is still widely spread in literature.

Apart from this classification, kimberlites are usually subdivided based on difference in their structure and mineralogy. According to structural and textural signatures two main types of kimberlite are commonly recognized: 1 - kimberlites with massive structure and 2 - volcanoclastic kimberlite (sometimes with subdivision to kimberlite breccia, tuff breccia and tuff). Based on mineral composition, olivine-, monticellite-, pyroxene-, melilite-, calcite- and phlogopite-olivine varieties can be distinguished (Kostrovitsky *et al.*, 2007). The petrochemical classification of kimberlite is much more complex. To the first order, contents of $TiO_2$, FeO and $K_2O$ should be taken into account. $Na_2O$ and $P_2O_5$ concentrations also are usually used for this classification.

Within the YKP four genetic types of kimberlites and related rocks have been recognized: 1 - diamondiferous kimberlites of the southern fields (Malo-Botuobinskoe, Daldyn, Alakit, Upper Muna and Nakyn); 2 – non-diamondiferous or diamond-poor kimberlites of the northern fields of the YKP; 3 - Group II kimberlites (orangeites) of the Ingashi field in Sayan; and 4 - carbonatites that form individual pipes within kimberlitic fields of the Anabar region (Ilupin *et al.*, 1990).

Diamondiferous and diamond-poor kimberlitic pipes of the southern and northern fields are Group I kimberlites according to Smith's classification. Among them there are pipes of both massive and volcanoclastic structure. The pipes of the southern area (except the Upper Muna field) are largely filled by breccia-type kimberlites, while massive kimberlites are more widely spread within the northern fields. In terms of mineral composition, all types mentioned above are found in the northern area. The southern fields are essentially dominated by olivine kimberlites with carbonate-olivine varieties. The Upper Muna field is the only one containing monticellite-olivine kimberlites.

According to their chemical composition, the following contrasting types of kimberlites and related rocks have been recognized in the YKP: 1 - high Mg, low Ti, low K; 2 - high Mg, low Ti, high K; 3 - Mg-Fe, high Ti, low K; 4 - Fe-Ti, low K; 5 - Fe-Ti, high K (Kostrovitsky *et al.*, 2007).

***Ages of kimberlitic magmatism***

Across the Siberian Craton kimberlite magmatism is restricted to four main stages: (1) Proterozoic (The Ingashi veins only); (2) Middle Paleozoic (the majority of kimberlites of the Daldyn-Olenek and Vilyui-Markha zones); (3) Lower Mesozoic (kimberlites and related rocks of the Olenek-Anabar zone as well as the Kotui and Kharamai fields); (4) Upper Mesozoic (some kimberlites from the Kuoika and Upper Molodo fields) (Kostrovitsky *et al.*, 2007).

A significant body of isotopic-geochronological data are reported in the literature. However, many analyses are controversial, even if the dated samples are from the same kimberlitic body. Thus, for this review the most reliable ages (U-Pb or fission track methods) have been used where possible. Apart from those, Rb-Sr, K-Ar and Ar-Ar data are also available, but the type of analysed sample, analytical procedure and geological conditions (stage of alteration, late processes *etc*) need to be considered when using these results (Table 2.2).

According to the recently published study by Smelov and Zaitsev (2013) five main epochs of kimberlite magmatism can be recognized within the YKP: Ordovician-Silurian, Devonian-Carboniferous, Triassic, Jurassic and Cretaceous. In general, there is a south-to-north younging of kimberlite magmatism. Thus, kimberlites of Ordovician to Carboniferous age are found in both southern and northern parts of the province, while Triassic, Jurassic and Cretaceous bodies occur only in the northern area.

Ordovician-Silurian kimberlites are found within the Magan (Malo-Botuobinskoe field), Khapchan (Chomurdakh field), and Birekta terranes (West Ukukit, Ogoner-Uryakh and Upper Motorchuna fields).

The Devonian-Carboniferous epoch is considered to be the main stage of the kimberlite magmatism within the YKP. The kimberlites of this age are widely spread across the province, within the Magan (Malo-Botuobiskoe field), Markha (Nakyn, Alakit-Markha and Upper Muna fields), Daldyn (Daldyn field), Hapchan (Chomurdakh and Severnoe fields) and Birekta (West and East Ukukit fields, Merchemdenskoe, Toluopka) terranes.

Triassic ages were determined for bodies of kimberlite within the Anabar shield (Serbian dike), and in the Magan (Kharamai field) and Hapchan terranes (Kuranakh, Luchakan, Middle and Lower Kuonamka).

Jurassic kimberlites are known mainly in the Birekta terrane (Kuoika, Upper Molodo). However, Rb-Sr isotopic data show ages of 140-180 Ma in the Kharamai field (Magan terrane). Moreover, U-Pb dating of zircons from two pipes of the Middle Kuonamka field (Khapchan terrane) reveals ages *ca* 150 Ma (Smelov & Zaitsev, 2013).

The Cretaceous epoch of kimberlite magmatism was defined by Smelov and others (Altukhova & Zaitsev, 2006, Smelov & Zaitsev, 2013) based on the Rb-Sr dating of the groundmass of two pipes from the Ary-Mastakh field (Daldyn terrane, Table 2.2). These data are consistent with some ages of pipes from the Kuoika and Molodo fields, but such young ages for both locations are not yet confirmed by U-Pb dating.

Table 2.2. Comparison of the isotopic data (Ma) for kimberlites, obtained by different dating techniques (Smelov & Zaitsev, 2013).

| **Locality** | **Isotopic methods** | | | | |
|---|---|---|---|---|---|
| | **Rb-Sr** | **U-Pb** | **Fission-track analysis** | **K-Ar** | **Ar-Ar** |
| ***Malo-Botuobiya field (1)*** | | | | | |
| Mir pipe | 348-382 | 360-367 | 358 | 403 | 372 |
| Tayezhnaya pipe | 372-440 | 403 | 397 | | 372 |
| Amakinskaya pipe | 333-353 | 450 | 486 | | |
| ***Nakyn field (27)*** | | | | | |
| Botuobiskaya pipe | 448-364 | | | | 440-365 |
| Nyurbinskaya pipe | 449-332 | | 404-396 | | 385-369; 994-1868 |
| ***Alakit-Markha field (2)*** | | | | | |
| Druzhba pipe | 431 | 358 | | | |

| Locality | Isotopic methods | | | | |
|---|---|---|---|---|---|
| | **Rb-Sr** | **U-Pb** | **Fission-track analysis** | **K-Ar** | **Ar-Ar** |
| Kollektivnaya pipe | | 347 | 385 | | |
| Radiovolnovaya pipe | | 229 | | 272-242 | |
| Komsomolskaya pipe | 358, 410-420 | 344-358 | | | |
| Yubileynaya-Vostochnaya pipe | 366-342 | 358 | | | 363 |
| Sytykanskaya pipe | | 344 | 384 | | |
| ***Daldyn field (3)*** | | | | | |
| Udachnaya-Zapadnaya pipe | 391-328; 599; 880 | 359-353 | | 315-424; 699-509 | |
| Udachnaya-Vostochnaya pipe | 402-327; 474; 716 | 367-336 | | | 380-354; 445; 595-510 |
| Dalnaya pipe | 404-315 | 355 | | | |
| Zagadochnaya pipe | 357-348 | | 370 | 454-420; 544-517 | |
| ***Upper-Muna field (4)*** | | | | | |
| Novinka pipe | 374 | 355 | | | |
| Interkosmos pipe | | 369 | 369 | 458 | |
| 325 let Yakutii pipe | | 345; 440-449 | 362 | | |
| Komsomolskaya-magnitnaya pipe | 402 | | | 382-334 | 427 |
| Rassvet pipe | | 344 | 374 | | |
| ***Chomurdakh field (5)*** | | | | | |
| Snezhinka pipe | 372-421 | | | 386-513 | |
| Perevalnaya-3 stock | 373-448 | | | 411 | |
| Chomur pipe | 353-439 | | 377 | 387-418 | |
| Svetlaya pipe | 378-381 | | | 370 | |
| Druzhba pipe | 380 | 412-429 | 448 | | |
| Uralskaya pipe | 440 | | | 406-441 | |
| ***West Ukukit field (6)*** | | | | | |
| Anomaly 23-1/65, stock | 389-367 | | | 445 | |
| Anomaly 23-2/65 | 434-366 | | | 418-374 | |
| Leningrad pipe | 380-350 | | | | 385 |
| ***East Ukukit field (7)*** | | | | | |
| Ukukit dike | 373 | | | 428 | |
| ***Ogoner-Yuryakh field (8)*** | | | | | |
| Aerogeologicheskaya pipe | 432 | 409 | 459 | | |
| ***Merchemden field (9)*** | | | | | |
| Vostok-6 body | 400 | 419 | 367 | | |

| Locality | Isotopic methods | | | | |
|---|---|---|---|---|---|
| | **Rb-Sr** | **U-Pb** | **Fission-track analysis** | **K-Ar** | **Ar-Ar** |
| ***Kuoyka field (11)*** | | | | | |
| Obnazhennaya pipe | 161-135 | | | 205-185, 288 | 418-397 |
| Lyudmila pipe | 174 | | | 169 | |
| Rubin pipe | 141 | | | 177 | |
| Anomaly 23/78 | 169 | | | 122 | |
| Dyanga dike | 249-227 | | | | |
| Dyanga pipe | 157-156 | 156 | | | |
| Ruslovaya pipe | 179-159 | | 158 | 381-341 | |
| Montichellitovaya pipe | | 170-148 | | 550-520 | |
| Irina pipe | | 148 | 165 | 509 | |
| Velikan-2 | | 159-128 | | 352 | |
| Pyatnitsa pipe | | 156 | 157 | | |
| Muza pipe | | 149 | 154 | | |
| Slyudyanka pipe | | 148 | 147 | | |
| Tokur pipe | | 152 | 153 | | |
| ***Molodo field (10)*** | | | | | |
| Molodo pipe | 140 | | 125 | | |
| Granatovaya pipe | 188-135, 509 | | | 195-186 | |
| Marichka pipe | | 159 | 171 | | |
| Khrizolitovaya pipe | | 156 | 150 | | |
| ***Luchakan field (14)*** | | | | | |
| Lykhchan-2 pipe | 229-220 | | | 227 | |
| Otritsatelnaya pipe | 160 | | | 229 | |
| ***Kuranakh field (13)*** | | | | | |
| Malokuonamskaya pipe | 170-239 | 224 | 223 | 263 | |
| Markiza pipe | 244-258 | | | 252 | |
| ***Biriginde field (15)*** | | | | | |
| Shkiper body | | 158 | 162 | | |
| Dike C-26 (Olobu) | | 240 | 193 | | |
| ***Ary-Mastakh field (18)*** | | | | | |
| Stock Arktika-1 | 235 | 232 | | 239 | |
| Polyarnaya pipe | 101 – 157 | | | | |
| Perm pipe | 100 | | | | |

## 2.3 Subcontinental lithospheric mantle of the Siberian craton

Cratons are commonly underlain by thick lithospheric roots, which vary in composition and thermal state, reflecting the tectonothermal history of the overlying crust. Thus, constraining the age and evolution of the sub-continental lithospheric mantle (SCLM) has important implications for our understanding of continent evolution over geological time. Geophysical data can give an indication of the physical properties of the rocks that exist at depth today, but our ability to correlate these data with real rock types is still limited (Kuskov *et al.*, 2014b). Apart from geophysical approach, studying xenoliths is the only way to obtain information about the SCLM (Griffin *et al.*, 1999a). Fragments of the lithosphere under Siberia have been sampled as xenoliths and xenocrysts, brought up to the surface by kimberlitic magmas. Numerous kimberlite pipes of various ages have been described within the Siberian craton, providing invaluable 'snapshots' of the evolution of the Siberian SCLM over time.

### *Composition of the lithospheric mantle based on xenoliths study*

The investigation of xenoliths and xenocrysts from diamond-bearing kimberlites has provided unique information on the composition and structure of the lithospheric mantle and shown that the root of the Siberian craton is composed mainly of peridotites depleted in basaltic components (primarily, Fe, Ca, and Al), which is related to the early stage of crustal development (Sobolev, 1977). They are composed of olivine and orthopyroxene with subordinate garnet and clinopyroxene (harzburgites and garnet lherzolites). Spinel-bearing lherzolites are dominant at shallower levels. The use of multimineralic and single mineral garnet thermobarometry has allowed model reconstructions of the composition and structure of the Siberian lithospheric mantle (Ashchepkov *et al.*, 2010, Boyd *et al.*, 1997, Griffin *et al.*, 1996, Griffin *et al.*, 2003, Ionov *et al.*, 2010). The mineral assemblage from which a given garnet macrocryst was derived can be estimated from the relationship between CaO and $Cr_2O_3$ contents. This allows distinction of the lherzolite paragenesis (olivine + orthopyroxene + clinopyroxene + garnet ± spinel) from the harzburgite paragenesis (lacking clinopyroxene). This 'thermodynamic' definition emphasises the important distinction between rocks in which the garnet is Ca-saturated through equilibrium with Cpx, and those in which the Ca content of the garnet is not buffered by the mineral assemblage (Griffin *et al.*, 1999a).

According to published results from xenolith studies the distribution of rock types in the Siberian Craton lithosphere varies underneath different part of the Craton. Thus Griffin *et al.* (1999a) reported that harzburgitic rocks are generally restricted to the southern half of the Olenek trend (Fig. 2.2.1), within the areas underlain by Archean crustal terranes. The low-Ca

harzburgites are concentrated in a restricted depth range, with most being derived from 150 to 180 km depth. Garnets from calcic harzburgites show a wider vertical distribution, with discontinuities between some fields clearly visible. These discontinuities correspond to the terrane boundaries mapped in the crustal rocks (cf. Figs. 2.1.1 and 2.2.1). Wehrlitic garnets show a more restricted lateral distribution, being concentrated at the southern end of the traverse (Malo-Botuobiya and Alakit-Markha fields).

Low-Cr lherzolitic garnets (<1.5% $Cr_2O_3$), occur mainly at shallow depths in the southern part of the traverse, but make up most of the lithospheric mantle beneath the north-central part of the traverse. Their distribution indicates a significant difference in mantle composition between the southern and the northern parts of the traverse. The deep 'slab' of such rocks dipping southwards beneath the harzburgitic part of the lithosphere is interpreted as reflecting a high proportion of asthenosphere-derived material in the lower lithosphere beneath this part of the traverse.

The depth distribution of harzburgitic garnets in the kimberlite fields of the Olenek trend is shown in more detail in Fig. 2.3.1. The maximum proportion of such garnets is significantly higher in the Alakit-Markha and Daldyn fields than in the fields to the north and south.

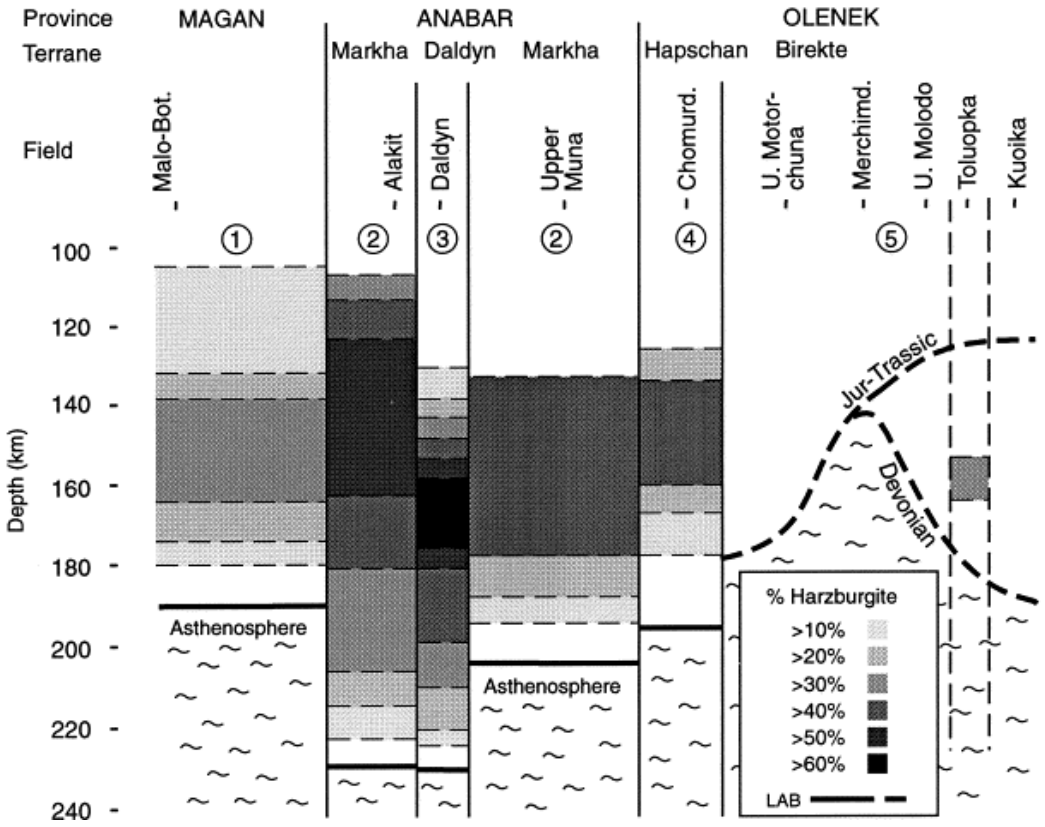



Figure 2.3.1 Detailed distribution of harzburgitic garnets within each field along the Olenek trend (Griffin *et al.*, 1999a)

***Re-Os and platinum-group elements data***

Another valuable tool used in xenolith studies is the Re-Os isotopic system. This can be applied to both whole-rock samples (bulk analysis) and sulfides or Platinum-Group minerals (in-situ analysis) to constrain the chemical history and evolution of the SCLM (Pernet-Fisher *et al.*, 2015). Model-age calculations are commonly used to provide age estimates for depletion events within the lithosphere. *Mantle separation model age* ($T_{MA}$) assumes that Re and Os contents of the sample were not modified after their formation and is calculated using the measured Re/Os of sulfide and assuming separation from the source. A more commonly used Os isotopic model age is *Rhenium-depletion model age* ($T_{RD}$) which assumes no Re in the sample and represents the time of separation of the sulfide from a reservoir, assuming zero Re/Os and which are by definition minimum age. However, such age calculations are sensitive to the effects of metasomatism. Depending on melt/rock ratios and the degree of S-saturation of metasomatic fluids, sulfides (the main host for Os in these rocks) can either be dissolved by metasomatic fluids or precipitated along silicate grain boundaries; in either case they can perturb the Re-Os system. The use of PGE patterns in conjunction with Re abundances can identify samples that are likely to have undergone Re-enrichment, thus altering Re/Os ratios. Extensive melting will result in residues that display highly fractionated P-PGE/I-PGE values (i.e., Pt/Ir > 1). Therefore, residues that display enhanced Re concentrations (i.e., large Re-spikes), coupled with strong P-PGE depletions, are not likely to be consistent with the observed level of melt depletion.

Xenoliths from the Udachnaya pipe have been extensively studied over the past several decades, resulting in a large suite of melt-extraction ages from samples that display variable extents of metasomatism, i.e., large ranges in Re/Os (Griffin *et al.*, 2002a, Ionov *et al.*, 2006, Pearson *et al.*, 2002).

Griffin *et al.* (2002a) presented a plot of $T_{MA}$ versus $T_{RD}$ (Fig. 2.3.2) showing that some of the sulfides scatter into the quadrant with ($T_{MA} > 0$, $T_{RD} < 0$); in whole-rock xenolith studies this pattern commonly is interpreted as reflecting the addition of Re to the sample near the time of eruption. These sulfides may have been introduced into the lithosphere shortly before kimberlite eruption. However, other sulfides define a trend extending into the quadrant with ($T_{MA} < 0$, $T_{RD} < 0$), implying a multistage growth in which the Re/Os of the earlier stage(s) was less than that of the analyzed sample. In whole-rock studies this is commonly ascribed to a recent loss of Re; however, it is difficult to see a mechanism for causing Re loss in individual sulfide inclusions within olivine.

A plot of $T_{MA}$ versus $^{187}Re/^{188}Os$ (Fig. 2.3.2b) shows these two trends in another perspective. A broad scatter of data from Group 3C sulfides (extending well outside the range

of the figure) shows a trend of increasing $T_{MA}$ with increasing Re/Os, as would be expected from addition of Re to samples with $^{187}Os/^{188}Os$ < CHUR. This positive correlation also is observed in whole rock Re-Os data for peridotite xenoliths from both Siberia and South Africa (Pearson *et al.*, 1995a, Pearson *et al.*, 1995b, Pearson *et al.*, 1995c), where it has been interpreted as the effect of young Re addition. These Group 3C sulfides may be the material by which such Re addition occurs.

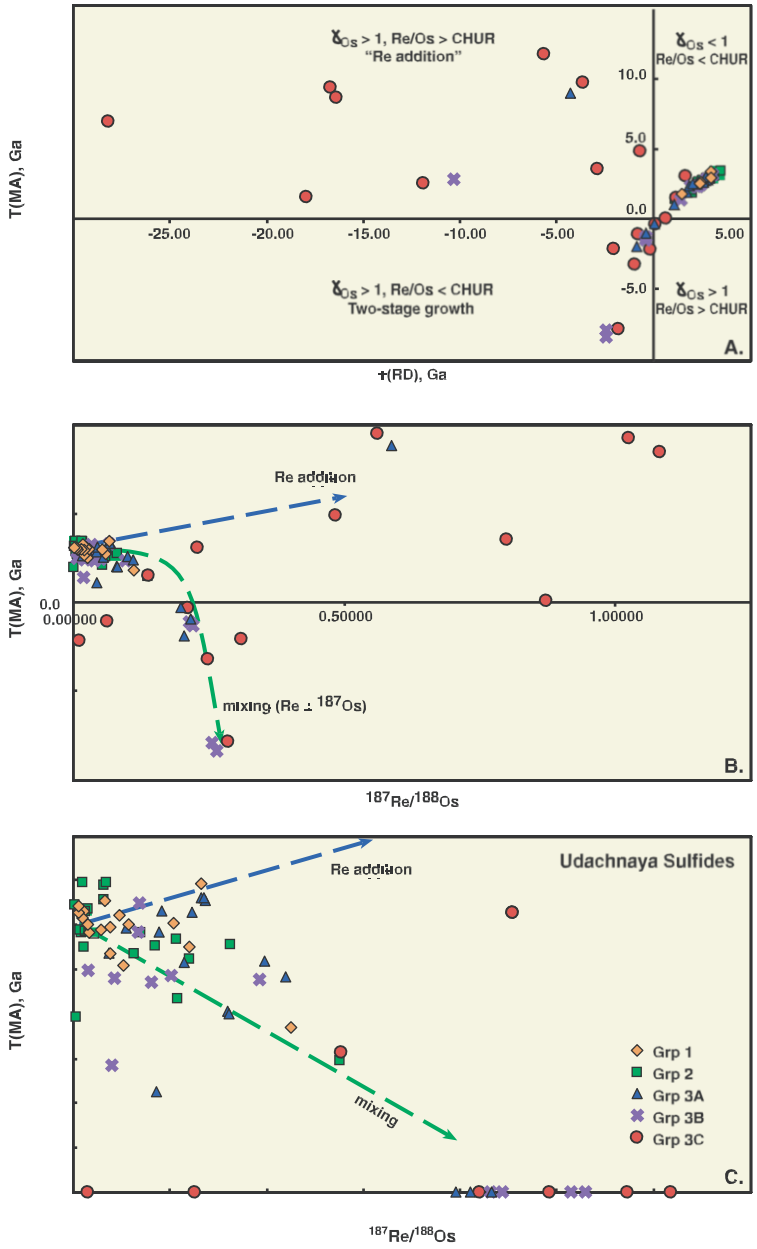



Figure 2.3.2. (a) $T_{MA}$ versus $T_{RD}$, showing scatter of some sulfides into upper left quadrant, and others into lower left. (b) $T_{MA}$ versus $^{187}Re/^{188}Os$, showing the broad positive trend produced by late Re addition, and the better- defined negative trend inferred to result from addition of sulfide melts derived from eclogites. (c) Expanded view of Fig.2.3.2b. Samples with negative $T_{MA}$ are plotted on the X axis (Griffin *et al.*, 2002a).

However, many of the other data points, including some Group 2 as well as Group 3 sulfides, define a negative trend between sulfides with high γOs and low Re/Os (Groups 1 and 2), and others with very high γOs and relatively modest Re/Os (<CHUR). As noted above, the trace element systematics of the Group 3 sulfides suggest a mixing process, in which Group 3A and 3B sulfides have acquired a hybrid PGE pattern by reaction between residual sulfides and sulfide melts more similar to some Group 3C sulfides. It was suggested that the Re-Os data may be explained by a similar mixing process (Griffin *et al.*, 2002a).

The existence of sulfides with $^{187}Os/^{188}Os$ > CHUR (up to γOs = 400), but $T_{MA}$ > 4.5 Ga, requires a two-stage evolution involving an older source that has Re/Os higher than most estimates for the convecting mantle, and presumably must reside within the lithosphere. An appropriate candidate for this source is represented by eclogite xenoliths from Udachnaya, the Re-Os systematics of which have been studied by Pearson et al. (Pearson *et al.*, 1995a, Pearson *et al.*, 1995b). These eclogite xenoliths scatter about a 2.9 Ma Re-Os isochron; four of them define a 3.2 Ga isochron. They have a mean Os content of 0.1 ppb and a mean $^{187}Re/^{188}Os$ = 99 (range 12 – 211), and are capable of generating extremely high $^{187}Os/^{188}Os$ within 10 – 100 Ga after their separation from the primitive mantle. Similar high Re/Os ratios and very radiogenic Os have been described from inclusions of eclogitic (low-Ni (Bulanova *et al.*, 1996)) sulfides in African diamonds (Pearson *et al.*, 1999, Shirey *et al.*, 2001). While PGE patterns are not available for the Udachnaya eclogites, we assume that they have the low Os/Pt characteristic of most basaltic rocks.

Five sulfide inclusions in Udachnaya diamonds (Pearson *et al.*, 1999) have $^{187}Re/^{188}Os$ = 0.031 – 0.175 and their $T_{MA}$ model ages range from 2.93 – 3.37 Ga, consistent with most of the data on low-Re/Os sulfides from this study. The PGE patterns of these inclusions (Freydier *et al.*, 1997) indicate that they are Group 1 or Group 2 sulfides; their Os contents are 70 – 110 ppm, while Pt contents were below the detection of the proton microprobe (ca 50 ppm). The inclusions analysed by Pearson were previously analysed by proton microprobe (Bulanova *et al.*, 1996) and have very high Os contents. Pearson's methods will dissolve sulfides, but not PGMs, so the difference suggests that the PGEs in the sulfides actually exist as micronuggets, rather than being in the structure of the sulfide.

On the basis of the data presented above, and the assumption that the formation of residual sulfides coincided with melt extraction from the peridotitic mantle, (Griffin *et al.*, 2002a) suggested that much of the SCLM beneath the Udachnaya pipe was stabilized between 3.5 and 3.0 Ga ago by one or more major melt-extraction events. Eclogites were formed either by the intrusion of mafic melts, or by subduction of crustal basalts, between 3.2 and 2.9 Ga (Pearson *et al.*, 1995a, Pearson *et al.*, 1995b), and would rapidly have evolved highly

radiogenic Os-isotope compositions. To explain the range of observed Os-isotope compositions in the enclosed sulfides, authors suggested that partial remelting of these eclogites at ca 2.9 Ga produced melts with high $^{187}Os/^{188}Os$ and moderate Re/Os, which penetrated the surrounding mantle wall rocks and reacted to varying degrees with discrete grains of Os-rich MSS. The heat required for this melting event may also have produced depletion in some mantle peridotites, so that it is recorded in the Os isotope compositions of many enclosed sulfides. It is plausible that the 2.9 Ga event recorded by the eclogites dates the intrusion, or the subduction and recrystallization, of their basaltic protoliths and their emplacement into the mantle root.

The major peak of $T_{MA}$ values around 2.9 Ga, and the scarcity of younger model ages, suggests that this event signaled the end of major lithosphere formation in this area. Several individual inclusions with low Re/Os and $T_{MA} < 2.6$ Ga may represent new additions to the lithosphere, but we cannot exclude the possibility that these too reflect mixing of sulfide generations.

This scenario is consistent with the limited data on crustal formation in the Daldyn terrane. These suggest a major crust-forming event around 3.0 Ga, and minor igneous activity related to the major terrane boundaries and associated with the amalgamation of the craton around 1.8 – 2.0 Ga (Rosen *et al.*, 1994).

***Thickness of the lithosphere***

The compositional spectrum of garnet peridotites and the thickness of the lithosphere may vary from craton to craton depending on the stabilization age, tectonic history, and thermal regime (Artemieva & Mooney, 2001, King, 2005, Kopylova & Russell, 2000, Kuskov *et al.*, 2014a). Petrological investigations have shown that the degree of depletion of the ultrabasic rocks decreases with depth (Boyd *et al.*, 1997, Gaul, 2000, Griffin *et al.*, 1996). The maximum thickness of a depleted mainly diamond-bearing harzburgite layer was established under the Anabar province (Rosen *et al.*, 2006). Although these rocks do not show a strictly regular distribution, it can be supposed that the lithospheric mantle beneath ancient cratons is strongly depleted up to 150–200 km depths. It is believed that the chemical (petrological) boundary (CBL) lies within this depth interval (Afonso *et al.*, 2008, Forte, 2000, King, 2005, O'Reilly & Griffin, 2010).

In particular, geochemical studies of xenoliths obtained from Paleozoic kimberlites (e.g., Udachnaya) suggest that a thick (~200 km), old (~3–1.8 Ga), diamondiferous lithosphere was present at this time (Boyd *et al.*, 1997, Griffin *et al.*, 2002a, Pearson *et al.*, 1995b). In contrast, xenoliths brought up by Mesozoic kimberlite pipes (e.g., Obnazhennaya) appear to sample a

significantly thinner (~150 km), diamond-barren lithosphere (Ashchepkov *et al.*, 2014, Griffin *et al.*, 1999b, Howarth *et al.*, 2014). This was also confirmed by petrological-geophysical modelling of the upper mantle based on seismic data combined with geochemical composition of xenoliths (Kuskov *et al.*, 2014a, Kuskov *et al.*, 2014b). This modelling shows significant heterogeneity in the distribution of seismic velocities, temperature, and density; the relief of seismic boundaries; and the degree of layering in the Siberian upper mantle.

***Thermal state of the lithosphere***

Mapping of the present-day thermal state of the lithospheric mantle indicates that the bottom of the thermal lithosphere (thermal boundary layer) of the craton, which weakly depends on the composition of the rocks, is close to the 1450 ± 100°C isotherm and lies at a depth of 300 ± 30 km (Kuskov *et al.*, 2014a).

The cratonic mantle (including that beneath the Yakutian kimberlite province) is characterized by elevated P-wave velocities and low values of temperature and density; the mantle heat flow is estimated as 11–17 mW/m$^2$. At depths of 100–200 km, temperature in the central part of the craton is somewhat lower than at its periphery and 300–400°C lower than that in the tectonically younger mantle surrounding the craton. The temperature profiles lie between the conductive geotherms of 32.5 and 35 mW/m$^2$, which is consistent with the data from seismic tomography (Deen *et al.*, 2006), xenolith thermobarometry (Ashchepkov *et al.*, 2010) and heat flow measurements for most Precambrian provinces (Artemieva & Mooney, 2001, Rosen *et al.*, 2009).

Based on data from geothermometry, tomography, mineral physics, and electromagnetic measurements, it was suggested that the cold ancient lithosphere of cratons has low heat flow averaging 38–40 mW/m2 (Artemieva, 2009, Rudnick *et al.*, 1998) and comprises high velocity anomalies but no partial melting zones (Egorkin, 2004).

According to the garnet-xenocryst study of Griffin *et al.* (1999a) the variations in the geotherm across the region in Devonian time were quite significant (Fig. 2.3.3). To show the difference the authors used the 1000 ºC isotherm, which is, within the uncertainties of measurement, flat across the southern part of the traverse, including the Malo-Botuobiya, Alakit and Daldyn fields. It lies at 175–180 km depth, reflecting a low geotherm, near the 35 mW/m$^2$ conductive model of Pollack and Chapman (1977). The data from the Devonian Upper Muna and Chomurdakh fields give a somewhat higher paleogeotherm, reflected in the 1000ºC isotherm rising to *ca* 160 km depth. Within the Mesozoic kimberlite fields of Birekte terrane, the paleogeotherm lies near the 40 mW/m$^2$ conductive model of Pollack and Chapman (1977),

bringing the 1000ºC isotherm up to *ca* 130 km depth. The Devonian geotherm beneath the Toluopka field was lower, and this isotherm therefore would have been deeper (140–150 km) during Devonian time (Fig. 2.3.3).

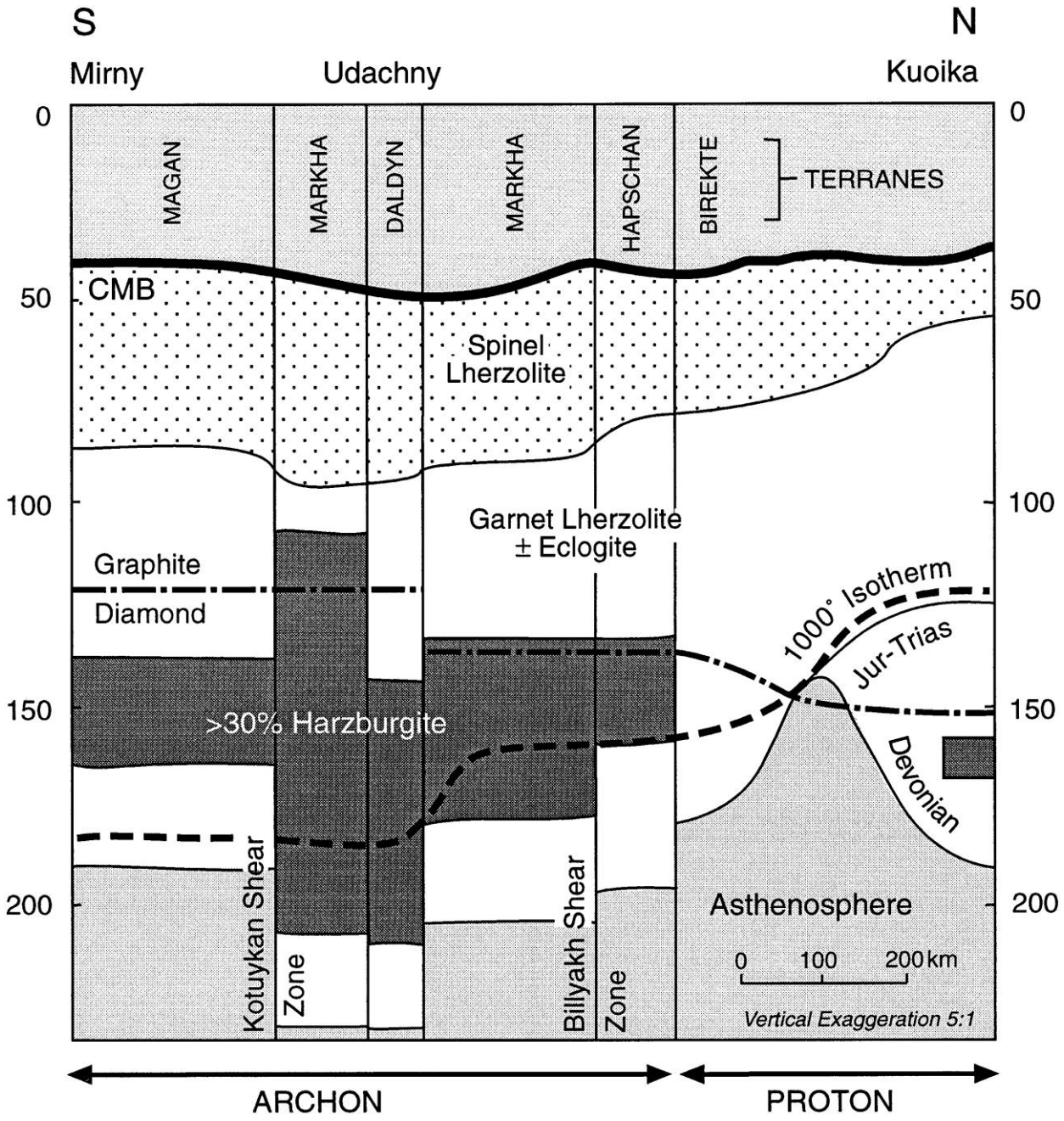



Figure 2.3.3. Variation in lithosphere structure, composition and thermal state along the Olenek trend. The depth variation of the 1000ºC isotherm reflects lateral variation in the paleogeotherm, and is mirrored by variation in depth to the graphite–diamond transition. Variation in depth to the spinel–garnet lherzolite transition reflects variations in both the geotherm and the mean degree of depletion; the transition has been observed in the Malo-Botuobiya and Daldyn fields, and is estimated in the others (Griffin *et al.*, 1999a).

# Chapter 3. Samples, analytical methods and techniques.

Most of analytical work was carried out at the CCFS/GEMOC Geochemical Analysis Unit (GAU), Macquarie University, Sydney. Colour cathodoluminescence imaging was performed in Department of Bio-Geosphere Science, Okayama University of Science, Kitaku, Okayama, Japan. The analysis of zircon oxygen-isotope compositions has been done at the Ion Probe Facility at The University of Western Australia Centre for Microscopy, Characterisation and Analysis (CMCA) in Perth. High-resolution U-Pb SHRIMP dating was performed at the John De Laeter Centre for Isotope Research, Curtin University, Perth.

## 3.1. Samples: location, types, and preparation

***Zircon samples*** from 38 kimberlite pipes in 13 fields of the Siberian Craton (Table. 3.1, Figure 3.1.1) were involved in the project. Samples have been supplied as heavy-mineral concentrates, mineral specimens or whole-rock samples by Dr. V.G. Malkovets, Prof. W.L. Griffin, Dr. Z.V. Spetsius, Dr. N. Vladykin and others.

There are 3 different types of zircon samples studied (Table 3.1): "HMC" – zircons extracted from the heavy-mineral concentrate collected from the weathered crust of kimberlite pipe; "kimberlite" – zircon grains hand-picked directly from the crushed kimberlite, usually based on their morphology and large size; "xenoliths" – zircons extracted from different types of xenoliths hosted by kimberlite.

To extract zircons from the whole-rock samples they were processed using the SelFrag electrostatic disaggregation facility. The disaggregated rock was sieved using 200 μm disposable nylon mesh, then panned to separate the denser fraction. Some separates were processed using hand and roll magnets, and then by heavy liquid separation using sodium polytungstate to further purify the zircon concentrate. Zircons were hand-picked under the binocular microscope, mounted in 25 mm epoxy discs and polished.

***Sulfide inclusions in silicate minerals*** were obtained only from the Udachnaya pipe (Daldyn field, #3). Olivine xenocrysts containing sulfide inclusions were hand-picked under the binocular microscope, mounted individually in epoxy discs, and polished until the sulfide inclusion exposed. Some of them were later cut from the individual discs and mounted together (up to 7 olivine grains per mount). Prior to analytical work included in this study, electron microprobe analyses, back-scattered electron (BSE) imaging and element mapping have been performed for all inclusions. This work has been done by Dr Vladimir Malkovets.

***Rutile inclusions*** in garnet xenocrysts were found only in kimberlite of Internationalaya pipe (Malo-Botuobinskoe field, #1). The preparation procedure is similar to those for sulfide inclusions.

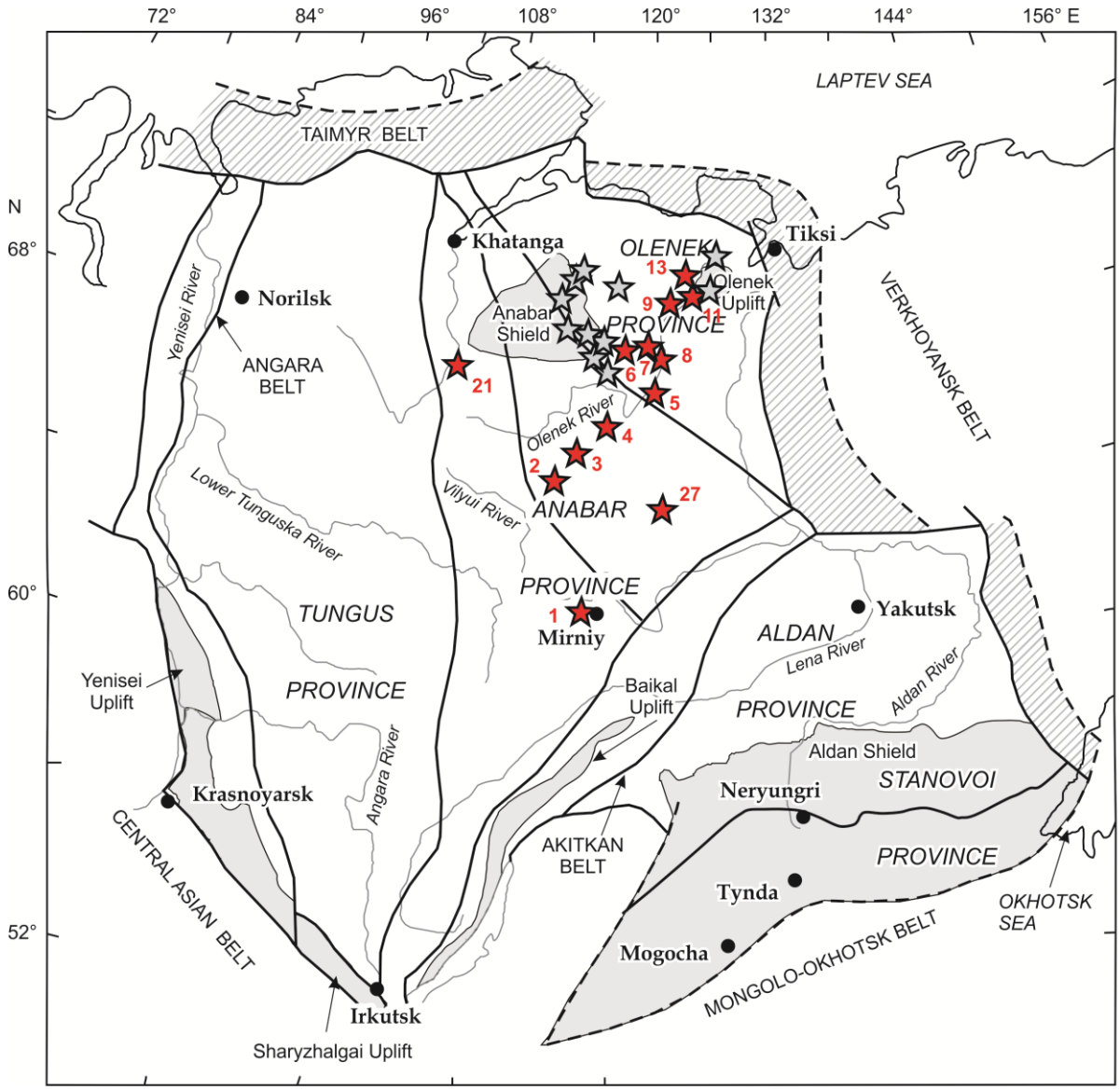



Figure 3.1.1. Map of the Siberian Craton showing sample locations. Numbers of fields are given according to the Table 3.1.

Table 3.1. Samples location, types and analytical work performed.

| Province | Terrane | Field | Pipe | Type of samples | Zircons | | | | Rutile | Sulfides | |
|---|---|---|---|---|---|---|---|---|---|---|---|
| | | | | | U-Pb* | TE | O | Hf | U-Pb | Re-Os | PGE |
| Anabar | Magan | Malo-Botuobinskoe (#1) | Mir | HMC | 29 (23) | 22 | | | | | |
| | | | Sputnik | HMC | 70 (59) | 57 | 26 | 58 | | | |
| | | | Internationalnaya | HMC | 54 (44) | 44 | | | 9 | | |
| | | | Amakinskaya | kimberlite | 6 | | | | | | |
| | | Kharamai (#21) | Eclogit | kimberlite | 10 | | | | | | |
| | | | Evenkiya | kimberlite | 11 (10) | | | | | | |
| | Markha | Upper Muna (#4) | Zimnyaya | HMC | 38 (29) | 26 | 31 | 28 | | | |
| | | | 325 years of Yakutia | kimberlite | 29 | 29 | | 19 | | | |
| | | | Zapolyarnaya | xenoliths | 78 (63) | | | 55 | | | |
| | | Daldyn (#3) | Udachnaya Eastern | HMC | 10 | 10 | | 9 | | | |
| | | | Zarnitsa | HMC | 10 | 10 | | 9 | | | |
| | | | Popugaeva | HMC | 22 | 22 | | 17 | | | |
| | | | Zagadochnaya | HMC | 37 | 37 | | 27 | | | |
| | | | Kusova | HMC | 50 (47) | 45 | | 39 | | | |
| | | | Udachnaya | xenoliths | 82 (81) | 81 | 65 | 40 | | 10 | 10 |
| | | Alakit-Markha (#2) | Kismet | HMC | 35 (34) | 31 | | 20 | | | |
| | | | Geochemical | HMC | 6 | 6 | | 6 | | | |
| | | | Vostok | HMC | 36 (35) | 34 | | 28 | | | |
| | | | Veselaya | HMC | 4 | 4 | | 4 | | | |
| | | | Krasnopresnenskaya | HMC | 5 | 5 | | 5 | | | |
| | | | Markha | HMC | 97 (85) | 85 | | | | | |
| | | | Aikhal | kimberlite | 53 | 9 | 25 | 18 | | | |
| | | Nakyn (#27) | Nurbinskaya | kimberlite | 65 (60) | 79 | 32 | 65 | | | |
| | | | Botuobinskaya | xenoliths | 41 | | | 41 | | | |

| Province | Terrane | Field | Pipe | Type of samples | Zircons | | | | Rutile | Sulfides | |
|---|---|---|---|---|---|---|---|---|---|---|---|
| | | | | | U-Pb* | TE | O | Hf | U-Pb | Re-Os | PGE |
| Anabar | Daldyn | Chomurdakh (#5) | Druzhba | kimberlite | 6 | | | | | | |
| | | | Rassvet | kimberlite | 12 (10) | 10 | | | | | |
| | | | Khairgastakh | kimberlite | 10 | | | | | | |
| | | Kuranakh (#13) | Malokuonapka | kimberlite | 36 (32) | 20 | | | | | |
| Olenek | Khapchan | Ukukit (##6-7) | Babie Leto | HMC | 34 (32) | | | | | | |
| | | Ogoner-Yuryakh (#8) | Baltiiskaya | HMC | 12 (10) | 10 | | 10 | | | |
| | | | Aerogeological | HMC | 15 (12) | 12 | | 10 | | | |
| | Birekta | Merchemdenskoe (#9) | Vostok-6 | kimberlite | 10 | | | | | | |
| | | | Operatorskaya | HMC | 21 (15) | 15 | | 10 | | | |
| | | Kuoika (#11) | Khrizolit | kimberlite | 10 (9) | | | | | | |
| | | | Pyatnitsa | Kimberlite | 11 | | | | | | |
| | | | Ruslovaya | HMC+kimberlite | 60 (55) | 25 | 27 | 35 | | | |
| | | | Olivinovaya | HMC | 35 (31) | 23 | 22 | 30 | | | |
| | | | Vtorogodnitsa | HMC | 44 (30) | 25 | 15 | 26 | | | |
| ***Total for the craton*** | | | | | ***1194 (1075)*** | ***776*** | ***243*** | ***609*** | ***9*** | ***10*** | ***10*** |

* U-Pb analyses: total (used)

## 3.2. Analytical methods used for zircon studies

***Quantitative crystallographic orientation analysis***

To examine the internal crystallographic structure of grains, electron backscattered diffraction analysis (EBSD) was performed using a Zeiss EVO15 scanning electron microscope. Mechano-chemically polished sample mounts were analysed at an accelerating voltage of 20 kV, beam current of 8 nA and at a working distance of ~9–14 mm. Electron backscatter diffraction patterns were automatically acquired and indexed using Oxford Instruments AzTEC. The EBSD patterns were collected in regular grids where the sampling step size varied from 5 to 10 μm for detailed microstructural areas and 1 to 3 μm for whole-grain mapping. Minimal post-acquisition processing (Piazolo *et al.*, 2006, Prior *et al.*, 2002) was required, as 90-95% of the mapped area was automatically indexed.

*Cathodoluminescence (CL) imaging*

All grains were imaged using cathodoluminescence (CL) to obtain detailed pictures of the internal structure. CL imaging was performed on polished, carbon-coated samples using a Zeiss EVO15 scanning electron microscope operating at 10kV with 12 mm working distance.

CL color imaging was carried out using a Luminoscope (ELM-3R) consisting of a cooled charge-coupled device (CCD) camera, a cold cathode discharge tube and a vacuum chamber, in which the sample was placed. This was operated with an excitation voltage of 7.5 kV and beam current of 0.5 mA at vacuum conditions under 80 Torr. A magnet was used to control the diameter of electron beam spot at a few-mm size on the sample surface. CL images were converted to digital data using a Nikon imaging system (DS-5Mc).

A Mini-CL detector (Gatan) consisting of multi-alkali photomultiplier tube (Hamamatsu-R1463) installed in a JSM-5410LV SEM was used to obtain the CL scanning images at high magnification with operating conditions of 15 kV and 0.05-1.0 nA. This detector has a high sensitivity in the blue region rather than in the red region.

***LAM-ICPMS trace-element analysis and U-Pb dating***

*In situ* trace-element and U-Pb isotopic analyses of zircon were obtained simultaneously using an Agilent 7700cx quadrupole ICPMS. Ablation was performed using Photon Machines Excite 193 nm excimer laser ablation system (fitted with a two-stage HeLeX cell). Counting times were 60 s on a gas background followed by up to 120 s of ablation/analysis, depending on the size of the zircon grain. Analyses were carried out using a spot size of 40-85 μm, pulse

rate of 5 Hz, and laser energy of ~3-10 J cm-2. The carrier gas was He in the sample cell, with Ar added downstream.

Zircon grains were analysed in runs of ~10-12 analyses bracketed by 4 analyses each of the GJ-1 Red zircon standard (ID-TIMS $^{207}Pb/^{206}Pb$ age = 608.5 ± 0.4 Ma;(Jackson *et al.*, 2004)) and NIST 610 glass (Norman *et al.*, 1996). The GJ-1 zircon and NIST 610 glass were used as calibration standards for U-Pb isotopic and trace-element analyses (Elhlou et al., 2006) respectively to correct for instrument sensitivity and drift. Two other well-characterized zircon standards, 91500 (Elhlou *et al.*, 2006, Wiedenbeck *et al.*, 1995)) and Mud Tank ($^{206}Pb/^{238}U$ age = 732 ± 5 Ma (Black & Gulson, 1978, Elhlou *et al.*, 2006))), were used as secondary standards to assess the accuracy and precision of U-Pb results (Fig. 3.2.1, 3.2.2, Appendix 1.1).

The measured values of the U/Pb isotope ratios were processed using the GLITTER software package (Griffin *et al.*, 2008). GLITTER calculates the relevant isotopic ratios for each mass sweep and displays them as time-resolved data. This allows isotopically homogeneous segments of the signal to be selected for integration. GLITTER then corrects the integrated ratios for ablation-related fractionation and instrumental mass bias by calibration of each selected time segment against the identical time segments in the standard zircon analyses.

We have employed a common-Pb correction procedure (Andersen, 2002) and the analyses presented here have been corrected assuming recent lead-loss with a common-lead composition corresponding to present-day average orogenic lead as given by the second-stage growth curve (Stacey & Kramers, 1975) for $^{238}U/^{204}Pb$=9.74. No correction has been applied to analyses that are concordant within 2σ analytical error in $^{206}Pb/^{238}U$ and $^{207}Pb/^{235}U$, or which have less than 0.2% common lead. Only zircons that are less than 15% discordant were taken into consideration for evaluation of the U-Pb age. $^{207}Pb/^{206}Pb$ ages (2σ) for grains older than 1.0 Ga were used for the figures and for calculation of the weighted average age, and $^{206}Pb/^{238}U$ (2σ) ages were used for grains younger than 1.0 Ga.

*In-situ* LAM-ICP-MS U–Pb dating of rutile was performed using the procedure and instrumental setup equal to the one used for zircons. To avoid ablation of the rutile-garnet interface, rutile grains with diameter > 30 μm were chosen for in situ U–Pb dating. Samples of rutile were bracketed at the beginning and end by the R19 rutile standard (493 ± 10 Ma; (Zack *et al.*, 2011)), which was used as a calibration standard in order to match the matrix for robust in situ U–Pb dating of rutile. The R10 rutile standard was used as a secondary independent control and yielded a $^{207}Pb/^{206}Pb$ age of 1065 ± 72 Ma and $^{206}Pb/^{238}U$ age of 1108 ± 16 Ma; both are within the analytical error of the reported age for this reference material (1090 ± 5 Ma; (Luvizotto *et al.*, 2009); (Zack *et al.*, 2011)).

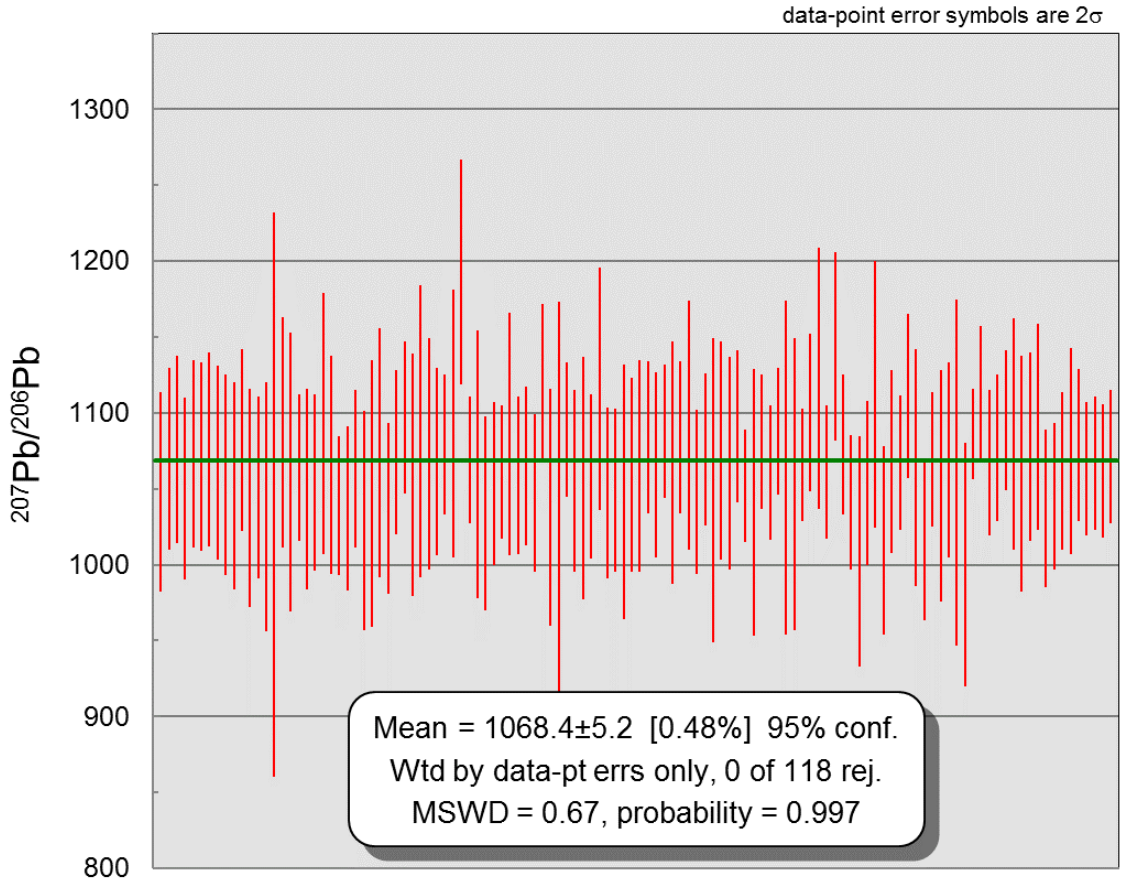



Figure 3.2.1. The weighted mean age of the 91500 zircon standard.

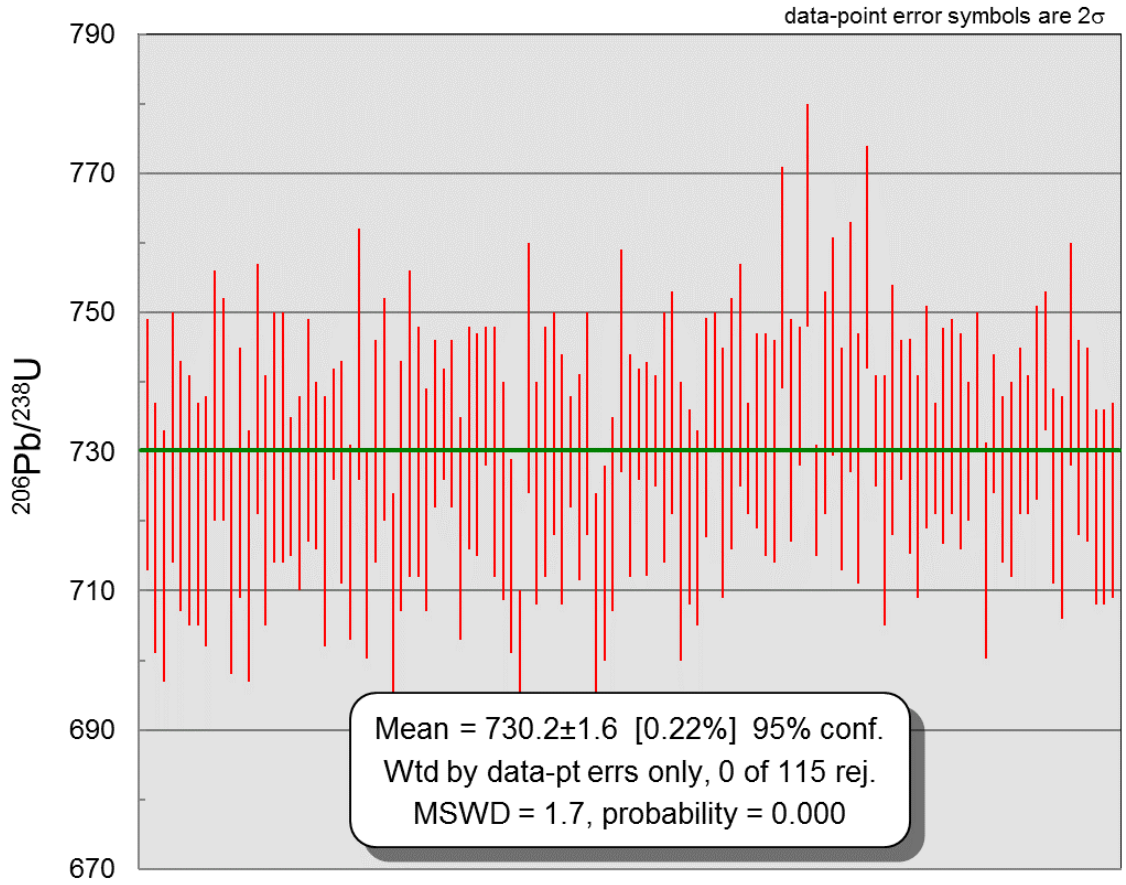



Figure 3.2.2 The weighted mean age of the MudTank zircon standard.

***SHRIMP U-Pb dating***

Thin zones in some zircon grains were dated using the sensitive high-resolution ion microprobe (SHRIMP II) at the John de Laeter Centre of Mass Spectrometry, Curtin University, Perth, Western Australia. The SHRIMP analytical procedure is described by Kennedy and De Laeter (1994). A spot size of 5 μm was used. The peak-hopping U–Pb data collection routine consisted of six scans through the mass stations. For sample analyses the Pb/U reference standard TEMORA-2 was used (ID TIMS $^{206}Pb/^{238}U$ age 416.8 ± 1.3 Ma (Black *et al.*, 2004)). The OG1 standard (3465.4 ± 0.6 Ma, Owens Gully Diorite, East Pilbara Terrane; (Stern *et al.*, 2009)) is an additional standard currently employed at the John de Laeter Centre of Mass Spectrometry for monitoring SHRIMP instrumental mass fractionation (IMF) of Pb isotopes (Stern *et al.*, 2009).

***Zircon Hf-isotope analyses***

*In situ* Hf-isotope analyses of zircon were carried out using a Nu Plasma multi-collector ICPMS (MC-ICPMS) system, in conjunction with two different laser ablation microprobes: a New Wave UP 213 nm system and 193 Photon Machine system. Zircon grains mounted in epoxy, and previously analysed for U-Pb isotopic compositions, were analysed using a spot size of 40-60 μm, pulse frequency of 5 Hz and laser energy of 5 J/cm$^{-2}$, and counting times of 30 s background and 60-150 s sample. These conditions gave Hf signal intensities in the range 1.5 to 11 volts for reference materials.

Zircon standards Mud Tank ($^{176}Hf/^{177}Hf$ = 0.282522 ± 42; (Griffin *et al.*, 2007) and Temora-2 ($^{176}Hf/^{177}Hf$ = 0.282680 ± 11; (Woodhead & Hergt, 2005)) were used as reference materials to assess accuracy and to monitor instrument stability; results of repeat analyses obtained in this study, compared with long term averages for the GAU are presented in Appendix 1.2. Interferences of $^{176}Yb$ and $^{176}Lu$ on the $^{176}Hf$ signal were corrected using the single-isotope method outlined by Griffin *et al.* (2004), Pearson *et al.* (2008) and Belousova *et al.* (2009), with a $^{176}Yb/^{172}Yb$ ratio of 0.587 and a $^{176}Lu/^{175}Lu$ ratio of 0.02669 (the Yb ratio has been empirically determined at the GAU; the Lu ratio is from De Biévre and Taylor (1993)). The efficacy of the correction is attested by the accuracy and reproducibility of the results for the two reference zircons with widely different REE contents (average $^{176}Yb/^{176}Hf$ = 0.0044 ± 12 for Mud Tank, 0.032 ± 12 for Temora-2; average $^{176}Lu/^{176}Hf$ = 0.000107 ± 25 for Mud Tank, 0.00102 ± 29 for Temora-2), together with the absence of any correlation between $^{176}Yb/^{177}Hf$ and the corrected $^{176}Hf/^{177}Hf$ (r2 of 0.04 and 0.005 for Mud Tank and Temora-2 respectively). During analysis, ablation was made in the same domains previously analysed for U-Pb and

trace elements, using the internal structure revealed in the CL images to guide the choice of analytical spots, and monitoring elemental and isotopic ratios throughout the analysis in order to detect the presence of multiple domains. Initial $^{176}Hf/^{177}Hf$, εHf, and model ages were calculated using the $^{176}Lu$ decay constant from (Scherer *et al.*, 2001).

***Zircon O-isotope analysis***

Oxygen isotope ratios were determined on the polished surfaces of zircon grains, using the CAMECA IMS 1280 at the Centre for Microscopy Characterisation and Analysis at the University of Western Australia. Analytical procedures was closely followed those described by Kita *et al.* (2009). Oxygen $^{16}O$ and $^{18}O$ isotopes were collected using dual Faraday cup detector. The Temora-2 zircon standard ($\delta^{18}O$=8.2±0.01 (Black *et al.*, 2004)) was measured as unknown sample every 2-5 analyses to control the instrument stability. Measured values of Temora-2 were used to correct instrumental time-dependent drift. Oxygen-isotope results are recorded as $\delta^{18}O$ values (relative to SMOW). Propagated uncertainties on $\delta^{18}O$ include contributions from internal precision, instrumental mass fractionation determination and the reference value of the standard.

## 3.3. Analytical methods used for sulfide inclusion studies *in-situ* Re-Os dating

Sulfide inclusions in silicate minerals were selected for in situ Re–Os isotope analysis at GEMOC using analytical methods described in detail by Pearson *et al.* (2002) and Griffin *et al.* (2002a). A New Wave/Merchantek UP 213 laser microprobe was coupled with a Nu Plasma Multicollector ICP-MS. Two different analytical routines were used: one for high-Os minerals (i.e. PGM) and another for low-Os minerals (i.e. BM-sulfides). During the analysis of PGM all ion beams were collected in Faraday cups. The laser was fired at a frequency of 4 Hz, with energies of 1–2 mJ/pulse and a spot size of 10-15 μm. The analysis of BM-sulfides used a mix of Faraday cups and ion counters. The laser was fired at a frequency of 5 Hz, with energies of 1–2 mJ/pulse and a spot size of 20–80 μm. During ablation runs, a standard NiS bead (PGE-A) with 199 ppm Os (Lorand & Alard, 2001) and $^{187}Os/^{188}Os$=0.1064 (Pearson *et al.*, 2002) was analyzed between samples to monitor any drift in the Faraday cups and ion counters. These variations typically were less than 0.1% over a long day's analytical session. During the analyses, a dry aerosol of Ir was bled into the gas line between the ablation cell and the ICP-MS to provide a mass-bias correction with a precision independent of the abundance of Os in the unknown.

The overlap of $^{187}Re$ on $^{187}Os$ was corrected by measuring the $^{185}Re$ peak and using $^{187}Re/^{185}Re=1.6742$. All the analyzed grains have $^{187}Re/^{188}Os$ lower than 0.5, thus ensuring that the isobaric interference of $^{187}Re$ on $^{187}Os$ was precisely corrected (Nowell *et al.*, 2008). The data were collected using the Nu Plasma time-resolved software, which allows the selection of the most stable intervals of the signal for integration. The selected interval was divided into 40 replicates to provide a measure of the standard error. Under the ablation conditions described above, for grains PGM having sizes of 5 μm and contents of Os>1 wt.%, a typical run duration of ~75 s was achieved and a signal intensity of Os>0.2 V was obtained in the Faraday cups, giving a precision for $^{187}Os/^{188}Os$ ranging from 1E-4 to 1.6E-3 (2SE). For BM-sulfides, which are generally larger than the PGM, and have Os contents from much lower to slightly higher than the standard (i.e. 199 ppm Os), the run durations (65–790 s) and signal intensities (0.02–1.4 V) obtained give a range of precision for $^{187}Os/^{188}Os$ from 2E-4 to 2E-3 (2SE); these values are quite similar to, or better than, that obtained for the PGE-A standard. Eight analyses of PGE-A done together with the BM-sulfide samples gave 150–999 s run durations, 0.03–0.14 V signal intensity, and internal precision for $^{187}Os/^{188}Os$ ranging from 9.80E-5 to 5.20E-4 (2SE), using mixed Faraday-ion counters. The accuracy of the data presented here is illustrated by independent analyses (different instruments, operating protocols) of Os–Ir alloys from chromitites in the Luobusa (Tibet) ophiolite. Shi *et al.* (2007) reported a mean $^{187}Os/^{188}Os=0.12646$ ±11 (1SE, n=148); Pearson *et al.* (2007) later reported $^{187}Os/^{188}Os=0.12653$±7 (1SE, n=80).

In both routines several tests were carried out to verify the low contents of Re and Os in the host chromite and silicates compared to the PGM. These tests showed that the partial inclusion of chromite or silicate in the ablated volume gave negligible contributions to the sampled Re and Os budgets (Ahmed *et al.*, 2006). γOs and model ages have been calculated relative to the Os-isotope evolution of Enstatite Chondrite (present day $^{187}Os/^{188}Os=0.1281$, $^{187}Re/^{188}Os=0.421$ (Walker *et al.*, 2002)). The quoted uncertainties on TMA and TRD model ages include the uncertainties in the measured $^{187}Os/^{188}Os$ and $^{187}Re/^{188}Os$, calculated according to the equation of (Sambridge & Lambert, 1997).

# Chapter 4. The Magan terrane

According to Smelov and Timofeev (2007), the Magan terrane is included within the larger Tungus terrane. However, other studies suggested that the Magan terrane, together with the Daldyn and Markha terranes, are part of the Anabar tectonic province (Gladkochub *et al.*, 2006, Rosen *et al.*, 1994, Rosen *et al.*, 2002, Rosen *et al.*, 2000).

The Magan tonalite–trondhjemite gneiss terrane consists mainly of granulite facies, homogeneous biotite and biotite–amphibole orthogneiss, derived from tonalite, granodiorite and granite with lesser amounts of garnet-bearing, highly aluminous gneisses and carbonate rocks. The average Sm–Nd model age for the basement rocks of the Magan terrane is ~2.94 Ga according to Rosen *et al.* (1994).

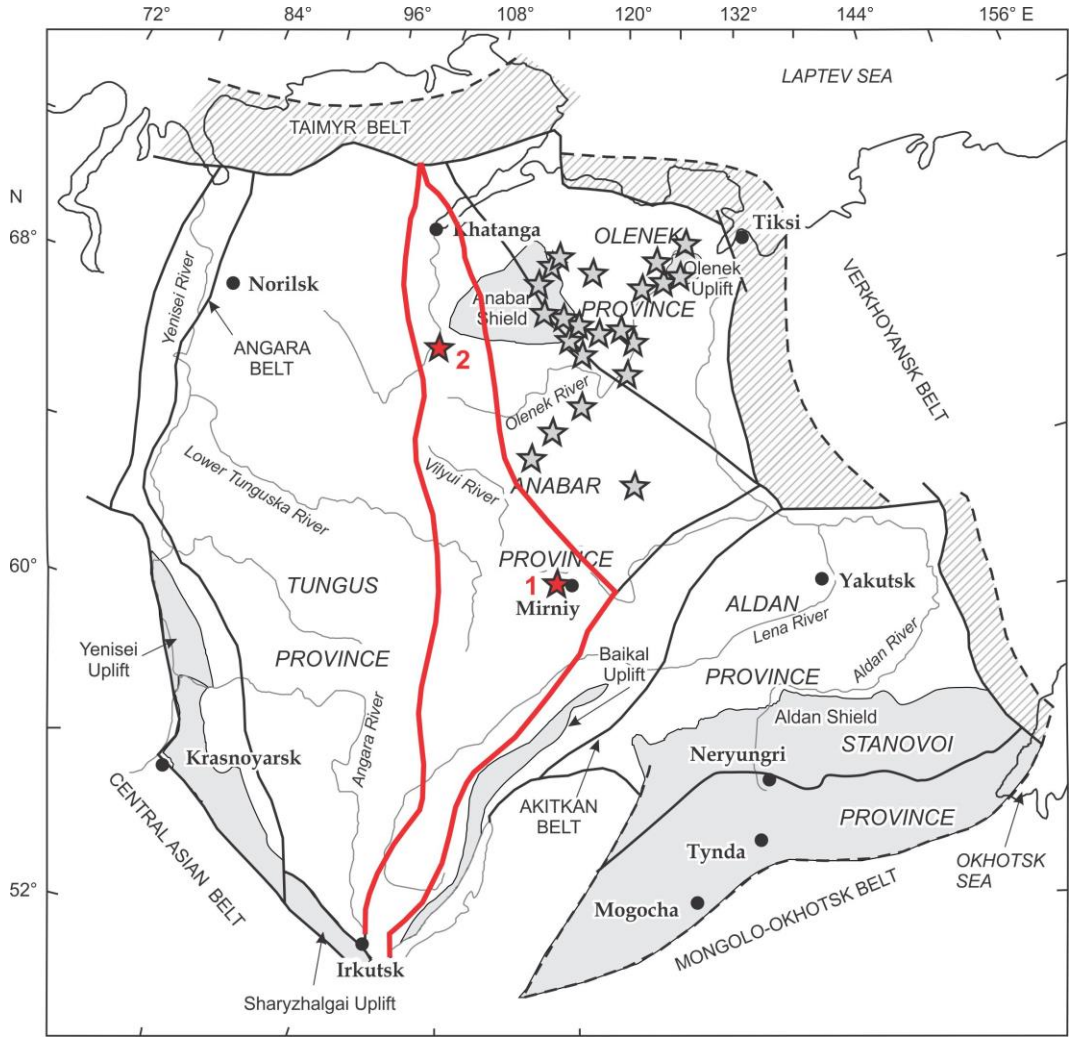



Figure 4. The location of the Magan terrane and studied kimberlite fields. Red stars are for kimberlite fields studied within this work: 1 – Malo-Botuobia; 2 – Kharamai.

There are only two kimberlite fields within the terrane: the Malo-Botuobia (or Malo-Botuobinskoe) and Kharamai (Fig. 4). Both of those contain diamond-bearing kimberlite bodies, some of which are highly diamondiferous such as the Mir, Sputnik and Internationalnaya pipes within the Malo-Botuobia field. Summary of the samples and analytical work done is shown in Table 4.

Table 4. Analytical work done for samples from the Magan terrane.

| Field | Pipe | Type of samples* | Zircons | | | | Rutile |
|---|---|---|---|---|---|---|---|
| | | | U-Pb | TE | O | Hf | U-Pb |
| Malo-Botuobia | Mir | HMC | 29 (23) | 22 | | | |
| | Sputnik | HMC | 70 (59) | 57 | 26 | 58 | |
| | Internationalnaya | HMC | 54 (44) | 44 | | | 9 |
| | Amakinskaya | kimberlite | 6 | | | | |
| Kharamai | Eclogit | kimberlite | 10 | | | | |
| | Evenkiya | kimberlite | 11 (10) | | | | |
| *Total for the terrane* | | | *180 (152)* | *123* | *26* | *58* | *9* |

* Type of samples: HMC - heavy mineral concentrate from weathered kimberlite; kimberlite - hand-picked zircons from crushed kimberlite.

^ U-Pb analyses: total (used)

## 4.1. The Malo-Botuobia kimberlite field

This field is located at the junction between the Tungus and Viluy depressions in the southern part of the terrane. Within the field carbonate and carbonate-terrigenous rocks of Early Palaeozoic to Early Mesozoic age host the Devonian kimberlite bodies and Triassic dolerite intrusions.

Seven pipes and one vein-type kimberlite body have been found within the Malo-Botuobia field. All pipes have complex structure and multi-stage intrusion history, and each of them is diamondiferous. The kimberlite bodies are intruded into Late Cambrian and Early Ordovician sedimentary rocks, and some of them are covered with Early Jurassic terrigenous sediments. The Mir pipe contains xenoliths of Middle Palaeozoic dolerite dikes, which are cut by kimberlite. According to the field observations, the age of pipes was suggested to be Late Devonian – Early Carboniferous (Zaitsev & Smelov, 2010).

The kimberlite bodies have been dated previously by various techniques. The majority of obtained ages fall into the range 350-380 Ma, however slightly younger (333-350 Ma) and older (up to 450 Ma) ages have been also reported (Smelov & Zaitsev, 2013).

This project involved samples from four out of the seven kimberlites of the Malo-Botuobia field: the Mir, Sputnik, Internationalnaya (Inter) and Amakinskaya pipes. The

samples include zircons from the heavy mineral concentrates (Mir, Sputnik, Inter) and from the crushed kimberlite rocks (Amakinskaya). Additional studies have been carried out on rutile from xenoliths of the Mir pipe and rutile inclusions in garnet megacrysts from the Inter pipe.

### *Zircon U-Pb data*

#### The Mir pipe

Twenty-nine zircons were dated by LA-ICPMS, giving a range of ages from 366 to 2915 Ma (Table 4.1.1). Six analyses revealed discordance more than 20% and were not further considered. The probability plot (Fig. 4.1.1) shows a major peak with the weighted mean age of 382.1±4 Ma (MSWD = 1.6, probability = 0.17; Fig. 4.1.2). The second major peak is slightly broader and gives a weighted mean age of 1834±26 (MSWD = 1.7, probability = 0.12; Fig 4.1.3). The youngest obtained age is 366±4 Ma. The oldest zircon found among the samples from the Mir pipe has an age of 2915±24 Ma (Appendix 2.1). Duplicate analyses of grains show the same age within the analytical error *ca* 486 and 488 Ma, 885 and 905 Ma, and 1972 and 1977 Ma.

Table 4.1.1. A summary of U-Pb age data for zircons from the Malo-Botuobia kimberlite field, Magan terrane.

| Pipe | Range of U-Pb ages, Ma (n = number of analyses) | Major peak mean age, Ma | Second peak mean age, Ma | Minor peaks ages, Ma |
|---|---|---|---|---|
| **Mir** | 366 – 2915 (n = 23) | 382.1±4 | 1834±26 | 486-488<br>885-905<br>1972-1977 |
| **Sputnik** | 361-2764 (n = 59) | 390.3±4.1 | 1860±12 | 437-470<br>831-850<br>2290-2359 |
| **Internationalnaya** | 353-2930 (n = 44) | 374.9±3.9 | 1874±19 | 494-505<br>822<br>2490-2647 |
| **Amakinskaya** | 368-379 (n = 6) | 373.3±4.7 | n/a | n/a |

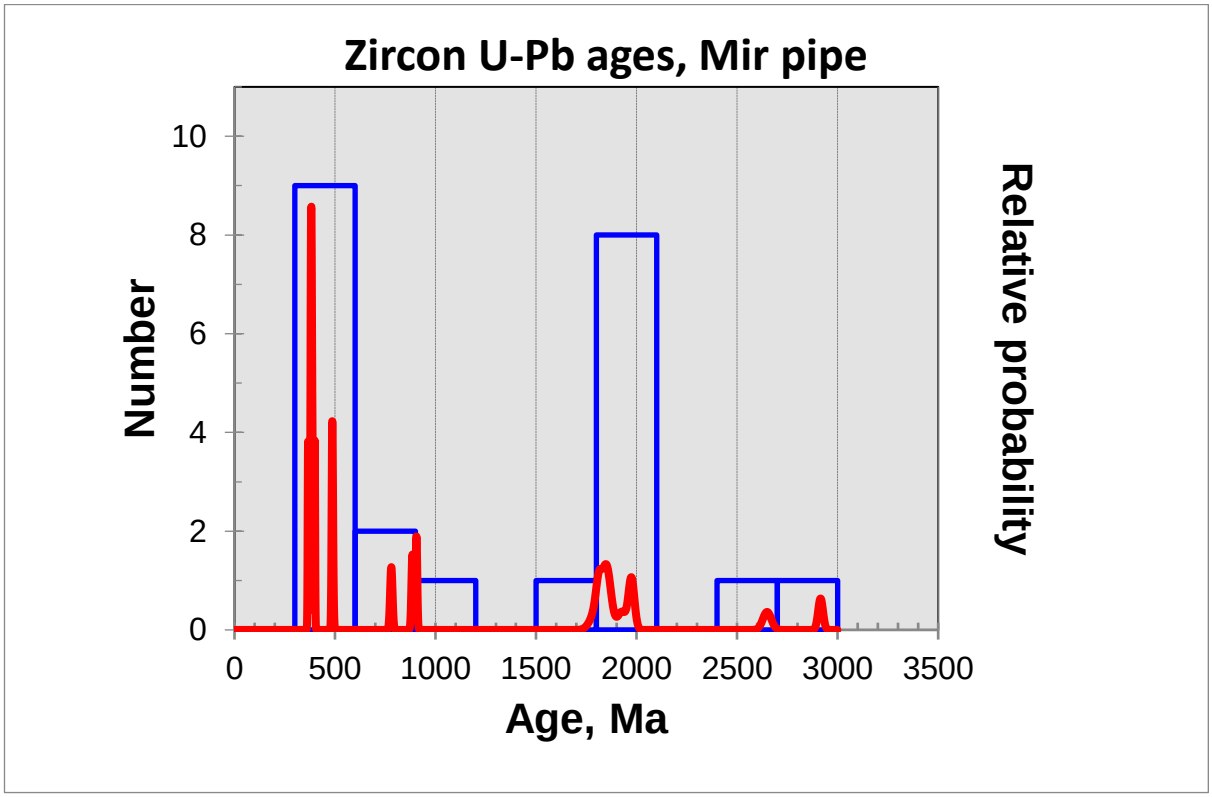



Figure 4.1.1. Probability plot of zircon U-Pb ages, Mir pipe, Magan terrane.

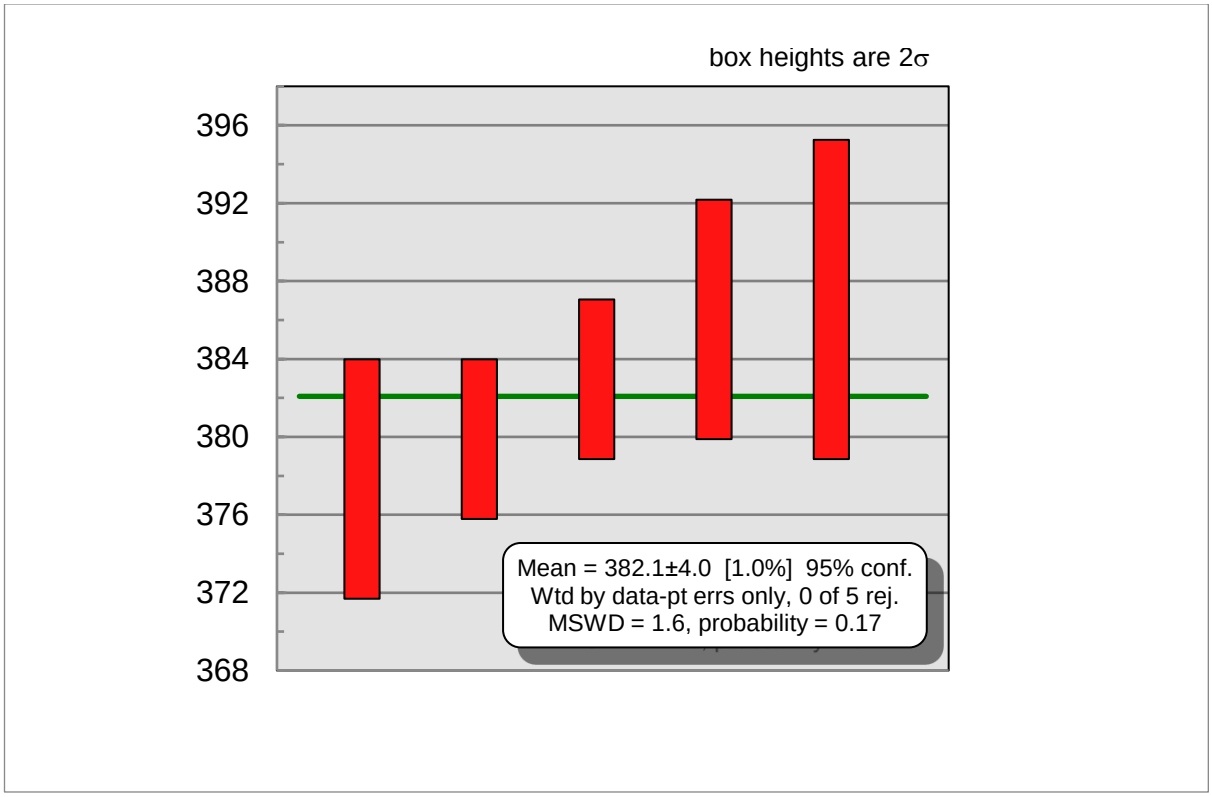



Figure 4.1.2. The weighted mean age of the youngest major population, for zircons from the Mir pipe, Magan terrane.

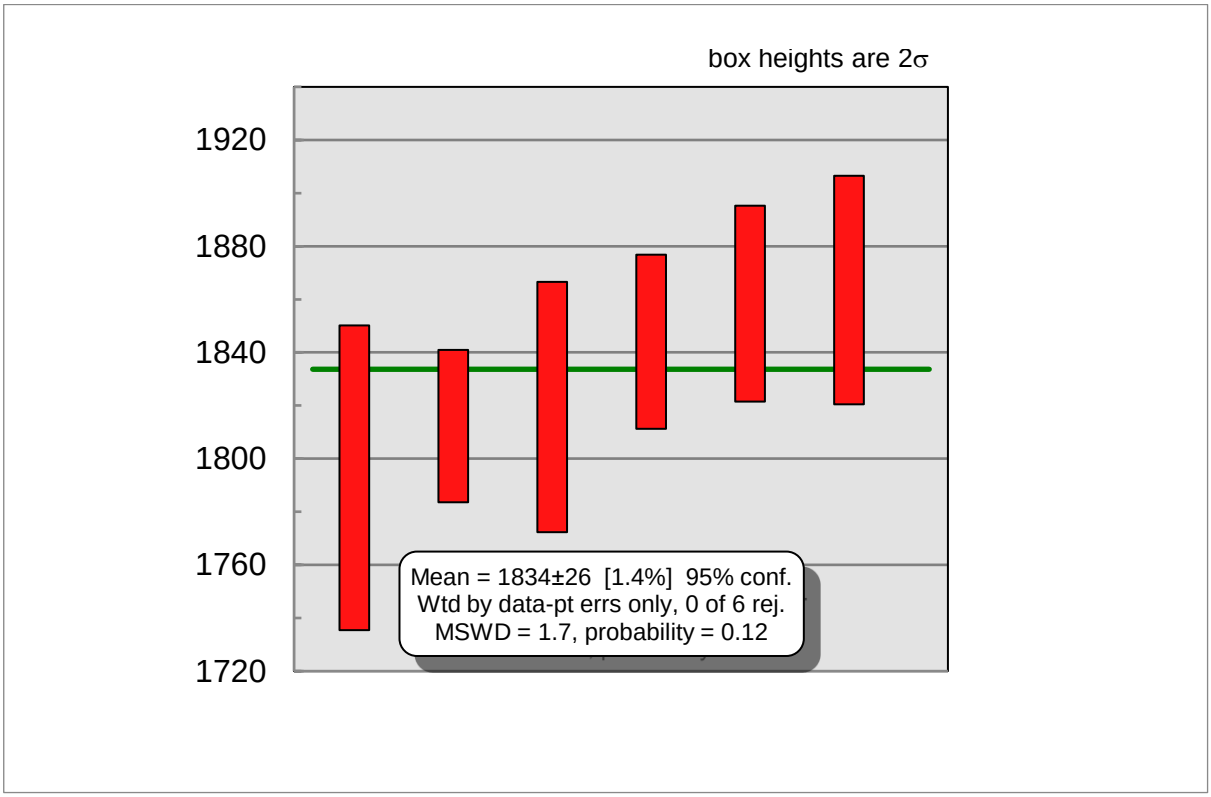



Figure 4.1.3. The weighted mean age of the second major peak for zircons from the Mir pipe, Magan terrane.

**The Sputnik pipe**

Seventy zircon grains were recovered from a heavy-mineral concentrate collected from the streams draining the pipe. Fifty-nine grains show less than 20% discordance and thus were selected for further consideration.

The distribution of ages is similar to the one described for that of the Mir pipe: ages vary from 361 to 2764 Ma (Fig. 4.1.4, Table 4.1), with two major age populations revealing the weighted mean ages of 390.3±4.1 (MSWD = 1.2, probability = 0.30; Fig. 4.1.5) and 1860±12 Ma (MSWD = 1.03, probability = 0.42; Fig. 4.1.6). The youngest zircon has an age of 361±10 Ma, and the oldest one shows the age of 2764±76 Ma.

Minor age peaks are also observed at ~440, 840 and 2330 Ma.

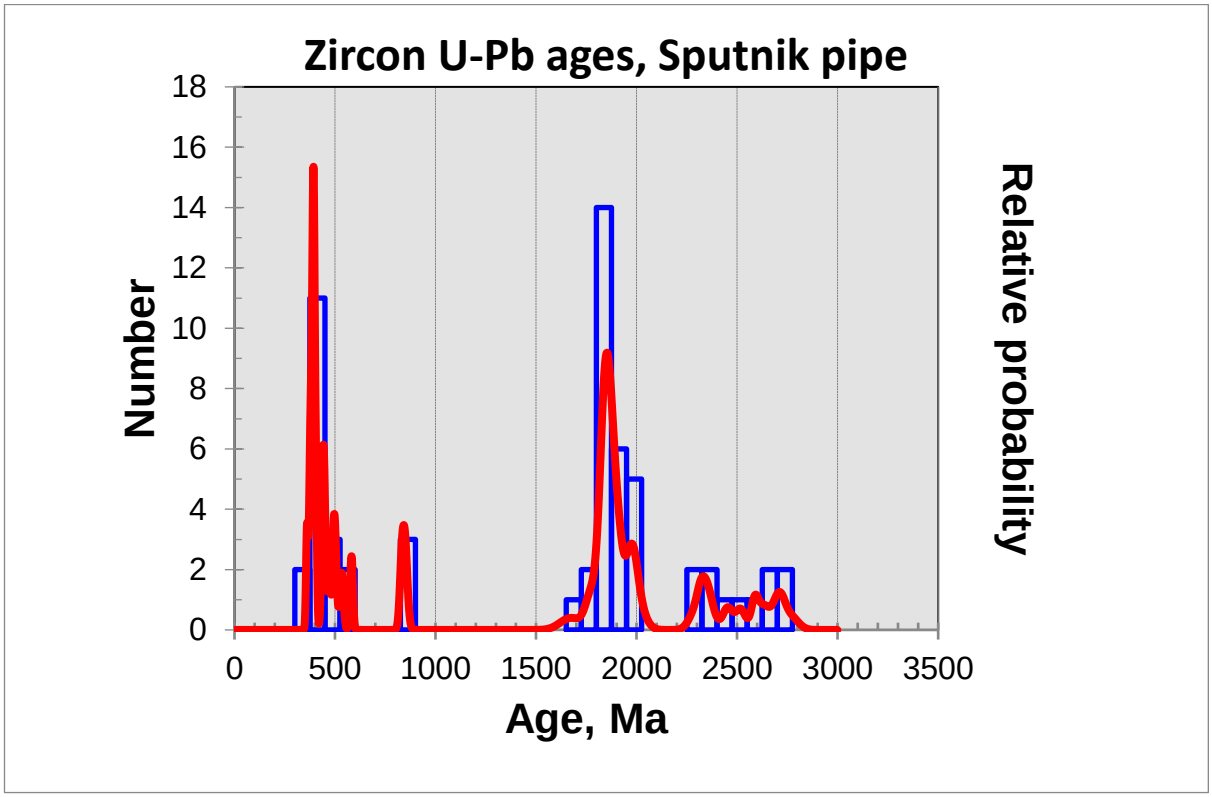



Figure 4.1.4. Probability plot of zircon U-Pb ages, Sputnik pipe, Magan terrane.

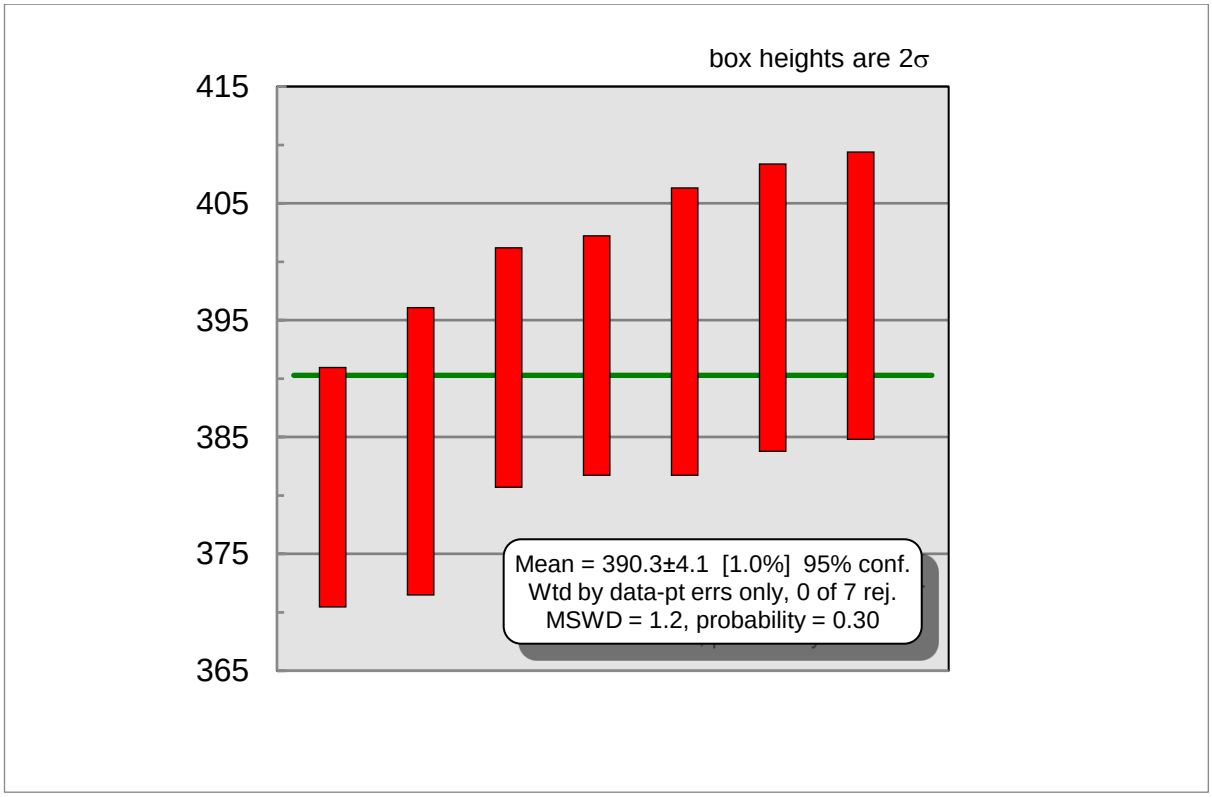



Figure 4.1.5. The weighted mean age of the youngest major population of zircons from the Sputnik pipe, Magan terrane.

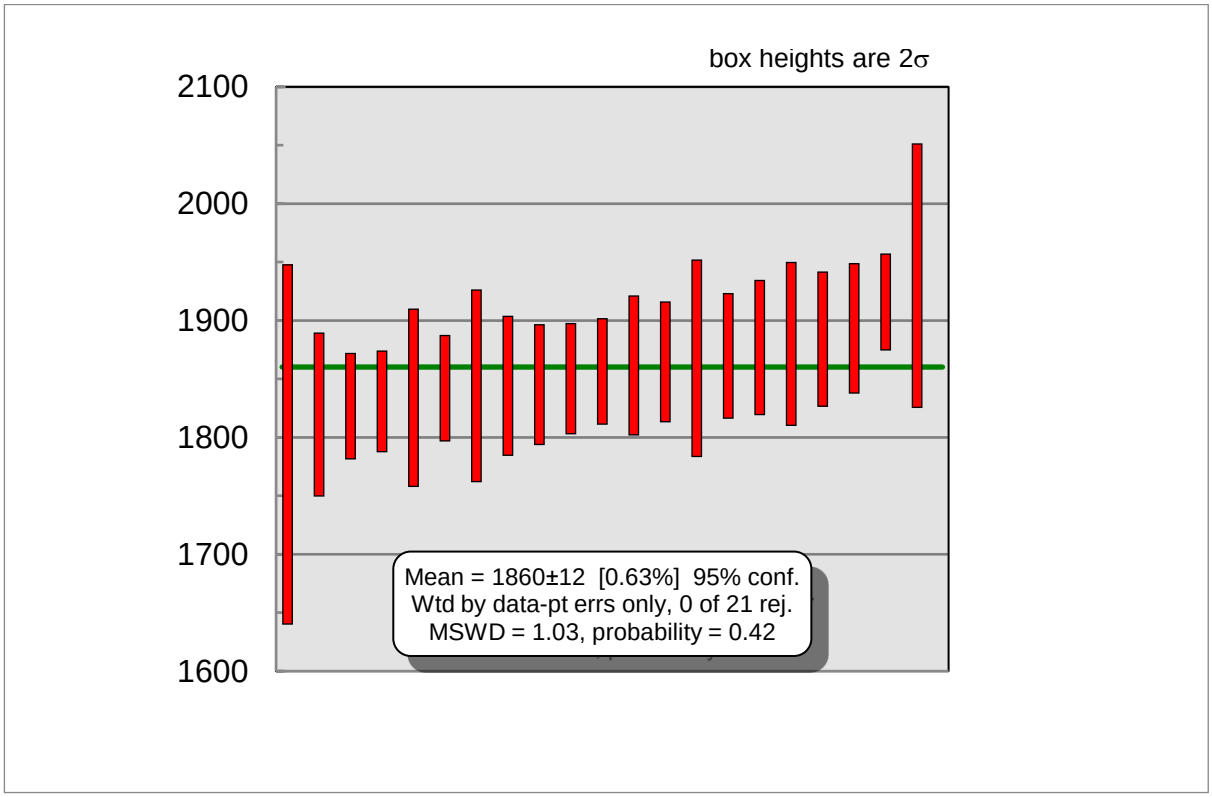



Figure 4.1.6. The weighted mean age of the main population of zircons from the, Sputnik pipe, Magan terrane.

**The Amakinskaya pipe**

Only 6 zircon grains from the Amakinskaya pipe were available for analysing; all of them represent a single population with a weighted mean age of 373.3±4.7 Ma (MSWD = 0.58, probability = 0.72; Fig. 4.1.7).

**The Internationalnaya pipe**

A total of 54 zircons from the Internationalnaya pipe were dated during this study, 10 of them were rejected because of their discordance higher than 20%.

The probability plot (Fig.4.1.8) shows the age distribution a pattern similar to those observed for the Mir and Sputnik pipes. The obtained ages spread over range from 353 to 2930 Ma. The major peak represented by 6 grains reveals gives a weighted mean age of 374.9±3.9 Ma (MSWD = 1.04, probability = 0.39; Fig. 4.1.9). The second largest age population is slightly wider, yielding a mean age of 1874±19 (MSWD = 0.57, probability = 0.87; Fig 4.1.10). The youngest zircon found within the set gives an age of 353±12 Ma. The oldest obtained age is 2930±58 Ma (Table 4.1.3). The other minor peaks are also present on the probability plot with ages at around 494-505 Ma and 2567-2688 Ma.




Figure 4.1.7. The weighted mean U-Pb age for zircons from the Amakinskaya pipe, Magan terrane

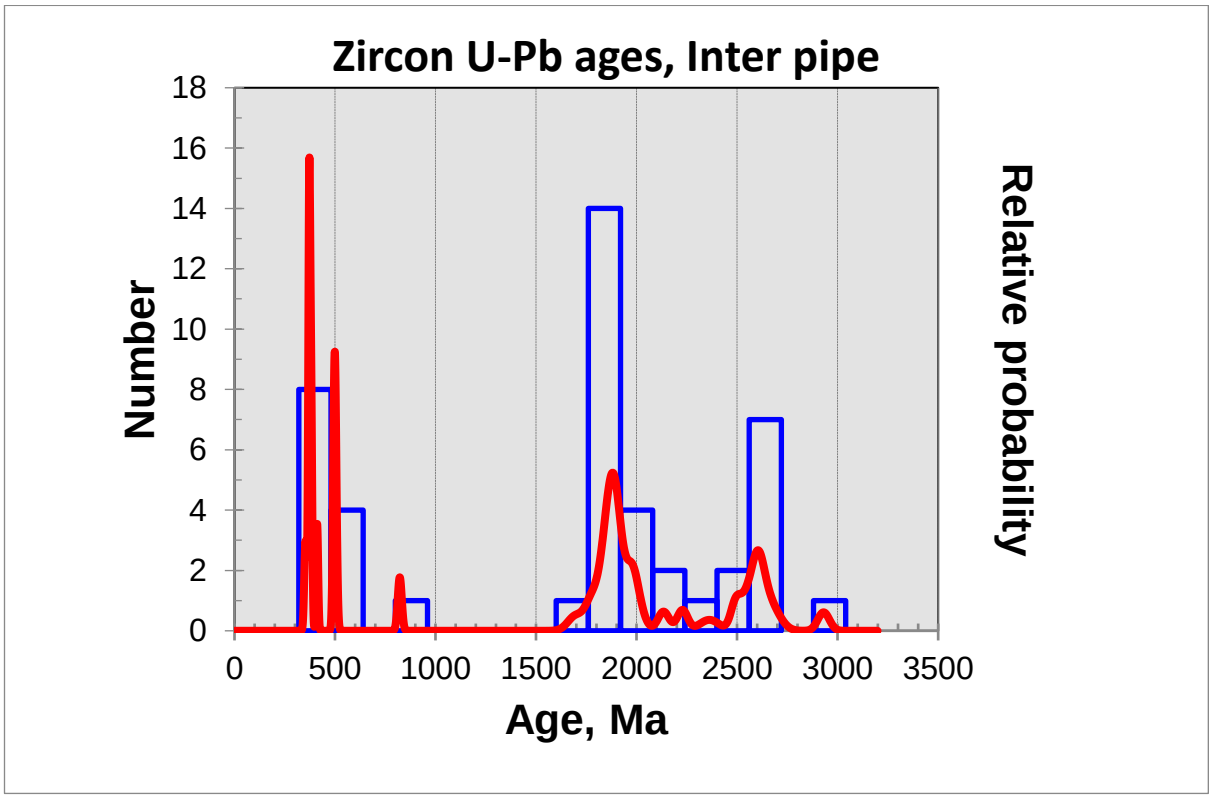



Figure 4.1.8. Probability plot of zircon U-Pb ages, Internationalnaya pipe, Magan terrane.

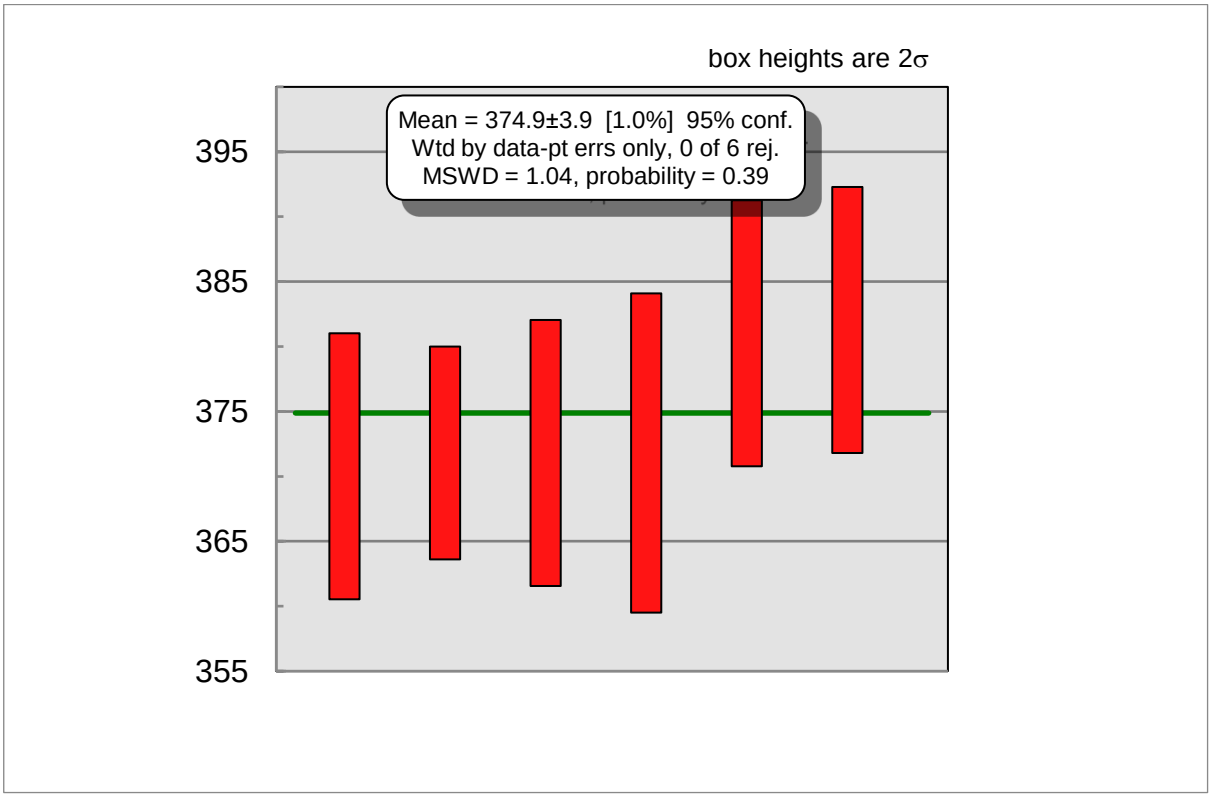



Figure 4.1.9. The weighted mean age of the major peak, Internationalnaya pipe, Magan terrane




Figure 4.1.10. The weighted mean age of the second major peak, Internationalnaya pipe, Magan terrane.

***Rutile U-Pb data***

Rutile inclusions in garnet xenocrysts from the Internationalnaya pipe have been dated using the same LA-ICPMS U-Pb technique (Malkovets *et al.*, 2016).

**The Internationalnaya pipe**

Nine rutile inclusions were found in garnet megacrysts: seven inclusions in four peridotitic garnets, and two in one eclogitic garnet. Because of the high contents of common Pb in rutile, we applied the approach suggested previously for the dating of perovskite (Batumike *et al.*, 2008, Giuliani *et al.*, 2014, Yaxley *et al.*, 2013). This regression technique treats a population of rutile analyses from a single sample as representing mixtures between the common-Pb and radiogenic-Pb components. The intercepts of the regression line through the raw data on an inverse Concordia (Tera–Wasserburg) plot provide both an estimate of the $^{207}Pb/^{206}Pb$ of the common-Pb component (upper intercept) and the inferred crystallization age (lower intercept). Thus, the lower intercept for all of rutiles from the Internationalnaya pipe 368.9±9.5 Ma (MSWD=0.55; Fig 4.1.11). The peridotitic rutile inclusions have U contents of 3.6-27.8 ppm *vs* 10.9 ppm and 22.6 ppm in eclogitic rutiles.

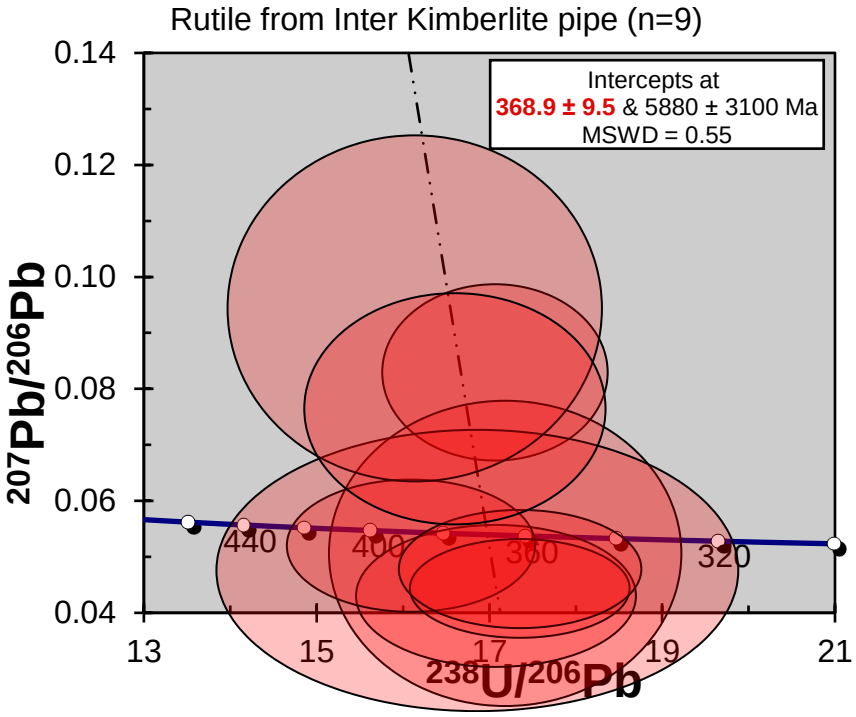



Figure 4.1.11. U-Pb age of rutile inclusions from Internationalnaya pipe, Magan terrane

***Zircon trace-element data***

**The Mir pipe**

Twenty-two dated zircons from the Mir pipe were analysed for their trace-element composition. Chondrite-normalized REE patterns for all analyzed grains are typical of zircons, with depletion in light rare earth elements (LREE) and enrichment in heavy rare earths (HREE, Fig. 4.1.12). All data is shown in the Appendix 2.2.

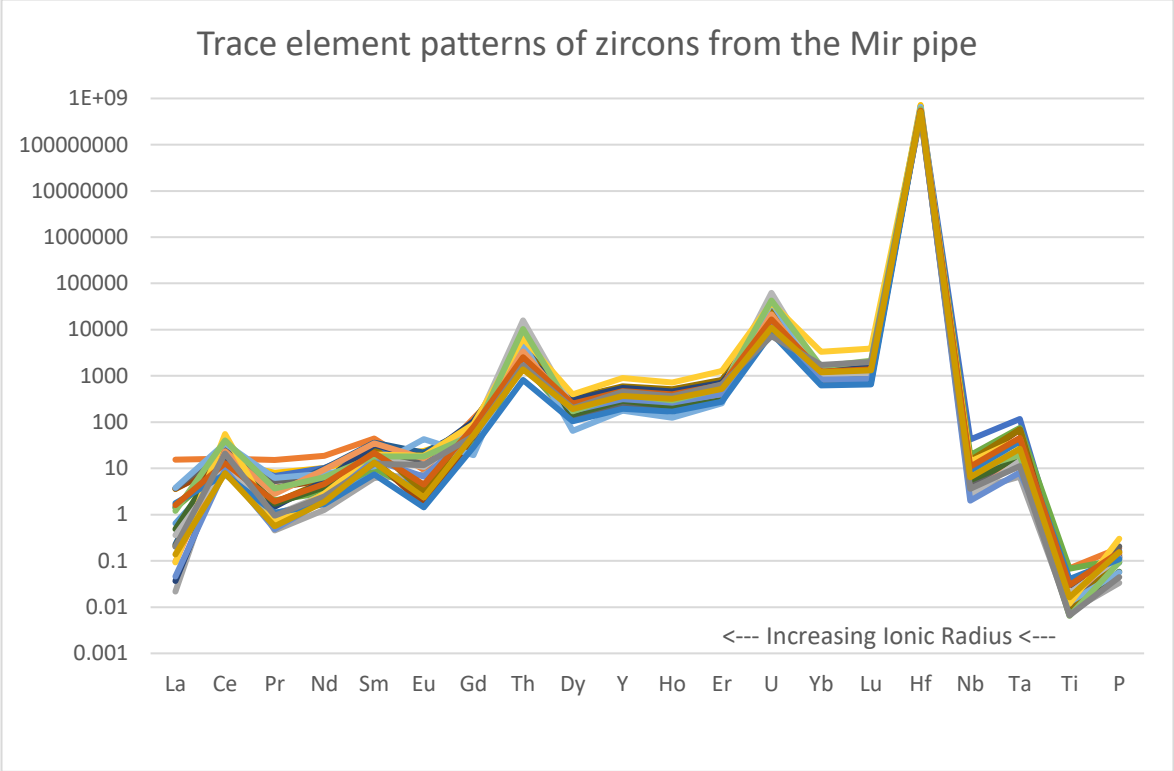
Positive Ce- and negative Eu-anomalies are presented for the most of grains (Fig. 4.1.12). Eu-minima commonly indicates crystallization of plagioclase before zircons were crystallized, while Ce-maxima may reflect high oxidation state of the parental melt (Guo *et al.*, 1996, Hinton & Upton, 1991). Positive Eu-anomaly found for a single grain might occur due to an inclusion or a crack within the analytical spot.

Concentrations of some elements differ by orders of magnitude, while others are relatively uniform for all grains (Fig. 4.1.12). Total content of REE vary from 325 to 880 ppm, with the only grain reveal 1615 ppm of REE. Yttrium ranges from 396 to 2010 ppm, Th – from 33 to 636, U – from 73 to 624 ppm. Concentrations of Hf vary from 0.8 to 1.3 wt.%.

Th/U ratios range widely between 0.14 and 1.02, and Ta/Nb shows a relatively narrow interval of values between 2.2 and 6.48. Nb/Ta ratio is higher typically in zircons from more fractionated rocks like granitoids than in kimberlitic zircons (Belousova *et al.*, 2002). Th/U ratios in zircon also reflect the fractionation degree of the parental melt when zircon crystallizes in equilibrium with the melt. However, when zircon crystallizes in disequilibrium with the melt, U and Th are more easily able to enter the zircon lattice, and their contents and Th/U ratios depend mainly on the degree of disequilibrium (Wang *et al.*).

Comparison of the trace-element composition of zircons from different age groups shows no regularity or correlations between different age populations/groups and concentrations of trace elements (Fig. 4.1.13).

Zircon trace element composition allows to suggest the most likely type of parental melt for analysed zircons. Based on the large set of samples with known origin statistical CART classification (Belousova *et al.*, 2002) uses some elements to discriminate zircons crystallized from melts of different composition. For example, mantle-derived zircons (kimberlitic or carbonatitic) commonly have low Lu (<20.7 ppm) and U (<130 ppm), but high Ta (>0.5). Crustal zircons, in opposite, shows high U (over wt%) and Lu (over 2000 ppm) (Belousova *et al.*, 2002).



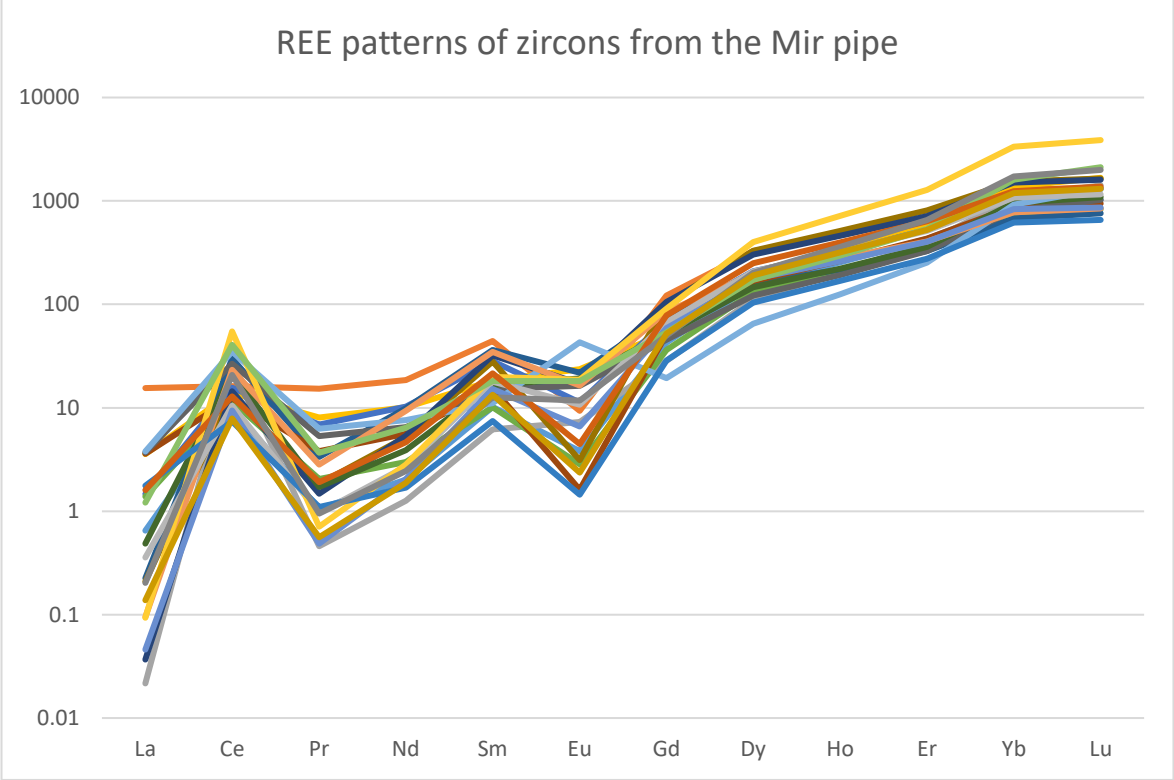




Figure 4.1.12 Trace-element and rare-earth-element patterns of zircons from the Mir pipe.

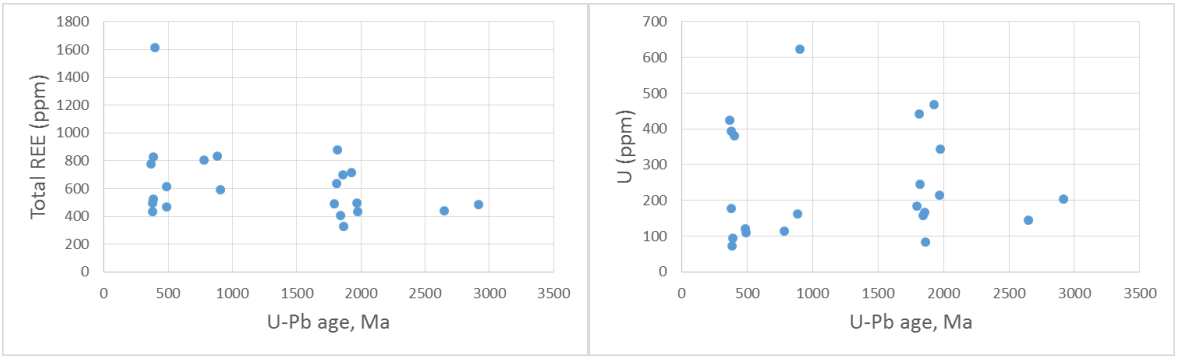



Figure 4.1.13. Total REE and U contents *vs* U-Pb age for zircons from the Mir pipe.

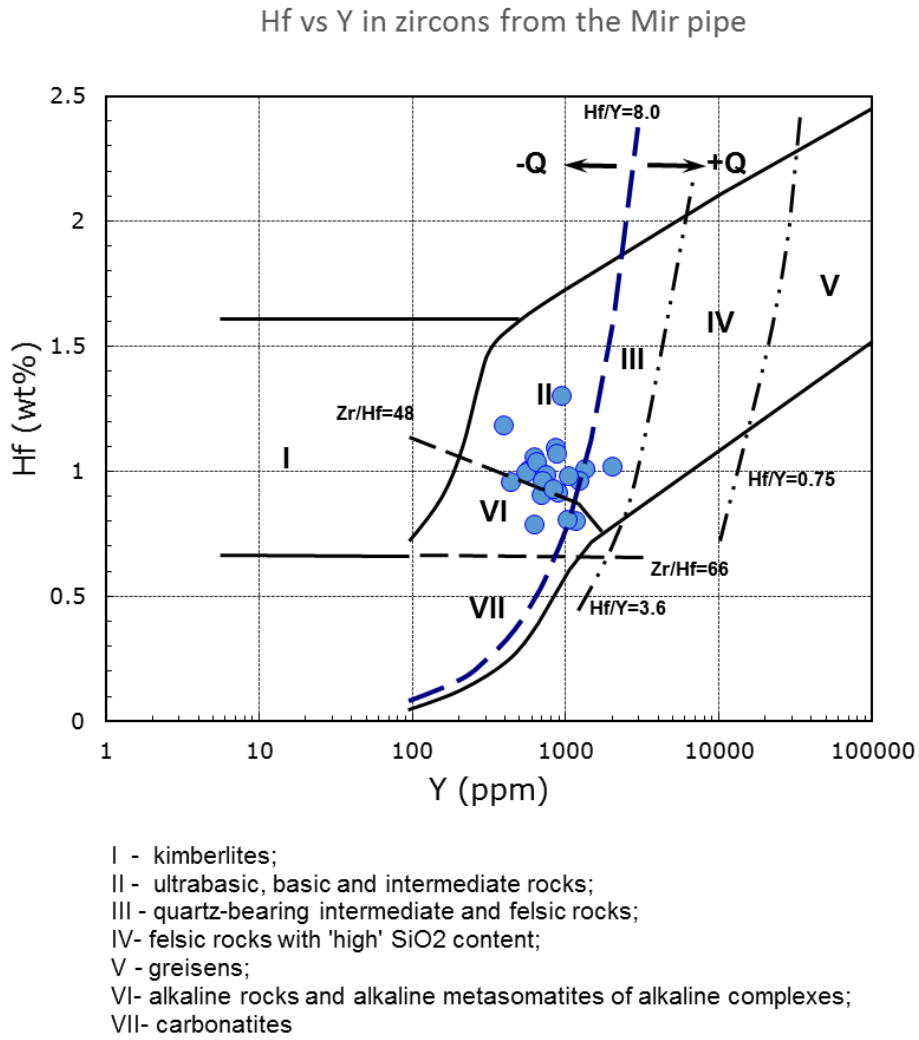



Figure 4.1.14. Hf *vs* Y discrimination diagram for zircons from the Mir pipe.

Thus, according to the CART classification all zircon grains from the Mir pipe have trace-element compositions similar to that of zircons crystallized from mafic or intermediate parental melt. This is confirmed by Hf *vs* Y discrimination diagram (Fig. 4.1.14) showing most of grains located within the fields of ultramafic to intermediate or alkaline rocks with low $SiO_2$ content.

**The Sputnik pipe**

Fifty-seven zircons were analysed for trace-element composition (Appendix 2.2). Similar to the previous samples, all analyzed grains have chondrite-normalized trace-element patterns typical of zircons (Fig. 4.1.15).

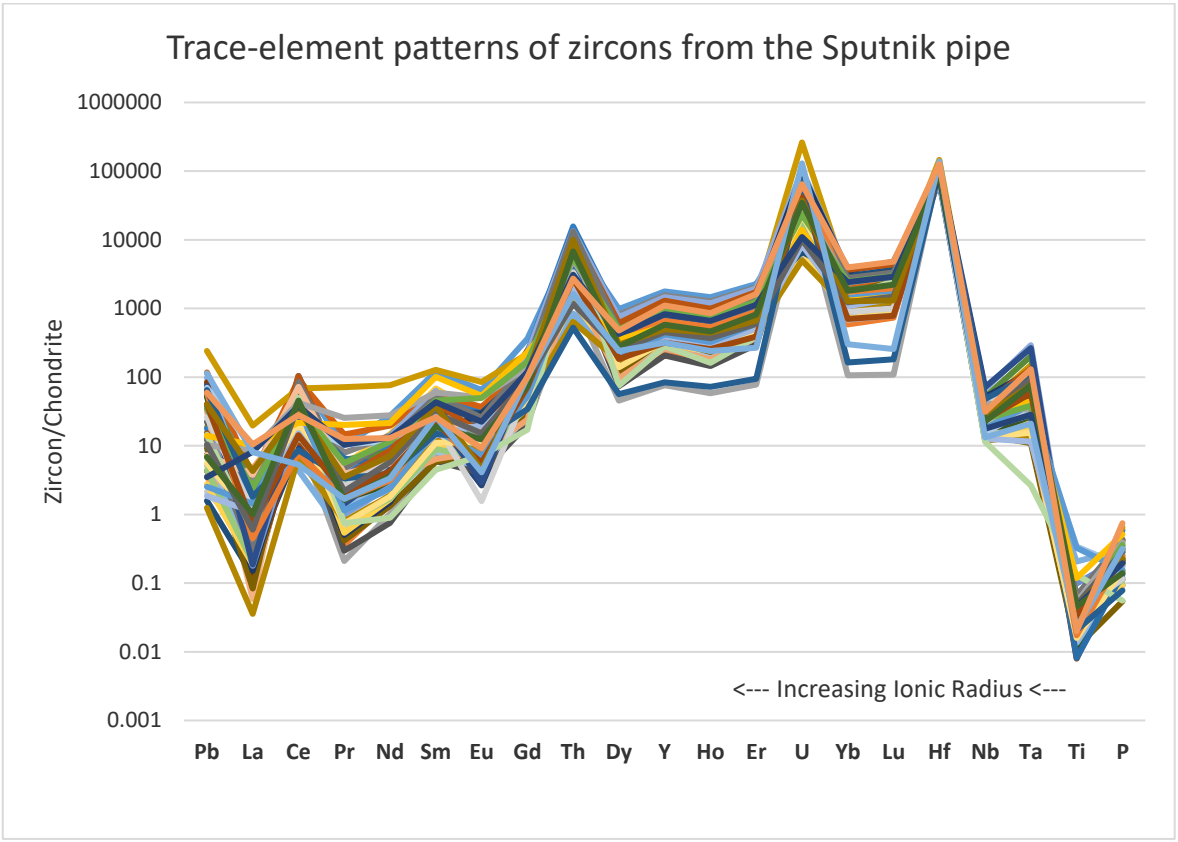
Chondrite-normalized REE pattern demonstrates negative Eu and positive Ce anomalies for the most of zircons, indicating plagioclase crystallization before zircons and high oxidation state of the parental melt.

The zircons show wide range of concentrations for the majority of elements. Thus, the concentrations of yttrium are in the range from 173 to 3986 ppm, Th vary from 21 to 626 ppm, U – from 50 to 2616 ppm. Hafnium concentrations are relatively high – from 1.26 to 2.63 wt%. Total REE also diverge in wide range from 100 to 2596 ppm. Some of zircons demonstrate relative enrichment in LREE (La up to 10 ppm, Ce up to 100 ppm), which is common for zircons from felsic rocks or in strongly metamict zircons.

The variations in Th/U and Nb/Ta ratios are also significant – 0.03-2.19 and 2.03-53.73 respectively.

Comparison of the trace element composition of zircons from different age groups reveals no correlation between total REE contents and age of zircons (Fig. 4.1.16). However, low Lu concentrations typical for mantle-derived zircons are found only in grains with age ca 1.85 Ga (Fig. 4.1.16).

According to the CART classification (Belousova *et al.*, 2002), 54 of the analyzed grains have trace element compositions typical of zircons from granitic rocks (high LREE, U, Hf and Nb) and only 3 grains show composition similar to carbonatitic zircons (Lu<20.7 ppm, Ta>0.5 ppm). The discriminant diagram Y *vs* Yb/Sm shows only few grains located out of the field of zircons from granitoids, and 3 zircons are situated within or close to carbonatites field (Fig. 4.1.17).



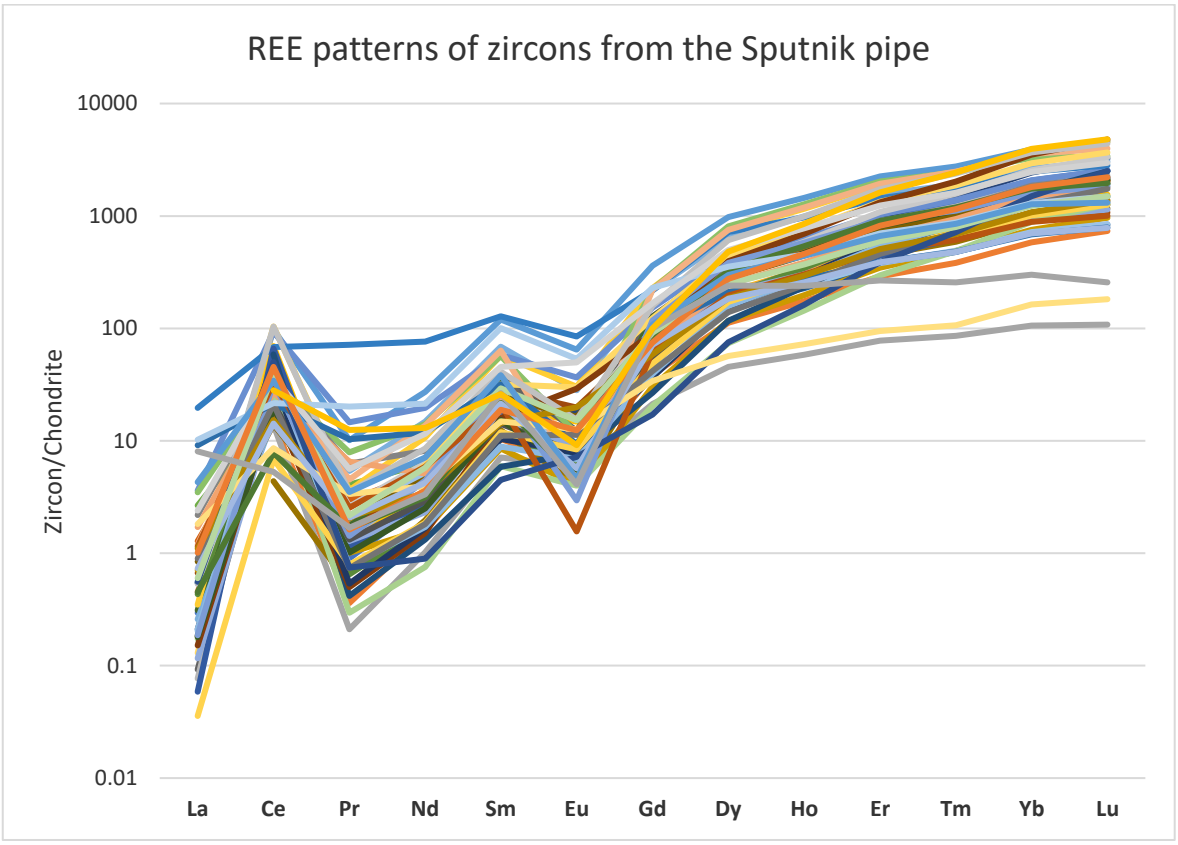




Figure. 4.1.15. Trace-element and rare-earth-element patterns of zircons from the Sputnik pipe.

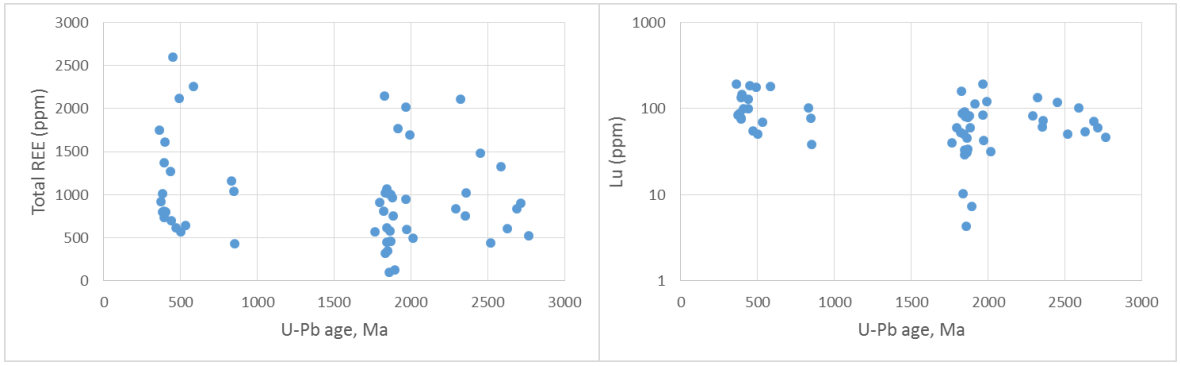



Figure 4.1.16. Total REE and Lu contents *vs* U-Pb age for zircons from the Sputnik pipe.

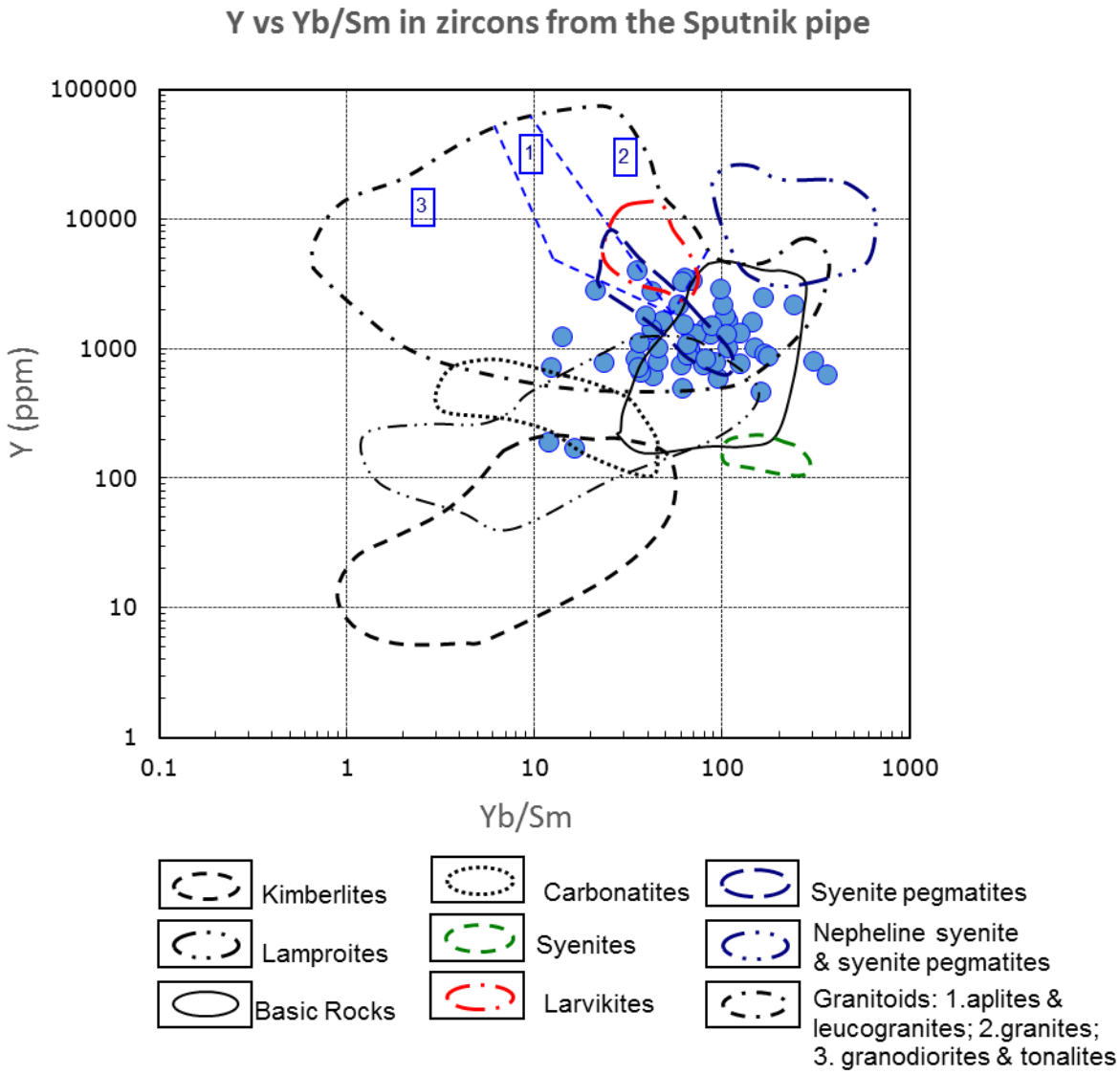



Figure 4.1.17. Y *vs* Yb/Sm discriminant diagram for zircons from the Sputnik pipe.

**The Internationalnaya pipe**

Trace-element compositions have been studied for 44 zircons from the Internationalnaya kimberlite pipe. Five grains were rejected because of inclusions or cracks affected the spectra.

The plot of chondrite-normalized REE concentrations shows patterns with minor to significant enrichment in HREE. Negative Eu and positive Ce anomalies are observed for the most of zircons; however, a few grains show none Eu-anomaly (Fig. 4.1.18) implying there was no plagioclase crystallized from the melt prior to zircons.

The concentrations of the most of elements vary in a wide interval. Total REE content ranges from 164 to 2532 ppm. The most of the light rare earth elements vary tenths to tens ppm, while HREE diverge from first ppm to hundreds ppm. Uranium ranges from 27 to 1127 ppm; Th – from 24 to 610; Hf concentration ranges from 0.8 to 2.56 wt%.

The Th/U ratio shows ranges from 0.07 to 1.3, Nb/Ta from 1.95 to 24.8.

The lowest concentrations (less than 500 ppm) are found only in zircons older than 1.8 Ga (Fig. 4.1.19). Low Lu contents typical for mantle-derived zircons are also found only in grains of Paleoproterozoic or Archean age (Fig. 4.1.19).

Similar to the zircons from the Sputnik pipe, only a few grains have trace-element signatures typical for zircons from carbonatitic rocks (low Lu and U, high Y and Th); the composition of the majority of grains is consistent with their crystallisation in magmas of mafic to felsic composition (Fig. 4.1.20).

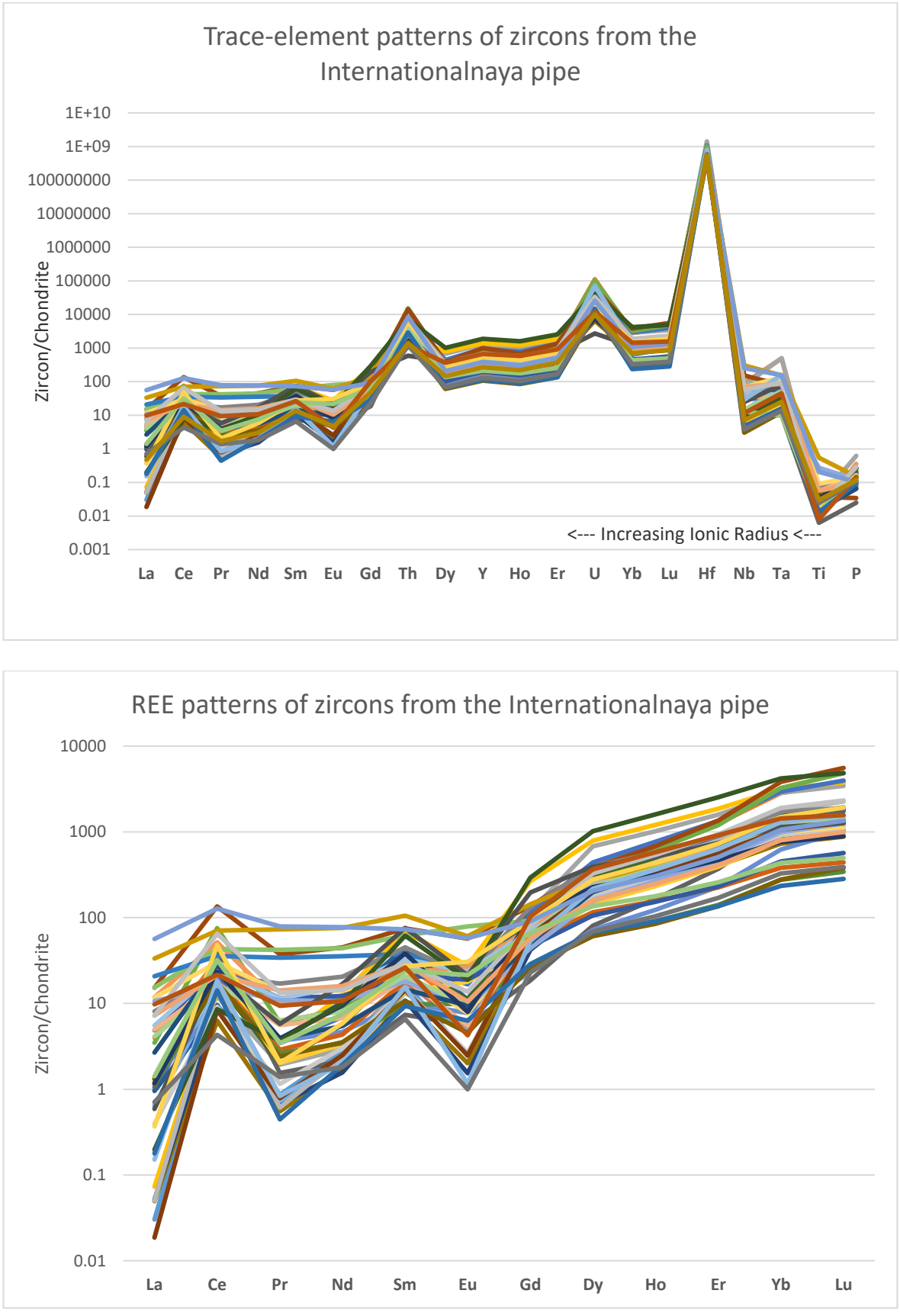



Figure. 4.1.18. Trace-element and rare-earth-element patterns of zircons from the Internationalnaya pipe.

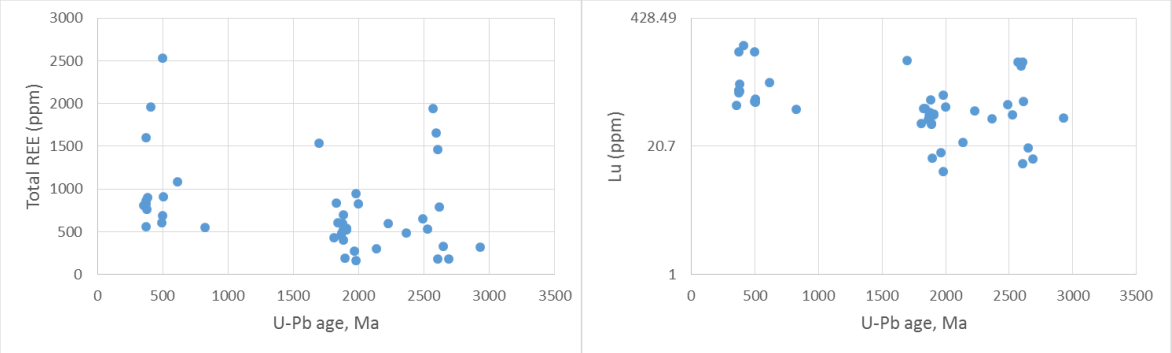



Figure 4.1.19. Total REE and Lu contents *vs* U-Pb age for zircons from the Internationalnaya pipe.

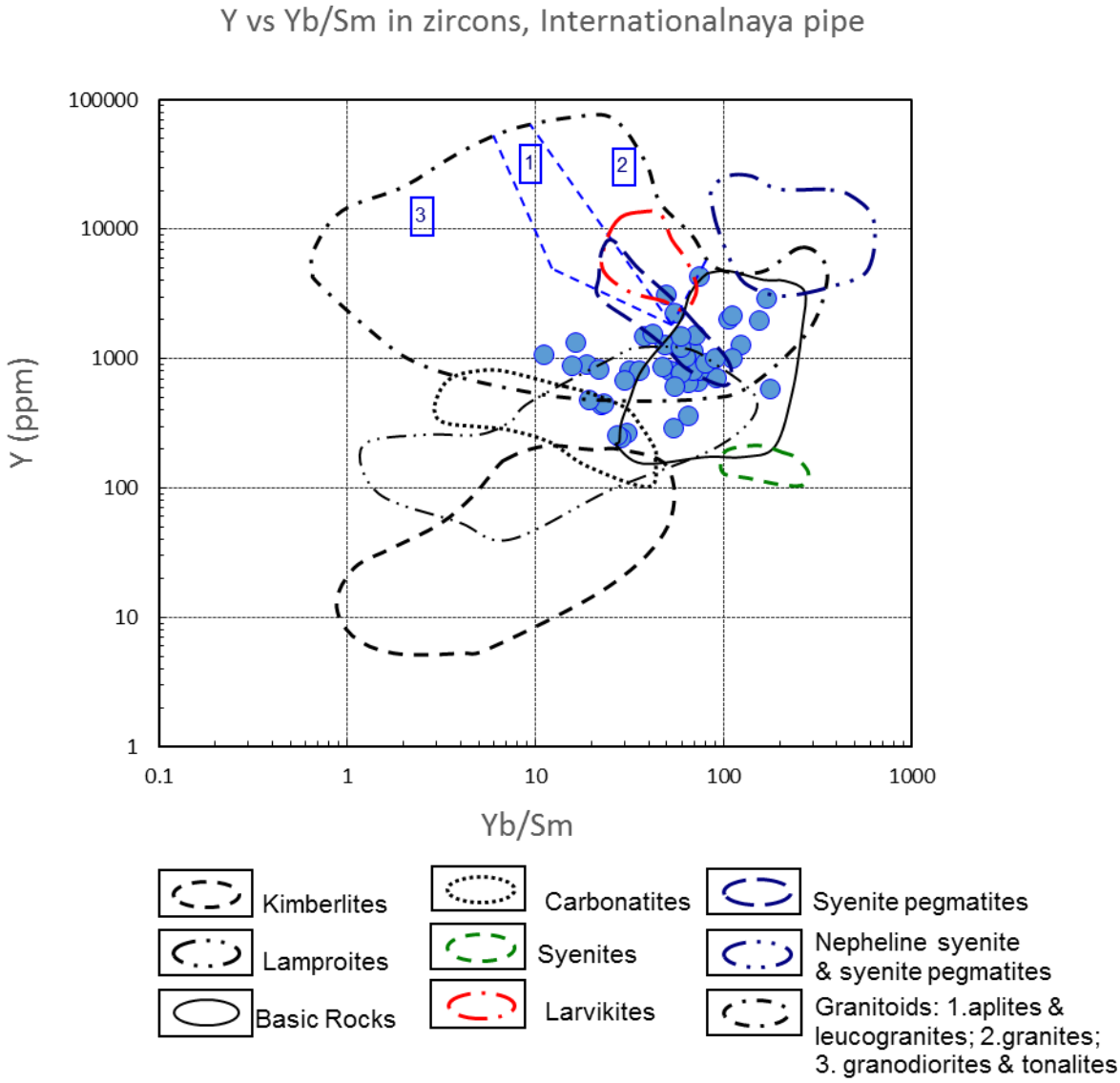



Figure. 4.1.20. Y *vs* Yb/Sm discrimination plot for zircons from the Internationalnaya pipe.

***Oxygen isotopes data***

**Sputnik pipe**

Oxygen isotopic composition was analysed in 26 zircons of different age groups (Appendix 2.3). $\delta^{18}O$ ranges significantly from 4.4±0.2 to 9.8±0.2‰. Young zircons have the widest range of $\delta^{18}O$ from 4.4±0.2 to 9.6±0.2‰; however six out of seven grains of the main population (mean age of 390 Ma) reveal $\delta^{18}O$ close or within the mantle values (5.3±0.6‰, (Valley *et al.*, 2003)). Mantle oxygen composition is also common for all grains older than 2.5 Ga. At the same time, supracrustal oxygen compositions ($\delta^{18}O$ > 6.6‰) are more typical in zircons from the second age group (1.76 – 2 Ga) (Fig. 4.1.21).

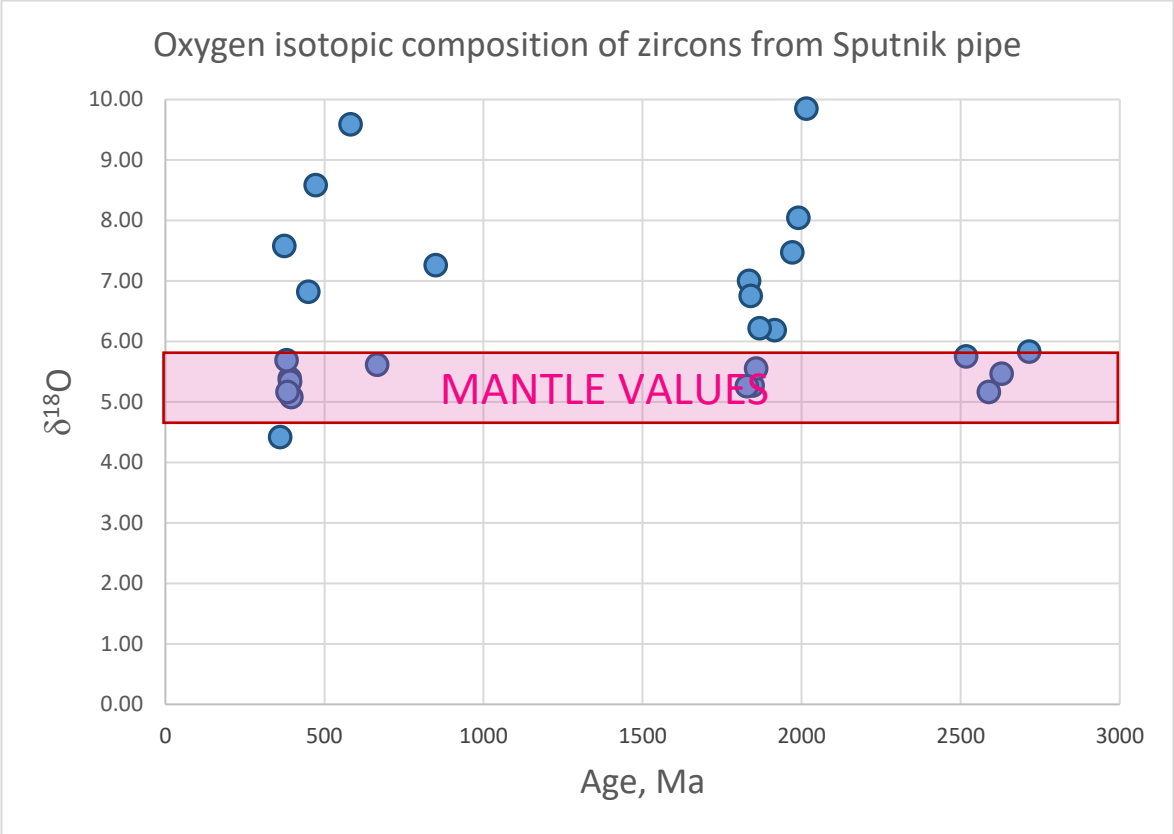



Figure 4.1.21. $\delta^{18}O$ *vs* U-Pb age for zircons from the Sputnik pipe.

***Hafnium-isotope data***

**The Sputnik pipe**

Lu-Hf isotopes have been studied in 58 zircon grains from the Sputnik pipe (Appendix 2.3). All grains were dated prior to analysis for Hf-isotope composition.

Studied zircons show large range in their Hf-isotope composition. The ranges of calculated, initial $^{176}Hf/^{177}Hf$ ratios, εHf values and model ages also vary significantly for zircons of different age groups (Table 4.1.2, Fig. 4.1.22). Thus, for zircons younger than 1 Ga initial Hf ratios differ in the interval 0.28177 – 0.28284, εHf ranges from -26 up to +14. This wide range of εHf values implies involving both reworking of the ancient crust (low negative εHf) and addition of the juvenile material (with positive εHf close to depleted mantle values). This is also reflected in crustal model ages falling into the wide interval from 600 Ma to 2.8 Ga.

The group of 1.76-2.0 Ga zircons also shows relatively wide range of Hf-data: initial Hf values are within the range of 0.28114 – 0.28165, εHf varies from about -16 to +5 and crustal model ages differ from ca 2.3 to 3.4 Ga.

Far less variation is found in the oldest zircon populations (2.3 – 2.76 Ga): initial Hf ranges from 0.2807 – 0.28133, εHf values are from -11 to +2 and crustal model ages are between 2.8 and 3.9 Ga.

Table. 4.1.2. Summary table of Hf-isotopic data for zircons from Sputnik pipe

| Age group | Range of U-Pb ages, Ma (n = number of grains) | Initial Hf values | εHf values | $T_{(DM)}^{C}$ range, Ga |
|---|---|---|---|---|
| **Group 1** | 361 – 850 (n = 21) | 0.28177 – 0.28284 | -26 – +13 | 0.6 – 2.8 |
| **Group 2** | 1767-2015 (n = 26) | 0.28114 – 0.28165 | -16 - +5 | 2.3 – 3.4 |
| **Group 3** | 2290 - 2764 (n = 11) | 0.2807 - 0.28133 | -11 - +2 | 2.8 – 3.9 |

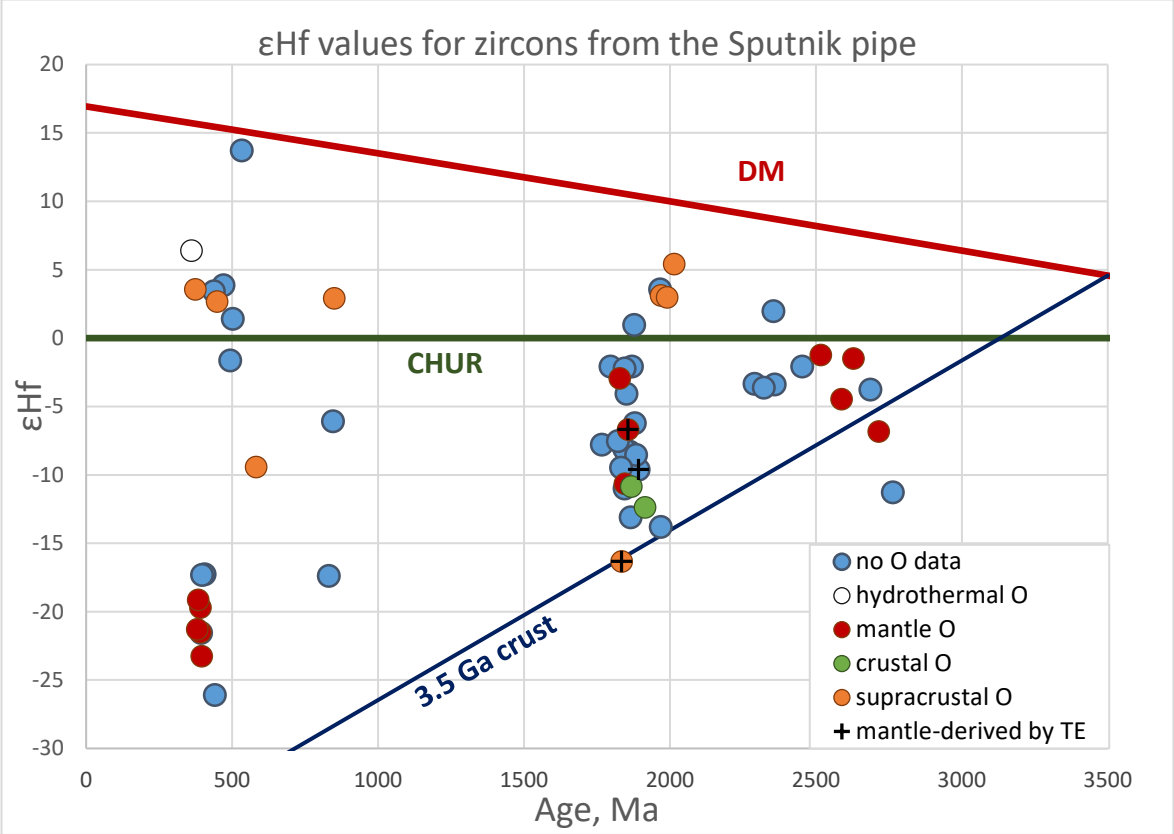



Figure 4.1.22. εHf *vs* U-Pb age plot for zircons from the Sputnik pipe. The data points are color-coded according to the zircon O-isotope composition (where these data are available) and grains with trace-element (TE) composition typical of mantle-derived zircons are also shown with black crosses. Reference lines: DM – depleted mantle reservoir, CHUR – chondrite reservoir, 3.5 Ga crust - evolution of the average continental crust ($^{176}Lu/^{178}Hf$ = 0.015, (Griffin *et al.*, 2002b)).

## 4.2. The Kharamai kimberlite field

The Kharamai field is located in the northern part of the Magan terrane, about 30 km SW from the Anabar shield. This part of the Magan terrane was suggested to be the "bridge" between the Magan and Tunguss terranes (Rosen *et al.*, 2000) or the result of re-working of the edge of the Tunguss terrane (Smelov & Timofeev, 2007).

The basement rocks are commonly overlaid by 1-2 km of Cambrian carbonate sediments, which are intruded by gabbro-dolerite dykes and sills of the Permian-Triassic Siberian Trap formation. More than 160 kimberlitic bodies are found within this field, including 90 pipes, some of which are diamondiferous (e.g. the Achtakh, Boloto, Evenkiya, Burustakh pipes etc.).

Because of the wide distribution of the Quaternary glacial deposits in the region, structural elements could be observed only from the geophysical data. Assuming a latitudinal strike of the field, the inferred Kharamai fault was suggested as a controling factor on the linear kimberlite distribution. This fault could be related to the wide (up to 30 km) Arga-Salinsk tectonic zone, marked by the mafic intrusives and local faults.

The age of the kimberlites of the Kharamai field is impossible to determine by geological observation. However, kimberlites intrude both Cambrian sedimentary rocks and the later dykes and sills, thus kimberlites could not be older than Early Mesozoic.

Previously, the kimberlites have been dated by Rb-Sr and U-Pb isotopic systematics. In most cases the Rb-Sr method gave ages the 135-186 Ma (Brakhfogel, 1995). Much older ages were obtained by zircon U-Pb SHRIMP and fission track methods: 290-233 Ma (Griffin *et al.*, 2005, Griffin *et al.*, 1999a, Kinny *et al.*, 1997).

Samples from only two kimberlite pipes of the Kharamai field were studied during this project: U-Pb ages were determined for zircon grains collected from the crushed kimberlite from Eclogit and Evenkiya pipes.

### *Zircon U-Pb data*

#### The Eclogit pipe

In total 10 U-Pb analyses have been done on zircons from the Eclogit pipe. All analyses are concordant and give the Concordia age of 235.4±0.81 Ma (MSWD = 0.42, probability = 0.51, Fig. 4.2.1). The youngest obtained age is 234±4 Ma, and the oldest is 238±6 Ma. Concentrations of U are within the range 12-26 ppm, Th – 3.7 - 9.6 ppm, which is typical of kimberlitic zircons.

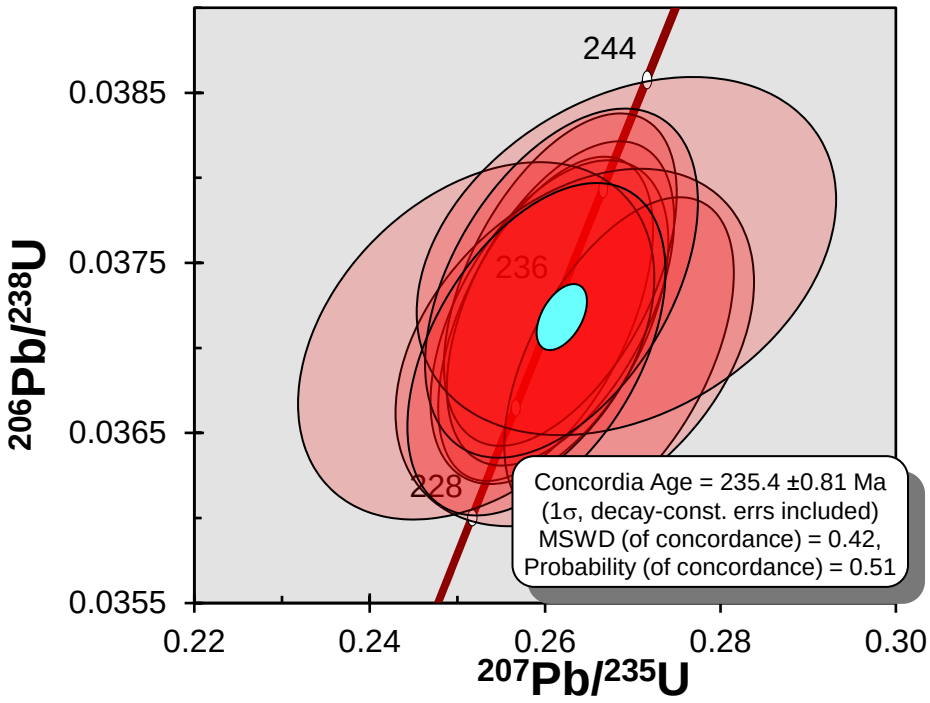



Figure 4.2.1. The Concordia diagram: U-Pb age of zircons from the Eclogit pipe, Magan terrane.

**The Evenkiya pipe**

Eleven zircons from the Evenkiya pipe were dated by U-Pb method. One analysis was rejected because of the high discordance, 10 others give a Concordia age of 238±0.98 (MSWD = 0.60, probability = 0.44; Fig. 4.2.2). Ages differ within the narrow interval 233 – 241 Ma; concentrations of uranium are from 4.64 to 37.95 ppm, Th - from 1.25 to 8.37 ppm, again consistent with their mantle origin.

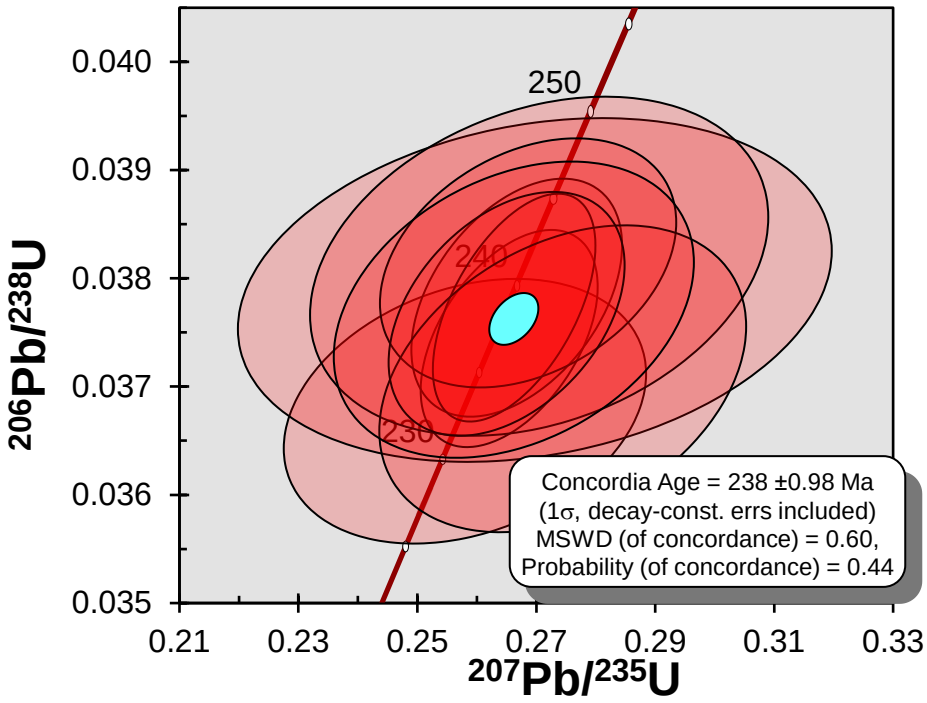



Figure 4.2.2. The U-Pb age of zircons from the Evenkiya pipe, Magan terrane.

# Chapter 5. The Markha terrane

The Markha terrane is located in the Markha River basin within the Anabar tectonic province (Fig. 5) (Rosen *et al.*, 1994). The terrane was distinguished by geophysical data as the basement rocks are not exposed at the surface. The previous crustal xenoliths study suggested that this terrane is the granite-greenstone complex buried under the cover sequences of Palaeozoic age. According to other studies, the Markha terrane also called Tyungsky (Smelov & Timofeev, 2007).

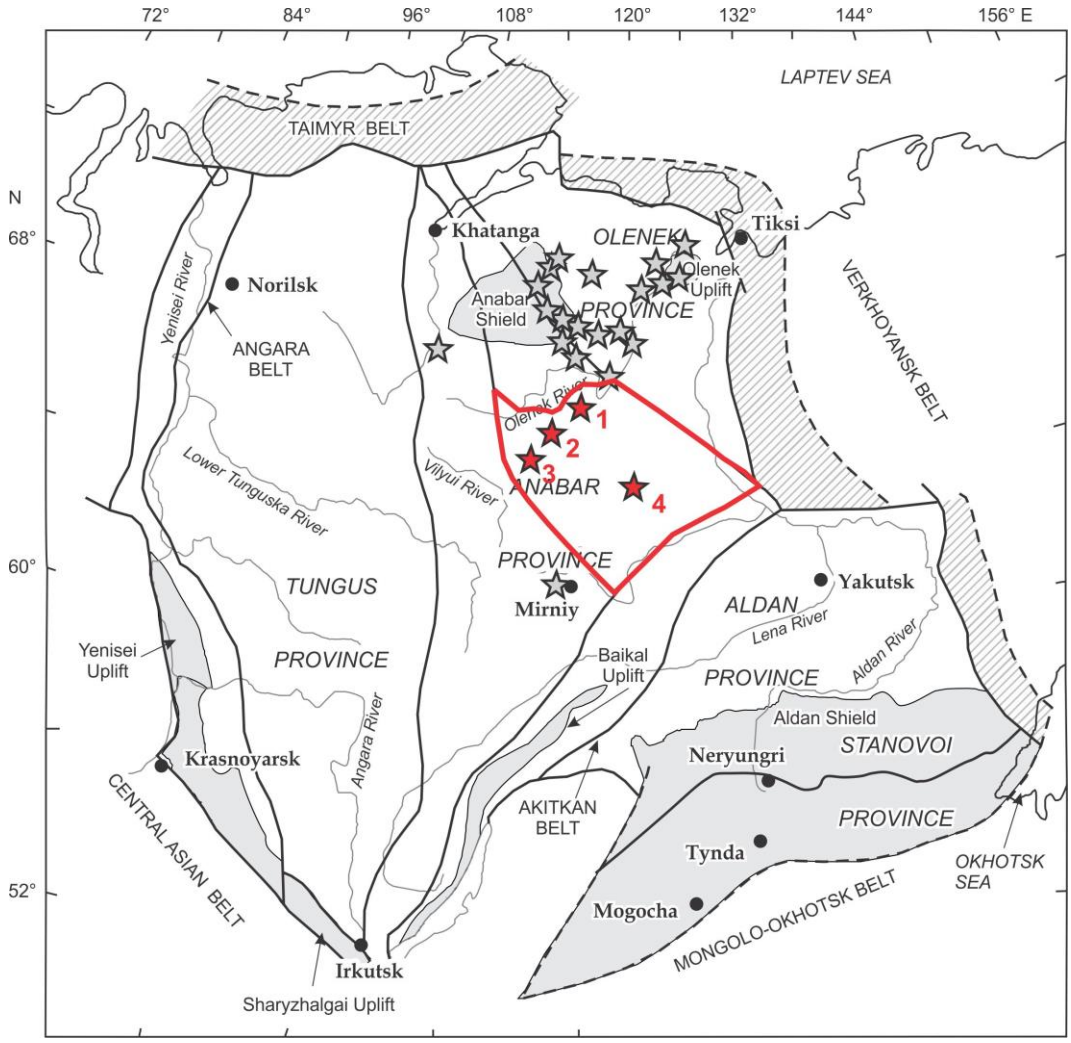



Figure 5. The location of the Markha terrane and studied kimberlite fields. Red stars are for kimberlite fields studied: 1 – Upper Muna; 2 – Daldyn, 3 – Alakhit-Markha, 4 - Nakyn.

The most common crustal xenoliths reported from kimberlitic pipes within the terrane are of two-pyroxene-garnet-hornblende mafic granulites and two-pyroxene-plagioclase-olivine composition. In addition, plagioclase-garnet-orthopyroxene-quartz and garnet-sillimanite-granulites were found as well. These xenoliths assemblages suggest that basement protoliths in

this region are dominantly mafic to intermediate volcanic and intrusives with some metasediments.

Very limited geochronological data are available for this terrane. The whole rock Sm/Nd isochron age of 1756±6 Ma was determined for the garnet amphibolite xenolith with $T_{DM}$ model age of 2920 Ma (Neymark *et al.*, 1993). Other garnet gneiss and amphibolite xenoliths gave Sm/Nd model ages ranging from 3.3 to 3.1 Ga (Rosen *et al.*, 1994).

The Markha terrane includes four kimberlite fields: Upper Muna (or Muna), Daldyn, Alakhit-Markha and Nakyn. Summary of studied samples from the terrane is shown in Table 5.

Table 5. Analytical work done for samples from the Markha terrane.

| Field | Pipe | Type of samples* | Zircons | | | | Sulfides | |
|---|---|---|---|---|---|---|---|---|
| | | | U-Pb^ | TE | O | Hf | Re-Os | PGE |
| Upper Muna | Zimnyaya | HMC | 38 (29) | 26 | 31 | 28 | | |
| | 325 years of Yakutia | kimberlite | 29 | 29 | | 19 | | |
| | Zapolyarnaya | xenoliths | 78 (63) | | | 55 | | |
| Daldyn | Udachnaya Eastern | HMC | 10 | 10 | | 9 | | |
| | Zarnitsa | HMC | 10 | 10 | | 9 | | |
| | Popugaeva | HMC | 22 | 22 | | 17 | | |
| | Zagadochnaya | HMC | 37 | 37 | | 27 | | |
| | Kusova | HMC | 50 (47) | 45 | | 39 | | |
| | Udachnaya | xenoliths | 82 (81) | 81 | 65 | 40 | 10 | 10 |
| Alakit-Markha | Kismet | HMC | 35 (34) | 31 | | 20 | | |
| | Geochemical | HMC | 6 | 6 | | 6 | | |
| | Vostok | HMC | 36 (35) | 34 | | 28 | | |
| | Veselaya | HMC | 4 | 4 | | 4 | | |
| | Krasnopresnenskaya | HMC | 5 | 5 | | 5 | | |
| | Markha | HMC | 97 (85) | 85 | | | | |
| | Aikhal | kimberlite | 53 | 9 | 25 | 18 | | |
| Nakyn | Nurbinskaya | kimberlite | 65 (60) | 79 | 32 | 65 | | |
| | Botuobinskaya | xenoliths | 41 | | | 41 | | |
| *Total for the terrane* | | | *698 (650)* | *513* | *153* | *430* | *10* | *10* |

* Type of samples: HMC - heavy mineral concentrate from weathered kimberlite; kimberlite - hand-picked zircons from crushed kimberlite; xenoliths – zircons extracted from xenoliths.

^ U-Pb analyses: total (used)

## 5.1. The Upper Muna kimberlite field

The field is located in the basin of the upper Muna River and its right tributary stream Uulakh-Muna. Twenty one kimberlite bodies were found within the field, which are hosted by carbonate and terrigenous-carbonate rocks of the Middle Cambrian – Early Ordovician age. The field observations confirmed that kimberlite bodies intruded into the Late Cambrian rocks of the Chukukskaya series (Zaitsev & Smelov, 2010).

Previous isotopic geochronological studies revealed two main age intervals of kimberlite eruptions: 334-382 and 426-458 Ma. Although a lot of Rb-Sr, K-Ar and U-Pb geochronological data are available for kimberlite pipes within the field, the ages determined by different techniques varies significantly for almost every individual pipe (Zaitsev & Smelov, 2010).

### *Zircon U-Pb data*

Zircons were collected from heavy mineral concentrates from two pipes - Zimnyaya and 325 years of Yakutia, as well as recovered from xenoliths from the Zapolyarnaya pipe (Tables 5.1.1, 5.1.2).

#### The Zimnyaya pipe

Thirty-eight zircons were recovered from the heavy mineral concentrate collected from the weathered kimberlite of the Zimnyaya pipe. Nine U-Pb analyses were rejected later because of their high discordance. In 5 grains both the rim and core were dated (Appendix 3.1), but only one zircon shows difference in ages outside of analytical uncertainty (sample 8008-11: core 2649 Ma, rim 1848 Ma).

Table 5.1.1. U-Pb ages of zircons from heavy-mineral concentrates from the Upper-Muna kimberlite field.

| Pipe | Range of U-Pb ages, Ma (n = number of analyses) | Major peak age range or mean age, Ma | Second peak age range, Ma | Minor peaks age ranges, Ma |
|---|---|---|---|---|
| **Zimnyaya** | 176 – 2745 (n = 29) | 260-334 | 2541-2745 | 176-202<br>405-455 |
| **325 years of Yakutia** | 341-374 (n = 29) | 357.7±1.5 | n/a | n/a |

Zircons from the Zimnyaya pipe could be generally subdivided into two main age groups: one represented by grains older than 2.5 Ga and the other by populations younger than 500 Ma (Fig 5.1.1).

For the younger group three age intervals could be identified: 176-202 Ma (6 grains), 260-334 Ma (14 grains) and 405-455 Ma (3 grains) (Fig. 5.1.2). Due to the scattered ages within each interval, it is not possible to calculate statistically meaningful mean age for each group.

The older group consists of 6 zircons ranging from 2541±40 to 2745±44 Ma. Four grains of this group are lying on the discordia with the upper intercept of 2613±29 and lower intercept at 1350±420 Ma (Fig. 5.1.3).

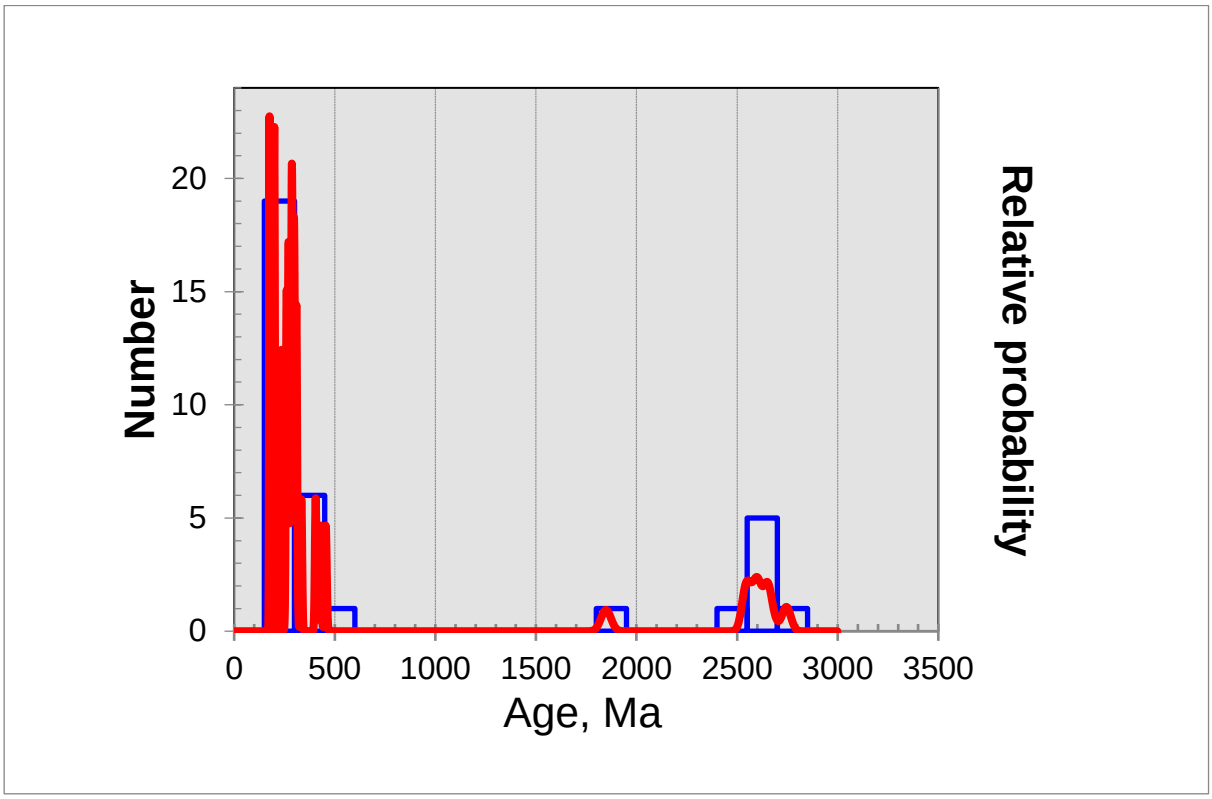



Figure 5.1.1. Probability plot of zircon U-Pb ages, Zimnyaya pipe, Markha terrane.

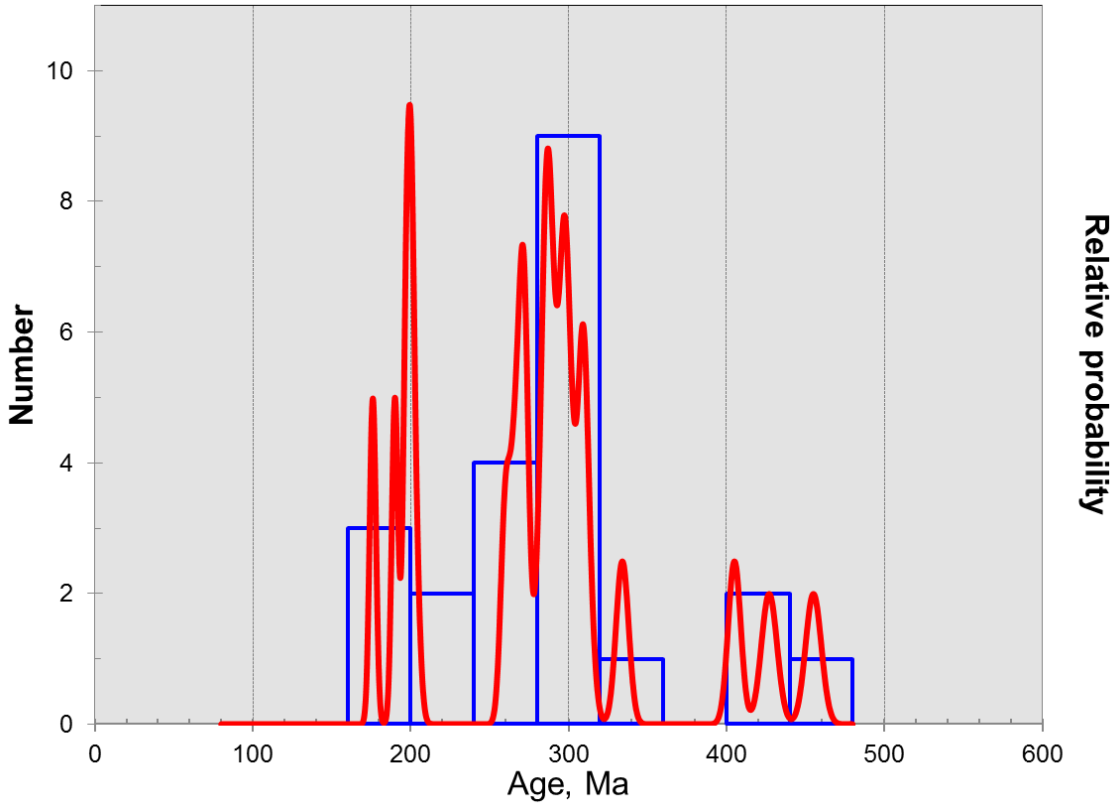



Figure 5.1.2. U-Pb age of young zircons from the Zimnyaya pipe, Markha terrane.

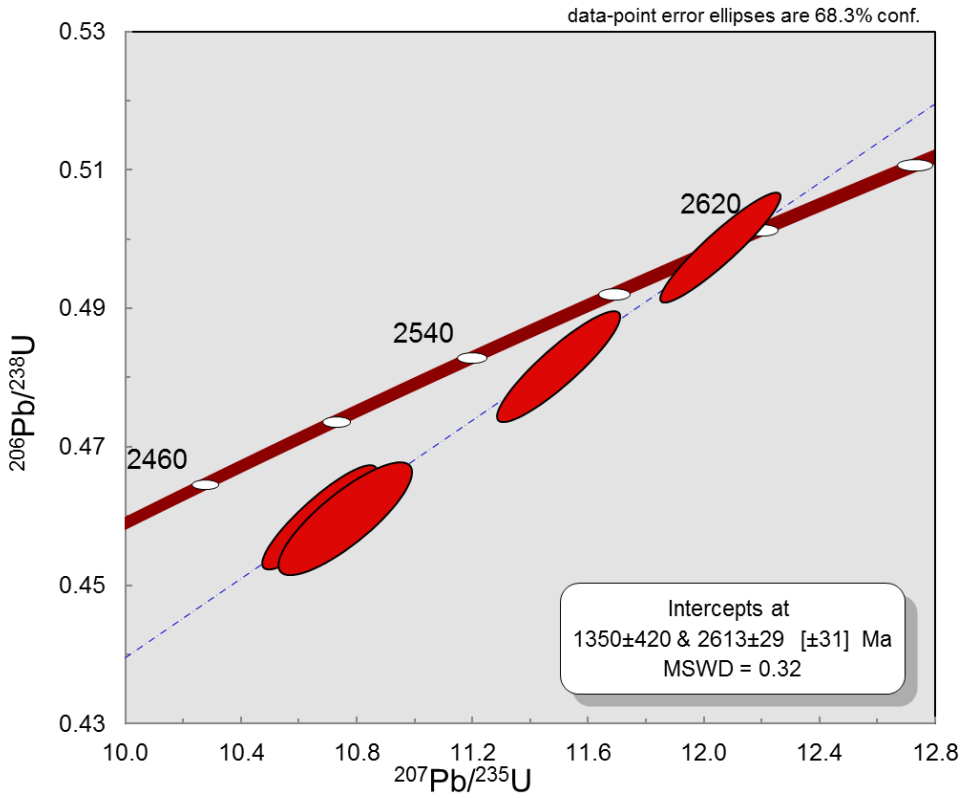



Figure. 5.1.3. U-Pb age of the old zircon population from the Zimnyaya pipe, Markha terrane.

**The 325 years of Yakutia**

Twenty-nine zircons were extracted from the crushed whole-rock kimberlite. All grains are concordant and consist of a single age population with the calculated concordia age of 357.7±1.5 Ma (MSWD = 1.5, probability = 0.21; Fig. 5.1.4). The youngest obtained age is 341±14 Ma and the oldest 374±14 Ma. This is in a good agreement with age of pipe (342-365 Ma) determined by different techniques and reported previously by Zaitsev and Smelov (2010).

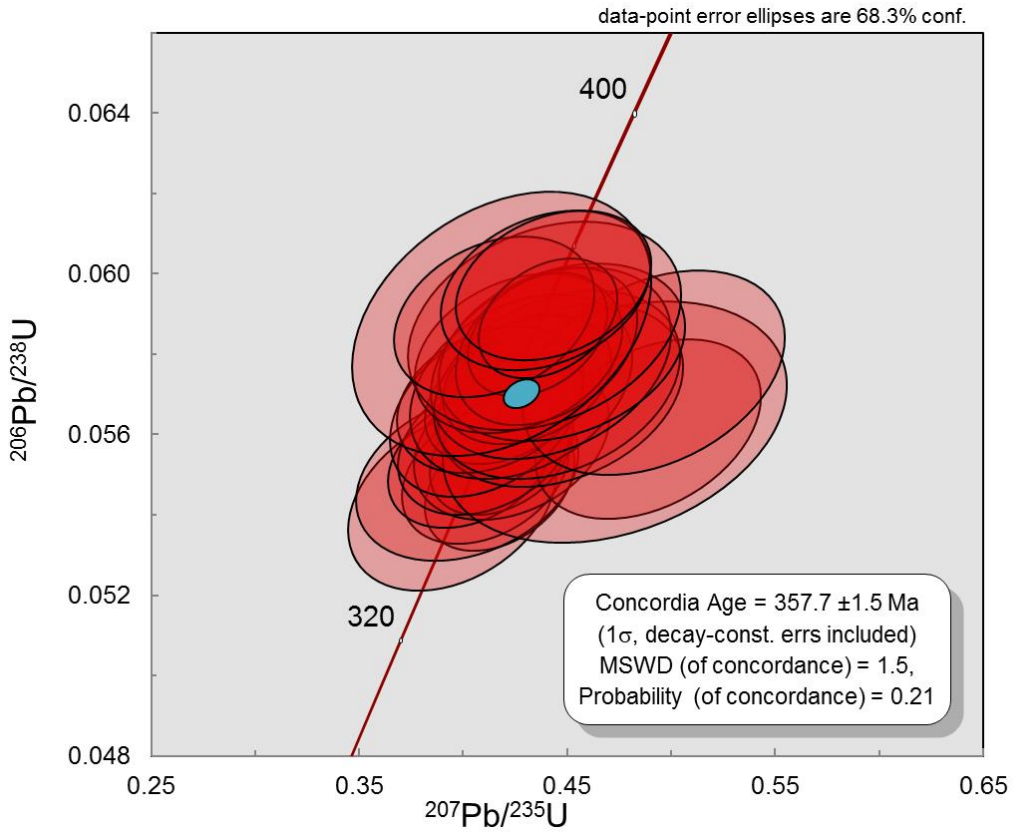



Figure 5.1.4. U-Pb age of zircons from the kimberlite pipe "325 years of Yakutia", Markha terrane.

**The Zapolyarnaya pipe**

Zircons were extracted from four crustal xenoliths from the Zapolyarnaya pipe (Table 5.1.2.)

Twenty one zircons were extracted from the mafic granulite xenolith ZP-10-04 (Cpx+Pl±Grt). All of them were dated, however, 6 U-Pb analyses were rejected due to the high discordance. The rest 15 grains form a regression line with upper intercept at 2711±14 Ma and the lower one at 379±110 Ma (MSWD = 0.59; Fig. 5.1.5). Eight zircons represent a single age population with a weighted mean age of 2709±9 Ma (MSWD = 0.40, probability = 0.91; Fig. 5.1.6).

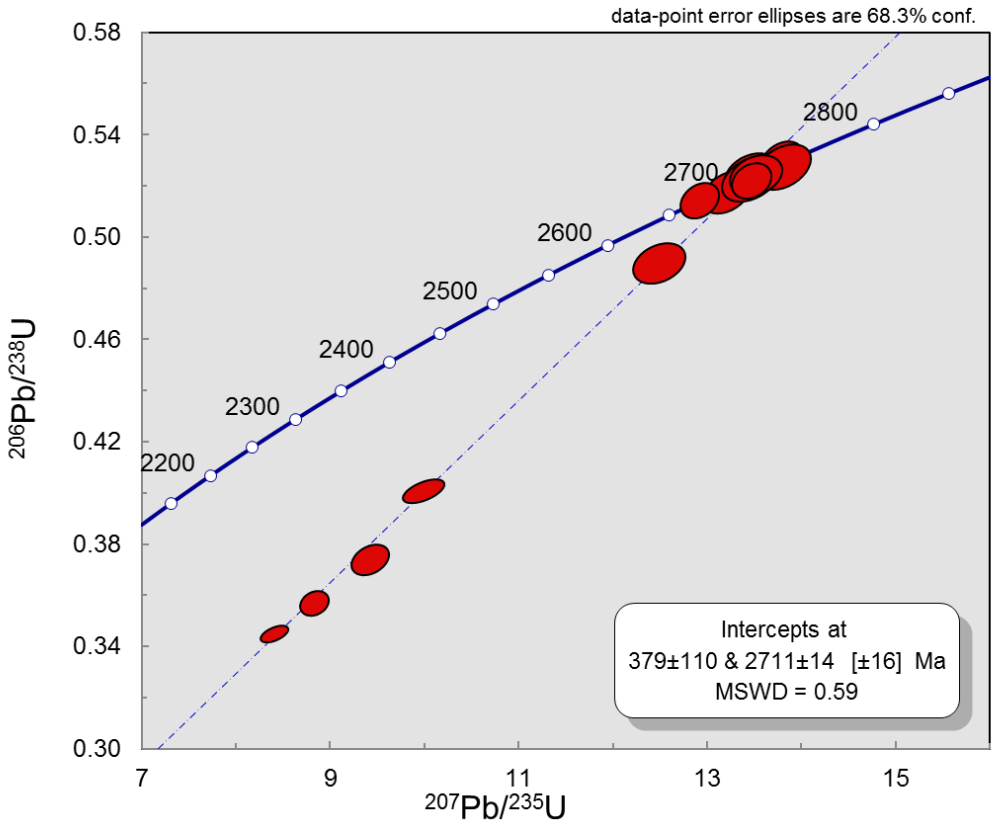



Figure 5.1.5. U-Pb age of zircons from the sample ZP-10-04, Zapolyarnaya pipe, Markha terrane.

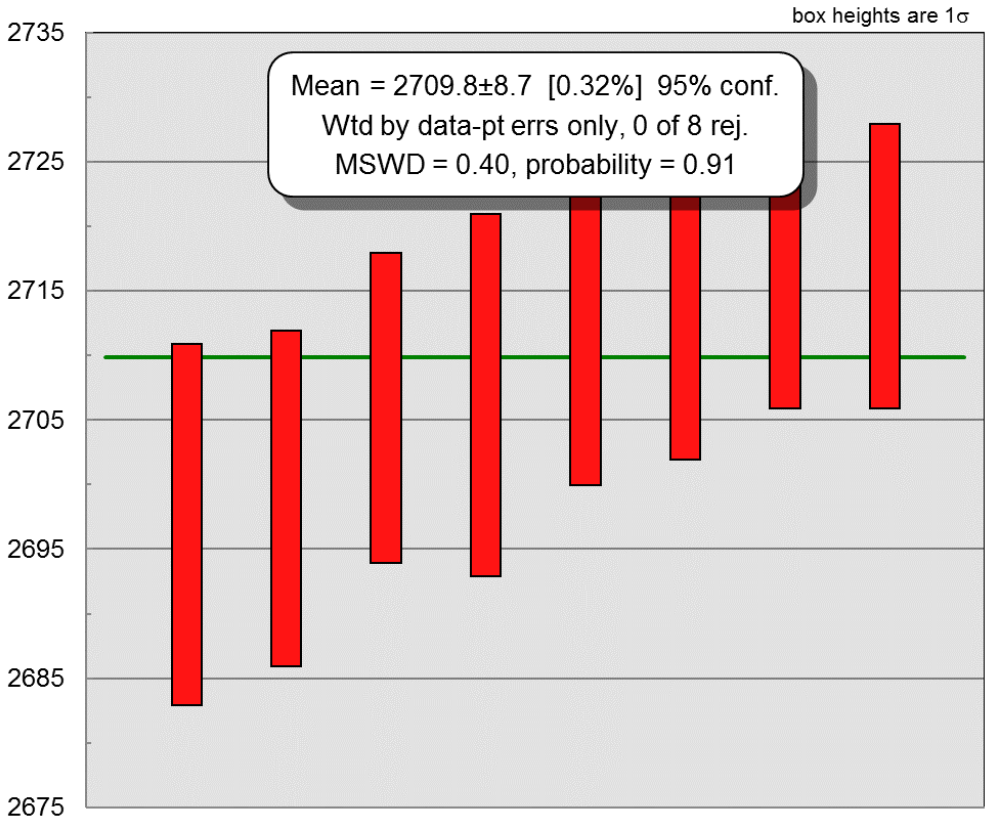



Figure 5.1.6. The weighted mean age of the oldest zircons, sample ZP-10-04, Zapolyarnaya pipe.

Table 5.1.2. A summary of U-Pb ages of zircons from xenoliths from the Zapolyarnaya kimberlite pipe

| Sample number (number of analyses) | Youngest age obtained | Oldest age obtained | Main peak mean age | Secondary peaks mean ages |
|---|---|---|---|---|
| **ZP-10-04 (15)** | n/a | 2717±11 | 2709.8±8.7 (8) | n/a |
| **ZP-11-04 (13)** | n/a | 2728±18 | 2713.3±3.9 | n/a |
| **ZP-16-04 (25)** | 1838±60 | 3200±36 | 1935±16 (8) | 3174±16 (6)<br>1864±28 (4) |
| **ZP-201-04 (10)** | n/a | 2726±18 | n/a | 2713±6.8 (3) |

Sample ZP-11-04 represents garnet-biotite gneiss (Grt+Bt+Cpx+Hbl+Pl±Qtz), and includes 21 zircon grains. Eight grains are highly discordant and rejected. Seven oldest grains consist of a population with the concordia age of 2713.3±3.9 Ma (MSWD = 0.062, probability = 0.80, Fig. 5.1.7). Other grains are lying on the regression line with the upper intercept at 2712±13 Ma and the lower intercept at 492±33 Ma (MSWD = 1.02, Fig. 5.1.8).

Sample ZP-16-04 contains 25 zircons, all analyses have discordance less than 15%. The probability plot represents range of ages from 1838 to 3200 Ma with two main age peaks (Fig. 5.1.9): the youngest group has a weighted mean age of 1935±16 Ma (MSWD = 0.19, probability = 0.99; Fig. 5.1.10) and the oldest population reveals age of 3174±16 Ma (MSWD = 3174±16, probability = 0.47; Fig. 5.1.11).

Eleven zircons were dated from the sample ZP-201-04, one of them was rejected due to discordance over 20%. Ten grains are falling along the regression line with the upper intercept age of 2687±16 Ma and lower intercept at 275±98 (MSWD=0.90, Fig. 5.1.12). Three oldest grains are concordant and give the concordia age of 2713±6.8 Ma (MSWD = 0.014, probability = 0.91; Fig. 5.1.13).

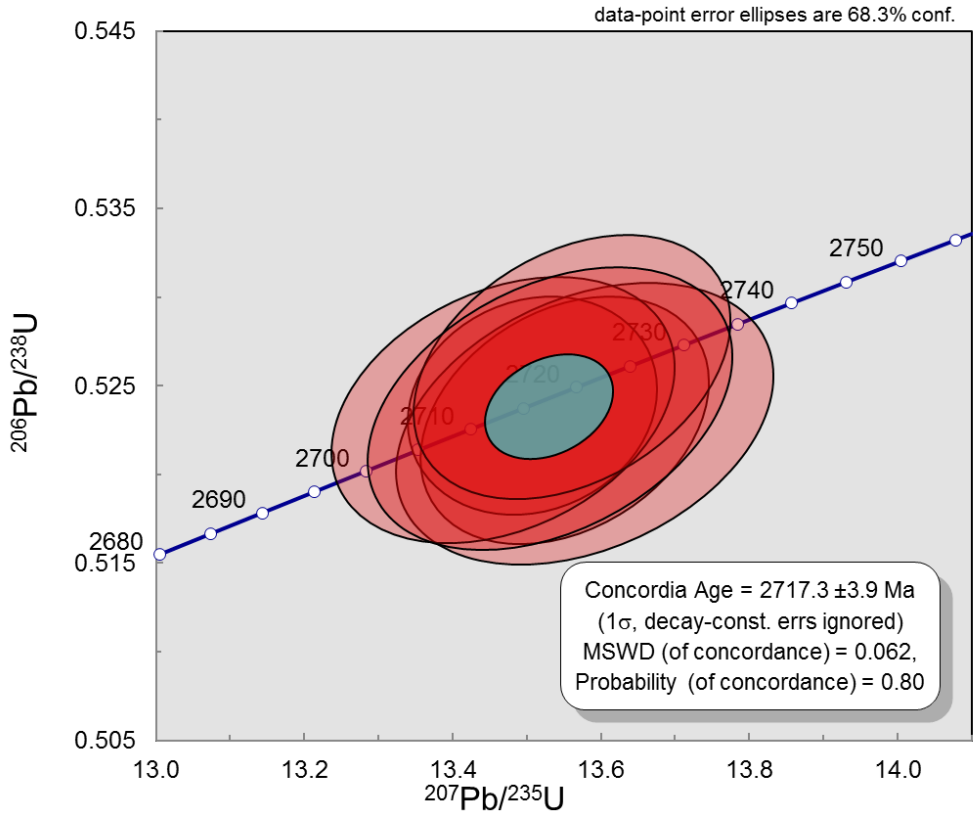



Figure 5.1.7. Concordia age for oldest zircons from the sample ZP-11-04, Zapolyarnaya pipe.

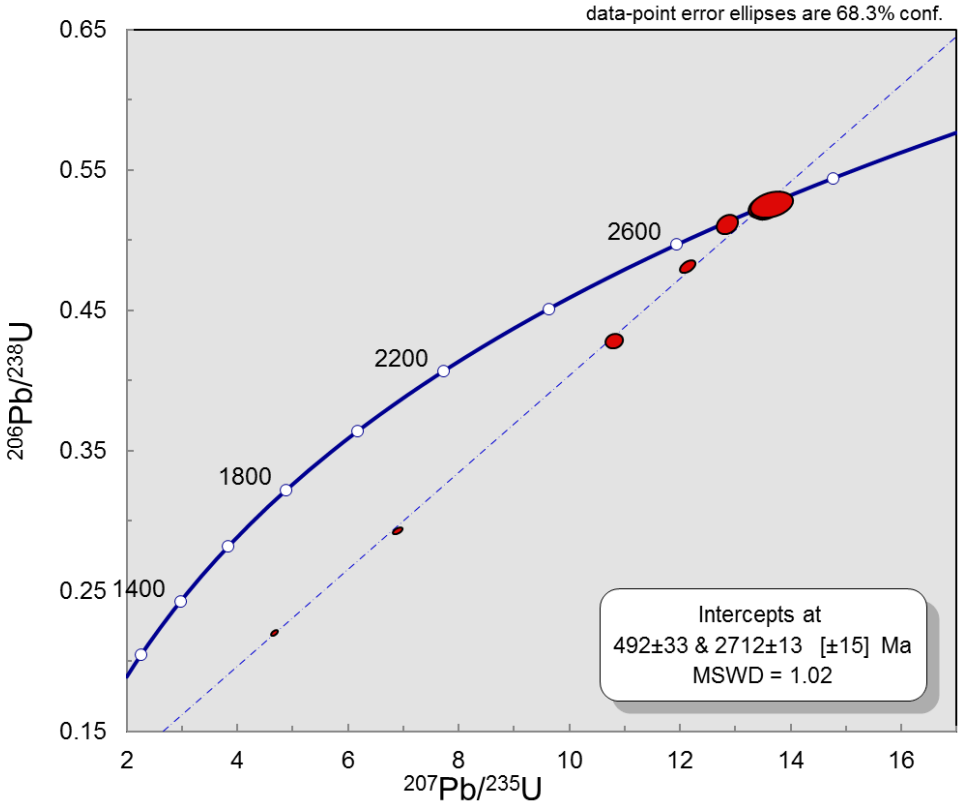



Figure 5.1.8. U-Pb concordia for zircons from the sample ZP-11-04, Zapolyarnaya pipe.

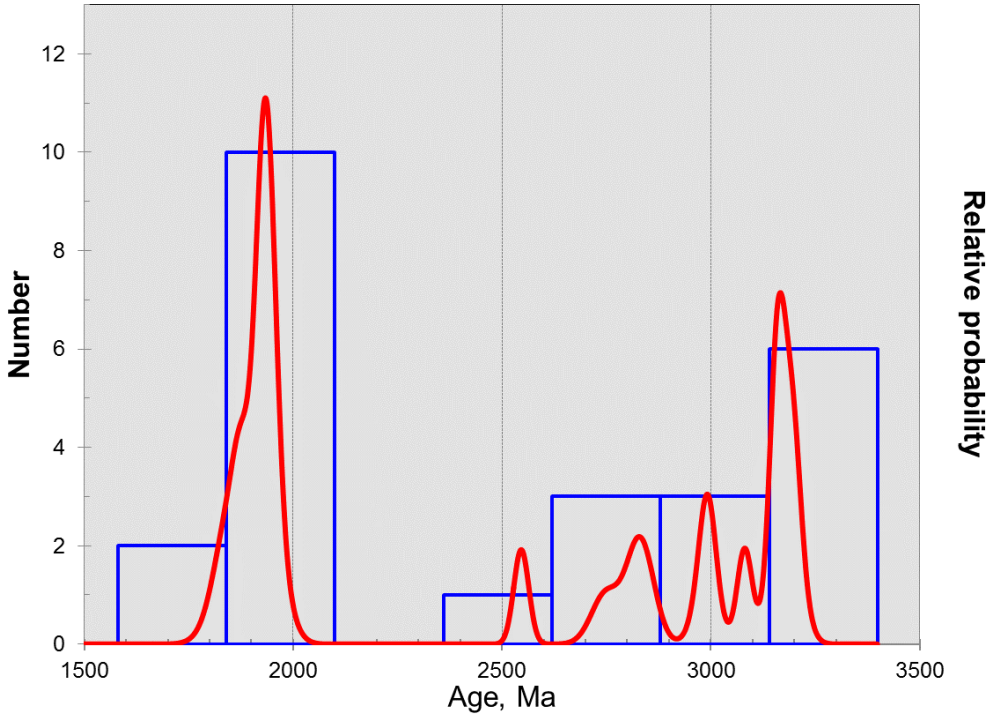



Figure 5.1.9. Probability plot of zircon U-Pb ages, sample ZP-16-04, Zapolyarnaya pipe.

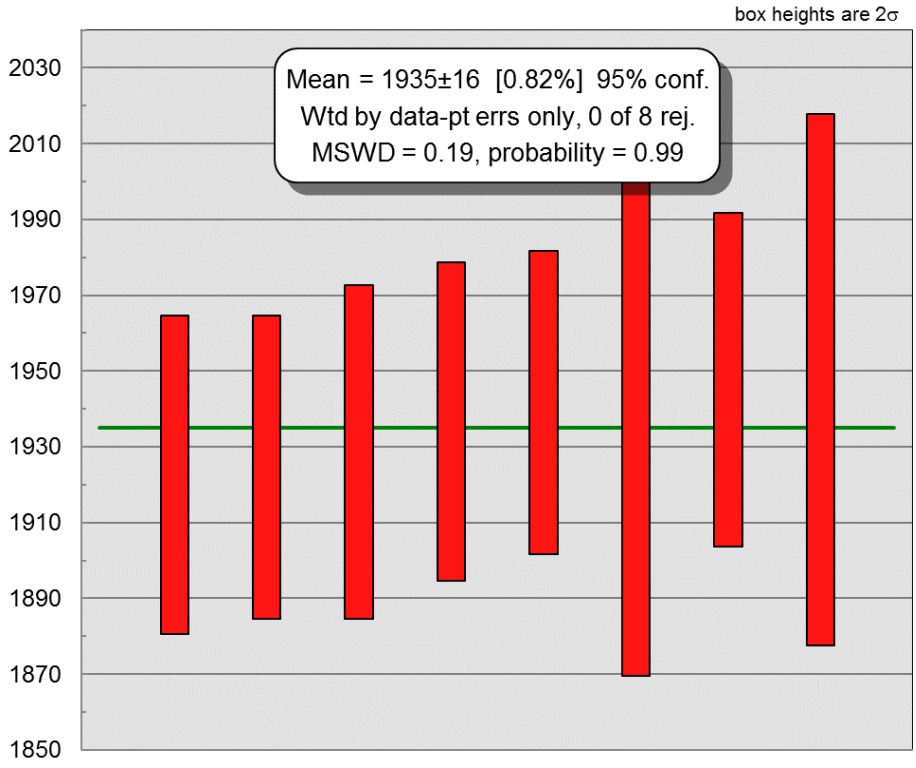



Figure. 5.1.10. The weighted mean age of the main population from the sample ZP-16-04, Zapolyarnaya pipe.

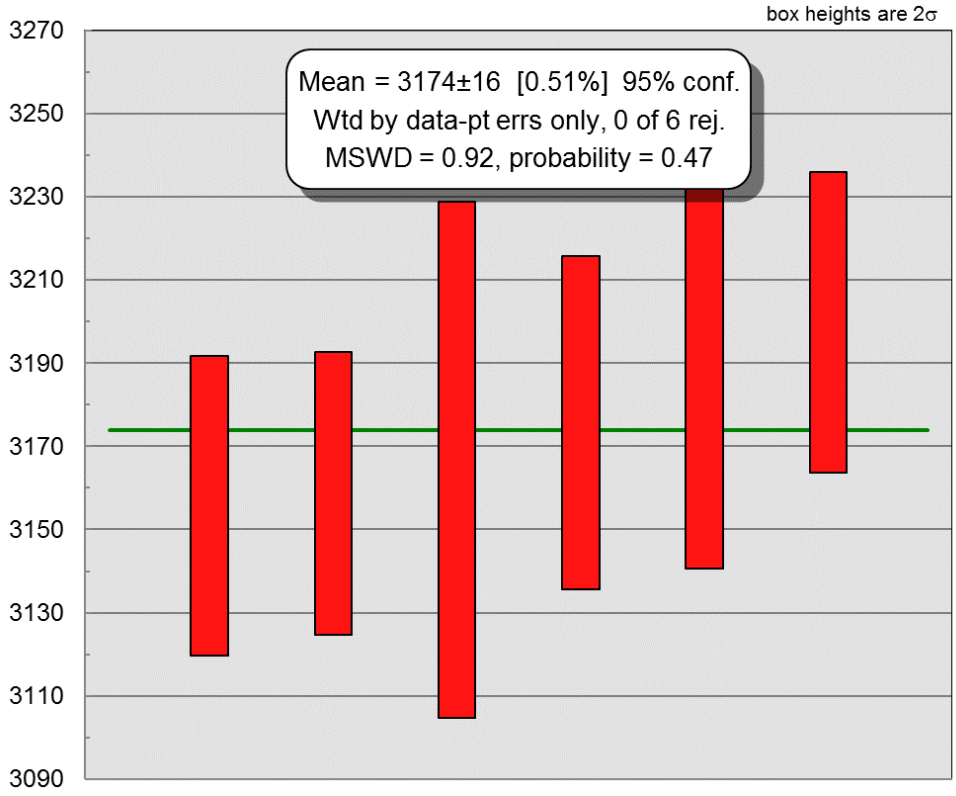



Figure 5.1.11. The weighted mean age of the second main population, sample ZP-16-04, Zapolyarnaya pipe.

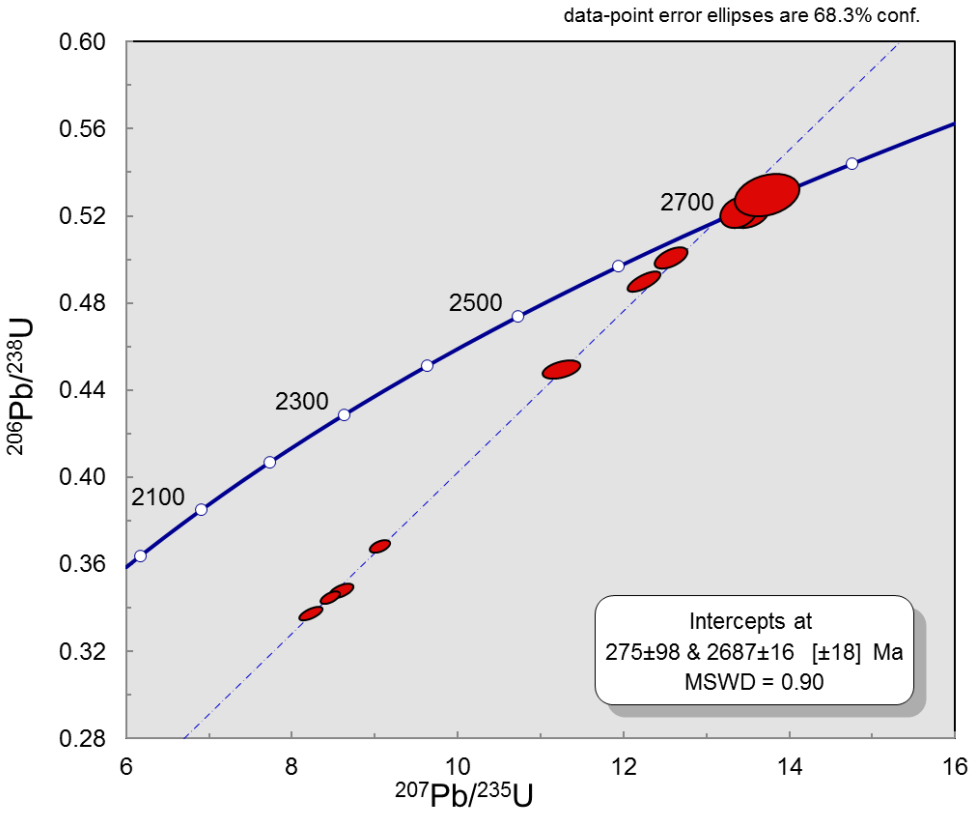



Figure 5.1.12. U-Pb concordia for zircons from the sample ZP-201-04, Zapolyarnaya pipe.

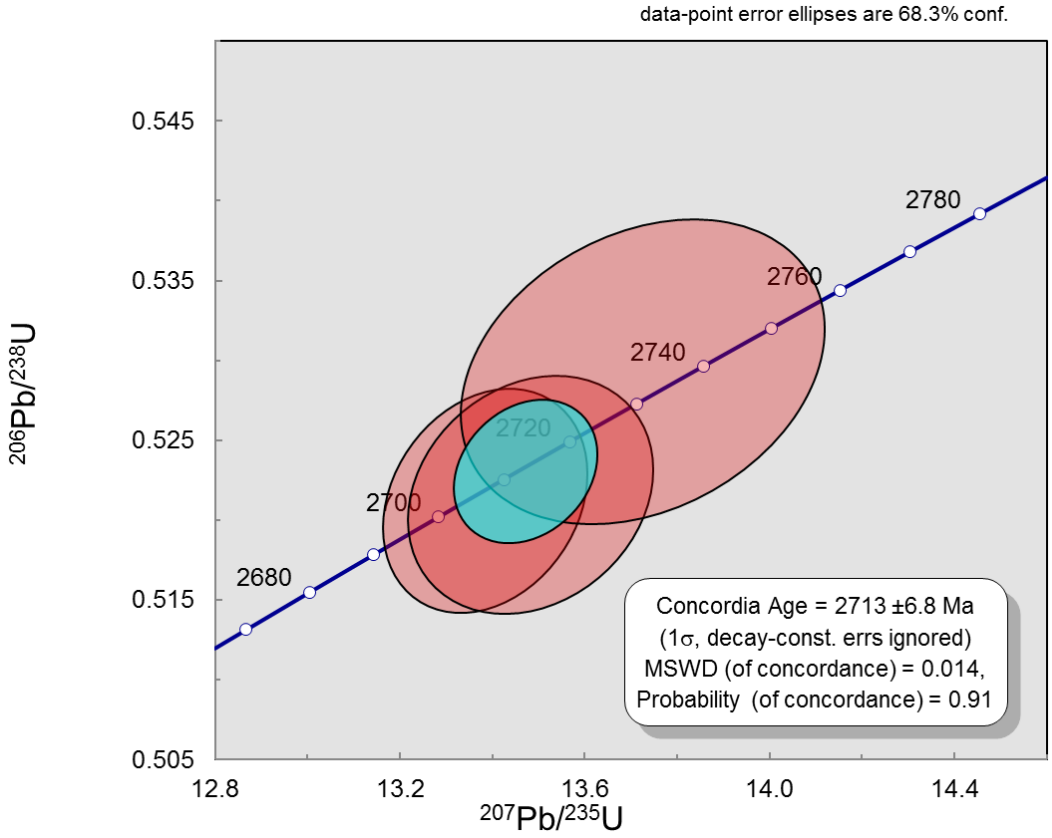


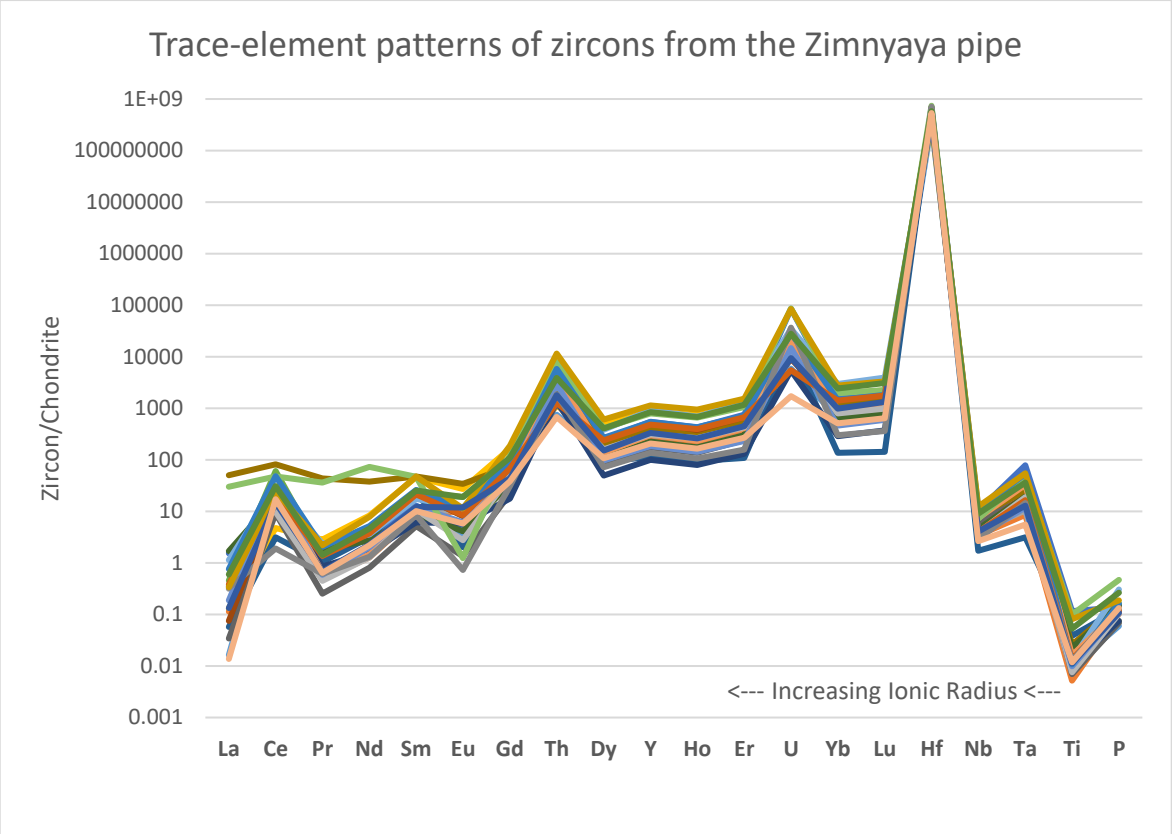

Figure 5.1.13. U-Pb age of oldest zircons from the sample ZP-201-04, Zapolyarnaya pipe.

***Zircon trace-element data***

**The Zimnyaya pipe**

Trace-element composition has been analysed for 26 zircon grains from the Zimnyaya pipe (Appendix 3.2). Majority of analysed grains have similar trace-element patterns (Fig. 5.1.14), however they show significant variations in concentration of most of elements. Chondrite-normalized rare-earth element plot reveals typical zircon patterns with enrichment in HREE and depletion in LREE (Fig. 5.1.14). Most of zircons show distinguished negative Eu anomaly indicating plagioclase crystallization prior to zircons. Ce-maxima well-defined for the majority of zircons is usually related to the high oxidation state of the parental melt. Two outstanding grains (8008-11C and 8008-27) have flatter REE patterns, without significant Ce anomaly and only one of them has well-pronounced Eu minima.

The total contents of the REE range from 142 to 1622 ppm; higher concentrations are common for zircons younger than 500 Ma, while old ones rarely reach 600-800 ppm (Fig. 5.1.15). Y concentrations vary from 226 to 2568 ppm; U and Th also change significantly – from 17 to 860 and from 27 to 460 ppm correspondingly. Th/U ratio varies from 0.2 to 1.5; the values of Nb/Ta ratio are within the 1.65 – 6.82 interval.



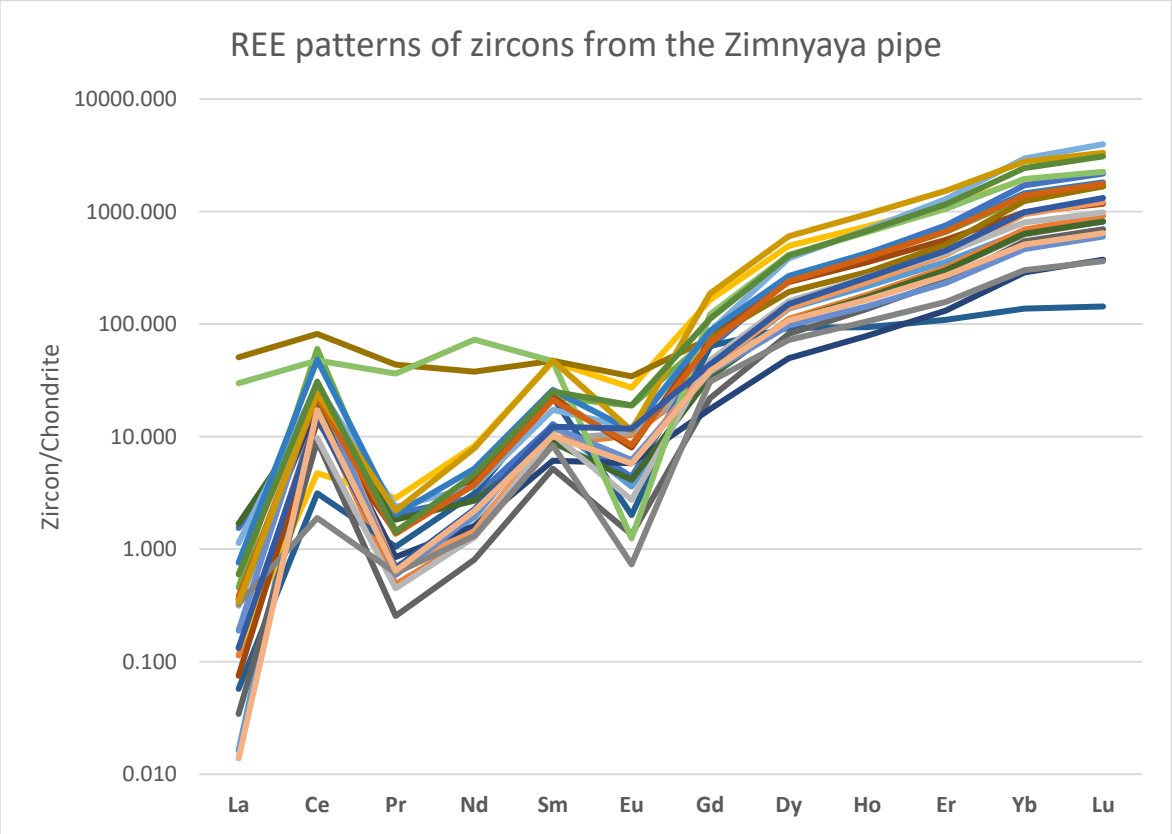




Figure 5.1.14. Trace-element and rare-earth element patterns of zircons from the Zimnyaya pipe.

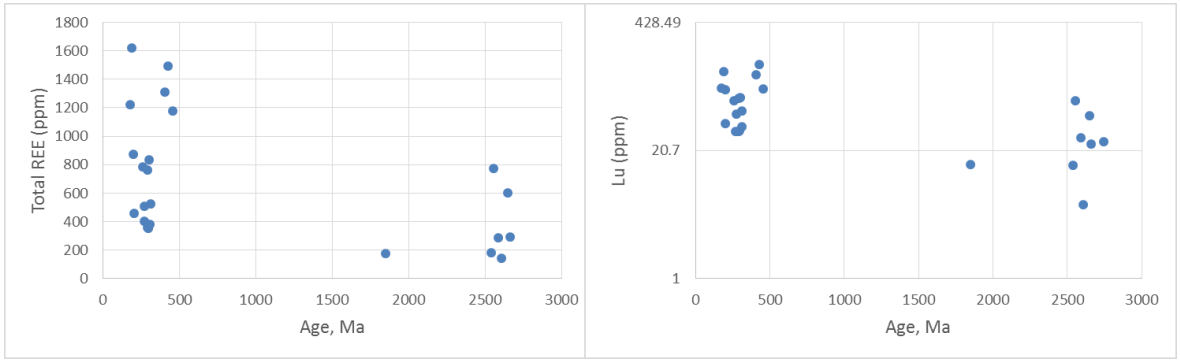



Figure 5.1.15. Total REE and U contents *vs* U-Pb age for zircons from the Zimnyaya pipe.

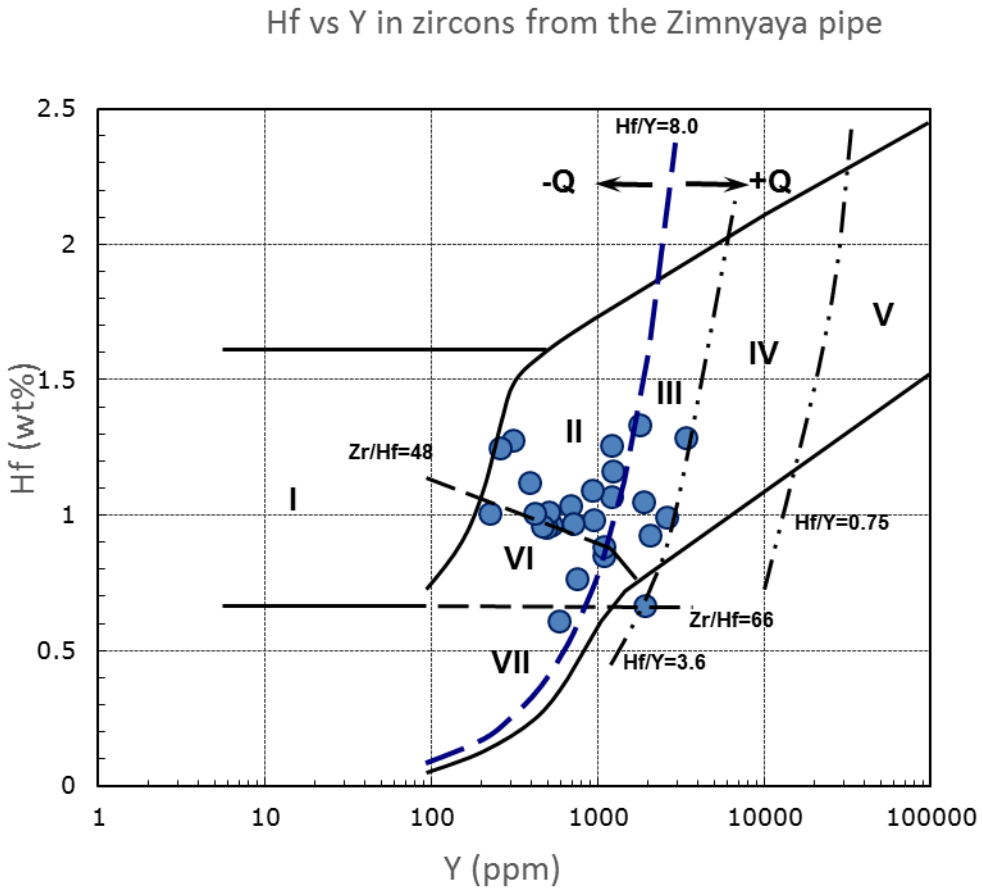
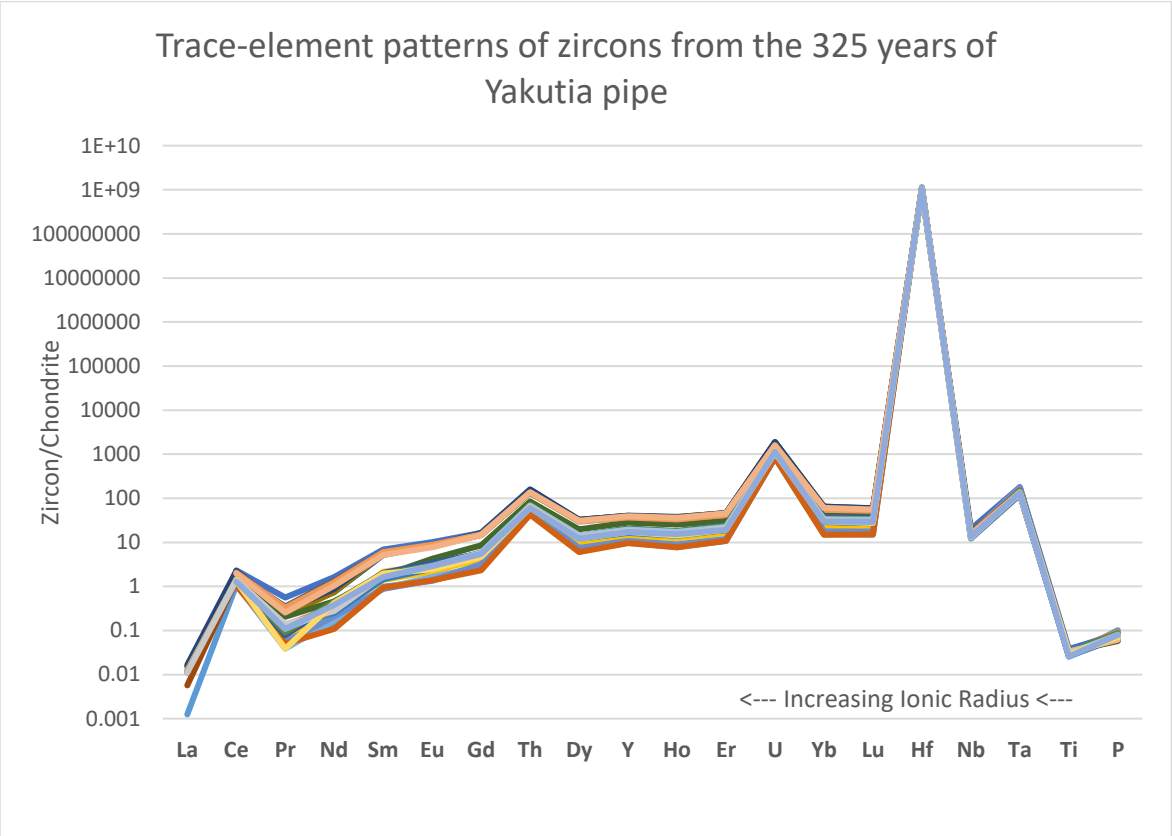



Figure 5.1.16. Y *vs* Yb/Sm discrimination diagram for zircons from the Zimnyaya pipe.

According to the CART classification (Belousova *et al.*, 2002), two grains have trace-element composition similar to zircons from carbonatites (low Lu and U, Y>170 ppm) while all others show signatures typical of zircons crystallised from mafic to felsic melt (Fig. 5.1.16).

**The 325 years of Yakutia pipe**



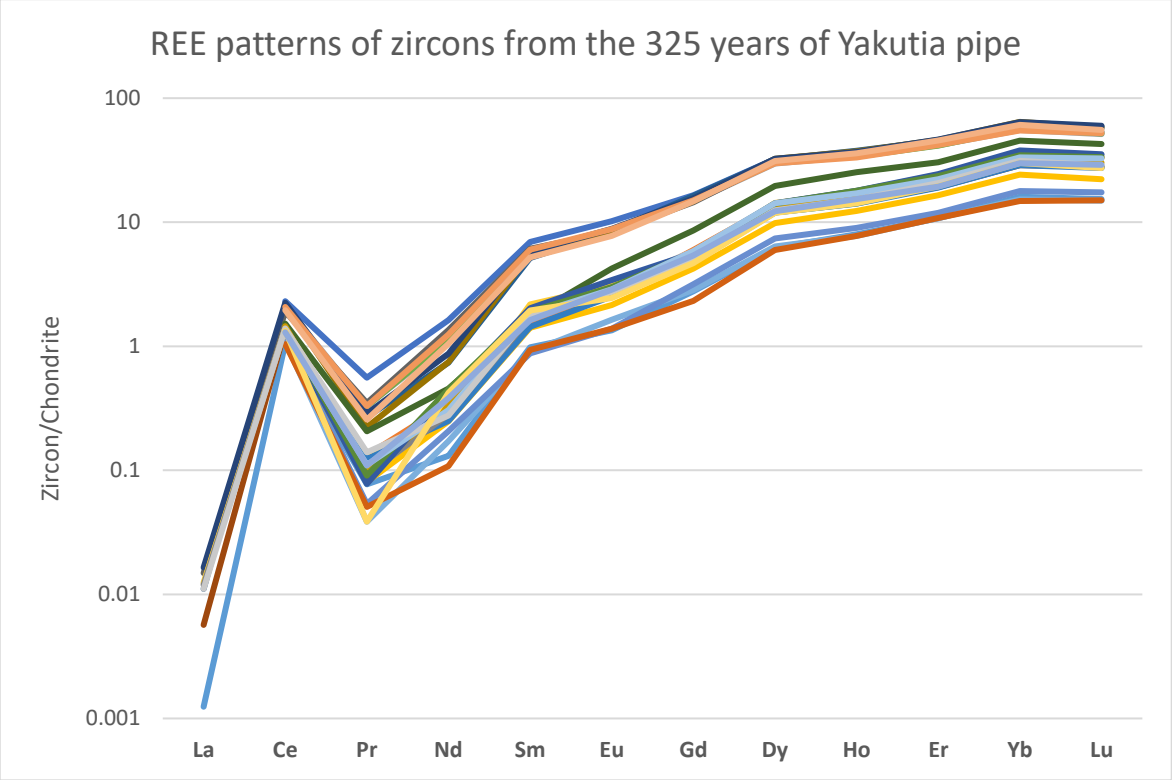




Figure 5.1.17. Trace-element and rare-earth element patterns of zircons from the 325 years of Yakutia pipe.

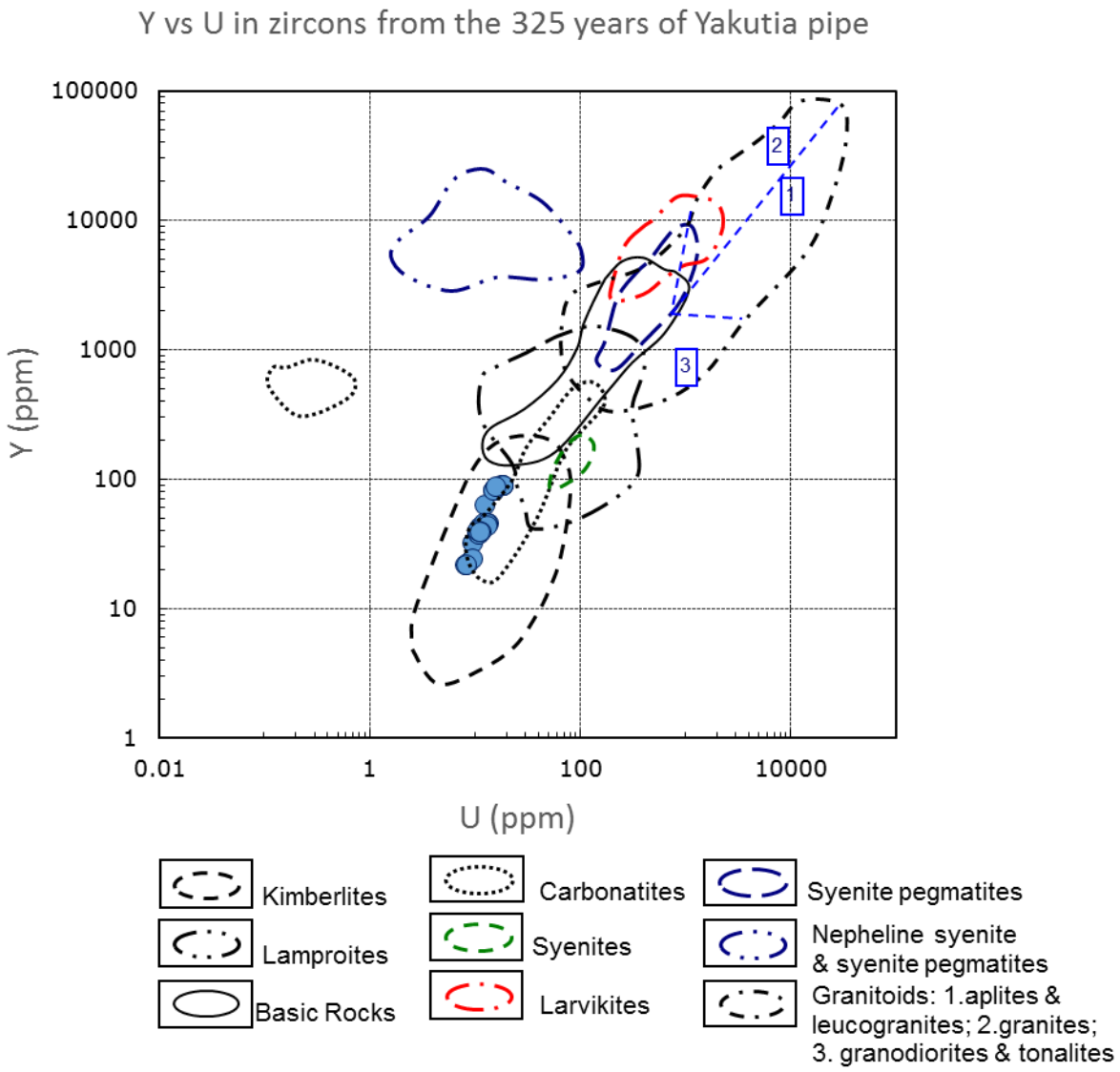



Figure 5.1.18. Y *vs* U discrimination diagram for zircons from the 325 years of Yakutia pipe.

The whole set of zircon grains collected from the pipe was analysed for their trace-element composition. All grains show comparable trace-element distribution patterns (Fig. 5.1.17) and relatively low concentrations of most elements. The REE patterns of all analysed zircons look similar (Fig. 5.1.15), showing depletion in LREE and enrichment in HREE typical for zircons. There is no Eu-minima, however positive Ce-anomaly is well developed.

Total concentrations of the rare-earth elements are low in all analysed grains and range from 12 to 55 ppm. Yttrium, Th and U contents are also low, raise only up to first (Th) or tens ppm (Y and U). Similar to element concentration behaviour, Th/U and Nb/Ta ratios show almost no variations: Th/U values from 0.2 to 0.36, Nb/Ta – from 1.08 to 1.46.

Low concentrations of Lu, U and Y together with depletion in REE content are common signature of kimberlitic zircons (Belousova et al., 2002). Application of the statistical CART

classification indicates that trace-element composition of all analysed zircons from this pipe are typical of grains from kimberlitic rocks worldwide (Fig. 5.1.18). This is also in a good agreement with obtained U-Pb age of those zircons (358±2 Ma), which is close to the age of pipe determined previously (342-365 Ma) (Zaitsev & Smelov, 2010) .

***Oxygen isotope data***

**The Zimnyaya pipe**

Oxygen isotopic composition was analysed in 31 zircons from different age groups. $\delta^{18}O$ ranges significantly from 2.84±0.24 to 7.87±0.24‰. The younger zircons have the widest range of $\delta^{18}O$, while the older ones differ within the interval 4.85 – 7.73‰ (Fig. 5.1.19). Mantle values of $\delta^{18}O$ (5.3±0.6‰, (Valley *et al.*, 2003)) (within the analytical uncertainty) were obtained for grains from both young and old age groups; however, mantle oxygen composition is more common for older zircons. At the same time, supracrustal oxygen composition ($\delta^{18}O$ > 6.6‰) is more typical of young zircons, there is only a single grain from the old population revealing this isotopic signature (Fig. 5.1.19). The values below 5‰ observed for a few grains of the younger age population are considered to represent the input of meteoric water, usually due to hydrothermal alteration of the rock or its protolith (Bindeman & Valley, 2001, Valley *et al.*, 2003).

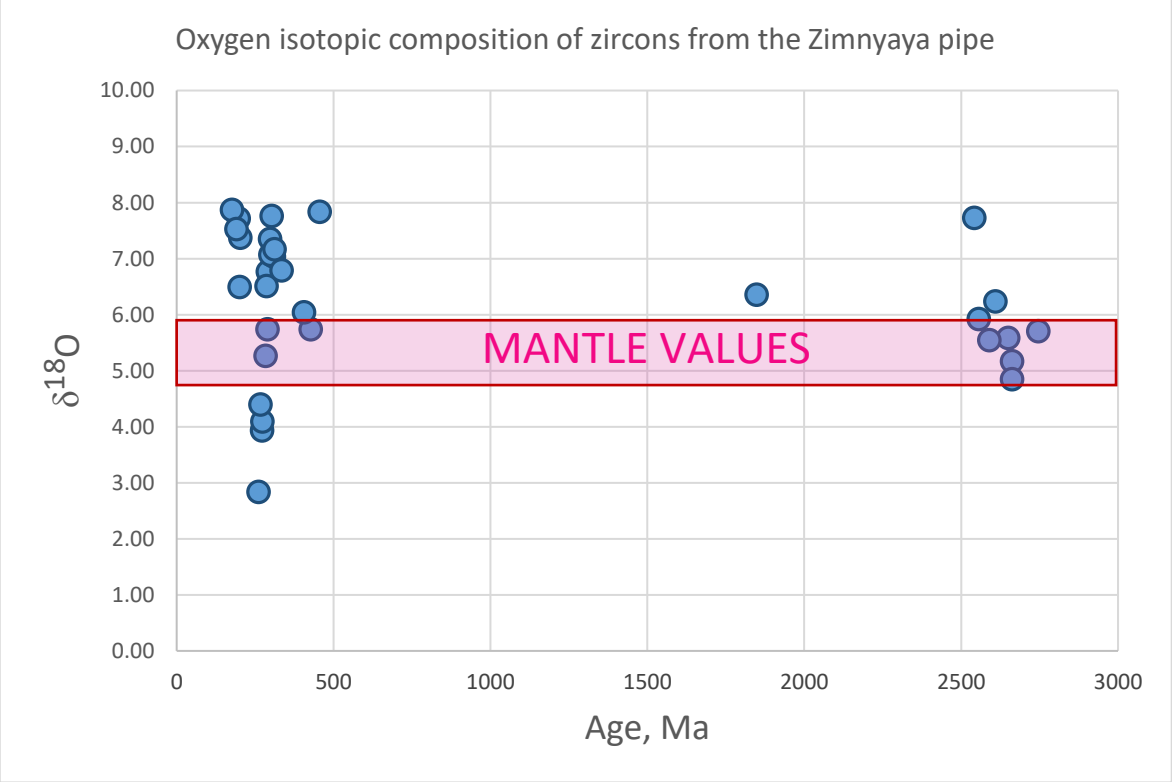



Figure 5.1.19. $\delta^{18}O$ *vs* U-Pb age for zircons from the Zimnyaya pipe.

***Hafnium-isotope data***

**The Zimnyaya pipe**

Lu-Hf isotopes have been studied in thirty zircon grains from the Zimnyaya pipe. All grains were dated prior to analysing for the Hf-isotope systematics.

The ranges of calculated initial $^{176}Hf/^{177}Hf$ ratios, εHf values and model ages vary significantly for zircons of different age groups (Table 5.1.3, Fig. 5.1.20). Thus, for youngest zircons (176 - 311 Ma) initial Hf ratios differ in the interval 0.281933 – 0.283120, εHf ranges from -24.1 up to +18.5 and calculated crustal model ages are as old as 2.59 Ga.

The group of 405-455 Ma zircons shows significantly less variations in Hf-isotope data: initial Hf values are within the range of 0.282610 – 0.283163 and εHf varies from +3.3 to +22.

The Archean zircons (2.54 – 2.74 Ga) reveal the narrow interval of the initial Hf, εHf values and crustal model ages: 0.280920 – 0.281115, -7.2 to +1.4 and +3.01 to +3.49 accordingly.

A single grain that shows a significant difference in U-Pb age between core and rim (2649 *vs* 1848 Ma) has similar initial Hf-isotope ratios in both domains (core 0.280934, rim 0.281031). This finding indicates that younger age of the rim is most likely due to Pb-loss process caused by thermal event at ca 1.85 Ga.

Table. 5.1.3. A summary table of Hf-isotope data for zircons from the Zimnyaya pipe

| Age group | Range of U-Pb ages, Ma (n = number of grains) | Initial Hf values | εHf values | $T_{(DM)}^{C}$ range, Ga |
|---|---|---|---|---|
| **Group 1** | 176 – 311 (n = 19) | 0.281933 – 0.283120 | -24.1 – +10.3 | Up to 2.59 |
| **Group 2** | 405 - 455 (n = 2) | 0.282610 – 0.283163 | +3.3 - +8.5 | Up to 1.13 |
| **Group 3** | 2541 - 2745 (n = 7) | 0.280920 - 0.281115 | -7.2 - +1.4 | 3.04 – 3.49 |

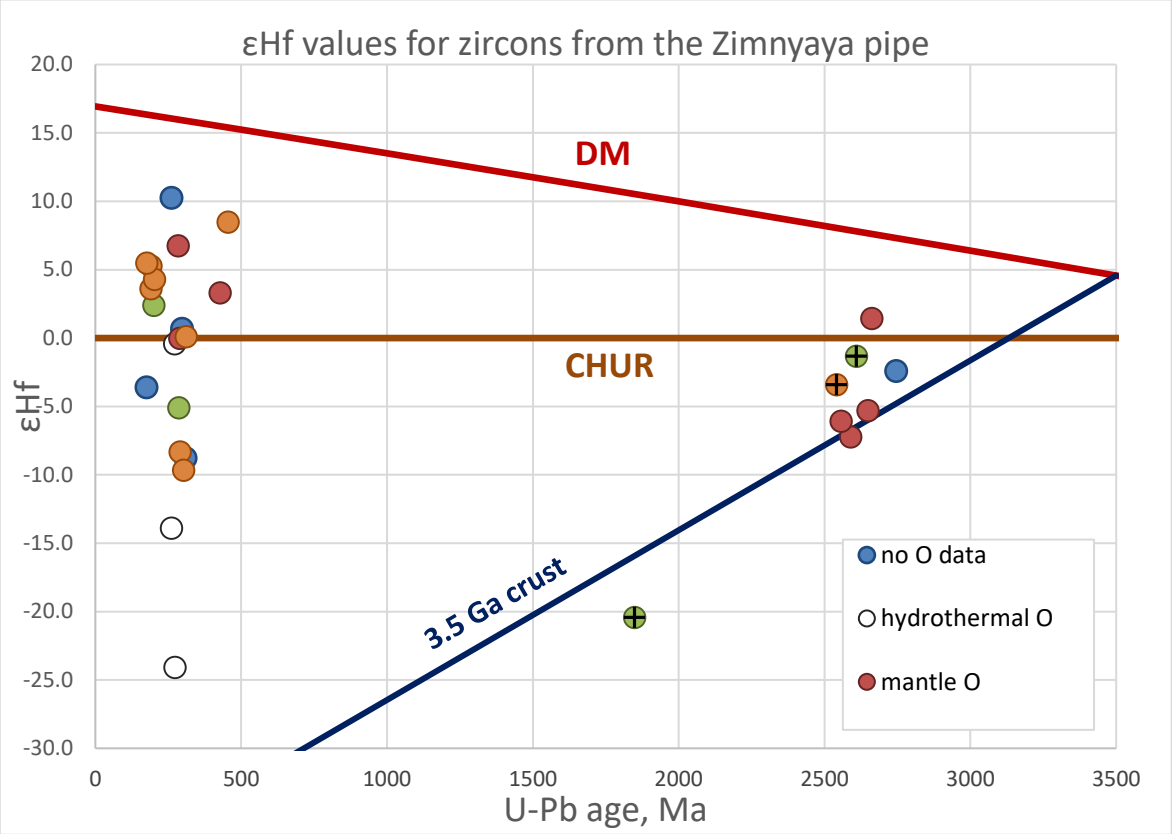



Figure 5.1.20. εHf *vs* U-Pb age plot for zircons from the Zimnyaya pipe. The data points are color-coded according to the zircon O-isotope composition (where these data are available). Grains with trace-element (TE) composition typical of mantle-derived zircons are also shown with black crosses. The reference line is shown for evolution of the average continental crust.

**The 325 years of Yakutia pipe**

Nineteen zircons from the pipe were analysed for their Hf composition. All grains have close values of εHf (2.3 – 4.1), initial Hf ratios (0.282628 – 0.282672) and model ages ($T_{DM}$ from 0.8 to 0.86 Ga and $T_{DM}^{C}$ from 1.09 to 1.19 Ga) (Fig. 5.1.21).

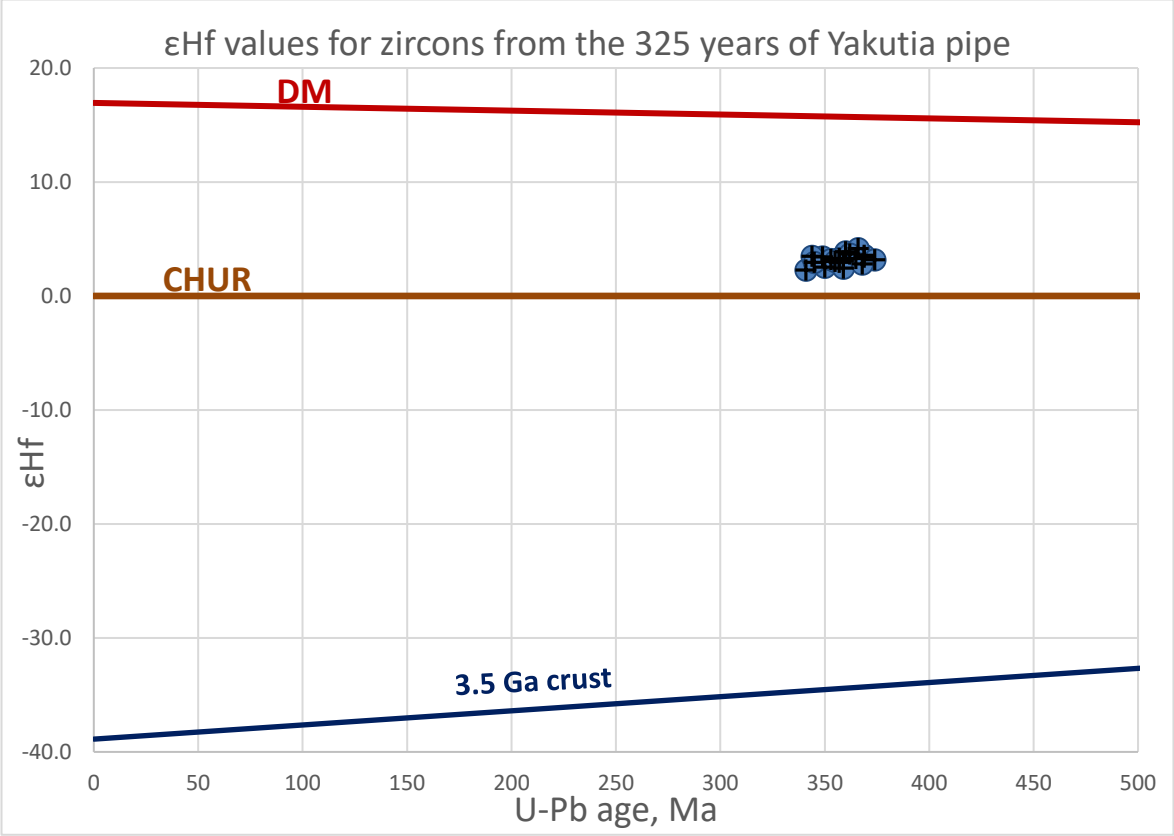



Figure 5.1.21. εHf *vs* U-Pb age plot for zircons from the 325 years of Yakutia pipe. Grains with trace-element (TE) composition typical of mantle-derived zircons are shown with black crosses. The reference line is shown for evolution of the average continental crust.

**The Zapolyarnaya pipe**

Lu-Hf isotopic composition was studied in zircons from all 4 xenoliths. Samples ZP-10-04, ZP-11-04 and ZP-16-04 show comparable isotopic signatures, while sample ZP-201-04 is different in Hf isotopic composition (Table 5.1.4, Fig. 5.1.22).

Sample ZP-16-04 shows two distinctive groups in terms of Hf-isotope composition: younger zircons (1838 – 1948 Ma) have lower εHf values (-15.8 to -31.3), while εHf within the older population (2546 – 3200 Ma) are closer to CHUR values (-16.2 to -3.1). Initial Hf for the young grains vary from 0.280675 to 0.281103 with the average value of 0.28099. The older zircons have average initial Hf of 0.280614 with a range of values 0.280531 – 0.280846. Calculated crustal model ages for both groups are overlapping: 3.59 – 4.54 Ga for younger and 3.76 – 4.26 Ga for older grains.

Samples ZP-10-04, ZP-11-04 and ZP-201-04 consist of a single age group and demonstrate far less variations in Hf isotopic composition. εHf for all grains ranges between -9.7 and +0.3; initial Hf ratios vary from 0.280862 to 0.281047 and crustal model ages fall into the 3.2 – 3.62 Ga interval.

Table. 5.1.4. A summary table of Hf-isotope data for zircons from the Zapolyarnaya pipe

| Sample number | Range of U-Pb ages, Ma (n = number of grains) | Initial Hf values | εHf values | $T_{(DM)}^{C}$ range, Ga |
|---|---|---|---|---|
| **ZP-10-04** | 2621-2740 (n = 15) | 0.28091 – 0.281047 | -6 – +0.3 | 3.2 – 3.54 |
| **ZP-11-04** | 2387 - 2728 (n = 6) | 0.280862 – 0.280983 | -9.7 - -2.9 | 3.39 – 3.6 |
| **ZP-201-04** | 2622 – 2721(n = 9) | 0.28088 - 0.281025 | -7.5 - -0.6 | 3.24 – 3.62 |
| **ZP-16-04 Young group** | 1838 - 1948 (n = 10) | 0.280675 - 0.281103 | -31.3 - -15.8 | 3.59 – 4.54 |
| **ZP-16-04 Old group** | 2546 – 3200 (n = 15) | 0.280531 - 0.280846 | -16.2 - -3.1 | 3.76 – 4.26 |

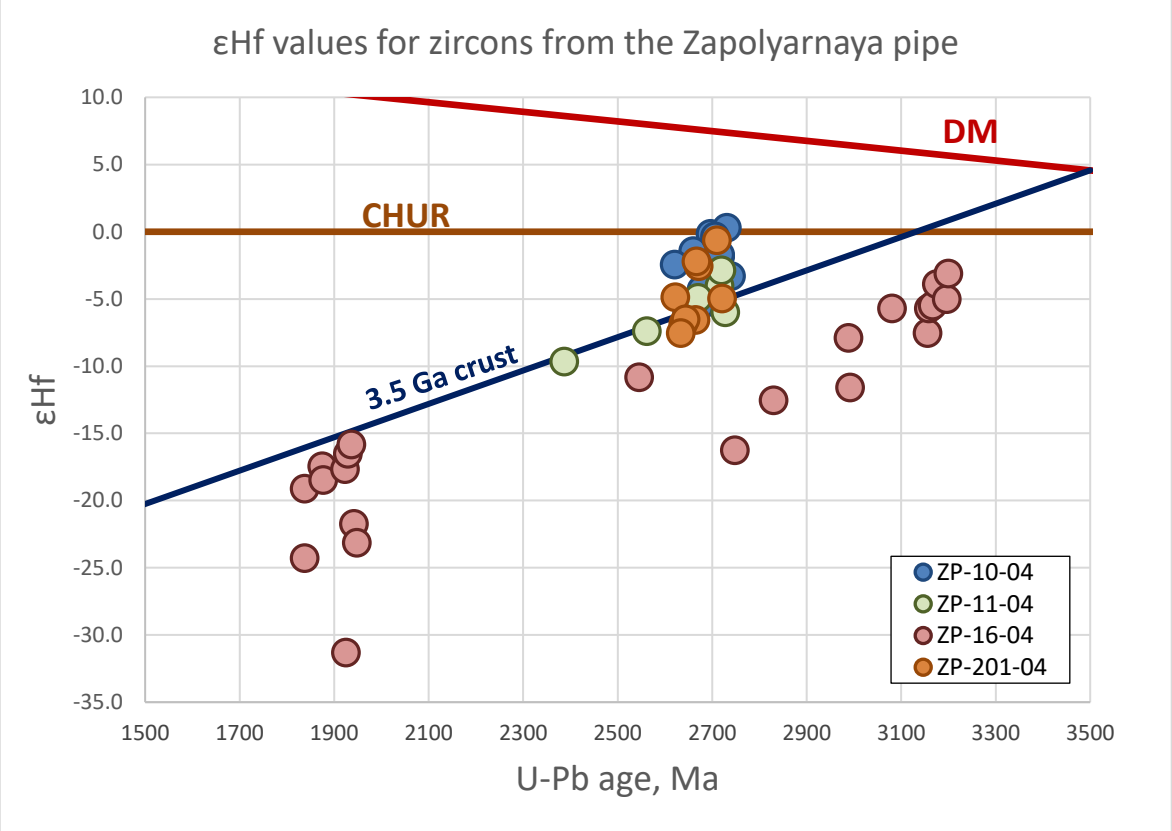



Figure 5.1.22. εHf *vs* U-Pb age plot for zircons from the Zapolyarnaya pipe. The reference line is shown for evolution of the average continental crust.

## 5.2. The Daldyn kimberlite field

The Daldyn kimberlite field is one of the most famous and economically important field within the Siberian Craton. It contains high-grade diamondiferous pipes such as Udachnaya, Zarnitsa, Popugaeva and others.

The field is situated between the Sytykan and Markha Rivers, within the Daldyn River basin. More than 80 kimberlitic bodies including pipes, dykes and veins have been found within the field. Kimberlites are intruded into the Early-Palaeozoic carbonate sequences, which are also hosting Triassic mafic dykes (Zaitsev & Smelov, 2010).

Sub-latitude faults and tectonic zones or their intersections with differently oriented tectonic structures (NW or near SN) commonly control the localization of kimberlite bodies. These bodies form chains or clusters with a general Northeast strike direction.

According to the geological observations, kimberlites are hosted by Late-Cambrian – Early-Ordovician rocks, with xenoliths of those found in Zarnitsa, Udachnaya and some other pipes. At the same time, the Early-Triassic mafic dyke cuts kimberlites of the Leningradskaya pipe. Thus, kimberlites should be formed in between the Middle Ordovician and Permian time (Brakhfogel, 1984).

Significant amount of various isotopic geochronological studies have been performed on samples from the Daldyn field. Rb-Sr, K-Ar and Ar-Ar techniques give wide intervals of ages for both whole rock and single minerals. Some of the reported ages (450-880 Ma) are much older than the observed geological/structural age of kimberlites. The most reliable results were obtained by U-Pb dating of perovskite and zircon, these ages fall into the narrow interval between 353 and 367 Ma (Zaitsev & Smelov, 2010).

### *Zircon U-Pb data*

The collection of zircon includes grains recovered from the heavy mineral concentrates of the crushed kimberlite rock and weathered crust of kimberlite of 5 pipes: Udachnaya Eastern, Popugaeva, Zarnitsa, Zagadochnaya and Kusova (Table 5.2.1). In addition, zircons were extracted from granulite xenoliths found in kimberlite of the Udachnaya pipe.

Table 5.2.1. U-Pb ages of zircons from heavy-mineral concentrates, Daldyn kimberlite field

| Pipe | Range of U-Pb ages, Ma (n = number of analyses) | Major age peak, Ma | Upper intercept, Ma | Lower intercept, Ma |
|---|---|---|---|---|
| **Udachnaya Eastern** | 1864 - 2643 (n = 10) | 2622±8.5* | 1776±57 | 2646±49 |
| **Zarnitsa** | 1860 - 2639 (n = 10) | 1973±26^ | 1938±40 | 2649±170 |
| **Popugaeva** | 1822 – 3317 (22) | 1934±5.4* | 3417±110 | 1940±39 |
| **Zagadochnaya** | 1834 – 2708 (37) | 1928±11^ | n/a | n/a |
| **Kusova** | 1851 – 2660 (47) | 1914±11^ | n/a | n/a |

***concordia age
^weighted mean age

**The Udachnaya Eastern pipe**

Only 7 zircons were collected from the heavy-mineral concentrate from this pipe. Three of them show distinct core-rim zoning, thus two U-Pb analyses were performed on each of these grains.

All analysed grains (or parts of grain) are lying on the regression line with upper intercept with concordia at 2646±49 and lower intercept at 1776±57 (Fig. 5.2.1). Three grains define a single age population with the concordia age of 2622±8.5 (MSWD = 1.1, probability = 0.29; Fig. 5.2.2). Two grains showing distinct core-rim zoning revealed difference in domain ages (1940±84 and 2367±56; 1864±74 and 2049±68) and one grain has ages of core and rim that are within the analytical uncertainty (Fig. 5.2.3).

**The Zarnitsa pipe**

Nine zircons from the Zarnitsa pipe were dated, all of them have discordance less than 10%. A single grain shows distinct core and rim, thus two analyses have been performed on this grain.

The ages obtained fall into a wide interval 1860-2639 Ma. The regression line crosses concordia at 2649±170 Ma and 1938±40 Ma (Fig. 5.2.4). Eight out of ten analyses form an age population with the weighted mean age of 1973±26 Ma (MSWD = 1.13, probability = 0.34, Fig. 5.2.5). The core and rim in the single grain have ages 1860±134 and 1954±60 Ma accordingly, which might be considered coeval assuming the analytical uncertainty.

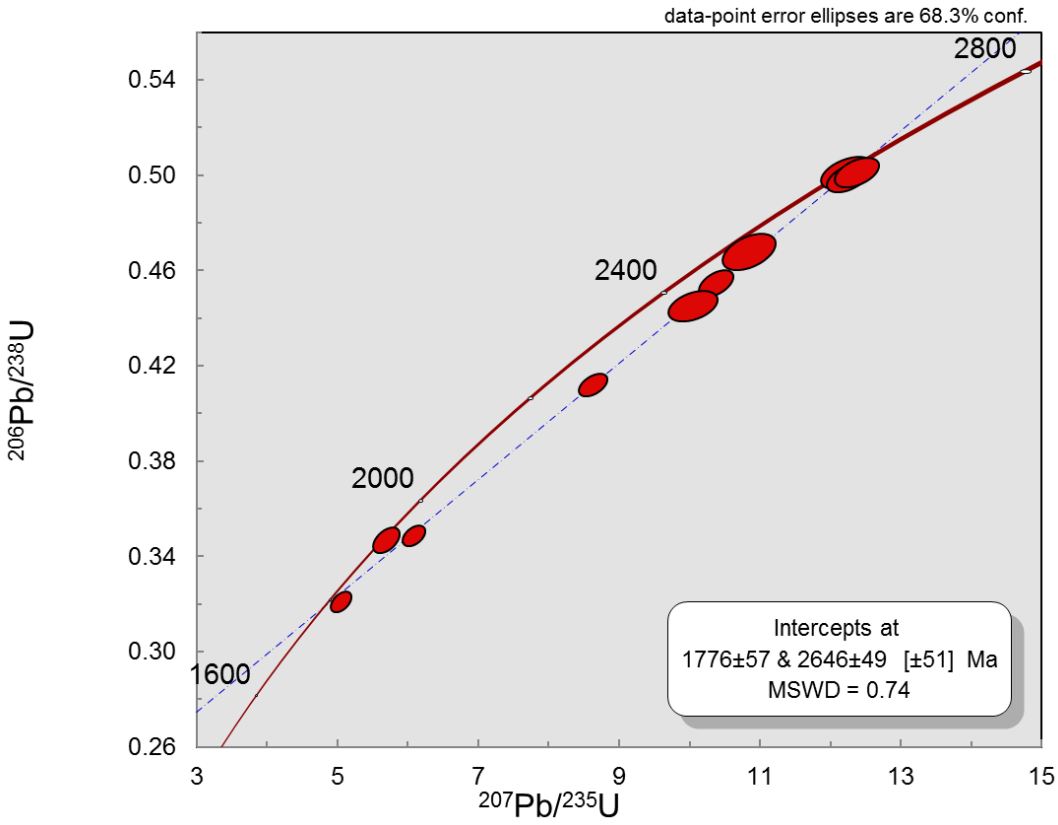



Figure 5.2.1. U-Pb concordia for zircons from the Udachnaya Eastern pipe.

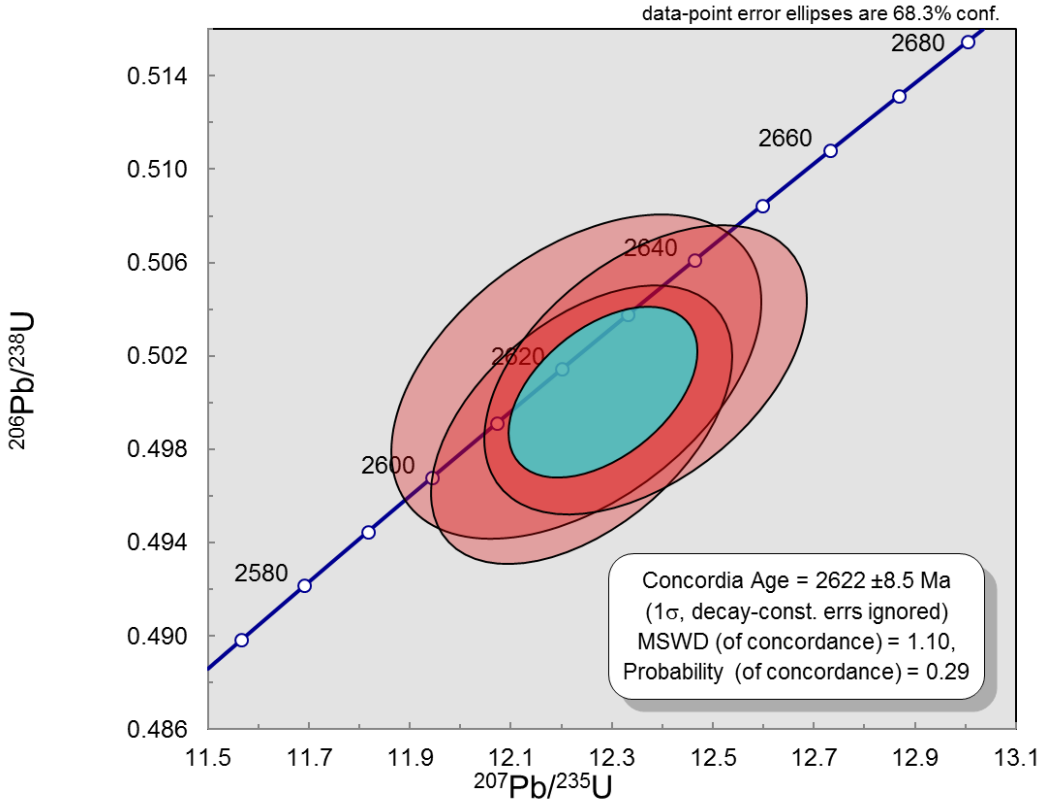



Figure 5.2.2. U-Pb age of oldest zircons from the Udachnaya Eastern pipe.

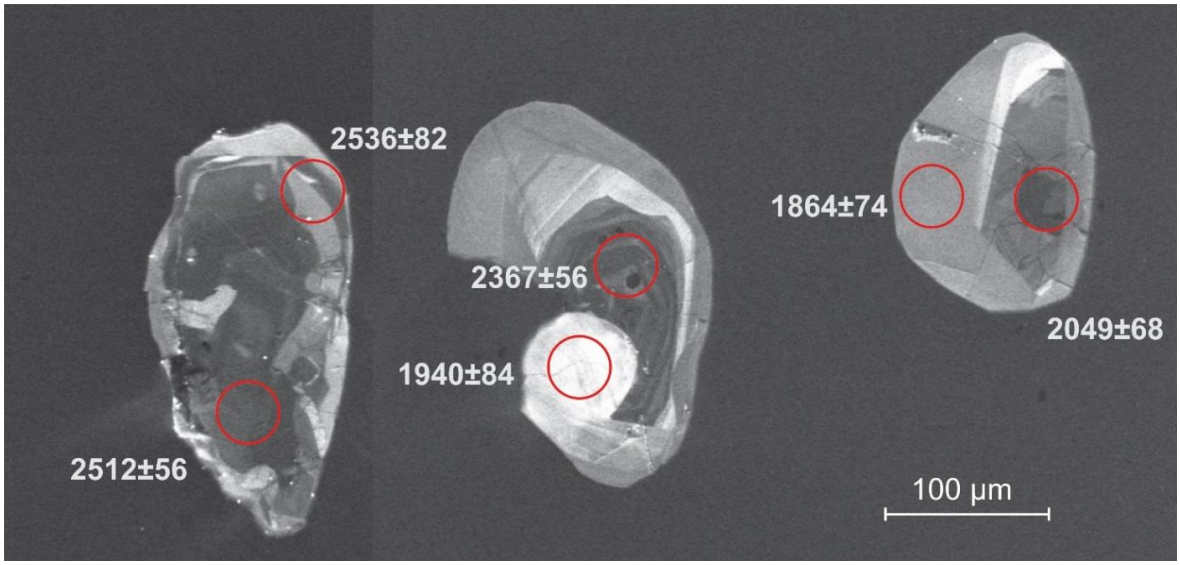



Figure 5.2.3. U-Pb ages for the different domains as revealed on CL images for zircon grains from the Udachnaya Eastern pipe.

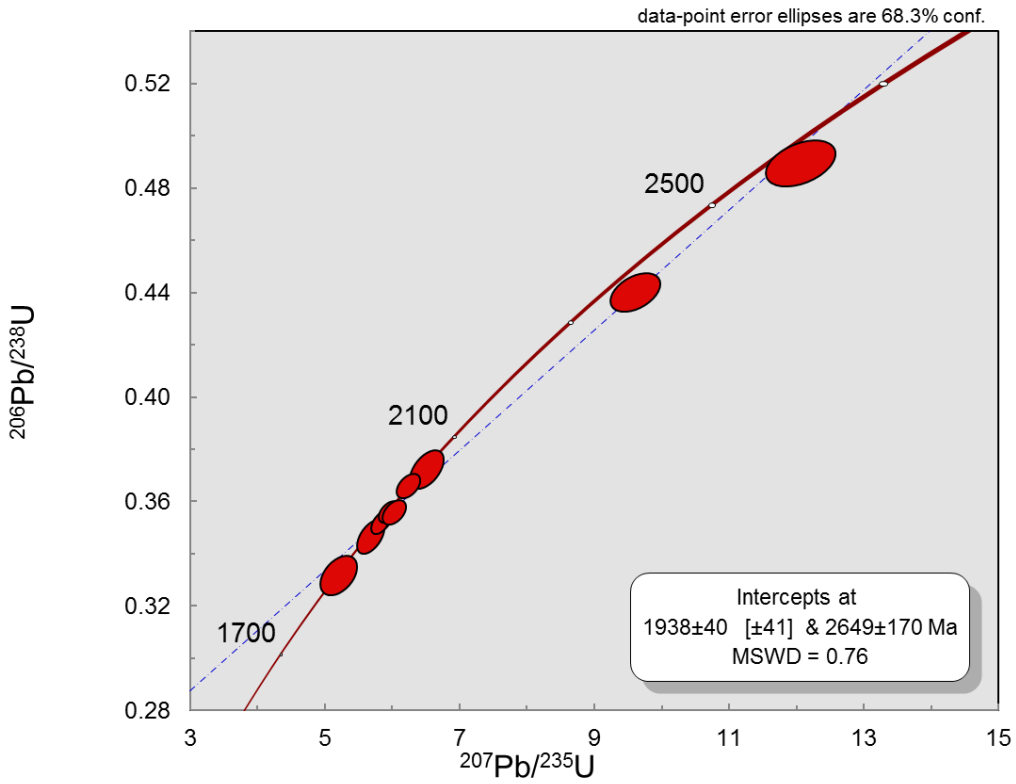



Figure 5.2.4. U-Pb concordia for zircons from the Zarnitsa pipe.

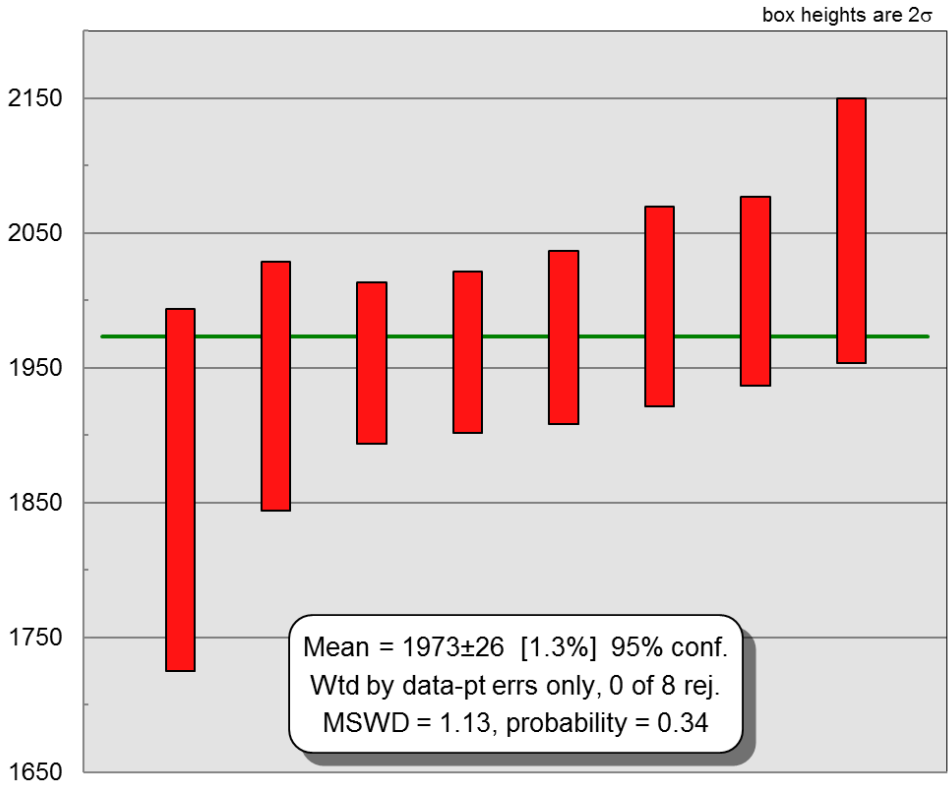



Figure 5.2.5. The weighted mean age of the main age population, Zarnitsa pipe.

**The Popugaeva pipe**

In total 19 zircon grains were picked out from the heavy-mineral concentrate of the Popugaeva pipe. All grains have discordance less than 20%. Cathodoluminescence imaging revealed inherited cores within three grains, thus 2 analyses have been performed on each of these grains.

Twenty-two U-Pb analyses give range of ages from 1822±108 to 3317±28 Ma (Fig. 5.2.6), with the concordia age of 1934±5.4 Ma (MSWD = 0.79, probability = 0.37; Fig. 5.2.7) for the main population.

One grain with a distinct core-rim structure yielded equal ages (within the analytical uncertainty) for both domains (1993±88 and 1942±90 Ma). Two other zircons reveal significant age difference between core and rim within the grain: 3317±28 and 2083±36 Ma; 2763±40 and 2359±56 Ma correspondingly (Fig. 5.2.8).

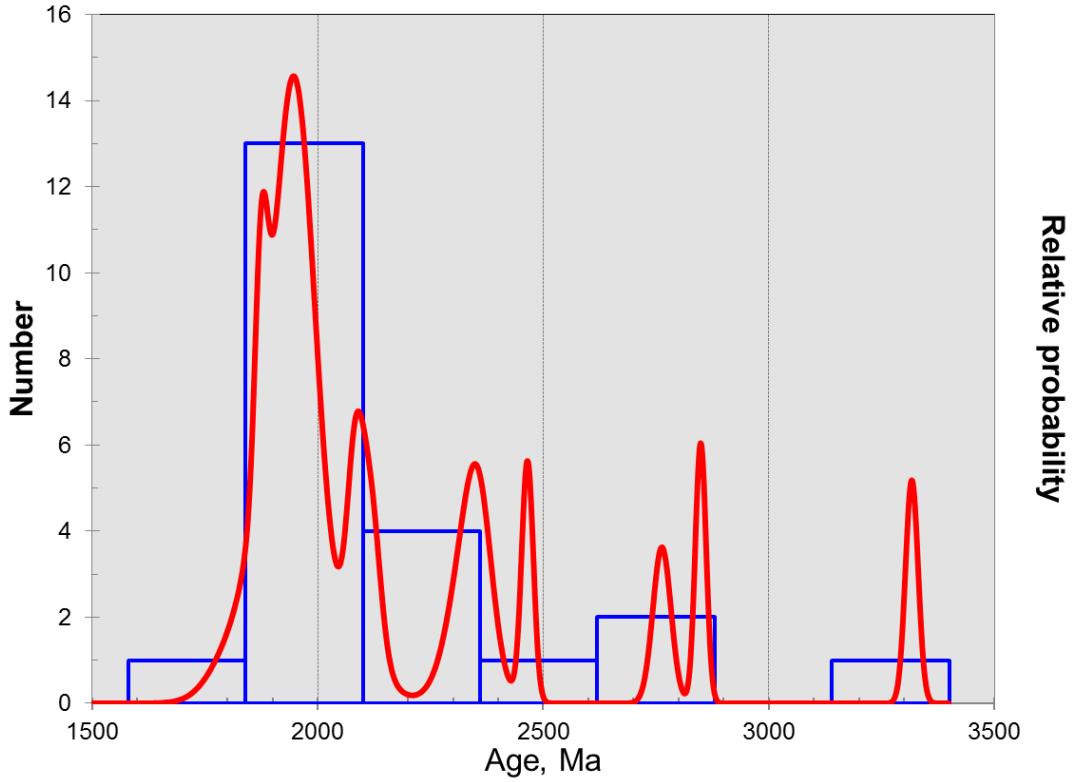



Figure 5.2.6. U-Pb ages of zircons from the Popugaeva pipe.

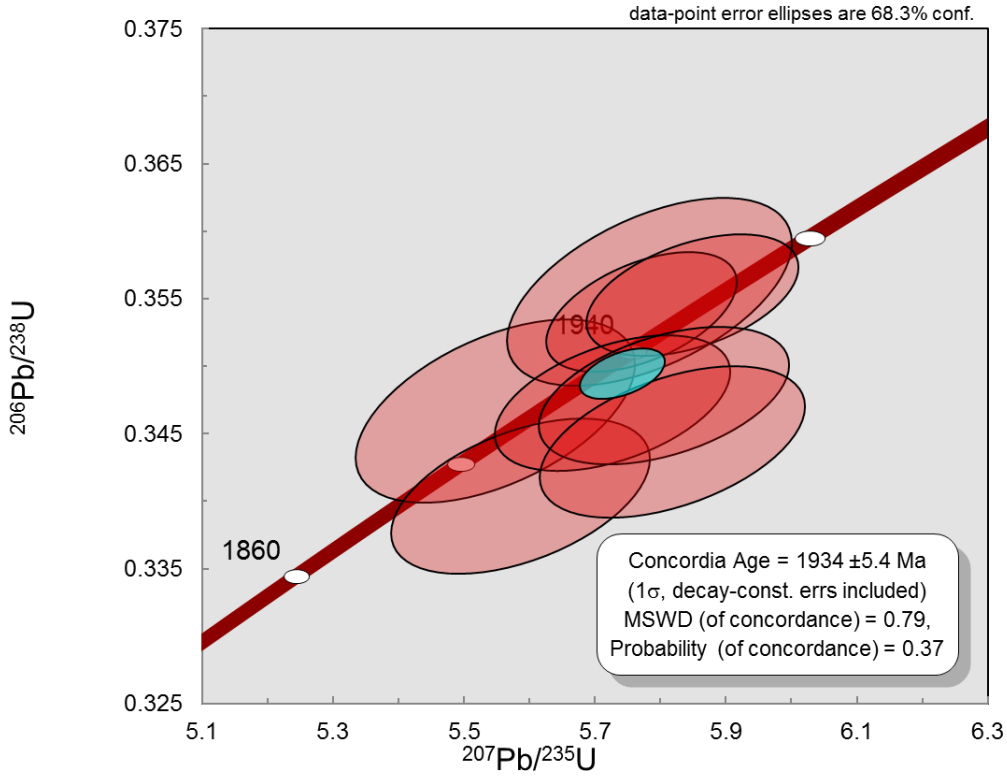



Figure 5.2.7. U-Pb concordia for zircons from the main age peak, Popugaeva pipe.

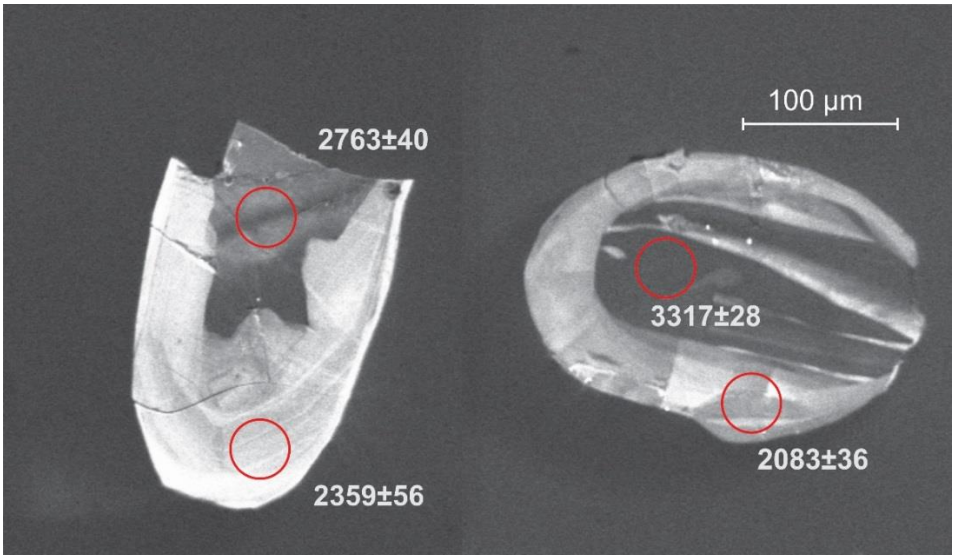



Figure 5.2.8. U-Pb ages of different domains recognised on CL images of zircon grains from the Popugaeva pipe.

**The Zagadochnaya pipe**

Thirty-seven U-Pb analyses were performed on 36 zircons representing the Zagadochnaya pipe. A single grain containing core and rim was large enough to place the analytical spots within each domain. The discordance of all obtained ages is less than 20%.

The youngest zircon from the pipe has an age of 1834±74 Ma, and the oldest one - 2708±72 Ma. The probability plot shows several age peaks (Fig. 5.2.9). The main peak is represented by the group of grains with the weighted mean age of 1928±11 Ma (MSWD = 1.12, probability = 0.35, Fig. 5.2.10). Minor peaks are found at 2023±16, 2181±24, 2332±16, 2396±19, 2473±24 and 2623±20 Ma (Fig. 5.2.11).

A single grain from the Zagadochnaya pipe was analysed with two spots placed within the distinct rim and core. The core gives the age much older than the age of the rim: 2624±32 and 1875±60 Ma correspondingly.

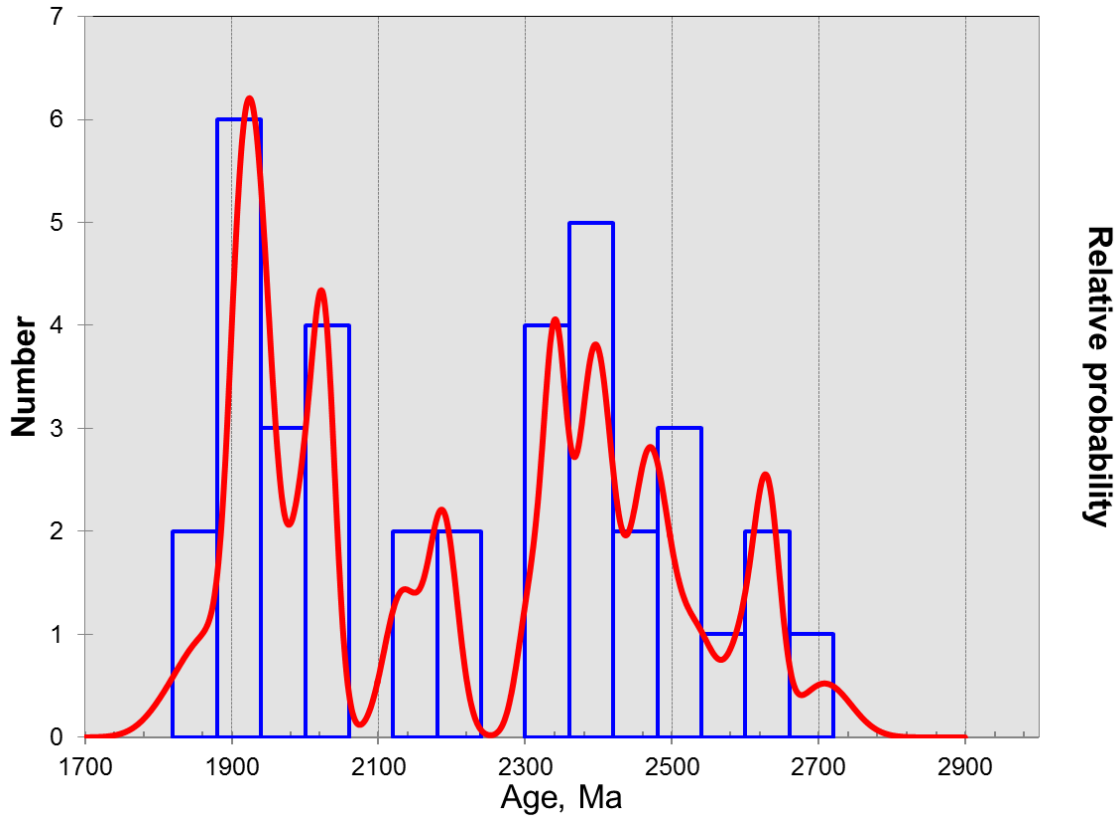



Figure 5.2.9. U-Pb ages of zircons from the Zagadochnaya pipe.

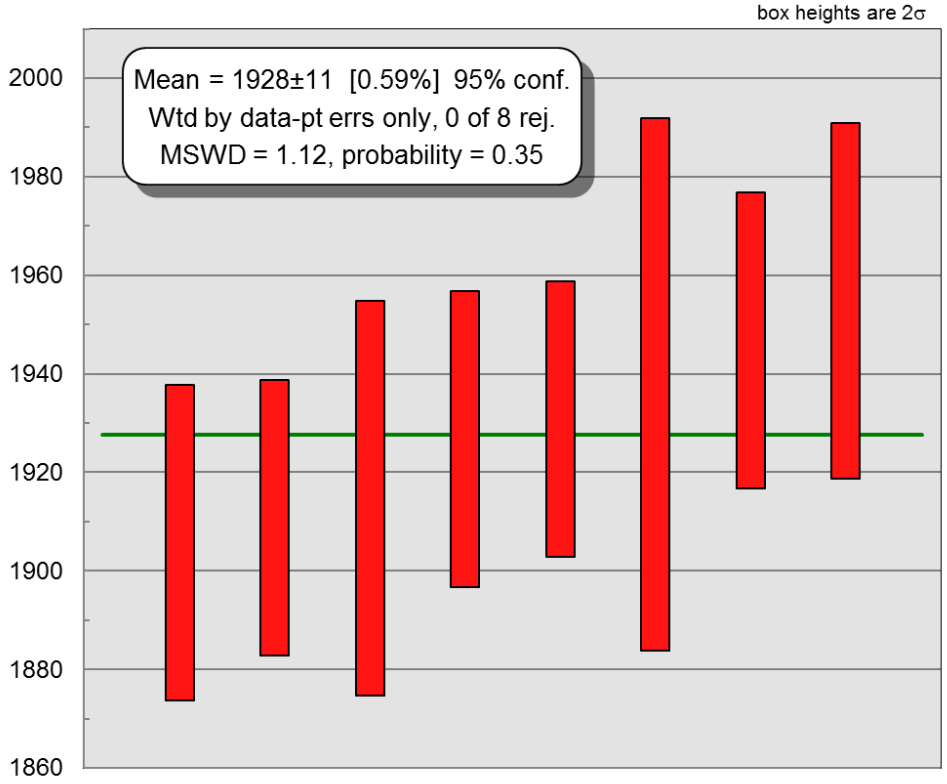



Figure 5.2.10. The weighted mean age of the main age population, Zagadochnaya pipe.

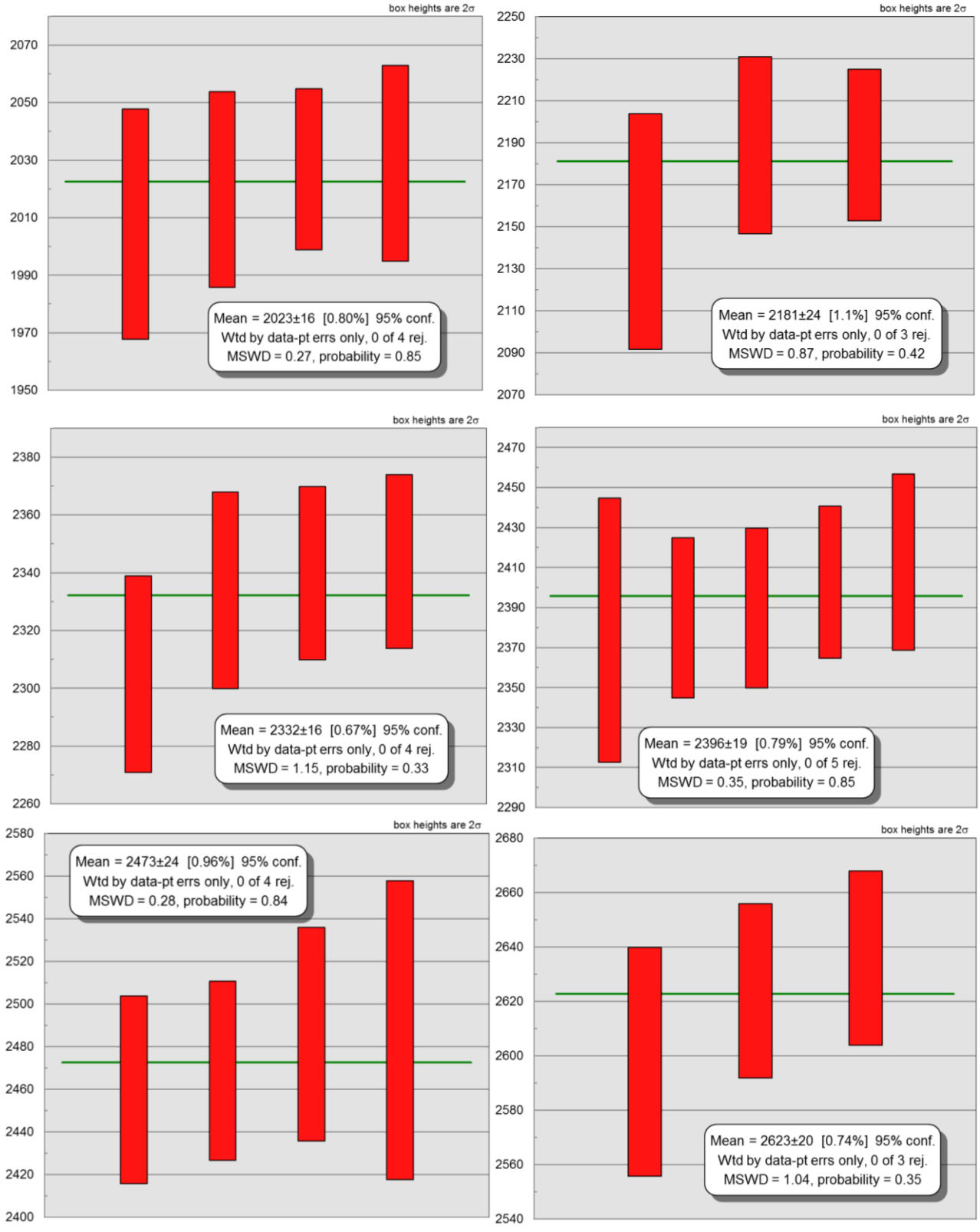



Figure 5.2.11. The weighted mean ages of the minor age populations, Zagadochnaya pipe.

**The Kusova pipe**

In total 49 grains have been collected and analysed by U-Pb method. Three of those were rejected because of discordance more than 20%. One grain include 2 analytical spots within distinct core and rim.

Ages obtained fall into the interval 1851 – 2660 Ma and reveal several age peaks (Fig. 5.2.12). The main age population consist of 10 grains with weighted mean age 1914±11 Ma (MSWD = 0.93, probability = 0.50, Fig. 5.2.13). Minor age peak has the mean age 2514±15 (MSWD = 0.54, probability = 0.70, Fig. 5.2.14). U-Pb analyses within core and rim of the single grain give ages 2528±28 and 2066±48 Ma.




Figure 5.2.12. U-Pb ages of zircons from the Kusova pipe.

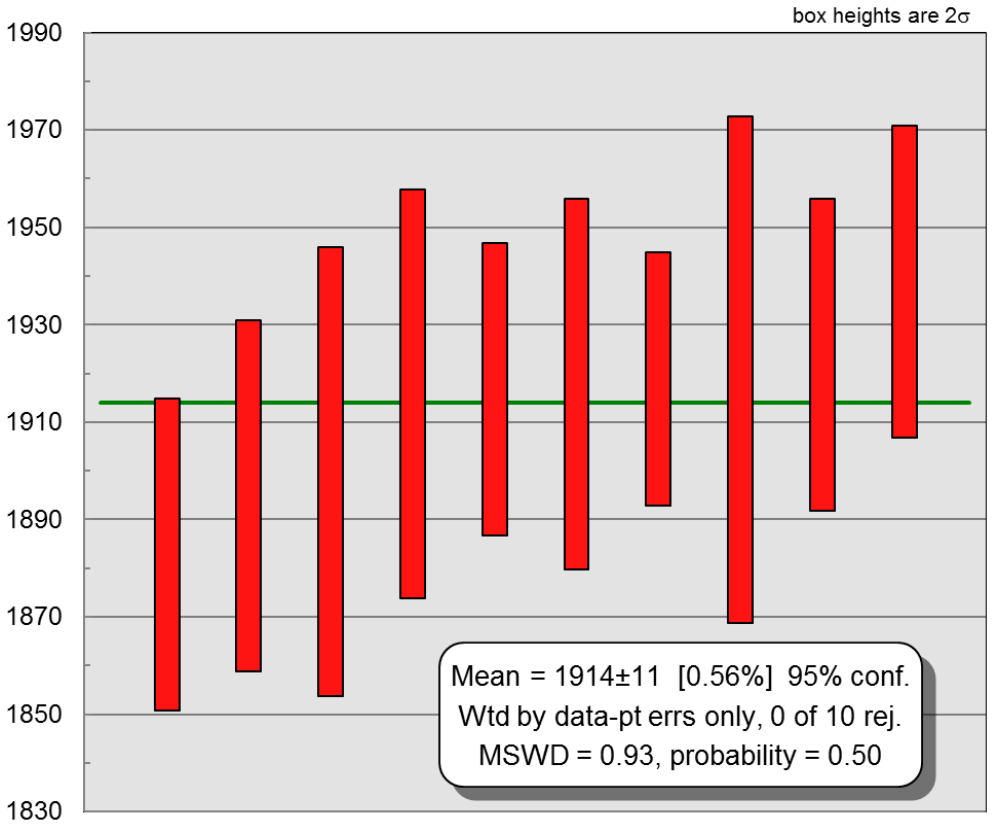



Figure 5.2.13. The weighted mean age of the main age population, Kusova pipe.

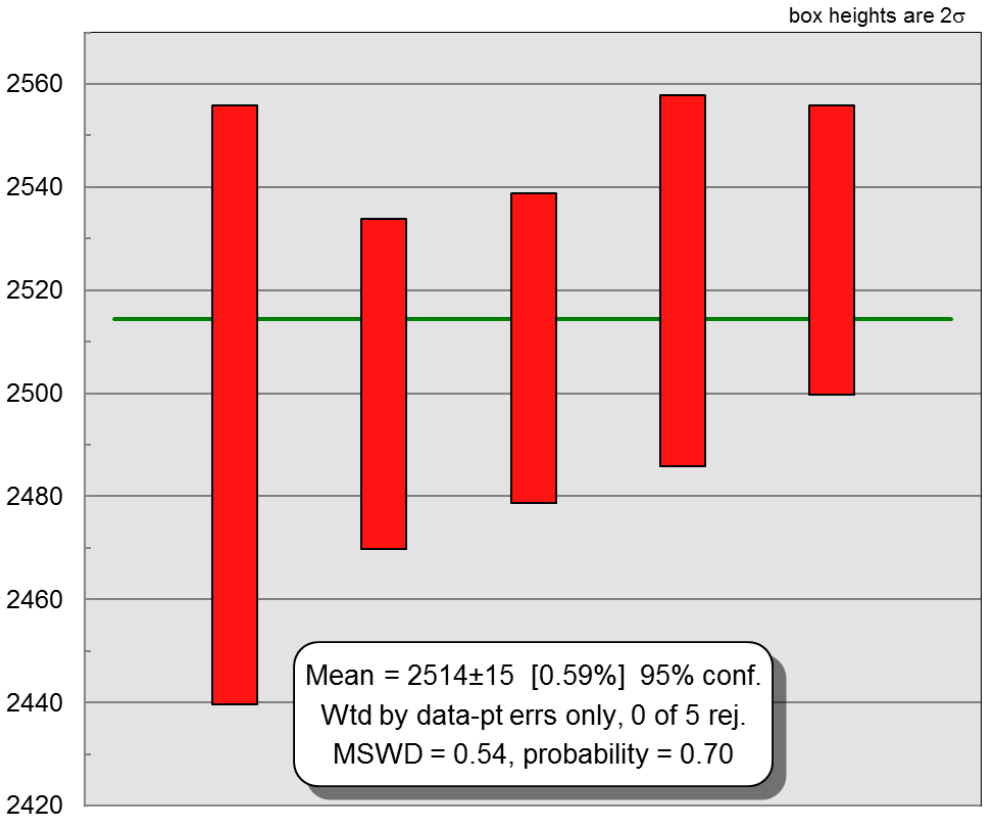



Figure 5.2.14. The weighted mean age of the minor age population, Kusova pipe.

**The Udachnaya pipe**

In total 82 zircon grains were extracted from two xenoliths found in the Udachnaya pipe: 29 grains was picked from the sample OCYB-2 and 53 zircons – from the sample OCYB-5. The sample OCYB-2 presents the xenolith of mafic garnet granulite, mainly consists of garnet, plagioclase and clinopyroxene, with accessory of amphibole and biotite. In the OCYB-5 xenolith plagioclase, garnet and amphibole are predominant, clinopyroxene content is ~5%.

Sample OCYB-2. Twenty-nine zircons were studied by U-Pb technique; one grain was rejected because of high discordance. Twenty-eight grains form a single age population with weighted mean age of 1847±10 Ma (MSWD = 0.26, probability = 1.0; Fig. 5.2.15).

Sample OCYB-5 represented by 53 zircon grains. Two analytical spots were placed within a single grain to date distinct core and rim revealed by CL imaging; however, the core age was rejected because of its high discordance. The range of obtained ages is 1731 – 2567 Ma. Forty-five zircons consist the main age population with weighed mean age of 1850±12 Ma (MSWD = 0.53, probability = 0.996; Fig. 5.2.16). This population together with other grains lie on the regression line crossing concordia at 1830±15 and 2723±73 Ma (MSWD = 0.77; Fig. 5.2.17). However, this regression line should be considered carefully because of discordance of some grains.

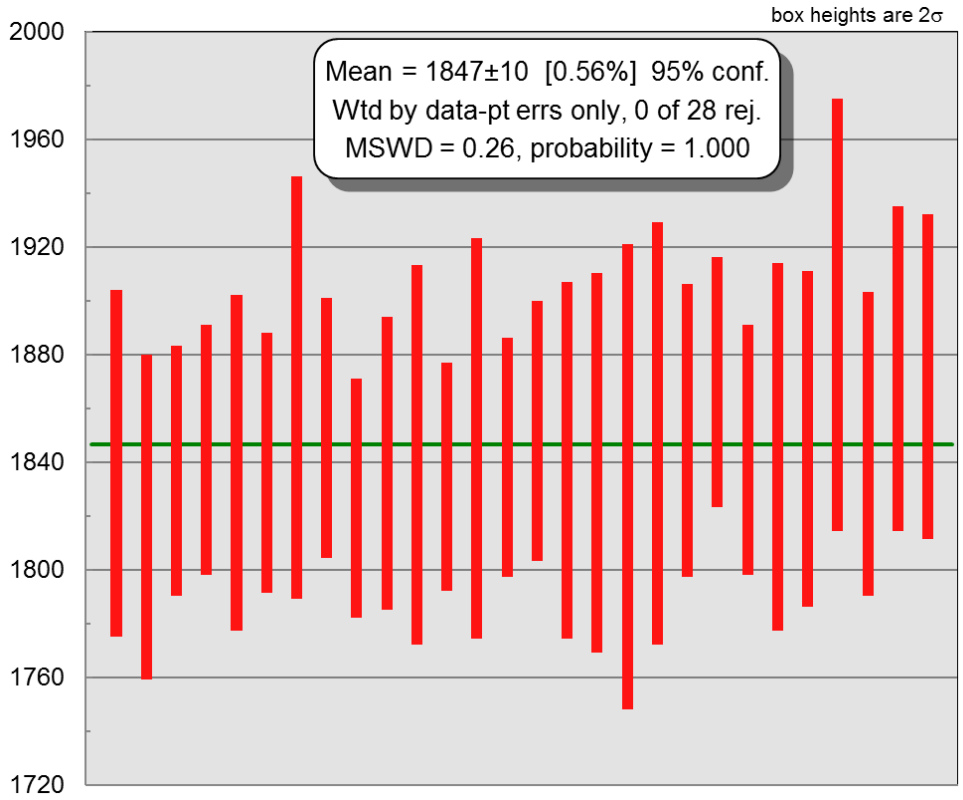



Figure 5.2.15. The weighted mean age of zircons from the xenolith OCYB-2, Udachnaya pipe.

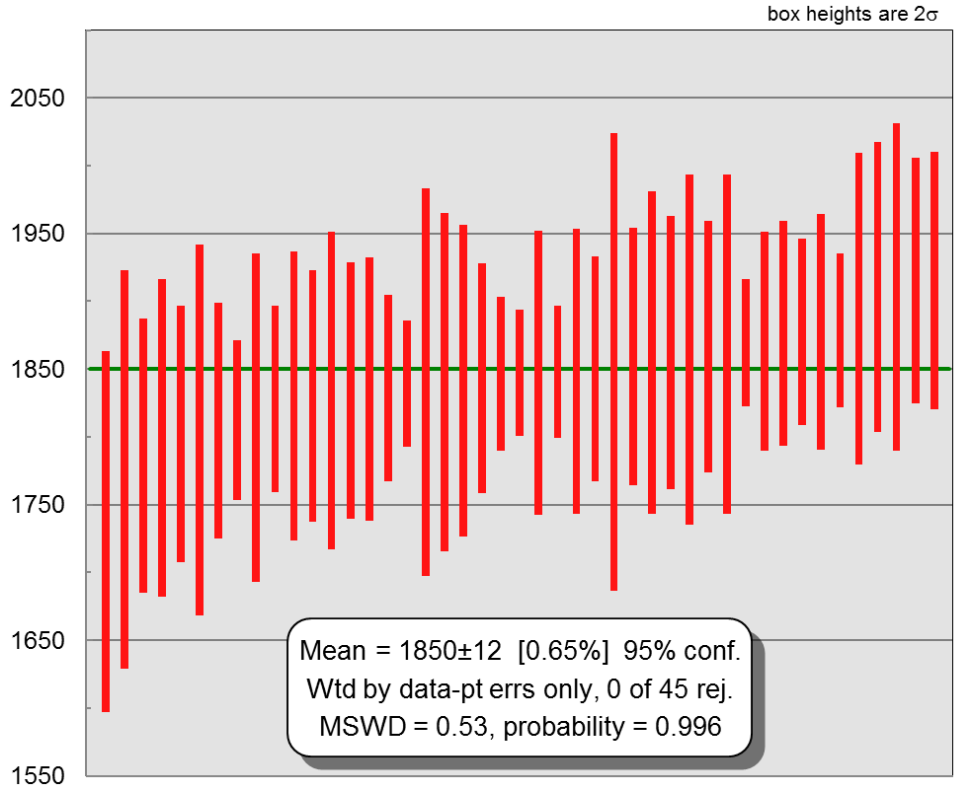



Figure 5.2.16. The weighted mean age of the main age population, sample OCYB-5, Udachnaya pipe.

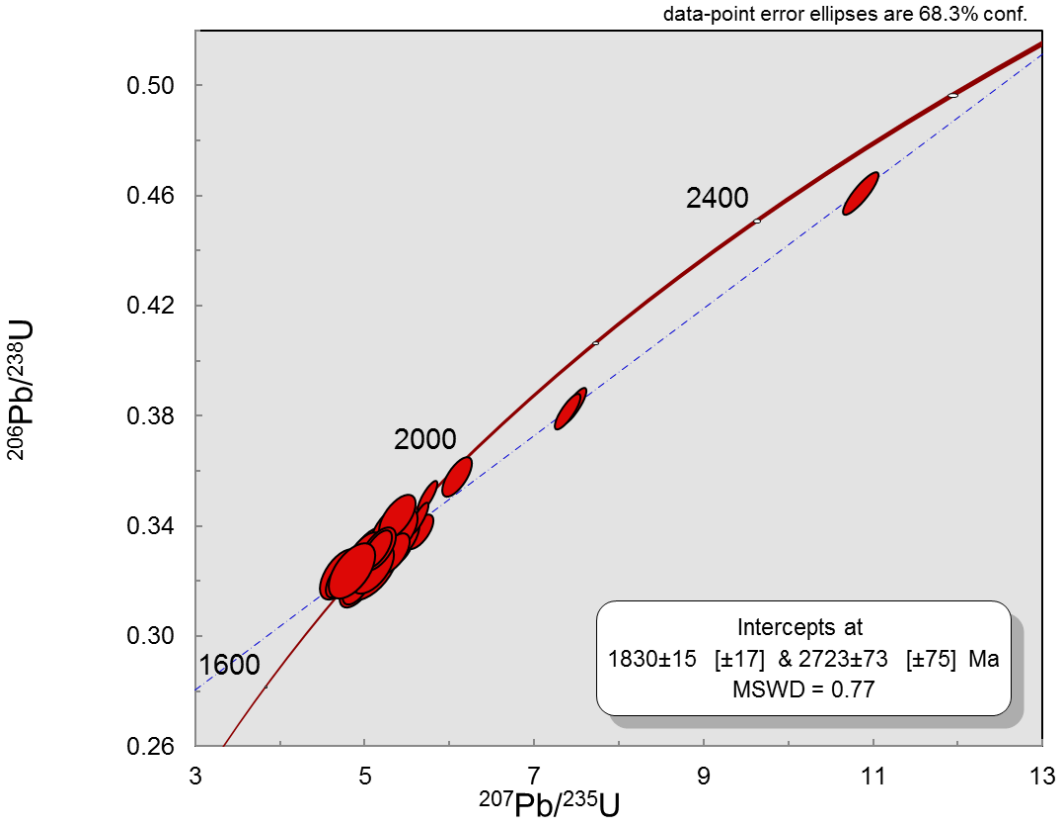



Figure 5.2.17. U-Pb concordia for zircons from the sample OCYB-5, Udachnaya pipe.

***Zircon trace-element data***

**The Udachnaya Eastern pipe**

The trace-element composition has been analysed for all 7 zircons collected from the Udachnaya Eastern pipe. Analyses of the rim and core were perfomed in the same spots as U-Pb dating. All grains show variations in concentrations of the majority of elements, however, only few of them differ significantly (Fig. 5.2.18).

The REE patterns (Fig. 5.2.18) shows more variety in elements behaviour, especially for the LREE. Some zircons are depleted in LREE and have distinct positive Ce-anomaly, while others have higher contents of LREE and show minor or even no Ce-anomaly. This behaviour is not typical for zircons, but may reflect alteration processes or inclusion of mineral with high LREE content. On the other hand, enrichment in HREE and negative Eu-anomaly are found for all analysed zircons.

Total REE contents are within the range 667 – 1442 ppm, except of a single analysis showing 3018 ppm. This spot is placed in the grain rim with U-Pb age of 1864 Ma. The core of this grain (U-Pb age 2049 Ma), in opposite, reveals the lowest total REE content (667 ppm). The rim is enriched in all trace elements, and has extremely high Ti concentration (2552 ppm *vs* 23 ppm in core) indicating possible presence of rutile inclusion within the analytical spot. Two other zircons in which both rim and core were studied do not show significant difference in total REE content within the grain.

Zircon grains from the Udachnaya Eastern pipe show significant variations in Th/U (0.27 – 1.97) and Nb/Ta ratios does not differ much (2.35 – 7.03).

The CART classification indicate trace-element composition of studied grain is similar to those of zircons from intermediate to felsic rocks (high Lu, Y and U). Localization of the majority of zircons within the granitoid field of the Y *vs* Yb/Sm discrimination diagram (Fig. 5.2.19) confirms the results of the CART classification.

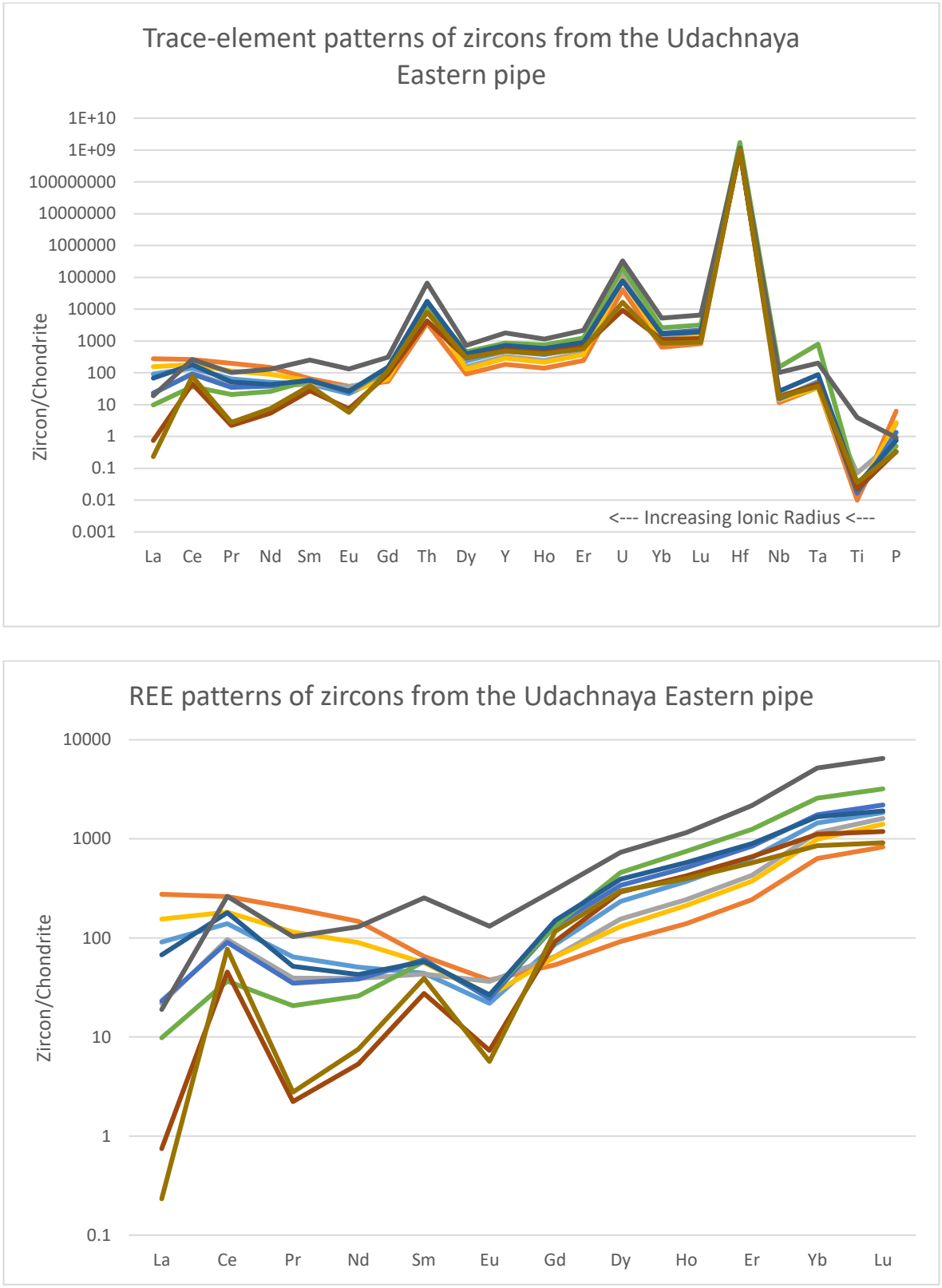



Figure 5.2.18. Trace-element and rare-earth element patterns of zircons from the Udachnaya Eastern pipe.

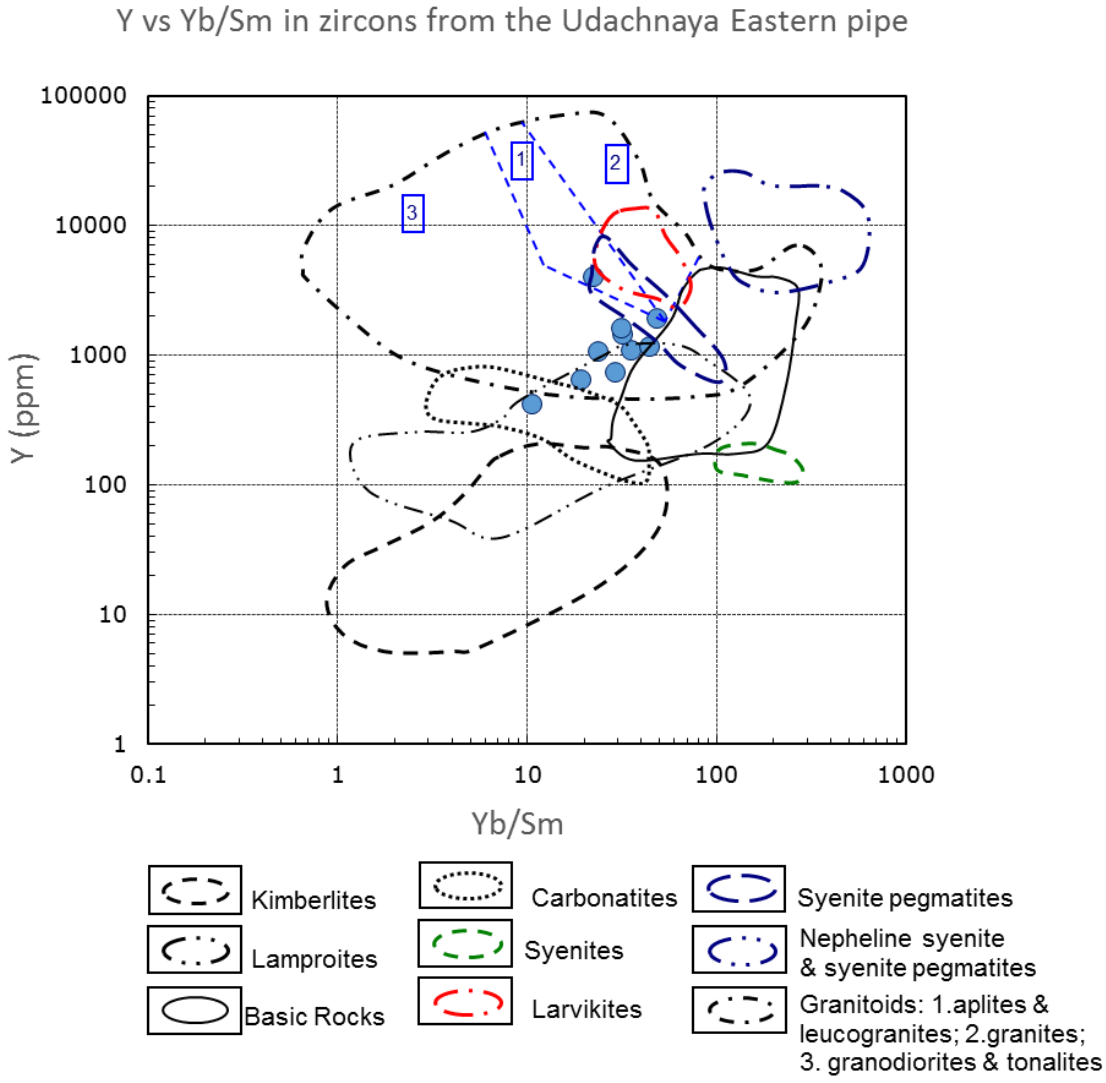
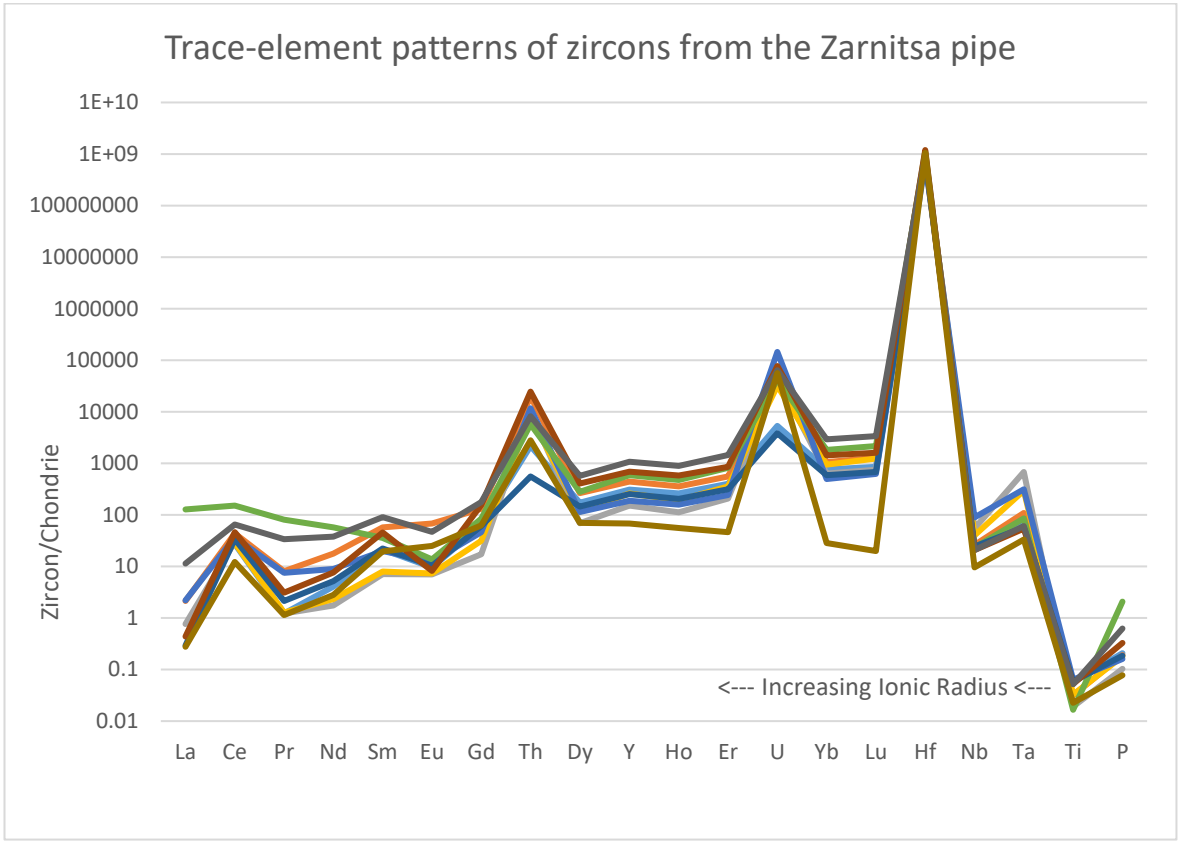



Figure 5.2.19. Y *vs* Yb/Sm discrimination diagram for zircons from the Udachnaya Eastern pipe.

**The Zarnitsa pipe**

In total ten analyses of the trace-element composition were obtained for 9 zircon grains from this pipe. A single grain has been analysed in two spots placed within a core and rim of the grain.

The trace-element patterns are similar for all analyses, except the zircons grain MVG458_Z-15. This grain has has generally low content of the majority of elements and the lowest concentrations of total REE (91 ppm), as well as the most of analysed elements (Fig. 5.2.20). Moreover, while all other grains show typical zircon pattern with enrichment in HREE, this grain is slightly depleted in HREE (Fig. 5.2.20).



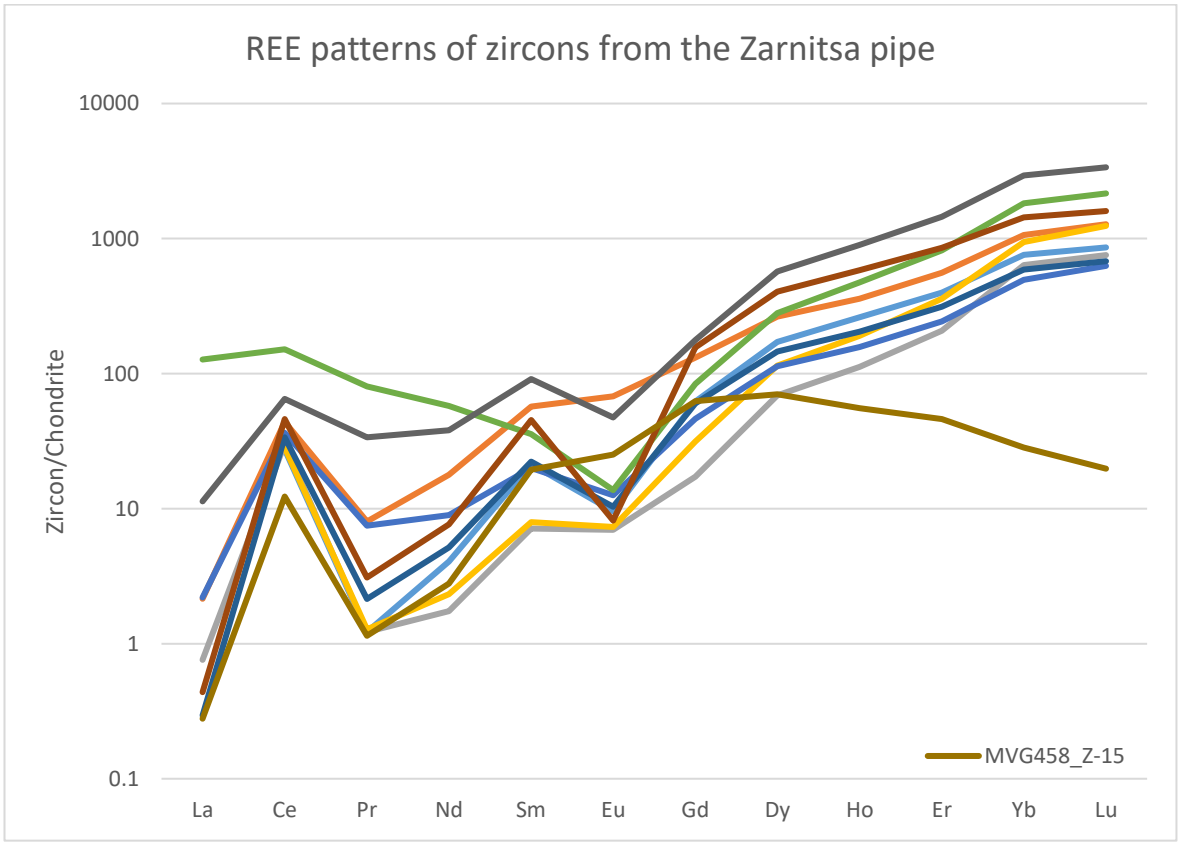




Figure 5.2.20. Trace-element and rare-earth element patterns of zircons from the Zarnitsa pipe.

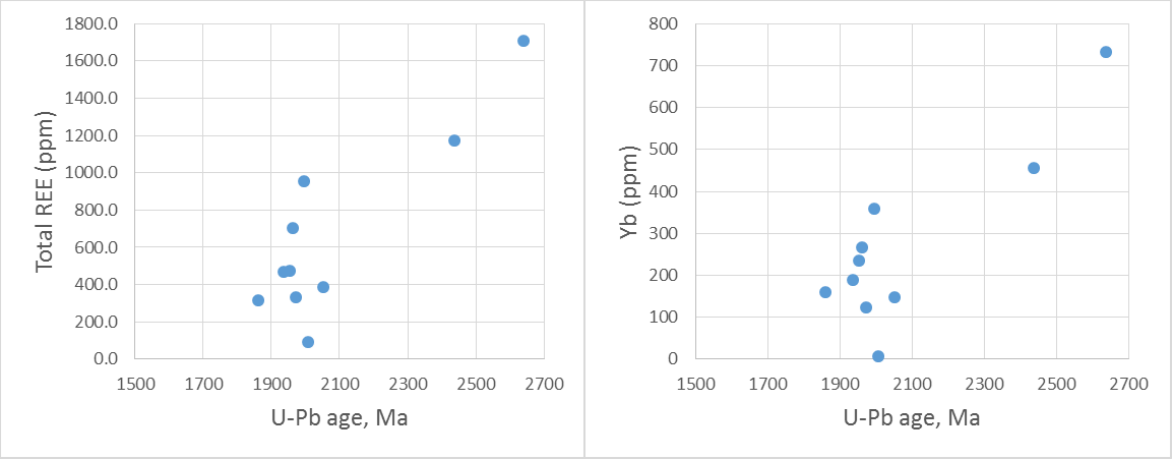



Figure 5.2.21. Total REE and Yb concentrations *vs* U-Pb age of zircons from the Zarnitsa pipe.

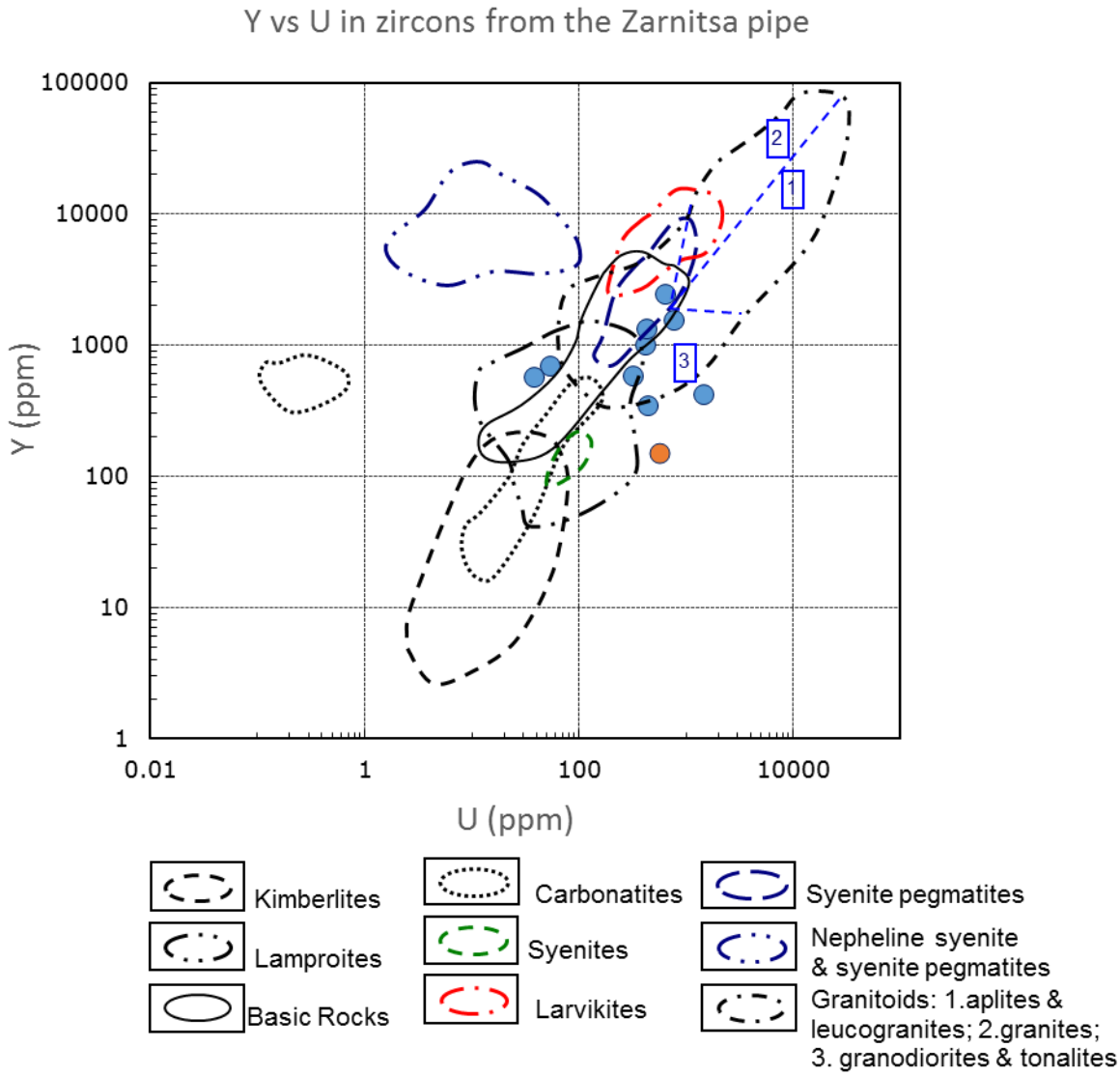



Figure 5.2.22. Y *vs* U discrimination diagram for zircons from the Zarnitsa pipe. Grain MVG458_Z-15 showed in orange color.

This pattern may reflect crystallization in unusual for zircons conditions; for example, other mineral phase competing for HREE might crystallize at the same time.

Apart from that, zircon MVG458_Z-15 has a less distinctive negative Eu-anomaly. All other grains show more variations in concentration of elements with the larger ionic radius, however even those differences rarely extend one order of magnitude. Total REE contents vary from 315 to 1707 ppm; Y concentrations differ from 343 to 2431 ppm, U – from 38 to 1453 and Th from 22 to 988 ppm. In general, higher contents of REE are common for older grains (Fig. 5.2.21). The ratios Th/U and Nb/Ta are within the intervals 0.2 – 1.8 and 1.01 – 5.32 correspondingly.

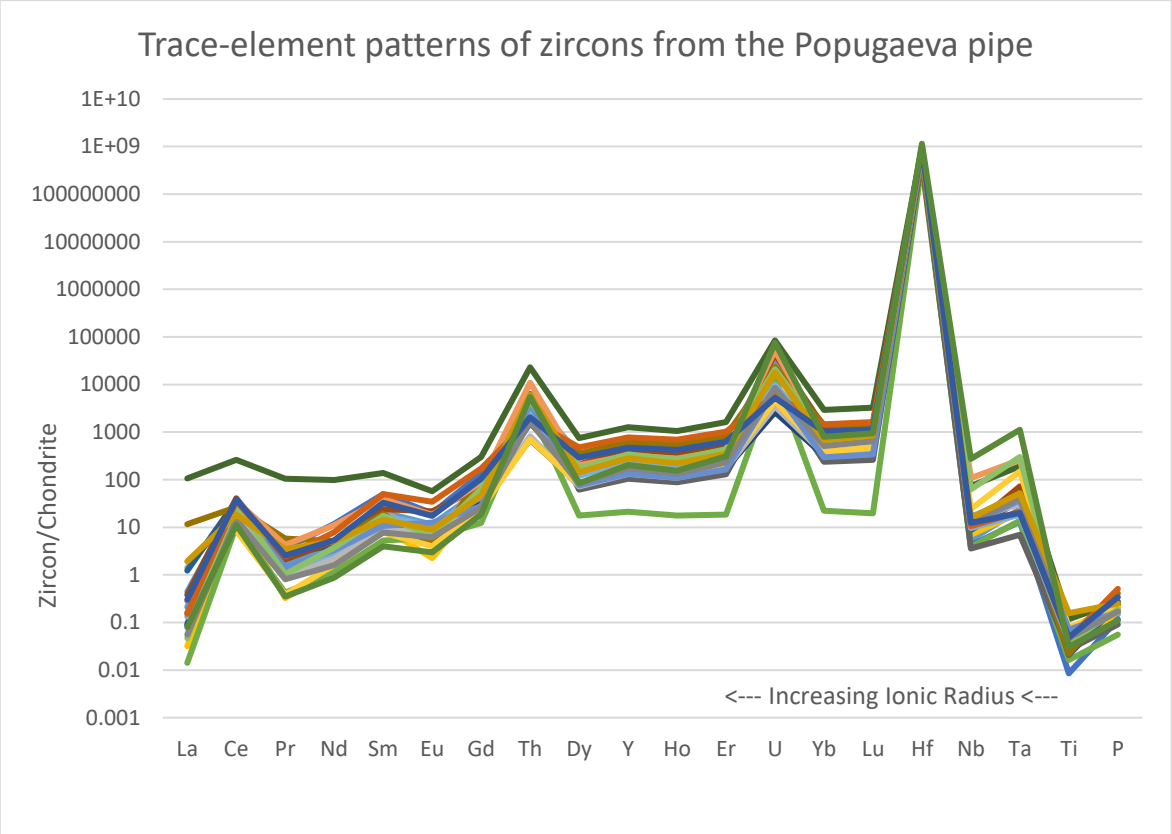
According to the CART classification, the grain MVG458_Z-15 has composition of trace elements similar to zircons from kimberlites, however, uranium concentration in the grain (560 ppm) is much higher than in kimberlitic zircons (<60 ppm). Y *vs* U discrimination diagram shows this grain located closer to the lamproites field (Fig. 5.2.22). Other grains shows trace-element signatures of zircons crystallized from intermediate to felsic parental melt.

**The Popugaeva pipe**

Analysing of the trace-element composition has been performed for all 19 grains recovered from this pipe. The grains with distinctive core and rim were analysed for the composition of both domains. In total 22 analyses have been collected for zircons from the Popugaeva pipe.

All grains show similar trace-element patterns with rare exceptions (Fig. 5.2.23). The grain MVG-458_P_02 shows significant enrichment in LREE, probably reflecting intensive alteration of the grain. This zircon also has highest REE contents (total REE 2164 ppm), as well as Th, U and Y concentrations. Another zircon grain (MVG-458_P_18), in opposite, reveals low REE concentration (total REE 36 ppm), especially HREE.

The chondrite-normalized plot of the REE composition of the rest of zircons demonstrate typical zircon patterns with depletion in LREE and enrichment in HREE. The most of grains are characterised by well-defined negative Eu-anomaly and positive Ce-anomaly. Total REE contents diverge from 160 to 1038 ppm, Y from 235 to 1744 ppm, Th and U are within ranges 28 – 915 and 26 - 849 ppm correspondingly. In general, lower concentrations of REE ($\Sigma$<500 ppm) are more common for younger zircons (1822 - 2117 Ma), while all grains older than 2.5 Ga have total REE contents higher than 500 ppm (Fig. 5.2.24).



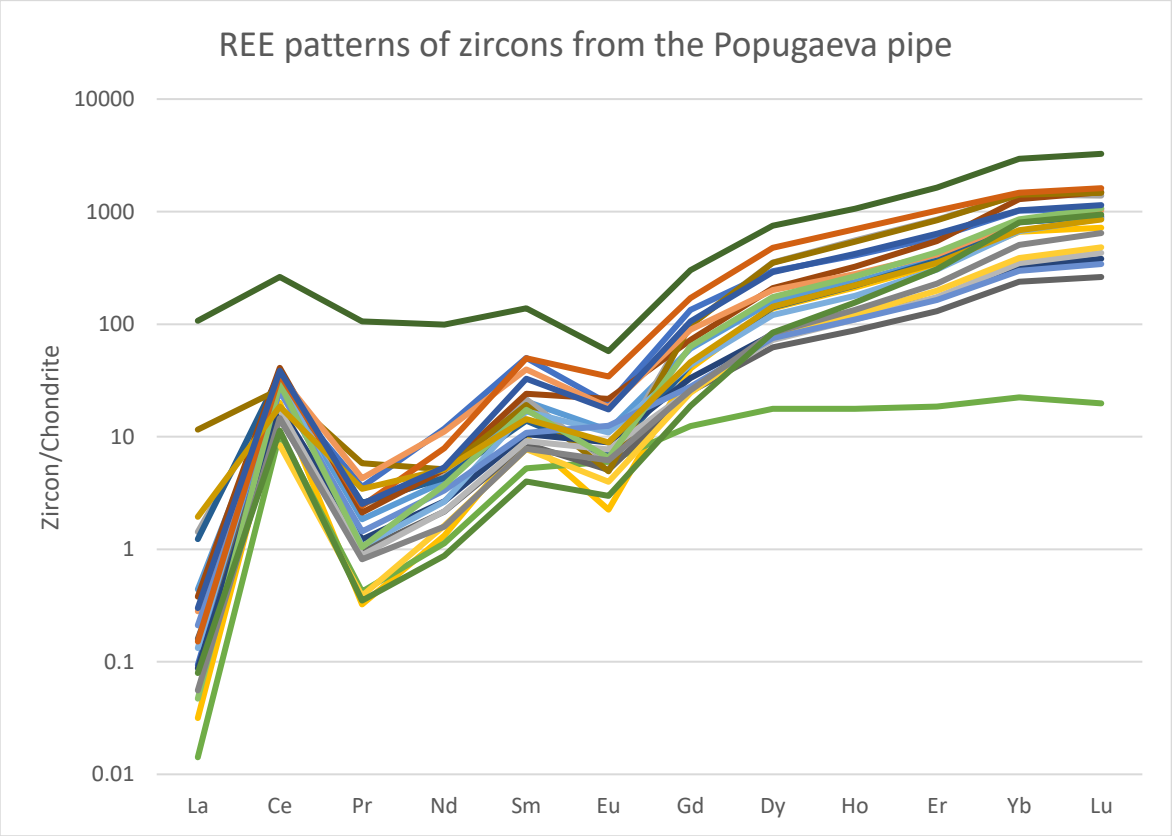




Figure 5.2.23. Trace-element and rare-earth element patterns of zircons from the Popugaeva pipe.

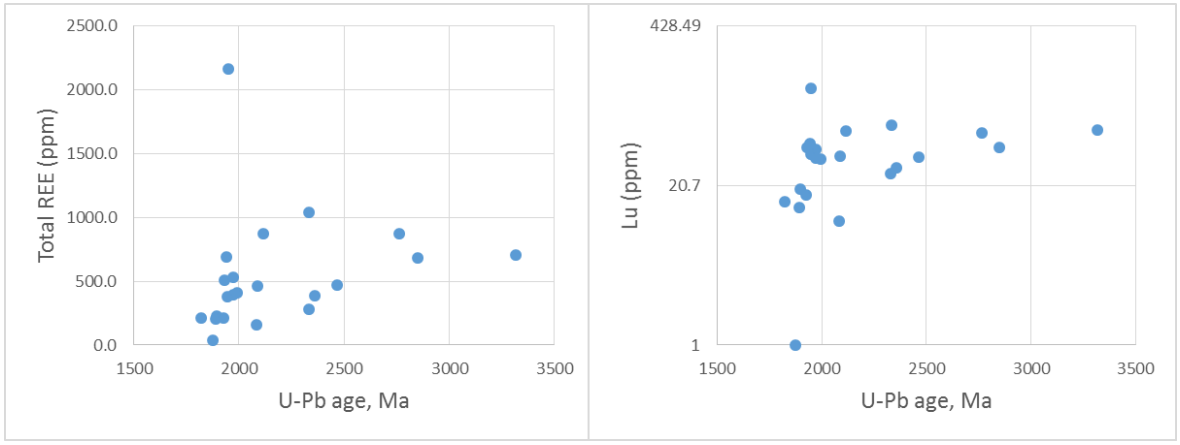



Figure 5.2.24. Total REE and Lu concentrations *vs* U-Pb age of zircons from the Popugaeva pipe.

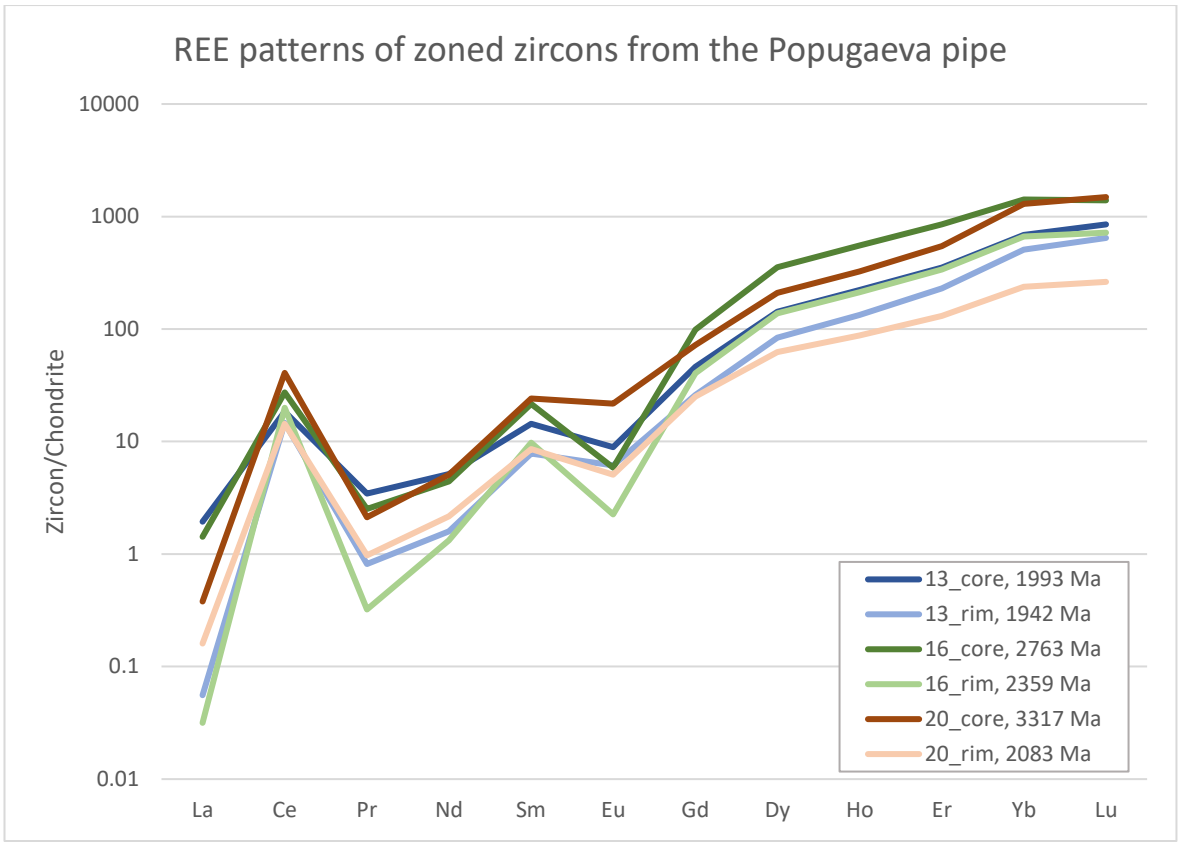



Figure 5.2.25. Rare-earth element patterns of zoned zircons from the Popugaeva pipe.

For zircon grains with defined core and rim zoning, REE patterns in general are similar, however, concentrations of the REE in cores are higher than in rims for all three grains (Fig. 5.2.25).

The Th/U ratios of all zircons from the Popugaeva pipe fall within the interval 0.28 – 2.79, Nb/Ta – 1.74 – 7.82.

According to CART classification, 5 grains have trace-element composition resembling zircons from carbonatites (Lu<20.7 ppm, low Ta and U); one zircon (MVG-458_P_18) shows signatures of kimberlitic origin (Lu<2 ppm, U< 60 ppm) and 13 grains have composition of trace element close to those of zircons crystallized from intermediate rocks. All mantle-derived zircons reveal U-Pb ages in the range of 1822 – 2083 Ma (Fig. 5.2.24).

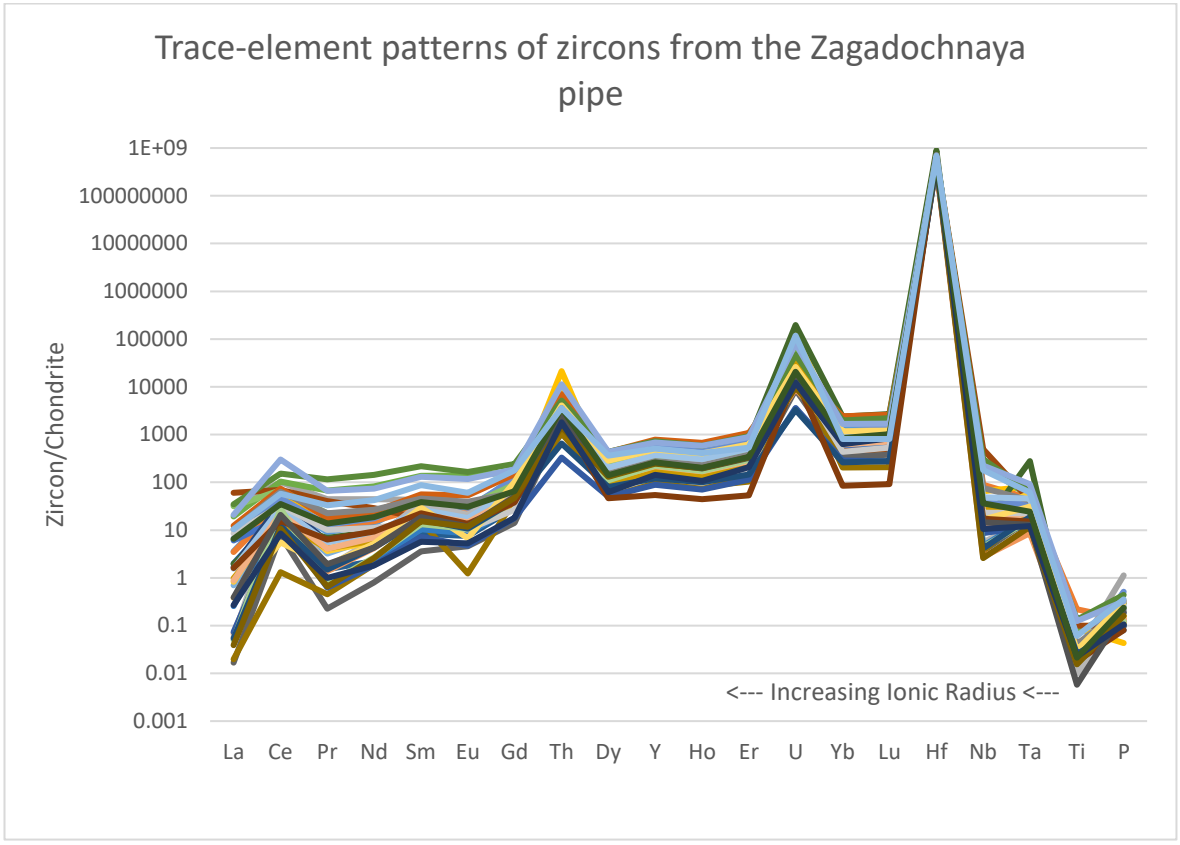
**The Zagadochnaya pipe**

The trace-element composition was analysed in thirty-six zircon grains. A single grain with core-rim zoning has been analysed with two analytical spots placed in each of domains.

The chondrite-normalized plot shows significant variations in concentrations of the most of trace elements (Fig. 5.2.26). Total REE contents vary from 101 to 1451 ppm. Y ranges from 152 to 1751 ppm, U – from 33 to 1977, Th from 13 to 856 ppm. LREE concentrations show more variety than HREE, which may be the result of different intensity of alteration. The Th/U ratio is in the range 0.03 – 1.2, Nb/Ta – 0.56 – 144.

The chondrite-normalised REE plot (Fig. 5.2.26) demonstrates two distinctive patterns: grains of the first group are more depleted in LREE, their negative Eu- and positive Ce-anomaly are well-defined; second group of zircons is less depleted in LREE, their anomalies are not significant, and thus they has flatter shape of patterns. Despite of the visible difference in REE patterns, there is no correlation with total REE contents (Fig. 5.2.27). According to the CART statistical classification, most of zircons from the first group have trace-element composition close to those of zircons from intermediate and felsic rocks, while the second population mostly consists of zircons with composition of trace elements typical for zircons from mafic rocks or carbonatite. The Hf *vs* Y discrimination diagram generally confirms CART classification (Fig. 5.2.28).

A single grain in which the core (U-Pb age of 2624 Ma) and rim (U-Pb age of 1875 Ma) were analysed reveals a difference in REE composition: the core is depleted in LREE, but shows significant positive Ce-anomaly (Fig. 5.2.29). LREE enrichment of the rim supports the suggestion of alteration processes affecting the LREE behaviour.



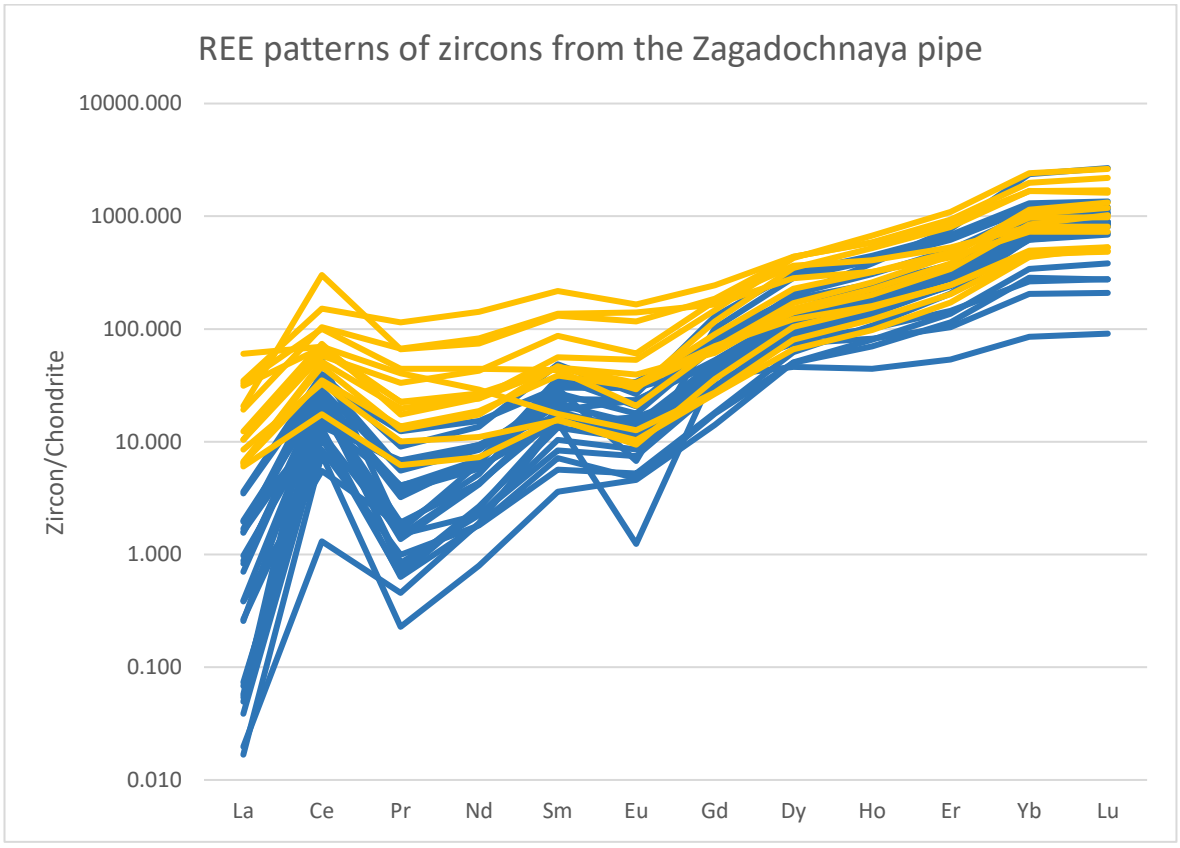




Figure 5.2.26. Trace-element and rare-earth element patterns of zircons from the Zagadochnaya pipe. Grains with elevated LREE abundances are shown in yellow.

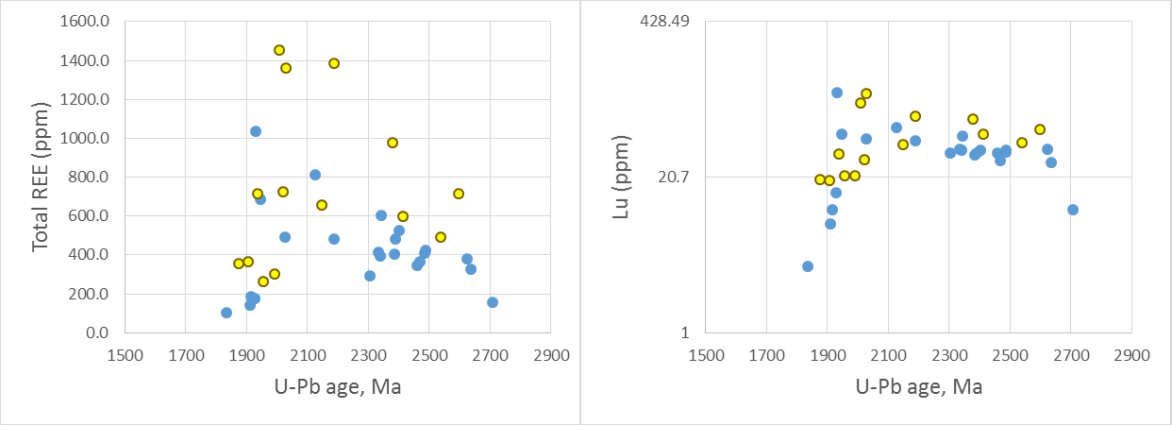
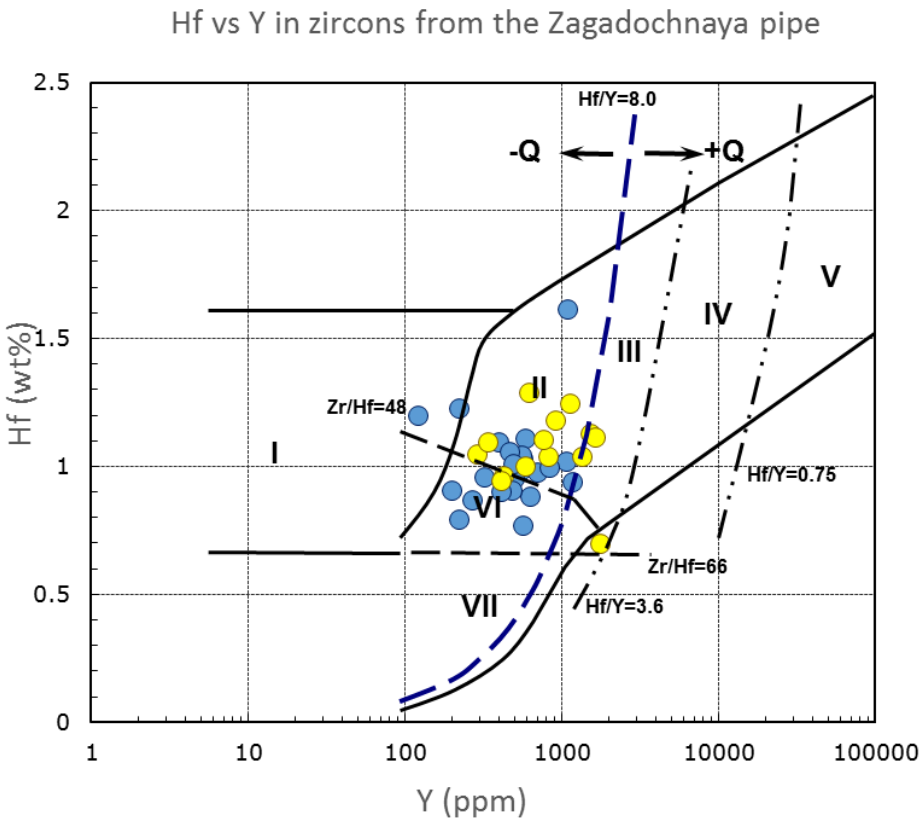



Figure 5.2.27. Total REE and Lu concentrations *vs* U-Pb age of zircons from the Zagadochnaya pipe. Data points are color-coded according to the REE patterns at the Fig. 5.2.26.




I - kimberlites;
II - ultrabasic, basic and intermediate rocks;
III - quartz-bearing intermediate and felsic rocks;
IV- felsic rocks with 'high' SiO2 content;
V - greisens;
VI- alkaline rocks and alkaline metasomatites of alkaline complexes;
VII- carbonatites

Figure 5.2.28. Hf *vs* Y discrimination diagram for zircons from the Zagadochnaya pipe. Data points are color-coded according to the REE patterns at the Fig. 5.2.26.

**The Kusova pipe**

Forty-five analyses of the trace-element composition were collected for zircons from the pipe. Core and rim analyses have been done on the grain with a distinctive zoning structure.

The concentrations of trace elements range more significantly for elements with larger ionic radius (Fig. 5.2.30). Total REE contents diverge from 32 to 1463 ppm. Uranium vary from 14 to 1789 ppm, Th – from 7 to 886 ppm. The concentrations of Y differ from 59 to 1972 ppm. Ratios Th/U and Nb/Ta also diverge significantly: Th/U is from 0.13 to 6.13 and Nb/Ta – from 1.8 to 200.

The REE plot show two general trends (Fig. 5.2.30). First group of zircons demonstrates almost flat patterns due to minor or even no depletion in LREE. These grains show slight Eu- and Ce-anomalies and high concentrations of HREE. Second group has more distinctive Eu-minima and Ce-maxima, grains are depleted in LREE and enriched in HREE. The concentrations of Lu are higher in zircons from the first group. There is no regularity in U-Pb age of zircons from different groups (Fig. 5.2.31). The statistical CART classification shows grains from the first group has trace-element composition similar to zircons from mafic, carbonatitic or kimberlitic rocks. The composition of grains from the second group is typical for zircons crystallized from the intermediate to felsic parental melt (Fig. 5.2.32).

The core (U-Pb age 2528 Ma) and rim (2066 Ma) analysed in the single grain has different REE composition (Fig. 5.2.29): the core is enriched in U, Th and all REE, especially in LREE. At the same time, the rim has more noticeable Eu- and Ce-anomalies. This core-rim behaviour of REE is not common for alteration processes, but may reflect crystallization of zircon rim around the inherited core.

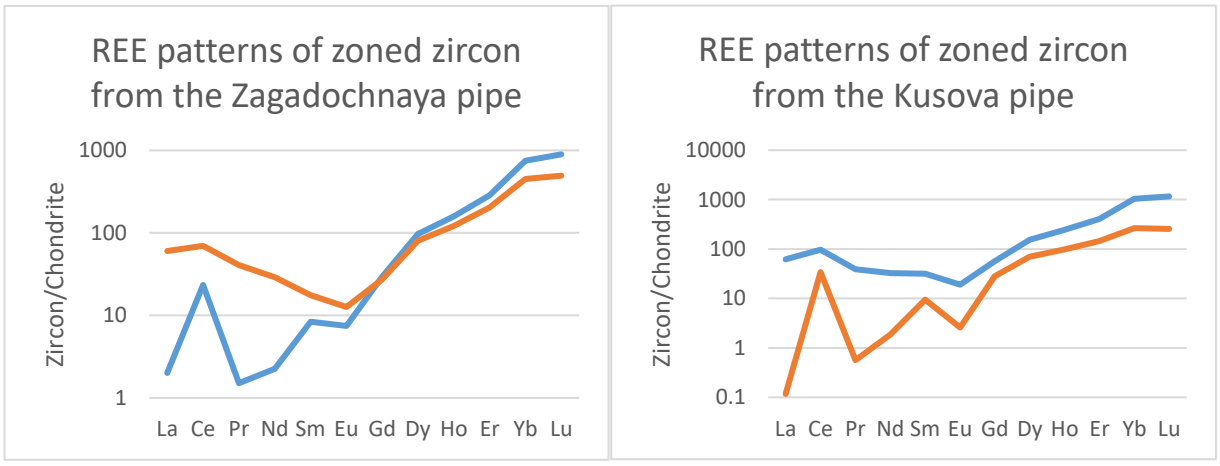
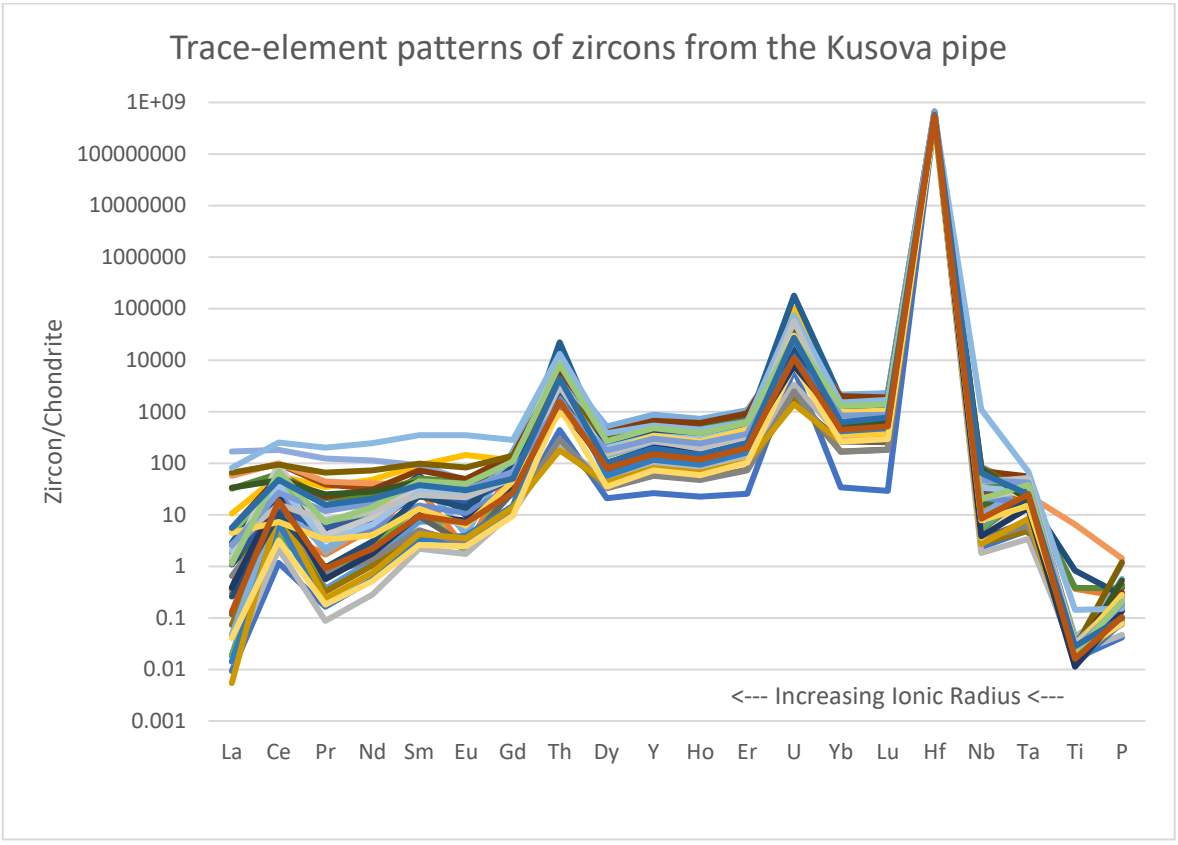



Figure 5.2.29. Rare-earth element patterns of zoned zircons from the Zagadochnaya and the Kusova pipes. Core patterns are shown in blue and rims are in orange.



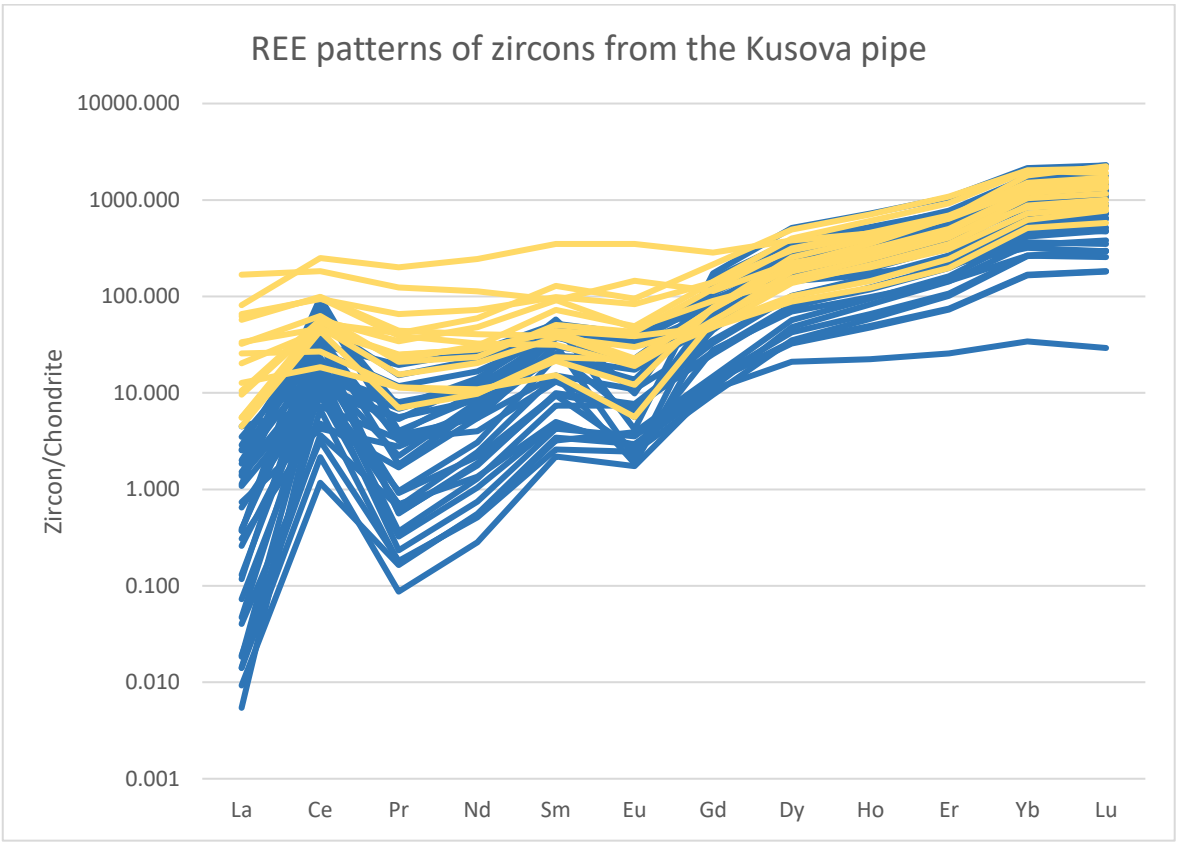




Figure 5.2.30. Trace-element and rare-earth element patterns of zircons from the Kusova pipe.

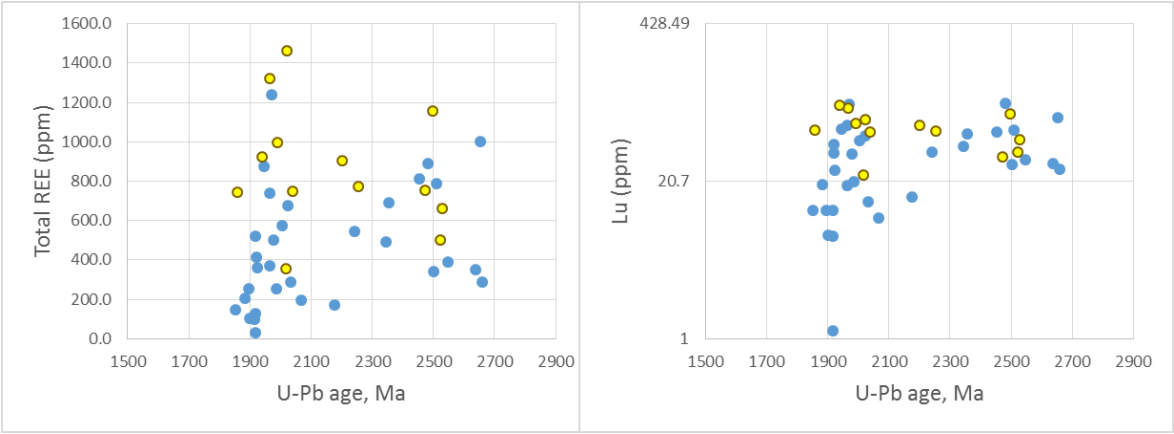
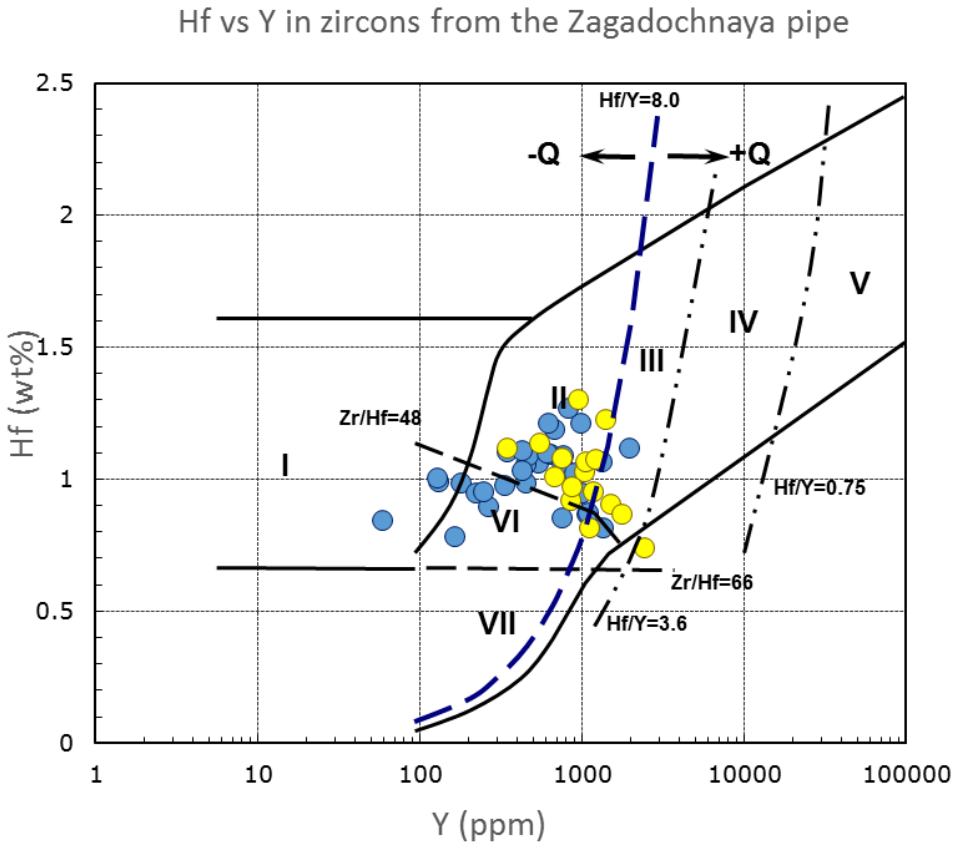



Figure 5.2.31. Total REE and Lu concentrations *vs* U-Pb age for zircons from the Kusova pipe. Data points are color-coded according to the REE patterns (Fig. 5.2.30).




I - kimberlites;
II - ultrabasic, basic and intermediate rocks;
III - quartz-bearing intermediate and felsic rocks;
IV- felsic rocks with 'high' SiO2 content;
V - greisens;
VI- alkaline rocks and alkaline metasomatites of alkaline complexes;
VII- carbonatites

Figure 5.2.32. Hf *vs* Y discrimination diagram for zircons from the Kusova pipe. Data points are color-coded according to the REE patterns (Fig. 5.2.30).

**The Udachnaya pipe**

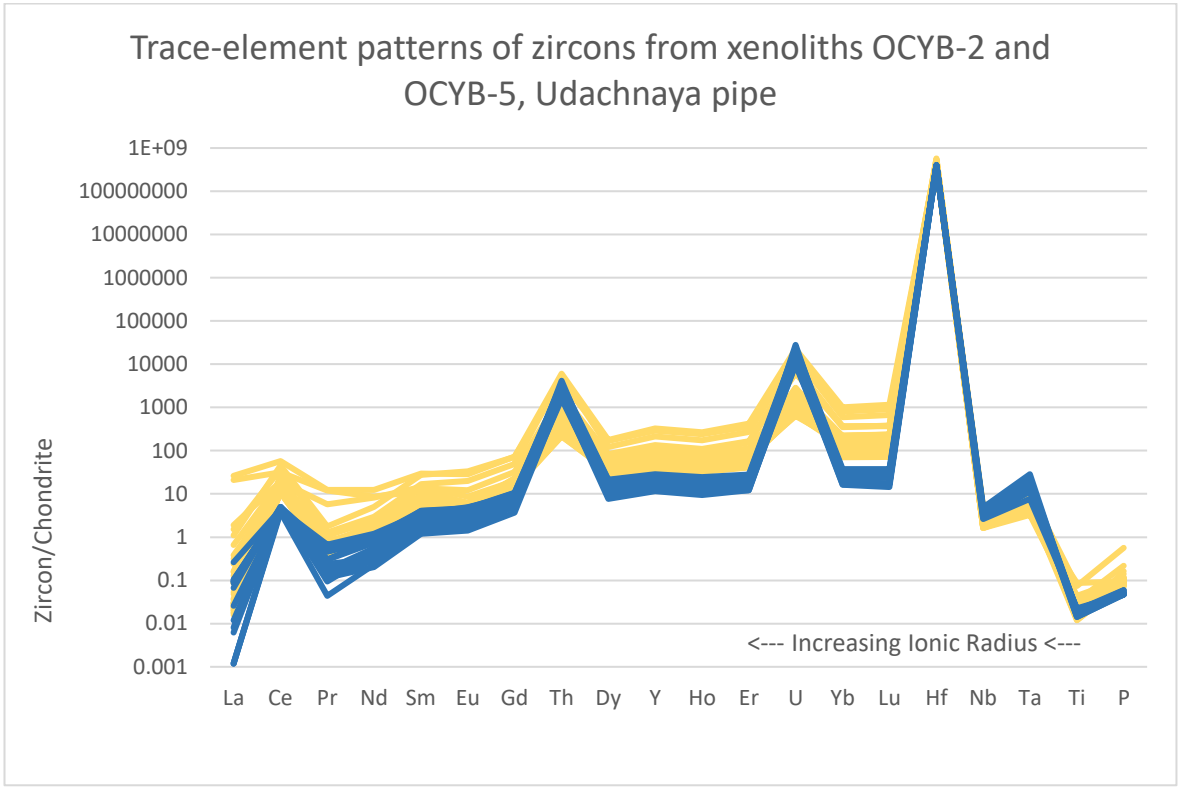
Zircons from both samples OCYB-2 (16 grains, U-Pb ages 1820 – 1895 Ma) and OCYB-5 (40 grains, U-Pb ages 1732 – 2235 Ma) were analysed for their trace-element composition.

The chondrite-normalized trace-element plot shows significant variations in composition of zircons from different samples (Fig. 5.2.33). In general, zircons from xenolith OCYB-5 have higher concentrations of the majority of trace elements except Th (8-239 ppm), U (6-223 ppm) and Nb (0.6-2 ppm). Total REE contents diverge from 65 to 572 ppm (Fig. 5.2.34). The concentrations of all elements are more scattered in grains from the sample OCYB-5 than in zircons from OCYB-2. Thus, for zircons from OCYB-2 total REE concentrations are within the narrow interval 17 – 38 ppm (Fig. 5.2.34), and variations in other element contents rarely reach one order of magnitude (Lu, Th, U, Nb and Ho). At the same time, for OCYB-5 only few elements differ within one order (Ce, Sm and Dy), others vary in much wider ranges. Ratios Th/U and Nb/Ta are also in agreement with this trend. For sample OCYB-5 Th/U ratio vary from 0.8 to 2.34, Nb-Ta – from 2.92 to 8.44. In zircons from OCYB-2 Th/U is in interval 0.5 – 0.8, Nb/Ta – 2.12 – 4.25.

The REE plot confirms the general difference between zircons from two studied samples (Fig. 5.2.33). Zircons from xenolith OCYB-5 have higher concentration of all rare-earth elements. Grains from sample OCYB-2 are more depleted in REE and show lack of Eu-minima, indicating an absence of plagioclase crystallized prior to the zircons. Considering the mineral composition of xenoliths (about 40% of plagioclase) this leaves no doubt plagioclase occurred after zircon crystallization or during later metamorphism.

According to CART classification, all zircons of OCYB-2 xenolith have trace-element composition typical for grains from kimberlitic rocks (Lu<2 ppm). However, this classification ignores U and Hf contents. All zircons from OCYB-2 show U concentrations from 96 to 277 ppm, while typical kimbelitic zircons have less than 60 ppm of uranium (Belousova *et al.*, 2002). Hf contents in studied grains, in opposite, are lower (Hf<0.73 wt%), than those in kimberlitic zircons (1.2 – 2 wt%). The discrimination diagram Y *vs* U (Fig. 5.2.35) shows all data points located in between kimberlitic and lamproitic rocks. Thus, despite of some variations in trace-element composition, zircons from the xenolith OCYB-2 could be mantle-derived or possibly originate from low-fractionated mafic/syenitic magmas.

The sample OCYB-5 contains zircon grains with trace-element signatures similar to those of zircons from carbonatites and two grains with composition of trace elements suggesting mafic to intermediate parental melt according to the CART classification.



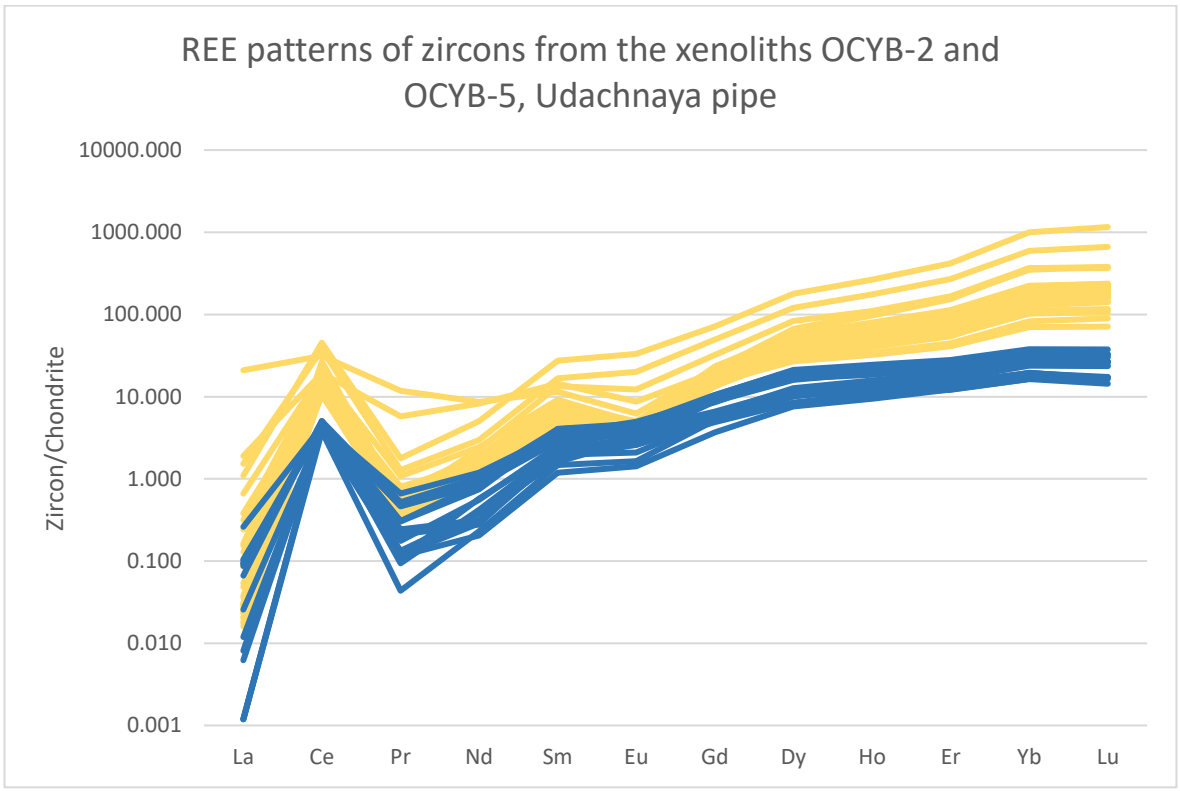




Figure 5.2.33. Trace-element and rare-earth element patterns of zircons from xenoliths, Udachnaya pipe.

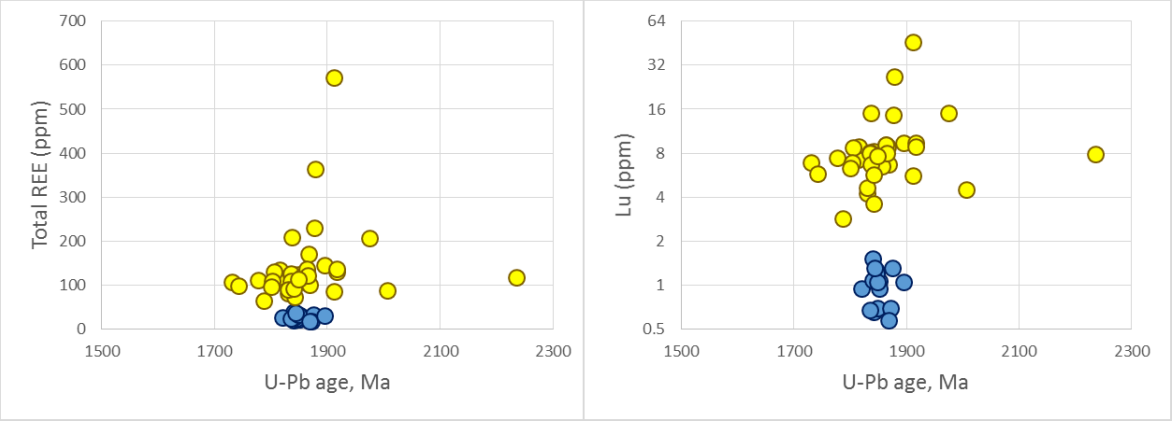



Figure 5.2.34. Total REE and Lu concentrations *vs* U-Pb age of zircons from the Udachnaya pipe. Data points are color-coded according to the TE patterns (Fig. 5.2.33).

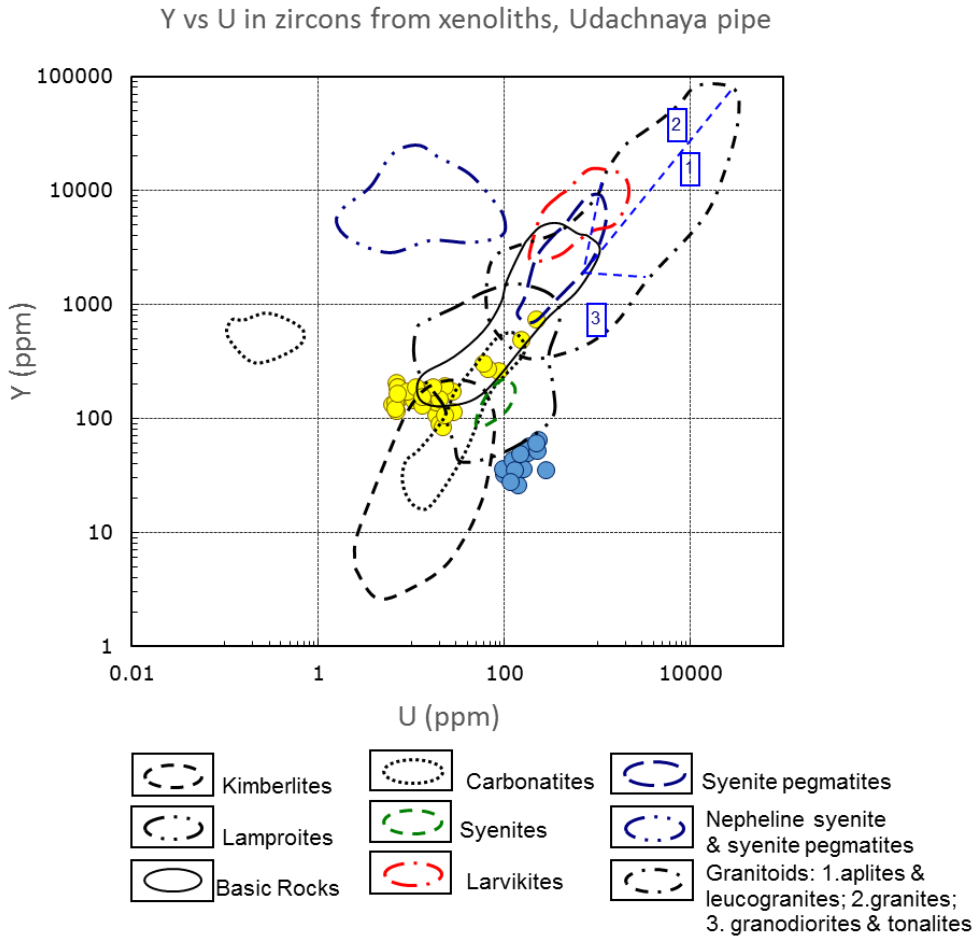



Figure 5.2.35. Y *vs* U discrimination diagram for zircons from the Udachnaya pipe. Data points are color-coded according to the TE patterns (Fig. 5.2.33).

The plot Y *vs* U shows the most of grains located within or close to kimberlitic, lamproitic and carbonatitic fields (Fig. 5.2.35). This is also confirmed by low (<20.7 ppm) concentrations of Lu and U (<100 ppm) found in the most of grains (Fig. 5.2.34).

***Oxygen isotopic data***

**The Udachnaya pipe**

Zircons from both xenoliths OCYB-2 and OCYB-5 were analysed for their oxygen isotopic composition. In total 16 zircon grains from OCYB-2 sample and 49 grains from OCYB-5 were studied.

The grains from OCYB-2 sample have values of $\delta^{18}O$ within or close to the mantle range (5.3±0.6‰, (Valley *et al.*, 2003), Fig. 5.2.36). They diverge from 5.26±0.22 to 5.93±0.24‰.

Sample OCYB-5 contains zircons with more supracrustal values of $\delta^{18}O$ – from 5.94±0.30 to 7.49±0.25.

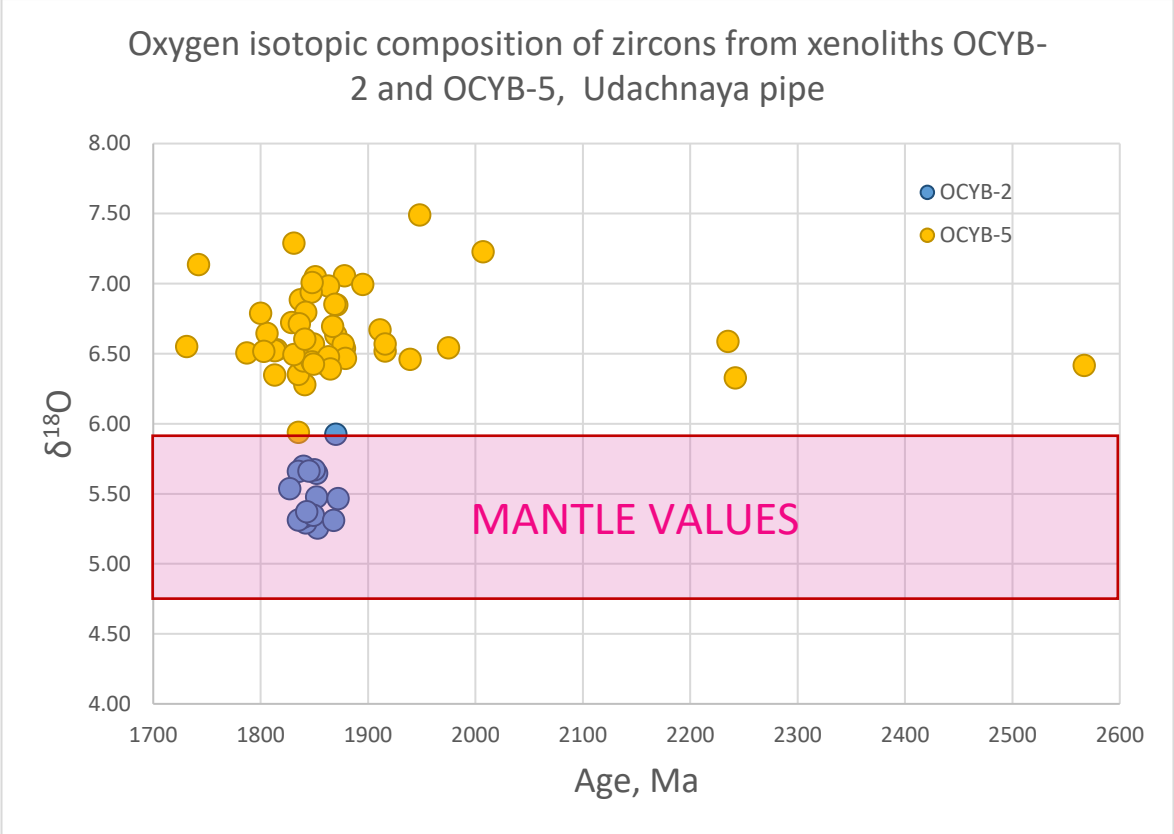



Figure 5.2.36. $\delta^{18}O$ *vs* U-Pb age for zircons from xenoliths OCYB-2 and OCYB-5, Udachnaya pipe.

***Hafnium-isotope data***

**The Udachnaya Eastern pipe**

Lu-Hf isotopes have been studied in 7 zircon grains from the pipe (9 analyses in total). All grains were dated prior to analysing for their Hf-systematics.

The calculated initial $^{176}Hf/^{177}Hf$ ratios fall into the narrow interval 0.281009 – 0.281098. εHf values and model ages vary more: εHf ranges from -1 to -19 (Fig. 5.2.37), crustal model age – from 3.28 to 3.74 Ga.

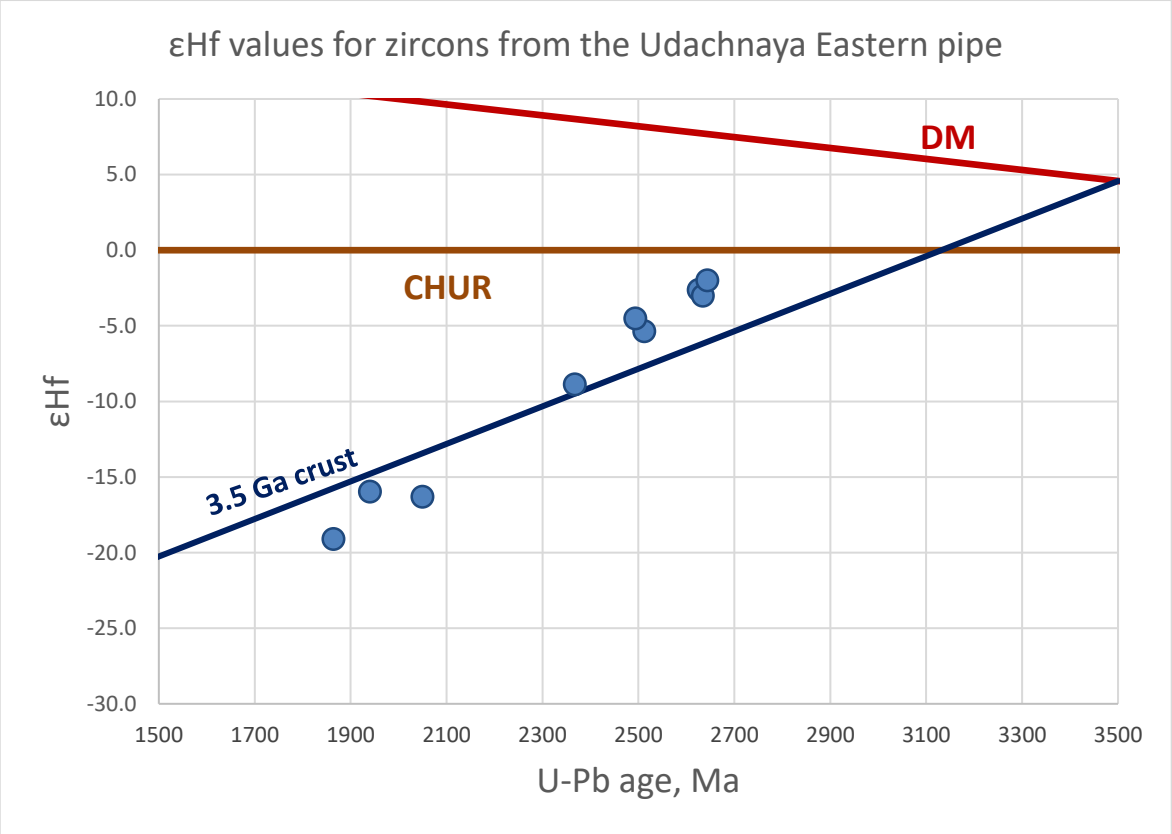



Figure 5.2.37. εHf *vs* U-Pb age plot for zircons from the Udachnaya Eastern pipe. The reference line is shown for evolution of the average continental crust.

**The Zarnitsa pipe**

Nine zircons from the Zarnitsa pipe were studied for their Lu-Hf isotopic composition.

Values of εHf fall into the range between +1.8 and -20.9 (Fig. 5.2.38). Calculated initial $^{176}Hf/^{177}Hf$ ranges from 0.280921 to 0.281445. The oldest estimated crustal model age is 3.96 Ga and the youngest one – 2.82 Ga.

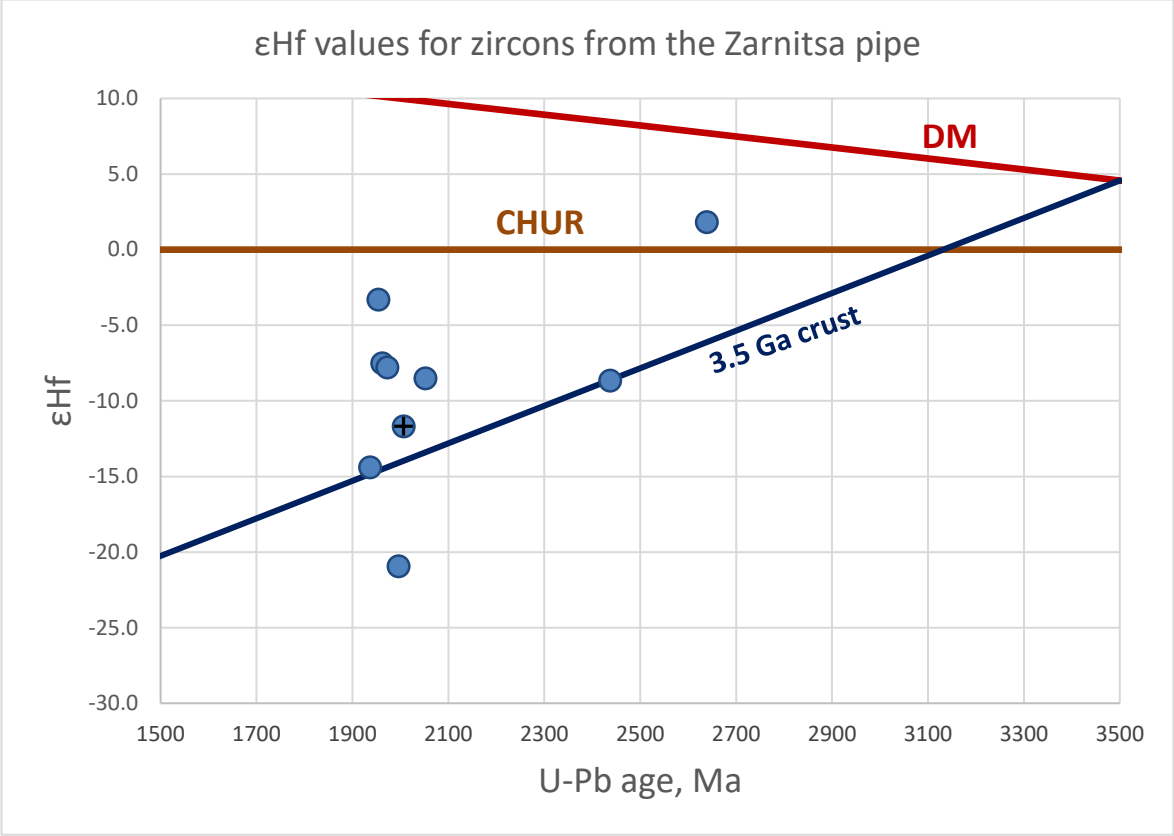



Figure 5.2.38. εHf *vs* U-Pb age plot for zircons from the Zarnitsa pipe. Grains with trace-element (TE) composition typical of mantle-derived zircons are shown with black crosses (here and further for all εHf plots). The reference line is shown for evolution of the average continental crust.

**The Popugaeva pipe**

Lu-Hf isotopes were analysed in 17 zircons from the Popugaeva pipe. Two grains contain two analytical spots each because of difference in ages of their cores and rims.

Lu-Hf isotopic signatures are different for zircons with age of 1800-2000 Ma in comparison to those older than 2000 Ma.

For the relatively young zircons calculated initial $^{176}Hf/^{177}Hf$ ratios form the range from 0.280970 to 0.281502. εHf values are scattered between -2.6 and -23.2 (Fig. 5.2.39). Calculated crustal model ages are within the interval 2.73 – 3.93 Ga.

Zircons older than 2000 Ma have wider range of εHf values – from -1 to -37.8. Initial $^{176}Hf/^{177}Hf$ ratio for this group diverge in between 0.280359 and 0.280967. The youngest calculated crustal model ages is 3.38 Ga. The oldest crustal model ages are out of geologically reasonable interval (from 4.7 to 5.09 Ga), $T_{DM}$ ages are within the range 3.63 – 3.93 Ga.

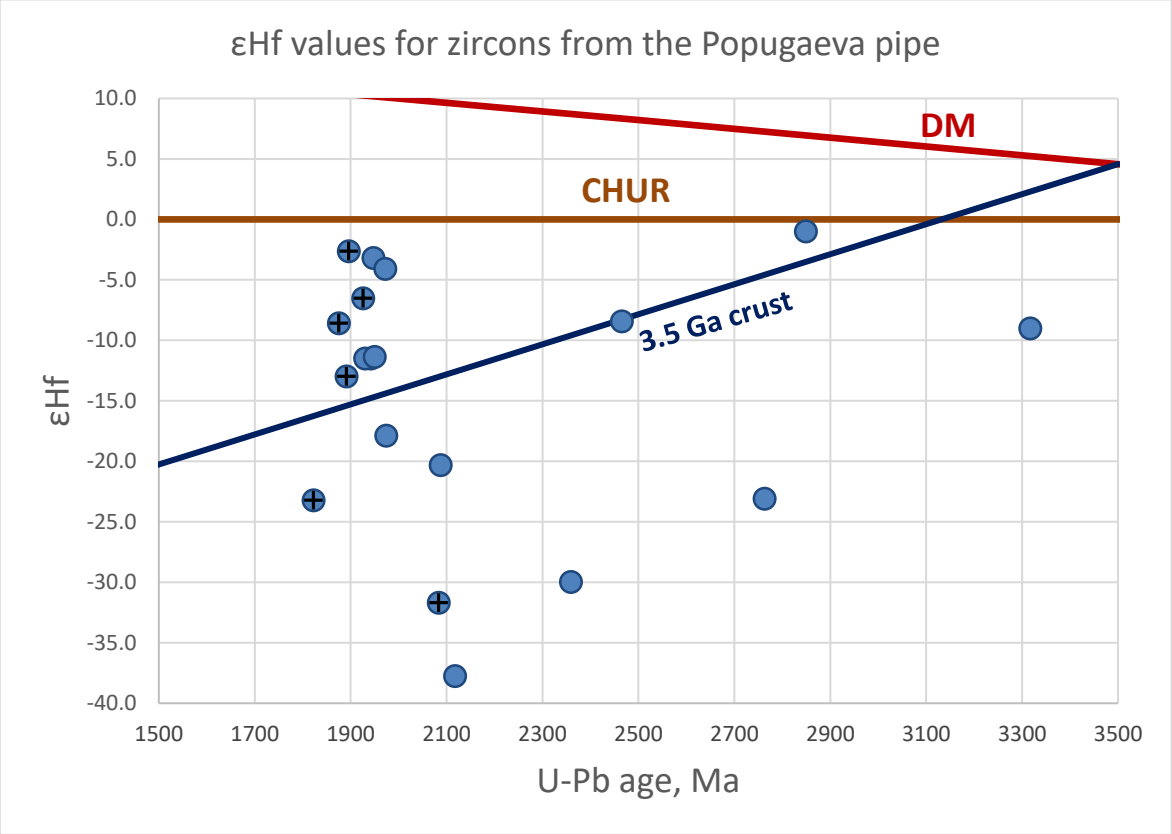



Figure 5.2.39. εHf *vs* U-Pb age plot for zircons from the Popugaeva pipe.

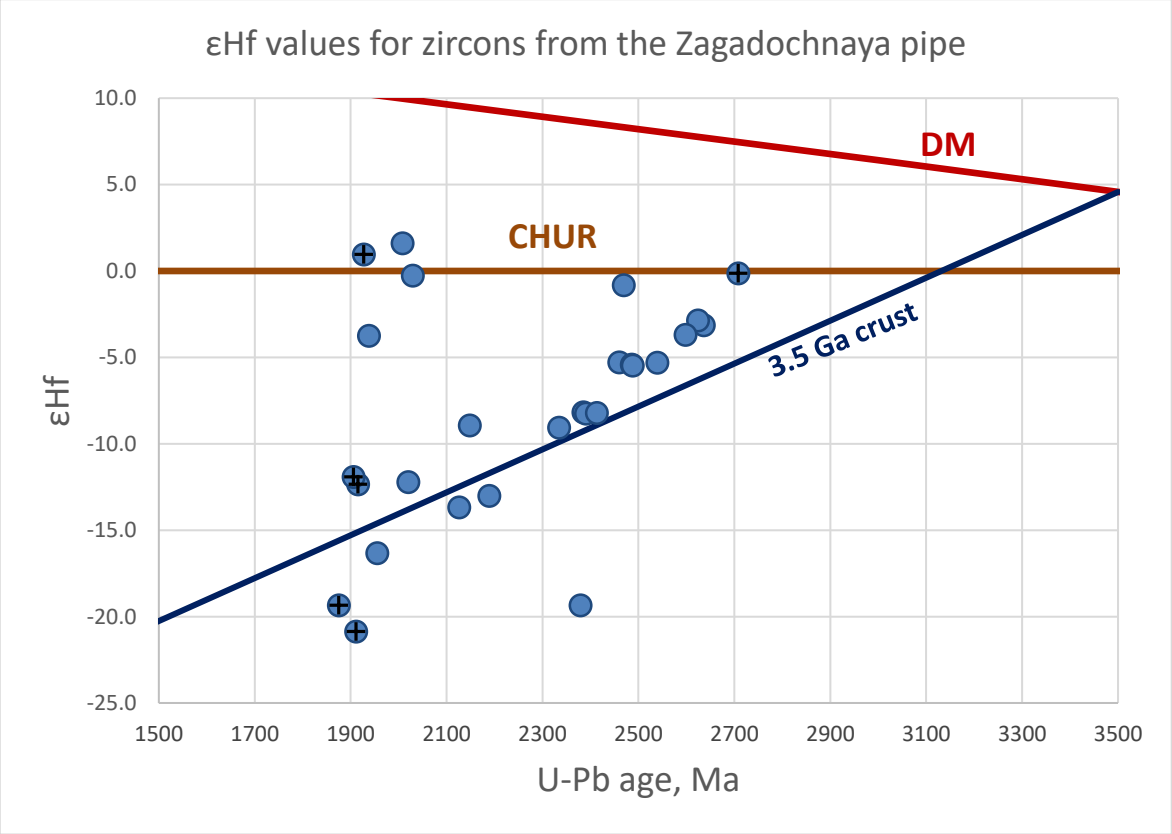



Figure 5.2.40. εHf *vs* U-Pb age plot for zircons from the Zagadochnaya pipe.

**The Zagadochnaya pipe**

Twenty-seven zircons were studied for Lu-Hf isotopic systematics. Within this set of grains there is no obvious correlation between U-Pb age of zircons and their Hf composition (Fig. 5.2.40). Obtained εHf values show a wide range from +1.6 to -20.9. Calculated initial $^{176}Hf/^{177}Hf$ fall from 0.280717 t 0.281583. The estimated crustal model ages vary from 2.53 to 4.16 Ga.

**The Kusova pipe**

In total 39 zircon grains were studied for their Lu-Hf isotopic systematic.

The εHf plot (Fig. 5.2.41) demonstrates two distinctive group of zircons: one with all negative εHf values and U-Pb ages from 1900 to 2660 Ma; and another group with εHf positive or close to 0 and U-Pb ages from 1897 to 2176 Ma.

The first group shows εHf values from -1.6 to -23.1. The lowest initial $^{176}Hf/^{177}Hf$ ratio is 0.280877, the highest – 0.281293. Calculated crustal $T_{DM}$ ages are within the range 3.16 – 4.07 Ga.

The second group has less variable εHf – from -1.2 to +4.4. Initial $^{176}Hf/^{177}Hf$ ratio vary from 0.281479 to 0.281667. Crustal $T_{DM}$ ages calculated for this group fall into the range 2.37 – 2.66 Ga.

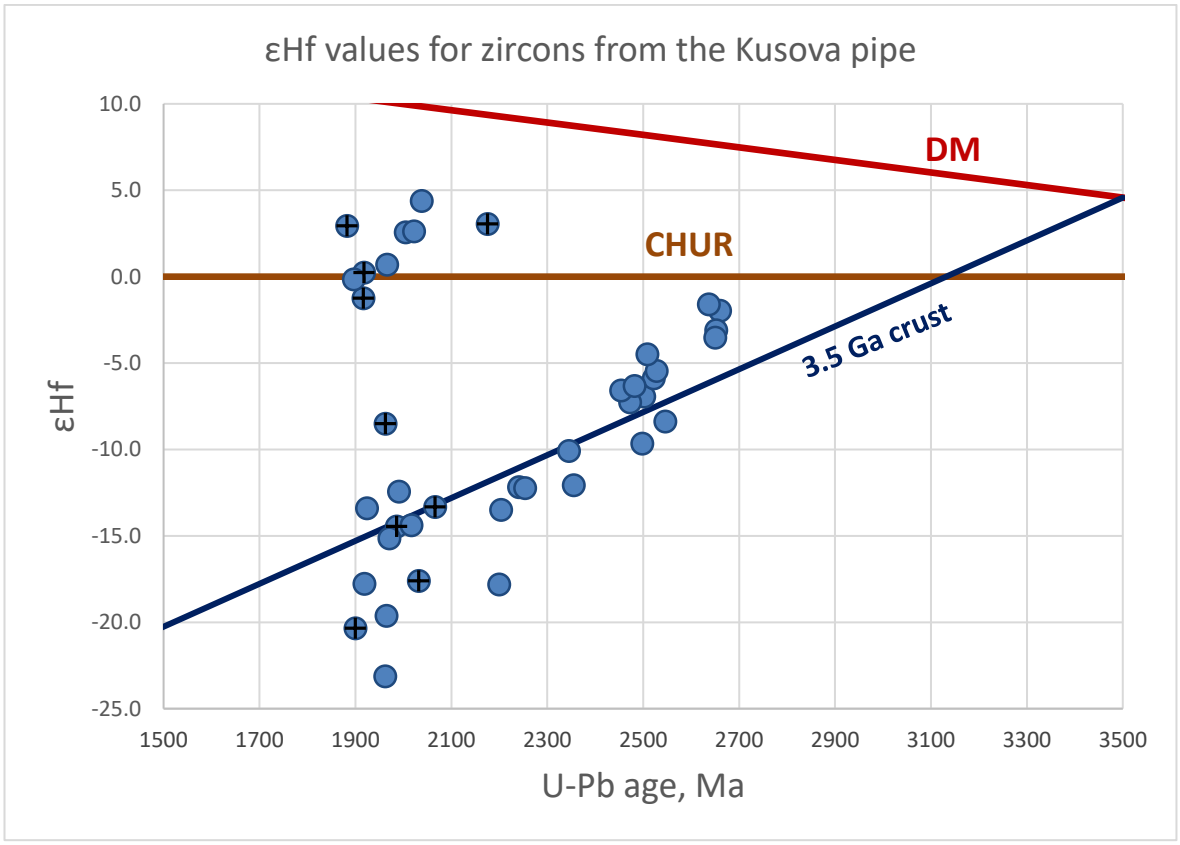



Figure 5.2.41. εHf *vs* U-Pb age plot for zircons from the Kusova pipe.

**The Udachnaya pipe**

Lu-Hf isotopic systematic was studied in zircons from both crustal xenoliths OCYB-2 and OCYB-5.

In sample OCYB-2 twelve grains were analysed. They form a uniform population at the εHf plot (Fig. 5.2.42). The εHf values are within the narrow interval -0.6 - +4.4. Calculated initial $^{176}Hf/^{177}Hf$ ratio ranges from 0.281608 to 0.281728. Crustal model ages for these grains are from 2.25 to 2.54 Ga.

Twenty-eight zircons from the sample OCYB-5 have wider range of εHf – from -23 to -3.9. Their initial $^{176}Hf/^{177}Hf$ ratio vary in interval 0.280950 – 0.281266. Calculated crustal model ages fall in between 3.26 and 3.98 Ga.

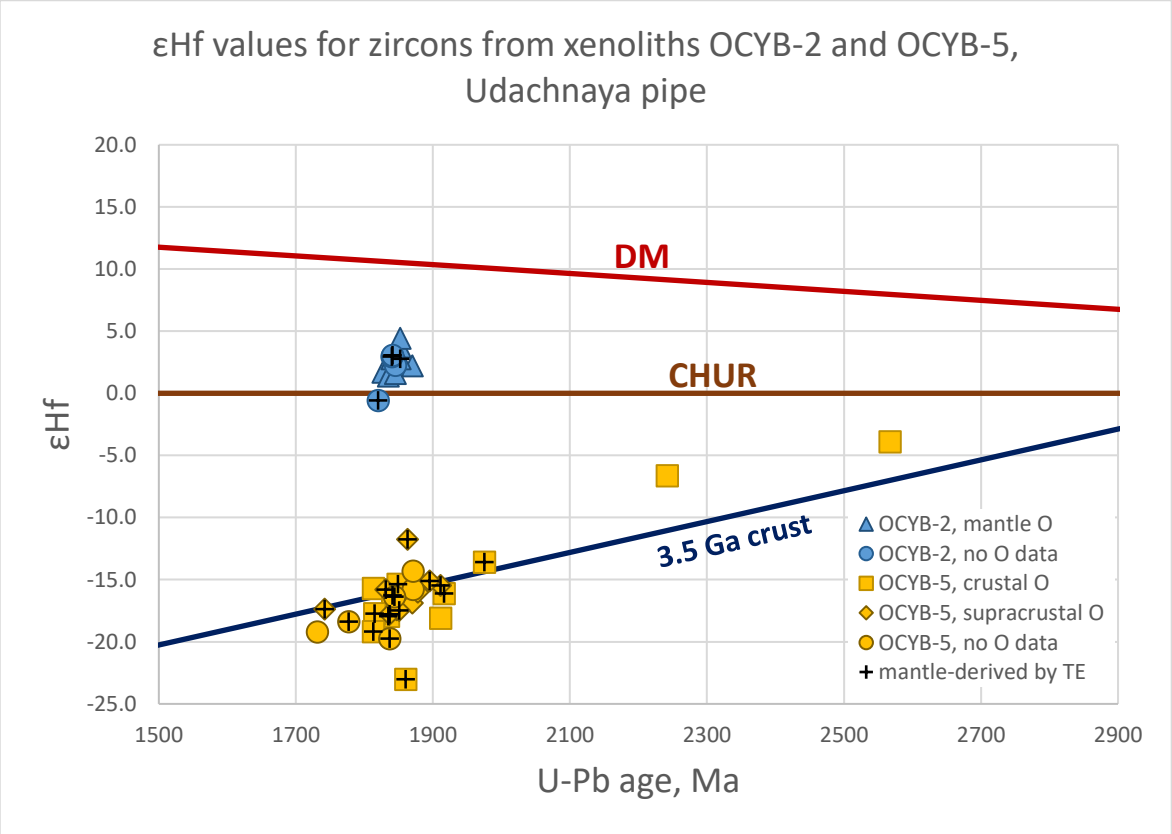



Figure 5.2.42. εHf *vs* U-Pb age plot for zircons from xenoliths OCYB-2 and OCYB-5, Udachnaya pipe. Different markers are used according to the zircon O-isotope composition (where these data are available).

***Sulfide Re-Os and PGE data***

**The Udachnaya pipe**

Re-Os isotopic compositions for 2 types of "primary" Fe-Ni monosulfide solid solution (MSS) sulfides from harzburgite-dunite xenoliths from the Udachnaya kimberlite pipe have been determined by laser ablation MC-ICP-MS. The model ages ($T_{RD}$) obtained for sulfides during this work fall into two main intervals - 3.0 - 3.5 Ga and 2.8 - 2.98 Ga and are well correlated with previous results for subcontinental lithospheric mantle under the Siberian Craton (Griffin *et al.*, 2002a, Pearson *et al.*, 1999, Pearson *et al.*, 1995b, Pearson *et al.*, 2002).

The Udachnaya kimberlite pipe has brought to the surface a wide range of uniquely fresh mantle xenoliths. One of the most interesting types is the megacrystalline pyrope harzburgite-dunites, which consist primarily of ultracoarse olivine (up to 10 cm), orthopyroxene and subcalcic Cr-pyrope; some of them also contain diamond ± chromite. Their constituent minerals are very similar in composition to the mineral inclusions in the Udachnaya diamonds. Based on this observation it was proposed that harzburgite-dunite xenoliths with high-chromium subcalcic pyrope represent fragments of the host rocks of the Siberian diamonds (Malkovets *et al.*, 2007, Pokhilenko *et al.*, 2014).

The lithospheric mantle of the Siberian craton experienced melting in the Archaean (Pearson et al 1995; Griffin et al. 2014) and is characterized by extreme depletion of incompatible major elements indicating extensive (~40%) melt extraction (Boyd *et al.*, 1997). Mantle that has experienced such high-degree melting usually would not be expected to have residual sulfides. However, our first detailed mineralogical study of the megacrystalline pyrope harzburgite-dunite xenoliths has revealed abundant enclosed and intergranular sulfides. The sulfides can be subdivided into several groups: 1) "primary" Fe-Ni MSS sulfides enclosed in olivine (no cracks around sulfides have been found); 2) Fe-Ni MSS sulfides enclosed in olivine but with djerfisherite ($K_6Na(Fe^{2+},Cu,Ni)_{25}S_{26}Cl$) rims (these sulfides are located in cracks cutting olivine crystals); 3) interstitial Fe-Ni MSS sulfides with djerfisherite rims; 4) numerous interstitial grains of djerfisherite. Sulfides of the first three groups reach 500 microns in diameter, while most interstitial djerfisherites rarely reach 100 microns.

The Os concentrations of the Fe-Ni MSS sulfides of different groups vary over a wide range from 4 to 2475 ppm. Chondrite-normalised PGE abundance patterns are generally characterized by depletion in PPGE relative to IPGE (Fig 5.2.43, 5.2.44). There is no difference in the concentrations of PGE between Fe-Ni MSS cores and their djerfisherite rims (Fig. 5.2.44). This suggests that the kimberlitic fluid responsible for crystallisation of the djerfisherite rims around primary Fe-Ni MSS sulfides did not transport significant amounts of PGE.

Re-Os isotopic compositions have been determined by laser ablation MC-ICP-MS for 13 sulfides (4 of group 1 and 9 of group 2) in eight xenoliths. All Group 1 sulfides have very low $^{187}Re/^{188}Os$ (<0.09), whereas Group 2 sulfides have a wider range (0.02-1.2). Modelling by Griffin *et al.* (2002a) suggested that sulfides with $^{187}Re/^{188}Os$ <0.07 are unlikely to have been disturbed by any metasomatic events.

For Group 1 sulfides $T_{CHUR}$ ages fall mainly between 3.2 and 3.9 Ga and $T_{RD}$ (Re-depletion) ages between 3 and 3.51 Ga (±0.03 Ga, mean 2s analytical uncertainty). $T_{RD}$ model ages for Group 2 sulfides fall into two intervals: 2.83-2.98 Ga and 1.87-2.12 Ga.

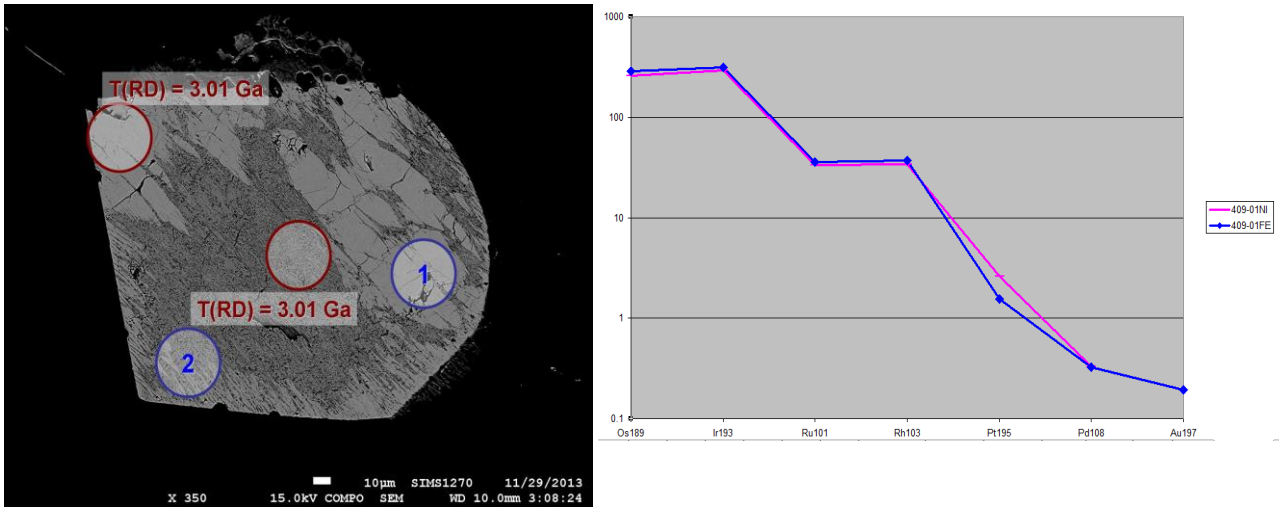



Figure 5.2.43. $T_{RD}$ model age and chondrite-normalised PGE patterns of the Group 1 sulfide inclusion. Red circles show Re-Os analysing spots, blue circles – PGE composition analysing spots.

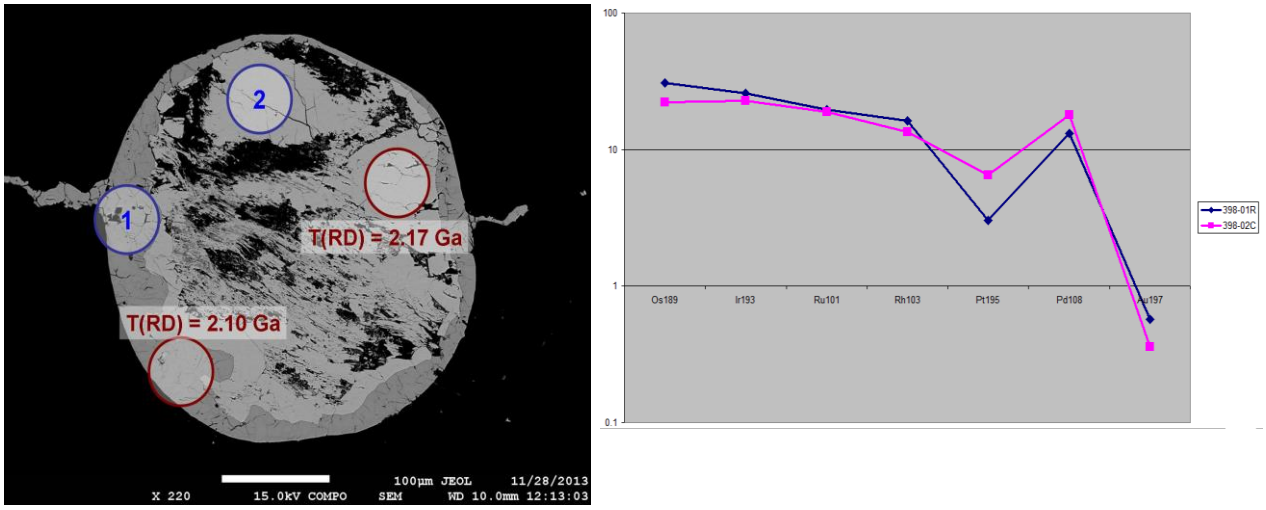



Figure 5.2.44. $T_{RD}$ model age and chondrite-normalised PGE patterns of the Group 2 sulfide inclusion.

## 5.3 The Alakit-Markha kimberlite field

The field is located within the basin of Alakit and Markha rivers. The kimberlite bodies are hosted by Ordivician and Silurian sedimentary rocks and are covered by sedimentary units of Middle to Late Carboniferous and Permian age and Low Triassic mafic sills.

More than 80 kimberlite bodies have been discovered within the field, those include pipe, dykes and stocks. Geological evidences that allow constraining the age of kimberlite magmatism include xenoliths of Late-Devonian sedimentary rocks, intrusion of Permian-Triassic dolerite in the Komsomolskaya kimberlite pipe and finding of the kimberlite-originated minerals in the Early-Carboniferous sediments. Thus, based on geological observation the age of kimberlite magmatism within the Alakit-Markha field was determined as 364-350 Ma (Zaitsev & Smelov, 2010).

This age is also confirmed by various isotopic geochronological studies (Rb-Sr, U-Pb, K-Ar, Ar-Ar techniques). Most of results are within that time interval assuming the analytical uncertainty; however, there are also ages reported in the range from 229 to 439 Ma.

### *Zircon U-Pb data*

Zircons were collected from heavy-mineral concentrate from weathered crust of a kimberlite pipe. Six pipes were sampled by this approach: Kismet, Vostok, Veselaya, Krasnopresnenskaya, Markha and Geochemical. The zircons from the Aikhal pipe were picked directly from crushed kimberlite. The summary of U-Pb ages of the Alakit-Markha field is given in Table 5.3.1.

#### The Kismet pipe

In total 35 grains were dated, one analysis was rejected because of its high discordance.

All grains fall into the interval of ages between 1766 and 2064 Ma. The weighted mean age calculated on 32 out of 34 analyses give age of 1894±12 Ma (MSWD = 1.01, probability = 0.45, Fig. 5.3.1).

#### The Geochemical pipe

Only 6 zircons were recovered from the heavy-mineral concentrate from this pipe. Their U-Pb ages range from 1866 to 1994 Ma and form a single population with weighed mean age of 1930±53 Ma (MSWD = 0.37, probability = 0.87; Fig. 5.3.2).

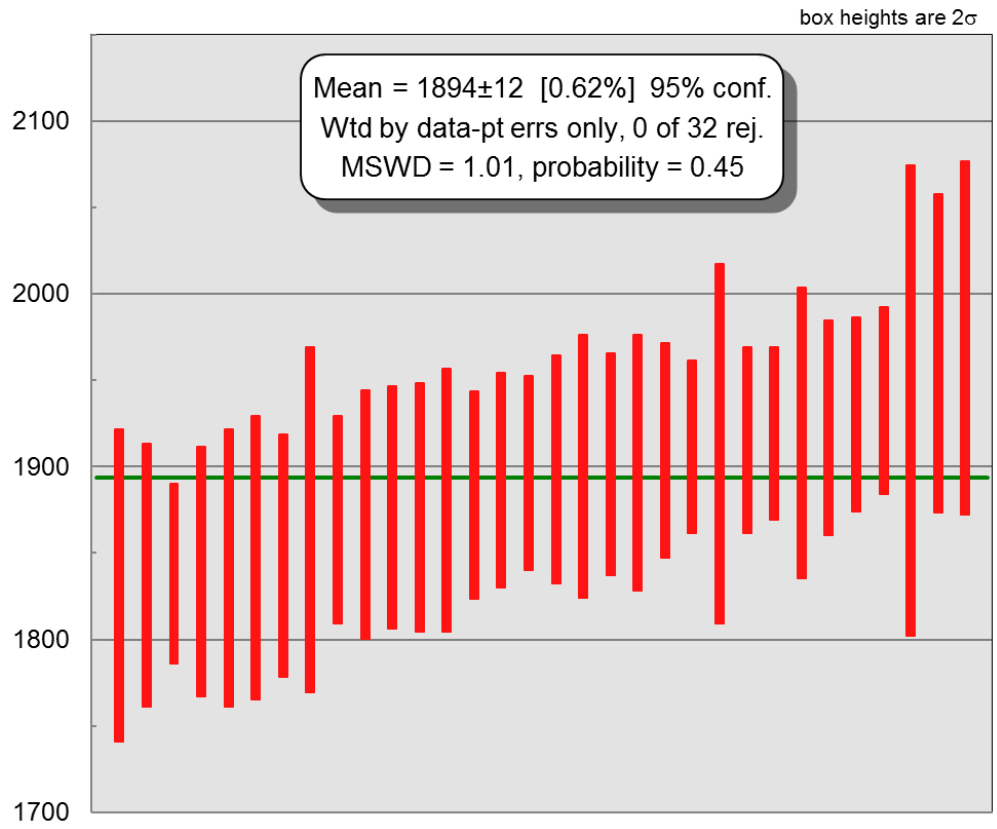



Figure 5.3.1. The weighted mean age of zircons from the Kismet pipe.

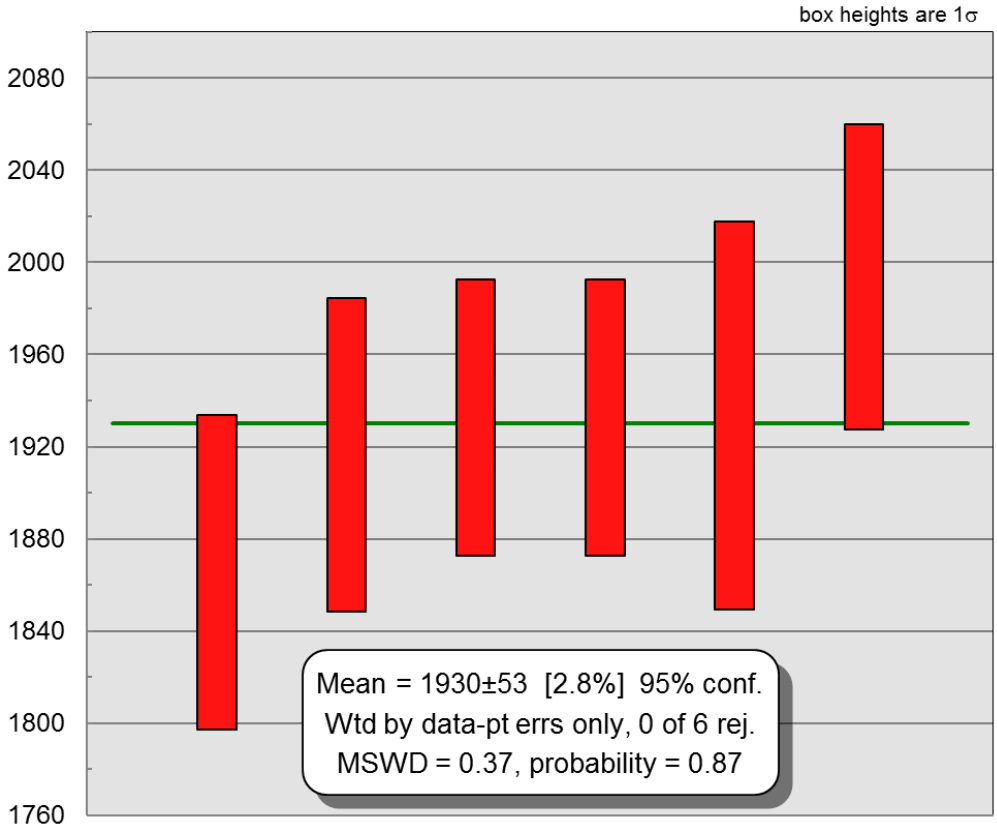



Figure 5.3.2. The weighted mean age of zircons from the Geochemical pipe.

Table 5.3.1. U-Pb ages of zircons from heavy-mineral concentrate, Alakit-Markha kimberlite field

| Pipe | Range of U-Pb ages, Ma (n = number of analyses) | Major peak mean age, Ma | Upper intercept, Ma | Lower intercept, Ma |
|---|---|---|---|---|
| **Kismet** | 1766 - 2064 (n = 34) | 1894±12 (n=32) | 1896±19 | 155±440 |
| **Geochemical** | 1866 – 1994 (n=6) | 1930±53 (n=6) | n/a | n/a |
| **Vostok** | 1794 – 2427 (n = 35) | 1923±13 (n=23) | 2447±74 | 1861±26 |
| **Veselaya** | 490 - 2645 (4) | n/a | n/a | n/a |
| **Krasnopresnenskaya** | 1876 - 2311 (n = 5) | 1908±88 (n=3) | 2640±170 | 1856±45 |
| **Markha** | 260 – 3414 (n = 85) | 1870.3±9.9 (n = 19) | n/a | n/a |
| **Aikhal** | 1845 – 2027 (53) | 1938.1±7.6 (n = 49) | n/a | n/a |

**The Vostok pipe**

Thirty-six zircons from the Vostok pipe were dated, one grain has discordance more than 20% and was rejected.

The youngest obtained age is 1794±100 Ma, the oldest – 2427±62 Ma. The probability plot shows 3 age peaks (Fig. 5.3.3). Twenty-three grains form a main age peak with weighted mean age of 1923±13 Ma (MSWD = 0.72, probability = 0.83; Fig. 5.3.4). Two minor peaks have mean ages of 2249±36 Ma (MSWD = 0.30, probability = 0.88) and 2398±33 Ma (MSWD = 0.67, probability = 0.65). A single grain has been analysed in two spots placed in rim and core and revealed 1965±80 and 2365±108 Ma correspondingly.

**The Veselaya pipe**

Only 4 zircon were collected from the pipe. All of them have discordance less than 10%. The obtained ages are very different: 490±8; 778±18; 1971±64 and 2645±76 Ma.

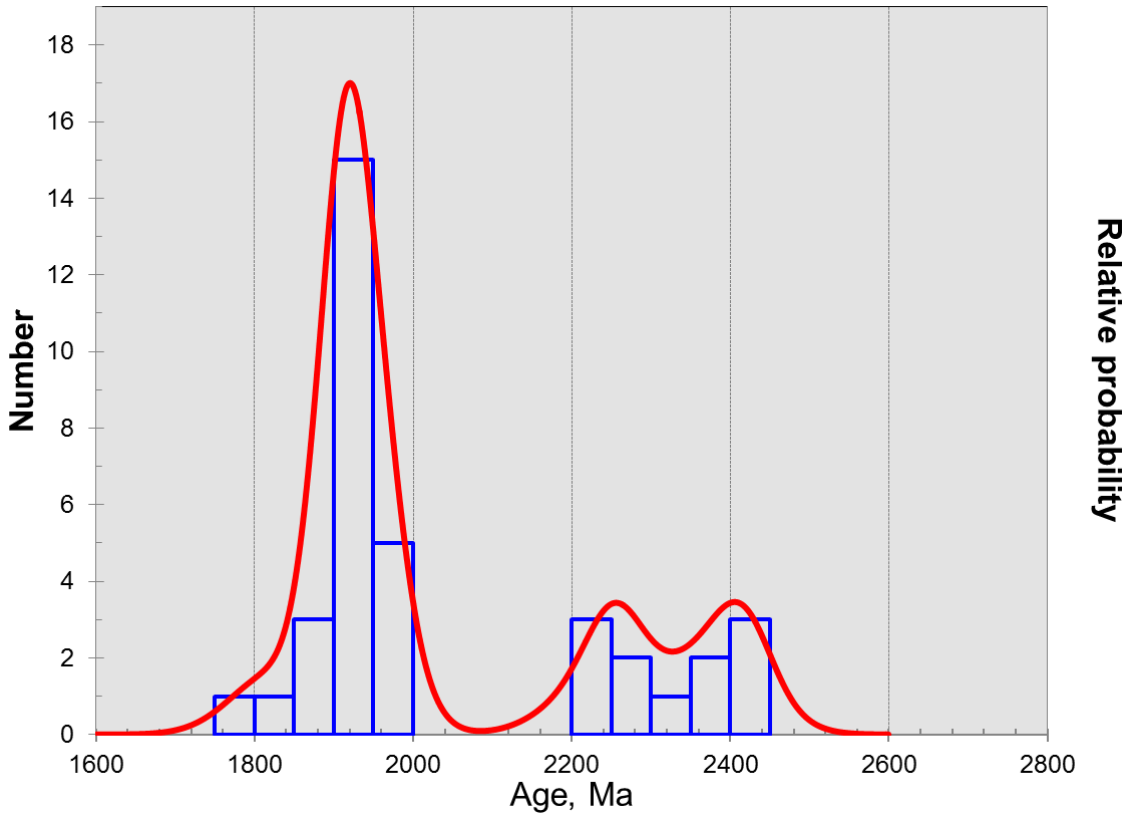



Figure 5.3.3. The U-Pb ages of zircons from the Vostok pipe.

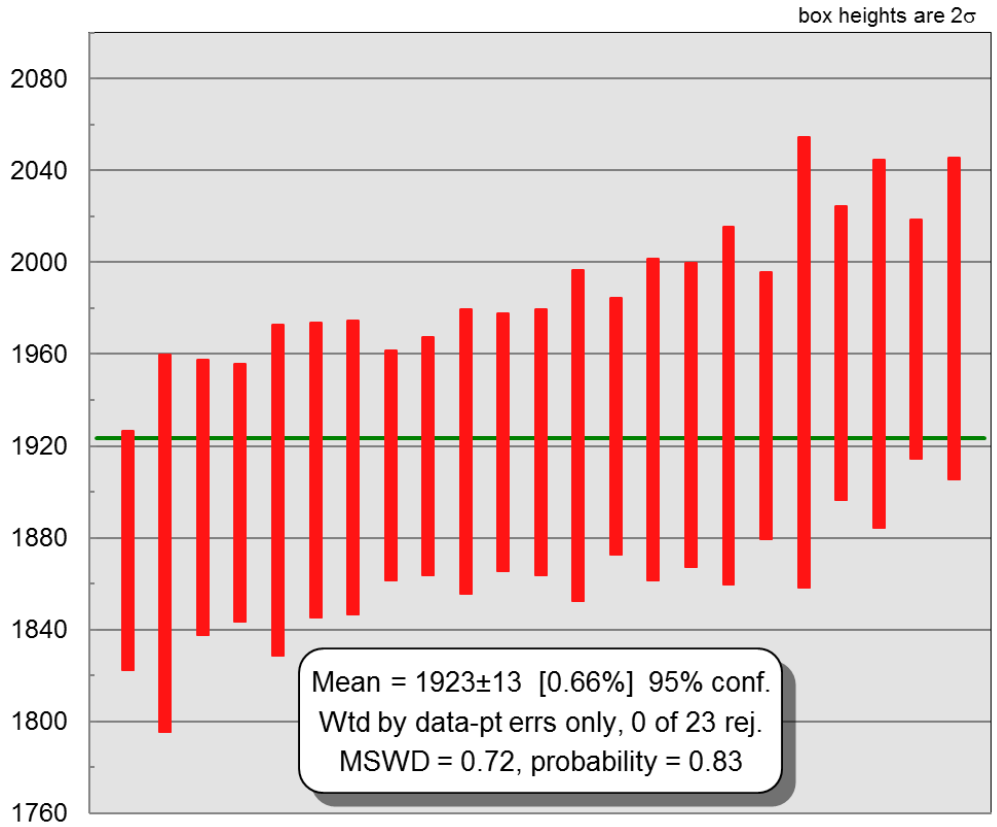



Figure 5.3.4. The weighted mean age of the main age peak, Vostok pipe.

**The Krasnopresnenskaya pipe**

Five zircons grains were studied; all of them have discordance less than 10%.

The U-Pb ages range from 1876±52 to 2311±78 Ma. All grains are lying on the regression line with upper intercept with concordia at 2640±170 Ma and lower intercept at 1856±45 Ma (MSWD = 0.58; Fig. 5.3.5).

**The Markha pipe**

In total 97 zircon grains were analysed for the U-Pb age, 13 were rejected later because of the high discordance. A single grain has been analysed twice to obtain age of observed core and rim.

Eighty-five U-Pb age data vary in a wide interval from 260 to 3414 Ma. The probability plot (Fig. 5.3.6) demonstrates a few age peaks: main one has the weighted mean age of 1870.3±9.9 (MSWD = 1.12, probability = 0.32; Fig. 5.3.7.), while minor peaks are scattered from 290 to 805 Ma and from 2000 to 3000 Ma. The grain with core and rim shows identical ages of those domains (2093±24 *vs* 2097±52 Ma).

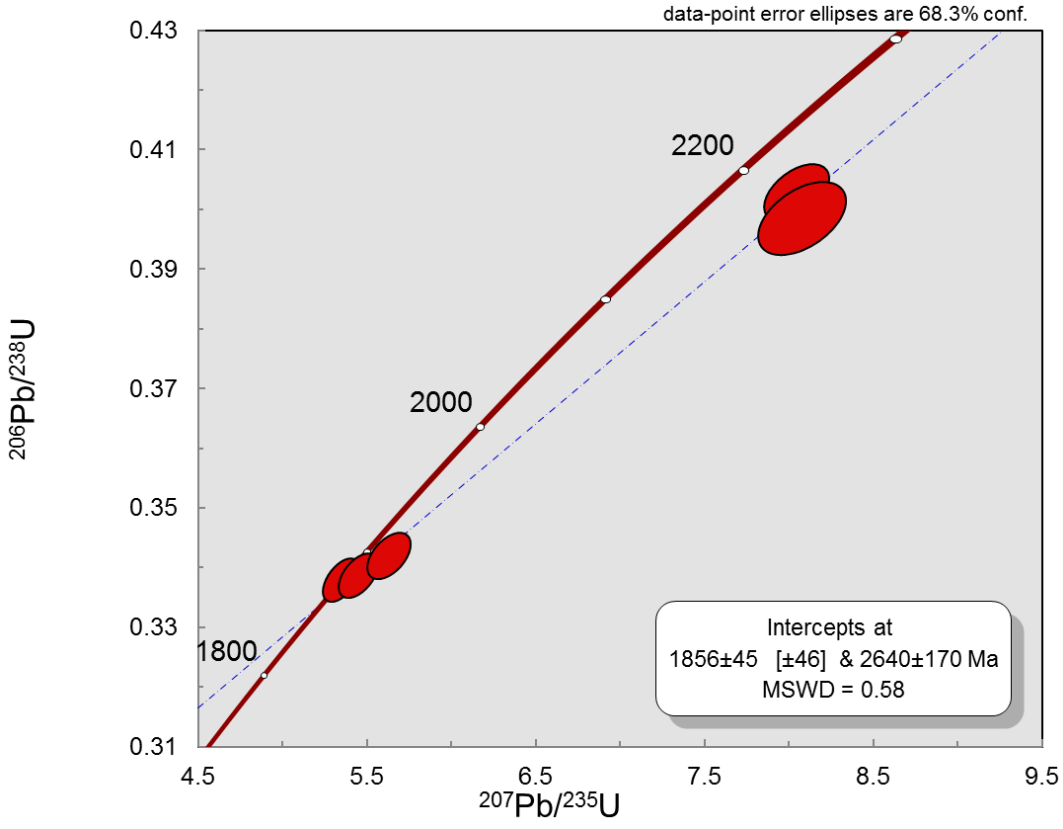



Figure 5.3.5. U-Pb concordia for zircons from the Krasnopresnenskaya pipe.

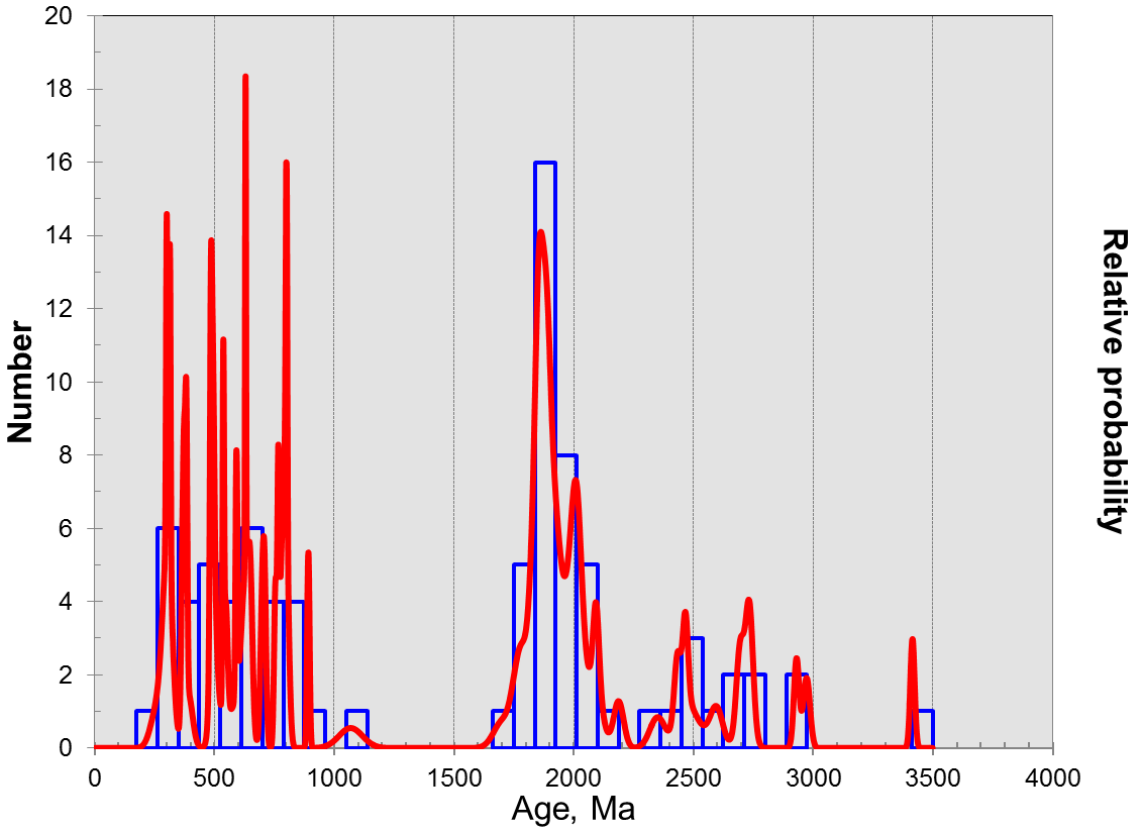



Figure 5.3.6. The U-Pb ages of zircons from the Markha pipe.

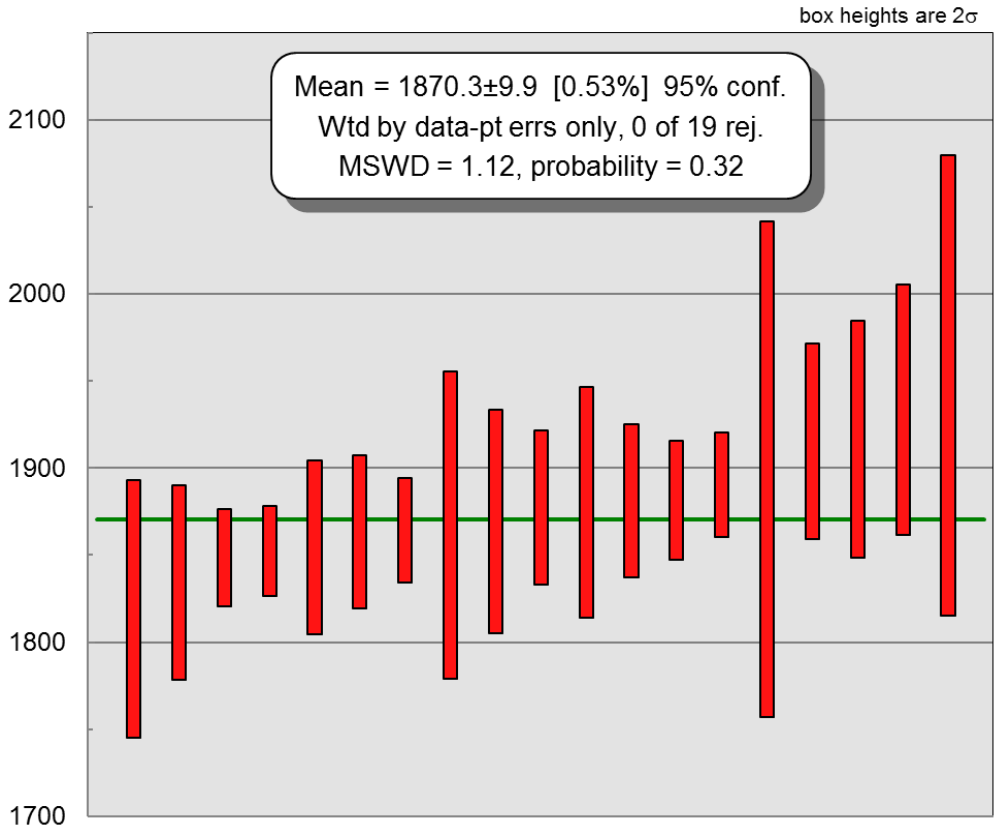



Figure 5.3.7. The weighted mean age of the main age peak, Markha pipe.

**The Aikhal pipe**

The U-Pb age were determined on 36 zircon grains from the crushed kimberlite rock of the Aikhal pipe. Some of grains showed distinctive core and rim, so 2 or even 3 analytical spots were placed within individual grains. In total 53 analyses of U-Pb ages have been done, all of them have discordance less than 10%.

The youngest obtained age is 1845±42 Ma, the oldest - 2027±56 Ma. The probability plot shows all analyses forming a single age peak (Fig. 5.3.8). The weighted mean age is calculated for 43 analyses and gives the age of 1940±6.5 Ma (MSWD = 0.95, probability = 0.56; Fig. 5.3.9).

All zircons showing core-rim zoning reveal no age difference within the grain when considering the analytical uncertainty.

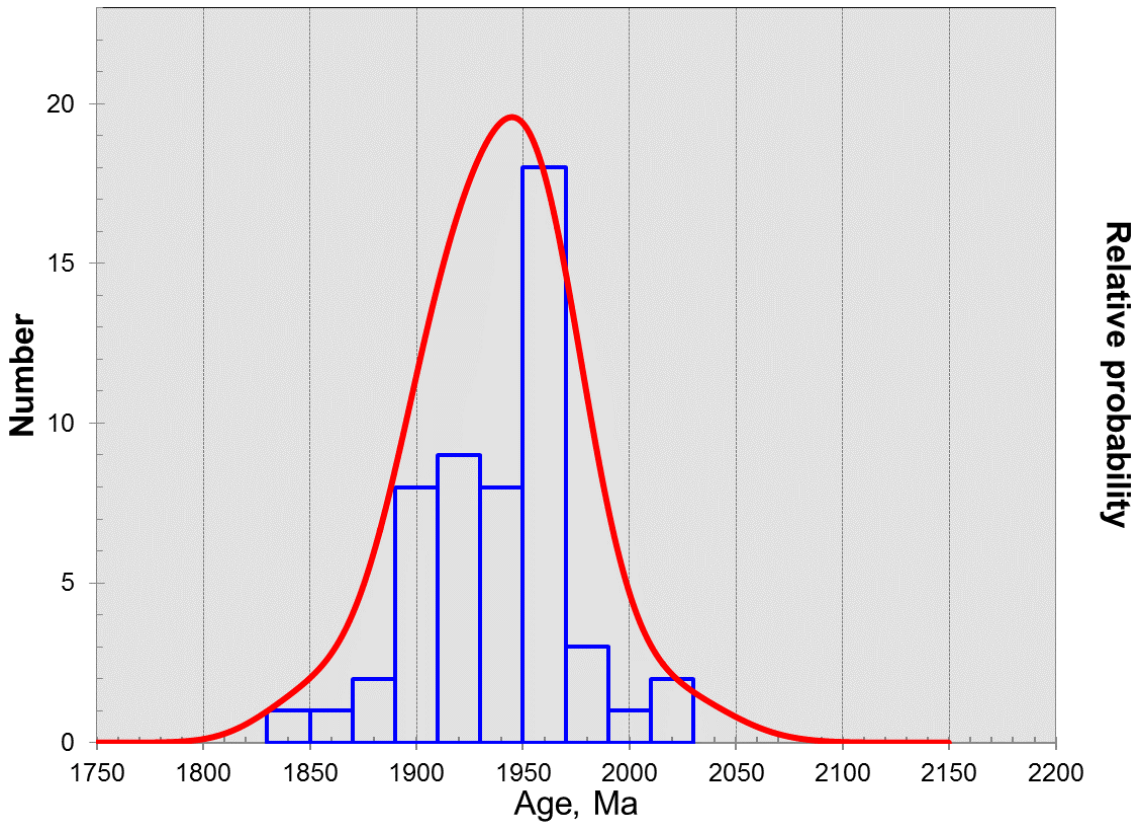



Figure 5.3.8. The U-Pb ages of zircons from the Aikhal pipe.

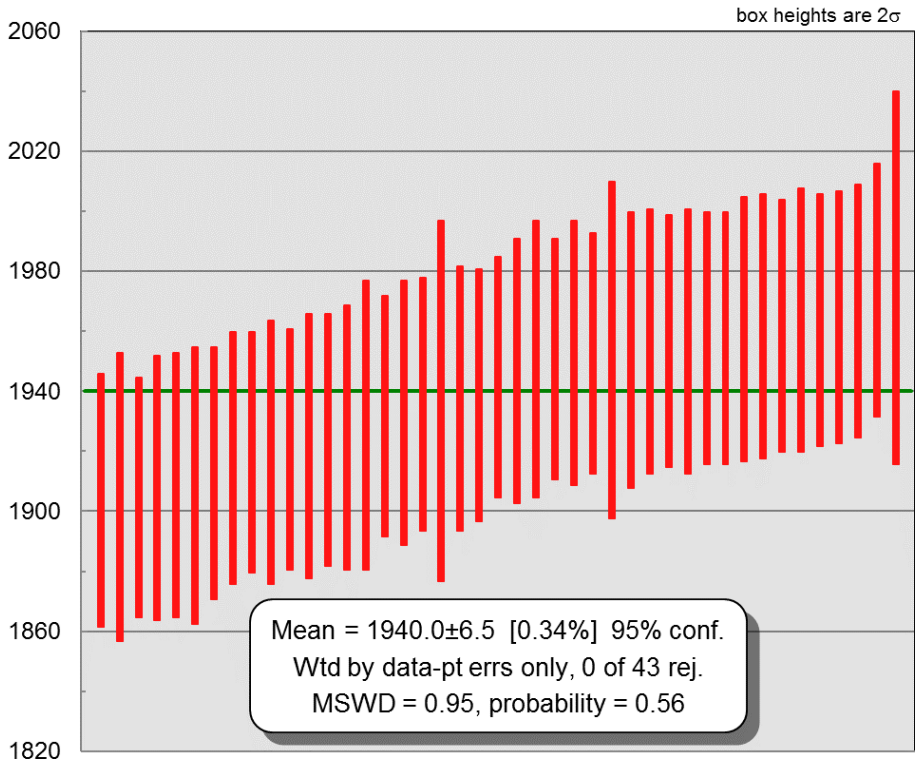



Figure 5.3.9. The weighted mean age of the main age peak, Aikhal pipe.

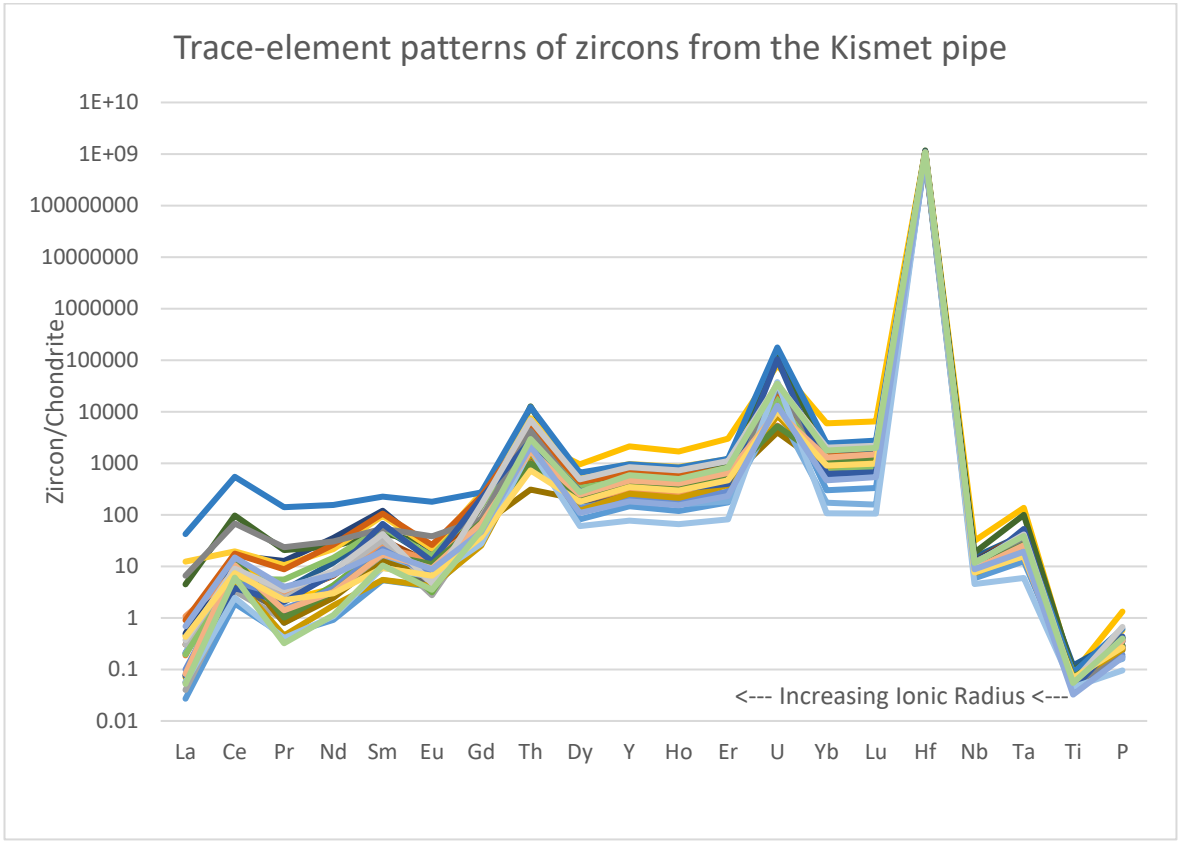
***Zircon trace-element data***

**The Kismet pipe**

Trace-element composition was studied on 31 zircon grains from the Kismet pipe.

Most of trace elements have significant variations in concentrations. Elements with larger ionic radius vary more, however even those with small radius diverge in orders of magnitude (Fig. 5.3.10). The total REE concentrations range from 95 to 3084 ppm. Y varies from 174 to 2169 ppm. A single grain contains 4780 ppm of Y, however, this grain also has the highest concentration of phosphorus (1734 ppm) , which may reflect the presence of microinclusion of apatite or monazite (Whitehouse & Kamber, 2002). U contents are within the range 40 – 1771 ppm, Th – from 12 to 509 ppm. Th/U ranges from 0.1 to 0.9, Nb/Ta – from 2.0 to 9.5. Narrow interval of U-Pb ages (1832 – 2064 Ma) makes it hard to find any regulations between zircon age and composition.

The chondrite-normalized REE plot shows typical zircon patterns with depletion in LREE and enrichment in HREE. Some grains are less depleted in LREE and thus have flatter patterns. Also these grains show less defined Eu- and Ce-anomalies. LREE enrichment has been reported previously for metamict zircons, as well as the result of zircon alteration (Belousova *et al.*, 2002, Hoskin, 2005).



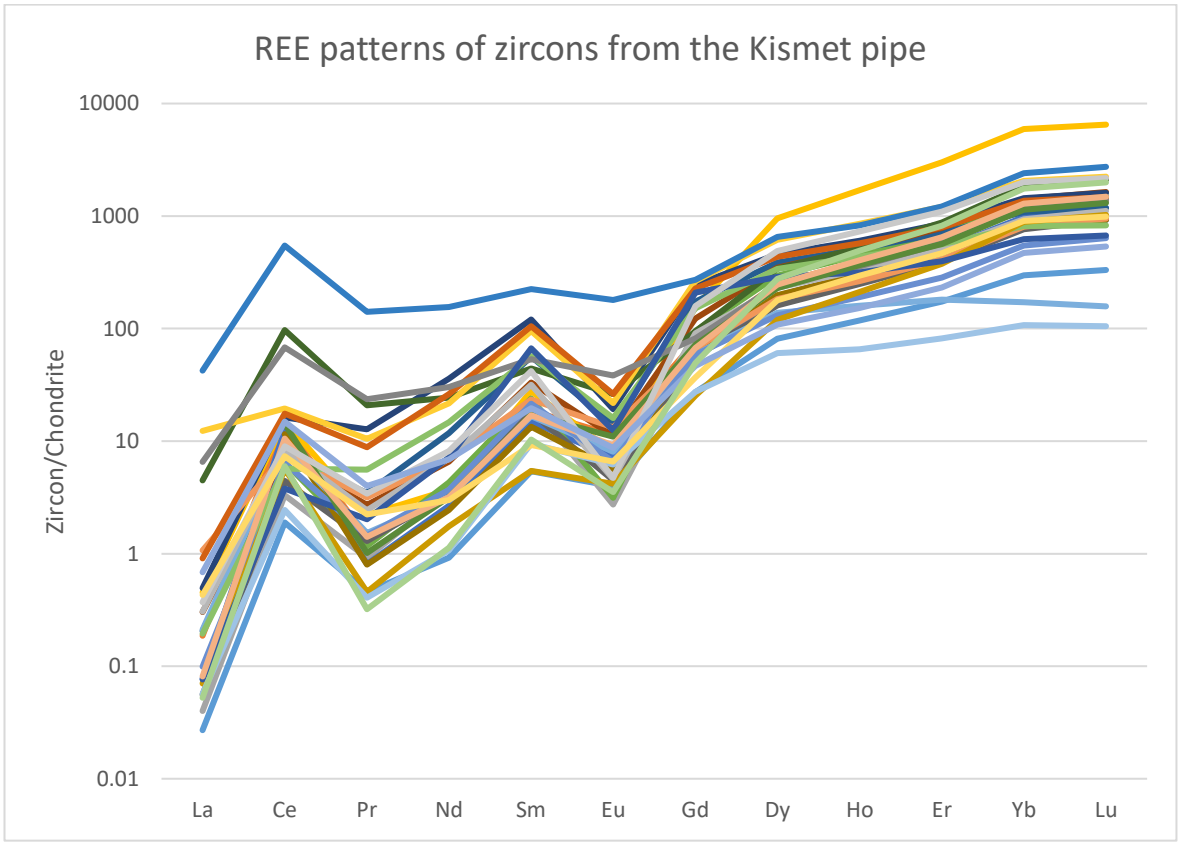




Figure 5.3.10. Trace-element and rare-earth element patterns of zircons from the Kismet pipe.

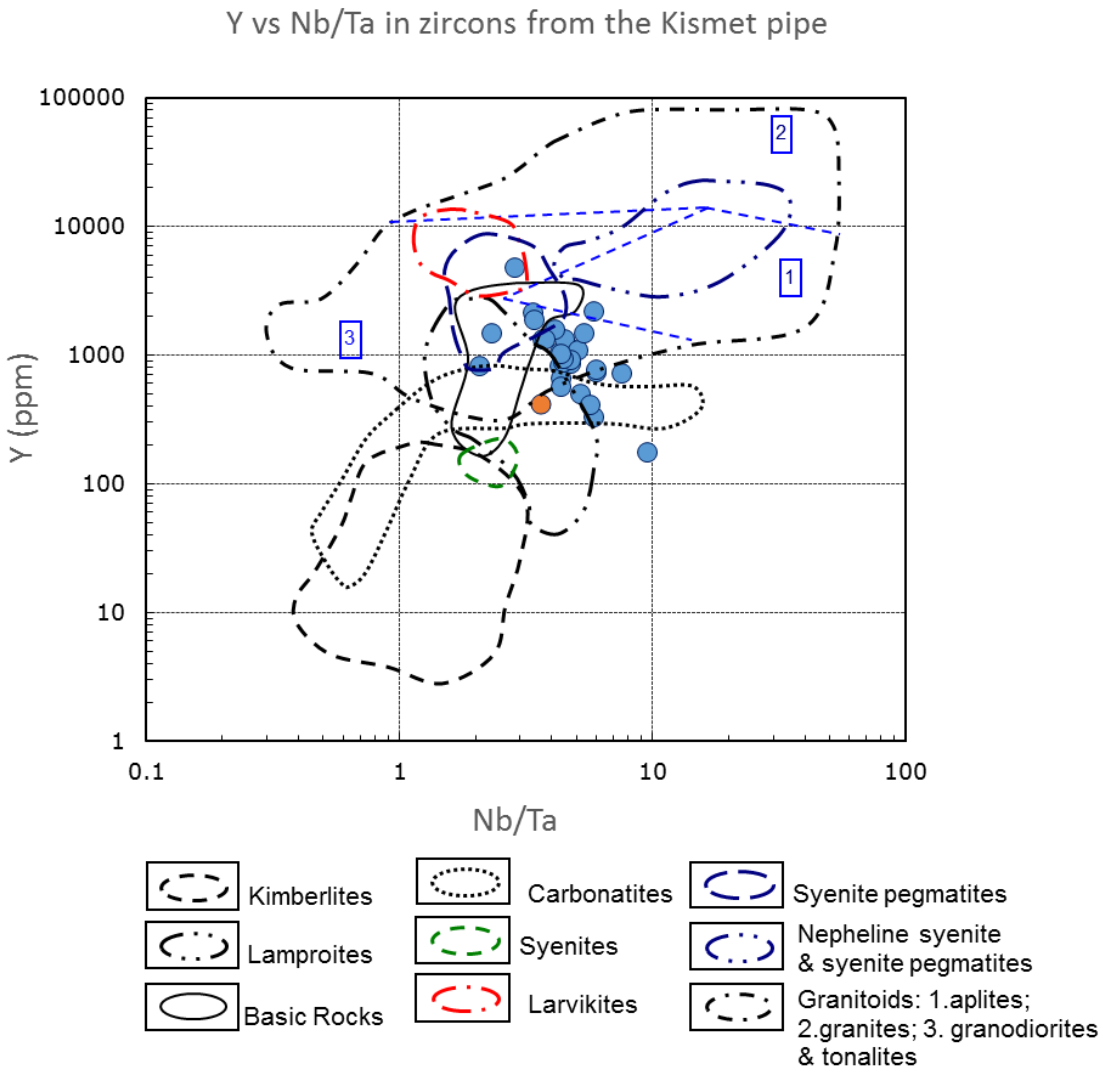
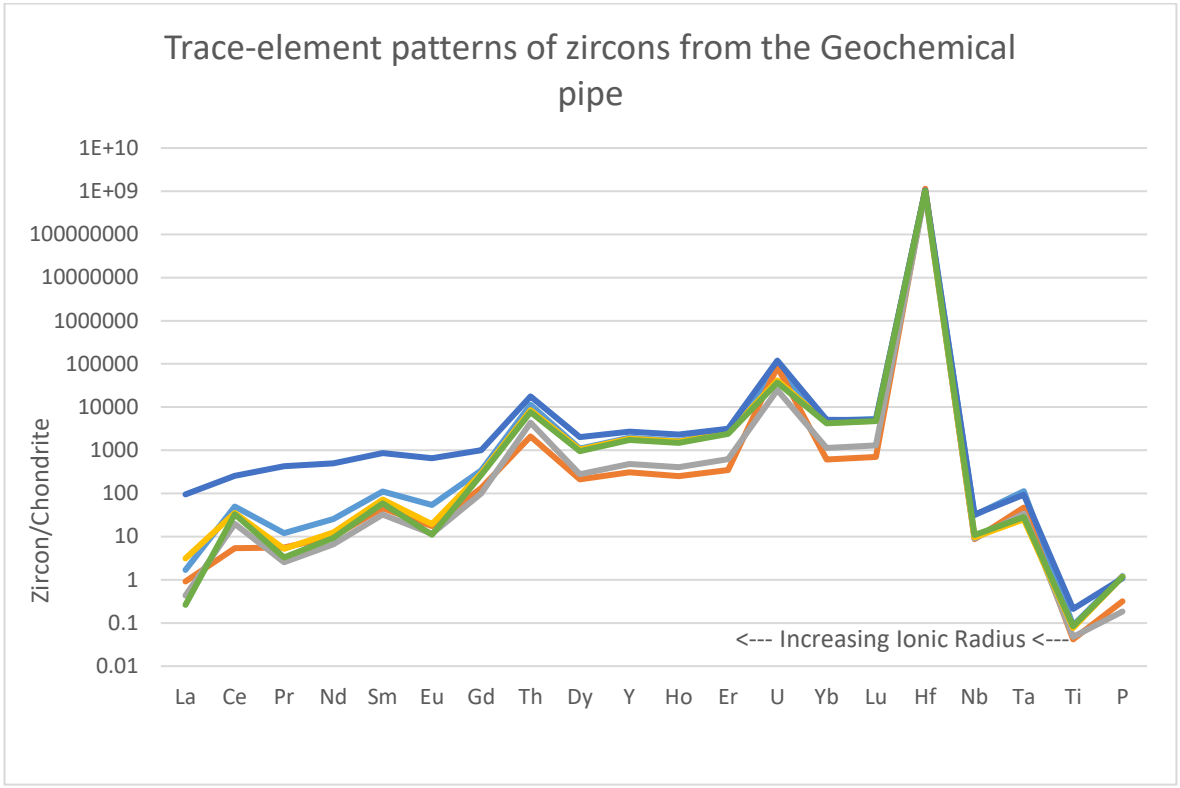



Figure 5.3.11. Y *vs* Nb/Ta discrimination diagram for zircons from the Kismet pipe. A grain classified as "carbonatitic" is shown in orange color.

According to CART statistical classification, the most of grains (22 out of 31) demonstrate trace-element signatures of zircons crystallized from intermediate to felsic parental melts. The composition of 8 zircons is similar to those from mafic rocks, and 1 grain shows trace-element composition typical for zircons from carbonatites (Lu<20.7 ppm). The discrimination diagram Y *vs* Nb/Ta confirms possible carbonatitic origin of this grain (Fig. 5.3.11).

**The Geochemical pipe**

Each of six zircons (U-Pb age 1866 – 1994 Ma) from the pipe was analysed for its trace-element composition. All grain have similar trace-element patterns (Fig. 5.3.12), except one enriched in LREE (MVG459_Gch-05).



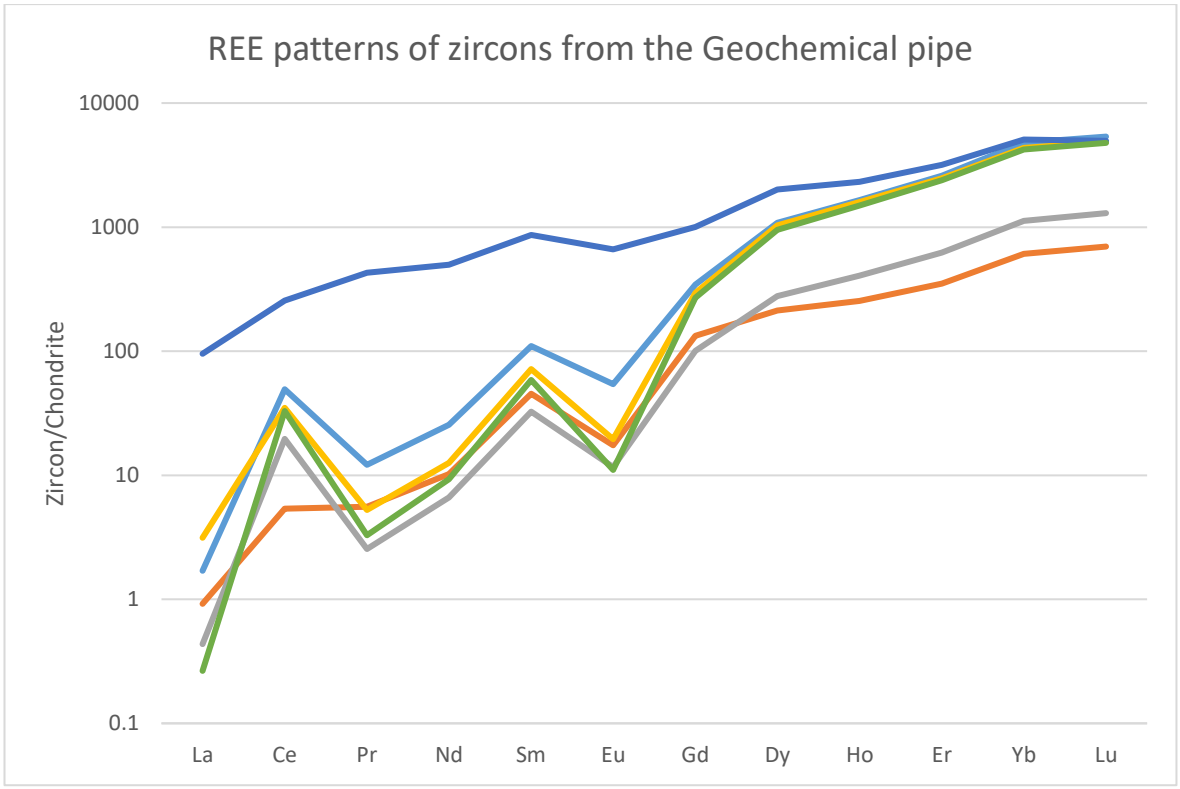
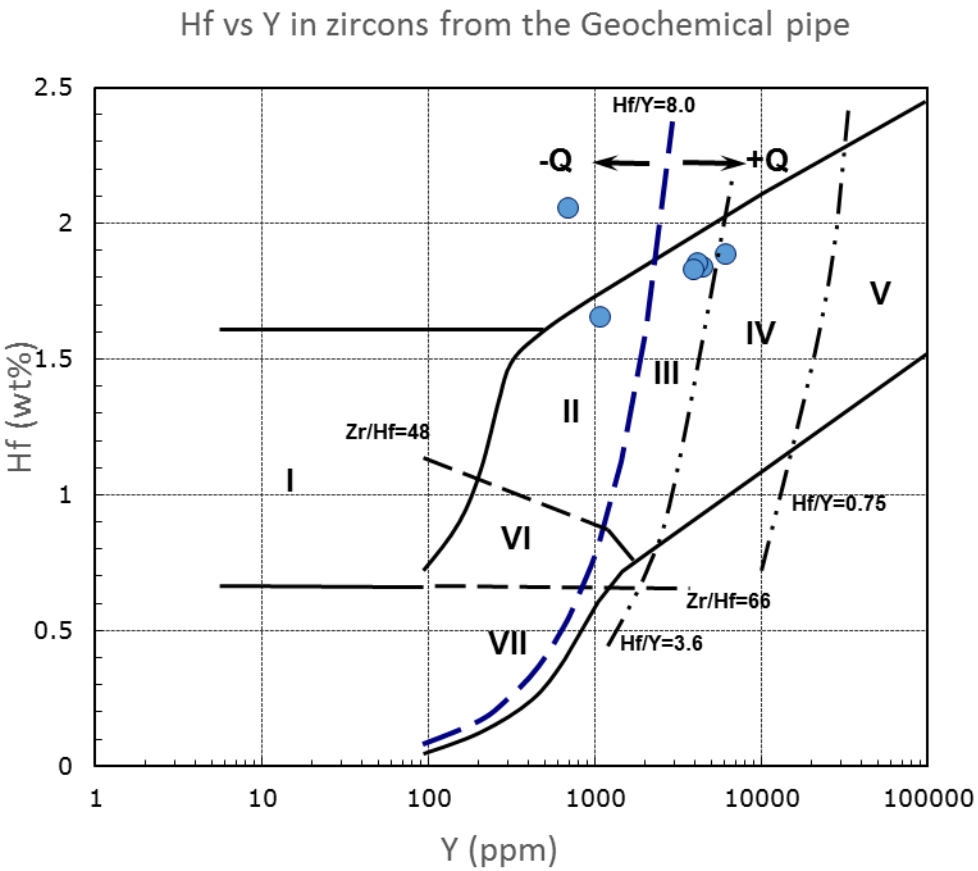




Figure 5.3.12. Trace-element and rare-earth element patterns of zircons from the Geochemical pipe.




I - kimberlites;
II - ultrabasic, basic and intermediate rocks;
III - quartz-bearing intermediate and felsic rocks;
IV- felsic rocks with 'high' SiO2 content;
V - greisens;
VI- alkaline rocks and alkaline metasomatites of alkaline complexes;
VII- carbonatites

Figure 5.3.13. Hf *vs* Y discrimination diagram for zircons from the Geochemical pipe.

Concentrations of the most of elements vary in one order of magnitude or less, if the LREE-enriched grains is not included in comparison. The trace-element patterns of all grains are similar for elements with ionic radius smaller than that of Th. Total REE contents diverge from 438 to 2827 ppm (4502 ppm in MVG459_Gch-05). This grain also has highest concentrations of all analysed elements, except Ta, Hf and P. Titanium content is about three times higher than in other grains, which may reflect microinclusion of rutile affected TE pattern.

Ratios Th/U and Nb/Ta range from 0.1 to 0.83 and from 2.3 to 4.8 correspondingly.

The REE plot show well defined negative Eu- and positive Ce-anomalies implying plagioclase crystallization prior to zircons and high oxidation state of the parental melt. The lack of Ce-maxima in the grain MVG459_Gch-05 may be due to LREE enrichment hiding the Ce-anomaly.

Application of CART classification shows that all analysed grains have trace-element features similar to those for zircons crystallized from intermediate to felsic rocks. Zircons from these rocks typically have high U, Y and Hf contents (Fig. 5.3.13).

**The Vostok pipe**

In total 34 zircon grains were studied for their trace-element composition.

The chondrite-normalised trace-element plot shows significant variations in element concentration, especially for larger ionic radius elements (Fig. 5.3.14). Thus, contents of La, Ce, Pr and Nd vary in up to 3 orders of magnitude, while Ti, Y and Nb diverge in one order of magnitude. Total REE contents range from 70 to 3828 ppm. Concentrations of Y fall in the interval 120-3984 ppm, Th – from 30 to 755 ppm and U ranges 148 to 2292 ppm. Th/U and Nb/Ta ratios are also variable – from 0.03 to 1.19 for Th/U and 1.1-11.7 for Ta/Nb.

In general, zircons of the main age population (mean age 1923 Ma) have lower total REE content, than older grains (2206 – 2427 Ma) (Fig. 5.3.15). The same pattern is observed for the most of trace elements, including Y, Th and U.

The rare-earth elements behave differently as well. The most of grains show typical zircon patterns with enrichment in HREE, depletion in LREE and well defined Ce and Eu-anomalies (Fig. 5.3.14). However, some zircons are less depleted in LREE than others are. In addition, these grains usually are characterized by slightly expressed or even absent Eu-minima.

According to CART classification, two grains reveal trace-element composition typical for zircons from carbonatitic rocks (Lu<20.7 ppm, Ta>0.5 ppm). However, Hf (2.2-2.3 wt%) and U (780-1200 ppm) concentrations in these grains both are too high to confirm carbonatitic origin (Hf<0.8 wt %, U<130 ppm) (Fig. 5.3.16). All other zircons show composition of trace elements similar to those from intermediate to felsic rocks.

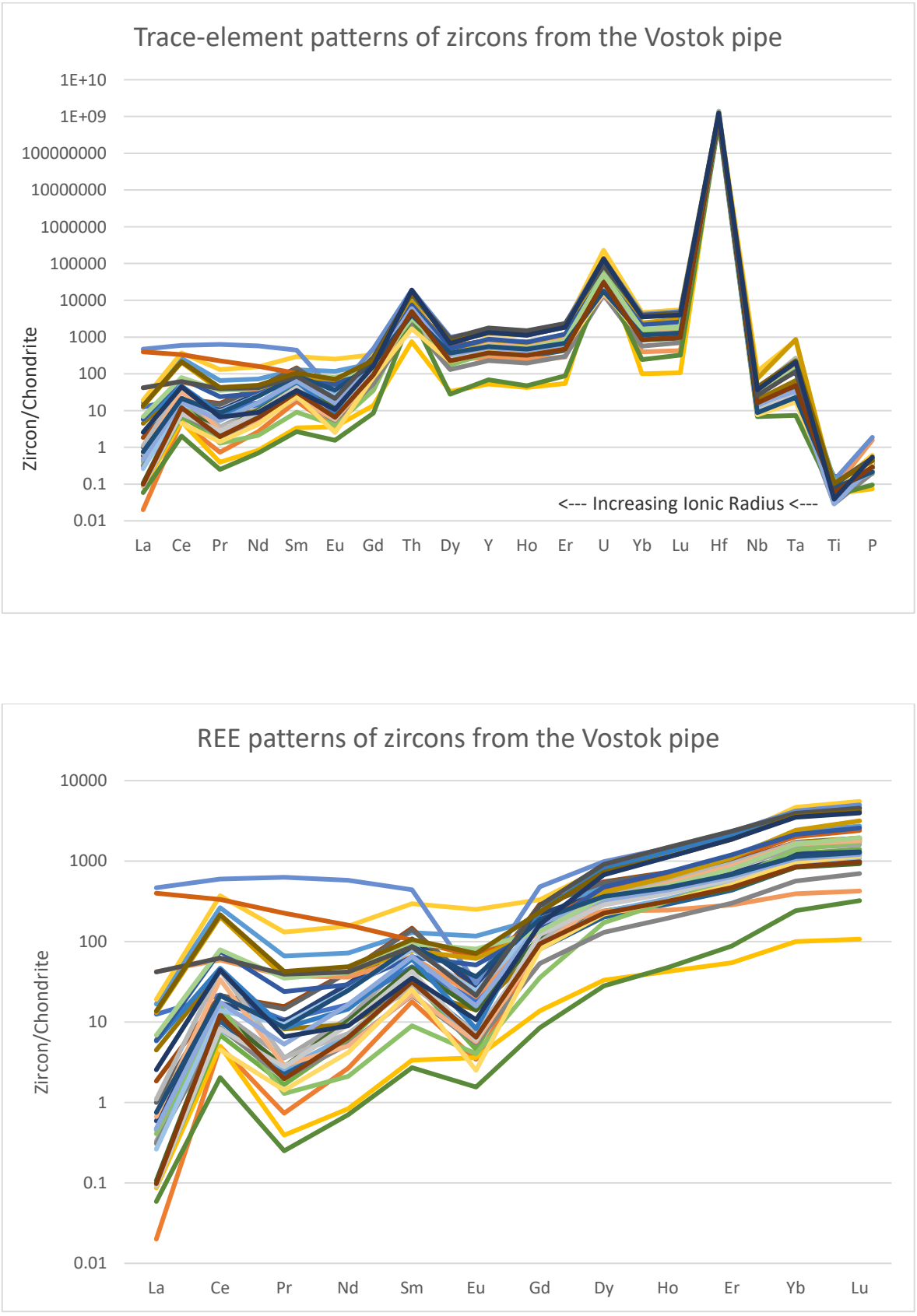



Figure 5.3.14. Trace-element and rare-earth element patterns of zircons from the Vostok pipe.

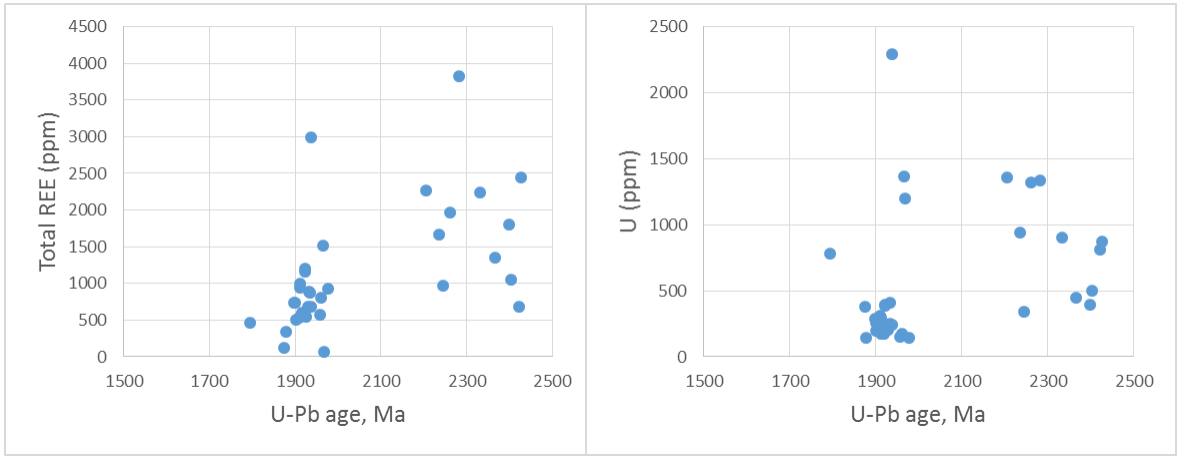
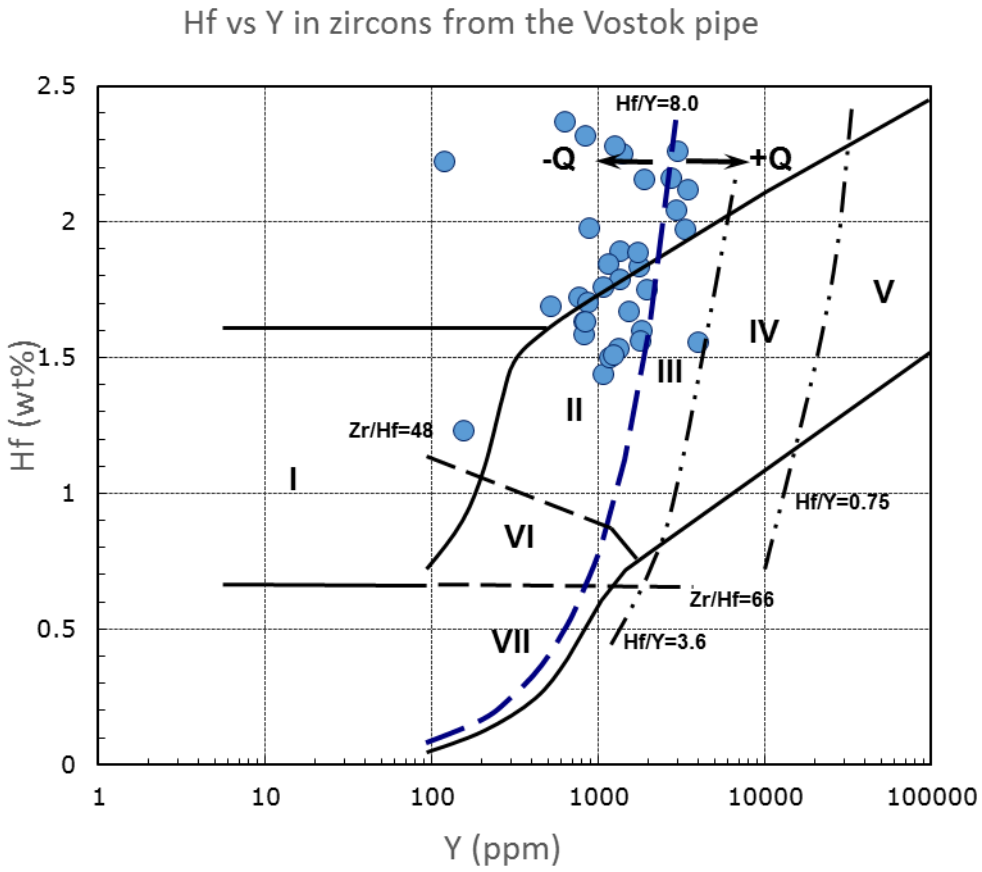



Figure 5.3.15. Total REE and U concentrations *vs* U-Pb age of zircons from the Vostok pipe.




I - kimberlites;
II - ultrabasic, basic and intermediate rocks;
III - quartz-bearing intermediate and felsic rocks;
IV- felsic rocks with 'high' SiO2 content;
V - greisens;
VI- alkaline rocks and alkaline metasomatites of alkaline complexes;
VII- carbonatites

Figure 5.3.16. Hf *vs* Y discrimination diagram for zircons from the Vostok pipe.

**The Veselaya pipe**

The trace-element composition was studied in all four zircon grains from the Veselaya pipe.

Concentrations of the most of trace elements do not vary much; fluctuations usually are within one order of magnitude. The chondrite-normalised trace-element plot shows the most variations in content of Pr (from 0.06 to 1 ppm), Nd (1.25 – 14.9 ppm), Sm (2.31 – 22.7 ppm) and Eu (from 0.65 to 9.9 ppm) (Fig. 3.5.17).

Total REE contents range from 730 to 2805 ppm; the highest one is found in the youngest zircon (490 Ma) (Fig. 5.3.18). The youngest grain also shows highest concentrations of all other analysed elements except La and Hf. Th/U ratio diverge in a range 0.5 – 2.0, while Nb/Ta interval is much more narrow – 3.3-6.6.

The REE patterns of all analysed grains are enriched in HREE and depleted in LREE, show distinctive Eu-minima and Ce-maxima.

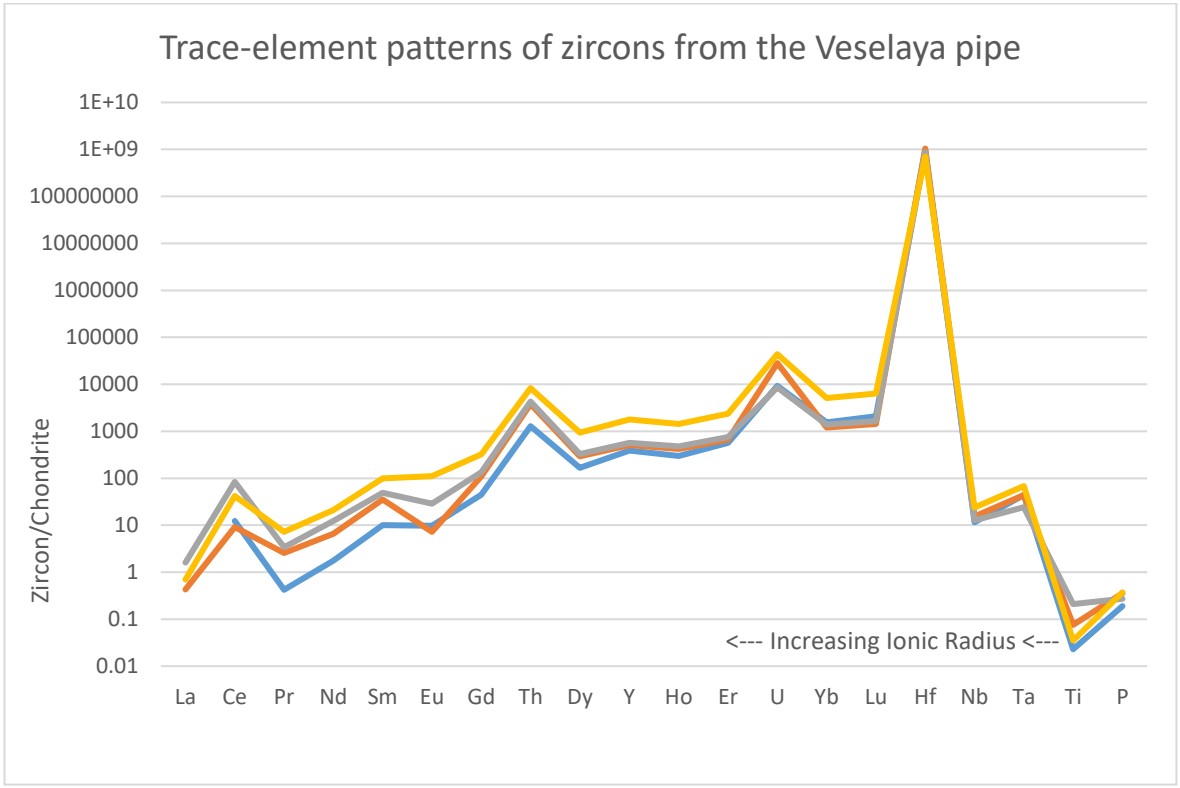
CART classification indicates that all grains have trace-element composition similar to those of zircons from granitoids. However, the discrimination diagram Hf *vs* Y shows three grains located within the ultramafic/mafic/intermediate rocks field, and only one – within the granitoid field (Fig. 5.3.19). Mafic or intermediate composition of the parental melt of those 3 grains is also in line with their U contents, which are lower (86 – 281 ppm) than expected for zircons from felsic rocks.

**The Krasnopresnenskaya pipe**

Five zircons from the pipe were analysed for their trace-element composition.

The chondrite-normalised trace-element plot show no significant difference in trace-element patterns (Fig. 5.3.20). Some variations are found in concentrations of Ta (0.3 – 1.9 ppm), Th (31 – 449 ppm), U ( 220 – 1277 ppm) and light rare-earth elements (up to 1 order of magnitude). Other elements reveal approximately equal concentrations in all grains. Total REE contents vary from 669 to 1218 ppm.

The rare-earth element plot demonstrates typical zircon patterns for all analysed grains. They are characterised by LREE-depletion, negative Eu- and positive Ce-anomaly.



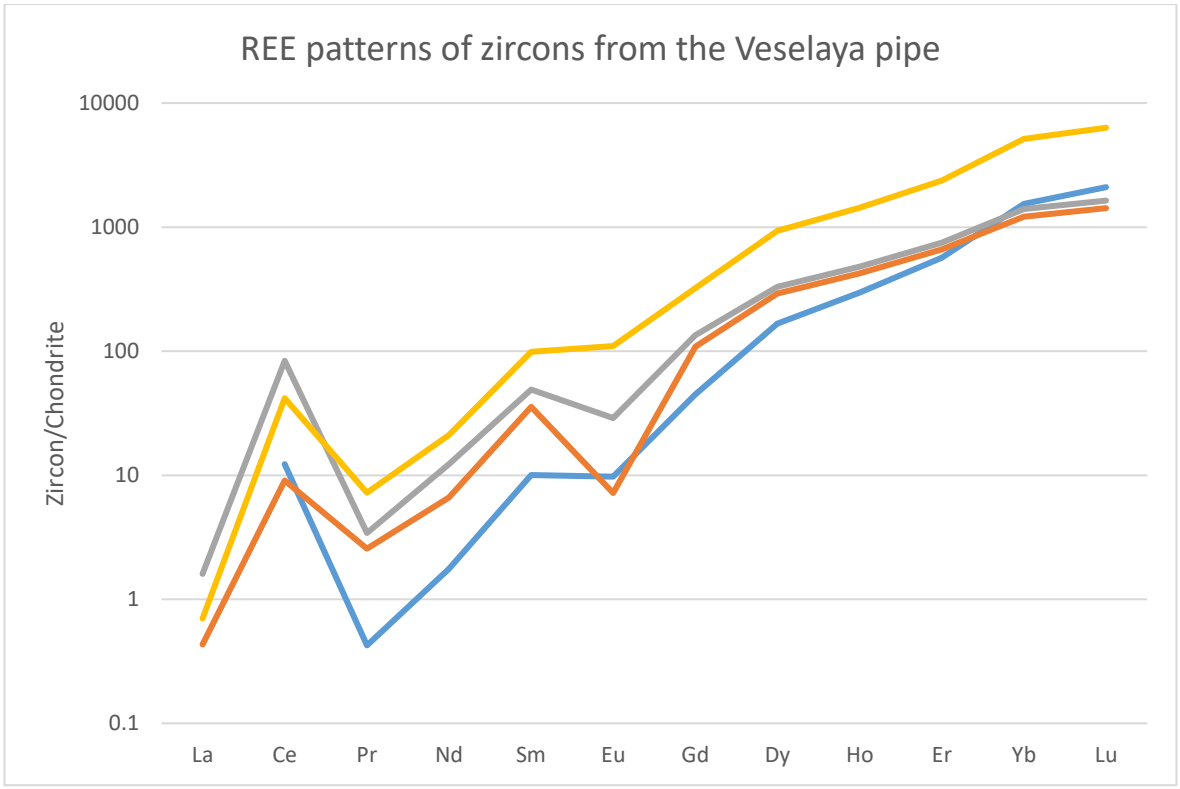




Figure 5.3.17. Trace-element and rare-earth element patterns of zircons from the Veselaya pipe.

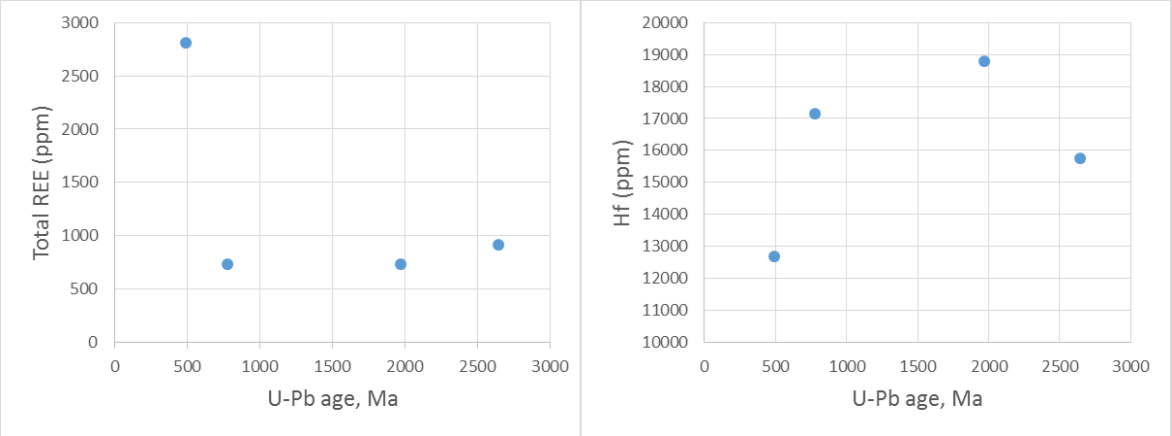
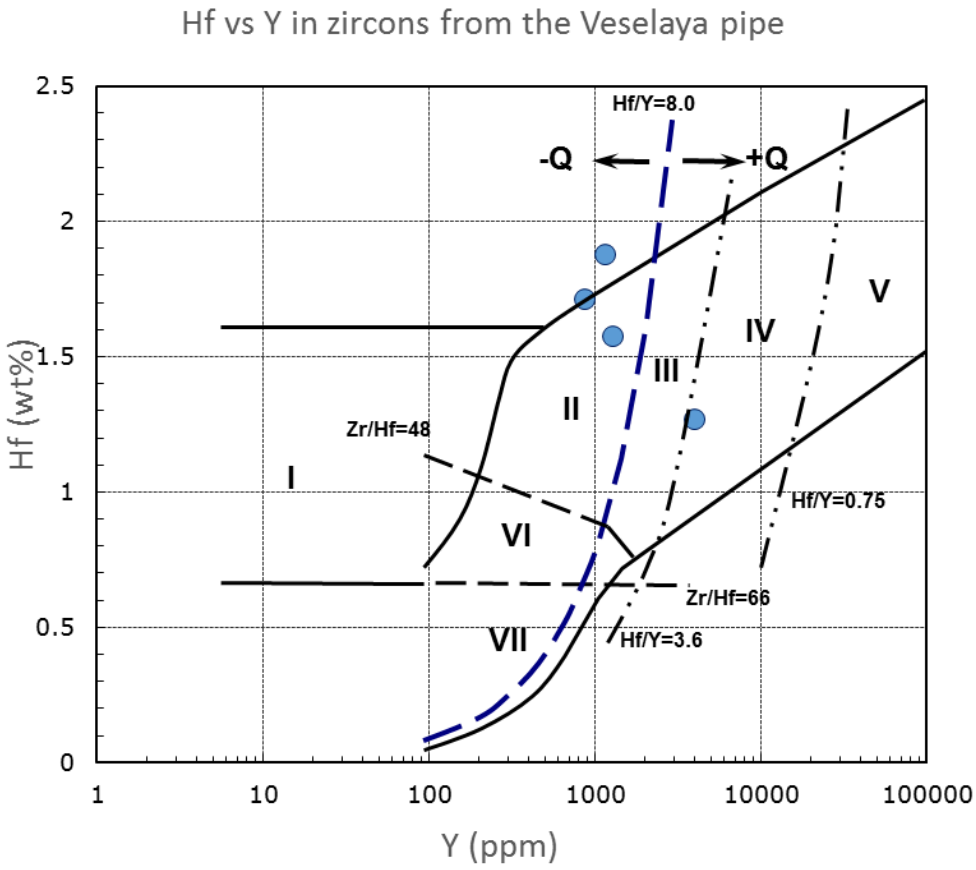
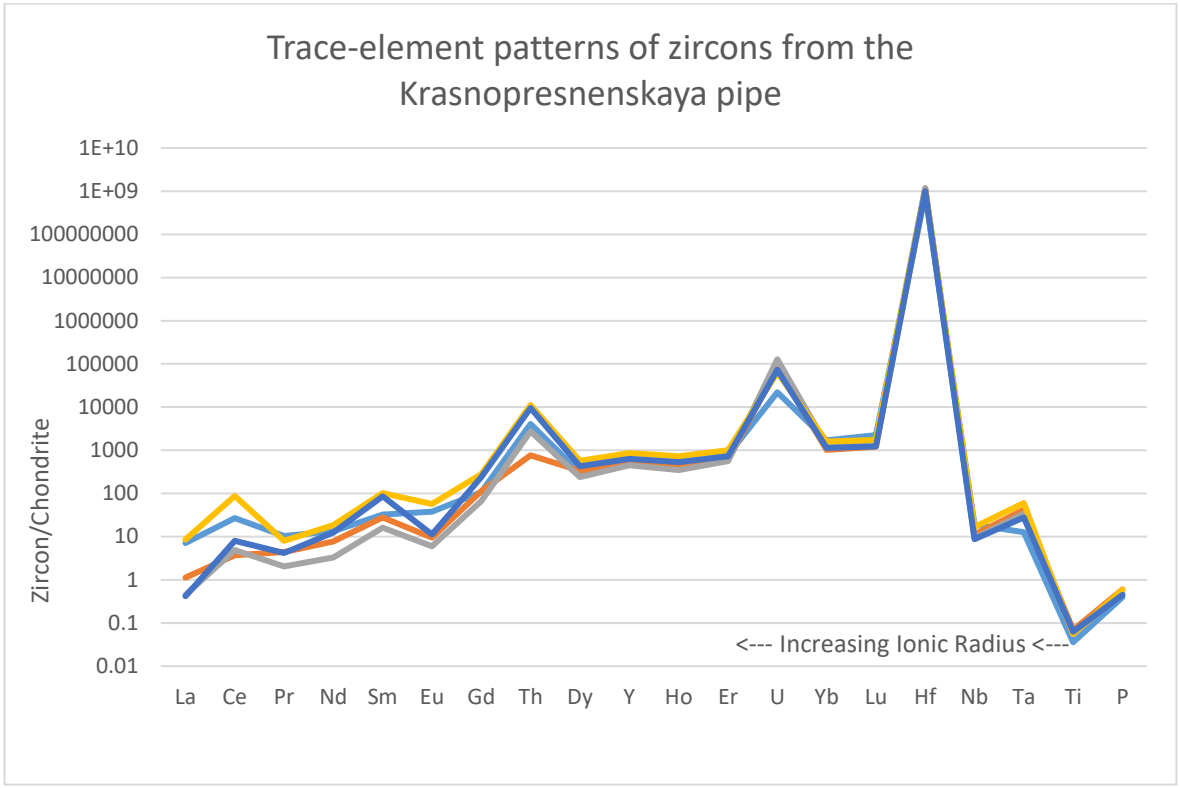



Figure 5.3.18. Total REE and Hf concentrations *vs* U-Pb age of zircons from the Veselaya pipe.




I - kimberlites;
II - ultrabasic, basic and intermediate rocks;
III - quartz-bearing intermediate and felsic rocks;
IV- felsic rocks with 'high' SiO2 content;
V - greisens;
VI- alkaline rocks and alkaline metasomatites of alkaline complexes;
VII- carbonatites

Figure 5.3.19. Hf *vs* Y discrimination diagram for zircons from the Veselaya pipe.



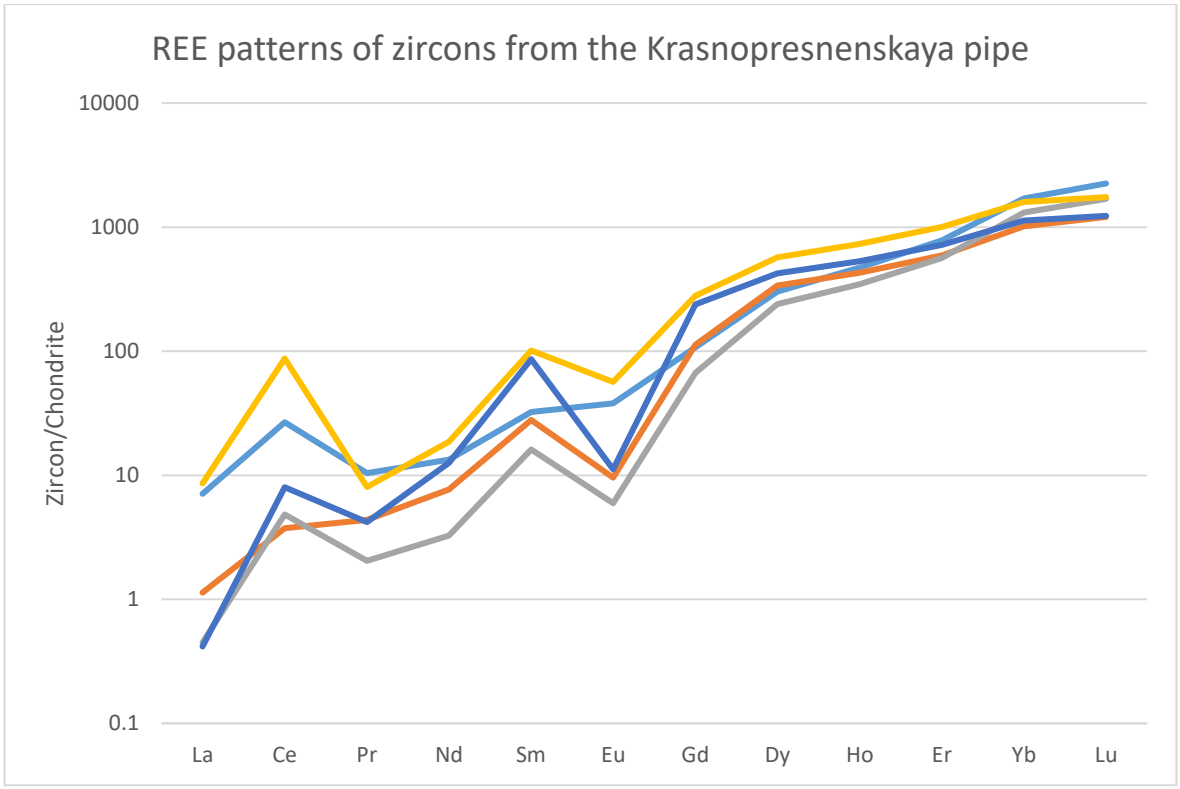




Figure 5.3.20. Trace-element and rare-earth element patterns of zircons from the Krasnopresnenskaya pipe.

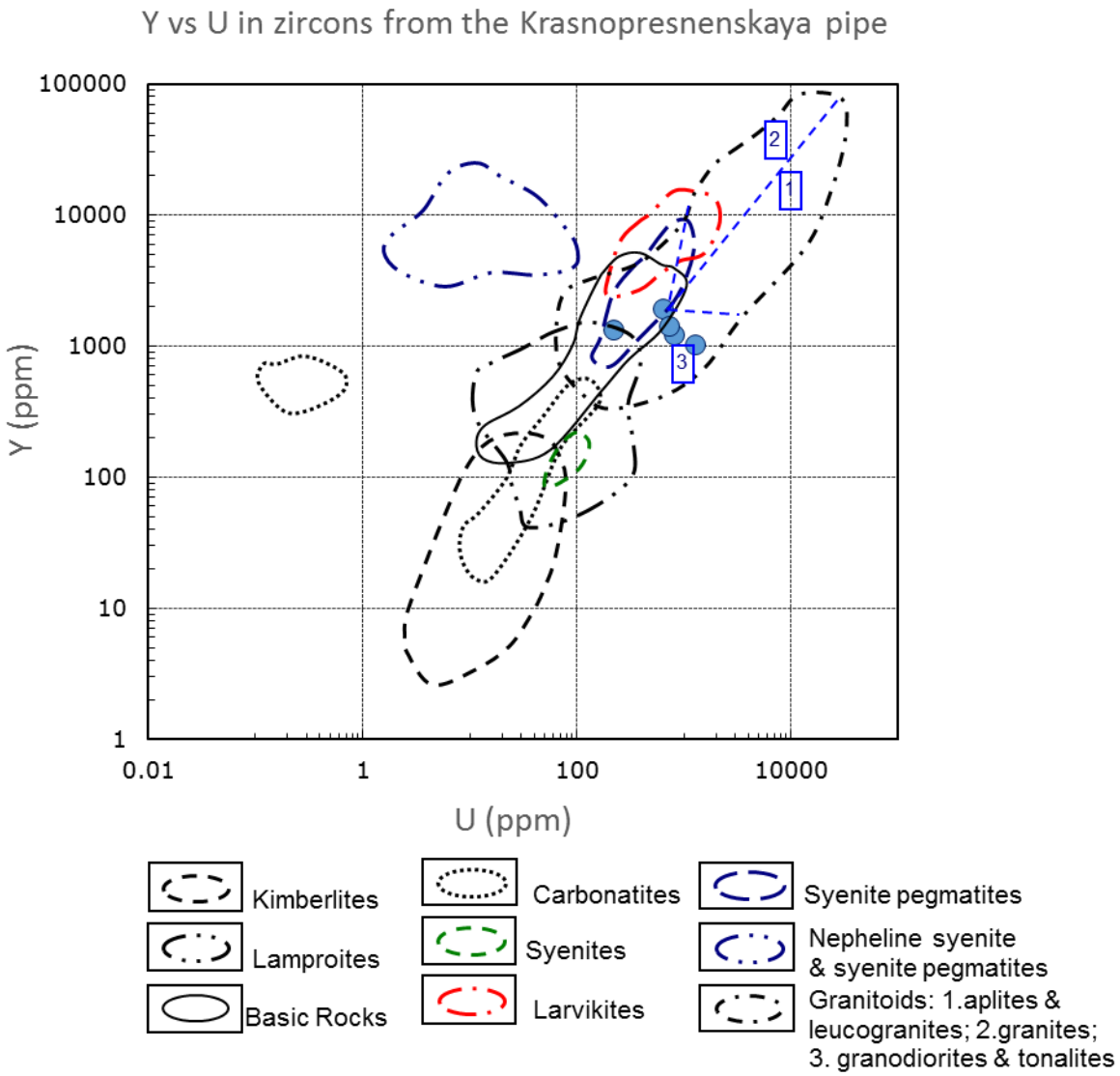



Figure 5.3.21. Y *vs* U discrimination diagram for zircons from the Krasnopresnenskaya pipe.

According to the CART classification, all grains from the Krasnopresnenskaya pipe show trace-element signatures of zircons from mafic to intermediate rocks. At the discrimination diagram Y *vs* U zircons are located within the same fields as predicted by the CART classification (Fig. 5.3.21).

**The Markha pipe**

The trace-element composition was studied in 85 zircons from the Markha pipe.

The chondrite-normalised plot shows wide range of trace element concentrations (Fig. 5.3.22). The only element varying in one order of magnitude is Hf (0.65 – 2.3 wt%); all other trace

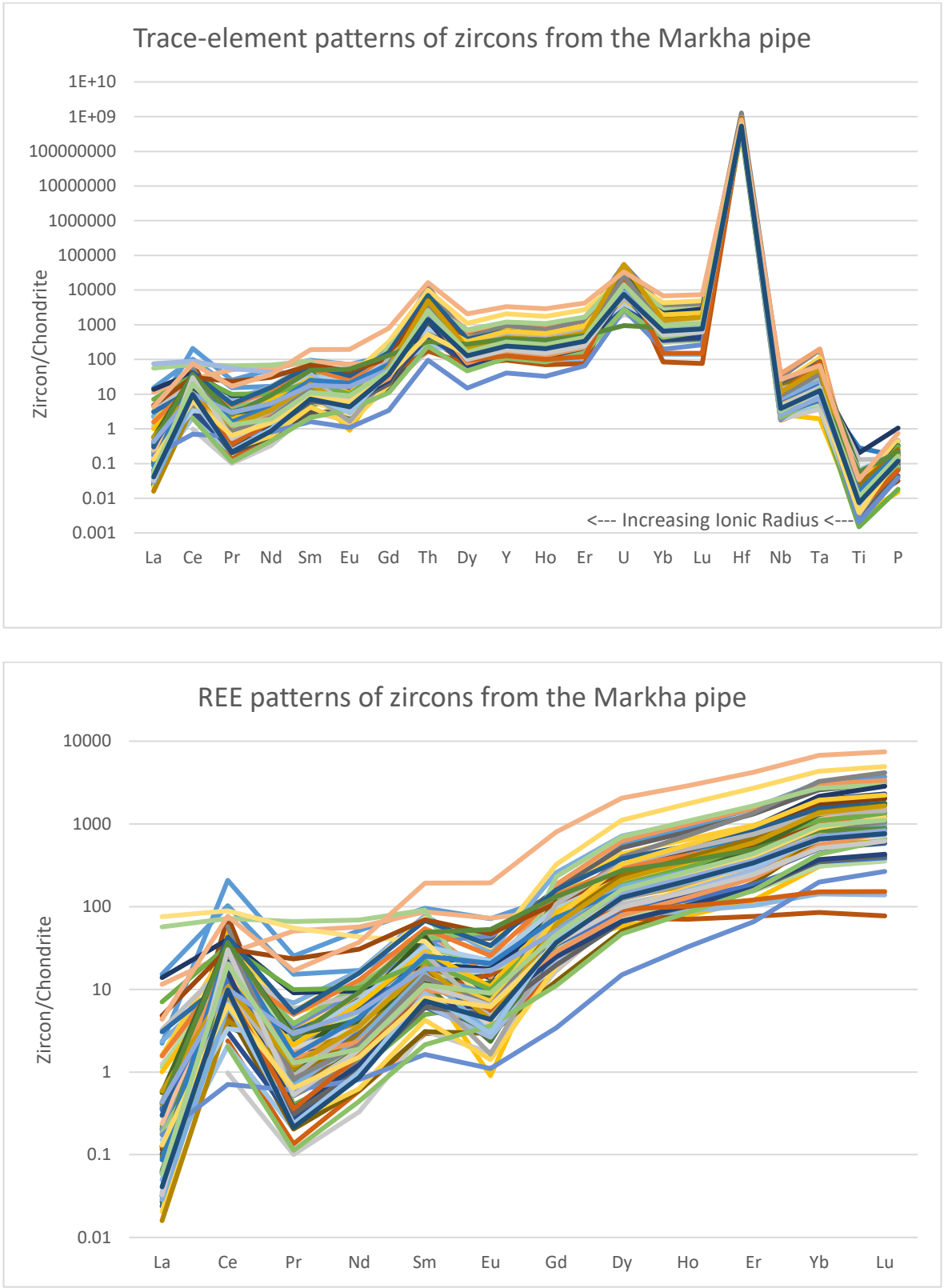



Figure 5.3.22. Trace-element and rare-earth element patterns of zircons from the Markha pipe.

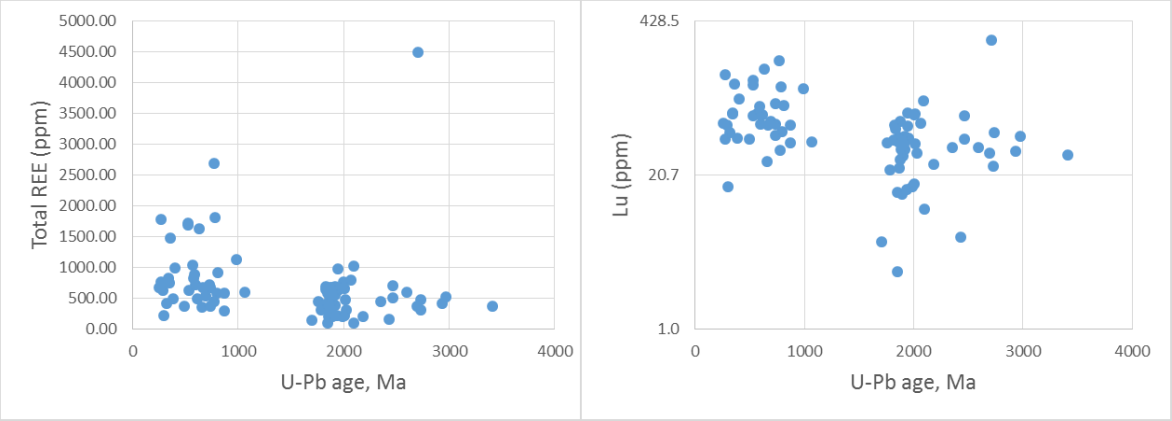



Figure 5.3.23. Total REE and Lu concentrations *vs* U-Pb age of zircons from the Markha pipe.

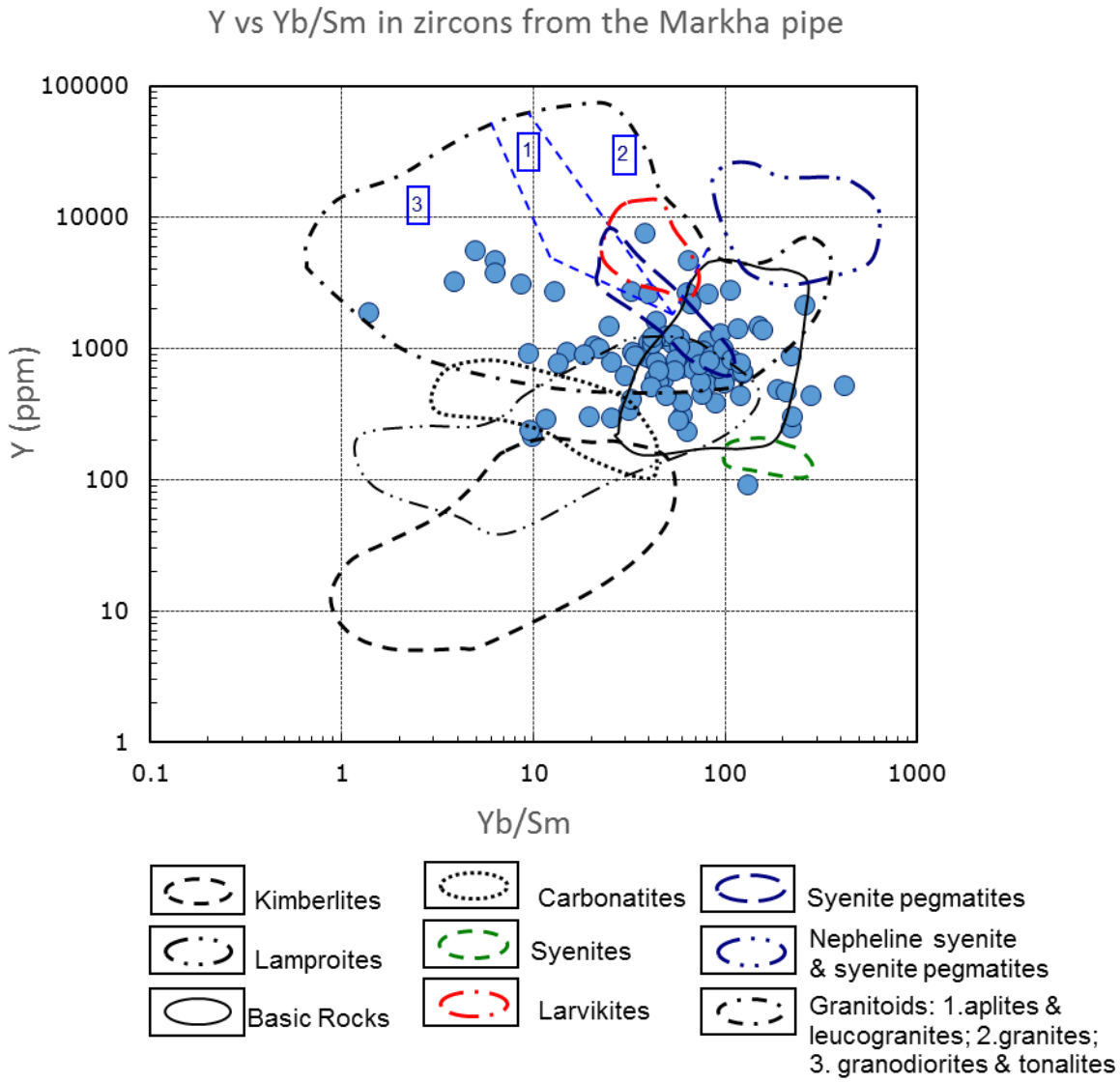



Figure 5.3.24. Y *vs* Yb/Sm discrimination diagram for zircons from the Markha pipe.

elements diverge in 2-4 orders of magnitude. Total REE contents range from 88 to 4498 ppm, Y varies from 92 to 7465, U – from 9.5 to 552 ppm, Th falls in range 3.8 – 662 ppm). Ratios Th/U and Nb/Ta show intervals of values 0.03-1.95 and 1.6 – 16.5 correspondingly. In general, zircons younger than 1000 Ma have total REE contents higher, than older grains (Fig. 5.3.23), however, this difference is not significant.

The REE plot demonstrate scattered patterns, however they all reflect typical zircon REE features – depletion in LREE and enrichment in HREE (Fig. 5.3.22). The majority of analysed grains also show well defined Eu-minima and Ce-maxima, indicating previous plagioclase crystallization and high oxidation state of the zircons parental melt.

Using CART statistical classification it was shown that 10 zircons have trace-element signatures common for zircons from carbonitites (Lu<20.7 ppm). Seven studied grains demonstrate composition of trace elements similar to zircons from syenite; and all others are close in their trace element characteristics to zircons crystallized from intermediate parental melts. The localization of data points at the Y *vs* Yb/Sm discrimination diagram confirms classification results (Fig. 5.3.24).

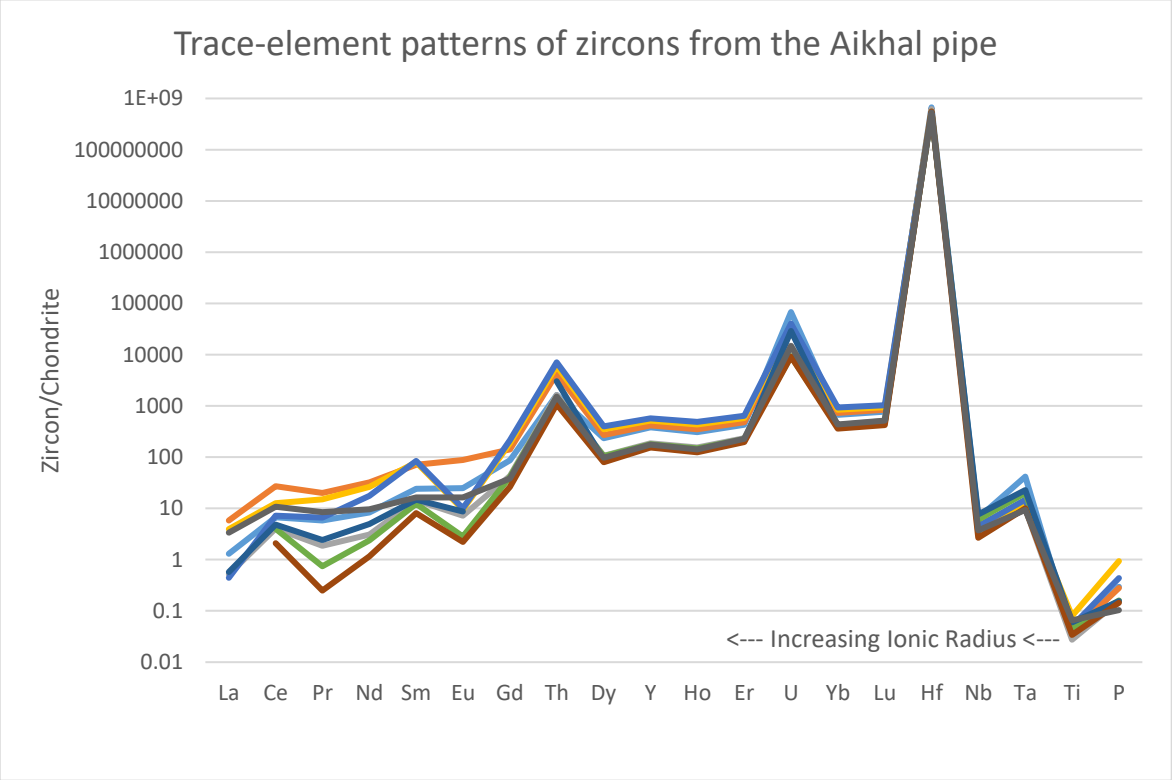
**The Aikhal pipe**

Only 9 grains from the Aikhal pipe with U-Pb ages from 1885 to 1991 Ma were analysed for their trace-element composition.

Concentrations of all trace elements are relatively low; however, some elements show fluctuations in their content (Fig. 5.3.25). Total REE contents range from 211 to 737 ppm, Y varies in the interval 347 – 1293 ppm, U and Th diverge from 92 to 682 ppm and from 43 to 285 ppm correspondingly.

The rare-earth element plot shows depletion in LREE and enrichment in HREE, typical for zircons. The negative Eu-anomaly and positive Ce-anomaly are more or less defined for all grains.

According to CART classification, 5 grains have trace-element composition typical for zircons from carbonatites; the rest 4 grains show trace-element signatures of zircons crystallized from intermediate parental melt. The grains classified as carbonatitic, however, have Hf and U contents higher than found in typical carbonatitic zircon, which indicates their more likely derivation from mafic or alkaline rock types (Fig. 5.3.26).



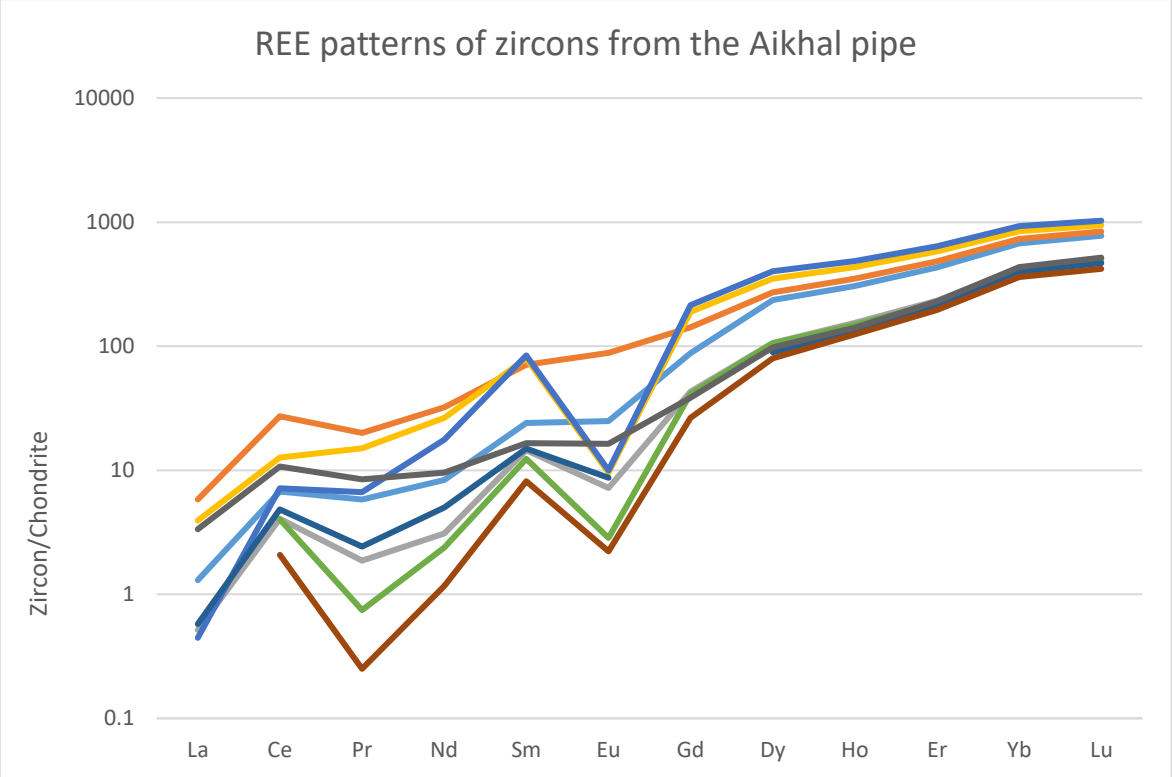




Figure 5.3.25. Trace-element and rare-earth element patterns of zircons from the Aikhal pipe.

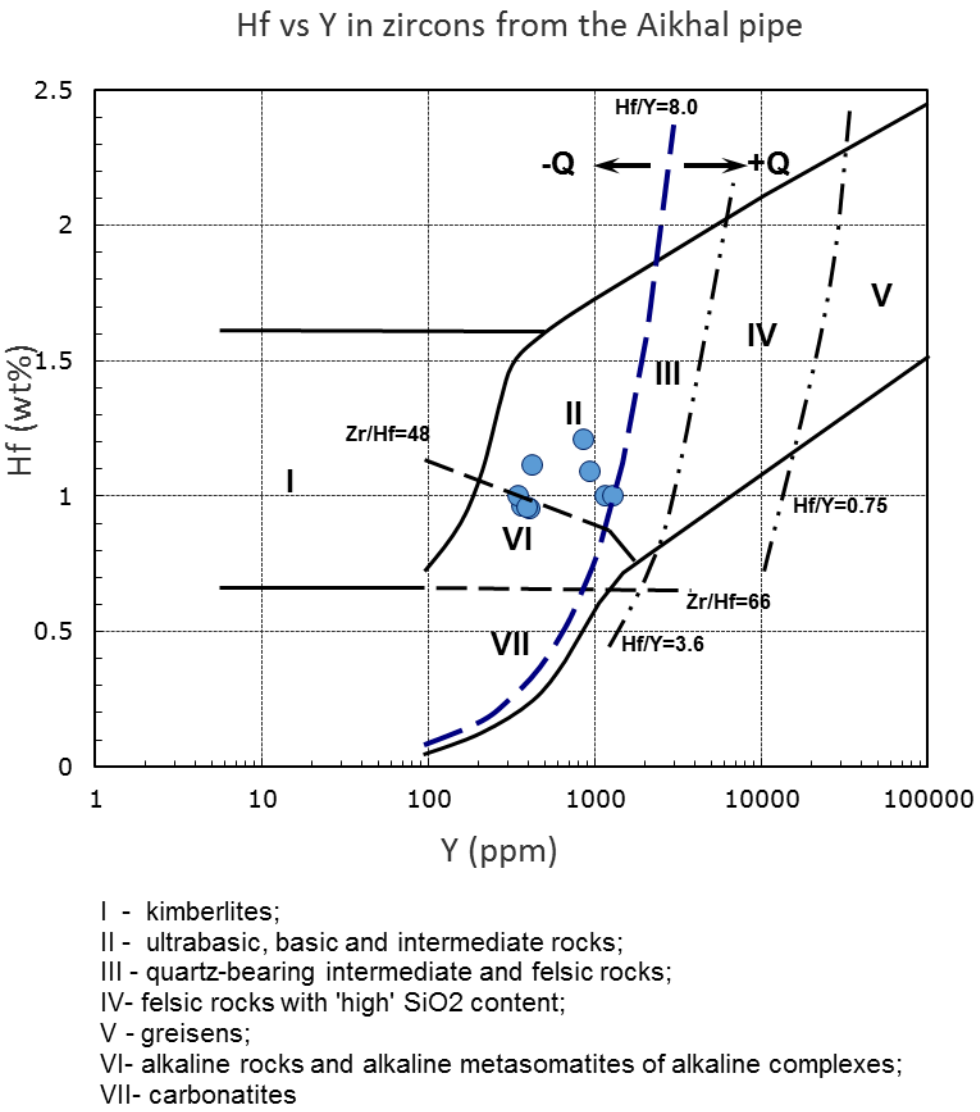



Figure 5.3.26. Hf *vs* Y discrimination diagram for zircons from the Aikhal pipe.

***Oxygen isotopic data***

**The Aikhal pipe**

Oxygen isotopic composition was analysed in 25 zircons from the Aikhal pipe. $\delta^{18}O$ ranges in relatively narrow interval of supracrustal values from 8.14±0.27 to 10.64±0.21‰ (Fig. 5.3.27).

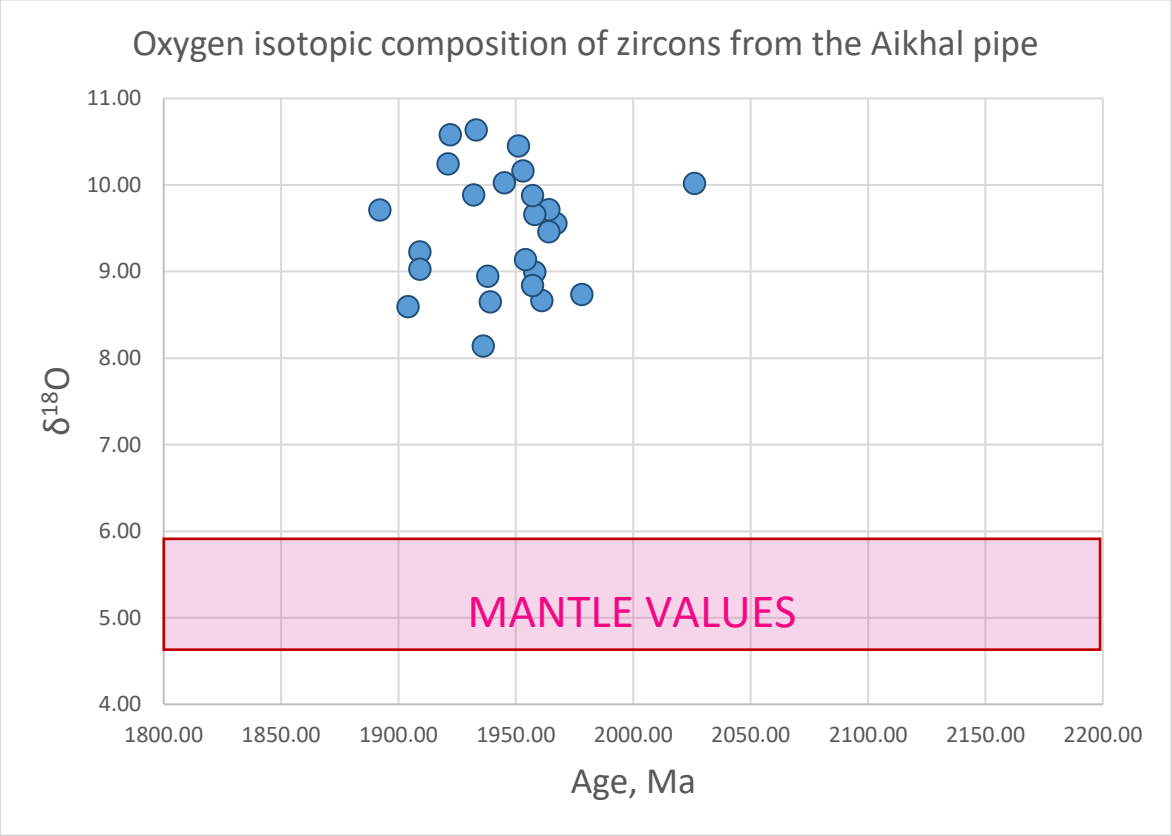



Figure 5.3.27. $\delta^{18}O$ *vs* U-Pb age for zircons from the Aikhal pipe.

***Hafnium-isotope data***

**The Kismet pipe**

Lu-Hf isotopes were analysed in 20 zircons from the Kismet pipe (Table 5.3.2).

The εHf plot shows all grains forming a single population with εHf values from -34 to +2.9 (Fig. 5.3.28). The most of zircons have εHf within the interval -20 - -5. Calculated initial $^{176}Hf/^{177}Hf$ ratios vary from 0.280607 to 0.281641. Crustal model ages are within the interval 2.4 – 4.7 Ga with the main peak age at ~3.2 Ga.

**The Geochemical pipe**

All 6 zircon grains were studied for their Lu-Hf isotope composition.

εHf values show variations in the range -13.2 - -3.7 (Fig. 5.3.29). The $^{176}Hf/^{177}Hf$ ratios calculated for these grains diverge from 0.281191 to 0.281415. Estimated crustal model ages fall into the interval 2.88 – 3.41 Ga.

Table. 5.3.2. Summary table of Hf-isotopic data for zircons from the Alakit-Markha kimberlite field.

| Age group | Range of U-Pb ages, Ma (n = number of grains) | Initial Hf values | εHf values | $T_{(DM)}^{C}$ range, Ga |
|---|---|---|---|---|
| **Kismet** | 1766 – 1939 (n = 20) | 0.280607 – 0.281641 | -34 - +2.9 | 2.4 – 4.7 |
| **Geochemical** | 1866 - 1994 (n = 6) | 0.281191 – 0.281415 | -13.2 - -3.7 | 2.88 – 3.41 |
| **Vostok** | 1875 - 2427 (n = 28) | 0.281089 - 0.281499 | -12.4 - +3.7 | 2.70 – 3.45 |
| **Veselaya** | 490 – 2645 (n = 4) | 0.281026 - 0.282517 | -7.6 - +5.1 | 1.35 – 3.29 |
| **Krasnopresnenskaya** | 1876 – 2311 (n = 5) | 0.281087 - 0.281580 | -8.3 - +0.4 | 2.55 – 3.40 |
| **Aikhal** | 1845 – 1991 (n = 18) | 0.281051 - 0.281413 | -19.8 - -4.2 | 2.81 – 3.62 |

**The Vostok pipe**

Twenty-eight zircons from the Vostok pipe were analysed for Lu-Hf isotopic composition.

At the εHf plot zircons form two distinctive groups (Fig. 5.3.30). The first one includes zircons grains younger than 2000 Ma, which have εHf values from -7.8 to -12.4. Two grains of the same age show higher εHf of -3.9 and -3.2. Initial $^{176}Hf/^{177}Hf$ values for this group are within the range 0.281181 – 0.281499. Calculated crustal model ages vary from 2.75 to 3.40 Ga.

Second group of grains with U-Pb ages older than 2000 Ma has more scattered εHf values – from -10.2 to +3.7, but more narrow interval of initial $^{176}Hf/^{177}Hf$ ratios – 0.281089 – 0.281374. Crustal model ages for these zircons range from 2.7 to 3.45 Ga.

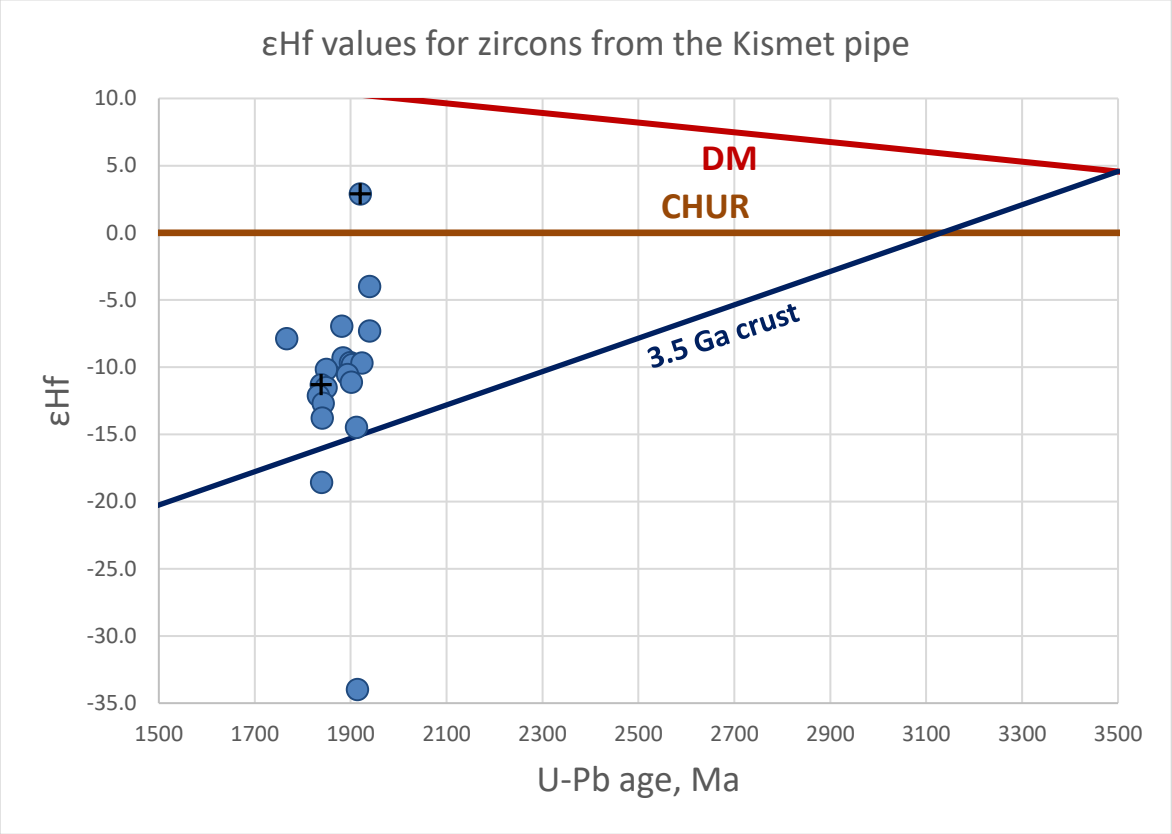



Figure 5.3.28. εHf *vs* U-Pb age plot for zircons from the Kismet pipe. Grains with trace-element (TE) composition typical of mantle-derived zircons are shown with black crosses (here and further for all εHf plots).

**The Veselaya pipe**

Four zircons from the Veselaya pipe show significantly different Hf-isotopic characteristics (Fig. 5.3.31). The εHf ranges from -7.6 to +5.1. Initial $^{176}Hf/^{177}Hf$ ratios are from 0.281026 to 0.282517. Calculated crustal model ages diverge in the interval 1.35 – 3.29 Ga.

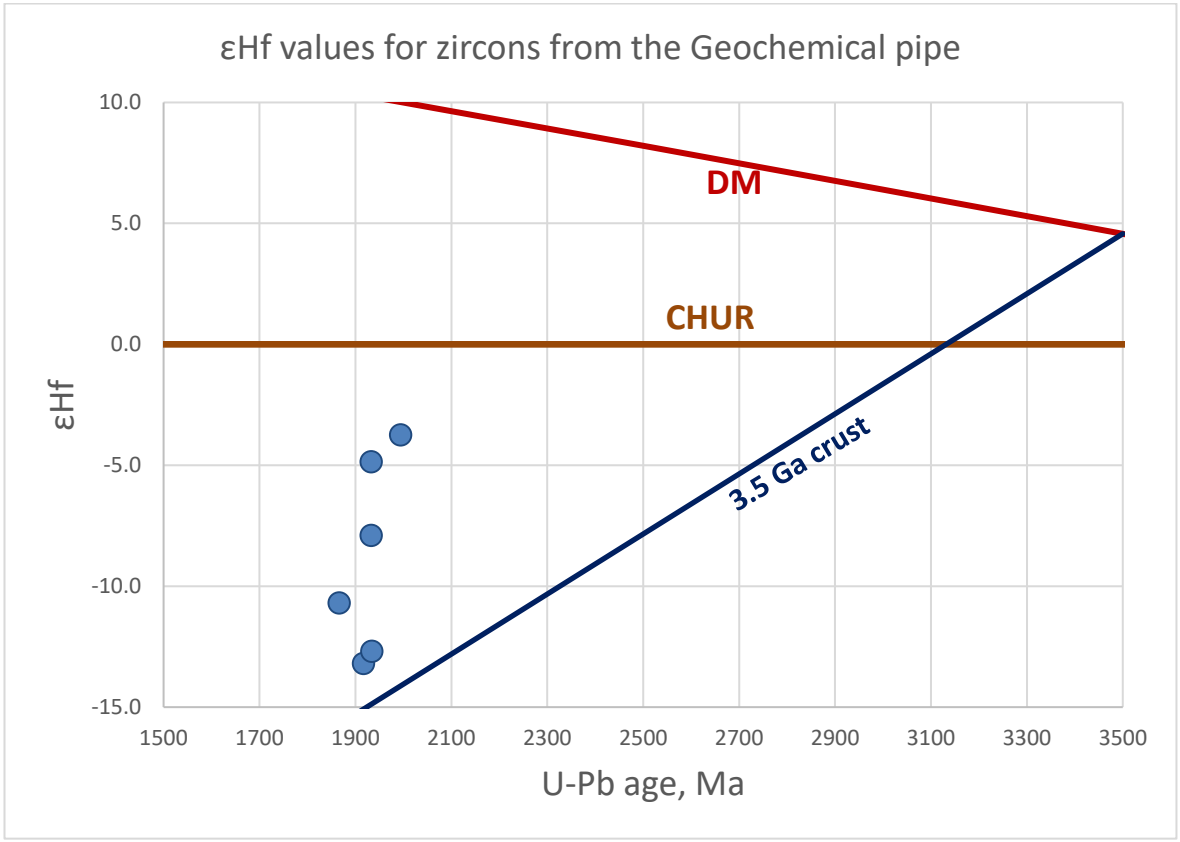



Figure 5.3.29. εHf *vs* U-Pb age plot for zircons from the Geochemical pipe.

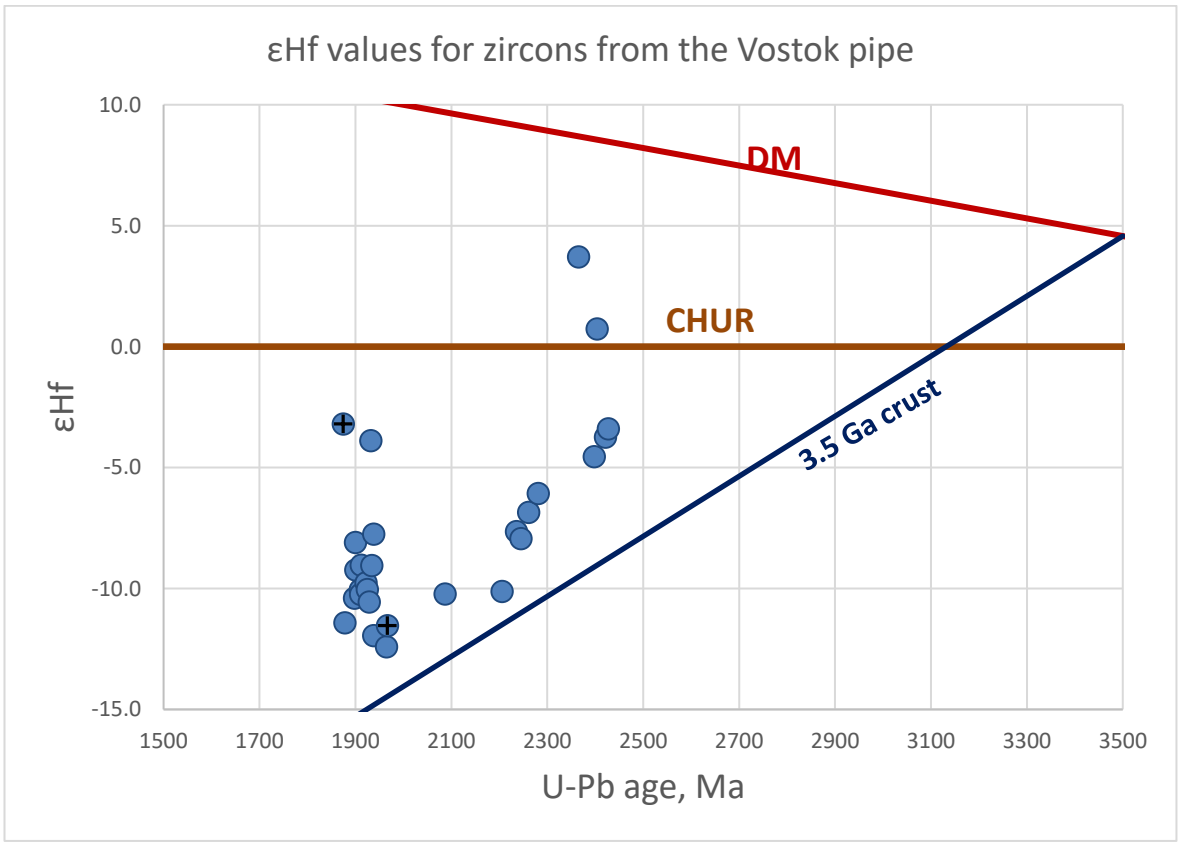



Figure 5.3.30. εHf *vs* U-Pb age plot for zircons from the Vostok pipe.

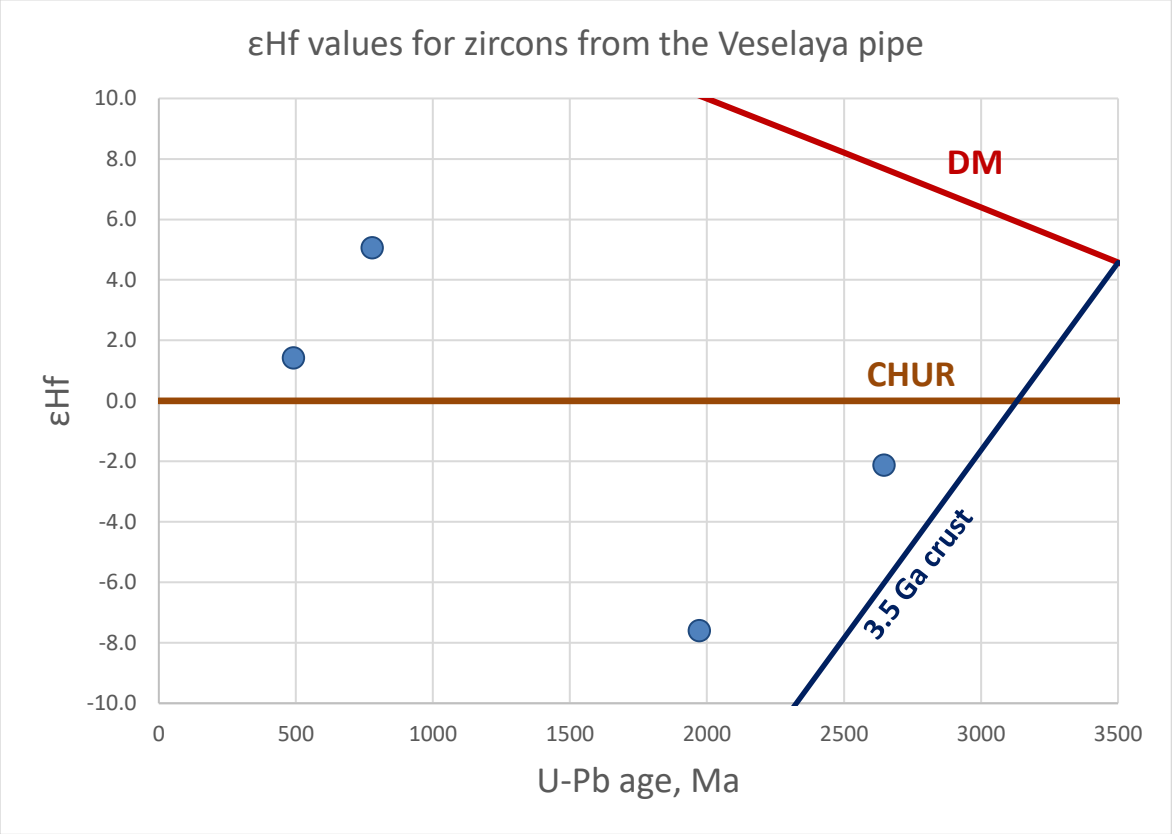



Figure 5.3.31. εHf *vs* U-Pb age plot for zircons from the Veselaya pipe.

**The Krasnopresnenskaya pipe**

The Lu-Hf isotopes were studied in five zircon grains from the pipe.

The range of εHf values is -8.3 - +0.4 (Fig. 5.3.32). Calculated initial $^{176}Hf/^{177}Hf$ ratios are from 0.281087 to 0.281580. Crustal model ages range from 2.55 to 3.40 Ga.

**The Aikhal pipe**

In total 18 analyses of Lu-Hf isotopic composition were obtained for zircons from the Aikhal pipe. All grains form a single population at the εHf plot (Fig. 5.3.33). The values of εHf vary from -19.8 to -4.2. Calculated initial $^{176}Hf/^{177}Hf$ ratios are within the interval 0.281051 – 0.281413. Estimated crustal model ages range from 2.81 to 3.62 Ga.

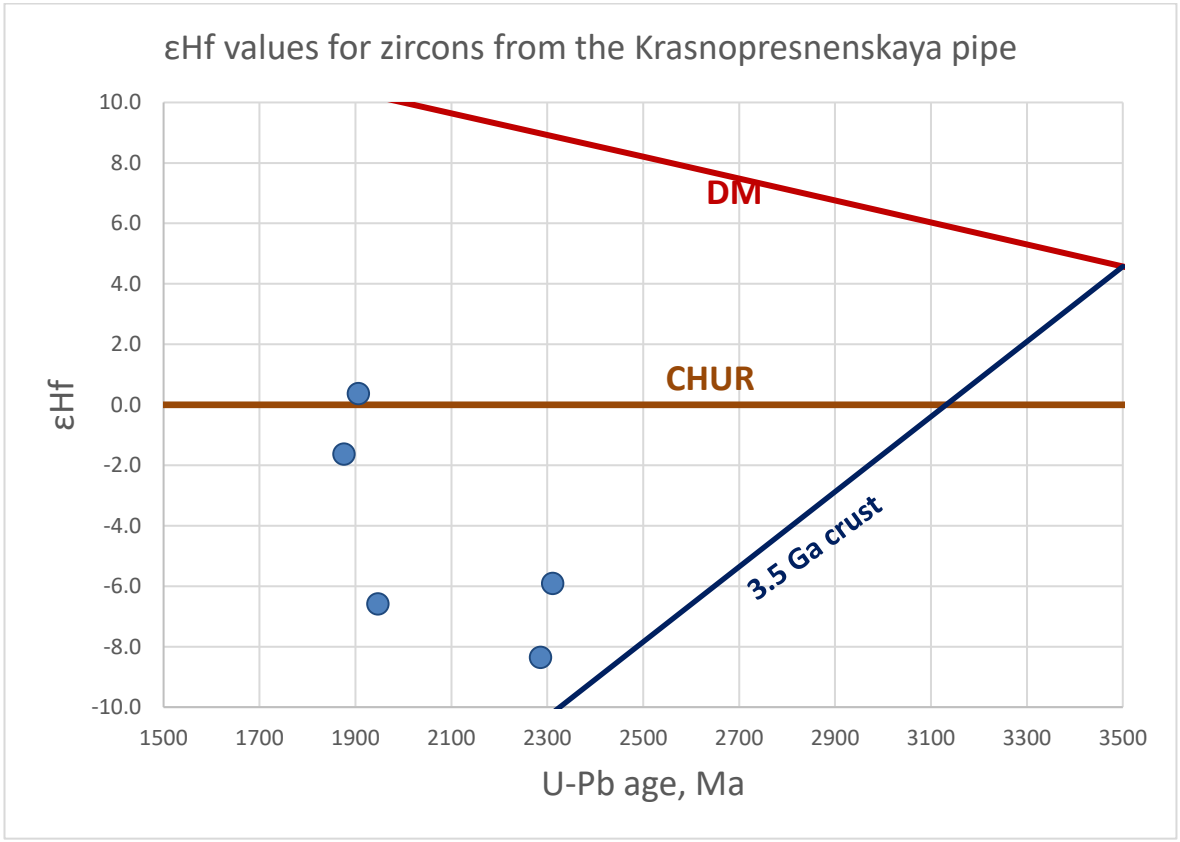



Figure 5.3.32. εHf *vs* U-Pb age plot for zircons from the Krasnopresnenskaya pipe.

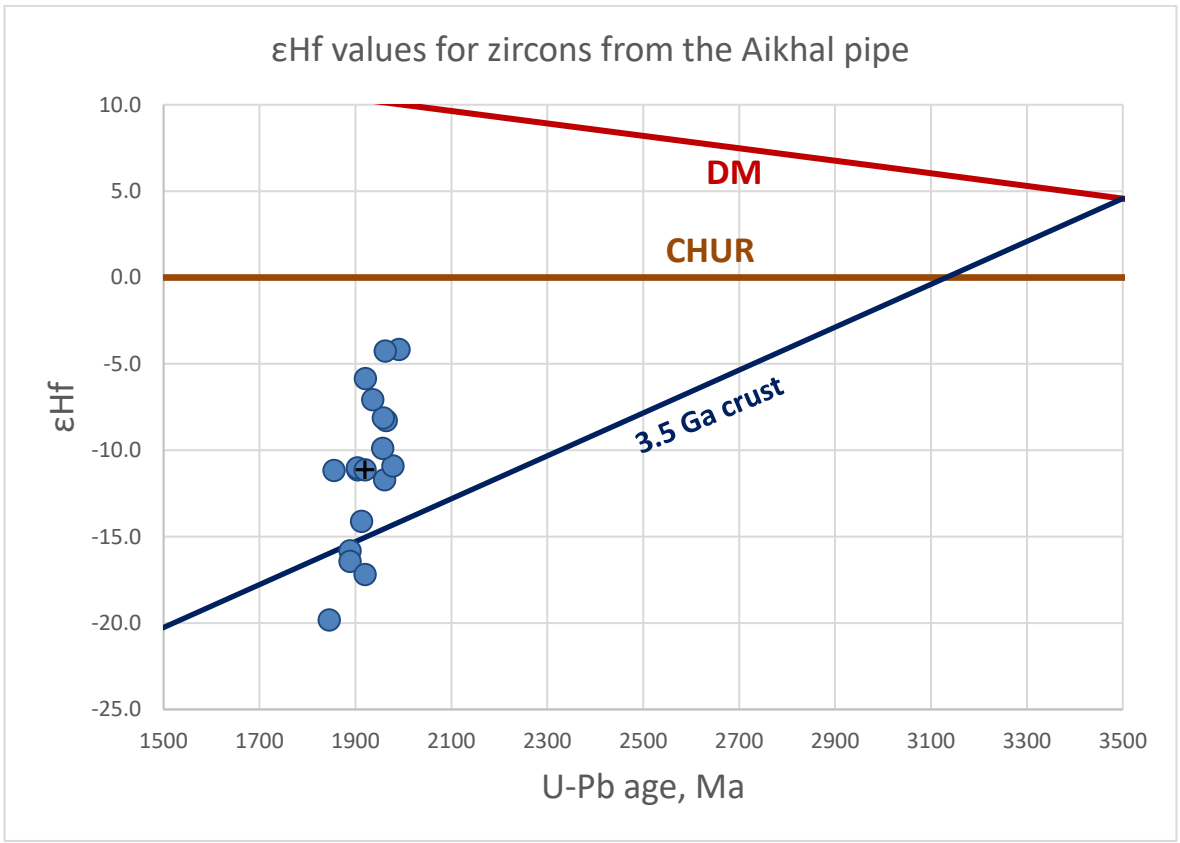



Figure 5.3.33. εHf *vs* U-Pb age plot for zircons from the Aikhal pipe.

## 5.4. The Nakyn kimberlite field

The Nakyn field is located at the middle part of the Marha river. The pipe is located within the Vilui-Markha deep fault zone, a NE-trending structure associated with the middle Paleozoic Vilui rift system (Agashev *et al.*, 2001). Only four kimberlite bodies were found within the field, all of them are diamondiferous.

The kimberlites are intruded into early Paleozoic terrigenous-carbonate sequences and are covered by 30-80 m of Jurassic terrigenous sediments. Apart from kimberlites within the field, intrusions of gabbro-dolerite and alkaline-mafic rocks as well as explosive breccia are found. Magmatic rocks are hosted by Cambrian to Silurian terrigenous sequences (Zaitsev & Smelov, 2010).

Geological age determination is based on finding of xenoliths of the Ordovician – Middle Devonian sedimentary rocks in the kimberlites. There is no direct contact between kimberlite and gabbro-dolerite; however, xenoliths of the later are reported founded in kimberlites. Both kimberlites and gabbro-dolerites are cut by alkaline-mafic rocks, which also found in a significant amount of clasts in the explosive breccia.

Isotopic geochronological studies (Rb-Sr, Sm-Nd, Ar-Ar and K-Ar systematics) were applied to various magmatic rocks of the Nakyn field. The range of obtained data even for a single pipe or dyke is wider than analytical uncertainty of used techniques. The most recent results give an age of 364 Ma for the Nurbinskaya and Botuobinskaya kimberlites determined by Rb-Sr dating on kimberlitic phlogopite (Agashev *et al.*, 2001). This age falls into the 353-367 Ma range defined as the main emplacement event of the Siberian diamondiferous kimberlites (Kinny & Friend, 1997).

### *Zircon U-Pb data*

Zircons were collected from two pipes: Nurbinskaya and Botuobinskaya. Zircons from the Nurbinskaya pipe were hand-picked from the crushed kimberlite. Zircon grains from the Botuobinskaya pipe were extracted from crustal xenoliths.

#### The Nurbinskaya pipe

Forty-eight zircon grains were collected from a heavy mineral concentrate of the crushed whole-rock kimberlite from the Nurbinskaya pipe. All grains are clear, transparent, yellowish or brownish in color and 2-5 mm in size. Five grains have an unusual "mosaic" internal structure revealed by CL imaging (Fig. 5.4.1). These were selected for more detailed investigation using

EBSD analysis, U-Pb SHRIMP dating and analyzing of O-isotopes and trace element composition. Several grains without such structural features have been used for comparison.

All 48 grains have been dated by laser ablation ICP-MS (Table 5.4.1). One or two analytical spots per grain were done depending on the complexity of their internal structure. 65 analyses were collected; 5 with discordance over 15% have been rejected.

The undeformed zircons define two main age populations: Devonian and Archean (Fig. 5.4.2). The younger population (n=18) has ages between 365 Ma and 375 Ma (mean age 370.7±2.3 Ma, Fig. 5.4.3). The older population (n=23) ranges in age from 2681 to 2744 Ma (mean age 2709.0±8.6 Ma, Fig. 5.4.4). A single grain yielded an age of 3745±42 Ma; 6 grains give ages of 1100-1622 Ma and two spots within a single zircon show ages of 495 and 509 Ma.

While the undeformed grains show identical within-grain ages (±2SD) (Appendix 3A.1), each of five mosaic grains shows significant within-grain variations. Two analyses of grain NU-19-03 give 404±10 and 518±12 Ma. The range in age within grains NU-25-08 and NU-26-08 was less significant (383 to 414 Ma and 370 to 392 Ma respectively), but still outside the analytical error. As laser-ablation analyses used a spot size of ca 30 μm, the results probably reflect a mixture of older blocks and younger interblock material.

To confirm these age variations within the mosaic zircons, 15 SHRIMP U-Pb analyses were carried out on structural elements defined on CL images (Appendix 3A.2). Analyses within the blocks yielded ages of 414±9 to 457±30 Ma while interblock material gives ages from 354±29 to 385±12 Ma.

Table 5.4.1. U-Pb ages of zircons from the Nurbinskaya kimberlite field

| Type of grains | Sample type | Main population age, Ma (number of grains) | Youngest age, Ma | Oldest age, Ma |
|---|---|---|---|---|
| **Undeformed** | Archean population | 2709.0±8.6 (23) | 2681±38 | 2744±68 |
| | Devonian population | 370.7±2.3 (18) | 365±10 | 375±10 |
| **Mosaic** | blocks | n/a (6) | 414±9 | 457±30 |
| | interblocks | n/a (5) | 354±29 | 385±12 |

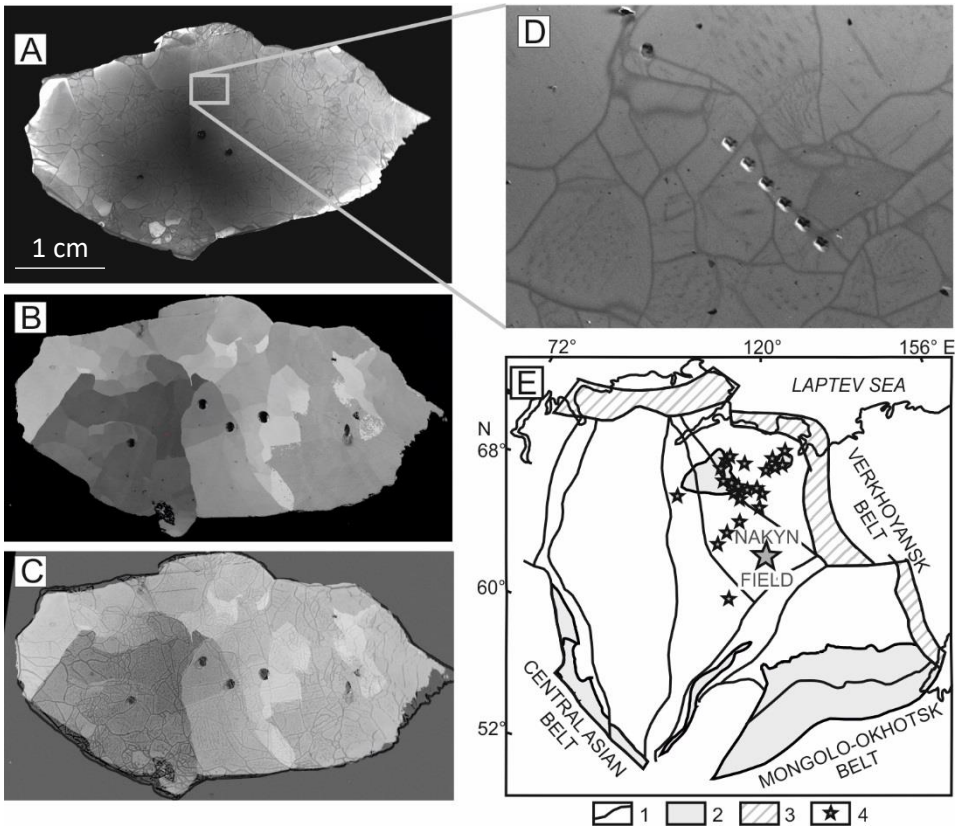



Figure 5.4.1. Mosaic structure by cathodoluminescence (A and D) imaging and EBSD mapping (B). Figure C combine EBSD map with traced CL-image.

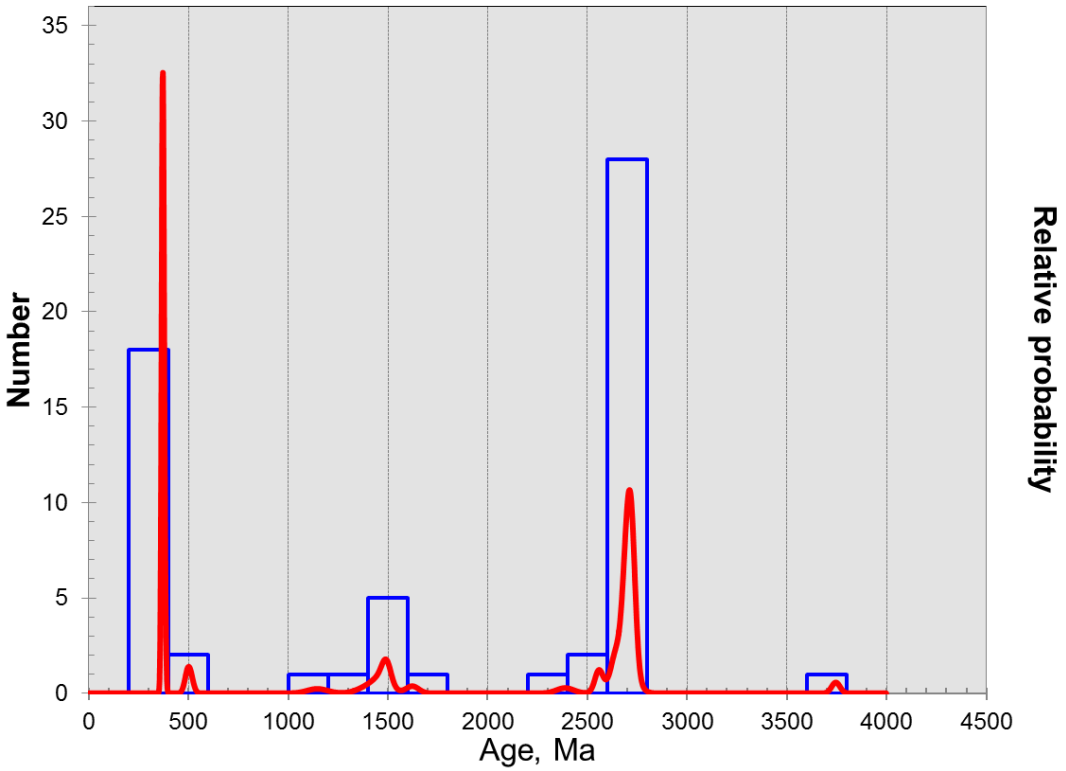



Figure 5.4.2. U-Pb ages of zircons from the Nurbinskaya pipe.

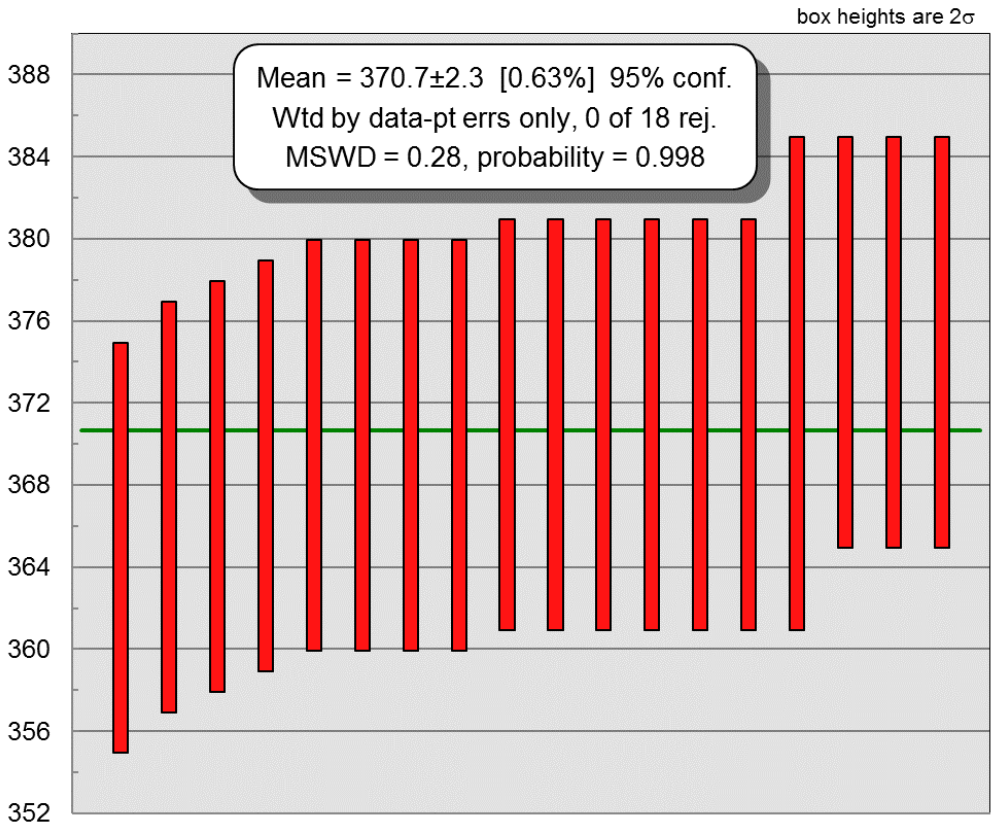



Figure 5.4.3. The weighted mean age of the youngest age peak, Nurbinskaya pipe.

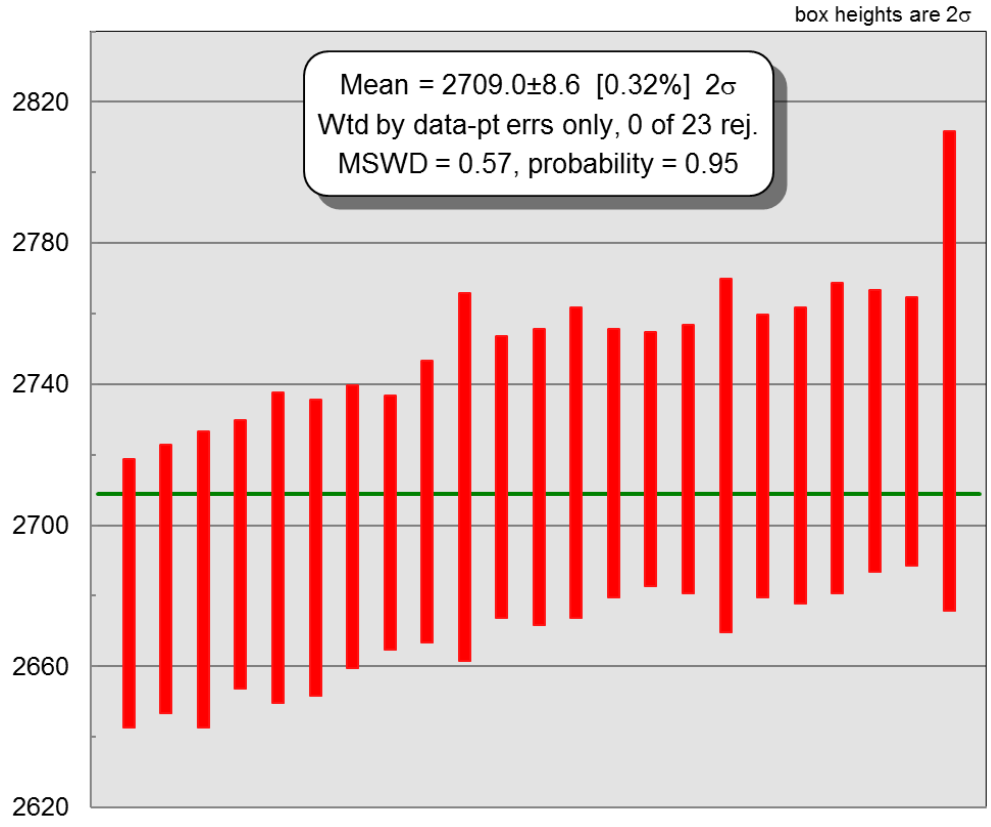



Figure 5.4.4. The weighted mean age of the oldest age peak, Nurbinskaya pipe.

**The Botuobinskaya pipe**

Zircons were extracted from two crustal xenoliths from the Botuobinskaya pipe. Twenty zircon grains from the sample BT-07-03 and twenty-one from xenolith BT-39-03 were analysed for their U-Pb age. All analysed grains have discordance less than 10%.

Sample BT-07-03 show the range of U-Pb ages from 2630 to 2942 Ma (Fig. 5.4.5). The major peak with the weighted mean age of 2787±11 (MSWD = 1.3, probability = 0.26; Fig. 5.4.6) was calculated out of 7 grains.

All zircons from the sample BT-39-03 lie on the regression line with upper intercept with concordia at 2748±33 Ma and lower intercept at 2028±58 Ma (MSWD = 0.64; Fig. 5.4.7). The youngest obtained age is 2026±11 Ma, the oldest - 2770±11 Ma. The main age population yielded the weighted mean age of 2745.2±7.5 Ma (MSWD = 1.17, probability = 0.31; Fig. 5.4.8).

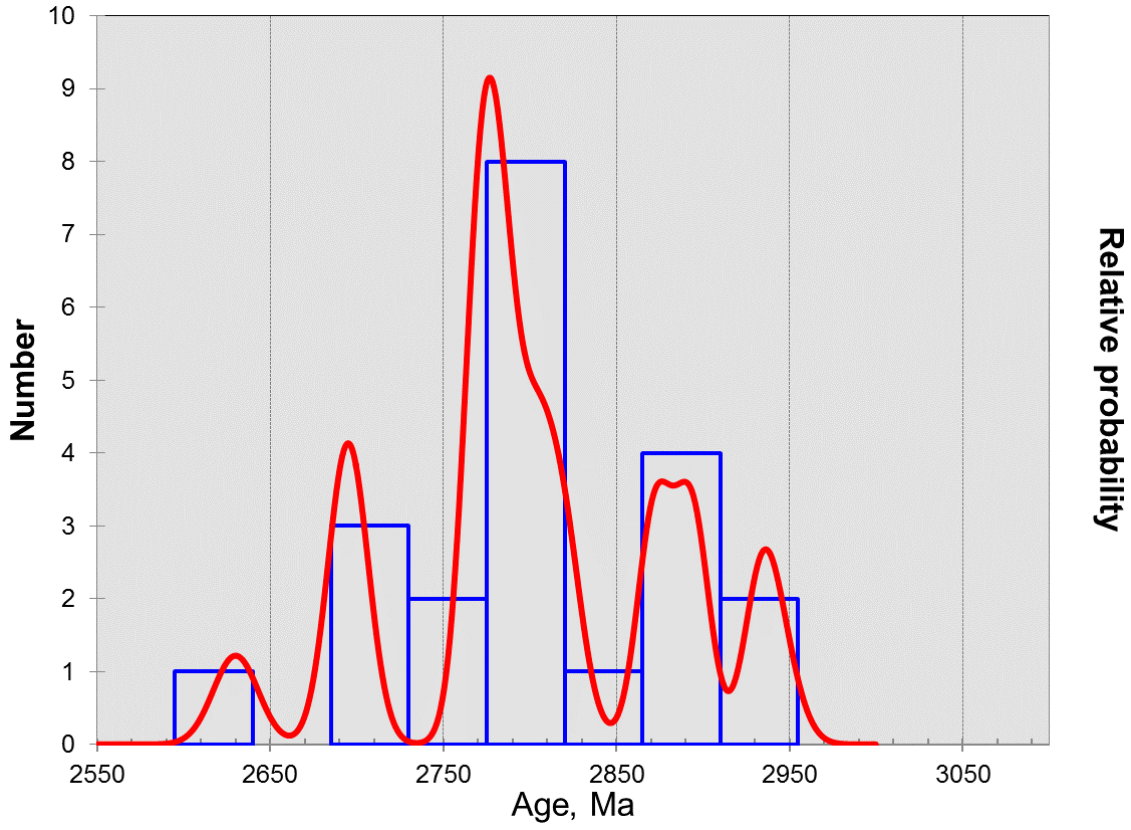



Figure 5.4.5. U-Pb ages of zircons from xenolith BT-07-03, Botuobinskaya pipe.

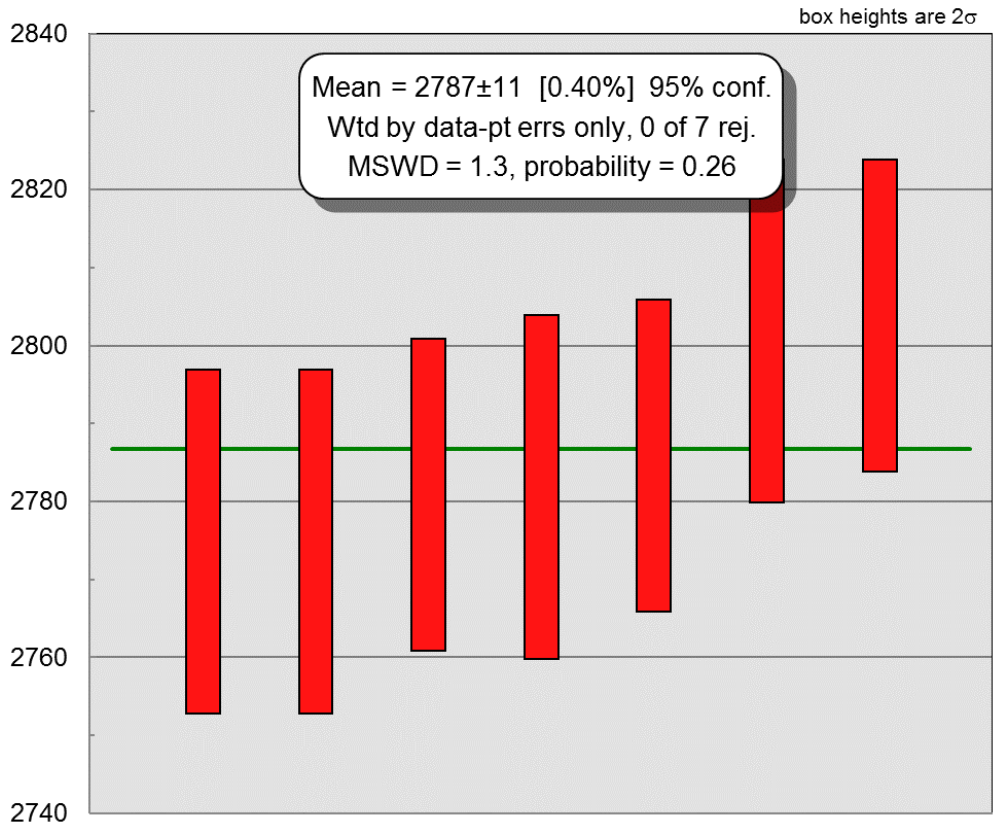



Figure 5.4.6. The weighted mean age of the major age peak, sample BT-07-03, Botuobinskaya pipe.

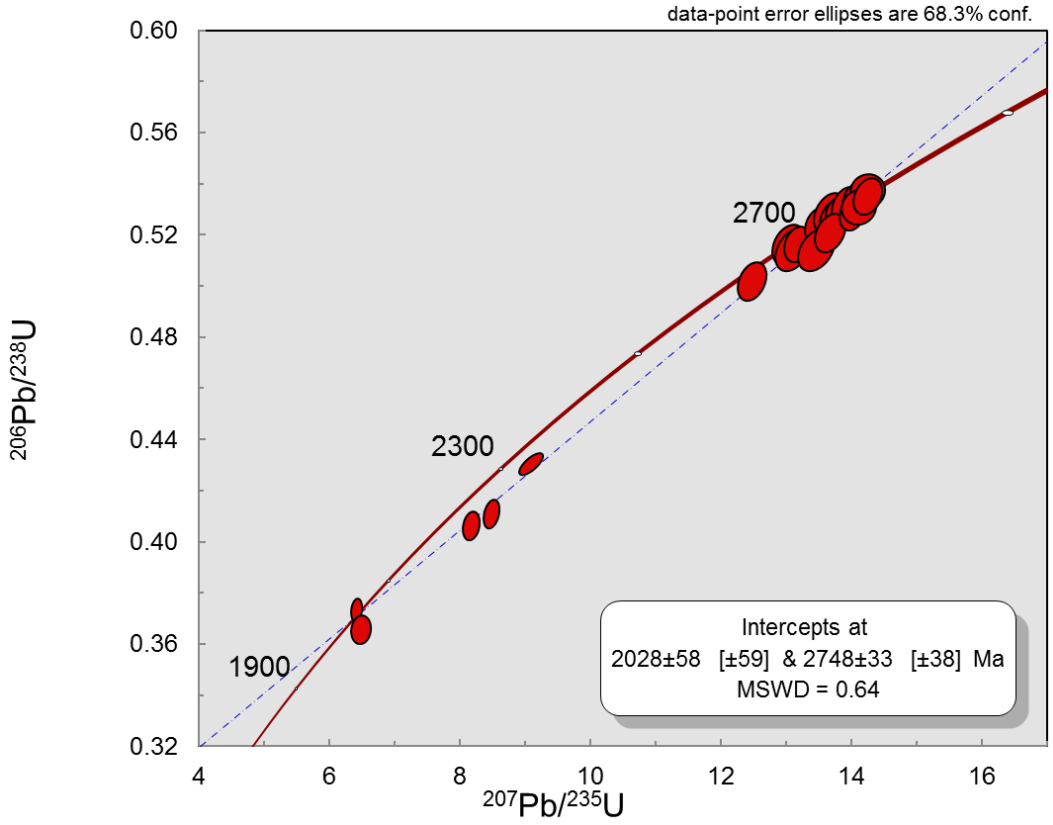



Figure 5.4.7. U-Pb concordia for zircons from sample BT-39-03, Botuobinskaya pipe.

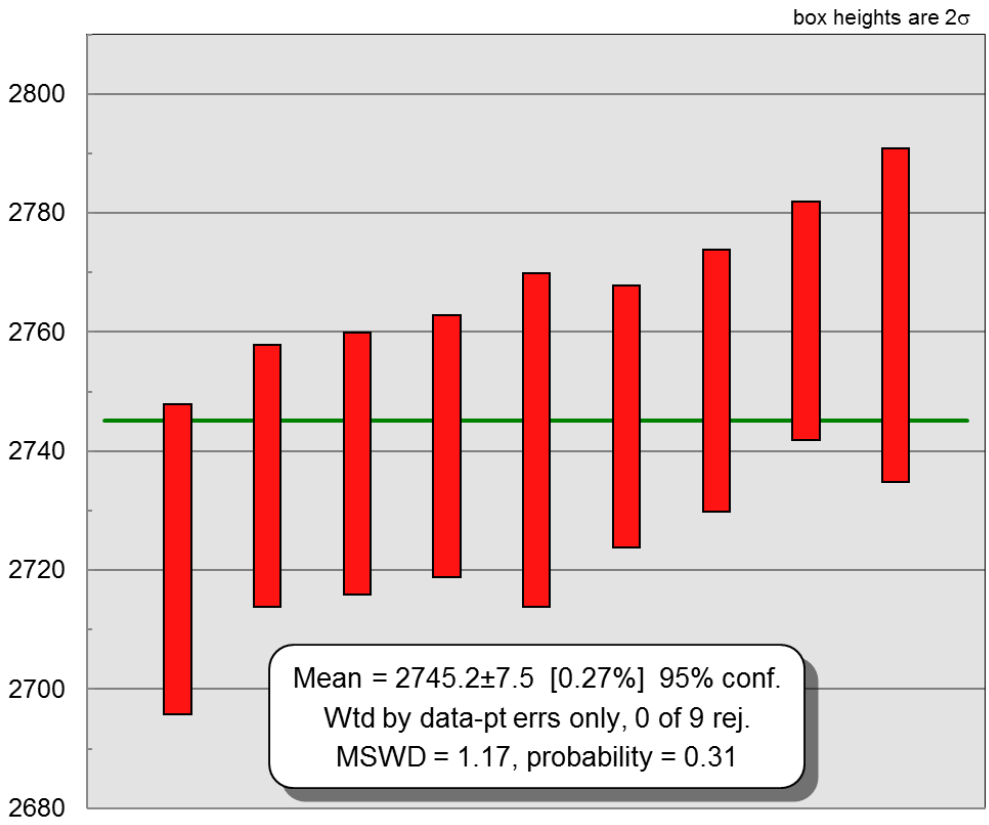



Figure 5.4.8. The weighted mean age of the major age peak, sample BT-39-03, Botuobinskaya pipe.

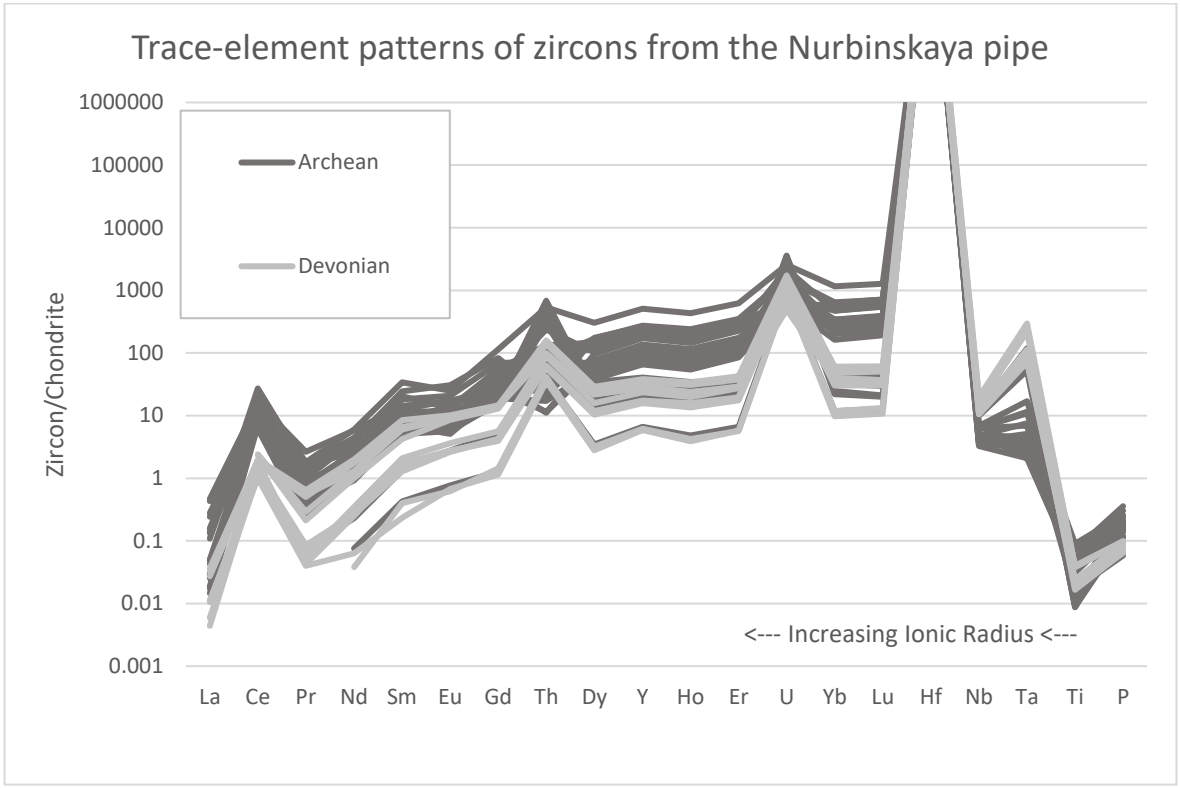
***Trace-element data***

**The Nurbinskaya pipe**

In total 79 trace-element analyses were performed on zircons from the Nurbinskaya pipe (Appendix 3A.3). Mosaic grains were analyzed in spots placed within blocks and interblock materials as well as using rastering profiles following or crossing structural elements.

All analyzed grains have chondrite-normalized trace-element patterns typical of zircons, with depletion in light rare earth elements (LREE) and enrichment in heavy rare earths (Fig. 5.4.7, 5.4.8). However, the total concentrations of trace elements are relatively low.

Undeformed grains from different age populations (mean ages 2.7 Ga and 370 Ma, and grains of ages 495 – 1622 Ma) show notable variation in the concentrations of some elements (Fig. 5.4.7). In general, ancient population (mean age 2.7 Ga) has higher concentrations of trace elements except for Nb and Ta. Thus, total REE contents in Archean zircons diverge from 102 to 723 ppm, while Devonian population shows the range 7.5 – 52 ppm (Fig. 5.4.8). Devonian grains have Y (13 – 86 ppm), Th (1.4 – 6.3 ppm) and U (8.2 – 17.2 ppm) lower than Archean ones (148 – 1147 ppm, 0.4 – 21.2 ppm and 5.2 – 26 ppm correspondingly).



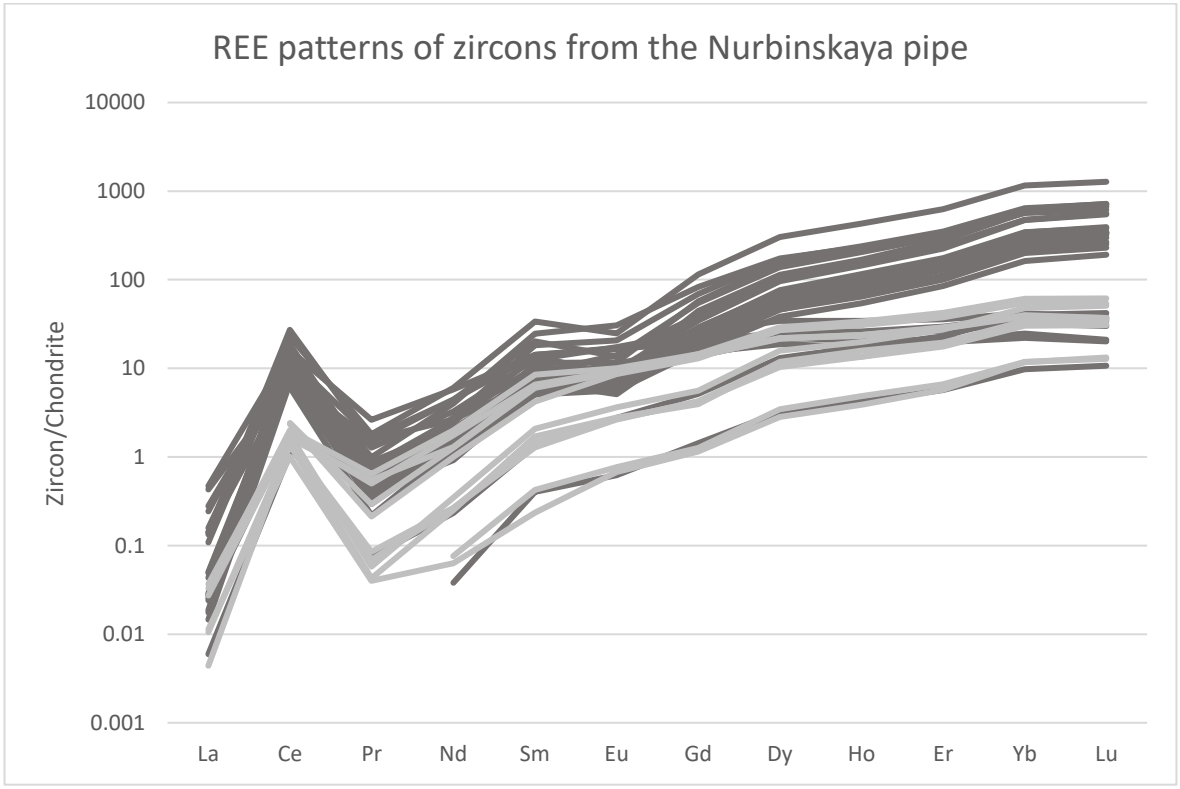




Figure 5.4.9. Trace-element and rare-earth element patterns of undeformed zircons from the Nurbinskaya pipe.

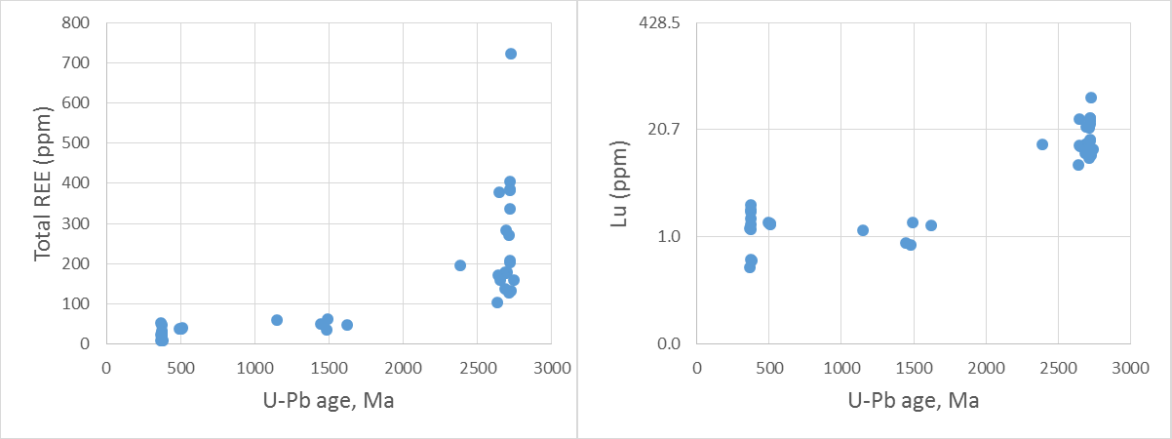



Figure 5.4.10. Total REE and Lu concentrations *vs* U-Pb age of undeformed zircons from the Nurbinskaya pipe.

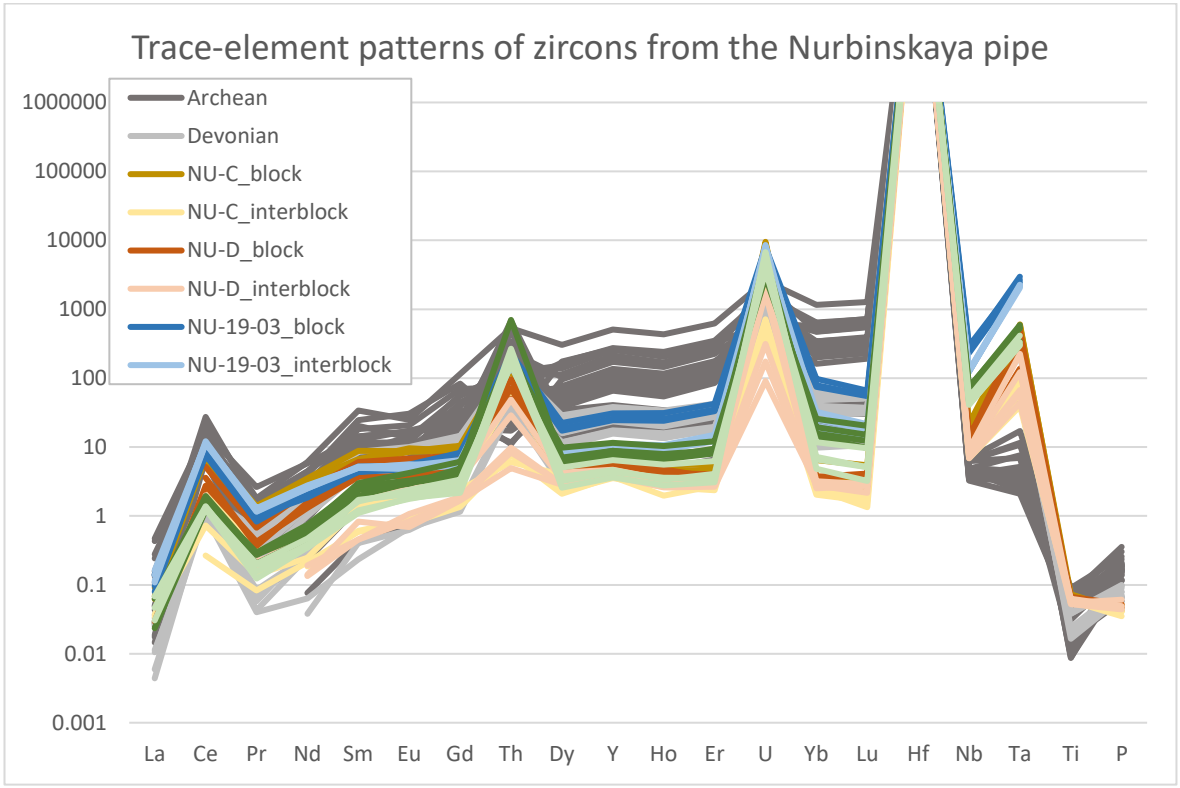
The REE patterns are similar in both populations, but young zircons are more depleted then old ones, especially in HREE. Archean zircons show minor or no Eu-anomaly, while all Devonian grains lack Eu-minima (Fig. 5.4.7).

Th/U ratio for all undeformed grains ranges from 0.06 to 0.83, Nb/Ta – from 0.83 to 24.3. All Devonian grains have low Nb/Ta ratio (0.83 – 1.85), similar to the ratio of 1.44 – 1.62 Ga zircons (1.3 – 2.38), while ancient grains show much higher Nb/Ta values – 5.0 – 24.3.

The trace-element compositions of the mosaic grains are similar to those of the young undeformed ones (Fig. 5.4.9). All mosaic grains have Th/U from 0.03 to 0.5, Nb/Ta – 0.34 - 2.19.

The REE pattern is generally flat and repeating the patterns of undeformed Devonian grains. Equally to those, mosaic grains show a moderate positive Ce-anomaly and no Eu-anomaly. However, most of them are also more depleted in HREE than zircons from young population. Rastering profiles across blocks and interstitial areas show that blocks generally have higher concentrations of REE than interblock material (Fig. 5.4.9.).

According to CART statistical classification, all underfomed zircons younger than 2 Ga and mosaic grains have a trace-element composition typical of kimberlitic zircons. The ancient population of zircons has more variable trace-element signatures: 13 grains were classified as “carbonatitic”, 6 zircons have typical “kimberlitic” trace-element composition, and 7 grains show similarity to zircons from intermediate rocks. This illustrated well by Y *vs* Yb/Sm discrimination diagram (Fig. 5.4.10).



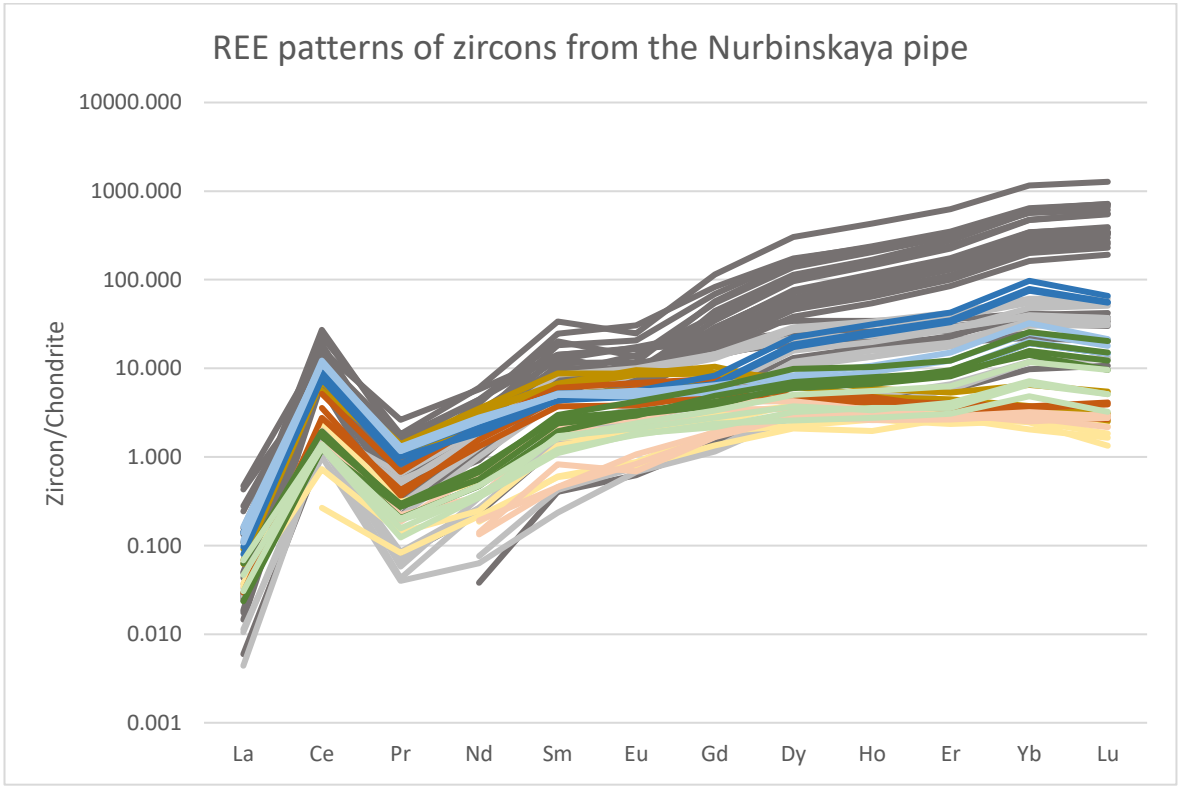




Figure 5.4.11. Trace-element and rare-earth element patterns of mosaic and undeformed zircons from the Nurbinskaya pipe.

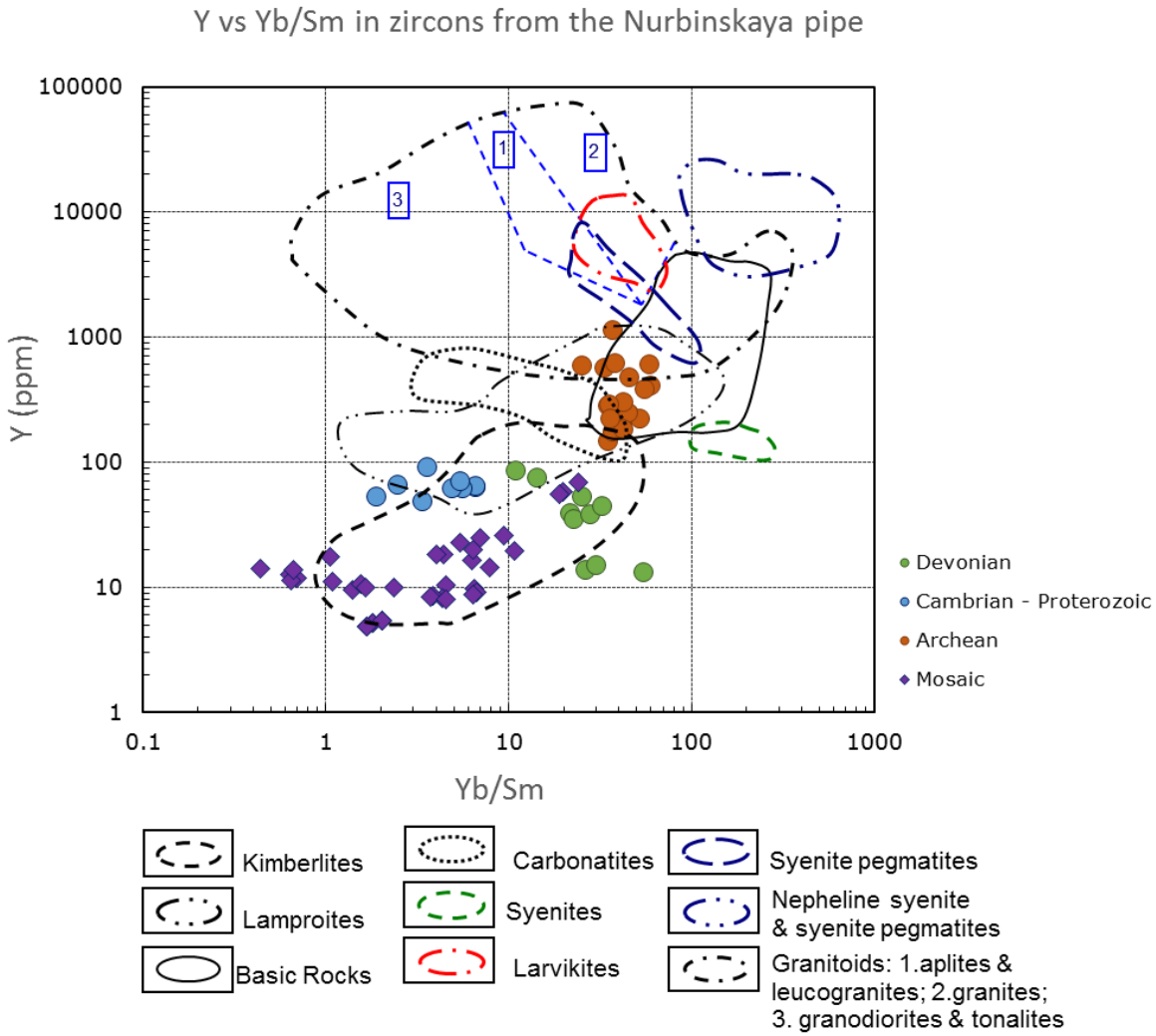



Figure 5.4.12. Y *vs* Yb/Sm discrimination diagram for zircons from the Nurbinskaya pipe.

***Hafnium-isotope data***

**The Nurbinskaya pipe**

Hf isotopes were analyzed in 39 undeformed and 5 mosaic zircon grains (Appendix 3A.5).

Undeformed Devonian zircons have εHf ranging from 6.4 to 12, while the Archean grains have εHf of *ca* -4 to +2.7 (Fig. 5.4.11). The grains with ages in between these two populations have εHf values from -23.2 (U-Pb age 1146 Ma) to -6.6 (U-Pb age 2388 Ma). Calculated initial $^{176}Hf/^{177}Hf$ for Devonian population gives the range 0.282729 – 0.282894; Archean zircons reveal values from 0.280968 to 0.281113. Crustal model ages calculated for Archean zircons fall in the range 3.04 – 3.42 Ga. The same interval of crustal model ages was determined for zircons with U-Pb ages between 1146 and 1622 Ma. All grains of Devonian U-Pb age have estimated crustal model ages from 0.58 to 0.9 Ga.

Five mosaic grains were analyzed within blocks and by rastering the laser beam along profiles that crossed structural elements and followed interblock zones. The profiles crossing structural boundaries and those within interblock areas both have flat and stable signals, without any steps in Hf-isotope composition. εHf for spots and traverses showed no significant variation. Initial $^{176}Hf/^{177}Hf$ for mosaic grains was calculated using the age of 370 Ma for spots and lines in interstitial areas, and 400 and 450 Ma for the profile and spots within the block, respectively. All εHf values fall in a narrow range from -30.3 to -35.9 (Fig. 5.4.11), and Hf crustal model ages are close to those of the Archean population (3.3-3.6 Ga).

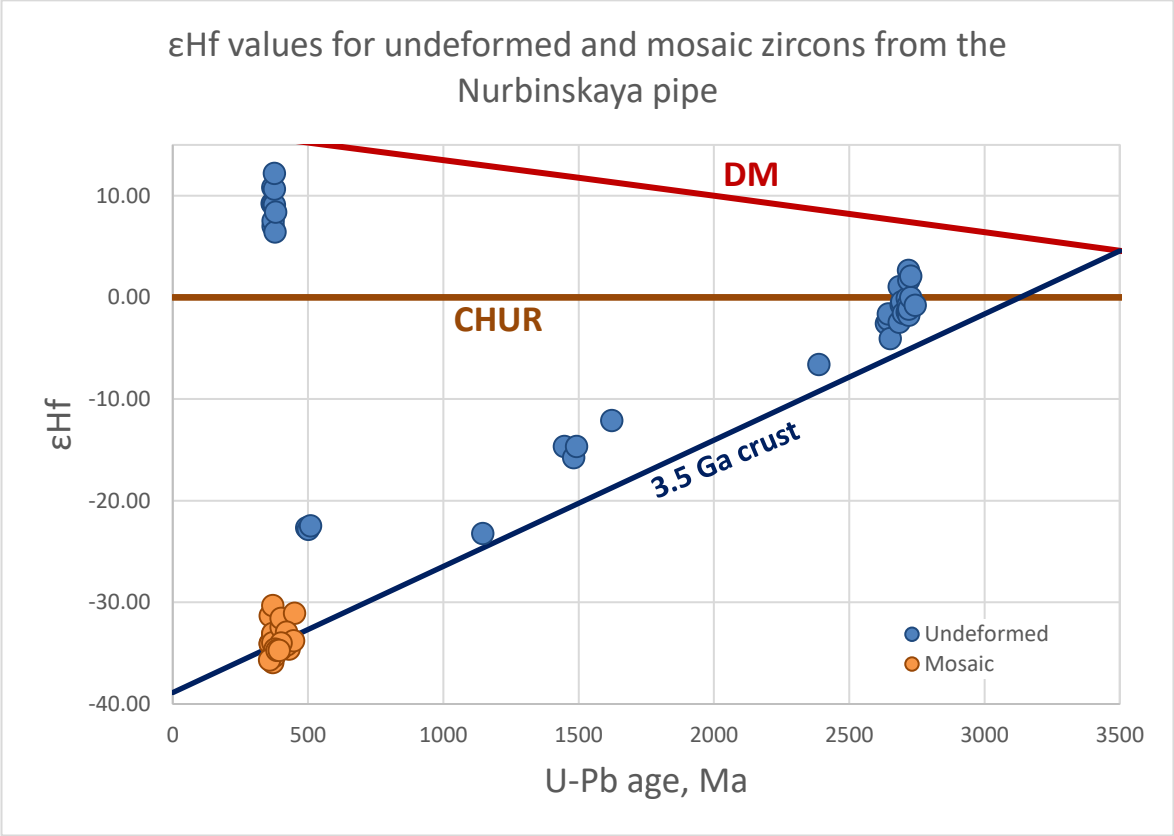



Figure 5.4.13. εHf *vs* U-Pb age plot for undeformed and mosaic zircons from the Nurbinskaya pipe.

**The Botuobinskaya pipe**

Lu-Hf isotopic composition was studied in zircons from both xenoliths BT-07-03 and BT-39-03. In total 20 grains from sample BT-07-03 and 21 – from sample BT-39-03 were analysed.

Zircons from xenolith BT-07-03 show relatively narrow interval of εHf values from -3.0 to +2.6 (Fig. 5.4.12). Calculated initial $^{176}Hf/^{177}Hf$ for these grains diverge from 0.280907 to 0.281064. Calculation of crustal model ages gives the range 3.11 – 3.42 Ga.

Sample BT-39-03 contains zircons with more variable εHf ranging from -15.6 to +2.1. However, the interval of the initial $^{176}Hf/^{177}Hf$ ratios is narrower: from 0.280987 to 0.281083. Crustal model ages are close to those of the sample BT-07-03 and fall in between 3.12 and 3.65 Ga.

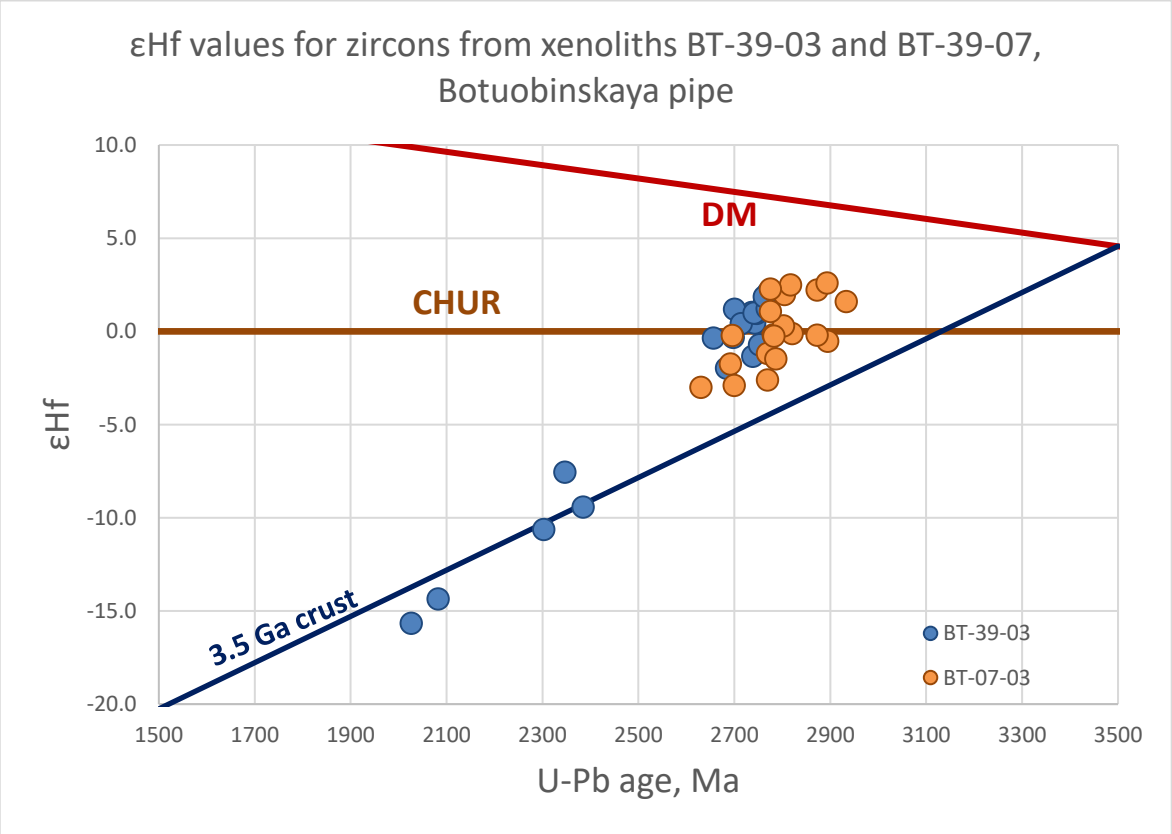



Figure 5.4.14. εHf *vs* U-Pb age plot for zircons from xenoliths BT-07-03 and BT-39-03, Botuobinskaya pipe.

***Oxygen isotopic data***

**The Nurbinskaya pipe**

Only mosaic zircons from the Nurbinskaya pipe were analysed for their oxygen isotopic composition (Appendix 3A.4). Analytical spots have been placed along profiles crossing blocks and interstitial zones within 4 areas. The distance between spots is 20 and 25 μm (Fig. 5.4.1D).

The first profile within grain NU-19-03 (n=12) has an average $\delta^{18}O$=6.0±0.3‰. The second profile (n=9) has an average $\delta^{18}O$=5.6±0.3‰. The profiles within grains NU-25-08 and

NU-26-08 show average $\delta^{18}O$=5.8±0.27‰ (n=5) and 5.7±0.3‰ (n=6), respectively (Fig. 5.4.13). No significant difference in $\delta^{18}O$ was found between blocks and interstitial areas.

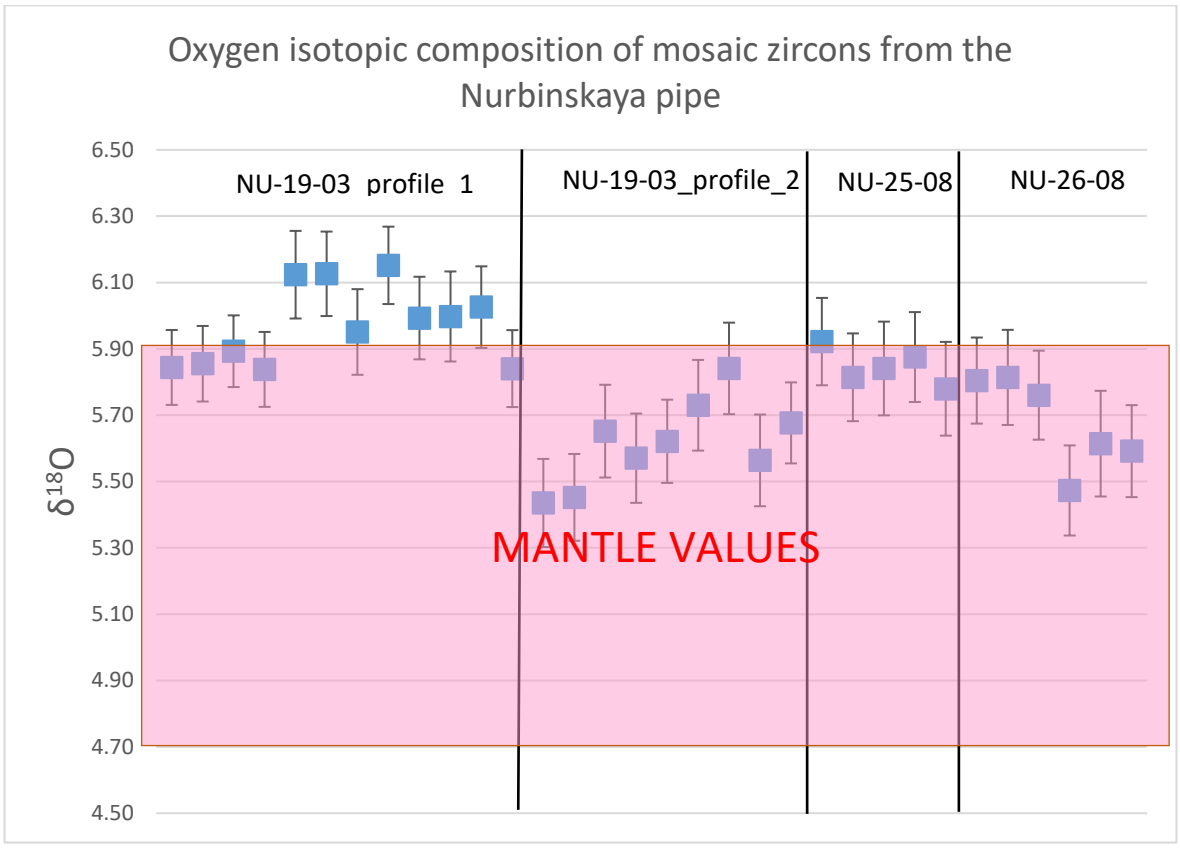



Figure 5.4.15. $\delta^{18}O$ plot for zircons from the Nurbinskaya pipe. Bars show 2σ error.

# Chapter 6. The Daldyn terrane.

The Daldyn terrane is a slice of high grade rocks thrusted over the Magan province in the west along the Kotuykan shear zone (Fig. 6) (Rosen *et al.*, 1994). Phanerozoic cratonic sediments cover the terrane, which is exposed only in the Anabar shield. The exposed or outcropped rocks are represented by enderbite-mafic granulite and enderbite-charnockite complexes folded into dominantly linear isoclinal folds with north-western strikes and generally north-east dips (Rosen, 1989). These rocks can be traced by magnetic and gravity anomalies under the sedimentary cover into both north and south of the Anabar shield (Zaitsev & Smelov, 2010).

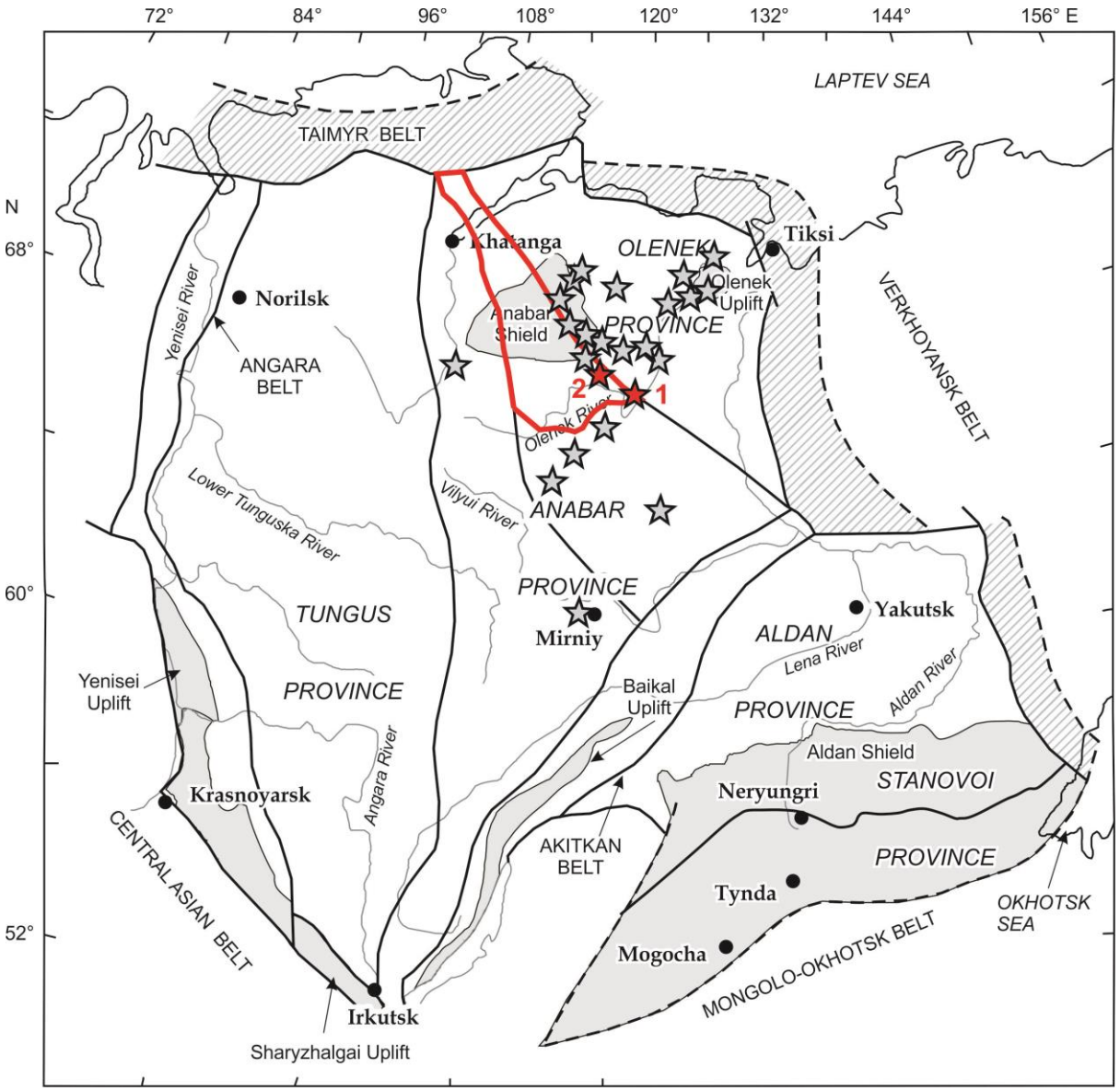



Figure 6. The location of the Daldyn terrane and studied kimberlite fields. Red stars are for kimberlite fields studied: 1 – Chomurdakh; 2 – Kuranakh.

Only a few isotopic geochronological studies have been done for the rocks of this terrane. In summary, isotopic ages from the Daldyn terrane suggest a crustal formation age of about 3.1 Ga followed by major deformation and metamorphic processes at 2.7-2.8 and 1.9 Ga (Zaitsev & Smelov, 2010).

There are three kimberlitic fields found within the terrane: Chomurdakh, Kuranakh and Birigindinskoe, all of them are poorly diamondiferous. This study includes samples from two kimberlitic fields – Chomurdakh and Kuranakh (Table 6). All analytical data are presented in the Appendix 4.

A previous study of crustal xenoliths from kimberlitic pipes of the Daldyn terrane shows two main types of sampled rocks: garnet, two-pyroxene mafic granulites and garnet-scapolite-zoisite-plagioclase granulites (Rosen *et al.*, 1994).

Table 6. Analytical work done for samples from the Daldyn terrane.

| **Field** | **Pipe** | **Type of samples*** | **Zircons** | | | |
|---|---|---|---|---|---|---|
| | | | **U-Pb^** | **TE** | **O** | **Hf** |
| Chomurdakh | Druzhba | kimberlite | 6 | | | |
| | Rassvet | kimberlite | 12 (10) | 10 | | |
| | Khairgastakh | kimberlite | 10 | | | |
| Kuranakh | Malokuonapka | kimberlite | 36 (32) | 20 | | |
| *Total for the terrane* | | | *64 (58)* | *30* | | |

* Type of samples: kimberlite - hand-picked zircons from crushed kimberlite.
^ U-Pb analyses: total (used)

## 6.1. The Chomurdakh kimberlite field

The Chomurdakh field is located within the basin of a middle part of the Olenek river.

According to Zaitsev and Smelov (2010) 42 kimberlite bodies (25 pipes and 17 dykes) are discovered within the field, 6 of them are diamondiferous. Kimberlites are intruded into Middle to Late Cambrian carbonate sequence presented mostly by limestone and carboniferous mudstone. The age of the host rock is the only geological evidence of the kimberlite age observed at the Chomurdakh field.

Kimberlites were studied previously by K-Ar, Rb-Sr and U-Pb isotopic geochronological techniques. The majority of results fall into 2 main time intervals: 353-390 and 405-440 Ma, however, younger ages (217 Ma, U-Pb) are also reported for this field.

### *Zircon U-Pb data*

Zircons were recovered from the crushed kimberlite rock of three pipes: Druzhba, Rassvet and Khairgastakh (Table 6.1.1). Zircon grains were picked up by hand based on their large size (>2 mm) and morphology, typical of kimberlitic zircons (clear, transparent grains, yellowish, pinkish or brownish in color). All data are given in the Appendix 4.1.

#### The Druzhba pipe

Only 6 zircon grains were recovered from the pipe and analysed for U-Pb age. The obtained ages form a single population ranging from 406 to 424 Ma and give the intercept with concordia at 412±5.5 Ma (MSWD = 0.75; Fig. 6.1.1). The weighted mean approach to calculate the age for this population produced the same result – 412.2±5.2 Ma (MSWD = 0.81, Fig. 6.1.2).

Table 6.1.1. A summary of U-Pb age results for zircons from the Chomurdakh kimberlite field, Daldyn terrane.

| Pipe | Range of U-Pb ages, Ma (n = number of analyses) | Major population age, Ma | Minor peaks ages, Ma |
|---|---|---|---|
| **Druzhba** | 406-424 (n = 6) | 412.±5.5 | |
| **Rassvet** | 405 - 478 (n = 10) | 446±3.3 | |
| **Khairgastakh** | 176 - 434 (n = 10) | 416±2.5 | 176±6 |

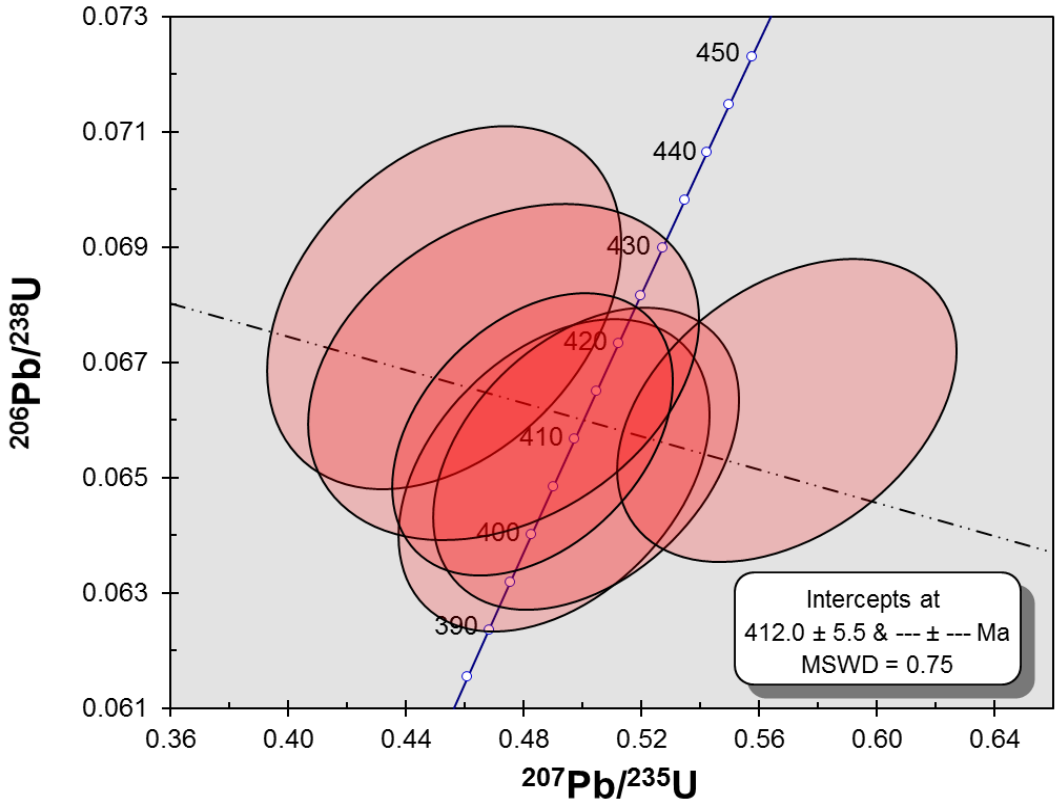



Figure 6.1.1. U-Pb concordia for zircons from the Druzhba pipe.

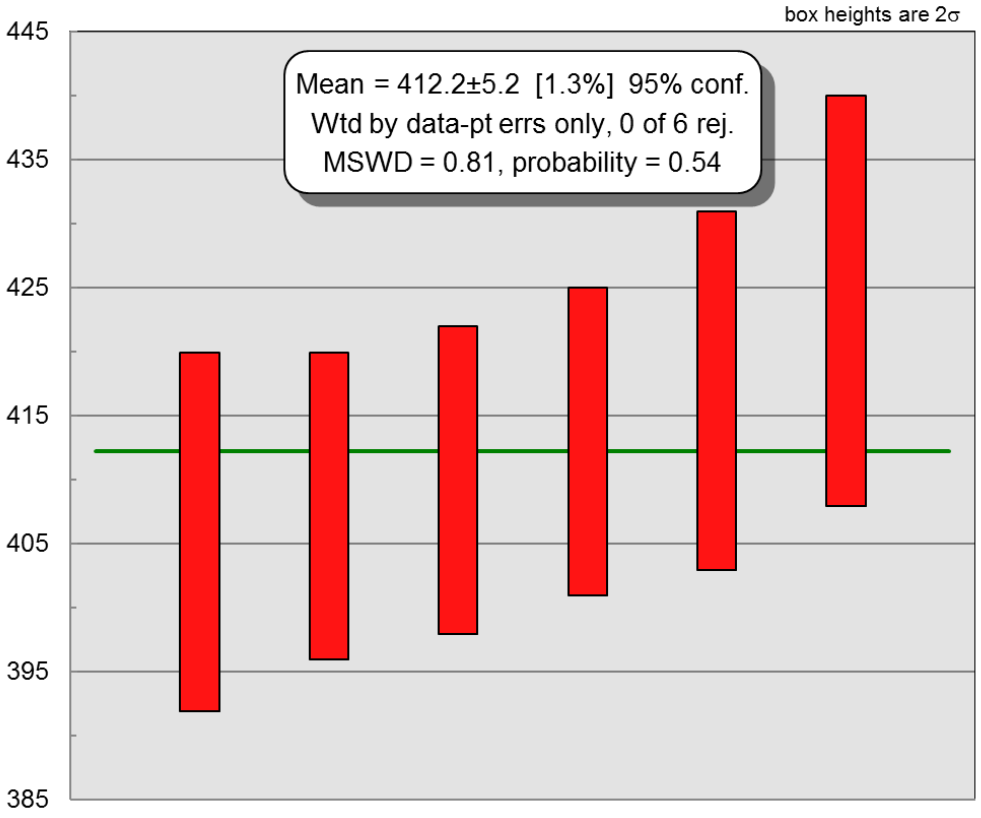



Figure 6.1.2. The weighted mean age of zircons from the Druzhba pipe.

**The Rassvet pipe**

In total 12 U-Pb analyses were obtained for zircons from the Rassvet pipe. Two of them were rejected later because of high discordance.

Ten U-Pb ages give range from 405±34 to 478±30 Ma. The calculated concordia age is 446±3.3 Ma (MSWD = 0.0026, probability = 0.96; Fig. 6.1.3.).

**The Khairgastakh pipe**

Ten zircon grains from the Khairgastakh pipe were dated by U-Pb technique, all of them are concordant.

Nine grains give range of ages from 402±16 to 434±18 Ma. The concordant age of this population is 416±2.5 Ma (MSWD = 0.15, probability = 0.70; Fig. 6.1.4).

A single zircon reveals an age of 176±6 Ma.

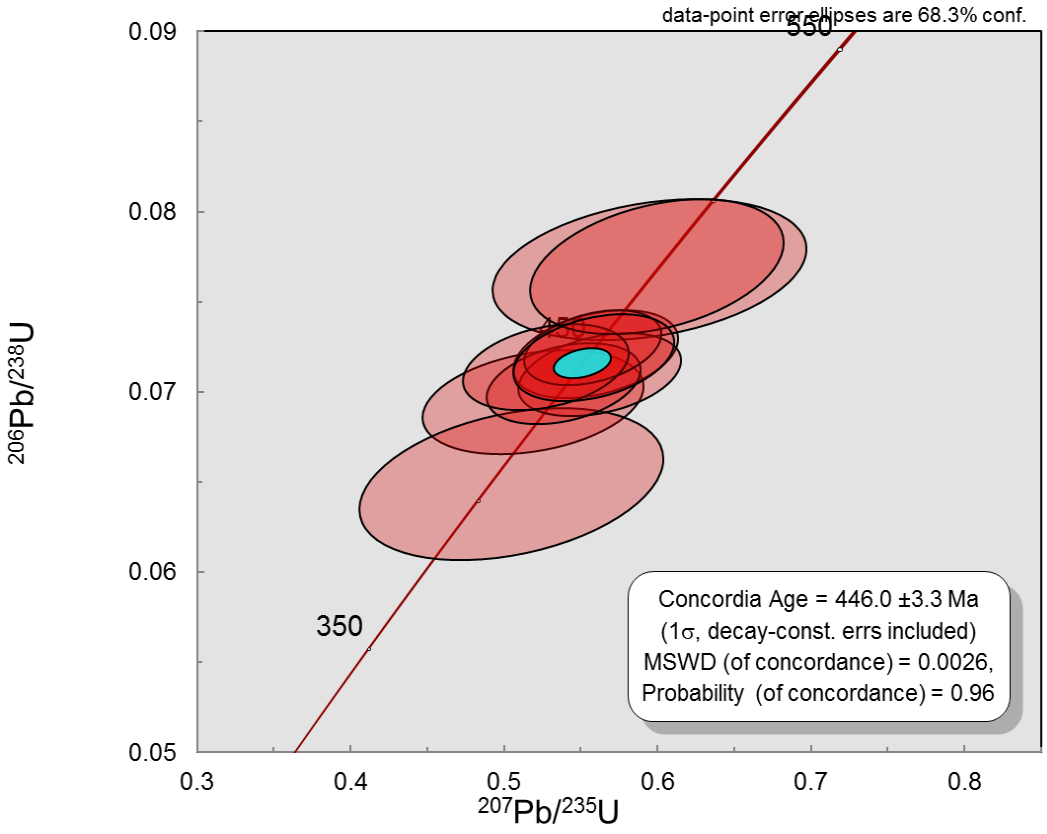



Figure 6.1.3. U-Pb concordia for zircons from the Rassvet pipe.

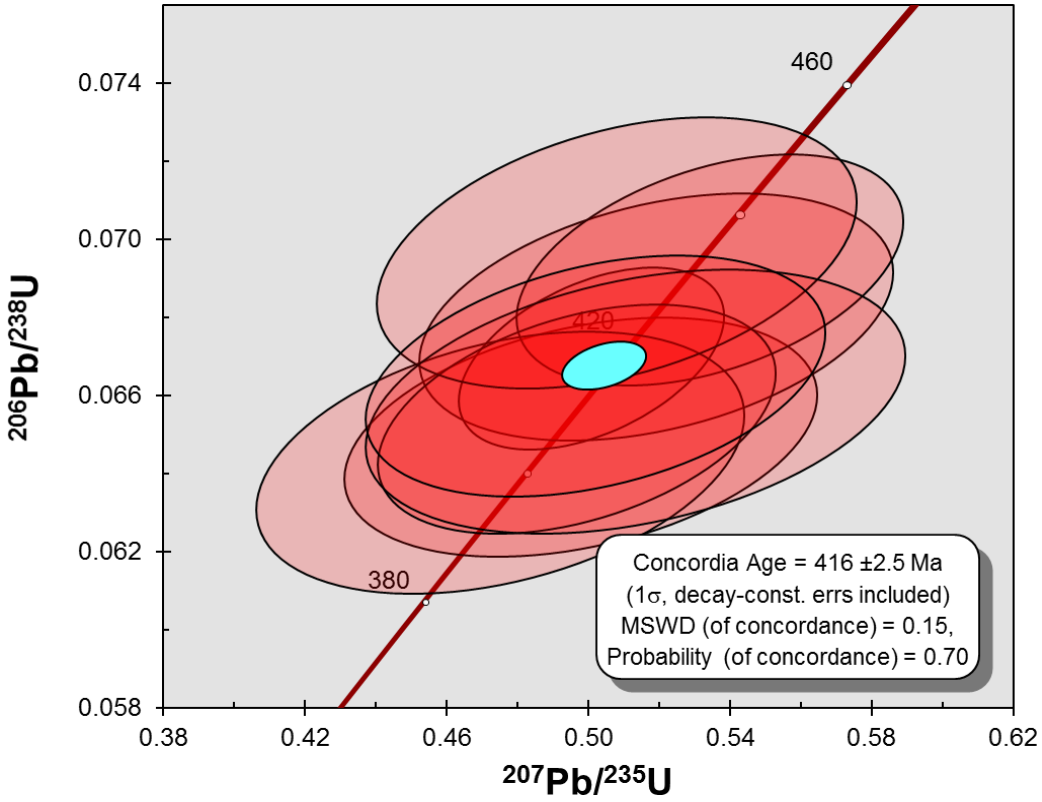



Figure 6.1.4. U-Pb concordia for zircons from the Khairgastakh pipe.

***Zircon trace-element data***

Trace-element composition was analysed only in zircons from the Rassvet pipe.

**The Rassvet pipe**

All 10 dated zircons from the Rassvet pipe were analysed for their trace-element composition.

The chondrite-normalised trace-element patterns of all analysed grains are generally similar with some minor variations in concentrations of light rare-earth elements (Fig. 6.1.5). Thus, Y concentrations diverge from 18.9 to 73 ppm, Th and U range from 1.5 to 4.8 ppm and from 7.4 to 13 ppm correspondingly. Total REE contents vary from 10 to 45 ppm. The most variable element is Sm, it differs from 0.05 to 1.15 ppm. All other elements range within an order of magnitude.

Th/U ratio varies from 0.21 to 0.37; Nb/Ta ranges from 0.82 to 1.56.

The REE plot demonstrates typical zircon patterns with depletion in LREE and enrichment in HREE. The positive Ce-anomaly is well defined, while Eu-minima is lacking for all grains. The absence of Eu-anomaly indicates no plagioclase crystallized before zircons.

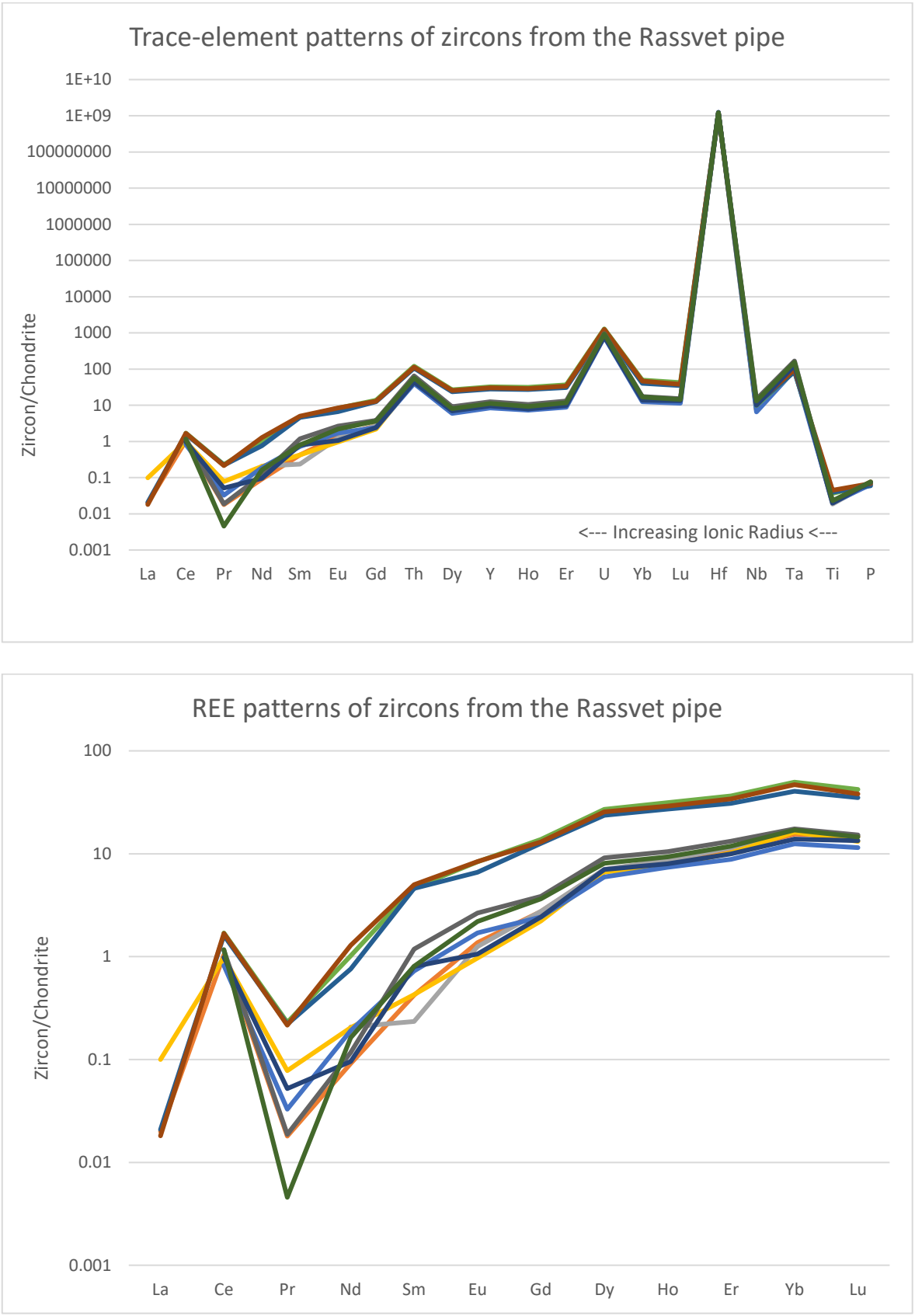



Figure 6.1.5. Trace-element and rare-earth element patterns of zircons from the Rassvet pipe.

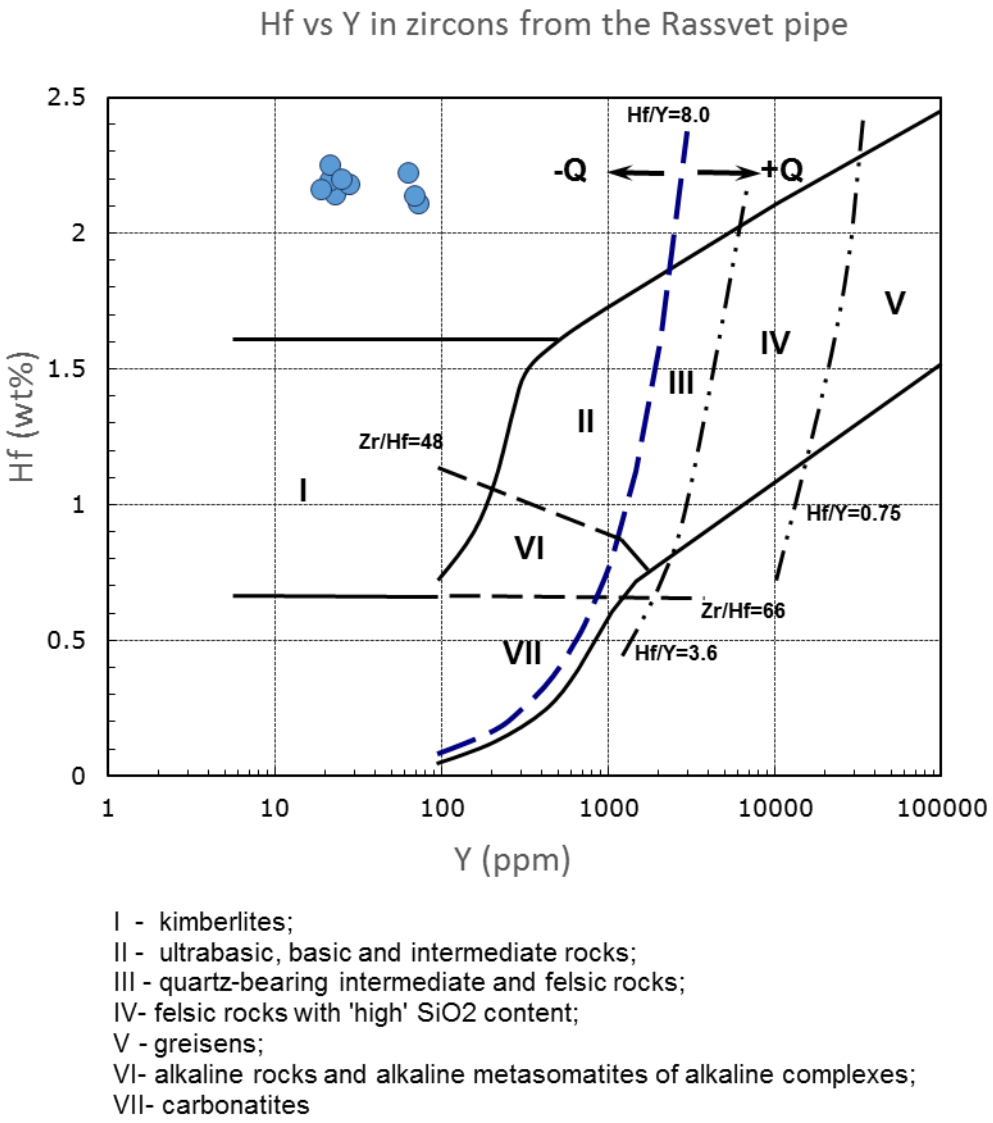



Figure 6.1.6. Hf *vs* Y discrimination diagram for zircons from the Rassvet pipe.

According to the CART statistical classification, all analysed grains have composition of trace elements typical for zircons from kimberlites, consistent with their low REE, Lu, U, Th, and Y concentrations. However, Hf contents (2.1 – 2.25 wt%) in these grains are higher than in typical kimberlitic zircons, thus at the discrimination plot Hf *vs* Y they are located above the kimberlitic field (Fig. 6.1.6). Unlike Hf, all other trace-element characteristics of zircons from the Rassvet pipe indicate their kimberlitic parental melt. The discrimination diagram Y *vs* Nb/Ta illustrates typical location of data points within the kimberlitic field (Fig. 6.1.7).

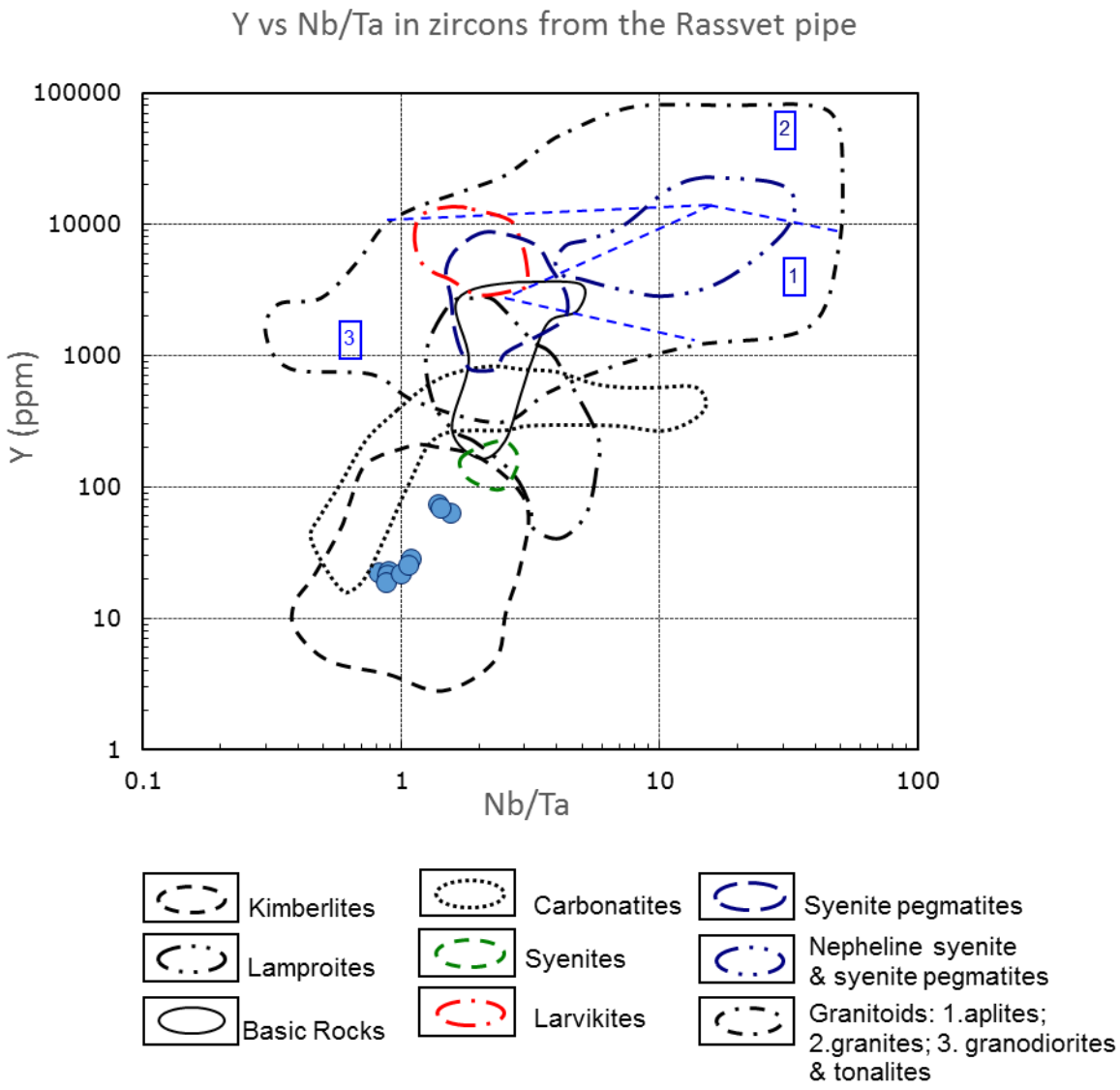



Figure 6.1.7. Y *vs* Nb/Ta discrimination diagram for zircons from the Rassvet pipe.

## 6.2. The Kuranakh kimberlite field

The Kuranakh field is the closest to the exposed basement rocks at the Anabar shield. The field is located within the basins of the Malokuonapka, Kuranakh and the Senku rivers. Twenty-five kimberlite bodies were found within the field, 6 of them contain diamonds.

Kimberlite pipes and dykes are hosted by various limestones of Late to Middle Cambrian age. There are no observed intrusions crosscutting kimberlites, however some of them are buried under the Quaternary sediments.

According to previous isotopic geochemical studies, kimberlite magmatism of the Kuranakh field has occurred twice - in Triassic and Jurassic time. Most of dated pipes give ages within 240-220 Ma time interval, however there are a few kimberlite bodies revealed *ca* 170 Ma age (Zaitsev & Smelov, 2010).

***Zircon U-Pb data***

Only one pipe from the field was sampled for zircons. This is Malokuonapka pipe, which is also mentioned in the literature as the Malokuonamskaya pipe.

**The Malokunapka pipe**

In total 36 zircon grains were analysed for U-Pb ages. Four of them were rejected because of their high discordance.

All analysed zircons form a single age population with range of ages from 202±30 to 234±12 Ma. The concordia age of this group is calculated at 221.9±1.5 Ma (MSWD = 1.6, probability = 0.21, Fig. 6.2.1).

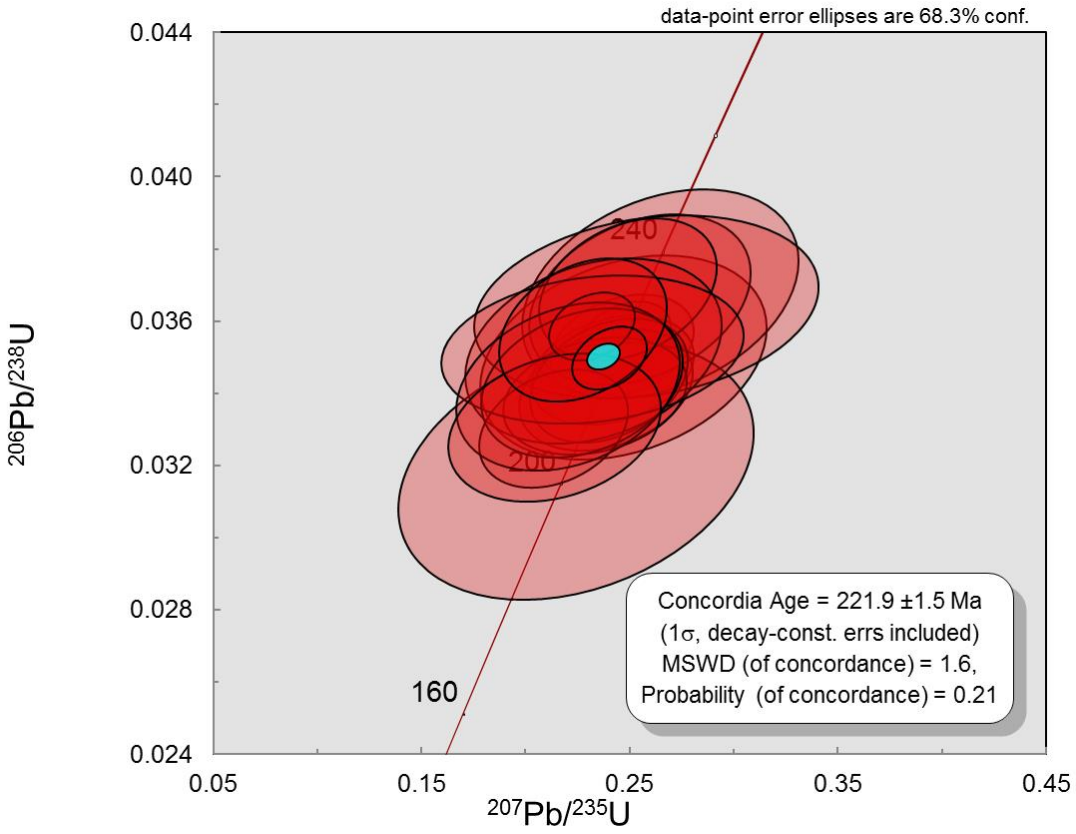



Figure 6.2.1. U-Pb concordia for zircons from the Malokuonapka pipe.

***Zircon trace-element data***

**The Malokuonapka pipe**

The trace-element composition was analysed for twenty zircons from the Malokuonapka pipe.

All analysed grains show similar chondrite-normalised trace-element patterns with some variations in concentrations of light rare-earth elements (Fig. 6.2.2). Y, Th and U diverge from 13.5 to 135 ppm, 0.9 to 10.5 ppm and 5.3 to 47 ppm, respectively. Total REE contents vary in interval 6.5 – 83 ppm. The Th/U and Nb/Ta ratios change within the intervals 0.17 – 0.33 and 0.9 – 1.83 correspondingly.

The REE plot demonstrates relatively low concentrations of all rare-earth elements. All zircon patterns are depleted in LREE and enriched in HREE. Not a single grain shows negative Eu-anomaly, however positive Ce-anomaly is typical for all zircons.

According to the CART statistical classification, 20 analysed grains have composition of trace elements typical of zircons from kimberlites and 2 show trace-element signatures similar to those of zircons from carbonatites. The grains classified as “kimberlitic” show Lu<2 ppm and U<30 ppm, while both “carbonatitic” grains have higher Lu (3.3 and 5.1 ppm) and U (33 and 47 ppm). The location of the data points within the kimberlitic and carbonatitic fields at the Y *vs* Nb/Ta discrimination diagram is in a good agreement with the results of the CART classification (Fig. 6.2.3).

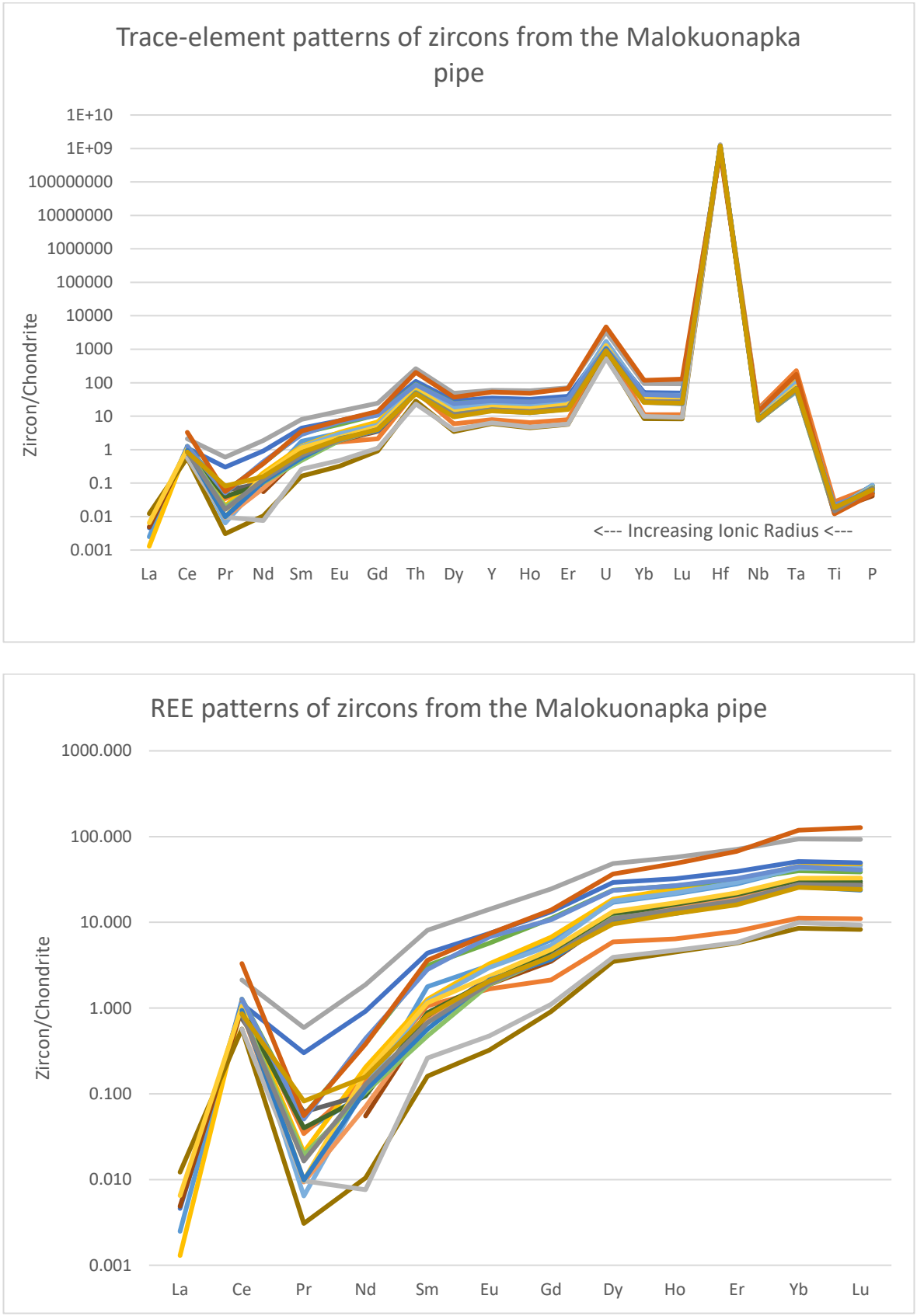



Figure 6.2.2. Trace-element and rare-earth element patterns of zircons from the Malokuonapka pipe.

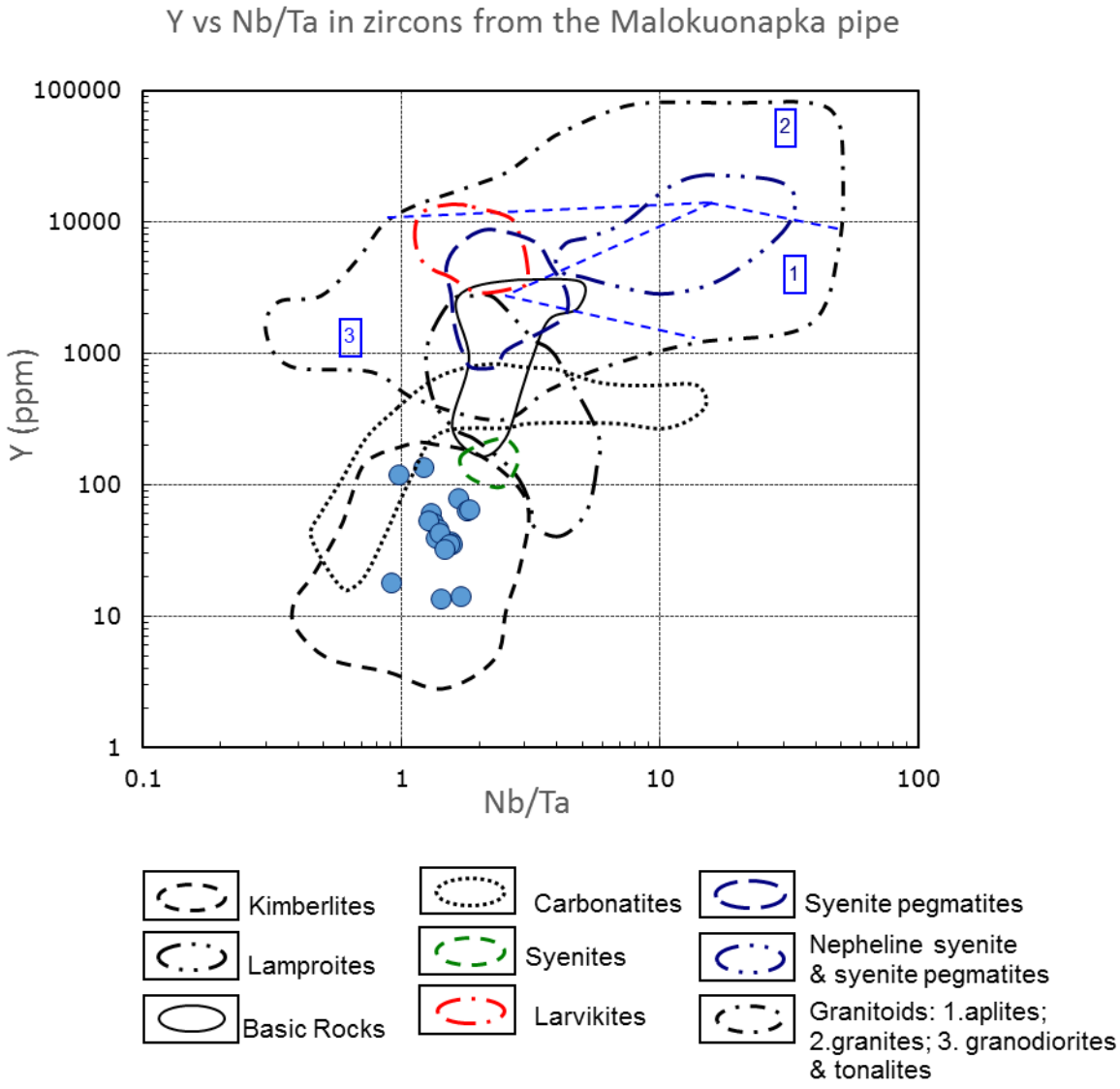



Figure 6.2.3. Y vs Nb/Ta discrimination plot for zircons from the Malokuonapka pipe.

# Chapter 7. The Khapchan terrane

The Khapchan granulite-gneiss terrane is included in the Olenek tectonic province (Fig. 7). It is exposed in the eastern part of the Anabar shield and according to geophysical data extends to North and South under the sedimentary cover (Rosen *et al.*, 2002, Smelov & Zaitsev, 2013).

The terrane is considered to be a fold belt, which was affected by granulite–facies metamorphism. Up to 40% of the terrane volume consists of carbonate rocks including marble, calciphyre and carbonate-silicate rocks. Subsidiary enderbites and schists are also present. In the central and southern parts, the rocks of the terrane are deformed into linear folds; dome-shaped structures are found in the northern area.

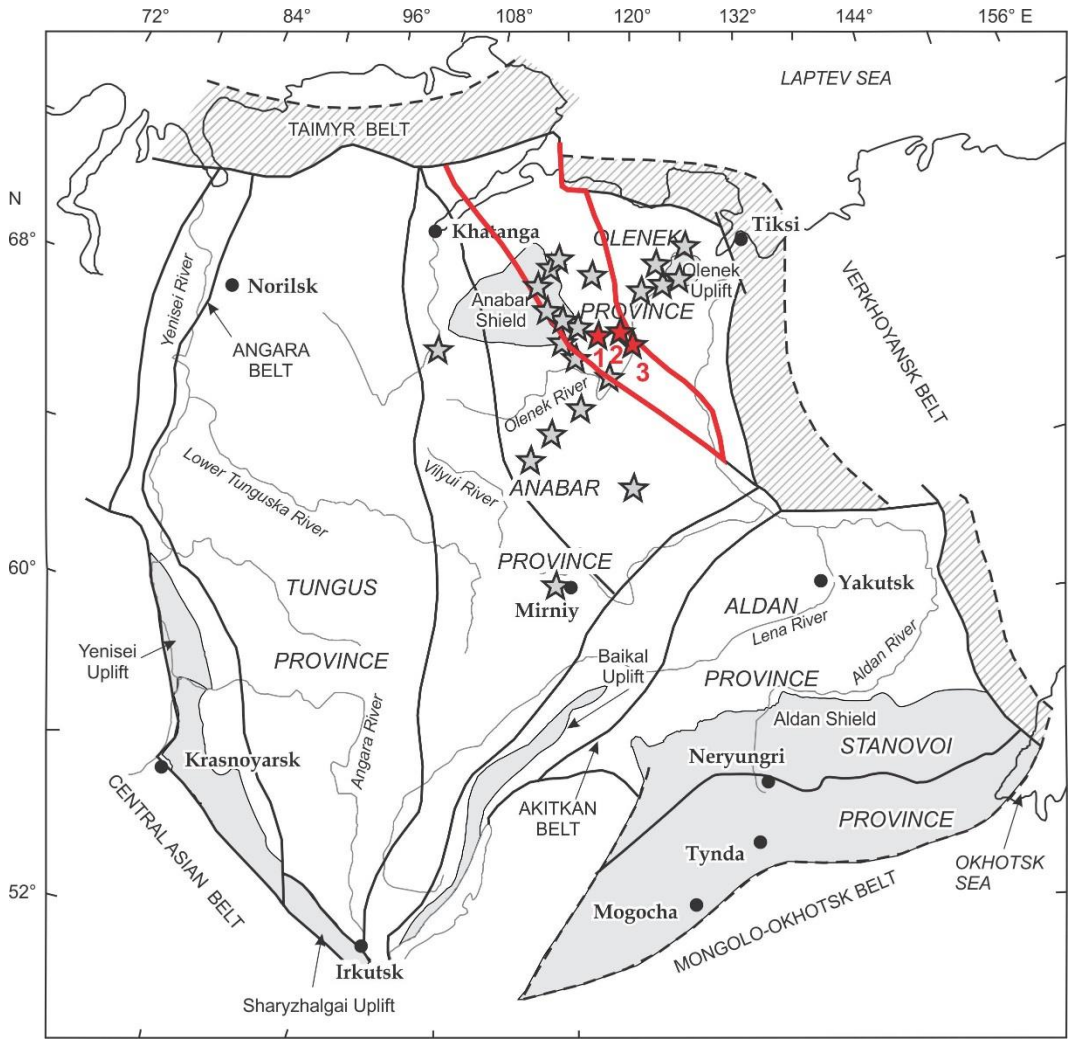



Figure 7. The location of the Khapchan terrane and studied kimberlite fields: 1 – West Ukukit; 2 – East Ukukit; 3 – Ogoner-Yuryakh.

The clastic material was derived from sources *ca* 2.5 Ga old, according to Sm-Nd model ages reported by (Rosen *et al.*, 2000). The source of the clastic material seems to be the basement of the nearby Birekta terrane, which now completely buried under the sedimentary cover. The rocks of the Khapchan belt accumulated on its passive margin, represented by the western part of the modern Birekta terrane (Deen *et al.*, 2006). The granulite metamorphism has been dated at 1.97 Ga by U-Pb in zircon from a monzodiorite dyke (Smelov & Timofeev, 2007, Zaitsev & Smelov, 2010). Kimberlite magmatism is widespread across the Khapchan terrane; ten fields containing more than 250 kimberlite bodies are known. High-grade diamond-bearing pipes are not common, but there are diamondiferous kimberlites within the terrane.

This study includes zircon samples from three fields (Fig. 7, Table 7): West-Ukukit, East-Ukukit and Ogoner-Yuryakh.

Table 7. Analytical work done for samples from the Khapchan terrane.

| Field | Pipe | Type of samples* | Number of analysis in zircons | | | |
|---|---|---|---|---|---|---|
| | | | U-Pb^ | TE | O | Hf |
| Ukukit | Babie Leto | HMC | 34 (32) | | | |
| Ogoner-Yuryakh | Baltiiskaya | HMC | 12 (10) | 10 | | 10 |
| | Aerogeological | HMC | 15 (12) | 12 | | 10 |
| *Total for the terrane* | | | *61 (54)* | *22* | | *20* |

* Type of samples: HMC - heavy mineral concentrate from weathered kimberlite

^ U-Pb analyses: total (used)

## 7.1 The Ukukit kimberlite field

According to the available literature (Zaitsev & Smelov, 2010) the West and East Ukukit fields are nearly identical in geological structure, age and features of the kimberlitic magmatism, so it seems reasonable to combine them into a single field; this Ukukit field includes more than 150 kimberlite bodies.

The Ukukit field is located in the basins of the Ukukit and Omonos rivers. Multiple kimberlite bodies together with rare dolerite dykes and porphyritic picrites are intruded into the Cambrian carbonate rocks. Thus, the earliest possible geological age of the kimberlites is Late Cambrian.

A great deal of isotopic-geochronological data have been reported for kimberlites of the Ukukit field. According to Rb-Sr, K-Ar and Ar-Ar dating the kimberlitic magmatism within the field has occurred during 2 main age intervals: 350-380 and 407-445 Ma (Zaitsev & Smelov, 2010).

***Zircon U-Pb data***

In this study the Ukukit kimberlite field is represented by a single kimberlite pipe, which is the Babie Leto pipe. Zircons were collected from heavy-mineral concentrate from the altered kimberlite of the Babie Leto pipe.

In total 34 zircons were analysed for their U-Pb age. Two analyses were rejected because of high discordance. The remaining 32 grains show a range of ages from 385 to 459 Ma (Appendix 5.1). Twenty-nine zircons form a single age population with weighted mean age 416.5±2.6 Ma (MSWD = 0.75; Fig. 7.1.1).

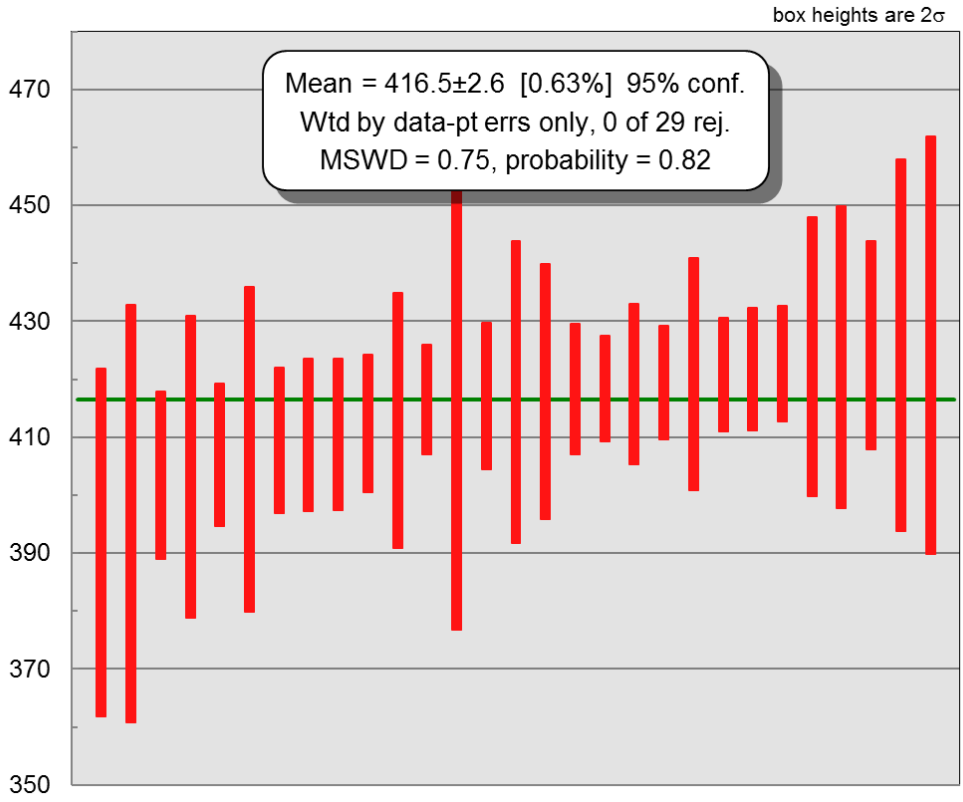



Figure 7.1.1. The weighted mean age of zircons from the Babie Leto pipe.

## 7.2 The Ogoner-Yuryakh kimberlite field

The field is situated within the basin of the Olenek and Merchemden rivers. It contains 20 kimberlite bodies including 9 pipes and 11 dykes. They are located in two separate areas: four diamondiferous pipes are found on the western bank of the Olenek river; others are further to the east. The kimberlite bodies are hosted by limestones of Late Cambrian age; sediments with Early Jurassic fossils cover some of them. Thus, geological evidence limits the age of kimberlite magmatism to between Late Cambrian and Early Jurassic.

A very few results of isotopic-geochronological studies are reported from this field. All of them show relatively good consistency despite the use of different analytical techniques. The ages of kimberlite determined by the Rb-Sr, K-Ar and U-Pb methods ranges from 409 to 453 Ma (Zaitsev & Smelov, 2010).

### *Zircon U-Pb data*

The analysed zircons were collected from heavy-mineral concentrates from altered kimberlite rocks from two pipes: Baltiiskaya and Aerogeological.

#### The Baltiiskaya pipe

Twelve U-Pb analyses were obtained; two of them showed discordance more than 20% and were rejected. The zircons show a wide range of ages – from 287 to 2592 Ma (Fig. 7.2.1). Four grains form the main age peak with a weighted mean age of 289.3±3.9 Ma (Lower Permian; MSWD = 0.31, probability = 0.82; Fig. 7.2.2). Another three zircons revealed identical ages (within the analytical error) with mean age 1876±37 Ma (MSWD = 0.06, probability = 0.94, Fig. 7.2.3).

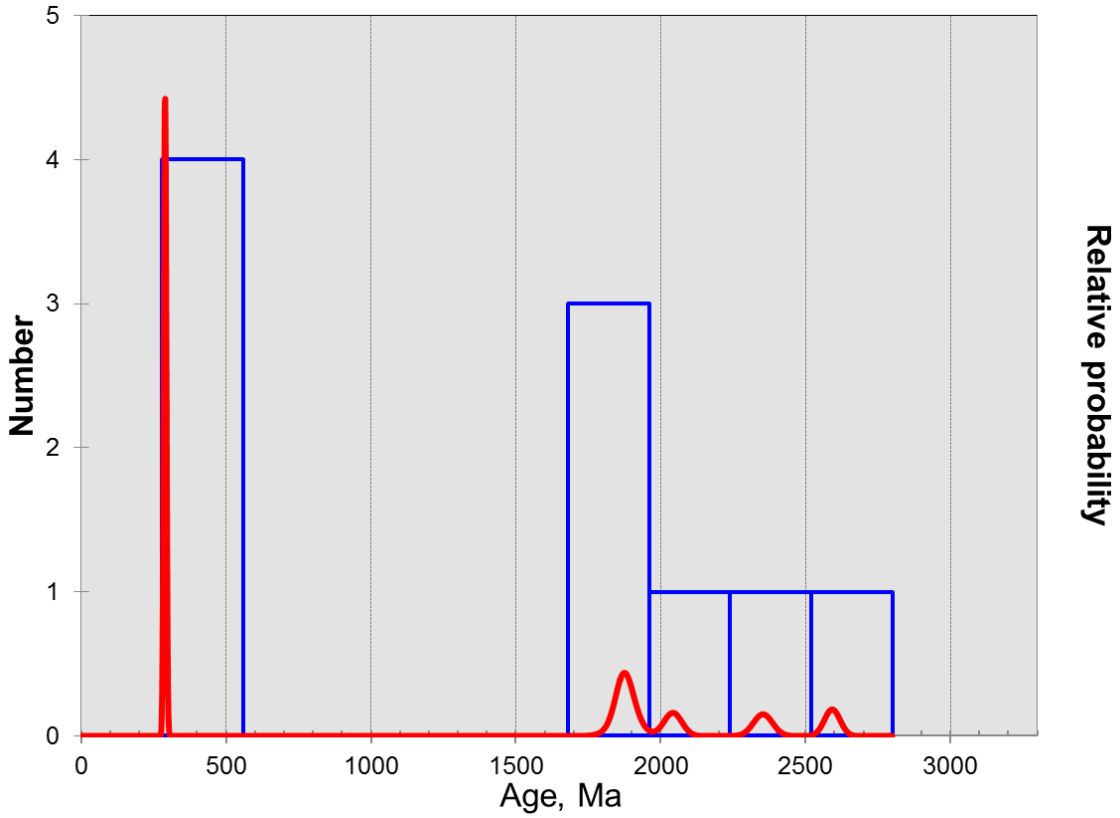



Figure 7.2.1. Probability plot of zircon U-Pb ages, Baltiiskaya pipe.

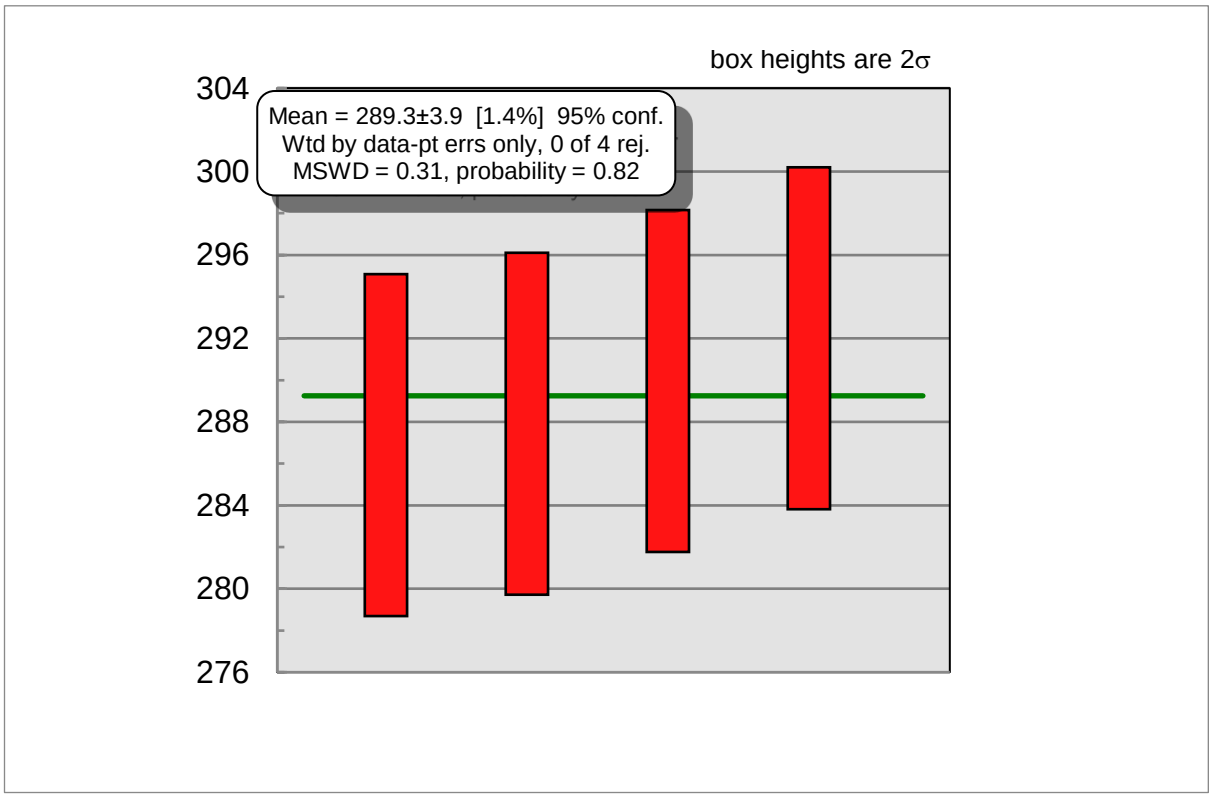



Figure 7.2.2. The weighted mean age of the major peak, Baltiiskaya pipe.

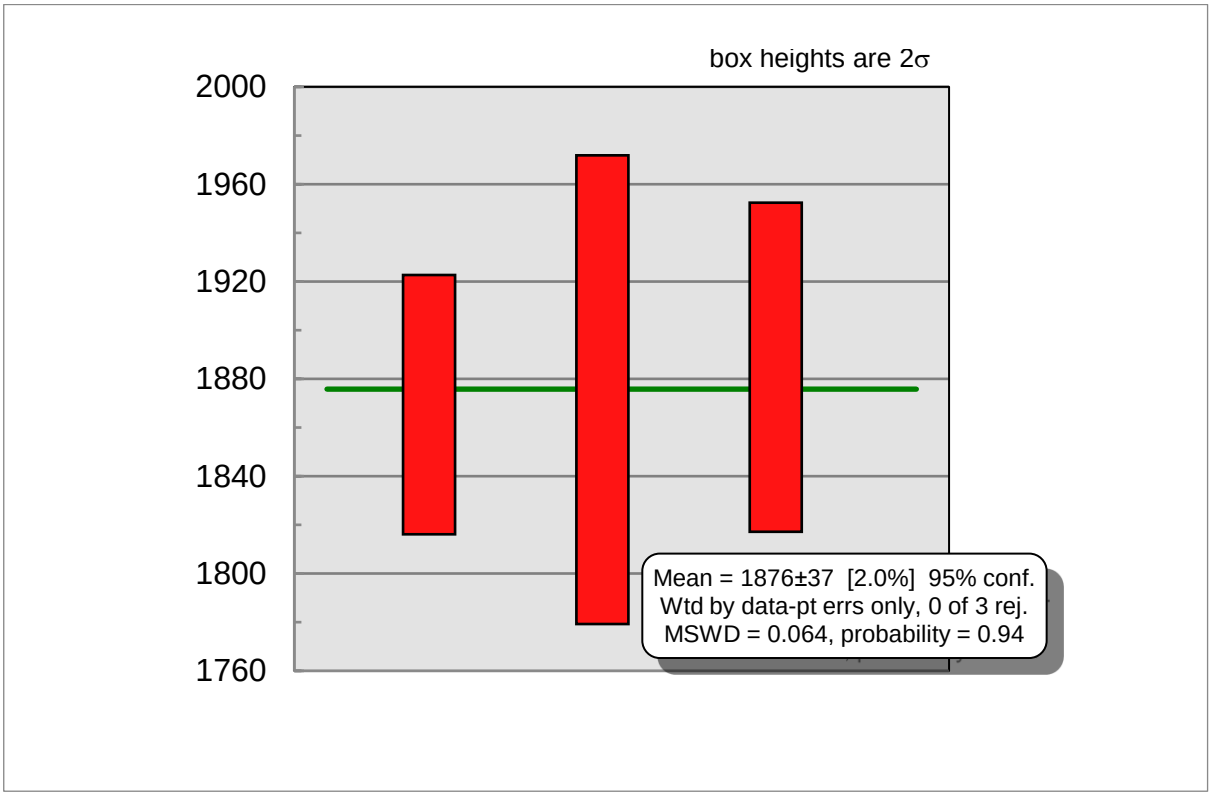



Figure 7.2.3. The weighted mean age of the second peak, Baltiiskaya pipe.

**The Aerogeological pipe**

Fifteen zircons from this pipe were dated, out of those 3 analyses were rejected because of high discordance. The U-Pb and $^{207}Pb/^{206}Pb$ ages fall into a wide interval from 227 to 2829 Ma (Fig. 7.2.4). Three grains show close ages and give a concordia age of 295.9±2.4 Ma (Lowest Permian; MSWD = 0.07, probability = 0.79; Fig. 7.2.5).

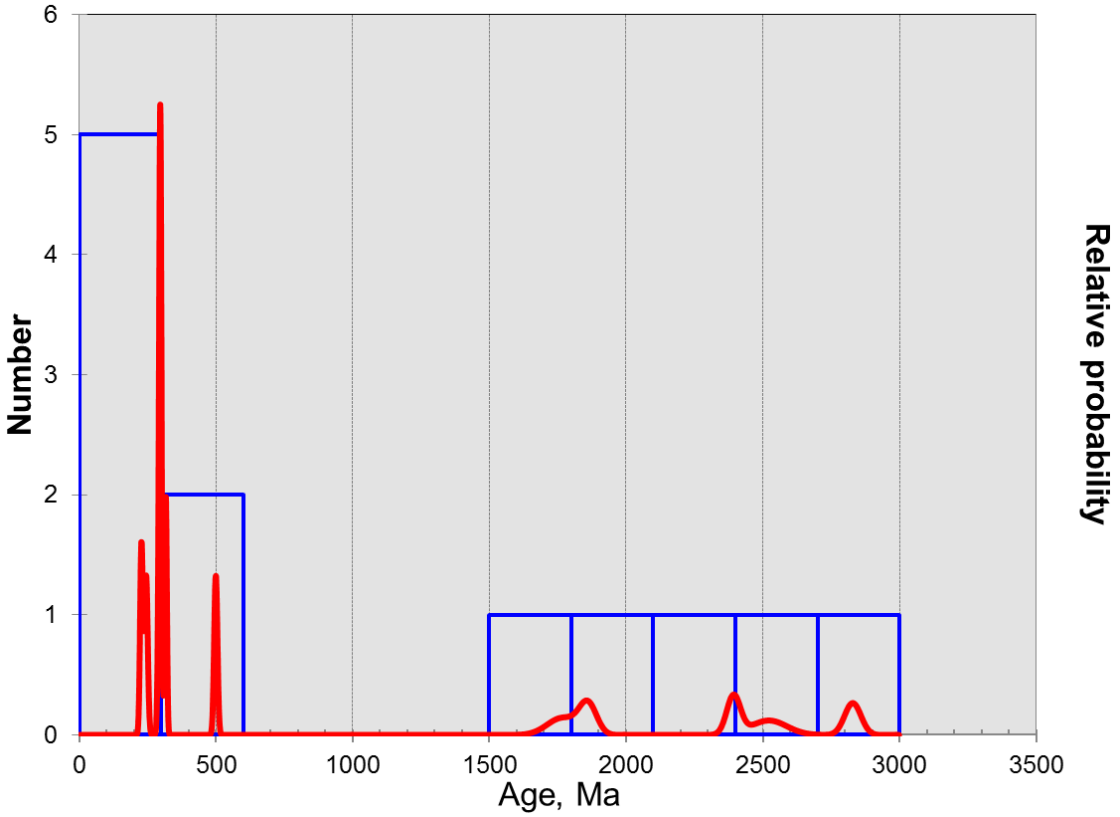



Figure 7.2.4. Probability plot of zircon U-Pb ages, Aerogeological pipe.

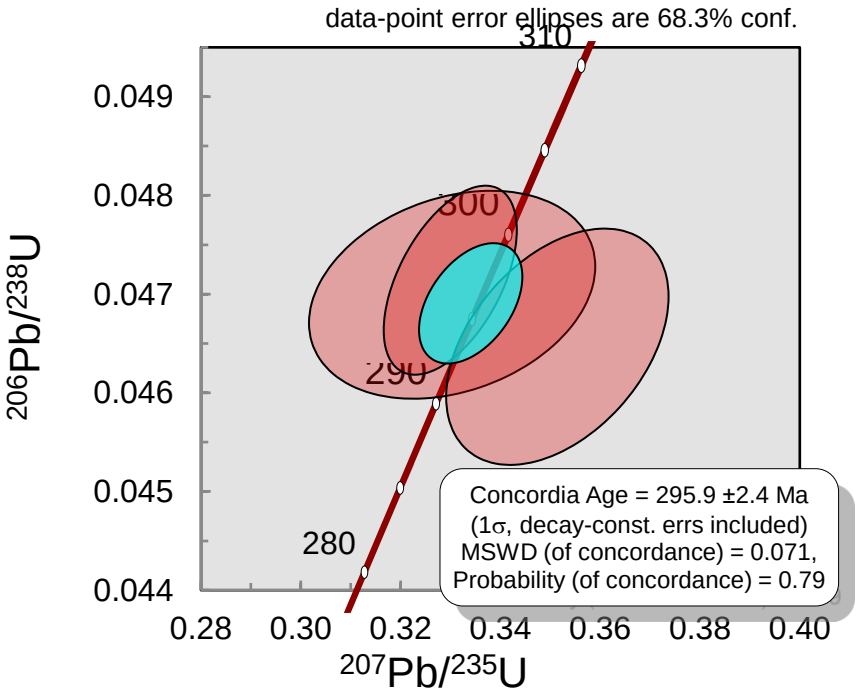
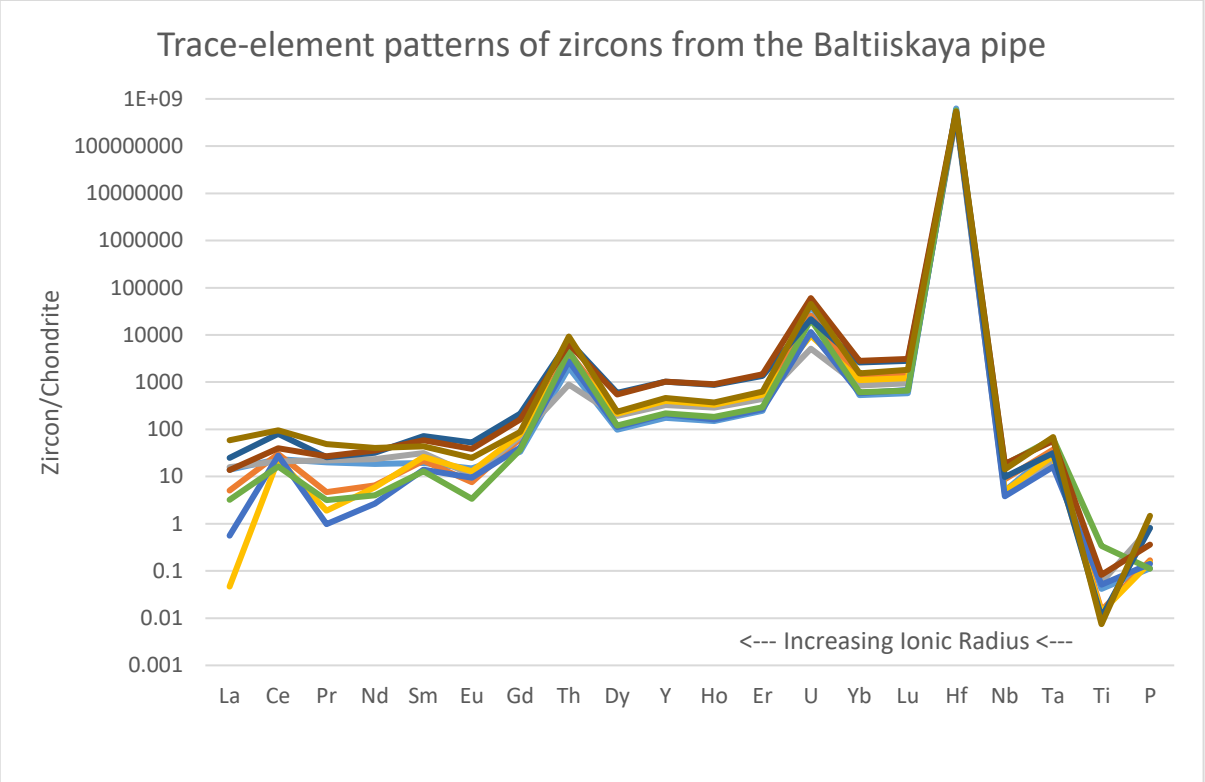



Figure 7.2.5. U-Pb concordia for zircons from the main age group, Aerogeological pipe.

***Zircon trace-element data***

**The Baltiiskaya pipe**



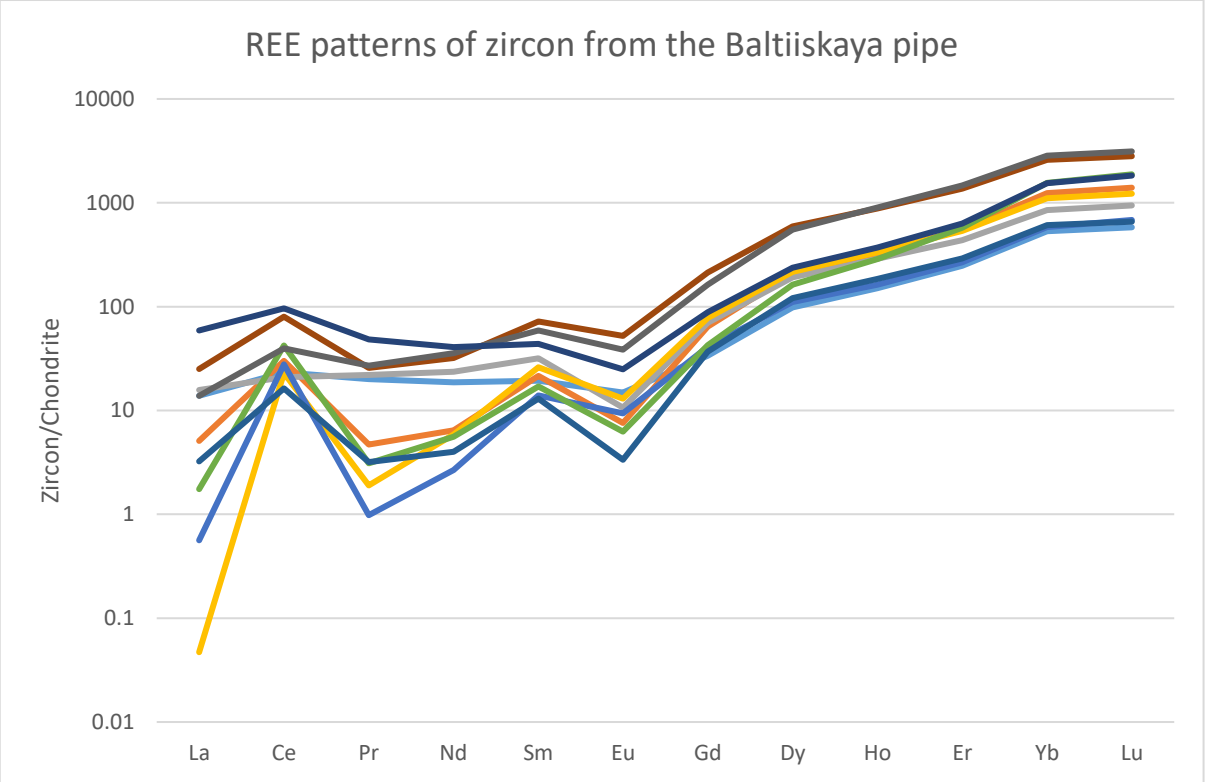




Figure 7.2.6. Trace-element and rare-earth element patterns of zircons from the Baltiiskaya pipe.

Trace-element compositions were analysed in 10 zircons from the Baltiiskaya pipe. One analyses was rejected because of extremely high Ti, Ca and P contents indicating the analytical spot located within mineral inclusion or crack.

The chondrite-normalised trace-element patterns of the analysed grains show significant variations in the concentrations of titanium and light rare-earth elements (Fig. 7.2.6). The concentrations of Y vary from 396 to 2308 ppm, U and Th diverge from 35 to 372 and from 51 to 603 ppm respectively. Total REE contents fall in the interval 329 – 1632 ppm. The lowest REE concentrations are found in the oldest zircon (2592 Ma), while grains from the major and the second main (mean age 1876 Ma) populations show similar levels of the REE (Fig. 7.2.7).

Th/U varies from 0.19 to 1.39; Nb/Ta ranges from 1.74 to 4.07.

For most of the grains the REE plot shows typical zircon patterns with depletion in LREE and enrichment in HREE. The negative Eu-anomaly is well defined, while some grains do not have a Ce-maxima.

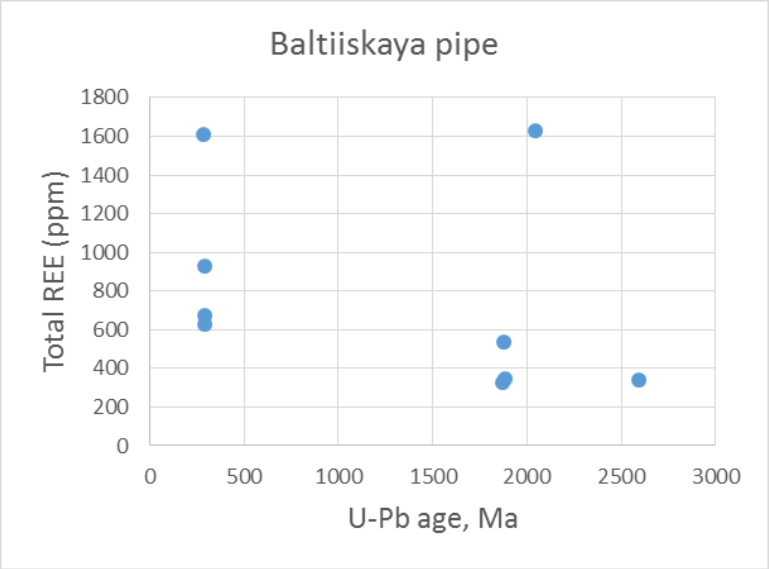



Figure 7.2.7 Total REE concentration vs U-Pb age of zircons from the Baltiiskaya pipe

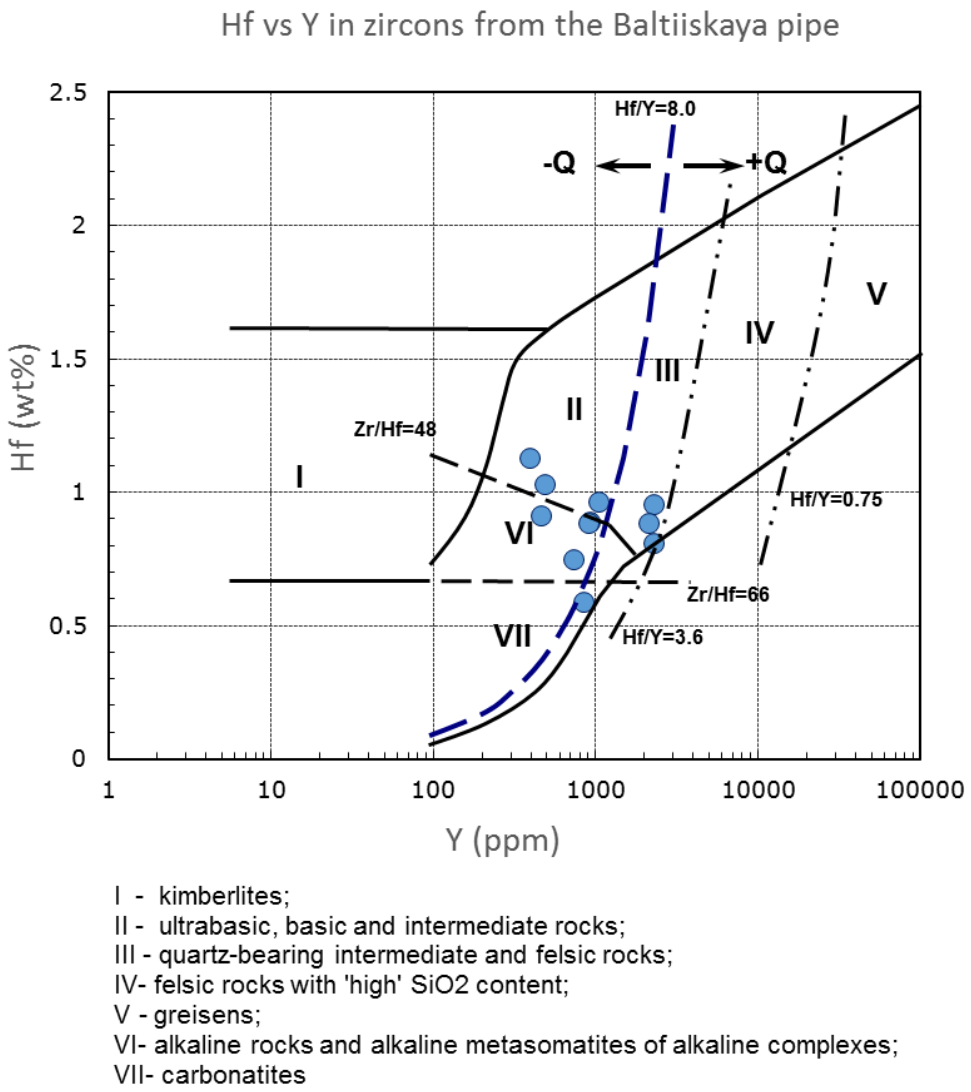



Figure 7.2.8. Hf vs Y discrimination diagram for zircons from the Baltiiskaya pipe.

The lack of Ce-maxima could indicate lower oxidation state of the parental melt, however, it is also often may be hided when LREE enrichment is related to alteration processes.

According to the CART statistical classification (Belousova *et al.*, 2002), the most of analysed grains have of trace-element compositions typical of zircons from rocks with mafic or intermediate compositions, rarely from felsic rocks. Zircons from mafic and intermediate rocks usually have lower U and Y concentrations than those from felsic rocks. The discrimination diagram Hf vs Y illustrates well the compositional difference of zircons from these types of rocks (Fig. 7.2.8).

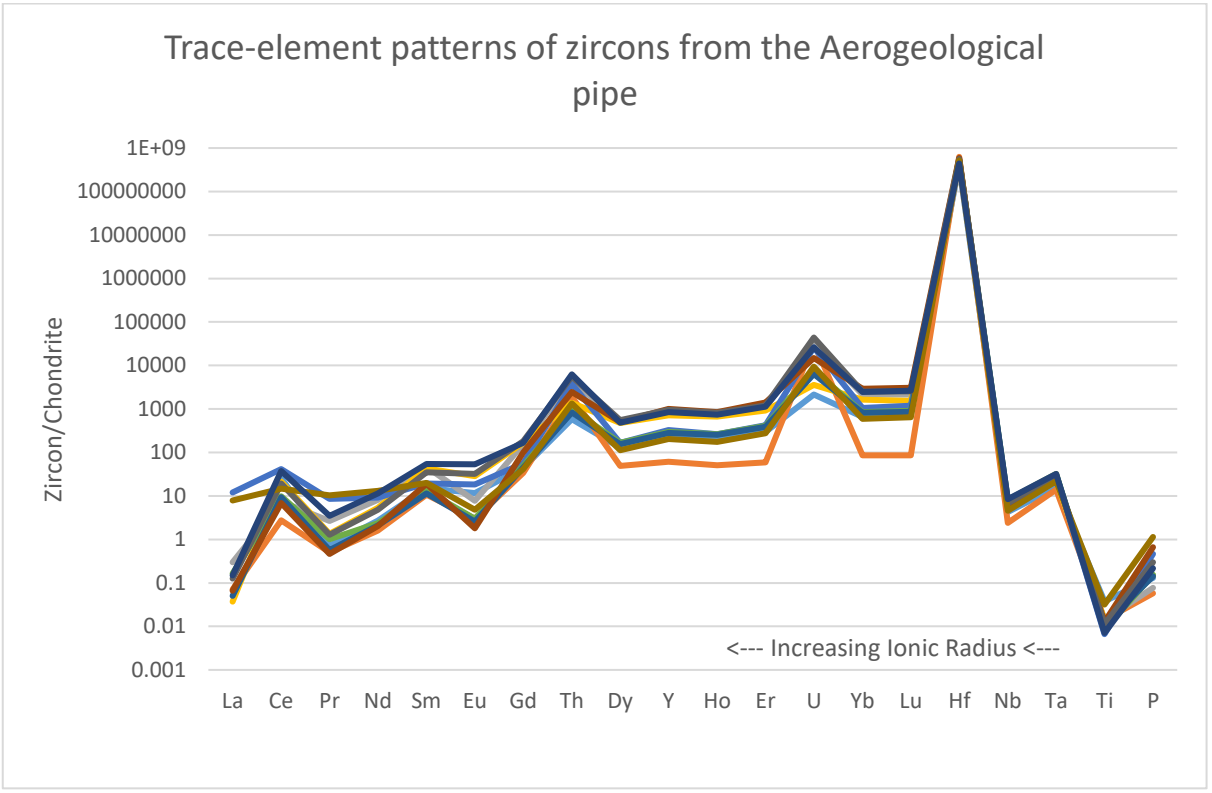
**The Aerogeological pipe**

The trace-element compositions were analysed in twelve zircons from the pipe.

All grains show similar chondrite-normalised trace-element patterns with variations in concentrations of some elements (Fig. 7.2.9). Thus, Y concentrations diverge from 137 to 2242 ppm, Th – from 23.5 to 248 ppm, U ranges from 21.5 to 441 ppm. Total REE contents differ within the range 80 – 1520 ppm. Th/U and Nb/Ta vary within the intervals 0.23 – 1.53 and 2.15 – 3.71 respectively. In general, older zircons (1767 – 2460 Ma) have lower levels of REE (Fig. 7.2.10), however, one of the highest total REE contents was found in the oldest grain (2829 Ma). The grains from the main age population (260 Ma), as well as other Palaeozoic grains (227 – 499 Ma) show total REE concentrations higher than 380 ppm. A single grain with low Lu, indicating its mantle origin, reveals U-Pb age of 2393 Ma.

The REE plot shows zircon patterns depleted in LREE and enriched in HREE. A few grains have flatter REE patterns. The negative Eu-anomaly is seen in all grains, as well as the Ce-maxima.

According to the CART statistical classification, most of the analysed zircons from the Aerogeologica pipe have trace-element compositions similar to those of zircons from intermediate rocks. A single grain has a trace-element signature typical of zircons from carbonatites (Lu<20.7 ppm, low U and Y), however, its Hf content (1.13 wt%) is higher than in typical carbonatitic zircons (<0.65 wt%). This grain is plotted within the kimberlitic field at the discrimination diagram Hf vs Y (Fig. 7.2.11). Well-developed Eu-minima observed at the REE plot together with low Lu, Y and U concentrations indicates derivation from low-fractionated mafic rocks.. Three zircons show trace-element evidence of having crystallized from higher fractioned felsic parental melt.



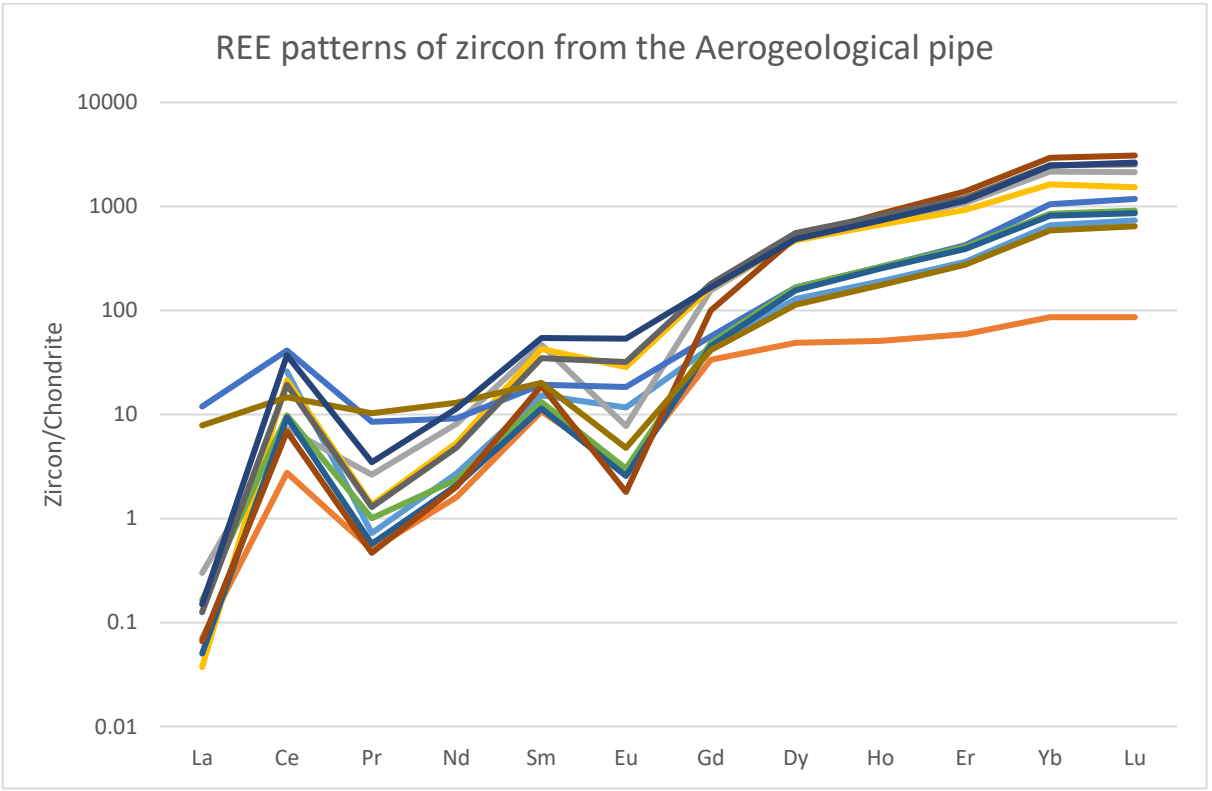




Figure 7.2.9. Trace-element and rare-earth element patterns of zircons from the Aerogeological pipe.

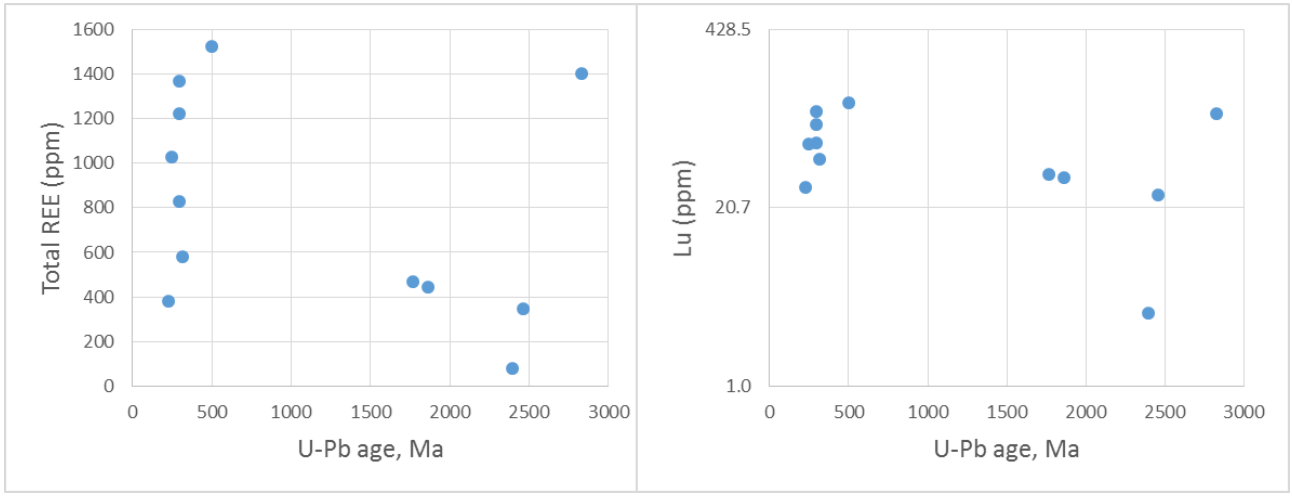
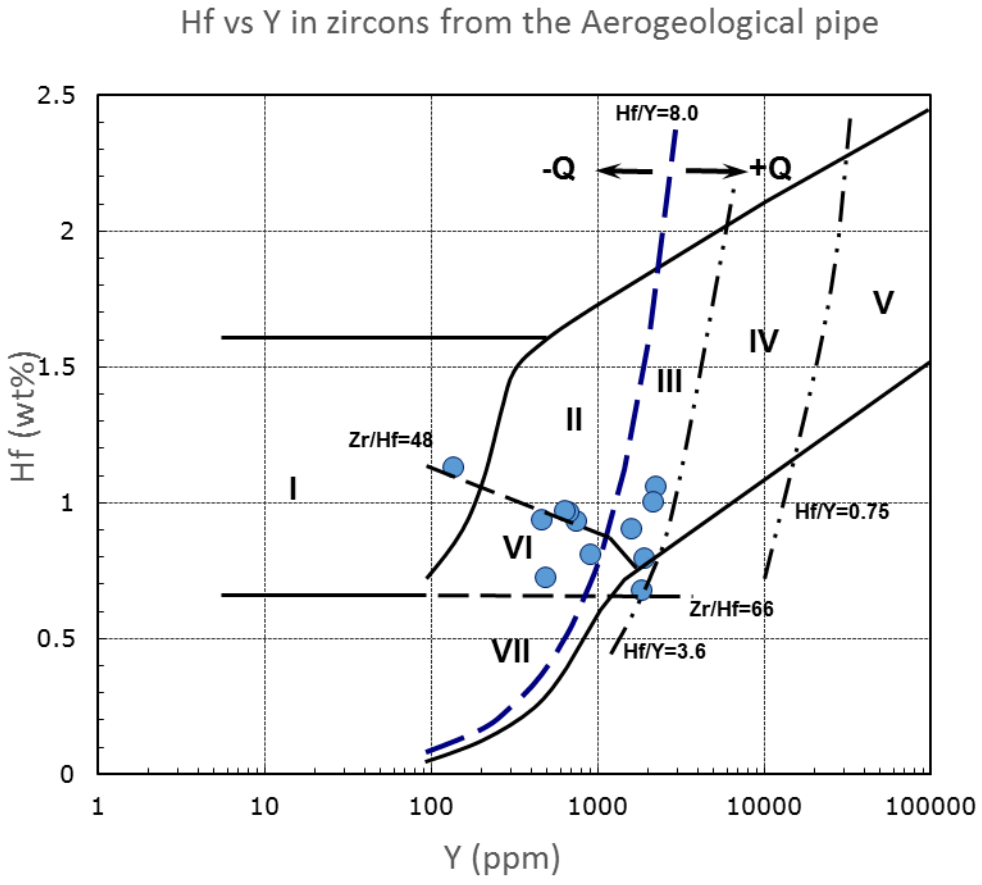



Figure 7.2.10. Total REE and Lu concentrations vs U-Pb age of zircons from the Aerogeological pipe.




I - kimberlites;
II - ultrabasic, basic and intermediate rocks;
III - quartz-bearing intermediate and felsic rocks;
IV- felsic rocks with 'high' SiO2 content;
V - greisens;
VI- alkaline rocks and alkaline metasomatites of alkaline complexes;
VII- carbonatites

Figure 7.2.11. Hf vs Y discrimination diagram for zircons from the Aerogeological pipe.

***Hafnium-isotope data***

**The Baltiiskaya pipe**

Ten grains dated by U-Pb technique were analysed for their Hf-isotopic composition.

The ranges of calculated initial $^{176}Hf/^{177}Hf$ ratios, εHf values and model ages vary significantly for zircons of different age populations (Appendix 5.3, Fig. 7.2.12). Thus, initial Hf ratios vary in the interval 0.2811085 – 0.282446, εHf ranges from -20.5 up to +9.6 and calculated crustal model ages fall in the wide interval from 1.64 to 3.19 Ga.

All zircons from the youngest age group (mean age 289.3±3.9 Ma) have εHf values below -5, while all older grains show εHf higher than -5 (Fig. 7.2.12). Positive εHf indicates the mantle input in zircon-produced melt, while low negative values mean reworking of the older crust without any significant contribution of mantle material. For example, three young zircons from the Baltiiskaya pipe with lowest εHf probably were crystallized from pre-existed "crustal" protolith without mantle input, while the top data point may reflect mixing of that "crustal" melt with mantle-derived material.

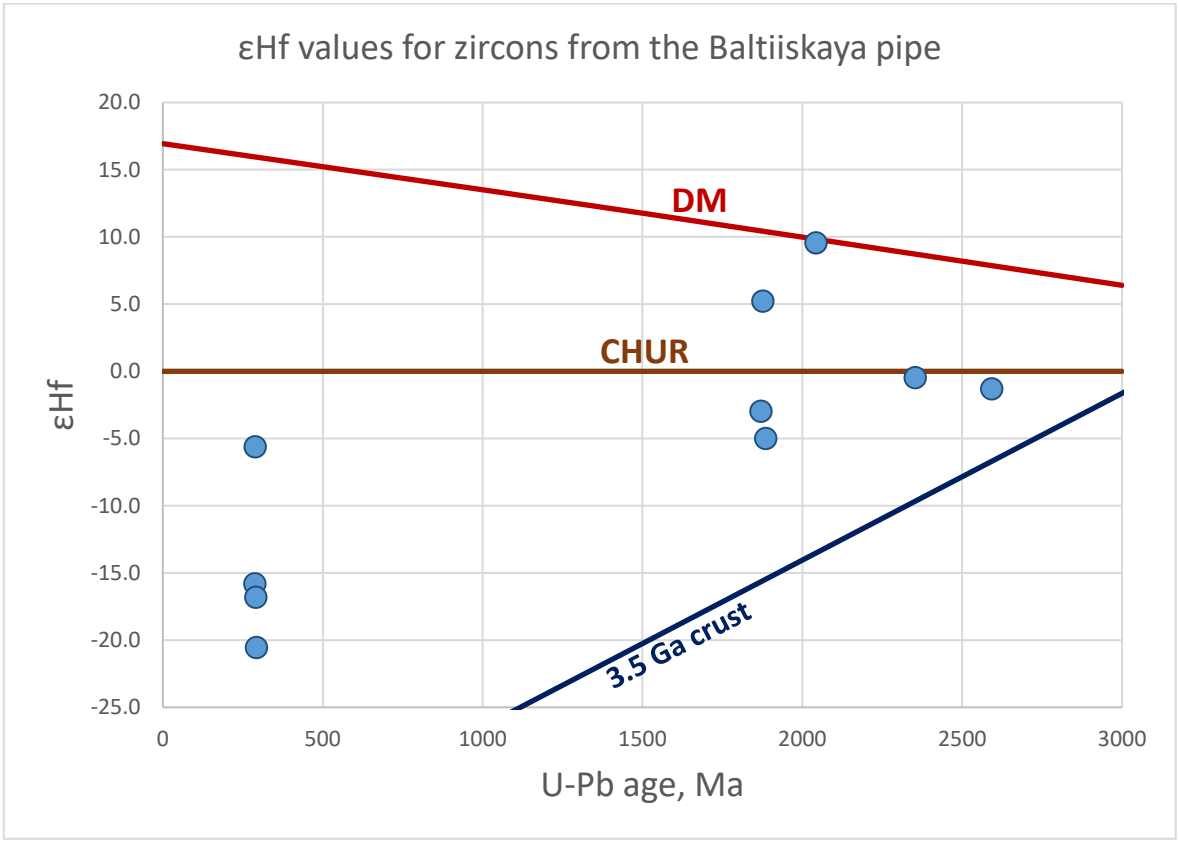



Figure 7.2.12. εHf vs U-Pb age plot for zircons from the Baltiiskaya pipe.

**The Aerogeological pipe**

Lu-Hf isotopes were studied in 10 previously-dated zircon grains from the pipe.

The group of zircons with U-Pb ages younger than 500 Ma shows wide range of Hf-data: initial Hf values are within the range of 0.282110 – 0.282602, εHf varies from -17.3 to +1.0 (Fig. 7.2.13) and crustal model ages range from 1.29 to 2.38 Ga.

Zircons with ages of 1860 – 2829 Ma have εHf close to CHUR (-1.8 – +1.1; Fig. 7.2.13) except for the oldest grain with εHf = +6.3. Their calculated initial Hf ranges from 0.281143 to 0.281630, and crustal model ages vary from 2.47 to 3.07 Ga.

Similar to the Baltiiskaya pipe, wide range of εHf values for young zircons may reflect mixing of both crustal and mantle-derived sources.

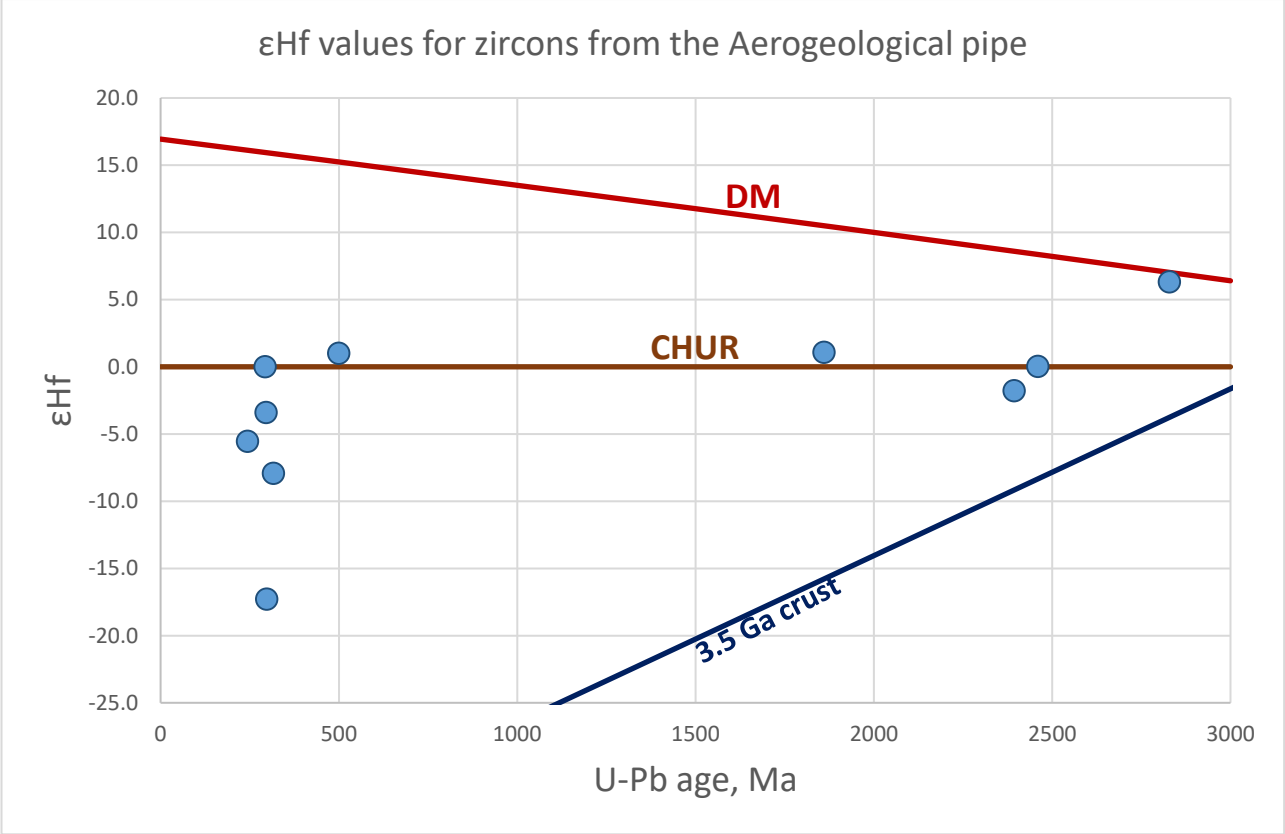



Figure 7.2.13. εHf vs U-Pb age plot for zircons from the Aerogeological pipe. Grain with trace-element (TE) composition typical of mantle-derived zircons is shown with black cross.

# Chapter 8. The Birekta terrane

The terrane is located in the north-eastern part of the Siberian Craton (Fig. 8) and included within the Olenek Province. It was defined entirely from geophysical data, as it completely buried under the thick sedimentary cover. Up to 10 km of Mesoproterozoic and Phanerozoic sediments covering the basement rocks consist of carbonate and carbonate-terrigenous sequences (Zaitsev & Smelov, 2010).

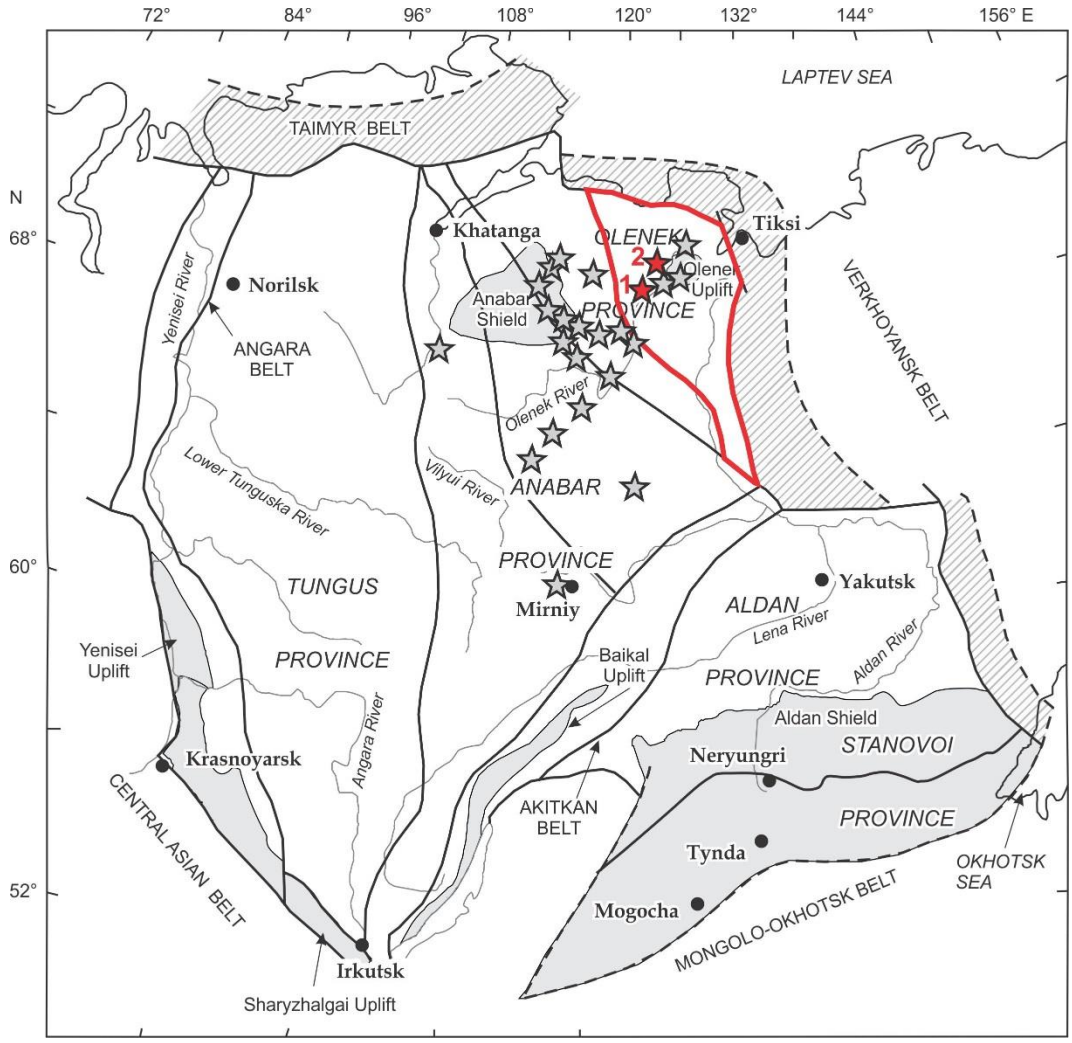



Figure 8. The location of the Birekta terrane and studied kimberlite fields: 1 – Merchemden; 2 – Kuoika.

According to geophysical data, mineralogical studies of clasts in the sedimentary cover, and investigation of the very limited outcrops in the Olenek uplift, the basement of the Birekta terrane is considered to be a granite-greenstone complex similar to Archean terranes of the Aldan province (Rosen *et al.*, 1994). The age of the basement has been estimated based on the

Paleoproterozoic ages of zircons from granitic rocks exposed at the Olenek uplift (2036±11 and 2111±20; (Wingate *et al.*, 2009, Zaitsev & Smelov, 2010).

The terrane contains at least 5 kimberlite fields. At the moment, economically important diamondiferous pipes are not known within the Birekta terrane. However, diamonds have been reported from kimberlitic pipes and alluvial deposits of diamonds are well known.

The current project includes zircon samples from 2 kimberlite fields: Merchemden and Kuoika (Table 8).

Table 8. Analytical work done for samples from the Birekta terrane.

| Field | Pipe | Type of samples* | Number of analysis in zircons | | | |
|---|---|---|---|---|---|---|
| | | | U-Pb^ | TE | O | Hf |
| Merchemdenskoe | Vostok-6 | kimberlite | 10 | | | |
| | Operatorskaya | HMC | 21 (15) | 15 | | 10 |
| Kuoika | Khrizolit | kimberlite | 10 (9) | | | |
| | Pyatnitsa | Kimberlite | 11 | | | |
| | Ruslovaya | HMC+kimberlite | 60 (55) | 25 | 27 | 35 |
| | Olivinovaya | HMC | 35 (31) | 23 | 22 | 30 |
| | Vtorogodnitsa | HMC | 44 (30) | 25 | 15 | 26 |
| *Total for the terrane* | | | *191 (161)* | *88* | *64* | *101* |

* Type of samples: HMC - heavy mineral concentrate from weathered kimberlite; kimberlite - hand-picked zircons from a crushed kimberlite rock.

^ U-Pb analyses: total (used)

## 8.1. The Merchemden kimberlite field

The field is located within the lower part of the Merchemden river, and contains 32 kimberlite bodies at the modern erosion surface. Kimberlites are intruded into Late Proterozoic and Cambrian carbonate rocks and terrigenous Permian and Jurassic sediments. Magmatic rocks are represented by kimberlites and basaltic traps. According to Zaitsev and Smelov (2010) there are no reliable geological evidences on the age of kimberlites. Most of isotopic-geochronological results were obtained by the Rb-Sr technique, and gave ages of 347-387 Ma, consistent with zircon fission-track dating results. An older interval of kimberlitic magmatism also have been reported: K-Ar, Rb-Sr and U-Pb SHRIMP analyses revealed ages 419-495 Ma (Zaitsev & Smelov, 2010).

Two pipes from the field were sampled for zircons – Vostok-6 and Operatorskaya.

### *Zircon U-Pb data*

#### The Vostok-6 pipe

Zircons were recovered from crushed kimberlite of the Vostok-6 pipe. In total 10 grains were mounted and analysed for their U-Pb age.

All analyses are concordant and form a single age population with a concordia age of 406±2.6 Ma (MSWD = 0.53, probability = 0.47; Fig. 8.1.1).

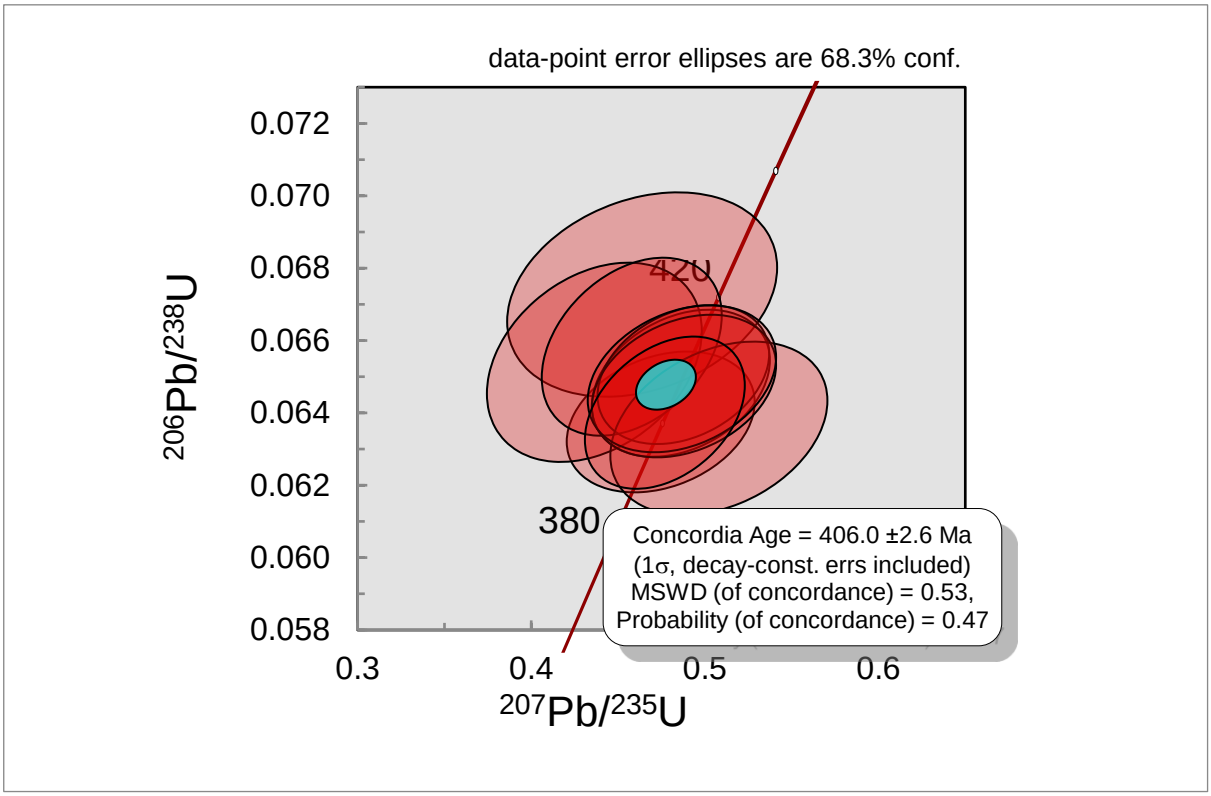



Figure 8.1.1. The U-Pb concordia for zircons from the Vostok-6 pipe.

**The Operatorskaya pipe**

Twenty-one zircon grains were picked out from heavy-mineral concentrate from the weathered kimberlite of the Operatorskaya pipe. All grains were dated, and 6 analyses were rejected because of high discordance.

The $^{207}Pb/^{206}Pb$ ages fall into the interval 1950 – 3058 Ma (Fig. 8.1.2). The main age population reveals a concordia age of 2721±6.2 Ma (MSWD = 0.20, probability = 0.66; Fig. 8.1.3). The second main peak shows a weighted mean age of 1967±34 (MSWD = 0.36, probability = 0.70, Fig. 8.1.4).

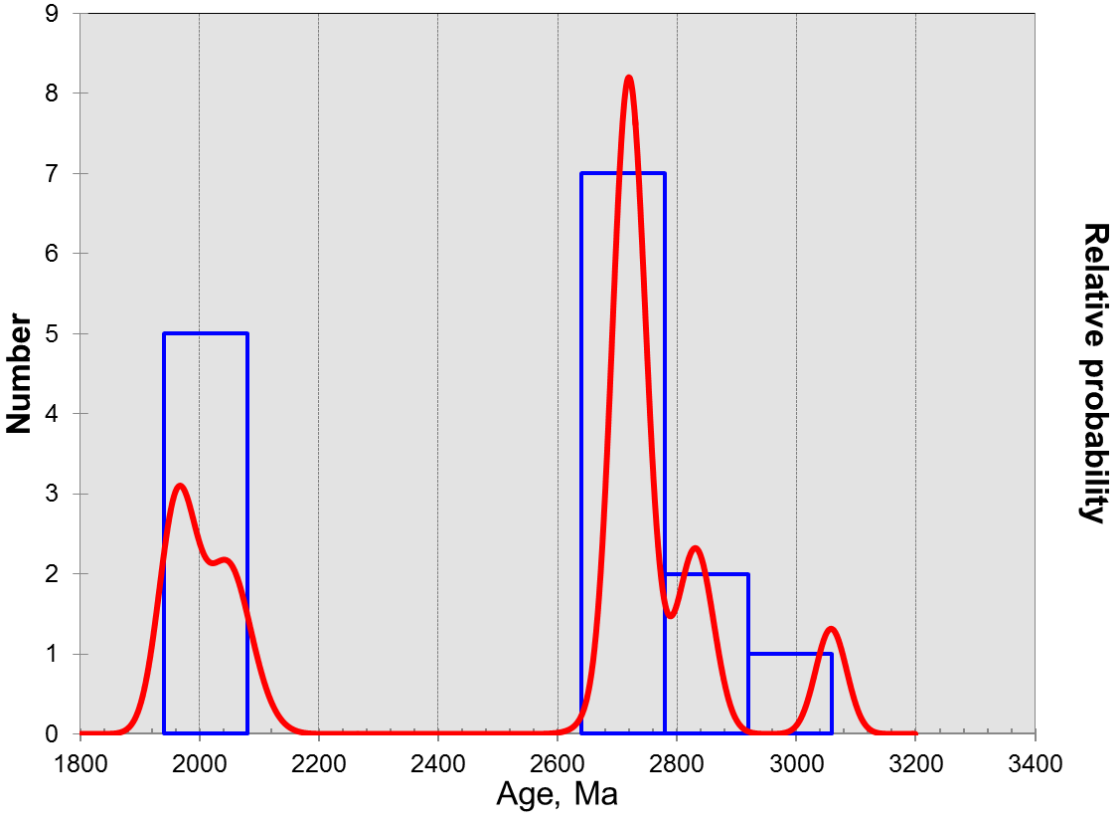



Figure 8.1.2. Probability plot of zircon U-Pb ages, Operatorskaya pipe.

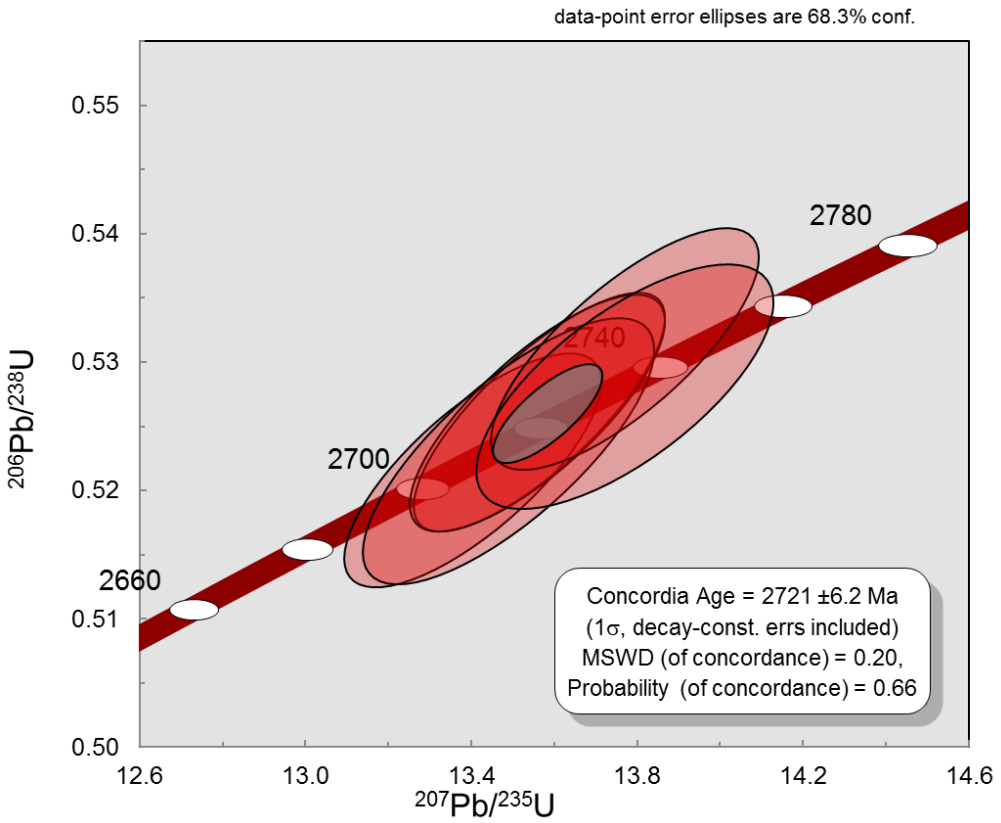



Figure 8.1.3. The U-Pb concordia for zircons from the main age population, Operatorskaya pipe.

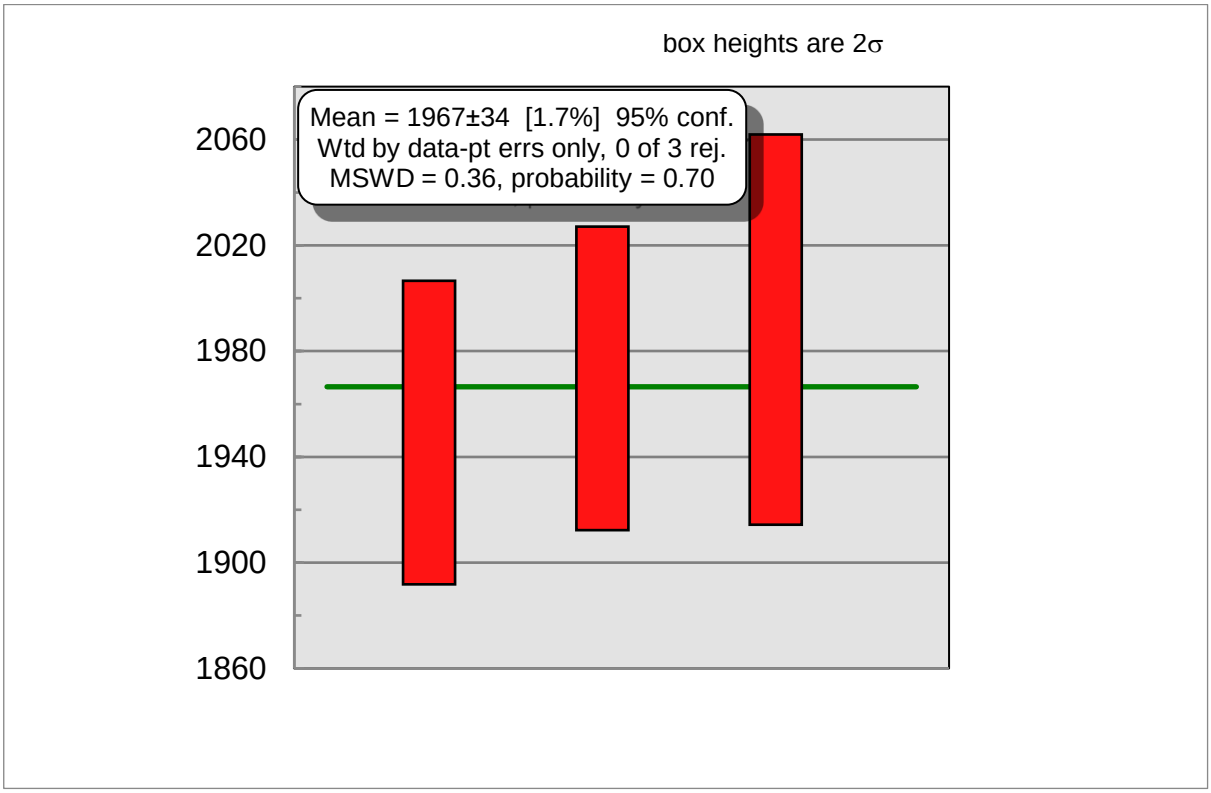



Figure 8.1.4 Weighted mean age of the second main peak, Operatorskaya pipe.

***Zircon trace-element data***

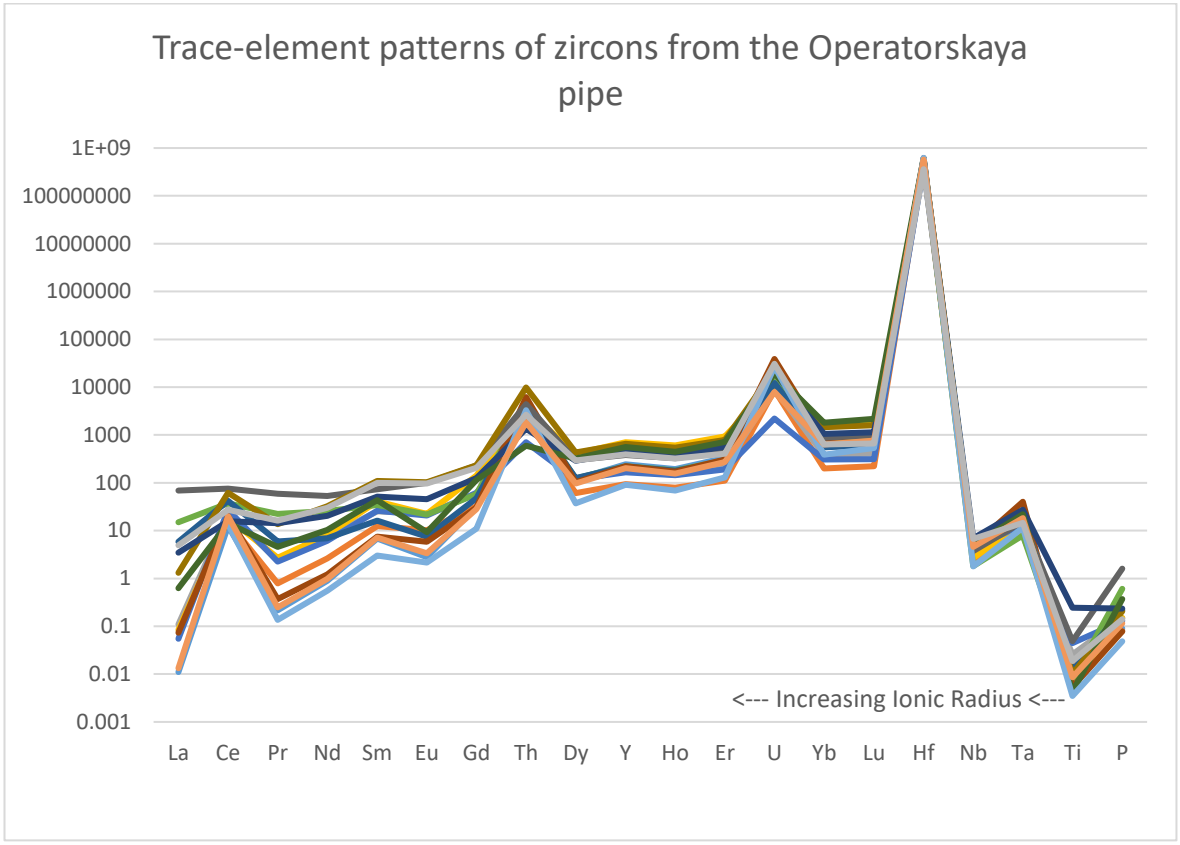
**The Operatorskaya pipe**

All 15 concordant zircons were analyzed for trace-element composition.

The chondrite-normalised trace-element patterns of all analysed grains are generally similar with minor variations in the concentrations of light rare-earth elements (Fig. 8.1.5). Concentrations of Y range from 204.5 to 1583 ppm, Th and U contents vary from 24 to 395ppm and from 22 to 391 ppm respectively. Total REE diverge within the range 147 – 1027 ppm (Fig. 8.1.6). There is no correlation found between U-Pb age of zircons and their REE content.

Th/U varies from 0.12 to 1.75; Nb/Ta ranges from 1.52 to 5.81.

The REE plot shows typical zircon patterns with depletion in LREE and enrichment in HREE (Fig. 8.1.5). The positive Ce-anomaly and Eu-minima are well defined in most grains. The grain showing the highest LREE also contains unusually high P and Ca, indicating mineral (likely apatite) inclusion affected the trace-element pattern.



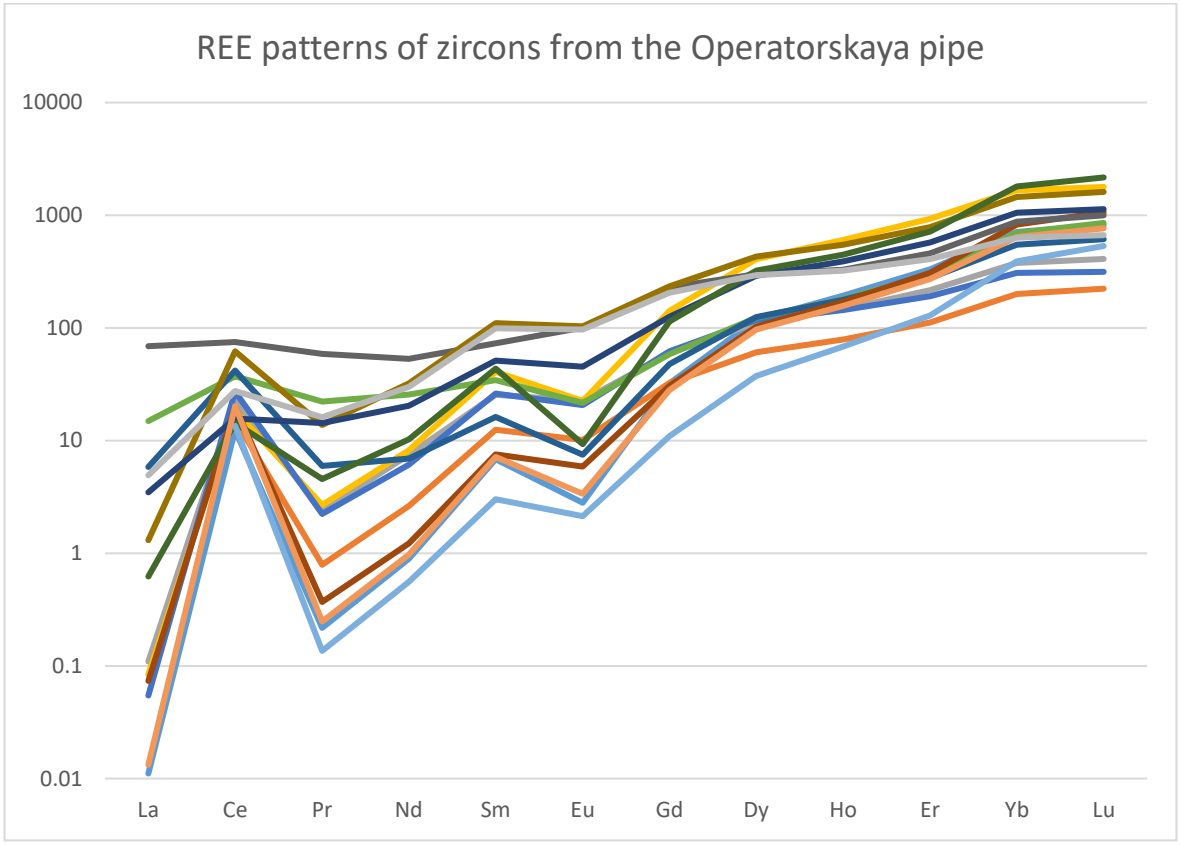




Figure 8.1.5. Trace-element and rare-earth element patterns of zircons from the Operatorskaya pipe.

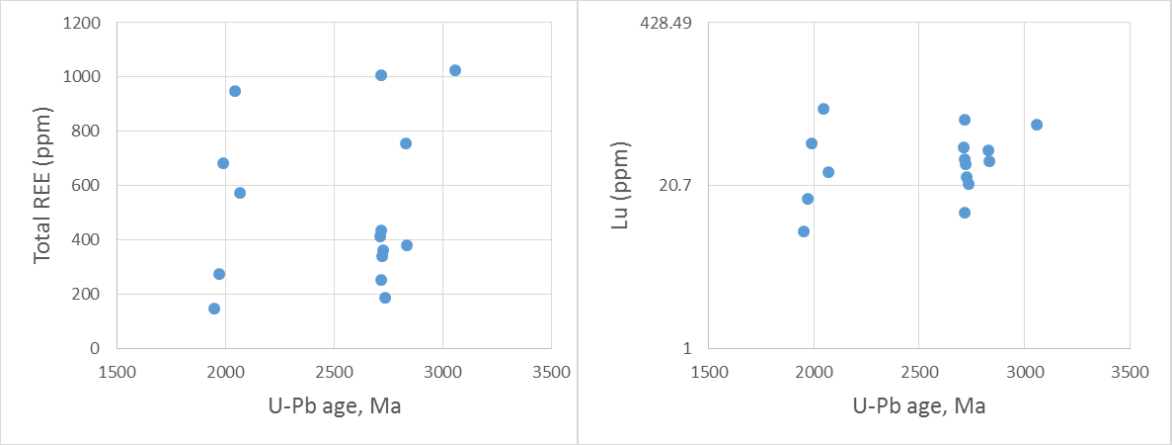



Figure 8.1.6. Total REE and Lu concentrations vs U-Pb age of zircons from the Operatorskaya pipe.

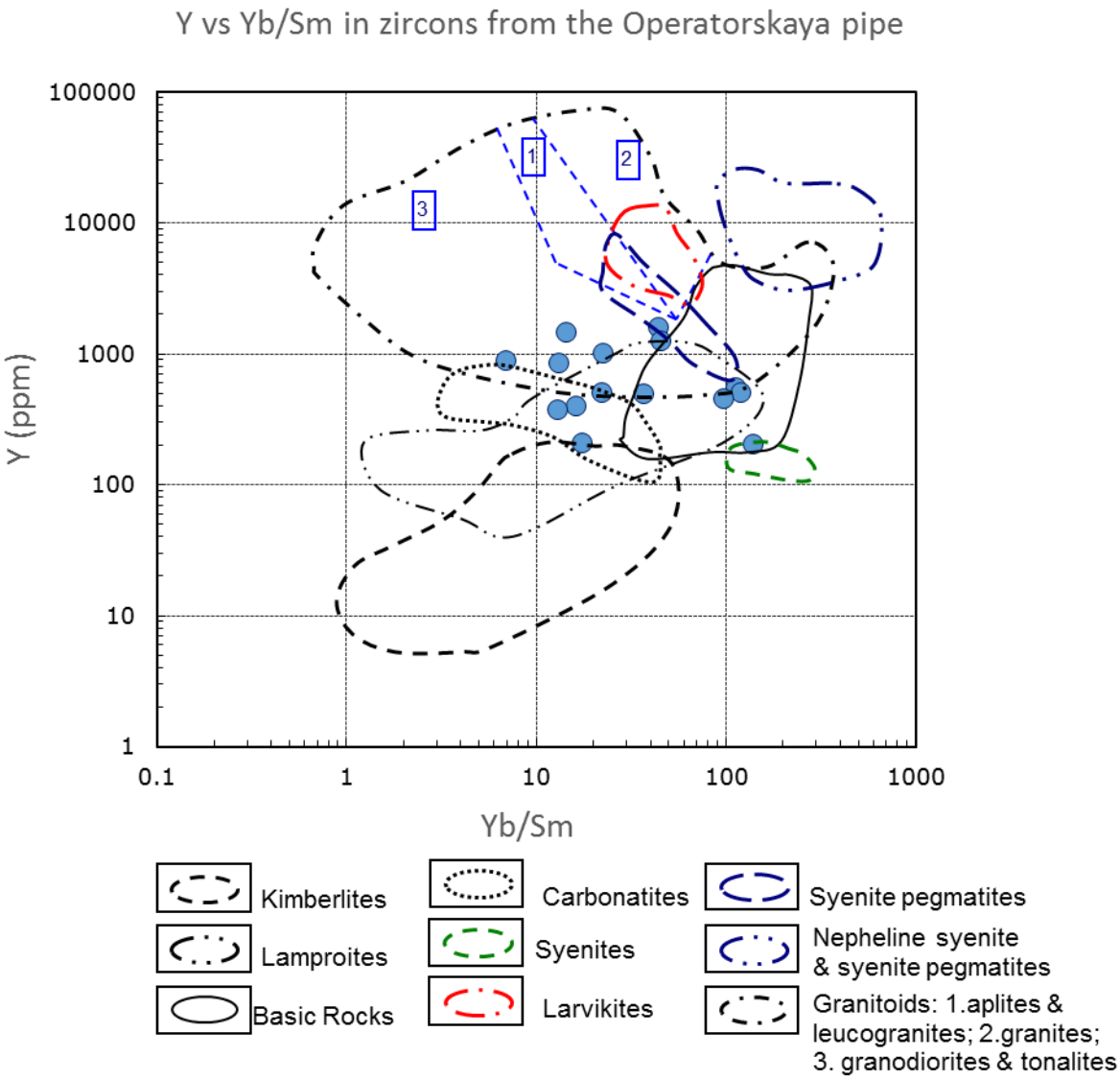



Figure 8.1.7. Y vs Yb/Sm discrimination diagram for zircons from the Operatorskaya pipe.

According to the CART statistical classification, three zircons show trace-element signatures of carbonatitic parental melts (Lu<20.7 ppm, low U, Y and Hf), while the rest of the

grains have trace-element compositions typical of zircons from intermediate to felsic rocks (high Y, Hf and U). The results of the CART classification correlate well with location of zircon data points at the discrimination diagrams, for example, Y vs Yb/Sm plot (Fig. 8.1.7).

***Hafnium-isotope data***

**The Operatorskaya pipe**

Lu-Hf isotopic compositions were analyzed in 10 dated zircons from the pipe.

The range of εHf values is from -6.2 to +4.4. Negative values are common for grains of the main age population (U-Pb age 2721 Ma), while both younger and older zircons show positive εHf values (Fig. 8.1.8). Crustal model ages vary from 2.38 to 3.61 Ga. while initial Hf ratios vary in the interval 0.280857 – 0.281630 (Appendix 4.3).

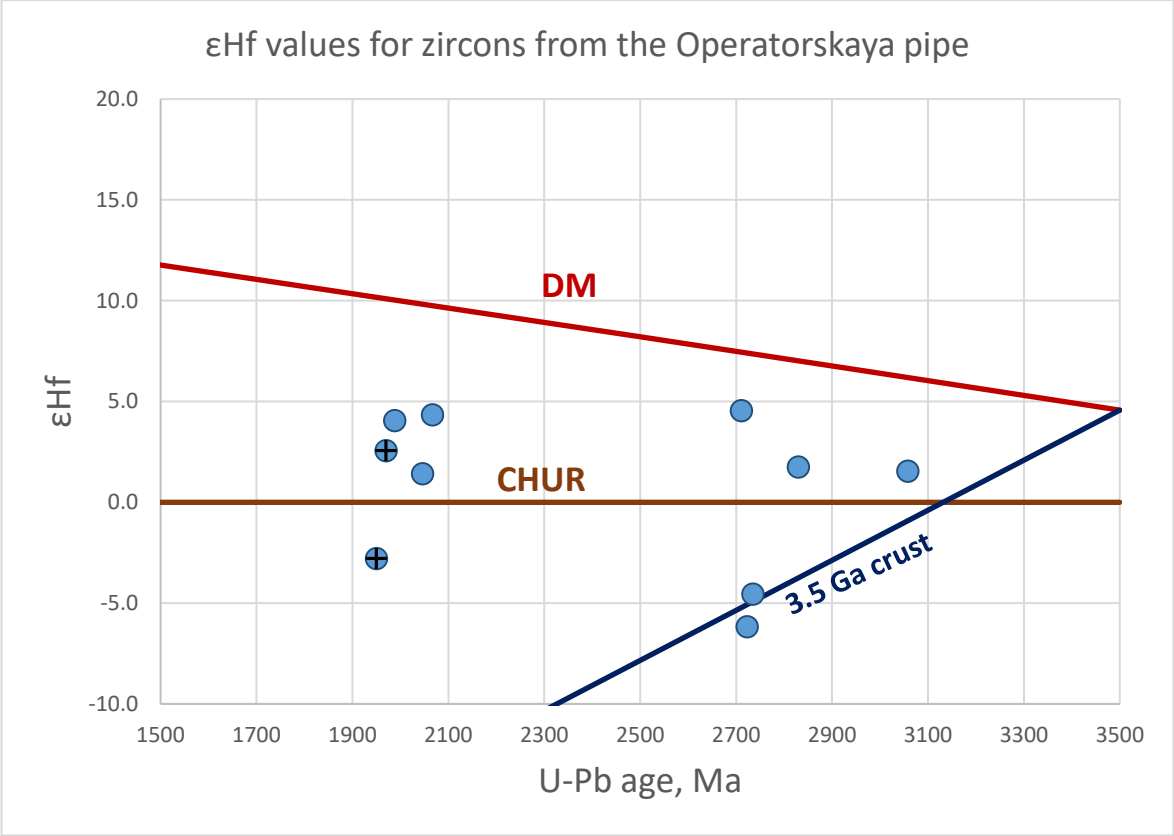



Figure 8.1.8. εHf *vs* age plot for zircons from the Operatorskaya pipe. Grains with trace-element (TE) composition typical of mantle-derived zircons are also shown with black crosses. The reference line is shown for evolution of the average continental crust.

## 8.2. The Kuoika kimberlite field

The field is located within the basins of the Olenek and Benchim rivers, whereas SW boundary lies adjacent to the Merchemden field. The Kuoika field contains more than 50 kimberlite bodies including pipes and dykes, hosted by a Cambrian sedimentary sequence, Late-Proterozoic dolomites and Early-Permian terrigenous rocks. A few pipes are intruded into Permian-Triassic dolerite sills. Thus, according to geological observations, the kimberlites are considered to be Mesozoic in age, probably Late Jurassic (Zaitsev & Smelov, 2010).

Geochronological studies have been done by different techniques and show a wide range of results. Thus, a Jurassic age was determined by U-Pb in zircons and perovskite, and by whole-rock K-Ar and Rb-Sr methods. At the same time, Rb-Sr, K-Ar and Ar-Ar techniques have given Paleozoic ages for some pipes (Kinny *et al.*, 1997).

The current study includes zircon samples from 5 kimberlitic pipes of the Kuoika field: Khrizolit, Pyatnitsa, Ruslovaya, Olivinovaya and Vtorogodnitsa.

### *Zircon U-Pb data*

Zircons were recovered from crushed kimberlite rocks of the Khrizolit, Pytnitsa and Ruslovaya pipes, and from heavy-mineral concentrates collected from the altered kimberlite of the Ruslovaya, Olivinovaya and Vtorogodnisa pipes.

#### The Khrizolit pipe

In total 10 U-Pb age determination were obtained; one was rejected because of high discordance.

U-Pb ages range from 154 to 160 Ma and form a single age population with an Upper Jurassic concordia age of 157.2±0.8 Ma (MSWD = 0.026, probability = 0.87; Fig. 8.2.1).

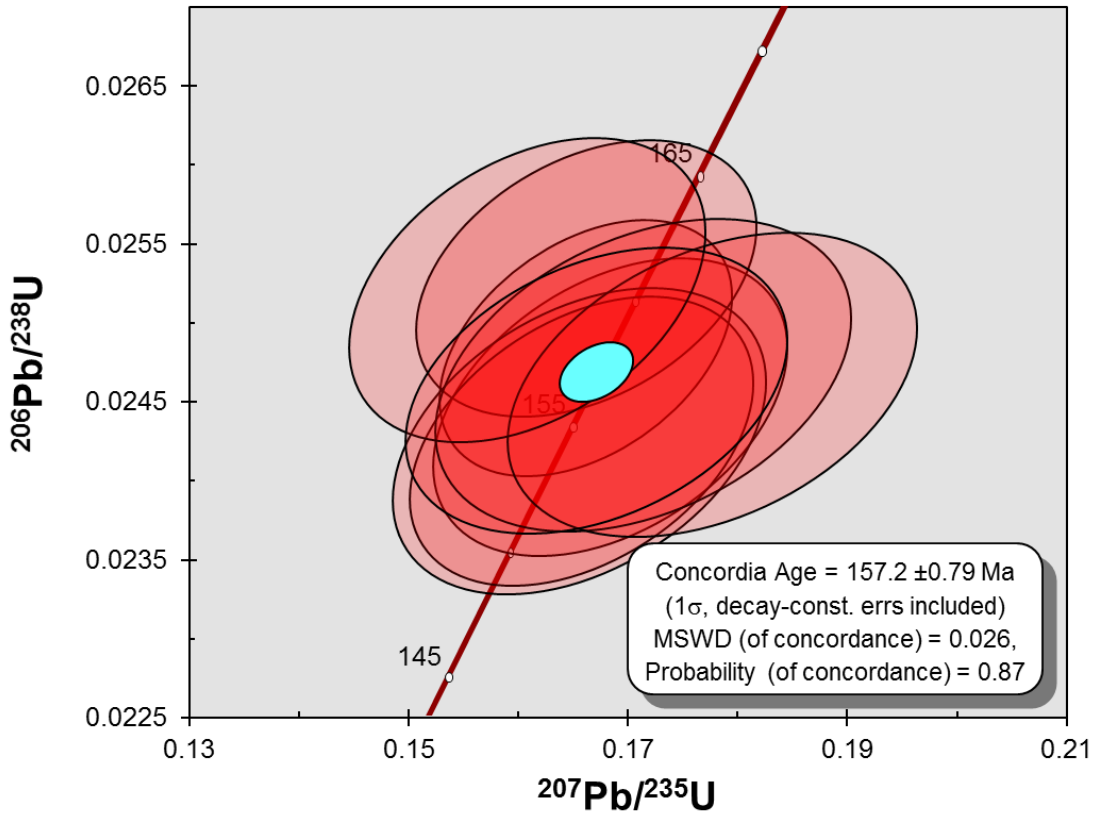



Figure 8.2.1. The U-Pb concordia for zircons from the Khrizolit pipe.

**The Pyatnitsa pipe**

Eleven U-Pb analyses were obtained for zircons collected from crushed kimberlite of the Pyatnitsa pipe. All analyses are concordant and form a single age group.

The range of U-Pb ages is from 137 to 153 Ma. The concordia age of the population is Uppermost Jurassic: 148.1±0.77 (MSWD = 0.0032, probability = 0.95; Fig. 8.2.2).

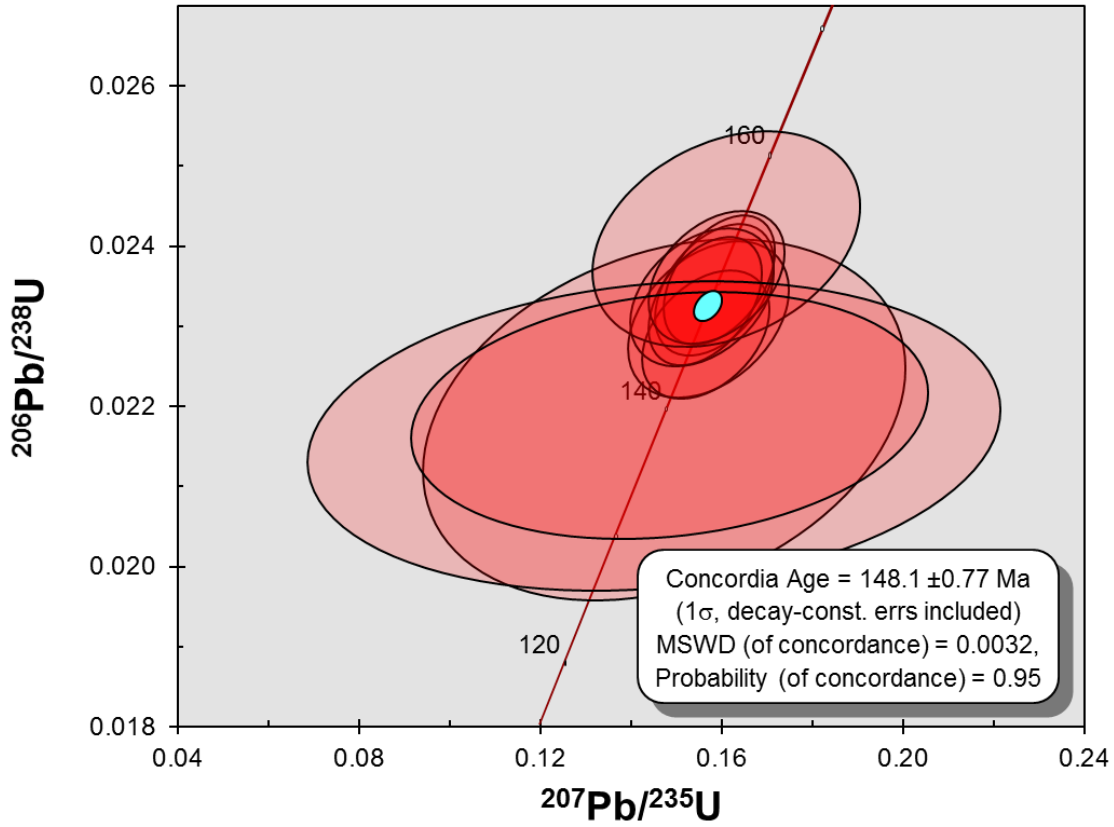



Figure 8.2.2. The U-Pb concordia for zircons from the Pyatnitsa pipe.

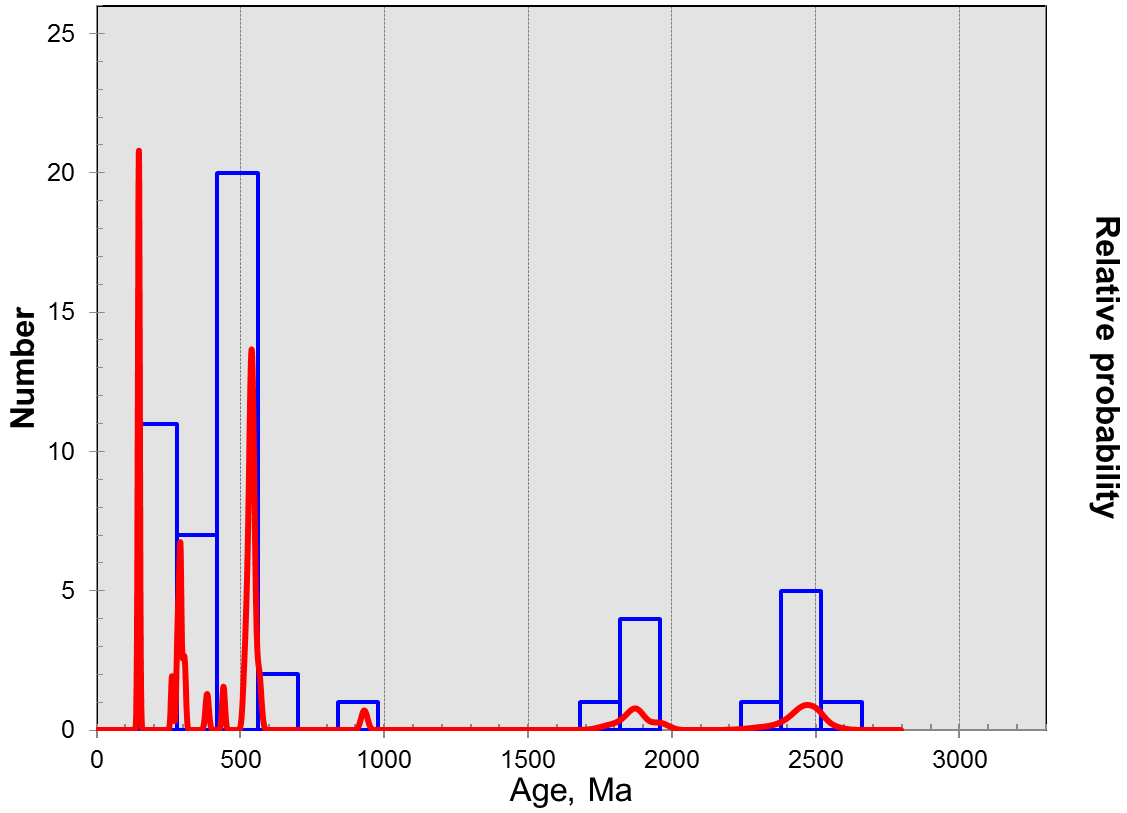



Figure 8.2.3. Probability plot of the U-Pb ages of zircons from the Ruslovaya pipe.

**The Ruslovaya pipe**

In total 60 zircons were analyzed for their U-Pb ages. Five analyses have discordance more than 20% and were not taken for further consideration.

U-Pb ages of zircons from the Ruslovaya pipe vary in a wide interval from 143 to 2534 Ma. The probability plot shows several age peaks; the major ones are younger than 1000 Ma Fig. 8.2.3). The youngest age population is represented by 9 zircon grains. The concordia age of this group is 145.4±0.98 Ma (MSWD = 0.15, probability = 0.70; Fig. 8.2.4).

The major peak is represented by 17 U-Pb analyses and shows a lowermost-Cambrian mean age of 537.2±3.3 Ma (MSWD = 1.08, probability = 0.37; Fig. 8.2.5).

The oldest age population consists of 6 grains with a weighted mean age of 2479±28 Ma (MSWD = 1.05, probability = 0.39; Fig. 8.2.6).

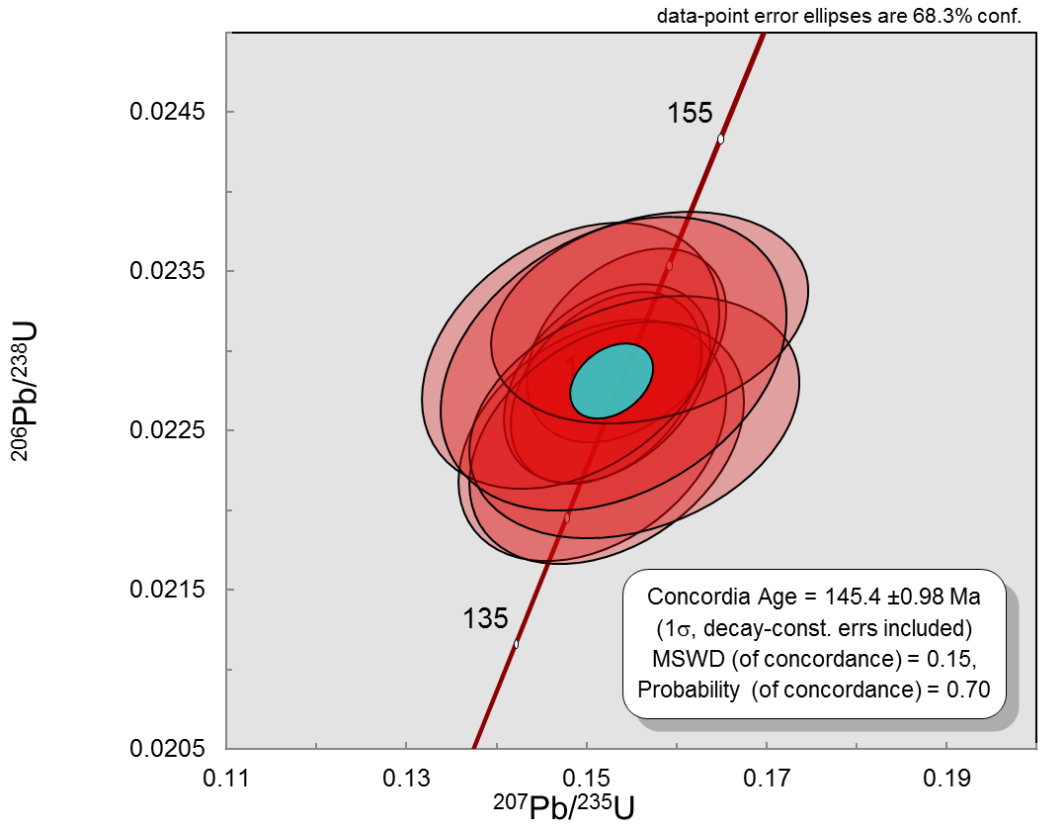



Figure 8.2.4. U-Pb concordia of zircons from the youngest age population, Ruslovaya pipe.

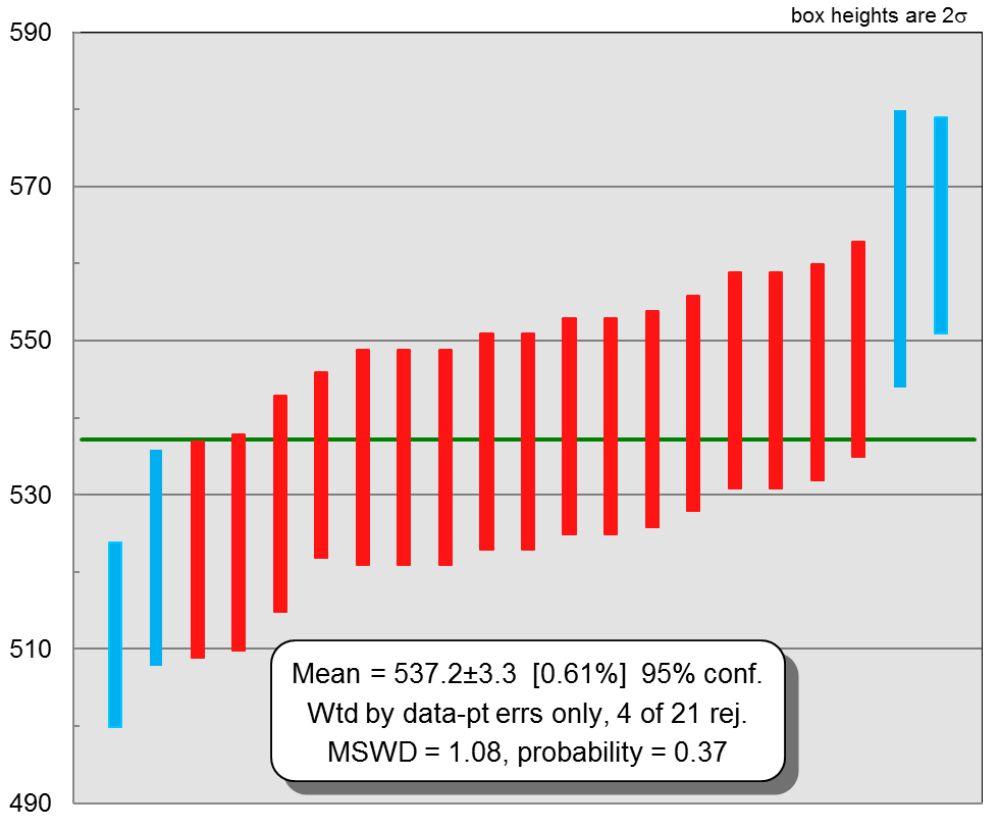



Figure 8.2.5. The weighted mean age of zircons of the major age population, Ruslovaya pipe.

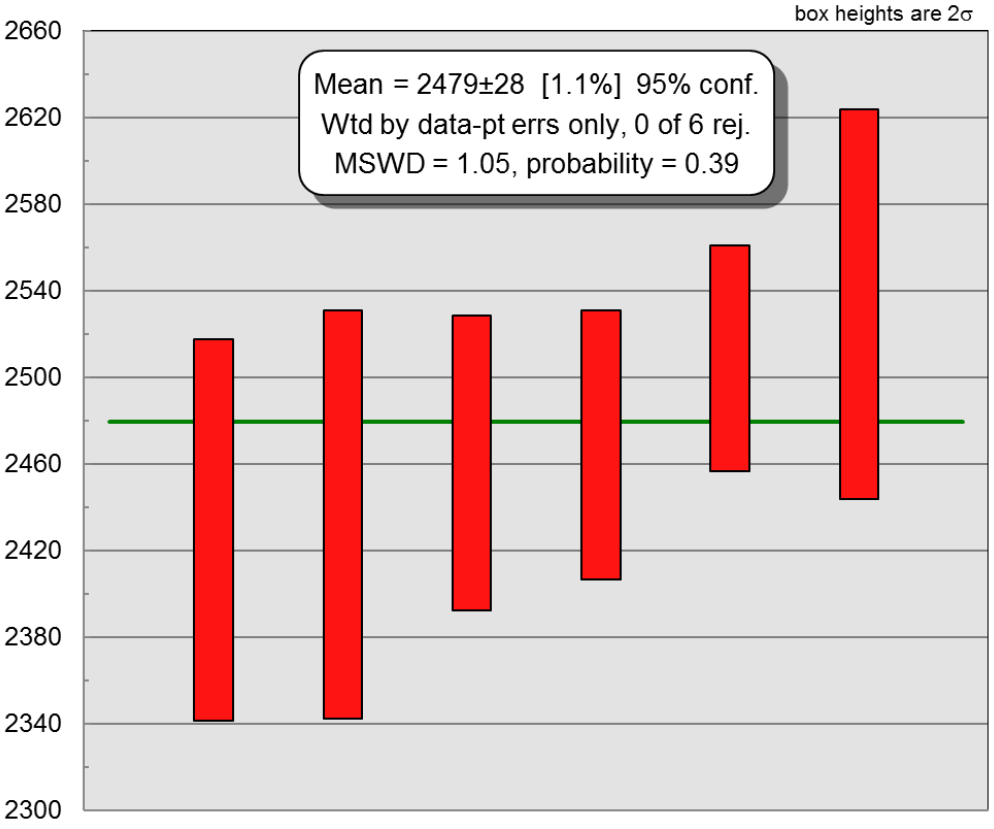



Figure 8.2.6. The weighted mean age of zircons of the oldest age population, Ruslovaya pipe.

**The Olivinovaya pipe**

Thirty-five grains were dated by U-Pb technique, of which four were rejected because of high discordance.

The obtained ages range from 141 to 2685 Ma and form two main age peaks on the probability plot (Fig. 8.2.7).

Nineteen zircons have U-Pb ages from 141 to 596 Ma, but it is hard to determine statistically meaningful age populations because of the relatively even distribution of ages in this range (Fig. 8.2.8).

The major peak for zircons older than 1000 Ma consists of 6 analyses and yields the mean age 1842±25 Ma (MSWD = 1.01, probability = 0.41; Fig. 8.2.9).

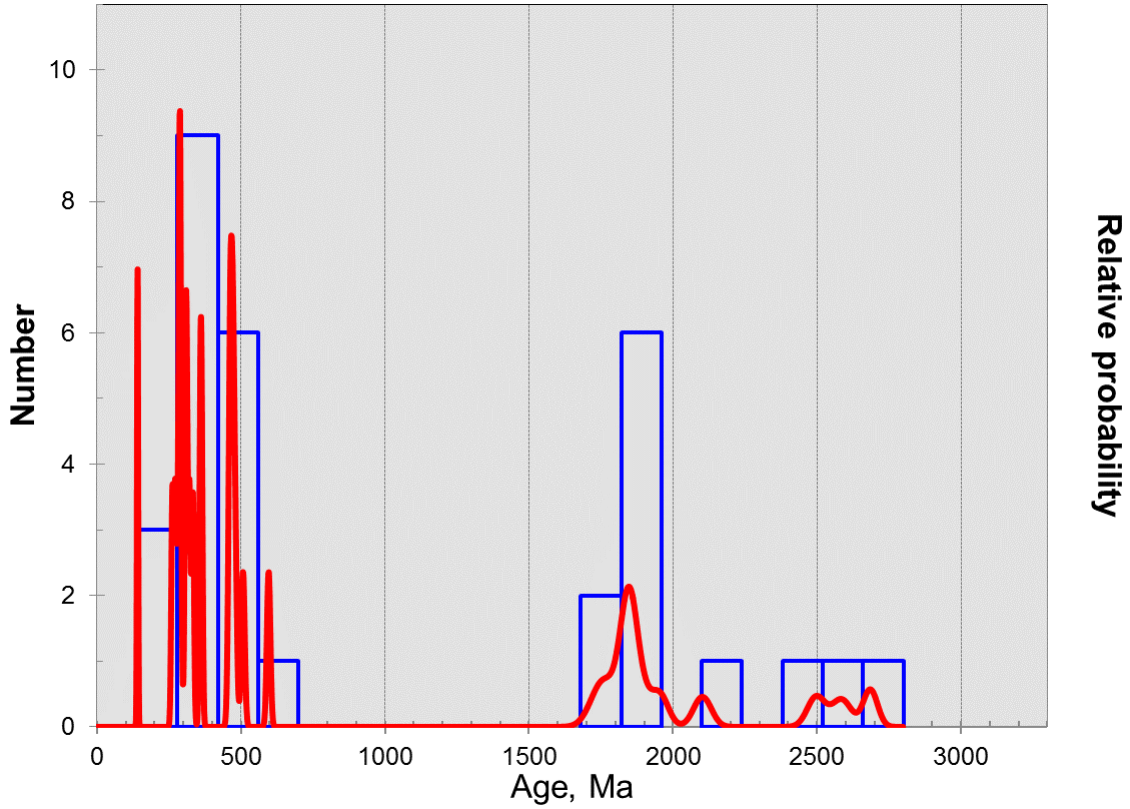



Figure 8.2.7. Probability plot of the U-Pb ages of zircons from the Olivinovaya pipe.

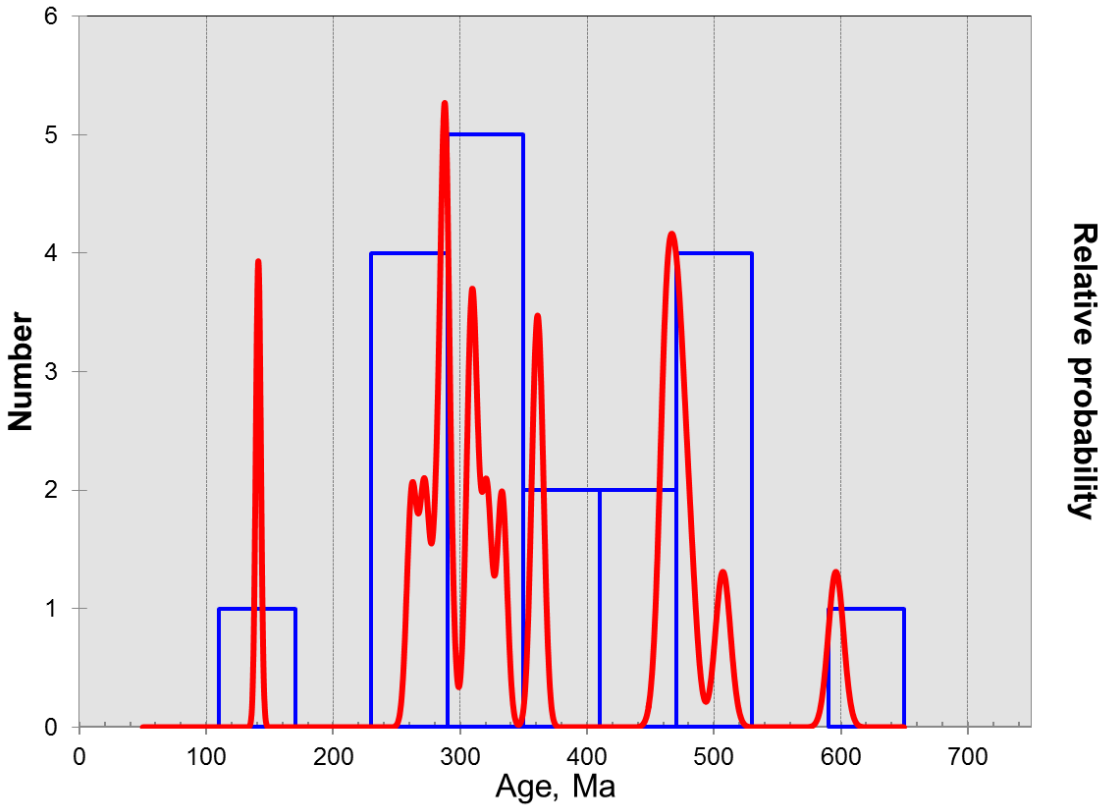



Figure 8.2.8. Probability plot of the U-Pb ages of young zircons from the Olivinovaya pipe.

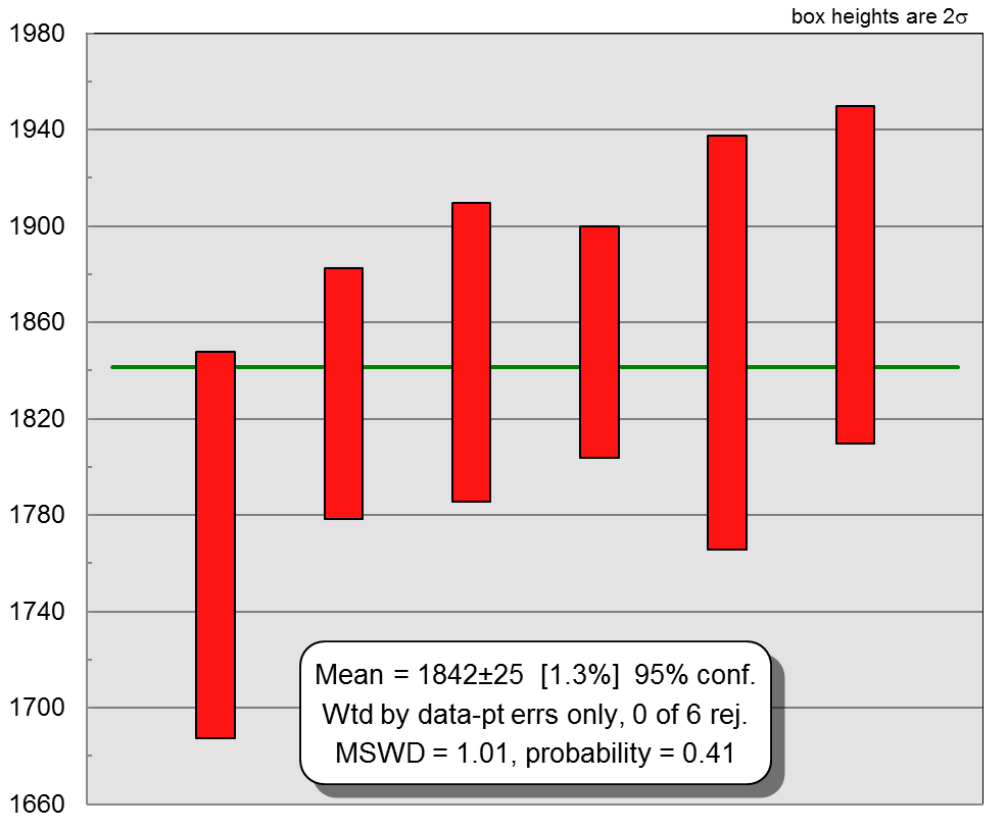



Figure 8.2.9. The weighted mean age of zircons of the oldest age population, Olivinovaya pipe.

**The Vtorogodnitsa pipe**

In total 44 zircons were collected from the pipe and dated. Fourteen analyses were rejected because of high discordance.

Zircon ages vary from 148 to 2804 Ma, defining a few distinctive age peaks (Fig. 8.2.10). As in the Olivinovaya pipe, younger ages (up to 470 Ma) are quite scattered and do not form uniform age populations (Fig. 8.2.11). The youngest double peak as shown in Fig. 8.2.11 reflects ages 148±4 and 157±4 Ma, the second youngest peak shows the age interval from 238±10 to 262±6 Ma. None of these peaks produces weighted mean age with acceptable MSWD (less than 2).

Among the grains older than 1500 Ma one distinctive age population is recognized. It consists of 8 analyses with a weighted mean age of 1884±22 Ma (MSWD = 0.54, probability = 0.81; Fig. 8.2.12).

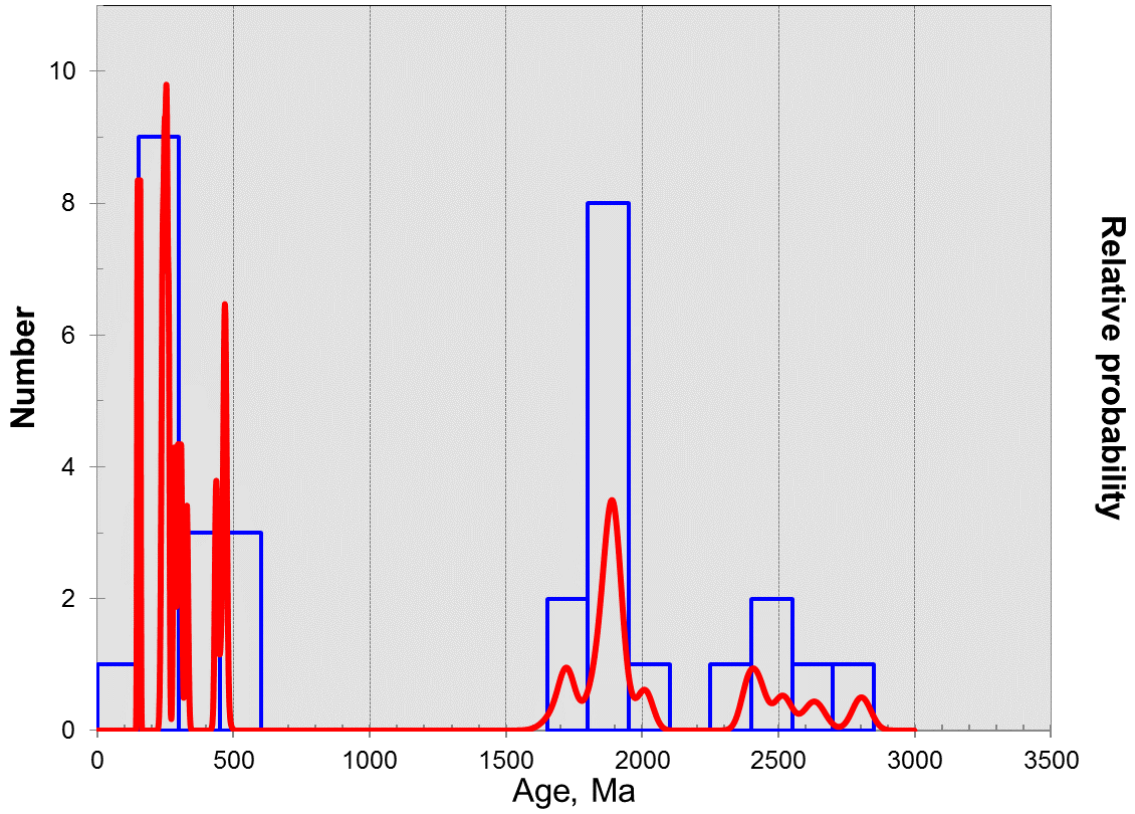



Figure 8.2.10. Probability plot of the U-Pb ages of zircons from the Vtorogodnitsa pipe.

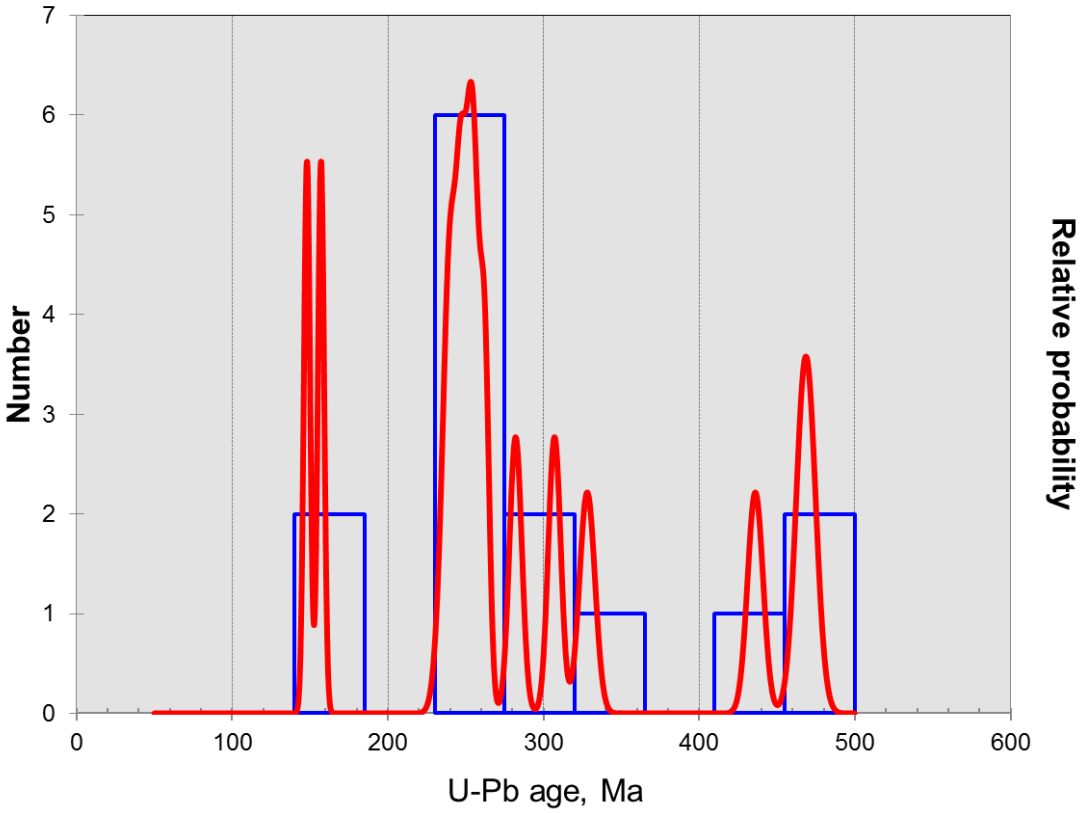



Figure 8.2.11. Probability plot of the U-Pb ages of young zircons from the Vtorogodnitsa pipe.

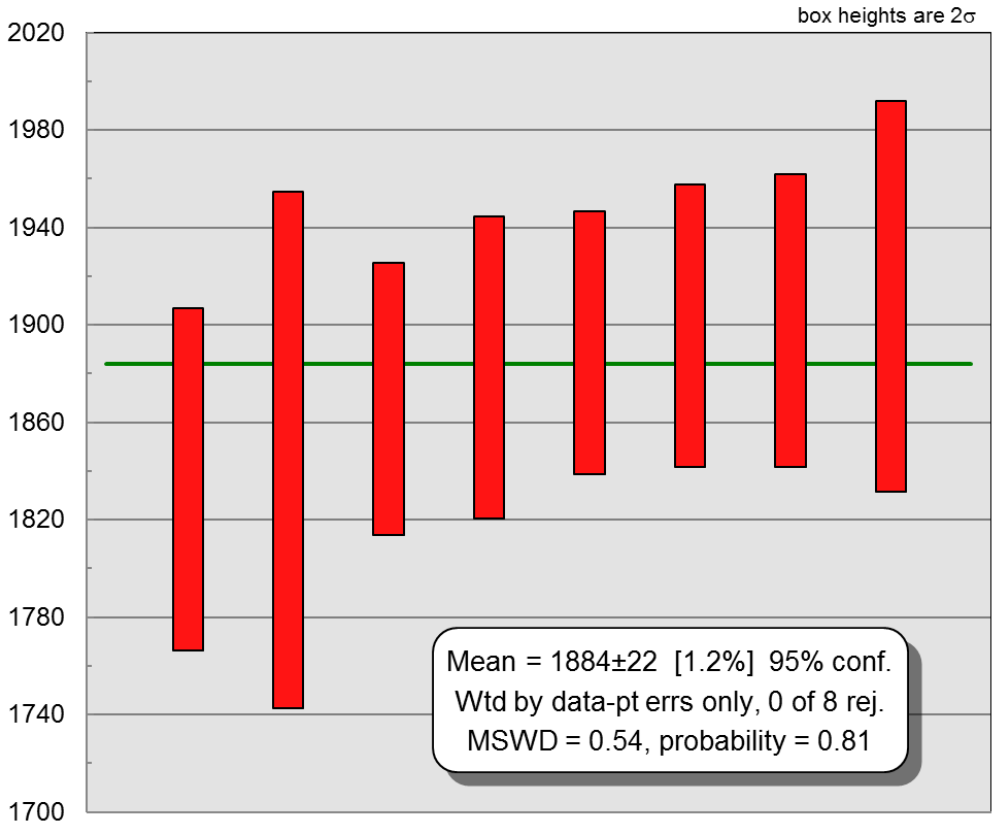



Figure 8.2.12. The weighted mean age of zircons of the oldest age population, Vtorogodnitsa pipe.

***Zircon trace-element data***

**The Ruslovaya pipe**

Twenty-five zircons from the pipe were studied for their trace-element composition.

Concentrations of trace elements are variable (Fig. 8.2.13). Thus, Y ranges from 665 to 4356 ppm, U – from 97 to 1494 ppm, Th – from 42 to 586 ppm. Total REE contents diverge within the interval 452 – 3001 ppm. The most variable concentrations are found among light rare-earth elements (from tenths to hundreds of ppm). In general, higher concentrations of REE (752 – 3001 ppm) are found in younger (261 – 930 Ma) zircons, while the most of older grains (1794 – 2534 Ma) having REE content under 1000 ppm (Fig. 8.2.14). However, the highest U concentrations, in opposite, were found in older grains.

Th/U and Nb/Ta range from 0.05 to 1.8 and from 1.07 to 4.75 respectively.

The chondrite-normalised REE plot shows relative enrichment in HREE and depletion in LREE, common feature of all zircons (Fig. 8.2.13). The Eu-minima is well-defined in all grains, while the positive Ce-anomaly is insignificant in some of the zircons. The presence of Eu-minima indicates that plagioclase was already crystallized from the zircon parental melt, while the Ce-maxima reflects the oxidation state of the melt.

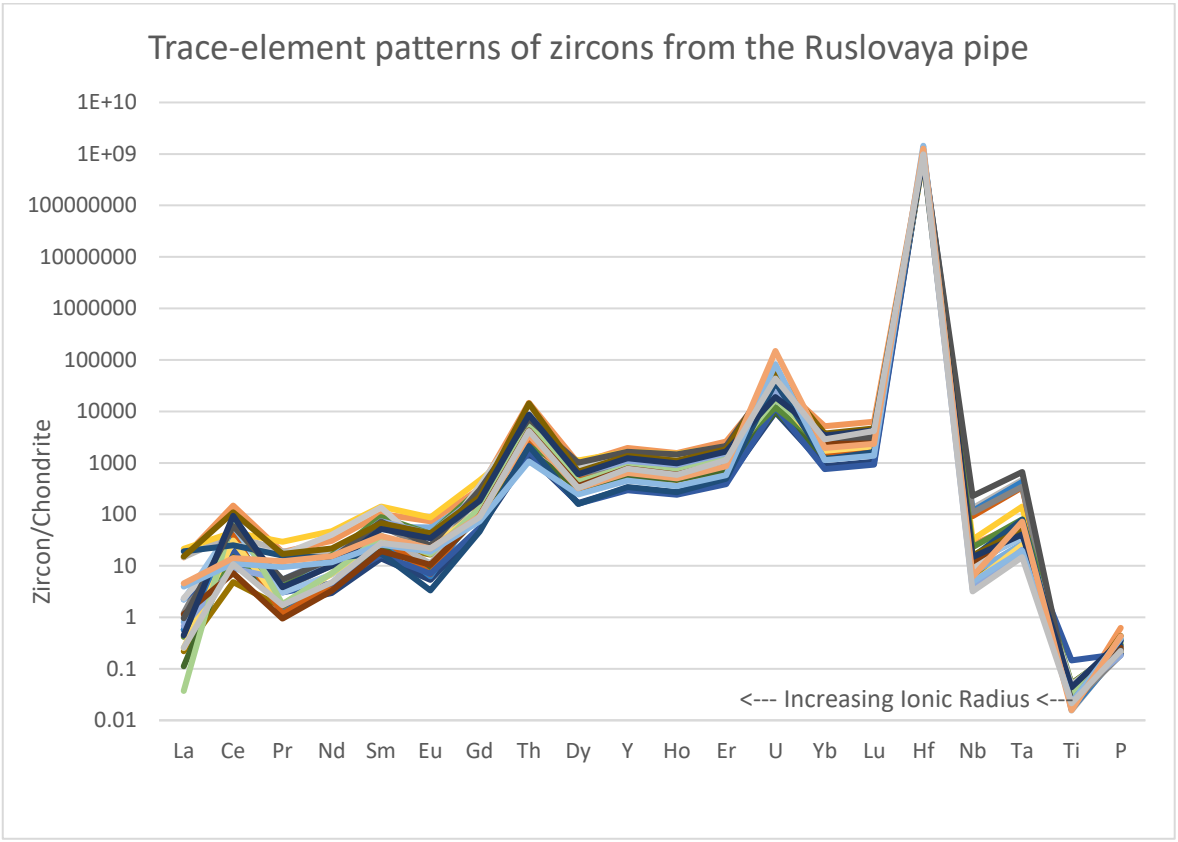
The CART statistical analysis classifies all grains as coming from intermediate or felsic rocks. High Y, U and Lu concentrations are common for zircons from these types of rocks, as well as high Hf content. The discrimination diagram Hf *vs* Y confirms the results of the CART classification (Fig. 8.2.15).

**The Olivinovaya pipe**

Twenty-three zircon grains from the pipe were studied for their trace-element composition.

The chondrite-normalised trace-element patterns of all analysed grains are generally similar, with some variations in the concentrations of rare-earth elements (Fig. 8.2.16). Total REE contents vary from 220 to 5570 ppm. Apart from REE the most of analysed trace elements range over one order of magnitude. Wide ranges of concentrations are also found for Y, Th and U: 269 – 7358 ppm, 48 – 1274 ppm and 65 – 897 ppm respectively. The highest concentrations of rare-earth elements are found for three younger zircons (<500 Ma), however, in general both young and old grains have close levels of REE and U (Fig. 8.2.17).

Th/U varies from 0.15 to 2.75; Nb/Ta ranges from 1.63 to 9.42.



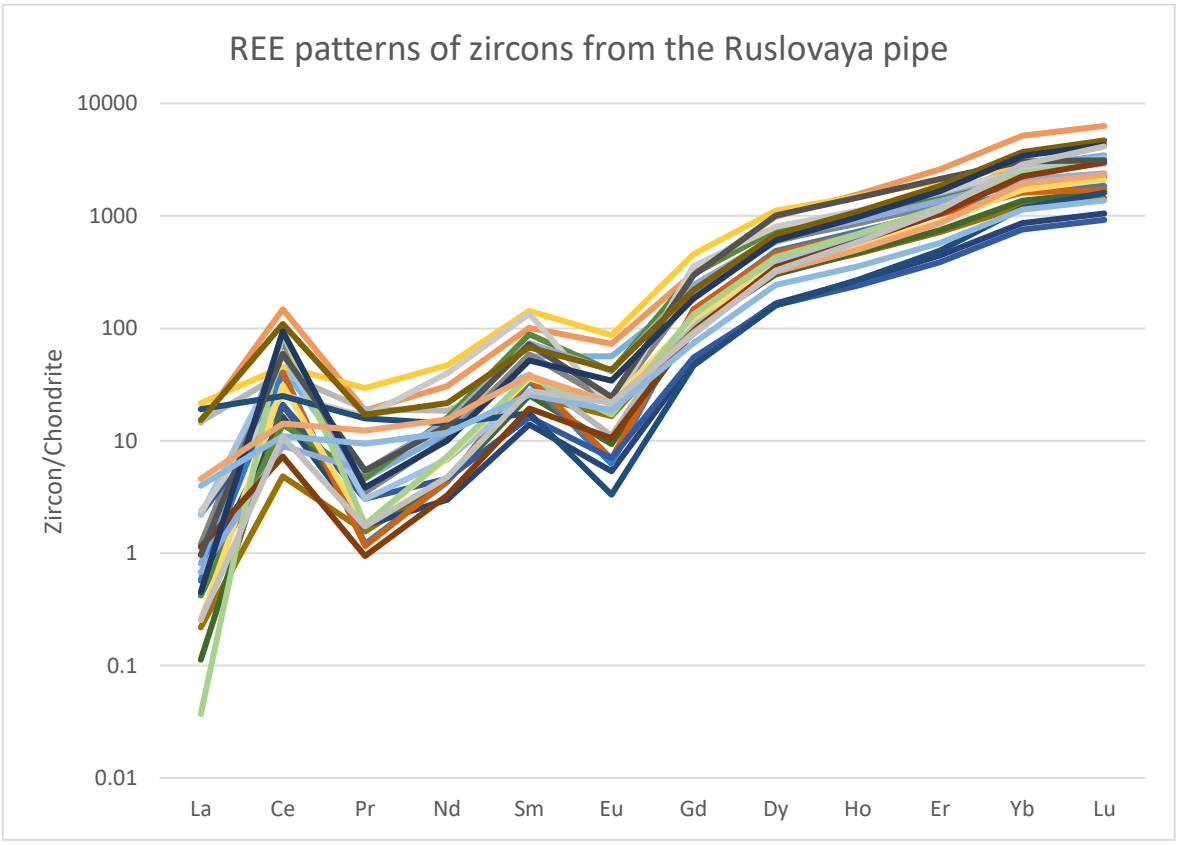




Figure 8.2.13. Trace-element and rare-earth element patterns of zircons, Ruslovaya pipe.

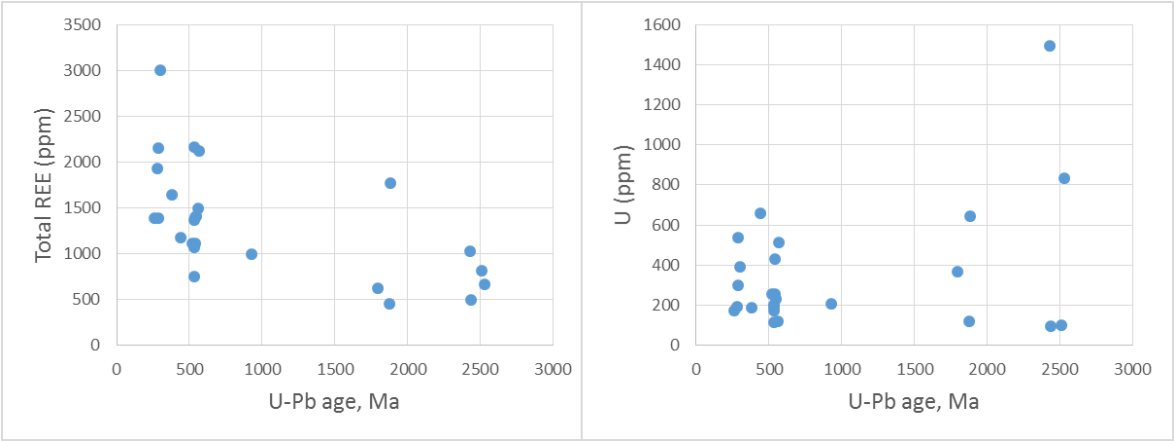
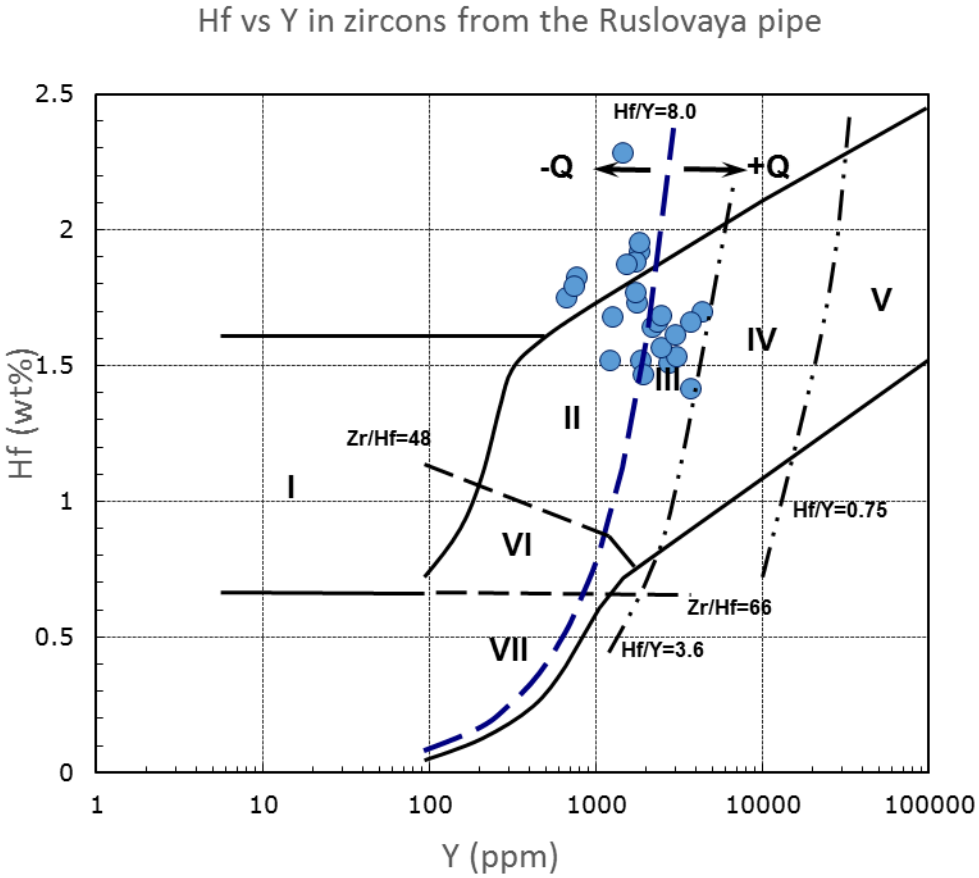
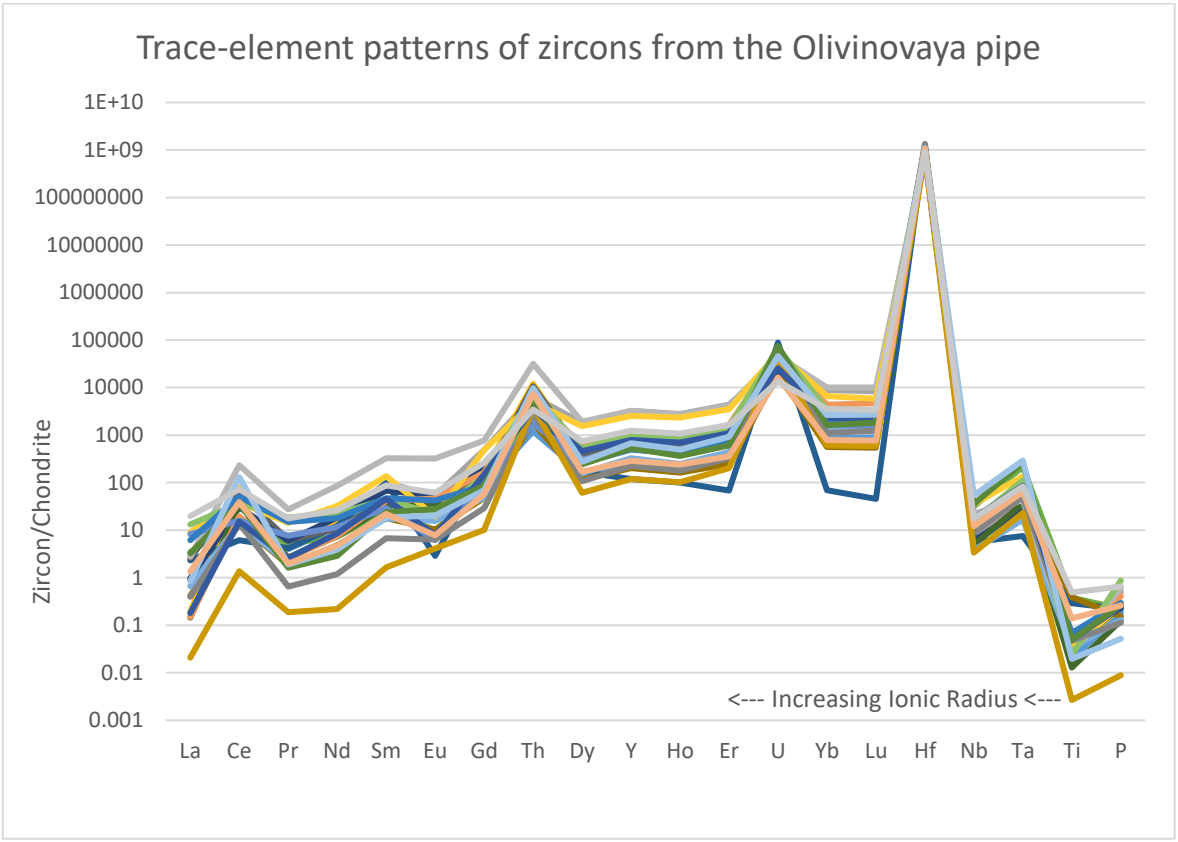



Figure 8.2.14. Total REE and U concentrations *vs* U-Pb age of zircons from the Ruslovaya pipe.




I - kimberlites;
II - ultrabasic, basic and intermediate rocks;
III - quartz-bearing intermediate and felsic rocks;
IV- felsic rocks with 'high' SiO2 content;
V - greisens;
VI- alkaline rocks and alkaline metasomatites of alkaline complexes;
VII- carbonatites

Figure 8.2.15. Hf *vs* Y discrimination diagram for zircons from the Ruslovaya pipe.



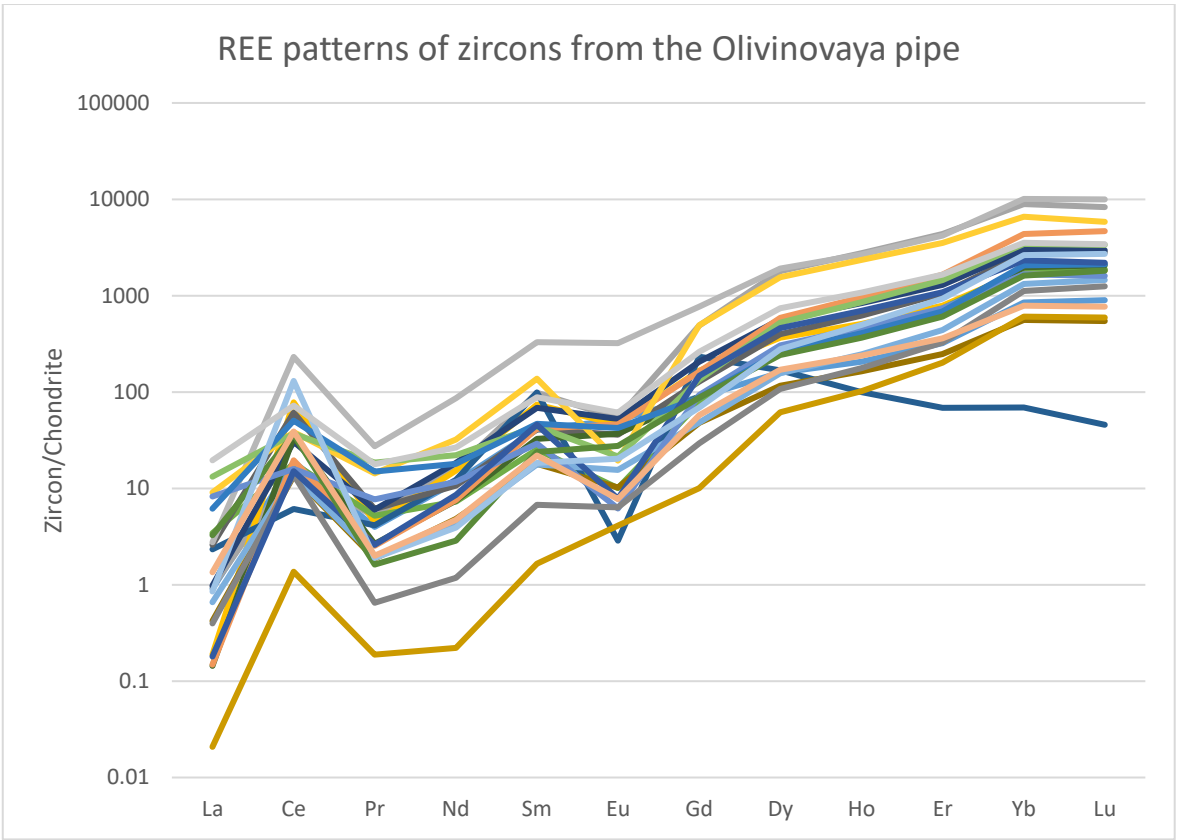




Figure 8.2.16. Trace-element and rare-earth element patterns of zircons, Olivinovaya pipe.

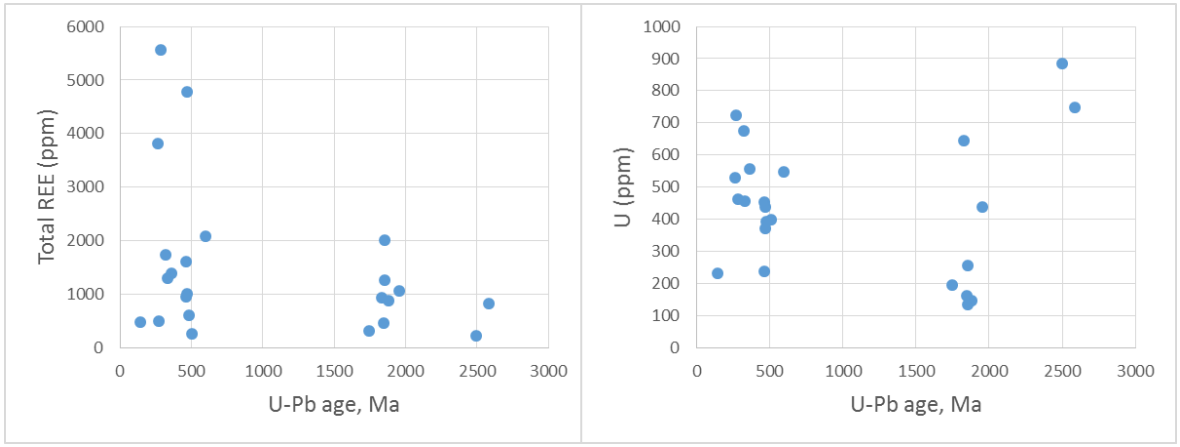



Figure 8.2.17. Total REE and U concentrations *vs* U-Pb age of zircons from the Olivinovaya pipe.

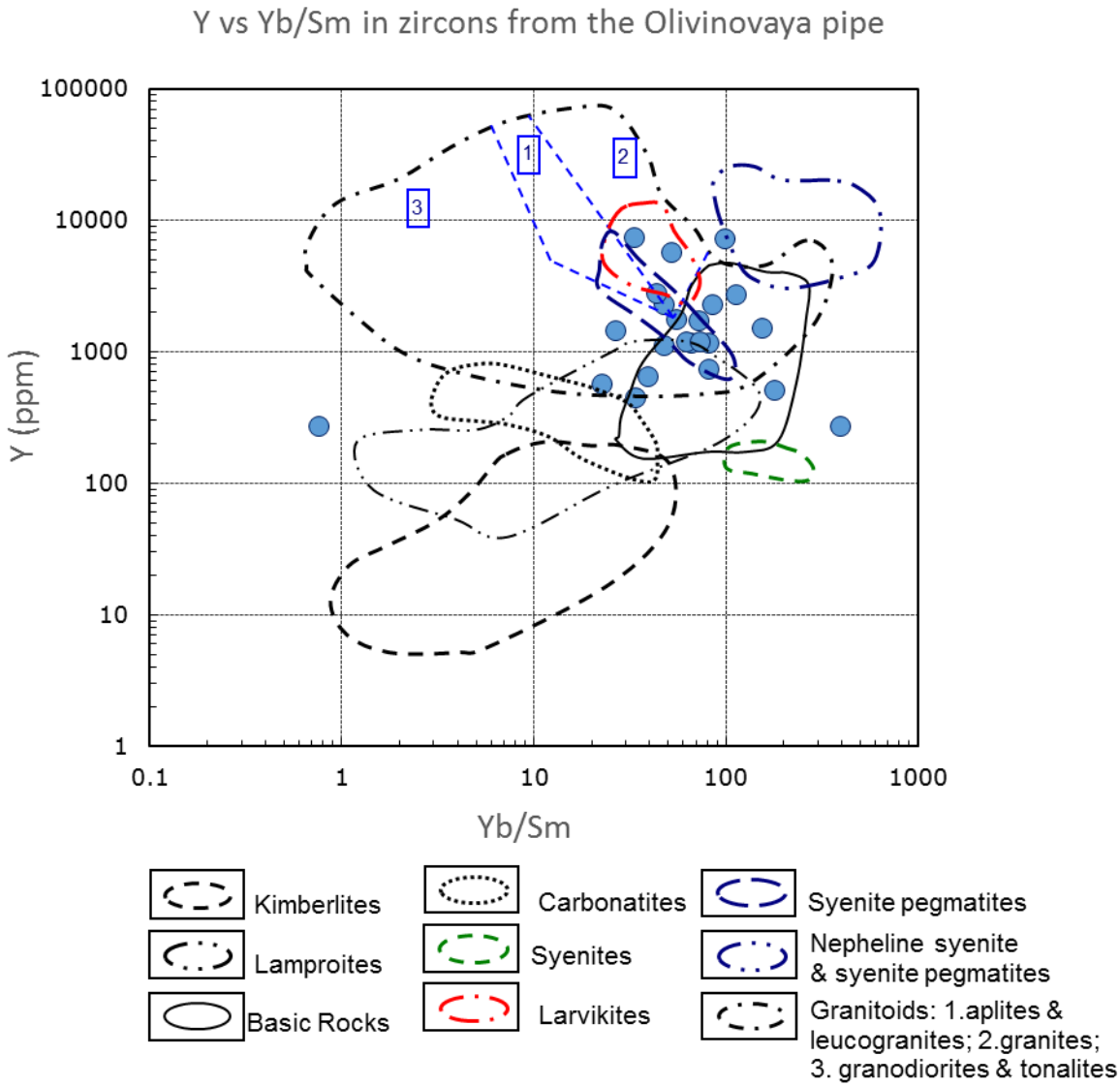



Figure 8.2.18. Y vs Yb/Sm discrimination diagram for zircons from the Olivinovaya pipe.

The REE plot shows typical zircon patterns with depletion in LREE and enrichment in HREE (Fig. 8.2.14). However, a single grain (U-Pb age of 2497 Ma) shows much less HREE enrichment comparing to other grains. The ration Yb/Sm demonstrates the degree of HREE

enrichment; all other grains have Yb/Sm from 22.7 to 398, while the outstanding zircon shows Yb/Sm=0.8. The depletion in HREE is not common for zircons and usually reflects the simultaneous crystallization of zircons and another mineral phase competing for HREE. The positive Ce-anomaly and Eu-minima are well defined for all grains.

According to the CART statistical classification, one grain with a different REE pattern has the trace-element composition typical of kimberlitic zircons (Lu<2 ppm, low REE, low Y and Ta). However, concentration of U (885 ppm) is much higher than in typical kimberlitic zircons (<60 ppm) and more common for zircons from mafic rocks. The depletion in HREE may indicate crystallization in garnet-bearing rocks, as garnet is the most common phase competing for HREE. Thus, low REE indicates mantle origin of the parental melt of these zircons, but high U excludes kimberlitic or carbonatitic origin. The rest of the grains show trace-element signatures of zircons crystallized from intermediate to felsic parental melts (high Y, U, REE) (Fig. 8.2.18).

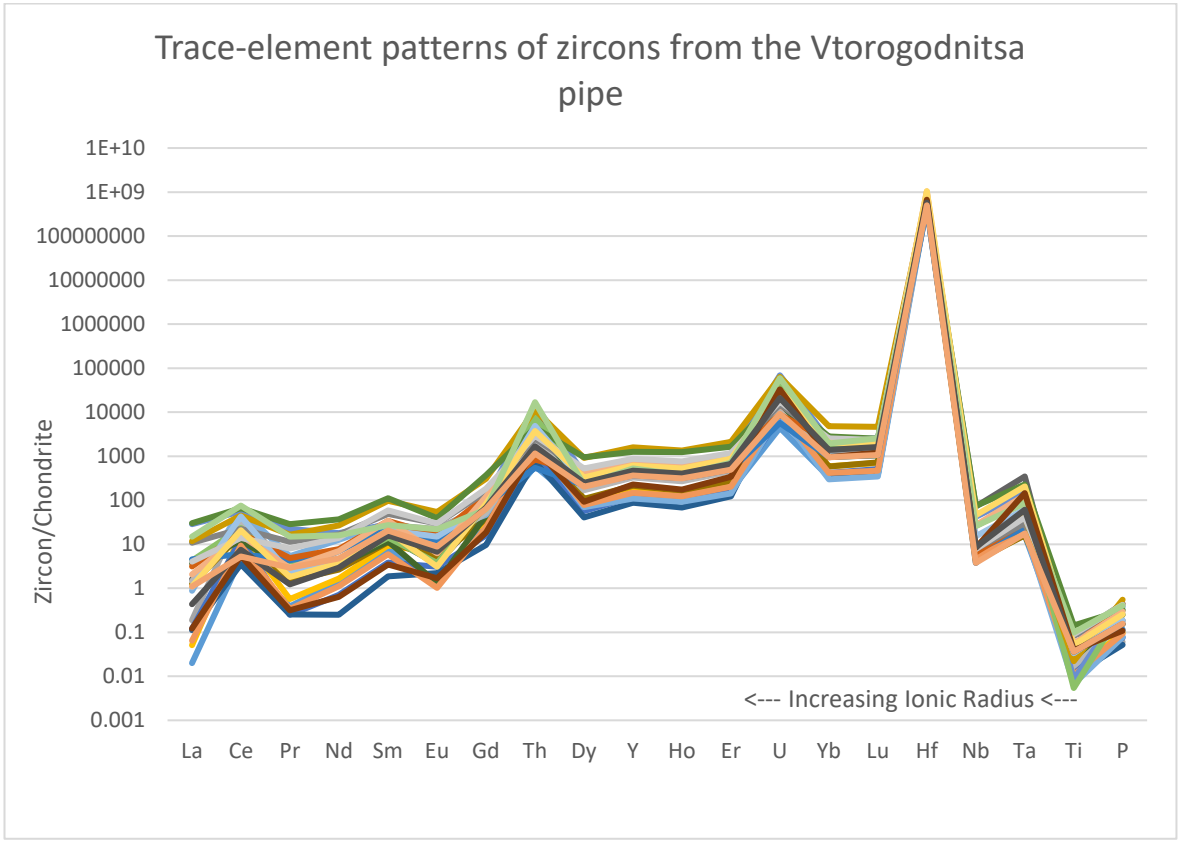
**The Vtorogodnitsa pipe**

Trace-element compositions were analysed in 25 zircon grains from the pipe.

All of them have chondrite-normalised trace-element patterns typical of zircons (Fig. 8.2.19). Concentrations of trace elements diverge quite significantly, especially for LREE. Thus, Y ranges from 198 to 3587 ppm, Th – from 23.5 to 674 ppm, U contents fall within the range 44 – 686 ppm. Total REE vary from 159 to 2570 ppm. Generally, lower REE contents are found in grain from the older age population (2388 – 2631 Ma). Zircons with ages younger than 500 Ma and 1723 – 2010 Ma show close levels of the total REE (Fig. 8.2.20). Low concentrations of Lu (<20.7 ppm) indicating mantle origin of the zircons parental melt are found only for grains from older populations (Fig. 8.2.20). Th/U ratio varies from 0.14 to 1.18, Nb/Ta – from 0.72 to 4.65.

The Ce- and Eu-anomalies are well defined in all of the analysed zircons reflecting high oxidation state of the parental magmas and crystallization of plagioclase prior to zircons.

The CART statistical analysis shows that 4 zircons have trace-element compositions similar to zircons from carbonatites (Lu<20.7 ppm), but their Hf contents are higher than those reported for carbonatitic zircons (Belousova *et al.*, 2002) (Fig. 8.2.21). Others have the typical trace-element signature of zircons from intermediate to felsic rocks (high Y, U, Lu and Hf) (Fig. 8.2.21).



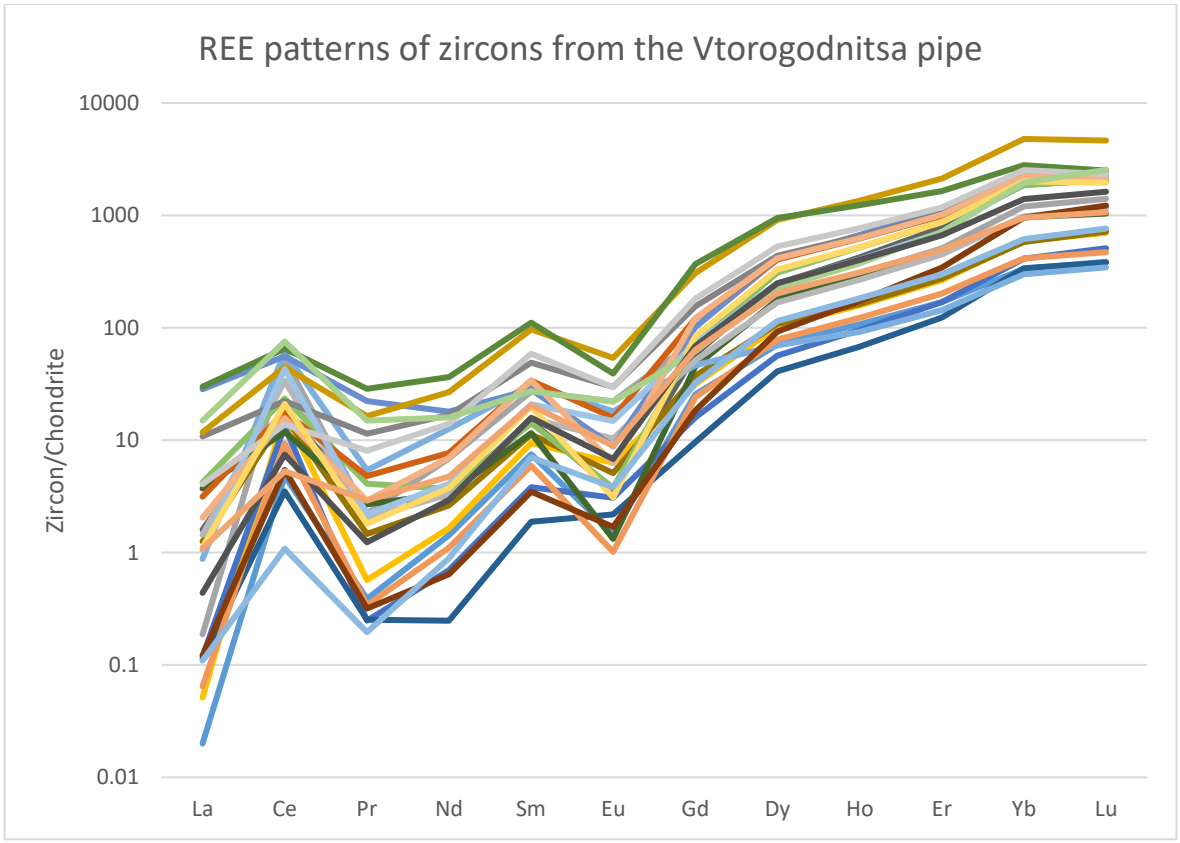




Figure 8.2.19. Trace-element and rare-earth element patterns of zircons, Vtorogodnitsa pipe.

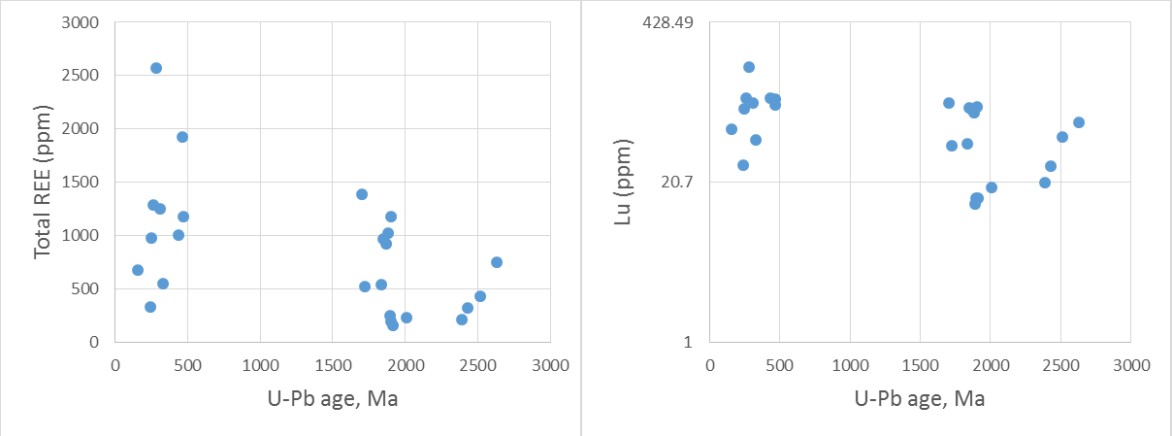
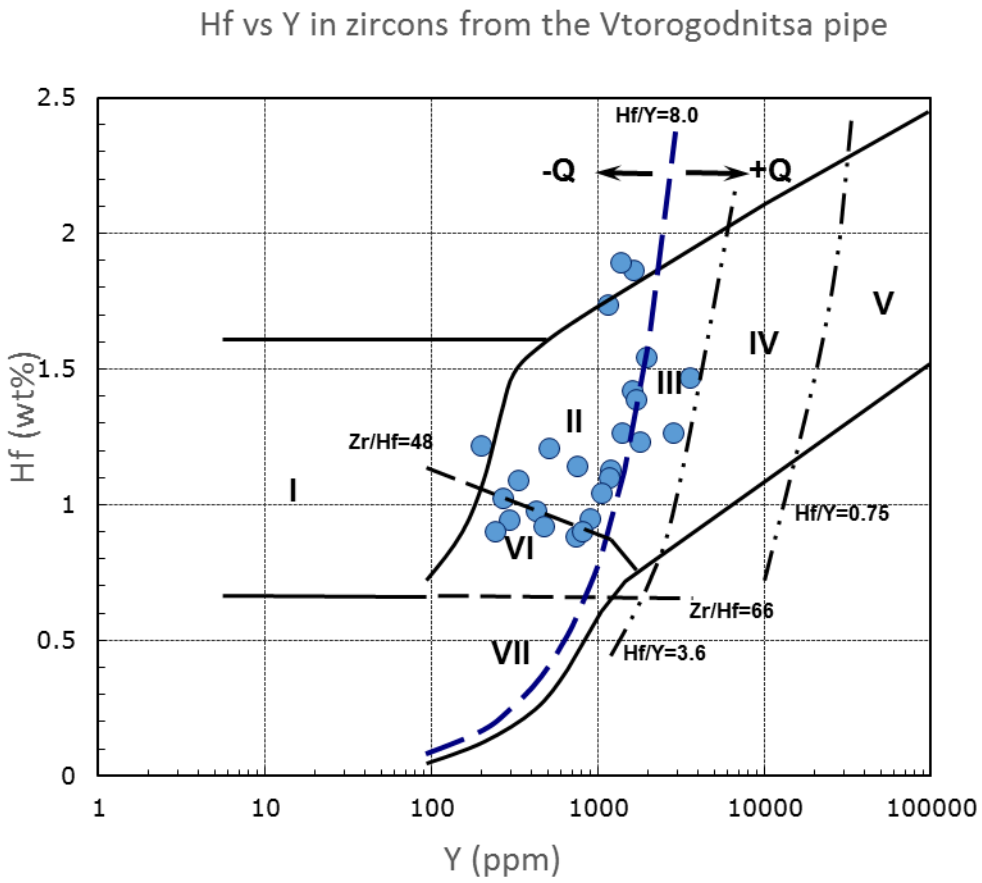



Figure 8.2.20. Total REE and Lu concentrations vs U-Pb age of zircons from the Vtorogodnitsa pipe.




I - kimberlites;
II - ultrabasic, basic and intermediate rocks;
III - quartz-bearing intermediate and felsic rocks;
IV- felsic rocks with 'high' SiO2 content;
V - greisens;
VI- alkaline rocks and alkaline metasomatites of alkaline complexes;
VII- carbonatites

Figure 8.2.21. Hf vs Y discrimination diagram for zircons from the Vtorogodnitsa pipe.

***Oxygen-isotopes data***

**The Ruslovaya pipe**

Isotopic composition of oxygen was analysed in 27 zircons from different age groups. The obtained values of $\delta^{18}O$ diverge from 4.02±0.59 to 9.27±0.62‰ (Fig. 8.2.22). Eight zircons have mantle oxygen isotopic composition (5.3±0.6‰, (Valley, 2003)). Supracrustal (>6.6‰) values are typical for zircons from the main age population (mean age 537 Ma), however a single grain of this age shows $\delta^{18}O$ of 4.92±0.6‰. The values below 5‰ observed for two grains are considered to represent the input of meteoric water, indicating hydrothermal origin of zircons or hydrothermal alteration of the rocks protolith (Bindeman & Valley, 2001, Valley *et al.*, 2003).

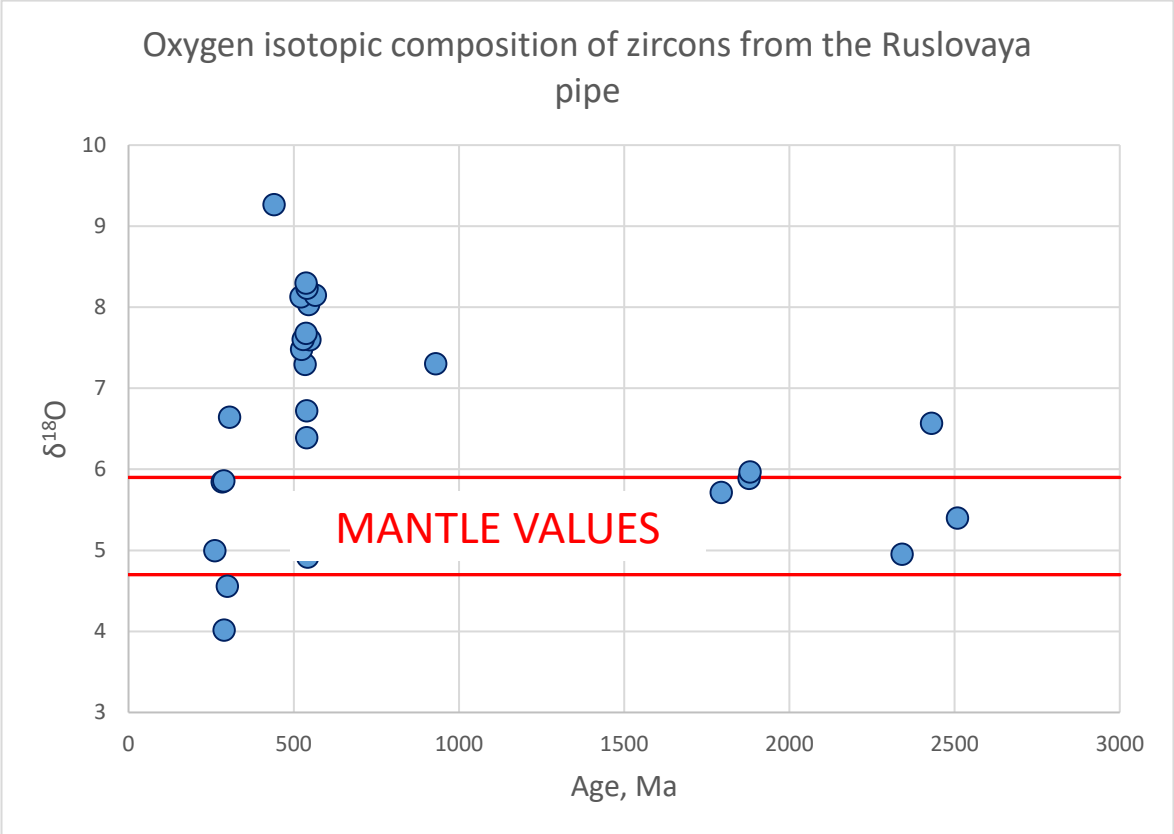



Figure 8.2.22. $\delta^{18}O$ vs U-Pb age for zircons from the Ruslovaya pipe.

**The Olivinovaya pipe**

Twenty-two zircons were analysed for their oxygen isotopic composition. The range of $\delta^{18}O$ values is from 4.39±0.6 to 8.54±0.6‰. Zircons older than 1500 Ma have oxygen composition within or close to mantle range of values, while the most of Palaeozoic ones show crustal or supracrustal oxygen composition. In total six grains reveal mantle $\delta^{18}O$ values within the analytical uncertainty (Fig. 8.2.23).

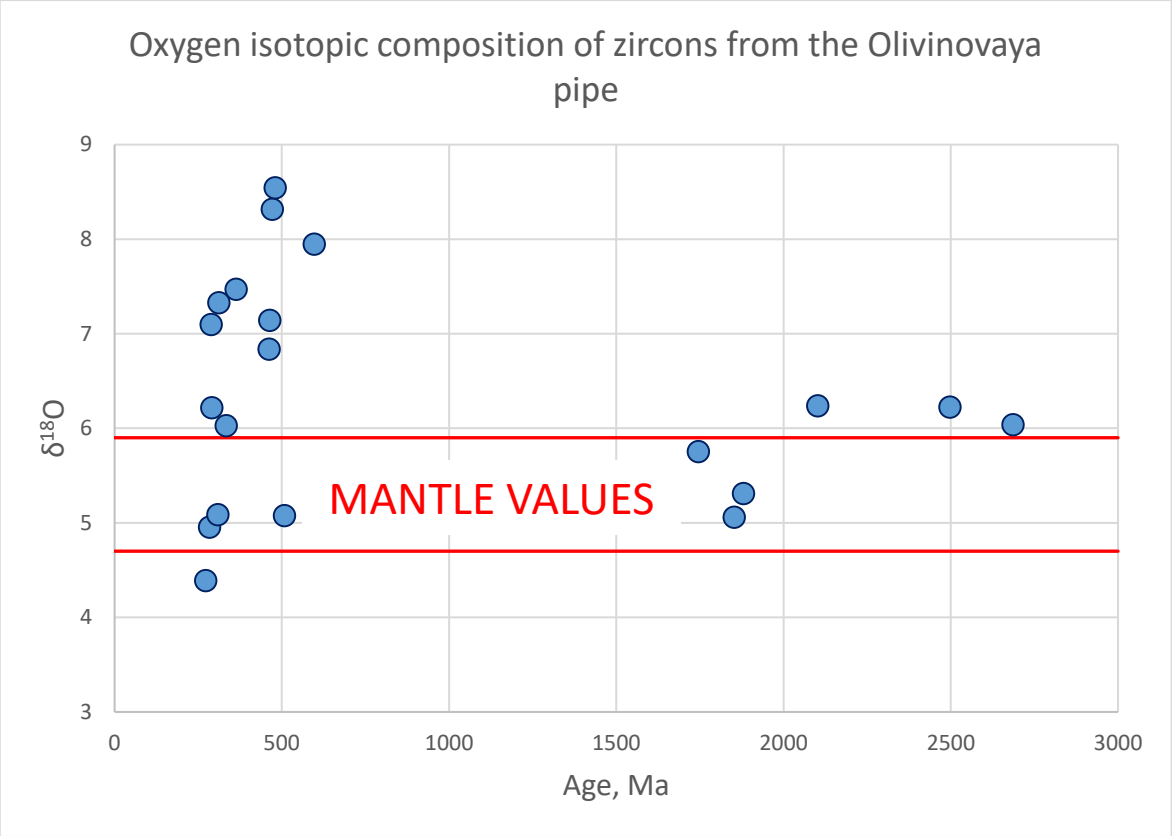



Figure 8.2.23. $\delta^{18}O$ vs U-Pb age for zircons from the Olivinovaya pipe.

**The Vtorogodnitsa pipe**

Fifteen zircon grains from the pipe were analysed for the isotopic composition of oxygen. The majority of them show $\delta^{18}O$ within the mantle range of values (Fig. 8.2.24). The lowest $\delta^{18}O$ of 3.95±0.62‰ is found for the grain with age 238 Ma. Usually values lower than 4.9 are considered to reflect the input of meteoric water or hydrothermal origin of zircon. Only two zircon have crustal oxygen isotopic composition, and another two show supracrustal oxygen signatures.

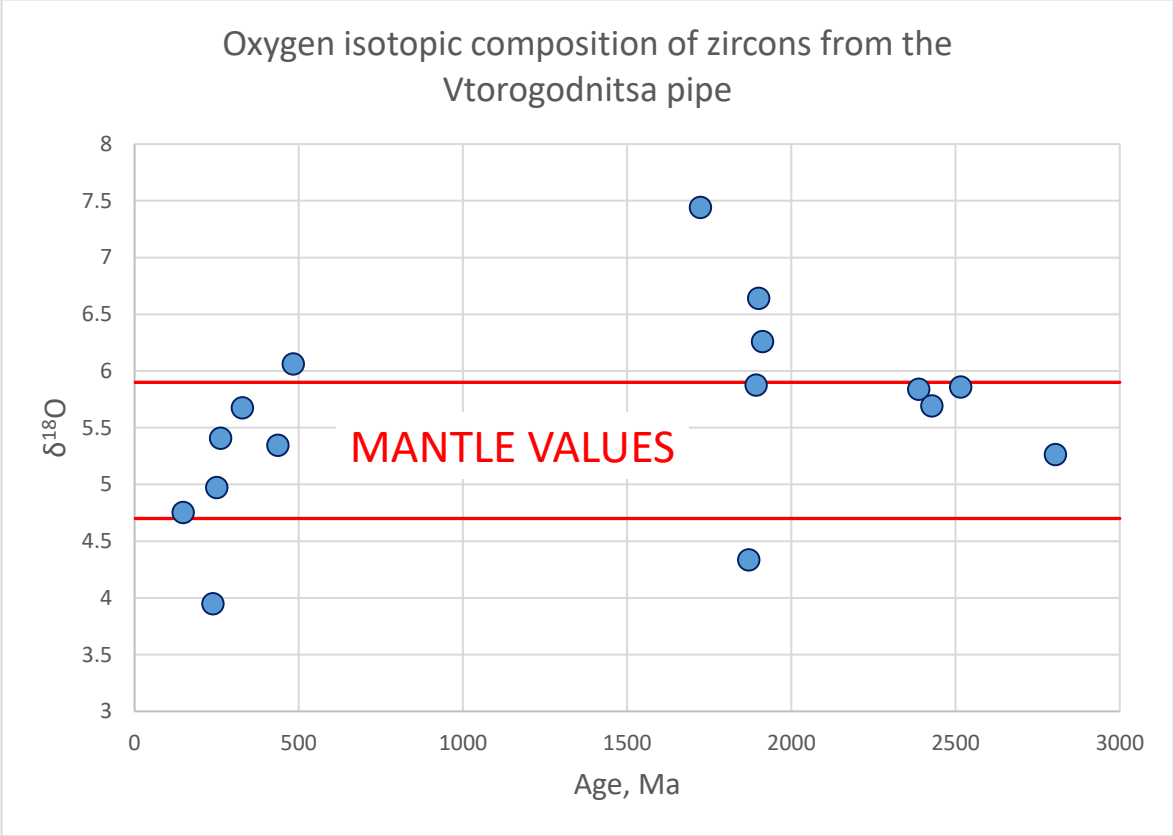



Figure 8.2.24. $\delta^{18}O$ vs U-Pb age for zircons from the Vtorogodnitsa pipe.

***Hafnium-isotopes data***

**The Ruslovaya pipe**

Thirty-five zircons of different age populations have been analyzed for their Lu-Hf isotopic systematic.

Young zircons (<1000 Ma) show the most variable Hf isotopic composition. The εHf values range from -29.4 to +15.5, and the most of these grains have positive εHf, indicating significant mantle input (Fig. 8.2.25). Despite of mantle Hf isotopic composition, a lot of those zircons show supracrustal $\delta^{18}O$ values. Such combination of isotopic signatures may occur in case of reworking of sedimentary material with a high proportion of juvenile component, for example, in subduction zones. On the other hand, mantle oxygen values together with negative εHf possibly indicate reworking of the old mantle-derived protolith that had no interaction with surface weathering processes and no contribution of sedimentary material.

Grains with ages older than 1794 Ma reveal less variation in εHf: from -13.5 to +1. Their crustal model ages vary from 2.44 to 3.48 Ga, while $T_{DM}^{C}$ for the young zircons ranges from 0.5 to 2.92 Ga. Initial Hf ratios vary in the interval 0.280990 – 0.281636 for old zircons and 0.281762 – 0.282921 for the young ones (Appendix 6.3).

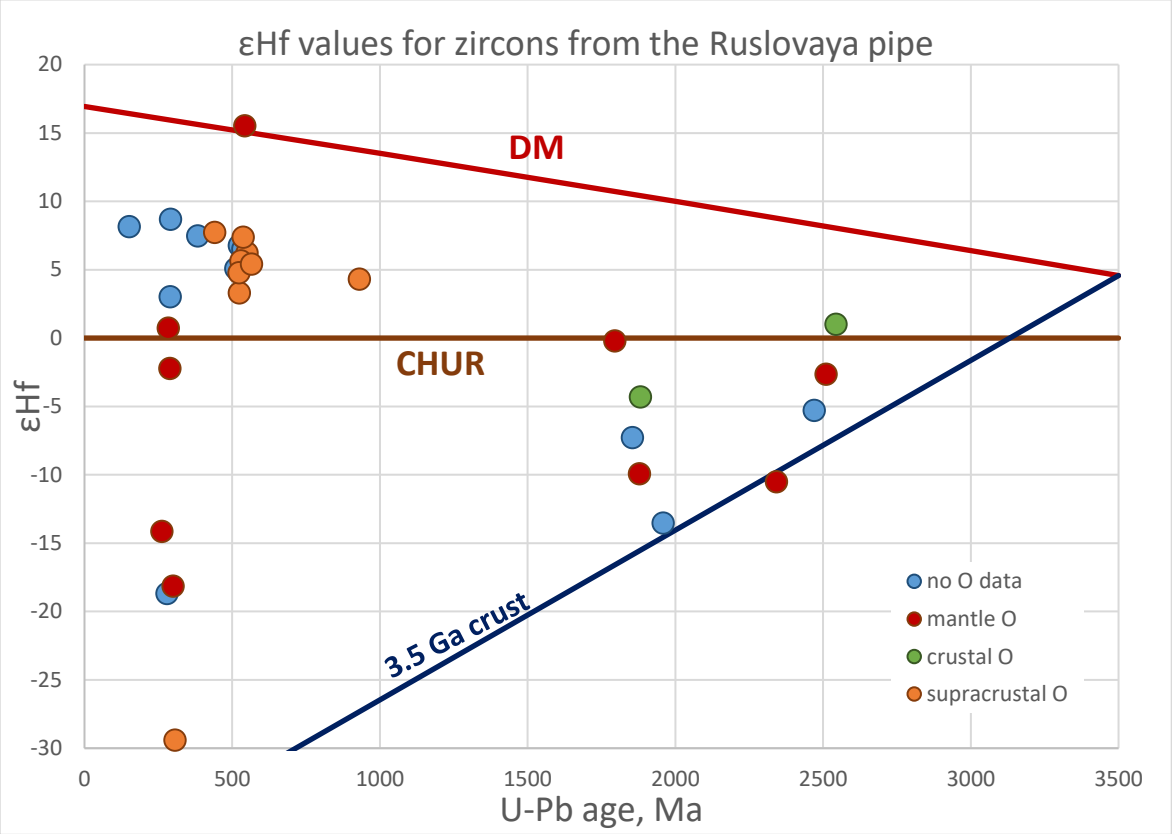



Figure 8.2.25. εHf *vs* age plot for zircons from the Ruslovaya pipe. The data points are color-coded according to the zircon O-isotope composition (where these data are available). The reference line is shown for evolution of the average continental crust.

**The Olivinovaya pipe**

Lu-Hf isotopic compositions were analyzed in 30 dated zircons from the pipe.

The range of εHf values is from -22.5 to +11.8. As in to the Ruslovaya pipe, young grains show more variation in εHf values, than the old ones. (Fig. 8.2.26). A significant amount of positive εHf among the Palaeozoic zircons demonstrates highly active processes in the mantle during this time.

Crustal model ages of the young zircons vary from 0.49 to 2.41 Ga, whereas old grains have $T_{DM}^{C}$ from 2.34 to 3.4 Ga. Calculated initial Hf ratios differ in the interval 0.281038 – 0.282953 (Appendix 6.3).

Two grains with trace-element composition typical for mantle-derived zircons are shown at the Fig.8.2.26. One of them is lying directly on the evolution line of the 3.5 Ga crust, and it also reveals mantle oxygen composition. This implies reworking of the 3.5 Ga mantle-derived protolith without interaction with sedimentary material.

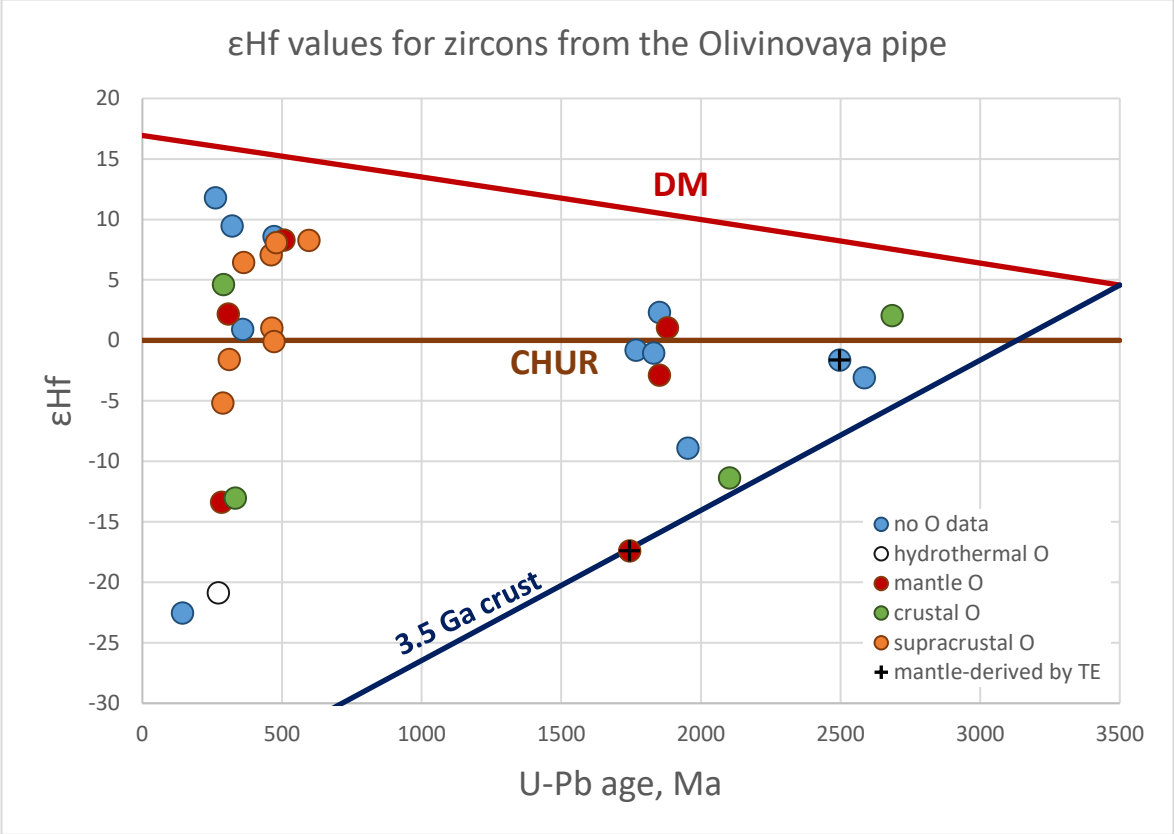



Figure 8.2.26. εHf *vs* age plot for zircons from the Olivinovaya pipe. The data points are color-coded according to the zircon O-isotope composition (where these data are available). Grains with trace-element (TE) composition typical of mantle-derived zircons are also shown with black crosses. The reference line is shown for evolution of the average continental crust.

**The Vtorogodnitsa pipe**

In total 26 zircons from the pipe were analysed for Hf-isotope compositions.

Unlike the other two pipes from the field, the zircons from the Vtorogodnitsa pipe show similar ranges of εHf values for young and old grains (Fig. 8.2.27). In general, εHf ranges from -19.4 to +8.4. Negative values are more common than positive ones for both young and old zircons. This implies less input of the juvenile material comparing to the other pipes of the Kuoika field.

Calculated initial Hf ratios vary in the interval 0.280696 – 0.282726. Crustal model ages of young zircons range from 0.86 to 2.31 Ga; old grains reveal a 2.23 – 4.04 Ga range in crustal model age.

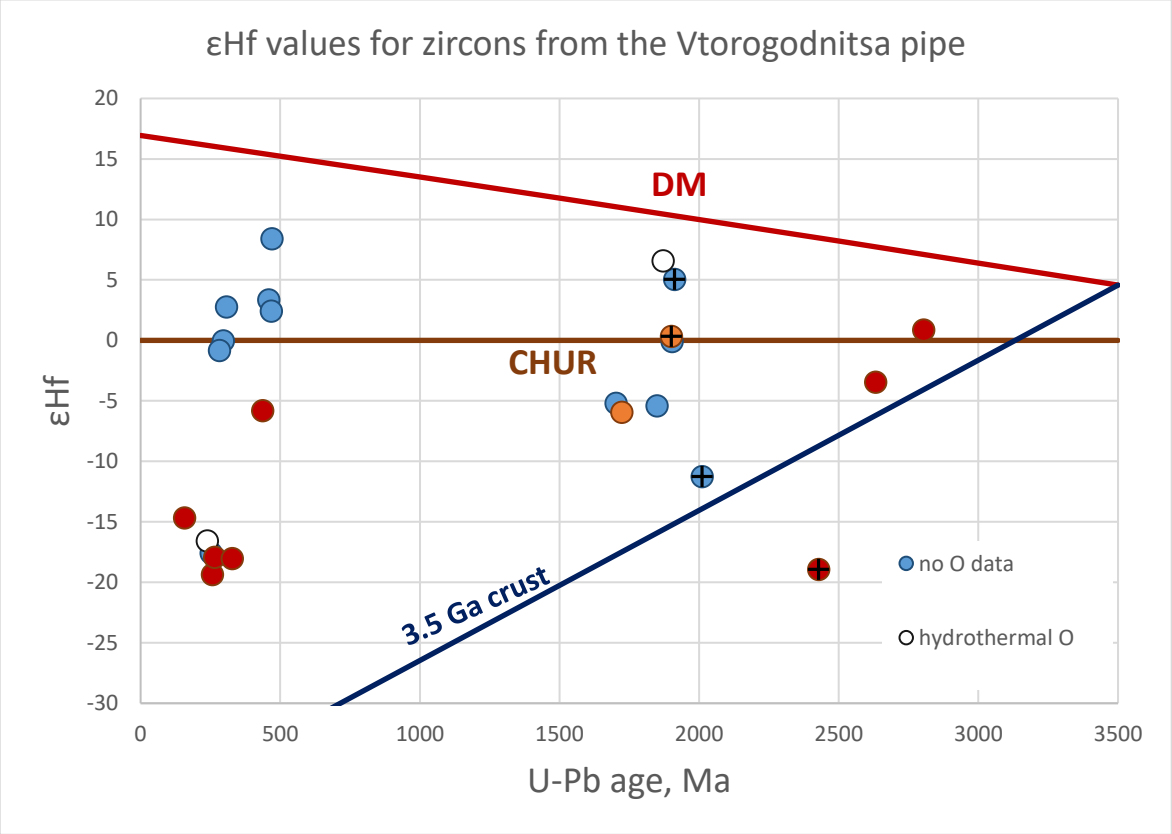



Figure 8.2.27. εHf *vs* age plot for zircons from the Vtorogodnitsa pipe. The data points are color-coded according to the zircon O-isotope composition (where these data are available). Grains with trace-element (TE) composition typical of mantle-derived zircons are also shown with black crosses. The reference line is shown for evolution of the average continental crust.

# Chapter 9. Discussion

## 9.1. Zircons from kimberlites: what are we dating?

Dating kimberlites by the U-Pb zircon technique is a well-known approach. Kimberlitic zircons have distinctive morphologies and trace-element compositions (Belousova *et al.*, 2002, Hanchar & Miller, 1993), making them easy to recognize. However, Kamenetsky *et al.* (2014) showed that in some cases such zircons show evidence of chemical abrasion during interaction with the kimberlitic melt. This finding raises questions about whether these zircons actually crystallized from the host kimberlitic melt. However, their distinctive trace-element composition and morphological signatures strongly suggest their mantle origin.

It has been previously proposed that the U–Pb systematics of kimberlitic zircon could be reset at mantle temperatures, thus dating kimberlite emplacement times (Davis *et al.*, 1980, LeCheminant *et al.*, 1997). However, several reports of multiple age populations of mantle-derived zircons in kimberlite pipes have shown that zircon can preserve ages older than those of the entraining magmas (Belousova *et al.*, 2001, Kinny, 1989, Konzett *et al.*, 2000, Konzett *et al.*, 1998, Liati *et al.*, 2004, Liu *et al.*, 2010, Simonetti & Neal, 2010, Zheng *et al.*, 2004). This strongly suggests that zircon can retain radiogenic Pb at mantle conditions for extended timespans (e.g., over 1.3 Ga in the case of Jurassic Timber Creek kimberlite (Belousova *et al.*, 2001) and *ca* 2.5 Ga in the case of the Neogene Hannuoba basalt (Liu *et al.*, 2010)).

In general, U-Pb dating of zircons from kimberlites provides a way to determine not only the age of the kimberlite, but also the age of rocks intruded by kimberlitic pipe, due to the common presence of xenoliths and xenocrysts of those rocks.

The trace-element composition of zircons is a powerful tool for identifying the type of parental melt from which the zircon crystallized. Together with crystal-morphology studies, this is a reliable approach to define the source of zircons and to constrain their possible links with kimberlitic magmatism. Considering other data such as Re-Os dating of sulfide inclusions in diamonds and silicate xenocrysts, the hafnium and oxygen isotopic composition of zircons, and U-Pb dating of rutile and apatite, the structure and evolution of the whole lithosphere under tcertain kimberlite fields can be reconstructed.

Thus, the multi-parameter study of zircons gives information about the age and type of their parental melt (i.e. crustal *vs* mantle). These combined characteristics provide a credible basis for defining zircons of different origins and reconstructing their spatial and temporal relationships.

## 9.2. The Magan terrane: lithospheric structure, age and evolution.

***Zircon U-Pb data***

The summarised probability plot of U-Pb ages of zircons from the Magan terrane (Fig. 9.2.1) shows 3 well-defined age peaks. The patterns of age peaks before 1000 Ma and after are distinctly different.

The pattern of age peaks younger than 1000 Ma (Fig. 9.2.2) is characterised by extremely sharp peaks representing a significant number of zircons in a narrow age interval. This could be explained by the presence of magmatic rocks of these ages.

The youngest peak represents ages from 233 to 241 Ma obtained from zircons of the Kharamai field. These grains were hand-picked from crushed kimberlite based on their "kimberlitic" morphology (large size, light colour, no crystal faces, no inclusions). The age of kimberlite magmatism of the Kharamai field was determined by several techniques. The most reliable data obtained by the U-Pb method (242±23 Ma (Griffin *et al.*, 1999a) and 245±3 Ma (Kinny *et al.*, 1997)) and fission track dating of zircons (226 – 290 Ma; (Komarov & Ilupin, 1990)) show ages that are very similar to those revealed from "kimberlitic" zircons.

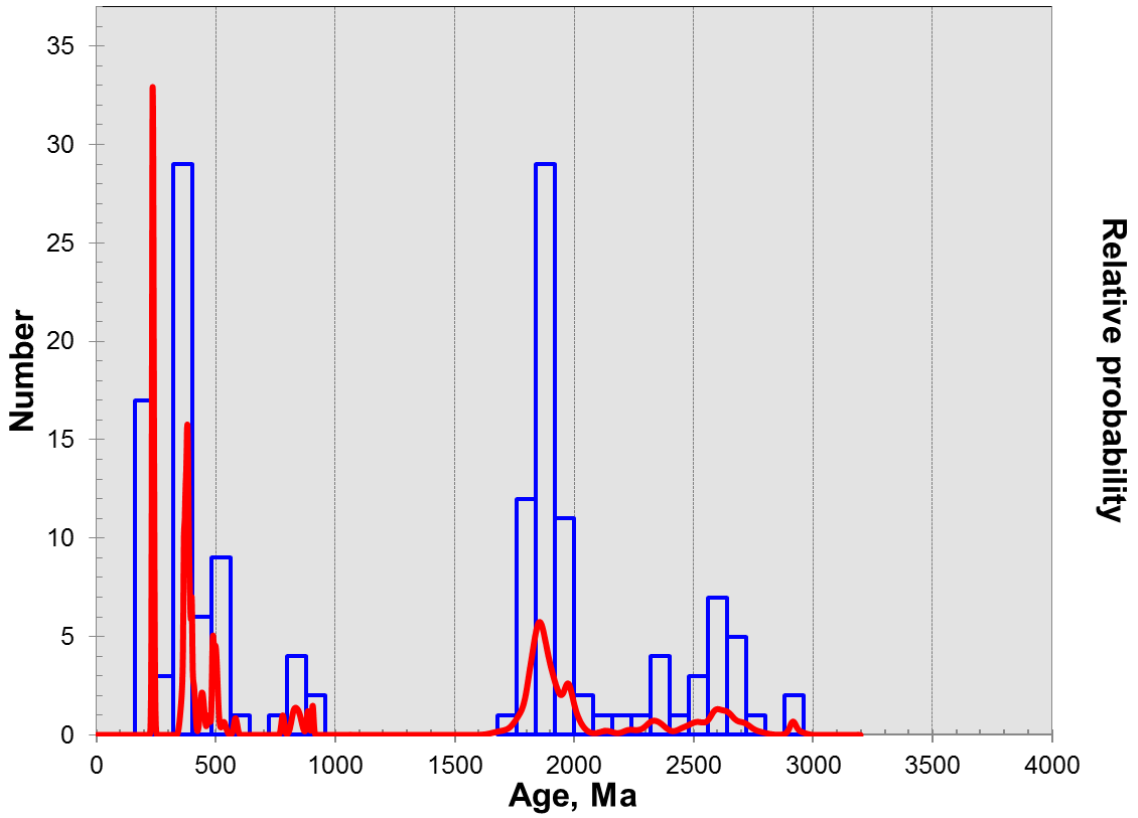



Figure 9.2.1. Probability plot of U-Pb ages of zircons from the Magan terrane.

The second youngest peak consists of zircons with U-Pb ages 353 – 406 (with a secondary peak at *ca* 399 Ma). This includes the ages of zircons from the Amakinskaya pipe with typical "kimberlitic" morphology. According to the review by Zaitsev and Smelov (2010), kimberlite ages obtained for Malo-Botuobinskoe field by Rb-Sr, K-Ar, and U-Pb techniques range in the interval 350-380 Ma, which is again in a good agreement with the data collected during this study.

Kimberlite of the Mir pipe cuts a dolerite sill and dyke of Middle Paleozoic age (possibly Silurian), and xenoliths of this rock are found in the kimberlite. The presence of Late Ordovician – Early Silurian zircons in heavy-mineral concentrates from the Sputnik pipe may indicate the presence of the same rocks within the sequence hosting the Sputnik kimberlite.

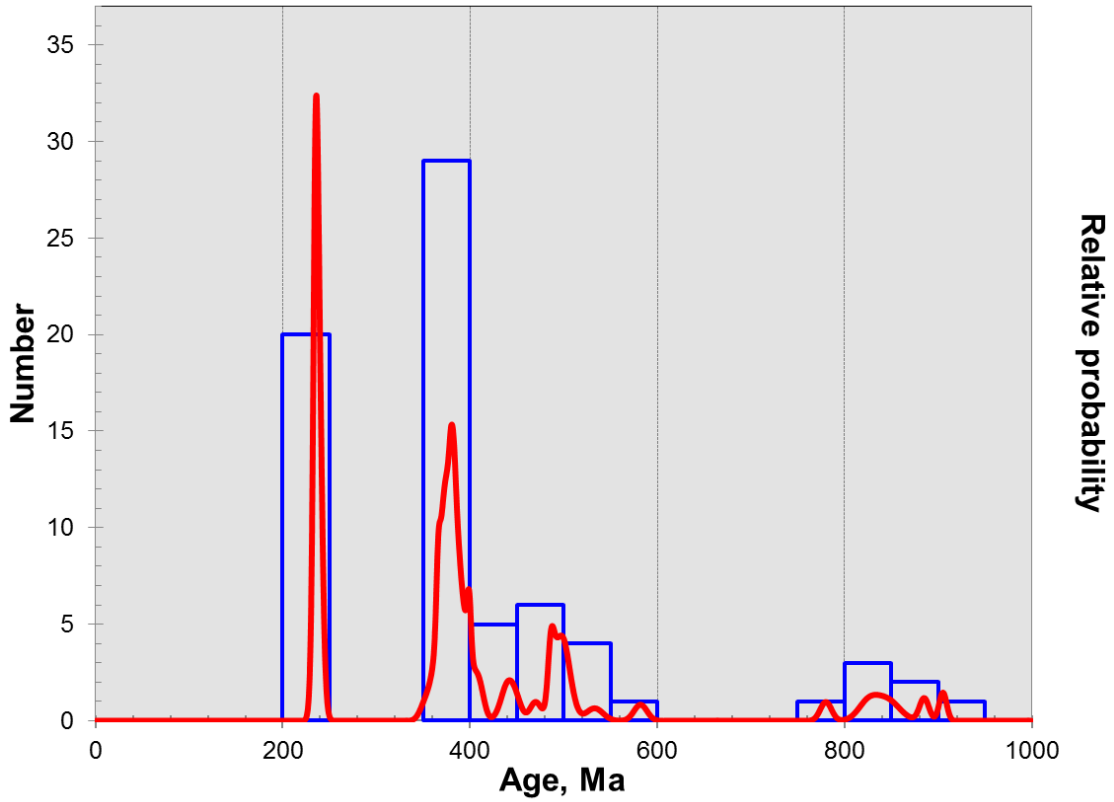



Figure 9.2.2. Probability plot of zircon U-Pb ages (<1000 Ma), Magan terrane.

The zircon ages of 470 – 580 Ma and 780 – 900 Ma could be explained by presence of the magmatic rocks of this age under the sedimentary cover. Another possible explanation is the detrital origin of these zircons in the sedimentary rocks hosting the kimberlite. Kimberlites of the Malo-Botuobinskoe field are intruded into Early Cambrian carbonate and terrigenous-carbonate rocks, so it is unlikely to find detrital Late Cambrian – Early Ordovician zircons in that sediments. Thus, the most likely source of these zircons is buried magmatic rocks.

The interval of ages 780 – 900 Ma is reported for granite complex and mafic dykes on the Yenisey Ridge at the western boundary of the Craton (Romanova *et al.*, 2012, Vernikovskaya *et al.*, 2010, Vernikovsky *et al.*, 2016, Vernikovsky *et al.*, 2007). These rocks might represent the source of detrital zircons in the Early Cambrian sediments, later picked up by kimberlites.

The probability plot of U-Pb ages older than 1500 Ma (Fig. 9.2.3) shows much smoother peaks compared to the peaks observed on the plot for younger zircons. Since the analytical uncertainty for old ages is much higher (2σ ranges from 28 to 150 Ma) than this for young ones (2σ up to 26 Ma) the shape of peaks might be explained in part by normal (Gaussian) distribution.

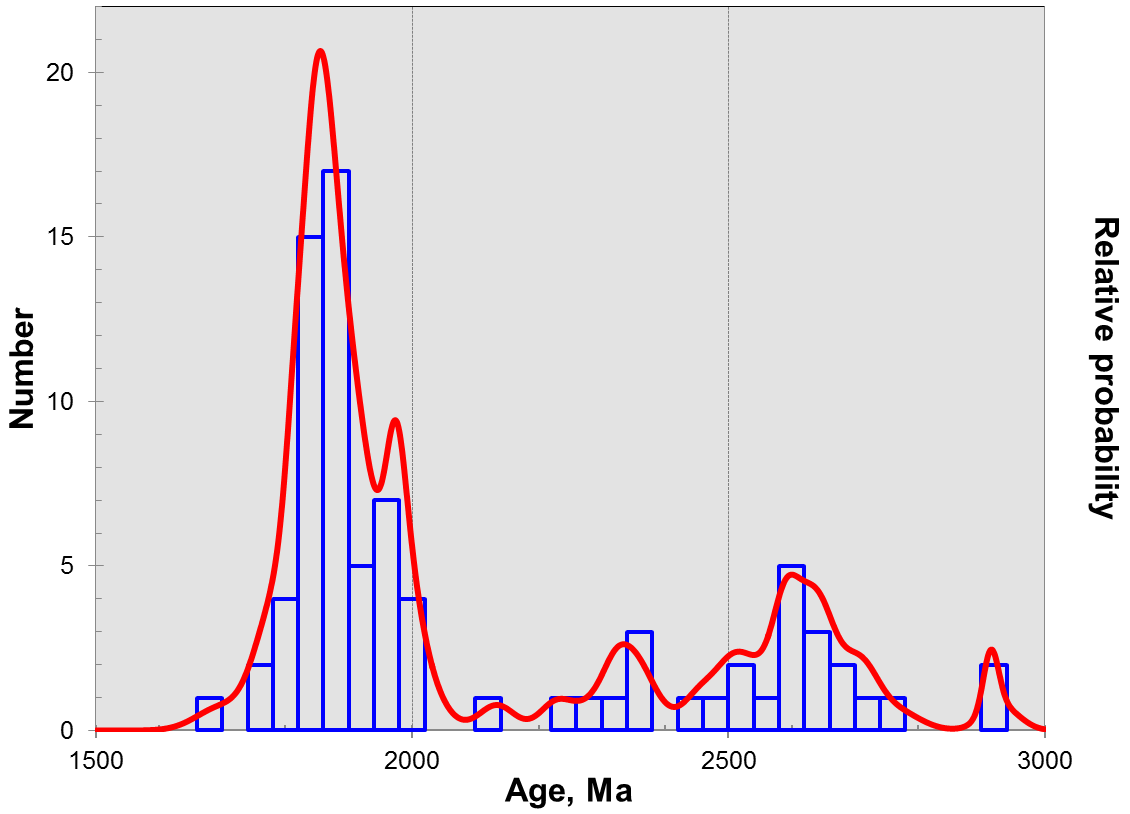



Figure 9.2.3. Probability plot of zircon U-Pb ages (>1500 Ma), Magan terrane.

The main age peak of this interval represents 55 zircons with U-Pb ages from 1695 to 2015 Ma. Most of the grains (n=34) fall into the interval 1820 – 1908 Ma (mean age 1857.5±9.2, MSWD = 0.65, probability 0.94). This age is well-known from metamorphic and magmatic rocks across the Siberian Craton (Table 2.1). Granites and various metamorphic rocks of this age are found within the Sharyzhalgay uplift at the southern boundary of the Magan terrane (Aftalion *et al.*, 1991, Poller *et al.*, 2005, Sal'nikova *et al.*, 2007), while biotite granites and rocks retrograded from granulite to amphibolite grade, found within the Kotuykan shear zone

(eastern boundary of the Magan terrane), give U-Pb ages 1870 – 1840 Ma (Rosen *et al.*, 1994, Stepanov, 1974).

A secondary peak is observed at *ca* 1960 Ma (13 zircons within the range 1915 – 2015 Ma). Anorthosites and syntectonic migmatites of the same age are known within the Kotuykan shear zone (Stepanov, 1974, Sukhanov & Rachkov, 1988). Also, granites and charnokites within the Sharyzhalgay uplift reveal ages 1950 – 1965 Ma (Aftalion *et al.*, 1991).

In general, this age is suggested to represent the time of collision between the Tunguss, Magan and Daldyn terranes. Moreover, the most widespread Early Proterozoic orogenic events in the Siberian craton occurred between 2.0 and 1.8 Ga (Aftalion *et al.*, 1991, Griffin *et al.*, 1999a, Kinny *et al.*, 1997, Rosen *et al.*, 1994).

The ages in the range 2100 – 2400 Ma are rarely mentioned in previous studies on the Magan terrane. Sukhanov *et al.* (1990) reported a Sm-Nd age of 2180 ± 20 Ma for monzodiorite from the Kotuykan shear zone. A Sm-Nd model age ($T_{DM}$) of 2.3-2.4 was calculated for granites of the Sharyzhalgay uplift by Aftalion *et al.* (1991). At the same time, no magmatic or metamorphic rocks of this age are known within the craton margins, so a detrital origin of these zircons is unlikely.

The wide interval of ages from 2450 to 2760 has been described previously for the terrane (Aftalion *et al.*, 1991, Bibikova *et al.*, 1989b, Dobretsov, 1986, Griffin *et al.*, 1999a, Rosen *et al.*, 2000, Sklyarov *et al.*, 1998, Smelov & Timofeev, 2007). The mafic and felsic granulites of the Sharyzhalgay uplift contain magmatic zircons of 2.7-2.6 Ga age; metamorphic zircons with ages of 2.57-2.40 Ga are found in the gneissic granitoids and high-grade rocks (Turkina *et al.*, 2012). Zircon with a U-Pb age of 2.7 Ga is also reported in monzodiorite of the Kotuykan shear zone (Sukhanov & Rachkov, 1988). Generally, the period 2.8-2.6 Ga is considered as the first major period of deformation and granulite-facies metamorphism of the primary Archean crust of the terrane (Aftalion *et al.*, 1991, Bibikova *et al.*, 1989b, Rosen *et al.*, 1994, Rosen *et al.*, 2000, Turkina *et al.*, 2012).

Two zircons gave ages of 2915±24 and 2930±58 Ma. A clinopyroxene amphibolite xenolith from the Mir pipe has yielded a Sm-Nd $T_{DM}$ model age of about 3000 Ma (Neymark *et al.*, 1993). This provides a minimum age for at least some of basement rocks in the region according to Rosen *et al.* (1994). Thus, zircon U-Pb ages confirm the presence of Archean crust under the Magan terrane.

***Zircon trace-element data***

The trace-element composition of zircons from the Magan terrane was analysed only in grains collected from heavy-mineral concentrates. In general for the terrane, ranges of concentrations of trace elements are similar for all pipes, as well as the distribution of predicted rock types according to the CART classification.

All zircon grains are enriched in trace elements relative to chondrite, except P, Ti, La and sometimes Pr. Typical zircon REE patterns with relative depletion in LREE and enrichment in HREE are seen in all grains.

A well-defined negative Eu anomaly is typical for almost all analysed grains. The presence of the Eu-minimum indicates that zircons were crystallized from melts in which $Eu^{2+}$ has fractionated into plagioclase. Thus, the Eu-minimum is an evidence of more fractionated and evolved parental melts (Belousova *et al.*, 2002).

A positive Ce-anomaly is observed in most of the studied zircons. Previous studies have suggest that the Ce-maximum is related to higher oxidation state of parental melt (Schreiber *et al.*, 1980). In general, oxidation of $Ce^{3+}$ to $Ce^{4+}$ requires oxidizing conditions at the Earth surface. As a result, zircons from primary mantle-derived rocks tend to lack Ce anomalies (Luo *et al.*, 2004). However, it was shown previously that zircons from all types have positive Ce anomalies, but kimberlitic and carbonatitic zircons show the least pronounced ones (Belousova *et al.*, 2002).

There is no clear correlation between trace-element composition and U-Pb age in these zircons. On the contrary, zircons with young “kimberlitic” ages show trace-element signatures similar to those of zircons crystallized from granitic or intermediate parental melt, while most of grains with mantle-type compositions have ages much older than the age of the host kimberlites (Appendix 2). The plot of Lu versus U-Pb age (Fig. 9.2.4) shows the classification of zircons reflecting their “mantle-derived” and “crustal” origin based on their Lu-content (Belousova *et al.*, 2002), where the “mantle-derived” group incorporates zircons with trace-element composition typical of grains derived from kimberlites and carbonatites.

The lack of zircons with both “mantle-derived” trace-element compositions, and ages corresponding to kimberlite eruption times suggests either re-setting of the U-Pb system during the interaction of these grains with kimberlitic melt, or the generation of zircons during other processes accompanying the kimberlite eruption. This also may be related to the specifics of the sampling procedure. Zircons were collected from heavy-mineral concentrate from the streams draining kimberlitic pipes. “Mantle-derived” zircons are generally large (up to 10 mm),

and bigger grains are easier to wash out and lose during the panning. This may result in the lack of large “mantle-derived” zircons in heavy-mineral concentrates.

The only common feature of zircons from all analysed kimberlite pipes is that most zircons with ages 1.8-2.0 Ga have trace-element compositions typical of zircons that crystallized from intermediate (<65% $SiO_2$) melts. The presence of a few grains with typical “carbonatitic” (Fig. 9.2.4) trace-element features seems to mark a mantle input in the event of this age.

All grains older than 2000 Ma show trace-element compositions typical for zircons from intermediate or felsic rocks. Moreover, they all have well-defined (or strong) positive Ce anomalies suggesting derivation from high-fractionated crustal rocks. These features indicate that oldest zircons found within the terrane support the existence of continental crust at this early stage of evolution of the Megan terrane.

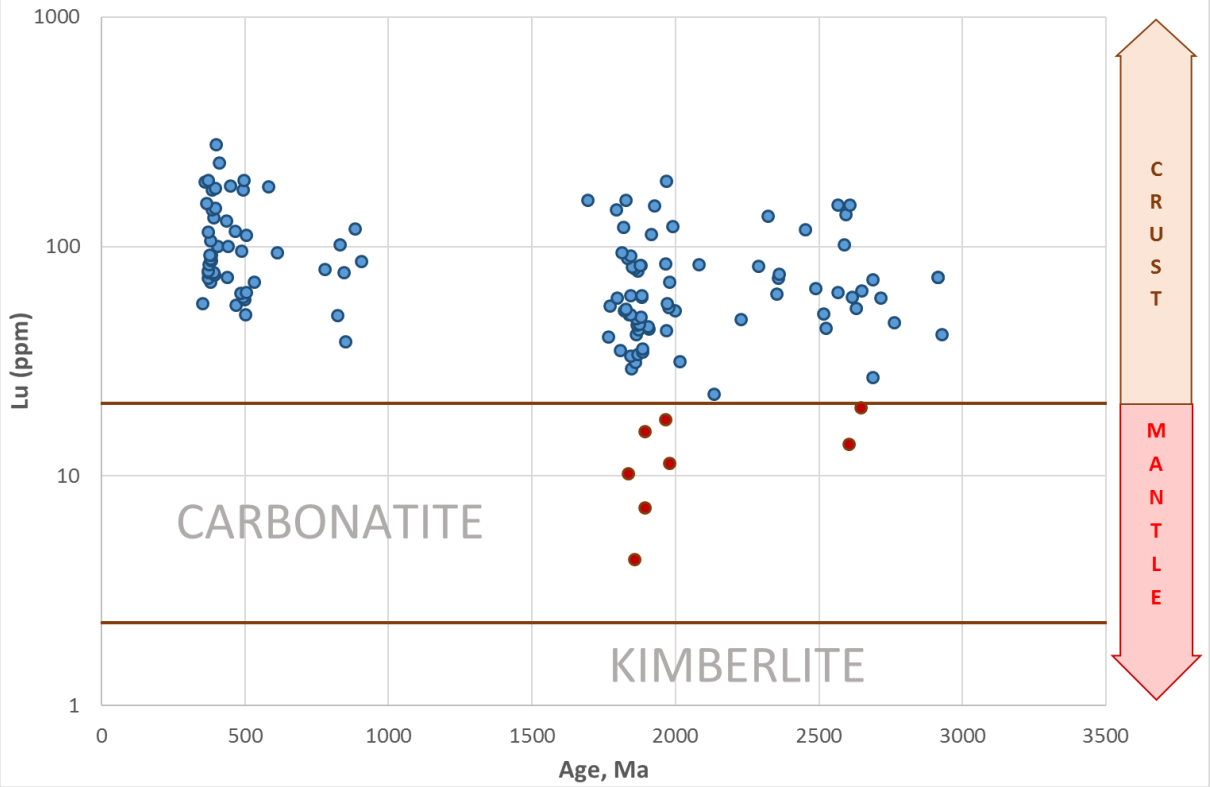



Figure 9.2.4. Lu vs U-Pb age plot for zircons from the Magan terrane.

***Oxygen-isotope data***

The isotopic composition of oxygen in zircons from the Sputnik pipe is shown in Fig. 4.1.21. The plot demonstrates the presence of zircons with mantle values of $\delta^{18}O$ (5.0±0.5‰)

in all three major age populations. When combined with the hafnium-isotope data (Fig. 9.2.5), these again support the mantle input during major magmatic/metamorphic events that reworked the ancient crust. Mantle $\delta^{18}O$ values in young zircons (384-396 Ma) with low εHf (-17 to –23) clearly show that the protolith for those zircons did not interact with (meta-)sedimentary rocks, since its separation from the depleted mantle at *ca* 2.6 Ga ($T_{DM}^{C}$ model age).

The combination of supracrustal $\delta^{18}O$ (>6.6‰) and relatively juvenile εHf values in some zircons may indicate that the upper mantle was variably re-enriched in $^{18}O$ with a minor contribution of recycled sediment, or by metasomatism induced by sediment-derived fluids or melts (Hiess *et al.*, 2009).

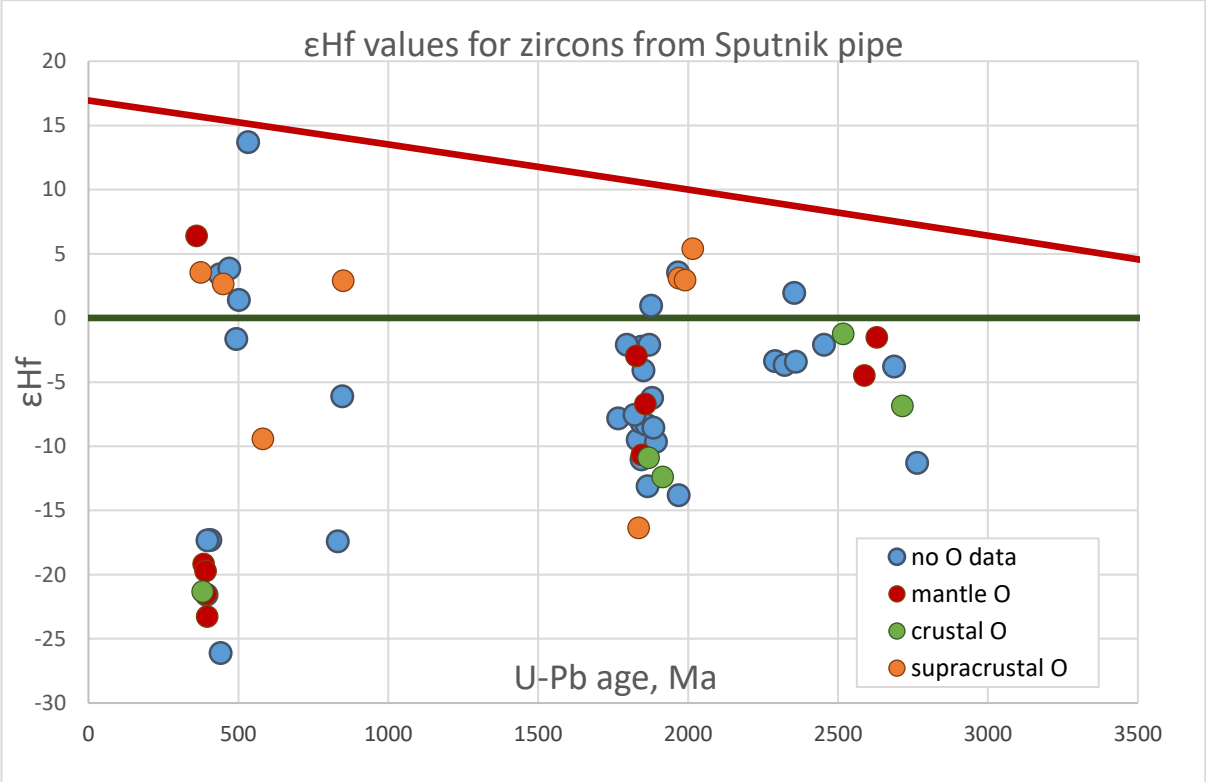



Figure 9.2.5. εHf vs U-Pb age plot for zircons classified by their oxygen-isotopic composition, Sputnik pipe, Magan terrane.

***Hafnium-isotopic composition***

The Lu-Hf isotopic systematics were analysed only in zircons from the Sputnik pipe. The range of the Hf-isotope composition reflects a wide variety of zircon origins.

The epsilon-Hf plot (Fig. 4.1.22) with a large proportion of zircons with negative (and thus evolved) εHf signature clearly shows several episodes in which the ancient crust was reworked to generate new melts. At the same time, the presence of positive εHf values indicates an input of mantle material during those events (Griffin *et al.*, 2000). This input is more

significant for grains of younger populations, but the age of those zircons is still slightly older than the age of kimberlite. This difference suggests some pre-kimberlite process in the mantle which involved the reworking of the lower crust and crystallization of zircon with strong juvenile signatures (εHf up to +13). According to their trace-element and oxygen isotopic composition (where the data are available) those zircons are not mantle-derived, which also supports the hypothesis of lower-crust reworking.

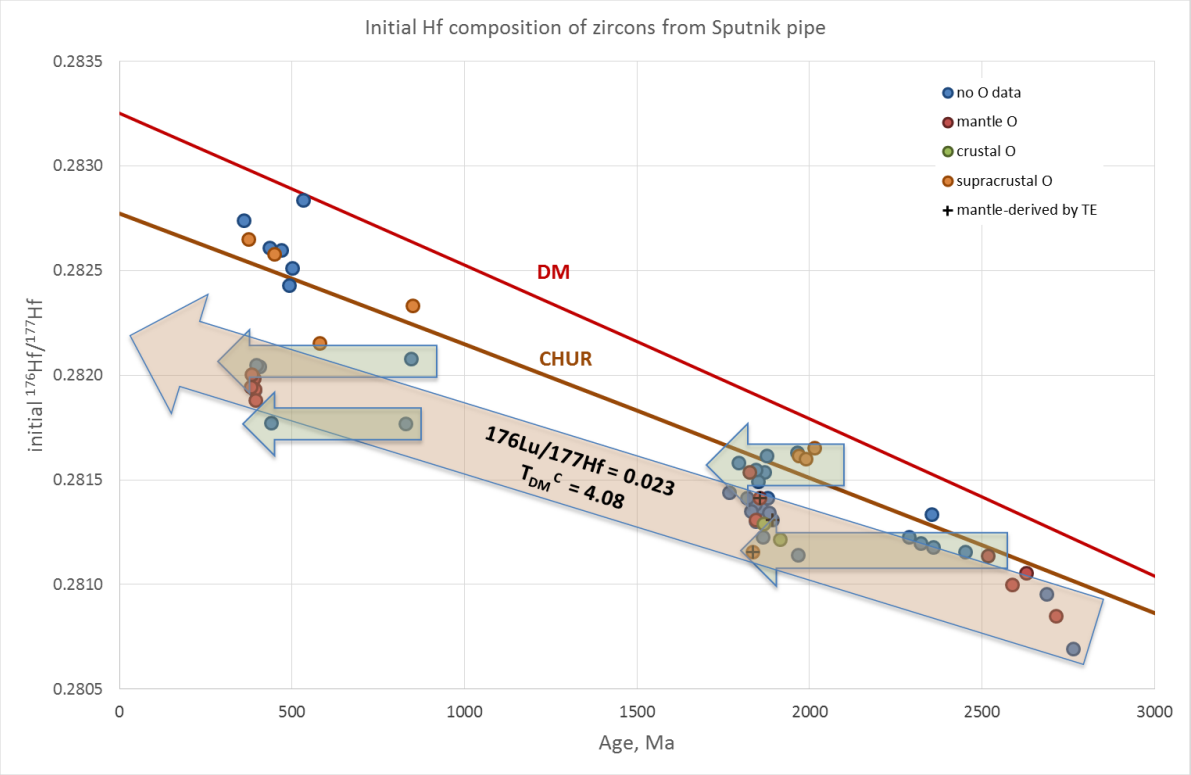



Figure 9.2.6. Initial $^{176}Hf/^{177}Hf$ *vs* U-Pb age plot for zircons from the Sputnik pipe, Magan terrane.

The initial-hafnium plot (Fig. 9.2.6) helps to understand the implication of the Lu-Hf systematics. Zircons are placed on the plot based on their U-Pb age (horizontal axis) and calculated initial $^{176}Hf/^{177}Hf$ ratio (vertical axis). Two distinct types of trends are observed in the plot: horizontal and sloping trends. Horizontal trends incorporate zircons of different age with the same values of the initial $^{176}Hf/^{177}Hf$ ratio. Thus, horizontal trends show the result of possible Pb-loss processes causing rejuvenation of the U-Pb age. In contrast, sloping trends indicate the evolution of the $^{176}Hf/^{177}Hf$ ratio of the primary protolith. The slope of such trends depends on the initial Lu-Hf ratio of the reservoir. For example, the DM and CHUR reference lines show evolution of the initial $^{176}Hf/^{177}Hf$ ratio of the depleted mantle ($^{176}Lu/^{177}Hf = 0.0384$)

and chondrite ($^{176}Lu/^{177}Hf$ = 0.0332) reservoirs correspondingly (Blichert-Toft & Albarède, 1997, Griffin *et al.*, 2004).

Zircons lying along those sloping trends can be interpreted as crystallizing at different times, but from melts derived from the same protolith (or protoliths with the same initial Lu-Hf ratio). The intercept of such trends with DM line gives the minimum age of the primary protolith, known as $T_{DM}^{C}$ crustal model age (Griffin *et al.*, 2004).

Thus, for zircons from the Sputnik pipe, four Pb-loss trends may be observed. Two of them are related to the major reworking event at 1.8-1.9 Ga, and two others are related to the time of the major kimberlite eruption event at 380-400 Ma.

At the same time, the sloping trend includes zircons of all major age-populations. The slope of this trend corresponds to initial Lu-Hf ratio of 0.023, which is close to estimated lower crustal (0.022 (Amelin *et al.*, 1999)) values. This trend represents a crustal evolution line that crosses the DM reference line at about 4.08 Ga, indicating the protolith could be as old as Hadean.

In summary, the zircon data obtained for the Magan terrane indicate that the earliest reworking of the pre-existing crust started at *ca* 2.9 Ga. The protolith of this crust was probably separated from the depleted mantle as early as 4.08 billion years ago ($T_{DM}^{C}$ model age, maximum estimate) and was reworked again at 1.8-2.0 Ga and later just before and during the kimberlite eruption event at 350-380 Ma. The integrated information on zircon trace-element, hafnium-isotope and oxygen-isotope compositions implies a contribution of juvenile material in all three events recognized in the evolution history of this terrane. Hafnium and oxygen isotopic data also suggest two reservoirs, compositionally distinct, that existed in the lithosphere (lithospheric mantle?) close to the time of major kimberlite eruption at 350-380 Ma. Thus, some zircons crystallized from melts which were not contaminated by sedimentary rocks (mantle $\delta^{18}O$ values *vs* low εHf), while others crystallized from melts that had interacted with sediments (as evidenced by supracrustal $\delta^{18}O$ *and* positive εHf values).

## 9.3. The Markha terrane: lithosphere structure, age and evolution.

***Zircon U-Pb data***

The summary probability plot (Fig. 9.3.1) shows results for more than 860 U-Pb analyses for zircons from the Markha terrane. Three main age peaks are observed in the plot are 350-400 Ma, 1.8 – 1.9 Ga and 2.6 – 2.8 Ga.

For the grains younger than 1500 Ma (Fig. 9.3.2) the main age population is represented by zircons with U-Pb ages from 350 to 450 Ma (Sablukov *et al.*, 2007). This is close to 350-380 Ma interval, which is well-known as the time of the main kimberlite emplacement events (Brakhfogel, 1984, Kostrovitsky *et al.*, 2007, Zaitsev & Smelov, 2010) for the Siberian Craton. Kimberlites with ages 410-460 Ma are also known within the terrane (Smelov & Zaitsev, 2013).

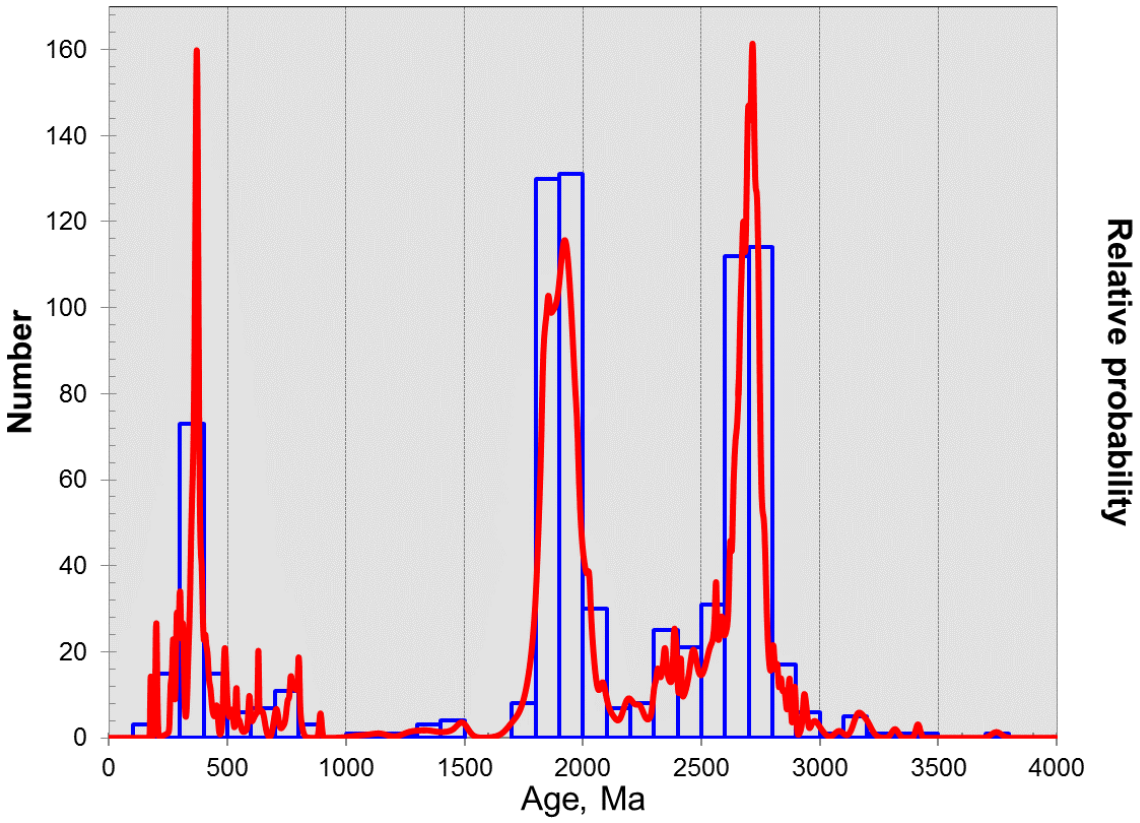



Figure 9.3.1. Probability plot of zircon U-Pb ages from the Markha terrane.

The younger ages define a distinctive peak at *ca* 300 Ma. All ages younger than 350 Ma are found within the Upper Muna (Zimnyaya pipe) and Alakit-Markha (Markha pipe) fields. Kimberlites of both of these fields are intruded into Late-Devonian – Early Carboniferous sedimentary sequences and are not covered by younger sediments; this excludes a detrital origin for zircons of those ages. There is no evidence of igneous rocks younger than the kimberlites within the Upper Muna field, but dolerites of Permian-Triassic age are found in the Alakit-Markha area. As both the Zimnyaya and Markha pipes are located within depressions, the

samples could be contaminated by younger zircons from the streams draining pipes. Thus, 170-350 Ma zircon ages are probably derived from the post-kimberlite intrusions, which might not be exposed at the surface or not recognised previously.

The scattered ages in the interval from 450 to 900 Ma have rarely been reported in previous studies. A dolerite sill within the Nakyn field gave a Rb-Sr age of 650-703 Ma (Sablukov *et al.*, 2007). Ages from 500 to 880 Ma were obtained by Ar-Ar, K-Ar and Rb-Sr techniques for whole-rock kimberlites and mineral separates from the Daldyn kimberlite field (Pearson *et al.*, 1997, Zaitsev & Smelov, 2010). Those ages are suggested to be associated with the intraplate magmatism related to the breakup of Laurasia in the Neoproterozoic time (Pisarevsky & Natapov, 2003, Yarmolyuk & Kovalenko, 2001) and accretion of island arcs to the Siberian supercontinent (Metelkin *et al.*, 2012, Pease *et al.*, 2001).

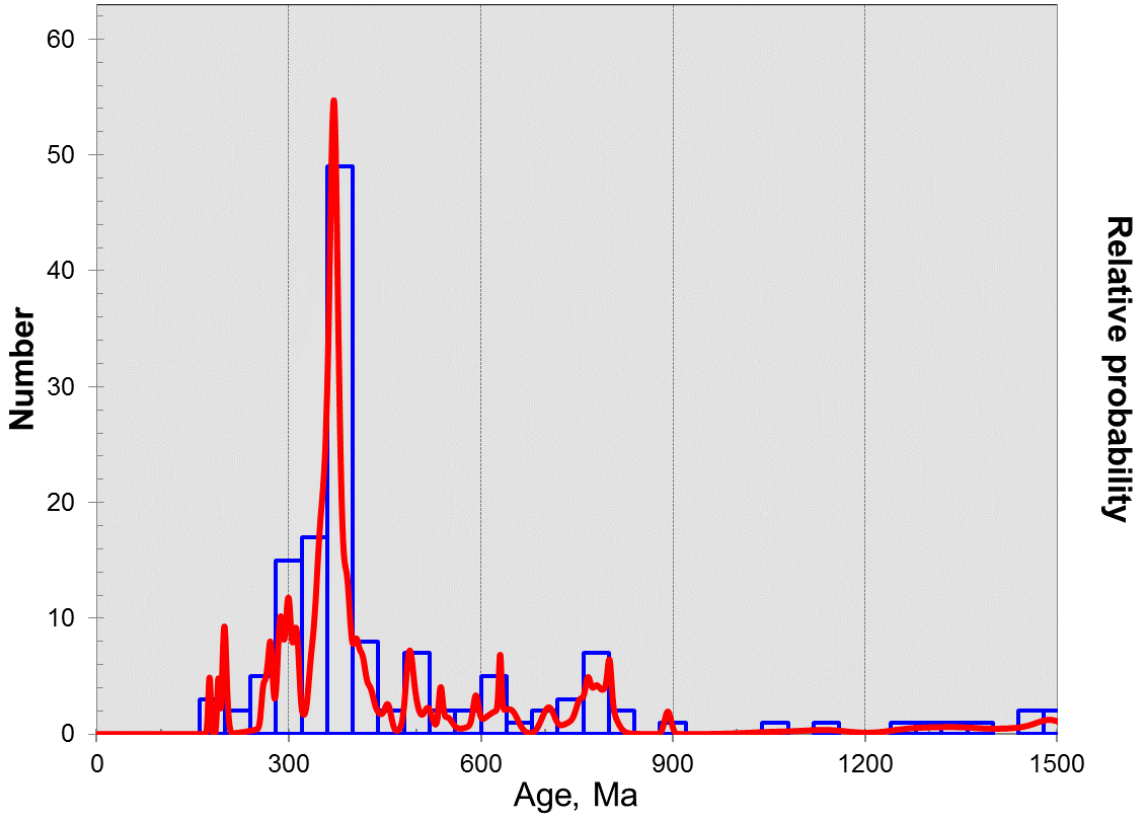



Figure 9.3.2. Probability plot of zircon with U-Pb ages <1500 Ma, Markha terrane.

Zircons older than 1500 Ma form two main populations (Fig. 9.3.3). The first is represented by zircons with Proterozoic ages from 1700 to 2100 Ma. This population has two distinct age peaks: one includes 130 zircons with mean age 1847±3.3 Ma (MSWD = 1.06, probability = 0.32); the second includes 98 grains with a mean age of 953±4.3 (MSWD = 0.92, probability = 0.70). The 1.95 Ga age is widely accepted as the peak of events accompanying

accretion of the Siberian Craton (Rosen, 2003, Rosen *et al.*, 1994, Turkina *et al.*, 2012). Granulite-facies metamorphism and granite emplacement at around 1.85 Ga were reported previously (Donskaya *et al.*, 2005, Gladkochub *et al.*, 2005, Poller *et al.*, 2005).

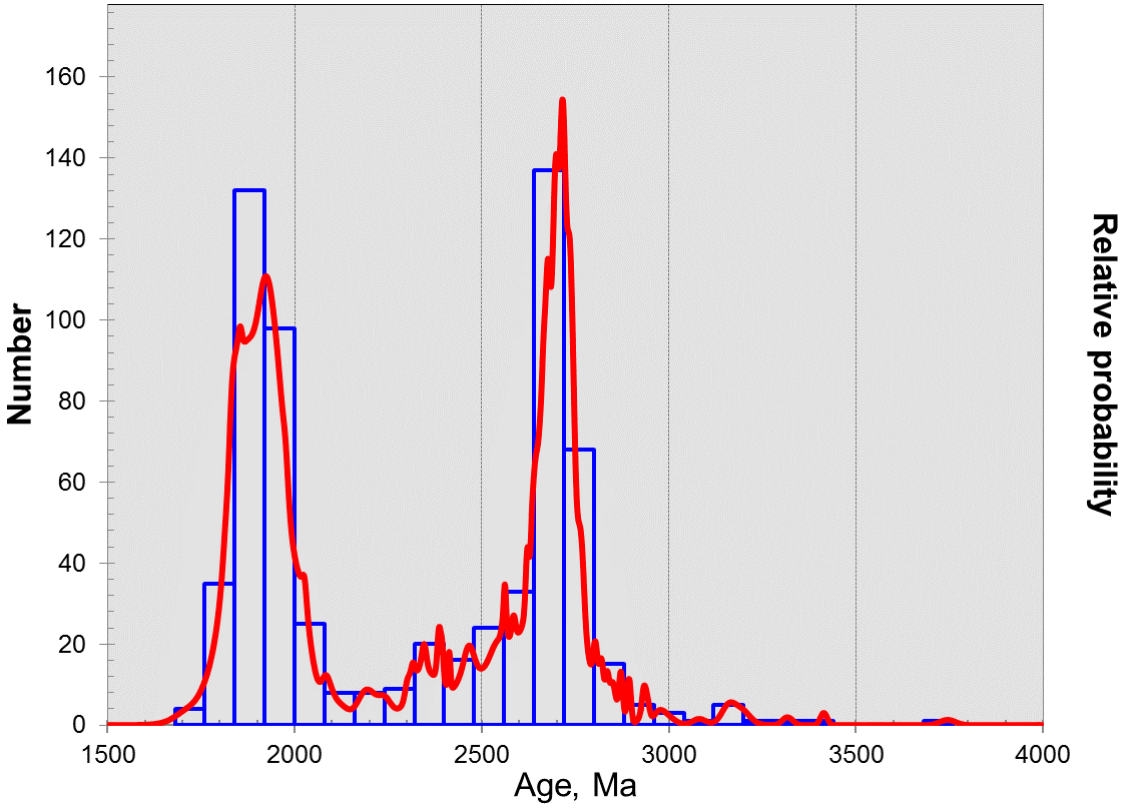



Figure 9.3.3. Probability plot of zircon U-Pb ages (>1500 Ma) from the Markha terrane.

The second peak includes Archean zircons with Pb-Pb ages from 2650 to 2750 Ma. This age interval is commonly suggested as the major period of granitoid magmatism, deformations and metamorphism (Poller *et al.*, 2005, Rosen, 2003, Smelov & Timofeev, 2007, Turkina *et al.*, 2012).

Minor magmatic and/or metamorphic processes continued during the time interval between the two major Archean and Proterozoic age peaks; this is reflected in numerous zircons with ages between 2000 and 2600 Ma. This finding supports the hypothesis that Neoarchean amalgamation of the Siberian craton core started at 2.7 Ga and was completed only by ~ 2.0 to 1.85 Ga (Smelov & Timofeev, 2007, Turkina *et al.*, 2012).

Zircons with U-Pb ages older than 2.8 Ga might represent relics of the primary crust, not affected by reworking at 2.7 or 1.9 Ga. This is consistent with previous studies that reported Nd

model ages ranging from 3.1 to 3.3 Ga for the crustal protolith of the Markha terrane (Poller *et al.*, 2005, Rosen *et al.*, 1994, Smelov & Timofeev, 2007, Turkina *et al.*, 2012).

***Zircon trace-element data***

Trace elements were analysed in zircons collected from heavy-mineral concentrates, crushed kimberlites and xenoliths.

Compared to the data obtained for the Magan terrane, the zircons from the Markha terrane show much more variation in their trace-element composition.

Zircons of different ages have distinct trace-element signatures. Most zircons with the age of kimberlite emplacement (350-380 Ma) have trace-element compositions typical of kimberlitic zircons. They show relatively low concentrations of REE, lack of negative Eu anomalies and much flatter (less fractionated) REE patterns. However, some zircons of this age interval (350-380 Ma) show different compositions of trace elements. Within the samples from the Alakit-Markha and Upper Muna fields, zircon grains with signatures of intermediate or felsic parental melt were also found. Those grains are characterised by much higher concentrations of Th and U; they also show well defined Eu minima and steeper, thus more fractionated REE patterns. On the plot of Lu versus U-Pb age these zircons lie above the "mantle" field (Fig. 9.3.4).

Zircons with both "mantle" and "crustal" trace-element signatures were crystallizing well before the kimberlite emplacement at 350-380 Ma – and present from about 800 Ma. "Crustal" origin is also determined for grains younger than main kimberlitic event, while in between 800 and 1800 Ma only "kimberlitic" type of zircon parental melt is found. Rare zircons with trace-element compositions similar to those of zircons from carbonatitic rocks originated earlier than 1500 million of years ago.

Ancient zircons (>1500 Ma) also have variable trace-element characteristics, but "carbonatitic" compositions occur more widely among this age population. "Carbonatitic" zircons are close in composition to "kimberlitic" ones, but they show slightly higher contents of most of trace elements including Lu (up to 2.7 ppm for kimberlitic and up to 20.7 ppm for carbonatitic;(Belousova *et al.*, 2002)). This indicates the similarity in composition of mantle sources for kimberlites and carbonatites, which was also confirmed experimentally (Foley *et al.*, 2009, Pokhilenko *et al.*, 2015, Safonov *et al.*, 2011).

A large set of "crustal" zircons was also found in the age population at 1.7 – 3.0 Ga (Fig. 9.3.4). Their trace-element compositions are characterised by strongly fractionated REE

patterns, well-defined Ce maxima and Eu minima and high concentrations of REE, Y, U and Th (hundreds to thousands of ppm). According to the CART statistical analysis, those zircons are likely to have crystallized from intermediate to felsic parental melts. This is consistent with the suggested amalgamation of the Craton core starting at 2.7 Ga and ending about 1.8 billion years ago.

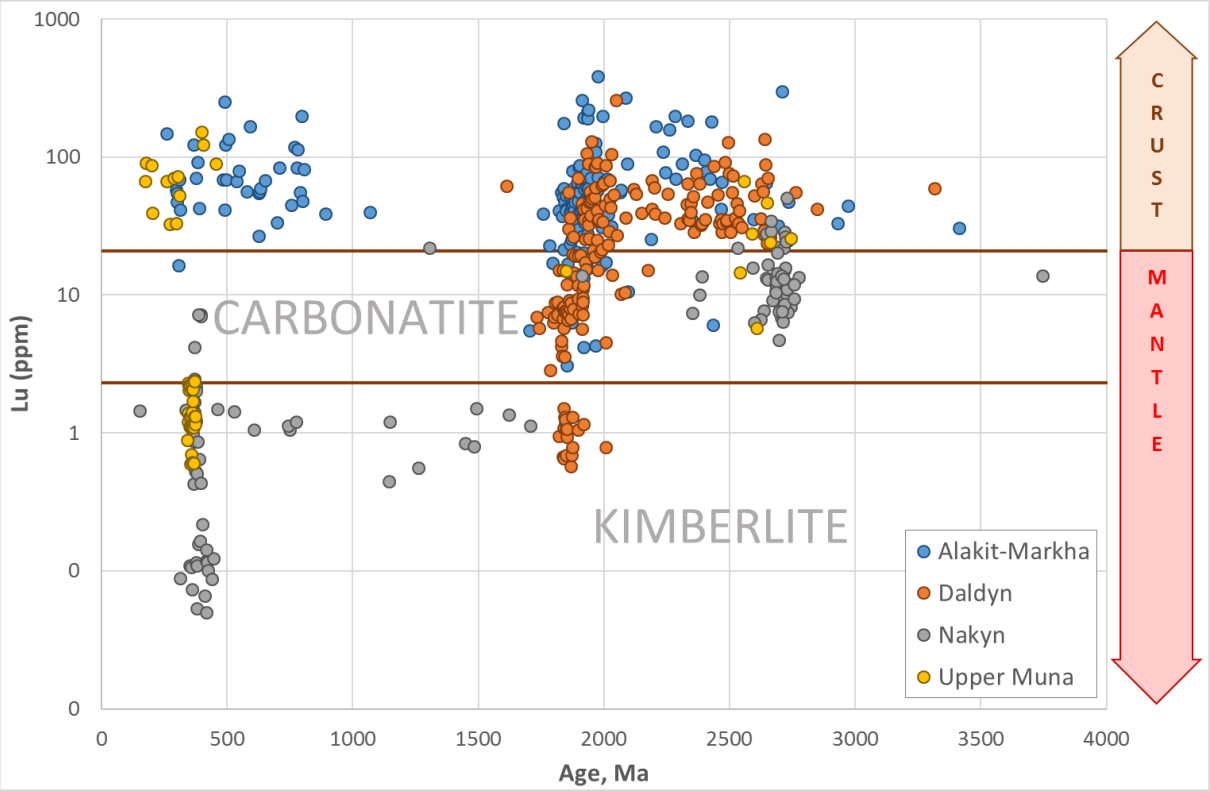



Figure 9.3.4. Lu (ppm) *vs* U-Pb age plot for zircons from different kimberlite fields.

***Oxygen isotopic data***

A summary of the isotopic composition of oxygen in zircons from the Markha terrane is presented in Fig. 9.3.5. The majority of analysed zircons show elevated $\delta^{18}O$, implying the involvement of supracrustal sources. However, a few zircons with mantle values of $\delta^{18}O$ (5.3±0.6‰ (Valley, 2003)) are present in the age populations representing all major tectonic/magmatic events.

The low $\delta^{18}O$ values (<4.5‰) of 3 grains from the Zimnyaya pipe (Upper Muna field) might indicate interaction with hydrothermally altered country rocks (Monani & Valley, 2001). The U-Pb age of those grains (260-270 Ma) is younger than the age of kimberlite and their trace-element signatures suggest a crustal origin of the parental melt, which is in good agreement with their oxygen-isotope composition.

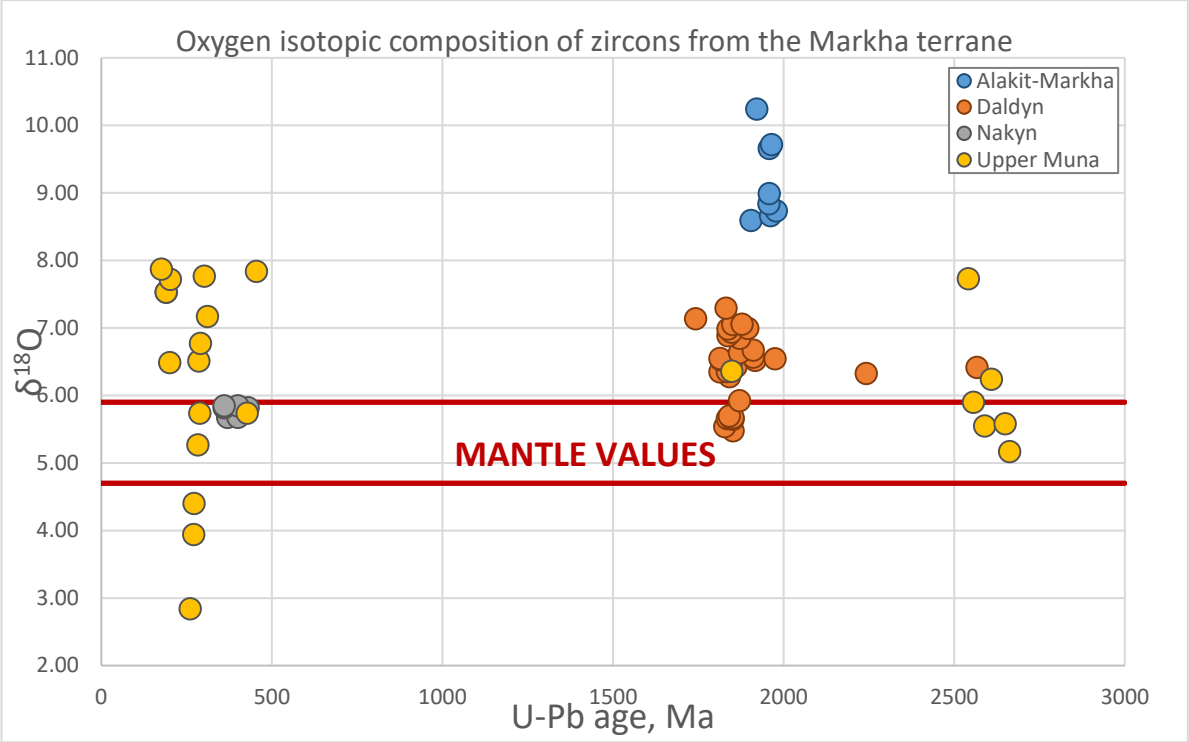



Figure 9.3.5. Oxygen composition of zircons from the Markha terrane.

***Hafnium-isotopic data***

The summary of hafnium-isotopic data is presented in Figures 9.3.6 and 9.3.7.

The plot of εHf *vs* U-Pb age shows vertical arrays, implying that both reworking of the primary crust and juvenile additions are involved. The higher the value of εHf, the more juvenile the Hf-composition. Thus, positive values imply mantle input, while low negative εHf indicate reworking of crustal rocks without necessary addition of any juvenile component. The dotted lines show the evolution in the Hf-isotopic composition of average crust generated 1.5, 2.5 and 3.5 billion years ago.

The hafnium-isotope composition of zircons from the Markha terrane indicates a significant input of juvenile material at the time of kimberlite emplacement. In addition, reworking of the existing crust was happening before and after kimberlite eruption. These data support the results of the trace-element analyses, showing crystallization of "crustal" zircons during that time. The calculated crustal model ages for zircons from melts generated by reworking of the ancient crust fall into the interval 1.8 – 3.5 Ga.

Unique results were obtained on zircons from the Nurbinskaya pipe in the Nakyn field (Fig. 5.4.13). Young zircons (U-Pb age from 360 to 450 Ma) with mosaic structure visible in CL-imaging have extremely low εHf values from -30 to -37, even though their internal and external morphology, and trace-element composition indicates kimberlitic origin. In the initial Hf and εHf plots these zircons lie on the same evolution line with Archean (U-Pb age *ca* 2709 Ma) zircons from the same pipe, which also have "mantle-derived" trace-element signatures. This is interpreted as re-melting of the same well-preserved protolith in Archean and Devonian time, so that zircons crystallized at different times inherited their Hf-isotope composition from the same protolith.

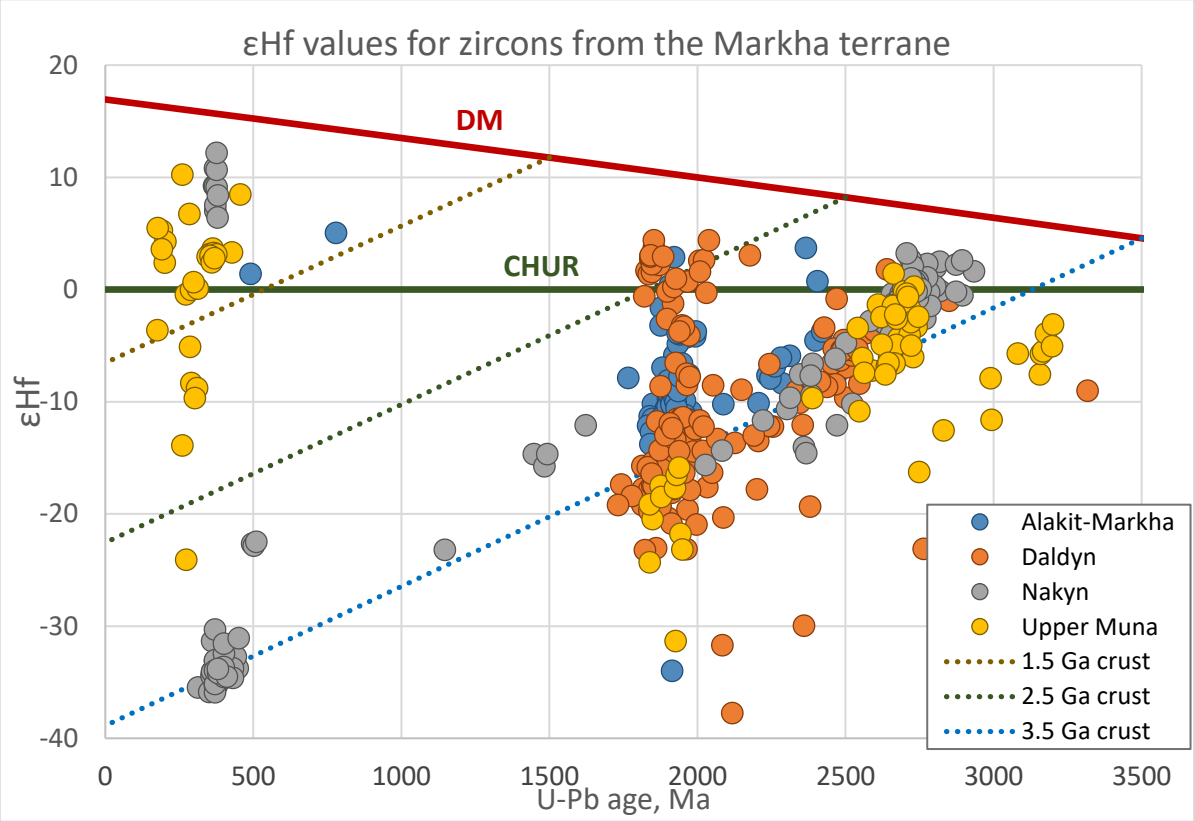



Figure 9.3.6. εHf vs U-Pb age plot for zircons from the Markha terrane.

In general for the terrane, zircons older than 1.6 Ga show that the major event at 1.8 – 2.0 Ga involved reworking of the Archean (2.5-3.5 Ga) crust. The positive εHf values shown by some zircons of that age indicate a contribution of juvenile material. The majority of zircons with U-Pb ages between 2.0 and 2.9 Ga define a continuous trend indicating the major crustal generation at least by 2.7-2.8 Ga, with strong reworking (and Pb-loss) during 1.8 - 1.9 Ga event.

As in the Magan terrane, several horizontal trends indicating Pb-loss processes are observed from the initial Hf plot (Fig. 9.3.7). Two of them were likely to be caused by

Paleoproterozoic deformation and metamorphism, as they do not extend to Mesoproterozoic time. The upper trend might indicate Pb-loss during an event prior to the kimberlite emplacement (450 - 400 Ma - the age of blocks in mosaic zircons from Nurbinskaya pipe).

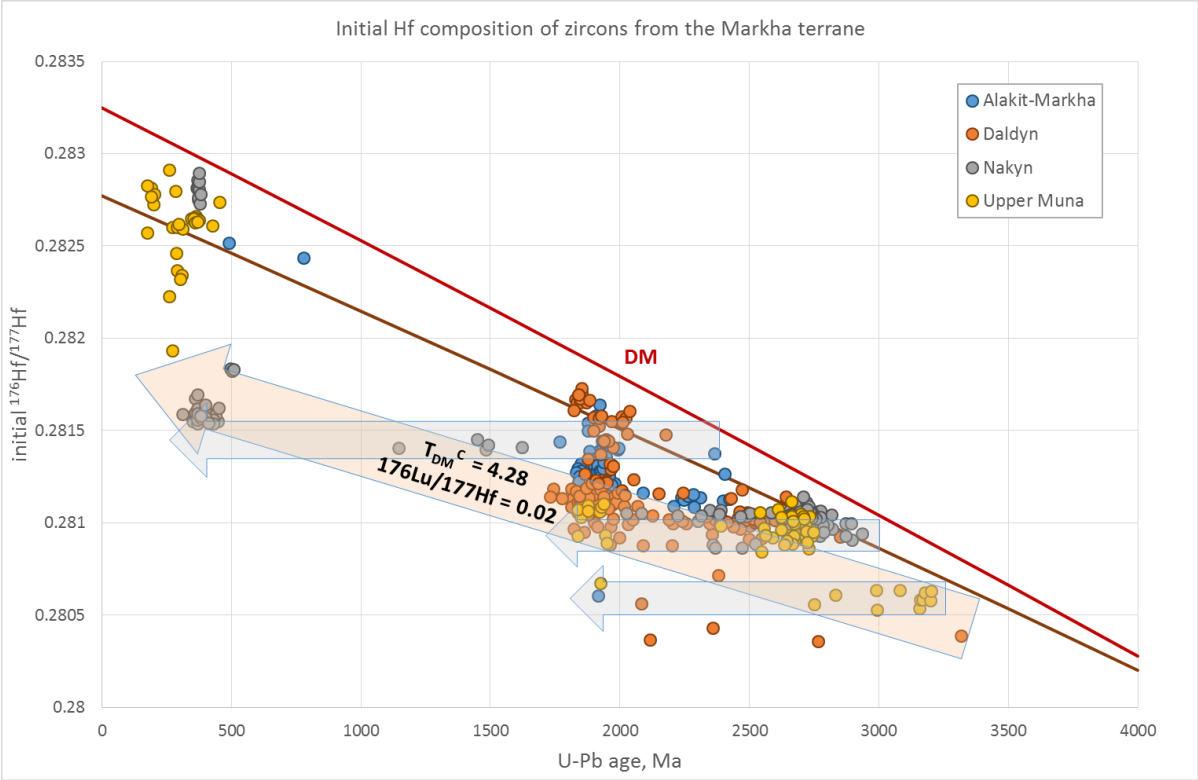



Figure 9.3.7. Initial Hf *vs* U-Pb age plot for zircons from the Markha terrane.

To evaluate the time of crust formation in the terrane, mosaic zircons from the Nakyn field and the oldest grains from the Upper Muna field were included in the model (Fig. 9.3.7). The evolution line connecting these zircons corresponds $^{176}Lu/^{177}Hf = 0.02$, which is close to a lower crustal value (0.022), and intersects the depleted mantle line at 4.28 Ga. This provides with evidence for the first possible generation of the crustal protolith as early as 4.28 Ga.

Comparison of Hf- and O-isotopic data shows a high proportion of reworking of old crust with significant interaction with sedimentary rocks. Supracsrustal (>6.6‰) values of $\delta^{18}O$ are seen even in grains with juvenile Hf-isotope compositions (Fig. 9.3.8). This suggests that the mantle reservoir that produced the parental melts of such zircons was contaminated by rocks with crustal oxygen composition.

On the other hand, the mantle oxygen-isotope signature found in zircons lying in the "crustal" range of εHf suggests reworking of the protolith without addition of sedimentary material. Moreover, Devonian mosaic zircons from the Nurbinskaya pipe show $\delta^{18}O$ values close to the mantle value (average 5.8±0.3‰), kimberlitic trace-element compositions,

extremely low εHf (from -30 to -34) and estimated crustal model ages of 3.3 – 3.5 Ga. Reworking of the mantle-derived Archean protolith in Paleozoic time is consistent with the mantle O-isotope and trace-element compositions of the mosaic grains and also explains the unusually low εHf values found in these zircons.

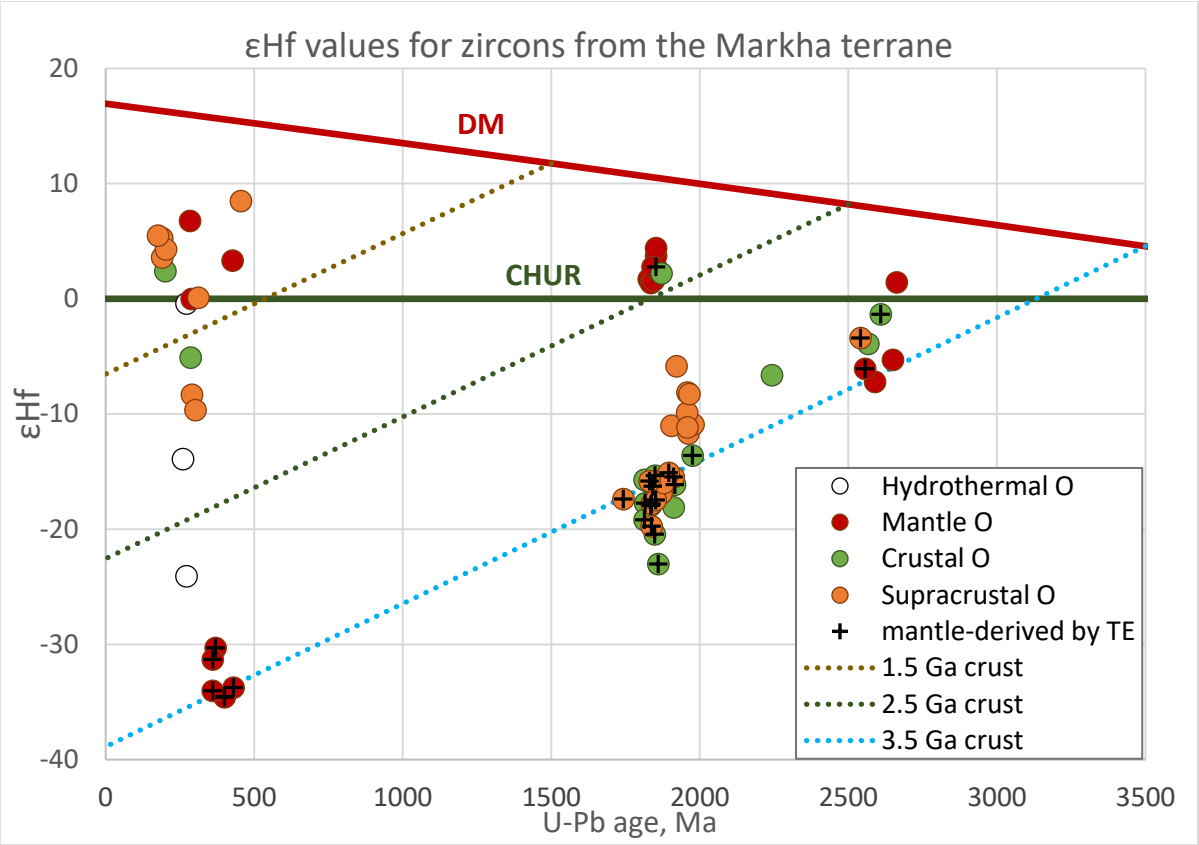



Figure 9.3.8. εHf vs U-Pb age plot for zircons analysed for their oxygen-isotopic composition, Markha terrane.

Thus, the variation of oxygen-isotope composition indicates a high degree of reworking of the preexisting crust during major deformation events. Mantle values of $\delta^{18}O$ support the involvement of juvenile material, while supracrustal and even hydrothermal signatures reflect large-scale processes that affected all levels of the crust.

***Sulfide Re-Os data***

Enclosed sulfides in harzburgite-dunite xenoliths from the Udachnaya pipe (Daldyn field) provide unique data about mantle composition and activity. Two groups of enclosed sulfides were selected for Re-Os and composition of platinum-group element (PGE) analyses. These include "primary" Fe-Ni monosulfide solid solution (MSS) sulfides enclosed in olivine (no

cracks around sulfides have been found); and Fe-Ni MSS sulfides enclosed in olivine but with djerfisherite (K-rich "secondary" sulfide) rims (these sulfides are located in cracks cutting olivine crystals).

All Group 1 sulfides have very low $^{187}Re/^{188}Os$ (<0.09), whereas Group 2 sulfides have a wider range (0.02-1.2). A previous study of sulfide inclusions in megacrystic olivines from the Udachnaya pipe suggested that the Re-Os systematics of enclosed sulfides with $^{187}Re/^{188}Os$ <0.07 are unlikely to have been disturbed by any metasomatic events (Griffin *et al.*, 2002a).

Model ages ($T_{CHUR}$ and $T_{RD}$) calculated for sulfides from Groups 1 and 2 are in good agreement with all available isotopic data. For Group 1 sulfides $T_{CHUR}$ ages fall mainly between 3.2 and 3.9 Ga and $T_{RD}$ (Re-depletion) ages between 3 and 3.51 Ga (±0.03 Ga, mean 2s analytical uncertainty). $T_{RD}$ model ages for Group 2 sulfides fall into two intervals: 2.83-2.98 Ga and 1.87-2.12 Ga.

These ages correlate well with the zircon U-Pb dating results and Hf model ages presented here. The main interval of Hf crustal model ages for zircons from the Udachnaya pipe ranges from 3.2 to 3.8 Ga. The main age population according to U-Pb data shows ages from 1.8 to 2.0 Ga. The correlation between Hf crustal model ages and Re-depletion ages indicates similar time interval for the primary crust formation (Hf $T_{DM}^{C}$) and separation of sulfides from the mantle reservoir (Re-Os $T_{RD}$). At the same time, U-Pb ages of zircons corresponding to $T_{RD}$ ages of the Group 2 sulfides demonstrate simultaneous crustal (zircons) and mantle (sulfides) processes.

These new U-Pb, Re-Os and Hf isotopic data, integrated with a previous study of sulfide inclusions in megacrystic olivines from the Udachnaya pipe (Griffin *et al.*, 1999a, Griffin *et al.*, 2002a, Pearson *et al.*, 1999), suggest that most of the subcontinental lithospheric mantle beneath the Daldyn kimberlite field formed at 3-3.5 Ga, and that lithosphere formation culminated at ca 2.9 Ga (Griffin *et al.*, 2002a). The occurrence of Group 1 and Group 2 sulfides with different model ages within a single xenolith suggests a later metasomatic input at 1.87-2.12 Ga, which may be related to global tectonic events that affected the Siberian craton (See Chapter 6 and Chapter 9.3).

The database for the Markha terrane includes a wide range of results on zircons and sulfide inclusions. According to Lu-Hf and Re-Os model ages, the protolith of the Markha terrane basement separated from the mantle 3.5 to 3.9 billion years ago. The first major reworking events affecting it started at 2.9 and likely were continuously active until the culmination or re-activation at about 1.85 Ga. However, the set of zircons with mantle oxygen signatures and very low εHf values indicates that some parts of the SCLM were not involved

in the major deformation and metamorphism, and survived uncontaminated by crustal material until the major Devonian kimberlite emplacement event.

## 9.4. The Daldyn terrane

### *Zircon U-Pb and trace-element data*

Only a very limited set of samples from the Daldyn terrane (Chomurdakh and Kuranakh fields) was available for this study. Fig. 9.4.1. shows the relative-probability plot of zircon U-Pb ages.

The two main age peaks are obvious from the plot (Fig. 9.4.1). The youngest peak consists of 29 zircons with a weighted mean age of 219.8±1.9 Ma (MSWD = 0.81, probability = 0.75). The second peak is more broader and includes ages from 402 to 451 Ma (24 zircons), however most of the grains show ages from 402 – 424 Ma (n = 14).

The trace-element compositions of all examined zircons are similar to those of zircons crystallized from mantle-derived (mainly "kimberlitic" with only 2 classified as "carbonatitic") melts. Fig. 9.4.2 shows that there are no zircons with "crustal" trace-element signatures identified among the studied samples from the Daldyn terrane.

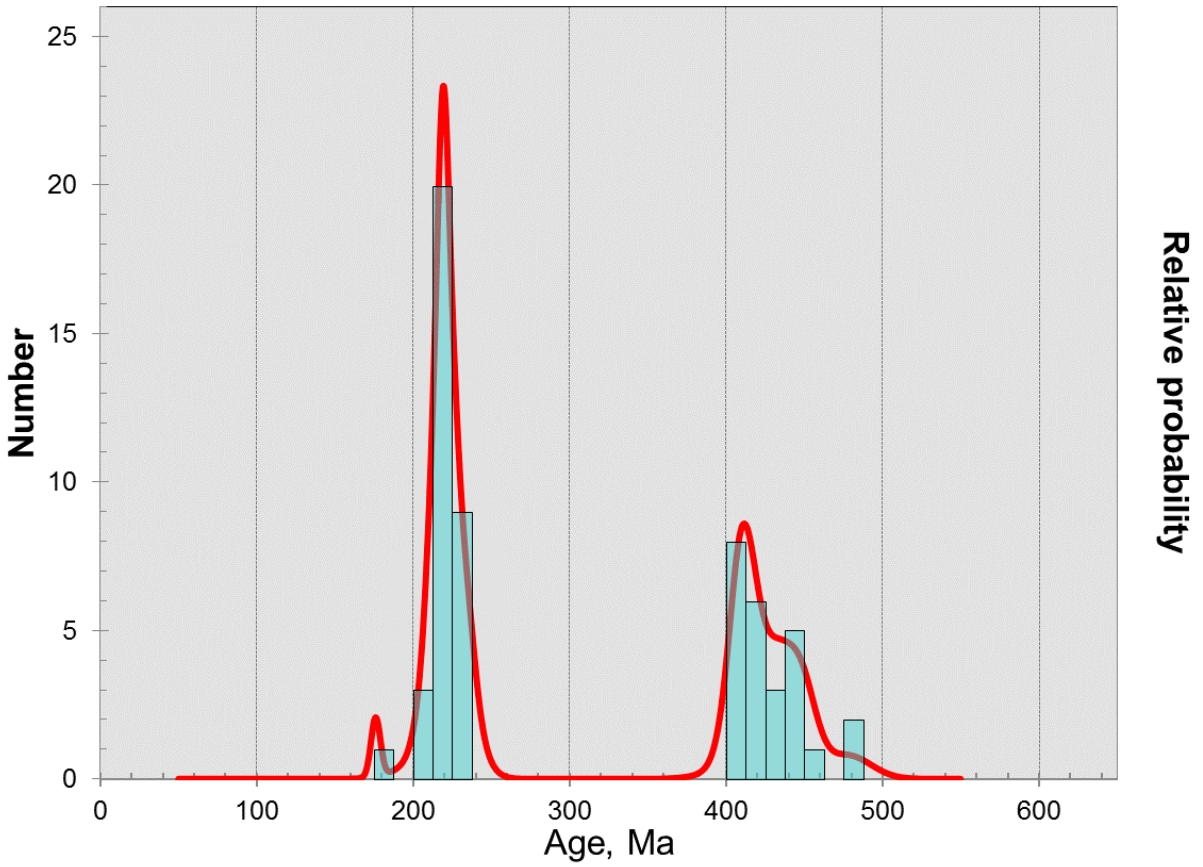



Figure 9.4.1. Probability plot of zircon U-Pb ages, Daldyn terrane.

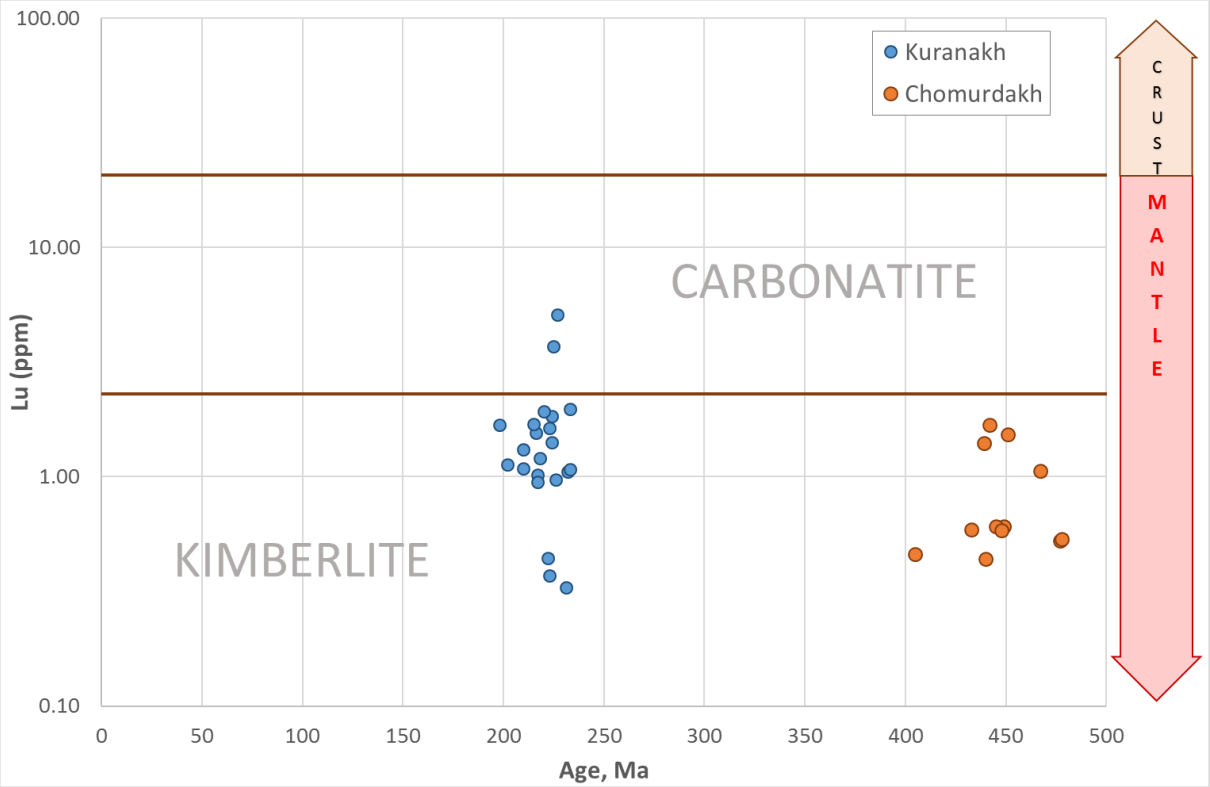



Figure 9.4.2. Lu *vs* U-Pb age of zircons from the Daldyn terrane.

Zaitsev and Smelov (2010) determined 5 epochs of kimberlite magmatism in the Daldyn terrane: 460-420, 400-360, 240-220, 180-160 and 100-80 Ma. These data were obtained mostly by Rb-Sr and K-Ar techniques, which are known to be affected by low-temperature processes. Zircon U-Pb dating is more reliable due to the higher closure temperature and trace-element analyses provide information about the parental rock type of analysed grains. The U-Pb and trace-element data confirm the presence of at least two kimberlitic events: 200-220 and 400-450 Ma. Only a single zircon from the Khairgastakh pipe gave an age different from these two intervals - 176±6 Ma (Table 6.1.1).

The ages determined by the U-Pb technique are similar to those reported by Zaitsev and Smelov (2010), but the Palaeozoic interval obtained in this study (400 – 450 Ma) is scattered between two epochs 460-420 and 400-360 Ma, mentioned by Zaitsev and Smelov (2010). The concordance of the U-Pb analyses suggests that these zircons were not affected by later thermal processes. However, younger kimberlitic events might reset Rb-Sr (closure temperature 650°C) and K-Ar (closure temperature 300-400°C) systematics and thus result in younger ages (400-420 *vs* 360-400 Ma).

## 9.5. The Khapchan terrane

### *Zircon U-Pb and trace-element data*

U-Pb ages of zircons from the Khapchan terrane scatter over a wide time interval from 227 to 2829 Ma (Appendix 5.1, Fig. 9.5.1), but most grains show Phanerozoic ages up to 499 Ma.

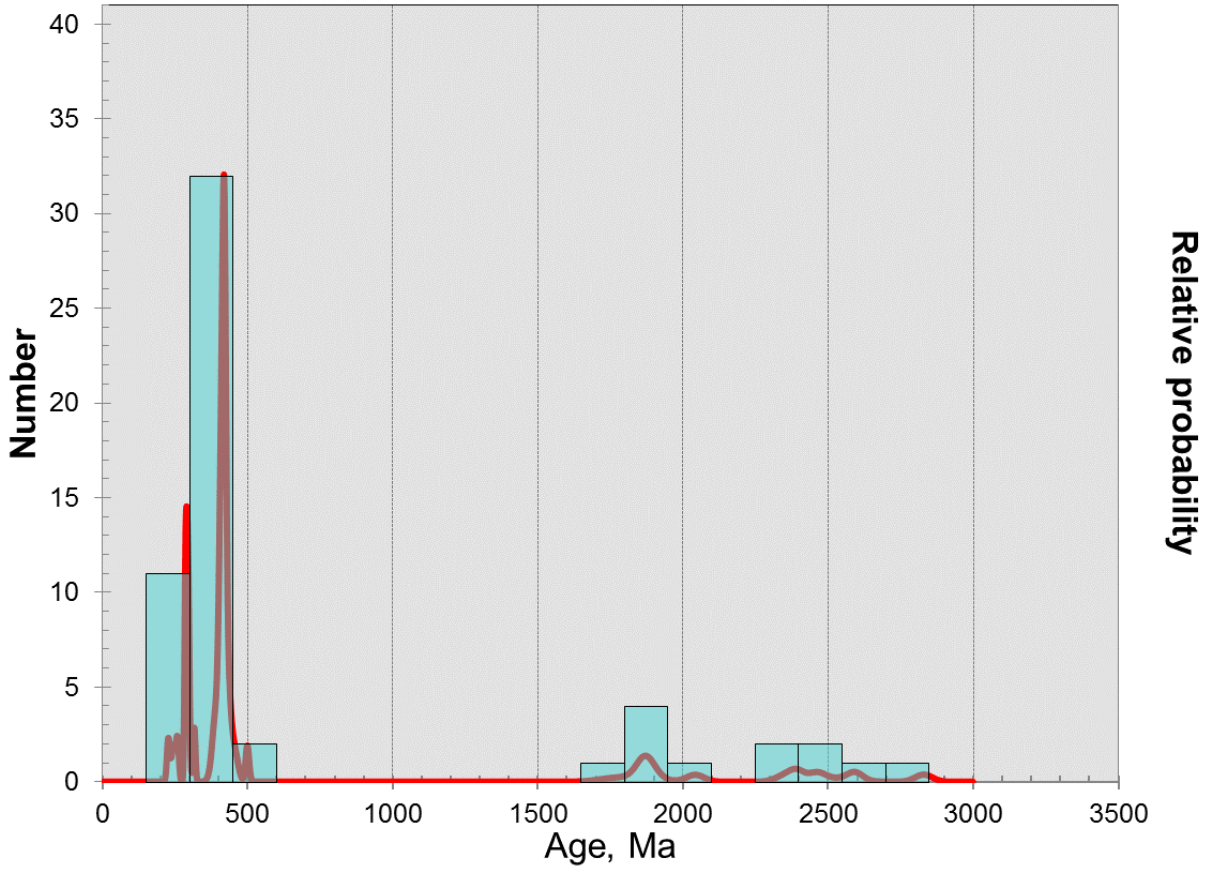



Figure 9.5.1. Probability plot of zircon U-Pb ages, Khapchan terrane.

The probability plot for the young zircons shows two distinct age peaks (Fig. 9.5.2). The first peak represents 8 zircons with a weighted mean age of 290.4±3.8 Ma (MSWD = 1.3, probability = 0.22). The second population consists of 27 grains with a mean age of 416.8±2.6 Ma (MSWD = 0.66, probability = 0.90). All of these grains were collected from heavy-mineral concentrate from the altered kimberlite of the Babie Leto pipe, based on their "kimberlitic" morphology.

Zircons older than 1500 Ma show only one minor age peak at 1875 Ma (5 zircons). Single ages from 2353 to 2829 Ma do not define any age populations.

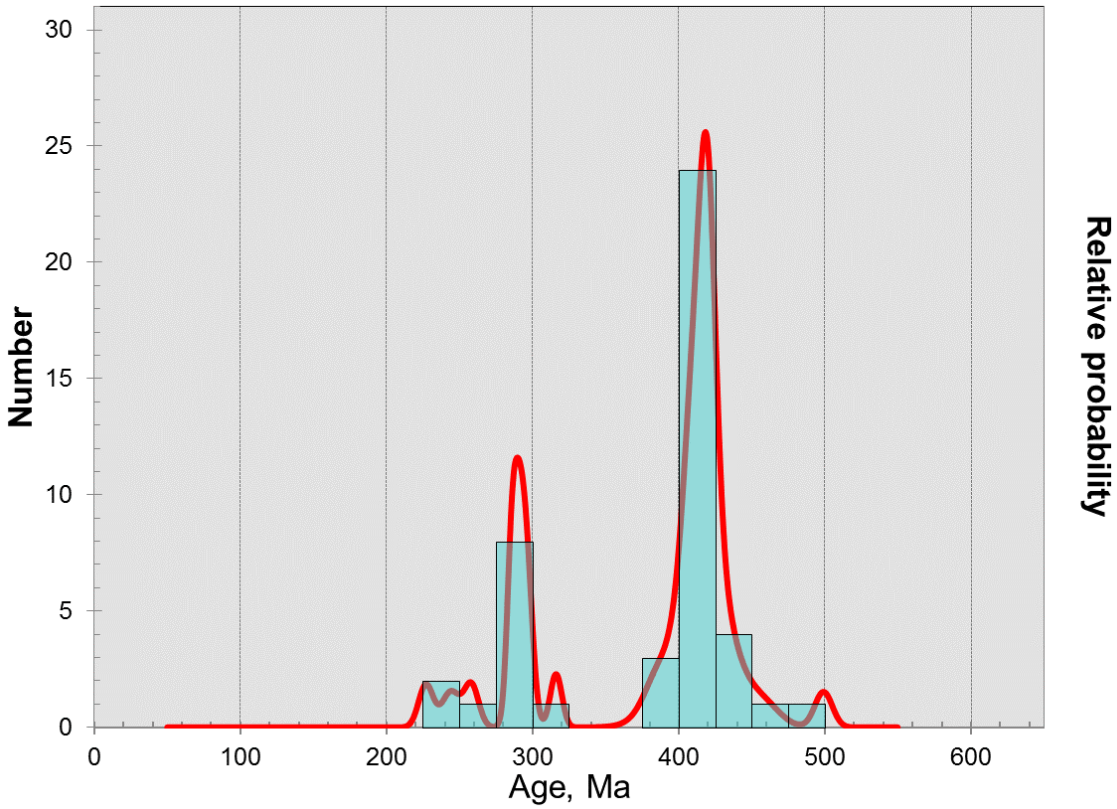



Figure 9.5.2. Probability plot of young zircon U-Pb ages, Khapchan terrane.

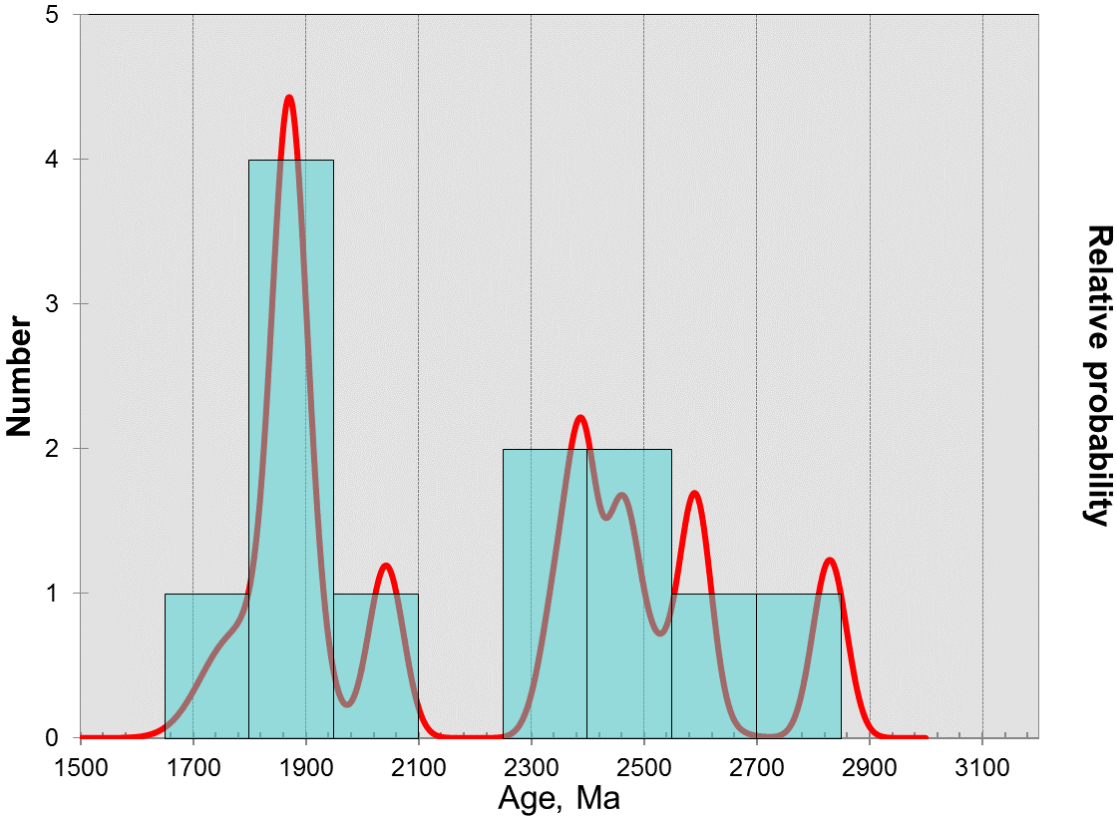



Figure 9.5.3. Probability plot of old zircon U-Pb ages, Khapchan terrane.

According to the kimberlite ages reported in literature two main epoch of kimberlitic magmatism are recognized in the Khapchan terrane: 360-400 and 420-460 Ma (Smelov & Zaitsev, 2013). Thus, the second peak of young ages measured here corresponds well with kimberlite age.

Younger ages (300-320 Ma) are also reported for kimberlites of the terrane (Zaitsev & Smelov, 2010). However, despite the narrow age interval, well-defined peak and weighted mean age similar to ones known for kimberlite, it is unlikely that these zircons were crystallized from the kimberlitic melt. Their trace-element composition is typical of zircons from "crustal" intermediate or felsic parental melt (Fig. 9.5.4), none of them shows "kimberlitic" trace-element signatures. This age population might be related to post-kimberlitic intrusions that cut the kimberlites, which are not reported in the literature.

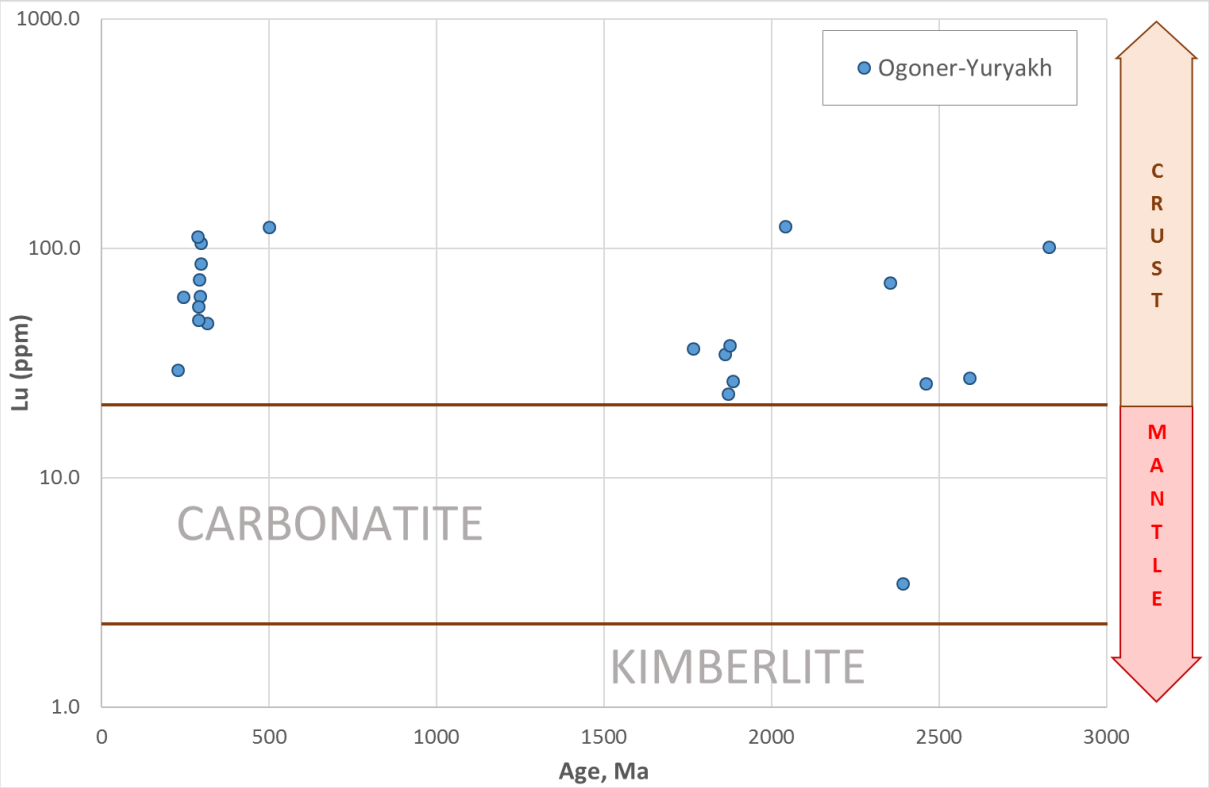



Figure 9.5.4. Lu vs U-Pb age of zircons from the Khapchan terrane.

***Hafnium-isotopic data***

The isotopic composition of hafnium was studied only in zircons from the Ogoner-Yuryakh field within the Khapchan terrane.

The number of studied samples is limited, but may still be representative due to the diversity in the U-Pb ages. The data are presented in Fig. 7.2.12, 7.2.13 and summarised in Fig. 9.5.5.

Low, mainly negative εHf values obtained for young zircons imply reworking of much older protoliths. In Fig. 9.5.5 two separate groups of young zircons are observed: first shows initial Hf ratios from 0.28235 to 0.2826 (εHf from -7.9 to +1.0); the second group has initial $^{177}Hf/^{178}Hf$ from 0.282 to 0.2822 (εHf from -20.5 to -15.8).

Crustal model ages and initial Lu/Hf ratio are calculated using the lowest available data point. The estimated crustal model age is ca 3.36 Ga, and the $^{176}Lu/^{177}Hf$ ratio = 0.022, which corresponds to a lower-crust composition.

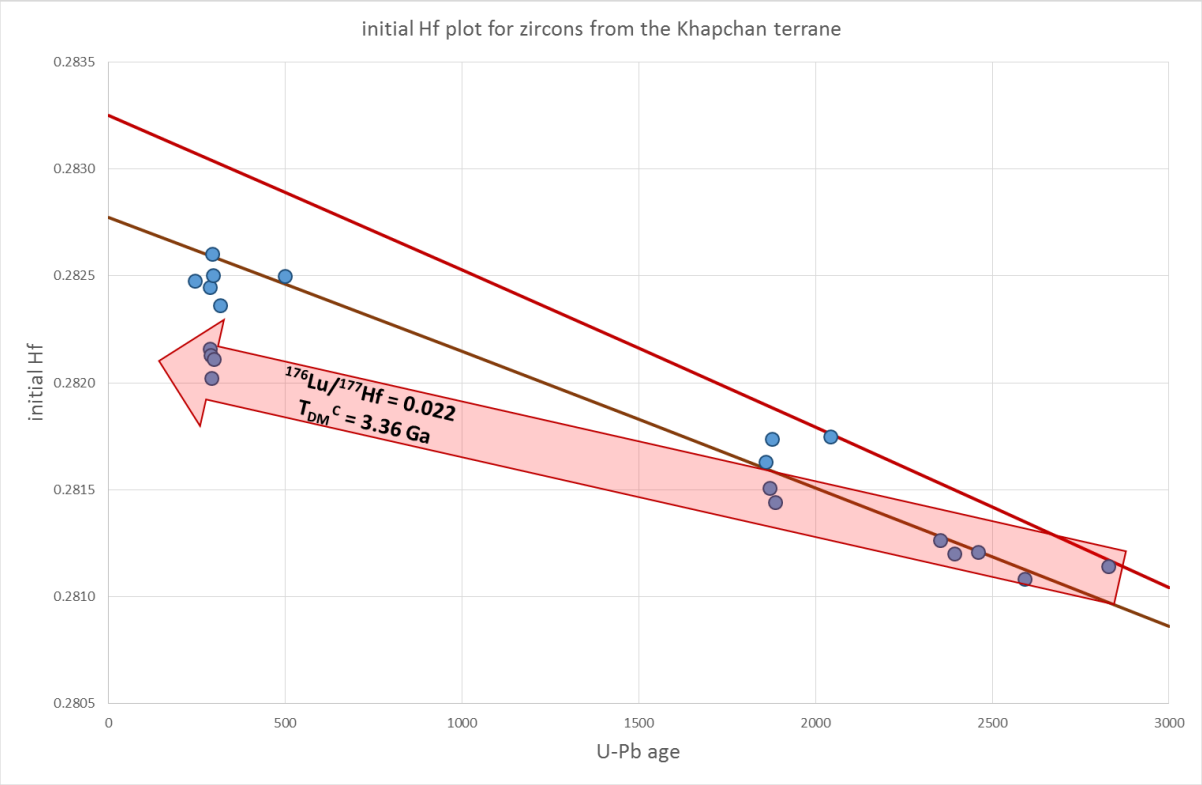



Figure 9.5.5. Initial Hf *vs* U-Pb age plot for zircons from the Khapchan terrane.

Thus, the U-Pb and Hf model ages indicate the presence of Archean crust in the basement of the Khapchan terrane. According to the Hf model ages, the SCLM under the terrane experienced melting at *ca* 3.4 billion years ago, and may have produced the primary crust of the terrane. Differences in the Hf-isotope composition of the young zircons also might be explained by mixing of the old subcontinental lithospheric mantle with asthenosphere at the time of kimberlite emplacement or the presence of two reservoirs different in composition. The trace-

element signatures of young zircons suggest post-kimberlite magmatic processes which were not reported previously.

## 9.6. The Birekta terrane

***Zircon U-Pb data***

U-Pb ages were analysed for about 200 zircon grains from the Birekta terrane. Figure 9.6.1 shows the relative -probability plot for zircon ages ranging from 138 to 3058 Ma.

As in other terranes two distinct groups of zircons are observed: one group includes grains with U-Pb age younger than 600 Ma; and another represents zircons older than 1500 Ma.

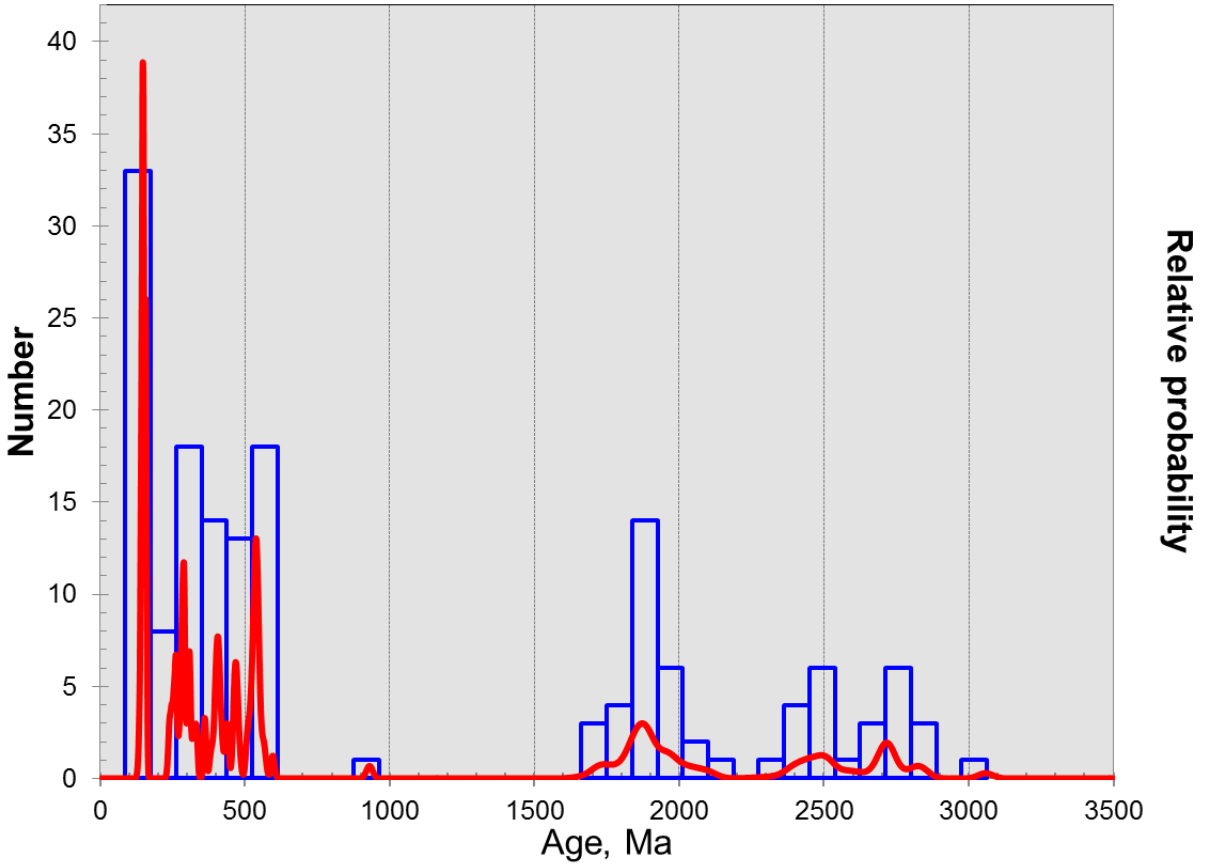



Figure 9.6.1. Relative-probability plot of zircon U-Pb ages, Birekta terrane.

The young zircons define several age peaks (Fig. 9.6.2). The youngest peak includes 36 grains with ages from 138 to 161 Ma. Concordia ages of zircons from the Khrizolit (157±0.8 Ma, Fig. 8.2.1), Pyatnitsa (148±0.8 Ma, Fig. 8.2.2) and Ruslovaya (145±1 Ma, Fig. 8.2.4) pipes within the Kuoika kimberlite field fall into that interval.

The second major peak is represented by 17 zircons with a weighted mean age of 537±3 Ma (Ruslovaya pipe, Fig. 8.2.5). Other young ages scatter between 230 and 596 Ma. This includes age of zircons from the Vostok-6 pipe (Concordia age 406±2.6 Ma, n=10) and ranges of ages from the pipes Olivinovaya (262 – 596 Ma), Ruslovaya (279 – 565 Ma) and Vtorogodnitsa (238 – 470 Ma).

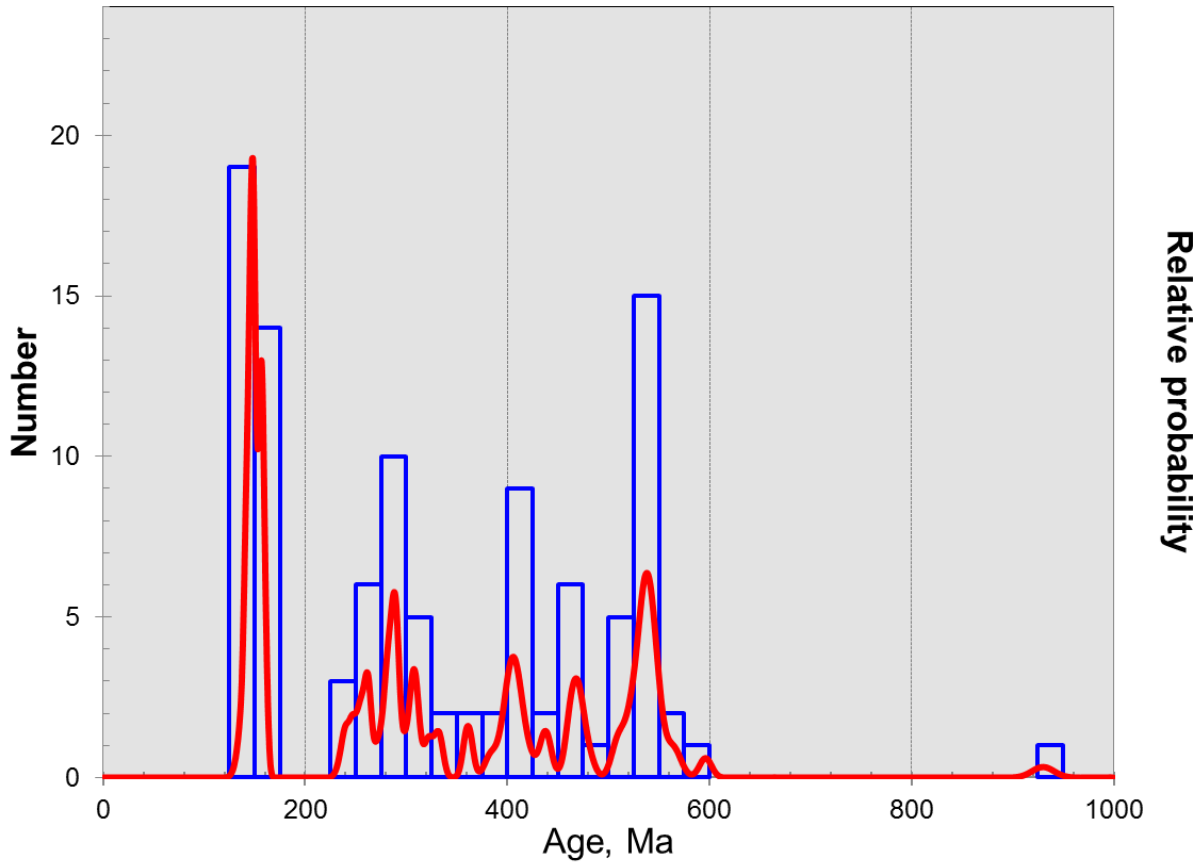



Figure 9.6.2. Relative-probability plot of zircon U-Pb ages (<1000 Ma), Birekta terrane.

Kimberlitic ages of 150-170, 330-340 and 415-440 Ma are known from the terrane (Smelov & Zaitsev, 2013). Thus, apart from the oldest age population, the Phanerozoic zircons might be related to the deep processes associated with the production of the host kimberlite.

U-Pb ages older than 1500 Ma comprise 3 distinct age peaks at the probability plot (Fig. 9.6.3). The main peak represents the range of ages from 1702 to 2102 Ma (29 U-Pb analyses). Sixteen of these grains form a unique age population with a weighted mean age of 1870±15 (MSWD = 0.62, probability = 0.86). The second and third peaks are at *ca* 2480 and 2750 Ma (Fig. 9.6.3).

The 1.8-1.9 Ga interval is commonly observed among zircon ages from all terranes. This age is commonly taken as dating the assembly of the Siberian Craton (Griffin *et al.*, 1999a, Neymark *et al.*, 1993, Pearson *et al.*, 1999, Rosen *et al.*, 1994, Rosen *et al.*, 2000, Yanshin & Borukaev, 1988).

The Archean zircon U-Pb ages obtained in this study were not reported previously. The Birekta terrane was considered as a terrane with Proterozoic crust (Rosen *et al.*, 1994, Rosen *et al.*, 2002, Smelov & Timofeev, 2007, Zaitsev & Smelov, 2010). Archean U-Pb ages were measured on zircons from several kimberlite pipes in both Kuoika and Merchemden fields.

They represent a uniform population despite a limited number of analyses, and thus an origin by contamination by zircons from sedimentary rocks is unlikely. The presence of an Archean crust in the basement of the Birekta terrane is more consistent with the U-Pb results.

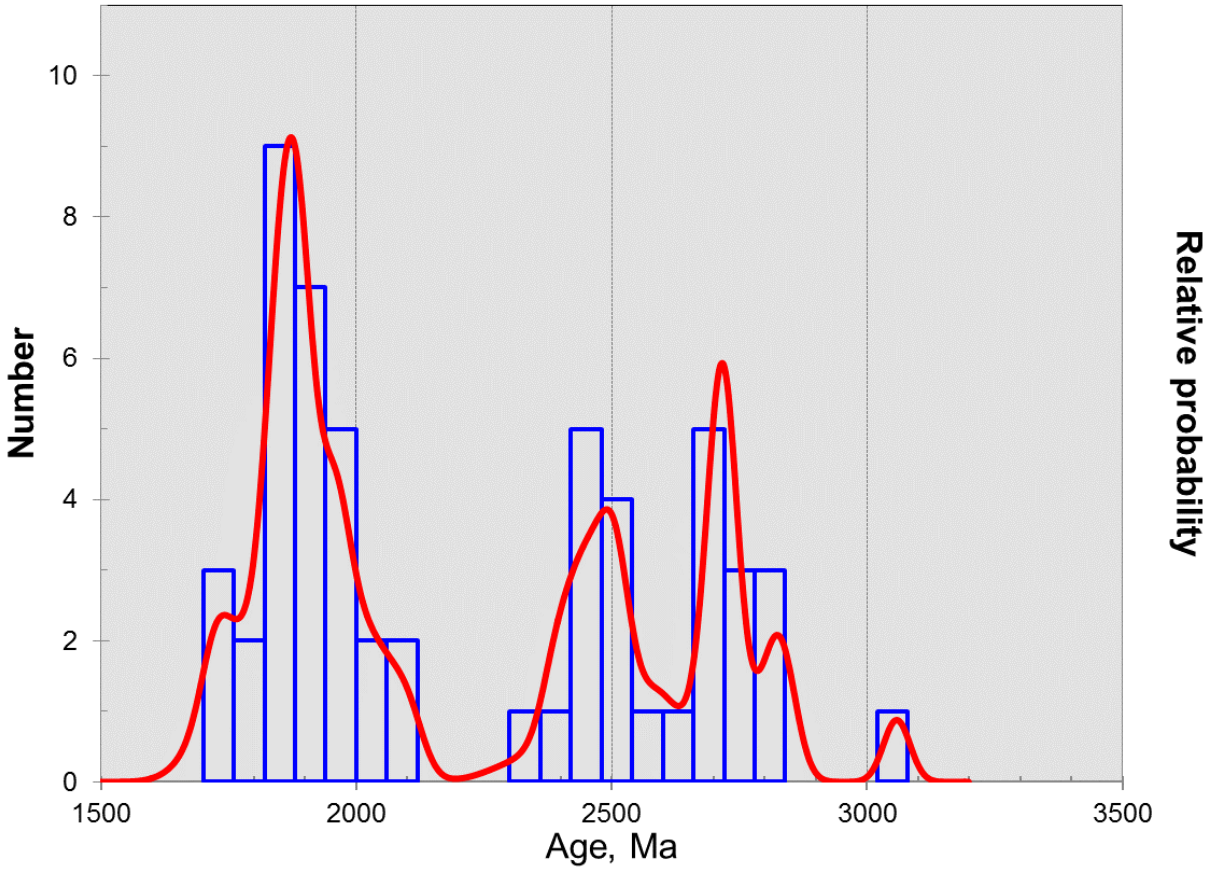



Figure 9.6.3. Relative probability plot of zircon U-Pb ages (>1500 Ma), Birekta terrane.

***Zircon trace-element data***

The trace-element signatures of zircons from the Birekta terrane do not show significant variation. All zircons have REE patterns with depletion in LREE and enrichment in HREE, well-defined Ce maxima and Eu minima. According to their trace-element content, most of the zircons have "crustal" origins, and crystallized from intermediate to felsic parental melts. Only rare grains from Archean and Paleoproterozoic populations show trace-element signatures typical of mantle-derived zircons (Fig. 9.6.4).

The U-Pb ages of zircons from the Phanerozoic population coincide with epochs of kimberlitic magmatism within the terrane, but none of those zircons have "kimberlitic" or "carbonatitic" trace-element signatures. This might indicate that in addition to kimberlite emplacement, other magmatic processes were happening at the same time. Such processes could be related to pre-kimberlite activity in the crust, or dykes intruding after kimberlite

eruption. In addition, trap magmatism is widespread within the Birekta terrane; however, the reported age interval is 245-255 Ma (Reichow *et al.*, 2009, Saunders & Reichow, 2009) which partially coincides with ages obtained in this study.

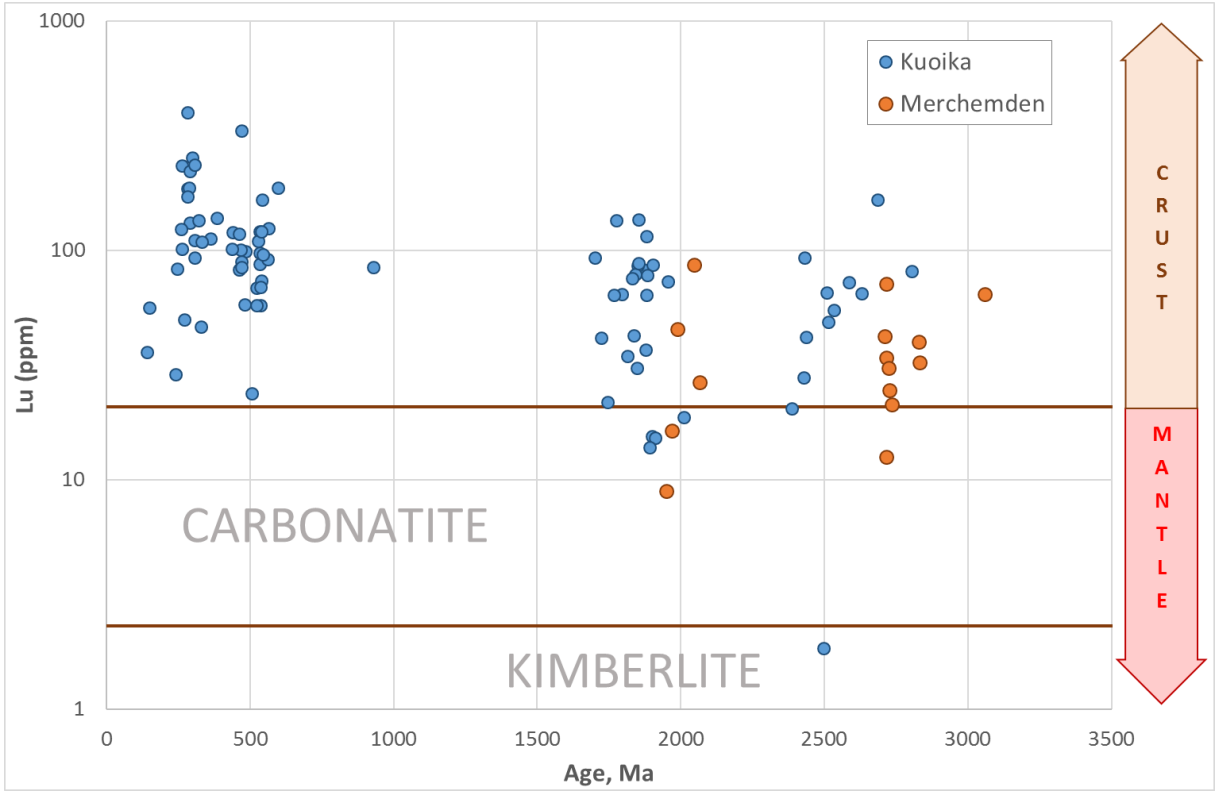



Figure 9.6.4. Lu *vs* U-Pb age of zircons from the Birekta terrane.

Thus, the trace-element compositions of zircons from the Birekta terrane indicate zircon-producing activity in the crust both in Archean-Proterozoic and Palaeozoic-Mesozoic time. Archean and Paleoproterozoic events also involved a minor input of mantle material producing zircons with "kimberlitic" or "carbonatitic" trace-element compositions. Despite the coincidence of the ages and the timing of kimberlite emplacement reported previously, none of Mesozoic and Palaeozoic zircons shows mantle-derived trace-element signatures. This implies that either there was magmatic activity in the crust simultaneous with kimberlite intrusion, or that previous dating of kimberlites is not precise. If there were simultaneous magmatic processes, kimberlitic zircons should be present as well, but no kimberlitic zircons were found. Kimberlites were dated by whole-rock Rb-Sr and K-Ar methods, and these have limitations due to closure temperatures much lower than those for U-Pb systematic. Thus, post-kimberlitic magmatic processes might have affected the isotopic systematics of the kimberlite and resulted in younger Rb-Sr and K-Ar ages. Resetting of the U-Pb system of older zircons caused by

heating in the hosting kimberlitic melt also may explain the coincident age of kimberlite, however this should be reflected in Pb-loss trends on the initial-Hf plot (see below).

***Oxygen isotopic data***

The plot of $\delta^{18}O$ *vs* U-Pb age (Fig. 9.6.5) shows the presence of zircons with mantle oxygen composition (5.3 ± 0.6‰) in all age groups. The highest $\delta^{18}O$ values (up to 9.3‰) are found in Palaeozoic zircons, indicating significant contamination of parental melts by material with a sedimentary signature. Zircons with the lowest $\delta^{18}O$, usually interpreted as result of hydrothermal material or meteoric water input (Monani & Valley, 2001), also are found within the Palaeozoic population. Despite the crustal trace-element signatures of most of the grains, mantle oxygen composition is common for zircons from the terrane. This implies that the parental melts of those zircons were not interacting with sedimentary rocks and, thus atmospheric oxygen.

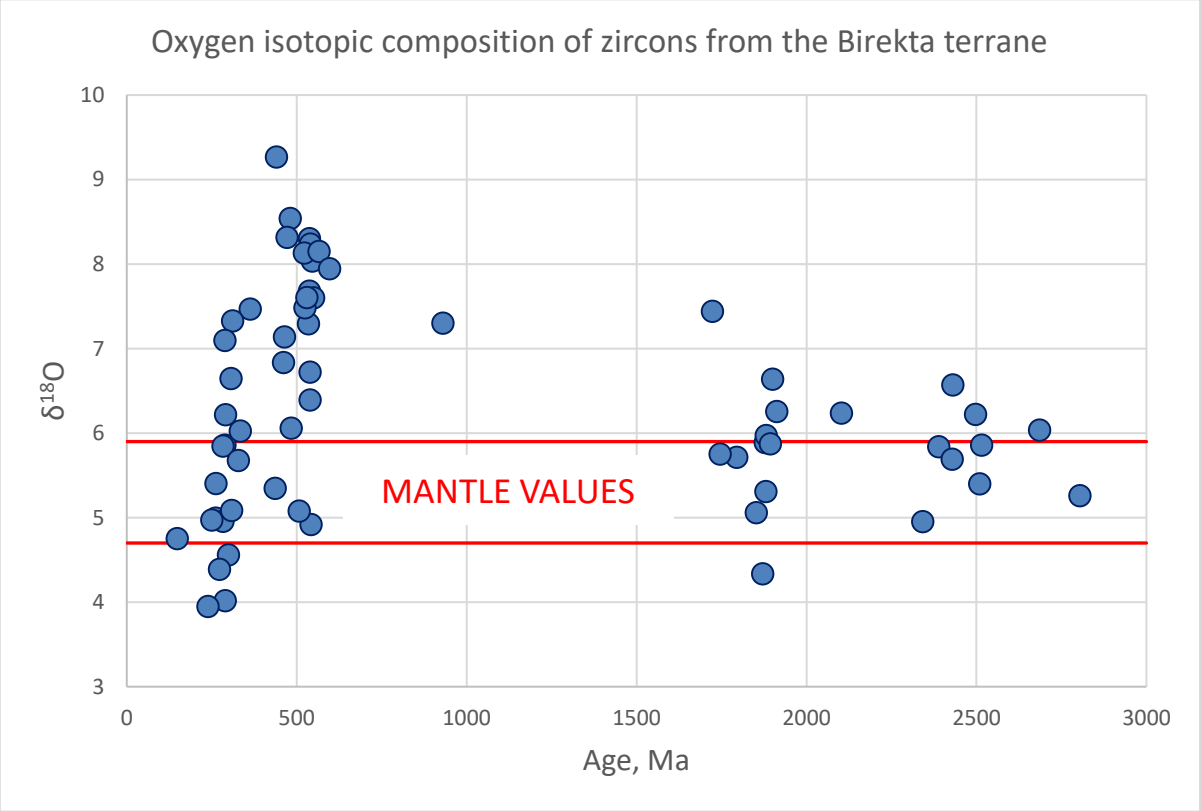



Figure 9.6.5. $\delta^{18}O$ *vs* U-Pb age of zircons from the Birekta terrane.

***Hafnium isotopic composition***

The isotopic composition of hafnium in zircons from the Birekta terrane is summarized in Fig. 9.6.6. The dotted lines show the evolution of the Hf-isotopic composition of average

crust, separated from the depleted mantle 1.0, 2.5 and 3.5 billion years ago. The plot also indicates reworking of Archean crust at ca 1.8 Ga and 300 Ma.

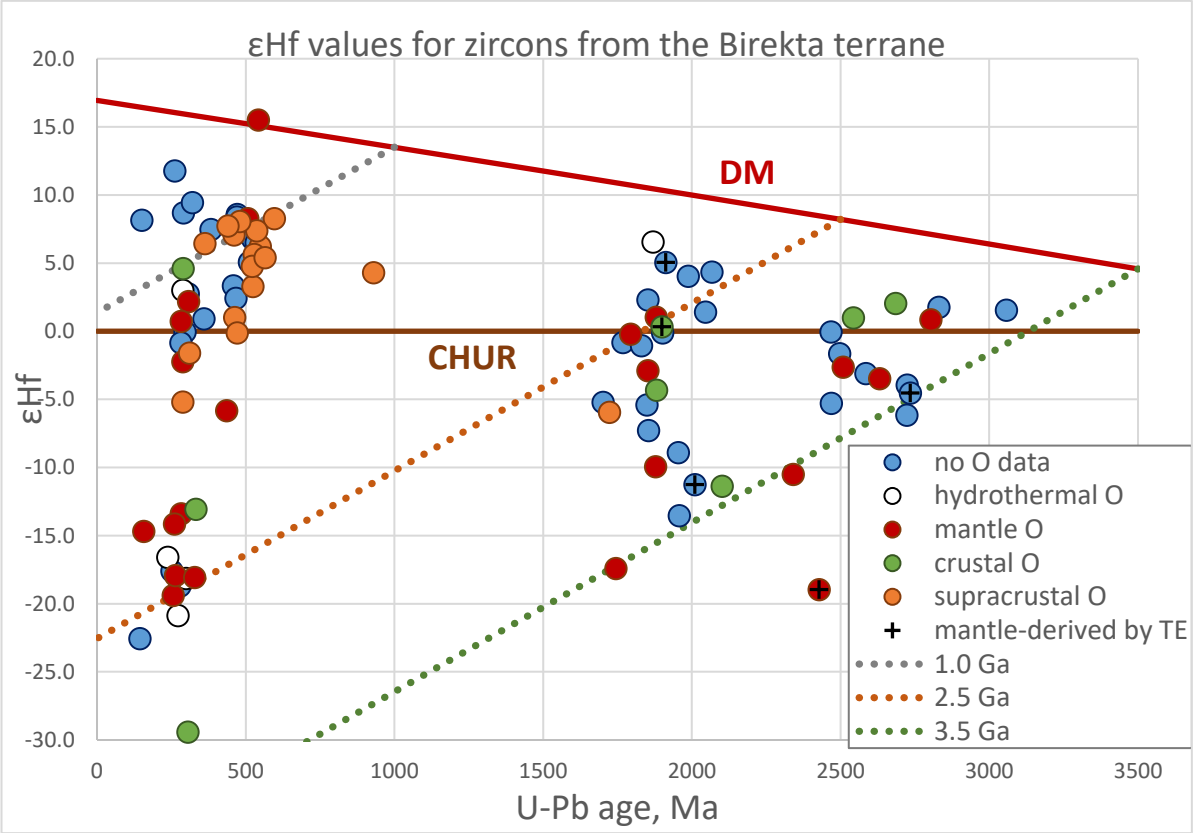



Figure 9.6.6. εHf vs U-Pb age of zircons from the Birekta terrane.

The population of zircons with Cambrian ages (mean age 537 Ma) have εHf values (+3 - +8) that might be interpreted as a reflection of reworking of the Proterozoic crust. The calculated $T_{DM}^{C}$ crustal model ages for these zircons fall into the interval 0.9-1.1 Ga. Ages from 948 to 1025 Ma are reported for the mafic sills and dykes of the Verkhoyansk fold belt located on the eastern boundary of the terrane (Rainbird *et al.*, 1998, Semikhatov *et al.*, 2000). However, in general the Neoproterozoic record in the Verkhoyansk orogenic belt indicates that the eastern edge of the Siberian Craton remained a passive continental margin during the Neoproterozoic and Palaeozoic (Vernikovsky *et al.*, 2004).

Integration of trace-element, Hf- and O-isotope data indicates reworking of the ancient crust without interacting with sedimentary rocks at 260-300 Ma (mantle O and very negative εHf). At the same time, some of zircons have mantle O composition and εHf near 0, but their trace-element signatures suggest crustal origins. This supports previous suggestions, but the Hf-isotope compositions demonstrate input of juvenile material into originally crustal melts. On

the other hand, the supracrustal oxygen composition of zircons with juvenile Hf implies contamination of mantle material by atmospheric oxygen from sa edimentary rocks.

The initial Hf plot (Fig. 9.6.7) shows that zircons of age *ca* 300 Ma lie on the same evolution line with Archean zircons. This line corresponds to evolution of a reservoir with initial $^{176}Lu/^{177}Hf = 0.024$ separated from the depleted mantle 3.84 billion years ago.

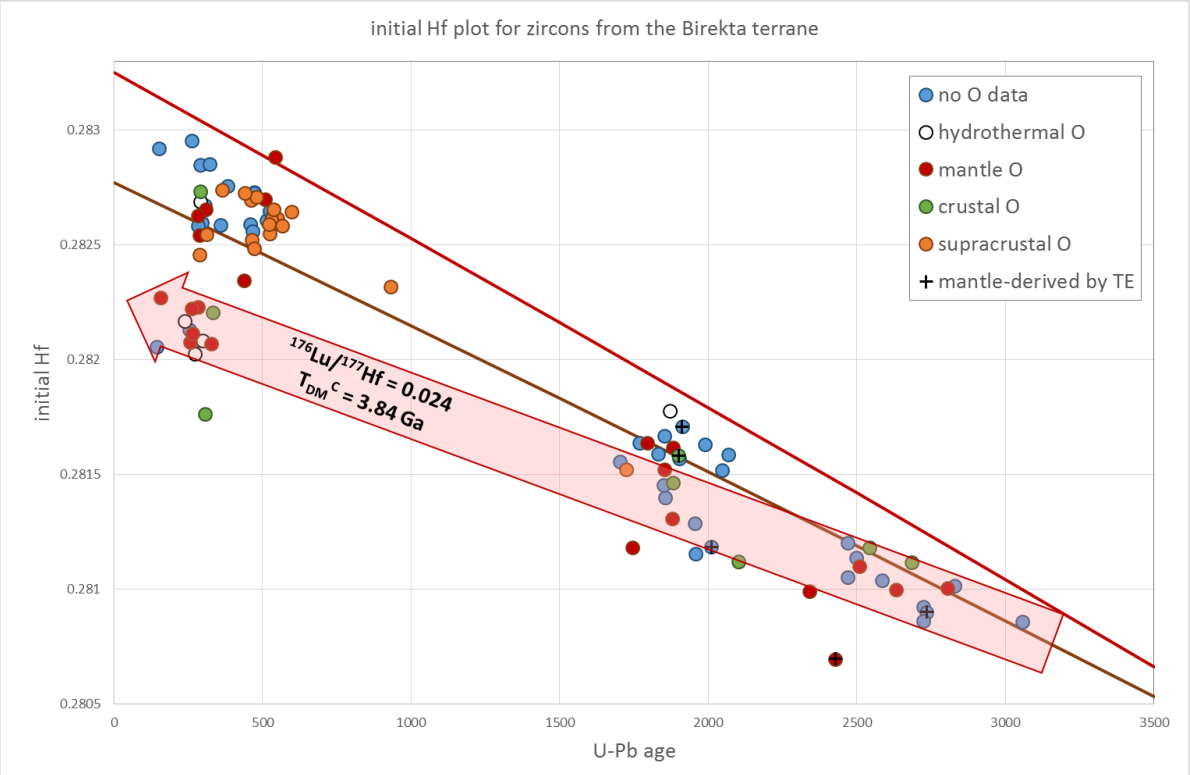



Figure 9.6.7. Initial Hf *vs* U-Pb age plot for zircons from the Birekta terrane.

Thus, zircons, crystallized in Archean, Paleoproterozoic and Palaeozoic-Mesozoic time have hafnium-isotopic compositions consistent with derivation from a single old protolith. Therefore, the hafnium isotopic data confirm the suggestion of an Archean age for the basement of the Birekta terrane. The trace-element compositions of zircons imply a significant involvement of old crust during all reworking events. Moreover, the U-Pb ages of zircons and their trace-element composition evidence extensive pre- and post-kimberlitic (intruded into kimberlite) magmatic activity.

## 9.7. The Siberian Craton Lithosphere

***U-Pb age data***

The summary of U-Pb ages of zircons from the Siberian Craton is presented in Figures 9.7.1, 9.7.2 and 9.7.3.

In general, all five terranes show major peaks in Palaeozoic-Mesozoic and Proterozoic-Archean time. No zircons are found within the interval between 1000 and 1700 Ma, except a few grains from the Markha terrane, which give those ages most likely because of Pb-loss (Fig. 9.3.7).

For better visualization of the age distribution, probability plots of U-Pb ages were created separately for ages older than 1500 Ma (Fig. 9.7.2) and younger than 1000 Ma (Fig. 9.7.3).

Due to the limited amount of samples from the Daldyn and Khapchan terranes it is difficult to compare their Precambrian geological history with other terranes (Fig. 9.7.1). However, zircons older than 1500 Ma from the Magan, Markha and Birekta terranes show a similar age distribution (Fig. 9.7.2). Thus, kimberlites from all four terranes (including the Khapchan) contain significant numbers of zircons with U-Pb ages 1.8 – 2.0 Ga. This age is commonly considered as the time of accretion of the Siberian Craton, accompanied by extensive tectonic, magmatic and metamorphic processes (Rosen, 2003, Rosen *et al.*, 1994, Turkina *et al.*, 2012).

The minor age peak at *ca* 2.3 - 2.4 Ga coincides for the Magan, Markha and Khapchan terranes, but is slightly offset in the Birekta terrane (~2.45 Ga). This age was previously considered as the time of Birekta crust formation (Bibikova *et al.*, 1989b, Neymark *et al.*,

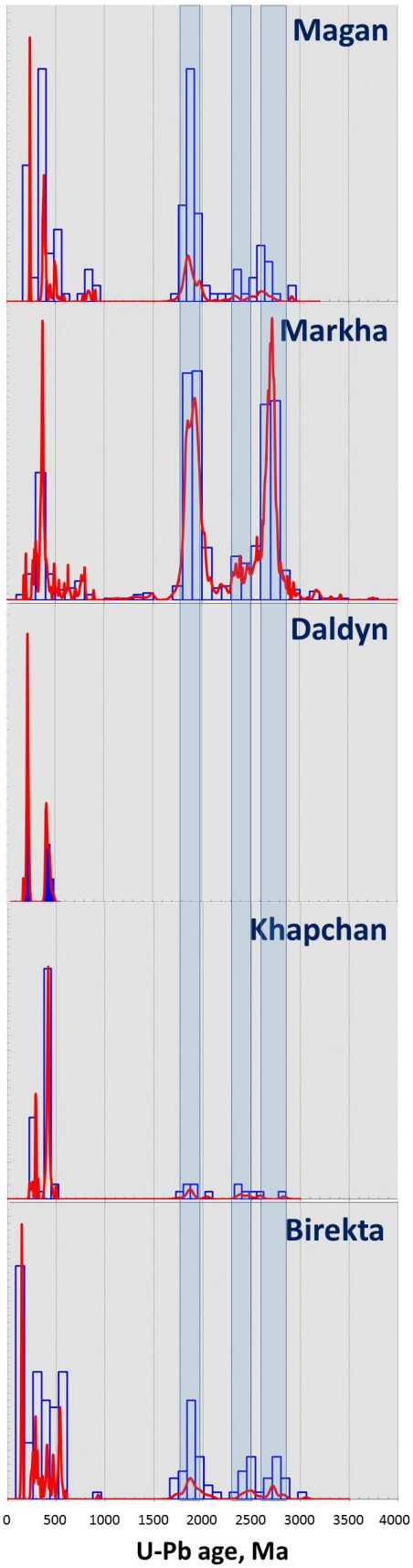



Figure 9.7.1. U-Pb ages of zircons from the Siberian Craton.

1993, Rosen *et al.*, 1994, Yanshin & Borukaev, 1988), but the number of zircons of this age is minor to support this possibility with high confidence.

The distinct peak at *ca* 2.7 Ga is found at the Magan, Markha and Birekta terrane (Fig. 9.7.2). The limited number of zircons from the Khapchan terrane does not allow confirmation this age peak, but close ages are obtained even among the few available grains. Older zircons (up to 3.7 Ga) are present in kimberlites from Magan, Markha and Birekta terranes.

The crust of the Khapchan and Birekta terranes was previously reported to be Proterozoic by many researchers (Griffin *et al.*, 1999a, Rosen *et al.*, 1994, Rosen *et al.*, 2006, Rosen *et al.*, 2000, Smelov & Zaitsev, 2013, Yanshin & Borukaev, 1988, Zaitsev & Smelov, 2010). This conclusion was based mainly on Sm-Nd model ages obtained from the whole-rock samples of lower-crustal xenoliths (Rosen *et al.*, 1991, Rosen *et al.*, 2000). The presence of zircons with Archean U-Pb ages in kimberlites from the Khapchan and Birekta terranes indicates the age of their crust older than previously suggested. While the data for the Khapchan terrane are not statistically significant, the results of zircon U-Pb dating for the Birekta terrane are more reliable and must be considered in future tectonic reconstructions involving the age of the terrane. Moreover, the coincidence of the major age peaks (2.7 and 1.8-1.9 Ga) at the Magan, Markha and Birekta terranes demonstrates that the tectonic and magmatic events at those times affected all three terranes.

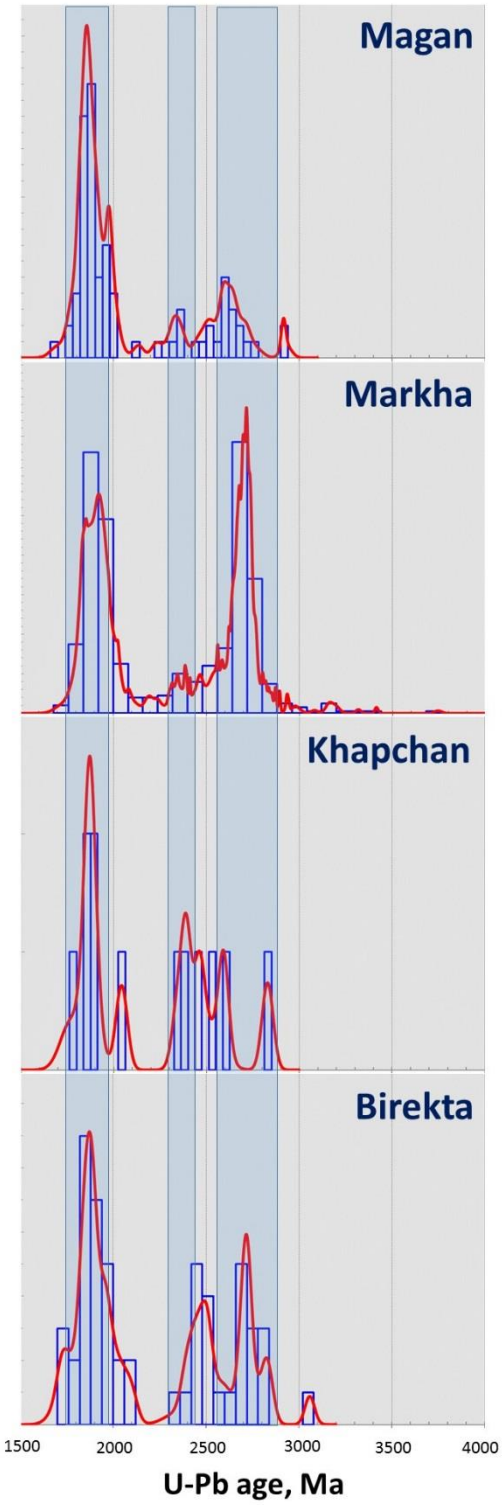



Figure 9.7.2. U-Pb ages (>1.5 Ga) of zircons from the Siberian Craton.

The similarity of Archean zircon age peaks is difficult to explain if the Siberian Craton was assembled in the Proterozoic time (1.8 – 1.9 Ga). If so, a global magmatic/tectonic event at *ca* 2.7

would need to affect the Magan, Markha and Birekta terranes separately and cause zircon crystallization in their crust. The age peak at 2.7 Ga corresponds to the existence of the supercontinent Kenorland assembled at 2.5 (?) – 2.7 Ga (Aspler *et al.*, 2002, Ernst *et al.*, 2013, Griffin *et al.*, 2014, Rosen, 2011). As reported by Condie *et al.* (2009) an alleged global mantle event is trackable in most existing Archean terranes. However, very limited data are available about the Archean structure of the Siberian craton and its position within the Kenorland supercontinent. Nevertheless, zircon U-Pb data obtained in this study suggest a close spatial relationship between at least 4 terranes (Magan, Markha, Khapchan and Birekta) at 2.7 Ga.

The magmatic history of the Siberian craton during Neoproterozoic – Palaeozoic time is characterized by multiple events, which may vary in time in different terranes. The probability plots of zircon U-Pb age data show some age peaks that coincide for two or three terranes, and also a variety of peaks that are individual for each terrane. This diversity may be explained by (i) better preservation of young zircons during the minor events and (ii) the larger set of young zircons and thus statistically higher amount of grains of each age interval.

In general, the Magan and Markha terranes show similar distribution of the age peaks. Thus, the main peak is observed at *ca* 370 Ma at both terranes, as well as a minor peak at *ca* 450-480 Ma. Zircon crystallization at *ca* 300 Ma is registered in the Markha, Khapchan and Birekta terranes. The youngest zircons, 140-150 Ma, are found only within the kimberlitic pipes of the Birekta terrane.

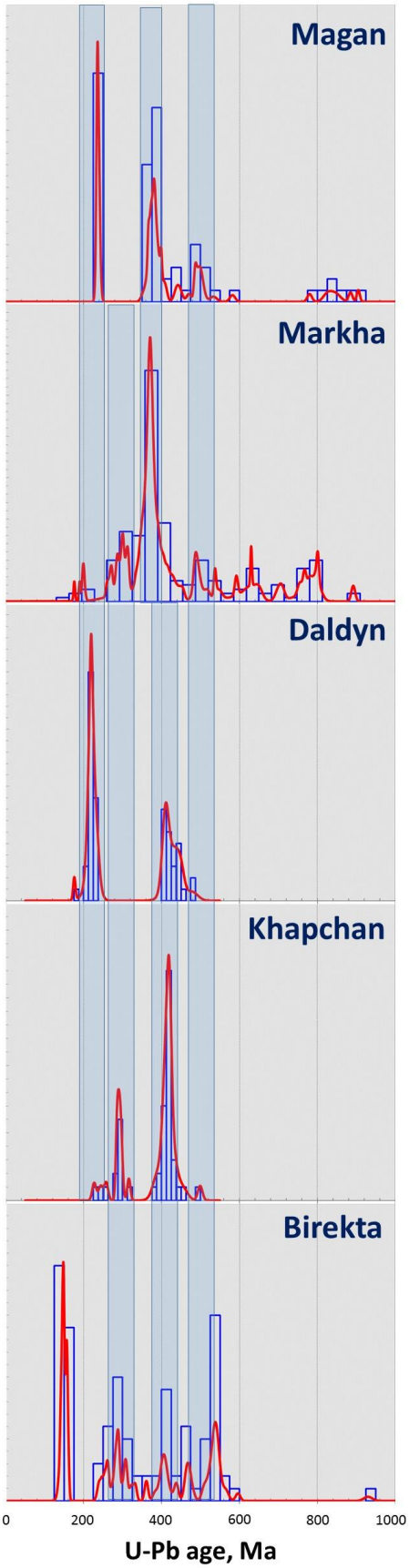



Figure 9.7.3. U-Pb ages (<1 Ga) of zircons from the Siberian Craton.

Some of observed peaks coincide well with the reported age stages of kimberlite magmatism across the craton (450–430, 420–400, 380–350, 250–230, 170–150, 110–100, and 60–50 Ma, (Smelov & Zaitsev, 2013). However, the trace-element composition of zircon should be used to divide grains crystallized in crustal melts from the mantle-derived ones.

***Trace-element data***

Combination of the trace-element composition data with U-Pb dating of zircons gives information not only about the time of zircon crystallization, but also provides with the evidence of the origin of zircon parental melt. As the result, mantle activity could be tracked through time.

Figure 9.7.4 shows the concentrations of, U and Lu, plotted versus the age of zircons. Belousova *et al.* (2002) showed that mantle-derived zircons have Lu-contents less than 20.7 ppm and U contents less than 130 ppm. Thus, Lu was used to discriminate zircons with analysed trace-element composition, and U concentrations were applied if the trace-element data are not available.

Mantle-derived zircons are found within all five studied terranes. They commonly occur in Palaeozoic-Mesozoic time reflecting kimberlitic magmatism. In general, there is a good agreement between the ages of Palaeozoic-Mesozoic mantle-derived zircons and previously reported ages of kimberlites. Thus, in

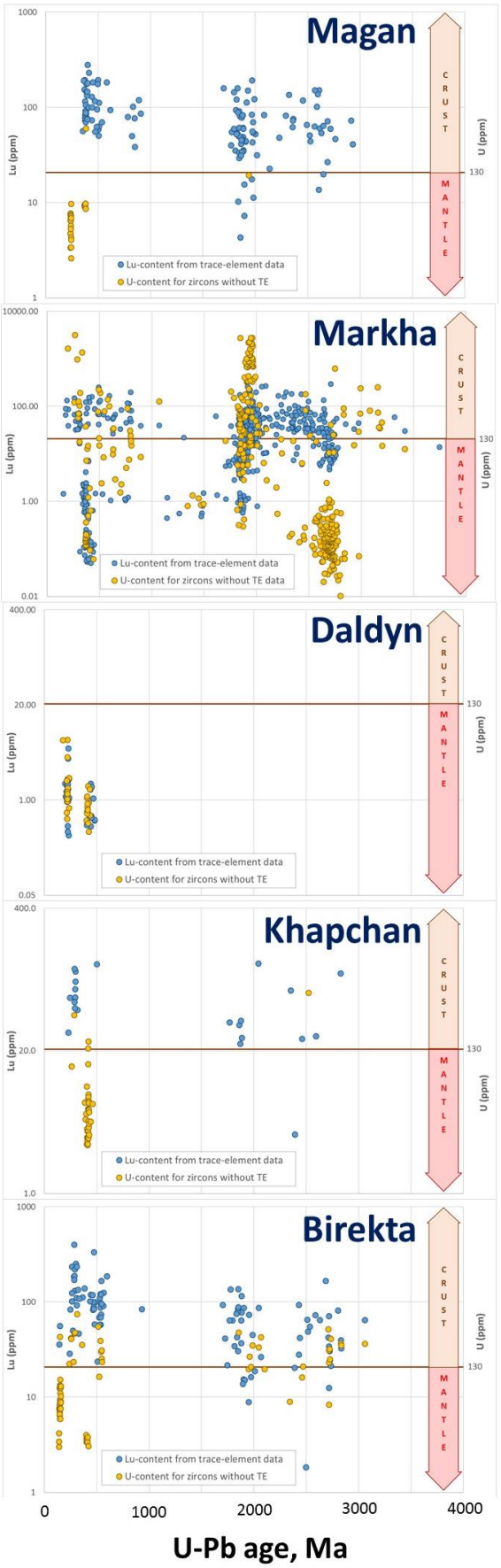



Figure 9.7.4. Lu and U *vs* age of zircons from the Siberian Craton.

both the Magan and Markha terranes mantle-derived zircons are found at 370 – 400 Ma. The interval 400-450 Ma is presented by zircons with low Lu and U in all studied terranes. In the Birekta terrane the youngest ages (140-150 Ma) are found in zircons with mantle U-content, but, the reported ages of Birekta kimberlites are much more scattered (130 – 180 Ma (Zaitsev & Smelov, 2010)).

This new data indicate than mantle-derived zircons were crystallizing during all the main stages of the Siberian craton evolution. In the Magan, Markha and Birekta terranes they are found at *ca* 2.7, 1.8 – 1.9 Ga and, of course, at the times of kimberlite emplacement (Fig. 9.7.4).

Similarly the temporal distribution of mantle-derived zircons in the Magan, Markha and Birekta, especially in Proterozoic-Archean time, could be considered as the evidence of shared tectono-magmatic history of those terranes.

***Hf-isotopes data***

Similar to U-Pb and trace-element data, the results of the Hf-isotope study indicate the comparable evolution of the studied terranes. The probability plots of the crustal model ages ($T_{DM}^{C}$) show overlapping peaks in the Magan, Markha and Birekta terranes (Fig. 9.7.5).

The youngest peak (~1 Ga) corresponds to the age of protolith of the Palaeozoic zircons. Two-stage model ages were calculated for both crustal and mantle-derived zircons as it was shown that the most of them lie on the same crustal evolution lines with Archean grains (Fig. 9.2.5, 9.3.7, 9.5.5, 9.6.7).

The second matching age peak (~2.5 Ga) is related to zircons crystallized at 1.8 – 1.9 Ga. This peak coincides for all four terranes where Hf-isotope data are available. A similar pattern may be expected for the Archean Magan and Markha

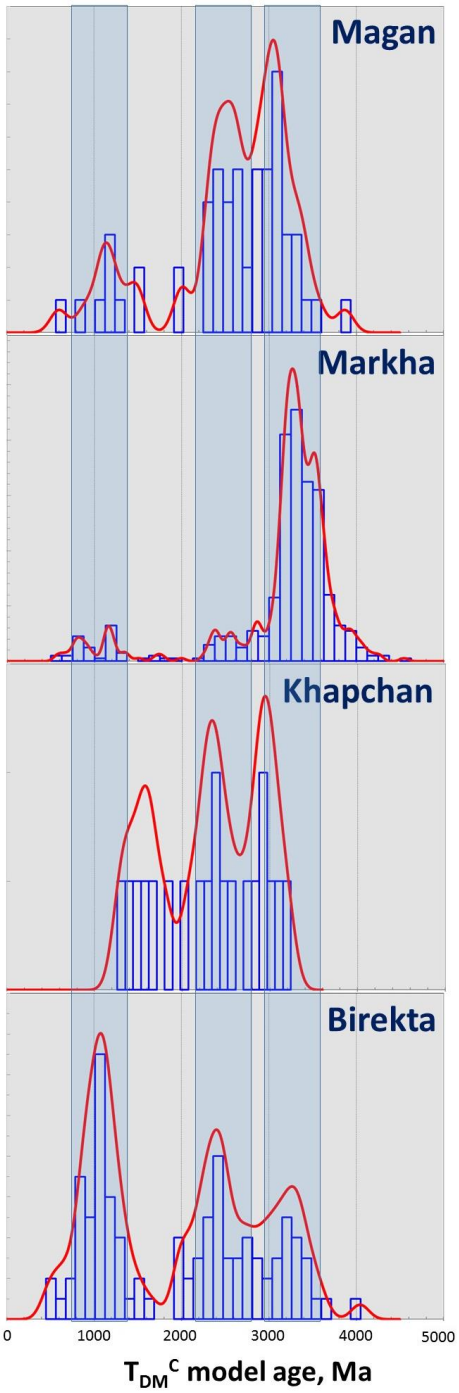



Figure 9.7.5. Hf crustal model ages of zircons from the Siberian Craton.

terranes if the Siberian craton was assembled in Proterozoic time. However,the crustal model ages older than 2.5 Ga for the Khapchan and Birekta terranes indicate the existence of their crust in Archean time.

The peak at *ca* 3.3 Ga is the major one for the Magan and Markha terranes, but it is also well defined in the Birekta terrane. This age corresponds to the major event of primary crust formation at all three terranes, and thus not only confirms the Archean age of the Birekta terrane, but also suggests the close timing of the tectonic/magmatic events in the terranes.

In summary, the comprehensive study of zircons from kimberlitic pipes of the Siberian craton shows a complex tectono-magmatic history in all studied terranes from Archean time until kimberlite emplacement. Based on the U-Pb, trace-element and Hf-isotope data, the Khapchan and Birekta terranes, previously considered as Proterozoic, are shown to have an Archean crust. Moreover, the distribution of U-Pb ages and Hf crustal model ages indicates a common tectonic history for the Magan, Markha and Birekta terranes in Archean and Proterozoic time, contradicting the assumed Proterozoic assembly of the Siberian craton. The trace-element composition of zircons from different age populations also indicates coincidence in the peaks of mantle-derived magmatic activity among the studied terranes. This implies a close spatial relationship, and thus supports the accretion of the Siberian craton at least 2.5-2.7 billion of years ago.

The comparison of the data obtained for sulfides (Re-Os and PGE) and zircons (U-Pb, Hf- and O-isotopes, trace-element composition) demonstrates inseparable connection between mantle and crustal processes and time coincidence of the major events in subcontinental lithospheric mantle and crust of the Siberian craton.

# Chapter 10. Conclusions

This study provides an integrated set of data including U-Pb age, trace-element composition, oxygen and hafnium isotopic composition on zircon grains separated from kimberlites from several terranes across the Siberian Craton. These data are combined with results on Re-Os systematics and platinum-group element compositions of sulfides from mantle xenoliths from the same localities. The main conclusions of this comprehensive study are listed below.

1. This multifaceted study of zircons and sulfides from kimberlitic pipes (including entrained mantle and lower crustal xenoliths) provides information not only about age of kimberlite itself, but also on the age and composition of rocks sampled by the kimberlites on their way to the surface. These data also provide some insights into the age and origin of the kimberlite protolith.

2. These new data suggest that the protolith of the primary crust of the ***Magan terrane*** was separated from the depleted mantle at least 3.6 Ga billion years ago and could be as old as 4.08 Ga. The reworking of this crust started at *ca* 2.9 Ga with the major reworking taking place at 1.8-1.9 Ga. The input of juvenile (mantle-derived) material can be recognized for both of these events, as well as for the duration of the kimberlite emplacement at 350-380 Ma. Two compositionally distinct domains in the lithospheric mantle were sampled at the time of kimberlite eruption: one contained sedimentary components and the other one did not.

3. Most of the subcontinental lithospheric mantle beneath the ***Markha terrane*** formed at 3-3.5 Ga, and lithosphere formation culminated at ca 2.9 Ga. Reworking of the primary crust was probably continuous until about 1.85 Ga. However, some parts of the SCLM were not involved in the major deformation and metamorphism, and survived, uncontaminated by crustal material, until the major Devonian kimberlite emplacement event.

4. The U-Pb data confirm at least two distinct kimberlitic events in the ***Daldyn terrane***: at 200-220 and 400-450 Ma. The difference in the Palaeozoic ages of kimberlites obtained in this study (400-450 Ma, U-Pb) and those reported previously (360-400 and 420-460 Ma, Rb-Sr and K-Ar) suggests that more detailed investigation is needed for kimberlites from this age interval.

5. The subcontinental lithospheric mantle under the ***Khapchan terrane*** experienced melting ca 3.4 billion years ago and this event may have produced the primary crust

of the terrane. This study demonstrates for the first time, the presence of the Archean crust in the Khapchan terrane, based on the U-Pb zircon ages. This crust was reworked during the 1.8-1.9 Ga event and at the time of kimberlite emplacement (*ca* 420 Ma). Moreover, post-kimberlitic magmatic processes (U-Pb age 290 Ma), which were not reported previously, are now suggested to have taken place within this terrane.

6. Archean crust was also recognized in the ***Birekta terrane*** for the first time. Zircon studies indicate that the primary crustal protolith separated from the depleted mantle at ca 3.84 Ga, while zircon crystallization was intermittently continuous since 2.7 Ga. The major crustal growth and reworking events happened at 1.8 – 1.9 Ga and in Palaeozoic time. In addition, extensive pre- and post-kimberlitic (intruded into kimberlite) magmatic events are confirmed.

7. In general, the integrated information for all the studied terranes within the ***Siberian craton*** implies a common tectono-magmatic history. The major across-craton events include formation of the primary crust starting at least *ca* 3.5 billion years ago, which is the most conservative estimation based on the Lu/Hf ratio of the average continental crust. Modeling implying more mafic protolith composition would give the age of the primary crust as old as 4 b.y. Further crustal growth and reworking of the 3.5 b.y. primary crust are recorded at 2.7 Ga and 1.8-1.9 Ga and might be related to the assembly of the Kenorland (2.7-2.5 Ga) and Nuna (1.8 Ga) supercontinents. Widespread magmatic activity, including kimberlite emplacement, occurred in Palaeozoic-Mesozoic time, and is recognised in both crustal and upper-mantle levels of the Siberian lithosphere.

8. The Proterozoic assembly of the Siberian craton, as it was assumed previously, is challenged by the new data collected during this work. These new data demonstrate a shared tectonic history for all terranes in Archean-Proterozoic time and also support the concurrence of the mantle-derived and crustal magmatism recorded within individual terranes. This implies their close spatial relationship, and thus suggests that the ***assembly of the Siberian craton*** occurred at least 2.5-2.7 billion years ago.

9. The Archean age of the Khapchan and Birekta terranes indicates that economically important ***diamond-bearing kimberlitic pipes*** could be found within these domains, which were previously considered to be non-prospective for diamond exploration because of their inferred Proterozoic age based on more limited data.

# References


Afonso, J. C., Fernàndez, M., Ranalli, G., Griffin, W. L. & Connolly, J. A. D. (2008). Integrated geophysical-petrological modeling of the lithosphere and sublithospheric upper mantle: Methodology and applications. *Geochemistry, Geophysics, Geosystems* **9**.

Aftalion, M., Bibikova, E. V., Bowes, D. R., Hopgood, A. M. & Perchuk, L. L. (1991). Timing of Early Proterozoic Collisional and Extensional Events in the Granulite-Gneiss-Charnockite-Granite Complex, Baikal lake, USSR - a U-Pb, Rb-Sr, and Sm-Nd Isotopic Study. Journal of Geology 99, 851-862.

Agashev, A. M., Watanabe, T., Bydaev, D. A., Pokhilenko, N. P., Fomin, A. S., Maehara, K. & Maeda, J. (2001). Geochemistry of kimberlites from the Nakyn field, Siberia: Evidence for unique source composition. Geology 29, 267-270.

Ahmed, A. H., Hanghoj, K., Kelemen, P. B., Hart, S. R. & Arai, S. (2006). Osmium isotope systematics of the Proterozoic and Phanerozoic ophiolitic chromitites: In situ ion probe analysis of primary Os-rich PGM. Earth and Planetary Science Letters 245, 777-791.

Altukhova, Z. A. & Zaitsev, A. I. (2006). Features of material composition and age of kimberlite rocks from Dyuken, Luchakan and Ary-Mastakh fields of Yakutian province. Lithosphere 2, 34-64.

Amelin, Y., Lee, D. C., Halliday, A. N. & Pidgeon, R. T. (1999). Nature of the Earth's earliest crust from hafnium isotopes in single detrital zircons. Nature 399, 252-255.

Andersen, T. (2002). Correction of common lead in U-Pb analyses that do not report Pb-204. Chemical Geology 192, 59-79.

Artemieva, I. M. (2009). The continental lithosphere: Reconciling thermal, seismic, and petrologic data. Lithos 109, 23-46.

Artemieva, I. M. & Mooney, W. D. (2001). Thermal thickness and evolution of Precambrian lithosphere: A global study. J. Geophys. Res. 106, 16387.

Ashchepkov, I. V., Pokhilenko, N. P., Vladykin, N. V., Logvinova, A. M., Afanasiev, V. P., Pokhilenko, L. N., Kuligin, S. S., Malygina, E. V., Alymova, N. A., Kostrovitsky, S. I., Rotman, A. Y., Mityukhin, S. I., Karpenko, M. A., Stegnitsky, Y. B. & Khemelnikova, O. S. (2010). Structure and evolution of the lithospheric mantle beneath Siberian craton, thermobarometric study. Tectonophysics 485, 17-41.

Ashchepkov, I. V., Vladykin, N. N., Ntaflos, T., Kostrovitsky, S. I., Prokopiev, S. A., Downes, H., Smelov, A. P., Agashev, A. M., Logvinova, A. M., Kuligin, S. S., Tychkov, N. S., Salikhov, R. F., Stegnitsky, Y. B., Alymova, N. V., Vavilov, M. A., Minin, V. A., Babushkina, S. A., Ovchinnikov, Y. I., Karpenko, M. A., Tolstov, A. V. & Shmarov, G. P. (2014). Layering of the lithospheric mantle beneath the Siberian Craton: Modeling using thermobarometry of mantle xenolith and xenocrysts. Tectonophysics 634, 55-75.

Aspler, L. B., Chiarenzelli, J. R., Cousens, B. L., McNicoll, V. J. & Davis, W. J. (2002). Paleoproterozoic intracratonic basin processes, from breakup of Kenorland to assembly of Laurentia: Hurwitz Basin, Nunavut, Canada (vol 141, pg 287, 2001). Sedimentary Geology 151, 335-336.

Baadsgaard, H., Nutman, A. P. & Samsonov, A. V. (1990). Geochronology of the Olondo Greenstone Belt. VII Intern. Conf. on Geochronology, Cosmochronology and Isotope Geology. Canberra, Australia: Geol. Soc. Australia, 6.

Batumike, J. M., Griffin, W. L., Belousova, E. A., Pearson, N. J., O'Reilly, S. Y. & Shee, S. R. (2008). LAM-ICPMS U-Pb dating of kimberlitic perovskite: Eocene-Oligocene kimberlites from the Kundelungu Plateau, DR Congo. Earth and Planetary Science Letters 267, 609-619.

Belousova, E. A., Griffin, W. L., O'Reilly, S. Y. & Fisher, N. I. (2002). Igneous zircon: trace element composition as an indicator of source rock type. Contributions to Mineralogy and Petrology 143, 602-622.

Belousova, E. A., Griffin, W. L., Shee, S. R., Jackson, S. E. & O'Reilly, S. Y. (2001). Two age populations of zircons from the Timber Creek kimberlites, Northern Territory, as determined by laser-ablation ICP-MS analysis. Australian Journal of Earth Sciences 48, 757-765.

Belousova, E. A., Reid, A. J., Griffin, W. L. & O'Reilly, S. Y. (2009). Rejuvenation vs. recycling of Archean crust in the Gawler Craton, South Australia: Evidence from U-Pb and Hf isotopes in detrital zircon. Lithos 113, 570-582.

Berezhnaya, N. G., Bibikova, E. V., Sochava, A. V., Kirnozova, T. I., Makarov, V. A. & Bogomolov, E. S. (1988). Isotopic age of the Chiney Subseries of the Udokan Group in the Kodaro-Udokan Depression. Doklady Akademii Nauk Sssr 302, 1209-1212.

Bibikova, E. V., Drugova, G. M., Duk, V. L., Levskii, L. K. & Levchenkov, O. A. (1986). The geochronology of the Aldan-Vitim shield. Methods of isotopic chronology and geochronological scale. Moscow: Nauka, 135-189.

Bibikova, E. V., Gavrikova, S. N., Kirnozova, T. V. & Fedchuk, V. (1989a). Early Proterozoic granites in the southern Aldan Shield: Isotopes and isotopic ages. Isotopes in Nature. Leipzig: German Democratic Republic Academy of Sciences, Central Institute of Isotope and Radiation Research, 13-14.

Bibikova, E. V., Gracheva, T. V., Dook, V. L., Kitsul, V. I. & Makarov, V. A. (1984). Isotopic Age of the Ungra Magmatic Complex of the Aldanian Shield. Doklady Akademii Nauk Sssr 276, 206-209.

Bibikova, E. V., Gracheva, T. V., Drugova, G. M., Makarov, V. A. & Morozova, I. M. (1989b). U-Pb Age of Granulites from Kurulta Complex (Aldanian Shield). Doklady Akademii Nauk Sssr 305, 949-952.

Bibikova, E. V., Karpenko, S. F., Sumin, L. V., Bogdanovsky, D. G., Kirnizova, T. I., Lyalikov, A. V., Makarov, V. A., Arakalyants, M. M., Korikovsky, S. P., Fedorovsky, V. S., Petrova, Z. I. & Levitsky, V. I. (1990a). U/Pb, Sm/Nd and K/Ar age of metamorphic and magmatic rocks in the Olkhon area, western Baikalia. Precambrian Geology and Geochronology of the Siberian Platform and Surroundings. Leningrad: Nauka Press, 171-183.

Bibikova, E. V., Khiltova, V. J., Gracheva, T. V. & Makarov, V. A. (1982). Age of Greenstone Belts of the Prisayanie. Doklady Akademii Nauk Sssr 267, 1171-1174.

Bibikova, E. V., Kirnozova, T. I. & Makarov, V. A. (1990b). Age boundaries in the evolution of the Sharyzhalgay Complex in western Baikalia (U/Pb system in zircons). Precambrian Geology and Geochronology of the Siberian Platform and Surrounding Areas. Leningrad: Nauka, 162-169.

Bindeman, I. N. & Valley, J. W. (2001). Low-delta O-18 rhyolites from Yellowstone: Magmatic evolution based on analyses of zircons and individual phenocrysts. Journal of Petrology 42, 1491-1517.

Black, L. P. & Gulson, B. L. (1978). The age of the Mud Tank Carbonatite, Strangways Range, Northern Territory. Bureau of Mineral Resources, Geology and Geophysics.

Black, L. P., Kamo, S. L., Allen, C. M., Davis, D. W., Aleinikoff, J. N., Valley, J. W., Mundil, R., Campbell, I. H., Korsch, R. J., Williams, I. S. & Foudoulis, C. (2004). Improved (206)Pb/(238)U microprobe geochronology by the monitoring of a trace-element-related matrix effect; SHRIMP, ID-TIMS, ELA-ICP-MS and oxygen isotope documentation for a series of zircon standards. Chemical Geology 205, 115-140.

Blichert-Toft, J. & Albarède, F. (1997). The Lu-Hf isotope geochemistry of chondrites and the evolution of the mantle-crust system. Earth and Planetary Science Letters 148, 243-258.

Boyd, F. R., Pokhilenko, N. P., Pearson, D. G., Mertzman, S. A., Sobolev, N. V. & Finger, L. W. (1997). Composition of the Siberian cratonic mantle: evidence from Udachnaya peridotite xenoliths. Contributions to Mineralogy and Petrology 128, 228-246.

Brakhfogel, F. F. (1984). Geological aspects of kimberlite magmatism in the northeastern part of the Siberian Platform. Report of the Academy of Sciences of the USSR, Orden of Lenin Siberian Department. Yakutsk: Institute of Geology, 128.

Brakhfogel, F. F. (1995). The age division of the kimberlitic and related magmatites in the NE of the Siberian platform (methods and results). In: Sobolev, N. V. (ed.) 6th International Kimberlite Conference. Novosibirsk, 60-62.

Bulanova, G. P., Griffin, W. L., Ryan, C. G., Shestakova, O. Y. & Barnes, S. J. (1996). Trace elements in sulfide inclusions from Yakutian diamonds. Contributions to Mineralogy and Petrology 124, 111-125.

Chernykh, A. I. (2000). Geological structure and petrologo-geochemical features of Precambrian ophiolitic and paleoisland-arc complexes of Yenisei Range. Novosibirsk, 21.

Condie, K. C., Belousova, E., Griffin, W. L. & Sircombe, K. N. (2009). Granitoid events in space and time: Constraints from igneous and detrital zircon age spectra. Gondwana Research 15, 228-242.

Davis, G. L., Sobolev, N. V. & Kharkiv, A. D. (1980). New data on the age of Yakutian kimberlites obtained by the uranium-lead method on zircons. Doklady Akademii Nauk Sssr 254, 175-179.

De Biévre, P. & Taylor, P. D. P. (1993). Table of the isotopic compositions of the elements. International Journal of Mass Spectrometry and Ion Processes 123, 149-166.

Deen, T. J., Griffin, W. L., Begg, G., O'Reilly, S. Y., Natapov, L. M. & Hronsky, J. (2006). Thermal and compositional structure of the subcontinental lithospheric mantle: Derivation from shear wave seismic tomography. Geochemistry Geophysics Geosystems 7.

Dobretsov, N. L. (1986). Early Precambrian of Southern Yakutia. Moscow: Nauka.

Donskaya, T. V., Gladkochub, D. P., Kovach, V. P. & Mazukabzov, A. M. (2005). Petrogenesis of Early Proterozoic postcollisional granitoids in the southern Siberian craton. Petrology 13, 229-252.

Dook, V. L. (1989). Precambrian of the Aldan Shield: structural evolution and geological history. Moscow: Geol. Inst., Russian Acad. Sci. Publ.

Egorkin, A. V. (2004). Mantle structure of the Siberian platform. Izvestiya-Physics of the Solid Earth 40, 385-394.

Elhlou, S., Belousova, E., Griffin, W. L., Pearson, N. J. & O'Reilly, S. Y. (2006). Trace element and isotopic composition of GJ-red zircon standard by laser ablation. Geochimica Et Cosmochimica Acta 70, A158-A158.

England, P. C. & Thompson, A. B. (1984). PRESSURE TEMPERATURE TIME PATHS OF REGIONAL METAMORPHISM .1. HEAT-TRANSFER DURING THE EVOLUTION OF REGIONS OF THICKENED CONTINENTAL-CRUST. Journal of Petrology 25, 894-928.

Ernst, R. E., Bleeker, W., Soderlund, U. & Kerr, A. C. (2013). Large Igneous Provinces and supercontinents: Toward completing the plate tectonic revolution. Lithos 174, 1-14.

Foley, S. F., Yaxley, G. M., Rosenthal, A., Buhre, S., Kiseeva, E. S., Rapp, R. P. & Jacob, D. E. (2009). The composition of near-solidus melts of peridotite in the presence of CO2 and H2O between 40 and 60 kbar. Lithos 112, 274-283.

Forte, A. M. (2000). Geodynamic Evidence for a Chemically Depleted Continental Tectosphere. Science 290, 1940-1944.

Freydier, C., Ruiz, J., Chesley, J., McCandless, T. & Munizaga, F. (1997). Re-Os isotope systematics of sulfides from felsic igneous rocks: Application to base metal porphyry mineralization in Chile. Geology 25, 775-778.

Frost, B. R., Avchenko, O. V., Chamberlain, K. R. & Frost, C. D. (1998). Evidence for extensive Proterozoic remobilization of the Aldan shield and implications for Proterozoic plate tectonic reconstructions of Siberia and Laurentia. Precambrian Research 89, 1-23.

Gafarov, R. A., Leites, A. M. & Fedorovskii, V. S. (1978). Tectonic dissection of Siberian Platform basement and stages of continental crust formation. Geotectonics 1, 43-58.

Gamaleya, Y. N. (1968). Formation analysis of the southeastern Siberian Platform. Geotectonics 6, 34-45.

Gaul, O. (2000). Mapping olivine composition in the lithospheric mantle. *Earth and Planetary Science Letters* **182**, 223-235.

Genshaft, N. S. (1996). Inner factors of tectonic mobility of platforms. *Geotectonics* **4**, 13-24.

Giuliani, A., Phillips, D., Maas, R., Woodhead, J. D., Kendrick, M. A., Greig, A., Armstrong, R. A., Chew, D., Kamenetsky, V. S. & Fiorentini, M. L. (2014). LIMA U-Pb ages link lithospheric mantle metasomatism to Karoo magmatism beneath the Kimberley region, South Africa. *Earth and Planetary Science Letters* **401**, 132-147.

Gladkochub, D., Pisarevsky, S., Donskaya, T., Natapov, L., Mazukabzov, A., Stanevich, A. & Sklyarov, E. (2006). The Siberian Craton and its evolution in terms of the Rodinia hypothesis. *Episodes* **29**, 169-174.

Gladkochub, D. P., Donskaya, T. V., Mazukabzov, A. M., Sal'nikova, E. B., Sklyarov, E. V. & Yakovleva, S. Z. (2005). The age and geodynamic interpretation of the Kitoi granitoid complex (southern Siberian craton). *Russian Geology and Geophysics* **46**, 1121-1133.

Glebovitsky, V. A. & Drugova, G. M. (1993). Tectonothermal Evolution of the Western Aldan Shield, Siberia. *Precambrian Research* **62**, 493-505.

Gorokhov, I. M., Timofeev, V. F., Bizunok, M. B., Berezkin, V. I., Dook, V. L., Krylov, I. N., Kutyavin, E. P., Melnikov, N. N. & Smelov, A. P. (1989). Rb/Sr sustems in metasediments of the Khani graben, Olekma greenstone belt. *Isotopic Geochronology of the Precambrian*. Leningrad: Nauka, 110-125.

Griffin, W. L., Belousova, E. A., O'Neill, C., O'Reilly, S. Y., Malkovets, V., Pearson, N. J., Spetsius, S. & Wilde, S. A. (2014). The world turns over: Hadean-Archean crust-mantle evolution. *Lithos* **189**, 2-15.

Griffin, W. L., Belousova, E. A., Shee, S. R., Pearson, N. J. & O'Reilly, S. Y. (2004). Archean crustal evolution in the northern Yilgam Craton: U-Pb and Hf-isotope evidence from detrital zircons. *Precambrian Research* **131**, 231-282.

Griffin, W. L., Kaminsky, F. V., Ryan, C. G., O'Reilly, S. Y., Win, T. T. & Ilupin, I. P. (1996). Thermal state and composition of the lithospheric mantle beneath the Daldyn kimberlite field, Yakutia. *Tectonophysics* **262**, 19-33.

Griffin, W. L., Natapov, L. M., O'Reilly, S. Y., van Achterbergh, E., Cherenkova, A. F. & Cherenkov, V. (2005). The Kharamai kimberlite field, Siberia: Modification of the lithospheric mantle by the Siberian Trap event. *Lithos* **81**, 167-187.

Griffin, W. L., O'Reilly, S. Y., Abe, N., Aulbach, S., Davies, R. M., Pearson, N. J., Doyle, B. J. & Kivi, K. (2003). The origin and evolution of Archean lithospheric mantle. *Precambrian Research* **127**, 19-41.

Griffin, W. L., Pearson, N. J., Belousova, E., Jackson, S. E., van Achterbergh, E., O'Reilly, S. Y. & Shee, S. R. (2000). The Hf isotope composition of cratonic mantle: LAM-MC-ICPMS analysis of zircon megacrysts in kimberlites. *Geochimica Et Cosmochimica Acta* **64**, 133-147.

Griffin, W. L., Pearson, N. J., Belousova, E. A. & Saeed, A. (2007). Reply to "Comment to short-communication 'Comment: Hf-isotope heterogeneity in zircon 91500' by W.L. Griffin, N.J. Pearson, E.A. Belousova and A. Saeed (Chemical geology 233 (2006) 358-363)" by F. Corfu. *Chemical Geology* **244**, 354-356.

Griffin, W. L., Powell, W. J., Pearson, N. J. & O'Reilly, S. Y. (2008). GLITTER: data reduction software for laser ablation ICP-MS. *Laser Ablation-ICP-MS in the Earth Sciences: Mineralogical Association of Canada Short Course Series* **40**, 204-207.

Griffin, W. L., Ryan, C. G., Kaminsky, F. V., O'Reilly, S. Y., Natapov, L. M., Win, T. T., Kinny, P. D. & Ilupin, I. P. (1999a). The Siberian lithosphere traverse: mantle terranes and the assembly of the Siberian Craton. *Tectonophysics* **310**, 1-35.

Griffin, W. L., Shee, S. R., Ryan, C. G., Win, T. T. & Wyatt, B. A. (1999b). Harzburgite to lherzolite and back again: metasomatic processes in ultramafic xenoliths from the Wesselton kimberlite, Kimberley, South Africa. *Contributions to Mineralogy and Petrology* **134**, 232-250.

Griffin, W. L., Spetsius, Z. V., Pearson, N. J. & O'Reilly, S. Y. (2002a). In situ Re-Os analysis of sulfide inclusions in kimberlitic olivine: New constraints on depletion events in the Siberian lithospheric mantle. *Geochemistry Geophysics Geosystems* **3**.

Griffin, W. L., Wang, X., Jackson, S. E., Pearson, N. J., O'Reilly, S. Y., Xu, X. S. & Zhou, X. M. (2002b). Zircon chemistry and magma mixing, SE China: In-situ analysis of Hf isotopes, Tonglu and Pingtan igneous complexes. *Lithos* **61**, 237-269.

Guo, J. F., OReilly, S. Y. & Griffin, W. L. (1996). Zircon inclusions in corundum megacrysts .1. Trace element geochemistry and clues to the origin of corundum megacrysts in alkali basalts. *Geochimica Et Cosmochimica Acta* **60**, 2347-2363.

Hanchar, J. M. & Miller, C. F. (1993). Zircon Zonation Patterns as Revealed by Cathodoluminescence and Backscattered Electron Images - Implications for Interpretation of Complex Crustal Histories. *Chemical Geology* **110**, 1-13.

Hiess, J., Bennett, V. C., Nutman, A. P. & Williams, I. S. (2009). In situ U-Pb, O and Hf isotopic compositions of zircon and olivine from Eoarchaean rocks, West Greenland: New insights to making old crust. *Geochimica Et Cosmochimica Acta* **73**, 4489-4516.

Hinton, R. W. & Upton, B. G. J. (1991). The Chemistry of Zircon - Variations within and between Large Crystals from Syenite and Alkali Basalt Xenoliths. *Geochimica Et Cosmochimica Acta* **55**, 3287-3302.

Hoskin, P. W. O. (2005). Trace-element composition of hydrothermal zircon and the alteration of Hadean zircon from the Jack Hills, Australia. *Geochimica Et Cosmochimica Acta* **69**, 637-648.

Howarth, G. H., Barry, P. H., Pernet-Fisher, J. F., Baziotis, I. P., Pokhilenko, N. P., Pokhilenko, L. N., Bodnar, R. J., Taylor, L. A. & Agashev, A. M. (2014). Superplume metasomatism: Evidence from Siberian mantle xenoliths. *Lithos* **184-187**, 209-224.

Ilupin, I. P., Vaganov, V. I. & Prokpuck, B. I. (1990). *Kimberlites*. Moscow: Nedra.

Ionov, D. A., Doucet, L. S. & Ashchepkov, I. V. (2010). Composition of the Lithospheric Mantle in the Siberian Craton: New Constraints from Fresh Peridotites in the Udachnaya-East Kimberlite. *Journal of Petrology* **51**, 2177-2210.

Ionov, D. A., Shirey, S. B., Weis, D. & Brügmann, G. (2006). Os–Hf–Sr–Nd isotope and PGE systematics of spinel peridotite xenoliths from Tok, SE Siberian craton: Effects of pervasive metasomatism in shallow refractory mantle. *Earth and Planetary Science Letters* **241**, 47-64.

Iskanderova, A. D., Mirkina, S. L., Neymark, L. A., Chukhonia, A. P. & Khoreva, B. Y. (1980). New data on lead isotopic studies of Archean metamorphic rocks and granitic gneisses in the Stanovoy area of the Aldan shield. *Geochronology of Eastern Siberia and the Far East*. Moscow: Nauka, 132-153.

Jackson, S. E., Pearson, N. J., Griffin, W. L. & Belousova, E. A. (2004). The application of laser ablation-inductively coupled plasma-mass spectrometry to in situ U-Pb zircon geochronology. *Chemical Geology* **211**, 47-69.

Kamenetsky, V. S., Belousova, E. A., Giuliani, A., Kamenetsky, M. B., Goemann, K. & Griffin, W. L. (2014). Chemical abrasion of zircon and ilmenite megacrysts in the Monastery kimberlite: Implications for the composition of kimberlite melts. *Chemical Geology* **383**, 76-85.

Kennedy, A. & De Laeter, J. R. (1994). The performance of the WA SHRIMP II ion microprobe. *8 INT C GEOCHR COSM* **1107**, 166-166.

Kharkiv, A. D., Zinchuk, N. N. & Kryuchkov, A. I. (1998). *Primary diamond deposits of the world*. Moscow: Nedra.

Khorev, B. Y. (1987). Map of metamorphic complexes and granitoids of the USSR, Scale 1:10000000. In: Khorev, B. Y. (ed.). Leningrad.

King, S. (2005). Archean cratons and mantle dynamics. *Earth and Planetary Science Letters* **234**, 1-14.

Kinny, P. D. (1989). Archaean mantle xenocrysts in a Permian kimberlite: two generations of kimberlitic zircon in Jwaneng DK2, southern Botswana. *Kimberlites and related rocks* **14**, 833-842.

Kinny, P. D. & Friend, C. R. L. (1997). U-Pb isotopic evidence for the accretion of different crustal blocks to form the Lewisian Complex of northwest Scotland. *Contributions to Mineralogy and Petrology* **129**, 326-340.

Kinny, P. D., Griffin, B. J., Heaman, L. M., Brakhfogel, F. F. & Spetsius, Z. V. (1997). SHRIMP U-Pb ages of perovskite from Yakutian kimberlites. *Geologiya I Geofizika* **38**, 91-99.

Kita, N. T., Ushikubo, T., Fu, B. & Valley, J. W. (2009). High precision SIMS oxygen isotope analysis and the effect of sample topography. *Chemical Geology* **264**, 43-57.

Kitsul, V. I. (1986). Metamorphism. In: Dobretsov, N. L. (ed.) *Early Precambrian of South Yakutia*. Moscow: Nauka, 152-193.

Komarov, A. N. & Ilupin, I. P. (1990). Geochronology of kimberlites of the Siberian Platform by the fission-track method. *Geokhimiya* **3**, 365-372.

Konzett, J., Armstrong, R. A. & Gunther, D. (2000). Modal metasomatism in the Kaapvaal craton lithosphere: constraints on timing and genesis from U-Pb zircon dating of metasomatized peridotites and MARID-type xenoliths. *Contributions to Mineralogy and Petrology* **139**, 704-719.

Konzett, J., Armstrong, R. A., Sweeney, R. J. & Compston, W. (1998). The timing of MARID metasomatism in the Kaapvaal mantle: An ion probe study of zircons from MARID xenoliths. *Earth and Planetary Science Letters* **160**, 133-145.

Kopylova, M. G. & Russell, J. K. (2000). Chemical stratification of cratonic lithosphere: constraints from the Northern Slave craton, Canada. *Earth and Planetary Science Letters* **181**, 71-87.

Kostrovitsky, S. I., Morikiyo, T., Serov, I. V., Yakovlev, D. A. & Amirzhanov, A. A. (2007). Isotope-geochemical systematics of kimberlites and related rocks from the Siberian Platform. *Russian Geology and Geophysics* **48**, 272-290.

Kovach, V. P. (1994). Granitoid complexes of central part of Aldan granulite-gneiss area: geology and petrology. St. Petersburg.

Kovach, V. P., Kotov, A. B., Berezkin, V. I., Sal'nikova, E. B., Velikoslavinskii, S. D., Smelov, A. P. & Zagornaya, N. Y. (1999). Age limits of high-grade metamorphic supracrustal complexes in the central Aldan Shield: Sm-Nd isotopic data. *Stratigraphy and Geological Correlation* **7**, 1-14.

Krylov, I. N., Gorokhov, I. M., Kutyavin, E. P., Melnikov, N. N. & Varshavskaya, E. S. (1980). Rb/Sr dating of polymetamorphic rocks in the Sharyzhalgay Series (SW Baikalia). *Geochronology of Eastern Siberia and the Far East*. Moscow: Nauka, 80-94.

Kuskov, O. L., Kronrod, V. A., Prokof'ev, A. A. & Pavlenkova, N. I. (2014a). Petrological-geophysical models of the internal structure of the lithospheric mantle of the Siberian Craton. *Petrology* **22**, 17-44.

Kuskov, O. L., Kronrod, V. A., Prokofyev, A. A. & Pavlenkova, N. I. (2014b). Thermo-chemical structure of the lithospheric mantle underneath the Siberian craton inferred from long-range seismic profiles. *Tectonophysics* **615**, 154-166.

LeCheminant, A. N., Heaman, E. A., Kretschmar, U. & LeCouteur, P. C. (1997). Complex origin and multiple ages of mantle zircon megacrysts from Canadian and South African kimberlites. *7th International Kimberlite Conference*. University of Cape Town: University of Cape Town, South Africa, 486-488.

Levchenkov, D. A., Morozova, I. M., Drugova, G. M., Dook, V. L. & Levskii, L. K. (1987). U/Pb dating of the oldest rocks in the Aldan Shield. *Isotopic Dating of Metamorphic and Metasomatic Processes*. Moscow: Nauka Press, 116-138.

Liati, A., Franz, L., Gebauer, D. & Fanning, C. M. (2004). The timing of mantle and crustal events in South Namibia, as defined by SHRIMP-dating of zircon domains from a garnet peridotite xenolith of the Gibeon Kimberlite Province. *Journal of African Earth Sciences* **39**, 147-157.

Liu, Y., Gao, S., Hu, Z., Gao, C., Zong, K. & Wang, D. (2010). Continental and Oceanic Crust Recycling-induced Melt-Peridotite Interactions in the Trans-North China Orogen: U-Pb Dating, Hf Isotopes and Trace Elements in Zircons from Mantle Xenoliths. *Journal of Petrology* **51**, 537-571.

Lorand, J. P. & Alard, O. (2001). Platinum-group element abundances in the upper mantle: New constraints from in situ and whole-rock analyses of Massif Central xenoliths (France). Geochimica Et Cosmochimica Acta 65, 2789-2806.

Luo, Y., Gao, S., Yuan, H. L., Liu, X. M., Gunther, D., Jin, Z. M. & Sun, M. (2004). Ce anomaly in minerals of eclogite and garnet pyroxenite from Dabie-Sulu ultrahigh pressure metamorphic belt: Tacking subducted sediment formed under oxidizing conditions. Science in China Series D-Earth Sciences 47, 920-930.

Lutz, B. G. & Oksman, V. K. (1990). Severely eroded zones of Anabar Shield faults. Moscow: Nauka.

Luvizotto, G. L., Zack, T., Meyer, H. P., Ludwig, T., Triebold, S., Kronz, A., Munker, C., Stockli, D. F., Prowatke, S., Klemme, S., Jacob, D. E. & von Eynatten, H. (2009). Rutile crystals as potential trace element and isotope mineral standards for microanalysis. Chemical Geology 261, 346-369.

Malkovets, V. G., Griffin, W. L., O'Reilly, S. Y. & Wood, B. J. (2007). Diamond, subcalcic garnet, and mantle metasomatism: Kimberlite sampling patterns define the link. Geology 35, 339-342.

Malkovets, V. G., Rezvukhin, D. I., Belousova, E. A., Griffin, W. L., Sharygin, I. S., Tretiakova, I. G., Gibsher, A. A., O'Reilly, S. Y., Kuzmin, D. V., Litasov, K. D., Logvinova, A. M., Pokhilenko, N. P. & Sobolev, N. V. (2016). Cr-rich rutile: A powerful tool for diamond exploration. Lithos 265, 304-311.

Mekhonoshin, A. S. (1999). Mafic-ultramafic magmatism of the Onot greenstone belt (East Sayan). Geologiya I Geofizika 40, 1772-1784.

Metelkin, D. V., Vernikovsky, V. A. & Kazansky, A. Y. (2012). Tectonic evolution of the Siberian paleocontinent from the Neoproterozoic to the Late Mesozoic: paleomagnetic record and reconstructions. Russian Geology and Geophysics 53, 675-688.

Mitchell, R. H. (1995). Kimberlites, Orangeites, and Related Rocks: Springer My Copy UK.

Monani, S. & Valley, J. W. (2001). Oxygen isotope ratios of zircon: magma genesis of low delta O-18 granites from the British Tertiary Igneous Province, western Scotland. Earth and Planetary Science Letters 184, 377-392.

Morozova, I. M., Bogomolov, E. S., Jakovleva, S. Z., Belyatski, B. V. & Berezhnaya, N. G. (1989). U/Pb dating of granite-gneiss and tonalite-trondhjemite gneisses. In: Rudnik, V. A. (ed.) The Oldest Rocks of the Aldan-Stanovik Shield, eastern Siberia, USSR. Excursion Guide, IGCP 280. Leningrad-Mainz, 105-107.

Neymark, L. A., Larin, A. M., Nemchin, A. A., Ovchinnikova, G. V. & Rytsk, E. Y. (1998). Anorogenic nature of magmatism in the Northern Baikal volcanic belt: Evidence from geochemical, geochronological (U-Pb), and isotopic (Pb, Nd) data. Petrology 6, 124-148.

Neymark, L. A., Larin, A. M., Ovchinnikova, G. V. & Yakovleva, S. Z. (1992). U/Pb age of the Zhugzhur anorthosite. Doklady Russian Academy of Sciences 323, 514-518.

Neymark, L. A., Nemchin, A. A., Rosen, O. M., Serenko, V. P., Spetsius, Z. V. & Shuleshko, I. K. (1993). Sm-Nd Isotope Systematics of Lower Crystal Xenoliths from the Yakutian Kimberlites. Doklady Akademii Nauk 327, 374-378.

Norman, M. D., Pearson, N. J., Sharma, A. & Griffin, W. L. (1996). Quantitative analysis of trace elements in geological materials by laser ablation ICPMS: Instrumental operating conditions and calibration values of NIST glasses. Geostandards Newsletter-the Journal of Geostandards and Geoanalysis 20, 247-261.

Nowell, G. M., Pearson, D. G., Parman, S. W., Luguet, A. & Hanski, E. (2008). Precise and accurate Os-186/Os-188 and Os-187/Os-188 measurements by Multi-collector Plasma Ionisation Mass Spectrometry, part II: Laser ablation and its application to single-grain Pt-Os and Re-Os geochronology. Chemical Geology 248, 394-426.

Nozhkin, A. D. (1999). Early proterozoic margin-continental complexes of the Angara fold belt and their metallogeny. Geologiya I Geofizika 40, 1524-1544.

Nozhkin, A. D., Turkina, O. M., Bibikova, E. V. & Ponomarchuk, V. A. (2001). Structure, composition, and formation conditions of metasedimentary-volcanogenic complexes of the Kan greenstone belt (northwestern Sayan region). Geologiya I Geofizika 42, 1058-1078.

Nutman, A. P., Chernyshev, I. V., Baadsgaard, H. & Smelov, A. P. (1992a). The Aldan Shield of Siberia, Ussr - the Age of Its Archean Components and Evidence for Widespread Reworking in the Midproterozoic. Precambrian Research 54, 195-210.

Nutman, A. P., Gavrikova, S. N. & Chernyshev, I. V. (1992b). Late Archean crust formation and mid-Proterozoic reworking in the Stanovik block of the Aldan Shield, USSR. In: Glover, J. E. & Ho, S. E. (eds.) The Archaean: Terrains, Processes and Metallogeny : Proceedings Volume for the Third International Archaean Symposium Held in Perth, Western Australia, 17th to 21st September, 1990: Geology Department (Key Centre) & University Extension, The University of Western Australia, 89-92.

O'Reilly, S. Y. & Griffin, W. L. (2010). The continental lithosphere–asthenosphere boundary: Can we sample it? Lithos 120, 1-13.

Pearson, D. G., Carlson, R. W., Shirey, S. B., Boyd, F. R. & Nixon, P. H. (1995a). Stabilization of Archean Lithospheric Mantle - a Re-Os Isotope Study of Peridotite Xenoliths from the Kaapvaal Craton. Earth and Planetary Science Letters 134, 341-357.

Pearson, D. G., Kelley, S. P., Pokhilenko, N. P. & Boyd, F. R. (1997). Laser Ar-40/Ar-39 dating of phlogopites from southern African and Siberian kimberlites and their xenoliths: Constraints on eruption ages, melt degassing and mantle volatile compositions. Geologiya I Geofizika 38, 100-111.

Pearson, D. G., Parman, S. W. & Nowell, G. M. (2007). A link between large mantle melting events and continent growth seen in osmium isotopes. Nature 449, 202-205.

Pearson, D. G., Shirey, S. B., Bulanova, G. P., Carlson, R. W. & Milledge, H. J. (1999). Re-Os isotope measurements of single sulfide inclusions in a Siberian diamond and its nitrogen aggregation systematics. Geochimica Et Cosmochimica Acta 63, 703-711.

Pearson, D. G., Shirey, S. B., Carlson, R. W., Boyd, F. R., Pokhilenko, N. P. & Shimizu, N. (1995b). Re-Os, Sm-Nd, and Rb-Sr isotope evidence for thick Archaean lithospheric mantle beneath the Siberian craton modified by multistage metasomatism. Geochimica Et Cosmochimica Acta 59, 959-977.

Pearson, D. G., Snyder, G. A., Shirey, S. B., Taylor, L. A., Carlson, R. W. & Sobolev, N. V. (1995c). Archean Re-Os Age for Siberian Eclogites and Constraints on Archean Tectonics. Nature 374, 711-713.

Pearson, N. J., Alard, O., Griffin, W. L., Jackson, S. E. & O'Reilly, S. Y. (2002). In situ measurement of Re-Os isotopes in mantle sulfides by laser ablation multicollector-inductively coupled plasma mass spectrometry: Analytical methods and preliminary results. Geochimica Et Cosmochimica Acta 66, 1037-1050.

Pearson, N. J., Griffin, W. L. & O'Reilly, S. Y. (2008). Precision of in situ isotope ratio measurements by LAM-MC-ICPMS. Geochimica Et Cosmochimica Acta 72, A732-A732.

Pease, V., Gee, D. G., Vernikovsky, V., Vernikovskaya, A. & Kireev, S. (2001). Geochronological evidence for late-Grenvillian magmatic and metamorphic events in central Taimyr, northern Siberia. Terra Nova 13, 270-280.

Pernet-Fisher, J. F., Howarth, G. H., Pearson, D. G., Woodland, S., Barry, P. H., Pokhilenko, N. P., Pokhilenko, L. N., Agashev, A. M. & Taylor, L. A. (2015). Plume impingement on the Siberian SCLM: Evidence from Re-Os isotope systematics. Lithos 218, 141-154.

Petrov, A. F., Gusev, G. S., Tret'yakov, F. F. & Oksman, V. S. (1985). Archean (Aldan) and Lower Proterozoic (Karelian) Megacomplexes. Structure and evolution of the Earth's crust of Yakutia. Moscow: Nauka, 9-39.

Piazolo, S., Bestmann, M., Prior, D. J. & SpierS, C. J. (2006). Temperature dependent grain boundary migration in deformed-then-annealed material: Observations from experimentally deformed synthetic rocksalt. Tectonophysics 427, 55-71.

Pisarevsky, S. A. & Natapov, L. M. (2003). Siberia and Rodinia. Tectonophysics 375, 221-245.

Pokhilenko, L. N., Mal'kovets, V. G., Kuz'min, D. V. & Pokhilenko, N. P. (2014). New data on the mineralogy of megacrystalline pyrope peridotite from the Udachnaya kimberlite pipe, Siberian Craton, Yakutian diamondiferous province. Doklady Earth Sciences 454, 179-184.

Pokhilenko, N. P., Agashev, A. M., Litasov, K. D. & Pokhilenko, L. N. (2015). Carbonatite metasomatism of peridotite lithospheric mantle: implications for diamond formation and carbonatite-kimberlite magmatism. Russian Geology and Geophysics 56, 280-295.

Pollack, H. N. & Chapman, D. S. (1977). On the regional variation of heat flow, geotherms, and lithospheric thickness. Tectonophysics 38, 279-296.

Poller, U., Gladkochub, D., Donskaya, T., Mazukabzov, A., Sklyarov, E. & Todt, W. (2005). Multistage magmatic and metamorphic evolution in the Southern Siberian Craton: Archean and Palaeoproterozoic zircon ages revealed by SHRIMP and TIMS. Precambrian Research 136, 353-368.

Popov, N. V. & Smelov, A. P. (1996). The Aldan Shield metamorphic assemblages. Russian Geology and Geophysics 37, 138-149.

Popov, N. V., Smelov, A. P., Dobretsov, N. N., Bogomolova, L. M. & Kartavchenko, V. G. (1990). The Olondo Greenstone Belt. Yakutsk: Yakutsk Scientific Center.

Prior, D. J., Wheeler, J., Peruzzo, L., Spiess, R. & Storey, C. (2002). Some garnet micro structures: an illustration of the potential of orientation maps and misorientation analysis in microstructural studies. Journal of Structural Geology 24, 999-1011.

Puchtel, I. S., Samsonov, A. V., Simon, A. K. & Zhuravlev, D. Z. (1989). Geology, geochemistry and Sm/Nd geochronology of the oldest rocks from the Olekma granite-greenstone terrane. In: Rudnik, V. A. (ed.) The Oldest Rocks of the Aldan-Stanovik Shield, Eastern Siberia, USSR. Excursion Guide, IGCP 280. Leningrad-Mainz, 57-63.

Rainbird, R. H., Stern, R. A., Khudoley, A. K., Kropachev, A. P., Heaman, L. M. & Sukhorukov, V. I. (1998). U-Pb geochronology of Riphean sandstone and gabbro from southeast Siberia and its bearing on the Laurentia-Siberia connection. Earth and Planetary Science Letters 164, 409-420.

Reichow, M. K., Pringle, M. S., Al'Mukhamedov, A. I., Allen, M. B., Andreichev, V. L., Buslov, M. M., Davies, C. E., Fedoseev, G. S., Fitton, J. G., Inger, S., Medvedev, A. Y., Mitchell, C., Puchkov, V. N., Safonova, I. Y., Scott, R. A. & Saunders, A. D. (2009). The timing and extent of the eruption of the Siberian Traps large igneous province: Implications for the end-Permian environmental crisis. Earth and Planetary Science Letters 277, 9-20.

Romanova, I. V., Vernikovskaya, A. E., Vernikovsky, V. A., Matushkin, N. Y. & Larionov, A. N. (2012). Neoproterozoic alkaline magmatism and associated igneous rocks in the western framing of the Siberian craton: petrography, geochemistry, and geochronology. Russian Geology and Geophysics 53, 1176-1196.

Rosen, O. M. (1989). 2 Geochemically Different Types of Precambrian Crust in the Anabar Shield, North Siberia. Precambrian Research 45, 129-142.

Rosen, O. M. (1992). Geochemistry of granulites and the Archean sialic crust formation in the Anabar shield, North Siberia. High grade metamorphism. Athens, Greece: Theophrastus Publications S.A., 66-102.

Rosen, O. M. (1995). Metamorphic effects of tectonic movements at the lower crust level, Proterozoic collision zones and terranes of the Anabar shield. *Geotectonics* **29**, 91-101.

Rosen, O. M. (2003). The Siberian craton: Tectonic zonation and stages of evolution. Geotectonics 37, 175-192.

Rosen, O. M. (2011). Stabilization and breakdown of Archean Cratons: Formation of sedimentary basins, mafic magmatism, and metallogenic productivity. Geotectonics 45, 1-22.

Rosen, O. M., Bibikova, E. V. & Zhuravlev, A. B. (1991). Early crust of the Anabar Shield: age and formation models. Early Earth's Crust: the Composition and Age. Moscow: Nauka Press, 199-224.

Rosen, O. M., Condie, K. C., Natapov, L. M. & Nozhkin, A. D. (1994). Archean and Early Proterozoic evolution of the Siberian craton: a preliminary assessment. In: Condie, K. C. (ed.) Archean Crustal Evolution. Amsterdam: Elsevier Science & Technology Books, 411-459.

Rosen, O. M. & Fedorovskii, V. S. (2001). Collisional Granitoids and Stratification of the Earth Crust. Moscow: Nauchniy Mir.

Rosen, O. M., Levskii, L. K., Zhuravlev, D. Z., Rotman, A. Y., Spetsius, Z. V., Makeev, A. F., Zinchuk, N. N., Manakov, A. V. & Serenko, V. P. (2006). Paleoproterozoic accretion in the Northeast Siberian craton: Isotopic dating of the Anabar collision system. Stratigraphy and Geological Correlation 14, 581-601.

Rosen, O. M., Nozhkin, A. D. & Condie, K. C. (1993). Active margin of the Tungus protocontinent in the early Proterozoic, the earliest shoreline of the Paleoasian ocean? 4th International Symposium on Dynamic Evolution of Paleoasian Ocean. Novosibirsk: UIGGM, 117.

Rosen, O. M., Serenko, V. P., Spetsius, Z. V., Manakov, A. V. & Zinchuk, N. N. (2002). Yakutian kimberlite province: Position in the structure of the Siberian craton and composition of the upper and lower crust. Geologiya I Geofizika 43, 3-26.

Rosen, O. M., Soloviev, A. V. & Zhuravlev, D. Z. (2009). Thermal evolution of the northeastern Siberian platform in the light of apatite fission-track dating of the deep drill core. Izvestiya, Physics of the Solid Earth 45, 914-931.

Rosen, O. M., Zhuravlev, D. Z., Sukhanov, M. K., Bibikova, E. V. & Zlobin, V. L. (2000). Early Proterozoic terranes, collision zones, and associated anorthosites in the northeast of the Siberian craton: isotope geochemistry and age characteristics. Russian Geology and Geophysics 41, 163–180.

Rublev, A. G., Chukhonin, A. D., Neymark, A. P. & Zaitsev, V. S. (1981). Age of the Kodar Massif. Geology and Mineralogy of the Precambrian in Baikal-Amur Railway area. Proceedings of the All Union Geol. Institute: Ministry of Geology, 54-60.

Rudnick, R. L., McDonough, W. F. & O'Connell, R. J. (1998). Thermal structure, thickness and composition of continental lithosphere. Chemical Geology 145, 395-411.

Rumyantsev, M. Y. (2001). Petrology and geochemistry of Late Riphean island-arc complexes of northeastern Sayan. Novosibirsk, 20.

Rumyantsev, M. Y., Turkina, O. M., Nozhkin, A. D., Gracheva, T. V. & Shevchenko, D. O. (2000). New data on the age of the Shumikha Paleoisland-arc complex (East Sayan): Late Riphean-Vendian crust formation on the southwestern margin of the Siberian Platform. Geologiya I Geofizika 41, 1790-1797.

Rundkvist, D. V. & Mitrofanov, F. P. (1988). Precambrian geology of the USSR. Leningrad: Nauka.

Sablukov, S. M., Sablukova, L. I., Stegnitsky, Y. B. & Banzeruck, V. I. (2007). Lithospheric mantle characteristics of the Nakyn field in Yakutia from datas on mantle xenoliths and basalts in the Nyurbinskaya pipe. In: Vladykin, N. V. (ed.) VII International Conference "Alkaline magmatism, its cources and plume". Irkutsk - Napoli: Publishing House of the Institute of Geography SB RAS, 140-156.

Safonov, O. G., Kamenetsky, V. S. & Perchuk, L. L. (2011). Links between Carbonatite and Kimberlite Melts in Chloride-Carbonate-Silicate Systems: Experiments and Application to Natural Assemblages. Journal of Petrology 52, 1307-1331.

Sal'nikova, E. B., Kotov, A. B., Levitskii, V. I., Reznitskii, L. Z., Mel'nikov, A. I., Kozakov, I. K., Kovach, V. P., Barash, I. G. & Yakovleva, S. Z. (2007). Age constraints of high-temperature metamorphic events in crystalline complexes of the Irkut block, the Sharyzhalgai ledge of the Siberian platform basement: Results of the U-Pb single zircon dating. Stratigraphy and Geological Correlation 15, 343-358.

Sambridge, M. & Lambert, D. D. (1997). Propagating errors in decay equations: Examples from the Re-Os isotopic system. Geochimica Et Cosmochimica Acta 61, 3019-3024.

Saunders, A. & Reichow, M. (2009). The Siberian Traps and the End-Permian mass extinction: a critical review. Chinese Science Bulletin 54, 20-37.

Scherer, E., Munker, C. & Mezger, K. (2001). Calibration of the lutetium-hafnium clock. Science 293, 683-687.

Schreiber, H. D., Lauer, H. V., Jr. & Thanyasiri, T. (1980). The redox state of cerium in basaltic magmas: an experimental study of iron-cerium interactions in silicate melts. Geochimica Et Cosmochimica Acta 44, 1599-1612.

Semikhatov, M. A., Ovchinnikova, G. V., Gorokhov, I. M., Kuznetsov, A. B., Vasil'eva, I. M., Gorokhovskii, B. M. & Podkovyrov, V. N. (2000). Isotope age of the Middle-Upper Riphean boundary: Pb-Pb geochronology of the Lakhanda Group carbonates, Eastern Siberia. Doklady Earth Sciences 372, 625-629.

Sharkov, E. V., Bogina, M. M., Quick, J. E. & Mekhonoshin, A. S. (1995). Tectonic blocks of the Precambrian lower crust and upper mantle, Southern Sayan mountains, East Siberia. International Geology Review 37, 81-91.

Shepel, A. B. (1980). K/Ar age of phlogopites in scarn-magnetite deposits of the Aldan Shield and its geological interpretation. Geochronology of East Siberia. Moscow: Nauka, 38-47.

Shi, R. D., Alard, O., Zhi, X. C., O'Reilly, S. Y., Pearson, N. J., Griffin, W. L., Zhang, M. & Chen, X. M. (2007). Multiple events in the Neo-Tethyan oceanic upper mantle: Evidence from Ru-Os-Ir alloys in the Luobusa and Dongqiao ophiolitic podiform chromitites, Tibet. Earth and Planetary Science Letters 261, 33-48.

Shirey, S. B., Carlson, R. W., Richardson, S. H., Menzies, A., Gurney, J. J., Pearson, D. G., Harris, J. W. & Wiechert, U. (2001). Archean emplacement of eclogitic components into the lithospheric mantle during formation of the Kaapvaal Craton. Geophysical Research Letters 28, 2509-2512.

Shuldiner, V. I. & Panchenko, I. V. (1985). Isotopic age of granulites in the western Stanovoy area and its geological meaning. Geologiya I Geofizika 11, 39-45.

Simonetti, A. & Neal, C. R. (2010). In-situ chemical, U-Pb dating, and Hf isotope investigation of megacrystic zircons, Malaita (Solomon Islands): Evidence for multi-stage alkaline magmatic activity beneath the Ontong Java Plateau. Earth and Planetary Science Letters 295, 251-261.

Skinner, E. M. W. (1986). Contrasting Group 1 and 2 kimberlite petrology: Towards a genetic model for kimberlites. Fourth International Kimberlite Conference. Perth, Australia, 202-204.

Sklyarov, E. V., Gladkochub, D. P., Mazukabzov, A. M. & Men'shagin, Y. A. (1998). Metamorphism of the ancient ophiolites of the Sharyzhalgai massif. Geologiya I Geofizika 39, 1733-1749.

Smelov, A. P. & Timofeev, V. F. (2007). The age of the North Asian Cratonic basement: An overview. Gondwana Research 12, 279-288.

Smelov, A. P. & Zaitsev, A. I. (2013). The Age and Localization of Kimberlite Magmatism in the Yakutian Kimberlite Province: Constraints from Isotope Geochronology—An Overview. In: Pearson, D. G., Grütter, H. S., Harris, J. W., Kjarsgaard, B. A., O'Brien, H., Rao, N. V. C. & Sparks, S. (eds.) Proceedings of 10th International Kimberlite Conference: Springer India, 225-234.

Smelov, A. P., Zedgenizov, A. N., Parfenov, L. M. & Timofeev, V. F. (1998). Precambian terranes of Aldan-Stanovoi Shield. Metallogeny, petroleum potential, and geodynamics of North-Asian Craton and adjacent orogenic belts. Irkutsk: Santai, 119-120.

Smith, C. B. (1983). Pb, Sr and Nd isotopic evidence for sources of southern African Cretaceous kimberlites. Nature 304, 51-54.

Smith, C. B., Gurney, J. J., Skinner, E. M. W., Clement, C. R. & Ebrahim, N. (1985). Geochemical character of southern African kimberlites: a new approach based on isotopic constraints. Transactions of the Geological Society of South Africa 88, 267-280.

Sobolev, N. V. (1977). Deep-Seated Inclusions in Kimberlites and the Problem of the Composition of the Upper Mantle: Wiley-Blackwell.

Spiridonov, V. G., Sukhanov, M. K., Karpenko, S. F. & Lyalikov, A. V. (1991). Sm-Nd Isotope System of Oldest Granulites of Anabar Shield. Doklady Akademii Nauk Sssr 319, 1209-1212.

Stacey, J. S. & Kramers, J. D. (1975). Approximation of terrestrial lead isotope evolution by a two-stage model. Earth and Planetary Science Letters 26, 207-221.

Stepanov, L. L. (1974). Radiogenic age of polymetamorphic rocks in the Anabar Shield. Early Precambrian Rocks and Related Ore Deposits of the Central Arctic. Leningrad: Nauka, 77-84.

Stern, R. A., Bodorkos, S., Kamo, S. L., Hickman, A. H. & Corfu, F. (2009). Measurement of SIMS Instrumental Mass Fractionation of Pb Isotopes During Zircon Dating. Geostandards and Geoanalytical Research 33, 145-168.

Sukhanov, M. K. & Rachkov, V. S. (1988). Anorthosites and related rocks. In: Markov, M. S. (ed.) Archean of the Anabar Shield and Problems of Early Evolution of the Earth. Moscow: Nauka, 62-83.

Sukhanov, M. K., Spiridonov, V. G. & Karpenko, S. F. (1990). 1st Dating Results of the Anabar Shield Anorthosites by the Sm-Nd Isochrone Method. Doklady Akademii Nauk Sssr 310, 448-453.

Tauson, L. V., Sobachenko, V. N., Pliusnin, G. S., Sandimirova, G. P., Nikolaev, V. M., Pakholchenko, I. A. & Rekhviashvili, O. I. (1983). The Rubidium-Strontium Age of Rapakivi-Like Granites and Metasomatites in the Katugino-Aianskaia Zone (Northeast Transbaikalia). Doklady Akademii Nauk Sssr 273, 1233-1236.

Turkina, O. M., Berezhnaya, N. G., Lepekhina, E. N. & Kapitonov, I. N. (2012). U-Pb (SHRIMP II), Lu-Hf isotope and trace element geochemistry of zircons from high-grade metamorphic rocks of the Irkut terrane, Sharyzhalgay Uplift: Implications for the Neoarchaean evolution of the Siberian Craton. Gondwana Research 21, 801-817.

Valley, J. W. (2003). Oxygen isotopes in zircon. Zircon 53, 343-385.

Valley, J. W., Bindeman, I. N. & Peck, W. H. (2003). Empirical calibration of oxygen isotope fractionation in zircon. Geochimica Et Cosmochimica Acta 67, 3257-3266.

Vernikovskaya, A. E., Vernikovsky, V. A., Matushkin, N. Y., Romanova, I. V., Berejnaya, N. G., Larionov, A. N. & Travin, A. V. (2010). Middle Paleozoic and Early Mesozoic anorogenic magmatism of the South Yenisei Ridge: first geochemical and geochronological data. Russian Geology and Geophysics 51, 548-562.

Vernikovsky, V. A. (1996). Geodynamic evolution of Taimyr folded area. Novosibirsk: Publishing House SB RAS.

Vernikovsky, V. A., Metelkin, D. V., Vernikovskaya, A. E., Matushkin, N. Y., Kazansky, A. Y., Kadilnikov, P. I., Romanova, I. V., Wingate, M. T. D., Larionov, A. N. & Rodionov, N. V. (2016). Neoproterozoic tectonic structure of the Yenisei Ridge and formation of the western margin of the Siberian craton based on new geological, paleomagnetic, and geochronological data. Russian Geology and Geophysics 57, 47-68.

Vernikovsky, V. A., Vernikovskaya, A. E., Pease, V. L. & Gee, D. G. (2004). Neoproterozoic Orogeny along the margins of Siberia. Geological Society, London, Memoirs 30, 233-248.

Vernikovsky, V. A., Vernikovskaya, A. E., Sal'nikova, E. B., Kotov, A. B., Chernykh, A. I., Kovach, V. P., Berezhnaya, N. G. & Yakovleva, S. Z. (1999). New U-Pb data on the formation of the Predivinsk paleoisland-arc complex (Yenisei Ridge). Geologiya I Geofizika 40, 255-259.

Vernikovsky, V. A., Vernikovskaya, A. E., Wingate, M. T. D., Popov, N. V. & Kovach, V. P. (2007). The 880-864 Ma granites of the Yenisey Ridge, western Siberian margin: Geochemistry, SHRIMP geochronology, and tectonic implications. Precambrian Research 154, 175-191.

Walker, R. J., Horan, M. F., Morgan, J. W., Becker, H., Grossman, J. N. & Rubin, A. E. (2002). Comparative Re-187-Os-187 systematics of chondrites: Implications regarding early solar system processes. Geochimica Et Cosmochimica Acta 66, 4187-4201.

Wang, X., Griffin, W. L., Chen, J., Huang, P. & Li, X. (2011). U and Th contents and Th/U ratios of zircon in felsic and mafic magmatic rocks : improved zircon-melt distribution coefficients.

Whitehouse, M. J. & Kamber, B. S. (2002). On the overabundance of light rare earth elements in terrestrial zircons and its implication for Earth's earliest magmatic differentiation. Earth and Planetary Science Letters 204, 333-346.

Wiedenbeck, M., Alle, P., Corfu, F., Griffin, W. L., Meier, M., Oberli, F., Vonquadt, A., Roddick, J. C. & Speigel, W. (1995). 3 Natural Zircon Standards for U-Th-Pb, Lu-Hf, Trace-Element and Ree Analyses. Geostandards Newsletter 19, 1-23.

Wingate, M. T. D., Pisarevsky, S. A., Gladkochub, D. P., Donskaya, T. V., Konstantinov, K. M., Mazukabzov, A. M. & Stanevich, A. M. (2009). Geochronology and paleomagnetism of mafic igneous rocks in the Olenek Uplift, northern Siberia: Implications for Mesoproterozoic supercontinents and paleogeography. Precambrian Research 170, 256-266.

Woodhead, J. D. & Hergt, J. M. (2005). A preliminary appraisal of seven natural zircon reference materials for in situ Hf isotope determination. Geostandards and Geoanalytical Research 29, 183-195.

Yanshin, A. L. & Borukaev, C. B. (1988). Tectonics and evolution of the Earth’s crust in Siberia: Nauka.

Yarmolyuk, V. V. & Kovalenko, V. I. (2001). Late Riphean breakup between Siberia and Laurentia: Evidence from intraplate magmatism. Doklady Earth Sciences 379, 525-528.

Yaxley, G. M., Kamenetsky, V. S., Nichols, G. T., Maas, R., Belousova, E., Rosenthal, A. & Norman, M. (2013). The discovery of kimberlites in Antarctica extends the vast Gondwanan Cretaceous province. Nature Communications 4.

Zack, T., Stockli, D. F., Luvizotto, G. L., Barth, M. G., Belousova, E., Wolfe, M. R. & Hinton, R. W. (2011). In situ U-Pb rutile dating by LA-ICP-MS: Pb-208 correction and prospects for geological applications. Contributions to Mineralogy and Petrology 162, 515-530.

Zaitsev, A. I. & Smelov, A. P. (2010). Isotope geochronology of rocks of kimberlite formation in the Yakutian province. Yakutsk: DPMGI SB RAS.

Zheng, J. P., Griffin, W. L., O'Reilly, S. Y., Lu, F. X., Yu, C. M., Zhang, M. & Li, H. M. (2004). U-Pb and Hf-isotope analysis of zircons in mafic xenoliths from Fuxian kimberlites: evolution of the lower crust beneath the North China craton. *Contributions to Mineralogy and Petrology* **148**, 79-103.

Zonenshain, L. P., Kuz'min, V. I. & Natapov, L. M. (1989). Geology of the USSR, a plate tectonic synthesis.

**Appendix 1.1. Zircon U-Pb age data for 91500 and MudTank standards obtained during this study**

| Analysis No. | RATIOS | | | | | | | | AGES (Ma) | | | | | | | | | | CONCENTRATIONS (ppm) | |
|---|---|---|---|---|---|---|---|---|---|---|---|---|---|---|---|---|---|---|---|---|
| | $^{207}Pb/^{206}Pb$ | ± 2σ | $^{207}Pb/^{235}U$ | ± 2σ | $^{206}Pb/^{238}U$ | ± 2σ | $^{208}Pb/^{232}Th$ | ± 2σ | $^{207}Pb/^{206}Pb$ | ± 2σ | $^{207}Pb/^{235}U$ | ± 2σ | $^{206}Pb/^{238}U$ | ± 2σ | $^{208}Pb/^{232}Th$ | ± 2σ | Used Age | ± 2σ | Th | U |
| 91500-001 | 0.07425 | 0.00234 | 1.84554 | 0.06012 | 0.18030 | 0.00456 | 0.05536 | 0.00282 | 1048 | 66 | 1062 | 22 | 1069 | 24 | 1089 | 54 | 1048 | 66 | 29.98 | 79.20 |
| 91500-002 | 0.07506 | 0.00222 | 1.81993 | 0.05710 | 0.17585 | 0.00446 | 0.05258 | 0.00250 | 1070 | 60 | 1053 | 20 | 1044 | 24 | 1036 | 48 | 1070 | 60 | 39.65 | 104.07 |
| 91500-003 | 0.07529 | 0.00228 | 1.84841 | 0.05884 | 0.17806 | 0.00450 | 0.05244 | 0.00256 | 1076 | 62 | 1063 | 20 | 1056 | 24 | 1033 | 50 | 1076 | 62 | 32.69 | 87.62 |
| 91500-004 | 0.07431 | 0.00218 | 1.79273 | 0.05566 | 0.17500 | 0.00440 | 0.05354 | 0.00254 | 1050 | 60 | 1043 | 20 | 1040 | 24 | 1054 | 48 | 1050 | 60 | 33.34 | 94.33 |
| 91500-005 | 0.07515 | 0.00224 | 1.84662 | 0.05848 | 0.17820 | 0.00452 | 0.05347 | 0.00244 | 1073 | 62 | 1062 | 20 | 1057 | 24 | 1053 | 46 | 1073 | 62 | 30.13 | 86.80 |
| 91500-006 | 0.07508 | 0.00228 | 1.82003 | 0.05782 | 0.17580 | 0.00438 | 0.05369 | 0.00264 | 1071 | 62 | 1053 | 20 | 1044 | 24 | 1057 | 50 | 1071 | 62 | 33.14 | 89.09 |
| 91500-007 | 0.07527 | 0.00232 | 1.84270 | 0.05936 | 0.17757 | 0.00446 | 0.05396 | 0.00260 | 1076 | 64 | 1061 | 22 | 1054 | 24 | 1062 | 50 | 1076 | 64 | 29.76 | 85.78 |
| 91500-008 | 0.07495 | 0.00230 | 1.83792 | 0.05726 | 0.17782 | 0.00426 | 0.05228 | 0.00258 | 1067 | 64 | 1059 | 20 | 1055 | 24 | 1030 | 50 | 1067 | 64 | 33.98 | 90.26 |
| 91500-009 | 0.07465 | 0.00236 | 1.82135 | 0.05992 | 0.17699 | 0.00448 | 0.05437 | 0.00268 | 1059 | 66 | 1053 | 22 | 1051 | 24 | 1070 | 52 | 1059 | 66 | 29.09 | 84.06 |
| 91500-010 | 0.07438 | 0.00248 | 1.82609 | 0.06082 | 0.17808 | 0.00428 | 0.05376 | 0.00292 | 1052 | 68 | 1055 | 22 | 1056 | 24 | 1058 | 56 | 1052 | 68 | 31.63 | 84.92 |
| 91500-011 | 0.07552 | 0.00220 | 1.87105 | 0.05846 | 0.17971 | 0.00456 | 0.05383 | 0.00238 | 1082 | 60 | 1071 | 20 | 1065 | 24 | 1060 | 46 | 1082 | 60 | 29.77 | 87.30 |
| 91500-012 | 0.07411 | 0.00262 | 1.80512 | 0.06308 | 0.17667 | 0.00426 | 0.05097 | 0.00304 | 1044 | 72 | 1047 | 22 | 1049 | 24 | 1005 | 58 | 1044 | 72 | 36.86 | 97.39 |
| 91500-013 | 0.07436 | 0.00220 | 1.78224 | 0.05568 | 0.17386 | 0.00436 | 0.05131 | 0.00228 | 1051 | 60 | 1039 | 20 | 1033 | 24 | 1011 | 44 | 1051 | 60 | 28.65 | 86.15 |
| 91500-014 | 0.07389 | 0.00296 | 1.90274 | 0.07456 | 0.18675 | 0.00460 | 0.05517 | 0.00386 | 1038 | 82 | 1082 | 26 | 1104 | 24 | 1085 | 74 | 1038 | 82 | 34.10 | 91.73 |
| 91500-015 | 0.07416 | 0.00670 | 1.92844 | 0.16696 | 0.18863 | 0.00692 | 0.06178 | 0.00994 | 1046 | 186 | 1091 | 58 | 1114 | 38 | 1212 | 190 | 1046 | 186 | 8.93 | 24.46 |
| 91500-016 | 0.07571 | 0.00284 | 1.84640 | 0.06944 | 0.17690 | 0.00454 | 0.05147 | 0.00316 | 1087 | 76 | 1062 | 24 | 1050 | 24 | 1014 | 60 | 1087 | 76 | 25.29 | 75.04 |
| 91500-017 | 0.07473 | 0.00334 | 1.87171 | 0.08066 | 0.18165 | 0.00456 | 0.05332 | 0.00430 | 1061 | 92 | 1071 | 28 | 1076 | 24 | 1050 | 82 | 1061 | 92 | 27.50 | 73.64 |
| 91500-018 | 0.07485 | 0.00172 | 1.88018 | 0.04622 | 0.18221 | 0.00410 | 0.05511 | 0.00136 | 1064 | 48 | 1074 | 16 | 1079 | 22 | 1084 | 26 | 1064 | 48 | 33.58 | 84.21 |
| 91500-019 | 0.07430 | 0.00240 | 1.79617 | 0.05586 | 0.17539 | 0.00278 | 0.05605 | 0.00242 | 1050 | 66 | 1044 | 20 | 1042 | 16 | 1102 | 46 | 1050 | 66 | 33.08 | 88.74 |
| 91500-020 | 0.07445 | 0.00206 | 1.83391 | 0.05468 | 0.17864 | 0.00450 | 0.05161 | 0.00168 | 1054 | 58 | 1058 | 20 | 1060 | 24 | 1017 | 32 | 1054 | 58 | 33.81 | 91.26 |
| 91500-021 | 0.07594 | 0.00320 | 1.87046 | 0.07558 | 0.17866 | 0.00336 | 0.05308 | 0.00322 | 1093 | 86 | 1071 | 26 | 1060 | 18 | 1045 | 62 | 1093 | 86 | 34.89 | 92.60 |
| 91500-022 | 0.07490 | 0.00264 | 1.84196 | 0.06472 | 0.17839 | 0.00438 | 0.05398 | 0.00250 | 1066 | 72 | 1061 | 24 | 1058 | 24 | 1063 | 48 | 1066 | 72 | 34.90 | 93.51 |
| 91500-023 | 0.07390 | 0.00166 | 1.76540 | 0.03780 | 0.17328 | 0.00228 | 0.05267 | 0.00160 | 1039 | 46 | 1033 | 14 | 1030 | 12 | 1037 | 30 | 1039 | 46 | 38.22 | 100.52 |
| 91500-024 | 0.07385 | 0.00192 | 1.80083 | 0.04422 | 0.17686 | 0.00238 | 0.05458 | 0.00198 | 1037 | 54 | 1046 | 16 | 1050 | 14 | 1074 | 38 | 1037 | 54 | 37.62 | 101.49 |
| 91500-025 | 0.07480 | 0.00188 | 1.81147 | 0.04660 | 0.17566 | 0.00386 | 0.05483 | 0.00154 | 1063 | 52 | 1050 | 16 | 1043 | 22 | 1079 | 30 | 1063 | 52 | 39.81 | 108.53 |
| 91500-026 | 0.07356 | 0.00258 | 1.78690 | 0.06258 | 0.17619 | 0.00426 | 0.05422 | 0.00248 | 1029 | 72 | 1041 | 22 | 1046 | 24 | 1067 | 48 | 1029 | 72 | 43.36 | 110.83 |
| 91500-027 | 0.07421 | 0.00318 | 1.83574 | 0.07808 | 0.17945 | 0.00490 | 0.05497 | 0.00316 | 1047 | 88 | 1058 | 28 | 1064 | 26 | 1082 | 60 | 1047 | 88 | 41.79 | 111.13 |
| 91500-028 | 0.07522 | 0.00300 | 1.84861 | 0.07194 | 0.17830 | 0.00440 | 0.05399 | 0.00290 | 1074 | 82 | 1063 | 26 | 1058 | 24 | 1063 | 56 | 1074 | 82 | 45.04 | 120.83 |
| 91500-029 | 0.07383 | 0.00208 | 1.80313 | 0.05040 | 0.17714 | 0.00389 | 0.05264 | 0.00184 | 1037 | 56 | 1047 | 18 | 1051 | 21 | 1037 | 35 | 1037 | 56 | 45.85 | 122.27 |
| 91500-030 | 0.07521 | 0.00194 | 1.86702 | 0.04858 | 0.18006 | 0.00392 | 0.05460 | 0.00162 | 1074 | 54 | 1069 | 18 | 1067 | 22 | 1075 | 32 | 1074 | 54 | 58.14 | 479.07 |
| 91500-031 | 0.07608 | 0.00186 | 1.88394 | 0.04702 | 0.17960 | 0.00390 | 0.05480 | 0.00158 | 1097 | 50 | 1075 | 16 | 1065 | 22 | 1078 | 30 | 1097 | 50 | 61.29 | 508.76 |
| 91500-032 | 0.07463 | 0.00288 | 1.83149 | 0.06872 | 0.17801 | 0.00426 | 0.05312 | 0.00352 | 1059 | 80 | 1057 | 24 | 1056 | 24 | 1046 | 68 | 1059 | 80 | 30.65 | 81.48 |
| 91500-033 | 0.07574 | 0.00358 | 1.83037 | 0.08526 | 0.17528 | 0.00474 | 0.05324 | 0.00404 | 1088 | 96 | 1056 | 30 | 1041 | 26 | 1048 | 78 | 1088 | 96 | 29.03 | 78.03 |
| 91500-034 | 0.07515 | 0.00280 | 1.79763 | 0.06676 | 0.17352 | 0.00436 | 0.05345 | 0.00250 | 1073 | 76 | 1045 | 24 | 1031 | 24 | 1052 | 48 | 1073 | 76 | 30.15 | 81.15 |
| 91500-035 | 0.07498 | 0.00226 | 1.87518 | 0.06012 | 0.18139 | 0.00466 | 0.05521 | 0.00208 | 1068 | 62 | 1072 | 22 | 1075 | 26 | 1086 | 40 | 1068 | 62 | 31.66 | 84.59 |
| 91500-036 | 0.07540 | 0.00168 | 1.83695 | 0.03836 | 0.17671 | 0.00214 | 0.05295 | 0.00156 | 1079 | 46 | 1059 | 14 | 1049 | 12 | 1043 | 30 | 1079 | 46 | 31.77 | 84.97 |
| 91500-037 | 0.07594 | 0.00326 | 1.90191 | 0.07812 | 0.18164 | 0.00346 | 0.05451 | 0.00332 | 1093 | 88 | 1082 | 28 | 1076 | 18 | 1073 | 64 | 1093 | 88 | 32.33 | 86.87 |
| 91500-038 | 0.07985 | 0.00292 | 1.94568 | 0.06806 | 0.17675 | 0.00306 | 0.05516 | 0.00280 | 1193 | 74 | 1097 | 24 | 1049 | 16 | 1085 | 54 | 1193 | 74 | 32.97 | 88.66 |
| 91500-039 | 0.07503 | 0.00150 | 1.86839 | 0.03584 | 0.18063 | 0.00230 | 0.05465 | 0.00150 | 1069 | 42 | 1070 | 12 | 1070 | 12 | 1075 | 28 | 1069 | 42 | 35.70 | 91.86 |

| Analysis No. | RATIOS | | | | | | | | AGES (Ma) | | | | | | | | | | CONCENTRATIONS (ppm) | |
|---|---|---|---|---|---|---|---|---|---|---|---|---|---|---|---|---|---|---|---|---|
| | $^{207}Pb/^{206}Pb$ | ± 2σ | $^{207}Pb/^{235}U$ | ± 2σ | $^{206}Pb/^{238}U$ | ± 2σ | $^{208}Pb/^{232}Th$ | ± 2σ | $^{207}Pb/^{206}Pb$ | ± 2σ | $^{207}Pb/^{235}U$ | ± 2σ | $^{206}Pb/^{238}U$ | ± 2σ | $^{208}Pb/^{232}Th$ | ± 2σ | Used Age | ± 2σ | Th | U |
| 91500-040 | 0.07490 | 0.00322 | 1.84209 | 0.07724 | 0.17836 | 0.00462 | 0.05491 | 0.00314 | 1066 | 88 | 1061 | 28 | 1058 | 26 | 1080 | 60 | 1066 | 88 | 37.26 | 95.75 |
| 91500-041 | 0.07374 | 0.00230 | 1.79561 | 0.05580 | 0.17663 | 0.00410 | 0.05324 | 0.00204 | 1034 | 64 | 1044 | 20 | 1049 | 22 | 1048 | 40 | 1034 | 64 | 36.57 | 96.61 |
| 91500-042 | 0.07444 | 0.00198 | 1.82441 | 0.04780 | 0.17776 | 0.00379 | 0.05383 | 0.00166 | 1053 | 54 | 1054 | 17 | 1055 | 21 | 1060 | 32 | 1053 | 54 | 39.53 | 100.58 |
| 91500-043 | 0.07472 | 0.00160 | 1.85195 | 0.04342 | 0.17978 | 0.00404 | 0.05532 | 0.00114 | 1061 | 44 | 1064 | 16 | 1066 | 22 | 1088 | 22 | 1061 | 44 | 38.22 | 101.25 |
| 91500-044 | 0.07567 | 0.00292 | 1.85407 | 0.06970 | 0.17772 | 0.00432 | 0.05258 | 0.00272 | 1086 | 80 | 1065 | 24 | 1055 | 24 | 1036 | 52 | 1086 | 80 | 45.10 | 116.99 |
| 91500-045 | 0.07465 | 0.00188 | 1.82441 | 0.04714 | 0.17728 | 0.00392 | 0.05445 | 0.00156 | 1059 | 52 | 1054 | 16 | 1052 | 22 | 1072 | 30 | 1059 | 52 | 47.32 | 125.24 |
| 91500-046 | 0.07486 | 0.00190 | 1.82922 | 0.04626 | 0.17724 | 0.00378 | 0.05322 | 0.00154 | 1065 | 52 | 1056 | 16 | 1052 | 20 | 1048 | 30 | 1065 | 52 | 57.38 | 472.27 |
| 91500-047 | 0.07421 | 0.00188 | 1.81819 | 0.04576 | 0.17771 | 0.00376 | 0.05345 | 0.00156 | 1047 | 52 | 1052 | 16 | 1054 | 20 | 1052 | 30 | 1047 | 52 | 58.33 | 484.64 |
| 91500-048 | 0.07694 | 0.01918 | 1.86825 | 0.61174 | 0.17611 | 0.00314 | 0.05362 | 0.01970 | 1120 | 52 | 1070 | 26 | 1046 | 18 | 1056 | 37 | 1120 | 52 | 31.60 | 83.19 |
| 91500-049 | 0.07388 | 0.00276 | 1.81095 | 0.06762 | 0.17784 | 0.00448 | 0.05546 | 0.00264 | 1038 | 78 | 1049 | 24 | 1055 | 24 | 1091 | 50 | 1038 | 78 | 31.11 | 83.81 |
| 91500-050 | 0.07397 | 0.00472 | 1.83052 | 0.11036 | 0.17963 | 0.00458 | 0.05778 | 0.00518 | 1041 | 132 | 1056 | 40 | 1065 | 26 | 1135 | 98 | 1041 | 132 | 36.28 | 97.17 |
| 91500-051 | 0.07578 | 0.00166 | 1.88933 | 0.04542 | 0.18085 | 0.00410 | 0.05734 | 0.00126 | 1089 | 44 | 1077 | 16 | 1072 | 22 | 1127 | 24 | 1089 | 44 | 36.58 | 97.91 |
| 91500-052 | 0.07450 | 0.00214 | 1.89244 | 0.05926 | 0.18424 | 0.00478 | 0.05560 | 0.00184 | 1055 | 60 | 1078 | 20 | 1090 | 26 | 1094 | 36 | 1055 | 60 | 37.80 | 98.97 |
| 91500-053 | 0.07456 | 0.00286 | 1.84438 | 0.06916 | 0.17942 | 0.00432 | 0.05502 | 0.00270 | 1057 | 80 | 1061 | 24 | 1064 | 24 | 1083 | 52 | 1057 | 80 | 41.32 | 107.86 |
| 91500-054 | 0.07460 | 0.00196 | 1.84656 | 0.05048 | 0.17953 | 0.00412 | 0.05701 | 0.00174 | 1058 | 54 | 1062 | 18 | 1064 | 22 | 1121 | 34 | 1058 | 54 | 39.49 | 109.56 |
| 91500-055 | 0.07681 | 0.00300 | 1.88966 | 0.07328 | 0.17844 | 0.00454 | 0.05469 | 0.00284 | 1116 | 80 | 1077 | 26 | 1058 | 24 | 1076 | 54 | 1116 | 80 | 44.49 | 113.20 |
| 91500-056 | 0.07421 | 0.00209 | 1.83649 | 0.05186 | 0.17949 | 0.00400 | 0.05443 | 0.00183 | 1047 | 56 | 1059 | 19 | 1064 | 22 | 1071 | 35 | 1047 | 56 | 43.43 | 113.67 |
| 91500-057 | 0.07427 | 0.00194 | 1.84534 | 0.04616 | 0.18025 | 0.00258 | 0.05470 | 0.00210 | 1049 | 54 | 1062 | 16 | 1068 | 14 | 1076 | 40 | 1049 | 54 | 46.31 | 122.31 |
| 91500-058 | 0.07424 | 0.00302 | 1.75383 | 0.06864 | 0.17134 | 0.00416 | 0.04275 | 0.00238 | 1048 | 84 | 1029 | 26 | 1019 | 22 | 846 | 46 | 1048 | 84 | 50.41 | 130.66 |
| 91500-059 | 0.07466 | 0.00234 | 1.88700 | 0.05760 | 0.18332 | 0.00406 | 0.05669 | 0.00214 | 1059 | 64 | 1077 | 20 | 1085 | 22 | 1115 | 40 | 1059 | 64 | 46.68 | 372.03 |
| 91500-060 | 0.07487 | 0.00256 | 1.85214 | 0.06538 | 0.17943 | 0.00470 | 0.05332 | 0.00234 | 1065 | 70 | 1064 | 24 | 1064 | 26 | 1050 | 44 | 1065 | 70 | 29.86 | 80.53 |
| 91500-061 | 0.07558 | 0.00186 | 1.86467 | 0.02414 | 0.17897 | 0.00142 | 0.05494 | 0.00192 | 1084 | 50 | 1069 | 8 | 1061 | 8 | 1081 | 36 | 1084 | 50 | 31.08 | 81.95 |
| 91500-062 | 0.07490 | 0.00229 | 1.84301 | 0.05513 | 0.17850 | 0.00394 | 0.05387 | 0.00204 | 1066 | 61 | 1061 | 20 | 1059 | 22 | 1061 | 39 | 1066 | 61 | 36.94 | 94.81 |
| 91500-063 | 0.07573 | 0.00164 | 1.85422 | 0.04376 | 0.17760 | 0.00398 | 0.05533 | 0.00116 | 1088 | 44 | 1065 | 16 | 1054 | 22 | 1088 | 22 | 1088 | 44 | 37.70 | 102.06 |
| 91500-064 | 0.07493 | 0.00292 | 1.83242 | 0.06986 | 0.17739 | 0.00434 | 0.05537 | 0.00292 | 1067 | 80 | 1057 | 26 | 1053 | 24 | 1089 | 56 | 1067 | 80 | 41.78 | 108.54 |
| 91500-065 | 0.07557 | 0.00182 | 1.86395 | 0.04296 | 0.17892 | 0.00246 | 0.05536 | 0.00188 | 1084 | 50 | 1068 | 16 | 1061 | 14 | 1089 | 36 | 1084 | 50 | 41.45 | 109.29 |
| 91500-066 | 0.07588 | 0.00304 | 1.85757 | 0.07370 | 0.17756 | 0.00458 | 0.05509 | 0.00294 | 1092 | 82 | 1066 | 26 | 1054 | 26 | 1084 | 56 | 1092 | 82 | 42.53 | 110.07 |
| 91500-067 | 0.07424 | 0.00196 | 1.83286 | 0.05044 | 0.17907 | 0.00414 | 0.05772 | 0.00178 | 1048 | 54 | 1057 | 18 | 1062 | 22 | 1134 | 34 | 1048 | 54 | 46.43 | 128.17 |
| 91500-068 | 0.07527 | 0.00186 | 1.85548 | 0.04586 | 0.17879 | 0.00380 | 0.05378 | 0.00148 | 1076 | 50 | 1065 | 16 | 1060 | 20 | 1059 | 28 | 1076 | 50 | 55.76 | 459.70 |
| 91500-069 | 0.07428 | 0.00360 | 1.84222 | 0.08526 | 0.17989 | 0.00370 | 0.05627 | 0.00374 | 1049 | 100 | 1061 | 30 | 1066 | 20 | 1106 | 72 | 1049 | 100 | 31.18 | 83.04 |
| 91500-070 | 0.07524 | 0.00264 | 1.86877 | 0.06298 | 0.18013 | 0.00404 | 0.05199 | 0.00218 | 1075 | 72 | 1070 | 22 | 1068 | 22 | 1024 | 42 | 1075 | 72 | 33.88 | 85.42 |
| 91500-071 | 0.07496 | 0.00254 | 1.91604 | 0.06776 | 0.18538 | 0.00492 | 0.05458 | 0.00238 | 1067 | 70 | 1087 | 24 | 1096 | 26 | 1074 | 46 | 1067 | 70 | 32.76 | 87.37 |
| 91500-072 | 0.07583 | 0.00182 | 1.85515 | 0.02382 | 0.17747 | 0.00144 | 0.05599 | 0.00188 | 1091 | 50 | 1065 | 8 | 1053 | 8 | 1101 | 36 | 1091 | 50 | 33.61 | 88.51 |
| 91500-073 | 0.07438 | 0.00137 | 1.60599 | 0.02897 | 0.15656 | 0.00309 | 1.60599 | 0.02897 | 1052 | 37 | 973 | 11 | 938 | 17 | 973 | 11 | 1052 | 37 | 36.87 | 97.78 |
| 91500-074 | 0.07400 | 0.00314 | 1.83701 | 0.06500 | 0.18005 | 0.00418 | 0.05430 | 0.00128 | 1041 | 88 | 1059 | 24 | 1067 | 22 | 1069 | 24 | 1041 | 88 | 38.68 | 106.03 |
| 91500-075 | 0.07546 | 0.00162 | 1.88358 | 0.04480 | 0.18106 | 0.00412 | 0.05510 | 0.00116 | 1081 | 44 | 1075 | 16 | 1073 | 22 | 1084 | 22 | 1081 | 44 | 41.21 | 106.44 |
| 91500-076 | 0.07471 | 0.00165 | 1.85676 | 0.04426 | 0.18026 | 0.00403 | 0.05529 | 0.00125 | 1061 | 44 | 1066 | 16 | 1068 | 22 | 1088 | 24 | 1061 | 44 | 41.43 | 109.67 |
| 91500-077 | 0.07574 | 0.00156 | 1.86878 | 0.03680 | 0.17897 | 0.00228 | 0.05314 | 0.00152 | 1088 | 42 | 1070 | 14 | 1061 | 12 | 1047 | 30 | 1088 | 42 | 42.21 | 109.72 |
| 91500-078 | 0.07484 | 0.00402 | 1.82526 | 0.09546 | 0.17690 | 0.00512 | 0.05202 | 0.00392 | 1064 | 110 | 1055 | 34 | 1050 | 28 | 1025 | 76 | 1064 | 110 | 51.13 | 137.26 |
| 91500-079 | 0.07443 | 0.00344 | 1.86322 | 0.08594 | 0.18155 | 0.00522 | 0.05538 | 0.00340 | 1053 | 96 | 1068 | 30 | 1075 | 28 | 1089 | 66 | 1053 | 96 | 27.85 | 75.50 |

| Analysis No. | RATIOS | | | | | | | | AGES (Ma) | | | | | | | | | | CONCENTRATIONS (ppm) | |
|---|---|---|---|---|---|---|---|---|---|---|---|---|---|---|---|---|---|---|---|---|
| | $^{207}Pb/^{206}Pb$ | ± 2σ | $^{207}Pb/^{235}U$ | ± 2σ | $^{206}Pb/^{238}U$ | ± 2σ | $^{208}Pb/^{232}Th$ | ± 2σ | $^{207}Pb/^{206}Pb$ | ± 2σ | $^{207}Pb/^{235}U$ | ± 2σ | $^{206}Pb/^{238}U$ | ± 2σ | $^{208}Pb/^{232}Th$ | ± 2σ | Used Age | ± 2σ | Th | U |
| 91500-080 | 0.07489 | 0.00140 | 1.69914 | 0.03215 | 0.16457 | 0.00337 | 1.69914 | 0.03215 | 1066 | 37 | 1008 | 12 | 982 | 19 | 1008 | 12 | 1066 | 37 | 34.40 | 85.79 |
| 91500-081 | 0.07617 | 0.00190 | 1.84508 | 0.02468 | 0.17567 | 0.00142 | 0.05410 | 0.00196 | 1100 | 52 | 1062 | 8 | 1043 | 8 | 1065 | 38 | 1100 | 52 | 32.66 | 86.73 |
| 91500-082 | 0.07707 | 0.00326 | 1.91229 | 0.07720 | 0.17996 | 0.00340 | 0.05694 | 0.00334 | 1123 | 86 | 1085 | 26 | 1067 | 18 | 1119 | 64 | 1123 | 86 | 32.56 | 87.19 |
| 91500-083 | 0.07473 | 0.00162 | 1.85270 | 0.04368 | 0.17982 | 0.00402 | 0.05460 | 0.00116 | 1061 | 44 | 1064 | 16 | 1066 | 22 | 1075 | 22 | 1061 | 44 | 37.49 | 94.05 |
| 91500-084 | 0.07790 | 0.00234 | 1.93411 | 0.05782 | 0.18003 | 0.00414 | 0.05238 | 0.00180 | 1144 | 62 | 1093 | 20 | 1067 | 22 | 1032 | 34 | 1144 | 62 | 36.20 | 95.72 |
| 91500-085 | 0.07539 | 0.00172 | 1.81489 | 0.03964 | 0.17461 | 0.00232 | 0.05375 | 0.00170 | 1079 | 46 | 1051 | 14 | 1037 | 12 | 1058 | 32 | 1079 | 46 | 40.49 | 106.27 |
| 91500-086 | 0.07400 | 0.00164 | 1.83225 | 0.04345 | 0.17960 | 0.00400 | 0.05138 | 0.00110 | 1041 | 44 | 1057 | 16 | 1065 | 22 | 1013 | 21 | 1041 | 44 | 40.99 | 108.16 |
| 91500-087 | 0.07283 | 0.00270 | 1.80946 | 0.06598 | 0.18020 | 0.00440 | 0.05253 | 0.00250 | 1009 | 76 | 1049 | 24 | 1068 | 24 | 1035 | 48 | 1009 | 76 | 42.58 | 110.19 |
| 91500-088 | 0.07446 | 0.00196 | 1.83689 | 0.04926 | 0.17893 | 0.00398 | 0.05450 | 0.00166 | 1054 | 54 | 1059 | 18 | 1061 | 22 | 1073 | 32 | 1054 | 54 | 43.43 | 114.15 |
| 91500-089 | 0.07663 | 0.00332 | 1.88198 | 0.07778 | 0.17813 | 0.00344 | 0.05479 | 0.00336 | 1112 | 88 | 1075 | 28 | 1057 | 18 | 1078 | 64 | 1112 | 88 | 31.86 | 83.77 |
| 91500-090 | 0.07306 | 0.00216 | 1.80665 | 0.05102 | 0.17935 | 0.00272 | 0.05421 | 0.00230 | 1016 | 62 | 1048 | 18 | 1063 | 14 | 1067 | 44 | 1016 | 62 | 32.15 | 84.06 |
| 91500-091 | 0.07497 | 0.00220 | 1.87924 | 0.06024 | 0.18181 | 0.00478 | 0.05411 | 0.00198 | 1068 | 60 | 1074 | 22 | 1077 | 26 | 1065 | 38 | 1068 | 60 | 38.39 | 103.39 |
| 91500-092 | 0.07495 | 0.00166 | 1.86289 | 0.04453 | 0.18027 | 0.00404 | 0.05257 | 0.00116 | 1067 | 44 | 1068 | 16 | 1069 | 22 | 1036 | 22 | 1067 | 44 | 40.72 | 103.46 |
| 91500-093 | 0.07659 | 0.00204 | 1.87713 | 0.05024 | 0.17776 | 0.00388 | 0.05584 | 0.00172 | 1111 | 54 | 1073 | 18 | 1055 | 22 | 1098 | 32 | 1111 | 54 | 41.21 | 106.21 |
| 91500-094 | 0.07485 | 0.00286 | 1.83484 | 0.06886 | 0.17780 | 0.00440 | 0.05373 | 0.00270 | 1064 | 78 | 1058 | 24 | 1055 | 24 | 1058 | 52 | 1064 | 78 | 42.75 | 111.52 |
| 91500-095 | 0.07303 | 0.00186 | 1.80301 | 0.02430 | 0.17907 | 0.00144 | 0.05569 | 0.00192 | 1015 | 52 | 1047 | 8 | 1062 | 8 | 1095 | 36 | 1015 | 52 | 20.30 | 291.77 |
| 91500-096 | 0.07504 | 0.00167 | 1.86243 | 0.04453 | 0.18001 | 0.00403 | 0.05339 | 0.00116 | 1070 | 44 | 1068 | 16 | 1067 | 22 | 1051 | 22 | 1070 | 44 | 35.41 | 93.16 |
| 91500-097 | 0.07438 | 0.00276 | 1.86529 | 0.07050 | 0.18189 | 0.00480 | 0.05673 | 0.00280 | 1052 | 76 | 1069 | 24 | 1077 | 26 | 1115 | 54 | 1052 | 76 | 36.29 | 94.53 |
| 91500-098 | 0.07502 | 0.00230 | 1.85949 | 0.05416 | 0.17976 | 0.00282 | 0.05317 | 0.00232 | 1069 | 64 | 1067 | 20 | 1066 | 16 | 1047 | 44 | 1069 | 64 | 39.96 | 101.47 |
| 91500-099 | 0.07473 | 0.00416 | 1.85410 | 0.09810 | 0.17998 | 0.00422 | 0.05899 | 0.00462 | 1061 | 114 | 1065 | 34 | 1067 | 24 | 1158 | 88 | 1061 | 114 | 37.22 | 102.16 |
| 91500-100 | 0.07250 | 0.00278 | 1.78136 | 0.06744 | 0.17821 | 0.00444 | 0.05460 | 0.00270 | 1000 | 80 | 1039 | 24 | 1057 | 24 | 1075 | 52 | 1000 | 80 | 39.96 | 104.62 |
| 91500-101 | 0.07567 | 0.00112 | 1.86344 | 0.01544 | 0.17862 | 0.00126 | 0.05585 | 0.00104 | 1086 | 30 | 1068 | 6 | 1059 | 6 | 1098 | 20 | 1086 | 30 | 19.96 | 288.36 |
| 91500-102 | 0.07670 | 0.00168 | 1.88327 | 0.04122 | 0.17809 | 0.00246 | 0.05441 | 0.00158 | 1113 | 44 | 1075 | 14 | 1057 | 14 | 1071 | 30 | 1113 | 44 | 21.92 | 317.11 |
| 91500-103 | 0.07495 | 0.00174 | 1.86577 | 0.04324 | 0.18056 | 0.00256 | 0.05408 | 0.00170 | 1067 | 48 | 1069 | 16 | 1070 | 14 | 1065 | 32 | 1067 | 48 | 40.56 | 106.21 |
| 91500-104 | 0.07532 | 0.00174 | 1.85346 | 0.04272 | 0.17848 | 0.00252 | 0.05546 | 0.00174 | 1077 | 48 | 1065 | 16 | 1059 | 14 | 1091 | 34 | 1077 | 48 | 40.41 | 106.24 |
| 91500-105 | 0.07600 | 0.00168 | 1.84564 | 0.04040 | 0.17613 | 0.00242 | 0.05434 | 0.00156 | 1095 | 46 | 1062 | 14 | 1046 | 14 | 1070 | 30 | 1095 | 46 | 38.48 | 100.75 |
| 91500-106 | 0.07564 | 0.00278 | 1.85807 | 0.06564 | 0.17818 | 0.00310 | 0.05631 | 0.00292 | 1086 | 76 | 1066 | 24 | 1057 | 16 | 1107 | 56 | 1086 | 76 | 36.15 | 94.48 |
| 91500-107 | 0.07469 | 0.00286 | 1.85987 | 0.06812 | 0.18062 | 0.00316 | 0.05556 | 0.00292 | 1060 | 78 | 1067 | 24 | 1070 | 18 | 1093 | 56 | 1060 | 78 | 34.46 | 88.23 |
| 91500-108 | 0.07536 | 0.00224 | 1.88502 | 0.05466 | 0.18144 | 0.00288 | 0.05584 | 0.00230 | 1078 | 62 | 1076 | 20 | 1075 | 16 | 1098 | 44 | 1078 | 62 | 38.09 | 99.47 |
| 91500-109 | 0.07586 | 0.00250 | 1.88231 | 0.06012 | 0.18005 | 0.00296 | 0.05739 | 0.00280 | 1091 | 68 | 1075 | 22 | 1067 | 16 | 1128 | 54 | 1091 | 68 | 38.63 | 101.22 |
| 91500-110 | 0.07382 | 0.00184 | 1.82116 | 0.04470 | 0.17897 | 0.00376 | 0.05415 | 0.00154 | 1037 | 52 | 1053 | 16 | 1061 | 20 | 1066 | 30 | 1037 | 52 | 55.49 | 455.54 |
| 91500-111 | 0.07412 | 0.00170 | 1.79217 | 0.04234 | 0.17537 | 0.00380 | 0.05246 | 0.00148 | 1045 | 48 | 1043 | 16 | 1042 | 20 | 1033 | 28 | 1045 | 48 | 32.23 | 93.18 |
| 91500-112 | 0.07477 | 0.00188 | 1.87839 | 0.04722 | 0.18221 | 0.00392 | 0.05654 | 0.00188 | 1062 | 52 | 1073 | 16 | 1079 | 22 | 1112 | 36 | 1062 | 52 | 25.13 | 69.57 |
| 91500-113 | 0.07524 | 0.00252 | 1.84744 | 0.06024 | 0.17813 | 0.00404 | 0.06359 | 0.00270 | 1075 | 68 | 1063 | 22 | 1057 | 22 | 1246 | 52 | 1075 | 68 | 5.91 | 94.01 |
| 91500-114 | 0.07538 | 0.00186 | 1.87839 | 0.04672 | 0.18075 | 0.00388 | 0.05577 | 0.00158 | 1079 | 50 | 1073 | 16 | 1071 | 22 | 1097 | 30 | 1079 | 50 | 57.17 | 458.16 |
| 91500-115 | 0.07478 | 0.00158 | 1.87346 | 0.03832 | 0.18173 | 0.00358 | 0.05677 | 0.00128 | 1063 | 44 | 1072 | 14 | 1076 | 20 | 1116 | 24 | 1063 | 44 | 39.40 | 109.89 |
| 91500-116 | 0.07496 | 0.00158 | 1.83744 | 0.03672 | 0.17778 | 0.00340 | 0.05644 | 0.00126 | 1067 | 44 | 1059 | 14 | 1055 | 18 | 1110 | 24 | 1067 | 44 | 35.14 | 100.78 |
| 91500-117 | 0.07477 | 0.00158 | 1.85092 | 0.03698 | 0.17956 | 0.00344 | 0.05624 | 0.00124 | 1062 | 44 | 1064 | 14 | 1065 | 18 | 1106 | 24 | 1062 | 44 | 32.89 | 93.25 |
| 91500-118 | 0.07509 | 0.00158 | 1.87377 | 0.03770 | 0.18100 | 0.00348 | 0.05753 | 0.00126 | 1071 | 44 | 1072 | 14 | 1072 | 18 | 1131 | 24 | 1071 | 44 | 33.75 | 93.41 |
| MT-001 | 0.06350 | 0.00248 | 1.05154 | 0.04198 | 0.12011 | 0.00326 | 0.04028 | 0.00222 | 725 | 84 | 730 | 20 | 731 | 18 | 798 | 44 | 731 | 18 | 60.99 | 100.03 |

| Analysis No. | RATIOS | | | | | | | | AGES (Ma) | | | | | | | | | | CONCENTRATIONS (ppm) | |
|---|---|---|---|---|---|---|---|---|---|---|---|---|---|---|---|---|---|---|---|---|
| | $^{207}Pb/^{206}Pb$ | ± 2σ | $^{207}Pb/^{235}U$ | ± 2σ | $^{206}Pb/^{238}U$ | ± 2σ | $^{208}Pb/^{232}Th$ | ± 2σ | $^{207}Pb/^{206}Pb$ | ± 2σ | $^{207}Pb/^{235}U$ | ± 2σ | $^{206}Pb/^{238}U$ | ± 2σ | $^{208}Pb/^{232}Th$ | ± 2σ | Used Age | ± 2σ | Th | U |
| MT-002 | 0.06390 | 0.00230 | 1.03941 | 0.03902 | 0.11797 | 0.00316 | 0.03511 | 0.00184 | 738 | 78 | 724 | 20 | 719 | 18 | 697 | 36 | 719 | 18 | 138.14 | 147.04 |
| MT-003 | 0.06312 | 0.00202 | 1.02034 | 0.03410 | 0.11725 | 0.00300 | 0.03514 | 0.00154 | 712 | 70 | 714 | 18 | 715 | 18 | 698 | 30 | 715 | 18 | 65.37 | 99.10 |
| MT-004 | 0.06299 | 0.00202 | 1.04408 | 0.03480 | 0.12022 | 0.00304 | 0.03497 | 0.00162 | 708 | 70 | 726 | 18 | 732 | 18 | 695 | 32 | 732 | 18 | 139.99 | 143.05 |
| MT-005 | 0.06382 | 0.00206 | 1.04784 | 0.03506 | 0.11907 | 0.00298 | 0.03617 | 0.00162 | 736 | 70 | 728 | 18 | 725 | 18 | 718 | 32 | 725 | 18 | 85.11 | 109.97 |
| MT-006 | 0.06427 | 0.00194 | 1.05159 | 0.03352 | 0.11867 | 0.00296 | 0.03596 | 0.00142 | 751 | 66 | 730 | 16 | 723 | 18 | 714 | 28 | 723 | 18 | 117.23 | 125.18 |
| MT-007 | 0.06408 | 0.00224 | 1.04501 | 0.03666 | 0.11826 | 0.00290 | 0.03656 | 0.00176 | 744 | 76 | 726 | 18 | 721 | 16 | 726 | 34 | 721 | 16 | 61.61 | 94.56 |
| MT-008 | 0.06472 | 0.00222 | 1.05490 | 0.03812 | 0.11822 | 0.00316 | 0.03555 | 0.00170 | 765 | 74 | 731 | 18 | 720 | 18 | 706 | 34 | 720 | 18 | 123.44 | 139.27 |
| MT-009 | 0.06391 | 0.00216 | 1.06849 | 0.03760 | 0.12129 | 0.00314 | 0.03673 | 0.00160 | 739 | 74 | 738 | 18 | 738 | 18 | 729 | 32 | 738 | 18 | 50.78 | 80.25 |
| MT-010 | 0.06404 | 0.00230 | 1.06794 | 0.03806 | 0.12095 | 0.00292 | 0.03675 | 0.00182 | 743 | 78 | 738 | 18 | 736 | 16 | 729 | 36 | 736 | 16 | 83.55 | 106.19 |
| MT-011 | 0.06495 | 0.00280 | 1.04928 | 0.04390 | 0.11718 | 0.00290 | 0.03560 | 0.00224 | 773 | 92 | 729 | 22 | 714 | 16 | 707 | 44 | 714 | 16 | 71.04 | 105.29 |
| MT-012 | 0.06334 | 0.00202 | 1.04289 | 0.03482 | 0.11942 | 0.00304 | 0.03690 | 0.00158 | 720 | 70 | 725 | 18 | 727 | 18 | 732 | 30 | 727 | 18 | 94.20 | 116.21 |
| MT-013 | 0.06384 | 0.00198 | 1.03254 | 0.03370 | 0.11732 | 0.00296 | 0.03552 | 0.00142 | 736 | 68 | 720 | 16 | 715 | 18 | 705 | 28 | 715 | 18 | 103.23 | 118.37 |
| MT-014 | 0.06484 | 0.00276 | 1.08584 | 0.04498 | 0.12146 | 0.00298 | 0.03764 | 0.00242 | 769 | 92 | 746 | 22 | 739 | 18 | 747 | 48 | 739 | 18 | 125.49 | 144.18 |
| MT-015 | 0.06524 | 0.00210 | 1.06810 | 0.03612 | 0.11876 | 0.00304 | 0.03601 | 0.00148 | 782 | 70 | 738 | 18 | 723 | 18 | 715 | 28 | 723 | 18 | 91.09 | 109.94 |
| MT-016 | 0.06490 | 0.00374 | 1.07572 | 0.05932 | 0.12022 | 0.00328 | 0.03559 | 0.00308 | 771 | 124 | 742 | 30 | 732 | 18 | 707 | 60 | 732 | 18 | 48.97 | 75.52 |
| MT-017 | 0.06346 | 0.00222 | 1.05272 | 0.03784 | 0.12032 | 0.00310 | 0.03528 | 0.00132 | 724 | 76 | 730 | 18 | 732 | 18 | 701 | 26 | 732 | 18 | 102.56 | 114.27 |
| MT-018 | 0.06261 | 0.00166 | 1.02678 | 0.02594 | 0.11896 | 0.00164 | 0.03720 | 0.00106 | 695 | 58 | 717 | 12 | 725 | 10 | 738 | 20 | 725 | 10 | 112.92 | 121.34 |
| MT-019 | 0.06663 | 0.00336 | 1.09173 | 0.05244 | 0.11885 | 0.00242 | 0.03878 | 0.00240 | 826 | 108 | 749 | 26 | 724 | 14 | 769 | 46 | 724 | 14 | 115.41 | 126.73 |
| MT-020 | 0.06362 | 0.00148 | 1.05672 | 0.02616 | 0.12047 | 0.00272 | 0.03782 | 0.00088 | 729 | 50 | 732 | 12 | 733 | 16 | 750 | 18 | 733 | 16 | 132.79 | 127.41 |
| MT-021 | 0.06457 | 0.00226 | 1.06450 | 0.03574 | 0.11960 | 0.00192 | 0.03776 | 0.00152 | 760 | 76 | 736 | 18 | 728 | 12 | 749 | 30 | 728 | 12 | 120.96 | 127.92 |
| MT-022 | 0.06426 | 0.00240 | 1.04663 | 0.03914 | 0.11814 | 0.00296 | 0.03631 | 0.00152 | 750 | 80 | 727 | 20 | 720 | 18 | 721 | 30 | 720 | 18 | 138.38 | 142.75 |
| MT-023 | 0.06329 | 0.00144 | 1.05271 | 0.02252 | 0.12065 | 0.00144 | 0.03830 | 0.00100 | 718 | 50 | 730 | 12 | 734 | 8 | 760 | 20 | 734 | 8 | 150.67 | 144.27 |
| MT-024 | 0.06342 | 0.00234 | 1.04351 | 0.03816 | 0.11936 | 0.00292 | 0.03664 | 0.00158 | 722 | 80 | 726 | 18 | 727 | 16 | 727 | 30 | 727 | 16 | 140.21 | 145.06 |
| MT-025 | 0.06399 | 0.00160 | 1.03842 | 0.02606 | 0.11771 | 0.00250 | 0.03678 | 0.00092 | 741 | 54 | 723 | 12 | 717 | 14 | 730 | 18 | 717 | 14 | 150.07 | 147.40 |
| MT-026 | 0.06358 | 0.00242 | 1.07202 | 0.04118 | 0.12230 | 0.00316 | 0.03772 | 0.00168 | 728 | 82 | 740 | 20 | 744 | 18 | 748 | 32 | 744 | 18 | 152.21 | 153.61 |
| MT-027 | 0.06278 | 0.00184 | 1.01539 | 0.02929 | 0.11732 | 0.00256 | 0.03621 | 0.00114 | 701 | 62 | 712 | 15 | 715 | 15 | 719 | 22 | 715 | 15 | 164.17 | 167.77 |
| MT-028 | 0.06476 | 0.00252 | 1.07016 | 0.04080 | 0.11987 | 0.00290 | 0.03635 | 0.00166 | 767 | 84 | 739 | 20 | 730 | 16 | 722 | 32 | 730 | 16 | 221.54 | 186.63 |
| MT-029 | 0.06354 | 0.00166 | 1.05985 | 0.02774 | 0.12099 | 0.00262 | 0.03678 | 0.00098 | 726 | 56 | 734 | 14 | 736 | 16 | 730 | 20 | 736 | 16 | 88.99 | 1088.10 |
| MT-030 | 0.06573 | 0.00186 | 1.05257 | 0.03052 | 0.11616 | 0.00264 | 0.03572 | 0.00118 | 798 | 60 | 730 | 16 | 708 | 16 | 709 | 24 | 708 | 16 | 205.45 | 2705.22 |
| MT-031 | 0.06344 | 0.00290 | 1.04066 | 0.04632 | 0.11899 | 0.00298 | 0.03507 | 0.00226 | 723 | 100 | 724 | 24 | 725 | 18 | 697 | 44 | 725 | 18 | 47.99 | 79.07 |
| MT-032 | 0.06363 | 0.00432 | 1.05854 | 0.06914 | 0.12062 | 0.00366 | 0.03562 | 0.00260 | 729 | 148 | 733 | 34 | 734 | 22 | 707 | 50 | 734 | 22 | 94.70 | 99.77 |
| MT-033 | 0.06333 | 0.00206 | 1.04751 | 0.03578 | 0.11998 | 0.00312 | 0.03354 | 0.00114 | 719 | 70 | 728 | 18 | 730 | 18 | 667 | 22 | 730 | 18 | 81.14 | 107.43 |
| MT-034 | 0.06226 | 0.00210 | 1.01868 | 0.03398 | 0.11868 | 0.00276 | 0.03734 | 0.00136 | 683 | 74 | 713 | 18 | 723 | 16 | 741 | 26 | 723 | 16 | 95.77 | 121.56 |
| MT-035 | 0.06496 | 0.00288 | 1.08082 | 0.04596 | 0.12068 | 0.00224 | 0.03822 | 0.00206 | 773 | 96 | 744 | 22 | 734 | 12 | 758 | 40 | 734 | 12 | 116.09 | 126.07 |
| MT-036 | 0.06399 | 0.00148 | 1.06320 | 0.02312 | 0.12052 | 0.00144 | 0.03644 | 0.00094 | 741 | 50 | 735 | 12 | 734 | 8 | 723 | 18 | 734 | 8 | 135.29 | 133.09 |
| MT-037 | 0.06522 | 0.00230 | 1.08407 | 0.03670 | 0.12056 | 0.00194 | 0.03670 | 0.00152 | 781 | 76 | 746 | 18 | 734 | 12 | 729 | 30 | 734 | 12 | 139.63 | 135.55 |
| MT-038 | 0.06382 | 0.00188 | 1.03877 | 0.03084 | 0.11806 | 0.00270 | 0.03703 | 0.00116 | 736 | 64 | 723 | 16 | 719 | 16 | 735 | 22 | 719 | 16 | 101.89 | 139.20 |
| MT-039 | 0.06436 | 0.00138 | 1.06718 | 0.02512 | 0.12026 | 0.00270 | 0.03748 | 0.00076 | 753 | 46 | 737 | 12 | 732 | 16 | 744 | 14 | 732 | 16 | 157.13 | 148.26 |
| MT-040 | 0.06217 | 0.00226 | 1.02833 | 0.03754 | 0.11999 | 0.00294 | 0.03663 | 0.00148 | 680 | 80 | 718 | 18 | 731 | 16 | 727 | 28 | 731 | 16 | 165.20 | 148.77 |
| MT-041 | 0.06404 | 0.00148 | 1.07129 | 0.02372 | 0.12134 | 0.00160 | 0.03752 | 0.00102 | 743 | 50 | 739 | 12 | 738 | 10 | 744 | 20 | 738 | 10 | 145.83 | 157.03 |

| Analysis No. | RATIOS | | | | | | | | AGES (Ma) | | | | | | | | | | CONCENTRATIONS (ppm) | |
|---|---|---|---|---|---|---|---|---|---|---|---|---|---|---|---|---|---|---|---|---|
| | $^{207}Pb/^{206}Pb$ | ± 2σ | $^{207}Pb/^{235}U$ | ± 2σ | $^{206}Pb/^{238}U$ | ± 2σ | $^{208}Pb/^{232}Th$ | ± 2σ | $^{207}Pb/^{206}Pb$ | ± 2σ | $^{207}Pb/^{235}U$ | ± 2σ | $^{206}Pb/^{238}U$ | ± 2σ | $^{208}Pb/^{232}Th$ | ± 2σ | Used Age | ± 2σ | Th | U |
| MT-042 | 0.06395 | 0.00284 | 1.05658 | 0.04596 | 0.11985 | 0.00308 | 0.03775 | 0.00188 | 740 | 96 | 732 | 22 | 730 | 18 | 749 | 36 | 730 | 18 | 162.54 | 174.33 |
| MT-043 | 0.06304 | 0.00193 | 1.03361 | 0.03156 | 0.11892 | 0.00272 | 0.03414 | 0.00114 | 710 | 64 | 721 | 16 | 724 | 16 | 679 | 22 | 724 | 16 | 169.85 | 179.48 |
| MT-044 | 0.06364 | 0.00160 | 1.02976 | 0.02586 | 0.11737 | 0.00250 | 0.03526 | 0.00090 | 730 | 54 | 719 | 12 | 715 | 14 | 700 | 18 | 715 | 14 | 105.20 | 1317.59 |
| MT-045 | 0.06582 | 0.00168 | 1.03524 | 0.02668 | 0.11408 | 0.00246 | 0.03536 | 0.00104 | 801 | 54 | 722 | 14 | 696 | 14 | 702 | 20 | 696 | 14 | 272.22 | 3484.58 |
| MT-046 | 0.06467 | 0.00234 | 1.08763 | 0.04030 | 0.12198 | 0.00320 | 0.03693 | 0.00126 | 764 | 78 | 747 | 20 | 742 | 18 | 733 | 24 | 742 | 18 | 70.80 | 92.74 |
| MT-047 | 0.06476 | 0.00272 | 1.06139 | 0.04334 | 0.11887 | 0.00292 | 0.03751 | 0.00172 | 767 | 90 | 735 | 22 | 724 | 16 | 744 | 34 | 724 | 16 | 76.00 | 101.20 |
| MT-048 | 0.06670 | 0.00262 | 1.10250 | 0.04318 | 0.11991 | 0.00304 | 0.03709 | 0.00162 | 828 | 84 | 755 | 20 | 730 | 18 | 736 | 32 | 730 | 18 | 92.04 | 112.72 |
| MT-049 | 0.06352 | 0.00158 | 1.05641 | 0.02680 | 0.12063 | 0.00264 | 0.03852 | 0.00098 | 726 | 54 | 732 | 14 | 734 | 16 | 764 | 20 | 734 | 16 | 89.62 | 114.66 |
| MT-050 | 0.06413 | 0.01904 | 1.05415 | 0.60524 | 0.11923 | 0.00312 | 0.03643 | 0.01946 | 746 | 66 | 731 | 30 | 726 | 18 | 723 | 38 | 726 | 18 | 124.25 | 126.47 |
| MT-051 | 0.06545 | 0.00142 | 1.08165 | 0.02258 | 0.11987 | 0.00154 | 0.03827 | 0.00094 | 789 | 46 | 744 | 12 | 730 | 8 | 759 | 18 | 730 | 8 | 124.71 | 133.19 |
| MT-052 | 0.06495 | 0.00179 | 1.06779 | 0.02918 | 0.11925 | 0.00258 | 0.03786 | 0.00106 | 773 | 57 | 738 | 14 | 726 | 15 | 751 | 21 | 726 | 15 | 124.06 | 133.46 |
| MT-053 | 0.06445 | 0.00146 | 1.07228 | 0.02670 | 0.12068 | 0.00278 | 0.03744 | 0.00080 | 756 | 48 | 740 | 14 | 734 | 16 | 743 | 16 | 734 | 16 | 142.65 | 149.81 |
| MT-054 | 0.06349 | 0.00246 | 1.01688 | 0.03792 | 0.11617 | 0.00272 | 0.03231 | 0.00154 | 725 | 84 | 712 | 20 | 708 | 16 | 643 | 30 | 708 | 16 | 153.39 | 173.05 |
| MT-055 | 0.06469 | 0.00338 | 1.04488 | 0.05188 | 0.11718 | 0.00246 | 0.03750 | 0.00258 | 764 | 112 | 726 | 26 | 714 | 14 | 744 | 50 | 714 | 14 | 251.89 | 254.91 |
| MT-056 | 0.06413 | 0.00166 | 1.04642 | 0.02702 | 0.11836 | 0.00252 | 0.03676 | 0.00108 | 746 | 56 | 727 | 14 | 721 | 14 | 730 | 22 | 721 | 14 | 135.40 | 1632.25 |
| MT-057 | 0.06444 | 0.00224 | 1.08540 | 0.03666 | 0.12221 | 0.00278 | 0.04425 | 0.00166 | 756 | 76 | 746 | 18 | 743 | 16 | 875 | 32 | 743 | 16 | 16.15 | 113.99 |
| MT-058 | 0.06562 | 0.00146 | 1.08095 | 0.02610 | 0.11949 | 0.00268 | 0.03883 | 0.00080 | 794 | 48 | 744 | 12 | 728 | 16 | 770 | 16 | 728 | 16 | 88.68 | 120.12 |
| MT-059 | 0.06239 | 0.00186 | 1.03737 | 0.02408 | 0.12059 | 0.00142 | 0.03736 | 0.00190 | 688 | 66 | 723 | 12 | 734 | 8 | 741 | 38 | 734 | 8 | 120.77 | 127.38 |
| MT-060 | 0.06326 | 0.00182 | 1.04194 | 0.03002 | 0.11946 | 0.00266 | 0.03679 | 0.00109 | 717 | 61 | 725 | 15 | 728 | 15 | 730 | 21 | 728 | 15 | 119.42 | 132.87 |
| MT-061 | 0.06394 | 0.00142 | 1.06073 | 0.02256 | 0.12034 | 0.00154 | 0.03638 | 0.00092 | 740 | 48 | 734 | 12 | 733 | 8 | 722 | 18 | 733 | 8 | 127.21 | 134.83 |
| MT-062 | 0.06373 | 0.00202 | 1.05643 | 0.03544 | 0.12022 | 0.00310 | 0.03575 | 0.00130 | 733 | 68 | 732 | 18 | 732 | 18 | 710 | 26 | 732 | 18 | 160.17 | 146.45 |
| MT-063 | 0.06694 | 0.00150 | 1.11835 | 0.02706 | 0.12118 | 0.00272 | 0.03935 | 0.00088 | 836 | 48 | 762 | 12 | 737 | 16 | 780 | 18 | 737 | 16 | 144.00 | 146.64 |
| MT-064 | 0.06450 | 0.00382 | 1.05007 | 0.06008 | 0.11810 | 0.00348 | 0.03811 | 0.00262 | 758 | 128 | 729 | 30 | 720 | 20 | 756 | 52 | 720 | 20 | 140.30 | 159.03 |
| MT-065 | 0.06444 | 0.00160 | 1.05316 | 0.02636 | 0.11855 | 0.00252 | 0.03635 | 0.00094 | 756 | 54 | 730 | 14 | 722 | 14 | 722 | 18 | 722 | 14 | 144.71 | 1772.33 |
| MT-066 | 0.06379 | 0.00160 | 1.03815 | 0.02602 | 0.11804 | 0.00250 | 0.03635 | 0.00098 | 735 | 54 | 723 | 12 | 719 | 14 | 722 | 20 | 719 | 14 | 155.42 | 1903.23 |
| MT-067 | 0.06412 | 0.00212 | 1.06524 | 0.03458 | 0.12051 | 0.00274 | 0.03588 | 0.00119 | 746 | 69 | 736 | 17 | 734 | 16 | 713 | 23 | 734 | 16 | 52.28 | 83.22 |
| MT-068 | 0.06347 | 0.00152 | 1.06423 | 0.02456 | 0.12163 | 0.00162 | 0.03781 | 0.00100 | 724 | 52 | 736 | 12 | 740 | 10 | 750 | 20 | 740 | 10 | 81.09 | 106.14 |
| MT-069 | 0.06463 | 0.00256 | 1.06399 | 0.04274 | 0.11940 | 0.00320 | 0.03662 | 0.00164 | 762 | 86 | 736 | 22 | 727 | 18 | 727 | 32 | 727 | 18 | 77.80 | 107.88 |
| MT-070 | 0.06342 | 0.00262 | 1.05457 | 0.04260 | 0.12061 | 0.00300 | 0.03686 | 0.00162 | 722 | 90 | 731 | 22 | 734 | 18 | 732 | 32 | 734 | 18 | 115.30 | 123.65 |
| MT-071 | 0.06398 | 0.00214 | 1.07463 | 0.03482 | 0.12185 | 0.00270 | 0.03719 | 0.00124 | 741 | 72 | 741 | 18 | 741 | 16 | 738 | 24 | 741 | 16 | 119.85 | 126.58 |
| MT-072 | 0.06207 | 0.00186 | 1.02489 | 0.02406 | 0.11977 | 0.00142 | 0.03793 | 0.00190 | 677 | 66 | 716 | 12 | 729 | 8 | 752 | 36 | 729 | 8 | 120.33 | 127.79 |
| MT-073 | 0.06851 | 0.00314 | 1.13803 | 0.04984 | 0.12048 | 0.00232 | 0.03822 | 0.00214 | 884 | 96 | 772 | 24 | 733 | 14 | 758 | 42 | 733 | 14 | 125.95 | 134.09 |
| MT-074 | 0.06416 | 0.00142 | 1.06243 | 0.02566 | 0.12010 | 0.00272 | 0.03835 | 0.00080 | 747 | 48 | 735 | 12 | 731 | 16 | 761 | 16 | 731 | 16 | 146.28 | 144.03 |
| MT-075 | 0.06407 | 0.00140 | 1.05911 | 0.02528 | 0.11990 | 0.00268 | 0.03860 | 0.00084 | 744 | 48 | 733 | 12 | 730 | 16 | 766 | 16 | 730 | 16 | 158.40 | 153.23 |
| MT-076 | 0.06352 | 0.00182 | 1.08732 | 0.03064 | 0.12418 | 0.00270 | 0.03849 | 0.00114 | 726 | 62 | 747 | 14 | 755 | 16 | 763 | 22 | 755 | 16 | 97.35 | 1161.01 |
| MT-077 | 0.06548 | 0.00210 | 1.08664 | 0.03428 | 0.12037 | 0.00270 | 0.03853 | 0.00126 | 790 | 68 | 747 | 16 | 733 | 16 | 764 | 24 | 733 | 16 | 57.92 | 82.14 |
| MT-078 | 0.06462 | 0.00178 | 1.08132 | 0.02856 | 0.12137 | 0.00174 | 0.03831 | 0.00118 | 762 | 60 | 744 | 14 | 738 | 10 | 760 | 22 | 738 | 10 | 64.66 | 96.35 |
| MT-079 | 0.06289 | 0.00200 | 1.09137 | 0.03452 | 0.12584 | 0.00290 | 0.03726 | 0.00114 | 705 | 70 | 749 | 16 | 764 | 16 | 739 | 22 | 764 | 16 | 88.14 | 108.39 |
| MT-080 | 0.06487 | 0.00188 | 1.06098 | 0.02412 | 0.11862 | 0.00142 | 0.03797 | 0.00194 | 770 | 62 | 734 | 12 | 723 | 8 | 753 | 38 | 723 | 8 | 100.00 | 115.96 |
| MT-081 | 0.06395 | 0.00138 | 1.06788 | 0.02530 | 0.12113 | 0.00272 | 0.03803 | 0.00076 | 740 | 46 | 738 | 12 | 737 | 16 | 754 | 14 | 737 | 16 | 106.81 | 121.54 |

| Analysis No. | RATIOS | | | | | | | | AGES (Ma) | | | | | | | | | | CONCENTRATIONS (ppm) | |
|---|---|---|---|---|---|---|---|---|---|---|---|---|---|---|---|---|---|---|---|---|
| | $^{207}Pb/^{206}Pb$ | ± 2σ | $^{207}Pb/^{235}U$ | ± 2σ | $^{206}Pb/^{238}U$ | ± 2σ | $^{208}Pb/^{232}Th$ | ± 2σ | $^{207}Pb/^{206}Pb$ | ± 2σ | $^{207}Pb/^{235}U$ | ± 2σ | $^{206}Pb/^{238}U$ | ± 2σ | $^{208}Pb/^{232}Th$ | ± 2σ | Used Age | ± 2σ | Th | U |
| MT-082 | 0.07498 | 0.00170 | 1.26661 | 0.03072 | 0.12252 | 0.00274 | 0.04172 | 0.00093 | 1068 | 45 | 831 | 14 | 745 | 16 | 826 | 18 | 745 | 16 | 119.59 | 131.30 |
| MT-083 | 0.06346 | 0.00356 | 1.04750 | 0.05606 | 0.11974 | 0.00262 | 0.03972 | 0.00258 | 724 | 122 | 728 | 28 | 729 | 16 | 787 | 50 | 729 | 16 | 150.41 | 141.45 |
| MT-084 | 0.06395 | 0.00216 | 1.07943 | 0.03822 | 0.12243 | 0.00322 | 0.03696 | 0.00140 | 740 | 74 | 743 | 18 | 745 | 18 | 734 | 28 | 745 | 18 | 146.99 | 142.06 |
| MT-085 | 0.06238 | 0.00252 | 1.02955 | 0.04084 | 0.11970 | 0.00296 | 0.03645 | 0.00162 | 687 | 88 | 719 | 20 | 729 | 18 | 724 | 32 | 729 | 18 | 174.83 | 155.21 |
| MT-086 | 0.06379 | 0.00224 | 1.09706 | 0.03686 | 0.12474 | 0.00274 | 0.03963 | 0.00148 | 735 | 76 | 752 | 18 | 758 | 16 | 786 | 28 | 758 | 16 | 110.03 | 1234.34 |
| MT-087 | 0.06560 | 0.00186 | 1.08943 | 0.02400 | 0.12045 | 0.00142 | 0.03709 | 0.00184 | 794 | 60 | 748 | 12 | 733 | 8 | 736 | 36 | 733 | 8 | 32.44 | 86.49 |
| MT-088 | 0.06457 | 0.00280 | 1.05648 | 0.04476 | 0.11868 | 0.00302 | 0.03746 | 0.00176 | 760 | 94 | 732 | 22 | 723 | 18 | 743 | 34 | 723 | 18 | 111.43 | 122.99 |
| MT-089 | 0.06424 | 0.00208 | 1.07158 | 0.03648 | 0.12099 | 0.00312 | 0.03686 | 0.00136 | 750 | 70 | 740 | 18 | 736 | 18 | 732 | 26 | 736 | 18 | 129.01 | 132.99 |
| MT-090 | 0.06502 | 0.00154 | 1.08456 | 0.02492 | 0.12098 | 0.00164 | 0.03893 | 0.00106 | 775 | 50 | 746 | 12 | 736 | 10 | 772 | 20 | 736 | 10 | 128.30 | 138.02 |
| MT-091 | 0.06416 | 0.00145 | 1.06176 | 0.02572 | 0.12004 | 0.00269 | 0.03879 | 0.00085 | 747 | 47 | 735 | 13 | 731 | 15 | 769 | 16 | 731 | 15 | 128.11 | 140.87 |
| MT-092 | 0.06403 | 0.00208 | 1.05152 | 0.03392 | 0.11911 | 0.00274 | 0.03783 | 0.00130 | 743 | 70 | 730 | 16 | 725 | 16 | 751 | 26 | 725 | 16 | 121.20 | 145.58 |
| MT-093 | 0.06250 | 0.00388 | 1.04135 | 0.06162 | 0.12084 | 0.00288 | 0.03841 | 0.00288 | 691 | 136 | 725 | 30 | 735 | 16 | 762 | 56 | 735 | 16 | 189.17 | 162.19 |
| MT-094 | 0.06375 | 0.00114 | 1.05168 | 0.01552 | 0.11966 | 0.00126 | 0.03767 | 0.00104 | 733 | 38 | 730 | 8 | 729 | 8 | 747 | 20 | 729 | 8 | 31.40 | 85.63 |
| MT-095 | 0.06353 | 0.00148 | 1.05337 | 0.02616 | 0.12028 | 0.00270 | 0.03325 | 0.00068 | 726 | 49 | 731 | 13 | 732 | 16 | 661 | 13 | 732 | 16 | 67.89 | 95.99 |
| MT-096 | 0.06308 | 0.00302 | 1.04964 | 0.04802 | 0.12069 | 0.00236 | 0.03808 | 0.00212 | 711 | 104 | 729 | 24 | 735 | 14 | 755 | 42 | 735 | 14 | 103.21 | 120.82 |
| MT-097 | 0.06332 | 0.00145 | 1.04892 | 0.02578 | 0.12015 | 0.00270 | 0.03574 | 0.00077 | 719 | 48 | 728 | 13 | 731 | 16 | 710 | 15 | 731 | 16 | 115.22 | 127.13 |
| MT-098 | 0.06412 | 0.00156 | 1.05952 | 0.02566 | 0.11985 | 0.00170 | 0.03718 | 0.00100 | 746 | 52 | 734 | 12 | 730 | 10 | 738 | 20 | 730 | 10 | 19.58 | 283.51 |
| MT-099 | 0.06424 | 0.00164 | 1.07674 | 0.02726 | 0.12157 | 0.00174 | 0.03813 | 0.00110 | 750 | 56 | 742 | 14 | 740 | 10 | 756 | 22 | 740 | 10 | 129.58 | 133.19 |
| MT-100 | 0.06455 | 0.00158 | 1.04521 | 0.02707 | 0.11744 | 0.00268 | 0.03263 | 0.00072 | 760 | 51 | 727 | 13 | 716 | 15 | 649 | 14 | 716 | 15 | 125.30 | 139.20 |
| MT-101 | 0.06397 | 0.00166 | 1.06378 | 0.02726 | 0.12061 | 0.00174 | 0.03794 | 0.00112 | 741 | 56 | 736 | 14 | 734 | 10 | 753 | 22 | 734 | 10 | 137.11 | 134.92 |
| MT-102 | 0.06339 | 0.00428 | 1.04200 | 0.06802 | 0.11922 | 0.00200 | 0.03658 | 0.00056 | 721 | 146 | 725 | 34 | 726 | 12 | 726 | 10 | 726 | 12 | 131.44 | 131.04 |
| MT-103 | 0.06552 | 0.00292 | 1.07621 | 0.04596 | 0.11915 | 0.00226 | 0.03837 | 0.00200 | 791 | 96 | 742 | 22 | 726 | 14 | 761 | 38 | 726 | 14 | 129.99 | 119.61 |
| MT-104 | 0.06602 | 0.00254 | 1.09574 | 0.04040 | 0.12036 | 0.00206 | 0.03739 | 0.00164 | 807 | 82 | 751 | 20 | 733 | 12 | 742 | 32 | 733 | 12 | 141.00 | 127.53 |
| MT-105 | 0.06399 | 0.00192 | 1.05955 | 0.03110 | 0.12011 | 0.00186 | 0.03797 | 0.00132 | 741 | 64 | 734 | 16 | 731 | 10 | 753 | 26 | 731 | 10 | 122.54 | 131.37 |
| MT-106 | 0.06425 | 0.00304 | 1.07286 | 0.04874 | 0.12116 | 0.00238 | 0.04003 | 0.00252 | 750 | 102 | 740 | 24 | 737 | 14 | 793 | 48 | 737 | 14 | 149.34 | 130.73 |
| MT-107 | 0.06421 | 0.00194 | 1.08172 | 0.03196 | 0.12223 | 0.00188 | 0.03926 | 0.00166 | 749 | 66 | 744 | 16 | 743 | 10 | 778 | 32 | 743 | 10 | 191.11 | 159.62 |
| MT-108 | 0.06382 | 0.00156 | 1.04781 | 0.02546 | 0.11910 | 0.00250 | 0.03673 | 0.00096 | 736 | 52 | 728 | 12 | 725 | 14 | 729 | 18 | 725 | 14 | 219.66 | 2673.96 |
| MT-109 | 0.06369 | 0.00168 | 1.04033 | 0.02876 | 0.11847 | 0.00278 | 0.03930 | 0.00124 | 731 | 58 | 724 | 14 | 722 | 16 | 779 | 24 | 722 | 16 | 70.12 | 116.24 |
| MT-110 | 0.06389 | 0.00170 | 1.07696 | 0.02852 | 0.12227 | 0.00264 | 0.03901 | 0.00120 | 738 | 58 | 742 | 14 | 744 | 16 | 773 | 24 | 744 | 16 | 54.76 | 79.57 |
| MT-111 | 0.06437 | 0.00160 | 1.06737 | 0.02674 | 0.12027 | 0.00258 | 0.03731 | 0.00098 | 754 | 54 | 737 | 14 | 732 | 14 | 740 | 20 | 732 | 14 | 161.03 | 1934.34 |
| MT-112 | 0.06375 | 0.00132 | 1.05575 | 0.02096 | 0.12013 | 0.00230 | 0.03767 | 0.00076 | 733 | 44 | 732 | 10 | 731 | 14 | 747 | 14 | 731 | 14 | 147.51 | 156.40 |
| MT-113 | 0.06400 | 0.00136 | 1.04555 | 0.02108 | 0.11850 | 0.00226 | 0.03672 | 0.00078 | 742 | 46 | 727 | 10 | 722 | 14 | 729 | 16 | 722 | 14 | 151.88 | 149.88 |
| MT-114 | 0.06405 | 0.00136 | 1.04671 | 0.02112 | 0.11853 | 0.00228 | 0.03638 | 0.00076 | 743 | 46 | 727 | 10 | 722 | 14 | 722 | 14 | 722 | 14 | 128.62 | 133.70 |
| MT-115 | 0.06417 | 0.00136 | 1.04921 | 0.02136 | 0.11860 | 0.00230 | 0.03678 | 0.00076 | 747 | 46 | 728 | 10 | 723 | 14 | 730 | 14 | 723 | 14 | 153.11 | 145.74 |

**Appendix 1.2. Compilation for Hf standards MudTank and Temora-II, GAU, 2005-2016**

| Standard | Ratio | Long term (2005-2014) | | Long term (2015-2016) | | Reference value | |
|---|---|---|---|---|---|---|---|
| | | Average | 1σ | Average | 1σ | Average | 1σ |
| | | n=6093 | | n=1150 | | | |
| Mud Tank | $^{176}Hf/^{177}Hf$ | 0.282528 | 0.000026 | 0.282531 | 0.000020 | 0.282522 | 0.000042 |
| | $^{178}Hf/^{177}Hf$ | 1.46717 | 0.00024 | 1.46719 | 0.00098 | | |
| | $^{180}Hf/^{177}Hf$ | 1.88667 | 0.00026 | 1.88662 | 0.00010 | | |
| | $^{176}Yb/^{177}Hf$ | 0.0034 | 0.0025 | 0.0065 | 0.0018 | | |
| | $^{176}Lu/^{177}Hf$ | 0.00008 | 0.00005 | 0.00012 | 0.00003 | | |
| | | n=399 | | n=599 | | | |
| Temora-II | $^{176}Hf/^{177}Hf$ | 0.282686 | 0.000034 | 0.282686 | 0.000028 | 0.282680 | 0.000011 |
| | $^{178}Hf/^{177}Hf$ | 1.46714 | 0.00037 | 1.46718 | 0.00133 | | |
| | $^{180}Hf/^{177}Hf$ | 1.88673 | 0.00035 | 1.88656 | 0.00016 | | |
| | $^{176}Yb/^{177}Hf$ | 0.035 | 0.014 | 0.052 | 0.018 | | |
| | $^{176}Lu/^{177}Hf$ | 0.00109 | 0.00038 | 0.00126 | 0.00044 | | |

Reference values from: MT - Griffin *et al.* (2007), Temora-2 - Woodhead and Hergt (2005)

**Appendix 2.1. Zircon U-Pb age data for samples from the Magan terrane**

| Analysis No. | RATIOS | | | | | | | | AGES (Ma) | | | | | | | | | | CONCENTRATIONS (ppm) | |
|---|---|---|---|---|---|---|---|---|---|---|---|---|---|---|---|---|---|---|---|---|
| | $^{207}Pb/^{206}Pb$ | ± 2σ | $^{207}Pb/^{235}U$ | ± 2σ | $^{206}Pb/^{238}U$ | ± 2σ | $^{208}Pb/^{232}Th$ | ± 2σ | $^{207}Pb/^{206}Pb$ | ± 2σ | $^{207}Pb/^{235}U$ | ± 2σ | $^{206}Pb/^{238}U$ | ± 2σ | $^{208}Pb/^{232}Th$ | ± 2σ | Used Age | ± 2σ | Th | U |
| **Malo-Botuobinskoe field, Internationalnaya pipe** | | | | | | | | | | | | | | | | | | | | |
| INT1-01 | 0.14003 | 0.00406 | 8.23819 | 0.24452 | 0.42674 | 0.01020 | 0.12521 | 0.00550 | 2228 | 52 | 2258 | 26 | 2291 | 46 | 2384 | 98 | 2228 | 52 | 47.00 | 98.51 |
| INT1-03 | 0.1084 | 0.00360 | 4.44251 | 0.14730 | 0.29726 | 0.00722 | 0.08826 | 0.00426 | 1773 | 62 | 1720 | 28 | 1678 | 36 | 1710 | 80 | 1773 | 62 | 74.75 | 99.05 |
| INT1-07 | 0.17508 | 0.00700 | 10.82271 | 0.43504 | 0.44849 | 0.01188 | 0.13104 | 0.00976 | 2607 | 68 | 2508 | 38 | 2389 | 52 | 2489 | 174 | 2607 | 68 | 223.23 | 1009.39 |
| INT1-08 | 0.17388 | 0.00844 | 11.36583 | 0.55220 | 0.47403 | 0.01418 | 0.09755 | 0.01008 | 2595 | 82 | 2554 | 46 | 2501 | 62 | 1881 | 186 | 2595 | 82 | 53.94 | 426.23 |
| INT1-09 | 0.171 | 0.00590 | 11.71725 | 0.40498 | 0.49699 | 0.01232 | 0.13524 | 0.00796 | 2567 | 60 | 2582 | 32 | 2601 | 54 | 2564 | 142 | 2567 | 60 | 75.19 | 109.08 |
| INT1-11 | 0.1039 | 0.00422 | 3.97823 | 0.16190 | 0.2777 | 0.00738 | 0.08092 | 0.00600 | 1695 | 76 | 1630 | 34 | 1580 | 38 | 1573 | 112 | 1695 | 76 | 302.72 | 590.15 |
| INT1-12 | 0.05225 | 0.00242 | 0.42689 | 0.01946 | 0.05926 | 0.00156 | 0.01824 | 0.00136 | 296 | 108 | 361 | 14 | 371 | 10 | 365 | 26 | 371 | 10 | 558.25 | 790.13 |
| INT1-13 | 0.12156 | 0.00366 | 5.90976 | 0.18340 | 0.35263 | 0.00860 | 0.104 | 0.00480 | 1979 | 54 | 1963 | 26 | 1947 | 40 | 2000 | 88 | 1979 | 54 | 104.77 | 171.56 |
| INT1-14C | 0.05557 | 0.00214 | 0.50463 | 0.01956 | 0.06588 | 0.00166 | 0.02049 | 0.00114 | 435 | 88 | 415 | 14 | 411 | 10 | 410 | 22 | 411 | 10 | 908.70 | 888.10 |
| INT1-14R | 0.0549 | 0.00202 | 0.44966 | 0.01660 | 0.05941 | 0.00144 | 0.01731 | 0.00082 | 408 | 84 | 377 | 12 | 372 | 8 | 347 | 16 | 372 | 8 | 274.39 | 446.37 |
| INT1-15 | 0.11058 | 0.00504 | 4.90138 | 0.21630 | 0.32139 | 0.00868 | 0.0943 | 0.00636 | 1809 | 84 | 1802 | 38 | 1797 | 42 | 1821 | 118 | 1809 | 84 | 60.87 | 67.73 |
| INT1-16 | 0.11446 | 0.00484 | 5.03431 | 0.21342 | 0.31896 | 0.00878 | 0.09552 | 0.00700 | 1871 | 78 | 1825 | 36 | 1785 | 42 | 1844 | 130 | 1871 | 78 | 118.35 | 243.63 |
| INT1-18C | 0.17592 | 0.00792 | 10.99535 | 0.48452 | 0.45337 | 0.01230 | 0.12765 | 0.01036 | 2615 | 76 | 2523 | 42 | 2410 | 54 | 2428 | 186 | 2615 | 76 | 106.51 | 169.77 |
| INT1-18R | 0.16681 | 0.00564 | 10.04393 | 0.34306 | 0.43679 | 0.01066 | 0.12117 | 0.00720 | 2526 | 58 | 2439 | 32 | 2336 | 48 | 2312 | 130 | 2526 | 58 | 80.22 | 242.61 |
| INT1-19 | 0.05382 | 0.00244 | 0.44019 | 0.01964 | 0.05933 | 0.00152 | 0.01854 | 0.00108 | 364 | 104 | 370 | 14 | 372 | 10 | 371 | 22 | 372 | 10 | 262.68 | 311.66 |
| INT1-20 | 0.05417 | 0.00210 | 0.45553 | 0.01768 | 0.061 | 0.00150 | 0.01934 | 0.00116 | 378 | 90 | 381 | 12 | 382 | 10 | 387 | 24 | 382 | 10 | 270.78 | 662.48 |
| INT1-21C | 0.11505 | 0.00426 | 5.35088 | 0.19914 | 0.33738 | 0.00852 | 0.09397 | 0.00588 | 1881 | 68 | 1877 | 32 | 1874 | 42 | 1815 | 108 | 1881 | 68 | 236.03 | 210.12 |
| INT1-21RI | 0.11392 | 0.00444 | 5.20094 | 0.20372 | 0.33118 | 0.00846 | 0.09053 | 0.00628 | 1863 | 72 | 1853 | 34 | 1844 | 40 | 1752 | 116 | 1863 | 72 | 343.94 | 444.92 |
| INT1-22C | 0.21314 | 0.00740 | 16.1841 | 0.56598 | 0.55079 | 0.01336 | 0.15494 | 0.00964 | 2930 | 58 | 2888 | 34 | 2828 | 56 | 2912 | 168 | 2930 | 58 | 71.11 | 201.78 |
| INT1-23 | 0.16331 | 0.00464 | 10.07809 | 0.29902 | 0.44766 | 0.01058 | 0.12634 | 0.00602 | 2490 | 48 | 2442 | 28 | 2385 | 48 | 2405 | 108 | 2490 | 48 | 76.85 | 938.58 |
| INT1-23R | 0.12059 | 0.00508 | 6.2334 | 0.26474 | 0.3748 | 0.01046 | 0.1036 | 0.00720 | 1965 | 76 | 2009 | 38 | 2052 | 50 | 1992 | 132 | 1965 | 76 | 291.10 | 228.94 |
| INT1-24R | 0.123 | 0.00498 | 5.53642 | 0.22784 | 0.32632 | 0.00888 | 0.06686 | 0.00484 | 2000 | 74 | 1906 | 36 | 1821 | 44 | 1308 | 92 | 2000 | 74 | 508.41 | 891.11 |
| INT1-25C | 0.13269 | 0.00408 | 6.70519 | 0.21130 | 0.36655 | 0.00874 | 0.10819 | 0.00558 | 2134 | 56 | 2073 | 28 | 2013 | 42 | 2076 | 102 | 2134 | 56 | 150.54 | 516.87 |
| INT1-25R | 0.17493 | 0.00530 | 11.17781 | 0.34500 | 0.46346 | 0.01100 | 0.11932 | 0.00582 | 2605 | 52 | 2538 | 28 | 2455 | 48 | 2278 | 106 | 2605 | 52 | 97.29 | 143.93 |
| INT1-27 | 0.05962 | 0.00264 | 0.65515 | 0.02864 | 0.0797 | 0.00206 | 0.02487 | 0.00134 | 590 | 98 | 512 | 18 | 494 | 12 | 497 | 26 | 494 | 12 | 197.27 | 197.58 |
| INT1-28 | 0.11681 | 0.00544 | 5.38572 | 0.24718 | 0.33444 | 0.00938 | 0.08514 | 0.00680 | 1908 | 86 | 1883 | 40 | 1860 | 46 | 1652 | 126 | 1908 | 86 | 133.95 | 160.32 |
| INT1-30 | 0.1166 | 0.00396 | 5.42516 | 0.18540 | 0.33749 | 0.00818 | 0.09958 | 0.00564 | 1905 | 62 | 1889 | 30 | 1875 | 40 | 1919 | 104 | 1905 | 62 | 91.77 | 160.70 |
| INT1-31 | 0.11466 | 0.00518 | 5.14422 | 0.23200 | 0.32545 | 0.00910 | 0.08539 | 0.00702 | 1875 | 84 | 1843 | 38 | 1816 | 44 | 1656 | 130 | 1875 | 84 | 202.60 | 389.86 |
| INT1-33 | 0.0667 | 0.00312 | 1.25108 | 0.05768 | 0.13605 | 0.00364 | 0.04242 | 0.00308 | 828 | 100 | 824 | 26 | 822 | 20 | 840 | 60 | 822 | 20 | 74.87 | 179.51 |
| INT1-34 | 0.05633 | 0.00242 | 0.62688 | 0.02666 | 0.08073 | 0.00208 | 0.02559 | 0.00182 | 465 | 98 | 494 | 16 | 500 | 12 | 511 | 36 | 500 | 12 | 255.08 | 635.11 |
| INT1-35 | 0.05592 | 0.00274 | 0.46943 | 0.02254 | 0.06089 | 0.00162 | 0.02045 | 0.00108 | 449 | 112 | 391 | 16 | 381 | 10 | 409 | 22 | 381 | 10 | 139.30 | 219.67 |
| INT2-01 | 0.11248 | 0.00334 | 5.17701 | 0.15702 | 0.33384 | 0.00788 | 0.09503 | 0.00428 | 1840 | 56 | 1849 | 26 | 1857 | 38 | 1835 | 80 | 1840 | 56 | 109.68 | 193.30 |
| INT2-02 | 0.11168 | 0.00726 | 5.137 | 0.32126 | 0.3336 | 0.01220 | 0.08542 | 0.00700 | 1827 | 120 | 1842 | 54 | 1856 | 58 | 1657 | 130 | 1827 | 120 | 46.22 | 46.93 |
| INT2-03 | 0.18386 | 0.00918 | 13.02418 | 0.62648 | 0.51386 | 0.01636 | 0.13973 | 0.00996 | 2688 | 84 | 2681 | 46 | 2673 | 70 | 2644 | 176 | 2688 | 84 | 80.04 | 25.88 |
| INT2-04 | 0.11541 | 0.00376 | 5.29531 | 0.17402 | 0.3328 | 0.00812 | 0.09952 | 0.00470 | 1886 | 60 | 1868 | 28 | 1852 | 40 | 1918 | 86 | 1886 | 60 | 123.51 | 97.53 |
| INT2-05 | 0.05714 | 0.00324 | 0.63305 | 0.03496 | 0.08037 | 0.00226 | 0.02649 | 0.00228 | 497 | 128 | 498 | 22 | 498 | 14 | 528 | 44 | 498 | 14 | 379.73 | 527.31 |
| INT2-06 | 0.11511 | 0.00356 | 5.28034 | 0.16714 | 0.33271 | 0.00790 | 0.09435 | 0.00488 | 1882 | 58 | 1866 | 28 | 1852 | 38 | 1822 | 90 | 1882 | 58 | 325.59 | 699.63 |
| INT2-07 | 0.15143 | 0.00844 | 8.90049 | 0.48560 | 0.42634 | 0.01318 | 0.10003 | 0.01024 | 2362 | 98 | 2328 | 50 | 2289 | 60 | 1927 | 188 | 2362 | 98 | 707.91 | 850.50 |
| INT2-09C | 0.05497 | 0.00420 | 0.45081 | 0.03318 | 0.05948 | 0.00200 | 0.01779 | 0.00154 | 411 | 176 | 378 | 24 | 372 | 12 | 356 | 30 | 372 | 12 | 428.81 | 314.06 |

| Analysis No. | RATIOS | | | | | | | | AGES (Ma) | | | | | | | | | | CONCENTRATIONS (ppm) | |
|---|---|---|---|---|---|---|---|---|---|---|---|---|---|---|---|---|---|---|---|---|
| | $^{207}Pb/^{206}Pb$ | ± 2σ | $^{207}Pb/^{235}U$ | ± 2σ | $^{206}Pb/^{238}U$ | ± 2σ | $^{208}Pb/^{232}Th$ | ± 2σ | $^{207}Pb/^{206}Pb$ | ± 2σ | $^{207}Pb/^{235}U$ | ± 2σ | $^{206}Pb/^{238}U$ | ± 2σ | $^{208}Pb/^{232}Th$ | ± 2σ | Used Age | ± 2σ | Th | U |
| INT2-09R | 0.05384 | 0.00380 | 0.41807 | 0.02854 | 0.05633 | 0.00182 | 0.01377 | 0.00122 | 364 | 162 | 355 | 20 | 353 | 12 | 276 | 24 | 353 | 12 | 631.66 | 450.11 |
| INT2-10 | 0.17937 | 0.00876 | 12.11129 | 0.57804 | 0.48978 | 0.01424 | 0.12799 | 0.01120 | 2647 | 82 | 2613 | 44 | 2570 | 62 | 2434 | 200 | 2647 | 82 | 197.09 | 192.69 |
| INT2-11 | 0.1216 | 0.00540 | 5.8374 | 0.25510 | 0.34822 | 0.00936 | 0.10395 | 0.00826 | 1980 | 80 | 1952 | 38 | 1926 | 44 | 1999 | 152 | 1980 | 80 | 209.59 | 229.50 |
| INT2-12 | 0.05693 | 0.00324 | 0.63992 | 0.03552 | 0.08153 | 0.00232 | 0.02658 | 0.00200 | 489 | 128 | 502 | 22 | 505 | 14 | 530 | 40 | 505 | 14 | 64.90 | 155.99 |
| INT2-13 | 0.116 | 0.00540 | 5.46057 | 0.24942 | 0.34151 | 0.00956 | 0.09774 | 0.00792 | 1895 | 86 | 1894 | 40 | 1894 | 46 | 1885 | 146 | 1895 | 86 | 80.74 | 166.45 |
| INT2-14 | 0.11538 | 0.00434 | 4.9693 | 0.18634 | 0.31238 | 0.00792 | 0.09331 | 0.00584 | 1886 | 70 | 1814 | 32 | 1752 | 38 | 1803 | 108 | 1886 | 70 | 81.99 | 138.55 |
| ~~INT1-02~~ | ~~0.07468~~ | ~~0.00364~~ | ~~0.65076~~ | ~~0.03072~~ | ~~0.06321~~ | ~~0.00172~~ | ~~0.0198~~ | ~~0.00088~~ | ~~1060~~ | ~~100~~ | ~~509~~ | ~~18~~ | ~~395~~ | ~~10~~ | ~~396~~ | ~~18~~ | | | ~~893.46~~ | ~~121.47~~ |
| ~~INT1-04~~ | ~~0.06234~~ | ~~0.00346~~ | ~~0.70017~~ | ~~0.03760~~ | ~~0.08147~~ | ~~0.00230~~ | ~~0.02771~~ | ~~0.00162~~ | ~~686~~ | ~~122~~ | ~~539~~ | ~~22~~ | ~~505~~ | ~~14~~ | ~~552~~ | ~~32~~ | ~~505~~ | ~~14~~ | ~~63.76~~ | ~~97.27~~ |
| ~~INT1-10~~ | ~~0.05723~~ | ~~0.00356~~ | ~~0.46886~~ | ~~0.02834~~ | ~~0.05942~~ | ~~0.00176~~ | ~~0.01925~~ | ~~0.00126~~ | ~~500~~ | ~~140~~ | ~~390~~ | ~~20~~ | ~~372~~ | ~~10~~ | ~~385~~ | ~~24~~ | ~~372~~ | ~~10~~ | ~~191.91~~ | ~~142.44~~ |
| ~~INT1-17~~ | ~~0.04605~~ | ~~0.04924~~ | ~~0.3698~~ | ~~0.39376~~ | ~~0.05825~~ | ~~0.00568~~ | ~~0.01866~~ | ~~0.00106~~ | ~~0~~ | ~~1810~~ | ~~320~~ | ~~292~~ | ~~365~~ | ~~34~~ | ~~374~~ | ~~22~~ | ~~365~~ | ~~34~~ | ~~208.98~~ | ~~23.07~~ |
| ~~INT1-22R~~ | ~~0.17071~~ | ~~0.00638~~ | ~~7.79119~~ | ~~0.29262~~ | ~~0.33107~~ | ~~0.00818~~ | ~~0.07913~~ | ~~0.00544~~ | ~~2565~~ | ~~64~~ | ~~2207~~ | ~~34~~ | ~~1844~~ | ~~40~~ | ~~1539~~ | ~~102~~ | ~~2565~~ | ~~64~~ | ~~316.72~~ | ~~954.24~~ |
| ~~INT1-24C~~ | ~~0.12884~~ | ~~0.00616~~ | ~~3.8053~~ | ~~0.17990~~ | ~~0.21425~~ | ~~0.00602~~ | ~~0.03827~~ | ~~0.00334~~ | ~~2082~~ | ~~86~~ | ~~1594~~ | ~~38~~ | ~~1251~~ | ~~32~~ | ~~759~~ | ~~66~~ | ~~2082~~ | ~~86~~ | ~~678.83~~ | ~~708.12~~ |
| ~~INT1-26~~ | ~~0.06117~~ | ~~0.00286~~ | ~~0.59343~~ | ~~0.02724~~ | ~~0.07037~~ | ~~0.00186~~ | ~~0.02427~~ | ~~0.00136~~ | ~~645~~ | ~~102~~ | ~~473~~ | ~~18~~ | ~~438~~ | ~~12~~ | ~~485~~ | ~~26~~ | ~~438~~ | ~~12~~ | ~~245.18~~ | ~~243.23~~ |
| ~~INT1-29~~ | ~~0.07178~~ | ~~0.00346~~ | ~~0.73947~~ | ~~0.03512~~ | ~~0.07472~~ | ~~0.00208~~ | ~~0.02107~~ | ~~0.00148~~ | ~~980~~ | ~~100~~ | ~~562~~ | ~~20~~ | ~~465~~ | ~~12~~ | ~~421~~ | ~~30~~ | ~~465~~ | ~~12~~ | ~~557.85~~ | ~~474.76~~ |
| ~~INT1-32~~ | ~~0.09473~~ | ~~0.00644~~ | ~~1.01842~~ | ~~0.06596~~ | ~~0.07798~~ | ~~0.00264~~ | ~~0.02422~~ | ~~0.00196~~ | ~~1523~~ | ~~132~~ | ~~713~~ | ~~34~~ | ~~484~~ | ~~16~~ | ~~484~~ | ~~38~~ | | | ~~878.10~~ | ~~114.29~~ |
| ~~INT2-08~~ | ~~0.06818~~ | ~~0.00376~~ | ~~0.93977~~ | ~~0.05050~~ | ~~0.09997~~ | ~~0.00296~~ | ~~0.02738~~ | ~~0.00230~~ | ~~874~~ | ~~116~~ | ~~673~~ | ~~26~~ | ~~614~~ | ~~18~~ | ~~546~~ | ~~46~~ | ~~614~~ | ~~18~~ | ~~636.18~~ | ~~625.18~~ |
| **Malo-Botuobinskoe field, Mir pipe** | | | | | | | | | | | | | | | | | | | | |
| mir-02 | 0.21125 | 0.00316 | 16.38927 | 0.22720 | 0.56272 | 0.00576 | 0.15495 | 0.00400 | 2915 | 24 | 2900 | 14 | 2878 | 24 | 2912 | 70 | 2915 | 24 | 151.84 | 248.18 |
| mir-03 | 0.06497 | 0.00234 | 1.15177 | 0.03924 | 0.12858 | 0.00202 | 0.04124 | 0.00214 | 773 | 78 | 778 | 18 | 780 | 12 | 817 | 42 | 780 | 12 | 133.25 | 230.55 |
| mir-04 | 0.05447 | 0.00272 | 0.4648 | 0.02202 | 0.06191 | 0.00116 | 0.02033 | 0.00104 | 391 | 114 | 388 | 16 | 387 | 8 | 407 | 20 | 387 | 8 | 164.06 | 161.15 |
| mir-05 | 0.11804 | 0.00268 | 5.09451 | 0.10866 | 0.31304 | 0.00370 | 0.06971 | 0.00332 | 1927 | 42 | 1835 | 18 | 1756 | 18 | 1362 | 62 | 1927 | 42 | 64.73 | 651.60 |
| mir-06 | 0.11083 | 0.00172 | 4.8299 | 0.07064 | 0.31611 | 0.00330 | 0.0799 | 0.00218 | 1813 | 28 | 1790 | 12 | 1771 | 16 | 1554 | 40 | 1813 | 28 | 228.43 | 646.91 |
| mir-08 | 0.11273 | 0.00194 | 4.98495 | 0.08046 | 0.32075 | 0.00348 | 0.09054 | 0.00268 | 1844 | 32 | 1817 | 14 | 1793 | 16 | 1752 | 50 | 1844 | 32 | 94.77 | 213.26 |
| mir-12 | 0.12141 | 0.00204 | 5.97193 | 0.09404 | 0.35677 | 0.00380 | 0.10179 | 0.00304 | 1977 | 30 | 1972 | 14 | 1967 | 18 | 1959 | 56 | 1977 | 30 | 361.28 | 502.26 |
| mir-13 | 0.10968 | 0.00326 | 4.59845 | 0.12914 | 0.30409 | 0.00448 | 0.08537 | 0.00490 | 1794 | 56 | 1749 | 24 | 1712 | 22 | 1656 | 92 | 1794 | 56 | 490.10 | 792.91 |
| mir-14 | 0.17955 | 0.00454 | 11.98117 | 0.28472 | 0.48406 | 0.00630 | 0.13979 | 0.00666 | 2649 | 42 | 2603 | 22 | 2545 | 28 | 2645 | 118 | 2649 | 42 | 186.40 | 221.54 |
| mir-16 | 0.11123 | 0.00270 | 4.80407 | 0.10998 | 0.31328 | 0.00400 | 0.08459 | 0.00382 | 1820 | 46 | 1786 | 20 | 1757 | 20 | 1641 | 72 | 1820 | 46 | 305.83 | 501.60 |
| mir-17 | 0.06864 | 0.00130 | 1.39272 | 0.02468 | 0.14717 | 0.00162 | 0.04442 | 0.00112 | 888 | 40 | 886 | 10 | 885 | 10 | 878 | 22 | 885 | 10 | 169.32 | 212.36 |
| mir-18 | 0.05575 | 0.00210 | 0.46415 | 0.01664 | 0.06039 | 0.00098 | 0.01938 | 0.00084 | 442 | 86 | 387 | 12 | 378 | 6 | 388 | 16 | 378 | 6 | 211.08 | 350.32 |
| mir-19 | 0.05423 | 0.00104 | 0.45398 | 0.00824 | 0.06071 | 0.00066 | 0.01866 | 0.00048 | 381 | 44 | 380 | 6 | 380 | 4 | 374 | 10 | 380 | 4 | 518.69 | 615.82 |
| mir-21 | 0.1211 | 0.00192 | 5.93322 | 0.08736 | 0.35536 | 0.00370 | 0.09916 | 0.00260 | 1972 | 28 | 1966 | 12 | 1960 | 18 | 1911 | 48 | 1972 | 28 | 174.17 | 280.09 |
| mir-22 | 0.06933 | 0.00114 | 1.44021 | 0.02210 | 0.15066 | 0.00156 | 0.04541 | 0.00122 | 909 | 34 | 906 | 10 | 905 | 8 | 898 | 24 | 905 | 8 | 850.93 | 794.00 |
| mir-24 | 0.05542 | 0.00116 | 0.48778 | 0.00958 | 0.06384 | 0.00072 | 0.01962 | 0.00056 | 429 | 48 | 403 | 6 | 399 | 4 | 393 | 12 | 399 | 4 | 344.27 | 491.47 |
| mir-25 | 0.05741 | 0.00178 | 0.61977 | 0.01824 | 0.0783 | 0.00110 | 0.02453 | 0.00088 | 507 | 70 | 490 | 12 | 486 | 6 | 490 | 18 | 486 | 6 | 114.47 | 161.24 |
| mir-26 | 0.05405 | 0.00120 | 0.43549 | 0.00904 | 0.05844 | 0.00066 | 0.01779 | 0.00056 | 373 | 52 | 367 | 6 | 366 | 4 | 356 | 12 | 366 | 4 | 521.73 | 521.07 |
| mir-27 | 0.11391 | 0.00258 | 5.22754 | 0.11088 | 0.33286 | 0.00420 | 0.098 | 0.00382 | 1863 | 42 | 1857 | 18 | 1852 | 20 | 1890 | 70 | 1863 | 42 | 46.81 | 113.35 |
| mir-28 | 0.11361 | 0.00224 | 5.12316 | 0.09450 | 0.32707 | 0.00374 | 0.08852 | 0.00304 | 1858 | 36 | 1840 | 16 | 1824 | 18 | 1714 | 56 | 1858 | 36 | 95.85 | 183.24 |
| mir-30 | 0.05587 | 0.00240 | 0.47538 | 0.01938 | 0.06172 | 0.00106 | 0.0184 | 0.00080 | 447 | 98 | 395 | 14 | 386 | 6 | 369 | 16 | 386 | 6 | 104.16 | 104.54 |
| mir-31 | 0.05678 | 0.00212 | 0.61517 | 0.02172 | 0.07858 | 0.00122 | 0.02385 | 0.00114 | 483 | 84 | 487 | 14 | 488 | 8 | 476 | 22 | 488 | 8 | 76.18 | 146.33 |
| mir-33 | 0.05585 | 0.00124 | 0.47151 | 0.00992 | 0.06123 | 0.00070 | 0.01944 | 0.00070 | 446 | 50 | 392 | 6 | 383 | 4 | 389 | 14 | 383 | 4 | 572.23 | 700.56 |
| ~~mir-07~~ | ~~0.06058~~ | ~~0.00124~~ | ~~0.64513~~ | ~~0.01248~~ | ~~0.07725~~ | ~~0.00088~~ | ~~0.02258~~ | ~~0.00068~~ | ~~624~~ | ~~46~~ | ~~505~~ | ~~8~~ | ~~480~~ | ~~6~~ | ~~451~~ | ~~14~~ | ~~480~~ | ~~6~~ | ~~566.77~~ | ~~623.37~~ |

| Analysis No. | RATIOS | | | | | | | | AGES (Ma) | | | | | | | | | | CONCENTRATIONS (ppm) | |
|---|---|---|---|---|---|---|---|---|---|---|---|---|---|---|---|---|---|---|---|---|
| | $^{207}Pb/^{206}Pb$ | ± 2σ | $^{207}Pb/^{235}U$ | ± 2σ | $^{206}Pb/^{238}U$ | ± 2σ | $^{208}Pb/^{232}Th$ | ± 2σ | $^{207}Pb/^{206}Pb$ | ± 2σ | $^{207}Pb/^{235}U$ | ± 2σ | $^{206}Pb/^{238}U$ | ± 2σ | $^{208}Pb/^{232}Th$ | ± 2σ | Used Age | ± 2σ | Th | U |
| ~~mir 11~~ | ~~0.06252~~ | ~~0.00230~~ | ~~0.69894~~ | ~~0.02432~~ | ~~0.08109~~ | ~~0.00134~~ | ~~0.02545~~ | ~~0.00150~~ | ~~692~~ | ~~80~~ | ~~538~~ | ~~14~~ | ~~503~~ | ~~8~~ | ~~508~~ | ~~30~~ | ~~503~~ | ~~8~~ | ~~202.65~~ | ~~552.79~~ |
| ~~mir 15~~ | ~~0.07908~~ | ~~0.00206~~ | ~~1.11041~~ | ~~0.02724~~ | ~~0.10185~~ | ~~0.00136~~ | ~~0.02957~~ | ~~0.00108~~ | ~~1174~~ | ~~52~~ | ~~758~~ | ~~14~~ | ~~625~~ | ~~8~~ | ~~589~~ | ~~22~~ | ~~625~~ | ~~8~~ | ~~374.93~~ | ~~164.06~~ |
| ~~mir 23~~ | ~~0.0858~~ | ~~0.00268~~ | ~~1.74468~~ | ~~0.05014~~ | ~~0.14747~~ | ~~0.00178~~ | ~~0.04376~~ | ~~0.00066~~ | ~~1334~~ | ~~62~~ | ~~1025~~ | ~~18~~ | ~~887~~ | ~~10~~ | ~~866~~ | ~~12~~ | ~~887~~ | ~~10~~ | ~~84.92~~ | ~~250.86~~ |
| ~~mir 29~~ | ~~0.06305~~ | ~~0.00222~~ | ~~0.59659~~ | ~~0.01974~~ | ~~0.06864~~ | ~~0.00108~~ | ~~0.0192~~ | ~~0.00088~~ | ~~710~~ | ~~76~~ | ~~475~~ | ~~12~~ | ~~428~~ | ~~6~~ | ~~384~~ | ~~18~~ | ~~428~~ | ~~6~~ | ~~289.26~~ | ~~273.73~~ |
| ~~mir 32~~ | ~~0.16227~~ | ~~0.00500~~ | ~~6.16191~~ | ~~0.17944~~ | ~~0.27542~~ | ~~0.00404~~ | ~~0.06113~~ | ~~0.00362~~ | ~~2479~~ | ~~54~~ | ~~1999~~ | ~~26~~ | ~~1568~~ | ~~20~~ | ~~1199~~ | ~~68~~ | ~~2479~~ | ~~54~~ | ~~542.19~~ | ~~529.36~~ |
| **Malo-Botuobinskoe field, Amakinskaya pipe** | | | | | | | | | | | | | | | | | | | | |
| MVG250-A-01 | 0.055094 | 0.00401 | 0.45764 | 0.03284 | 0.060245 | 0.00197 | 0.018101 | 0.00155 | 415.9 | 158 | 382.6 | 23 | 377.1 | 12 | 362.6 | 31 | 377.1 | 12 | 1.54 | 38.39 |
| MVG250-A-02 | 0.055709 | 0.00382 | 0.457768 | 0.03096 | 0.059598 | 0.00190 | 0.018664 | 0.00150 | 440.5 | 149 | 382.7 | 22 | 373.2 | 12 | 373.8 | 30 | 373.2 | 12 | 1.50 | 36.06 |
| MVG250-A-03 | 0.056375 | 0.00401 | 0.456787 | 0.03196 | 0.058766 | 0.00191 | 0.018657 | 0.00158 | 466.4 | 155 | 382 | 22 | 368.1 | 12 | 373.6 | 31 | 368.1 | 12 | 1.47 | 35.94 |
| MVG250-A-04 | 0.051122 | 0.00406 | 0.418843 | 0.03273 | 0.059422 | 0.00199 | 0.017727 | 0.00163 | 246.3 | 178 | 355.2 | 23 | 372.1 | 12 | 355.2 | 32 | 372.1 | 12 | 1.36 | 34.88 |
| MVG250-A-05 | 0.056869 | 0.00386 | 0.462832 | 0.03106 | 0.059028 | 0.00185 | 0.021357 | 0.00154 | 485.8 | 148 | 386.2 | 22 | 369.7 | 11 | 427.1 | 31 | 369.7 | 11 | 1.61 | 33.98 |
| MVG250-A-06 | 0.057434 | 0.00390 | 0.480609 | 0.03218 | 0.060693 | 0.00191 | 0.021389 | 0.00160 | 507.8 | 147 | 398.5 | 22 | 379.8 | 12 | 427.8 | 32 | 379.8 | 12 | 1.47 | 31.24 |
| **Malo-Botuobinskoe field, Sputnik pipe** | | | | | | | | | | | | | | | | | | | | |
| SPUT-01 | 0.05697 | 0.00222 | 0.56609 | 0.02252 | 0.07206 | 0.00194 | 0.02095 | 0.00080 | 490 | 88 | 455 | 14 | 449 | 12 | 419 | 16 | 449 | 12 | 257.10 | 176.04 |
| SPUT-02 | 0.11287 | 0.00310 | 5.29237 | 0.15884 | 0.34005 | 0.00872 | 0.09442 | 0.00402 | 1846 | 50 | 1868 | 26 | 1887 | 42 | 1824 | 74 | 1846 | 50 | 61.18 | 271.30 |
| SPUT-03 | 0.11352 | 0.00268 | 5.15951 | 0.13774 | 0.32961 | 0.00814 | 0.09082 | 0.00298 | 1857 | 44 | 1846 | 22 | 1836 | 40 | 1757 | 56 | 1857 | 44 | 44.71 | 274.43 |
| SPUT-04 | 0.15073 | 0.00412 | 8.82225 | 0.26432 | 0.42449 | 0.01110 | 0.10814 | 0.00402 | 2354 | 48 | 2320 | 28 | 2281 | 50 | 2075 | 74 | 2354 | 48 | 87.52 | 102.78 |
| SPUT-05 | 0.06779 | 0.00222 | 1.28624 | 0.04446 | 0.13761 | 0.00364 | 0.0395 | 0.00172 | 862 | 70 | 840 | 20 | 831 | 20 | 783 | 34 | 831 | 20 | 193.05 | 255.89 |
| SPUT-06 | 0.12069 | 0.00376 | 5.96107 | 0.19876 | 0.3582 | 0.00948 | 0.09143 | 0.00452 | 1966 | 56 | 1970 | 28 | 1974 | 44 | 1768 | 84 | 1966 | 56 | 76.52 | 308.92 |
| SPUT-07 | 0.11281 | 0.00490 | 5.13728 | 0.22234 | 0.33021 | 0.00944 | 0.08723 | 0.00560 | 1845 | 80 | 1842 | 36 | 1839 | 46 | 1690 | 104 | 1845 | 80 | 47.89 | 52.81 |
| SPUT-10 | 0.12093 | 0.00332 | 5.97719 | 0.17744 | 0.35847 | 0.00902 | 0.09677 | 0.00390 | 1970 | 50 | 1973 | 26 | 1975 | 42 | 1867 | 72 | 1970 | 50 | 99.37 | 143.07 |
| SPUT-13 | 0.06885 | 0.00238 | 1.33021 | 0.04826 | 0.14015 | 0.00378 | 0.03235 | 0.00116 | 894 | 74 | 859 | 22 | 846 | 22 | 644 | 22 | 846 | 22 | 159.97 | 162.77 |
| SPUT-14 | 0.19255 | 0.00868 | 14.05105 | 0.62958 | 0.52929 | 0.01606 | 0.14439 | 0.01092 | 2764 | 76 | 2753 | 42 | 2738 | 68 | 2726 | 192 | 2764 | 76 | 32.14 | 44.09 |
| SPUT-15R | 0.05581 | 0.00368 | 0.53917 | 0.03496 | 0.07016 | 0.00244 | 0.01582 | 0.00096 | 445 | 150 | 438 | 24 | 437 | 14 | 317 | 20 | 437 | 14 | 104.02 | 159.25 |
| SPUT-16 | 0.18691 | 0.00552 | 13.41635 | 0.43646 | 0.52071 | 0.01398 | 0.09849 | 0.00348 | 2715 | 50 | 2709 | 30 | 2702 | 60 | 1899 | 64 | 2715 | 50 | 341.01 | 150.48 |
| SPUT-17 | 0.12232 | 0.00318 | 5.82105 | 0.16866 | 0.34519 | 0.00874 | 0.07884 | 0.00256 | 1990 | 48 | 1950 | 26 | 1912 | 42 | 1534 | 48 | 1990 | 48 | 167.73 | 375.60 |
| SPUT-18 | 0.14519 | 0.00518 | 7.78279 | 0.29116 | 0.38883 | 0.01056 | 0.08547 | 0.00438 | 2290 | 62 | 2206 | 34 | 2117 | 50 | 1658 | 82 | 2290 | 62 | 192.79 | 392.97 |
| SPUT-19 | 0.11282 | 0.00350 | 5.13594 | 0.17110 | 0.33022 | 0.00874 | 0.0658 | 0.00242 | 1845 | 58 | 1842 | 28 | 1839 | 42 | 1288 | 46 | 1845 | 58 | 98.47 | 128.11 |
| SPUT-20 | 0.06032 | 0.00196 | 0.78557 | 0.02714 | 0.09447 | 0.00248 | 0.02027 | 0.00072 | 615 | 72 | 589 | 16 | 582 | 14 | 406 | 14 | 582 | 14 | 477.20 | 411.84 |
| SPUT-21 | 0.17312 | 0.00374 | 11.7832 | 0.30616 | 0.49367 | 0.01246 | 0.12792 | 0.00346 | 2588 | 36 | 2587 | 24 | 2587 | 54 | 2433 | 62 | 2588 | 36 | 399.42 | 572.03 |
| SPUT-22 | 0.14792 | 0.00346 | 8.4516 | 0.23540 | 0.41444 | 0.01084 | 0.1159 | 0.00366 | 2322 | 42 | 2281 | 26 | 2235 | 50 | 2216 | 66 | 2322 | 42 | 193.07 | 382.60 |
| SPUT-23 | 0.1173 | 0.00254 | 5.36324 | 0.13484 | 0.33162 | 0.00804 | 0.09699 | 0.00274 | 1915 | 40 | 1879 | 22 | 1846 | 38 | 1871 | 50 | 1915 | 40 | 170.44 | 1422.71 |
| SPUT-24 | 0.11315 | 0.00278 | 5.2094 | 0.15218 | 0.33391 | 0.00898 | 0.10008 | 0.00328 | 1851 | 46 | 1854 | 24 | 1857 | 44 | 1928 | 60 | 1851 | 46 | 142.98 | 324.84 |
| SPUT-25 | 0.11198 | 0.00252 | 4.76949 | 0.12820 | 0.30893 | 0.00792 | 0.08931 | 0.00256 | 1832 | 42 | 1780 | 22 | 1735 | 40 | 1729 | 48 | 1832 | 42 | 318.41 | 669.41 |
| SPUT-26 | 0.06661 | 0.00352 | 1.29404 | 0.06920 | 0.1409 | 0.00462 | 0.03891 | 0.00234 | 826 | 112 | 843 | 30 | 850 | 26 | 772 | 46 | 850 | 26 | 54.71 | 153.15 |
| SPUT-27 | 0.11266 | 0.00272 | 5.11659 | 0.14514 | 0.32943 | 0.00864 | 0.0953 | 0.00288 | 1843 | 44 | 1839 | 24 | 1836 | 42 | 1840 | 54 | 1843 | 44 | 209.54 | 242.82 |
| SPUT-30 | 0.05589 | 0.00274 | 0.48148 | 0.02362 | 0.06249 | 0.00178 | 0.01956 | 0.00074 | 448 | 112 | 399 | 16 | 391 | 10 | 392 | 14 | 391 | 10 | 56.82 | 75.50 |
| SPUT-31 | 0.11422 | 0.00510 | 4.67538 | 0.16824 | 0.29688 | 0.00788 | 0.08552 | 0.00232 | 1868 | 82 | 1763 | 30 | 1676 | 40 | 1659 | 44 | 1868 | 82 | 79.88 | 239.29 |
| SPUT-32 | 0.11176 | 0.00260 | 5.1565 | 0.13934 | 0.33465 | 0.00844 | 0.09523 | 0.00296 | 1828 | 44 | 1845 | 22 | 1861 | 40 | 1839 | 54 | 1828 | 44 | 373.55 | 678.35 |
| SPUT-34 | 0.05411 | 0.00270 | 0.46758 | 0.02326 | 0.06267 | 0.00180 | 0.01972 | 0.00102 | 376 | 114 | 390 | 16 | 392 | 10 | 395 | 20 | 392 | 10 | 189.41 | 188.13 |
| SPUT-35 | 0.05363 | 0.00274 | 0.46827 | 0.02384 | 0.06333 | 0.00182 | 0.02136 | 0.00084 | 356 | 118 | 390 | 16 | 396 | 12 | 427 | 16 | 396 | 12 | 107.83 | 67.43 |

| Analysis No. | RATIOS | | | | | | | | AGES (Ma) | | | | | | | | | | CONCENTRATIONS (ppm) | |
|---|---|---|---|---|---|---|---|---|---|---|---|---|---|---|---|---|---|---|---|---|
| | $^{207}Pb/^{206}Pb$ | ± 2σ | $^{207}Pb/^{235}U$ | ± 2σ | $^{206}Pb/^{238}U$ | ± 2σ | $^{208}Pb/^{232}Th$ | ± 2σ | $^{207}Pb/^{206}Pb$ | ± 2σ | $^{207}Pb/^{235}U$ | ± 2σ | $^{206}Pb/^{238}U$ | ± 2σ | $^{208}Pb/^{232}Th$ | ± 2σ | Used Age | ± 2σ | Th | U |
| SPUT-36 | 0.11407 | 0.00306 | 4.70554 | 0.14352 | 0.29919 | 0.00798 | 0.07827 | 0.00324 | 1865 | 50 | 1768 | 26 | 1687 | 40 | 1523 | 60 | 1865 | 50 | 252.56 | 968.89 |
| SPUT-37 | 0.1659 | 0.00484 | 10.84548 | 0.35328 | 0.47419 | 0.01310 | 0.11127 | 0.00524 | 2517 | 50 | 2510 | 30 | 2502 | 58 | 2132 | 96 | 2517 | 50 | 129.01 | 452.81 |
| SPUT-38 | 0.06138 | 0.00246 | 0.54982 | 0.02254 | 0.06497 | 0.00178 | 0.01909 | 0.00104 | 653 | 88 | 445 | 14 | 406 | 10 | 382 | 20 | 406 | 10 | 237.13 | 352.78 |
| SPUT-39 | 0.05359 | 0.00180 | 0.4256 | 0.01516 | 0.0576 | 0.00156 | 0.01793 | 0.00096 | 354 | 78 | 360 | 10 | 361 | 10 | 359 | 20 | 361 | 10 | 93.60 | 765.51 |
| SPUT-40 | 0.17742 | 0.00520 | 12.37345 | 0.39470 | 0.50583 | 0.01340 | 0.13739 | 0.00682 | 2629 | 50 | 2633 | 30 | 2639 | 58 | 2602 | 122 | 2629 | 50 | 136.84 | 251.99 |
| SPUT-43 | 0.05477 | 0.00234 | 0.45123 | 0.01962 | 0.05975 | 0.00170 | 0.01897 | 0.00110 | 403 | 98 | 378 | 14 | 374 | 10 | 380 | 22 | 374 | 10 | 130.72 | 253.98 |
| SPUT-44 | 0.05267 | 0.00288 | 0.44605 | 0.02420 | 0.06142 | 0.00188 | 0.01972 | 0.00096 | 315 | 128 | 375 | 16 | 384 | 12 | 395 | 20 | 384 | 12 | 101.73 | 111.53 |
| SPUT-45 | 0.11498 | 0.00426 | 5.40423 | 0.20608 | 0.34088 | 0.00938 | 0.09534 | 0.00590 | 1880 | 68 | 1886 | 32 | 1891 | 46 | 1841 | 108 | 1880 | 68 | 219.45 | 260.05 |
| SPUT-46 | 0.05738 | 0.00306 | 0.49828 | 0.02622 | 0.06299 | 0.00184 | 0.01849 | 0.00120 | 506 | 120 | 411 | 18 | 394 | 12 | 370 | 24 | 394 | 12 | 235.37 | 288.47 |
| SPUT-47 | 0.18376 | 0.00676 | 12.95928 | 0.49130 | 0.51149 | 0.01384 | 0.14034 | 0.00924 | 2687 | 62 | 2677 | 36 | 2663 | 60 | 2654 | 164 | 2687 | 62 | 241.93 | 594.23 |
| SPUT-48 | 0.05593 | 0.00246 | 0.61302 | 0.02754 | 0.07952 | 0.00234 | 0.02381 | 0.00154 | 450 | 100 | 485 | 18 | 493 | 14 | 476 | 30 | 493 | 14 | 493.45 | 536.60 |
| SPUT-50 | 0.06029 | 0.00390 | 0.67264 | 0.04266 | 0.08091 | 0.00266 | 0.02598 | 0.00162 | 614 | 144 | 522 | 26 | 502 | 16 | 518 | 32 | 502 | 16 | 20.23 | 38.98 |
| SPUT-51 | 0.15119 | 0.00598 | 8.99963 | 0.35992 | 0.43176 | 0.01164 | 0.10349 | 0.00702 | 2359 | 70 | 2338 | 36 | 2314 | 52 | 1990 | 128 | 2359 | 70 | 201.79 | 321.11 |
| SPUT-52 | 0.05716 | 0.00276 | 0.50086 | 0.02452 | 0.06355 | 0.00190 | 0.01892 | 0.00126 | 498 | 108 | 412 | 16 | 397 | 12 | 379 | 24 | 397 | 12 | 408.47 | 312.90 |
| SPUT-53 | 0.12403 | 0.00472 | 6.30314 | 0.24362 | 0.36859 | 0.00974 | 0.09614 | 0.00678 | 2015 | 70 | 2019 | 34 | 2023 | 46 | 1855 | 126 | 2015 | 70 | 20.27 | 404.99 |
| SPUT-55 | 0.10804 | 0.00286 | 4.70165 | 0.13834 | 0.31566 | 0.00806 | 0.08646 | 0.00322 | 1767 | 50 | 1768 | 24 | 1768 | 40 | 1676 | 60 | 1767 | 50 | 107.05 | 205.00 |
| SPUT-56 | 0.06006 | 0.00434 | 0.71335 | 0.05054 | 0.08617 | 0.00318 | 0.02245 | 0.00182 | 606 | 160 | 547 | 30 | 533 | 18 | 449 | 36 | 533 | 18 | 121.81 | 227.68 |
| SPUT-57 | 0.05727 | 0.00226 | 0.59681 | 0.02412 | 0.07559 | 0.00204 | 0.02223 | 0.00086 | 502 | 88 | 475 | 16 | 470 | 12 | 444 | 18 | 470 | 12 | 125.42 | 105.90 |
| SPUT-58 | 0.11874 | 0.00714 | 5.53953 | 0.29576 | 0.33835 | 0.00942 | 0.09708 | 0.00270 | 1937 | 110 | 1907 | 46 | 1879 | 46 | 1873 | 50 | 1937 | 110 | 74.63 | 115.33 |
| SPUT-59 | 0.05581 | 0.00184 | 0.54436 | 0.01908 | 0.07076 | 0.00188 | 0.02049 | 0.00088 | 445 | 74 | 441 | 12 | 441 | 12 | 410 | 18 | 441 | 12 | 278.83 | 482.16 |
| SPUT-61 | 0.11434 | 0.00326 | 5.11535 | 0.16132 | 0.32458 | 0.00854 | 0.08295 | 0.00362 | 1870 | 52 | 1839 | 26 | 1812 | 42 | 1611 | 68 | 1870 | 52 | 224.99 | 573.32 |
| SPUT-63 | 0.10981 | 0.00888 | 4.63504 | 0.34442 | 0.30612 | 0.00980 | 0.08854 | 0.00298 | 1796 | 150 | 1756 | 62 | 1722 | 48 | 1715 | 56 | 1796 | 150 | 35.12 | 86.17 |
| SPUT-64 | 0.11482 | 0.00354 | 4.98161 | 0.16672 | 0.31481 | 0.00854 | 0.09457 | 0.00462 | 1877 | 56 | 1816 | 28 | 1764 | 42 | 1826 | 86 | 1877 | 56 | 183.00 | 310.24 |
| SPUT-66 | 0.15978 | 0.00436 | 9.91278 | 0.30432 | 0.45002 | 0.01226 | 0.09076 | 0.00376 | 2453 | 48 | 2427 | 28 | 2395 | 54 | 1756 | 70 | 2453 | 48 | 231.37 | 238.55 |
| SPUT-67C | 0.11584 | 0.00336 | 5.3577 | 0.17064 | 0.33555 | 0.00886 | 0.05376 | 0.00312 | 1893 | 54 | 1878 | 28 | 1865 | 42 | 1058 | 60 | 1893 | 54 | 21.13 | 663.88 |
| SPUT-67R | 0.11384 | 0.00358 | 5.17537 | 0.17308 | 0.32979 | 0.00866 | 0.08314 | 0.00432 | 1862 | 58 | 1849 | 28 | 1837 | 42 | 1614 | 80 | 1862 | 58 | 101.44 | 387.49 |
| SPUT-68 | 0.11526 | 0.00350 | 5.10968 | 0.16656 | 0.32157 | 0.00852 | 0.08653 | 0.00388 | 1884 | 56 | 1838 | 28 | 1797 | 42 | 1677 | 72 | 1884 | 56 | 37.90 | 78.07 |
| SPUT-69 | 0.11131 | 0.00402 | 4.6642 | 0.17490 | 0.304 | 0.00834 | 0.08833 | 0.00538 | 1821 | 68 | 1761 | 32 | 1711 | 42 | 1711 | 100 | 1821 | 68 | 408.58 | 366.83 |
| SPUT-71 | 0.05521 | 0.00218 | 0.46375 | 0.01866 | 0.06093 | 0.00162 | 0.01899 | 0.00096 | 421 | 90 | 387 | 12 | 381 | 10 | 380 | 20 | 381 | 10 | 206.04 | 253.46 |
| SPUT-72 | 0.1122 | 0.00454 | 5.0957 | 0.21412 | 0.3294 | 0.00964 | 0.09023 | 0.00684 | 1835 | 74 | 1835 | 36 | 1835 | 46 | 1746 | 126 | 1835 | 74 | 64.97 | 1325.24 |
| SPUT-75 | 0.12082 | 0.00480 | 6.03923 | 0.24768 | 0.36257 | 0.01070 | 0.09588 | 0.00726 | 1968 | 72 | 1982 | 36 | 1994 | 50 | 1851 | 134 | 1968 | 72 | 134.08 | 626.01 |
| ~~SPUT-08~~ | ~~0.12777~~ | ~~0.05206~~ | ~~1.45934~~ | ~~0.58094~~ | ~~0.08284~~ | ~~0.00720~~ | ~~0.02359~~ | ~~0.00170~~ | ~~2068~~ | ~~792~~ | ~~914~~ | ~~240~~ | ~~513~~ | ~~42~~ | ~~471~~ | ~~34~~ | ~~2068~~ | ~~792~~ | ~~44.30~~ | ~~16.19~~ |
| ~~SPUT-09~~ | ~~0.06034~~ | ~~0.00306~~ | ~~0.6323~~ | ~~0.03190~~ | ~~0.07603~~ | ~~0.00222~~ | ~~0.0229~~ | ~~0.00138~~ | ~~616~~ | ~~112~~ | ~~498~~ | ~~20~~ | ~~472~~ | ~~14~~ | ~~458~~ | ~~28~~ | ~~472~~ | ~~14~~ | ~~132.49~~ | ~~143.19~~ |
| ~~SPUT-11~~ | ~~0.23679~~ | ~~0.01116~~ | ~~3.34869~~ | ~~0.15272~~ | ~~0.1026~~ | ~~0.00322~~ | ~~0.11258~~ | ~~0.00822~~ | ~~3099~~ | ~~76~~ | ~~1492~~ | ~~36~~ | ~~630~~ | ~~18~~ | ~~2156~~ | ~~150~~ | ~~3099~~ | ~~76~~ | ~~116.53~~ | ~~211.60~~ |
| ~~SPUT-12~~ | ~~0.06774~~ | ~~0.00272~~ | ~~1.01458~~ | ~~0.04242~~ | ~~0.10865~~ | ~~0.00314~~ | ~~0.0272~~ | ~~0.00118~~ | ~~861~~ | ~~86~~ | ~~711~~ | ~~22~~ | ~~665~~ | ~~18~~ | ~~542~~ | ~~24~~ | ~~665~~ | ~~18~~ | ~~157.11~~ | ~~229.49~~ |
| ~~SPUT-41~~ | ~~0.06978~~ | ~~0.00354~~ | ~~0.63896~~ | ~~0.03250~~ | ~~0.06646~~ | ~~0.00212~~ | ~~0.01687~~ | ~~0.00126~~ | ~~922~~ | ~~106~~ | ~~502~~ | ~~20~~ | ~~415~~ | ~~12~~ | ~~338~~ | ~~26~~ | ~~415~~ | ~~12~~ | ~~269.45~~ | ~~439.11~~ |
| ~~SPUT-42~~ | ~~0.06692~~ | ~~0.00286~~ | ~~0.55545~~ | ~~0.02402~~ | ~~0.0602~~ | ~~0.00172~~ | ~~0.01898~~ | ~~0.00094~~ | ~~835~~ | ~~92~~ | ~~449~~ | ~~16~~ | ~~377~~ | ~~10~~ | ~~380~~ | ~~18~~ | ~~377~~ | ~~10~~ | ~~80.25~~ | ~~113.26~~ |
| ~~SPUT-49~~ | ~~0.06421~~ | ~~0.00216~~ | ~~0.69906~~ | ~~0.02474~~ | ~~0.07896~~ | ~~0.00212~~ | ~~0.02403~~ | ~~0.00110~~ | ~~749~~ | ~~72~~ | ~~538~~ | ~~14~~ | ~~490~~ | ~~12~~ | ~~480~~ | ~~22~~ | ~~490~~ | ~~12~~ | ~~446.77~~ | ~~372.61~~ |
| ~~SPUT-54~~ | ~~0.0716~~ | ~~0.00306~~ | ~~0.75109~~ | ~~0.03302~~ | ~~0.07607~~ | ~~0.00224~~ | ~~0.02~~ | ~~0.00102~~ | ~~975~~ | ~~90~~ | ~~569~~ | ~~20~~ | ~~473~~ | ~~14~~ | ~~400~~ | ~~20~~ | ~~473~~ | ~~14~~ | ~~330.37~~ | ~~299.17~~ |
| ~~SPUT-60~~ | ~~0.0666~~ | ~~0.00634~~ | ~~0.55539~~ | ~~0.05078~~ | ~~0.0605~~ | ~~0.00252~~ | ~~0.01838~~ | ~~0.00172~~ | ~~825~~ | ~~204~~ | ~~449~~ | ~~34~~ | ~~379~~ | ~~16~~ | ~~368~~ | ~~34~~ | ~~379~~ | ~~16~~ | ~~103.87~~ | ~~126.57~~ |
| ~~SPUT-62~~ | ~~0.07017~~ | ~~0.00506~~ | ~~1.001~~ | ~~0.07024~~ | ~~0.10343~~ | ~~0.00388~~ | ~~0.02464~~ | ~~0.00206~~ | ~~933~~ | ~~152~~ | ~~704~~ | ~~36~~ | ~~634~~ | ~~22~~ | ~~492~~ | ~~40~~ | ~~634~~ | ~~22~~ | ~~258.53~~ | ~~257.18~~ |

| Analysis No. | RATIOS | | | | | | | | AGES (Ma) | | | | | | | | | | CONCENTRATIONS (ppm) | |
|---|---|---|---|---|---|---|---|---|---|---|---|---|---|---|---|---|---|---|---|---|
| | $\frac{^{207}Pb}{^{206}Pb}$ | ± 2σ | $\frac{^{207}Pb}{^{235}U}$ | ± 2σ | $\frac{^{206}Pb}{^{238}U}$ | ± 2σ | $\frac{^{208}Pb}{^{232}Th}$ | ± 2σ | $\frac{^{207}Pb}{^{206}Pb}$ | ± 2σ | $\frac{^{207}Pb}{^{235}U}$ | ± 2σ | $\frac{^{206}Pb}{^{238}U}$ | ± 2σ | $\frac{^{208}Pb}{^{232}Th}$ | ± 2σ | Used Age | ± 2σ | Th | U |
| ~~SPUT-70~~ | ~~0.07982~~ | ~~0.00502~~ | ~~0.93505~~ | ~~0.05688~~ | ~~0.08498~~ | ~~0.00284~~ | ~~0.02722~~ | ~~0.00204~~ | ~~1193~~ | ~~128~~ | ~~670~~ | ~~30~~ | ~~526~~ | ~~16~~ | ~~543~~ | ~~40~~ | ~~526~~ | ~~16~~ | ~~118.79~~ | ~~99.58~~ |

**Appendix 2.2. Zircon trace-element data (ppm) for the samples from the Magan terrane**

| Analysis No. | P | Ca | Ti | Y | Nb | La | Ce | Pr | Nd | Sm | Eu | Gd | Dy | Ho | Er | Yb | Lu | Hf | Ta | Th | U | Th/U | Nb/Ta |
|---|---|---|---|---|---|---|---|---|---|---|---|---|---|---|---|---|---|---|---|---|---|---|---|
| **Malo-Botuobinskoe field, Internationalnaya pipe** | | | | | | | | | | | | | | | | | | | | | | | |
| INT1-01 | 231 | | 22.5 | 958 | 4.5 | 0.01 | 9.3 | 0.1 | 1.9 | 4.0 | 0.2 | 22.5 | 86.8 | 31.7 | 140.3 | 249 | 48.1 | 16940 | 1.5 | 59.1 | 133.7 | 0.44 | 2.98 |
| INT1-07 | 357 | | 25.7 | 1999 | 33.4 | 1.47 | 30.1 | 1.4 | 8.7 | 6.7 | 0.8 | 31.2 | 150.7 | 61.8 | 313.1 | 709 | 151.2 | 21318 | 14.8 | 230.6 | 1126.9 | 0.20 | 2.26 |
| INT1-08 | 810 | | 19.9 | 2933 | 29.6 | 0.24 | 11.6 | 0.3 | 2.1 | 4.2 | 0.4 | 36.6 | 257.4 | 91.7 | 397.3 | 715 | 137.6 | 25596 | 15.1 | 42.8 | 509.1 | 0.08 | 1.96 |
| INT1-09 | 310 | | 10.3 | 3134 | 3.3 | 0.03 | 13.4 | 0.5 | 9.0 | 15.8 | 2.5 | 82.3 | 300.3 | 109.2 | 465.3 | 788 | 151.6 | 16998 | 1.0 | 88.4 | 149.5 | 0.59 | 3.33 |
| INT1-11 | 343 | | 10.5 | 2161 | 10.7 | 0.37 | 19.7 | 0.5 | 4.9 | 6.7 | 1.5 | 35.8 | 167.2 | 69.3 | 336.6 | 740 | 158.7 | 19167 | 1.2 | 267.6 | 471.7 | 0.57 | 8.92 |
| INT1-12 | 171 | | 7.9 | 1952 | 11.0 | 1.29 | 72.6 | 0.8 | 6.1 | 5.2 | 2.6 | 27.3 | 127.7 | 55.9 | 301.2 | 811 | 193.4 | 18190 | 1.7 | 610.5 | 1018.0 | 0.60 | 6.33 |
| INT1-13 | 114 | <28.35 | 9.7 | 1493 | 3.6 | 0.35 | 8.0 | 0.5 | 7.4 | 10.4 | 1.0 | 42.7 | 142.6 | 50.7 | 220.1 | 393 | 70.1 | 9153 | 0.6 | 81.4 | 158.6 | 0.51 | 6.18 |
| INT1-14C | 45 | 132 | 22.8 | 2313 | 52.6 | 5.26 | 132.9 | 4.9 | 29.8 | 16.3 | 5.0 | 41.7 | 147.4 | 63.1 | 351.0 | 994 | 231.2 | 10068 | 2.2 | 587.0 | 626.9 | 0.94 | 24.12 |
| INT1-14R | 32 | <37.98 | 4.1 | 590 | 3.4 | 0.40 | 38.0 | 0.2 | 1.5 | 1.7 | 0.5 | 5.8 | 30.8 | 14.9 | 93.4 | 300 | 73.0 | 11339 | 0.3 | 179.7 | 348.8 | 0.52 | 11.32 |
| INT1-15 | 156 | <50.08 | 14.8 | 675 | 2.8 | 0.02 | 6.1 | 0.1 | 1.3 | 2.5 | 0.2 | 15.0 | 60.2 | 22.6 | 101.3 | 183 | 35.4 | 10640 | 0.9 | 53.3 | 64.9 | 0.82 | 3.20 |
| INT1-16 | 158 | 29 | 17.3 | 714 | 4.9 | 0.02 | 9.1 | 0.1 | 1.1 | 2.5 | 0.1 | 13.2 | 61.3 | 23.1 | 110.0 | 227 | 43.3 | 10116 | 1.7 | 67.7 | 147.0 | 0.46 | 2.84 |
| INT1-18C | 267 | <42.77 | 6.5 | 1273 | 4.4 | 0.48 | 17.3 | 0.3 | 4.0 | 6.6 | 1.0 | 31.6 | 117.2 | 43.6 | 188.9 | 322 | 60.3 | 8724 | 1.6 | 73.3 | 131.6 | 0.56 | 2.85 |
| INT1-18R | 202 | <40.72 | 6.7 | 809 | 5.3 | 0.24 | 14.1 | 0.1 | 1.5 | 3.1 | 0.4 | 16.7 | 71.7 | 27.2 | 124.7 | 230 | 44.0 | 9968 | 2.1 | 52.0 | 191.0 | 0.27 | 2.52 |
| INT1-19 | 456 | 1066 | 8.2 | 1149 | 4.4 | 4.40 | 50.1 | 1.4 | 7.7 | 5.4 | 2.4 | 23.4 | 91.4 | 34.7 | 165.5 | 370 | 78.4 | 9040 | 0.9 | 202.1 | 261.3 | 0.77 | 5.12 |
| INT1-20 | 198 | <36.43 | 7.2 | 1296 | 4.1 | 0.02 | 14.8 | 0.1 | 1.7 | 3.6 | 0.8 | 19.8 | 98.0 | 40.2 | 200.9 | 436 | 91.4 | 9434 | 1.4 | 191.1 | 525.4 | 0.36 | 2.91 |
| INT1-21RI | 126 | 119 | 17.2 | 697 | 13.5 | 7.90 | 46.7 | 3.7 | 20.5 | 9.1 | 2.9 | 19.7 | 60.5 | 22.0 | 102.0 | 210 | 41.4 | 11836 | 2.1 | 244.1 | 334.5 | 0.73 | 6.51 |
| INT1-22C | 86 | 85 | 9.4 | 370 | 4.1 | 0.50 | 8.7 | 0.5 | 3.3 | 2.4 | 0.7 | 7.3 | 27.8 | 11.2 | 58.2 | 157 | 41.2 | 12957 | 0.6 | 54.2 | 167.2 | 0.32 | 6.92 |
| INT1-22R | 127 | 643 | 65.1 | 1052 | 38.9 | 8.49 | 56.4 | 8.7 | 47.0 | 20.3 | 9.5 | 38.3 | 99.8 | 34.1 | 147.4 | 296 | 62.9 | 13015 | 4.5 | 259.5 | 832.6 | 0.31 | 8.74 |
| INT1-23 | 360 | 268 | 28.5 | 808 | 19.8 | 26.12 | 86.8 | 13.4 | 66.3 | 20.0 | 19.0 | 26.4 | 69.5 | 25.9 | 127.2 | 321 | 65.8 | 13333 | 2.7 | 53.8 | 702.6 | 0.08 | 7.28 |
| INT1-23R | 191 | <39.14 | 11.5 | 435 | 2.3 | 0.43 | 17.5 | 0.4 | 3.1 | 4.2 | 0.5 | 16.3 | 44.0 | 14.0 | 56.4 | 95 | 17.7 | 12964 | 0.5 | 146.9 | 134.1 | 1.10 | 4.63 |
| INT1-24R | 195 | 298 | 353.4 | 1079 | 116.0 | 12.58 | 68.7 | 10.3 | 54.5 | 24.5 | 5.6 | 44.9 | 106.8 | 34.5 | 146.8 | 273 | 52.4 | 11234 | 4.7 | 289.0 | 545.1 | 0.53 | 24.58 |
| INT1-25C | 236 | 161 | 19.9 | 449 | 10.6 | 1.80 | 24.2 | 1.6 | 8.7 | 4.9 | 1.7 | 14.4 | 40.5 | 13.8 | 58.1 | 113 | 22.7 | 10496 | 1.9 | 116.3 | 417.3 | 0.28 | 5.70 |
| INT1-25R | 97 | <35.50 | 13.4 | 269 | 3.0 | 0.43 | 16.4 | 0.4 | 2.4 | 2.2 | 0.9 | 8.0 | 24.3 | 8.2 | 35.1 | 69 | 13.7 | 10352 | 0.7 | 65.7 | 102.8 | 0.64 | 4.21 |
| INT1-27 | 154 | 122 | 11.9 | 805 | 17.6 | 2.05 | 23.5 | 1.6 | 11.2 | 7.6 | 2.1 | 22.0 | 66.4 | 24.4 | 113.5 | 269 | 59.9 | 10586 | 1.2 | 161.9 | 178.8 | 0.91 | 14.59 |
| INT1-28 | 195 | 177 | 36.1 | 809 | 14.4 | 1.83 | 16.5 | 0.8 | 4.8 | 4.4 | 0.5 | 18.9 | 73.0 | 27.4 | 120.5 | 230 | 43.6 | 10106 | 0.9 | 78.8 | 106.0 | 0.74 | 15.19 |
| INT1-30 | 157 | <34.60 | 15.8 | 800 | 4.2 | 0.15 | 8.8 | 0.2 | 2.1 | 3.3 | 0.2 | 16.7 | 70.9 | 26.6 | 121.4 | 231 | 44.6 | 9785 | 1.4 | 68.1 | 130.4 | 0.52 | 3.03 |
| INT1-31 | 192 | 410 | 59.5 | 856 | 25.7 | 4.33 | 29.0 | 1.9 | 10.0 | 5.2 | 0.7 | 17.8 | 76.1 | 28.7 | 131.6 | 246 | 46.0 | 10872 | 3.9 | 119.4 | 248.1 | 0.48 | 6.54 |
| INT1-33 | 159 | 178 | 177.5 | 774 | 4.5 | 3.96 | 14.7 | 1.5 | 7.5 | 4.2 | 0.8 | 13.7 | 59.3 | 24.1 | 118.2 | 248 | 49.9 | 11638 | 0.6 | 56.6 | 149.2 | 0.38 | 7.20 |
| INT1-34 | 163 | 211 | 8.4 | 1032 | 5.5 | 1.53 | 15.8 | 0.9 | 5.7 | 4.8 | 0.9 | 19.8 | 87.3 | 33.6 | 156.6 | 304 | 58.9 | 10517 | 1.6 | 178.7 | 484.9 | 0.37 | 3.48 |
| INT1-35 | 100 | 89 | 13.2 | 837 | 7.2 | 5.76 | 40.1 | 2.2 | 12.2 | 5.2 | 1.8 | 14.7 | 62.1 | 25.7 | 133.8 | 324 | 70.2 | 10012 | 1.2 | 97.4 | 165.9 | 0.59 | 6.24 |
| INT2-02 | 227 | 266 | 90.0 | 1529 | 88.0 | 10.40 | 67.7 | 9.6 | 58.6 | 33.6 | 7.2 | 82.5 | 176.7 | 52.5 | 200.5 | 299 | 53.2 | 10630 | 5.8 | 93.5 | 47.9 | 1.95 | 15.09 |
| INT2-03 | 324 | 775 | 233.4 | 447 | 3.1 | 2.35 | 21.1 | 1.6 | 11.0 | 7.2 | 2.0 | 16.4 | 43.9 | 14.3 | 62.6 | 133 | 26.8 | 12538 | 1.0 | 104.1 | 385.8 | 0.27 | 3.06 |
| INT2-04 | 186 | <37.18 | 21.9 | 817 | 4.2 | 0.44 | 22.4 | 0.5 | 6.8 | 8.8 | 0.7 | 30.5 | 86.5 | 28.4 | 117.7 | 191 | 35.7 | 9976 | 1.1 | 88.7 | 76.0 | 1.17 | 3.85 |
| INT2-05 | 349 | <37.19 | 11.8 | 4272 | 3.3 | 0.07 | 8.2 | 0.5 | 7.1 | 14.2 | 1.7 | 91.3 | 387.5 | 144.4 | 632.1 | 1050 | 194.2 | 8090 | 1.0 | 285.1 | 423.3 | 0.67 | 3.16 |
| INT2-06 | 454 | 891 | 34.1 | 1076 | 18.1 | 12.83 | 48.4 | 4.9 | 21.9 | 9.6 | 1.4 | 25.7 | 94.5 | 35.2 | 163.2 | 321 | 61.1 | 12981 | 4.1 | 235.5 | 547.3 | 0.43 | 4.43 |
| INT2-07 | 191 | 211 | 82.5 | 1748 | 49.8 | 6.77 | 46.6 | 5.3 | 34.8 | 23.2 | 2.4 | 66.4 | 185.9 | 60.9 | 251.2 | 424 | 75.7 | 10491 | 3.4 | 376.4 | 487.7 | 0.77 | 14.52 |
| INT2-08 | 1805 | 5665 | 16.9 | 1539 | 28.6 | 15.66 | 89.7 | 6.4 | 24.8 | 9.9 | 2.0 | 29.1 | 126.2 | 48.9 | 233.0 | 477 | 93.7 | 10646 | 3.1 | 292.5 | 325.7 | 0.90 | 9.32 |

| Analysis No. | P | Ca | Ti | Y | Nb | La | Ce | Pr | Nd | Sm | Eu | Gd | Dy | Ho | Er | Yb | Lu | Hf | Ta | Th | U | Th/U | Nb/Ta |
|---|---|---|---|---|---|---|---|---|---|---|---|---|---|---|---|---|---|---|---|---|---|---|---|
| INT2-09C | 215 | <35.18 | 9.9 | 1209 | 2.6 | 0.14 | 46.1 | 0.3 | 4.2 | 6.3 | 2.8 | 28.5 | 105.8 | 39.2 | 182.6 | 373 | 76.9 | 8828 | 0.6 | 236.9 | 182.4 | 1.30 | 4.10 |
| INT2-09R | 139 | 187 | 146.7 | 890 | 99.5 | 22.61 | 124.6 | 11.6 | 57.7 | 16.8 | 5.3 | 28.0 | 78.8 | 27.9 | 130.2 | 274 | 56.3 | 10870 | 4.8 | 322.7 | 250.9 | 1.29 | 20.65 |
| INT2-10 | 195 | 48 | 9.0 | 480 | 4.8 | 0.53 | 30.7 | 0.5 | 5.3 | 5.6 | 1.9 | 20.5 | 51.9 | 16.1 | 64.6 | 109 | 19.9 | 8255 | 0.3 | 109.1 | 114.7 | 0.95 | 16.15 |
| INT2-11 | 120 | 45 | 8.5 | 255 | 1.7 | 0.07 | 13.6 | 0.1 | 1.4 | 2.1 | 0.6 | 9.0 | 25.4 | 8.2 | 34.0 | 59 | 11.3 | 10164 | 0.5 | 116.6 | 147.5 | 0.79 | 3.62 |
| INT2-12 | 189 | 73 | 5.2 | 1496 | 4.3 | 3.62 | 20.7 | 1.3 | 7.6 | 6.0 | 0.4 | 32.0 | 139.2 | 52.3 | 229.0 | 358 | 62.9 | 7746 | 1.3 | 48.2 | 121.2 | 0.40 | 3.18 |
| INT2-13 | 141 | <27.37 | 16.1 | 292 | 1.4 | 0.26 | 4.1 | 0.2 | 1.3 | 1.5 | 0.1 | 7.1 | 26.2 | 9.4 | 42.6 | 82 | 15.6 | 10606 | 0.4 | 47.8 | 106.6 | 0.45 | 3.45 |
| INT2-14 | 153 | 36 | 19.4 | 612 | 2.7 | 0.18 | 8.7 | 0.2 | 2.1 | 3.1 | 0.4 | 14.9 | 55.5 | 20.1 | 92.3 | 174 | 34.7 | 9732 | 0.7 | 55.4 | 100.5 | 0.55 | 3.58 |
| **Malo-Botuobinskoe field, Mir pipe** | | | | | | | | | | | | | | | | | | | | | | | |
| mir-02 | 285 | 28 | 9.0 | 1255 | 2.7 | 0.12 | 14.6 | 0.1 | 2.0 | 4.0 | 0.5 | 24.1 | 106.0 | 41.1 | 191.8 | 397 | 73.1 | 16037 | 1.1 | 193.6 | 332.4 | 0.58 | 2.43 |
| mir-03 | 433 | 385 | 21.5 | 1516 | 4.0 | 3.50 | 18.3 | 1.3 | 8.9 | 7.6 | 0.3 | 36.9 | 143.2 | 53.3 | 234.8 | 441 | 79.5 | 17106 | 1.1 | 180.8 | 325.6 | 0.56 | 3.77 |
| mir-04 | 108 | <22.41 | 10.0 | 2042 | 3.4 | 0.02 | 86.8 | 0.2 | 3.0 | 4.6 | 2.0 | 29.3 | 139.0 | 60.4 | 322.4 | 833 | 175.8 | 13510 | 0.5 | 249.2 | 257.1 | 0.97 | 6.49 |
| mir-05 | 664 | 96 | 12.4 | 2159 | 7.4 | 3.88 | 28.3 | 3.0 | 18.1 | 8.1 | 3.4 | 30.0 | 167.4 | 69.5 | 355.9 | 790 | 150.6 | 24749 | 2.2 | 107.7 | 1135.6 | 0.09 | 3.40 |
| mir-06 | 361 | 104 | 31.8 | 1509 | 26.8 | 0.80 | 26.0 | 1.4 | 11.4 | 10.5 | 1.5 | 37.4 | 139.4 | 50.4 | 234.7 | 522 | 93.7 | 19991 | 6.3 | 271.2 | 803.2 | 0.34 | 4.25 |
| mir-08 | 253 | 64 | 80.8 | 1045 | 13.2 | 0.91 | 20.1 | 0.5 | 3.8 | 4.2 | 0.5 | 20.6 | 91.1 | 35.1 | 163.9 | 344 | 60.9 | 18444 | 4.1 | 122.1 | 288.9 | 0.42 | 3.21 |
| mir-12 | 218 | <19.33 | 23.8 | 1101 | 2.6 | 0.16 | 51.6 | 0.8 | 12.1 | 14.8 | 3.4 | 43.8 | 108.3 | 34.6 | 145.4 | 303 | 54.3 | 19333 | 1.1 | 428.4 | 625.7 | 0.68 | 2.27 |
| mir-13 | 520 | 522 | 27.6 | 3069 | 10.1 | 11.43 | 51.1 | 4.2 | 28.2 | 20.9 | 0.8 | 81.5 | 293.5 | 105.2 | 456.2 | 930 | 144.5 | 15912 | 5.2 | 465.6 | 788.5 | 0.59 | 1.96 |
| mir-14 | 321 | 882 | 9.5 | 896 | 2.9 | 1.49 | 43.1 | 0.9 | 6.2 | 5.5 | 2.4 | 23.4 | 75.4 | 27.8 | 132.1 | 319 | 64.2 | 18365 | 0.8 | 210.7 | 263.7 | 0.80 | 3.81 |
| mir-16 | 502 | 841 | 12.2 | 2483 | 13.6 | 19.40 | 70.1 | 6.6 | 34.6 | 17.6 | 1.1 | 64.4 | 239.0 | 86.3 | 381.5 | 754 | 121.1 | 18185 | 5.0 | 317.7 | 546.8 | 0.58 | 2.69 |
| mir-17 | 325 | <22.24 | 24.4 | 2293 | 2.0 | 0.02 | 26.2 | 0.4 | 6.7 | 13.4 | 2.8 | 60.7 | 214.4 | 77.2 | 331.0 | 694 | 119.7 | 17983 | 0.8 | 234.8 | 307.4 | 0.76 | 2.44 |
| mir-18 | 136 | 29 | 7.0 | 1365 | 4.0 | 0.15 | 39.2 | 0.4 | 4.6 | 7.8 | 3.6 | 33.4 | 115.6 | 42.1 | 187.9 | 519 | 91.6 | 18970 | 0.9 | 231.6 | 401.5 | 0.58 | 4.37 |
| mir-19 | 184 | 92 | 37.6 | 1069 | 11.3 | 11.02 | 111.9 | 5.5 | 31.1 | 11.8 | 10.2 | 23.1 | 78.9 | 32.0 | 165.6 | 527 | 105.8 | 19436 | 1.9 | 679.2 | 844.1 | 0.80 | 5.79 |
| mir-21 | 306 | 34 | 46.7 | 1196 | 2.5 | 0.71 | 44.7 | 1.0 | 12.7 | 14.2 | 2.5 | 44.8 | 118.9 | 39.6 | 161.2 | 325 | 56.2 | 18782 | 1.0 | 236.3 | 397.3 | 0.59 | 2.49 |
| mir-22 | 283 | <25.07 | 24.0 | 1651 | 1.8 | 0.69 | 20.4 | 0.4 | 4.8 | 7.9 | 2.0 | 39.5 | 146.7 | 54.0 | 237.3 | 497 | 85.9 | 16969 | 0.8 | 1197.8 | 1167.3 | 1.03 | 2.25 |
| mir-24 | 697 | 22 | 15.3 | 3595 | 9.6 | 1.13 | 97.4 | 0.6 | 6.1 | 8.9 | 3.3 | 51.2 | 271.6 | 115.0 | 570.7 | 1491 | 278.5 | 18750 | 2.4 | 473.4 | 706.2 | 0.67 | 4.03 |
| mir-25 | 273 | <21.31 | 43.8 | 1271 | 1.4 | 0.29 | 17.1 | 0.2 | 3.1 | 6.4 | 1.1 | 32.9 | 119.9 | 42.6 | 181.3 | 377 | 62.4 | 17690 | 0.4 | 148.1 | 218.0 | 0.68 | 3.24 |
| mir-26 | 218 | <24.00 | 7.2 | 1571 | 6.2 | 0.76 | 69.3 | 0.9 | 7.8 | 7.1 | 2.8 | 29.6 | 116.1 | 47.4 | 240.2 | 723 | 154.5 | 19755 | 1.0 | 739.0 | 773.3 | 0.96 | 6.07 |
| mir-27 | 260 | 119 | 55.5 | 808 | 6.7 | 1.73 | 14.3 | 0.4 | 2.5 | 3.1 | 0.2 | 16.2 | 72.1 | 27.7 | 126.6 | 282 | 48.4 | 17787 | 2.2 | 62.5 | 158.3 | 0.39 | 3.03 |
| mir-28 | 316 | 95 | 167.7 | 1463 | 9.7 | 24.20 | 28.9 | 0.8 | 5.5 | 6.5 | 0.5 | 32.2 | 134.0 | 50.4 | 225.3 | 470 | 80.0 | 18439 | 2.9 | 140.2 | 280.3 | 0.50 | 3.32 |
| mir-30 | 106 | 26 | 8.0 | 1930 | 2.3 | 0.15 | 35.6 | 0.3 | 3.5 | 6.0 | 2.1 | 30.7 | 148.3 | 62.0 | 306.4 | 801 | 145.0 | 14701 | 0.6 | 130.2 | 136.7 | 0.95 | 3.96 |
| mir-31 | 365 | <21.42 | 19.4 | 1518 | 4.5 | 0.09 | 13.8 | 0.1 | 2.4 | 5.6 | 0.4 | 29.2 | 132.9 | 52.3 | 239.6 | 546 | 95.8 | 16966 | 1.4 | 100.8 | 202.6 | 0.50 | 3.09 |
| **Malo-Botuobinskoe field, Sputnik pipe** | | | | | | | | | | | | | | | | | | | | | | | |
| SPUT-01 | 511 | | 42.3 | 3986 | 7.2 | 0.20 | 93.9 | 1.4 | 19.4 | 27.5 | 5.8 | 111.7 | 372.0 | 130.7 | 563.5 | 975 | 184.0 | 14500 | 1.3 | 378.0 | 259.0 | 1.46 | 5.66 |
| SPUT-02 | 243 | | 6.2 | 495 | 6.4 | | 13.8 | 0.1 | 1.1 | 2.4 | 0.5 | 12.0 | 42.6 | 15.7 | 72.5 | 146 | 29.4 | 19885 | 1.3 | 81.8 | 351.4 | 0.23 | 4.73 |
| SPUT-03 | 156 | | 7.1 | 171 | 6.6 | | 13.4 | 0.0 | 0.7 | 1.6 | 0.5 | 6.6 | 17.2 | 5.2 | 19.4 | 26.5 | 4.3 | 20519 | 3.3 | 55.9 | 367.9 | 0.15 | 2.03 |
| SPUT-04 | 240 | | 7.2 | 997 | 9.5 | 0.07 | 66.8 | 0.2 | 2.6 | 4.7 | 1.3 | 21.7 | 79.6 | 30.1 | 142.7 | 311 | 61.9 | 15429 | 1.6 | 104.5 | 128.7 | 0.81 | 6.08 |
| SPUT-05 | 450 | | 15.5 | 1628 | 7.0 | 0.11 | 35.6 | 0.1 | 2.1 | 4.8 | 0.7 | 27.0 | 127.5 | 50.1 | 242.9 | 515 | 101.5 | 17321 | 1.7 | 229.8 | 320.1 | 0.72 | 4.22 |
| SPUT-06 | 563 | | 8.7 | 1305 | 6.3 | 0.98 | 17.3 | 0.6 | 4.5 | 6.1 | 1.4 | 30.3 | 110.8 | 40.7 | 191.9 | 414 | 84.2 | 16957 | 0.6 | 87.4 | 356.2 | 0.25 | 11.37 |
| SPUT-07 | 266 | | 30.8 | 620 | 8.8 | 0.20 | 23.6 | 0.2 | 3.1 | 4.1 | 0.5 | 17.0 | 58.8 | 20.5 | 91.7 | 177 | 33.4 | 18423 | 1.8 | 78.0 | 112.7 | 0.69 | 4.80 |
| SPUT-10 | 270 | | 20.3 | 837 | 5.9 | 0.25 | 47.9 | 0.2 | 3.9 | 6.5 | 1.8 | 26.2 | 77.9 | 26.6 | 113.9 | 226 | 42.9 | 16333 | 0.9 | 127.2 | 185.2 | 0.69 | 6.38 |

| Analysis No. | P | Ca | Ti | Y | Nb | La | Ce | Pr | Nd | Sm | Eu | Gd | Dy | Ho | Er | Yb | Lu | Hf | Ta | Th | U | Th/U | Nb/Ta |
|---|---|---|---|---|---|---|---|---|---|---|---|---|---|---|---|---|---|---|---|---|---|---|---|
| SPUT-13 | 410 | | 22.4 | 1629 | 5.1 | 0.03 | 25.4 | 0.3 | 4.6 | 8.6 | 1.1 | 39.8 | 143.3 | 51.8 | 226.3 | 415 | 77.2 | 17360 | 0.7 | 198.7 | 202.9 | 0.98 | 7.25 |
| SPUT-14 | 404 | | 134.8 | 743 | 5.1 | | 4.2 | 0.1 | 1.4 | 2.9 | 0.4 | 15.7 | 63.0 | 24.3 | 112.3 | 226 | 46.7 | 15636 | 0.5 | 33.7 | 61.5 | 0.55 | 10.76 |
| SPUT-15R | 401 | | 18.0 | 1598 | 6.7 | 0.08 | 33.1 | 0.2 | 2.1 | 4.2 | 1.6 | 23.5 | 116.3 | 47.9 | 249.8 | 609 | 129.5 | 16844 | 1.2 | 105.9 | 172.1 | 0.61 | 5.82 |
| SPUT-16 | 473 | | 27.9 | 1405 | 7.4 | 0.12 | 43.9 | 0.2 | 3.9 | 7.8 | 0.5 | 39.1 | 137.1 | 47.4 | 198.1 | 326 | 59.5 | 17879 | 1.0 | 388.9 | 177.5 | 2.19 | 7.29 |
| SPUT-17 | 298 | | 16.2 | 2732 | 5.0 | 0.10 | 15.1 | 0.8 | 10.5 | 15.8 | 2.5 | 67.3 | 240.6 | 88.9 | 389.6 | 662 | 122.1 | 15999 | 0.7 | 234.8 | 541.6 | 0.43 | 6.79 |
| SPUT-18 | 309 | | 64.4 | 1014 | 10.2 | 0.17 | 37.6 | 0.4 | 3.0 | 3.7 | 0.8 | 17.5 | 76.4 | 30.7 | 157.5 | 390 | 82.0 | 19493 | 2.7 | 205.5 | 444.2 | 0.46 | 3.79 |
| SPUT-19 | 452 | | 43.0 | 1428 | 12.2 | 0.03 | 37.6 | 0.2 | 3.2 | 5.1 | 0.7 | 27.4 | 122.1 | 46.5 | 221.3 | 466 | 91.3 | 17559 | 3.4 | 97.9 | 155.3 | 0.63 | 3.59 |
| SPUT-20 | 767 | | 9.3 | 3346 | 10.4 | 0.13 | 99.6 | 0.5 | 7.7 | 13.3 | 2.7 | 70.7 | 282.0 | 104.4 | 475.2 | 918 | 182.7 | 18344 | 3.3 | 626.0 | 546.6 | 1.15 | 3.19 |
| SPUT-21 | 399 | | 18.3 | 1784 | 11.4 | 1.34 | 89.1 | 2.0 | 13.9 | 13.3 | 3.3 | 47.5 | 163.4 | 57.0 | 257.4 | 521 | 101.8 | 18151 | 2.7 | 480.8 | 692.1 | 0.69 | 4.16 |
| SPUT-22 | 564 | | 10.9 | 3499 | 14.4 | 1.29 | 32.8 | 1.1 | 10.0 | 13.0 | 1.0 | 69.0 | 307.4 | 114.7 | 506.5 | 822 | 135.9 | 15402 | 3.2 | 204.7 | 430.3 | 0.48 | 4.45 |
| SPUT-23 | 840 | | 23.3 | 2818 | 14.3 | 7.26 | 65.4 | 10.0 | 54.0 | 29.4 | 7.6 | 67.6 | 272.6 | 87.5 | 360.5 | 620 | 112.6 | 26325 | 4.5 | 88.3 | 2616.4 | 0.03 | 3.17 |
| SPUT-24 | 365 | | 26.2 | 1435 | 12.0 | 0.47 | 16.8 | 0.4 | 3.8 | 5.4 | 0.5 | 27.8 | 123.3 | 47.1 | 218.7 | 442 | 81.2 | 17823 | 3.3 | 144.7 | 345.2 | 0.42 | 3.70 |
| SPUT-25 | 332 | | 25.7 | 1300 | 19.2 | 0.81 | 34.7 | 0.9 | 5.8 | 5.4 | 0.8 | 22.5 | 106.6 | 41.3 | 203.0 | 463 | 88.9 | 19468 | 6.1 | 361.4 | 796.9 | 0.45 | 3.15 |
| SPUT-26 | 231 | | 223.9 | 583 | 6.7 | 0.26 | 20.3 | 0.1 | 1.2 | 2.0 | 0.4 | 9.4 | 44.4 | 17.7 | 87.0 | 187 | 38.5 | 20790 | 0.9 | 100.8 | 157.3 | 0.64 | 7.16 |
| SPUT-27 | 244 | | 28.7 | 748 | 8.7 | 0.02 | 63.5 | 0.2 | 2.0 | 4.2 | 0.8 | 16.8 | 63.7 | 23.5 | 111.3 | 256 | 50.4 | 18601 | 2.1 | 236.2 | 286.9 | 0.82 | 4.11 |
| SPUT-30 | 174 | | 17.0 | 1008 | 7.1 | 0.16 | 35.3 | 0.1 | 1.3 | 2.5 | 0.6 | 14.9 | 74.1 | 31.1 | 159.4 | 380 | 77.2 | 16990 | 1.3 | 75.4 | 104.8 | 0.72 | 5.54 |
| SPUT-31 | 195 | | 39.2 | 654 | 7.0 | 0.08 | 19.2 | 0.3 | 3.7 | 4.9 | 0.7 | 19.1 | 63.4 | 21.7 | 94.8 | 180 | 33.9 | 17325 | 1.1 | 51.5 | 71.3 | 0.72 | 6.06 |
| SPUT-32 | 420 | | 20.6 | 3288 | 25.0 | 0.44 | 31.4 | 0.6 | 9.7 | 14.6 | 0.5 | 68.5 | 285.5 | 106.9 | 484.8 | 889 | 159.2 | 18031 | 8.8 | 532.1 | 1032.7 | 0.52 | 2.85 |
| SPUT-34 | 383 | | 19.9 | 1776 | 6.8 | 0.20 | 37.7 | 0.4 | 4.5 | 6.1 | 1.4 | 30.6 | 131.5 | 53.0 | 271.1 | 636 | 133.6 | 15017 | 1.3 | 216.6 | 233.8 | 0.93 | 5.30 |
| SPUT-35 | 120 | | 13.3 | 2152 | 5.2 | 0.05 | 39.7 | 0.3 | 4.3 | 7.3 | 2.7 | 38.1 | 163.3 | 66.6 | 335.0 | 733 | 146.7 | 12623 | 0.4 | 77.9 | 66.8 | 1.17 | 12.31 |
| SPUT-36 | 286 | | 5.2 | 887 | 5.3 | 0.04 | 19.0 | 0.2 | 1.6 | 3.7 | 0.8 | 20.6 | 78.5 | 27.2 | 121.4 | 241 | 45.6 | 19579 | 1.7 | 260.4 | 1017.5 | 0.26 | 3.04 |
| SPUT-37 | 193 | | 10.1 | 465 | 5.8 | 0.06 | 27.3 | 0.0 | 0.5 | 1.4 | 0.4 | 6.3 | 28.1 | 13.0 | 74.3 | 221 | 50.9 | 18841 | 2.0 | 131.0 | 487.4 | 0.27 | 2.85 |
| SPUT-38 | 71 | | 7.6 | 801 | 5.4 | 0.03 | 56.2 | 0.1 | 0.9 | 1.4 | 0.7 | 8.3 | 44.3 | 21.1 | 124.3 | 413 | 99.9 | 17127 | 0.3 | 291.8 | 454.0 | 0.64 | 16.50 |
| SPUT-39 | 255 | | 6.8 | 2168 | 19.3 | 0.06 | 20.0 | 0.1 | 1.1 | 3.7 | 2.6 | 28.0 | 150.3 | 62.4 | 329.8 | 876 | 191.4 | 17719 | 3.6 | 120.3 | 941.3 | 0.13 | 5.38 |
| SPUT-40 | 259 | | 7.7 | 809 | 5.5 | 0.09 | 20.7 | 0.2 | 2.1 | 3.3 | 0.7 | 16.2 | 67.0 | 25.6 | 123.5 | 268 | 53.8 | 17668 | 0.8 | 159.6 | 311.2 | 0.51 | 6.88 |
| SPUT-43 | 229 | | 9.8 | 1284 | 4.9 | 0.31 | 13.4 | 0.3 | 3.2 | 5.7 | 1.5 | 26.8 | 106.0 | 39.9 | 188.1 | 414 | 83.7 | 16616 | 0.6 | 145.8 | 292.2 | 0.50 | 8.42 |
| SPUT-44 | 121 | | 12.9 | 919 | 5.5 | 0.07 | 33.9 | 0.1 | 1.2 | 2.4 | 0.7 | 11.5 | 59.4 | 26.2 | 144.2 | 399 | 86.4 | 14509 | 0.5 | 120.9 | 132.5 | 0.91 | 10.66 |
| SPUT-45 | 367 | | 27.5 | 1326 | 11.7 | 0.07 | 18.7 | 0.1 | 1.8 | 3.5 | 0.5 | 22.0 | 105.9 | 42.2 | 204.0 | 440 | 82.5 | 18462 | 3.1 | 273.5 | 330.6 | 0.83 | 3.74 |
| SPUT-46 | 145 | | 18.0 | 863 | 7.3 | 0.08 | 38.6 | 0.1 | 1.2 | 2.0 | 0.6 | 12.2 | 60.1 | 25.5 | 135.6 | 357 | 75.1 | 16850 | 1.1 | 149.4 | 185.6 | 0.81 | 6.73 |
| SPUT-47 | 177 | | 5.3 | 1082 | 8.6 | 0.63 | 26.0 | 0.9 | 3.6 | 5.7 | 1.0 | 21.2 | 93.5 | 34.8 | 164.3 | 373 | 71.9 | 22613 | 2.5 | 165.4 | 432.7 | 0.38 | 3.50 |
| SPUT-48 | 543 | | 23.1 | 2906 | 15.3 | 0.20 | 99.8 | 0.5 | 6.1 | 9.5 | 1.4 | 49.4 | 232.4 | 89.4 | 433.2 | 922 | 176.2 | 18030 | 4.0 | 462.3 | 524.9 | 0.88 | 3.85 |
| SPUT-50 | 298 | | 36.3 | 781 | 4.6 | 0.01 | 6.6 | 0.1 | 1.3 | 2.7 | 0.8 | 15.0 | 65.3 | 25.4 | 121.0 | 253 | 50.4 | 15511 | 0.4 | 25.7 | 50.0 | 0.51 | 11.12 |
| SPUT-51 | 281 | | 15.5 | 1526 | 26.7 | 0.07 | 31.8 | 0.2 | 3.2 | 6.5 | 0.3 | 36.5 | 145.1 | 52.0 | 227.6 | 403 | 72.6 | 19638 | 8.0 | 240.2 | 548.1 | 0.44 | 3.36 |
| SPUT-53 | 382 | | 31.9 | 783 | 5.7 | 3.38 | 20.6 | 1.4 | 8.4 | 7.3 | 0.8 | 30.2 | 80.2 | 24.6 | 97.6 | 172 | 31.6 | 21416 | 1.1 | 114.8 | 649.1 | 0.18 | 5.14 |
| SPUT-55 | 150 | | 23.9 | 802 | 16.0 | 0.42 | 32.0 | 0.4 | 4.2 | 4.9 | 0.1 | 19.4 | 74.5 | 27.1 | 120.8 | 222 | 40.2 | 16285 | 3.0 | 134.4 | 264.7 | 0.51 | 5.37 |
| SPUT-56 | 202 | | 10.4 | 756 | 4.9 | 0.33 | 20.4 | 0.1 | 1.3 | 2.6 | 1.0 | 13.0 | 52.9 | 21.9 | 114.8 | 318 | 69.7 | 16870 | 0.5 | 121.6 | 235.8 | 0.52 | 10.43 |
| SPUT-57 | 230 | | 31.4 | 834 | 4.8 | 0.41 | 14.7 | 0.3 | 2.5 | 3.3 | 1.8 | 18.3 | 70.8 | 26.6 | 126.7 | 270 | 55.4 | 13319 | 0.3 | 74.3 | 83.9 | 0.89 | 13.75 |
| SPUT-59 | 72 | | 85.6 | 633 | 4.3 | 0.21 | 48.3 | 0.1 | 0.6 | 1.0 | 0.6 | 5.3 | 28.7 | 14.6 | 96.7 | 374 | 100.1 | 19070 | 0.1 | 368.8 | 650.1 | 0.57 | 53.73 |
| SPUT-61 | 325 | | 11.4 | 1488 | 9.0 | 0.17 | 7.5 | 0.2 | 2.2 | 5.0 | 0.4 | 26.6 | 125.2 | 48.3 | 225.2 | 437 | 78.5 | 20645 | 2.4 | 250.0 | 682.1 | 0.37 | 3.80 |

| Analysis No. | P | Ca | Ti | Y | Nb | La | Ce | Pr | Nd | Sm | Eu | Gd | Dy | Ho | Er | Yb | Lu | Hf | Ta | Th | U | Th/U | Nb/Ta |
|---|---|---|---|---|---|---|---|---|---|---|---|---|---|---|---|---|---|---|---|---|---|---|---|
| SPUT-63 | 666 | | 77.5 | 1231 | 11.5 | 3.78 | 20.8 | 2.8 | 15.2 | 23.1 | 4.8 | 71.2 | 134.7 | 40.8 | 175.0 | 325 | 59.6 | 16299 | 1.3 | 56.2 | 141.0 | 0.40 | 8.56 |
| SPUT-64 | 472 | | 41.3 | 1569 | 17.4 | 22.4 | 75.0 | 7.8 | 32.7 | 12.6 | 0.9 | 37.0 | 140.0 | 53.4 | 240.0 | 471 | 82.6 | 17677 | 4.7 | 212.7 | 413.5 | 0.51 | 3.68 |
| SPUT-66 | 467 | | 23.8 | 2189 | 9.2 | 0.89 | 35.5 | 0.8 | 8.2 | 10.5 | 4.5 | 51.9 | 189.3 | 69.7 | 310.1 | 615 | 118.7 | 14087 | 1.2 | 220.1 | 232.7 | 0.95 | 7.97 |
| SPUT-67C | 101 | | 13.6 | 189 | 18.0 | 0.67 | 8.3 | 0.5 | 2.8 | 3.4 | 1.1 | 10.5 | 21.5 | 6.5 | 23.7 | 40.7 | 7.3 | 18051 | 3.2 | 21.1 | 705.9 | 0.03 | 5.60 |
| SPUT-67R | 284 | | 21.8 | 712 | 8.9 | 0.27 | 13.7 | 0.3 | 3.0 | 4.9 | 0.5 | 22.1 | 69.8 | 23.1 | 97.2 | 175 | 31.3 | 17768 | 1.7 | 109.7 | 414.8 | 0.26 | 5.13 |
| SPUT-68 | 375 | | 31.9 | 1022 | 11.4 | 0.22 | 38.6 | 0.3 | 4.1 | 6.7 | 1.4 | 28.4 | 94.4 | 33.2 | 149.6 | 308 | 59.9 | 20799 | 2.8 | 46.8 | 100.9 | 0.46 | 4.14 |
| SPUT-69 | 294 | | 29.5 | 1117 | 10.5 | 1.59 | 33.0 | 0.5 | 5.1 | 8.8 | 0.4 | 33.5 | 113.7 | 39.8 | 166.3 | 317 | 52.5 | 19261 | 2.3 | 396.7 | 373.7 | 1.06 | 4.58 |
| SPUT-71 | 182 | | 29.8 | 1301 | 8.5 | 0.37 | 43.6 | 0.2 | 2.6 | 4.3 | 1.1 | 23.1 | 104.6 | 41.5 | 204.4 | 453 | 88.3 | 17098 | 2.3 | 271.6 | 344.7 | 0.79 | 3.73 |
| SPUT-72 | 410 | | 14.7 | 711 | 5.0 | 2.98 | 5.1 | 0.2 | 2.4 | 6.1 | 0.4 | 31.0 | 91.3 | 21.5 | 66.7 | 75.0 | 10.3 | 24848 | 0.6 | 64.7 | 1293.2 | 0.05 | 7.89 |
| SPUT-75 | 970 | | 13.0 | 2491 | 11.8 | 3.85 | 27.1 | 1.8 | 9.2 | 6.0 | 0.8 | 31.0 | 182.4 | 76.8 | 404.7 | 986 | 192.2 | 22858 | 3.9 | 108.5 | 646.7 | 0.17 | 3.01 |

**Appendix 2.3. Zircon Hf and O isotopes data for the samples from the Magan terrane**

| Analysis No. | Lu-Hf RATIOS | | | | $Hf_{initial}$ | εHf(T) | ± SE | $T_{DM}$ (Ga) | $T_{DM}^{Crustal}$ (Ga) | U-Pb AGE | Oxygen | |
|---|---|---|---|---|---|---|---|---|---|---|---|---|
| | $^{176}Hf/^{177}Hf$ | 1SE | $^{176}Lu/^{177}Hf$ | $^{176}Yb/^{177}Hf$ | | | | | | (Ma) | $\delta^{18}O$ | 2σ |
| **Malo-Botuobinskoe field, Sputnik pipe** | | | | | | | | | | | | |
| Sputnik-01 | 0.282589 | 0.000008 | 0.001327 | 0.058783 | 0.282578 | 2.7 | 0.3 | 0.95 | 1.18 | 449 | 6.83 | 0.28 |
| Sputnik-02 | 0.281318 | 0.000008 | 0.000270 | 0.011229 | 0.281309 | -10.6 | 0.3 | 2.65 | 3.09 | 1846 | 5.28 | 0.21 |
| Sputnik-03 | 0.281415 | 0.000009 | 0.000070 | 0.003144 | 0.281413 | -6.7 | 0.3 | 2.51 | 2.87 | 1857 | 5.55 | 0.27 |
| Sputnik-04 | 0.281354 | 0.000010 | 0.000482 | 0.020147 | 0.281332 | 2.0 | 0.3 | 2.62 | 2.76 | 2354 | - | - |
| Sputnik-05 | 0.281789 | 0.000008 | 0.001261 | 0.046297 | 0.281769 | -17.4 | 0.3 | 2.07 | 2.66 | 831 | - | - |
| Sputnik-06 | 0.281666 | 0.000010 | 0.000956 | 0.039592 | 0.281630 | 3.6 | 0.3 | 2.22 | 2.36 | 1966 | - | - |
| Sputnik-07 | 0.281311 | 0.000008 | 0.000334 | 0.010878 | 0.281299 | -11.0 | 0.3 | 2.66 | 3.11 | 1845 | - | - |
| Sputnik-10 | 0.281627 | 0.000008 | 0.000315 | 0.013164 | 0.281615 | 3.1 | 0.3 | 2.24 | 2.39 | 1970 | 7.47 | 0.21 |
| Sputnik-13 | 0.282090 | 0.000011 | 0.000702 | 0.030938 | 0.282079 | -6.1 | 0.4 | 1.63 | 2.02 | 846 | - | - |
| Sputnik-14 | 0.280724 | 0.000009 | 0.000633 | 0.025904 | 0.280690 | -11.3 | 0.3 | 3.47 | 3.87 | 2764 | - | - |
| Sputnik-15R | 0.282623 | 0.000015 | 0.001972 | 0.068136 | 0.282607 | 3.4 | 0.5 | 0.92 | 1.13 | 437 | - | - |
| Sputnik-16 | 0.280885 | 0.000012 | 0.000711 | 0.032805 | 0.280848 | -6.8 | 0.4 | 3.26 | 3.57 | 2715 | 5.84 | 0.22 |
| Sputnik-17 | 0.281641 | 0.000010 | 0.001131 | 0.049080 | 0.281598 | 3.0 | 0.3 | 2.27 | 2.41 | 1990 | 8.05 | 0.22 |
| Sputnik-18 | 0.281253 | 0.000010 | 0.000639 | 0.024908 | 0.281225 | -3.3 | 0.4 | 2.76 | 3.02 | 2290 | - | - |
| Sputnik-19 | 0.281578 | 0.000009 | 0.000903 | 0.036757 | 0.281546 | -2.2 | 0.3 | 2.34 | 2.60 | 1845 | - | - |
| Sputnik-20 | 0.282167 | 0.000009 | 0.001332 | 0.054693 | 0.282152 | -9.4 | 0.3 | 1.54 | 2.00 | 582 | 9.59 | 0.23 |
| Sputnik-21 | 0.281043 | 0.000008 | 0.000913 | 0.037526 | 0.280998 | -4.5 | 0.3 | 3.07 | 3.33 | 2588 | 5.17 | 0.20 |
| Sputnik-22 | 0.281252 | 0.000013 | 0.001269 | 0.050900 | 0.281196 | -3.6 | 0.5 | 2.81 | 3.07 | 2322 | - | - |
| Sputnik-23 | 0.281256 | 0.000009 | 0.001133 | 0.048711 | 0.281215 | -12.4 | 0.3 | 2.79 | 3.25 | 1915 | 6.19 | 0.19 |
| Sputnik-24 | 0.281526 | 0.000007 | 0.001010 | 0.042520 | 0.281491 | -4.1 | 0.2 | 2.42 | 2.71 | 1851 | - | - |
| Sputnik-25 | 0.281472 | 0.000015 | 0.003495 | 0.172668 | 0.281351 | -9.5 | 0.5 | 2.66 | 3.01 | 1832 | - | - |
| Sputnik-26 | 0.282336 | 0.000007 | 0.000359 | 0.014163 | 0.282330 | 2.9 | 0.3 | 1.27 | 1.49 | 850 | 7.26 | 0.19 |
| Sputnik-27 | 0.281397 | 0.000008 | 0.000442 | 0.016066 | 0.281382 | -8.1 | 0.3 | 2.56 | 2.94 | 1843 | - | - |
| Sputnik-30 | 0.281988 | 0.000010 | 0.000728 | 0.032107 | 0.281983 | -19.7 | 0.4 | 1.77 | 2.44 | 391 | 5.39 | 0.20 |
| Sputnik-31 | 0.281298 | 0.000011 | 0.000285 | 0.013528 | 0.281288 | -10.9 | 0.4 | 2.68 | 3.12 | 1868 | 6.23 | 0.22 |
| Sputnik-32 | 0.281569 | 0.000009 | 0.000920 | 0.043317 | 0.281537 | -2.9 | 0.3 | 2.35 | 2.63 | 1828 | 5.26 | 0.25 |
| Sputnik-34 | 0.281942 | 0.000013 | 0.001533 | 0.061624 | 0.281931 | -21.5 | 0.5 | 1.87 | 2.54 | 392 | 5.34 | 0.24 |
| Sputnik-35 | 0.281892 | 0.000010 | 0.001735 | 0.076177 | 0.281879 | -23.2 | 0.4 | 1.95 | 2.64 | 396 | 5.09 | 0.23 |
| Sputnik-36 | 0.281238 | 0.000011 | 0.000310 | 0.012632 | 0.281227 | -13.1 | 0.4 | 2.76 | 3.25 | 1865 | - | - |
| Sputnik-37 | 0.281159 | 0.000007 | 0.000486 | 0.018912 | 0.281136 | -1.2 | 0.2 | 2.88 | 3.08 | 2517 | 5.76 | 0.24 |
| Sputnik-38 | 0.282051 | 0.000010 | 0.001232 | 0.046008 | 0.282042 | -17.3 | 0.4 | 1.70 | 2.31 | 406 | - | - |
| Sputnik-39 | 0.282747 | 0.000009 | 0.001208 | 0.048644 | 0.282739 | 6.4 | 0.3 | 0.72 | 0.89 | 361 | 4.42 | 0.23 |

| Analysis No. | Lu-Hf RATIOS | | | | $Hf_{initial}$ | εHf(T) | ± SE | $T_{DM}$ (Ga) | $T_{DM}^{Crustal}$ (Ga) | U-Pb AGE | Oxygen | |
|---|---|---|---|---|---|---|---|---|---|---|---|---|
| | $^{176}Hf/^{177}Hf$ | 1SE | $^{176}Lu/^{177}Hf$ | $^{176}Yb/^{177}Hf$ | | | | | | (Ma) | $\delta^{18}O$ | 2σ |
| Sputnik-40 | 0.281078 | 0.000009 | 0.000464 | 0.020879 | 0.281055 | -1.5 | 0.3 | 2.99 | 3.19 | 2629 | 5.47 | 0.26 |
| Sputnik-43 | 0.282654 | 0.000010 | 0.000506 | 0.020989 | 0.282650 | 3.6 | 0.4 | 0.84 | 1.07 | 374 | 7.58 | 0.21 |
| Sputnik-44 | 0.282012 | 0.000010 | 0.001292 | 0.051987 | 0.282003 | -19.1 | 0.4 | 1.76 | 2.40 | 384 | 5.17 | 0.23 |
| Sputnik-45 | 0.281440 | 0.000009 | 0.000817 | 0.036708 | 0.281411 | -6.2 | 0.3 | 2.52 | 2.86 | 1880 | - | - |
| Sputnik-46 | 0.281936 | 0.000010 | 0.001063 | 0.041732 | 0.281928 | -21.6 | 0.3 | 1.85 | 2.54 | 394 | - | - |
| Sputnik-47 | 0.281063 | 0.000014 | 0.002152 | 0.068380 | 0.280952 | -3.8 | 0.5 | 3.14 | 3.37 | 2687 | - | - |
| Sputnik-48 | 0.282443 | 0.000013 | 0.001538 | 0.070941 | 0.282429 | -1.6 | 0.5 | 1.16 | 1.47 | 493 | - | - |
| Sputnik-50 | 0.282514 | 0.000010 | 0.000523 | 0.022193 | 0.282509 | 1.4 | 0.4 | 1.03 | 1.30 | 502 | - | - |
| Sputnik-51 | 0.281210 | 0.000011 | 0.000701 | 0.035972 | 0.281178 | -3.4 | 0.4 | 2.83 | 3.08 | 2359 | - | - |
| Sputnik-52 | 0.282058 | 0.000009 | 0.001605 | 0.072786 | 0.282046 | -17.3 | 0.3 | 1.71 | 2.30 | 397 | - | - |
| Sputnik-53 | 0.281659 | 0.000010 | 0.000224 | 0.010779 | 0.281650 | 5.4 | 0.3 | 2.19 | 2.29 | 2015 | 9.85 | 0.25 |
| Sputnik-55 | 0.281452 | 0.000010 | 0.000368 | 0.017537 | 0.281440 | -7.8 | 0.3 | 2.48 | 2.86 | 1767 | - | - |
| Sputnik-56 | 0.282841 | 0.000009 | 0.000401 | 0.011026 | 0.282837 | 13.7 | 0.3 | 0.57 | 0.60 | 533 | - | - |
| Sputnik-57 | 0.282604 | 0.000012 | 0.000647 | 0.026435 | 0.282598 | 3.9 | 0.4 | 0.91 | 1.13 | 470 | - | - |
| Sputnik-59 | 0.281778 | 0.000010 | 0.000880 | 0.029553 | 0.281771 | -26.1 | 0.4 | 2.06 | 2.84 | 441 | - | - |
| Sputnik-61 | 0.281557 | 0.000008 | 0.000641 | 0.028835 | 0.281534 | -2.1 | 0.3 | 2.35 | 2.61 | 1870 | - | - |
| Sputnik-63 | 0.281606 | 0.000011 | 0.000708 | 0.032847 | 0.281582 | -2.1 | 0.4 | 2.29 | 2.55 | 1796 | - | - |
| Sputnik-64 | 0.281644 | 0.000011 | 0.000810 | 0.038060 | 0.281615 | 1.0 | 0.4 | 2.24 | 2.44 | 1877 | - | - |
| Sputnik-66 | 0.281211 | 0.000012 | 0.001217 | 0.055591 | 0.281154 | -2.1 | 0.4 | 2.86 | 3.08 | 2453 | - | - |
| Sputnik-67Core | 0.281308 | 0.000015 | 0.000032 | 0.001432 | 0.281307 | -9.6 | 0.5 | 2.65 | 3.07 | 1893 | - | - |
| Sputnik-67Rim | 0.281377 | 0.000019 | 0.000369 | 0.017842 | 0.281364 | -8.3 | 0.7 | 2.58 | 2.97 | 1862 | - | - |
| Sputnik-68 | 0.281362 | 0.000012 | 0.000523 | 0.021606 | 0.281343 | -8.5 | 0.4 | 2.61 | 3.00 | 1884 | - | - |
| Sputnik-69 | 0.281432 | 0.000009 | 0.000581 | 0.027826 | 0.281412 | -7.5 | 0.3 | 2.52 | 2.89 | 1821 | - | - |
| Sputnik-71 | 0.281954 | 0.000014 | 0.001449 | 0.065563 | 0.281944 | -21.3 | 0.5 | 1.85 | 2.52 | 381 | 5.69 | 0.23 |
| Sputnik-72 | 0.281183 | 0.000010 | 0.000792 | 0.048798 | 0.281155 | -16.3 | 0.4 | 2.87 | 3.41 | 1835 | 7.01 | 0.21 |
| Sputnik-75 | 0.281169 | 0.000009 | 0.000763 | 0.029816 | 0.281140 | -13.8 | 0.3 | 2.89 | 3.37 | 1968 | - | - |

**Appendix 3.1. Zircon U-Pb age data for samples from the Markha terrane**

| Analysis No. | RATIOS | | | | | | | | AGES (Ma) | | | | | | | | | | CONCENTRATIONS (ppm) | |
|---|---|---|---|---|---|---|---|---|---|---|---|---|---|---|---|---|---|---|---|---|
| | $^{207}Pb/^{206}Pb$ | ± 2σ | $^{207}Pb/^{235}U$ | ± 2σ | $^{206}Pb/^{238}U$ | ± 2σ | $^{208}Pb/^{232}Th$ | ± 2σ | $^{207}Pb/^{206}Pb$ | ± 2σ | $^{207}Pb/^{235}U$ | ± 2σ | $^{206}Pb/^{238}U$ | ± 2σ | $^{208}Pb/^{232}Th$ | ± 2σ | Used Age | ± 2σ | Th | U |
| **Upper Muna field, Zimnyaya pipe** | | | | | | | | | | | | | | | | | | | | |
| 8008-01 | 0.05516 | 0.00246 | 0.32617 | 0.01246 | 0.04288 | 0.00098 | 0.01338 | 0.00034 | 419 | 102 | 287 | 10 | 271 | 6 | 269 | 6 | 271 | 6 | 22.36 | 722.40 |
| 8008-02 | 0.05267 | 0.00168 | 0.35695 | 0.01138 | 0.04916 | 0.00110 | 0.01568 | 0.00050 | 315 | 74 | 310 | 8 | 309 | 6 | 314 | 10 | 309 | 6 | 66.09 | 1905.97 |
| 8008-02R | 0.05271 | 0.00148 | 0.34316 | 0.00960 | 0.04722 | 0.00102 | 0.01463 | 0.00044 | 316 | 66 | 300 | 8 | 297 | 6 | 294 | 8 | 297 | 6 | 146.74 | 4480.38 |
| 8008-06 | 0.05667 | 0.00176 | 0.57154 | 0.01776 | 0.07315 | 0.00166 | 0.02284 | 0.00084 | 479 | 70 | 459 | 12 | 455 | 10 | 456 | 16 | 455 | 10 | 49.41 | 983.77 |
| 8008-07 | 0.05310 | 0.00206 | 0.23079 | 0.00728 | 0.03152 | 0.00072 | 0.00988 | 0.00024 | 333 | 90 | 211 | 6 | 200 | 4 | 199 | 4 | 200 | 4 | 112.28 | 5045.55 |
| 8008-08 | 0.05935 | 0.00208 | 0.33712 | 0.00938 | 0.04120 | 0.00088 | 0.01274 | 0.00030 | 580 | 78 | 295 | 8 | 260 | 6 | 256 | 6 | 260 | 6 | 273.56 | 9283.61 |
| 8008-09 | 0.17536 | 0.00390 | 12.05966 | 0.27320 | 0.49883 | 0.01050 | 0.13815 | 0.00380 | 2609 | 38 | 2609 | 22 | 2609 | 46 | 2616 | 68 | 2609 | 38 | 723.59 | 2334.66 |
| 8008-10C | 0.17957 | 0.00406 | 12.58067 | 0.28940 | 0.50819 | 0.01076 | 0.13919 | 0.00394 | 2649 | 38 | 2649 | 22 | 2649 | 46 | 2634 | 70 | 2649 | 38 | 315.40 | 1008.64 |
| 8008-10R | 0.17320 | 0.00406 | 11.50015 | 0.28090 | 0.48161 | 0.01058 | 0.13130 | 0.00426 | 2589 | 40 | 2565 | 22 | 2534 | 46 | 2494 | 76 | 2589 | 40 | 290.56 | 1014.70 |
| 8008-11C | 0.16979 | 0.00462 | 10.76145 | 0.30604 | 0.45972 | 0.01078 | 0.12845 | 0.00550 | 2556 | 46 | 2503 | 26 | 2438 | 48 | 2443 | 98 | 2556 | 46 | 979.86 | 3736.54 |
| 8008-11R | 0.11301 | 0.00300 | 5.25876 | 0.13846 | 0.33757 | 0.00738 | 0.09879 | 0.00320 | 1848 | 50 | 1862 | 22 | 1875 | 36 | 1904 | 58 | 1848 | 50 | 286.27 | 1325.28 |
| 8008-12C | 0.05405 | 0.00266 | 0.34238 | 0.01624 | 0.04595 | 0.00114 | 0.01438 | 0.00070 | 373 | 114 | 299 | 12 | 290 | 8 | 289 | 14 | 290 | 8 | 112.13 | 3477.58 |
| 8008-12R | 0.05094 | 0.00224 | 0.31892 | 0.01372 | 0.04542 | 0.00110 | 0.01445 | 0.00056 | 238 | 104 | 281 | 10 | 286 | 6 | 290 | 12 | 286 | 6 | 49.68 | 1611.54 |
| 8008-13C | 0.05604 | 0.00196 | 0.52841 | 0.01876 | 0.06840 | 0.00170 | 0.02223 | 0.00116 | 454 | 80 | 431 | 12 | 427 | 10 | 444 | 22 | 427 | 10 | 182.31 | 4116.63 |
| 8008-14C | 0.05280 | 0.00180 | 0.31353 | 0.01060 | 0.04307 | 0.00100 | 0.01333 | 0.00050 | 320 | 80 | 277 | 8 | 272 | 6 | 268 | 10 | 272 | 6 | 112.09 | 3825.20 |
| 8008-14R | 0.05485 | 0.00234 | 0.31870 | 0.01144 | 0.04214 | 0.00098 | 0.01315 | 0.00034 | 406 | 98 | 281 | 8 | 266 | 6 | 264 | 6 | 266 | 6 | 99.75 | 3462.07 |
| 8008-18 | 0.05023 | 0.00328 | 0.22054 | 0.01396 | 0.03185 | 0.00092 | 0.01033 | 0.00052 | 206 | 156 | 202 | 12 | 202 | 6 | 208 | 10 | 202 | 6 | 28.41 | 1243.79 |
| 8008-18R | 0.05238 | 0.00230 | 0.22406 | 0.00966 | 0.03103 | 0.00078 | 0.00978 | 0.00040 | 302 | 102 | 205 | 8 | 197 | 4 | 197 | 8 | 197 | 4 | 48.75 | 2277.08 |
| 8008-27 | 0.05143 | 0.00168 | 0.19672 | 0.00648 | 0.02775 | 0.00064 | 0.00881 | 0.00040 | 260 | 76 | 182 | 6 | 176 | 4 | 177 | 8 | 176 | 4 | 173.43 | 9105.56 |
| 8008-29 | 0.05464 | 0.00220 | 0.36113 | 0.01436 | 0.04794 | 0.00118 | 0.01546 | 0.00076 | 398 | 92 | 313 | 10 | 302 | 8 | 310 | 16 | 302 | 8 | 178.65 | 5443.04 |
| 8008-30 | 0.05305 | 0.00302 | 0.33516 | 0.01870 | 0.04583 | 0.00128 | 0.01535 | 0.00076 | 331 | 132 | 293 | 14 | 289 | 8 | 308 | 16 | 289 | 8 | 66.37 | 2108.00 |
| 8008-32 | 0.16834 | 0.00402 | 10.67349 | 0.26058 | 0.45991 | 0.00994 | 0.12643 | 0.00436 | 2541 | 40 | 2495 | 22 | 2439 | 44 | 2406 | 78 | 2541 | 40 | 738.98 | 2654.71 |
| 8008-36 | 0.05544 | 0.00288 | 0.36134 | 0.01846 | 0.04730 | 0.00132 | 0.01546 | 0.00080 | 430 | 118 | 313 | 14 | 298 | 8 | 310 | 16 | 298 | 8 | 119.22 | 3941.25 |
| 8008-40 | 0.05557 | 0.00270 | 0.34353 | 0.01414 | 0.04484 | 0.00114 | 0.01397 | 0.00038 | 435 | 110 | 300 | 10 | 283 | 8 | 280 | 8 | 283 | 8 | 241.39 | 8131.06 |
| 8008-43C | 0.05114 | 0.00162 | 0.21056 | 0.00658 | 0.02987 | 0.00066 | 0.00957 | 0.00032 | 247 | 74 | 194 | 6 | 190 | 4 | 193 | 6 | 190 | 4 | 97.97 | 4562.90 |
| 8008-49 | 0.05451 | 0.00218 | 0.37130 | 0.01446 | 0.04941 | 0.00114 | 0.01606 | 0.00054 | 392 | 92 | 321 | 10 | 311 | 8 | 322 | 10 | 311 | 8 | 31.43 | 864.54 |
| 8008-51 | 0.05742 | 0.00154 | 0.51336 | 0.01366 | 0.06485 | 0.00140 | 0.02037 | 0.00064 | 508 | 60 | 421 | 10 | 405 | 8 | 408 | 12 | 405 | 8 | 120.43 | 2635.01 |
| 8008-59 | 0.19036 | 0.00492 | 14.31838 | 0.36850 | 0.54559 | 0.01204 | 0.14765 | 0.00478 | 2745 | 44 | 2771 | 24 | 2807 | 50 | 2784 | 84 | 2745 | 44 | 262.39 | 789.68 |
| 8008-60 | 0.05352 | 0.00222 | 0.39186 | 0.01622 | 0.05310 | 0.00134 | 0.01740 | 0.00098 | 351 | 96 | 336 | 12 | 334 | 8 | 349 | 20 | 334 | 8 | 72.14 | 1998.11 |
| ~~8008-19~~ | ~~0.17362~~ | ~~0.00688~~ | ~~6.36429~~ | ~~0.19998~~ | ~~0.26586~~ | ~~0.00642~~ | ~~0.07349~~ | ~~0.00224~~ | ~~2593~~ | ~~68~~ | ~~2027~~ | ~~28~~ | ~~1520~~ | ~~32~~ | ~~1433~~ | ~~42~~ | ~~2593~~ | ~~68~~ | ~~402.98~~ | ~~1581.17~~ |
| ~~8008-21~~ | ~~0.06089~~ | ~~0.00228~~ | ~~0.23114~~ | ~~0.00690~~ | ~~0.02753~~ | ~~0.00062~~ | ~~0.00849~~ | ~~0.00022~~ | ~~635~~ | ~~82~~ | ~~211~~ | ~~6~~ | ~~175~~ | ~~4~~ | ~~171~~ | ~~4~~ | ~~175~~ | ~~4~~ | ~~120.74~~ | ~~4891.04~~ |
| ~~8008-22~~ | ~~0.18104~~ | ~~0.00558~~ | ~~10.82712~~ | ~~0.24486~~ | ~~0.43376~~ | ~~0.00910~~ | ~~0.11943~~ | ~~0.00264~~ | ~~2662~~ | ~~52~~ | ~~2508~~ | ~~22~~ | ~~2323~~ | ~~40~~ | ~~2280~~ | ~~48~~ | ~~2662~~ | ~~52~~ | ~~489.99~~ | ~~1787.59~~ |
| ~~8008-33~~ | ~~0.16457~~ | ~~0.03824~~ | ~~6.24970~~ | ~~1.33510~~ | ~~0.27544~~ | ~~0.03242~~ | ~~0.07726~~ | ~~0.03176~~ | ~~2503~~ | ~~408~~ | ~~2011~~ | ~~186~~ | ~~1568~~ | ~~164~~ | ~~1504~~ | ~~596~~ | ~~2503~~ | ~~408~~ | ~~1.03~~ | ~~6.96~~ |
| ~~8008-43R~~ | ~~0.06518~~ | ~~0.00258~~ | ~~0.26888~~ | ~~0.00870~~ | ~~0.02992~~ | ~~0.00068~~ | ~~0.00915~~ | ~~0.00026~~ | ~~780~~ | ~~84~~ | ~~242~~ | ~~6~~ | ~~190~~ | ~~4~~ | ~~184~~ | ~~6~~ | ~~190~~ | ~~4~~ | ~~99.92~~ | ~~3361.17~~ |
| ~~8008-46~~ | ~~0.05617~~ | ~~0.00400~~ | ~~0.31924~~ | ~~0.02214~~ | ~~0.04123~~ | ~~0.00134~~ | ~~0.01344~~ | ~~0.00076~~ | ~~459~~ | ~~162~~ | ~~281~~ | ~~18~~ | ~~260~~ | ~~8~~ | ~~270~~ | ~~16~~ | ~~260~~ | ~~8~~ | ~~179.82~~ | ~~7108.30~~ |
| ~~8008-52~~ | ~~0.07075~~ | ~~0.02328~~ | ~~0.62262~~ | ~~0.19828~~ | ~~0.06383~~ | ~~0.00580~~ | ~~0.04560~~ | ~~0.00904~~ | ~~950~~ | ~~724~~ | ~~491~~ | ~~124~~ | ~~399~~ | ~~36~~ | ~~901~~ | ~~174~~ | ~~399~~ | ~~36~~ | ~~1.18~~ | ~~12.77~~ |
| ~~8008-53~~ | ~~0.05573~~ | ~~0.00224~~ | ~~0.28745~~ | ~~0.01120~~ | ~~0.03742~~ | ~~0.00086~~ | ~~0.01191~~ | ~~0.00052~~ | ~~442~~ | ~~92~~ | ~~257~~ | ~~8~~ | ~~237~~ | ~~6~~ | ~~239~~ | ~~10~~ | ~~237~~ | ~~6~~ | ~~101.66~~ | ~~3663.72~~ |
| ~~8008-53R~~ | ~~0.05418~~ | ~~0.00210~~ | ~~0.27531~~ | ~~0.01068~~ | ~~0.03686~~ | ~~0.00092~~ | ~~0.01194~~ | ~~0.00056~~ | ~~379~~ | ~~90~~ | ~~247~~ | ~~8~~ | ~~233~~ | ~~6~~ | ~~240~~ | ~~12~~ | ~~233~~ | ~~6~~ | ~~141.75~~ | ~~5850.26~~ |
| **Upper Muna field, 325 years of Yakutia pipe** | | | | | | | | | | | | | | | | | | | | |
| MVG124-01 | 0.05434 | 0.00934 | 0.42853 | 0.07054 | 0.0572 | 0.00304 | 0.01837 | 0.00332 | 385 | 394 | 362 | 50 | 359 | 18 | 368 | 66 | 359 | 18 | 1.98 | 8.92 |
| MVG124-02 | 0.05114 | 0.0081 | 0.4155 | 0.06358 | 0.05893 | 0.00264 | 0.01767 | 0.00274 | 247 | 362 | 353 | 46 | 369 | 16 | 354 | 54 | 369 | 16 | 2.75 | 12.86 |
| MVG124-03 | 0.05469 | 0.0062 | 0.41903 | 0.04552 | 0.05558 | 0.00206 | 0.01867 | 0.00174 | 400 | 262 | 355 | 32 | 349 | 12 | 374 | 34 | 349 | 12 | 5.38 | 14.88 |

| Analysis No. | RATIOS | | | | | | | | AGES (Ma) | | | | | | | | | | CONCENTRATIONS (ppm) | |
|---|---|---|---|---|---|---|---|---|---|---|---|---|---|---|---|---|---|---|---|---|
| | $^{207}Pb/^{206}Pb$ | ± 2σ | $^{207}Pb/^{235}U$ | ± 2σ | $^{206}Pb/^{238}U$ | ± 2σ | $^{208}Pb/^{232}Th$ | ± 2σ | $^{207}Pb/^{206}Pb$ | ± 2σ | $^{207}Pb/^{235}U$ | ± 2σ | $^{206}Pb/^{238}U$ | ± 2σ | $^{208}Pb/^{232}Th$ | ± 2σ | Used Age | ± 2σ | Th | U |
| MVG124-04 | 0.05275 | 0.0092 | 0.39525 | 0.06604 | 0.05435 | 0.00296 | 0.0172 | 0.00374 | 318 | 400 | 338 | 48 | 341 | 18 | 345 | 74 | 341 | 18 | 2.206 | 9.65 |
| MVG124-05 | 0.05452 | 0.007 | 0.43129 | 0.05346 | 0.05738 | 0.00212 | 0.01638 | 0.00166 | 393 | 296 | 364 | 38 | 360 | 12 | 328 | 34 | 360 | 12 | 6.33 | 17.67 |
| MVG124-06 | 0.05357 | 0.00666 | 0.42006 | 0.05034 | 0.05687 | 0.0021 | 0.01831 | 0.00192 | 353 | 288 | 356 | 36 | 357 | 12 | 367 | 38 | 357 | 12 | 5.34 | 15.46 |
| MVG124-07 | 0.05434 | 0.00566 | 0.44124 | 0.04408 | 0.0589 | 0.00196 | 0.01986 | 0.0018 | 385 | 240 | 371 | 32 | 369 | 12 | 397 | 36 | 369 | 12 | 6.14 | 18.63 |
| MVG124-08 | 0.06324 | 0.00976 | 0.4896 | 0.07172 | 0.05615 | 0.00296 | 0.01873 | 0.00324 | 716 | 338 | 405 | 48 | 352 | 18 | 375 | 64 | 352 | 18 | 2.516 | 10.9 |
| MVG124-09 | 0.05508 | 0.0084 | 0.42397 | 0.06214 | 0.05582 | 0.00256 | 0.0167 | 0.0023 | 415 | 352 | 359 | 44 | 350 | 16 | 335 | 46 | 350 | 16 | 5.34 | 15.26 |
| MVG124-10 | 0.05541 | 0.0066 | 0.41827 | 0.04754 | 0.05475 | 0.00216 | 0.01818 | 0.00192 | 429 | 274 | 355 | 34 | 344 | 14 | 364 | 38 | 344 | 14 | 6.13 | 18.59 |
| MVG124-11 | 0.05412 | 0.00576 | 0.43653 | 0.04442 | 0.0585 | 0.00204 | 0.0178 | 0.00186 | 376 | 246 | 368 | 32 | 366 | 12 | 357 | 36 | 366 | 12 | 6.26 | 18.83 |
| MVG125-01 | 0.05559 | 0.01 | 0.44285 | 0.07646 | 0.05778 | 0.00314 | 0.01493 | 0.00316 | 436 | 412 | 372 | 54 | 362 | 20 | 300 | 62 | 362 | 20 | 3.37 | 12.4 |
| MVG125-02 | 0.06098 | 0.01462 | 0.47346 | 0.10914 | 0.05632 | 0.00398 | 0.01918 | 0.00538 | 639 | 540 | 394 | 76 | 353 | 24 | 384 | 106 | 353 | 24 | 1.945 | 8.16 |
| MVG125-03 | 0.0549 | 0.0075 | 0.44054 | 0.05756 | 0.05821 | 0.00258 | 0.01915 | 0.0022 | 408 | 314 | 371 | 40 | 365 | 16 | 383 | 44 | 365 | 16 | 5.37 | 15.13 |
| MVG125-04 | 0.05423 | 0.0073 | 0.41154 | 0.05312 | 0.05505 | 0.00234 | 0.02051 | 0.00318 | 381 | 312 | 350 | 38 | 345 | 14 | 410 | 62 | 345 | 14 | 2.712 | 13.57 |
| MVG125-05 | 0.05394 | 0.0078 | 0.44411 | 0.06204 | 0.05972 | 0.00246 | 0.02213 | 0.00318 | 369 | 334 | 373 | 44 | 374 | 14 | 442 | 62 | 374 | 14 | 2.78 | 13.23 |
| MVG125-06 | 0.05693 | 0.01028 | 0.44735 | 0.07778 | 0.05699 | 0.00302 | 0.02034 | 0.00382 | 489 | 412 | 375 | 54 | 357 | 18 | 407 | 76 | 357 | 18 | 2.006 | 9.48 |
| MVG125-07 | 0.05274 | 0.00814 | 0.41142 | 0.06076 | 0.05658 | 0.0028 | 0.01699 | 0.0034 | 318 | 356 | 350 | 44 | 355 | 18 | 341 | 68 | 355 | 18 | 2.35 | 10.49 |
| MVG125-08 | 0.05645 | 0.01028 | 0.44562 | 0.07812 | 0.05726 | 0.0031 | 0.01821 | 0.0036 | 470 | 416 | 374 | 54 | 359 | 18 | 365 | 72 | 359 | 18 | 2.423 | 11.03 |
| MVG125-09 | 0.05429 | 0.0111 | 0.43956 | 0.08674 | 0.05872 | 0.00342 | 0.01692 | 0.00416 | 383 | 468 | 370 | 62 | 368 | 20 | 339 | 82 | 368 | 20 | 1.697 | 8.34 |
| MVG125-10 | 0.05597 | 0.0101 | 0.44798 | 0.0782 | 0.05805 | 0.00292 | 0.01763 | 0.00356 | 451 | 412 | 376 | 54 | 364 | 18 | 353 | 70 | 364 | 18 | 2.55 | 11.16 |
| MVG125-11 | 0.05312 | 0.00962 | 0.40246 | 0.07056 | 0.05495 | 0.00276 | 0.01918 | 0.00326 | 334 | 414 | 343 | 52 | 345 | 16 | 384 | 64 | 345 | 16 | 2.5 | 11.32 |
| MVG125-12 | 0.06203 | 0.01102 | 0.49211 | 0.08328 | 0.05755 | 0.00336 | 0.01959 | 0.00376 | 675 | 394 | 406 | 56 | 361 | 20 | 392 | 74 | 361 | 20 | 2.72 | 12.27 |
| MVG125-13 | 0.05275 | 0.00786 | 0.41377 | 0.05956 | 0.05689 | 0.00242 | 0.01641 | 0.00298 | 318 | 342 | 352 | 42 | 357 | 14 | 329 | 60 | 357 | 14 | 2.8 | 13.21 |
| MVG125-14 | 0.05352 | 0.00754 | 0.41156 | 0.05576 | 0.05578 | 0.00234 | 0.01825 | 0.00322 | 351 | 326 | 350 | 40 | 350 | 14 | 366 | 64 | 350 | 14 | 2.719 | 13.16 |
| MVG125-15 | 0.05293 | 0.00708 | 0.40394 | 0.0521 | 0.05536 | 0.00222 | 0.01927 | 0.00218 | 326 | 310 | 345 | 38 | 347 | 14 | 386 | 44 | 347 | 14 | 5.45 | 16.04 |
| MVG125-16 | 0.05339 | 0.00852 | 0.42715 | 0.06586 | 0.05803 | 0.00262 | 0.01721 | 0.00314 | 345 | 366 | 361 | 46 | 364 | 16 | 345 | 62 | 364 | 16 | 2.456 | 10.73 |
| MVG125-17 | 0.05175 | 0.01226 | 0.41925 | 0.09496 | 0.05877 | 0.00434 | 0.0193 | 0.00496 | 274 | 534 | 356 | 68 | 368 | 26 | 386 | 98 | 368 | 26 | 2.52 | 11.47 |
| MVG125-18 | 0.05359 | 0.00836 | 0.44027 | 0.06642 | 0.05959 | 0.00262 | 0.02208 | 0.00326 | 354 | 358 | 370 | 46 | 373 | 16 | 441 | 64 | 373 | 16 | 2.4 | 11.29 |
| **Upper Muna field, Zapolyarnaya pipe** | | | | | | | | | | | | | | | | | | | | |
| 20104-01 | 0.18213 | 0.0016 | 12.56557 | 0.13213 | 0.50038 | 0.00325 | 0.13769 | 0.00091 | 2672 | 8 | 2648 | 10 | 2615 | 14 | 2607 | 16 | 2672 | 8 | | |
| 20104-02 | 0.18133 | 0.00137 | 12.24094 | 0.12775 | 0.48961 | 0.00308 | 0.13479 | 0.00084 | 2665 | 7 | 2623 | 10 | 2569 | 13 | 2556 | 15 | 2665 | 7 | | |
| 20104-03 | 0.18754 | 0.0027 | 13.48562 | 0.17536 | 0.52157 | 0.00492 | 0.15343 | 0.00461 | 2721 | 14 | 2714 | 12 | 2706 | 21 | 2885 | 81 | 2721 | 14 | | |
| 20104-04 | 0.17848 | 0.00143 | 9.05624 | 0.08357 | 0.368 | 0.00179 | 0.10146 | 0.00052 | 2639 | 8 | 2344 | 8 | 2020 | 8 | 1953 | 10 | 2639 | 8 | | |
| 20104-06 | 0.18631 | 0.0023 | 13.38695 | 0.14638 | 0.52119 | 0.00463 | 0.15393 | 0.0035 | 2710 | 12 | 2707 | 10 | 2704 | 20 | 2894 | 61 | 2710 | 12 | | |
| 20104-07 | 0.18815 | 0.00364 | 13.7275 | 0.26023 | 0.52923 | 0.0063 | 0.14981 | 0.00719 | 2726 | 18 | 2731 | 18 | 2738 | 27 | 2822 | 126 | 2726 | 18 | | |
| 20104-08 | 0.17666 | 0.00148 | 8.22234 | 0.09131 | 0.33757 | 0.00215 | 0.09316 | 0.00059 | 2622 | 8 | 2256 | 10 | 1875 | 10 | 1800 | 11 | 2622 | 8 | | |
| 20104-09 | 0.18151 | 0.00217 | 11.2437 | 0.15102 | 0.44927 | 0.00281 | 0.12367 | 0.0008 | 2667 | 11 | 2544 | 13 | 2392 | 12 | 2357 | 14 | 2667 | 11 | | |
| 20104-10 | 0.17903 | 0.00165 | 8.58881 | 0.09586 | 0.34793 | 0.00213 | 0.0959 | 0.00059 | 2644 | 9 | 2295 | 10 | 1925 | 10 | 1851 | 11 | 2644 | 9 | | |
| 20104-11 | 0.17797 | 0.00127 | 8.45742 | 0.07481 | 0.34467 | 0.00192 | 0.09505 | 0.00054 | 2634 | 7 | 2281 | 8 | 1909 | 9 | 1835 | 10 | 2634 | 7 | | |
| ZP110401 | 0.18792 | 0.00202 | 13.5523 | 0.12849 | 0.52308 | 0.00462 | 0.14881 | 0.00213 | 2724 | 11 | 2719 | 9 | 2712 | 20 | 2804 | 37 | 2724 | 11 | | |
| ZP110402 | 0.18781 | 0.00197 | 13.61774 | 0.10461 | 0.52591 | 0.00375 | 0.14875 | 0.00186 | 2723 | 10 | 2723 | 7 | 2724 | 16 | 2803 | 33 | 2723 | 10 | | |
| ZP110404 | 0.18703 | 0.00195 | 13.50935 | 0.1109 | 0.5239 | 0.00408 | 0.14949 | 0.0018 | 2716 | 10 | 2716 | 8 | 2716 | 17 | 2816 | 32 | 2716 | 10 | | |
| ZP110407 | 0.18226 | 0.00204 | 12.85161 | 0.12347 | 0.51145 | 0.00437 | 0.14692 | 0.00248 | 2674 | 11 | 2669 | 9 | 2663 | 19 | 2771 | 44 | 2674 | 11 | | |
| ZP110407-1 | 0.18273 | 0.00212 | 10.79906 | 0.10325 | 0.42864 | 0.00343 | 0.11989 | 0.00233 | 2678 | 11 | 2506 | 9 | 2300 | 15 | 2289 | 42 | 2678 | 11 | | |
| ZP110412 | 0.18272 | 0.00125 | 12.1325 | 0.09079 | 0.48157 | 0.00283 | 0.13247 | 0.00081 | 2678 | 7 | 2615 | 7 | 2534 | 12 | 2514 | 15 | 2678 | 7 | | |
| ZP110415 | 0.18838 | 0.00245 | 13.57966 | 0.16818 | 0.52289 | 0.00525 | 0.14488 | 0.00387 | 2728 | 13 | 2721 | 12 | 2711 | 22 | 2735 | 68 | 2728 | 13 | | |

| Analysis No. | RATIOS | | | | | | | | AGES (Ma) | | | | | | | | | | CONCENTRATIONS (ppm) | |
|---|---|---|---|---|---|---|---|---|---|---|---|---|---|---|---|---|---|---|---|---|
| | $^{207}Pb/^{206}Pb$ | ± 2σ | $^{207}Pb/^{235}U$ | ± 2σ | $^{206}Pb/^{238}U$ | ± 2σ | $^{208}Pb/^{232}Th$ | ± 2σ | $^{207}Pb/^{206}Pb$ | ± 2σ | $^{207}Pb/^{235}U$ | ± 2σ | $^{206}Pb/^{238}U$ | ± 2σ | $^{208}Pb/^{232}Th$ | ± 2σ | Used Age | ± 2σ | Th | U |
| ZP110416 | 0.18657 | 0.00229 | 13.46945 | 0.15306 | 0.52365 | 0.00497 | 0.15021 | 0.00345 | 2712 | 12 | 2713 | 11 | 2715 | 21 | 2829 | 61 | 2712 | 12 | | |
| ZP110418 | 0.15368 | 0.00113 | 4.66643 | 0.04224 | 0.22022 | 0.00118 | 0.0616 | 0.00034 | 2387 | 8 | 1761 | 8 | 1283 | 6 | 1208 | 6 | 2387 | 8 | | |
| ZP110419 | 0.18699 | 0.00212 | 13.56264 | 0.14139 | 0.52608 | 0.00492 | 0.15579 | 0.0028 | 2716 | 11 | 2720 | 10 | 2725 | 21 | 2926 | 49 | 2716 | 11 | | |
| ZP110420 | 0.17046 | 0.00116 | 6.89332 | 0.05695 | 0.2933 | 0.00157 | 0.08122 | 0.00045 | 2562 | 6 | 2098 | 7 | 1658 | 8 | 1578 | 8 | 2562 | 6 | | |
| ZP110424 | 0.18743 | 0.00234 | 13.53296 | 0.16226 | 0.52374 | 0.00528 | 0.15618 | 0.00368 | 2720 | 12 | 2718 | 11 | 2715 | 22 | 2933 | 64 | 2720 | 12 | | |
| ZP110425 | 0.18836 | 0.00354 | 13.64936 | 0.2517 | 0.52563 | 0.00633 | 0.16449 | 0.0079 | 2728 | 18 | 2726 | 17 | 2723 | 27 | 3078 | 137 | 2728 | 18 | | |
| ZP100403 | 0.18486 | 0.00279 | 12.48551 | 0.18152 | 0.48993 | 0.00524 | 0.13023 | 0.0043 | 2697 | 14 | 2642 | 14 | 2570 | 23 | 2474 | 77 | 2697 | 14 | | |
| ZP100406 | 0.18505 | 0.00246 | 13.20553 | 0.17207 | 0.51769 | 0.00548 | 0.13831 | 0.00367 | 2699 | 13 | 2694 | 12 | 2689 | 23 | 2618 | 65 | 2699 | 13 | | |
| ZP100407 | 0.18078 | 0.00215 | 9.98959 | 0.14532 | 0.40076 | 0.00316 | 0.11036 | 0.00088 | 2660 | 11 | 2434 | 13 | 2173 | 15 | 2116 | 16 | 2660 | 11 | | |
| ZP100408 | 0.17941 | 0.00231 | 8.82988 | 0.10184 | 0.35698 | 0.00323 | 0.0868 | 0.00214 | 2647 | 12 | 2321 | 11 | 1968 | 15 | 1682 | 40 | 2647 | 12 | | |
| ZP100412 | 0.18871 | 0.00223 | 13.78793 | 0.14882 | 0.52998 | 0.00495 | 0.14087 | 0.00272 | 2731 | 11 | 2735 | 10 | 2741 | 21 | 2664 | 48 | 2731 | 11 | | |
| ZP100413 | 0.18589 | 0.00225 | 13.44578 | 0.14676 | 0.52466 | 0.0048 | 0.13958 | 0.00291 | 2706 | 12 | 2711 | 10 | 2719 | 20 | 2641 | 52 | 2706 | 12 | | |
| ZP100418 | 0.186 | 0.00266 | 13.45931 | 0.18319 | 0.52496 | 0.0054 | 0.13992 | 0.0042 | 2707 | 14 | 2712 | 13 | 2720 | 23 | 2647 | 74 | 2707 | 14 | | |
| ZP100420 | 0.18675 | 0.00278 | 13.4568 | 0.19801 | 0.52291 | 0.00591 | 0.13757 | 0.00431 | 2714 | 14 | 2712 | 14 | 2712 | 25 | 2605 | 77 | 2714 | 14 | | |
| ZP100421 | 0.17661 | 0.00168 | 8.3999 | 0.09673 | 0.34495 | 0.00211 | 0.0952 | 0.00059 | 2621 | 9 | 2275 | 10 | 1910 | 10 | 1838 | 11 | 2621 | 9 | | |
| ZP100422 | 0.18712 | 0.00204 | 13.56176 | 0.12774 | 0.5257 | 0.00454 | 0.14425 | 0.00215 | 2717 | 11 | 2720 | 9 | 2723 | 19 | 2724 | 38 | 2717 | 11 | | |
| ZP100424 | 0.1898 | 0.00267 | 13.80242 | 0.19041 | 0.52756 | 0.00576 | 0.14643 | 0.00423 | 2740 | 14 | 2736 | 13 | 2731 | 24 | 2762 | 75 | 2740 | 14 | | |
| ZP100426 | 0.18693 | 0.0027 | 13.51462 | 0.18184 | 0.52444 | 0.00521 | 0.14152 | 0.00435 | 2715 | 13 | 2716 | 13 | 2718 | 22 | 2675 | 77 | 2715 | 13 | | |
| ZP100427 | 0.18216 | 0.00213 | 12.91715 | 0.13545 | 0.51434 | 0.00466 | 0.13557 | 0.00263 | 2673 | 11 | 2674 | 10 | 2675 | 20 | 2570 | 47 | 2673 | 11 | | |
| ZP100429 | 0.18276 | 0.00267 | 9.42021 | 0.13384 | 0.37391 | 0.00403 | 0.10408 | 0.00331 | 2678 | 13 | 2380 | 13 | 2048 | 19 | 2001 | 61 | 2678 | 13 | | |
| ZP100432 | 0.18711 | 0.00218 | 13.4664 | 0.13729 | 0.52202 | 0.00459 | 0.14242 | 0.00273 | 2717 | 11 | 2713 | 10 | 2708 | 19 | 2691 | 48 | 2717 | 11 | | |
| MVG63-29 | 0.25187 | 0.00884 | 21.24333 | 0.56020 | 0.61171 | 0.01418 | 0.16328 | 0.00388 | 3197 | 56 | 3150 | 26 | 3077 | 56 | 3057 | 68 | 3197 | 56 | | |
| MVG63-30 | 0.11479 | 0.00262 | 5.25687 | 0.12844 | 0.33216 | 0.00758 | 0.09492 | 0.00284 | 1877 | 42 | 1862 | 20 | 1849 | 36 | 1833 | 52 | 1877 | 42 | | |
| MVG63-31C | 0.24717 | 0.00942 | 19.99129 | 0.60198 | 0.58659 | 0.01368 | 0.15685 | 0.00372 | 3167 | 62 | 3091 | 30 | 2976 | 56 | 2945 | 66 | 3167 | 62 | | |
| MVG63-31R | 0.1192 | 0.00478 | 5.65436 | 0.23948 | 0.34374 | 0.01068 | 0.09368 | 0.00756 | 1944 | 74 | 1924 | 36 | 1905 | 52 | 1810 | 140 | 1944 | 74 | | |
| MVG63-32 | 0.11904 | 0.00254 | 5.7021 | 0.12504 | 0.34743 | 0.00734 | 0.10262 | 0.00382 | 1942 | 40 | 1932 | 18 | 1922 | 36 | 1975 | 70 | 1942 | 40 | | |
| MVG63-33 | 0.24545 | 0.00542 | 19.9712 | 0.48260 | 0.59014 | 0.01354 | 0.15718 | 0.00548 | 3156 | 36 | 3090 | 24 | 2990 | 54 | 2951 | 96 | 3156 | 36 | | |
| MVG63-35C | 0.22119 | 0.00748 | 15.77248 | 0.42438 | 0.51718 | 0.01064 | 0.13972 | 0.00314 | 2989 | 56 | 2863 | 26 | 2687 | 46 | 2643 | 56 | 2989 | 56 | | |
| MVG63-35R | 0.11945 | 0.00286 | 5.86239 | 0.14916 | 0.35599 | 0.00816 | 0.10381 | 0.00438 | 1948 | 44 | 1956 | 22 | 1963 | 38 | 1996 | 80 | 1948 | 44 | | |
| MVG63-36 | 0.11469 | 0.00356 | 5.25695 | 0.17388 | 0.33249 | 0.00890 | 0.09236 | 0.00496 | 1875 | 58 | 1862 | 28 | 1850 | 44 | 1786 | 92 | 1875 | 58 | | |
| MVG63-38 | 0.20043 | 0.00768 | 13.30197 | 0.41036 | 0.48133 | 0.01094 | 0.13125 | 0.00306 | 2830 | 64 | 2701 | 30 | 2533 | 48 | 2493 | 54 | 2830 | 64 | | |
| MVG63-40 | 0.11792 | 0.00262 | 5.57861 | 0.13084 | 0.34312 | 0.00756 | 0.10542 | 0.00432 | 1925 | 40 | 1913 | 20 | 1902 | 36 | 2026 | 78 | 1925 | 40 | | |
| MVG63-42 | 0.11779 | 0.00266 | 5.87401 | 0.13172 | 0.36175 | 0.00742 | 0.11208 | 0.00492 | 1923 | 42 | 1957 | 20 | 1990 | 36 | 2147 | 90 | 1923 | 42 | | |
| MVG63-43 | 0.24598 | 0.00528 | 21.16758 | 0.47450 | 0.62417 | 0.01342 | 0.177 | 0.00520 | 3159 | 34 | 3146 | 22 | 3126 | 54 | 3294 | 90 | 3159 | 34 | | |
| MVG63-44 | 0.16881 | 0.00360 | 11.02443 | 0.26006 | 0.47369 | 0.01082 | 0.13689 | 0.00400 | 2546 | 36 | 2525 | 22 | 2500 | 48 | 2593 | 72 | 2546 | 36 | | |
| MVG63-45 | 0.22154 | 0.00500 | 15.67684 | 0.35734 | 0.51328 | 0.01078 | 0.14108 | 0.00490 | 2992 | 38 | 2857 | 22 | 2671 | 46 | 2668 | 86 | 2992 | 38 | | |
| MVG63-46 | 0.23427 | 0.00504 | 19.50825 | 0.45916 | 0.60401 | 0.01370 | 0.17675 | 0.00528 | 3081 | 36 | 3067 | 22 | 3046 | 56 | 3290 | 90 | 3081 | 36 | | |
| MVG63-47 | 0.25246 | 0.00562 | 21.80829 | 0.49310 | 0.62656 | 0.01326 | 0.17836 | 0.00584 | 3200 | 36 | 3175 | 22 | 3136 | 52 | 3317 | 100 | 3200 | 36 | | |
| MVG63-48 | 0.11822 | 0.00278 | 5.75627 | 0.14348 | 0.35318 | 0.00802 | 0.10809 | 0.00380 | 1929 | 44 | 1940 | 22 | 1950 | 38 | 2075 | 70 | 1929 | 44 | | |
| MVG63-49 | 0.11871 | 0.00268 | 5.75557 | 0.13978 | 0.35167 | 0.00800 | 0.10397 | 0.00332 | 1937 | 42 | 1940 | 22 | 1943 | 38 | 1999 | 60 | 1937 | 42 | | |
| MVG63-51 | 0.11234 | 0.00366 | 5.12926 | 0.17734 | 0.33126 | 0.00908 | 0.09556 | 0.00560 | 1838 | 60 | 1841 | 30 | 1844 | 44 | 1845 | 104 | 1838 | 60 | | |
| MVG63-52C | 0.20062 | 0.00790 | 13.49457 | 0.42494 | 0.48784 | 0.01156 | 0.13301 | 0.00334 | 2831 | 66 | 2715 | 30 | 2561 | 50 | 2524 | 60 | 2831 | 66 | | |
| MVG63-52R | 0.11237 | 0.00496 | 5.18434 | 0.23100 | 0.33465 | 0.01042 | 0.09128 | 0.00684 | 1838 | 82 | 1850 | 38 | 1861 | 50 | 1766 | 126 | 1838 | 82 | | |
| MVG63-53 | 0.19062 | 0.00764 | 13.06799 | 0.54058 | 0.49722 | 0.01472 | 0.12004 | 0.01086 | 2748 | 68 | 2685 | 40 | 2602 | 64 | 2291 | 196 | 2748 | 68 | | |

| Analysis No. | RATIOS | | | | | | | | AGES (Ma) | | | | | | | | | | CONCENTRATIONS (ppm) | |
|---|---|---|---|---|---|---|---|---|---|---|---|---|---|---|---|---|---|---|---|---|
| | $^{207}Pb/^{206}Pb$ | ± 2σ | $^{207}Pb/^{235}U$ | ± 2σ | $^{206}Pb/^{238}U$ | ± 2σ | $^{208}Pb/^{232}Th$ | ± 2σ | $^{207}Pb/^{206}Pb$ | ± 2σ | $^{207}Pb/^{235}U$ | ± 2σ | $^{206}Pb/^{238}U$ | ± 2σ | $^{208}Pb/^{232}Th$ | ± 2σ | Used Age | ± 2σ | Th | U |
| MVG63-54 | 0.24868 | 0.00626 | 21.93517 | 0.59184 | 0.63982 | 0.01514 | 0.17884 | 0.00836 | 3176 | 40 | 3181 | 26 | 3188 | 60 | 3326 | 144 | 3176 | 40 | | |
| MVG63-55 | 0.11948 | 0.00454 | 5.86855 | 0.23068 | 0.35635 | 0.01020 | 0.08537 | 0.01534 | 1948 | 70 | 1957 | 34 | 1965 | 48 | 1656 | 286 | 1948 | 70 | | |
| ~~20104-05~~ | ~~0.13193~~ | ~~0.00204~~ | ~~2.87595~~ | ~~0.05575~~ | ~~0.1581~~ | ~~0.00119~~ | ~~0.04489~~ | ~~0.00033~~ | ~~2124~~ | ~~15~~ | ~~1376~~ | ~~15~~ | ~~946~~ | ~~7~~ | ~~888~~ | ~~6~~ | ~~2124~~ | ~~15~~ | | |
| ~~ZP110409~~ | ~~0.17645~~ | ~~0.00128~~ | ~~10.23818~~ | ~~0.07778~~ | ~~0.42082~~ | ~~0.00229~~ | ~~0.11615~~ | ~~0.00067~~ | ~~2620~~ | ~~7~~ | ~~2457~~ | ~~7~~ | ~~2264~~ | ~~10~~ | ~~2221~~ | ~~12~~ | ~~2620~~ | ~~7~~ | | |
| ~~ZP110410~~ | ~~0.17922~~ | ~~0.00227~~ | ~~9.85663~~ | ~~0.11461~~ | ~~0.39891~~ | ~~0.00377~~ | ~~0.11009~~ | ~~0.00266~~ | ~~2646~~ | ~~12~~ | ~~2421~~ | ~~11~~ | ~~2164~~ | ~~17~~ | ~~2111~~ | ~~48~~ | ~~2646~~ | ~~12~~ | | |
| ~~ZP110414~~ | ~~0.17467~~ | ~~0.00151~~ | ~~9.58003~~ | ~~0.10098~~ | ~~0.39778~~ | ~~0.0024~~ | ~~0.1099~~ | ~~0.00067~~ | ~~2603~~ | ~~8~~ | ~~2395~~ | ~~10~~ | ~~2159~~ | ~~11~~ | ~~2107~~ | ~~12~~ | ~~2603~~ | ~~8~~ | | |
| ~~ZP110421~~ | ~~0.17245~~ | ~~0.0013~~ | ~~6.19545~~ | ~~0.05876~~ | ~~0.26056~~ | ~~0.00156~~ | ~~0.07207~~ | ~~0.00044~~ | ~~2582~~ | ~~7~~ | ~~2004~~ | ~~8~~ | ~~1493~~ | ~~8~~ | ~~1407~~ | ~~8~~ | ~~2582~~ | ~~7~~ | | |
| ~~ZP110422~~ | ~~0.1774~~ | ~~0.00116~~ | ~~10.08998~~ | ~~0.07813~~ | ~~0.41252~~ | ~~0.00233~~ | ~~0.1138~~ | ~~0.00066~~ | ~~2629~~ | ~~6~~ | ~~2443~~ | ~~7~~ | ~~2226~~ | ~~11~~ | ~~2178~~ | ~~12~~ | ~~2629~~ | ~~6~~ | | |
| ~~ZP110423~~ | ~~0.16797~~ | ~~0.00139~~ | ~~8.57299~~ | ~~0.08924~~ | ~~0.37016~~ | ~~0.00238~~ | ~~0.10265~~ | ~~0.00068~~ | ~~2538~~ | ~~8~~ | ~~2294~~ | ~~9~~ | ~~2030~~ | ~~11~~ | ~~1975~~ | ~~12~~ | ~~2538~~ | ~~8~~ | | |
| ~~ZP110426~~ | ~~0.18191~~ | ~~0.00286~~ | ~~12.81006~~ | ~~0.1705~~ | ~~0.51082~~ | ~~0.00401~~ | ~~0.14427~~ | ~~0.0052~~ | ~~2670~~ | ~~15~~ | ~~2666~~ | ~~13~~ | ~~2660~~ | ~~17~~ | ~~2724~~ | ~~92~~ | ~~2670~~ | ~~15~~ | | |
| ~~ZP110428~~ | ~~0.17513~~ | ~~0.00109~~ | ~~10.51539~~ | ~~0.08905~~ | ~~0.43547~~ | ~~0.00237~~ | ~~0.12028~~ | ~~0.00066~~ | ~~2607~~ | ~~6~~ | ~~2481~~ | ~~8~~ | ~~2330~~ | ~~11~~ | ~~2296~~ | ~~12~~ | ~~2607~~ | ~~6~~ | | |
| ~~ZP100401~~ | ~~0.16135~~ | ~~0.00161~~ | ~~6.37501~~ | ~~0.07669~~ | ~~0.28656~~ | ~~0.00178~~ | ~~0.07978~~ | ~~0.00053~~ | ~~2470~~ | ~~9~~ | ~~2029~~ | ~~11~~ | ~~1624~~ | ~~9~~ | ~~1551~~ | ~~10~~ | ~~2470~~ | ~~9~~ | | |
| ~~ZP100404~~ | ~~0.18341~~ | ~~0.00224~~ | ~~10.7876~~ | ~~0.11038~~ | ~~0.42659~~ | ~~0.0035~~ | ~~0.11949~~ | ~~0.00257~~ | ~~2684~~ | ~~12~~ | ~~2505~~ | ~~10~~ | ~~2290~~ | ~~16~~ | ~~2281~~ | ~~46~~ | ~~2684~~ | ~~12~~ | | |
| ~~ZP100410~~ | ~~0.15558~~ | ~~0.00902~~ | ~~9.60062~~ | ~~0.71106~~ | ~~0.44755~~ | ~~0.00785~~ | ~~0.12504~~ | ~~0.00159~~ | ~~2408~~ | ~~54~~ | ~~2397~~ | ~~68~~ | ~~2384~~ | ~~35~~ | ~~2381~~ | ~~29~~ | ~~2408~~ | ~~54~~ | | |
| ~~ZP100414~~ | ~~0.17396~~ | ~~0.00348~~ | ~~10.73899~~ | ~~0.29494~~ | ~~0.44773~~ | ~~0.00427~~ | ~~0.12374~~ | ~~0.00103~~ | ~~2596~~ | ~~19~~ | ~~2501~~ | ~~26~~ | ~~2385~~ | ~~19~~ | ~~2358~~ | ~~19~~ | ~~2596~~ | ~~19~~ | | |
| ~~ZP100428~~ | ~~0.16645~~ | ~~0.00238~~ | ~~9.55823~~ | ~~0.17589~~ | ~~0.41647~~ | ~~0.00328~~ | ~~0.11559~~ | ~~0.00088~~ | ~~2522~~ | ~~14~~ | ~~2393~~ | ~~17~~ | ~~2244~~ | ~~15~~ | ~~2211~~ | ~~16~~ | ~~2522~~ | ~~14~~ | | |
| ~~ZP100435~~ | ~~0.17168~~ | ~~0.00484~~ | ~~10.78749~~ | ~~0.40791~~ | ~~0.45572~~ | ~~0.00511~~ | ~~0.12611~~ | ~~0.00116~~ | ~~2574~~ | ~~27~~ | ~~2505~~ | ~~35~~ | ~~2421~~ | ~~23~~ | ~~2401~~ | ~~21~~ | ~~2574~~ | ~~27~~ | | |
| **Daldyn field, Udachnaya Eastern pipe** | | | | | | | | | | | | | | | | | | | | |
| MVG458_UE-1c | 0.16546 | 0.0054 | 10.37668 | 0.32506 | 0.45482 | 0.00724 | 0.12521 | 0.00778 | 2512 | 56 | 2469 | 30 | 2417 | 32 | 2384 | 140 | 2512 | 56 | 455.16 | 745.86 |
| MVG458_UE-1r | 0.16786 | 0.00808 | 10.83534 | 0.4992 | 0.46787 | 0.01002 | 0.13076 | 0.01214 | 2536 | 82 | 2509 | 42 | 2474 | 44 | 2484 | 218 | 2536 | 82 | 151.87 | 417.77 |
| MVG458_UE-2 | 0.17705 | 0.0073 | 12.23181 | 0.48454 | 0.50113 | 0.00916 | 0.12777 | 0.01006 | 2625 | 70 | 2622 | 38 | 2619 | 40 | 2430 | 180 | 2625 | 70 | 680.19 | 1377.63 |
| MVG458_UE-3 | 0.17792 | 0.00598 | 12.24293 | 0.39338 | 0.49907 | 0.00788 | 0.13624 | 0.0089 | 2634 | 58 | 2623 | 30 | 2610 | 34 | 2582 | 158 | 2634 | 58 | 352.05 | 665.12 |
| MVG458_UE-4 | 0.17891 | 0.0064 | 12.3693 | 0.42248 | 0.50143 | 0.0082 | 0.13579 | 0.0094 | 2643 | 60 | 2633 | 32 | 2620 | 36 | 2574 | 168 | 2643 | 60 | 497.09 | 638.44 |
| MVG458_UE-5 | 0.16356 | 0.00792 | 10.03948 | 0.45818 | 0.4452 | 0.00846 | 0.12738 | 0.01204 | 2493 | 84 | 2438 | 42 | 2374 | 38 | 2423 | 216 | 2493 | 84 | 341.20 | 1193.15 |
| MVG458_UE-6c | 0.15182 | 0.00494 | 8.62628 | 0.2684 | 0.41208 | 0.00634 | 0.11244 | 0.0069 | 2367 | 56 | 2299 | 28 | 2224 | 28 | 2154 | 126 | 2367 | 56 | 578.30 | 600.87 |
| MVG458_UE-6r | 0.11891 | 0.00542 | 5.68588 | 0.24468 | 0.3468 | 0.00726 | 0.09478 | 0.00702 | 1940 | 84 | 1929 | 38 | 1919 | 34 | 1830 | 130 | 1940 | 84 | 137.36 | 70.30 |
| MVG458_UE-7c | 0.12642 | 0.00472 | 6.07906 | 0.21508 | 0.34877 | 0.00562 | 0.10035 | 0.00722 | 2049 | 68 | 1987 | 30 | 1929 | 26 | 1933 | 132 | 2049 | 68 | 1877.38 | 2205.16 |
| MVG458_UE-7r | 0.11396 | 0.00462 | 5.04462 | 0.19318 | 0.32106 | 0.00584 | 0.09266 | 0.00646 | 1864 | 74 | 1827 | 32 | 1795 | 28 | 1791 | 120 | 1864 | 74 | 255.16 | 121.82 |
| **Daldyn field, Zarnitsa pipe** | | | | | | | | | | | | | | | | | | | | |
| MVG458_Z-01 | 0.11873 | 0.00596 | 5.67074 | 0.26912 | 0.34647 | 0.00858 | 0.09866 | 0.00656 | 1937 | 92 | 1927 | 40 | 1918 | 42 | 1902 | 120 | 1937 | 92 | 85.80 | 50.44 |
| MVG458_Z-05 | 0.12042 | 0.0039 | 5.86259 | 0.18292 | 0.35312 | 0.00554 | 0.10423 | 0.00624 | 1962 | 60 | 1956 | 28 | 1949 | 26 | 2004 | 114 | 1962 | 60 | 700.23 | 353.48 |
| MVG458_Z-06 | 0.11377 | 0.00822 | 5.20276 | 0.35882 | 0.33178 | 0.00988 | 0.08943 | 0.01232 | 1860 | 134 | 1853 | 58 | 1847 | 48 | 1731 | 228 | 1860 | 134 | 481.31 | 510.13 |
| MVG458_Z-06r | 0.11987 | 0.004 | 5.81784 | 0.1861 | 0.35202 | 0.00562 | 0.10252 | 0.00628 | 1954 | 60 | 1949 | 28 | 1944 | 26 | 1973 | 116 | 1954 | 60 | 267.24 | 247.11 |
| MVG458_Z-07 | 0.12111 | 0.0042 | 5.94785 | 0.19814 | 0.35621 | 0.00562 | 0.1063 | 0.00732 | 1973 | 64 | 1968 | 28 | 1964 | 26 | 2042 | 134 | 1973 | 64 | 412.72 | 1213.35 |
| MVG458_Z-08 | 0.15829 | 0.00832 | 9.60565 | 0.48568 | 0.44023 | 0.00984 | 0.12576 | 0.01344 | 2437 | 92 | 2398 | 46 | 2352 | 44 | 2394 | 242 | 2437 | 92 | 253.83 | 455.09 |
| MVG458_Z-09 | 0.12668 | 0.00684 | 6.50604 | 0.33256 | 0.37249 | 0.00974 | 0.11094 | 0.00944 | 2052 | 98 | 2047 | 44 | 2041 | 46 | 2126 | 172 | 2052 | 98 | 19.22 | 31.33 |
| MVG458_Z-10 | 0.12269 | 0.00494 | 6.01961 | 0.23316 | 0.35584 | 0.00622 | 0.10558 | 0.00854 | 1996 | 74 | 1979 | 34 | 1962 | 30 | 2029 | 156 | 1996 | 74 | 882.73 | 655.75 |
| MVG458_Z-11 | 0.17855 | 0.01046 | 12.05444 | 0.68048 | 0.48973 | 0.01162 | 0.13737 | 0.01704 | 2639 | 100 | 2609 | 52 | 2570 | 50 | 2602 | 302 | 2639 | 100 | 361.70 | 676.62 |
| MVG458_Z-15 | 0.12348 | 0.0047 | 6.23416 | 0.22784 | 0.36618 | 0.00616 | 0.10567 | 0.00814 | 2007 | 70 | 2009 | 32 | 2011 | 30 | 2030 | 148 | 2007 | 70 | 86.08 | 410.99 |
| **Daldyn field, Popugaeva pipe** | | | | | | | | | | | | | | | | | | | | |
| MVG458_P-01 | 0.11138 | 0.00646 | 5.30322 | 0.29072 | 0.34536 | 0.00984 | 0.10349 | 0.00678 | 1822 | 108 | 1869 | 46 | 1912 | 48 | 1990 | 124 | 1822 | 108 | 23.59 | 21.34 |
| MVG458_P-02 | 0.11961 | 0.00514 | 5.72703 | 0.23714 | 0.34731 | 0.00666 | 0.10104 | 0.00826 | 1950 | 78 | 1935 | 36 | 1922 | 32 | 1946 | 152 | 1950 | 78 | 1028.56 | 908.61 |
| MVG458_P-03 | 0.1212 | 0.00426 | 6.103 | 0.20514 | 0.36524 | 0.00652 | 0.10267 | 0.00578 | 1974 | 64 | 1991 | 30 | 2007 | 30 | 1975 | 106 | 1974 | 64 | 77.91 | 72.25 |
| MVG458_P-04 | 0.12109 | 0.00554 | 5.8063 | 0.25284 | 0.34784 | 0.00672 | 0.10025 | 0.00894 | 1972 | 84 | 1947 | 38 | 1924 | 32 | 1931 | 164 | 1972 | 84 | 269.35 | 299.91 |

| Analysis No. | RATIOS | | | | | | | | AGES (Ma) | | | | | | | | | | CONCENTRATIONS (ppm) | |
|---|---|---|---|---|---|---|---|---|---|---|---|---|---|---|---|---|---|---|---|---|
| | $^{207}Pb/^{206}Pb$ | ± 2σ | $^{207}Pb/^{235}U$ | ± 2σ | $^{206}Pb/^{238}U$ | ± 2σ | $^{208}Pb/^{232}Th$ | ± 2σ | $^{207}Pb/^{206}Pb$ | ± 2σ | $^{207}Pb/^{235}U$ | ± 2σ | $^{206}Pb/^{238}U$ | ± 2σ | $^{208}Pb/^{232}Th$ | ± 2σ | Used Age | ± 2σ | Th | U |
| MVG458_P-05 | 0.11799 | 0.0062 | 5.78415 | 0.2872 | 0.35555 | 0.0092 | 0.1032 | 0.00708 | 1926 | 96 | 1944 | 42 | 1961 | 44 | 1985 | 130 | 1926 | 96 | 26.74 | 26.68 |
| MVG458_P-07 | 0.11606 | 0.00622 | 5.54836 | 0.28122 | 0.34674 | 0.00896 | 0.10192 | 0.00788 | 1896 | 98 | 1908 | 44 | 1919 | 42 | 1962 | 144 | 1896 | 98 | 24.23 | 36.37 |
| MVG458_P-08 | 0.11574 | 0.00526 | 5.29575 | 0.22882 | 0.33187 | 0.00716 | 0.09616 | 0.00656 | 1891 | 84 | 1868 | 36 | 1847 | 34 | 1856 | 120 | 1891 | 84 | 122.69 | 57.65 |
| MVG458_P-10 | 0.11823 | 0.0041 | 5.7716 | 0.19156 | 0.35408 | 0.00586 | 0.10311 | 0.00652 | 1930 | 64 | 1942 | 28 | 1954 | 28 | 1983 | 120 | 1930 | 64 | 147.10 | 158.15 |
| MVG458_P-12 | 0.14886 | 0.00866 | 8.61294 | 0.4736 | 0.41966 | 0.01152 | 0.1155 | 0.01118 | 2333 | 102 | 2298 | 50 | 2259 | 52 | 2209 | 202 | 2333 | 102 | 46.40 | 35.41 |
| MVG458_P-13_R | 0.11906 | 0.00582 | 5.58728 | 0.26068 | 0.34039 | 0.0076 | 0.09161 | 0.00738 | 1942 | 90 | 1914 | 40 | 1889 | 36 | 1772 | 136 | 1942 | 90 | 61.66 | 75.12 |
| MVG458_P-13C | 0.12251 | 0.00586 | 5.8187 | 0.26674 | 0.34445 | 0.0074 | 0.09485 | 0.00784 | 1993 | 88 | 1949 | 40 | 1908 | 36 | 1832 | 144 | 1993 | 88 | 198.28 | 139.17 |
| MVG458_P-13R | 0.14874 | 0.00618 | 8.32586 | 0.32908 | 0.406 | 0.00856 | 0.10972 | 0.00728 | 2331 | 72 | 2267 | 36 | 2197 | 40 | 2104 | 132 | 2331 | 72 | 67.02 | 40.80 |
| MVG458_P-14 | 0.11941 | 0.00452 | 5.8494 | 0.21306 | 0.35529 | 0.00594 | 0.10369 | 0.00784 | 1947 | 70 | 1954 | 32 | 1960 | 28 | 1994 | 144 | 1947 | 70 | 171.84 | 576.34 |
| MVG458-P_15 | 0.16086 | 0.0025 | 9.47673 | 0.14514 | 0.42736 | 0.0051 | 0.11915 | 0.0033 | 2465 | 26 | 2385 | 14 | 2294 | 24 | 2275 | 60 | 2465 | 26 | 308.81 | 417.41 |
| MVG458-P_16c | 0.19238 | 0.00458 | 12.07345 | 0.2417 | 0.45517 | 0.00582 | 0.1246 | 0.00162 | 2763 | 40 | 2610 | 18 | 2418 | 26 | 2373 | 30 | 2763 | 40 | 292.47 | 324.68 |
| MVG458-P_16r | 0.15111 | 0.0048 | 7.94558 | 0.22678 | 0.38135 | 0.0053 | 0.10684 | 0.00148 | 2359 | 56 | 2225 | 26 | 2083 | 24 | 2052 | 26 | 2359 | 56 | 103.32 | 91.49 |
| MVG458-P_17 | 0.20284 | 0.00302 | 15.66276 | 0.22924 | 0.56014 | 0.00664 | 0.15416 | 0.0039 | 2849 | 24 | 2856 | 14 | 2867 | 28 | 2898 | 68 | 2849 | 24 | 142.73 | 101.64 |
| MVG458-P_18 | 0.11468 | 0.0018 | 5.37683 | 0.08238 | 0.34009 | 0.00402 | 0.10032 | 0.00266 | 1875 | 28 | 1881 | 14 | 1887 | 20 | 1932 | 48 | 1875 | 28 | 170.70 | 181.46 |
| MVG458-P_19 | 0.12918 | 0.00782 | 6.75945 | 0.3905 | 0.37951 | 0.00678 | 0.10798 | 0.00174 | 2087 | 108 | 2080 | 52 | 2074 | 32 | 2073 | 32 | 2087 | 108 | 88.09 | 51.30 |
| MVG458-P_20 | 0.27184 | 0.00474 | 22.94711 | 0.39256 | 0.61233 | 0.00746 | 0.16441 | 0.0055 | 3317 | 28 | 3225 | 16 | 3079 | 30 | 3077 | 96 | 3317 | 28 | 246.46 | 721.83 |
| MVG458-P_20r | 0.12887 | 0.00256 | 6.45349 | 0.12374 | 0.36326 | 0.00466 | 0.10117 | 0.00354 | 2083 | 36 | 2040 | 16 | 1998 | 22 | 1948 | 64 | 2083 | 36 | 338.47 | 115.08 |
| MVG458-P_21 | 0.13142 | 0.00312 | 6.56351 | 0.14894 | 0.36229 | 0.00482 | 0.10592 | 0.00498 | 2117 | 42 | 2054 | 20 | 1993 | 22 | 2035 | 92 | 2117 | 42 | 175.67 | 264.09 |
| **Daldyn field, Zagadochnaya pipe** | | | | | | | | | | | | | | | | | | | | |
| MVG458-Zag_01 | 0.13206 | 0.00322 | 6.61081 | 0.13954 | 0.36305 | 0.00444 | 0.10307 | 0.00132 | 2126 | 44 | 2061 | 18 | 1997 | 20 | 1983 | 24 | 2126 | 44 | 222.03 | 474.16 |
| MVG458-Zag_02 | 0.15345 | 0.00344 | 8.4556 | 0.18152 | 0.39968 | 0.0052 | 0.09475 | 0.00422 | 2385 | 40 | 2281 | 20 | 2168 | 24 | 1830 | 78 | 2385 | 40 | 126.96 | 824.09 |
| MVG458-Zag_03 | 0.17417 | 0.00426 | 11.05711 | 0.2333 | 0.46042 | 0.00574 | 0.12724 | 0.00166 | 2598 | 42 | 2528 | 20 | 2441 | 26 | 2421 | 30 | 2598 | 42 | 525.83 | 918.89 |
| MVG458-Zag_04 | 0.11667 | 0.00204 | 5.47879 | 0.09326 | 0.3406 | 0.00402 | 0.09764 | 0.00324 | 1906 | 32 | 1897 | 14 | 1890 | 20 | 1883 | 60 | 1906 | 32 | 1276.24 | 2403.48 |
| MVG458-Zag_05 | 0.12239 | 0.00228 | 6.3871 | 0.11538 | 0.3785 | 0.00464 | 0.09972 | 0.00348 | 1991 | 34 | 2030 | 16 | 2069 | 22 | 1921 | 64 | 1991 | 34 | 61.69 | 209.19 |
| MVG458-Zag_06 | 0.12435 | 0.00228 | 5.66231 | 0.1008 | 0.33025 | 0.00396 | 0.09171 | 0.0032 | 2020 | 34 | 1926 | 16 | 1840 | 20 | 1774 | 60 | 2020 | 34 | 222.56 | 724.00 |
| MVG458-Zag_07c | 0.17688 | 0.00332 | 11.72141 | 0.213 | 0.48062 | 0.00586 | 0.13583 | 0.00488 | 2624 | 32 | 2582 | 18 | 2530 | 26 | 2574 | 86 | 2624 | 32 | 214.08 | 352.37 |
| MVG458-Zag_07r | 0.11467 | 0.00372 | 5.03438 | 0.14862 | 0.31843 | 0.00422 | 0.09169 | 0.00126 | 1875 | 60 | 1825 | 26 | 1782 | 20 | 1773 | 24 | 1875 | 60 | 110.04 | 200.66 |
| MVG458-Zag_08 | 0.11805 | 0.00198 | 5.68618 | 0.09298 | 0.34937 | 0.00426 | 0.10521 | 0.00278 | 1927 | 30 | 1929 | 14 | 1932 | 20 | 2022 | 50 | 1927 | 30 | 97.83 | 114.87 |
| MVG458-Zag_09 | 0.11698 | 0.0018 | 5.61541 | 0.0851 | 0.34818 | 0.00406 | 0.10304 | 0.00286 | 1911 | 28 | 1918 | 14 | 1926 | 20 | 1982 | 52 | 1911 | 28 | 59.69 | 363.68 |
| MVG458-Zag_10 | 0.12488 | 0.00194 | 6.29083 | 0.09632 | 0.36539 | 0.00426 | 0.10623 | 0.00292 | 2027 | 28 | 2017 | 14 | 2008 | 20 | 2041 | 54 | 2027 | 28 | 142.93 | 392.79 |
| MVG458-Zag_11 | 0.11832 | 0.0018 | 5.79598 | 0.08766 | 0.35532 | 0.0041 | 0.10753 | 0.00306 | 1931 | 28 | 1946 | 14 | 1960 | 20 | 2064 | 56 | 1931 | 28 | 102.84 | 2671.06 |
| MVG458-Zag_12 | 0.15396 | 0.0036 | 9.12624 | 0.21064 | 0.43002 | 0.00602 | 0.12058 | 0.00562 | 2390 | 40 | 2351 | 22 | 2306 | 28 | 2301 | 102 | 2390 | 40 | 251.72 | 683.34 |
| MVG458-Zag_13 | 0.16306 | 0.00656 | 10.45289 | 0.3856 | 0.46493 | 0.00742 | 0.1293 | 0.00206 | 2488 | 70 | 2476 | 34 | 2461 | 32 | 2458 | 36 | 2488 | 70 | 125.99 | 132.04 |
| MVG458-Zag_14 | 0.15507 | 0.0033 | 8.91766 | 0.18602 | 0.41718 | 0.0055 | 0.12015 | 0.0049 | 2403 | 38 | 2330 | 20 | 2248 | 26 | 2293 | 88 | 2403 | 38 | 354.49 | 353.93 |
| MVG458-Zag_15 | 0.13698 | 0.00318 | 7.10157 | 0.13988 | 0.37601 | 0.00458 | 0.10637 | 0.00138 | 2189 | 42 | 2124 | 18 | 2058 | 22 | 2043 | 26 | 2189 | 42 | 467.05 | 1279.76 |
| MVG458-Zag_16 | 0.15292 | 0.00574 | 8.60137 | 0.29436 | 0.40795 | 0.00624 | 0.11416 | 0.00186 | 2379 | 66 | 2297 | 32 | 2206 | 28 | 2185 | 34 | 2379 | 66 | 347.13 | 644.65 |
| MVG458-Zag_17 | 0.13374 | 0.00414 | 6.79509 | 0.1891 | 0.36848 | 0.00504 | 0.10448 | 0.00156 | 2148 | 56 | 2085 | 24 | 2022 | 24 | 2009 | 28 | 2148 | 56 | 126.18 | 281.01 |
| MVG458-Zag_18 | 0.17813 | 0.00334 | 12.44132 | 0.2307 | 0.50664 | 0.0064 | 0.1468 | 0.00524 | 2636 | 32 | 2638 | 18 | 2642 | 28 | 2769 | 92 | 2636 | 32 | 96.94 | 164.27 |
| MVG458-Zag_19 | 0.12502 | 0.0024 | 6.57682 | 0.12478 | 0.38158 | 0.00482 | 0.1148 | 0.00418 | 2029 | 34 | 2056 | 16 | 2084 | 22 | 2197 | 76 | 2029 | 34 | 383.18 | 306.03 |
| MVG458-Zag_20 | 0.15601 | 0.0039 | 8.91458 | 0.19044 | 0.41443 | 0.00536 | 0.11575 | 0.0016 | 2413 | 44 | 2329 | 20 | 2235 | 24 | 2214 | 30 | 2413 | 44 | 296.16 | 1376.58 |
| MVG458-Zag_21 | 0.16041 | 0.004 | 10.0032 | 0.21154 | 0.45228 | 0.006 | 0.12598 | 0.00176 | 2460 | 44 | 2435 | 20 | 2405 | 26 | 2398 | 32 | 2460 | 44 | 283.40 | 671.80 |
| MVG458-Zag_22 | 0.18612 | 0.00796 | 14.15328 | 0.56858 | 0.55156 | 0.01346 | 0.14965 | 0.01194 | 2708 | 72 | 2760 | 38 | 2832 | 56 | 2819 | 210 | 2708 | 72 | 21.62 | 59.46 |
| MVG458-Zag_23 | 0.12352 | 0.00276 | 4.96337 | 0.10564 | 0.29142 | 0.00378 | 0.08386 | 0.00348 | 2008 | 40 | 1813 | 18 | 1649 | 18 | 1628 | 64 | 2008 | 40 | 238.64 | 526.30 |
| MVG458-Zag_24 | 0.14985 | 0.0025 | 9.13456 | 0.14956 | 0.44212 | 0.00544 | 0.10472 | 0.00298 | 2344 | 30 | 2352 | 14 | 2360 | 24 | 2013 | 54 | 2344 | 30 | 124.63 | 165.51 |

| Analysis No. | RATIOS | | | | | | | | AGES (Ma) | | | | | | | | | | CONCENTRATIONS (ppm) | |
|---|---|---|---|---|---|---|---|---|---|---|---|---|---|---|---|---|---|---|---|---|
| | $^{207}Pb/^{206}Pb$ | ± 2σ | $^{207}Pb/^{235}U$ | ± 2σ | $^{206}Pb/^{238}U$ | ± 2σ | $^{208}Pb/^{232}Th$ | ± 2σ | $^{207}Pb/^{206}Pb$ | ± 2σ | $^{207}Pb/^{235}U$ | ± 2σ | $^{206}Pb/^{238}U$ | ± 2σ | $^{208}Pb/^{232}Th$ | ± 2σ | Used Age | ± 2σ | Th | U |
| MVG458-Zag_25 | 0.16125 | 0.00394 | 10.12905 | 0.2116 | 0.45558 | 0.0058 | 0.12684 | 0.00166 | 2469 | 42 | 2447 | 20 | 2420 | 26 | 2414 | 30 | 2469 | 42 | 120.99 | 183.54 |
| MVG458-Zag_26 | 0.11992 | 0.00242 | 5.5286 | 0.10778 | 0.33441 | 0.0043 | 0.09435 | 0.00344 | 1955 | 36 | 1905 | 16 | 1860 | 20 | 1822 | 64 | 1955 | 36 | 173.88 | 284.57 |
| MVG458-Zag_27 | 0.1194 | 0.00196 | 5.83766 | 0.0932 | 0.35463 | 0.0042 | 0.10359 | 0.00294 | 1947 | 30 | 1952 | 14 | 1957 | 20 | 1992 | 54 | 1947 | 30 | 243.68 | 379.71 |
| MVG458-Zag_28 | 0.13699 | 0.0028 | 6.77413 | 0.13292 | 0.35869 | 0.00458 | 0.10016 | 0.00388 | 2189 | 36 | 2082 | 18 | 1976 | 22 | 1929 | 72 | 2189 | 36 | 708.64 | 1242.59 |
| MVG458-Zag_29 | 0.14944 | 0.00258 | 9.47661 | 0.15804 | 0.45996 | 0.00556 | 0.12902 | 0.00386 | 2340 | 30 | 2385 | 16 | 2439 | 24 | 2453 | 70 | 2340 | 30 | 147.82 | 183.63 |
| MVG458-Zag_31 | 0.11727 | 0.00254 | 5.70931 | 0.11832 | 0.35312 | 0.00486 | 0.10417 | 0.00342 | 1915 | 40 | 1933 | 18 | 1949 | 24 | 2003 | 62 | 1915 | 40 | 37.37 | 46.32 |
| MVG458-Zag_32 | 0.11211 | 0.0045 | 4.92782 | 0.18466 | 0.3188 | 0.00464 | 0.09201 | 0.00138 | 1834 | 74 | 1807 | 32 | 1784 | 22 | 1779 | 26 | 1834 | 74 | 116.54 | 182.76 |
| MVG458-Zag_33 | 0.16288 | 0.00472 | 10.07748 | 0.27388 | 0.44872 | 0.00666 | 0.12316 | 0.00664 | 2486 | 50 | 2442 | 26 | 2390 | 30 | 2348 | 120 | 2486 | 50 | 108.97 | 162.19 |
| MVG458-Zag_34 | 0.14897 | 0.00284 | 8.54346 | 0.15626 | 0.41599 | 0.0052 | 0.1163 | 0.00394 | 2334 | 34 | 2291 | 16 | 2242 | 24 | 2224 | 72 | 2334 | 34 | 84.97 | 138.85 |
| MVG458-Zag_35 | 0.14648 | 0.00276 | 8.08669 | 0.14628 | 0.40043 | 0.00496 | 0.11239 | 0.00378 | 2305 | 34 | 2241 | 16 | 2171 | 22 | 2153 | 68 | 2305 | 34 | 105.89 | 175.77 |
| MVG458-Zag_36 | 0.16808 | 0.0049 | 10.13883 | 0.26174 | 0.43748 | 0.00588 | 0.12131 | 0.0017 | 2539 | 50 | 2448 | 24 | 2339 | 26 | 2314 | 30 | 2539 | 50 | 214.54 | 302.74 |
| MVG458-Zag_37 | 0.11877 | 0.00354 | 5.0754 | 0.14202 | 0.30995 | 0.00446 | 0.06474 | 0.00378 | 1938 | 54 | 1832 | 24 | 1740 | 22 | 1268 | 72 | 1938 | 54 | 173.96 | 1377.69 |
| **Daldyn field, Kusova pipe** | | | | | | | | | | | | | | | | | | | | |
| MVG458-K_01 | 0.18074 | 0.00258 | 12.39883 | 0.17514 | 0.49758 | 0.00574 | 0.13698 | 0.00342 | 2660 | 24 | 2635 | 14 | 2603 | 24 | 2595 | 60 | 2660 | 24 | 100.28 | 305.75 |
| MVG458-K_02 | 0.12047 | 0.00190 | 5.80006 | 0.08938 | 0.34922 | 0.00416 | 0.10783 | 0.00276 | 1963 | 28 | 1946 | 14 | 1931 | 20 | 2070 | 50 | 1963 | 28 | 133.71 | 174.65 |
| MVG458-K_03 | 0.14113 | 0.00228 | 7.74119 | 0.12168 | 0.39785 | 0.00482 | 0.11078 | 0.00290 | 2241 | 28 | 2201 | 14 | 2159 | 22 | 2124 | 52 | 2241 | 28 | 168.41 | 127.98 |
| MVG458-K_05 | 0.12562 | 0.00328 | 5.93278 | 0.14996 | 0.34253 | 0.00500 | 0.10232 | 0.00528 | 2038 | 48 | 1966 | 22 | 1899 | 24 | 1969 | 96 | 2038 | 48 | 1279.37 | 1676.98 |
| MVG458-K_07 | 0.11745 | 0.00246 | 5.60229 | 0.11208 | 0.34599 | 0.00456 | 0.1051 | 0.00404 | 1918 | 38 | 1916 | 18 | 1915 | 22 | 2020 | 74 | 1918 | 38 | 26.71 | 99.01 |
| MVG458-K_08 | 0.11787 | 0.00208 | 5.68796 | 0.09748 | 0.35001 | 0.00432 | 0.10223 | 0.00304 | 1924 | 32 | 1930 | 14 | 1935 | 20 | 1967 | 56 | 1924 | 32 | 89.49 | 126.75 |
| MVG458-K_10 | 0.16252 | 0.00260 | 10.22515 | 0.15992 | 0.45633 | 0.00530 | 0.12882 | 0.00382 | 2482 | 28 | 2455 | 14 | 2423 | 24 | 2449 | 68 | 2482 | 28 | 1313.38 | 2508.35 |
| MVG458-K_11c | 0.16706 | 0.00272 | 10.27458 | 0.16360 | 0.44609 | 0.00528 | 0.12709 | 0.00380 | 2528 | 28 | 2460 | 14 | 2378 | 24 | 2418 | 68 | 2528 | 28 | 384.57 | 540.26 |
| MVG458-K_11r | 0.12765 | 0.00346 | 6.31918 | 0.16176 | 0.35907 | 0.00586 | 0.10185 | 0.00354 | 2066 | 48 | 2021 | 22 | 1978 | 28 | 1960 | 64 | 2066 | 48 | 158.27 | 25.24 |
| MVG458-K_12 | 0.1163 | 0.00296 | 5.35497 | 0.12908 | 0.33397 | 0.00508 | 0.10169 | 0.00404 | 1900 | 46 | 1878 | 20 | 1858 | 24 | 1957 | 74 | 1900 | 46 | 13.22 | 28.70 |
| MVG458-K_13 | 0.11923 | 0.00222 | 5.67373 | 0.10204 | 0.34517 | 0.00420 | 0.1026 | 0.00358 | 1945 | 34 | 1927 | 16 | 1911 | 20 | 1974 | 66 | 1945 | 34 | 346.25 | 366.51 |
| MVG458-K_15 | 0.1799 | 0.00308 | 11.95921 | 0.20126 | 0.48219 | 0.00592 | 0.13178 | 0.00402 | 2652 | 30 | 2601 | 16 | 2537 | 26 | 2502 | 72 | 2652 | 30 | 500.38 | 430.30 |
| MVG458-K_16 | 0.12099 | 0.00178 | 5.86843 | 0.08504 | 0.35182 | 0.00404 | 0.10352 | 0.00250 | 1971 | 26 | 1957 | 12 | 1943 | 20 | 1991 | 46 | 1971 | 26 | 402.19 | 292.91 |
| MVG458-K_18 | 0.14216 | 0.00394 | 7.75406 | 0.19110 | 0.39561 | 0.00500 | 0.1115 | 0.00142 | 2254 | 48 | 2203 | 22 | 2149 | 24 | 2137 | 26 | 2254 | 48 | 367.54 | 413.49 |
| MVG458-K_19 | 0.13593 | 0.00254 | 7.45045 | 0.13396 | 0.39758 | 0.00522 | 0.11578 | 0.00370 | 2176 | 34 | 2167 | 16 | 2158 | 24 | 2214 | 68 | 2176 | 34 | 12.55 | 43.34 |
| MVG458-K_21 | 0.12525 | 0.00272 | 6.30096 | 0.13220 | 0.36492 | 0.00484 | 0.10929 | 0.00444 | 2032 | 40 | 2019 | 18 | 2005 | 22 | 2096 | 80 | 2032 | 40 | 133.69 | 366.48 |
| MVG458-K_22 | 0.16448 | 0.00304 | 10.07583 | 0.18000 | 0.44434 | 0.00540 | 0.12617 | 0.00432 | 2502 | 32 | 2442 | 16 | 2370 | 24 | 2402 | 78 | 2502 | 32 | 105.94 | 263.90 |
| MVG458-K_23 | 0.14991 | 0.00440 | 8.20101 | 0.21598 | 0.39676 | 0.00520 | 0.11125 | 0.00150 | 2345 | 52 | 2253 | 24 | 2154 | 24 | 2132 | 28 | 2345 | 52 | 475.27 | 644.85 |
| MVG458-K_24 | 0.11518 | 0.00194 | 5.32964 | 0.08684 | 0.33564 | 0.00398 | 0.09842 | 0.00282 | 1883 | 32 | 1874 | 14 | 1866 | 20 | 1897 | 52 | 1883 | 32 | 188.09 | 220.03 |
| MVG458-K_26 | 0.17972 | 0.00306 | 12.33692 | 0.20368 | 0.49791 | 0.00602 | 0.14013 | 0.00418 | 2650 | 28 | 2630 | 16 | 2605 | 26 | 2651 | 74 | 2650 | 28 | 81.28 | 115.47 |
| MVG458-K_27 | 0.11734 | 0.00272 | 5.43046 | 0.11958 | 0.33569 | 0.00482 | 0.09825 | 0.00350 | 1916 | 42 | 1890 | 18 | 1866 | 24 | 1894 | 64 | 1916 | 42 | 15.08 | 31.07 |
| MVG458-K_28 | 0.1132 | 0.00314 | 5.26366 | 0.13790 | 0.33728 | 0.00546 | 0.0978 | 0.00384 | 1851 | 52 | 1863 | 22 | 1874 | 26 | 1886 | 70 | 1851 | 52 | 9.41 | 17.83 |
| MVG458-K_29 | 0.12332 | 0.00350 | 5.92721 | 0.14862 | 0.3486 | 0.00468 | 0.09965 | 0.00144 | 2005 | 52 | 1965 | 22 | 1928 | 22 | 1920 | 26 | 2005 | 52 | 77.47 | 240.89 |
| MVG458-K_30 | 0.13781 | 0.00246 | 7.5348 | 0.13046 | 0.39658 | 0.00472 | 0.11945 | 0.00392 | 2200 | 32 | 2177 | 16 | 2153 | 22 | 2281 | 70 | 2200 | 32 | 324.34 | 559.81 |
| MVG458-K_31 | 0.12457 | 0.00236 | 6.04594 | 0.11018 | 0.35205 | 0.00430 | 0.09802 | 0.00334 | 2023 | 34 | 1982 | 16 | 1944 | 20 | 1890 | 62 | 2023 | 34 | 202.79 | 231.81 |
| MVG458-K_33 | 0.15989 | 0.00296 | 9.68798 | 0.17426 | 0.43947 | 0.00554 | 0.1252 | 0.00412 | 2454 | 32 | 2406 | 16 | 2348 | 24 | 2384 | 74 | 2454 | 32 | 346.51 | 256.39 |
| MVG458-K_34 | 0.1174 | 0.00198 | 5.52897 | 0.09078 | 0.34159 | 0.00414 | 0.09846 | 0.00264 | 1917 | 30 | 1905 | 14 | 1894 | 20 | 1898 | 48 | 1917 | 30 | 69.91 | 111.59 |
| MVG458-K_35 | 0.16162 | 0.00298 | 9.75561 | 0.17342 | 0.43782 | 0.00528 | 0.11485 | 0.00386 | 2473 | 32 | 2412 | 16 | 2341 | 24 | 2197 | 70 | 2473 | 32 | 229.76 | 283.63 |
| MVG458-K_37 | 0.15076 | 0.00308 | 8.16699 | 0.16140 | 0.39292 | 0.00510 | 0.11373 | 0.00432 | 2355 | 36 | 2250 | 18 | 2136 | 24 | 2177 | 78 | 2355 | 36 | 161.93 | 260.80 |
| MVG458-K_38 | 0.16404 | 0.00552 | 9.1395 | 0.29554 | 0.40418 | 0.00690 | 0.11192 | 0.00760 | 2498 | 58 | 2352 | 30 | 2188 | 32 | 2144 | 138 | 2498 | 58 | 379.18 | 459.31 |
| MVG458-K_39 | 0.13817 | 0.00360 | 7.37464 | 0.18444 | 0.38718 | 0.00574 | 0.11259 | 0.00542 | 2204 | 46 | 2158 | 22 | 2110 | 26 | 2156 | 98 | 2204 | 46 | 117.20 | 139.13 |

| Analysis No. | RATIOS | | | | | | | | AGES (Ma) | | | | | | | | | | CONCENTRATIONS (ppm) | |
|---|---|---|---|---|---|---|---|---|---|---|---|---|---|---|---|---|---|---|---|---|
| | $^{207}Pb/^{206}Pb$ | ± 2σ | $^{207}Pb/^{235}U$ | ± 2σ | $^{206}Pb/^{238}U$ | ± 2σ | $^{208}Pb/^{232}Th$ | ± 2σ | $^{207}Pb/^{206}Pb$ | ± 2σ | $^{207}Pb/^{235}U$ | ± 2σ | $^{206}Pb/^{238}U$ | ± 2σ | $^{208}Pb/^{232}Th$ | ± 2σ | Used Age | ± 2σ | Th | U |
| MVG458-K_40 | 0.12235 | 0.00326 | 5.61074 | 0.13232 | 0.33258 | 0.00412 | 0.09514 | 0.00128 | 1991 | 48 | 1918 | 20 | 1851 | 20 | 1837 | 24 | 1991 | 48 | 163.07 | 354.91 |
| MVG458-K_41 | 0.17832 | 0.00328 | 11.83385 | 0.21054 | 0.48134 | 0.00600 | 0.13456 | 0.00446 | 2637 | 32 | 2591 | 16 | 2533 | 26 | 2552 | 80 | 2637 | 32 | 69.50 | 105.74 |
| MVG458-K_42 | 0.12415 | 0.00270 | 6.0269 | 0.12702 | 0.35211 | 0.00456 | 0.10083 | 0.00430 | 2017 | 40 | 1980 | 18 | 1945 | 22 | 1942 | 78 | 2017 | 40 | 233.15 | 721.49 |
| MVG458-K_43 | 0.1245 | 0.00334 | 5.37776 | 0.13754 | 0.3133 | 0.00434 | 0.08834 | 0.00464 | 2022 | 48 | 1881 | 22 | 1757 | 22 | 1711 | 86 | 2022 | 48 | 342.61 | 625.16 |
| MVG458-K_47 | 0.11767 | 0.00332 | 6.18711 | 0.1666 | 0.38138 | 0.00608 | 0.10331 | 0.00556 | 1921 | 52 | 2003 | 24 | 2083 | 28 | 1987 | 102 | 1921 | 52 | 35.43 | 159.13 |
| MVG458-K_48 | 0.11751 | 0.00172 | 5.53568 | 0.07944 | 0.34169 | 0.00390 | 0.07382 | 0.00196 | 1919 | 26 | 1906 | 12 | 1895 | 18 | 1440 | 36 | 1919 | 26 | 55.12 | 408.15 |
| MVG458-K_49 | 0.12147 | 0.00230 | 5.61372 | 0.10352 | 0.3352 | 0.00426 | 0.08745 | 0.00310 | 1978 | 34 | 1918 | 16 | 1864 | 20 | 1695 | 58 | 1978 | 34 | 96.07 | 418.22 |
| MVG458-K_51 | 0.16511 | 0.00288 | 9.91447 | 0.16842 | 0.43555 | 0.00528 | 0.12265 | 0.00386 | 2509 | 30 | 2427 | 16 | 2331 | 24 | 2338 | 70 | 2509 | 30 | 511.48 | 405.75 |
| MVG458-K_52 | 0.16885 | 0.00280 | 9.87479 | 0.15966 | 0.42418 | 0.00500 | 0.1089 | 0.00324 | 2546 | 28 | 2423 | 14 | 2279 | 22 | 2089 | 60 | 2546 | 28 | 254.25 | 381.19 |
| MVG458-K_53 | 0.12202 | 0.00368 | 5.80833 | 0.15732 | 0.34523 | 0.00464 | 0.09879 | 0.00138 | 1986 | 56 | 1948 | 24 | 1912 | 22 | 1904 | 26 | 1986 | 56 | 96.98 | 163.30 |
| MVG458-K_54 | 0.1136 | 0.00190 | 5.19318 | 0.08430 | 0.33157 | 0.00396 | 0.09121 | 0.00258 | 1858 | 30 | 1851 | 14 | 1846 | 20 | 1764 | 48 | 1858 | 30 | 145.46 | 241.48 |
| MVG458-K_55 | 0.16644 | 0.00356 | 9.826 | 0.20150 | 0.42825 | 0.00560 | 0.11616 | 0.00472 | 2522 | 36 | 2419 | 18 | 2298 | 26 | 2221 | 86 | 2522 | 36 | 126.82 | 284.95 |
| MVG458-K_56 | 0.11884 | 0.00204 | 5.66709 | 0.09442 | 0.34586 | 0.00412 | 0.097 | 0.00300 | 1939 | 32 | 1926 | 14 | 1915 | 20 | 1871 | 56 | 1939 | 32 | 238.91 | 454.89 |
| MVG458-K_57 | 0.11596 | 0.00228 | 5.83082 | 0.11084 | 0.3647 | 0.00462 | 0.09934 | 0.00366 | 1895 | 36 | 1951 | 16 | 2004 | 22 | 1914 | 68 | 1895 | 36 | 93.28 | 337.81 |
| MVG458-K_58 | 0.12058 | 0.00298 | 5.52426 | 0.11722 | 0.33227 | 0.00420 | 0.09519 | 0.00136 | 1965 | 46 | 1904 | 18 | 1849 | 20 | 1838 | 26 | 1965 | 46 | 126.65 | 687.56 |
| MVG458-K_59 | 0.12069 | 0.00366 | 5.3596 | 0.15420 | 0.32209 | 0.00490 | 0.09314 | 0.00560 | 1966 | 56 | 1878 | 24 | 1800 | 24 | 1800 | 104 | 1966 | 56 | 394.64 | 749.01 |
| ~~MVG458-K_32~~ | ~~0.12039~~ | ~~0.00370~~ | ~~3.35395~~ | ~~0.09420~~ | ~~0.20205~~ | ~~0.00254~~ | ~~0.05789~~ | ~~0.00074~~ | ~~1962~~ | ~~56~~ | ~~1494~~ | ~~22~~ | ~~1186~~ | ~~14~~ | ~~1138~~ | ~~14~~ | ~~1962~~ | ~~56~~ | ~~898.21~~ | ~~1085.33~~ |
| ~~MVG458-K_36~~ | ~~0.09931~~ | ~~0.00354~~ | ~~1.73441~~ | ~~0.05772~~ | ~~0.12666~~ | ~~0.00164~~ | ~~0.03702~~ | ~~0.00076~~ | ~~1611~~ | ~~68~~ | ~~1021~~ | ~~22~~ | ~~769~~ | ~~10~~ | ~~735~~ | ~~16~~ | ~~1611~~ | ~~68~~ | ~~254.33~~ | ~~851.50~~ |
| ~~MVG458-K_44~~ | ~~0.11612~~ | ~~0.00218~~ | ~~3.16295~~ | ~~0.05786~~ | ~~0.19757~~ | ~~0.00240~~ | ~~0.04785~~ | ~~0.00172~~ | ~~1897~~ | ~~34~~ | ~~1448~~ | ~~14~~ | ~~1162~~ | ~~12~~ | ~~945~~ | ~~34~~ | ~~1897~~ | ~~34~~ | ~~256.41~~ | ~~991.88~~ |
| **Daldyn field, Udachnaya pipe** | | | | | | | | | | | | | | | | | | | | |
| OCYB-2_10 | 0.11283 | 0.00276 | 5.16808 | 0.12924 | 0.33222 | 0.00724 | 0.09767 | 0.00294 | 1845 | 46 | 1847 | 22 | 1849 | 36 | 1884 | 54 | 1845 | 46 | 108.66 | 118.31 |
| OCYB-2_17 | 0.11247 | 0.00382 | 5.02027 | 0.17308 | 0.32376 | 0.00814 | 0.08749 | 0.00448 | 1840 | 62 | 1823 | 30 | 1808 | 40 | 1695 | 84 | 1840 | 62 | 115.37 | 175.06 |
| OCYB-2_2 | 0.11229 | 0.0028 | 4.98038 | 0.12638 | 0.32169 | 0.00698 | 0.09581 | 0.00324 | 1837 | 46 | 1816 | 22 | 1798 | 34 | 1849 | 60 | 1837 | 46 | 149.06 | 282.77 |
| OCYB-2_20 | 0.11169 | 0.0027 | 5.00955 | 0.1244 | 0.32531 | 0.0071 | 0.09715 | 0.00304 | 1827 | 44 | 1821 | 22 | 1816 | 34 | 1874 | 56 | 1827 | 44 | 201.02 | 344.33 |
| OCYB-2_24 | 0.11333 | 0.00298 | 5.08292 | 0.13518 | 0.3253 | 0.00712 | 0.09751 | 0.0037 | 1853 | 48 | 1833 | 22 | 1816 | 34 | 1881 | 68 | 1853 | 48 | 455.89 | 492.90 |
| OCYB-2_26 | 0.11262 | 0.00272 | 5.09768 | 0.1247 | 0.32831 | 0.00702 | 0.09745 | 0.00304 | 1842 | 44 | 1836 | 20 | 1830 | 34 | 1880 | 56 | 1842 | 44 | 115.21 | 214.68 |
| OCYB-2_3 | 0.11325 | 0.00288 | 5.13855 | 0.13194 | 0.32907 | 0.00718 | 0.10328 | 0.00346 | 1852 | 48 | 1843 | 22 | 1834 | 34 | 1987 | 64 | 1852 | 48 | 88.48 | 174.14 |
| OCYB-2_33 | 0.11246 | 0.0039 | 4.92463 | 0.16904 | 0.31761 | 0.00758 | 0.09239 | 0.00532 | 1840 | 64 | 1806 | 28 | 1778 | 38 | 1786 | 98 | 1840 | 64 | 197.99 | 295.43 |
| OCYB-2_4 | 0.11439 | 0.00286 | 5.23768 | 0.13136 | 0.33211 | 0.00716 | 0.09786 | 0.00292 | 1870 | 46 | 1859 | 22 | 1849 | 34 | 1887 | 54 | 1870 | 46 | 97.24 | 86.81 |
| OCYB-2_6 | 0.11281 | 0.00276 | 5.02432 | 0.12442 | 0.32305 | 0.00692 | 0.09588 | 0.0031 | 1845 | 46 | 1823 | 20 | 1805 | 34 | 1851 | 58 | 1845 | 46 | 132.12 | 254.79 |
| OCYB-2_7 | 0.11246 | 0.00288 | 5.03927 | 0.13176 | 0.32501 | 0.0072 | 0.09696 | 0.00342 | 1840 | 48 | 1826 | 22 | 1814 | 36 | 1870 | 64 | 1840 | 48 | 203.14 | 350.00 |
| OCYB-2_9 | 0.1122 | 0.00258 | 5.05699 | 0.11912 | 0.32689 | 0.00698 | 0.09732 | 0.0027 | 1835 | 42 | 1829 | 20 | 1823 | 34 | 1877 | 50 | 1835 | 42 | 223.38 | 339.49 |
| OCYB-2-11 | 0.11326 | 0.0033 | 5.17562 | 0.14978 | 0.33144 | 0.00738 | 0.09705 | 0.0043 | 1852 | 54 | 1849 | 24 | 1845 | 36 | 1872 | 80 | 1852 | 54 | 151.13 | 255.29 |
| OCYB-2-12 | 0.11124 | 0.00356 | 4.92318 | 0.15568 | 0.32102 | 0.0074 | 0.09075 | 0.00452 | 1820 | 60 | 1806 | 26 | 1795 | 36 | 1756 | 84 | 1820 | 60 | 118.47 | 212.18 |
| OCYB-2-13 | 0.11316 | 0.00482 | 5.15402 | 0.2104 | 0.33037 | 0.00806 | 0.09632 | 0.0071 | 1851 | 78 | 1845 | 34 | 1840 | 40 | 1859 | 130 | 1851 | 78 | 130.73 | 216.37 |
| OCYB-2-15 | 0.11292 | 0.00338 | 5.20191 | 0.15408 | 0.33414 | 0.00746 | 0.09657 | 0.00452 | 1847 | 56 | 1853 | 26 | 1858 | 36 | 1863 | 84 | 1847 | 56 | 166.38 | 294.96 |
| OCYB-2-18 | 0.11253 | 0.004 | 5.10835 | 0.1787 | 0.32931 | 0.00786 | 0.09375 | 0.00538 | 1841 | 66 | 1837 | 30 | 1835 | 38 | 1811 | 100 | 1841 | 66 | 118.29 | 178.64 |
| OCYB-2-19 | 0.11302 | 0.00382 | 5.19209 | 0.17262 | 0.33322 | 0.0077 | 0.09499 | 0.00536 | 1849 | 62 | 1851 | 28 | 1854 | 38 | 1834 | 98 | 1849 | 62 | 237.55 | 384.09 |
| OCYB-2-22 | 0.1147 | 0.00376 | 5.30478 | 0.1712 | 0.33546 | 0.00768 | 0.09886 | 0.0053 | 1875 | 60 | 1870 | 28 | 1865 | 38 | 1905 | 98 | 1875 | 60 | 146.25 | 265.28 |
| OCYB-2-23 | 0.11451 | 0.00376 | 5.30737 | 0.17142 | 0.33616 | 0.00768 | 0.09765 | 0.00522 | 1872 | 60 | 1870 | 28 | 1868 | 38 | 1883 | 96 | 1872 | 60 | 107.74 | 198.68 |
| OCYB-2-25 | 0.11284 | 0.0041 | 5.17414 | 0.18502 | 0.3326 | 0.00806 | 0.09177 | 0.0054 | 1846 | 68 | 1848 | 30 | 1851 | 38 | 1775 | 100 | 1846 | 68 | 95.88 | 145.47 |
| OCYB-2-27 | 0.11249 | 0.0042 | 5.11014 | 0.1869 | 0.3295 | 0.00792 | 0.09592 | 0.00608 | 1840 | 70 | 1838 | 32 | 1836 | 38 | 1851 | 112 | 1840 | 70 | 114.41 | 202.51 |
| OCYB-2-28 | 0.11216 | 0.00526 | 5.09936 | 0.2321 | 0.32982 | 0.00876 | 0.09541 | 0.00794 | 1835 | 86 | 1836 | 38 | 1838 | 42 | 1842 | 146 | 1835 | 86 | 172.93 | 190.56 |
| OCYB-2-29 | 0.11302 | 0.00446 | 5.09786 | 0.19768 | 0.32719 | 0.00808 | 0.09392 | 0.00658 | 1849 | 74 | 1836 | 32 | 1825 | 40 | 1814 | 122 | 1849 | 74 | 245.26 | 394.93 |

| Analysis No. | RATIOS | | | | | | | | AGES (Ma) | | | | | | | | | | CONCENTRATIONS (ppm) | |
|---|---|---|---|---|---|---|---|---|---|---|---|---|---|---|---|---|---|---|---|---|
| | $^{207}Pb/^{206}Pb$ | ± 2σ | $^{207}Pb/^{235}U$ | ± 2σ | $^{206}Pb/^{238}U$ | ± 2σ | $^{208}Pb/^{232}Th$ | ± 2σ | $^{207}Pb/^{206}Pb$ | ± 2σ | $^{207}Pb/^{235}U$ | ± 2σ | $^{206}Pb/^{238}U$ | ± 2σ | $^{208}Pb/^{232}Th$ | ± 2σ | Used Age | ± 2σ | Th | U |
| OCYB-2-30 | 0.11267 | 0.00428 | 5.06889 | 0.18836 | 0.32631 | 0.0078 | 0.0939 | 0.00626 | 1843 | 70 | 1831 | 32 | 1820 | 38 | 1814 | 116 | 1843 | 70 | 193.59 | 322.45 |
| OCYB-2-31 | 0.11427 | 0.0048 | 5.12241 | 0.20906 | 0.32515 | 0.00808 | 0.09273 | 0.00684 | 1868 | 78 | 1840 | 34 | 1815 | 40 | 1792 | 126 | 1868 | 78 | 152.06 | 163.93 |
| OCYB-2-32 | 0.116 | 0.005 | 5.32901 | 0.22346 | 0.33323 | 0.00842 | 0.09709 | 0.00748 | 1895 | 80 | 1874 | 36 | 1854 | 40 | 1873 | 138 | 1895 | 80 | 120.99 | 214.23 |
| OCYB-2-8 | 0.1125 | 0.00332 | 5.05369 | 0.1485 | 0.32583 | 0.00732 | 0.09355 | 0.00424 | 1840 | 54 | 1828 | 24 | 1818 | 36 | 1808 | 78 | 1840 | 54 | 200.80 | 321.54 |
| OCYB-5-01 | 0.11485 | 0.0042 | 5.18665 | 0.18436 | 0.32754 | 0.00832 | 0.09842 | 0.0034 | 1878 | 68 | 1850 | 30 | 1826 | 40 | 1897 | 62 | 1878 | 68 | 14.37 | 11.01 |
| OCYB-5-08 | 0.11445 | 0.0049 | 5.20044 | 0.21442 | 0.32956 | 0.00912 | 0.09779 | 0.00366 | 1871 | 80 | 1853 | 36 | 1836 | 44 | 1886 | 68 | 1871 | 80 | 13.65 | 8.94 |
| OCYB5-10 | 0.11097 | 0.00716 | 5.06262 | 0.31078 | 0.33092 | 0.01172 | 0.09833 | 0.00666 | 1815 | 120 | 1830 | 52 | 1843 | 56 | 1896 | 122 | 1815 | 120 | 13.34 | 8.81 |
| OCYB-5-11 | 0.11294 | 0.00336 | 5.11532 | 0.15 | 0.3285 | 0.0076 | 0.09715 | 0.00292 | 1847 | 56 | 1839 | 24 | 1831 | 36 | 1874 | 54 | 1847 | 56 | 21.37 | 17.64 |
| OCYB5-12 | 0.11733 | 0.0057 | 5.43721 | 0.25302 | 0.33619 | 0.00934 | 0.09873 | 0.0072 | 1916 | 90 | 1891 | 40 | 1868 | 46 | 1903 | 132 | 1916 | 90 | 48.37 | 36.81 |
| OCYB-5-13 | 0.11438 | 0.0028 | 5.2236 | 0.13214 | 0.33122 | 0.00728 | 0.09678 | 0.00314 | 1870 | 46 | 1856 | 22 | 1844 | 36 | 1867 | 58 | 1870 | 46 | 815.00 | 452.63 |
| OCYB5-14 | 0.11701 | 0.00674 | 5.3433 | 0.29788 | 0.33128 | 0.0095 | 0.0906 | 0.00938 | 1911 | 106 | 1876 | 48 | 1845 | 46 | 1753 | 174 | 1911 | 106 | 344.47 | 289.90 |
| OCYB-5-14 | 0.11303 | 0.00296 | 5.14331 | 0.13758 | 0.33002 | 0.00742 | 0.10196 | 0.00332 | 1849 | 48 | 1843 | 22 | 1838 | 36 | 1962 | 60 | 1849 | 48 | 50.04 | 76.90 |
| OCYB5-15 | 0.11085 | 0.00514 | 4.96422 | 0.22176 | 0.32482 | 0.0092 | 0.09815 | 0.0052 | 1813 | 86 | 1813 | 38 | 1813 | 44 | 1892 | 96 | 1813 | 86 | 25.81 | 21.06 |
| OCYB5-16 | 0.10596 | 0.00744 | 4.7114 | 0.31494 | 0.3225 | 0.01214 | 0.09983 | 0.00746 | 1731 | 132 | 1769 | 56 | 1802 | 60 | 1923 | 138 | 1731 | 132 | 19.91 | 17.56 |
| OCYB5-18 | 0.11375 | 0.00578 | 5.21168 | 0.25514 | 0.33227 | 0.01002 | 0.09546 | 0.00614 | 1860 | 94 | 1855 | 42 | 1849 | 48 | 1843 | 114 | 1860 | 94 | 29.08 | 27.46 |
| OCYB5-19 | 0.1213 | 0.00472 | 5.65395 | 0.2148 | 0.33801 | 0.00838 | 0.10026 | 0.0062 | 1975 | 70 | 1924 | 32 | 1877 | 40 | 1931 | 114 | 1975 | 70 | 106.86 | 101.87 |
| OCYB5-2 | 0.11196 | 0.00638 | 4.9133 | 0.26546 | 0.3184 | 0.01024 | 0.09909 | 0.0063 | 1831 | 106 | 1805 | 46 | 1782 | 50 | 1910 | 116 | 1831 | 106 | 17.76 | 15.76 |
| OCYB5-20 | 0.11254 | 0.00864 | 5.04071 | 0.36648 | 0.32481 | 0.01304 | 0.09475 | 0.00734 | 1841 | 142 | 1826 | 62 | 1813 | 64 | 1830 | 136 | 1841 | 142 | 14.67 | 9.32 |
| OCYB5-23 | 0.11215 | 0.00698 | 5.1051 | 0.30306 | 0.33016 | 0.01104 | 0.0947 | 0.0075 | 1835 | 116 | 1837 | 50 | 1839 | 54 | 1829 | 138 | 1835 | 116 | 21.65 | 18.31 |
| OCYB-5-25 | 0.11084 | 0.0035 | 5.11012 | 0.15866 | 0.33437 | 0.00792 | 0.09831 | 0.00318 | 1813 | 58 | 1838 | 26 | 1860 | 38 | 1895 | 58 | 1813 | 58 | 23.75 | 14.91 |
| OCYB-5-26 | 0.14118 | 0.00372 | 7.46845 | 0.20064 | 0.38368 | 0.00864 | 0.11049 | 0.00388 | 2242 | 46 | 2169 | 24 | 2093 | 40 | 2118 | 70 | 2242 | 46 | 80.21 | 86.77 |
| OCYB-5-27 | 0.17092 | 0.00426 | 10.85929 | 0.27718 | 0.4608 | 0.01018 | 0.13047 | 0.00438 | 2567 | 42 | 2511 | 24 | 2443 | 44 | 2479 | 78 | 2567 | 42 | 92.32 | 125.15 |
| OCYB5-28 | 0.11699 | 0.00762 | 5.40619 | 0.33466 | 0.33517 | 0.01212 | 0.09639 | 0.00672 | 1911 | 120 | 1886 | 54 | 1863 | 58 | 1860 | 124 | 1911 | 120 | 12.71 | 8.64 |
| OCYB5-29 | 0.1066 | 0.0052 | 4.71759 | 0.22238 | 0.32098 | 0.0092 | 0.09654 | 0.00628 | 1742 | 92 | 1770 | 40 | 1795 | 44 | 1863 | 116 | 1742 | 92 | 25.89 | 23.70 |
| OCYB5-3 | 0.11319 | 0.00506 | 5.219 | 0.22368 | 0.33447 | 0.00922 | 0.09939 | 0.00524 | 1851 | 82 | 1856 | 36 | 1860 | 44 | 1915 | 96 | 1851 | 82 | 31.43 | 22.68 |
| OCYB-5-31 | 0.11299 | 0.00276 | 5.17034 | 0.13062 | 0.33189 | 0.00728 | 0.09658 | 0.00316 | 1848 | 46 | 1848 | 22 | 1848 | 36 | 1863 | 58 | 1848 | 46 | 623.49 | 324.31 |
| OCYB5-34 | 0.11261 | 0.00696 | 4.99956 | 0.29734 | 0.32217 | 0.01076 | 0.08924 | 0.00808 | 1842 | 114 | 1819 | 50 | 1800 | 52 | 1728 | 150 | 1842 | 114 | 45.11 | 47.96 |
| OCYB-5-35 | 0.11182 | 0.0041 | 5.12873 | 0.18292 | 0.33266 | 0.00842 | 0.09965 | 0.00362 | 1829 | 68 | 1841 | 30 | 1851 | 40 | 1920 | 66 | 1829 | 68 | 15.07 | 9.32 |
| OCYB5-36 | 0.1143 | 0.00766 | 5.33849 | 0.3403 | 0.33874 | 0.01242 | 0.10035 | 0.00748 | 1869 | 124 | 1875 | 54 | 1881 | 60 | 1933 | 138 | 1869 | 124 | 11.31 | 8.14 |
| OCYB5-37 | 0.11039 | 0.0081 | 4.96007 | 0.34636 | 0.3259 | 0.01266 | 0.09688 | 0.00792 | 1806 | 136 | 1813 | 60 | 1818 | 62 | 1869 | 146 | 1806 | 136 | 15.09 | 9.47 |
| OCYB-5-38 | 0.14063 | 0.00378 | 7.40231 | 0.20256 | 0.38175 | 0.00856 | 0.10857 | 0.00422 | 2235 | 48 | 2161 | 24 | 2084 | 40 | 2083 | 76 | 2235 | 48 | 161.87 | 134.69 |
| OCYB5-39 | 0.11488 | 0.0054 | 5.30916 | 0.2405 | 0.33519 | 0.00978 | 0.0981 | 0.00476 | 1878 | 86 | 1870 | 38 | 1863 | 48 | 1891 | 88 | 1878 | 86 | 26.22 | 18.69 |
| OCYB5-4 | 0.11228 | 0.00414 | 5.06302 | 0.18092 | 0.32714 | 0.00786 | 0.09903 | 0.00562 | 1837 | 68 | 1830 | 30 | 1825 | 38 | 1909 | 104 | 1837 | 68 | 74.70 | 88.36 |
| OCYB5-40 | 0.11484 | 0.00516 | 5.37059 | 0.23604 | 0.33932 | 0.00956 | 0.0964 | 0.00622 | 1877 | 82 | 1880 | 38 | 1883 | 46 | 1860 | 114 | 1877 | 82 | 173.84 | 122.63 |
| OCYB-5-41 | 0.11247 | 0.00282 | 5.06572 | 0.13004 | 0.32667 | 0.00718 | 0.09541 | 0.00326 | 1840 | 46 | 1830 | 22 | 1822 | 34 | 1842 | 60 | 1840 | 46 | 249.38 | 192.10 |
| OCYB5-42 | 0.11494 | 0.0035 | 5.25516 | 0.16076 | 0.33162 | 0.00774 | 0.09488 | 0.00428 | 1879 | 56 | 1862 | 26 | 1846 | 38 | 1832 | 80 | 1879 | 56 | 289.84 | 199.05 |
| OCYB5-44 | 0.11301 | 0.00636 | 5.11992 | 0.27494 | 0.3286 | 0.01078 | 0.09588 | 0.00528 | 1848 | 104 | 1839 | 46 | 1832 | 52 | 1851 | 98 | 1848 | 104 | 15.15 | 11.66 |
| OCYB-5-45 | 0.11884 | 0.0031 | 5.74594 | 0.15152 | 0.35068 | 0.00766 | 0.10374 | 0.0039 | 1939 | 48 | 1938 | 22 | 1938 | 36 | 1995 | 72 | 1939 | 48 | 178.41 | 149.61 |
| OCYB5-46 | 0.10924 | 0.00586 | 4.90267 | 0.25142 | 0.3255 | 0.00996 | 0.09331 | 0.00596 | 1787 | 100 | 1803 | 44 | 1817 | 48 | 1803 | 110 | 1787 | 100 | 27.85 | 24.60 |
| OCYB5-48 | 0.11217 | 0.00564 | 5.0398 | 0.24276 | 0.32588 | 0.00986 | 0.09681 | 0.00528 | 1835 | 94 | 1826 | 40 | 1818 | 48 | 1868 | 98 | 1835 | 94 | 19.23 | 16.73 |
| OCYB5-49 | 0.1102 | 0.00556 | 4.9311 | 0.23858 | 0.32455 | 0.00978 | 0.09726 | 0.00534 | 1803 | 94 | 1808 | 40 | 1812 | 48 | 1876 | 98 | 1803 | 94 | 20.09 | 17.09 |
| OCYB5-5 | 0.1139 | 0.00726 | 5.3269 | 0.32258 | 0.33923 | 0.01136 | 0.0994 | 0.00872 | 1863 | 118 | 1873 | 52 | 1883 | 54 | 1915 | 160 | 1863 | 118 | 51.40 | 28.06 |
| OCYB5-50 | 0.11417 | 0.0057 | 5.13098 | 0.24706 | 0.32597 | 0.00976 | 0.09649 | 0.00624 | 1867 | 92 | 1841 | 40 | 1819 | 48 | 1862 | 116 | 1867 | 92 | 43.07 | 40.59 |
| OCYB5-51 | 0.11346 | 0.01028 | 5.07418 | 0.4336 | 0.32436 | 0.01514 | 0.09702 | 0.00812 | 1856 | 168 | 1832 | 72 | 1811 | 74 | 1872 | 150 | 1856 | 168 | 11.07 | 7.16 |

| Analysis No. | RATIOS | | | | | | | | AGES (Ma) | | | | | | | | | | CONCENTRATIONS (ppm) | |
|---|---|---|---|---|---|---|---|---|---|---|---|---|---|---|---|---|---|---|---|---|
| | $^{207}Pb/^{206}Pb$ | ± 2σ | $^{207}Pb/^{235}U$ | ± 2σ | $^{206}Pb/^{238}U$ | ± 2σ | $^{208}Pb/^{232}Th$ | ± 2σ | $^{207}Pb/^{206}Pb$ | ± 2σ | $^{207}Pb/^{235}U$ | ± 2σ | $^{206}Pb/^{238}U$ | ± 2σ | $^{208}Pb/^{232}Th$ | ± 2σ | Used Age | ± 2σ | Th | U |
| OCYB-5-55 | 0.11942 | 0.0031 | 5.64643 | 0.14858 | 0.34295 | 0.00754 | 0.10015 | 0.00364 | 1948 | 48 | 1923 | 22 | 1901 | 36 | 1929 | 66 | 1948 | 48 | 132.87 | 112.41 |
| OCYB5-56 | 0.12346 | 0.00484 | 6.09341 | 0.2331 | 0.35797 | 0.00938 | 0.10413 | 0.00558 | 2007 | 72 | 1989 | 34 | 1973 | 44 | 2002 | 102 | 2007 | 72 | 40.99 | 36.84 |
| OCYB5-58 | 0.11004 | 0.00684 | 4.99966 | 0.29568 | 0.32953 | 0.01118 | 0.09716 | 0.00676 | 1800 | 116 | 1819 | 50 | 1836 | 54 | 1874 | 124 | 1800 | 116 | 23.34 | 15.14 |
| OCYB5-59 | 0.11223 | 0.0058 | 4.97545 | 0.24632 | 0.32155 | 0.00966 | 0.0976 | 0.00634 | 1836 | 96 | 1815 | 42 | 1797 | 48 | 1882 | 116 | 1836 | 96 | 25.28 | 22.21 |
| OCYB5-6 | 0.11595 | 0.00714 | 5.3975 | 0.31576 | 0.33765 | 0.0117 | 0.10486 | 0.0063 | 1895 | 114 | 1884 | 50 | 1875 | 56 | 2016 | 116 | 1895 | 114 | 13.59 | 8.42 |
| OCYB5-60 | 0.11196 | 0.0055 | 4.91919 | 0.23304 | 0.31868 | 0.00928 | 0.09812 | 0.00618 | 1831 | 92 | 1806 | 40 | 1783 | 46 | 1892 | 114 | 1831 | 92 | 78.91 | 32.29 |
| OCYB5-61 | 0.11254 | 0.0075 | 5.08017 | 0.32182 | 0.32743 | 0.01202 | 0.1008 | 0.00686 | 1841 | 124 | 1833 | 54 | 1826 | 58 | 1941 | 126 | 1841 | 124 | 12.23 | 9.08 |
| OCYB5-62 | 0.11735 | 0.00602 | 5.34087 | 0.26298 | 0.33011 | 0.0099 | 0.09759 | 0.00658 | 1916 | 94 | 1875 | 42 | 1839 | 48 | 1882 | 122 | 1916 | 94 | 24.27 | 20.82 |
| OCYB5-63 | 0.11394 | 0.00622 | 5.3959 | 0.2824 | 0.34348 | 0.01082 | 0.10113 | 0.00654 | 1863 | 100 | 1884 | 44 | 1903 | 52 | 1947 | 120 | 1863 | 100 | 24.16 | 14.61 |
| OCYB5-64 | 0.11406 | 0.00784 | 5.1036 | 0.3328 | 0.32454 | 0.01206 | 0.09967 | 0.00738 | 1865 | 128 | 1837 | 56 | 1812 | 58 | 1920 | 136 | 1865 | 128 | 13.04 | 8.91 |
| OCYB5-65 | 0.11302 | 0.00634 | 5.16799 | 0.27756 | 0.33166 | 0.01054 | 0.09791 | 0.00688 | 1849 | 104 | 1847 | 46 | 1846 | 52 | 1888 | 126 | 1849 | 104 | 27.35 | 17.29 |
| OCYB5-7 | 0.11275 | 0.0051 | 5.15647 | 0.22452 | 0.33171 | 0.0092 | 0.10073 | 0.00576 | 1844 | 84 | 1845 | 38 | 1847 | 44 | 1940 | 106 | 1844 | 84 | 25.03 | 22.14 |
| OCYB5-9 | 0.10866 | 0.00854 | 4.85137 | 0.36142 | 0.32395 | 0.0133 | 0.09613 | 0.00764 | 1777 | 146 | 1794 | 62 | 1809 | 64 | 1855 | 140 | 1777 | 146 | 11.37 | 8.22 |
| ~~OCYB-2-16~~ | ~~0.12354~~ | ~~0.00694~~ | ~~3.20383~~ | ~~0.16956~~ | ~~0.18812~~ | ~~0.00598~~ | ~~0.06062~~ | ~~0.0034~~ | ~~2008~~ | ~~102~~ | ~~1458~~ | ~~40~~ | ~~1111~~ | ~~32~~ | ~~1190~~ | ~~64~~ | ~~2008~~ | ~~102~~ | ~~95.55~~ | ~~26.95~~ |
| **Alakhit-Markha field, Kismet pipe** | | | | | | | | | | | | | | | | | | | | |
| MVG459_Kis-01 | 0.11761 | 0.00324 | 5.5 | 0.14682 | 0.33919 | 0.00494 | 0.10059 | 0.00526 | 1920 | 50 | 1901 | 22 | 1883 | 24 | 1937 | 96 | 1920 | 50 | 82.05 | 259.55 |
| MVG459_Kis-02 | 0.1165 | 0.00468 | 5.37428 | 0.20468 | 0.3346 | 0.00682 | 0.09757 | 0.00558 | 1903 | 74 | 1881 | 32 | 1861 | 32 | 1882 | 102 | 1903 | 74 | 35.29 | 41.89 |
| MVG459_Kis-03 | 0.11504 | 0.00472 | 5.39854 | 0.2111 | 0.34055 | 0.0067 | 0.09646 | 0.0068 | 1881 | 76 | 1885 | 34 | 1889 | 32 | 1861 | 126 | 1881 | 76 | 47.07 | 84.96 |
| MVG459_Kis-04 | 0.11709 | 0.0032 | 5.60767 | 0.14832 | 0.34738 | 0.0049 | 0.10327 | 0.00572 | 1912 | 50 | 1917 | 22 | 1922 | 24 | 1986 | 104 | 1912 | 50 | 94.63 | 634.73 |
| MVG459_Kis-05 | 0.1126 | 0.00482 | 5.45554 | 0.222 | 0.35143 | 0.00748 | 0.10293 | 0.00638 | 1842 | 80 | 1894 | 34 | 1941 | 36 | 1980 | 116 | 1842 | 80 | 28.00 | 35.96 |
| MVG459_Kis-06 | 0.1183 | 0.00366 | 5.69621 | 0.16942 | 0.34923 | 0.00544 | 0.10401 | 0.006 | 1931 | 56 | 1931 | 26 | 1931 | 26 | 2000 | 110 | 1931 | 56 | 132.25 | 189.83 |
| MVG459_Kis-07 | 0.11525 | 0.00376 | 5.39068 | 0.16854 | 0.33924 | 0.0055 | 0.09804 | 0.00584 | 1884 | 60 | 1883 | 26 | 1883 | 26 | 1890 | 108 | 1884 | 60 | 117.54 | 150.55 |
| MVG459_Kis-08 | 0.12125 | 0.00676 | 5.97739 | 0.31848 | 0.35765 | 0.00894 | 0.08782 | 0.00904 | 1975 | 102 | 1973 | 46 | 1971 | 42 | 1701 | 168 | 1975 | 102 | 57.71 | 118.94 |
| MVG459_Kis-09 | 0.11582 | 0.00396 | 5.3876 | 0.1766 | 0.33739 | 0.00564 | 0.09762 | 0.00616 | 1893 | 62 | 1883 | 28 | 1874 | 28 | 1883 | 114 | 1893 | 62 | 111.19 | 137.85 |
| MVG459_Kis-10 | 0.1148 | 0.00432 | 5.47902 | 0.19726 | 0.34616 | 0.00632 | 0.09958 | 0.00674 | 1877 | 70 | 1897 | 30 | 1916 | 30 | 1919 | 124 | 1877 | 70 | 47.56 | 82.24 |
| MVG459_Kis-12 | 0.11198 | 0.00544 | 5.38175 | 0.24786 | 0.34858 | 0.00818 | 0.10494 | 0.00876 | 1832 | 90 | 1882 | 40 | 1928 | 40 | 2017 | 160 | 1832 | 90 | 9.55 | 29.71 |
| MVG459_Kis-13 | 0.11696 | 0.004 | 5.51862 | 0.1821 | 0.34222 | 0.00558 | 0.10137 | 0.00686 | 1910 | 62 | 1904 | 28 | 1897 | 26 | 1952 | 126 | 1910 | 62 | 195.85 | 230.78 |
| MVG459_Kis-14 | 0.11623 | 0.00414 | 5.69812 | 0.1951 | 0.35558 | 0.00574 | 0.10393 | 0.00768 | 1899 | 66 | 1931 | 30 | 1961 | 28 | 1999 | 140 | 1899 | 66 | 395.57 | 814.79 |
| MVG459_Kis-15 | 0.11437 | 0.00622 | 5.30443 | 0.27318 | 0.33648 | 0.00804 | 0.09593 | 0.00946 | 1870 | 100 | 1870 | 44 | 1870 | 38 | 1852 | 174 | 1870 | 100 | 59.92 | 74.28 |
| MVG459_Kis-16 | 0.11718 | 0.00666 | 5.44152 | 0.2967 | 0.33715 | 0.00774 | 0.10027 | 0.01144 | 1914 | 104 | 1891 | 46 | 1873 | 38 | 1931 | 210 | 1914 | 104 | 238.20 | 355.58 |
| MVG459_Kis-17 | 0.11479 | 0.0045 | 5.46671 | 0.20548 | 0.34541 | 0.00618 | 0.10202 | 0.00794 | 1877 | 72 | 1895 | 32 | 1913 | 30 | 1964 | 146 | 1877 | 72 | 103.60 | 154.26 |
| MVG459_Kis-19 | 0.1124 | 0.00314 | 5.22903 | 0.14098 | 0.3374 | 0.005 | 0.0986 | 0.00508 | 1839 | 52 | 1857 | 22 | 1874 | 24 | 1901 | 94 | 1839 | 52 | 182.64 | 226.15 |
| MVG459_Kis-20 | 0.11882 | 0.00348 | 5.66331 | 0.1601 | 0.34567 | 0.00524 | 0.10137 | 0.0056 | 1939 | 54 | 1926 | 24 | 1914 | 26 | 1952 | 102 | 1939 | 54 | 233.16 | 239.73 |
| MVG459_Kis-21 | 0.11434 | 0.00376 | 5.46059 | 0.17198 | 0.34637 | 0.00592 | 0.10263 | 0.00576 | 1870 | 60 | 1894 | 28 | 1917 | 28 | 1975 | 106 | 1870 | 60 | 53.29 | 88.64 |
| MVG459_Kis-22 | 0.1161 | 0.0035 | 5.51529 | 0.16044 | 0.34452 | 0.00542 | 0.10287 | 0.00562 | 1897 | 56 | 1903 | 26 | 1908 | 26 | 1979 | 102 | 1897 | 56 | 137.38 | 155.14 |
| MVG459_Kis-23 | 0.12067 | 0.00604 | 5.57809 | 0.26066 | 0.33525 | 0.00602 | 0.09604 | 0.00188 | 1966 | 92 | 1913 | 40 | 1864 | 30 | 1854 | 34 | 1966 | 92 | 264.42 | 876.40 |
| MVG459_Kis-24 | 0.11778 | 0.00396 | 5.57773 | 0.18064 | 0.34345 | 0.00572 | 0.10258 | 0.00648 | 1923 | 62 | 1913 | 28 | 1903 | 28 | 1974 | 118 | 1923 | 62 | 161.82 | 200.51 |
| MVG459_Kis-25 | 0.12753 | 0.00782 | 5.56372 | 0.32404 | 0.31643 | 0.00822 | 0.08768 | 0.00998 | 2064 | 110 | 1911 | 50 | 1772 | 40 | 1699 | 186 | 2064 | 110 | 184.15 | 281.43 |
| MVG459_Kis-26 | 0.11303 | 0.00428 | 5.38007 | 0.19468 | 0.34521 | 0.00654 | 0.10304 | 0.00642 | 1849 | 70 | 1882 | 30 | 1912 | 32 | 1982 | 118 | 1849 | 70 | 49.90 | 61.80 |
| MVG459_Kis-27 | 0.11734 | 0.00344 | 5.7497 | 0.16352 | 0.35538 | 0.00522 | 0.10266 | 0.00636 | 1916 | 54 | 1939 | 24 | 1960 | 24 | 1975 | 116 | 1916 | 54 | 87.68 | 770.76 |
| MVG459_Kis-28 | 0.11299 | 0.00496 | 5.43278 | 0.22658 | 0.34871 | 0.00756 | 0.10299 | 0.00696 | 1848 | 82 | 1890 | 36 | 1928 | 36 | 1981 | 128 | 1848 | 82 | 30.51 | 37.78 |
| MVG459_Kis-29 | 0.11759 | 0.00536 | 5.41335 | 0.23578 | 0.33401 | 0.00666 | 0.10115 | 0.00956 | 1920 | 84 | 1887 | 38 | 1858 | 32 | 1948 | 176 | 1920 | 84 | 71.06 | 343.53 |
| MVG459_Kis-30 | 0.11247 | 0.00434 | 5.40995 | 0.20008 | 0.34886 | 0.00658 | 0.10011 | 0.00682 | 1840 | 72 | 1886 | 32 | 1929 | 32 | 1928 | 126 | 1840 | 72 | 54.34 | 73.08 |
| MVG459_Kis-31 | 0.11885 | 0.00878 | 5.12602 | 0.36062 | 0.31284 | 0.00864 | 0.08748 | 0.01326 | 1939 | 136 | 1840 | 60 | 1755 | 42 | 1695 | 246 | 1939 | 136 | 424.95 | 2336.90 |

| Analysis No. | RATIOS | | | | | | | | AGES (Ma) | | | | | | | | | | CONCENTRATIONS (ppm) | |
|---|---|---|---|---|---|---|---|---|---|---|---|---|---|---|---|---|---|---|---|---|
| | $^{207}Pb/^{206}Pb$ | ± 2σ | $^{207}Pb/^{235}U$ | ± 2σ | $^{206}Pb/^{238}U$ | ± 2σ | $^{208}Pb/^{232}Th$ | ± 2σ | $^{207}Pb/^{206}Pb$ | ± 2σ | $^{207}Pb/^{235}U$ | ± 2σ | $^{206}Pb/^{238}U$ | ± 2σ | $^{208}Pb/^{232}Th$ | ± 2σ | Used Age | ± 2σ | Th | U |
| MVG459_Kis-32 | 0.11644 | 0.00402 | 5.61612 | 0.187 | 0.34982 | 0.00576 | 0.10283 | 0.0071 | 1902 | 64 | 1919 | 28 | 1934 | 28 | 1978 | 130 | 1902 | 64 | 218.76 | 258.66 |
| MVG459_Kis-33 | 0.10803 | 0.0043 | 4.73394 | 0.18072 | 0.31782 | 0.00598 | 0.17213 | 0.06208 | 1766 | 74 | 1773 | 32 | 1779 | 30 | 3210 | 1070 | 1766 | 74 | 0.26 | 90.70 |
| MVG459_Kis-35 | 0.11638 | 0.00484 | 5.52738 | 0.21992 | 0.34446 | 0.00674 | 0.10305 | 0.00834 | 1901 | 76 | 1905 | 34 | 1908 | 32 | 1982 | 152 | 1901 | 76 | 22.62 | 76.14 |
| MVG459_Kis-36 | 0.11238 | 0.00462 | 5.33645 | 0.21042 | 0.34442 | 0.00658 | 0.09916 | 0.00776 | 1838 | 76 | 1875 | 34 | 1908 | 32 | 1911 | 142 | 1838 | 76 | 67.16 | 96.13 |
| MVG459_Kis-37 | 0.11454 | 0.00446 | 5.33953 | 0.20022 | 0.33812 | 0.00598 | 0.10311 | 0.00828 | 1873 | 72 | 1875 | 32 | 1878 | 28 | 1983 | 152 | 1873 | 72 | 94.79 | 257.35 |
| ~~MVG459_Kis-34~~ | ~~0.11567~~ | ~~0.01084~~ | ~~3.1572~~ | ~~0.28712~~ | ~~0.19795~~ | ~~0.00454~~ | ~~0.05695~~ | ~~0.00272~~ | ~~1890~~ | ~~172~~ | ~~1447~~ | ~~70~~ | ~~1164~~ | ~~24~~ | ~~1120~~ | ~~52~~ | ~~1890~~ | ~~172~~ | ~~410.19~~ | ~~2092.54~~ |
| **Alakhit-Markha field, Geochemical pipe** | | | | | | | | | | | | | | | | | | | | |
| MVG459_Gch-01 | 0.11844 | 0.00382 | 5.64131 | 0.17532 | 0.34551 | 0.00534 | 0.09802 | 0.00608 | 1933 | 60 | 1922 | 26 | 1913 | 26 | 1890 | 112 | 1933 | 60 | 415.80 | 648.57 |
| MVG459_Gch-02 | 0.11844 | 0.00394 | 5.81331 | 0.185 | 0.35611 | 0.00548 | 0.10614 | 0.00714 | 1933 | 60 | 1948 | 28 | 1964 | 26 | 2039 | 130 | 1933 | 60 | 70.17 | 662.49 |
| MVG459_Gch-03 | 0.11409 | 0.0042 | 5.09469 | 0.17912 | 0.324 | 0.00548 | 0.09168 | 0.0063 | 1866 | 68 | 1835 | 30 | 1809 | 26 | 1773 | 116 | 1866 | 68 | 145.85 | 196.27 |
| MVG459_Gch-04 | 0.11739 | 0.0043 | 5.45801 | 0.19126 | 0.33735 | 0.00558 | 0.09921 | 0.00696 | 1917 | 68 | 1894 | 30 | 1874 | 26 | 1912 | 128 | 1917 | 68 | 278.99 | 316.82 |
| MVG459_Gch-05 | 0.12255 | 0.00448 | 4.61038 | 0.16114 | 0.27295 | 0.00442 | 0.06469 | 0.00458 | 1994 | 66 | 1751 | 30 | 1556 | 22 | 1267 | 86 | 1994 | 66 | 583.37 | 916.78 |
| MVG459_Gch-06 | 0.11852 | 0.00538 | 5.75959 | 0.2479 | 0.35249 | 0.00664 | 0.09914 | 0.00854 | 1934 | 84 | 1940 | 38 | 1946 | 32 | 1911 | 158 | 1934 | 84 | 253.50 | 288.15 |
| **Alakhit-Markha field, Vostok pipe** | | | | | | | | | | | | | | | | | | | | |
| MVG459_Vos-01 | 0.14068 | 0.00806 | 7.28625 | 0.39748 | 0.37567 | 0.00852 | 0.10806 | 0.01234 | 2236 | 102 | 2147 | 48 | 2056 | 40 | 2074 | 226 | 2236 | 102 | 390.20 | 1029.48 |
| MVG459_Vos-02 | 0.11841 | 0.00448 | 5.57724 | 0.20166 | 0.34165 | 0.00572 | 0.10087 | 0.00766 | 1932 | 70 | 1913 | 32 | 1895 | 28 | 1942 | 140 | 1932 | 70 | 107.07 | 314.78 |
| MVG459_Vos-04 | 0.11704 | 0.00324 | 5.55318 | 0.14880 | 0.34415 | 0.00504 | 0.1018 | 0.00516 | 1912 | 50 | 1909 | 24 | 1907 | 24 | 1959 | 94 | 1912 | 50 | 180.70 | 225.39 |
| MVG459_Vos-05 | 0.12073 | 0.00346 | 5.88153 | 0.16380 | 0.35335 | 0.00512 | 0.10902 | 0.00710 | 1967 | 52 | 1959 | 24 | 1951 | 24 | 2091 | 130 | 1967 | 52 | 26.08 | 922.95 |
| MVG459_Vos-06 | 0.12008 | 0.00638 | 5.70119 | 0.28688 | 0.34437 | 0.00816 | 0.10427 | 0.01000 | 1957 | 98 | 1932 | 44 | 1908 | 40 | 2005 | 184 | 1957 | 98 | 112.12 | 158.26 |
| MVG459_Vos-07 | 0.11627 | 0.00354 | 5.56289 | 0.16332 | 0.34703 | 0.00534 | 0.10378 | 0.00594 | 1900 | 56 | 1910 | 26 | 1920 | 26 | 1996 | 108 | 1900 | 56 | 106.07 | 191.25 |
| MVG459_Vos-08 | 0.11637 | 0.00460 | 5.56117 | 0.21128 | 0.34661 | 0.00636 | 0.10326 | 0.00764 | 1901 | 72 | 1910 | 32 | 1918 | 30 | 1986 | 140 | 1901 | 72 | 77.89 | 133.31 |
| MVG459_Vos-09 | 0.1177 | 0.00362 | 5.58544 | 0.16584 | 0.34421 | 0.00524 | 0.10275 | 0.00614 | 1922 | 56 | 1914 | 26 | 1907 | 26 | 1977 | 112 | 1922 | 56 | 243.15 | 301.46 |
| MVG459_Vos-10 | 0.11771 | 0.00376 | 5.57717 | 0.17176 | 0.34366 | 0.00534 | 0.10166 | 0.00634 | 1922 | 58 | 1913 | 26 | 1904 | 26 | 1957 | 116 | 1922 | 58 | 237.00 | 286.60 |
| MVG459_Vos-11 | 0.14147 | 0.00548 | 8.27077 | 0.30782 | 0.42405 | 0.00748 | 0.12384 | 0.00976 | 2245 | 68 | 2261 | 34 | 2279 | 34 | 2360 | 176 | 2245 | 68 | 148.35 | 304.34 |
| MVG459_Vos-12 | 0.11853 | 0.00430 | 5.60869 | 0.19580 | 0.34323 | 0.00582 | 0.10221 | 0.00724 | 1934 | 66 | 1917 | 30 | 1902 | 28 | 1967 | 132 | 1934 | 66 | 153.42 | 175.08 |
| MVG459_Vos-13 | 0.1179 | 0.00464 | 5.64916 | 0.21412 | 0.34757 | 0.00628 | 0.10519 | 0.00818 | 1925 | 72 | 1924 | 32 | 1923 | 30 | 2022 | 150 | 1925 | 72 | 112.60 | 160.52 |
| MVG459_Vos-14 | 0.11734 | 0.00338 | 5.37823 | 0.14730 | 0.33263 | 0.00490 | 0.10337 | 0.00568 | 1916 | 52 | 1881 | 24 | 1851 | 24 | 1988 | 104 | 1916 | 52 | 151.78 | 241.21 |
| MVG459_Vos-15 | 0.10966 | 0.00592 | 4.67923 | 0.23882 | 0.30948 | 0.00550 | 0.08952 | 0.00174 | 1794 | 100 | 1764 | 42 | 1738 | 28 | 1733 | 32 | 1794 | 100 | 213.37 | 663.06 |
| MVG459_Vos-16 | 0.117 | 0.00414 | 5.36716 | 0.17876 | 0.3328 | 0.00562 | 0.10113 | 0.00682 | 1911 | 64 | 1880 | 28 | 1852 | 28 | 1947 | 126 | 1911 | 64 | 78.85 | 146.26 |
| MVG459_Vos-17 | 0.11875 | 0.00502 | 5.45639 | 0.21414 | 0.33324 | 0.00526 | 0.09562 | 0.00170 | 1938 | 78 | 1894 | 34 | 1854 | 26 | 1846 | 32 | 1938 | 78 | 308.81 | 1645.65 |
| MVG459_Vos-18 | 0.11099 | 0.00476 | 4.7527 | 0.19132 | 0.3107 | 0.00628 | 0.72436 | 0.36110 | 1816 | 80 | 1777 | 34 | 1744 | 30 | 11013 | 4232 | 1816 | 80 | 0.06 | 59.60 |
| MVG459_Vos-19 | 0.14443 | 0.00878 | 8.10656 | 0.45800 | 0.40737 | 0.00944 | 0.12692 | 0.01722 | 2281 | 108 | 2243 | 52 | 2203 | 44 | 2415 | 308 | 2281 | 108 | 944.78 | 1508.59 |
| MVG459_Vos-20 | 0.15678 | 0.00928 | 9.38393 | 0.51472 | 0.4343 | 0.00994 | 0.13976 | 0.01910 | 2421 | 102 | 2376 | 50 | 2325 | 44 | 2644 | 338 | 2421 | 102 | 215.29 | 824.91 |
| MVG459_Vos-21 | 0.1488 | 0.00818 | 8.55489 | 0.43736 | 0.41733 | 0.00892 | 0.13464 | 0.01704 | 2332 | 96 | 2292 | 46 | 2248 | 40 | 2553 | 304 | 2332 | 96 | 637.78 | 950.37 |
| MVG459_Vos-22 | 0.15469 | 0.00584 | 9.45849 | 0.32910 | 0.44361 | 0.00710 | 0.12982 | 0.01112 | 2398 | 66 | 2384 | 32 | 2367 | 32 | 2467 | 198 | 2398 | 66 | 106.50 | 282.24 |
| MVG459_Vos-23 | 0.11487 | 0.00506 | 5.29583 | 0.21486 | 0.33447 | 0.00628 | 0.10287 | 0.00940 | 1878 | 82 | 1868 | 34 | 1860 | 30 | 1979 | 172 | 1878 | 82 | 63.86 | 98.05 |
| MVG459_Vos-24C | 0.12062 | 0.00524 | 5.66877 | 0.22398 | 0.34089 | 0.00576 | 0.10849 | 0.01096 | 1965 | 80 | 1927 | 34 | 1891 | 28 | 2082 | 200 | 1965 | 80 | 241.09 | 859.45 |
| MVG459_Vos-24R | 0.15164 | 0.00946 | 8.94741 | 0.50738 | 0.42816 | 0.00992 | 0.13537 | 0.01964 | 2365 | 108 | 2333 | 52 | 2297 | 44 | 2566 | 350 | 2365 | 108 | 307.56 | 398.94 |
| MVG459_Vos-25 | 0.11469 | 0.00320 | 5.36589 | 0.14526 | 0.33932 | 0.00494 | 0.09974 | 0.00528 | 1875 | 52 | 1879 | 24 | 1883 | 24 | 1922 | 98 | 1875 | 52 | 129.16 | 305.16 |
| MVG459_Vos-26 | 0.11816 | 0.00358 | 5.54833 | 0.16200 | 0.34056 | 0.00530 | 0.0989 | 0.00536 | 1929 | 56 | 1908 | 26 | 1889 | 26 | 1906 | 98 | 1929 | 56 | 140.69 | 165.25 |
| MVG459_Vos-27 | 0.12131 | 0.00468 | 5.84825 | 0.21596 | 0.34963 | 0.00668 | 0.10332 | 0.00650 | 1976 | 70 | 1954 | 32 | 1933 | 32 | 1987 | 120 | 1976 | 70 | 136.82 | 85.28 |
| MVG459_Vos-28 | 0.11879 | 0.00370 | 5.74466 | 0.17210 | 0.35074 | 0.00548 | 0.10177 | 0.00590 | 1938 | 58 | 1938 | 26 | 1938 | 26 | 1959 | 108 | 1938 | 58 | 126.74 | 188.36 |
| MVG459_Vos-29 | 0.11748 | 0.00392 | 5.60385 | 0.17964 | 0.34594 | 0.00570 | 0.10301 | 0.00642 | 1918 | 62 | 1917 | 28 | 1915 | 28 | 1982 | 118 | 1918 | 62 | 53.60 | 131.79 |
| MVG459_Vos-30 | 0.11614 | 0.00374 | 5.54031 | 0.17250 | 0.34598 | 0.00546 | 0.10187 | 0.00628 | 1898 | 60 | 1907 | 26 | 1915 | 26 | 1961 | 116 | 1898 | 60 | 196.74 | 224.97 |

| Analysis No. | RATIOS | | | | | | | | AGES (Ma) | | | | | | | | | | CONCENTRATIONS (ppm) | |
|---|---|---|---|---|---|---|---|---|---|---|---|---|---|---|---|---|---|---|---|---|
| | $^{207}Pb/^{206}Pb$ | ± 2σ | $^{207}Pb/^{235}U$ | ± 2σ | $^{206}Pb/^{238}U$ | ± 2σ | $^{208}Pb/^{232}Th$ | ± 2σ | $^{207}Pb/^{206}Pb$ | ± 2σ | $^{207}Pb/^{235}U$ | ± 2σ | $^{206}Pb/^{238}U$ | ± 2σ | $^{208}Pb/^{232}Th$ | ± 2σ | Used Age | ± 2σ | Th | U |
| MVG459_Vos-31 | 0.15522 | 0.00916 | 9.61777 | 0.54756 | 0.44948 | 0.01122 | 0.12017 | 0.01418 | 2404 | 102 | 2399 | 52 | 2393 | 50 | 2294 | 256 | 2404 | 102 | 128.56 | 312.36 |
| MVG459_Vos-32 | 0.12031 | 0.00426 | 5.74576 | 0.19560 | 0.34635 | 0.00588 | 0.1024 | 0.00684 | 1961 | 64 | 1938 | 30 | 1917 | 28 | 1970 | 126 | 1961 | 64 | 132.14 | 137.56 |
| MVG459_Vos-33 | 0.11693 | 0.00408 | 5.56513 | 0.18728 | 0.34515 | 0.00566 | 0.1029 | 0.00712 | 1910 | 64 | 1911 | 28 | 1911 | 28 | 1980 | 130 | 1910 | 64 | 162.81 | 242.05 |
| MVG459_Vos-34 | 0.15728 | 0.00560 | 9.60869 | 0.33022 | 0.44307 | 0.00718 | 0.12499 | 0.00936 | 2427 | 62 | 2398 | 32 | 2364 | 32 | 2380 | 168 | 2427 | 62 | 435.62 | 581.52 |
| MVG459_Vos-35 | 0.13832 | 0.00854 | 7.56035 | 0.44508 | 0.39644 | 0.00948 | 0.10726 | 0.01398 | 2206 | 110 | 2180 | 52 | 2153 | 44 | 2059 | 256 | 2206 | 110 | 97.93 | 833.33 |
| MVG459_Vos-36 | 0.14279 | 0.00520 | 7.86425 | 0.27722 | 0.39941 | 0.00652 | 0.11723 | 0.00900 | 2261 | 64 | 2216 | 32 | 2166 | 30 | 2241 | 162 | 2261 | 64 | 598.01 | 991.86 |
| ~~MVG459_Vos-03~~ | ~~0.12921~~ | ~~0.00768~~ | ~~5.57445~~ | ~~0.31386~~ | ~~0.31293~~ | ~~0.00706~~ | ~~0.0785~~ | ~~0.00956~~ | ~~2087~~ | ~~106~~ | ~~1912~~ | ~~48~~ | ~~1755~~ | ~~34~~ | ~~1527~~ | ~~180~~ | ~~2087~~ | ~~106~~ | ~~187.28~~ | ~~1205.32~~ |
| **Alakhit-Markha field, Veselaya pipe** | | | | | | | | | | | | | | | | | | | | |
| MVG459_Ves-01 | 0.06735 | 0.0045 | 1.1906 | 0.07588 | 0.12821 | 0.00332 | 0.04204 | 0.00352 | 849 | 142 | 796 | 36 | 778 | 18 | 832 | 68 | 778 | 18 | 46.57 | 79.57 |
| MVG459_Ves-02 | 0.121 | 0.00426 | 5.85705 | 0.198 | 0.3511 | 0.00578 | 0.10725 | 0.0072 | 1971 | 64 | 1955 | 30 | 1940 | 28 | 2059 | 132 | 1971 | 64 | 120.98 | 213.72 |
| MVG459_Ves-03 | 0.17911 | 0.00798 | 11.76976 | 0.4996 | 0.47662 | 0.00998 | 0.13638 | 0.01114 | 2645 | 76 | 2586 | 40 | 2513 | 44 | 2584 | 198 | 2645 | 76 | 154.85 | 74.66 |
| MVG459_Ves-04 | 0.05811 | 0.00252 | 0.63261 | 0.0263 | 0.07897 | 0.0014 | 0.02468 | 0.00172 | 534 | 98 | 498 | 16 | 490 | 8 | 493 | 34 | 490 | 8 | 258.12 | 325.55 |
| **Alakhit-Markha field, Krasnopresnenskaya pipe** | | | | | | | | | | | | | | | | | | | | |
| MVG459_Kpr-01 | 0.14699 | 0.0066 | 8.08028 | 0.34302 | 0.39863 | 0.00812 | 0.09319 | 0.00758 | 2311 | 78 | 2240 | 38 | 2163 | 38 | 1801 | 140 | 2311 | 78 | 123.78 | 154.84 |
| MVG459_Kpr-02 | 0.11473 | 0.00322 | 5.34584 | 0.14456 | 0.33798 | 0.00484 | 0.09393 | 0.00586 | 1876 | 52 | 1876 | 24 | 1877 | 24 | 1815 | 108 | 1876 | 52 | 27.48 | 688.04 |
| MVG459_Kpr-03 | 0.11668 | 0.0034 | 5.44754 | 0.15318 | 0.33866 | 0.00488 | 0.1026 | 0.00608 | 1906 | 54 | 1892 | 24 | 1880 | 24 | 1974 | 112 | 1906 | 54 | 95.99 | 1048.70 |
| MVG459_Kpr-04 | 0.14485 | 0.0048 | 8.04524 | 0.25586 | 0.40285 | 0.00634 | 0.11543 | 0.00748 | 2286 | 58 | 2236 | 28 | 2182 | 30 | 2208 | 136 | 2286 | 58 | 413.31 | 548.47 |
| MVG459_Kpr-05 | 0.1194 | 0.0037 | 5.62872 | 0.16758 | 0.34199 | 0.00512 | 0.09867 | 0.00596 | 1947 | 56 | 1921 | 26 | 1896 | 24 | 1902 | 110 | 1947 | 56 | 348.84 | 620.53 |
| **Alakhit-Markha field, Markha pipe** | | | | | | | | | | | | | | | | | | | | |
| 459_MRH-02 | 0.11486 | 0.00268 | 5.33425 | 0.12132 | 0.33689 | 0.00460 | 0.10034 | 0.00404 | 1878 | 44 | 1874 | 20 | 1872 | 22 | 1933 | 74 | 1878 | 44 | 98.62 | 174.25 |
| 459_MRH-04 | 0.06486 | 0.00228 | 1.17451 | 0.03968 | 0.13136 | 0.00210 | 0.04112 | 0.00188 | 770 | 76 | 789 | 18 | 796 | 12 | 814 | 36 | 796 | 12 | 290.59 | 151.22 |
| 459_MRH-05r | 0.07212 | 0.00310 | 1.28104 | 0.05268 | 0.12886 | 0.00244 | 0.04204 | 0.00208 | 989 | 90 | 837 | 24 | 781 | 14 | 832 | 40 | 781 | 14 | 79.67 | 71.16 |
| 459_MRH-06 | 0.18607 | 0.00544 | 13.01863 | 0.36604 | 0.50753 | 0.00754 | 0.13864 | 0.00762 | 2708 | 50 | 2681 | 26 | 2646 | 32 | 2624 | 136 | 2708 | 50 | 442.85 | 209.99 |
| 459_MRH-07 | 0.06074 | 0.00196 | 0.80486 | 0.02496 | 0.09612 | 0.00146 | 0.03041 | 0.00152 | 630 | 72 | 600 | 14 | 592 | 8 | 605 | 30 | 592 | 8 | 360.14 | 373.86 |
| 459_MRH-08 | 0.12307 | 0.00344 | 6.01614 | 0.16244 | 0.35457 | 0.00520 | 0.10337 | 0.00530 | 2001 | 50 | 1978 | 24 | 1956 | 24 | 1988 | 98 | 2001 | 50 | 77.78 | 161.84 |
| 459_MRH-09c | 0.16519 | 0.00946 | 7.2728 | 0.39860 | 0.31936 | 0.00816 | 0.04217 | 0.00454 | 2509 | 98 | 2145 | 48 | 1787 | 40 | 835 | 88 | 2509 | 98 | 381.94 | 150.33 |
| 459_MRH-10 | 0.12412 | 0.00304 | 6.13638 | 0.14484 | 0.35857 | 0.00496 | 0.10312 | 0.00430 | 2016 | 44 | 1995 | 20 | 1975 | 24 | 1984 | 78 | 2016 | 44 | 111.16 | 158.73 |
| 459_MRH-11 | 0.11219 | 0.00340 | 5.10101 | 0.14788 | 0.32976 | 0.00534 | 0.0961 | 0.00434 | 1835 | 56 | 1836 | 24 | 1837 | 26 | 1855 | 80 | 1835 | 56 | 48.36 | 59.33 |
| 459_MRH-12 | 0.11736 | 0.00358 | 5.40745 | 0.15724 | 0.33418 | 0.00542 | 0.0998 | 0.00454 | 1916 | 56 | 1886 | 24 | 1859 | 26 | 1923 | 84 | 1916 | 56 | 71.28 | 60.40 |
| 459_MRH-13 | 0.15035 | 0.00558 | 8.06323 | 0.28336 | 0.38893 | 0.00682 | 0.11147 | 0.00760 | 2350 | 64 | 2238 | 32 | 2118 | 32 | 2136 | 138 | 2350 | 64 | 112.82 | 127.66 |
| 459_MRH-14 | 0.05899 | 0.00204 | 0.63503 | 0.02112 | 0.07808 | 0.00120 | 0.02428 | 0.00120 | 567 | 78 | 499 | 14 | 485 | 8 | 485 | 24 | 485 | 8 | 208.30 | 317.04 |
| 459_MRH-15 | 0.0533 | 0.00392 | 0.43971 | 0.03090 | 0.05984 | 0.00150 | 0.01918 | 0.00112 | 342 | 170 | 370 | 22 | 375 | 10 | 384 | 22 | 375 | 10 | 90.01 | 68.96 |
| 459_MRH-18 | 0.11439 | 0.00400 | 5.20504 | 0.17322 | 0.33002 | 0.00578 | 0.09597 | 0.00522 | 1870 | 64 | 1853 | 28 | 1838 | 28 | 1852 | 96 | 1870 | 64 | 38.03 | 47.79 |
| 459_MRH-19 | 0.05283 | 0.00296 | 0.3484 | 0.01862 | 0.04783 | 0.00100 | 0.01508 | 0.00114 | 322 | 130 | 304 | 14 | 301 | 6 | 303 | 22 | 301 | 6 | 233.26 | 438.04 |
| 459_MRH-20 | 0.05482 | 0.00326 | 0.46226 | 0.02618 | 0.06117 | 0.00132 | 0.01868 | 0.00114 | 405 | 136 | 386 | 18 | 383 | 8 | 374 | 22 | 383 | 8 | 115.79 | 99.94 |
| 459_MRH2-01 | 0.11308 | 0.00166 | 5.19157 | 0.01812 | 0.33301 | 0.00114 | 0.09695 | 0.00112 | 1849 | 28 | 1851 | 2 | 1853 | 6 | 1870 | 20 | 1849 | 28 | 84.32 | 97.87 |
| 459_MRH2-02 | 0.11511 | 0.00218 | 5.31094 | 0.01372 | 0.33468 | 0.00080 | 0.09814 | 0.00074 | 1882 | 34 | 1871 | 2 | 1861 | 4 | 1892 | 14 | 1882 | 34 | 140.42 | 162.75 |
| 459_MRH2-03 | 0.12232 | 0.00322 | 5.99564 | 0.14170 | 0.35556 | 0.00506 | 0.10533 | 0.00452 | 1990 | 48 | 1975 | 20 | 1961 | 24 | 2024 | 82 | 1990 | 48 | 73.41 | 237.41 |
| 459_MRH2-04 | 0.11343 | 0.00310 | 5.22463 | 0.13772 | 0.33411 | 0.00484 | 0.0987 | 0.00462 | 1855 | 50 | 1857 | 22 | 1858 | 24 | 1903 | 84 | 1855 | 50 | 89.45 | 149.37 |
| 459_MRH2-05 | 0.12338 | 0.00350 | 6.13169 | 0.16534 | 0.36053 | 0.00528 | 0.10905 | 0.00572 | 2006 | 52 | 1995 | 24 | 1985 | 26 | 2092 | 104 | 2006 | 52 | 76.10 | 110.69 |
| 459_MRH2-06 | 0.18445 | 0.00324 | 13.22423 | 0.14324 | 0.52008 | 0.00496 | 0.1442 | 0.00502 | 2693 | 30 | 2696 | 10 | 2700 | 22 | 2723 | 88 | 2693 | 30 | 74.41 | 88.12 |
| 459_MRH2-07 | 0.12783 | 0.00484 | 6.4952 | 0.23054 | 0.36859 | 0.00682 | 0.10828 | 0.00772 | 2068 | 68 | 2045 | 32 | 2023 | 32 | 2078 | 140 | 2068 | 68 | 69.01 | 64.16 |
| 459_MRH2-08 | 0.11997 | 0.00534 | 5.15246 | 0.36890 | 0.31153 | 0.00804 | 0.06729 | 0.00776 | 1956 | 82 | 1845 | 60 | 1748 | 40 | 1316 | 146 | 1956 | 82 | 198.39 | 264.01 |
| 459_MRH2-09 | 0.06185 | 0.00424 | 0.87127 | 0.20556 | 0.10219 | 0.00622 | 0.03194 | 0.00608 | 669 | 150 | 636 | 112 | 627 | 36 | 635 | 120 | 627 | 36 | 112.51 | 84.05 |

| Analysis No. | RATIOS | | | | | | | | AGES (Ma) | | | | | | | | | | CONCENTRATIONS (ppm) | |
|---|---|---|---|---|---|---|---|---|---|---|---|---|---|---|---|---|---|---|---|---|
| | $^{207}Pb/^{206}Pb$ | ± 2σ | $^{207}Pb/^{235}U$ | ± 2σ | $^{206}Pb/^{238}U$ | ± 2σ | $^{208}Pb/^{232}Th$ | ± 2σ | $^{207}Pb/^{206}Pb$ | ± 2σ | $^{207}Pb/^{235}U$ | ± 2σ | $^{206}Pb/^{238}U$ | ± 2σ | $^{208}Pb/^{232}Th$ | ± 2σ | Used Age | ± 2σ | Th | U |
| 459_MRH-21 | 0.1611 | 0.00632 | 9.5806 | 0.35612 | 0.43142 | 0.00718 | 0.12658 | 0.00998 | 2467 | 68 | 2395 | 34 | 2312 | 32 | 2409 | 180 | 2467 | 68 | 203.72 | 547.72 |
| 459_MRH2-10 | 0.05233 | 0.00592 | 0.35299 | 0.24240 | 0.04893 | 0.00632 | 0.01592 | 0.00648 | 300 | 264 | 307 | 182 | 308 | 38 | 319 | 128 | 308 | 38 | 132.08 | 123.83 |
| 459_MRH2-11 | 0.05707 | 0.00262 | 0.62199 | 0.06152 | 0.07905 | 0.00292 | 0.02552 | 0.00262 | 494 | 104 | 491 | 38 | 490 | 18 | 509 | 52 | 490 | 18 | 387.14 | 629.00 |
| 459_MRH2-12 | 0.10745 | 0.00262 | 3.88483 | 0.06152 | 0.26221 | 0.00292 | 0.07601 | 0.00262 | 1757 | 46 | 1611 | 12 | 1501 | 14 | 1481 | 50 | 1757 | 46 | 198.84 | 594.74 |
| 459_MRH2-15 | 0.06578 | 0.00158 | 1.20055 | 0.01664 | 0.13239 | 0.00108 | 0.04129 | 0.00104 | 799 | 52 | 801 | 8 | 801 | 6 | 818 | 20 | 801 | 6 | 164.42 | 127.00 |
| 459_MRH2-16 | 0.05171 | 0.00158 | 0.3564 | 0.01664 | 0.04999 | 0.00108 | 0.01571 | 0.00104 | 273 | 72 | 310 | 12 | 314 | 6 | 315 | 20 | 314 | 6 | 916.74 | 571.89 |
| 459_MRH2-17 | 0.11329 | 0.00158 | 4.86014 | 0.01664 | 0.31113 | 0.00108 | 0.0897 | 0.00104 | 1853 | 26 | 1795 | 2 | 1746 | 6 | 1736 | 20 | 1853 | 26 | 9.71 | 306.96 |
| 459_MRH2-18 | 0.21325 | 0.00292 | 16.55112 | 0.01964 | 0.56298 | 0.00094 | 0.15364 | 0.00098 | 2930 | 22 | 2909.2 | 1 | 2879 | 4 | 2889 | 18 | 2930 | 22 | 125.56 | 112.10 |
| 459_MRH2-19 | 0.11402 | 0.00276 | 5.3258 | 0.11498 | 0.33882 | 0.00422 | 0.10124 | 0.00566 | 1864 | 44 | 1873 | 18 | 1881 | 20 | 1949 | 104 | 1864 | 44 | 51.12 | 59.54 |
| 459_MRH2-20 | 0.11512 | 0.00276 | 5.17526 | 0.11498 | 0.32605 | 0.00422 | 0.09385 | 0.00566 | 1882 | 44 | 1849 | 18 | 1819 | 20 | 1813 | 104 | 1882 | 44 | 127.95 | 110.97 |
| 459_MRH2-21 | 0.05343 | 0.00362 | 0.36247 | 0.16146 | 0.04921 | 0.00564 | 0.01593 | 0.00492 | 347 | 156 | 314 | 120 | 310 | 34 | 319 | 98 | 310 | 34 | 410.04 | 380.87 |
| 459_MRH2-22 | 0.07503 | 0.00360 | 1.78624 | 0.15580 | 0.17267 | 0.00510 | 0.05558 | 0.00496 | 1069 | 98 | 1040 | 56 | 1027 | 28 | 1093 | 94 | 1069 | 98 | 207.59 | 435.04 |
| 459_MRH2-23 | 0.16094 | 0.00210 | 9.82194 | 0.01374 | 0.44267 | 0.00080 | 0.12841 | 0.00080 | 2466 | 22 | 2418.2 | 1 | 2363 | 4 | 2442 | 14 | 2466 | 22 | 224.56 | 331.12 |
| 459_MRH2-24 | 0.0637 | 0.00214 | 1.0211 | 0.04900 | 0.11628 | 0.00246 | 0.03792 | 0.00280 | 732 | 72 | 714 | 24 | 709 | 14 | 752 | 54 | 709 | 14 | 13.38 | 33.18 |
| 459_MRH2-25 | 0.11739 | 0.00432 | 5.21269 | 0.25428 | 0.32208 | 0.00620 | 0.09664 | 0.00658 | 1917 | 68 | 1855 | 42 | 1800 | 30 | 1865 | 122 | 1917 | 68 | 68.88 | 322.91 |
| 459_MRH2-26 | 0.11926 | 0.00436 | 5.78504 | 0.06672 | 0.35186 | 0.00302 | 0.10239 | 0.00288 | 1945 | 66 | 1944 | 10 | 1943 | 14 | 1970 | 52 | 1945 | 66 | 162.59 | 523.14 |
| 459_MRH2-27 | 0.28934 | 0.00338 | 27.41759 | 0.14476 | 0.68729 | 0.00466 | 0.19038 | 0.00542 | 3414 | 18 | 3398 | 6 | 3372 | 18 | 3522 | 92 | 3414 | 18 | 78.86 | 98.85 |
| 459_MRH2-28 | 0.11128 | 0.00448 | 4.45265 | 0.20864 | 0.29022 | 0.00590 | 0.08882 | 0.00782 | 1820 | 74 | 1722 | 38 | 1643 | 30 | 1720 | 146 | 1820 | 74 | 162.34 | 374.11 |
| 459_MRH2-29 | 0.11946 | 0.00864 | 5.62477 | 0.78878 | 0.3415 | 0.01060 | 0.102 | 0.01104 | 1948 | 132 | 1920 | 120 | 1894 | 50 | 1963 | 202 | ~~1948~~ | ~~132~~ | 395.04 | 322.35 |
| 459_MRH-23 | 0.06039 | 0.00272 | 0.88341 | 0.06334 | 0.1061 | 0.00292 | 0.03465 | 0.00256 | 618 | 100 | 643 | 34 | 650 | 18 | 688 | 50 | 650 | 18 | 21.13 | 38.45 |
| 459_MRH2-30 | 0.10436 | 0.00412 | 3.98684 | 0.14896 | 0.27706 | 0.00348 | 0.08055 | 0.00106 | 1703 | 74 | 1632 | 30 | 1577 | 18 | 1566 | 20 | 1703 | 74 | 124.77 | 127.39 |
| 459_MRH2-32c | 0.12996 | 0.00382 | 6.83205 | 0.14098 | 0.38126 | 0.00490 | 0.10404 | 0.00456 | 2097 | 52 | 2090 | 18 | 2082 | 22 | 2001 | 84 | 2097 | 52 | 5.72 | 37.23 |
| 459_MRH2-32r | 0.12965 | 0.00166 | 6.6512 | 0.01736 | 0.37211 | 0.00110 | 0.10724 | 0.00112 | 2093 | 24 | 2066 | 2 | 2039 | 6 | 2059 | 20 | 2093 | 24 | 69.32 | 184.32 |
| 459_MRH2-33 | 0.06382 | 0.00584 | 0.82652 | 0.29078 | 0.09393 | 0.00884 | 0.02856 | 0.00978 | 736 | 198 | 612 | 162 | 579 | 52 | 569 | 192 | 579 | 52 | 217.28 | 462.51 |
| 459_MRH2-34 | 0.21887 | 0.00370 | 17.18523 | 0.18290 | 0.56948 | 0.00554 | 0.15702 | 0.00564 | 2972 | 28 | 2945 | 10 | 2906 | 22 | 2948 | 98 | 2972 | 28 | 129.64 | 170.93 |
| 459_MRH2-36 | 0.17397 | 0.00536 | 11.92287 | 0.40960 | 0.49706 | 0.00790 | 0.13968 | 0.00718 | 2596 | 52 | 2598 | 32 | 2601 | 34 | 2643 | 128 | 2596 | 52 | 18.18 | 12.08 |
| 459_MRH2-37 | 0.06251 | 0.00500 | 0.88863 | 0.24780 | 0.1031 | 0.00522 | 0.03158 | 0.00370 | 692 | 174 | 646 | 134 | 633 | 30 | 628 | 72 | 633 | 30 | 143.31 | 188.50 |
| 459_MRH2-38 | 0.11631 | 0.00892 | 5.41673 | 0.57640 | 0.33778 | 0.01474 | 0.09719 | 0.00924 | 1900 | 142 | 1888 | 92 | 1876 | 72 | 1875 | 170 | ~~1900~~ | ~~142~~ | 176.89 | 173.40 |
| 459_MRH2-39 | 0.05799 | 0.00272 | 0.63572 | 0.03698 | 0.07951 | 0.00188 | 0.02512 | 0.00186 | 529 | 106 | 500 | 22 | 493 | 12 | 501 | 36 | 493 | 12 | 264.93 | 138.77 |
| 459_MRH-24 | 0.18907 | 0.00306 | 13.57123 | 0.02110 | 0.52067 | 0.00104 | 0.14479 | 0.00096 | 2734 | 28 | 2720.3 | 1 | 2702 | 4 | 2733 | 16 | 2734 | 28 | 26.91 | 89.37 |
| 459_MRH2-40 | 0.11509 | 0.00406 | 5.23528 | 0.18192 | 0.32993 | 0.00572 | 0.09963 | 0.00608 | 1881 | 66 | 1858 | 30 | 1838 | 28 | 1920 | 112 | 1881 | 66 | 108.38 | 262.16 |
| 459_MRH2-43 | 0.05947 | 0.00526 | 0.65689 | 0.13580 | 0.08012 | 0.00402 | 0.02478 | 0.00300 | 584 | 196 | 513 | 84 | 497 | 24 | 495 | 60 | 497 | 24 | 137.04 | 110.88 |
| 459_MRH2-45 | 0.06604 | 0.00266 | 1.21049 | 0.06302 | 0.13294 | 0.00304 | 0.04182 | 0.00270 | 808 | 86 | 805 | 28 | 805 | 18 | 828 | 52 | 805 | 18 | 98.89 | 110.30 |
| 459_MRH2-46 | 0.06385 | 0.00258 | 1.09324 | 0.04112 | 0.12419 | 0.00208 | 0.041 | 0.00162 | 737 | 88 | 750 | 20 | 755 | 12 | 812 | 32 | 755 | 12 | 44.73 | 55.22 |
| 459_MRH2-47 | 0.06507 | 0.00328 | 1.02686 | 0.05734 | 0.11447 | 0.00272 | 0.03466 | 0.00204 | 777 | 108 | 717 | 28 | 699 | 16 | 689 | 40 | 699 | 16 | 9.26 | 25.64 |
| 459_MRH2-48 | 0.11853 | 0.00466 | 5.52316 | 0.07606 | 0.33797 | 0.00342 | 0.09676 | 0.00308 | 1934 | 72 | 1904 | 12 | 1877 | 16 | 1867 | 56 | 1934 | 72 | 96.92 | 108.91 |
| 459_MRH2-49 | 0.05378 | 0.00270 | 0.43402 | 0.04070 | 0.05853 | 0.00204 | 0.01885 | 0.00162 | 362 | 116 | 366 | 28 | 367 | 12 | 377 | 32 | 367 | 12 | 158.93 | 201.38 |
| 459_MRH-25 | 0.12501 | 0.00392 | 6.15402 | 0.05474 | 0.35695 | 0.00258 | 0.10205 | 0.00206 | 2029 | 56 | 1998 | 8 | 1968 | 12 | 1964 | 38 | 2029 | 56 | 81.85 | 159.35 |
| 459_MRH2-50 | 0.068 | 0.00318 | 1.22246 | 0.14316 | 0.13039 | 0.00492 | 0.04044 | 0.00454 | 869 | 100 | 811 | 66 | 790 | 28 | 801 | 88 | 790 | 28 | 178.80 | 175.72 |
| 459_MRH2-51 | 0.15784 | 0.00256 | 9.43966 | 0.01982 | 0.43379 | 0.00108 | 0.12244 | 0.00092 | 2433 | 28 | 2381.7 | 2 | 2323 | 4 | 2335 | 16 | 2433 | 28 | 56.42 | 63.68 |
| 459_MRH2-52 | 0.05953 | 0.00338 | 0.72753 | 0.05806 | 0.08864 | 0.00268 | 0.02748 | 0.00216 | 587 | 126 | 555 | 34 | 547 | 16 | 548 | 42 | 547 | 16 | 162.35 | 319.78 |
| 459_MRH2-53 | 0.05439 | 0.00398 | 0.46823 | 0.23096 | 0.06244 | 0.00596 | 0.01939 | 0.00580 | 387 | 168 | 390 | 160 | 390 | 36 | 388 | 116 | 390 | 36 | 209.49 | 109.23 |
| 459_MRH2-54 | 0.11743 | 0.00286 | 5.32194 | 0.03346 | 0.32869 | 0.00170 | 0.10058 | 0.00140 | 1917 | 44 | 1872 | 6 | 1832 | 8 | 1937 | 26 | 1917 | 44 | 419.40 | 429.74 |
| 459_MRH2-55 | 0.0581 | 0.00196 | 0.69599 | 0.01626 | 0.08689 | 0.00098 | 0.02786 | 0.00100 | 534 | 76 | 536 | 10 | 537 | 6 | 555 | 20 | 537 | 6 | 81.07 | 76.21 |

| Analysis No. | RATIOS | | | | | | | | AGES (Ma) | | | | | | | | | | CONCENTRATIONS (ppm) | |
|---|---|---|---|---|---|---|---|---|---|---|---|---|---|---|---|---|---|---|---|---|
| | $^{207}Pb/^{206}Pb$ | ± 2σ | $^{207}Pb/^{235}U$ | ± 2σ | $^{206}Pb/^{238}U$ | ± 2σ | $^{208}Pb/^{232}Th$ | ± 2σ | $^{207}Pb/^{206}Pb$ | ± 2σ | $^{207}Pb/^{235}U$ | ± 2σ | $^{206}Pb/^{238}U$ | ± 2σ | $^{208}Pb/^{232}Th$ | ± 2σ | Used Age | ± 2σ | Th | U |
| 459_MRH2-56 | 0.0616 | 0.00528 | 0.86586 | 0.22728 | 0.10196 | 0.00694 | 0.03151 | 0.00742 | 660 | 188 | 633 | 124 | 626 | 40 | 627 | 146 | 626 | 40 | 127.71 | 183.72 |
| 459_MRH2-57 | 0.12383 | 0.00244 | 6.17371 | 0.02806 | 0.36165 | 0.00152 | 0.10743 | 0.00158 | 2012 | 36 | 2001 | 4 | 1990 | 8 | 2062 | 28 | 2012 | 36 | 226.50 | 202.23 |
| 459_MRH2-58 | 0.10906 | 0.00244 | 4.8673 | 0.02806 | 0.32368 | 0.00152 | 0.09368 | 0.00158 | 1784 | 42 | 1797 | 4 | 1808 | 8 | 1810 | 30 | 1784 | 42 | 352.96 | 486.69 |
| 459_MRH2-59 | 0.18884 | 0.00426 | 13.77593 | 0.20432 | 0.52916 | 0.00580 | 0.14622 | 0.00724 | 2732 | 38 | 2734 | 14 | 2738 | 24 | 2758 | 128 | 2732 | 38 | 100.53 | 154.31 |
| 459_MRH-26 | 0.05169 | 0.00578 | 0.29368 | 0.39712 | 0.04121 | 0.00848 | 0.01278 | 0.00856 | 272 | 262 | 261 | 312 | 260 | 52 | 257 | 170 | 260 | 52 | 475.29 | 425.30 |
| 459_MRH-27 | 0.05135 | 0.00510 | 0.3347 | 0.23954 | 0.04728 | 0.00664 | 0.01533 | 0.00776 | 257 | 234 | 293 | 182 | 298 | 40 | 308 | 154 | 298 | 40 | 249.60 | 260.94 |
| 459_MRH-28 | 0.1118 | 0.00202 | 5.10741 | 0.01104 | 0.33134 | 0.00066 | 0.09515 | 0.00058 | 1829 | 34 | 1837.3 | 2 | 1845 | 4 | 1837 | 10 | 1829 | 34 | 72.34 | 86.32 |
| 459_MRH-29 | 0.05992 | 0.00226 | 0.8478 | 0.01418 | 0.10263 | 0.00082 | 0.0318 | 0.00074 | 601 | 84 | 623 | 8 | 630 | 4 | 633 | 14 | 630 | 4 | 104.09 | 98.22 |
| 459_MRH-30 | 0.13676 | 0.00330 | 7.43873 | 0.14494 | 0.39454 | 0.00514 | 0.11878 | 0.00454 | 2187 | 42 | 2166 | 18 | 2144 | 24 | 2269 | 82 | 2187 | 42 | 9.63 | 29.77 |
| 459_MRH-32 | 0.11422 | 0.00540 | 5.23569 | 0.27938 | 0.33246 | 0.00818 | 0.09792 | 0.00802 | 1868 | 88 | 1858 | 46 | 1850 | 40 | 1888 | 148 | 1868 | 88 | 94.63 | 178.24 |
| 459_MRH-34 | 0.06534 | 0.00478 | 1.13759 | 0.03056 | 0.12631 | 0.00154 | 0.04045 | 0.00134 | 785 | 158 | 771 | 14 | 767 | 8 | 801 | 26 | 767 | 8 | 202.94 | 351.46 |
| 459_MRH-37 | 0.06802 | 0.00352 | 1.3916 | 0.03434 | 0.14838 | 0.00166 | 0.04721 | 0.00188 | 869 | 110 | 885 | 14 | 892 | 10 | 932 | 36 | 892 | 10 | 38.70 | 77.06 |
| 459_MRH-38 | 0.11408 | 0.00186 | 4.99019 | 0.02408 | 0.31725 | 0.00142 | 0.0914 | 0.00190 | 1865 | 30 | 1818 | 4 | 1776 | 6 | 1768 | 36 | 1865 | 30 | 25.57 | 57.81 |
| 459_MRH-39 | 0.11572 | 0.00186 | 5.2643 | 0.02408 | 0.32994 | 0.00142 | 0.09492 | 0.00190 | 1891 | 30 | 1863 | 4 | 1838 | 6 | 1833 | 36 | 1891 | 30 | 91.45 | 274.16 |
| 459_MRH-40 | 0.05801 | 0.00446 | 0.65264 | 0.18620 | 0.08161 | 0.00624 | 0.02557 | 0.00568 | 530 | 172 | 510 | 114 | 506 | 38 | 510 | 112 | 506 | 38 | 406.62 | 567.27 |
| 459_MRH-41 | 0.05217 | 0.00528 | 0.34174 | 0.23292 | 0.04752 | 0.00654 | 0.01525 | 0.00964 | 293 | 238 | 298 | 176 | 299 | 40 | 306 | 192 | 299 | 40 | 172.58 | 298.63 |
| ~~459_MRH-01~~ | ~~0.17564~~ | ~~0.01342~~ | ~~4.81003~~ | ~~0.34700~~ | ~~0.19862~~ | ~~0.00500~~ | ~~0.05484~~ | ~~0.00190~~ | ~~2612~~ | ~~130~~ | ~~1787~~ | ~~60~~ | ~~1168~~ | ~~26~~ | ~~1079~~ | ~~36~~ | ~~2612~~ | ~~130~~ | ~~264.04~~ | ~~964.38~~ |
| ~~459_MRH-03~~ | ~~0.10797~~ | ~~0.00796~~ | ~~2.64652~~ | ~~0.18880~~ | ~~0.17777~~ | ~~0.00330~~ | ~~0.0515~~ | ~~0.00170~~ | ~~1765~~ | ~~138~~ | ~~1314~~ | ~~52~~ | ~~1055~~ | ~~18~~ | ~~1015~~ | ~~32~~ | ~~1765~~ | ~~138~~ | ~~196.65~~ | ~~612.81~~ |
| ~~459_MRH-05c~~ | ~~0.06915~~ | ~~0.00446~~ | ~~1.33644~~ | ~~0.08230~~ | ~~0.14021~~ | ~~0.00360~~ | ~~0.04593~~ | ~~0.00438~~ | ~~903~~ | ~~136~~ | ~~862~~ | ~~36~~ | ~~846~~ | ~~20~~ | ~~908~~ | ~~84~~ | ~~846~~ | ~~20~~ | ~~377.83~~ | ~~257.36~~ |
| ~~459_MRH-09r~~ | ~~0.11759~~ | ~~0.00364~~ | ~~5.23583~~ | ~~0.15594~~ | ~~0.32297~~ | ~~0.00478~~ | ~~0.0822~~ | ~~0.00492~~ | ~~1920~~ | ~~56~~ | ~~1858~~ | ~~26~~ | ~~1804~~ | ~~24~~ | ~~1597~~ | ~~92~~ | ~~1920~~ | ~~56~~ | ~~438.17~~ | ~~977.45~~ |
| ~~459_MRH-22~~ | ~~0.04905~~ | ~~0.01918~~ | ~~0.34888~~ | ~~0.61174~~ | ~~0.05159~~ | ~~0.00314~~ | ~~0.01632~~ | ~~0.01970~~ | ~~150~~ | ~~714~~ | ~~304~~ | ~~460~~ | ~~324~~ | ~~20~~ | ~~327~~ | ~~392~~ | ~~324~~ | ~~20~~ | ~~290.41~~ | ~~302.02~~ |
| ~~459_MRH2-31~~ | ~~0.05715~~ | ~~0.00250~~ | ~~0.6156~~ | ~~0.03924~~ | ~~0.07813~~ | ~~0.00200~~ | ~~0.02489~~ | ~~0.00166~~ | ~~497~~ | ~~98~~ | ~~487~~ | ~~24~~ | ~~485~~ | ~~12~~ | ~~497~~ | ~~32~~ | ~~485~~ | ~~12~~ | ~~147.13~~ | ~~539.34~~ |
| ~~459_MRH2-35~~ | ~~0.18684~~ | ~~0.00286~~ | ~~9.52002~~ | ~~0.03546~~ | ~~0.36954~~ | ~~0.00172~~ | ~~0.07186~~ | ~~0.00214~~ | ~~2715~~ | ~~26~~ | ~~2389~~ | ~~4~~ | ~~2027~~ | ~~8~~ | ~~1403~~ | ~~40~~ | ~~2715~~ | ~~26~~ | ~~428.00~~ | ~~791.67~~ |
| ~~459_MRH2-41~~ | ~~0.11031~~ | ~~0.00274~~ | ~~2.95577~~ | ~~0.02876~~ | ~~0.19431~~ | ~~0.00150~~ | ~~0.03164~~ | ~~0.00136~~ | ~~1805~~ | ~~46~~ | ~~1396~~ | ~~8~~ | ~~1145~~ | ~~8~~ | ~~630~~ | ~~26~~ | ~~1805~~ | ~~46~~ | ~~571.33~~ | ~~603.12~~ |
| ~~459_MRH2-42~~ | ~~0.10183~~ | ~~0.00334~~ | ~~2.68557~~ | ~~0.14682~~ | ~~0.19128~~ | ~~0.00484~~ | ~~0.06459~~ | ~~0.00542~~ | ~~1658~~ | ~~62~~ | ~~1324~~ | ~~40~~ | ~~1128~~ | ~~26~~ | ~~1265~~ | ~~102~~ | ~~1658~~ | ~~62~~ | ~~105.75~~ | ~~56.53~~ |
| ~~459_MRH-31~~ | ~~0.05107~~ | ~~0.00350~~ | ~~0.34234~~ | ~~0.04744~~ | ~~0.04862~~ | ~~0.00230~~ | ~~0.01481~~ | ~~0.00200~~ | ~~244~~ | ~~162~~ | ~~299~~ | ~~36~~ | ~~306~~ | ~~14~~ | ~~297~~ | ~~40~~ | ~~306~~ | ~~14~~ | ~~239.49~~ | ~~123.47~~ |
| ~~459_MRH-35~~ | ~~0.06058~~ | ~~0.00330~~ | ~~0.62024~~ | ~~0.14656~~ | ~~0.07426~~ | ~~0.00494~~ | ~~0.02341~~ | ~~0.00520~~ | ~~624~~ | ~~120~~ | ~~490~~ | ~~92~~ | ~~462~~ | ~~30~~ | ~~468~~ | ~~102~~ | ~~462~~ | ~~30~~ | ~~126.32~~ | ~~174.85~~ |
| ~~459_MRH-36~~ | ~~0.05442~~ | ~~0.00280~~ | ~~0.35895~~ | ~~0.04672~~ | ~~0.04785~~ | ~~0.00228~~ | ~~0.0149~~ | ~~0.00292~~ | ~~388~~ | ~~118~~ | ~~311~~ | ~~34~~ | ~~301~~ | ~~14~~ | ~~299~~ | ~~58~~ | ~~301~~ | ~~14~~ | ~~372.48~~ | ~~397.20~~ |
| **Alakhit-Markha field, Aikhal pipe** | | | | | | | | | | | | | | | | | | | | |
| AIKH-01 | 0.12239 | 0.00268 | 5.93127 | 0.13230 | 0.35149 | 0.00730 | 0.1448 | 0.00382 | 1991 | 40 | 1966 | 20 | 1942 | 34 | 2733 | 68 | 1991 | 40 | 332.73 | 1015.15 |
| AIKH-02 | 0.1166 | 0.00260 | 5.59429 | 0.12678 | 0.34801 | 0.00728 | 0.1011 | 0.00260 | 1905 | 40 | 1915 | 20 | 1925 | 34 | 1947 | 48 | 1905 | 40 | 320.31 | 1406.88 |
| AIKH-03 | 0.11714 | 0.00262 | 5.56769 | 0.12672 | 0.34475 | 0.00724 | 0.09983 | 0.00264 | 1913 | 42 | 1911 | 20 | 1909 | 34 | 1923 | 48 | 1913 | 42 | 285.23 | 1270.94 |
| AIKH-04 | 0.12123 | 0.00278 | 5.8975 | 0.14024 | 0.35283 | 0.00764 | 0.09795 | 0.00282 | 1974 | 42 | 1961 | 20 | 1948 | 36 | 1889 | 52 | 1974 | 42 | 819.94 | 3797.82 |
| AIKH-05 | 0.1204 | 0.00286 | 5.96713 | 0.13990 | 0.35946 | 0.00736 | 0.1083 | 0.00336 | 1962 | 44 | 1971 | 20 | 1980 | 34 | 2078 | 62 | 1962 | 44 | 610.06 | 2431.71 |
| AIKH-06 | 0.1201 | 0.00274 | 5.83787 | 0.13470 | 0.35256 | 0.00738 | 0.10489 | 0.00296 | 1958 | 42 | 1952 | 20 | 1947 | 36 | 2016 | 54 | 1958 | 42 | 310.42 | 1312.47 |
| AIKH-10 | 0.11883 | 0.00278 | 5.69623 | 0.13638 | 0.3477 | 0.00746 | 0.10045 | 0.00308 | 1939 | 42 | 1931 | 20 | 1924 | 36 | 1935 | 56 | 1939 | 42 | 410.56 | 1854.92 |
| AIKH-10C | 0.12005 | 0.00288 | 5.91747 | 0.14416 | 0.35754 | 0.00762 | 0.10368 | 0.00338 | 1957 | 44 | 1964 | 22 | 1971 | 36 | 1994 | 62 | 1957 | 44 | 389.40 | 1691.64 |
| AIKH-11 | 0.11838 | 0.00262 | 5.83356 | 0.13236 | 0.35744 | 0.00754 | 0.10461 | 0.00278 | 1932 | 40 | 1951 | 20 | 1970 | 36 | 2011 | 50 | 1932 | 40 | 440.69 | 1882.49 |
| AIKH-12C | 0.11765 | 0.00258 | 5.64899 | 0.12684 | 0.34827 | 0.00734 | 0.10236 | 0.00270 | 1921 | 40 | 1924 | 20 | 1926 | 36 | 1970 | 50 | 1921 | 40 | 698.70 | 3049.16 |
| AIKH-12R | 0.11759 | 0.00262 | 5.43552 | 0.12424 | 0.33528 | 0.00710 | 0.0998 | 0.00274 | 1920 | 40 | 1890 | 20 | 1864 | 34 | 1923 | 50 | 1920 | 40 | 377.85 | 1696.14 |
| AIKH-13 | 0.11926 | 0.00266 | 5.80294 | 0.13210 | 0.35294 | 0.00742 | 0.10311 | 0.00282 | 1945 | 40 | 1947 | 20 | 1949 | 36 | 1983 | 52 | 1945 | 40 | 730.39 | 3153.68 |
| AIKH-14 | 0.11575 | 0.00276 | 5.56415 | 0.13638 | 0.34866 | 0.00760 | 0.10363 | 0.00326 | 1892 | 44 | 1911 | 22 | 1928 | 36 | 1993 | 60 | 1892 | 44 | 342.19 | 1498.04 |
| AIKH-15C | 0.1205 | 0.00278 | 6.02648 | 0.14032 | 0.36277 | 0.00760 | 0.10826 | 0.00318 | 1964 | 42 | 1980 | 20 | 1995 | 36 | 2078 | 58 | 1964 | 42 | 370.93 | 1506.32 |
| AIKH-15R | 0.12009 | 0.00272 | 5.82573 | 0.13550 | 0.35189 | 0.00748 | 0.1019 | 0.00294 | 1958 | 42 | 1950 | 20 | 1944 | 36 | 1961 | 54 | 1958 | 42 | 719.26 | 3153.44 |

| Analysis No. | RATIOS | | | | | | | | AGES (Ma) | | | | | | | | | | CONCENTRATIONS (ppm) | |
|---|---|---|---|---|---|---|---|---|---|---|---|---|---|---|---|---|---|---|---|---|
| | $^{207}Pb/^{206}Pb$ | ± 2σ | $^{207}Pb/^{235}U$ | ± 2σ | $^{206}Pb/^{238}U$ | ± 2σ | $^{208}Pb/^{232}Th$ | ± 2σ | $^{207}Pb/^{206}Pb$ | ± 2σ | $^{207}Pb/^{235}U$ | ± 2σ | $^{206}Pb/^{238}U$ | ± 2σ | $^{208}Pb/^{232}Th$ | ± 2σ | Used Age | ± 2σ | Th | U |
| AIKH-16 | 0.11977 | 0.00290 | 6.06523 | 0.15204 | 0.36732 | 0.00806 | 0.10605 | 0.00360 | 1953 | 44 | 1985 | 22 | 2017 | 38 | 2037 | 66 | 1953 | 44 | 1172.74 | 5039.11 |
| AIKH-18 | 0.12002 | 0.00278 | 5.92488 | 0.14028 | 0.35806 | 0.00764 | 0.10254 | 0.00310 | 1957 | 42 | 1965 | 20 | 1973 | 36 | 1973 | 56 | 1957 | 42 | 602.57 | 2626.63 |
| AIKH-20C | 0.11967 | 0.00268 | 6.11666 | 0.14028 | 0.37074 | 0.00786 | 0.10895 | 0.00308 | 1951 | 40 | 1993 | 20 | 2033 | 36 | 2090 | 56 | 1951 | 40 | 1094.14 | 4557.79 |
| AIKH-20C1 | 0.12042 | 0.00278 | 5.83968 | 0.13616 | 0.35175 | 0.00738 | 0.10304 | 0.00316 | 1962 | 42 | 1952 | 20 | 1943 | 36 | 1982 | 58 | 1962 | 42 | 841.85 | 3655.14 |
| AIKH-20R | 0.11862 | 0.00272 | 5.72739 | 0.13286 | 0.35024 | 0.00736 | 0.10275 | 0.00306 | 1936 | 42 | 1936 | 20 | 1936 | 36 | 1977 | 56 | 1936 | 42 | 350.33 | 1524.26 |
| AIKH-21C | 0.12003 | 0.00292 | 5.94566 | 0.14348 | 0.35929 | 0.00748 | 0.10618 | 0.00362 | 1957 | 44 | 1968 | 20 | 1979 | 36 | 2040 | 66 | 1957 | 44 | 342.12 | 1420.38 |
| AIKH-24 | 0.11877 | 0.00286 | 5.6716 | 0.13638 | 0.34636 | 0.00730 | 0.10073 | 0.00338 | 1938 | 44 | 1927 | 20 | 1917 | 34 | 1940 | 62 | 1938 | 44 | 507.24 | 2255.54 |
| AIKH-25C | 0.1177 | 0.00276 | 5.57913 | 0.13146 | 0.34384 | 0.00722 | 0.09958 | 0.00320 | 1922 | 44 | 1913 | 20 | 1905 | 34 | 1919 | 58 | 1922 | 44 | 605.31 | 2718.55 |
| AIKH-25R | 0.11843 | 0.00284 | 5.61935 | 0.13516 | 0.34415 | 0.00726 | 0.09778 | 0.00330 | 1933 | 44 | 1919 | 20 | 1907 | 34 | 1886 | 60 | 1933 | 44 | 603.93 | 2778.71 |
| AIKH-26 | 0.11687 | 0.00286 | 5.72319 | 0.14198 | 0.3552 | 0.00764 | 0.10506 | 0.00348 | 1909 | 44 | 1935 | 22 | 1959 | 36 | 2019 | 64 | 1909 | 44 | 190.94 | 811.86 |
| AIKH-27 | 0.1248 | 0.00316 | 6.20102 | 0.15936 | 0.36041 | 0.00786 | 0.10168 | 0.00370 | 2026 | 46 | 2005 | 22 | 1984 | 38 | 1957 | 68 | 2026 | 46 | 860.36 | 3935.75 |
| AIKH-28 | 0.11985 | 0.00364 | 5.8396 | 0.18272 | 0.35361 | 0.00848 | 0.10038 | 0.00492 | 1954 | 56 | 1952 | 28 | 1952 | 40 | 1933 | 90 | 1954 | 56 | 1298.00 | 6294.80 |
| AIKH-33 | 0.11986 | 0.00298 | 6.05058 | 0.15174 | 0.36615 | 0.00786 | 0.10735 | 0.00396 | 1954 | 46 | 1983 | 22 | 2011 | 38 | 2061 | 72 | 1954 | 46 | 1085.21 | 4603.68 |
| AIKH-34 | 0.11686 | 0.00290 | 5.57566 | 0.13848 | 0.34609 | 0.00738 | 0.10134 | 0.00364 | 1909 | 46 | 1912 | 22 | 1916 | 36 | 1951 | 66 | 1909 | 46 | 370.36 | 1649.42 |
| AIKH-35 | 0.11977 | 0.00264 | 6.0393 | 0.13436 | 0.36576 | 0.00758 | 0.10497 | 0.00278 | 1953 | 40 | 1982 | 20 | 2009 | 36 | 2018 | 50 | 1953 | 40 | 621.18 | 2627.39 |
| AIKH-38C | 0.11749 | 0.00268 | 5.71587 | 0.13156 | 0.35288 | 0.00742 | 0.10054 | 0.00278 | 1918 | 42 | 1934 | 20 | 1948 | 36 | 1936 | 52 | 1918 | 42 | 185.50 | 823.43 |
| AIKH-38R | 0.11783 | 0.00272 | 5.60209 | 0.12870 | 0.34486 | 0.00716 | 0.09851 | 0.00278 | 1924 | 42 | 1916 | 20 | 1910 | 34 | 1899 | 52 | 1924 | 42 | 335.93 | 1501.76 |
| AIKH-48C | 0.12215 | 0.00334 | 6.05967 | 0.16456 | 0.35982 | 0.00786 | 0.10465 | 0.00414 | 1988 | 50 | 1984 | 24 | 1981 | 38 | 2012 | 76 | 1988 | 50 | 218.12 | 944.75 |
| AIKH-48R1 | 0.11818 | 0.00304 | 5.63342 | 0.14092 | 0.34573 | 0.00718 | 0.10216 | 0.00368 | 1929 | 48 | 1921 | 22 | 1914 | 34 | 1966 | 68 | 1929 | 48 | 313.43 | 1348.56 |
| AIKH-48R2 | 0.11962 | 0.00304 | 5.63114 | 0.13928 | 0.34143 | 0.00706 | 0.10192 | 0.00364 | 1951 | 46 | 1921 | 22 | 1894 | 34 | 1962 | 66 | 1951 | 46 | 378.88 | 1631.85 |
| AIKH-49 | 0.12059 | 0.00284 | 5.94426 | 0.14212 | 0.35754 | 0.00762 | 0.1043 | 0.00318 | 1965 | 42 | 1968 | 20 | 1971 | 36 | 2005 | 58 | 1965 | 42 | 298.13 | 1288.39 |
| AIKH-53 | 0.11557 | 0.00260 | 5.44338 | 0.12472 | 0.34164 | 0.00718 | 0.10556 | 0.00316 | 1889 | 42 | 1892 | 20 | 1895 | 34 | 2028 | 58 | 1889 | 42 | 127.96 | 543.67 |
| AIKH-53R | 0.11279 | 0.00256 | 5.12214 | 0.11782 | 0.3294 | 0.00694 | 0.0954 | 0.00272 | 1845 | 42 | 1840 | 20 | 1835 | 34 | 1842 | 50 | 1845 | 42 | 671.32 | 3158.70 |
| AIKH-56 | 0.11758 | 0.00276 | 5.70023 | 0.13502 | 0.35165 | 0.00744 | 0.09992 | 0.00300 | 1920 | 44 | 1931 | 20 | 1942 | 36 | 1925 | 56 | 1920 | 44 | 445.55 | 1990.68 |
| AIKH-56R | 0.11682 | 0.00282 | 5.64769 | 0.13744 | 0.35067 | 0.00748 | 0.1016 | 0.00320 | 1908 | 44 | 1923 | 20 | 1938 | 36 | 1956 | 58 | 1908 | 44 | 181.23 | 797.17 |
| AIKH-56S | 0.1249 | 0.00388 | 6.08453 | 0.17880 | 0.35331 | 0.00756 | 0.10597 | 0.00482 | 2027 | 56 | 1988 | 26 | 1950 | 36 | 2036 | 88 | 2027 | 56 | 97.00 | 388.19 |
| AIKH-59C | 0.11662 | 0.00308 | 5.62809 | 0.14406 | 0.35002 | 0.00728 | 0.10104 | 0.00374 | 1905 | 48 | 1920 | 22 | 1935 | 34 | 1946 | 68 | 1905 | 48 | 298.60 | 1291.11 |
| AIKH-59R | 0.11874 | 0.00390 | 5.73102 | 0.18582 | 0.35013 | 0.00814 | 0.10721 | 0.00558 | 1937 | 60 | 1936 | 28 | 1935 | 38 | 2058 | 102 | 1937 | 60 | 326.86 | 1401.70 |
| AIKH-66 | 0.11341 | 0.00292 | 5.30168 | 0.14406 | 0.33909 | 0.00786 | 0.09887 | 0.00372 | 1855 | 48 | 1869 | 24 | 1882 | 38 | 1906 | 68 | 1855 | 48 | 339.78 | 1598.39 |
| AIKH-66R | 0.11531 | 0.00312 | 5.28247 | 0.14778 | 0.33228 | 0.00764 | 0.09889 | 0.00404 | 1885 | 50 | 1866 | 24 | 1849 | 36 | 1906 | 74 | 1885 | 50 | 196.83 | 922.22 |
| AIKH-6R | 0.11654 | 0.00268 | 5.49775 | 0.12768 | 0.34217 | 0.00718 | 0.09925 | 0.00288 | 1904 | 42 | 1900 | 20 | 1897 | 34 | 1913 | 52 | 1904 | 42 | 368.06 | 1652.61 |
| AIKH-75 | 0.11793 | 0.00288 | 5.72643 | 0.14106 | 0.35223 | 0.00752 | 0.0995 | 0.00332 | 1925 | 44 | 1935 | 22 | 1945 | 36 | 1917 | 62 | 1925 | 44 | 340.13 | 1526.99 |
| AIKH-76 | 0.11941 | 0.00282 | 5.86089 | 0.13946 | 0.35602 | 0.00754 | 0.10146 | 0.00320 | 1947 | 44 | 1955 | 20 | 1963 | 36 | 1953 | 58 | 1947 | 44 | 471.82 | 2081.11 |
| AIKH-76R | 0.11564 | 0.00286 | 5.15457 | 0.12988 | 0.32331 | 0.00704 | 0.09299 | 0.00324 | 1890 | 46 | 1845 | 22 | 1806 | 34 | 1797 | 60 | 1890 | 46 | 268.41 | 1318.12 |
| AIKH-7R | 0.12074 | 0.00274 | 5.7658 | 0.13354 | 0.34638 | 0.00734 | 0.09977 | 0.00284 | 1967 | 42 | 1941 | 20 | 1917 | 36 | 1922 | 52 | 1967 | 42 | 895.88 | 4046.28 |
| AIKH-8C | 0.1203 | 0.00296 | 5.77994 | 0.14450 | 0.34847 | 0.00760 | 0.10524 | 0.00338 | 1961 | 44 | 1943 | 22 | 1927 | 36 | 2022 | 62 | 1961 | 44 | 187.98 | 807.53 |
| AIKH-8R | 0.1215 | 0.00414 | 5.71385 | 0.19708 | 0.34112 | 0.00860 | 0.10102 | 0.00542 | 1978 | 62 | 1933 | 30 | 1892 | 42 | 1945 | 100 | 1978 | 62 | 187.91 | 897.19 |
| AIKH-9 | 0.1205 | 0.00284 | 6.11892 | 0.14582 | 0.36831 | 0.00782 | 0.1044 | 0.00322 | 1964 | 44 | 1993 | 20 | 2021 | 36 | 2007 | 58 | 1964 | 44 | 376.35 | 1619.37 |
| **Nakyn field, Botuobinskaya pipe** | | | | | | | | | | | | | | | | | | | | |
| BT070301 | 0.19317 | 0.00204 | 14.32275 | 0.12693 | 0.5378 | 0.00451 | 0.14586 | 0.00183 | 2769 | 9 | 2771 | 8 | 2774 | 19 | 2752 | 32 | 2769 | 9 | | |
| BT070303 | 0.19453 | 0.00206 | 14.47314 | 0.12803 | 0.53965 | 0.00451 | 0.14706 | 0.00181 | 2781 | 10 | 2781 | 8 | 2782 | 19 | 2773 | 32 | 2781 | 10 | | |
| BT070306 | 0.19926 | 0.0021 | 15.11588 | 0.13065 | 0.55021 | 0.00448 | 0.14875 | 0.00186 | 2820 | 10 | 2823 | 8 | 2826 | 19 | 2803 | 33 | 2820 | 10 | | |
| BT070308core | 0.18418 | 0.00199 | 12.97294 | 0.12707 | 0.51089 | 0.00466 | 0.14448 | 0.00221 | 2691 | 11 | 2678 | 9 | 2660 | 20 | 2728 | 39 | 2691 | 11 | | |
| BT070308rim | 0.21484 | 0.00257 | 17.20254 | 0.16614 | 0.58079 | 0.00459 | 0.18462 | 0.00362 | 2942 | 12 | 2946 | 9 | 2952 | 19 | 3424 | 62 | 2942 | 12 | | |

| Analysis No. | RATIOS | | | | | | | | AGES (Ma) | | | | | | | | | | CONCENTRATIONS (ppm) | |
|---|---|---|---|---|---|---|---|---|---|---|---|---|---|---|---|---|---|---|---|---|
| | $^{207}Pb/^{206}Pb$ | ± 2σ | $^{207}Pb/^{235}U$ | ± 2σ | $^{206}Pb/^{238}U$ | ± 2σ | $^{208}Pb/^{232}Th$ | ± 2σ | $^{207}Pb/^{206}Pb$ | ± 2σ | $^{207}Pb/^{235}U$ | ± 2σ | $^{206}Pb/^{238}U$ | ± 2σ | $^{208}Pb/^{232}Th$ | ± 2σ | Used Age | ± 2σ | Th | U |
| BT070309 | 0.19725 | 0.00209 | 14.62994 | 0.1302 | 0.53797 | 0.0045 | 0.15428 | 0.00202 | 2804 | 10 | 2791 | 8 | 2775 | 19 | 2900 | 35 | 2804 | 10 | | |
| BT070311 | 0.20846 | 0.00223 | 15.97426 | 0.14255 | 0.5558 | 0.00462 | 0.15118 | 0.00202 | 2894 | 10 | 2875 | 9 | 2849 | 19 | 2846 | 35 | 2894 | 10 | | |
| BT070312 | 0.19889 | 0.00291 | 14.94404 | 0.18641 | 0.54501 | 0.00472 | 0.1597 | 0.00479 | 2817 | 14 | 2812 | 12 | 2804 | 20 | 2995 | 83 | 2817 | 14 | | |
| BT070315 | 0.19389 | 0.00211 | 14.37646 | 0.13253 | 0.5378 | 0.00453 | 0.15084 | 0.00224 | 2775 | 11 | 2775 | 9 | 2774 | 19 | 2840 | 39 | 2775 | 11 | | |
| BT070316 | 0.1846 | 0.00214 | 13.07073 | 0.13309 | 0.51356 | 0.00454 | 0.14328 | 0.00277 | 2695 | 11 | 2685 | 10 | 2672 | 19 | 2706 | 49 | 2695 | 11 | | |
| BT070317 | 0.197 | 0.00221 | 14.83133 | 0.13757 | 0.54606 | 0.00444 | 0.15454 | 0.00262 | 2802 | 11 | 2804 | 9 | 2809 | 19 | 2905 | 46 | 2802 | 11 | | |
| BT070318 | 0.19313 | 0.00222 | 14.03805 | 0.13688 | 0.52722 | 0.00452 | 0.14619 | 0.0025 | 2769 | 10 | 2752 | 9 | 2730 | 19 | 2758 | 44 | 2769 | 10 | | |
| BT070319 | 0.19471 | 0.00219 | 14.30254 | 0.12571 | 0.53281 | 0.00406 | 0.15081 | 0.00239 | 2782 | 11 | 2770 | 8 | 2753 | 17 | 2839 | 42 | 2782 | 11 | | |
| BT070320 | 0.21362 | 0.00231 | 16.37425 | 0.14507 | 0.55599 | 0.00456 | 0.14728 | 0.00194 | 2933 | 10 | 2899 | 8 | 2850 | 19 | 2777 | 34 | 2933 | 10 | | |
| BT070322 | 0.20569 | 0.00219 | 15.88689 | 0.1365 | 0.56023 | 0.0045 | 0.15167 | 0.00193 | 2872 | 10 | 2870 | 8 | 2868 | 19 | 2854 | 34 | 2872 | 10 | | |
| BT070323 | 0.18507 | 0.00215 | 12.87164 | 0.11843 | 0.50451 | 0.00392 | 0.14017 | 0.00242 | 2699 | 11 | 2670 | 9 | 2633 | 17 | 2651 | 43 | 2699 | 11 | | |
| BT070324 | 0.20569 | 0.00217 | 15.62304 | 0.13696 | 0.55091 | 0.00454 | 0.14808 | 0.00188 | 2872 | 10 | 2854 | 8 | 2829 | 19 | 2791 | 33 | 2872 | 10 | | |
| BT070328 | 0.20843 | 0.00224 | 16.25546 | 0.14532 | 0.56568 | 0.00469 | 0.15289 | 0.00207 | 2893 | 10 | 2892 | 9 | 2890 | 19 | 2876 | 36 | 2893 | 10 | | |
| BT070329 | 0.19509 | 0.0021 | 14.45466 | 0.1281 | 0.5374 | 0.00438 | 0.15057 | 0.00212 | 2786 | 10 | 2780 | 8 | 2773 | 18 | 2835 | 37 | 2786 | 10 | | |
| BT070330 | 0.19388 | 0.00217 | 14.37299 | 0.13499 | 0.53772 | 0.00452 | 0.14958 | 0.00231 | 2775 | 11 | 2775 | 9 | 2774 | 19 | 2818 | 41 | 2775 | 11 | | |
| BT070331 | 0.17757 | 0.00247 | 12.26969 | 0.14138 | 0.50121 | 0.00404 | 0.14606 | 0.0041 | 2630 | 13 | 2625 | 11 | 2619 | 17 | 2756 | 72 | 2630 | 13 | | |
| BT390301 | 0.18927 | 0.00217 | 13.73856 | 0.1391 | 0.52652 | 0.00477 | 0.14707 | 0.00233 | 2736 | 11 | 2732 | 10 | 2727 | 20 | 2773 | 41 | 2736 | 11 | | |
| BT390303 | 0.12482 | 0.00134 | 6.4266 | 0.05656 | 0.37347 | 0.00304 | 0.11077 | 0.00143 | 2026 | 11 | 2036 | 8 | 2046 | 14 | 2123 | 26 | 2026 | 11 | | |
| BT390305 | 0.18772 | 0.00233 | 13.68242 | 0.15982 | 0.52866 | 0.00521 | 0.15014 | 0.00339 | 2722 | 13 | 2728 | 11 | 2736 | 22 | 2827 | 60 | 2722 | 13 | | |
| BT390309 | 0.14999 | 0.00164 | 8.49889 | 0.08283 | 0.41101 | 0.00368 | 0.11591 | 0.00177 | 2346 | 11 | 2286 | 9 | 2220 | 17 | 2217 | 32 | 2346 | 11 | | |
| BT390310 | 0.18998 | 0.00267 | 13.47177 | 0.18467 | 0.51434 | 0.00561 | 0.14157 | 0.00397 | 2742 | 14 | 2713 | 13 | 2675 | 24 | 2676 | 70 | 2742 | 14 | | |
| BT390311 | 0.18518 | 0.00216 | 13.18678 | 0.13282 | 0.51651 | 0.00462 | 0.1572 | 0.00274 | 2700 | 11 | 2693 | 10 | 2684 | 20 | 2951 | 48 | 2700 | 11 | | |
| BT390312 | 0.19048 | 0.00227 | 13.68388 | 0.15145 | 0.52107 | 0.005 | 0.14487 | 0.0029 | 2746 | 11 | 2728 | 10 | 2704 | 21 | 2735 | 51 | 2746 | 11 | | |
| BT390313 | 0.19237 | 0.0028 | 14.25702 | 0.17842 | 0.5374 | 0.00431 | 0.16449 | 0.00561 | 2763 | 14 | 2767 | 12 | 2773 | 18 | 3078 | 97 | 2763 | 14 | | |
| BT390314 | 0.18682 | 0.0021 | 13.4931 | 0.13212 | 0.52389 | 0.0046 | 0.14388 | 0.00238 | 2714 | 11 | 2715 | 9 | 2716 | 19 | 2717 | 42 | 2714 | 11 | | |
| BT390315 | 0.18329 | 0.00244 | 13.04633 | 0.16367 | 0.51628 | 0.00519 | 0.14459 | 0.00375 | 2683 | 12 | 2683 | 12 | 2683 | 22 | 2730 | 66 | 2683 | 12 | | |
| BT390316 | 0.19326 | 0.0022 | 14.25997 | 0.14445 | 0.53519 | 0.0048 | 0.14941 | 0.00274 | 2770 | 11 | 2767 | 10 | 2763 | 20 | 2815 | 48 | 2770 | 11 | | |
| BT390321 | 0.1899 | 0.00217 | 13.91569 | 0.14234 | 0.53151 | 0.00494 | 0.14267 | 0.00209 | 2741 | 11 | 2744 | 10 | 2748 | 21 | 2696 | 37 | 2741 | 11 | | |
| BT390323 | 0.19296 | 0.00279 | 14.12544 | 0.17326 | 0.53105 | 0.00452 | 0.15106 | 0.00447 | 2768 | 13 | 2758 | 12 | 2746 | 19 | 2844 | 78 | 2768 | 13 | | |
| BT390326 | 0.18947 | 0.00216 | 13.80351 | 0.12625 | 0.5284 | 0.0042 | 0.15187 | 0.00242 | 2738 | 11 | 2736 | 9 | 2735 | 18 | 2858 | 42 | 2738 | 11 | | |
| BT390328 | 0.19232 | 0.0021 | 14.02951 | 0.13252 | 0.52911 | 0.00464 | 0.14686 | 0.00199 | 2762 | 10 | 2752 | 9 | 2738 | 20 | 2770 | 35 | 2762 | 10 | | |
| BT390329 | 0.19113 | 0.00207 | 14.06164 | 0.12834 | 0.53361 | 0.00453 | 0.15186 | 0.00203 | 2752 | 11 | 2754 | 9 | 2757 | 19 | 2858 | 36 | 2752 | 11 | | |
| BT390330 | 0.18035 | 0.00225 | 12.48552 | 0.14454 | 0.50213 | 0.00498 | 0.14075 | 0.00278 | 2656 | 12 | 2642 | 11 | 2623 | 21 | 2662 | 49 | 2656 | 12 | | |
| BT390331 | 0.18485 | 0.00257 | 13.10465 | 0.17659 | 0.51422 | 0.00551 | 0.14668 | 0.00415 | 2697 | 12 | 2687 | 13 | 2675 | 23 | 2766 | 73 | 2697 | 12 | | |
| BT390332 | 0.12886 | 0.00228 | 6.49699 | 0.10137 | 0.36576 | 0.00366 | 0.11375 | 0.00374 | 2082 | 18 | 2045 | 14 | 2009 | 17 | 2178 | 68 | 2082 | 18 | | |
| BT390333 | 0.14617 | 0.00175 | 8.18973 | 0.08448 | 0.40637 | 0.0036 | 0.10974 | 0.00198 | 2302 | 13 | 2252 | 9 | 2198 | 17 | 2105 | 36 | 2302 | 13 | | |
| BT390335 | 0.15336 | 0.00141 | 9.10154 | 0.11574 | 0.43044 | 0.00276 | 0.12042 | 0.00075 | 2384 | 9 | 2348 | 12 | 2308 | 12 | 2298 | 13 | 2384 | 9 | | |

**Appendix 3.2. Zircon trace-element data (ppm) for the samples from the Markha terrane**

| Analysis No. | P | Ti | Y | Nb | La | Ce | Pr | Nd | Sm | Eu | Gd | Dy | Ho | Er | Yb | Lu | Hf | Ta | Th | U | Th/U | Nb/Ta | Total REE | U-Pb age |
|---|---|---|---|---|---|---|---|---|---|---|---|---|---|---|---|---|---|---|---|---|---|---|---|---|
| **Upper Muna field, Zimnyaya pipe** | | | | | | | | | | | | | | | | | | | | | | | | |
| 8008-01 | 77.8 | 6.4 | 584.9 | 2.11 | 0.01 | 25.66 | 0.08 | 1.37 | 2.99 | 0.32 | 12.40 | 52.02 | 19.60 | 89.35 | 167.56 | 32.55 | 6116 | 0.567 | 29.79 | 58.87 | 0.51 | 0.27 | 403.91 | 271 |
| 8008-02 | 133.8 | 3.4 | 523.5 | 1.29 | 0.04 | 15.72 | 0.07 | 0.91 | 1.94 | 0.93 | 10.56 | 42.35 | 16.36 | 79.55 | 173.58 | 36.59 | 9634 | 0.257 | 57.58 | 111.45 | 0.52 | 0.20 | 378.60 | 309 |
| 8008-02R | 91.2 | 4.8 | 488.1 | 1.52 | 0.12 | 20.48 | 0.10 | 1.14 | 2.18 | 0.97 | 10.88 | 40.28 | 15.42 | 74.70 | 155.88 | 32.91 | 9553 | 0.311 | 70.59 | 122.79 | 0.57 | 0.20 | 355.06 | 297 |
| 8008-06 | 96.1 | 9.3 | 1916.5 | 1.98 | 0.05 | 4.56 | 0.40 | 5.87 | 10.62 | 2.45 | 50.72 | 187.94 | 66.63 | 281.48 | 477.11 | 88.93 | 6663 | 0.502 | 43.72 | 155.92 | 0.28 | 0.25 | 1176.76 | 455 |
| 8008-07 | 178.6 | 75.9 | 1227.4 | 3.86 | 0.57 | 13.75 | 0.29 | 2.05 | 2.91 | 0.40 | 19.28 | 94.69 | 38.09 | 188.07 | 426.36 | 87.12 | 11629 | 2.334 | 268.16 | 850.5 | 0.32 | 0.60 | 873.57 | 200 |
| 8008-08 | 208.0 | 11.8 | 1091.4 | 3.73 | 0.17 | 57.78 | 0.20 | 3.10 | 5.19 | 1.70 | 23.25 | 93.55 | 35.53 | 165.14 | 331.08 | 67.04 | 8498 | 0.956 | 205.69 | 135.33 | 1.52 | 0.26 | 783.73 | 260 |
| 8008-09 | 162.6 | 25.2 | 256.8 | 0.64 | 0.02 | 3.00 | 0.15 | 2.22 | 5.16 | 0.18 | 19.83 | 35.20 | 8.45 | 27.26 | 34.41 | 5.74 | 12468 | 0.094 | 116.38 | 137.74 | 0.84 | 0.15 | 141.62 | 2609 |
| 8008-10C | 156.1 | 5.6 | 947.4 | 1.90 | 0.03 | 13.21 | 0.20 | 3.00 | 5.14 | 0.72 | 25.23 | 89.94 | 31.99 | 140.83 | 246.73 | 46.93 | 9812 | 0.59 | 71.16 | 91.65 | 0.78 | 0.31 | 603.95 | 2649 |
| 8008-10R | 89.1 | 4.6 | 390.5 | 2.18 | 0.01 | 8.80 | 0.04 | 0.57 | 1.20 | 0.12 | 6.79 | 31.10 | 12.32 | 60.60 | 135.99 | 27.90 | 11195 | 0.893 | 50.96 | 144.32 | 0.35 | 0.41 | 285.44 | 2589 |
| 8008-11C | 193.7 | 17.0 | 921.0 | 3.15 | 18.72 | 78.67 | 6.12 | 26.88 | 10.86 | 3.09 | 23.08 | 73.56 | 26.05 | 127.68 | 309.54 | 67.14 | 10911 | 0.74 | 236.99 | 297.49 | 0.80 | 0.23 | 771.39 | 2556 |
| 8008-11R | 97.9 | 7.0 | 226.0 | 1.35 | 0.13 | 18.82 | 0.12 | 1.14 | 1.40 | 0.52 | 5.46 | 18.88 | 7.10 | 32.94 | 72.18 | 14.95 | 10082 | 0.435 | 57.14 | 53.96 | 1.06 | 0.32 | 173.65 | 1848 |
| 8008-12C | 194.3 | 14.7 | 504.3 | 1.70 | 0.62 | 17.18 | 0.26 | 1.92 | 2.04 | 0.37 | 10.57 | 40.82 | 15.69 | 75.32 | 159.31 | 32.66 | 10141 | 0.581 | 99.64 | 135.33 | 0.74 | 0.34 | 356.76 | 290 |
| 8008-13C | 398.4 | 8.5 | 2052.4 | 4.55 | 0.42 | 27.14 | 0.33 | 2.55 | 3.99 | 1.07 | 26.70 | 145.53 | 62.15 | 323.73 | 739.54 | 158.65 | 9262 | 1.119 | 197.74 | 347.48 | 0.57 | 0.25 | 1491.80 | 427 |
| 8008-14C | 148.9 | 10.6 | 682.2 | 2.77 | 0.13 | 25.95 | 0.09 | 1.02 | 2.75 | 0.54 | 13.02 | 52.77 | 21.28 | 103.22 | 237.50 | 48.67 | 10359 | 0.976 | 175.98 | 207.12 | 0.85 | 0.35 | 506.95 | 272 |
| 8008-18 | 133.0 | 5.0 | 706.6 | 1.46 | | 9.36 | 0.06 | 0.91 | 2.43 | 0.25 | 14.74 | 60.53 | 23.71 | 107.20 | 199.82 | 39.37 | 9710 | 0.563 | 59.42 | 117.35 | 0.51 | 0.39 | 458.38 | 202 |
| 8008-21 | 191.3 | 37.8 | 1203.3 | 3.37 | 1.49 | 15.65 | 0.63 | 3.77 | 4.18 | 0.10 | 23.16 | 101.14 | 38.72 | 179.22 | 344.19 | 66.74 | 12584 | 1.499 | 221.36 | 701.98 | 0.32 | 0.44 | 778.99 | 175 |
| 8008-22 | 147.1 | 6.5 | 414.6 | 1.26 | 0.07 | 26.80 | 0.08 | 1.43 | 2.80 | 0.56 | 11.56 | 36.95 | 12.93 | 57.87 | 116.11 | 24.02 | 10078 | 0.357 | 117.35 | 146.87 | 0.80 | 0.28 | 291.18 | 2662 |
| 8008-27 | 611.7 | 65.1 | 1791.3 | 2.68 | 11.05 | 45.50 | 5.08 | 51.61 | 10.81 | 0.11 | 37.73 | 156.94 | 59.00 | 265.37 | 486.83 | 90.26 | 13332 | 1.414 | 313.41 | 859.85 | 0.36 | 0.53 | 1220.29 | 176 |
| 8008-29 | 212.2 | 7.0 | 1208.0 | 3.84 | 0.28 | 46.11 | 0.28 | 3.68 | 6.00 | 1.02 | 26.96 | 101.87 | 38.41 | 176.87 | 361.95 | 72.71 | 10705 | 1.615 | 233.42 | 286.27 | 0.82 | 0.42 | 836.14 | 302 |
| 8008-30 | 149.8 | 8.8 | 1089.0 | 1.50 | 0.14 | 21.45 | 0.19 | 2.66 | 4.89 | 0.76 | 21.00 | 91.19 | 35.37 | 166.82 | 349.59 | 70.51 | 8853 | 0.497 | 51.01 | 54.48 | 0.94 | 0.33 | 764.57 | 289 |
| 8008-32 | 170.6 | 8.3 | 307.1 | 1.08 | 0.12 | 1.82 | 0.09 | 0.93 | 1.93 | 0.07 | 9.54 | 27.45 | 9.51 | 39.32 | 75.35 | 14.51 | 12756 | 0.433 | 75.07 | 367.88 | 0.20 | 0.40 | 180.63 | 2541 |
| 8008-43C | 244.9 | 52.9 | 2568.3 | 4.63 | 0.13 | 23.30 | 0.31 | 5.59 | 10.95 | 1.02 | 57.94 | 229.39 | 85.23 | 382.00 | 693.04 | 133.13 | 9912 | 1.634 | 460.16 | 837.53 | 0.55 | 0.35 | 1622.02 | 190 |
| 8008-49 | 139.7 | 7.4 | 751.2 | 1.52 | 0.05 | 14.09 | 0.10 | 1.60 | 2.82 | 1.06 | 13.50 | 57.27 | 23.31 | 112.20 | 247.10 | 52.84 | 7656 | 0.388 | 72.17 | 94.41 | 0.76 | 0.26 | 525.93 | 311 |
| 8008-51 | 343.3 | 34.7 | 1891.2 | 3.41 | 0.22 | 29.60 | 0.20 | 3.28 | 5.79 | 1.71 | 34.46 | 153.89 | 60.91 | 290.93 | 607.91 | 123.82 | 10504 | 1.084 | 155.99 | 279.59 | 0.56 | 0.32 | 1312.72 | 405 |
| 8008-52 | 2202.3 | 5005.1 | 3395.6 | 6.86 | 15.58 | 77.05 | 9.19 | 65.84 | 76.06 | 21.95 | 184.53 | 416.50 | 107.84 | 510.82 | ###### | 152.94 | 12868 | 3.75 | 258.81 | 584.62 | 0.44 | 0.55 | 2642.70 | 399 |
| 8008-59 | 172.9 | 7.7 | 463.6 | 0.99 | 0.01 | 16.57 | 0.09 | 1.55 | 2.33 | 0.52 | 11.83 | 40.90 | 14.82 | 67.43 | 126.91 | 25.70 | 9613 | 0.166 | 27.09 | 17.1 | 1.58 | 0.17 | 308.65 | 2745 |
| **Upper Muna field, 325 years of Yakutia pipe** | | | | | | | | | | | | | | | | | | | | | | | | |
| MVG124-01 | 132.7 | 17.8 | 22.9 | 5.54 | 0.0005 | 1.01 | 0.01 | 0.09 | 0.23 | 0.12 | 0.86 | 2.36 | 0.72 | 2.69 | 4.01 | 0.62 | 19492 | 4.62 | 1.98 | 8.92 | 0.22 | 0.83 | 12.72 | 359 |
| MVG124-02 | 118.5 | 22.3 | 44.8 | 5.52 | <0 | 1.35 | 0.02 | 0.24 | 0.36 | 0.24 | 1.85 | 5.27 | 1.57 | 5.76 | 8.70 | 1.32 | 18254 | 4.39 | 2.75 | 12.9 | 0.21 | 0.80 | 26.68 | 369 |
| MVG124-03 | 85.2 | 23.5 | 81.9 | 5.91 | <0 | 2.04 | 0.05 | 0.78 | 1.35 | 0.76 | 4.58 | 11.3 | 3.07 | 10.5 | 13.9 | 2.05 | 18917 | 4.04 | 5.38 | 14.9 | 0.36 | 0.68 | 50.23 | 349 |
| MVG124-04 | 99.1 | 18.3 | 32.4 | 5.43 | <0 | 1.23 | 0.01 | 0.18 | 0.32 | 0.19 | 1.31 | 3.74 | 1.11 | 4.13 | 6.05 | 0.89 | 19739 | 4.21 | 2.21 | 9.65 | 0.23 | 0.78 | 19.17 | 341 |
| MVG124-05 | 106.4 | 24.9 | 89.7 | 7.48 | <0.01 | 2.22 | 0.08 | 1.16 | 1.59 | 0.92 | 5.11 | 12.3 | 3.23 | 11.4 | 14.8 | 2.29 | 18540 | 5.34 | 6.33 | 17.7 | 0.36 | 0.71 | 55.10 | 360 |
| MVG124-06 | 84.4 | 20.6 | 82.9 | 5.68 | <0 | 1.92 | 0.05 | 0.81 | 1.27 | 0.75 | 4.64 | 11.5 | 3.05 | 10.4 | 14.3 | 2.08 | 18610 | 3.90 | 5.34 | 15.5 | 0.35 | 0.69 | 50.74 | 357 |
| MVG124-07 | 84.6 | 20.0 | 90.4 | 6.33 | 0.0041 | 2.09 | 0.04 | 0.52 | 1.18 | 0.76 | 5.05 | 12.2 | 3.40 | 11.4 | 15.6 | 2.36 | 17617 | 4.74 | 6.14 | 18.6 | 0.33 | 0.75 | 54.58 | 369 |
| MVG124-08 | 98.1 | 17.8 | 38.8 | 5.26 | 0.0021 | 1.32 | 0.01 | 0.29 | 0.40 | 0.25 | 1.54 | 4.73 | 1.31 | 4.80 | 7.21 | 1.12 | 19470 | 3.86 | 2.52 | 10.9 | 0.23 | 0.73 | 22.99 | 352 |
| MVG124-09 | 88.8 | 20.6 | 83.3 | 5.47 | 0.0055 | 1.83 | 0.05 | 0.96 | 1.41 | 0.75 | 4.50 | 11.8 | 3.05 | 10.7 | 14.2 | 2.15 | 18671 | 4.06 | 5.34 | 15.3 | 0.35 | 0.74 | 51.41 | 350 |
| MVG124-10 | 84.8 | 19.4 | 90.1 | 6.32 | <0 | 2.04 | 0.03 | 0.53 | 1.29 | 0.73 | 4.57 | 12.3 | 3.36 | 11.6 | 16.1 | 2.32 | 17809 | 4.67 | 6.13 | 18.6 | 0.33 | 0.74 | 54.84 | 344 |
| MVG124-11 | 84.2 | 19.5 | 90.2 | 6.21 | 0.0061 | 2.16 | 0.04 | 0.62 | 1.33 | 0.80 | 4.82 | 12.3 | 3.32 | 11.6 | 16.0 | 2.39 | 17831 | 4.52 | 6.26 | 18.8 | 0.33 | 0.73 | 55.43 | 366 |
| MVG125-01 | 74.2 | 22.0 | 62.6 | 5.37 | <0.01 | 1.46 | 0.03 | 0.32 | 0.40 | 0.38 | 2.66 | 7.44 | 2.27 | 7.62 | 11.4 | 1.70 | 19909 | 3.95 | 3.37 | 12.4 | 0.27 | 0.74 | 35.66 | 362 |
| MVG125-02 | 101.1 | 16.5 | 21.8 | 5.78 | <0 | 1.05 | 0.01 | 0.12 | 0.21 | 0.15 | 0.88 | 2.43 | 0.70 | 2.71 | 3.82 | 0.60 | 20824 | 5.00 | 1.95 | 8.16 | 0.24 | 0.87 | 12.67 | 353 |
| MVG125-03 | 88.4 | 21.4 | 82.1 | 5.42 | <0 | 1.99 | 0.05 | 0.88 | 1.38 | 0.79 | 4.66 | 11.3 | 3.00 | 10.5 | 13.7 | 2.09 | 19313 | 3.94 | 5.37 | 15.1 | 0.35 | 0.73 | 50.37 | 365 |
| MVG125-04 | 103.7 | 17.6 | 45.6 | 4.47 | 0.0045 | 1.32 | 0.02 | 0.23 | 0.41 | 0.28 | 1.81 | 5.38 | 1.61 | 6.02 | 8.93 | 1.39 | 17132 | 3.58 | 2.71 | 13.6 | 0.20 | 0.80 | 27.39 | 345 |
| MVG125-05 | 110.8 | 18.2 | 44.9 | 5.26 | 0.0046 | 1.35 | 0.02 | 0.19 | 0.50 | 0.28 | 1.67 | 5.44 | 1.54 | 5.65 | 8.85 | 1.33 | 18504 | 4.31 | 2.78 | 13.2 | 0.21 | 0.82 | 26.81 | 374 |

| Analysis No. | P | Ti | Y | Nb | La | Ce | Pr | Nd | Sm | Eu | Gd | Dy | Ho | Er | Yb | Lu | Hf | Ta | Th | U | Th/U | Nb/Ta | Total REE | U-Pb age |
|---|---|---|---|---|---|---|---|---|---|---|---|---|---|---|---|---|---|---|---|---|---|---|---|---|
| MVG125-06 | 100.1 | 18.0 | 24.3 | 5.81 | <0 | 1.12 | 0.01 | 0.15 | 0.20 | 0.13 | 0.98 | 2.82 | 0.81 | 2.98 | 4.46 | 0.70 | 19084 | 5.37 | 2.01 | 9.48 | 0.21 | 0.92 | 14.35 | 357 |
| MVG125-07 | 103.7 | 18.5 | 38.4 | 5.24 | <0 | 1.33 | <0.01 | 0.21 | 0.41 | 0.25 | 1.48 | 4.54 | 1.28 | 4.86 | 7.48 | 1.11 | 19690 | 4.03 | 2.35 | 10.5 | 0.22 | 0.77 | 22.94 | 355 |
| MVG125-08 | 87.3 | 17.1 | 37.2 | 4.73 | <0 | 1.33 | 0.02 | 0.18 | 0.33 | 0.23 | 1.56 | 4.56 | 1.28 | 4.77 | 7.21 | 1.09 | 18464 | 3.60 | 2.42 | 11.0 | 0.22 | 0.76 | 22.55 | 359 |
| MVG125-09 | 90.5 | 18.2 | 21.6 | 5.77 | <0 | 1.00 | 0.01 | 0.08 | 0.22 | 0.13 | 0.72 | 2.27 | 0.70 | 2.71 | 3.70 | 0.60 | 19585 | 4.52 | 1.70 | 8.34 | 0.20 | 0.78 | 12.13 | 368 |
| MVG125-10 | 96.2 | 19.2 | 39.5 | 5.01 | 0.0044 | 1.35 | 0.01 | 0.20 | 0.39 | 0.27 | 1.47 | 4.85 | 1.34 | 4.91 | 7.66 | 1.12 | 19253 | 3.87 | 2.55 | 11.2 | 0.23 | 0.77 | 23.58 | 364 |
| MVG125-11 | 101.3 | 20.7 | 42.8 | 5.25 | <0.01 | 1.39 | 0.01 | 0.23 | 0.42 | 0.26 | 1.52 | 5.04 | 1.52 | 5.39 | 8.10 | 1.21 | 18419 | 4.03 | 2.50 | 11.3 | 0.22 | 0.77 | 25.10 | 345 |
| MVG125-12 | 105.5 | 20.2 | 46.0 | 5.32 | <0 | 1.29 | 0.01 | 0.30 | 0.47 | 0.31 | 1.74 | 5.39 | 1.62 | 6.10 | 9.48 | 1.42 | 18157 | 4.36 | 2.72 | 12.3 | 0.22 | 0.82 | 28.12 | 361 |
| MVG125-13 | 113.7 | 21.0 | 45.5 | 5.20 | <0.01 | 1.32 | 0.01 | 0.32 | 0.44 | 0.27 | 1.76 | 5.36 | 1.62 | 5.91 | 8.66 | 1.34 | 18408 | 4.44 | 2.80 | 13.2 | 0.21 | 0.85 | 27.01 | 357 |
| MVG125-14 | 105.1 | 19.3 | 43.5 | 4.77 | <0.01 | 1.25 | 0.02 | 0.22 | 0.41 | 0.26 | 1.81 | 5.41 | 1.54 | 5.56 | 8.33 | 1.31 | 18028 | 4.09 | 2.72 | 13.2 | 0.21 | 0.86 | 26.10 | 350 |
| MVG125-15 | 80.0 | 21.8 | 87.9 | 5.67 | <0.01 | 1.88 | 0.04 | 0.74 | 1.20 | 0.70 | 4.56 | 11.8 | 3.23 | 11.4 | 15.2 | 2.22 | 18769 | 4.09 | 5.45 | 16.0 | 0.34 | 0.72 | 53.03 | 347 |
| MVG125-16 | 94.5 | 20.2 | 40.3 | 5.15 | 0.0041 | 1.34 | 0.02 | 0.20 | 0.41 | 0.25 | 1.57 | 4.73 | 1.38 | 5.16 | 7.82 | 1.15 | 19314 | 3.85 | 2.46 | 10.7 | 0.23 | 0.75 | 24.02 | 364 |
| MVG125-17 | 91.1 | 18.5 | 39.0 | 4.99 | <0.01 | 1.28 | 0.01 | 0.30 | 0.45 | 0.22 | 1.45 | 4.51 | 1.28 | 4.88 | 7.50 | 1.10 | 18173 | 3.93 | 2.52 | 11.5 | 0.22 | 0.79 | 22.97 | 368 |
| MVG125-18 | 102.2 | 16.8 | 39.0 | 5.05 | <0.01 | 1.24 | 0.02 | 0.27 | 0.37 | 0.26 | 1.68 | 4.65 | 1.39 | 4.85 | 7.49 | 1.16 | 18883 | 3.96 | 2.40 | 11.3 | 0.21 | 0.78 | 23.37 | 373 |
| **Daldyn field, Udachnaya Eastern pipe** | | | | | | | | | | | | | | | | | | | | | | | | |
| UE-1c | 3408.7 | 7.2 | 1078.5 | 5.66 | 33.54 | 133.75 | 9.03 | 35.99 | 10.15 | 1.97 | 26.70 | 88.66 | 33.44 | 161.48 | 361.81 | 73.79 | 19719 | 1.60 | 496.9 | 850.3 | 0.58 | 0.28 | 970.31 | 2512 |
| UE-1r | 8136.7 | 6.5 | 416.2 | 4.34 | 102.39 | 250.99 | 27.87 | 104.22 | 14.95 | 3.38 | 16.59 | 34.84 | 12.52 | 60.99 | 158.69 | 33.14 | 19534 | 1.05 | 143.7 | 409.8 | 0.35 | 0.24 | 820.57 | 2536 |
| UE-2 | 1046.3 | 46.3 | 736.9 | 7.50 | 8.06 | 92.50 | 5.51 | 27.77 | 9.93 | 3.28 | 20.22 | 58.78 | 21.89 | 107.38 | 288.52 | 64.32 | 20596 | 1.07 | 639.9 | 1363.5 | 0.47 | 0.14 | 708.16 | 2625 |
| UE-3 | 3516.2 | 10.5 | 648.2 | 5.19 | 57.29 | 174.33 | 16.00 | 63.76 | 12.89 | 2.35 | 19.99 | 49.58 | 19.10 | 93.64 | 247.20 | 56.36 | 17912 | 1.07 | 423.5 | 846.1 | 0.50 | 0.21 | 812.49 | 2634 |
| UE-4 | 1763.8 | 10.6 | 1435.9 | 5.71 | 8.55 | 86.96 | 4.90 | 27.18 | 13.84 | 2.20 | 41.13 | 128.77 | 46.03 | 210.64 | 439.00 | 87.99 | 19010 | 1.42 | 574.2 | 777.7 | 0.74 | 0.25 | 1097.19 | 2643 |
| UE-5 | 642.1 | 21.0 | 1933.9 | 56.16 | 3.63 | 35.11 | 2.90 | 18.44 | 13.28 | 2.40 | 41.11 | 173.91 | 67.31 | 312.26 | 643.81 | 127.98 | 31216 | 23.84 | 573.0 | 2056.4 | 0.28 | 0.42 | 1442.14 | 2493 |
| UE-6c | 962.7 | 19.6 | 1629.3 | 9.89 | 24.91 | 172.86 | 7.25 | 30.34 | 13.31 | 2.39 | 46.29 | 149.04 | 52.03 | 224.28 | 418.31 | 76.59 | 16766 | 2.62 | 712.5 | 783.6 | 0.91 | 0.26 | 1217.60 | 2367 |
| UE-6r | 438.0 | 14.2 | 1158.1 | 6.56 | 0.28 | 43.46 | 0.31 | 3.80 | 6.33 | 0.66 | 28.49 | 110.70 | 38.21 | 165.04 | 278.75 | 47.46 | 17921 | 1.37 | 171.1 | 93.3 | 1.83 | 0.21 | 723.49 | 1940 |
| UE-7c | 1203.3 | 2552.3 | 4003.4 | 38.57 | 7.01 | 252.48 | 14.37 | 91.92 | 58.48 | 11.80 | 95.19 | 277.14 | 104.20 | 543.00 | 1302.7 | 259.61 | 20797 | 6.11 | 2646.8 | 3296.0 | 0.80 | 0.16 | 3017.85 | 2049 |
| UE-7r | 418.6 | 23.4 | 1062.5 | 6.48 | 0.09 | 73.86 | 0.39 | 5.34 | 9.00 | 0.51 | 36.06 | 113.10 | 35.70 | 142.92 | 213.62 | 36.53 | 18797 | 1.12 | 323.6 | 164.1 | 1.97 | 0.17 | 667.12 | 1864 |
| **Daldyn field, Zarnitsa pipe** | | | | | | | | | | | | | | | | | | | | | | | | |
| Z-01 | 270.4 | 37.3 | 697.9 | 9.31 | <0.0162 | 26.29 | 0.17 | 2.89 | 4.92 | 0.86 | 19.33 | 65.12 | 23.58 | 99.67 | 189.23 | 34.40 | 15469 | 2.28 | 86.5 | 53.6 | 1.61 | 0.24 | 466.46 | 1937 |
| Z-05 | 248.7 | 20.6 | 993.2 | 9.77 | 0.80 | 42.13 | 1.13 | 12.67 | 13.11 | 6.12 | 40.67 | 100.32 | 32.20 | 139.70 | 265.91 | 51.07 | 13927 | 3.29 | 796.6 | 423.5 | 1.88 | 0.34 | 705.82 | 1962 |
| Z-06 | 133.5 | 12.5 | 343.1 | 20.55 | 0.28 | 28.95 | 0.17 | 1.24 | 1.64 | 0.63 | 5.36 | 26.21 | 10.09 | 51.92 | 159.03 | 30.19 | 15378 | 20.29 | 399.3 | 446.9 | 0.89 | 0.99 | 315.71 | 1860 |
| Z-06r | 235.8 | 21.4 | 586.5 | 15.13 | <0.0217 | 27.21 | 0.18 | 1.65 | 1.83 | 0.66 | 9.77 | 43.57 | 17.13 | 89.45 | 235.35 | 49.66 | 16430 | 8.88 | 328.3 | 319.0 | 1.03 | 0.59 | 476.46 | 1954 |
| Z-07 | 208.0 | 41.5 | 419.9 | 33.43 | 0.81 | 35.06 | 1.05 | 6.36 | 4.59 | 1.13 | 14.35 | 43.20 | 14.14 | 60.82 | 123.46 | 25.11 | 12225 | 9.47 | 470.6 | 1453.3 | 0.32 | 0.28 | 330.08 | 1973 |
| Z-08 | 2689.0 | 10.8 | 1330.0 | 8.71 | 46.93 | 145.47 | 11.24 | 40.83 | 8.20 | 1.24 | 26.07 | 106.87 | 42.56 | 204.73 | 455.07 | 86.38 | 19954 | 2.55 | 227.5 | 424.9 | 0.54 | 0.29 | 1175.59 | 2437 |
| Z-09 | 240.5 | 38.4 | 570.7 | 9.11 | 0.11 | 32.46 | 0.30 | 3.67 | 5.12 | 0.93 | 18.71 | 55.40 | 18.44 | 78.43 | 147.12 | 27.19 | 15294 | 1.71 | 22.2 | 38.4 | 0.58 | 0.19 | 387.88 | 2052 |
| Z-10 | 424.3 | 34.4 | 1553.9 | 7.75 | 0.16 | 44.34 | 0.43 | 5.42 | 10.41 | 0.73 | 48.60 | 153.65 | 52.48 | 214.02 | 359.47 | 63.97 | 21495 | 1.61 | 987.6 | 770.0 | 1.28 | 0.21 | 953.69 | 1996 |
| Z-11 | 813.1 | 34.0 | 2431.5 | 7.84 | 4.19 | 62.29 | 4.72 | 27.06 | 20.97 | 4.25 | 55.11 | 216.74 | 80.63 | 363.69 | 732.53 | 134.84 | 16919 | 1.83 | 325.7 | 641.3 | 0.51 | 0.23 | 1707.02 | 2639 |
| Z-15 | 100.4 | 14.8 | 152.1 | 3.58 | 0.10 | 11.78 | 0.16 | 1.98 | 4.48 | 2.26 | 19.42 | 26.71 | 4.98 | 11.52 | 7.09 | 0.79 | 18977 | 1.00 | 112.3 | 560.5 | 0.20 | 0.28 | 91.27 | 2007 |
| **Daldyn field, Popugaeva pipe** | | | | | | | | | | | | | | | | | | | | | | | | |
| P_15 | 193.6 | 15.6 | 664.7 | 2.05 | 0.16 | 30.33 | 0.26 | 2.84 | 4.72 | 1.02 | 18.76 | 60.79 | 21.29 | 94.71 | 203.04 | 35.32 | 9943 | 0.72 | 219.9 | 307.7 | 0.71 | 0.35 | 473.25 | 2465 |
| P_16c | 356.7 | 23.9 | 1420.8 | 6.24 | 0.53 | 26.27 | 0.35 | 3.13 | 4.95 | 0.53 | 30.69 | 134.40 | 49.88 | 212.52 | 354.20 | 55.69 | 7987 | 1.37 | 200.9 | 233.0 | 0.86 | 0.22 | 873.14 | 2763 |
| P_16r | 213.3 | 19.8 | 557.5 | 2.63 | 0.01 | 19.22 | 0.05 | 0.94 | 2.25 | 0.20 | 12.55 | 52.43 | 19.06 | 84.37 | 165.60 | 28.75 | 10843 | 0.62 | 76.1 | 70.5 | 1.08 | 0.24 | 385.43 | 2359 |
| P_17 | 152.7 | 5.6 | 1066.9 | 1.58 | 0.03 | 25.59 | 0.50 | 8.37 | 11.52 | 1.77 | 41.38 | 112.56 | 36.77 | 148.50 | 255.18 | 42.32 | 9029 | 0.39 | 104.4 | 77.7 | 1.34 | 0.25 | 684.50 | 2849 |
| P_18 | 72.7 | 10.7 | 47.9 | 1.46 | 0.01 | 10.26 | 0.06 | 0.80 | 1.21 | 0.54 | 3.84 | 6.71 | 1.59 | 4.62 | 5.59 | 0.79 | 7921 | 0.41 | 125.4 | 139.6 | 0.90 | 0.28 | 36.02 | 1875 |
| P_19 | 316.7 | 13.6 | 600.4 | 3.29 | 0.46 | 34.65 | 0.36 | 3.06 | 3.19 | 0.61 | 13.56 | 53.74 | 19.83 | 91.63 | 202.55 | 36.17 | 10195 | 1.10 | 62.3 | 39.6 | 1.57 | 0.33 | 459.81 | 2087 |
| P_20 | 291.4 | 23.6 | 907.2 | 3.77 | 0.14 | 39.16 | 0.30 | 3.61 | 5.55 | 1.96 | 22.38 | 79.67 | 29.18 | 136.79 | 323.75 | 59.54 | 9319 | 2.17 | 211.7 | 434.9 | 0.49 | 0.58 | 702.02 | 3317 |
| P_20r | 117.7 | 17.7 | 235.2 | 1.34 | 0.06 | 13.77 | 0.14 | 1.54 | 1.98 | 0.46 | 7.80 | 23.66 | 7.91 | 32.70 | 59.52 | 10.50 | 10508 | 0.21 | 255.9 | 91.7 | 2.79 | 0.16 | 160.02 | 2083 |
| P_21 | 536.8 | 14.2 | 1378.8 | 4.14 | 4.29 | 25.27 | 0.82 | 3.65 | 4.41 | 0.44 | 30.35 | 132.95 | 48.57 | 209.14 | 354.18 | 58.75 | 10045 | 1.14 | 146.8 | 232.5 | 0.63 | 0.28 | 872.82 | 2117 |

| Analysis No. | P | Ti | Y | Nb | La | Ce | Pr | Nd | Sm | Eu | Gd | Dy | Ho | Er | Yb | Lu | Hf | Ta | Th | U | Th/U | Nb/Ta | Total REE | U-Pb age |
|---|---|---|---|---|---|---|---|---|---|---|---|---|---|---|---|---|---|---|---|---|---|---|---|---|
| P-01 | 242.4 | 44.0 | 314.6 | 5.90 | 0.03 | 17.40 | 0.17 | 1.89 | 2.43 | 0.80 | 10.30 | 30.83 | 10.54 | 42.72 | 81.16 | 15.24 | 14360 | 0.993 | 27.6 | 26.3 | 1.05 | 0.17 | 213.51 | 1822 |
| P-02 | 358.4 | 76.8 | 2872.9 | 27.38 | 39.65 | 252.00 | 14.78 | 70.48 | 31.88 | 5.18 | 93.68 | 284.09 | 95.52 | 409.06 | 737.45 | 130.46 | 17107 | 5.78 | 915.5 | 848.7 | 1.08 | 0.21 | 2164.23 | 1950 |
| P-03 | 251.9 | 26.5 | 528.2 | 3.61 | 0.05 | 34.32 | 0.15 | 1.88 | 3.85 | 0.98 | 13.49 | 45.82 | 16.09 | 76.16 | 167.29 | 34.55 | 16876 | 0.551 | 100.6 | 98.0 | 1.03 | 0.15 | 394.63 | 1974 |
| P-04 | 275.0 | 39.2 | 727.1 | 40.78 | 0.10 | 33.85 | 0.60 | 7.91 | 9.10 | 1.65 | 27.65 | 76.20 | 25.14 | 104.23 | 202.61 | 41.10 | 16976 | 7.79 | 436.6 | 511.1 | 0.85 | 0.19 | 530.14 | 1972 |
| P-05 | 244.3 | 42.4 | 299.2 | 5.53 | <0.0147 | 16.60 | 0.12 | 1.54 | 2.10 | 0.69 | 7.91 | 27.55 | 9.89 | 43.47 | 87.18 | 17.19 | 14779 | 0.927 | 33.1 | 34.8 | 0.95 | 0.17 | 214.25 | 1926 |
| P-07 | 279.9 | 50.5 | 339.6 | 9.00 | <0.0155 | 8.03 | 0.05 | 1.15 | 1.78 | 0.36 | 7.61 | 30.16 | 10.94 | 49.59 | 96.52 | 19.26 | 17257 | 4.49 | 28.4 | 44.9 | 0.63 | 0.50 | 225.45 | 1896 |
| P-08 | 219.3 | 46.0 | 302.1 | 4.44 | 0.08 | 24.43 | 0.20 | 2.37 | 2.49 | 1.13 | 8.60 | 28.67 | 9.88 | 41.09 | 74.42 | 13.69 | 15604 | 1.115 | 156.6 | 77.5 | 2.02 | 0.25 | 207.05 | 1891 |
| P-10 | 240.8 | 24.9 | 760.6 | 23.72 | 0.02 | 28.31 | 0.15 | 2.65 | 3.99 | 0.58 | 19.69 | 65.99 | 23.94 | 108.97 | 214.37 | 42.86 | 15585 | 8.96 | 186.6 | 210.8 | 0.88 | 0.38 | 511.52 | 1930 |
| P-12 | 659.3 | 29.6 | 1744.7 | 3.96 | 0.06 | 34.22 | 0.34 | 5.62 | 11.47 | 3.08 | 52.99 | 181.60 | 62.62 | 254.36 | 367.17 | 64.60 | 16824 | 0.635 | 72.9 | 60.1 | 1.21 | 0.16 | 1038.13 | 2333 |
| P-12R | 442.5 | 31.7 | 1060.5 | 4.67 | 0.11 | 36.96 | 0.36 | 3.79 | 7.53 | 1.57 | 32.76 | 110.42 | 37.86 | 158.76 | 256.42 | 45.67 | 17644 | 0.597 | 82.6 | 52.9 | 1.56 | 0.13 | 692.21 | 2331 |
| P-13_R | 220.0 | 30.9 | 395.7 | 4.56 | 0.02 | 14.04 | 0.11 | 1.13 | 1.80 | 0.55 | 8.04 | 31.75 | 12.02 | 57.39 | 126.88 | 25.79 | 13808 | 1.25 | 66.6 | 85.3 | 0.78 | 0.27 | 279.53 | 1942 |
| P-13C | 324.4 | 102.7 | 635.9 | 5.87 | 0.72 | 17.73 | 0.48 | 3.65 | 3.31 | 0.80 | 14.31 | 54.30 | 19.98 | 87.91 | 171.47 | 34.03 | 16530 | 1.56 | 244.0 | 180.0 | 1.36 | 0.27 | 408.69 | 1993 |
| P-14 | 143.3 | 20.2 | 459.5 | 103.15 | 0.03 | 10.90 | 0.05 | 0.62 | 0.92 | 0.27 | 5.80 | 32.02 | 13.98 | 77.10 | 199.58 | 37.68 | 20691 | 33.73 | 216.3 | 763.6 | 0.28 | 0.33 | 378.95 | 1947 |
| **Daldyn field, Zagadochnaya pipe** | | | | | | | | | | | | | | | | | | | | | | | | |
| Zag_01 | 387.1 | 17.3 | 1170.5 | 13.0 | 1.34 | 38.1 | 1.27 | 9.66 | 11.2 | 2.38 | 40.1 | 121 | 40.1 | 171 | 325 | 54.1 | 9371 | 1.03 | 153 | 337 | 0.45 | 0.08 | 814.81 | 2126 |
| Zag_02 | 178.0 | 142.6 | 494.3 | 33.1 | 1.29 | 32.0 | 1.73 | 10.8 | 6.93 | 2.70 | 14.6 | 42.0 | 15.4 | 73.6 | 173 | 32.2 | 10088 | 1.37 | 78.8 | 424 | 0.19 | 0.04 | 406.39 | 2385 |
| Zag_03 | 1459.4 | 17.8 | 763.7 | 6.59 | 12.2 | 96.7 | 6.21 | 31.5 | 9.96 | 1.87 | 21.1 | 64.3 | 23.3 | 111 | 286 | 52.9 | 11024 | 1.07 | 355 | 642 | 0.55 | 0.16 | 717.13 | 2598 |
| Zag_04 | 56.0 | 57.1 | 414.5 | 24.4 | 2.34 | 49.3 | 2.75 | 17.5 | 10.6 | 2.99 | 21.9 | 46.5 | 14.4 | 61.2 | 116 | 19.4 | 9419 | 2.45 | 856 | 1671 | 0.51 | 0.10 | 365.17 | 1906 |
| Zag_05 | 162.8 | 18.5 | 425.3 | 9.55 | 2.23 | 16.8 | 0.87 | 5.18 | 3.66 | 0.85 | 11.1 | 39.7 | 13.9 | 61.5 | 124 | 21.3 | 9605 | 0.74 | 43.0 | 155 | 0.28 | 0.08 | 300.73 | 1991 |
| Zag_06 | 302.4 | 47.3 | 911.9 | 86.8 | 7.12 | 99.8 | 9.37 | 58.6 | 31.3 | 12.6 | 51.3 | 107 | 29.0 | 108 | 182 | 29.1 | 11774 | 1.50 | 153 | 516 | 0.30 | 0.02 | 725.39 | 2020 |
| Zag_07c | 125.6 | 14.9 | 469.6 | 4.54 | 0.74 | 22.5 | 0.21 | 1.60 | 1.93 | 0.67 | 9.05 | 36.8 | 14.3 | 71.4 | 187 | 35.8 | 10541 | 0.70 | 147 | 251 | 0.59 | 0.15 | 382.12 | 2624 |
| Zag_07r | 127.7 | 65.3 | 339.7 | 184 | 22.3 | 66.8 | 5.68 | 20.6 | 4.05 | 1.14 | 8.48 | 30.6 | 11.0 | 50.8 | 113 | 19.7 | 10934 | 1.28 | 77.7 | 147 | 0.53 | 0.01 | 353.88 | 1875 |
| Zag_08 | 133.7 | 17.3 | 224.1 | 1.37 | 0.01 | 7.39 | 0.03 | 0.57 | 0.83 | 0.41 | 4.39 | 19.2 | 7.24 | 34.1 | 85.2 | 15.3 | 7920 | 0.51 | 71.1 | 86.8 | 0.82 | 0.37 | 174.65 | 1927 |
| Zag_09 | 207.0 | 17.2 | 221.0 | 1.37 | 0.01 | 1.26 | 0.06 | 1.35 | 3.43 | 0.11 | 13.1 | 28.3 | 7.38 | 25.9 | 51.2 | 8.36 | 12248 | 0.73 | 42.6 | 270 | 0.16 | 0.53 | 140.49 | 1911 |
| Zag_10 | 245.9 | 14.8 | 562.9 | 7.96 | 0.63 | 35.2 | 0.81 | 6.20 | 5.52 | 2.10 | 15.7 | 47.8 | 17.2 | 82.4 | 233 | 43.3 | 10439 | 0.77 | 104 | 305 | 0.34 | 0.10 | 489.84 | 2027 |
| Zag_11 | 383.3 | 8.2 | 1097.5 | 4.67 | 0.72 | 13.0 | 0.96 | 6.63 | 3.93 | 1.06 | 11.1 | 74.7 | 34.3 | 191 | 592 | 107 | 16127 | 8.31 | 73.4 | 1978 | 0.04 | 1.78 | 1036.73 | 1931 |
| Zag_12 | 268.5 | 10.1 | 632.2 | 5.18 | 0.26 | 24.6 | 0.45 | 4.95 | 7.64 | 3.06 | 24.6 | 66.2 | 21.5 | 90.0 | 207 | 33.1 | 8803 | 0.43 | 157 | 436 | 0.36 | 0.08 | 482.87 | 2390 |
| Zag_13 | 172.6 | 13.7 | 569.5 | 1.03 | 0.03 | 18.4 | 0.19 | 2.98 | 4.39 | 2.10 | 16.4 | 52.3 | 18.4 | 81.3 | 195 | 34.8 | 7663 | 0.26 | 84.3 | 91.7 | 0.92 | 0.25 | 426.13 | 2488 |
| Zag_14 | 260.9 | 6.5 | 697.7 | 2.09 | 0.02 | 50.7 | 0.23 | 4.56 | 8.44 | 1.86 | 27.3 | 70.7 | 22.5 | 93.1 | 209 | 35.2 | 9747 | 0.53 | 234 | 241 | 0.97 | 0.25 | 523.65 | 2403 |
| Zag_15 | 204.4 | 11.9 | 592.0 | 9.15 | 0.31 | 26.0 | 0.51 | 4.09 | 4.04 | 1.20 | 13.6 | 50.3 | 18.6 | 87.3 | 232 | 42.2 | 11081 | 1.73 | 326 | 921 | 0.35 | 0.19 | 480.15 | 2189 |
| Zag_16 | 668.7 | 14.5 | 1358.1 | 13.8 | 2.47 | 44.7 | 1.80 | 12.4 | 10.8 | 2.62 | 36.2 | 133 | 46.9 | 201 | 419 | 64.6 | 10353 | 1.06 | 222 | 427 | 0.52 | 0.08 | 975.63 | 2379 |
| Zag_17 | 319.8 | 15.8 | 818.7 | 11.6 | 11.6 | 65.7 | 3.15 | 17.1 | 10.5 | 2.87 | 27.8 | 86.4 | 28.7 | 120 | 242 | 39.2 | 10375 | 0.70 | 90.5 | 203 | 0.45 | 0.06 | 654.72 | 2148 |
| Zag_18 | 133.9 | 12.0 | 402.2 | 1.74 | 0.10 | 21.2 | 0.12 | 1.59 | 2.38 | 0.77 | 9.57 | 35.6 | 13.0 | 60.1 | 154 | 27.5 | 10925 | 0.56 | 71.7 | 125 | 0.57 | 0.32 | 326.35 | 2636 |
| Zag_19 | 423.7 | 18.1 | 1751.3 | 5.02 | 4.57 | 70.9 | 2.44 | 17.2 | 12.9 | 4.79 | 45.5 | 162 | 60.7 | 272 | 601 | 105 | 6984 | 0.44 | 279 | 229 | 1.22 | 0.09 | 1359.26 | 2029 |
| Zag_20 | 284.1 | 27.1 | 625.2 | 28.6 | 3.87 | 60.8 | 3.16 | 19.0 | 10.5 | 3.55 | 19.0 | 57.1 | 20.4 | 95.5 | 260 | 47.5 | 12893 | 1.25 | 204 | 967 | 0.21 | 0.04 | 600.35 | 2413 |
| Zag_21 | 150.2 | 11.9 | 411.3 | 9.94 | 0.36 | 14.5 | 0.57 | 4.28 | 3.36 | 1.49 | 9.09 | 32.3 | 12.2 | 60.9 | 173 | 33.3 | 9009 | 0.74 | 162 | 392 | 0.41 | 0.07 | 345.18 | 2460 |
| Zag_22 | 105.3 | 17.0 | 199.4 | 3.24 | 0.03 | 12.7 | 0.09 | 1.30 | 1.65 | 0.43 | 5.52 | 19.1 | 6.31 | 28.6 | 71.3 | 11.0 | 9037 | 0.36 | 13.3 | 36.4 | 0.36 | 0.11 | 157.94 | 2708 |
| Zag_23 | 572.8 | 86.9 | 1638.9 | 115 | 12.9 | 146 | 16.1 | 101 | 50.0 | 14.8 | 75.6 | 167 | 52.9 | 233 | 495 | 87.6 | 11149 | 1.94 | 207 | 469 | 0.44 | 0.02 | 1451.08 | 2008 |
| Zag_24 | 338.9 | 14.6 | 841.1 | 18.2 | 0.58 | 27.8 | 0.78 | 6.04 | 6.21 | 1.60 | 21.7 | 77.5 | 27.6 | 126 | 262 | 46.0 | 9930 | 1.37 | 95.0 | 131 | 0.73 | 0.08 | 604.27 | 2344 |
| Zag_25 | 174.1 | 10.7 | 485.6 | 4.75 | 0.33 | 21.6 | 0.57 | 4.93 | 4.94 | 1.31 | 15.6 | 44.8 | 15.3 | 69.6 | 156 | 28.5 | 9074 | 0.71 | 82.3 | 129 | 0.64 | 0.15 | 363.52 | 2469 |
| Zag_26 | 345.4 | 14.8 | 288.8 | 8.67 | 3.15 | 31.5 | 1.41 | 7.80 | 3.56 | 0.93 | 8.24 | 25.1 | 8.81 | 43.0 | 109 | 21.2 | 10467 | 0.68 | 110 | 186 | 0.59 | 0.08 | 263.07 | 1955 |
| Zag_27 | 393.1 | 20.0 | 1083.8 | 6.15 | 0.14 | 5.28 | 0.25 | 3.67 | 6.82 | 0.61 | 31.5 | 108 | 36.5 | 155 | 292 | 48.1 | 10194 | 0.94 | 163 | 261 | 0.62 | 0.15 | 687.32 | 1947 |
| Zag_28 | 420.7 | 81.3 | 1538.8 | 83.6 | 7.66 | 288 | 9.26 | 52.8 | 30.1 | 10.5 | 57.6 | 166 | 52.4 | 222 | 419 | 68.0 | 11285 | 2.75 | 452 | 802 | 0.56 | 0.03 | 1383.34 | 2189 |
| Zag_29 | 160.3 | 12.4 | 503.2 | 1.66 | 0.02 | 27.1 | 0.10 | 1.89 | 3.06 | 0.95 | 12.4 | 41.8 | 15.5 | 74.5 | 184 | 35.1 | 9532 | 0.49 | 102 | 130 | 0.78 | 0.29 | 396.55 | 2340 |
| Zag_31 | 132.1 | 16.6 | 270.8 | 1.54 | 0.02 | 11.4 | 0.21 | 3.07 | 3.79 | 0.97 | 12.7 | 30.4 | 9.08 | 36.3 | 65.9 | 11.1 | 8690 | 0.56 | 25.9 | 33.0 | 0.78 | 0.36 | 184.88 | 1915 |
| Zag_32 | 104.4 | 11.7 | 121.6 | 6.52 | 0.59 | 14.9 | 0.89 | 6.64 | 5.14 | 1.21 | 11.8 | 17.6 | 4.00 | 13.4 | 21.4 | 3.64 | 11999 | 0.45 | 91.6 | 148 | 0.62 | 0.07 | 101.10 | 1834 |
| Zag_33 | 244.0 | 3.8 | 569.3 | 5.51 | 0.14 | 20.0 | 0.27 | 3.05 | 4.30 | 1.07 | 15.5 | 50.9 | 17.7 | 80.9 | 181 | 34.0 | 10269 | 0.39 | 91.8 | 139 | 0.66 | 0.07 | 408.28 | 2486 |

| Analysis No. | P | Ti | Y | Nb | La | Ce | Pr | Nd | Sm | Eu | Gd | Dy | Ho | Er | Yb | Lu | Hf | Ta | Th | U | Th/U | Nb/Ta | Total REE | U-Pb age |
|---|---|---|---|---|---|---|---|---|---|---|---|---|---|---|---|---|---|---|---|---|---|---|---|---|
| Zag_34 | 208.0 | 10.1 | 555.9 | 0.97 | 0.01 | 10.3 | 0.09 | 1.84 | 3.52 | 1.07 | 14.6 | 49.4 | 17.8 | 84.1 | 195 | 35.8 | 9857 | 0.35 | 57.7 | 97.3 | 0.59 | 0.37 | 413.07 | 2334 |
| Zag_35 | 138.9 | 14.7 | 324.8 | 3.97 | 0.10 | 8.17 | 0.14 | 1.29 | 1.30 | 0.47 | 5.62 | 23.8 | 9.63 | 51.7 | 158 | 33.2 | 9568 | 0.37 | 72.1 | 123 | 0.59 | 0.09 | 293.73 | 2305 |
| Zag_36 | 306.1 | 14.0 | 585.2 | 13.5 | 2.41 | 33.6 | 1.91 | 13.3 | 8.87 | 2.74 | 20.2 | 53.3 | 18.1 | 85.3 | 211 | 40.9 | 10004 | 0.73 | 141 | 206 | 0.69 | 0.05 | 491.78 | 2539 |
| Zag_37 | 457.1 | 39.6 | 1141.4 | 68.0 | 3.86 | 55.7 | 4.65 | 30.2 | 20.1 | 5.45 | 55.2 | 139 | 36.7 | 132 | 202 | 32.4 | 12453 | 1.85 | 144 | 1187 | 0.12 | 0.03 | 716.58 | 1938 |
| **Daldyn field, Kusova pipe** | | | | | | | | | | | | | | | | | | | | | | | | |
| K_01 | 96.7 | 14.5 | 347.2 | 1.94 | 0.01 | 15.6 | 0.05 | 0.92 | 1.70 | 0.66 | 7.84 | 29.6 | 11.2 | 52.6 | 142 | 26.1 | 11037 | 0.91 | 63.2 | 195 | 0.32 | 0.47 | 287.95 | 2660 |
| K_02 | 335.7 | 238.2 | 641.6 | 4.60 | 0.11 | 4.63 | 0.24 | 3.90 | 7.18 | 0.19 | 28.0 | 75.0 | 22.3 | 80.0 | 128 | 18.9 | 10920 | 0.73 | 92.7 | 122 | 0.76 | 0.16 | 368.52 | 1963 |
| K_03 | 264.8 | 10.8 | 749.0 | 1.67 | 0.14 | 35.9 | 0.25 | 4.97 | 8.51 | 3.00 | 28.9 | 78.4 | 25.5 | 105 | 219 | 36.5 | 8509 | 0.40 | 107 | 82.5 | 1.30 | 0.24 | 545.89 | 2241 |
| K_05 | 134.0 | 22.4 | 858.2 | 19.4 | 3.89 | 55.1 | 4.82 | 34.0 | 21.0 | 13.1 | 35.4 | 84.5 | 27.5 | 119 | 296 | 53.3 | 9213 | 1.22 | 656 | 1034 | 0.63 | 0.06 | 747.39 | 2038 |
| K_07 | 54.4 | 10.7 | 59.1 | 0.89 | 0.00 | 1.13 | 0.02 | 0.40 | 0.79 | 0.27 | 3.37 | 8.02 | 2.01 | 6.39 | 8.54 | 1.17 | 8460 | 0.15 | 17.7 | 67.4 | 0.26 | 0.17 | 32.10 | 1918 |
| K_08 | 239.2 | 17.0 | 539.1 | 1.90 | 0.01 | 3.52 | 0.09 | 1.73 | 3.49 | 0.17 | 16.0 | 54.8 | 18.9 | 77.8 | 156 | 25.4 | 10599 | 0.46 | 56.8 | 81.4 | 0.70 | 0.24 | 358.21 | 1924 |
| K_10 | 217.2 | 18.4 | 976.8 | 6.35 | 1.07 | 50.5 | 2.14 | 15.8 | 9.61 | 2.92 | 18.6 | 64.9 | 26.5 | 140 | 467 | 91.9 | 12107 | 1.71 | 887 | 1789 | 0.50 | 0.27 | 890.91 | 2482 |
| K_11c | 571.2 | 11.9 | 680.1 | 10.0 | 23.0 | 92.5 | 5.45 | 23.0 | 7.24 | 1.71 | 17.5 | 58.8 | 22.0 | 102 | 260 | 46.4 | 10072 | 0.74 | 254 | 356 | 0.71 | 0.07 | 659.41 | 2528 |
| K_11r | 129.2 | 11.5 | 246.2 | 1.29 | 0.04 | 33.0 | 0.08 | 1.33 | 2.16 | 0.23 | 8.67 | 26.5 | 8.89 | 36.0 | 66.1 | 10.2 | 9537 | 0.22 | 99.1 | 16.2 | 6.13 | 0.17 | 193.24 | 2066 |
| K_12 | 107.1 | 19.6 | 131.0 | 1.07 | 0.03 | 9.04 | 0.05 | 0.74 | 1.10 | 0.26 | 4.12 | 13.0 | 4.45 | 18.7 | 42.1 | 7.32 | 9904 | 0.15 | 8.80 | 19.3 | 0.46 | 0.14 | 100.86 | 1900 |
| K_13 | 498.7 | 19.9 | 1325.6 | 12.7 | 0.40 | 9.99 | 0.75 | 9.32 | 13.3 | 0.89 | 47.5 | 143 | 47.2 | 187 | 357 | 56.6 | 10637 | 0.87 | 221 | 238 | 0.93 | 0.07 | 873.38 | 1945 |
| K_15 | 304.4 | 13.0 | 1346.8 | 5.65 | 0.14 | 75.2 | 0.53 | 7.24 | 10.0 | 3.01 | 38.1 | 128 | 45.1 | 194 | 430 | 70.1 | 8148 | 1.02 | 323 | 285 | 1.13 | 0.18 | 1000.88 | 2652 |
| K_16 | 747.0 | 14.5 | 1972.3 | 3.58 | 0.02 | 15.8 | 0.31 | 5.73 | 11.9 | 0.38 | 53.6 | 195 | 65.3 | 266 | 537 | 91.3 | 11188 | 1.30 | 292 | 221 | 1.32 | 0.36 | 1241.61 | 1971 |
| K_19 | 60.7 | 13.6 | 222.2 | 0.68 | 0.01 | 2.07 | 0.01 | 0.20 | 0.50 | 0.16 | 3.53 | 18.3 | 7.45 | 35.7 | 85.7 | 15.2 | 9488 | 0.10 | 9.41 | 33.8 | 0.28 | 0.15 | 168.82 | 2176 |
| K_21 | 212.9 | 21.5 | 464.1 | 16.7 | 0.56 | 14.4 | 0.96 | 8.41 | 8.75 | 1.88 | 22.3 | 57.7 | 15.7 | 54.3 | 90.9 | 14.0 | 10893 | 0.64 | 84.6 | 245 | 0.34 | 0.04 | 289.80 | 2032 |
| K_22 | 187.0 | 8.2 | 425.5 | 7.95 | 0.68 | 21.9 | 0.51 | 3.89 | 3.47 | 0.98 | 11.0 | 38.1 | 14.0 | 63.3 | 156 | 28.7 | 11064 | 0.52 | 83.6 | 214 | 0.39 | 0.07 | 342.23 | 2502 |
| K_23 | 225.0 | 28.1 | 605.8 | 13.9 | 1.67 | 42.2 | 0.98 | 6.98 | 5.38 | 1.98 | 14.8 | 52.3 | 19.1 | 87.6 | 219 | 40.1 | 10984 | 1.09 | 345 | 486 | 0.71 | 0.08 | 491.77 | 2345 |
| K_24 | 105.9 | 8.1 | 264.2 | 1.42 | 0.01 | 6.48 | 0.02 | 0.38 | 0.74 | 0.35 | 4.59 | 21.5 | 8.52 | 40.5 | 105 | 19.2 | 8958 | 0.62 | 141 | 172 | 0.82 | 0.44 | 207.00 | 1883 |
| K_26 | 5780.8 | 10.1 | 423.9 | 1.10 | 253 | 517 | 57.8 | 246 | 37.7 | 2.47 | 32.5 | 46.1 | 14.4 | 60.1 | 136 | 23.9 | 9330 | 0.30 | 63.7 | 93.1 | 0.68 | 0.27 | 1425.98 | 2650 |
| K_27 | 125.2 | 19.9 | 127.8 | 1.25 | 0.24 | 10.1 | 0.10 | 0.96 | 1.15 | 0.24 | 4.08 | 12.3 | 4.29 | 18.2 | 41.5 | 7.24 | 10029 | 0.18 | 11.6 | 24.9 | 0.47 | 0.15 | 100.44 | 1916 |
| K_28 | 108.6 | 10.3 | 180.2 | 1.02 | 0.00 | 12.5 | 0.03 | 0.53 | 0.98 | 0.32 | 4.30 | 16.1 | 5.90 | 26.7 | 66.3 | 11.9 | 9874 | 0.25 | 7.18 | 14.1 | 0.51 | 0.25 | 145.57 | 1851 |
| K_29 | 182.4 | 18.2 | 756.0 | 11.2 | 0.51 | 11.5 | 0.78 | 5.97 | 5.21 | 1.57 | 15.8 | 67.8 | 25.9 | 120 | 275 | 44.9 | 10618 | 1.50 | 54.6 | 176 | 0.31 | 0.13 | 574.77 | 2005 |
| K_30 | 487.5 | 249.2 | 1171.8 | 17.9 | 11.9 | 60.3 | 2.94 | 16.8 | 11.6 | 3.85 | 37.1 | 119 | 41.2 | 173 | 366 | 60.2 | 9546 | 0.71 | 247 | 442 | 0.56 | 0.04 | 904.58 | 2200 |
| K_31 | 383.4 | 24.9 | 908.8 | 12.5 | 0.74 | 36.6 | 0.45 | 4.53 | 6.94 | 2.05 | 26.7 | 87.3 | 30.7 | 134 | 298 | 49.6 | 10233 | 0.84 | 161 | 192 | 0.84 | 0.07 | 677.65 | 2023 |
| K_33 | 317.3 | 12.7 | 1096.1 | 7.71 | 0.53 | 93.2 | 0.57 | 6.33 | 9.08 | 3.64 | 34.6 | 107 | 35.8 | 149 | 320 | 53.2 | 8698 | 0.96 | 389 | 268 | 1.45 | 0.12 | 812.50 | 2454 |
| K_34 | 101.8 | 13.2 | 163.5 | 1.35 | 0.01 | 3.05 | 0.03 | 0.36 | 0.59 | 0.22 | 2.96 | 13.4 | 5.27 | 25.5 | 65.7 | 11.8 | 7828 | 0.54 | 49.3 | 81.6 | 0.60 | 0.40 | 128.80 | 1917 |
| K_35 | 1461.3 | 18.1 | 548.6 | 32.0 | 62.2 | 175 | 17.4 | 80.3 | 21.1 | 4.21 | 27.8 | 56.7 | 18.0 | 77.6 | 181 | 33.2 | 11345 | 1.00 | 183 | 235 | 0.78 | 0.03 | 754.74 | 2473 |
| K_37 | 355.5 | 541.9 | 1007.3 | 3.01 | 0.10 | 9.88 | 0.13 | 2.17 | 5.43 | 1.24 | 26.9 | 100 | 35.1 | 148 | 311 | 51.7 | 9466 | 0.62 | 106 | 178 | 0.59 | 0.21 | 692.41 | 2355 |
| K_38 | 406.3 | 21.6 | 1500.6 | 26.6 | 2.06 | 52.3 | 3.13 | 21.8 | 16.6 | 4.42 | 43.9 | 151 | 54.7 | 231 | 502 | 75.9 | 9071 | 1.68 | 250 | 298 | 0.84 | 0.06 | 1159.00 | 2498 |
| K_40 | 1563.8 | 16.9 | 1122.8 | 30.7 | 24.4 | 90.5 | 9.19 | 51.4 | 22.6 | 7.49 | 43.3 | 114 | 38.8 | 165 | 369 | 62.9 | 8152 | 0.79 | 116 | 263 | 0.44 | 0.03 | 998.18 | 1991 |
| K_41 | 175.8 | 7.4 | 450.9 | 1.42 | 0.14 | 22.2 | 0.08 | 1.25 | 2.28 | 0.69 | 10.2 | 38.7 | 14.4 | 66.7 | 166 | 29.2 | 10544 | 0.41 | 49.1 | 77.9 | 0.63 | 0.29 | 351.61 | 2637 |
| K_42 | 689.8 | 11.0 | 346.7 | 29.6 | 12.4 | 44.6 | 3.50 | 20.0 | 10.1 | 3.49 | 15.0 | 33.7 | 11.1 | 49.2 | 128 | 23.1 | 11182 | 0.59 | 142 | 486 | 0.29 | 0.02 | 354.15 | 2017 |
| K_43 | 197.3 | 93.5 | 1218.1 | 414 | 30.0 | 241 | 28.2 | 173 | 80.5 | 31.5 | 88.1 | 145 | 40.5 | 161 | 377 | 68.1 | 10743 | 2.06 | 530 | 741 | 0.71 | 0.00 | 1463.21 | 2022 |
| K_47 | 289.6 | 21.1 | 616.1 | 16.3 | 0.96 | 15.2 | 1.12 | 8.14 | 5.58 | 1.98 | 15.8 | 58.4 | 17.4 | 80.9 | 171 | 35.5 | 12101 | 1.55 | 123 | 570 | 0.22 | 0.09 | 411.61 | 1921 |
| K_48 | 363.9 | 16.7 | 762.8 | 2.93 | 1.66 | 7.00 | 0.46 | 2.85 | 3.02 | 0.56 | 13.9 | 64.9 | 23.8 | 113 | 247 | 42.0 | 10887 | 0.44 | 38.9 | 298 | 0.13 | 0.15 | 520.07 | 1919 |
| K_49 | 234.9 | 16.7 | 678.5 | 17.6 | 0.94 | 25.7 | 1.65 | 11.8 | 9.11 | 2.79 | 21.3 | 67.4 | 21.7 | 93.1 | 210 | 35.2 | 11867 | 1.27 | 57.1 | 254 | 0.22 | 0.07 | 500.47 | 1978 |
| K_51 | 269.7 | 13.5 | 1076.2 | 7.55 | 0.42 | 66.9 | 1.01 | 10.0 | 10.3 | 3.61 | 33.6 | 102 | 34.4 | 151 | 320 | 55.5 | 8651 | 1.14 | 331 | 271 | 1.22 | 0.15 | 789.22 | 2509 |
| K_52 | 130.4 | 18.4 | 429.9 | 24.5 | 2.06 | 46.0 | 2.17 | 14.5 | 8.66 | 2.70 | 15.5 | 38.4 | 13.0 | 60.9 | 155 | 31.0 | 10320 | 0.75 | 177 | 272 | 0.65 | 0.03 | 389.90 | 2546 |
| K_53 | 135.2 | 10.5 | 336.7 | 3.16 | 0.05 | 17.7 | 0.13 | 1.55 | 2.21 | 0.63 | 8.35 | 30.7 | 10.7 | 49.2 | 112 | 20.7 | 9768 | 0.74 | 63.0 | 110 | 0.57 | 0.24 | 253.91 | 1986 |
| K_54 | 433.2 | 13.3 | 1047.9 | 10.9 | 9.47 | 25.9 | 1.60 | 7.06 | 4.94 | 1.09 | 23.8 | 96.3 | 35.6 | 160 | 323 | 55.6 | 10650 | 1.41 | 108 | 185 | 0.58 | 0.13 | 744.26 | 1858 |
| K_55 | 582.7 | 10.2 | 761.2 | 2.45 | 4.70 | 17.7 | 1.60 | 7.76 | 3.52 | 0.51 | 17.0 | 69.1 | 24.4 | 107 | 209 | 36.3 | 10798 | 1.35 | 82.5 | 189 | 0.44 | 0.55 | 499.11 | 2522 |
| K_56 | 1081.0 | 16.2 | 1038.2 | 13.6 | 7.50 | 42.5 | 3.46 | 20.2 | 9.97 | 2.04 | 22.9 | 80.1 | 31.8 | 164 | 449 | 89.4 | 10266 | 1.28 | 168 | 331 | 0.51 | 0.09 | 922.39 | 1939 |

| Analysis No. | P | Ti | Y | Nb | La | Ce | Pr | Nd | Sm | Eu | Gd | Dy | Ho | Er | Yb | Lu | Hf | Ta | Th | U | Th/U | Nb/Ta | Total REE | U-Pb age |
|---|---|---|---|---|---|---|---|---|---|---|---|---|---|---|---|---|---|---|---|---|---|---|---|---|
| K_57 | 192.2 | 27.6 | 449.2 | 6.94 | 0.27 | 4.09 | 0.39 | 4.33 | 5.85 | 0.50 | 22.4 | 54.7 | 15.1 | 53.1 | 79.8 | 11.8 | 9848 | 0.62 | 60.8 | 229 | 0.27 | 0.09 | 252.28 | 1895 |
| K_58 | 257.7 | 14.2 | 831.8 | 31.5 | 1.30 | 30.4 | 2.73 | 19.0 | 12.0 | 3.67 | 23.9 | 77.0 | 27.6 | 134 | 350 | 60.3 | 12671 | 1.25 | 76.8 | 431 | 0.18 | 0.04 | 741.58 | 1965 |
| K_59 | 338.3 | 42.3 | 1776.6 | 66.4 | 3.55 | 50.8 | 5.80 | 42.3 | 29.6 | 8.53 | 66.4 | 188 | 63.5 | 271 | 507 | 84.7 | 8672 | 2.26 | 238 | 461 | 0.52 | 0.03 | 1321.42 | 1966 |
| **Daldyn field, Udachnaya pipe** | | | | | | | | | | | | | | | | | | | | | | | | |
| OCYB2-11 | 67.8 | 11.9 | 49.7 | 1.47 | 0.00 | 4.02 | 0.02 | 0.41 | 0.53 | 0.28 | 2.71 | 6.08 | 1.75 | 5.44 | 7.33 | 1.07 | 6922 | 0.58 | 100.43 | 176.79 | 0.57 | 0.40 | 29.63 | 1852 |
| OCYB2-12 | 61.3 | 13.0 | 37.8 | 1.41 | 0.04 | 3.9 | 0.07 | 0.60 | 0.72 | 0.30 | 1.87 | 4.5 | 1.29 | 4.41 | 6.60 | 0.95 | 7208 | 0.52 | 75.19 | 139.65 | 0.54 | 0.37 | 25.25 | 1820 |
| OCYB2-13 | 75.8 | 12.6 | 35.6 | 1.58 | <0.0045 | 3.64 | 0.01 | 0.16 | 0.34 | 0.15 | 1.60 | 4.13 | 1.18 | 4.06 | 5.96 | 0.94 | 7202 | 0.61 | 92.6 | 160.75 | 0.58 | 0.39 | 22.17 | 1851 |
| OCYB2-15 | 61.7 | 9.3 | 56.9 | 1.24 | 0.00 | 4.15 | 0.02 | 0.40 | 0.58 | 0.35 | 2.97 | 7.27 | 1.92 | 6.29 | 8.41 | 1.25 | 7344 | 0.48 | 113.68 | 210.21 | 0.54 | 0.39 | 33.61 | 1847 |
| OCYB2-18 | 60.9 | 14.7 | 32.0 | 0.99 | 0.00 | 3.93 | 0.02 | 0.21 | 0.45 | 0.19 | 1.62 | 3.87 | 1.06 | 3.32 | 4.89 | 0.66 | 6641 | 0.23 | 70.65 | 99.01 | 0.71 | 0.24 | 20.20 | 1841 |
| OCYB2-19 | 63.8 | 9.7 | 34.8 | 1.82 | 0.00 | 4.83 | 0.01 | 0.30 | 0.51 | 0.23 | 1.81 | 4.42 | 1.07 | 3.59 | 4.82 | 0.70 | 6796 | 0.86 | 164.61 | 277.6 | 0.59 | 0.47 | 22.29 | 1849 |
| OCYB2-22 | 67.0 | 13.1 | 56.4 | 1.33 | 0.04 | 4.5 | 0.06 | 0.61 | 0.66 | 0.43 | 2.65 | 7.04 | 1.86 | 6.17 | 8.21 | 1.31 | 7069 | 0.57 | 98.56 | 185.72 | 0.53 | 0.43 | 33.53 | 1875 |
| OCYB2-23 | 77.2 | 13.2 | 25.8 | 1.64 | 0.00 | 3.61 | 0.02 | 0.15 | 0.27 | 0.13 | 1.14 | 2.9 | 0.85 | 3.05 | 4.11 | 0.69 | 7245 | 0.67 | 73.13 | 141.19 | 0.52 | 0.41 | 16.91 | 1872 |
| OCYB2-25 | 63.8 | 13.9 | 36.1 | 1.03 | 0.01 | 3.69 | 0.03 | 0.20 | 0.55 | 0.24 | 1.60 | 3.82 | 1.21 | 4.26 | 6.98 | 1.21 | 7060 | 0.34 | 62.86 | 96.54 | 0.65 | 0.33 | 23.78 | 1846 |
| OCYB2-27 | 66.8 | 12.5 | 42.4 | 1.17 | 0.00 | 3.71 | 0.02 | 0.27 | 0.37 | 0.27 | 1.96 | 4.8 | 1.42 | 4.86 | 7.13 | 1.08 | 6974 | 0.39 | 73.47 | 122.12 | 0.60 | 0.33 | 25.90 | 1840 |
| OCYB2-28 | 64.8 | 13.1 | 35.0 | 1.32 | 0.04 | 4.52 | 0.07 | 0.63 | 0.82 | 0.35 | 2.05 | 4.61 | 1.21 | 3.72 | 4.85 | 0.68 | 6862 | 0.55 | 112.17 | 128.62 | 0.87 | 0.42 | 23.55 | 1835 |
| OCYB2-29 | 63.9 | 9.7 | 52.5 | 1.71 | 0.02 | 4.83 | 0.04 | 0.53 | 0.88 | 0.36 | 2.91 | 6.82 | 1.91 | 5.65 | 7.40 | 1.05 | 6703 | 0.73 | 139.21 | 229.28 | 0.61 | 0.42 | 32.41 | 1849 |
| OCYB2-30 | 60.7 | 9.3 | 60.1 | 1.17 | 0.03 | 4.4 | 0.04 | 0.61 | 0.93 | 0.42 | 3.27 | 7.9 | 2.05 | 6.58 | 8.63 | 1.31 | 7057 | 0.51 | 125.23 | 220.7 | 0.57 | 0.43 | 36.18 | 1843 |
| OCYB2-31 | 76.0 | 10.2 | 27.9 | 1.36 | 0.03 | 4.24 | 0.03 | 0.22 | 0.42 | 0.23 | 1.53 | 3.22 | 0.97 | 3.02 | 4.09 | 0.57 | 6807 | 0.60 | 102.88 | 117.41 | 0.88 | 0.44 | 18.58 | 1868 |
| OCYB2-32 | 66.9 | 13.5 | 48.5 | 1.43 | 0.10 | 4.2 | 0.09 | 0.85 | 0.81 | 0.45 | 2.87 | 6.3 | 1.67 | 5.50 | 6.95 | 1.05 | 6891 | 0.54 | 84.07 | 147.87 | 0.57 | 0.37 | 30.83 | 1895 |
| OCYB2-8 | 60.8 | 11.7 | 64.4 | 1.48 | 0.03 | 4.85 | 0.07 | 0.74 | 0.93 | 0.40 | 3.24 | 8.05 | 2.20 | 6.95 | 9.44 | 1.51 | 7183 | 0.61 | 141.64 | 236.11 | 0.60 | 0.41 | 38.41 | 1840 |
| OCYB5-10 | 145.6 | 16.3 | 187.5 | 0.71 | 0.01 | 11.43 | 0.10 | 1.40 | 1.86 | 0.43 | 6.42 | 19.72 | 6.40 | 25.73 | 53.03 | 8.86 | 7188 | 0.14 | 10.32 | 7.23 | 1.43 | 0.20 | 135.38 | 1815 |
| OCYB5-12 | 115.1 | 8.9 | 173.4 | 0.82 | 0.05 | 12.15 | 0.07 | 0.83 | 1.30 | 0.31 | 4.95 | 17.19 | 5.84 | 24.78 | 54.28 | 9.48 | 8248 | 0.18 | 36.72 | 28.06 | 1.31 | 0.22 | 131.22 | 1916 |
| OCYB5-14 | 282.4 | 21.4 | 729.7 | 1.96 | 0.41 | 43.6 | 0.25 | 3.58 | 6.31 | 2.98 | 22.27 | 67.65 | 23.77 | 104.88 | 249.97 | 46.34 | 8229 | 0.46 | 239.11 | 223.27 | 1.07 | 0.24 | 572.00 | 1911 |
| OCYB5-15 | 142.3 | 14.2 | 161.7 | 1.00 | <0.0099 | 12.5 | 0.09 | 1.20 | 1.66 | 0.36 | 5.83 | 16.68 | 5.52 | 22.06 | 43.77 | 7.22 | 7848 | 0.21 | 19.65 | 16.63 | 1.18 | 0.21 | 116.89 | 1813 |
| OCYB5-16 | 139.3 | 16.9 | 143.3 | 0.75 | 0.01 | 11.97 | 0.06 | 1.14 | 1.50 | 0.35 | 5.06 | 14.72 | 4.93 | 19.39 | 40.74 | 6.90 | 7379 | 0.15 | 12.58 | 10.61 | 1.19 | 0.21 | 106.77 | 1731 |
| OCYB5-18 | 120.9 | 17.6 | 143.9 | 0.84 | <0.0082 | 11.74 | 0.06 | 0.89 | 1.47 | 0.31 | 4.66 | 14.51 | 4.76 | 19.57 | 42.78 | 7.20 | 8454 | 0.17 | 19.26 | 18.43 | 1.05 | 0.21 | 107.96 | 1860 |
| OCYB5-19 | 150.2 | 12.9 | 272.3 | 1.10 | 0.12 | 19.52 | 0.04 | 0.76 | 1.37 | 0.26 | 6.65 | 25.37 | 9.33 | 40.03 | 87.63 | 15.15 | 10068 | 0.38 | 66.16 | 66.96 | 0.99 | 0.34 | 206.23 | 1975 |
| OCYB5-2 | 105.9 | 14.6 | 107.5 | 0.90 | 0.01 | 12.68 | 0.08 | 1.26 | 1.78 | 0.32 | 5.00 | 12.23 | 3.78 | 13.92 | 25.58 | 4.25 | 8239 | 0.18 | 18.94 | 18.51 | 1.02 | 0.20 | 80.89 | 1831 |
| OCYB5-20 | 137.9 | 15.9 | 171.0 | 0.64 | 0.01 | 10.81 | 0.08 | 1.09 | 1.74 | 0.38 | 5.85 | 17.75 | 5.80 | 23.59 | 49.25 | 8.22 | 7117 | 0.14 | 11.56 | 7.82 | 1.48 | 0.22 | 124.57 | 1841 |
| OCYB5-23 | 127.9 | 13.4 | 168.2 | 0.81 | 0.03 | 11.65 | 0.08 | 1.18 | 1.61 | 0.38 | 6.22 | 17.04 | 5.72 | 23.46 | 47.39 | 8.12 | 8261 | 0.17 | 18.04 | 16.34 | 1.10 | 0.21 | 122.88 | 1835 |
| OCYB5-28 | 128.4 | 17.0 | 115.5 | 0.76 | 0.01 | 10.2 | 0.05 | 0.78 | 1.12 | 0.29 | 4.17 | 11.73 | 3.88 | 15.80 | 32.09 | 5.66 | 7121 | 0.17 | 9.8 | 6.94 | 1.41 | 0.23 | 85.79 | 1911 |
| OCYB5-29 | 124.4 | 15.2 | 137.2 | 0.72 | 0.01 | 12.05 | 0.07 | 1.09 | 1.67 | 0.38 | 5.71 | 15.73 | 4.81 | 17.73 | 33.86 | 5.75 | 8493 | 0.14 | 19.76 | 18.81 | 1.05 | 0.20 | 98.86 | 1742 |
| OCYB5-3 | 123.0 | 7.9 | 149.4 | 0.85 | 0.09 | 12.5 | 0.11 | 1.11 | 1.39 | 0.29 | 4.85 | 15.12 | 5.03 | 20.74 | 43.53 | 7.36 | 7632 | 0.18 | 24.5 | 18.5 | 1.32 | 0.22 | 112.12 | 1851 |
| OCYB5-34 | 98.5 | 14.2 | 90.2 | 0.76 | 0.03 | 14.6 | 0.08 | 1.06 | 1.64 | 0.43 | 5.02 | 11.01 | 3.09 | 11.13 | 20.57 | 3.59 | 8248 | 0.18 | 20.52 | 20.29 | 1.01 | 0.23 | 72.26 | 1842 |
| OCYB5-36 | 123.5 | 15.2 | 133.0 | 0.61 | <0.0090 | 10.46 | 0.07 | 0.97 | 1.37 | 0.37 | 4.61 | 13.45 | 4.48 | 18.45 | 38.85 | 6.74 | 7103 | 0.10 | 8.46 | 6.35 | 1.33 | 0.16 | 99.81 | 1869 |
| OCYB5-37 | 141.8 | 14.7 | 186.3 | 0.62 | <0.0093 | 10.74 | 0.09 | 1.28 | 1.98 | 0.42 | 6.31 | 18.99 | 6.25 | 25.08 | 51.41 | 8.81 | 7091 | 0.11 | 11.03 | 7.19 | 1.53 | 0.18 | 131.36 | 1806 |
| OCYB5-39 | 127.9 | 14.4 | 159.1 | 0.68 | 0.01 | 11.64 | 0.07 | 1.01 | 1.53 | 0.30 | 5.30 | 16.22 | 5.34 | 21.92 | 46.34 | 7.88 | 7575 | 0.13 | 19.03 | 14.37 | 1.32 | 0.20 | 117.56 | 1878 |
| OCYB5-4 | 133.4 | 9.2 | 260.0 | 1.20 | 0.06 | 22.07 | 0.08 | 0.99 | 1.84 | 0.40 | 6.65 | 24.39 | 8.74 | 38.42 | 91.19 | 15.09 | 10346 | 0.38 | 75.96 | 88.06 | 0.86 | 0.31 | 209.92 | 1837 |
| OCYB5-40 | 180.1 | 14.3 | 304.7 | 0.98 | 0.01 | 25.62 | 0.07 | 1.63 | 3.08 | 1.10 | 9.99 | 31.6 | 9.92 | 41.47 | 91.33 | 14.64 | 7115 | 0.19 | 80.15 | 60.95 | 1.32 | 0.20 | 230.47 | 1877 |
| OCYB5-42 | 210.7 | 8.8 | 482.7 | 1.04 | 0.57 | 36.09 | 0.18 | 2.10 | 3.84 | 1.80 | 15.37 | 45.85 | 15.75 | 67.50 | 148.23 | 26.60 | 9809 | 0.33 | 214.2 | 153.87 | 1.39 | 0.32 | 363.88 | 1879 |
| OCYB5-44 | 142.5 | 17.1 | 170.0 | 0.71 | 0.01 | 11.66 | 0.09 | 1.16 | 1.75 | 0.41 | 6.08 | 18.3 | 5.86 | 23.52 | 48.15 | 7.75 | 7385 | 0.14 | 11.04 | 8.99 | 1.23 | 0.20 | 124.74 | 1848 |
| OCYB5-46 | 94.5 | 13.4 | 83.4 | 0.77 | <0.0090 | 13.28 | 0.07 | 1.15 | 1.57 | 0.40 | 4.60 | 10.21 | 2.89 | 10.24 | 17.63 | 2.84 | 8637 | 0.16 | 22.69 | 22.11 | 1.03 | 0.20 | 64.89 | 1787 |
| OCYB5-48 | 149.3 | 16.5 | 174.9 | 0.79 | 0.01 | 12.36 | 0.09 | 1.22 | 1.93 | 0.41 | 6.43 | 18.42 | 5.90 | 23.73 | 48.52 | 7.98 | 7673 | 0.16 | 14.27 | 13.12 | 1.09 | 0.20 | 127.00 | 1835 |
| OCYB5-49 | 135.1 | 18.6 | 144.1 | 0.72 | 0.14 | 12.44 | 0.06 | 1.25 | 1.70 | 0.39 | 5.27 | 15.02 | 4.88 | 19.90 | 41.39 | 6.93 | 7486 | 0.15 | 14.64 | 13.22 | 1.11 | 0.21 | 109.36 | 1803 |
| OCYB5-5 | 123.3 | 12.0 | 175.5 | 0.73 | 0.03 | 10.92 | 0.08 | 1.19 | 1.57 | 0.36 | 5.81 | 18.25 | 5.98 | 24.34 | 52.23 | 9.10 | 7391 | 0.12 | 25.8 | 15.48 | 1.67 | 0.16 | 129.86 | 1863 |
| OCYB5-50 | 139.1 | 28.7 | 192.0 | 0.89 | 7.75 | 30.1 | 1.66 | 6.12 | 2.64 | 0.56 | 6.85 | 20.96 | 6.60 | 26.21 | 52.03 | 8.85 | 8501 | 0.21 | 25.04 | 23.34 | 1.07 | 0.23 | 170.33 | 1867 |
| OCYB5-51 | 122.4 | 57.0 | 138.9 | 0.97 | 0.70 | 18.59 | 0.81 | 5.88 | 3.31 | 0.78 | 6.22 | 14.81 | 4.76 | 18.78 | 39.38 | 6.54 | 7007 | 0.11 | 9.59 | 6.88 | 1.39 | 0.12 | 120.56 | 1856 |

| Analysis No. | P | Ti | Y | Nb | La | Ce | Pr | Nd | Sm | Eu | Gd | Dy | Ho | Er | Yb | Lu | Hf | Ta | Th | U | Th/U | Nb/Ta | Total REE | U-Pb age |
|---|---|---|---|---|---|---|---|---|---|---|---|---|---|---|---|---|---|---|---|---|---|---|---|---|
| OCYB5-56 | 99.6 | 15.4 | 114.2 | 0.82 | 0.01 | 14.85 | 0.08 | 1.15 | 1.80 | 0.45 | 5.91 | 13.62 | 3.85 | 14.76 | 26.74 | 4.51 | 8789 | 0.17 | 29.98 | 28.46 | 1.05 | 0.21 | 87.73 | 2007 |
| OCYB5-58 | 124.6 | 17.6 | 129.0 | 0.72 | <0.0066 | 10.73 | 0.04 | 0.88 | 1.17 | 0.27 | 4.16 | 12.84 | 4.31 | 17.96 | 38.24 | 6.34 | 7292 | 0.18 | 18.82 | 13.09 | 1.44 | 0.25 | 96.94 | 1800 |
| OCYB5-59 | 112.6 | 9.8 | 147.7 | 0.77 | 0.06 | 12.84 | 0.07 | 1.07 | 1.41 | 0.39 | 5.46 | 15.73 | 5.06 | 20.21 | 40.36 | 6.71 | 8506 | 0.19 | 21.17 | 20.22 | 1.05 | 0.25 | 109.36 | 1836 |
| OCYB5-6 | 148.3 | 17.1 | 204.8 | 0.69 | 0.02 | 11.03 | 0.10 | 1.31 | 2.08 | 0.44 | 7.24 | 21.97 | 7.15 | 28.36 | 55.86 | 9.41 | 7223 | 0.12 | 10.67 | 6.95 | 1.54 | 0.18 | 144.97 | 1895 |
| OCYB5-60 | 97.2 | 12.0 | 106.2 | 0.75 | 0.25 | 18.4 | 0.15 | 1.73 | 2.11 | 0.42 | 5.61 | 11.68 | 3.64 | 13.58 | 27.72 | 4.66 | 7268 | 0.15 | 54.49 | 23.25 | 2.34 | 0.20 | 89.94 | 1831 |
| OCYB5-61 | 132.2 | 15.8 | 120.9 | 0.70 | 0.01 | 11.26 | 0.06 | 0.89 | 1.11 | 0.29 | 4.22 | 12.57 | 4.14 | 16.43 | 34.65 | 5.73 | 7145 | 0.18 | 8.65 | 6.8 | 1.27 | 0.25 | 91.36 | 1841 |
| OCYB5-62 | 138.0 | 12.4 | 186.4 | 0.82 | <0.0125 | 11.9 | 0.09 | 1.33 | 1.88 | 0.42 | 6.58 | 19.3 | 6.42 | 25.94 | 53.47 | 8.94 | 8078 | 0.18 | 18.49 | 17.11 | 1.08 | 0.22 | 136.27 | 1916 |
| OCYB5-63 | 134.2 | 17.9 | 187.4 | 0.61 | 0.01 | 10.92 | 0.08 | 1.17 | 1.75 | 0.38 | 6.06 | 19.21 | 6.32 | 26.09 | 54.72 | 9.12 | 7189 | 0.14 | 17.76 | 11.41 | 1.56 | 0.23 | 135.83 | 1863 |
| OCYB5-64 | 137.8 | 19.7 | 164.9 | 0.61 | 0.02 | 11.69 | 0.08 | 1.23 | 1.93 | 0.44 | 5.73 | 17.15 | 5.48 | 22.63 | 47.19 | 8.02 | 7018 | 0.13 | 9.61 | 7.14 | 1.35 | 0.21 | 121.59 | 1865 |
| OCYB5-65 | 117.1 | 17.5 | 152.9 | 0.64 | 0.01 | 10.84 | 0.06 | 0.93 | 1.39 | 0.33 | 5.10 | 15.46 | 5.23 | 21.58 | 45.11 | 7.70 | 7349 | 0.16 | 19.84 | 13.18 | 1.51 | 0.25 | 113.74 | 1849 |
| OCYB5-7 | 110.9 | 7.8 | 142.7 | 0.72 | 0.01 | 10.15 | 0.05 | 0.83 | 1.32 | 0.29 | 4.34 | 14.24 | 4.73 | 20.33 | 44.82 | 7.61 | 7853 | 0.15 | 19.33 | 17.89 | 1.08 | 0.20 | 108.72 | 1844 |
| OCYB5-9 | 125.2 | 14.8 | 147.2 | 0.63 | 0.01 | 10.73 | 0.07 | 1.11 | 1.61 | 0.40 | 4.91 | 14.9 | 4.95 | 20.56 | 44.18 | 7.46 | 7149 | 0.11 | 9.44 | 7.37 | 1.28 | 0.18 | 110.89 | 1777 |
| **Alakhit-Markha field, Kismet pipe** | | | | | | | | | | | | | | | | | | | | | | | | |
| MVG459_Kis-01 | 228.5 | 45.7 | 331.7 | 2.20 | 0.01 | 1.82 | 0.06 | 0.65 | 1.24 | 0.36 | 8.42 | 30.9 | 10.6 | 43.5 | 74.4 | 13.3 | 14695 | 0.38 | 98.8 | 327 | 0.30 | 0.17 | 185.28 | 1920 |
| MVG459_Kis-02 | 375.3 | 50.2 | 1051.8 | 4.35 | 0.07 | 13.4 | 0.19 | 2.36 | 4.28 | 1.02 | 23.8 | 95.4 | 35.5 | 157 | 292 | 55.4 | 16513 | 1.02 | 43.4 | 54.1 | 0.80 | 0.23 | 679.90 | 1903 |
| MVG459_Kis-03 | 377.0 | 54.1 | 733.1 | 2.88 | 0.01 | 3.18 | 0.13 | 2.54 | 4.94 | 0.25 | 20.5 | 68.3 | 24.2 | 106 | 209 | 40.4 | 17930 | 0.48 | 97.4 | 162 | 0.60 | 0.17 | 478.99 | 1881 |
| MVG459_Kis-04 | 1734.0 | 55.3 | 4779.3 | 11.7 | 0.17 | 14.4 | 0.31 | 2.63 | 6.37 | 0.72 | 48.2 | 363 | 153 | 749 | 1487 | 260 | 20057 | 4.10 | 115 | 806 | 0.14 | 0.35 | 3083.88 | 1912 |
| MVG459_Kis-05 | 363.3 | 45.6 | 813.3 | 3.89 | 0.03 | 11.9 | 0.11 | 1.89 | 3.44 | 0.65 | 18.1 | 74.4 | 27.4 | 127 | 245 | 47.1 | 17326 | 0.91 | 34.8 | 47.1 | 0.74 | 0.23 | 556.31 | 1842 |
| MVG459_Kis-06 | 516.7 | 34.2 | 1186.2 | 4.76 | | 6.22 | 0.16 | 3.05 | 5.51 | 0.28 | 29.6 | 112 | 40.5 | 176 | 321 | 60.0 | 17398 | 1.04 | 163 | 244 | 0.67 | 0.22 | 754.81 | 1931 |
| MVG459_Kis-07 | 525.7 | 77.9 | 1314.7 | 5.63 | 0.08 | 7.18 | 0.49 | 8.37 | 13.0 | 1.27 | 54.0 | 147 | 46.1 | 176 | 272 | 47.3 | 18900 | 1.25 | 145 | 196 | 0.74 | 0.22 | 773.11 | 1884 |
| MVG459_Kis-09 | 473.0 | 39.0 | 1336.8 | 4.80 | 0.11 | 7.03 | 0.38 | 4.68 | 7.60 | 1.00 | 38.1 | 132 | 45.7 | 197 | 353 | 65.4 | 18063 | 1.30 | 139 | 181 | 0.77 | 0.27 | 851.73 | 1893 |
| MVG459_Kis-10 | 357.3 | 63.6 | 664.9 | 3.42 | 0.02 | 4.27 | 0.18 | 2.40 | 4.11 | 0.40 | 17.4 | 61.0 | 22.5 | 98.0 | 191 | 36.9 | 17074 | 0.79 | 59.0 | 107 | 0.55 | 0.23 | 437.77 | 1877 |
| MVG459_Kis-12 | 306.6 | 44.1 | 860.2 | 3.21 | | 11.1 | 0.11 | 1.74 | 3.08 | 0.51 | 19.3 | 75.2 | 27.1 | 118 | 204 | 37.2 | 19559 | 0.68 | 12.3 | 40.0 | 0.31 | 0.21 | 496.87 | 1832 |
| MVG459_Kis-13 | 452.9 | 48.1 | 1567.1 | 4.79 | 0.18 | 15.6 | 1.78 | 25.4 | 27.7 | 1.73 | 75.9 | 174 | 54.5 | 214 | 360 | 64.3 | 15664 | 1.17 | 237 | 293 | 0.81 | 0.24 | 1015.14 | 1910 |
| MVG459_Kis-14 | 541.4 | 61.9 | 1463.1 | 6.92 | 1.66 | 93.2 | 2.91 | 17.3 | 10.2 | 2.36 | 29.3 | 130 | 47.1 | 220 | 460 | 84.4 | 21154 | 2.98 | 509 | 1147 | 0.44 | 0.43 | 1097.57 | 1899 |
| MVG459_Kis-15 | 208.9 | 50.8 | 420.4 | 3.37 | 0.08 | 8.76 | 0.21 | 2.27 | 3.84 | 0.73 | 18.4 | 52.6 | 14.4 | 45.2 | 42.9 | 6.29 | 18980 | 0.94 | 84.3 | 109 | 0.77 | 0.28 | 195.77 | 1870 |
| MVG459_Kis-16 | 336.8 | 36.9 | 718.9 | 3.52 | 0.40 | 7.17 | 0.44 | 4.93 | 5.38 | 1.19 | 20.7 | 69.6 | 23.7 | 102 | 201 | 38.0 | 16183 | 0.46 | 231 | 363 | 0.64 | 0.13 | 474.60 | 1914 |
| MVG459_Kis-17 | 347.5 | 31.5 | 882.7 | 4.54 | 0.11 | 8.05 | 0.34 | 4.97 | 7.26 | 0.42 | 28.2 | 87.3 | 29.9 | 127 | 234 | 44.4 | 17432 | 1.02 | 125 | 196 | 0.64 | 0.23 | 572.24 | 1877 |
| MVG459_Kis-19 | 1270.9 | 57.7 | 3040.3 | 3.41 | 0.15 | 28.3 | 0.35 | 5.17 | 10.4 | 1.06 | 56.9 | 269 | 105 | 474 | 985 | 176 | 20455 | 0.44 | 228 | 301 | 0.76 | 0.13 | 2111.21 | 1839 |
| MVG459_Kis-20 | 747.0 | 40.7 | 2169.3 | 3.45 | 4.55 | 18.7 | 1.47 | 15.4 | 21.9 | 1.96 | 82.0 | 234 | 77.0 | 302 | 514 | 89.6 | 16617 | 0.59 | 301 | 332 | 0.91 | 0.17 | 1362.59 | 1939 |
| MVG459_Kis-21 | 251.5 | 31.7 | 501.9 | 2.78 | 0.04 | 6.15 | 0.20 | 2.63 | 4.94 | 0.59 | 18.2 | 49.8 | 17.2 | 71.0 | 137 | 25.5 | 15526 | 0.53 | 65.5 | 117 | 0.56 | 0.19 | 332.98 | 1870 |
| MVG459_Kis-22 | 343.5 | 59.4 | 1101.1 | 2.78 | 0.07 | 5.48 | 0.78 | 10.4 | 13.0 | 1.45 | 47.0 | 128 | 39.1 | 140 | 203 | 33.1 | 15499 | 0.55 | 168 | 199 | 0.84 | 0.20 | 622.34 | 1897 |
| MVG459_Kis-23 | 794.7 | 56.2 | 2143.0 | 3.94 | 15.7 | 527 | 19.8 | 111 | 51.5 | 16.2 | 84.2 | 248 | 74.4 | 305 | 602 | 110 | 18109 | 1.17 | 492 | 1771 | 0.28 | 0.30 | 2163.70 | 1966 |
| MVG459_Kis-24 | 334.5 | 45.0 | 1463.5 | 3.72 | 0.34 | 16.8 | 1.23 | 18.6 | 24.2 | 2.35 | 70.4 | 166 | 51.6 | 198 | 342 | 58.7 | 15499 | 0.70 | 198 | 264 | 0.75 | 0.19 | 949.79 | 1923 |
| MVG459_Kis-25 | 317.9 | 30.0 | 917.4 | 4.58 | 2.42 | 65.5 | 3.31 | 21.5 | 12.3 | 3.44 | 25.4 | 92.5 | 32.2 | 143 | 310 | 55.4 | 18712 | 0.97 | 169 | 290 | 0.58 | 0.21 | 766.75 | 2064 |
| MVG459_Kis-26 | 319.9 | 40.6 | 572.8 | 2.74 | 0.03 | 5.43 | 0.06 | 1.24 | 1.25 | 0.38 | 7.83 | 45.5 | 19.1 | 94.3 | 221 | 40.9 | 19725 | 0.63 | 63.3 | 84.3 | 0.75 | 0.23 | 437.39 | 1849 |
| MVG459_Kis-27 | 566.6 | 27.7 | 828.6 | 3.31 | 0.03 | 3.63 | 0.28 | 5.08 | 15.4 | 1.13 | 64.8 | 109 | 28.5 | 99.4 | 156 | 26.9 | 20208 | 1.60 | 110 | 1033 | 0.11 | 0.48 | 510.59 | 1916 |
| MVG459_Kis-28 | 379.0 | 46.3 | 934.7 | 3.52 | | 13.7 | 0.14 | 2.26 | 3.97 | 0.99 | 22.2 | 87.0 | 33.0 | 141 | 285 | 52.4 | 17364 | 0.79 | 39.6 | 52.3 | 0.76 | 0.23 | 641.66 | 1848 |
| MVG459_Kis-29 | 123.6 | 29.5 | 173.9 | 1.69 | 0.02 | 2.34 | 0.06 | 0.76 | 2.18 | 0.56 | 8.51 | 23.0 | 5.89 | 20.4 | 26.9 | 4.21 | 18622 | 0.18 | 73.2 | 378 | 0.19 | 0.11 | 94.79 | 1920 |
| MVG459_Kis-30 | 464.4 | 37.6 | 1028.6 | 3.31 | 0.03 | 10.1 | 0.20 | 2.26 | 3.92 | 0.83 | 20.9 | 93.8 | 36.5 | 162 | 322 | 59.5 | 19355 | 0.76 | 69.3 | 99.8 | 0.69 | 0.23 | 711.61 | 1840 |
| MVG459_Kis-32 | 868.6 | 37.4 | 1884.6 | 4.25 | 0.14 | 8.62 | 0.48 | 5.79 | 9.67 | 0.42 | 49.2 | 186 | 65.6 | 273 | 502 | 87.0 | 18384 | 1.24 | 273 | 346 | 0.79 | 0.29 | 1187.74 | 1902 |
| MVG459_Kis-35 | 350.0 | 44.4 | 774.1 | 2.85 | 0.16 | 7.05 | 0.31 | 2.13 | 2.12 | 0.59 | 11.4 | 67.9 | 26.6 | 117 | 227 | 39.5 | 18943 | 0.47 | 29.0 | 105 | 0.28 | 0.17 | 501.51 | 1901 |
| MVG459_Kis-36 | 224.2 | 21.2 | 406.6 | 3.29 | 0.25 | 14.3 | 0.56 | 4.89 | 4.50 | 0.79 | 14.4 | 41.2 | 13.7 | 58.1 | 117 | 21.5 | 15557 | 0.58 | 85.2 | 131 | 0.65 | 0.18 | 291.36 | 1838 |
| MVG459_Kis-37 | 519.5 | 35.7 | 1315.7 | 4.37 | 0.02 | 5.77 | 0.04 | 0.80 | 2.38 | 0.32 | 15.3 | 105 | 44.3 | 206 | 439 | 79.6 | 19541 | 1.17 | 119 | 352 | 0.34 | 0.27 | 898.52 | 1873 |
| **Alakhit-Markha field, Geochemical pipe** | | | | | | | | | | | | | | | | | | | | | | | | |
| MVG459_Gch-01 | 1594.0 | 57.8 | 4414.9 | 11.8 | 0.63 | 47.4 | 1.70 | 18.1 | 25.3 | 4.87 | 107 | 412 | 149 | 648 | 1199 | 215 | 18407 | 3.39 | 457 | 763 | 0.60 | 0.29 | 2827.85 | 1933 |
| MVG459_Gch-02 | 410.0 | 27.3 | 690.9 | 3.26 | 0.34 | 5.15 | 0.78 | 7.23 | 10.4 | 1.57 | 41.3 | 80.7 | 22.8 | 87.6 | 152 | 27.9 | 20546 | 1.42 | 83.6 | 849 | 0.10 | 0.44 | 437.72 | 1933 |

| Analysis No. | P | Ti | Y | Nb | La | Ce | Pr | Nd | Sm | Eu | Gd | Dy | Ho | Er | Yb | Lu | Hf | Ta | Th | U | Th/U | Nb/Ta | Total REE | U-Pb age |
|---|---|---|---|---|---|---|---|---|---|---|---|---|---|---|---|---|---|---|---|---|---|---|---|---|
| MVG459_Gch-03 | 237.9 | 31.2 | 1078.9 | 3.39 | 0.16 | 18.9 | 0.36 | 4.71 | 7.50 | 1.05 | 31.2 | 105 | 36.6 | 156 | 281 | 51.9 | 16536 | 1.03 | 173 | 250 | 0.69 | 0.30 | 694.77 | 1866 |
| MVG459_Gch-04 | 1544.5 | 50.2 | 4157.1 | 3.61 | 1.16 | 33.6 | 0.74 | 8.93 | 16.5 | 1.76 | 91.2 | 392 | 143 | 619 | 1090 | 194 | 18528 | 0.75 | 339 | 412 | 0.82 | 0.21 | 2592.00 | 1917 |
| MVG459_Gch-05 | 1408.5 | 138.3 | 6107.2 | 12.2 | 35.3 | 246 | 59.9 | 354 | 198 | 59.4 | 312 | 766 | 208 | 794 | 1271 | 199 | 18857 | 2.79 | 708 | 1187 | 0.60 | 0.23 | 4502.55 | 1994 |
| MVG459_Gch-06 | 1506.1 | 55.0 | 3905.7 | 4.09 | 0.10 | 31.6 | 0.46 | 6.59 | 13.5 | 0.99 | 83.4 | 362 | 135 | 596 | 1058 | 191 | 18293 | 0.86 | 306 | 371 | 0.83 | 0.21 | 2478.24 | 1934 |
| **Alakhit-Markha field, Vostok pipe** | | | | | | | | | | | | | | | | | | | | | | | | |
| MVG459_Vos-01 | 530.5 | 48.2 | 1891.5 | 14.9 | 6.18 | 252 | 9.25 | 51.2 | 29.7 | 10.5 | 60.0 | 197 | 64.3 | 288 | 584 | 109 | 21549 | 7.32 | 311 | 942 | 0.33 | 0.49 | 1660.83 | 2236 |
| MVG459_Vos-02 | 597.4 | 42.9 | 1352.1 | 4.73 | 0.01 | 4.75 | 0.10 | 1.90 | 4.11 | 0.31 | 25.7 | 114 | 44.5 | 207 | 411 | 77.5 | 18920 | 1.31 | 132 | 408 | 0.32 | 0.28 | 891.44 | 1932 |
| MVG459_Vos-04 | 468.0 | 29.7 | 1526.4 | 4.01 | 0.12 | 12.9 | 0.50 | 7.92 | 15.3 | 1.27 | 60.5 | 162 | 52.4 | 204 | 362 | 63.9 | 16676 | 0.72 | 226 | 300 | 0.76 | 0.18 | 942.88 | 1912 |
| MVG459_Vos-05 | 96.6 | 35.5 | 119.1 | 3.29 | 0.03 | 4.81 | 0.06 | 0.59 | 0.77 | 0.32 | 4.27 | 12.6 | 3.83 | 13.6 | 25.0 | 4.28 | 22223 | 1.08 | 30.1 | 1201 | 0.03 | 0.33 | 70.07 | 1967 |
| MVG459_Vos-06 | 357.5 | 102.8 | 830.9 | 4.33 | 4.60 | 20.9 | 1.49 | 11.6 | 11.2 | 1.67 | 33.7 | 89.3 | 29.0 | 115 | 218 | 38.6 | 16321 | 0.75 | 94.6 | 155 | 0.61 | 0.17 | 574.40 | 1957 |
| MVG459_Vos-07 | 534.0 | 44.8 | 1161.6 | 3.43 | 0.04 | 6.60 | 0.23 | 4.20 | 7.72 | 0.41 | 34.4 | 114 | 39.4 | 164 | 309 | 56.1 | 18450 | 0.61 | 135 | 259 | 0.52 | 0.18 | 735.27 | 1900 |
| MVG459_Vos-08 | 373.7 | 39.7 | 764.1 | 4.35 | 0.17 | 9.91 | 0.32 | 4.77 | 7.35 | 0.65 | 25.1 | 76.4 | 26.2 | 108 | 210 | 39.0 | 17216 | 0.90 | 112 | 200 | 0.56 | 0.21 | 508.30 | 1901 |
| MVG459_Vos-09 | 476.6 | 36.3 | 1838.5 | 4.42 | 0.68 | 20.5 | 2.18 | 30.0 | 33.7 | 2.16 | 90.3 | 210 | 65.1 | 249 | 423 | 73.8 | 16006 | 1.09 | 302 | 398 | 0.76 | 0.25 | 1199.48 | 1922 |
| MVG459_Vos-10 | 380.0 | 33.5 | 1791.8 | 4.22 | 0.37 | 20.4 | 2.02 | 29.5 | 32.3 | 2.58 | 86.6 | 205 | 63.6 | 242 | 411 | 71.7 | 15620 | 1.07 | 301 | 385 | 0.78 | 0.25 | 1166.49 | 1922 |
| MVG459_Vos-11 | 435.3 | 31.9 | 1346.6 | 7.37 | 1.66 | 40.8 | 1.15 | 6.63 | 5.88 | 1.27 | 25.5 | 119 | 46.3 | 210 | 429 | 77.3 | 17884 | 1.98 | 158 | 338 | 0.47 | 0.27 | 963.58 | 2245 |
| MVG459_Vos-12 | 360.4 | 47.8 | 1324.7 | 3.52 | 0.22 | 16.6 | 1.42 | 21.2 | 24.9 | 2.56 | 68.6 | 154 | 47.1 | 176 | 304 | 52.1 | 15343 | 0.68 | 205 | 248 | 0.83 | 0.19 | 868.45 | 1934 |
| MVG459_Vos-13 | 286.5 | 35.8 | 830.0 | 3.85 | 0.04 | 11.9 | 0.39 | 7.33 | 10.9 | 1.26 | 35.6 | 90.5 | 29.1 | 113 | 209 | 37.2 | 15841 | 0.75 | 133 | 205 | 0.65 | 0.19 | 545.97 | 1925 |
| MVG459_Vos-14 | 537.8 | 44.4 | 879.2 | 4.20 | 0.17 | 7.68 | 0.36 | 4.84 | 7.21 | 0.54 | 28.3 | 89.1 | 30.8 | 133 | 255 | 47.7 | 19765 | 0.89 | 148 | 241 | 0.61 | 0.21 | 604.51 | 1916 |
| MVG459_Vos-15 | 2043.7 | 49.9 | 629.3 | 3.18 | 15.6 | 56.4 | 5.25 | 25.7 | 15.0 | 1.86 | 44.2 | 91.6 | 22.1 | 71.4 | 98.3 | 17.0 | 23663 | 0.77 | 209 | 779 | 0.27 | 0.24 | 464.30 | 1794 |
| MVG459_Vos-16 | 550.5 | 31.7 | 1366.9 | 14.4 | 0.41 | 41.8 | 0.51 | 5.09 | 6.45 | 0.67 | 30.3 | 140 | 51.9 | 232 | 420 | 71.8 | 25487 | 8.06 | 90.7 | 173 | 0.53 | 0.56 | 1000.75 | 1911 |
| MVG459_Vos-17 | 796.1 | 55.0 | 2738.8 | 44.0 | 7.05 | 356 | 18.3 | 111 | 67.8 | 22.6 | 103 | 313 | 104 | 503 | 1164 | 221 | 21601 | 24.5 | 690 | 2292 | 0.30 | 0.56 | 2990.56 | 1938 |
| MVG459_Vos-20 | 250.0 | 77.9 | 840.8 | 11.0 | 0.15 | 15.3 | 0.18 | 1.50 | 2.07 | 0.36 | 11.0 | 65.5 | 28.3 | 149 | 345 | 69.5 | 23150 | 7.00 | 209 | 814 | 0.26 | 0.64 | 687.65 | 2421 |
| MVG459_Vos-21 | 631.9 | 45.6 | 3320.7 | 12.6 | 2.15 | 44.7 | 1.18 | 10.2 | 13.9 | 0.74 | 72.6 | 305 | 117 | 533 | 955 | 183 | 19732 | 5.07 | 573 | 906 | 0.63 | 0.40 | 2238.82 | 2332 |
| MVG459_Vos-22 | 513.9 | 37.2 | 1750.7 | 10.1 | 147 | 320 | 31.6 | 114 | 23.9 | 5.85 | 50.7 | 172 | 61.8 | 275 | 502 | 96.0 | 18350 | 4.56 | 140 | 397 | 0.35 | 0.45 | 1800.25 | 2398 |
| MVG459_Vos-23 | 262.8 | 19.0 | 516.6 | 3.45 | 0.11 | 8.20 | 0.28 | 3.77 | 4.93 | 0.49 | 16.5 | 49.4 | 17.5 | 74.9 | 141 | 28.0 | 16892 | 0.60 | 86.3 | 142 | 0.61 | 0.17 | 345.16 | 1878 |
| MVG459_Vos-24C | 495.1 | 45.2 | 1729.2 | 27.8 | 4.85 | 196 | 5.08 | 29.3 | 17.7 | 5.54 | 41.7 | 155 | 56.7 | 275 | 605 | 126 | 18878 | 25.9 | 373 | 1366 | 0.27 | 0.93 | 1518.15 | 1965 |
| MVG459_Vos-24R | 494.7 | 46.8 | 1959.2 | 11.6 | 2.19 | 72.5 | 3.34 | 20.6 | 14.6 | 4.60 | 44.6 | 181 | 65.9 | 299 | 536 | 103 | 17490 | 3.33 | 295 | 445 | 0.66 | 0.29 | 1346.36 | 2365 |
| MVG459_Vos-25 | 124.2 | 32.6 | 155.9 | 2.58 | 0.02 | 1.95 | 0.04 | 0.50 | 0.62 | 0.14 | 2.62 | 10.7 | 4.27 | 22.0 | 60.6 | 12.9 | 12304 | 0.22 | 151 | 377 | 0.40 | 0.09 | 116.24 | 1875 |
| MVG459_Vos-26 | 279.9 | 41.5 | 1084.6 | 3.61 | 0.10 | 13.3 | 1.31 | 18.0 | 18.4 | 2.20 | 52.5 | 119 | 36.6 | 143 | 238 | 43.2 | 14407 | 0.75 | 166 | 206 | 0.80 | 0.21 | 686.09 | 1929 |
| MVG459_Vos-27 | 450.2 | 28.9 | 1412.3 | 13.5 | 0.25 | 32.4 | 0.40 | 3.57 | 5.05 | 0.51 | 26.9 | 123 | 47.4 | 217 | 406 | 71.6 | 22485 | 6.47 | 171 | 143 | 1.19 | 0.48 | 933.75 | 1976 |
| MVG459_Vos-28 | 402.3 | 39.7 | 1068.8 | 3.73 | 0.03 | 7.88 | 0.39 | 6.57 | 9.75 | 0.54 | 37.9 | 109 | 35.7 | 148 | 272 | 50.3 | 17597 | 0.87 | 153 | 240 | 0.64 | 0.23 | 677.42 | 1938 |
| MVG459_Vos-29 | 510.1 | 40.7 | 873.4 | 2.88 | 0 | 4.32 | 0.20 | 2.98 | 5.86 | 0.23 | 24.9 | 83.2 | 28.8 | 127 | 244 | 46.3 | 17025 | 0.51 | 68.0 | 176 | 0.39 | 0.18 | 567.77 | 1918 |
| MVG459_Vos-30 | 385.9 | 19.0 | 1166.8 | 5.69 | 0.18 | 16.8 | 0.74 | 11.7 | 15.0 | 1.42 | 51.6 | 125 | 39.4 | 159 | 266 | 48.1 | 15021 | 1.00 | 237 | 287 | 0.83 | 0.18 | 735.18 | 1898 |
| MVG459_Vos-31 | 300.3 | 47.8 | 1268.3 | 10.6 | 2.53 | 75.9 | 4.89 | 29.3 | 21.5 | 7.28 | 41.6 | 136 | 44.4 | 199 | 407 | 78.2 | 22782 | 4.16 | 131 | 504 | 0.26 | 0.39 | 1047.13 | 2404 |
| MVG459_Vos-32 | 277.7 | 51.1 | 1237.6 | 3.31 | 0.28 | 20.4 | 1.21 | 17.5 | 19.9 | 3.28 | 58.3 | 138 | 42.3 | 170 | 285 | 51.0 | 15107 | 0.68 | 161 | 177 | 0.91 | 0.21 | 806.62 | 1961 |
| MVG459_Vos-33 | 379.3 | 38.1 | 840.3 | 6.05 | 0.04 | 11.6 | 0.28 | 4.56 | 7.31 | 0.58 | 29.1 | 85.3 | 28.5 | 117 | 212 | 39.2 | 16324 | 1.44 | 198 | 309 | 0.64 | 0.24 | 535.60 | 1910 |
| MVG459_Vos-34 | 667.8 | 66.4 | 3983.7 | 9.60 | 15.5 | 59.7 | 5.49 | 29.6 | 19.8 | 1.92 | 87.1 | 347 | 133 | 586 | 983 | 181 | 15587 | 3.53 | 630 | 876 | 0.72 | 0.37 | 2449.06 | 2427 |
| MVG459_Vos-35 | 564.5 | 68.4 | 2975.2 | 16.1 | 5.06 | 207 | 5.93 | 34.5 | 24.3 | 6.38 | 72.1 | 278 | 102 | 463 | 909 | 166 | 20422 | 6.73 | 629 | 1360 | 0.46 | 0.42 | 2273.35 | 2206 |
| **Alakhit-Markha field, Veselaya pipe** | | | | | | | | | | | | | | | | | | | | | | | | |
| MVG459_Vos-36 | 708.2 | 25.3 | 3000.3 | 13.6 | 0.94 | 42.5 | 0.92 | 6.36 | 8.14 | 0.96 | 50.7 | 257 | 101 | 466 | 878 | 159 | 22607 | 6.28 | 754 | 1317 | 0.57 | 0.46 | 1971.50 | 2261 |
| MVG459_Ves-01 | 247.5 | 14.9 | 875.6 | 4.31 | | 11.8 | 0.06 | 1.25 | 2.31 | 0.87 | 13.9 | 63.3 | 26.6 | 142 | 384 | 84.0 | 17146 | 1.32 | 51.2 | 92.3 | 0.55 | 0.31 | 730.06 | 778 |
| MVG459_Ves-02 | 460.6 | 49.4 | 1149.7 | 5.78 | 0.16 | 8.72 | 0.36 | 4.69 | 8.16 | 0.65 | 33.8 | 111 | 38.0 | 165 | 303 | 56.9 | 18780 | 1.32 | 151 | 281 | 0.54 | 0.23 | 730.28 | 1971 |
| MVG459_Ves-03 | 354.4 | 137.0 | 1279.1 | 4.76 | 0.59 | 80.4 | 0.48 | 8.71 | 11.3 | 2.60 | 41.7 | 125 | 43.1 | 187 | 349 | 65.4 | 15752 | 0.72 | 171 | 86.1 | 1.99 | 0.15 | 915.84 | 2645 |
| MVG459_Ves-04 | 484.1 | 23.0 | 4020.6 | 8.87 | 0.26 | 40.1 | 1.01 | 14.9 | 22.7 | 9.91 | 100.0 | 355 | 129 | 594 | 1285 | 253 | 12699 | 2.03 | 330 | 436 | 0.76 | 0.23 | 2805.49 | 490 |
| **Alakhit-Markha field, Krasnopresnenskaya pipe** | | | | | | | | | | | | | | | | | | | | | | | | |
| MVG459_Kpr-01 | 516.1 | 23.4 | 1336.5 | 7.09 | 2.62 | 25.6 | 1.46 | 9.48 | 7.42 | 3.42 | 33.3 | 115 | 42.6 | 196 | 426 | 89.9 | 15064 | 0.38 | 162 | 220 | 0.74 | 0.05 | 952.47 | 2311 |
| MVG459_Kpr-02 | 774.8 | 45.0 | 1222.0 | 4.13 | 0.42 | 3.59 | 0.61 | 5.45 | 6.43 | 0.86 | 34.9 | 129 | 38.5 | 148 | 253 | 48.3 | 20909 | 1.26 | 30.7 | 823 | 0.04 | 0.31 | 668.54 | 1876 |

| Analysis No. | P | Ti | Y | Nb | La | Ce | Pr | Nd | Sm | Eu | Gd | Dy | Ho | Er | Yb | Lu | Hf | Ta | Th | U | Th/U | Nb/Ta | Total REE | U-Pb age |
|---|---|---|---|---|---|---|---|---|---|---|---|---|---|---|---|---|---|---|---|---|---|---|---|---|
| MVG459_Kpr-03 | 629.3 | 36.4 | 1019.7 | 3.45 | 0.17 | 4.65 | 0.29 | 2.32 | 3.72 | 0.54 | 20.8 | 91.0 | 31.2 | 141 | 328 | 67.6 | 21301 | 1.03 | 109 | 1277 | 0.09 | 0.30 | 691.33 | 1906 |
| MVG459_Kpr-04 | 759.5 | 36.5 | 1936.1 | 6.25 | 3.19 | 83.9 | 1.13 | 13.2 | 23.3 | 5.09 | 86.9 | 217 | 65.7 | 251 | 398 | 69.8 | 18304 | 1.80 | 449 | 640 | 0.70 | 0.29 | 1218.18 | 2286 |
| MVG459_Kpr-05 | 581.0 | 41.1 | 1418.5 | 3.26 | 0.15 | 7.70 | 0.59 | 8.93 | 19.8 | 1.01 | 73.6 | 161 | 47.8 | 180 | 283 | 49.3 | 18176 | 0.84 | 383 | 730 | 0.52 | 0.26 | 832.98 | 1947 |
| **Alakhit-Markha field, Markha pipe** | | | | | | | | | | | | | | | | | | | | | | | | |
| MRH-02 | 256.0 | 22.5 | 978.8 | 2.74 | 0.09 | 17.0 | 0.17 | 2.00 | 3.57 | 0.36 | 19.8 | 83.6 | 31.9 | 149 | 304 | 59.2 | 17026 | 0.88 | 132 | 249 | 0.53 | 0.32 | 671.13 | 1878 |
| MRH-04 | 575.9 | 27.0 | 4697.5 | 3.27 | 0.11 | 24.0 | 0.76 | 11.2 | 16.8 | 2.89 | 100 | 421 | 157 | 679 | 1083 | 198 | 14547 | 1.01 | 396 | 223 | 1.78 | 0.31 | 2693.35 | 796 |
| MRH-05r | 1370.9 | 132.2 | 1428.1 | 3.46 | 5.11 | 38.4 | 1.27 | 6.83 | 4.63 | 1.59 | 24.1 | 112 | 45.9 | 231 | 540 | 114 | 16241 | 0.75 | 122 | 111 | 1.09 | 0.22 | 1125.05 | 781 |
| MRH-06 | 980.1 | 22.3 | 7464.5 | 10.0 | 1.60 | 73.8 | 2.35 | 26.3 | 44.3 | 17.4 | 249 | 781 | 260 | 1054 | 1691 | 297 | 14713 | 1.99 | 662 | 339 | 1.95 | 0.20 | 4497.98 | 2708 |
| MRH-07 | 594.9 | 7.6 | 2160.3 | 11.7 | <0.01 | 54.8 | 0.07 | 0.96 | 3.11 | 0.51 | 26.5 | 151 | 65.3 | 340 | 815 | 166 | 23094 | 5.70 | 490 | 542 | 0.90 | 0.49 | 1623.41 | 592 |
| MRH-08 | 326.6 | 15.2 | 1060.4 | 5.71 | 0.03 | 27.7 | 0.12 | 2.00 | 3.75 | 0.58 | 20.3 | 89.9 | 35.0 | 166 | 346 | 67.3 | 16548 | 1.56 | 106 | 235 | 0.45 | 0.27 | 758.60 | 2001 |
| MRH-10 | 265.9 | 9.0 | 710.5 | 2.77 | 0.01 | 5.79 | 0.09 | 1.78 | 3.56 | 0.26 | 18.5 | 67.1 | 24.3 | 104 | 209 | 38.3 | 10763 | 0.76 | 87.0 | 133 | 0.66 | 0.27 | 472.54 | 2016 |
| MRH-11 | 249.2 | 35.3 | 1044.6 | 1.01 | 0.07 | 3.88 | 0.30 | 5.05 | 7.24 | 1.91 | 31.2 | 108 | 37.3 | 153 | 287 | 51.3 | 8222 | 0.25 | 38.6 | 50.5 | 0.76 | 0.24 | 686.47 | 1835 |
| MRH-12 | 249.9 | 34.9 | 1043.3 | 1.53 | 0.58 | 16.8 | 0.70 | 9.17 | 12.4 | 2.29 | 42.3 | 115 | 37.3 | 147 | 257 | 44.1 | 9157 | 0.33 | 60.5 | 54.6 | 1.11 | 0.22 | 684.72 | 1916 |
| MRH-13 | 259.7 | 10.6 | 615.4 | 1.06 | 0.03 | 31.4 | 0.22 | 3.24 | 5.80 | 1.86 | 22.7 | 59.7 | 19.6 | 83.2 | 175 | 35.3 | 8270 | 0.20 | 104 | 126 | 0.83 | 0.19 | 438.38 | 2350 |
| MRH-14 | 187.4 | 25.9 | 1614.6 | 9.45 | 0.59 | 30.9 | 0.73 | 6.16 | 9.38 | 0.52 | 44.1 | 166 | 58.6 | 240 | 407 | 68.6 | 8294 | 2.10 | 168 | 273 | 0.61 | 0.22 | 1032.41 | 485 |
| MRH-15 | 101.6 | 8.7 | 1127.2 | 1.34 | 0.01 | 21.8 | 0.14 | 2.72 | 4.76 | 1.49 | 23.9 | 98.4 | 37.8 | 175 | 387 | 70.3 | 8765 | 0.34 | 68.5 | 55.9 | 1.23 | 0.25 | 822.58 | 375 |
| MRH-18 | 228.5 | 44.3 | 928.6 | 0.91 | 0.06 | 3.22 | 0.37 | 5.16 | 7.60 | 2.00 | 29.8 | 97.5 | 32.9 | 136 | 249 | 43.9 | 8183 | 0.20 | 30.6 | 41.0 | 0.75 | 0.22 | 606.67 | 1870 |
| MRH-19 | 23.5 | 1.0 | 483.5 | 1.39 | 0.15 | 35.9 | 0.06 | 0.74 | 1.14 | 0.58 | 6.10 | 28.3 | 12.7 | 68.6 | 215 | 47.5 | 10381 | 0.12 | 140 | 283 | 0.50 | 0.08 | 416.63 | 301 |
| MRH-20 | 99.5 | 5.4 | 1285.3 | 1.47 | 0.01 | 21.6 | 0.18 | 2.83 | 5.18 | 1.25 | 24.3 | 105 | 42.5 | 206 | 492 | 92.2 | 9026 | 0.46 | 96.1 | 89.0 | 1.08 | 0.31 | 993.19 | 383 |
| MRH2-01 | 200.4 | 18.2 | 870.4 | 1.43 | 1.13 | 12.7 | 0.43 | 4.64 | 6.25 | 0.74 | 25.2 | 85.4 | 30.4 | 126 | 240 | 42.3 | 9566 | 0.39 | 54.0 | 74.5 | 0.73 | 0.27 | 575.59 | 1849 |
| MRH2-02 | 149.6 | 15.5 | 433.2 | 4.64 | <0.01 | 30.8 | 0.03 | 0.73 | 1.48 | 0.24 | 7.07 | 34.6 | 14.1 | 69.1 | 176 | 34.4 | 11653 | 1.83 | 110 | 138 | 0.80 | 0.39 | 368.77 | 1882 |
| MRH2-03 | 57.8 | 1.8 | 232.3 | 6.55 | <0.01 | 15.1 | 0.04 | 0.72 | 1.41 | 0.44 | 6.10 | 25.0 | 9.10 | 39.4 | 88.9 | 16.4 | 9435 | 2.62 | 54.2 | 189 | 0.29 | 0.40 | 202.44 | 1990 |
| MRH2-04 | 172.8 | 12.2 | 309.3 | 1.19 | <0.01 | 10.0 | 0.05 | 0.73 | 1.37 | 0.46 | 7.25 | 28.2 | 10.2 | 43.2 | 81.8 | 14.7 | 9968 | 0.42 | 69.3 | 125 | 0.56 | 0.35 | 197.87 | 1855 |
| MRH2-05 | 120.3 | 3.5 | 286.0 | 1.02 | <0.01 | 15.4 | 0.05 | 0.86 | 1.62 | 0.52 | 7.63 | 25.3 | 9.30 | 41.4 | 92.8 | 17.2 | 8784 | 0.24 | 51.4 | 80.1 | 0.64 | 0.24 | 212.04 | 2006 |
| MRH2-06 | 193.3 | 3.9 | 533.8 | 1.14 | <0.01 | 6.42 | 0.03 | 0.71 | 2.04 | 0.27 | 13.0 | 51.0 | 18.2 | 78.3 | 164 | 32.0 | 11089 | 0.27 | 58.3 | 74.6 | 0.78 | 0.24 | 365.74 | 2693 |
| MRH2-07 | 175.3 | 2.3 | 1279.0 | 5.25 | <0.01 | 9.61 | 0.13 | 2.53 | 6.17 | 0.42 | 33.5 | 124 | 45.2 | 187 | 332 | 57.8 | 9838 | 0.94 | 55.1 | 55.2 | 1.00 | 0.18 | 798.49 | 2068 |
| MRH2-08 | 225.2 | 18.0 | 930.1 | 4.07 | 1.78 | 29.5 | 3.26 | 21.7 | 15.9 | 4.21 | 34.2 | 97.4 | 32.1 | 130 | 239 | 42.6 | 9572 | 1.04 | 193 | 274 | 0.71 | 0.25 | 651.16 | 1956 |
| MRH2-09 | 232.4 | 13.0 | 1015.5 | 1.40 | 0.14 | 11.5 | 0.35 | 4.26 | 5.11 | 2.07 | 24.0 | 90.9 | 33.8 | 147 | 295 | 54.8 | 8084 | 0.33 | 88.5 | 70.9 | 1.25 | 0.24 | 669.37 | 627 |
| MRH-21 | 227.4 | 4.0 | 952.0 | 4.28 | 0.22 | 10.4 | 0.17 | 2.51 | 4.41 | 0.39 | 19.0 | 81.0 | 31.8 | 148 | 340 | 66.1 | 12077 | 1.65 | 196 | 552 | 0.36 | 0.38 | 704.14 | 2467 |
| MRH2-10 | 19.5 | 2.0 | 305.6 | 0.97 | 0.07 | 46.6 | 0.44 | 5.37 | 3.89 | 1.58 | 10.8 | 22.1 | 6.98 | 29.9 | 76.3 | 16.5 | 6468 | 0.06 | 98.0 | 99.6 | 0.98 | 0.06 | 220.38 | 308 |
| MRH2-11 | 86.5 | 1.8 | 448.1 | 0.80 | 0.01 | 12.9 | 0.09 | 1.37 | 2.42 | 1.08 | 9.69 | 35.6 | 13.5 | 67.2 | 184 | 41.7 | 10957 | 0.38 | 273 | 476 | 0.57 | 0.48 | 369.00 | 490 |
| MRH2-12 | 116.4 | 7.2 | 606.3 | 14.4 | 0.15 | 13.6 | 0.25 | 1.97 | 2.11 | 0.24 | 10.2 | 50.5 | 20.2 | 97.8 | 210 | 38.9 | 10436 | 6.06 | 140 | 450 | 0.31 | 0.42 | 446.28 | 1757 |
| MRH2-15 | 174.5 | 12.8 | 827.6 | 1.48 | 0.04 | 20.9 | 0.30 | 4.63 | 5.94 | 1.84 | 24.8 | 75.9 | 26.8 | 119 | 247 | 48.3 | 8468 | 0.43 | 119 | 98.3 | 1.21 | 0.29 | 574.98 | 801 |
| MRH2-16 | 90.1 | 12.4 | 909.6 | 1.68 | 0.82 | 200 | 3.53 | 36.6 | 22.0 | 6.42 | 41.6 | 77.4 | 23.0 | 96.3 | 206 | 41.7 | 7562 | 0.13 | 529 | 363 | 1.46 | 0.08 | 754.83 | 314 |
| MRH2-17 | 135.6 | 8.1 | 215.0 | 1.12 | 0.05 | 4.28 | 0.10 | 1.15 | 2.16 | 1.36 | 11.4 | 27.6 | 6.31 | 19.0 | 21.3 | 3.08 | 10228 | 0.38 | 7.07 | 240 | 0.03 | 0.34 | 97.75 | 1853 |
| MRH2-18 | 158.9 | 6.5 | 591.1 | 0.96 | 0.16 | 9.67 | 0.41 | 3.85 | 4.09 | 1.50 | 15.9 | 55.5 | 20.2 | 89.8 | 175 | 33.2 | 8905 | 0.24 | 90.7 | 86.5 | 1.05 | 0.25 | 408.79 | 2930 |
| MRH2-19 | 156.3 | 14.5 | 850.9 | 1.45 | 0.01 | 4.01 | 0.15 | 3.08 | 5.64 | 0.45 | 23.5 | 81.5 | 28.9 | 125 | 220 | 39.8 | 8968 | 0.36 | 37.8 | 47.0 | 0.80 | 0.25 | 532.69 | 1864 |
| MRH2-20 | 195.7 | 12.8 | 784.8 | 4.80 | 28.0 | 85.3 | 7.72 | 30.6 | 8.74 | 0.58 | 21.5 | 74.9 | 26.9 | 118 | 223 | 41.1 | 11095 | 1.17 | 96.5 | 89.4 | 1.08 | 0.24 | 666.37 | 1882 |
| MRH2-21 | 41.3 | 4.0 | 1000.6 | 3.88 | 0.04 | 72.7 | 0.12 | 1.95 | 3.49 | 1.48 | 16.8 | 70.5 | 28.7 | 145 | 339 | 68.4 | 8952 | 0.51 | 294 | 292 | 1.01 | 0.13 | 748.45 | 310 |
| MRH2-22 | 423.6 | 8.9 | 995.0 | 1.82 | <0.01 | 3.43 | 0.22 | 4.53 | 10.0 | 0.36 | 42.3 | 108 | 33.1 | 131 | 219 | 39.7 | 10989 | 0.52 | 150 | 335 | 0.45 | 0.29 | 591.34 | 1069 |
| MRH2-23 | 198.9 | 7.1 | 686.7 | 3.38 | <0.01 | 34.8 | 0.12 | 1.51 | 3.21 | 0.58 | 15.7 | 59.4 | 22.1 | 103 | 217 | 42.1 | 10519 | 1.15 | 165 | 260 | 0.64 | 0.34 | 499.81 | 2466 |
| MRH2-24 | 161.5 | 4.3 | 884.7 | 0.75 | 0.02 | 2.00 | 0.03 | 0.63 | 1.70 | 0.36 | 11.5 | 62.6 | 26.9 | 143 | 376 | 83.9 | 10732 | 0.15 | 9.96 | 26.3 | 0.38 | 0.21 | 708.64 | 709 |
| MRH2-25 | 88.2 | 10.2 | 552.2 | 2.60 | <0.01 | 7.43 | 0.08 | 1.28 | 2.39 | 0.15 | 11.4 | 46.9 | 17.4 | 82.9 | 178 | 34.6 | 10701 | 0.72 | 50.0 | 250 | 0.20 | 0.28 | 382.77 | 1917 |
| MRH2-26 | 405.6 | 6.2 | 827.0 | 3.69 | 2.61 | 32.3 | 1.39 | 7.33 | 4.99 | 0.89 | 18.3 | 69.8 | 26.9 | 127 | 275 | 54.0 | 9958 | 1.04 | 118 | 405 | 0.29 | 0.28 | 620.51 | 1945 |
| MRH2-27 | 154.3 | 4.9 | 548.1 | 1.43 | 0.02 | 9.42 | 0.03 | 0.61 | 1.66 | 0.39 | 11.4 | 48.9 | 18.5 | 84.4 | 164 | 30.5 | 9644 | 0.38 | 56.7 | 75.7 | 0.75 | 0.27 | 369.68 | 3414 |
| MRH2-28 | 122.6 | 4.9 | 468.8 | 7.44 | 0.01 | 11.8 | 0.04 | 0.44 | 0.98 | 0.13 | 5.90 | 35.1 | 15.0 | 78.2 | 203 | 40.9 | 10930 | 3.32 | 123 | 303 | 0.41 | 0.45 | 391.40 | 1820 |
| MRH2-29 | 185.5 | 9.7 | 1488.6 | 4.38 | 0.11 | 40.9 | 0.73 | 11.2 | 15.6 | 3.04 | 49.5 | 144 | 49.0 | 208 | 385 | 70.8 | 9540 | 1.21 | 282 | 245 | 1.15 | 0.28 | 977.97 | 1948 |

| Analysis No. | P | Ti | Y | Nb | La | Ce | Pr | Nd | Sm | Eu | Gd | Dy | Ho | Er | Yb | Lu | Hf | Ta | Th | U | Th/U | Nb/Ta | Total REE | U-Pb age |
|---|---|---|---|---|---|---|---|---|---|---|---|---|---|---|---|---|---|---|---|---|---|---|---|---|
| MRH-23 | 138.1 | 4.7 | 524.5 | 0.67 | <0.01 | 2.28 | 0.02 | 0.42 | 0.67 | 0.28 | 5.23 | 31.1 | 14.5 | 87.2 | 281 | 67.6 | 10095 | 0.13 | 16.3 | 31.8 | 0.51 | 0.20 | 489.92 | 650 |
| MRH2-30 | 145.4 | 4.5 | 236.7 | 1.13 | 0.02 | 8.90 | 0.10 | 1.60 | 3.72 | 0.61 | 14.1 | 29.4 | 7.94 | 25.9 | 35.6 | 5.56 | 12540 | 0.32 | 80.7 | 88.1 | 0.92 | 0.28 | 133.44 | 1703 |
| MRH2-32c | 50.8 | 1.4 | 92.4 | 0.71 | 0.06 | 0.68 | 0.08 | 0.58 | 0.37 | 0.10 | 1.06 | 5.68 | 2.93 | 16.3 | 49.4 | 10.7 | 12260 | 0.33 | 3.82 | 27.1 | 0.14 | 0.46 | 87.94 | 2097 |
| MRH2-32r | 254.7 | 2.8 | 1471.3 | 3.77 | | 8.48 | 0.08 | 1.29 | 3.25 | 0.65 | 22.6 | 124 | 50.6 | 234 | 485 | 89.1 | 10502 | 1.25 | 55.5 | 159 | 0.35 | 0.33 | 1018.90 | 2093 |
| MRH2-33 | 297.5 | 11.6 | 770.2 | 1.75 | 4.25 | 26.1 | 7.10 | 40.5 | 19.9 | 6.51 | 28.1 | 72.8 | 23.9 | 109 | 268 | 56.3 | 10010 | 0.70 | 232 | 533 | 0.44 | 0.40 | 662.95 | 579 |
| MRH2-34 | 212.2 | 7.1 | 712.5 | 1.21 | 0.02 | 19.3 | 0.18 | 1.35 | 2.59 | 0.81 | 14.3 | 61.1 | 23.7 | 109 | 240 | 44.4 | 9980 | 0.42 | 101 | 142 | 0.71 | 0.34 | 516.28 | 2972 |
| MRH2-36 | 276.9 | 37.6 | 900.3 | 1.63 | 0.16 | 35.4 | 0.36 | 6.57 | 11.3 | 4.76 | 40.9 | 103 | 32.2 | 123 | 207 | 35.2 | 8719 | 0.30 | 13.2 | 9.48 | 1.39 | 0.18 | 600.06 | 2596 |
| MRH2-37 | 188.6 | 11.8 | 667.6 | 1.23 | 0.08 | 10.1 | 0.14 | 1.58 | 2.29 | 0.98 | 11.2 | 48.3 | 20.3 | 101 | 283 | 59.7 | 8565 | 0.33 | 99.3 | 142 | 0.70 | 0.27 | 539.11 | 633 |
| MRH2-38 | 193.8 | 9.6 | 583.8 | 1.72 | 0.02 | 30.1 | 0.11 | 1.86 | 3.44 | 0.78 | 16.9 | 55.0 | 19.3 | 81.1 | 165 | 30.0 | 10470 | 0.46 | 134 | 141 | 0.95 | 0.27 | 402.97 | 1900 |
| MRH2-39 | 411.4 | 24.0 | 2612.6 | 2.81 | 0.87 | 12.2 | 0.96 | 11.9 | 17.9 | 2.52 | 79.6 | 271 | 93.8 | 388 | 716 | 123 | 8193 | 0.75 | 206 | 115 | 1.78 | 0.27 | 1717.69 | 493 |
| MRH-24 | 191.3 | 2.5 | 645.4 | 1.17 | 0.05 | 6.14 | 0.09 | 1.08 | 1.81 | 0.55 | 11.1 | 52.3 | 21.1 | 102 | 225 | 47.3 | 10677 | 0.23 | 21.3 | 78.0 | 0.27 | 0.20 | 468.54 | 2734 |
| MRH2-40 | 185.0 | 37.6 | 555.3 | 2.29 | 0.46 | 10.4 | 0.28 | 2.45 | 3.56 | 0.31 | 14.9 | 53.5 | 18.9 | 81.0 | 160 | 28.1 | 9720 | 0.67 | 90.0 | 234 | 0.38 | 0.29 | 373.57 | 1881 |
| MRH2-43 | 166.3 | 10.5 | 1100.6 | 2.13 | 0.16 | 31.5 | 0.51 | 6.98 | 8.75 | 3.99 | 32.7 | 103 | 36.4 | 161 | 363 | 69.0 | 7786 | 0.61 | 106 | 91.7 | 1.16 | 0.29 | 817.12 | 497 |
| MRH2-45 | 219.8 | 11.4 | 1376.9 | 1.02 | <0.01 | 6.53 | 0.03 | 0.76 | 2.73 | 0.52 | 21.0 | 111 | 43.6 | 209 | 431 | 81.3 | 10659 | 0.26 | 32.8 | 43.4 | 0.76 | 0.25 | 906.98 | 805 |
| MRH2-46 | 105.1 | 2.7 | 435.8 | 0.70 | <0.01 | 0.94 | 0.01 | 0.23 | 0.72 | 0.15 | 5.28 | 29.9 | 13.4 | 73.7 | 201 | 45.2 | 8906 | 0.11 | 6.83 | 20.1 | 0.34 | 0.16 | 370.59 | 755 |
| MRH2-47 | 234.7 | 23.6 | 675.6 | 0.99 | 0.22 | 11.6 | 0.29 | 2.78 | 3.43 | 0.63 | 16.2 | 61.1 | 21.9 | 97.1 | 186 | 33.4 | 10396 | 0.28 | 73.7 | 88.8 | 0.83 | 0.28 | 434.69 | 699 |
| MRH2-48 | 137.5 | 17.8 | 335.7 | 2.57 | 0.13 | 12.8 | 0.19 | 2.08 | 2.75 | 0.43 | 10.8 | 33.2 | 11.0 | 45.9 | 86.6 | 15.6 | 10376 | 0.64 | 116 | 157 | 0.74 | 0.25 | 221.47 | 1934 |
| MRH2-49 | 412.2 | 9.9 | 2188.0 | 2.00 | 0.05 | 34.8 | 0.30 | 5.44 | 9.80 | 3.70 | 50.2 | 195 | 72.0 | 329 | 645 | 123 | 8662 | 0.54 | 131 | 138 | 0.95 | 0.27 | 1469.67 | 367 |
| MRH-25 | 142.8 | 7.8 | 396.3 | 1.50 | 0.16 | 19.2 | 0.21 | 1.65 | 2.31 | 0.65 | 8.89 | 30.0 | 11.6 | 55.6 | 138 | 31.6 | 10859 | 0.43 | 74.6 | 161 | 0.46 | 0.29 | 299.64 | 2029 |
| MRH2-50 | 177.3 | 8.5 | 804.6 | 1.46 | | 11.2 | 0.12 | 2.00 | 3.31 | 0.79 | 16.7 | 66.1 | 25.8 | 125 | 276 | 55.4 | 8731 | 0.37 | 41.1 | 49.6 | 0.83 | 0.26 | 581.68 | 790 |
| MRH2-51 | 83.7 | 3.2 | 286.5 | 3.88 | | 9.01 | 0.05 | 1.11 | 3.26 | 0.51 | 16.3 | 35.4 | 9.12 | 30.0 | 37.8 | 6.08 | 10811 | 2.46 | 118 | 248 | 0.47 | 0.63 | 148.70 | 2433 |
| MRH2-52 | 196.2 | 14.2 | 1227.0 | 1.56 | 0.13 | 24.3 | 0.54 | 7.90 | 9.36 | 4.53 | 34.9 | 109 | 38.1 | 176 | 393 | 79.4 | 6633 | 0.39 | 153 | 85.3 | 1.79 | 0.25 | 876.85 | 547 |
| MRH2-53 | 148.1 | 21.2 | 679.9 | 2.19 | 0.02 | 11.4 | 0.26 | 3.63 | 4.90 | 0.83 | 17.9 | 60.2 | 21.5 | 98.6 | 219 | 42.5 | 9735 | 1.06 | 306 | 335 | 0.91 | 0.48 | 480.30 | 390 |
| MRH2-54 | 203.3 | 29.7 | 873.4 | 2.11 | 0.37 | 12.4 | 0.30 | 4.67 | 6.59 | 0.97 | 26.6 | 86.2 | 29.7 | 123 | 224 | 40.0 | 8882 | 0.56 | 53.6 | 53.8 | 1.00 | 0.27 | 555.22 | 1917 |
| MRH2-55 | 236.5 | 12.5 | 814.2 | 1.34 | 0.01 | 12.9 | 0.08 | 1.49 | 2.89 | 0.74 | 15.0 | 64.3 | 25.7 | 129 | 312 | 67.0 | 9053 | 0.45 | 92.8 | 143 | 0.65 | 0.33 | 631.31 | 537 |
| MRH2-56 | 207.2 | 35.5 | 513.6 | 1.37 | 0.08 | 21.2 | 0.24 | 2.40 | 3.50 | 0.52 | 13.4 | 47.5 | 16.4 | 73.3 | 144 | 26.9 | 9992 | 0.37 | 167 | 160 | 1.05 | 0.27 | 349.34 | 626 |
| MRH2-57 | 178.2 | 8.0 | 776.5 | 3.42 | 0.21 | 34.6 | 0.40 | 2.91 | 2.71 | 0.70 | 11.4 | 53.9 | 23.0 | 124 | 325 | 69.3 | 11197 | 1.15 | 221 | 328 | 0.67 | 0.34 | 648.21 | 2012 |
| MRH2-58 | 177.6 | 84.8 | 411.1 | 3.06 | 1.21 | 19.5 | 0.82 | 6.05 | 3.96 | 0.70 | 11.0 | 40.8 | 13.8 | 62.0 | 129 | 23.0 | 10061 | 0.89 | 55.2 | 90.8 | 0.61 | 0.29 | 311.76 | 1784 |
| MRH2-59 | 158.5 | 6.7 | 433.9 | 1.70 | 0.01 | 28.9 | 0.07 | 1.33 | 2.58 | 0.57 | 11.3 | 37.4 | 13.6 | 61.3 | 126 | 24.8 | 10302 | 0.46 | 104 | 79.6 | 1.30 | 0.27 | 308.22 | 2732 |
| MRH-26 | 553.3 | 4.5 | 2582.6 | 7.25 | 5.63 | 98.7 | 2.12 | 12.0 | 9.59 | 1.19 | 44.3 | 207 | 81.3 | 388 | 786 | 148 | 9964 | 1.59 | 360 | 346 | 1.04 | 0.22 | 1783.96 | 260 |
| MRH-27 | 190.7 | 7.5 | 956.0 | 2.18 | 0.01 | 30.4 | 0.17 | 2.53 | 4.28 | 1.47 | 21.2 | 82.0 | 30.7 | 142 | 297 | 57.6 | 8143 | 0.75 | 186 | 209 | 0.89 | 0.34 | 669.69 | 298 |
| MRH-28 | 299.6 | 33.5 | 869.9 | 4.65 | 0.07 | 27.0 | 0.12 | 1.74 | 3.35 | 0.44 | 17.1 | 75.9 | 29.1 | 137 | 287 | 55.5 | 9679 | 1.66 | 56.0 | 72.0 | 0.78 | 0.36 | 633.88 | 1829 |
| MRH-29 | 209.6 | 186.1 | 1183.2 | 1.13 | 0.08 | 9.29 | 0.25 | 3.68 | 5.27 | 0.93 | 27.3 | 105 | 38.7 | 170 | 305 | 56.5 | 9632 | 0.35 | 93.9 | 88.0 | 1.07 | 0.31 | 722.38 | 630 |
| MRH-30 | 106.1 | 6.1 | 246.3 | 0.80 | | 1.93 | 0.02 | 0.31 | 0.49 | 0.33 | 3.44 | 17.8 | 7.63 | 39.3 | 108 | 25.4 | 7398 | 0.23 | 9.71 | 27.6 | 0.35 | 0.29 | 204.49 | 2187 |
| MRH-32 | 182.1 | 43.0 | 661.4 | 4.40 | 0.02 | 8.14 | 0.08 | 1.36 | 2.64 | 0.21 | 13.3 | 57.6 | 21.8 | 103 | 211 | 40.5 | 10104 | 1.70 | 72.2 | 146 | 0.50 | 0.39 | 459.23 | 1868 |
| MRH-34 | 451.3 | 4.9 | 2720.5 | 8.31 | 21.0 | 69.0 | 9.24 | 49.1 | 21.0 | 0.44 | 71.3 | 266 | 97.0 | 414 | 676 | 118 | 12010 | 2.45 | 149 | 269 | 0.55 | 0.29 | 1812.95 | 767 |
| MRH-37 | 97.0 | 4.6 | 303.0 | 0.89 | <0.01 | 5.20 | 0.03 | 0.43 | 0.71 | 0.26 | 3.88 | 19.2 | 8.56 | 48.2 | 159 | 39.0 | 10734 | 0.29 | 29.6 | 63.3 | 0.47 | 0.33 | 284.70 | 892 |
| MRH-38 | 156.6 | 22.2 | 382.2 | 1.38 | <0.01 | 2.94 | 0.04 | 0.76 | 1.41 | 0.26 | 8.07 | 34.7 | 13.1 | 58.6 | 125 | 23.5 | 9163 | 0.44 | 17.6 | 43.0 | 0.41 | 0.32 | 268.19 | 1865 |
| MRH-39 | 131.1 | 20.0 | 295.8 | 1.42 | 0.42 | 18.0 | 0.42 | 3.51 | 3.03 | 1.53 | 9.77 | 29.1 | 9.46 | 38.7 | 76.9 | 14.2 | 9330 | 0.16 | 61.1 | 192 | 0.32 | 0.11 | 204.98 | 1891 |
| MRH-40 | 304.0 | 10.7 | 2631.0 | 1.88 | 0.14 | 16.5 | 0.50 | 6.73 | 11.8 | 1.26 | 57.4 | 238 | 89.3 | 388 | 749 | 134 | 10636 | 0.56 | 312 | 471 | 0.66 | 0.30 | 1691.88 | 506 |
| MRH-41 | 155.4 | 2.5 | 865.6 | 2.95 | 0.04 | 19.0 | 0.09 | 1.60 | 3.03 | 0.08 | 15.6 | 71.2 | 28.3 | 131 | 297 | 54.9 | 8918 | 0.79 | 125 | 241 | 0.52 | 0.27 | 621.05 | 299 |
| **Alakhit-Markha field, Aikhal pipe** | | | | | | | | | | | | | | | | | | | | | | | | |
| AIKH-01 | 383.9 | 23.6 | 857.6 | 2.459 | 0.481 | 6.47 | 0.814 | 5.94 | 5.54 | 2.247 | 27.13 | 89.5 | 27.57 | 107.9 | 167.98 | 31.08 | 12083 | 1.254 | 65.55 | 681.82 | 0.10 | 0.51 | 472.65 | 1991 |
| AIKH-12C | 365.4 | 24.9 | 936.5 | 1.891 | 2.151 | 26.07 | 2.8 | 22.8 | 16.25 | 7.96 | 43.99 | 103.33 | 31.48 | 120.71 | 183.02 | 33.6 | 10916 | 0.303 | 170.48 | 291.65 | 0.58 | 0.16 | 594.16 | 1921 |
| AIKH-12R | 205.7 | 17.9 | 421.5 | 1.269 | 0.191 | 3.9 | 0.262 | 2.2 | 3.33 | 0.648 | 13.31 | 40.41 | 13.9 | 58.25 | 105.17 | 20.32 | 11147 | 0.291 | 65.54 | 149.91 | 0.44 | 0.23 | 261.89 | 1920 |
| AIKH-20C | 1215.4 | 52.3 | 1158.5 | 1.781 | 1.454 | 12.12 | 2.106 | 18.77 | 18.37 | 0.859 | 58.55 | 133.53 | 39.15 | 145.21 | 210.99 | 37.76 | 10007 | 0.378 | 239.54 | 358.58 | 0.67 | 0.21 | 678.87 | 1951 |
| AIKH-20R | 564.1 | 32.8 | 1292.7 | 1.676 | 0.165 | 6.88 | 0.933 | 12.56 | 19.35 | 0.898 | 66.4 | 152.3 | 43.85 | 159.78 | 232.74 | 41.04 | 9999 | 0.443 | 284.97 | 405.77 | 0.70 | 0.26 | 736.90 | 1936 |

| Analysis No. | P | Ti | Y | Nb | La | Ce | Pr | Nd | Sm | Eu | Gd | Dy | Ho | Er | Yb | Lu | Hf | Ta | Th | U | Th/U | Nb/Ta | Total REE | U-Pb age |
|---|---|---|---|---|---|---|---|---|---|---|---|---|---|---|---|---|---|---|---|---|---|---|---|---|
| AIKH-38 | 208.0 | 30.2 | 403.1 | 2.273 | | 3.85 | 0.1044 | 1.69 | 2.84 | 0.256 | 12.81 | 40.04 | 13.39 | 55.75 | 98.73 | 19.26 | 9531 | 0.604 | 59.44 | 92.62 | 0.64 | 0.27 | 248.72 | 1924 |
| AIKH-48R2 | 201.1 | 39.1 | 363.7 | 2.87 | 0.213 | 4.65 | 0.339 | 3.55 | 3.43 | 0.784 | | 33.96 | 11.92 | 52.04 | 100.1 | 18.67 | 9655 | 0.688 | 121.09 | 289.89 | 0.42 | 0.24 | 229.66 | 1951 |
| AIKH-66 | 186.6 | 22.2 | 347.2 | 0.997 | | 1.999 | 0.0351 | 0.83 | 1.87 | 0.2 | 8.19 | 30.29 | 11.2 | 49 | 90.41 | 16.81 | 10026 | 0.302 | 42.83 | 91.94 | 0.47 | 0.30 | 210.83 | 1855 |
| AIKH-76R | 134.2 | 42.8 | 395.0 | 1.396 | 1.238 | 10.31 | 1.185 | 6.79 | 3.79 | 1.47 | 11.88 | 37.17 | 12.68 | 57.3 | 108.78 | 20.68 | 9574 | 0.282 | 61.1 | 148.6 | 0.41 | 0.20 | 273.27 | 1890 |

**Appendix 3.3. Zircon Hf and O isotopes data for the samples from the Markha terrane**

| Analysis No. | Lu-Hf RATIOS | | | | | | | | | U-Pb AGE | Oxygen | |
|---|---|---|---|---|---|---|---|---|---|---|---|---|
| | $^{176}Hf/^{177}Hf$ | 1SE | $^{176}Lu/^{177}Hf$ | $^{176}Yb/^{177}Hf$ | $Hf_{initial}$ | εHf(T) | ± SE | $T_{DM}$ (Ga) | $T_{DM}^{Crustal}$ (Ga) | (Ma) | $\delta^{18}O$ | 2σ |
| **Malo-Botuobinskoe field, Sputnik pipe** | | | | | | | | | | | | |
| 8008-01 | 0.282607 | 0.000012 | 0.000788 | 0.031214 | 0.282603 | -0.4 | 0.4 | 0.91 | 1.22 | 271 | 3.94 | 0.22 |
| 8008-02Core | 0.282347 | 0.000015 | 0.000750 | 0.029216 | 0.282343 | -8.8 | 0.5 | 1.27 | 1.74 | 309 | 7.04 | 0.21 |
| 8008-02Rim | 0.282623 | 0.000021 | 0.001015 | 0.036906 | 0.282617 | 0.7 | 0.7 | 0.89 | 1.18 | 297 | 7.35 | 0.24 |
| 8008-06 | 0.282756 | 0.000025 | 0.002073 | 0.090087 | 0.282738 | 8.5 | 0.9 | 0.72 | 0.85 | 455 | 7.84 | 0.22 |
| 8008-07 | 0.282733 | 0.000061 | 0.001548 | 0.057954 | 0.282727 | 2.4 | 2.2 | 0.75 | 1.00 | 200 | 6.49 | 0.28 |
| 8008-08 | 0.282239 | 0.000014 | 0.002107 | 0.083094 | 0.282229 | -13.9 | 0.5 | 1.47 | 2.00 | 260 | 2.84 | 0.24 |
| 8008-09 | 0.281075 | 0.000009 | 0.000061 | 0.002561 | 0.281072 | -1.3 | 0.3 | 2.96 | 3.16 | 2609 | 6.24 | 0.20 |
| 8008-10Core | 0.280958 | 0.000014 | 0.000472 | 0.017478 | 0.280934 | -5.3 | 0.5 | 3.15 | 3.43 | 2649 | 5.58 | 0.23 |
| 8008-10CRim | 0.280947 | 0.000012 | 0.000550 | 0.016597 | 0.280920 | -7.2 | 0.4 | 3.17 | 3.49 | 2589 | 5.55 | 0.30 |
| 8008-11Core | 0.280999 | 0.000014 | 0.000525 | 0.018760 | 0.280973 | -6.1 | 0.5 | 3.10 | 3.40 | 2556 | 5.92 | 0.24 |
| 8008-11Rim | 0.281039 | 0.000012 | 0.000222 | 0.008470 | 0.281031 | -20.4 | 0.4 | 3.02 | 3.66 | 1848 | 6.36 | 0.22 |
| 8008-12Core | 0.282372 | 0.000027 | 0.000893 | 0.026966 | 0.282367 | -8.3 | 1.0 | 1.24 | 1.70 | 290 | 6.77 | 0.20 |
| 8008-12Rim | 0.282464 | 0.000020 | 0.000487 | 0.017284 | 0.282461 | -5.1 | 0.7 | 1.10 | 1.51 | 286 | 6.51 | 0.19 |
| 8008-13 | 0.282625 | 0.000011 | 0.001872 | 0.067488 | 0.282610 | 3.3 | 0.4 | 0.91 | 1.13 | 427 | 5.74 | 0.25 |
| 8008-14C | 0.281937 | 0.000012 | 0.000718 | 0.027627 | 0.281933 | -24.1 | 0.4 | 1.84 | 2.59 | 272 | 4.09 | 0.29 |
| 8008-14R | - | - | - | - | - | - | - | - | - | 266 | 4.40 | 0.25 |
| 8008-18C | 0.282783 | 0.000051 | 0.001005 | 0.041520 | 0.282779 | 4.3 | 1.8 | 0.67 | 0.89 | 202 | 7.37 | 0.23 |
| 8008-18R | - | - | - | - | - | - | - | - | - | - | 7.72 | 0.24 |
| 8008-21 | 0.282578 | 0.000019 | 0.001513 | 0.050833 | 0.282573 | -3.6 | 0.7 | 0.97 | 1.33 | 175 | 7.22 | 0.24 |
| 8008-22C | 0.281132 | 0.000011 | 0.000335 | 0.012335 | 0.281115 | 1.4 | 0.4 | 2.90 | 3.04 | 2662 | 5.17 | 0.31 |
| 8008-22R | - | - | - | - | - | - | - | - | - | - | 4.85 | 0.21 |
| 8008-27 | 0.282832 | 0.000110 | 0.000830 | 0.031021 | 0.282829 | 5.5 | 3.9 | 0.59 | 0.80 | 176 | 7.87 | 0.27 |
| 8008-29 | 0.282332 | 0.000016 | 0.001748 | 0.046031 | 0.282322 | -9.7 | 0.6 | 1.33 | 1.78 | 302 | 7.77 | 0.24 |
| 8008-30 | 0.282609 | 0.000013 | 0.001127 | 0.042391 | 0.282603 | 0.0 | 0.5 | 0.91 | 1.21 | 289 | 5.74 | 0.23 |
| 8008-32 | 0.281073 | 0.000024 | 0.000300 | 0.008131 | 0.281058 | -3.4 | 0.9 | 2.98 | 3.23 | 2541 | 7.73 | 0.27 |
| 8008-40 | 0.282809 | 0.000084 | 0.002101 | 0.081680 | 0.282798 | 6.7 | 3.0 | 0.65 | 0.81 | 283 | 5.27 | 0.20 |
| 8008-43Core | 0.282819 | 0.000015 | 0.001297 | 0.052305 | 0.282814 | 5.3 | 0.5 | 0.62 | 0.82 | 190 | 7.53 | 0.23 |
| 8008-43Rim | 0.282773 | 0.000020 | 0.001545 | 0.059770 | 0.282768 | 3.6 | 0.7 | 0.69 | 0.92 | 190 | - | - |
| 8008-46 | 0.282917 | 0.000040 | 0.001141 | 0.043508 | 0.282911 | 10.3 | 1.4 | 0.48 | 0.58 | 260 | - | - |
| 8008-49 | 0.282597 | 0.000012 | 0.000852 | 0.030929 | 0.282592 | 0.1 | 0.4 | 0.92 | 1.22 | 311 | 7.17 | 0.30 |
| 8008-51 | - | - | - | - | - | - | - | - | - | 405 | 6.05 | 0.20 |
| 8008-57 | - | - | - | - | - | - | - | - | - | 2745 | 5.70 | 0.20 |
| 8008-58 | - | - | - | - | - | - | - | - | - | 334 | 6.79 | 0.22 |
| 8008-59 | 0.280986 | 0.000018 | 0.000645 | 0.020538 | 0.280952 | -2.4 | 0.6 | 3.12 | 3.34 | 2745 | - | - |
| **Upper Muna field, 325 years of Yakutia pipe** | | | | | | | | | | | | |
| MVG124-01 | 0.282646 | 0.000007 | 0.000020 | 0.001097 | 0.282646 | 3.1 | 0.2 | 0.84 | 1.15 | 359 | - | - |
| MVG124-02 | 0.282649 | 0.000009 | 0.000013 | 0.000699 | 0.282649 | 3.4 | 0.3 | 0.83 | 1.14 | 369 | - | - |
| MVG124-03 | 0.282662 | 0.000007 | 0.000019 | 0.001043 | 0.282662 | 3.4 | 0.2 | 0.82 | 1.12 | 349 | - | - |
| MVG124-04 | 0.282635 | 0.000006 | 0.000008 | 0.000440 | 0.282635 | 2.3 | 0.2 | 0.85 | 1.18 | 341 | - | - |
| MVG124-05 | 0.282668 | 0.000007 | 0.000021 | 0.001119 | 0.282668 | 3.9 | 0.3 | 0.81 | 1.10 | 360 | - | - |
| MVG124-06 | 0.282653 | 0.000007 | 0.000020 | 0.001084 | 0.282653 | 3.3 | 0.3 | 0.83 | 1.13 | 357 | - | - |
| MVG124-07 | 0.282654 | 0.000006 | 0.000023 | 0.001243 | 0.282654 | 3.6 | 0.2 | 0.83 | 1.12 | 369 | - | - |

| Analysis No. | Lu-Hf RATIOS | | | | | | | | | U-Pb AGE | Oxygen | |
|---|---|---|---|---|---|---|---|---|---|---|---|---|
| | $^{176}Hf/^{177}Hf$ | 1SE | $^{176}Lu/^{177}Hf$ | $^{176}Yb/^{177}Hf$ | $Hf_{initial}$ | εHf(T) | ± SE | $T_{DM}$ (Ga) | $T_{DM}^{Crustal}$ (Ga) | (Ma) | $\delta^{18}O$ | 2σ |
| MVG124-09 | 0.282636 | 0.000007 | 0.000021 | 0.001123 | 0.282636 | 2.5 | 0.2 | 0.85 | 1.18 | 350 | - | - |
| MVG124-10 | 0.282667 | 0.000007 | 0.000024 | 0.001230 | 0.282667 | 3.5 | 0.2 | 0.81 | 1.11 | 344 | - | - |
| MVG124-11 | 0.282672 | 0.000010 | 0.000024 | 0.001257 | 0.282672 | 4.1 | 0.3 | 0.80 | 1.09 | 366 | - | - |
| MVG125-01 | 0.282661 | 0.000008 | 0.000017 | 0.000873 | 0.282661 | 3.7 | 0.3 | 0.82 | 1.11 | 362 | - | - |
| MVG125-02 | 0.282653 | 0.000010 | 0.000005 | 0.000252 | 0.282653 | 3.2 | 0.3 | 0.83 | 1.14 | 353 | - | - |
| MVG125-03 | 0.282648 | 0.000009 | 0.000018 | 0.000953 | 0.282648 | 3.3 | 0.3 | 0.83 | 1.14 | 365 | - | - |
| MVG125-04 | 0.282651 | 0.000011 | 0.000015 | 0.000739 | 0.282651 | 2.9 | 0.4 | 0.83 | 1.15 | 345 | - | - |
| MVG125-05 | 0.282639 | 0.000010 | 0.000012 | 0.000612 | 0.282639 | 3.2 | 0.4 | 0.85 | 1.15 | 374 | - | - |
| MVG125-06 | 0.282644 | 0.000008 | 0.000006 | 0.000298 | 0.282644 | 3.0 | 0.3 | 0.84 | 1.15 | 357 | - | - |
| MVG125-07 | 0.282647 | 0.000007 | 0.000014 | 0.000691 | 0.282647 | 3.0 | 0.2 | 0.84 | 1.15 | 355 | - | - |
| MVG125-08 | 0.282628 | 0.000009 | 0.000010 | 0.000518 | 0.282628 | 2.4 | 0.3 | 0.86 | 1.19 | 359 | - | - |
| MVG125-09 | 0.282633 | 0.000007 | 0.000003 | 0.000181 | 0.282633 | 2.8 | 0.2 | 0.85 | 1.17 | 368 | - | - |
| **Daldyn field, Udachnaya Eastern pipe** | | | | | | | | | | | | |
| ZP1004-03 | 0.281075 | 0.000026 | 0.000549 | 0.019005 | 0.281047 | -0.2 | 0.9 | 3.00 | 3.21 | 2697 | - | - |
| ZP1004-06 | 0.280966 | 0.000032 | 0.001075 | 0.037503 | 0.280910 | -5.0 | 1.1 | 3.18 | 3.51 | 2699 | - | - |
| ZP1004-07 | 0.281090 | 0.000028 | 0.001075 | 0.043678 | 0.281035 | -1.5 | 1.0 | 3.02 | 3.26 | 2660 | - | - |
| ZP1004-08 | 0.280960 | 0.000027 | 0.000894 | 0.032916 | 0.280915 | -6.0 | 1.0 | 3.18 | 3.54 | 2647 | - | - |
| ZP1004-12 | 0.281057 | 0.000019 | 0.000383 | 0.015329 | 0.281037 | 0.3 | 0.7 | 3.01 | 3.20 | 2731 | - | - |
| ZP1004-13 | 0.281054 | 0.000029 | 0.000360 | 0.014192 | 0.281035 | -0.4 | 1.0 | 3.01 | 3.23 | 2706 | - | - |
| ZP1004-18 | 0.281005 | 0.000026 | 0.000322 | 0.013163 | 0.280988 | -2.0 | 0.9 | 3.07 | 3.33 | 2707 | - | - |
| ZP1004-20 | 0.280993 | 0.000028 | 0.000372 | 0.014458 | 0.280974 | -2.4 | 1.0 | 3.09 | 3.36 | 2714 | - | - |
| ZP1004-21 | 0.281081 | 0.000026 | 0.000967 | 0.035432 | 0.281033 | -2.5 | 0.9 | 3.02 | 3.29 | 2621 | - | - |
| ZP1004-22 | 0.281003 | 0.000024 | 0.000326 | 0.013118 | 0.280986 | -1.9 | 0.9 | 3.07 | 3.33 | 2717 | - | - |
| ZP1004-24 | 0.280967 | 0.000038 | 0.000699 | 0.028523 | 0.280930 | -3.3 | 1.4 | 3.15 | 3.44 | 2740 | - | - |
| ZP1004-26 | 0.281025 | 0.000026 | 0.000980 | 0.043746 | 0.280974 | -2.3 | 0.9 | 3.10 | 3.36 | 2715 | - | - |
| ZP1004-27 | 0.280981 | 0.000022 | 0.001394 | 0.059749 | 0.280910 | -5.6 | 0.8 | 3.19 | 3.53 | 2673 | - | - |
| ZP1004-29 | 0.280978 | 0.000029 | 0.000686 | 0.028524 | 0.280943 | -4.3 | 1.0 | 3.14 | 3.46 | 2678 | - | - |
| ZP1004-32 | 0.281003 | 0.000031 | 0.000242 | 0.009989 | 0.280990 | -1.7 | 1.1 | 3.07 | 3.32 | 2717 | - | - |
| ZP1104-08 | 0.281011 | 0.000032 | 0.000607 | 0.021473 | 0.280983 | -9.7 | 1.1 | 3.09 | 3.56 | 2387 | - | - |
| ZP1104-19 | 0.280940 | 0.000029 | 0.000270 | 0.009693 | 0.280926 | -4.0 | 1.0 | 3.15 | 3.47 | 2716 | - | - |
| ZP1104-20 | 0.280968 | 0.000025 | 0.000727 | 0.027266 | 0.280932 | -7.4 | 0.9 | 3.15 | 3.56 | 2562 | - | - |
| ZP1104-24 | 0.280985 | 0.000028 | 0.000573 | 0.018352 | 0.280955 | -2.9 | 1.0 | 3.12 | 3.40 | 2720 | - | - |
| ZP1104-25 | 0.280922 | 0.000024 | 0.001143 | 0.042079 | 0.280862 | -6.0 | 0.9 | 3.25 | 3.60 | 2728 | - | - |
| ZP1104-26 | 0.280969 | 0.000023 | 0.000750 | 0.028430 | 0.280931 | -4.9 | 0.8 | 3.15 | 3.49 | 2670 | - | - |
| ZP1604-01 | 0.280665 | 0.000023 | 0.001396 | 0.059778 | 0.280579 | -5.0 | 0.8 | 3.62 | 3.91 | 3197 | - | - |
| ZP1604-02 | 0.281074 | 0.000024 | 0.000190 | 0.007148 | 0.281067 | -18.5 | 0.9 | 2.97 | 3.71 | 1877 | - | - |
| ZP1604-03 | 0.280647 | 0.000022 | 0.001001 | 0.042566 | 0.280586 | -5.5 | 0.8 | 3.61 | 3.91 | 3167 | - | - |
| ZP1604-04 | 0.280958 | 0.000025 | 0.000673 | 0.027065 | 0.280933 | -21.8 | 0.9 | 3.16 | 3.97 | 1942 | - | - |
| ZP1604-05 | 0.280588 | 0.000025 | 0.000861 | 0.036897 | 0.280536 | -7.6 | 0.9 | 3.67 | 4.04 | 3156 | - | - |
| ZP1604-06 | 0.281107 | 0.000021 | 0.000274 | 0.010564 | 0.281097 | -17.5 | 0.7 | 2.93 | 3.65 | 1875 | - | - |
| ZP1604-07 | 0.280685 | 0.000028 | 0.000843 | 0.036135 | 0.280637 | -7.9 | 1.0 | 3.54 | 3.93 | 2989 | - | - |
| ZP1604-09 | 0.280652 | 0.000020 | 0.000750 | 0.030570 | 0.280611 | -12.5 | 0.7 | 3.58 | 4.09 | 2830 | - | - |
| ZP1604-10 | 0.280720 | 0.000026 | 0.001236 | 0.050090 | 0.280675 | -31.3 | 0.9 | 3.53 | 4.55 | 1925 | - | - |
| ZP1604-12 | 0.281066 | 0.000025 | 0.000150 | 0.006566 | 0.281061 | -17.7 | 0.9 | 2.98 | 3.70 | 1923 | - | - |

| Analysis No. | Lu-Hf RATIOS | | | | $Hf_{initial}$ | εHf(T) | ± SE | $T_{DM}$ (Ga) | $T_{DM}^{Crustal}$ (Ga) | U-Pb AGE | Oxygen | |
|---|---|---|---|---|---|---|---|---|---|---|---|---|
| | $^{176}Hf/^{177}Hf$ | 1SE | $^{176}Lu/^{177}Hf$ | $^{176}Yb/^{177}Hf$ | | | | | | (Ma) | $\delta^{18}O$ | 2σ |
| ZP1604-13 | 0.280637 | 0.000025 | 0.000855 | 0.036755 | 0.280585 | -5.7 | 0.9 | 3.61 | 3.92 | 3159 | - | - |
| ZP1604-14 | 0.280898 | 0.000026 | 0.001068 | 0.042981 | 0.280846 | -10.8 | 0.9 | 3.28 | 3.76 | 2546 | - | - |
| ZP1604-15 | 0.280587 | 0.000017 | 0.000978 | 0.043250 | 0.280531 | -11.6 | 0.6 | 3.69 | 4.16 | 2992 | - | - |
| ZP1604-16 | 0.280683 | 0.000023 | 0.000773 | 0.032537 | 0.280637 | -5.7 | 0.8 | 3.54 | 3.86 | 3081 | - | - |
| ZP1604-17 | 0.280691 | 0.000022 | 0.000973 | 0.042088 | 0.280631 | -3.1 | 0.8 | 3.55 | 3.79 | 3200 | - | - |
| ZP1604-18 | 0.281089 | 0.000017 | 0.000005 | 0.000297 | 0.281089 | -16.5 | 0.6 | 2.94 | 3.63 | 1929 | - | - |
| ZP1604-19 | 0.281103 | 0.000021 | 0.000006 | 0.000330 | 0.281103 | -15.8 | 0.7 | 2.92 | 3.60 | 1937 | - | - |
| ZP1604-21 | 0.281086 | 0.000022 | 0.000329 | 0.011957 | 0.281075 | -19.1 | 0.8 | 2.96 | 3.72 | 1838 | - | - |
| ZP1604-22 | 0.280945 | 0.000024 | 0.000463 | 0.017929 | 0.280929 | -24.3 | 0.9 | 3.16 | 4.04 | 1838 | - | - |
| ZP1604-23 | 0.280617 | 0.000025 | 0.001066 | 0.047950 | 0.280561 | -16.3 | 0.9 | 3.65 | 4.26 | 2748 | - | - |
| ZP1604-24 | 0.280673 | 0.000030 | 0.000791 | 0.035297 | 0.280625 | -3.9 | 1.1 | 3.55 | 3.82 | 3176 | - | - |
| ZP1604-25 | 0.280898 | 0.000027 | 0.000220 | 0.008251 | 0.280890 | -23.2 | 1.0 | 3.21 | 4.06 | 1948 | - | - |
| ZP20104-01 | 0.281045 | 0.000025 | 0.000969 | 0.037958 | 0.280995 | -2.6 | 0.9 | 3.07 | 3.34 | 2672 | - | - |
| ZP20104-02 | 0.280934 | 0.000028 | 0.000904 | 0.038483 | 0.280888 | -6.6 | 1.0 | 3.21 | 3.59 | 2665 | - | - |
| ZP20104-03 | 0.280937 | 0.000029 | 0.000789 | 0.031080 | 0.280896 | -5.0 | 1.0 | 3.20 | 3.53 | 2721 | - | - |
| ZP20104-04 | 0.280937 | 0.000029 | 0.000789 | 0.031080 | 0.280897 | -6.9 | 1.0 | 3.20 | 3.59 | 2639 | - | - |
| ZP20104-06 | 0.281050 | 0.000023 | 0.000484 | 0.016598 | 0.281025 | -0.6 | 0.8 | 3.02 | 3.25 | 2710 | - | - |
| ZP20104-08 | 0.281011 | 0.000028 | 0.000950 | 0.036103 | 0.280963 | -4.9 | 1.0 | 3.11 | 3.45 | 2622 | - | - |
| ZP20104-09 | 0.281058 | 0.000027 | 0.000967 | 0.029476 | 0.281009 | -2.2 | 1.0 | 3.05 | 3.31 | 2667 | - | - |
| ZP20104-10 | 0.280958 | 0.000033 | 0.001085 | 0.042272 | 0.280903 | -6.5 | 1.2 | 3.20 | 3.57 | 2644 | - | - |
| ZP20104-11 | 0.280910 | 0.000026 | 0.000586 | 0.022338 | 0.280880 | -7.6 | 0.9 | 3.22 | 3.63 | 2634 | - | - |
| **Daldyn field, Udachnaya Eastern pipe** | | | | | | | | | | | | |
| MVG458_UE-1c | 0.281053 | 0.000010 | 0.000628 | 0.024371 | 0.281023 | -5.4 | 0.3 | 3.03 | 3.39 | 2512 | - | - |
| MVG458_UE-2 | 0.281129 | 0.000007 | 0.002059 | 0.083687 | 0.281026 | -2.6 | 0.2 | 3.04 | 3.30 | 2625 | - | - |
| MVG458_UE-3 | 0.281043 | 0.000007 | 0.000674 | 0.024483 | 0.281009 | -3.0 | 0.3 | 3.05 | 3.34 | 2634 | - | - |
| MVG458_UE-4 | 0.281072 | 0.000009 | 0.000805 | 0.031595 | 0.281031 | -2.0 | 0.3 | 3.02 | 3.28 | 2643 | - | - |
| MVG458_UE-5 | 0.281102 | 0.000010 | 0.000901 | 0.030319 | 0.281059 | -4.5 | 0.3 | 2.99 | 3.32 | 2493 | - | - |
| MVG458_UE-6c | 0.281055 | 0.000010 | 0.000797 | 0.032926 | 0.281019 | -8.9 | 0.3 | 3.04 | 3.50 | 2367 | - | - |
| MVG458_UE-6r | 0.281110 | 0.000008 | 0.000328 | 0.014572 | 0.281098 | -16.0 | 0.3 | 2.93 | 3.61 | 1940 | - | - |
| MVG458_UE-7c | 0.281045 | 0.000009 | 0.000714 | 0.028841 | 0.281017 | -16.3 | 0.3 | 3.05 | 3.71 | 2049 | - | - |
| MVG458_UE-7r | 0.281077 | 0.000008 | 0.000511 | 0.023366 | 0.281059 | -19.1 | 0.3 | 2.99 | 3.74 | 1864 | - | - |
| **Daldyn field, Zarnitsa pipe** | | | | | | | | | | | | |
| MVG458_Z-01 | 0.281159 | 0.000008 | 0.000420 | 0.018847 | 0.281144 | -14.4 | 0.3 | 2.87 | 3.51 | 1937 | - | - |
| MVG458_Z-05 | 0.281335 | 0.000008 | 0.000367 | 0.015313 | 0.281321 | -7.5 | 0.3 | 2.63 | 3.09 | 1962 | - | - |
| MVG458_Z-06r | 0.281464 | 0.000011 | 0.000518 | 0.020685 | 0.281445 | -3.3 | 0.4 | 2.47 | 2.82 | 1954 | - | - |
| MVG458_Z-07 | 0.281316 | 0.000012 | 0.000255 | 0.010744 | 0.281306 | -7.8 | 0.4 | 2.65 | 3.12 | 1973 | - | - |
| MVG458_Z-08 | 0.281015 | 0.000008 | 0.000769 | 0.031411 | 0.280979 | -8.7 | 0.3 | 3.09 | 3.54 | 2437 | - | - |
| MVG458_Z-09 | 0.281247 | 0.000009 | 0.000322 | 0.014539 | 0.281234 | -8.5 | 0.3 | 2.75 | 3.23 | 2052 | - | - |
| MVG458_Z-10 | 0.280937 | 0.000010 | 0.000417 | 0.018911 | 0.280921 | -20.9 | 0.4 | 3.17 | 3.96 | 1996 | - | - |
| MVG458_Z-11 | 0.281190 | 0.000015 | 0.000974 | 0.034476 | 0.281141 | 1.8 | 0.5 | 2.87 | 3.03 | 2639 | - | - |
| MVG458_Z-15 | 0.281175 | 0.000009 | 0.000007 | 0.000533 | 0.281175 | -11.7 | 0.3 | 2.82 | 3.39 | 2007 | - | - |
| **Daldyn field, Popugaeva pipe** | | | | | | | | | | | | |
| MVG458_P-01 | 0.280975 | 0.000013 | 0.000157 | 0.006941 | 0.280970 | -23.2 | 0.5 | 3.10 | 3.96 | 1822 | - | - |
| MVG458_P-02 | 0.281255 | 0.000012 | 0.000937 | 0.041763 | 0.281220 | -11.4 | 0.4 | 2.78 | 3.33 | 1950 | - | - |

| Analysis No. | Lu-Hf RATIOS | | | | | | | | | U-Pb AGE | Oxygen | |
|---|---|---|---|---|---|---|---|---|---|---|---|---|
| | $^{176}Hf/^{177}Hf$ | 1SE | $^{176}Lu/^{177}Hf$ | $^{176}Yb/^{177}Hf$ | $Hf_{initial}$ | εHf(T) | ± SE | $T_{DM}$ (Ga) | $T_{DM}^{Crustal}$ (Ga) | (Ma) | $\delta^{18}O$ | 2σ |
| MVG458_P-03 | 0.281034 | 0.000010 | 0.000319 | 0.013799 | 0.281022 | -17.9 | 0.4 | 3.03 | 3.75 | 1974 | - | - |
| MVG458_P-04 | 0.281421 | 0.000009 | 0.000255 | 0.010260 | 0.281411 | -4.1 | 0.3 | 2.51 | 2.88 | 1972 | - | - |
| MVG458_P-05 | 0.281378 | 0.000010 | 0.000149 | 0.006271 | 0.281373 | -6.5 | 0.4 | 2.56 | 3.00 | 1926 | - | - |
| MVG458_P-07 | 0.281507 | 0.000011 | 0.000149 | 0.006223 | 0.281502 | -2.6 | 0.4 | 2.39 | 2.73 | 1896 | - | - |
| MVG458_P-08 | 0.281219 | 0.000011 | 0.000150 | 0.006816 | 0.281214 | -13.0 | 0.4 | 2.77 | 3.38 | 1891 | - | - |
| MVG458_P-10 | 0.281246 | 0.000011 | 0.000450 | 0.019775 | 0.281229 | -11.5 | 0.4 | 2.76 | 3.32 | 1930 | - | - |
| MVG458_P-13r | 0.281234 | 0.000014 | 0.000323 | 0.013829 | 0.281222 | -11.5 | 0.5 | 2.77 | 3.33 | 1942 | - | - |
| MVG458_P-14 | 0.281463 | 0.000008 | 0.000280 | 0.012470 | 0.281453 | -3.2 | 0.3 | 2.46 | 2.81 | 1947 | - | - |
| MVG458_P-15 | 0.280987 | 0.000011 | 0.000420 | 0.017625 | 0.280967 | -8.4 | 0.4 | 3.10 | 3.55 | 2465 | - | - |
| MVG458_P-16c | 0.280430 | 0.000012 | 0.001338 | 0.062885 | 0.280359 | -23.1 | 0.4 | 3.93 | 4.70 | 2763 | - | - |
| MVG458_P-16r | 0.280450 | 0.000010 | 0.000426 | 0.018828 | 0.280431 | -30.0 | 0.3 | 3.81 | 4.81 | 2359 | - | - |
| MVG458_P-17 | 0.280967 | 0.000010 | 0.000801 | 0.037007 | 0.280923 | -1.0 | 0.4 | 3.16 | 3.38 | 2849 | - | - |
| MVG458_P-18 | 0.281348 | 0.000016 | 0.000024 | 0.001218 | 0.281347 | -8.6 | 0.6 | 2.59 | 3.09 | 1875 | - | - |
| MVG458_P-19 | 0.280902 | 0.000016 | 0.000558 | 0.023960 | 0.280880 | -20.3 | 0.6 | 3.23 | 3.99 | 2087 | - | - |
| MVG458_P-20c | 0.280484 | 0.000012 | 0.001503 | 0.063147 | 0.280388 | -9.0 | 0.4 | 3.88 | 4.25 | 3317 | - | - |
| MVG458_P-20r | 0.280568 | 0.000011 | 0.000156 | 0.007059 | 0.280562 | -31.7 | 0.4 | 3.63 | 4.69 | 2083 | - | - |
| MVG458_P-21 | 0.280410 | 0.000015 | 0.001008 | 0.048540 | 0.280369 | -37.8 | 0.5 | 3.93 | 5.09 | 2117 | - | - |
| **Daldyn field, Zagadochnaya pipe** | | | | | | | | | | | | |
| MVG458_Zag-01 | 0.281087 | 0.000010 | 0.001131 | 0.047940 | 0.281041 | -13.7 | 0.3 | 3.02 | 3.61 | 2126 | - | - |
| MVG458_Zag-02 | 0.281044 | 0.000010 | 0.000380 | 0.015862 | 0.281027 | -8.2 | 0.4 | 3.02 | 3.47 | 2385 | - | - |
| MVG458_Zag-03 | 0.281060 | 0.000016 | 0.000940 | 0.039410 | 0.281013 | -3.7 | 0.6 | 3.05 | 3.35 | 2598 | - | - |
| MVG458_Zag-04 | 0.281239 | 0.000013 | 0.000152 | 0.006773 | 0.281234 | -11.9 | 0.5 | 2.75 | 3.33 | 1906 | - | - |
| MVG458_Zag-06 | 0.281162 | 0.000012 | 0.000272 | 0.012907 | 0.281152 | -12.2 | 0.4 | 2.86 | 3.43 | 2020 | - | - |
| MVG458_Zag-07c | 0.281049 | 0.000009 | 0.000585 | 0.023373 | 0.281020 | -2.9 | 0.3 | 3.03 | 3.32 | 2624 | - | - |
| MVG458_Zag-07r | 0.281055 | 0.000010 | 0.000291 | 0.012764 | 0.281045 | -19.3 | 0.3 | 3.00 | 3.77 | 1875 | - | - |
| MVG458_Zag-08 | 0.281598 | 0.000016 | 0.000422 | 0.017467 | 0.281583 | 1.0 | 0.6 | 2.28 | 2.53 | 1927 | - | - |
| MVG458_Zag-09 | 0.281014 | 0.000008 | 0.000972 | 0.038521 | 0.280979 | -20.9 | 0.3 | 3.11 | 3.89 | 1911 | - | - |
| MVG458_Zag-12 | 0.281055 | 0.000010 | 0.000731 | 0.029949 | 0.281022 | -8.2 | 0.4 | 3.04 | 3.48 | 2390 | - | - |
| MVG458_Zag-13 | 0.281069 | 0.000014 | 0.000709 | 0.029612 | 0.281035 | -5.5 | 0.5 | 3.02 | 3.38 | 2488 | - | - |
| MVG458_Zag-15 | 0.281047 | 0.000014 | 0.000667 | 0.027553 | 0.281019 | -13.0 | 0.5 | 3.04 | 3.62 | 2189 | - | - |
| MVG458_Zag-16 | 0.280740 | 0.000012 | 0.000511 | 0.021400 | 0.280717 | -19.3 | 0.4 | 3.44 | 4.16 | 2379 | - | - |
| MVG458_Zag-17 | 0.281179 | 0.000009 | 0.000461 | 0.020536 | 0.281160 | -8.9 | 0.3 | 2.85 | 3.33 | 2148 | - | - |
| MVG458_Zag-18 | 0.281068 | 0.000012 | 0.001275 | 0.056447 | 0.281004 | -3.1 | 0.4 | 3.06 | 3.35 | 2636 | - | - |
| MVG458_Zag-19 | 0.281564 | 0.000012 | 0.002135 | 0.095111 | 0.281482 | -0.3 | 0.4 | 2.44 | 2.69 | 2029 | - | - |
| MVG458_Zag-20 | 0.281045 | 0.000014 | 0.000808 | 0.030824 | 0.281008 | -8.2 | 0.5 | 3.06 | 3.49 | 2413 | - | - |
| MVG458_Zag-21 | 0.281151 | 0.000019 | 0.001952 | 0.076514 | 0.281059 | -5.3 | 0.7 | 3.00 | 3.34 | 2460 | - | - |
| MVG458_Zag-22 | 0.281071 | 0.000009 | 0.000587 | 0.018947 | 0.281041 | -0.1 | 0.3 | 3.00 | 3.21 | 2708 | - | - |
| MVG458_Zag-23 | 0.281595 | 0.000010 | 0.001225 | 0.052601 | 0.281548 | 1.6 | 0.4 | 2.34 | 2.55 | 2008 | - | - |
| MVG458_Zag-25 | 0.281198 | 0.000009 | 0.000405 | 0.017379 | 0.281179 | -0.8 | 0.3 | 2.82 | 3.07 | 2469 | - | - |
| MVG458_Zag-26 | 0.281087 | 0.000012 | 0.000246 | 0.010377 | 0.281078 | -16.3 | 0.4 | 2.96 | 3.64 | 1955 | - | - |
| MVG458_Zag-31 | 0.281223 | 0.000016 | 0.000201 | 0.009129 | 0.281216 | -12.3 | 0.6 | 2.77 | 3.36 | 1915 | - | - |
| MVG458_Zag-33 | 0.281069 | 0.000010 | 0.000640 | 0.026123 | 0.281039 | -5.4 | 0.4 | 3.01 | 3.37 | 2486 | - | - |
| MVG458_Zag-34 | 0.281058 | 0.000008 | 0.000505 | 0.020611 | 0.281036 | -9.1 | 0.3 | 3.02 | 3.48 | 2334 | - | - |
| MVG458_Zag-36 | 0.281027 | 0.000009 | 0.000417 | 0.016392 | 0.281007 | -5.3 | 0.3 | 3.05 | 3.41 | 2539 | - | - |

| Analysis No. | Lu-Hf RATIOS | | | | $Hf_{initial}$ | εHf(T) | ± SE | $T_{DM}$ (Ga) | $T_{DM}^{Crustal}$ (Ga) | U-Pb AGE | Oxygen | |
|---|---|---|---|---|---|---|---|---|---|---|---|---|
| | $^{176}Hf/^{177}Hf$ | 1SE | $^{176}Lu/^{177}Hf$ | $^{176}Yb/^{177}Hf$ | | | | | | (Ma) | $\delta^{18}O$ | 2σ |
| MVG458_Zag-37 | 0.281458 | 0.000008 | 0.000404 | 0.021220 | 0.281443 | -3.7 | 0.3 | 2.47 | 2.83 | 1938 | - | - |
| **Daldyn field, Kusova pipe** | | | | | | | | | | | | |
| MVG458_K-01 | 0.281038 | 0.000012 | 0.000331 | 0.013426 | 0.281021 | -2.0 | 0.4 | 3.03 | 3.29 | 2660 | - | - |
| MVG458_K-02 | 0.281302 | 0.000008 | 0.000244 | 0.012641 | 0.281293 | -8.5 | 0.3 | 2.67 | 3.16 | 1963 | - | - |
| MVG458_K-03 | 0.281034 | 0.000012 | 0.000592 | 0.025049 | 0.281009 | -12.2 | 0.4 | 3.05 | 3.61 | 2241 | - | - |
| MVG458_K-05 | 0.281643 | 0.000012 | 0.000931 | 0.040298 | 0.281607 | 4.4 | 0.4 | 2.25 | 2.40 | 2038 | - | - |
| MVG458_K-07 | 0.281569 | 0.000011 | 0.000024 | 0.001321 | 0.281568 | 0.2 | 0.4 | 2.30 | 2.57 | 1918 | - | - |
| MVG458_K-08 | 0.281195 | 0.000012 | 0.000398 | 0.017570 | 0.281180 | -13.4 | 0.4 | 2.82 | 3.43 | 1924 | - | - |
| MVG458_K-10 | 0.281082 | 0.000009 | 0.001398 | 0.052288 | 0.281016 | -6.3 | 0.3 | 3.05 | 3.43 | 2482 | - | - |
| MVG458_K-11c | 0.281030 | 0.000015 | 0.000420 | 0.016909 | 0.281010 | -5.4 | 0.5 | 3.05 | 3.41 | 2528 | - | - |
| MVG458_K-11r | 0.281097 | 0.000013 | 0.000178 | 0.008142 | 0.281090 | -13.3 | 0.5 | 2.94 | 3.54 | 2066 | - | - |
| MVG458_K-12 | 0.281014 | 0.000014 | 0.000383 | 0.016153 | 0.281000 | -20.3 | 0.5 | 3.06 | 3.85 | 1900 | - | - |
| MVG458_K-15 | 0.281057 | 0.000012 | 0.001231 | 0.054376 | 0.280995 | -3.1 | 0.4 | 3.07 | 3.36 | 2652 | - | - |
| MVG458_K-16 | 0.281146 | 0.000011 | 0.001209 | 0.052741 | 0.281101 | -15.1 | 0.4 | 2.95 | 3.58 | 1971 | - | - |
| MVG458_K-18 | 0.281021 | 0.000011 | 0.000521 | 0.021299 | 0.280999 | -12.2 | 0.4 | 3.07 | 3.62 | 2254 | - | - |
| MVG458_K-19 | 0.281496 | 0.000012 | 0.000404 | 0.016831 | 0.281479 | 3.1 | 0.4 | 2.42 | 2.59 | 2176 | - | - |
| MVG458_K-21 | 0.281021 | 0.000011 | 0.000748 | 0.032089 | 0.280992 | -17.6 | 0.4 | 3.08 | 3.78 | 2032 | - | - |
| MVG458_K-22 | 0.281008 | 0.000012 | 0.000475 | 0.019478 | 0.280985 | -6.9 | 0.4 | 3.08 | 3.48 | 2502 | - | - |
| MVG458_K-23 | 0.281029 | 0.000013 | 0.000660 | 0.025600 | 0.281000 | -10.1 | 0.5 | 3.07 | 3.56 | 2345 | - | - |
| MVG458_K-24 | 0.281676 | 0.000012 | 0.000246 | 0.009916 | 0.281667 | 3.0 | 0.4 | 2.17 | 2.37 | 1883 | - | - |
| MVG458_K-26 | 0.281020 | 0.000012 | 0.000710 | 0.030921 | 0.280984 | -3.5 | 0.4 | 3.08 | 3.38 | 2650 | - | - |
| MVG458_K-29 | 0.281603 | 0.000010 | 0.000676 | 0.028950 | 0.281577 | 2.6 | 0.3 | 2.29 | 2.49 | 2005 | - | - |
| MVG458_K-30 | 0.280909 | 0.000015 | 0.000774 | 0.033641 | 0.280877 | -17.8 | 0.5 | 3.24 | 3.93 | 2200 | - | - |
| MVG458_K-32 | 0.280937 | 0.000008 | 0.001483 | 0.070982 | 0.280882 | -23.1 | 0.3 | 3.26 | 4.07 | 1962 | - | - |
| MVG458_K-33 | 0.281075 | 0.000014 | 0.001039 | 0.045002 | 0.281026 | -6.6 | 0.5 | 3.03 | 3.42 | 2454 | - | - |
| MVG458_K-34 | 0.281536 | 0.000013 | 0.000242 | 0.009487 | 0.281527 | -1.2 | 0.5 | 2.36 | 2.66 | 1917 | - | - |
| MVG458_K-35 | 0.281029 | 0.000011 | 0.000722 | 0.026505 | 0.280995 | -7.3 | 0.4 | 3.07 | 3.48 | 2473 | - | - |
| MVG458_K-37 | 0.280961 | 0.000013 | 0.000533 | 0.022539 | 0.280937 | -12.1 | 0.5 | 3.15 | 3.69 | 2355 | - | - |
| MVG458_K-38 | 0.280993 | 0.000016 | 0.001716 | 0.056650 | 0.280911 | -9.7 | 0.6 | 3.20 | 3.65 | 2498 | - | - |
| MVG458_K-39 | 0.281012 | 0.000010 | 0.000384 | 0.015523 | 0.280996 | -13.5 | 0.3 | 3.07 | 3.66 | 2204 | - | - |
| MVG458_K-40 | 0.281210 | 0.000012 | 0.001212 | 0.051139 | 0.281164 | -12.4 | 0.4 | 2.86 | 3.42 | 1991 | - | - |
| MVG458_K-41 | 0.281068 | 0.000012 | 0.000429 | 0.018619 | 0.281046 | -1.6 | 0.4 | 3.00 | 3.25 | 2637 | - | - |
| MVG458_K-42 | 0.281111 | 0.000012 | 0.000485 | 0.020571 | 0.281092 | -14.4 | 0.4 | 2.94 | 3.57 | 2017 | - | - |
| MVG458_K-43 | 0.281591 | 0.000010 | 0.000605 | 0.024804 | 0.281568 | 2.6 | 0.4 | 2.30 | 2.50 | 2022 | - | - |
| MVG458_K-44 | 0.281577 | 0.000010 | 0.000177 | 0.008807 | 0.281571 | -0.2 | 0.4 | 2.30 | 2.57 | 1897 | - | - |
| MVG458_K-48 | 0.281084 | 0.000010 | 0.000641 | 0.028619 | 0.281061 | -17.8 | 0.3 | 2.99 | 3.70 | 1919 | - | - |
| MVG458_K-51 | 0.281092 | 0.000009 | 0.000886 | 0.036302 | 0.281050 | -4.5 | 0.3 | 3.00 | 3.33 | 2509 | - | - |
| MVG458_K-52 | 0.280957 | 0.000015 | 0.000849 | 0.032732 | 0.280916 | -8.4 | 0.5 | 3.18 | 3.61 | 2546 | - | - |
| MVG458_K-53 | 0.281124 | 0.000010 | 0.000356 | 0.015188 | 0.281111 | -14.4 | 0.4 | 2.92 | 3.55 | 1986 | - | - |
| MVG458_K-55 | 0.281045 | 0.000015 | 0.000901 | 0.036385 | 0.281002 | -5.9 | 0.5 | 3.06 | 3.43 | 2522 | - | - |
| MVG458_K-58 | 0.281007 | 0.000011 | 0.000757 | 0.032749 | 0.280979 | -19.6 | 0.4 | 3.10 | 3.85 | 1965 | - | - |
| MVG458_K-59 | 0.281588 | 0.000015 | 0.001018 | 0.044812 | 0.281550 | 0.7 | 0.5 | 2.33 | 2.57 | 1966 | - | - |
| **Daldyn field, Udachnaya pipe** | | | | | | | | | | | | |
| OCYB-2_03 | 0.281710 | 0.000024 | 0.000023 | 0.001572 | 0.281709 | 3.7 | 0.9 | 2.11 | 2.29 | 1852 | 5.65 | 0.26 |

| Analysis No. | Lu-Hf RATIOS | | | | | | | | | U-Pb AGE | Oxygen | |
|---|---|---|---|---|---|---|---|---|---|---|---|---|
| | $^{176}Hf/^{177}Hf$ | 1SE | $^{176}Lu/^{177}Hf$ | $^{176}Yb/^{177}Hf$ | $Hf_{initial}$ | εHf(T) | ± SE | $T_{DM}$ (Ga) | $T_{DM}^{Crustal}$ (Ga) | (Ma) | $\delta^{18}O$ | 2σ |
| OCYB-2_03 | 0.281729 | 0.000022 | 0.000023 | 0.001504 | 0.281728 | 4.4 | 0.8 | 2.08 | 2.25 | 1852 | 5.67 | 0.25 |
| OCYB-2_04 | 0.281655 | 0.000020 | 0.000015 | 0.000874 | 0.281654 | 2.2 | 0.7 | 2.18 | 2.40 | 1870 | 5.93 | 0.24 |
| OCYB-2_06 | 0.281673 | 0.000018 | 0.000018 | 0.001255 | 0.281672 | 2.3 | 0.6 | 2.16 | 2.38 | 1845 | - | - |
| OCYB-2_07 | 0.281690 | 0.000018 | 0.000013 | 0.000877 | 0.281690 | 2.8 | 0.6 | 2.14 | 2.34 | 1840 | 5.70 | 0.24 |
| OCYB-2_08 | 0.281696 | 0.000014 | 0.000035 | 0.002086 | 0.281695 | 2.9 | 0.5 | 2.13 | 2.33 | 1840 | - | - |
| OCYB-2_09 | 0.281655 | 0.000020 | 0.000036 | 0.002564 | 0.281654 | 1.4 | 0.7 | 2.18 | 2.43 | 1835 | 5.66 | 0.23 |
| OCYB-2_10 | 0.281654 | 0.000022 | 0.000019 | 0.001316 | 0.281653 | 1.6 | 0.8 | 2.18 | 2.42 | 1845 | 5.66 | 0.24 |
| OCYB-2_11 | 0.281683 | 0.000019 | 0.000023 | 0.001410 | 0.281682 | 2.8 | 0.7 | 2.15 | 2.35 | 1852 | 5.48 | 0.23 |
| OCYB-2_12 | 0.281609 | 0.000024 | 0.000021 | 0.001445 | 0.281608 | -0.6 | 0.9 | 2.24 | 2.54 | 1820 | - | - |
| OCYB-2_18 | 0.281698 | 0.000028 | 0.000025 | 0.001463 | 0.281697 | 3.0 | 1.0 | 2.13 | 2.33 | 1841 | - | - |
| OCYB-2_20 | 0.281669 | 0.000018 | 0.000025 | 0.001695 | 0.281668 | 1.7 | 0.6 | 2.16 | 2.40 | 1827 | 5.54 | 0.27 |
| OCYB-5_01 | 0.281142 | 0.000013 | 0.000156 | 0.008797 | 0.281136 | -16.0 | 0.5 | 2.88 | 3.56 | 1878 | 7.06 | 0.30 |
| OCYB-5_02 | 0.281173 | 0.000015 | 0.000019 | 0.001350 | 0.281172 | -15.8 | 0.5 | 2.83 | 3.51 | 1831 | 7.29 | 0.26 |
| OCYB-5_03 | 0.281123 | 0.000022 | 0.000296 | 0.015558 | 0.281113 | -17.5 | 0.8 | 2.91 | 3.63 | 1851 | 7.05 | 0.29 |
| OCYB-5_04 | 0.281123 | 0.000022 | 0.000296 | 0.015558 | 0.281113 | -17.8 | 0.8 | 2.91 | 3.64 | 1837 | 6.89 | 0.23 |
| OCYB-5_04 | 0.281071 | 0.000014 | 0.000384 | 0.020051 | 0.281058 | -19.8 | 0.5 | 2.99 | 3.76 | 1837 | 6.98 | 0.25 |
| OCYB-5_05 | 0.281273 | 0.000014 | 0.000203 | 0.011908 | 0.281266 | -11.8 | 0.5 | 2.71 | 3.28 | 1863 | - | - |
| OCYB-5_06 | 0.281157 | 0.000026 | 0.000181 | 0.011367 | 0.281150 | -15.1 | 0.9 | 2.86 | 3.52 | 1895 | 7.00 | 0.23 |
| OCYB-5_07 | 0.281155 | 0.000014 | 0.000206 | 0.011493 | 0.281148 | -16.4 | 0.5 | 2.86 | 3.56 | 1844 | - | - |
| OCYB-5_08 | 0.281155 | 0.000014 | 0.000206 | 0.011493 | 0.281148 | -15.8 | 0.5 | 2.86 | 3.54 | 1871 | 6.85 | 0.25 |
| OCYB-5_08 | 0.281196 | 0.000018 | 0.000213 | 0.012650 | 0.281188 | -14.3 | 0.6 | 2.81 | 3.45 | 1871 | - | - |
| OCYB-5_09 | 0.281140 | 0.000023 | 0.000159 | 0.008520 | 0.281135 | -18.4 | 0.8 | 2.88 | 3.63 | 1777 | - | - |
| OCYB-5_10 | 0.281135 | 0.000017 | 0.000199 | 0.011675 | 0.281128 | -17.8 | 0.6 | 2.89 | 3.62 | 1815 | 6.53 | 0.24 |
| OCYB-5_11 | 0.281121 | 0.000017 | 0.000121 | 0.007289 | 0.281117 | -17.4 | 0.6 | 2.90 | 3.62 | 1847 | 6.94 | 0.22 |
| OCYB-5_12 | 0.281116 | 0.000018 | 0.000204 | 0.011897 | 0.281109 | -16.1 | 0.6 | 2.92 | 3.60 | 1916 | 6.52 | 0.25 |
| OCYB-5_13 | 0.281130 | 0.000015 | 0.000365 | 0.021381 | 0.281117 | -16.9 | 0.5 | 2.91 | 3.61 | 1870 | 6.63 | 0.22 |
| OCYB-5_14 | 0.281083 | 0.000022 | 0.000747 | 0.043078 | 0.281056 | -18.1 | 0.8 | 3.00 | 3.72 | 1911 | 6.57 | 0.24 |
| OCYB-5_15 | 0.281178 | 0.000016 | 0.000136 | 0.008129 | 0.281173 | -15.4 | 0.6 | 2.83 | 3.50 | 1849 | 6.52 | 0.21 |
| OCYB-5_16 | 0.281093 | 0.000028 | 0.000122 | 0.007277 | 0.281089 | -19.2 | 1.0 | 2.94 | 3.71 | 1813 | 6.55 | 0.25 |
| OCYB-5_17 | 0.281147 | 0.000014 | 0.000160 | 0.009592 | 0.281142 | -19.2 | 0.5 | 2.87 | 3.64 | 1731 | - | - |
| OCYB-5_18 | 0.280959 | 0.000016 | 0.000248 | 0.013890 | 0.280950 | -23.0 | 0.6 | 3.13 | 3.98 | 1860 | 6.43 | 0.22 |
| OCYB-5_19 | 0.281146 | 0.000017 | 0.000121 | 0.007151 | 0.281141 | -13.6 | 0.6 | 2.87 | 3.49 | 1975 | 6.54 | 0.24 |
| OCYB-5_20 | 0.281159 | 0.000017 | 0.000177 | 0.010622 | 0.281153 | -16.3 | 0.6 | 2.86 | 3.55 | 1841 | 6.28 | 0.24 |
| OCYB-5_23 | 0.281115 | 0.000013 | 0.000157 | 0.009626 | 0.281110 | -18.0 | 0.5 | 2.91 | 3.65 | 1835 | 6.35 | 0.28 |
| OCYB-5_25 | 0.281195 | 0.000020 | 0.000240 | 0.014383 | 0.281187 | -15.7 | 0.7 | 2.81 | 3.49 | 1813 | 6.35 | 0.23 |
| OCYB-5_26 | 0.281169 | 0.000018 | 0.000123 | 0.007392 | 0.281164 | -6.6 | 0.6 | 2.84 | 3.26 | 2242 | 6.33 | 0.21 |
| OCYB-5_27 | 0.281044 | 0.000015 | 0.000343 | 0.019570 | 0.281027 | -3.9 | 0.5 | 3.02 | 3.34 | 2567 | 6.42 | 0.23 |
| OCYB-5_28 | 0.281135 | 0.000023 | 0.000132 | 0.007829 | 0.281130 | -15.5 | 0.8 | 2.88 | 3.55 | 1911 | 6.67 | 0.26 |
| OCYB-5_29 | 0.281191 | 0.000015 | 0.000156 | 0.009469 | 0.281186 | -17.4 | 0.5 | 2.81 | 3.54 | 1742 | 7.14 | 0.27 |
| **Alakhit-Markha field, Kismet pipe** | | | | | | | | | | | | |
| MVG459_Kis-01 | 0.281647 | 0.000012 | 0.000155 | 0.007267 | 0.281641 | 2.9 | 0.4 | 2.20 | 2.40 | 1920 | - | - |
| MVG459_Kis-31 | 0.281469 | 0.000010 | 0.000923 | 0.047651 | 0.281435 | -4.0 | 0.4 | 2.49 | 2.85 | 1939 | - | - |
| MVG459_Kis-33 | 0.281469 | 0.000010 | 0.000923 | 0.047651 | 0.281438 | -7.9 | 0.4 | 2.49 | 2.96 | 1766 | - | - |
| MVG459_Kis-03 | 0.281402 | 0.000017 | 0.000348 | 0.014880 | 0.281390 | -7.0 | 0.6 | 2.54 | 2.99 | 1881 | - | - |

| Analysis No. | Lu-Hf RATIOS | | | | $Hf_{initial}$ | εHf(T) | ± SE | $T_{DM}$ (Ga) | $T_{DM}^{Crustal}$ (Ga) | U-Pb AGE | Oxygen | |
|---|---|---|---|---|---|---|---|---|---|---|---|---|
| | $^{176}Hf/^{177}Hf$ | 1SE | $^{176}Lu/^{177}Hf$ | $^{176}Yb/^{177}Hf$ | | | | | | (Ma) | $\delta^{18}O$ | 2σ |
| MVG459_Kis-20 | 0.281363 | 0.000012 | 0.000573 | 0.025805 | 0.281342 | -7.3 | 0.4 | 2.61 | 3.06 | 1939 | - | - |
| MVG459_Kis-07 | 0.281337 | 0.000011 | 0.000440 | 0.021402 | 0.281321 | -9.3 | 0.4 | 2.64 | 3.14 | 1884 | - | - |
| MVG459_Kis-26 | 0.281332 | 0.000011 | 0.000352 | 0.015052 | 0.281320 | -10.2 | 0.4 | 2.64 | 3.17 | 1849 | - | - |
| MVG459_Kis-14 | 0.281328 | 0.000009 | 0.000736 | 0.033581 | 0.281301 | -9.7 | 0.3 | 2.67 | 3.18 | 1899 | - | - |
| MVG459_Kis-02 | 0.281313 | 0.000009 | 0.000499 | 0.021801 | 0.281295 | -9.8 | 0.3 | 2.67 | 3.19 | 1903 | - | - |
| MVG459_Kis-24 | 0.281305 | 0.000013 | 0.000543 | 0.025649 | 0.281285 | -9.7 | 0.5 | 2.69 | 3.20 | 1923 | - | - |
| MVG459_Kis-09 | 0.281303 | 0.000009 | 0.000618 | 0.028539 | 0.281281 | -10.5 | 0.3 | 2.69 | 3.23 | 1893 | - | - |
| MVG459_Kis-36 | 0.281302 | 0.000011 | 0.000196 | 0.008758 | 0.281295 | -11.3 | 0.4 | 2.67 | 3.23 | 1838 | - | - |
| MVG459_Kis-28 | 0.281302 | 0.000010 | 0.000556 | 0.023862 | 0.281283 | -11.5 | 0.3 | 2.69 | 3.25 | 1848 | - | - |
| MVG459_Kis-35 | 0.281272 | 0.000010 | 0.000345 | 0.017263 | 0.281260 | -11.1 | 0.4 | 2.72 | 3.27 | 1901 | - | - |
| MVG459_Kis-12 | 0.281285 | 0.000011 | 0.000260 | 0.012305 | 0.281276 | -12.1 | 0.4 | 2.69 | 3.28 | 1832 | - | - |
| MVG459_Kis-05 | 0.281268 | 0.000011 | 0.000417 | 0.018432 | 0.281253 | -12.7 | 0.4 | 2.73 | 3.32 | 1842 | - | - |
| MVG459_Kis-30 | 0.281240 | 0.000010 | 0.000458 | 0.020304 | 0.281224 | -13.8 | 0.4 | 2.77 | 3.39 | 1840 | - | - |
| MVG459_Kis-04 | 0.281228 | 0.000007 | 0.001931 | 0.094586 | 0.281158 | -14.5 | 0.3 | 2.89 | 3.49 | 1912 | - | - |
| MVG459_Kis-19 | 0.281154 | 0.000016 | 0.001843 | 0.096703 | 0.281090 | -18.6 | 0.6 | 2.99 | 3.69 | 1839 | - | - |
| MVG459_Kis-16 | 0.280619 | 0.000023 | 0.000323 | 0.017724 | 0.280607 | -34.0 | 0.8 | 3.58 | 4.70 | 1914 | - | - |
| **Alakhit-Markha field, Geochemical pipe** | | | | | | | | | | | | |
| MVG459_Gch-01 | 0.281399 | 0.000019 | 0.001899 | 0.087102 | 0.281329 | -7.9 | 0.7 | 2.65 | 3.09 | 1933 | - | - |
| MVG459_Gch-02 | 0.281431 | 0.000015 | 0.000438 | 0.019734 | 0.281415 | -4.9 | 0.5 | 2.51 | 2.90 | 1933 | - | - |
| MVG459_Gch-03 | 0.281308 | 0.000012 | 0.000394 | 0.018119 | 0.281294 | -10.7 | 0.4 | 2.67 | 3.22 | 1866 | - | - |
| MVG459_Gch-04 | 0.281270 | 0.000010 | 0.002181 | 0.100526 | 0.281191 | -13.2 | 0.4 | 2.85 | 3.41 | 1917 | - | - |
| MVG459_Gch-05 | 0.281477 | 0.000015 | 0.001856 | 0.073387 | 0.281407 | -3.7 | 0.5 | 2.54 | 2.88 | 1994 | - | - |
| MVG459_Gch-06 | 0.281248 | 0.000008 | 0.001478 | 0.067112 | 0.281194 | -12.7 | 0.3 | 2.83 | 3.40 | 1934 | - | - |
| **Alakhit-Markha field, Vostok pipe** | | | | | | | | | | | | |
| MVG459_Vos-25 | 0.281505 | 0.000016 | 0.000161 | 0.005957 | 0.281499 | -3.2 | 0.6 | 2.39 | 2.75 | 1875 | - | - |
| MVG459_Vos-23 | 0.281276 | 0.000013 | 0.000283 | 0.012249 | 0.281266 | -11.4 | 0.5 | 2.71 | 3.27 | 1878 | - | - |
| MVG459_Vos-30 | 0.281300 | 0.000012 | 0.000512 | 0.023294 | 0.281282 | -10.4 | 0.4 | 2.69 | 3.22 | 1898 | - | - |
| MVG459_Vos-07 | 0.281361 | 0.000013 | 0.000444 | 0.020066 | 0.281345 | -8.1 | 0.5 | 2.60 | 3.08 | 1900 | - | - |
| MVG459_Vos-08 | 0.281325 | 0.000013 | 0.000347 | 0.015373 | 0.281312 | -9.2 | 0.5 | 2.65 | 3.15 | 1901 | - | - |
| MVG459_Vos-33 | 0.281297 | 0.000013 | 0.000375 | 0.017858 | 0.281283 | -10.1 | 0.5 | 2.69 | 3.21 | 1910 | - | - |
| MVG459_Vos-16 | 0.281295 | 0.000011 | 0.000483 | 0.022674 | 0.281277 | -10.2 | 0.4 | 2.70 | 3.22 | 1911 | - | - |
| MVG459_Vos-04 | 0.281330 | 0.000011 | 0.000528 | 0.024023 | 0.281311 | -9.0 | 0.4 | 2.65 | 3.15 | 1912 | - | - |
| MVG459_Vos-09 | 0.281310 | 0.000013 | 0.000713 | 0.033257 | 0.281284 | -9.8 | 0.5 | 2.69 | 3.20 | 1922 | - | - |
| MVG459_Vos-13 | 0.281284 | 0.000011 | 0.000267 | 0.012225 | 0.281274 | -10.0 | 0.4 | 2.70 | 3.22 | 1925 | - | - |
| MVG459_Vos-26 | 0.281274 | 0.000013 | 0.000467 | 0.022622 | 0.281257 | -10.6 | 0.5 | 2.72 | 3.26 | 1929 | - | - |
| MVG459_Vos-02 | 0.281459 | 0.000013 | 0.000442 | 0.020971 | 0.281443 | -3.9 | 0.5 | 2.47 | 2.84 | 1932 | - | - |
| MVG459_Vos-12 | 0.281308 | 0.000013 | 0.000316 | 0.014411 | 0.281296 | -9.0 | 0.5 | 2.67 | 3.17 | 1934 | - | - |
| MVG459_Vos-17 | 0.281273 | 0.000012 | 0.001658 | 0.070502 | 0.281212 | -11.9 | 0.4 | 2.81 | 3.35 | 1938 | - | - |
| MVG459_Vos-28 | 0.281347 | 0.000014 | 0.000459 | 0.020732 | 0.281330 | -7.8 | 0.5 | 2.62 | 3.09 | 1938 | - | - |
| MVG459_Vos-24c | 0.281246 | 0.000009 | 0.001733 | 0.081111 | 0.281181 | -12.4 | 0.3 | 2.85 | 3.40 | 1965 | - | - |
| MVG459_Vos-05 | 0.281227 | 0.000014 | 0.000597 | 0.030755 | 0.281205 | -11.5 | 0.5 | 2.80 | 3.35 | 1967 | - | - |
| MVG459_Vos-03 | 0.281220 | 0.000018 | 0.001418 | 0.071375 | 0.281164 | -10.2 | 0.6 | 2.87 | 3.36 | 2087 | - | - |
| MVG459_Vos-35 | 0.281152 | 0.000012 | 0.001496 | 0.071214 | 0.281089 | -10.1 | 0.4 | 2.96 | 3.45 | 2206 | - | - |
| MVG459_Vos-01 | 0.281176 | 0.000008 | 0.000863 | 0.038991 | 0.281139 | -7.6 | 0.3 | 2.88 | 3.32 | 2236 | - | - |

| Analysis No. | Lu-Hf RATIOS | | | | | | | | | U-Pb AGE | Oxygen | |
|---|---|---|---|---|---|---|---|---|---|---|---|---|
| | $^{176}Hf/^{177}Hf$ | 1SE | $^{176}Lu/^{177}Hf$ | $^{176}Yb/^{177}Hf$ | $Hf_{initial}$ | εHf(T) | ± SE | $T_{DM}$ (Ga) | $T_{DM}^{Crustal}$ (Ga) | (Ma) | $\delta^{18}O$ | 2σ |
| MVG459_Vos-11 | 0.281160 | 0.000013 | 0.000818 | 0.036043 | 0.281125 | -7.9 | 0.5 | 2.90 | 3.34 | 2245 | - | - |
| MVG459_Vos-36 | 0.281192 | 0.000011 | 0.001087 | 0.050880 | 0.281145 | -6.8 | 0.4 | 2.88 | 3.29 | 2261 | - | - |
| MVG459_Vos-19 | 0.281185 | 0.000009 | 0.000712 | 0.029134 | 0.281154 | -6.1 | 0.3 | 2.86 | 3.25 | 2281 | - | - |
| MVG459_Vos-24r | 0.281406 | 0.000012 | 0.000706 | 0.030820 | 0.281374 | 3.7 | 0.4 | 2.56 | 2.70 | 2365 | - | - |
| MVG459_Vos-22 | 0.281162 | 0.000015 | 0.000908 | 0.041351 | 0.281120 | -4.5 | 0.5 | 2.91 | 3.25 | 2398 | - | - |
| MVG459_Vos-31 | 0.281295 | 0.000019 | 0.000657 | 0.028375 | 0.281265 | 0.7 | 0.7 | 2.71 | 2.92 | 2404 | - | - |
| MVG459_Vos-20 | 0.281156 | 0.000010 | 0.000607 | 0.027063 | 0.281128 | -3.7 | 0.4 | 2.89 | 3.22 | 2421 | - | - |
| MVG459_Vos-34 | 0.281224 | 0.000017 | 0.001947 | 0.088635 | 0.281134 | -3.4 | 0.6 | 2.90 | 3.20 | 2427 | - | - |
| **Alakhit-Markha field, Veselaya pipe** | | | | | | | | | | | | |
| MVG459_Ves-01 | 0.282448 | 0.000013 | 0.000762 | 0.028887 | 0.282437 | 5.1 | 0.5 | 1.13 | 1.35 | 778 | - | - |
| MVG459_Ves-02 | 0.281332 | 0.000011 | 0.000507 | 0.022803 | 0.281313 | -7.6 | 0.4 | 2.65 | 3.11 | 1971 | - | - |
| MVG459_Ves-03 | 0.281056 | 0.000011 | 0.000586 | 0.026131 | 0.281026 | -2.1 | 0.4 | 3.02 | 3.29 | 2645 | - | - |
| MVG459_Ves-04 | 0.282534 | 0.000014 | 0.001899 | 0.078980 | 0.282517 | 1.4 | 0.5 | 1.04 | 1.36 | 490 | - | - |
| **Alakhit-Markha field, Krasnopresnenskaya pipe** | | | | | | | | | | | | |
| MVG459_Kpr-01 | 0.281171 | 0.000013 | 0.000725 | 0.027943 | 0.281139 | -5.9 | 0.5 | 2.88 | 3.27 | 2311 | - | - |
| MVG459_Kpr-02 | 0.281551 | 0.000014 | 0.000228 | 0.010585 | 0.281543 | -1.6 | 0.5 | 2.33 | 2.65 | 1876 | - | - |
| MVG459_Kpr-03 | 0.281589 | 0.000016 | 0.000261 | 0.011700 | 0.281580 | 0.4 | 0.6 | 2.29 | 2.55 | 1906 | - | - |
| MVG459_Kpr-04 | 0.281113 | 0.000012 | 0.000604 | 0.027461 | 0.281087 | -8.3 | 0.4 | 2.95 | 3.40 | 2286 | - | - |
| MVG459_Kpr-05 | 0.281372 | 0.000012 | 0.000401 | 0.019024 | 0.281357 | -6.6 | 0.4 | 2.59 | 3.02 | 1947 | - | - |
| **Alakhit-Markha field, Aikhal pipe** | | | | | | | | | | | | |
| Aikhal-01 | 0.281406 | 0.000009 | 0.000240 | 0.009615 | 0.281397 | -4.2 | 0.3 | 2.53 | 2.83 | 1991 | - | - |
| Aikhal-02 | 0.281275 | 0.000012 | 0.000517 | 0.021468 | 0.281256 | -11.1 | 0.4 | 2.72 | 3.17 | 1905 | - | - |
| Aikhal-03 | 0.281174 | 0.000012 | 0.000189 | 0.007646 | 0.281167 | -14.1 | 0.4 | 2.84 | 3.35 | 1913 | - | - |
| Aikhal-06 | 0.281301 | 0.000010 | 0.000377 | 0.014837 | 0.281288 | -11.2 | 0.4 | 2.68 | 3.13 | 1958 | 8.99 | 0.22 |
| Aikhal-06rim | 0.281269 | 0.000009 | 0.000238 | 0.008727 | 0.281260 | -11.0 | 0.3 | 2.71 | 3.16 | 1904 | 8.59 | 0.24 |
| Aikhal-07 | - | - | - | - | - | - | - | - | - | 1967 | 9.56 | 0.26 |
| Aikhal-08core | 0.281215 | 0.000009 | 0.000292 | 0.011019 | 0.281204 | -11.7 | 0.3 | 2.79 | 3.25 | 1961 | 8.66 | 0.22 |
| Aikhal-08rim | 0.281229 | 0.000007 | 0.000363 | 0.014139 | 0.281215 | -10.9 | 0.3 | 2.78 | 3.21 | 1978 | 8.74 | 0.21 |
| Aikhal-09C | - | - | - | - | - | - | - | - | - | 1964 | 9.46 | 0.22 |
| Aikhal-09R | - | - | - | - | - | - | - | - | - | 1954 | 9.14 | 0.24 |
| Aikhal-10 | - | - | - | - | - | - | - | - | - | 1939 | 8.65 | 0.22 |
| Aikhal-11 | - | - | - | - | - | - | - | - | - | 1932 | 9.88 | 0.21 |
| Aikhal-12core | 0.281411 | 0.000009 | 0.000442 | 0.017994 | 0.281395 | -5.8 | 0.3 | 2.54 | 2.87 | 1921 | 10.24 | 0.22 |
| Aikhal-12rim | 0.281257 | 0.000008 | 0.000280 | 0.011281 | 0.281247 | -11.1 | 0.3 | 2.73 | 3.18 | 1920 | - | - |
| Aikhal-13 | - | - | - | - | - | - | - | - | - | 1945 | 10.03 | 0.22 |
| Aikhal-14 | - | - | - | - | - | - | - | - | - | 1892 | 9.71 | 0.20 |
| Aikhal-15core | 0.281313 | 0.000009 | 0.000389 | 0.015437 | 0.281298 | -8.3 | 0.3 | 2.67 | 3.05 | 1964 | 9.72 | 0.27 |
| Aikhal-15rim | 0.281322 | 0.000010 | 0.000417 | 0.015729 | 0.281306 | -8.1 | 0.3 | 2.65 | 3.04 | 1958 | 9.66 | 0.25 |
| Aikhal-16 | - | - | - | - | - | - | - | - | - | 1953 | 10.16 | 0.24 |
| Aikhal-18 | 0.281270 | 0.000011 | 0.000330 | 0.012701 | 0.281258 | -9.9 | 0.4 | 2.72 | 3.14 | 1957 | 8.84 | 0.20 |
| Aikhal-20Core | 0.281435 | 0.000012 | 0.000582 | 0.024107 | 0.281413 | -4.2 | 0.4 | 2.51 | 2.81 | 1962 | 10.45 | 0.20 |
| Aikhal-20Rim | 0.281364 | 0.000013 | 0.000357 | 0.015369 | 0.281351 | -7.1 | 0.5 | 2.59 | 2.96 | 1936 | - | - |
| Aikhal-21C | - | - | - | - | - | - | - | - | - | 1957 | 9.88 | 0.21 |
| Aikhal-21R | - | - | - | - | - | - | - | - | - | 1936 | 8.14 | 0.27 |

| Analysis No. | Lu-Hf RATIOS | | | | $Hf_{initial}$ | εHf(T) | ± SE | $T_{DM}$ (Ga) | $T_{DM}^{Crustal}$ (Ga) | U-Pb AGE | Oxygen | |
|---|---|---|---|---|---|---|---|---|---|---|---|---|
| | $^{176}Hf/^{177}Hf$ | 1SE | $^{176}Lu/^{177}Hf$ | $^{176}Yb/^{177}Hf$ | | | | | | (Ma) | $\delta^{18}O$ | 2σ |
| Aikhal-24 | - | - | - | - | - | - | - | - | - | 1938 | 8.95 | 0.23 |
| Aikhal-25C | - | - | - | - | - | - | - | - | - | 1922 | 10.58 | 0.25 |
| Aikhal-25R | - | - | - | - | - | - | - | - | - | 1933 | 10.64 | 0.21 |
| Aikhal-26C | - | - | - | - | - | - | - | - | - | 1909 | 9.23 | 0.24 |
| Aikhal-26R | - | - | - | - | - | - | - | - | - | 1909 | 9.03 | 0.23 |
| Aikhal-27 | - | - | - | - | - | - | - | - | - | 2026 | 10.02 | 0.22 |
| Aikhal-53Ca | 0.281147 | 0.000012 | 0.000338 | 0.014186 | 0.281135 | -15.8 | 0.4 | 2.88 | 3.43 | 1889 | - | - |
| Aikhal-53Core | 0.281134 | 0.000011 | 0.000451 | 0.015456 | 0.281118 | -16.4 | 0.4 | 2.91 | 3.46 | 1889 | - | - |
| Aikhal-53Rim | 0.281056 | 0.000009 | 0.000154 | 0.005212 | 0.281051 | -19.8 | 0.3 | 2.99 | 3.62 | 1845 | - | - |
| Aikhal-56 | 0.281090 | 0.000008 | 0.000377 | 0.013890 | 0.281076 | -17.2 | 0.3 | 2.96 | 3.53 | 1920 | - | - |
| **Nakyn field, Botuobinskaya pipe** | | | | | | | | | | | | |
| BT3903-01 | 0.281073 | 0.000027 | 0.000347 | 0.015033 | 0.281055 | 1.0 | 1.0 | 2.98 | 3.16 | 2736 | - | - |
| BT3903-03 | 0.281057 | 0.000025 | 0.000163 | 0.006471 | 0.281051 | -15.6 | 0.9 | 2.99 | 3.65 | 2026 | - | - |
| BT3903-05 | 0.281083 | 0.000023 | 0.000541 | 0.022400 | 0.281055 | 0.7 | 0.8 | 2.98 | 3.17 | 2722 | - | - |
| BT3903-09 | 0.281106 | 0.000026 | 0.000806 | 0.033757 | 0.281070 | -7.5 | 0.9 | 2.97 | 3.40 | 2346 | - | - |
| BT3903-10 | 0.281084 | 0.000029 | 0.000936 | 0.041546 | 0.281035 | 0.5 | 1.0 | 3.01 | 3.20 | 2742 | - | - |
| BT3903-11 | 0.281087 | 0.000022 | 0.000070 | 0.002952 | 0.281083 | 1.2 | 0.8 | 2.94 | 3.12 | 2700 | - | - |
| BT3903-12 | 0.281078 | 0.000035 | 0.000598 | 0.027631 | 0.281047 | 1.0 | 1.2 | 3.00 | 3.17 | 2746 | - | - |
| BT3903-13 | 0.281066 | 0.000033 | 0.000223 | 0.009259 | 0.281054 | 1.6 | 1.2 | 2.98 | 3.14 | 2763 | - | - |
| BT3903-14 | 0.281066 | 0.000033 | 0.000260 | 0.010717 | 0.281053 | 0.4 | 1.2 | 2.99 | 3.18 | 2714 | - | - |
| BT3903-15 | 0.281042 | 0.000023 | 0.000704 | 0.032610 | 0.281006 | -2.0 | 0.8 | 3.05 | 3.31 | 2683 | - | - |
| BT3903-16 | 0.281072 | 0.000036 | 0.000184 | 0.007831 | 0.281062 | 2.1 | 1.3 | 2.97 | 3.12 | 2770 | - | - |
| BT3903-21 | 0.281062 | 0.000023 | 0.000220 | 0.009697 | 0.281050 | 1.0 | 0.8 | 2.99 | 3.17 | 2741 | - | - |
| BT3903-23 | 0.281049 | 0.000025 | 0.000180 | 0.008223 | 0.281039 | 1.2 | 0.9 | 3.00 | 3.17 | 2768 | - | - |
| BT3903-26 | 0.280998 | 0.000025 | 0.000202 | 0.008573 | 0.280987 | -1.3 | 0.9 | 3.07 | 3.31 | 2738 | - | - |
| BT3903-28 | 0.281075 | 0.000023 | 0.000259 | 0.010985 | 0.281061 | 1.9 | 0.8 | 2.97 | 3.13 | 2762 | - | - |
| BT3903-29 | 0.281014 | 0.000025 | 0.000351 | 0.015033 | 0.280995 | -0.7 | 0.9 | 3.06 | 3.28 | 2752 | - | - |
| BT3903-30 | 0.281081 | 0.000030 | 0.000240 | 0.010148 | 0.281069 | -0.4 | 1.1 | 2.96 | 3.19 | 2656 | - | - |
| BT3903-31 | 0.281054 | 0.000021 | 0.000217 | 0.009379 | 0.281043 | -0.3 | 0.7 | 3.00 | 3.22 | 2697 | - | - |
| BT3903-32 | 0.281056 | 0.000027 | 0.000129 | 0.005662 | 0.281051 | -14.3 | 1.0 | 2.99 | 3.62 | 2082 | - | - |
| BT3903-33 | 0.281018 | 0.000025 | 0.000132 | 0.005647 | 0.281012 | -10.6 | 0.9 | 3.04 | 3.56 | 2302 | - | - |
| BT3903-35 | 0.280998 | 0.000024 | 0.000119 | 0.005010 | 0.280993 | -9.4 | 0.9 | 3.07 | 3.55 | 2384 | - | - |
| BT703-01 | 0.280957 | 0.000025 | 0.000486 | 0.018998 | 0.280931 | -2.6 | 0.9 | 3.15 | 3.42 | 2769 | - | - |
| BT703-03 | 0.281014 | 0.000033 | 0.000429 | 0.018875 | 0.280991 | -0.2 | 1.2 | 3.07 | 3.27 | 2781 | - | - |
| BT703-06 | 0.281003 | 0.000030 | 0.000654 | 0.025969 | 0.280968 | -0.1 | 1.1 | 3.10 | 3.30 | 2820 | - | - |
| BT703-08 | 0.281030 | 0.000031 | 0.000447 | 0.017229 | 0.281007 | -1.7 | 1.1 | 3.05 | 3.30 | 2691 | - | - |
| BT703-09 | 0.281049 | 0.000027 | 0.000225 | 0.009075 | 0.281037 | 2.0 | 1.0 | 3.01 | 3.15 | 2804 | - | - |
| BT703-11 | 0.280939 | 0.000028 | 0.000577 | 0.022658 | 0.280907 | -0.5 | 1.0 | 3.18 | 3.38 | 2894 | - | - |
| BT703-12 | 0.281053 | 0.000027 | 0.000189 | 0.007364 | 0.281043 | 2.5 | 1.0 | 3.00 | 3.13 | 2817 | - | - |
| BT703-15 | 0.281100 | 0.000038 | 0.000668 | 0.026463 | 0.281064 | 2.3 | 1.4 | 2.97 | 3.11 | 2775 | - | - |
| BT703-16 | 0.281060 | 0.000030 | 0.000248 | 0.010381 | 0.281047 | -0.2 | 1.1 | 2.99 | 3.21 | 2695 | - | - |
| BT703-17 | 0.281009 | 0.000024 | 0.000336 | 0.013350 | 0.280991 | 0.3 | 0.9 | 3.07 | 3.26 | 2802 | - | - |
| BT703-18 | 0.280989 | 0.000037 | 0.000332 | 0.014075 | 0.280971 | -1.2 | 1.3 | 3.09 | 3.33 | 2769 | - | - |
| BT703-19 | 0.281003 | 0.000028 | 0.000271 | 0.010016 | 0.280989 | -0.3 | 1.0 | 3.07 | 3.28 | 2782 | - | - |

| Analysis No. | Lu-Hf RATIOS | | | | $Hf_{initial}$ | εHf(T) | ± SE | $T_{DM}$ (Ga) | $T_{DM}^{Crustal}$ (Ga) | U-Pb AGE | Oxygen | |
|---|---|---|---|---|---|---|---|---|---|---|---|---|
| | $^{176}Hf/^{177}Hf$ | 1SE | $^{176}Lu/^{177}Hf$ | $^{176}Yb/^{177}Hf$ | | | | | | (Ma) | $\delta^{18}O$ | 2σ |
| BT703-20 | 0.280974 | 0.000026 | 0.000581 | 0.023987 | 0.280941 | 1.6 | 0.9 | 3.13 | 3.28 | 2933 | - | - |
| BT703-22 | 0.281039 | 0.000024 | 0.000735 | 0.030834 | 0.280999 | 2.2 | 0.9 | 3.06 | 3.19 | 2872 | - | - |
| BT703-23 | 0.280992 | 0.000028 | 0.000447 | 0.018482 | 0.280969 | -2.9 | 1.0 | 3.10 | 3.38 | 2699 | - | - |
| BT703-24 | 0.280953 | 0.000019 | 0.000406 | 0.016573 | 0.280931 | -0.2 | 0.7 | 3.15 | 3.35 | 2872 | - | - |
| BT703-28 | 0.281019 | 0.000023 | 0.000423 | 0.016768 | 0.280996 | 2.6 | 0.8 | 3.06 | 3.18 | 2893 | - | - |
| BT703-29 | 0.280960 | 0.000033 | 0.000152 | 0.005963 | 0.280952 | -1.5 | 1.2 | 3.12 | 3.36 | 2786 | - | - |
| BT703-30 | 0.281047 | 0.000034 | 0.000308 | 0.013692 | 0.281031 | 1.1 | 1.2 | 3.01 | 3.19 | 2775 | - | - |
| BT703-31 | 0.281017 | 0.000026 | 0.000105 | 0.004899 | 0.281012 | -3.0 | 0.9 | 3.04 | 3.33 | 2630 | - | - |

**Appendix 3.4. Re-Os data for the samples from the Markha terrane**

| Sample | Group | $^{187}Os/^{188}Os$ | 2σ | $^{187}Re/^{188}Os$ | 2σ | $T_{MA}$ (Ga) | 2σ (Ga) | $T_{RD}$ (Ga) | 2σ (Ga) |
|---|---|---|---|---|---|---|---|---|---|
| MVG-351 | 1 | 0.105763 | 0.000099 | 0.091524 | 0.000370 | 3.99 | 0.02 | 3.10 | 0.01 |
| MVG-403 core | 1 | 0.102831 | 0.000150 | 0.026190 | 0.001400 | 3.75 | 0.03 | 3.51 | 0.03 |
| MVG-406 | 1 | 0.105674 | 0.000057 | 0.052197 | 0.000390 | 3.54 | 0.01 | 3.12 | 0.01 |
| MVG-409 sulf1 | 1 | 0.108549 | 0.000070 | 0.018307 | 0.000090 | 3.12 | 0.01 | 3.01 | 0.01 |
| MVG-409 sulf1 | 1 | 0.108379 | 0.000110 | 0.018949 | 0.000055 | 3.11 | 0.02 | 3.01 | 0.01 |
| MVG-377 rim | 2 | 0.107691 | 0.000370 | 0.148121 | 0.000900 | 4.43 | 0.09 | 2.83 | 0.05 |
| MVG-387 core | 2 | 0.106255 | 0.000380 | 0.000430 | 0.000023 | 3.22 | 0.60 | 2.98 | 0.05 |
| MVG-392 core | 2 | 0.109363 | 0.000043 | 0.015306 | 0.000150 | 2.95 | 0.10 | 2.84 | 0.01 |
| MVG-392 rim | 2 | 0.107152 | 0.000340 | 0.021140 | 0.000460 | 3.06 | 0.05 | 2.91 | 0.05 |
| MVG-392 2c | 2 | 0.107864 | 0.000210 | 0.020951 | 0.001000 | 2.96 | 0.03 | 2.83 | 0.03 |
| MVG-392 2r | 2 | 0.109332 | 0.000190 | 0.015315 | 0.000210 | 2.99 | 0.03 | 2.87 | 0.03 |
| MVG-394 core | 2 | 0.111960 | 0.000096 | 0.005439 | 0.000011 | -1.09 | 0.05 | 2.17 | 0.10 |
| MVG-394 rim | 2 | 0.112620 | 0.002600 | 0.001958 | 0.000087 | -2.81 | 0.58 | 2.10 | 0.42 |
| MVG-398 rim | 2 | 0.114889 | 0.000570 | 1.186190 | 0.014000 | -1.09 | 0.05 | 2.07 | 0.10 |
| MVG-405 core | 2 | 0.114421 | 0.000770 | 0.425689 | 0.002200 | -45.80 | 5.06 | 1.87 | 0.21 |
| MVG-407 sulf1 | 2 | 0.112624 | 0.001100 | 0.306739 | 0.002600 | 8.48 | 0.78 | 2.12 | 0.20 |
| MVG-408 sulf2 | 2 | 0.113148 | 0.002400 | 0.706038 | 0.012000 | -2.81 | 0.58 | 2.04 | 0.42 |

**Appendix 3.5. Sulfide platinum-group element data (ppm) of the samples from the Markha terrane**

| Sample | Ru101 | Rh103 | Pd108 | Os189 | Ir193 | Pt195 | Au197 |
|---|---|---|---|---|---|---|---|
| 387-01 | 778.33 | 476.56 | 83.02 | 1009.19 | 367.73 | 13.75 | 97.94 |
| 406-01 | 287.46 | 28.76 | 1.168 | 767.63 | 306.39 | 0.481 | 0.0693 |
| 351-01 | 42.2 | 5.48 | 7.19 | 127.83 | 74.54 | 27.32 | <0.41 |
| 377-01R | 10.73 | 2.3 | 46.59 | 11.9 | 5.23 | 4.13 | 0.0358 |
| 377-02C | 22.46 | 4.06 | 10.74 | 14.76 | 8.88 | 10.94 | 0.028 |
| 392-01R | 1261.95 | 117.81 | 17.48 | 2443.82 | 944.25 | 321.8 | 0.563 |
| 392-02C | 1067.2 | 160.57 | 13.87 | 2274.67 | 805.84 | 0.855 | 0.0251 |
| 398-01R | 21.12 | 3.28 | 10.94 | 32.47 | 18.22 | 4.31 | 0.125 |
| 398-02C | 20.18 | 2.7 | 14.91 | 23.34 | 16.11 | 9.25 | 0.0778 |
| 392-03R | 1148.05 | 196.33 | 7.56 | 2122.24 | 914.76 | 60.37 | 0.288 |
| 403-01 | 1542.63 | 150.04 | 52.43 | 2475.67 | 1155.72 | 17.02 | 0.0935 |
| 407-03 | 6.66 | 1.542 | 0.0761 | 5.87 | 2.454 | 1.684 | 0.0427 |
| 407-01NI | 2.624 | 0.496 | 41.74 | 4.48 | 2.04 | 23.71 | 0.018 |
| 407-01FE | 6.31 | 1.666 | 0.289 | 11.05 | 4.81 | 2.135 | 0.0175 |
| 407-02 | 9.3 | 3.01 | 0.028 | 11.67 | 5.46 | 1.826 | 0.0263 |
| 408-01 | 3.7 | 1.13 | 9.53 | 4.6 | 1.791 | 0.511 | 0.0337 |
| 408-02NI | 3.45 | 0.705 | 2.085 | 4.39 | 2.045 | 2.078 | 0.0467 |
| 408-02FE | 5.07 | 0.993 | 0.488 | 5.87 | 2.74 | 2.28 | 0.0231 |
| 394-01 | 3.18 | 0.985 | 20.07 | 0.695 | 0.33 | 14.25 | 0.0258 |
| 394-02NI | 39.34 | 7.75 | 9.36 | 25.54 | 6.12 | 6.19 | <0.043 |
| 394-02FE | 47.09 | 9.09 | 0.246 | 27.85 | 7.48 | 1.43 | 0.0268 |
| 409-01NI | 35.97 | 6.87 | 0.27 | 269.44 | 205.87 | 3.74 | <0.072 |
| 409-01FE | 38.08 | 7.49 | 0.274 | 300.49 | 220.27 | 2.21 | 0.042 |
| 409-02 | 5.88 | 1.509 | 21.44 | 4.19 | 1.903 | 51.42 | 0.1061 |
| 412-01 | 4.59 | 0.967 | 15.72 | 2.28 | 0.892 | 1.98 | 0.318 |
| 412-02 | 6.22 | 1.454 | 0.534 | 2.67 | 1.205 | 0.95 | 0.047 |
| 405-01R | 15.47 | 2.6 | 5.25 | 24.93 | 10.1 | 6.04 | 0.0254 |
| 405-01C | 14.29 | 2.36 | 5.3 | 26.98 | 9.48 | 3.55 | <0.0166 |

**Appendix 3A.1. Zircon U-Pb age data for undeformed and mosaic grains from the Nurbinskaya kimberlitic pipe, Nakyn field, Siberia, Russia**

| Analysis No. | RATIOS | | | | | | | | AGES (Ma) | | | | | | | | | | CONCENTRATIONS (ppm) | |
|---|---|---|---|---|---|---|---|---|---|---|---|---|---|---|---|---|---|---|---|---|
| | $^{207}Pb/^{206}Pb$ | ± 2σ | $^{207}Pb/^{235}U$ | ± 2σ | $^{206}Pb/^{238}U$ | ± 2σ | $^{208}Pb/^{232}Th$ | ± 2σ | $^{207}Pb/^{206}Pb$ | ± 2σ | $^{207}Pb/^{235}U$ | ± 2σ | $^{206}Pb/^{238}U$ | ± 2σ | $^{208}Pb/^{232}Th$ | ± 2σ | Used Age | ± 2σ | Th | U |
| **Mosaic** | | | | | | | | | | | | | | | | | | | | |
| NU19-3-1 | 0.05899 | 0.00182 | 0.68111 | 0.02170 | 0.08375 | 0.00200 | 0.02775 | 0.00104 | 567 | 68 | 527 | 14 | 518 | 12 | 553 | 20 | 518 | 12 | 5.11 | 34.04 |
| NU19-3-2 | 0.05611 | 0.00172 | 0.50073 | 0.01578 | 0.06473 | 0.00154 | 0.02111 | 0.00082 | 457 | 70 | 412 | 10 | 404 | 10 | 422 | 16 | 404 | 10 | 3.76 | 29.22 |
| NU25-08-1 | 0.05584 | 0.00234 | 0.48377 | 0.02010 | 0.06284 | 0.00158 | 0.03249 | 0.00300 | 446 | 96 | 401 | 14 | 393 | 10 | 646 | 58 | 393 | 10 | 0.36 | 12.34 |
| NU25-08-2 | 0.05616 | 0.00252 | 0.51299 | 0.02272 | 0.06625 | 0.00170 | 0.0266 | 0.00318 | 459 | 102 | 420 | 16 | 414 | 10 | 531 | 62 | 414 | 10 | 0.38 | 14.59 |
| NU26-08 | 0.05395 | 0.00180 | 0.46622 | 0.01582 | 0.06269 | 0.00150 | 0.02149 | 0.00072 | 369 | 76 | 389 | 10 | 392 | 10 | 430 | 14 | 392 | 10 | 5.16 | 21.95 |
| NU-ZR-C_interblc | 0.05404 | 0.00956 | 0.45243 | 0.07726 | 0.06073 | 0.00310 | 0.01761 | 0.00716 | 373 | 406 | 379 | 54 | 380 | 18 | 353 | 142 | 380 | 18 | 1.38 | 16.32 |
| NU-ZR-C_interblc | 0.05614 | 0.00808 | 0.52386 | 0.07226 | 0.06769 | 0.00306 | 0.02677 | 0.00744 | 458 | 330 | 428 | 48 | 422 | 18 | 534 | 146 | 422 | 18 | 1.39 | 18.09 |
| NU-ZR-C_block_1 | 0.05286 | 0.00768 | 0.49065 | 0.06842 | 0.06731 | 0.00308 | 0.0138 | 0.00444 | 323 | 336 | 405 | 46 | 420 | 18 | 277 | 88 | 420 | 18 | 3.31 | 40.47 |
| NU-ZR-C_block_2 | 0.05716 | 0.00466 | 0.56614 | 0.04404 | 0.07184 | 0.00204 | 0.01993 | 0.00348 | 498 | 184 | 456 | 28 | 447 | 12 | 399 | 68 | 447 | 12 | 4.74 | 57.81 |
| NU-ZR-C_block_3 | 0.05352 | 0.00456 | 0.47339 | 0.03862 | 0.06417 | 0.00186 | 0.02283 | 0.00316 | 351 | 198 | 394 | 26 | 401 | 12 | 456 | 62 | 401 | 12 | 4.68 | 49.06 |
| NU-ZR-D_interblc | 0.05448 | 0.01234 | 0.45366 | 0.09988 | 0.06039 | 0.00344 | 0.02158 | 0.00998 | 391 | 518 | 380 | 70 | 378 | 20 | 432 | 198 | 378 | 20 | 0.76 | 10.45 |
| NU-ZR-D_interblc | 0.05407 | 0.00858 | 0.44732 | 0.06876 | 0.06 | 0.00262 | 0.01952 | 0.00508 | 374 | 366 | 375 | 48 | 376 | 16 | 391 | 100 | 376 | 16 | 1.24 | 18.87 |
| NU-ZR-D_interblc | 0.05267 | 0.00620 | 0.41414 | 0.04674 | 0.05703 | 0.00214 | 0.0105 | 0.00318 | 315 | 274 | 352 | 34 | 358 | 14 | 211 | 64 | 358 | 14 | 1.87 | 25.30 |
| NU-ZR-D_block_1 | 0.05396 | 0.00526 | 0.45774 | 0.04268 | 0.06153 | 0.00202 | 0.01433 | 0.00344 | 369 | 226 | 383 | 30 | 385 | 12 | 288 | 68 | 385 | 12 | 2.46 | 34.96 |
| NU-ZR-D_block_2 | 0.05454 | 0.00798 | 0.47267 | 0.06650 | 0.06286 | 0.00282 | 0.02177 | 0.00770 | 393 | 338 | 393 | 46 | 393 | 18 | 435 | 152 | 393 | 18 | 1.42 | 22.06 |
| **Undeformed** | | | | | | | | | | | | | | | | | | | | |
| MVG126-01 | 0.18454 | 0.00472 | 13.25525 | 0.33002 | 0.521 | 0.00916 | 0.15018 | 0.00604 | 2694 | 44 | 2698 | 24 | 2703 | 38 | 2828 | 106 | 2694 | 44 | 6.59 | 13.99 |
| MVG126-02 | 0.09272 | 0.00408 | 3.39353 | 0.14228 | 0.26549 | 0.00576 | 0.08176 | 0.00434 | 1482 | 86 | 1503 | 32 | 1518 | 30 | 1588 | 82 | 1482 | 86 | 8.40 | 18.26 |
| MVG126-03 | 0.18681 | 0.00578 | 13.30693 | 0.39414 | 0.51668 | 0.01064 | 0.13786 | 0.00860 | 2714 | 52 | 2702 | 28 | 2685 | 46 | 2610 | 152 | 2714 | 52 | 2.02 | 8.54 |
| MVG126-04 | 0.09987 | 0.00340 | 3.79146 | 0.12376 | 0.27537 | 0.00504 | 0.0832 | 0.00368 | 1622 | 64 | 1591 | 26 | 1568 | 26 | 1615 | 68 | 1622 | 64 | 9.31 | 20.41 |
| MVG126-05_2 | 0.0562 | 0.01282 | 0.61857 | 0.13686 | 0.07984 | 0.00486 | 0.02671 | 0.00296 | 460 | 520 | 489 | 86 | 495 | 30 | 533 | 58 | 495 | 30 | 2.69 | 3.12 |
| MVG126-05_3 | 0.05797 | 0.01236 | 0.65662 | 0.13442 | 0.08216 | 0.00542 | 0.02901 | 0.00342 | 529 | 484 | 513 | 82 | 509 | 32 | 578 | 68 | 509 | 32 | 2.90 | 3.53 |
| MVG126-06 | 0.19023 | 0.00762 | 13.88676 | 0.52432 | 0.5295 | 0.01374 | 0.14653 | 0.01954 | 2744 | 68 | 2742 | 36 | 2739 | 58 | 2764 | 344 | 2744 | 68 | 0.35 | 4.18 |
| MVG126-07 | 0.17906 | 0.00732 | 12.74175 | 0.49334 | 0.51613 | 0.01300 | 0.13866 | 0.01230 | 2644 | 70 | 2661 | 36 | 2683 | 56 | 2625 | 218 | 2644 | 70 | 1.55 | 7.76 |
| MVG126-08 | 0.15378 | 0.00754 | 9.21215 | 0.42400 | 0.4345 | 0.01246 | 0.1319 | 0.00946 | 2388 | 86 | 2359 | 42 | 2326 | 56 | 2504 | 168 | 2388 | 86 | 1.70 | 3.99 |
| MVG126-09 | 0.18748 | 0.00552 | 13.40861 | 0.38114 | 0.51876 | 0.00992 | 0.14937 | 0.00828 | 2720 | 50 | 2709 | 26 | 2694 | 42 | 2814 | 146 | 2720 | 50 | 3.07 | 10.86 |
| MVG126-10 | 0.17826 | 0.00964 | 12.81253 | 0.65090 | 0.5213 | 0.01718 | 0.15336 | 0.01302 | 2637 | 92 | 2666 | 48 | 2705 | 72 | 2884 | 228 | 2637 | 92 | 1.60 | 3.53 |
| NU18-01 | 0.35889 | 0.00990 | 37.81392 | 1.10468 | 0.76424 | 0.02078 | 0.79468 | 0.02608 | 3745 | 42 | 3715 | 28 | 3660 | 76 | 11821 | 294 | 3745 | 42 | 3.73 | 6.67 |
| NU18-01-2 | 0.18455 | 0.00454 | 13.03214 | 0.34148 | 0.5122 | 0.01228 | 0.15134 | 0.00418 | 2694 | 42 | 2682 | 24 | 2666 | 52 | 2848 | 74 | 2694 | 42 | 2.26 | 4.03 |
| NU18-01-3 | 0.18516 | 0.00448 | 13.30928 | 0.34402 | 0.52138 | 0.01240 | 0.15682 | 0.00422 | 2700 | 40 | 2702 | 24 | 2705 | 52 | 2944 | 74 | 2700 | 40 | 2.73 | 4.68 |
| NU18-02 | 0.18679 | 0.00434 | 13.46821 | 0.33888 | 0.52299 | 0.01234 | 0.16723 | 0.00764 | 2714 | 40 | 2713 | 24 | 2712 | 52 | 3125 | 132 | 2714 | 40 | 0.44 | 7.46 |
| NU18-03 | 0.1835 | 0.00408 | 12.80762 | 0.31188 | 0.50626 | 0.01174 | 0.11778 | 0.00314 | 2685 | 38 | 2666 | 22 | 2641 | 50 | 2251 | 56 | 2685 | 38 | 2.80 | 14.02 |
| NU18-04 | 0.05487 | 0.00264 | 0.45364 | 0.02158 | 0.05996 | 0.00158 | 0.01949 | 0.00096 | 407 | 110 | 380 | 16 | 375 | 10 | 390 | 20 | 375 | 10 | 5.52 | 15.07 |
| NU18-05 | 0.07795 | 0.00390 | 1.96925 | 0.08592 | 0.18322 | 0.00450 | 0.05494 | 0.00132 | 1146 | 102 | 1105 | 30 | 1085 | 24 | 1081 | 26 | 1146 | 102 | 19.49 | 32.29 |
| NU18-06 | 0.05637 | 0.00342 | 0.45566 | 0.02684 | 0.05863 | 0.00170 | 0.02153 | 0.00132 | 467 | 138 | 381 | 18 | 367 | 10 | 431 | 26 | 367 | 10 | 2.47 | 11.66 |
| NU18-07 | 0.18831 | 0.00450 | 13.50095 | 0.34652 | 0.52004 | 0.01236 | 0.17306 | 0.00508 | 2727 | 40 | 2715 | 24 | 2699 | 52 | 3226 | 88 | 2727 | 40 | 2.06 | 7.01 |
| NU18-08 | 0.05411 | 0.00242 | 0.44693 | 0.01976 | 0.05992 | 0.00154 | 0.01977 | 0.00092 | 376 | 102 | 375 | 14 | 375 | 10 | 396 | 18 | 375 | 10 | 3.53 | 15.64 |
| NU18-09 | 0.1875 | 0.00438 | 13.69693 | 0.34536 | 0.52987 | 0.01244 | 0.15362 | 0.00468 | 2720 | 40 | 2729 | 24 | 2741 | 52 | 2888 | 82 | 2720 | 40 | 2.42 | 11.05 |

| Analysis No. | RATIOS | | | | | | | | AGES (Ma) | | | | | | | | | | CONCENTRATIONS (ppm) | |
|---|---|---|---|---|---|---|---|---|---|---|---|---|---|---|---|---|---|---|---|---|
| | $^{207}Pb/^{206}Pb$ | ± 2σ | $^{207}Pb/^{235}U$ | ± 2σ | $^{206}Pb/^{238}U$ | ± 2σ | $^{208}Pb/^{232}Th$ | ± 2σ | $^{207}Pb/^{206}Pb$ | ± 2σ | $^{207}Pb/^{235}U$ | ± 2σ | $^{206}Pb/^{238}U$ | ± 2σ | $^{208}Pb/^{232}Th$ | ± 2σ | Used Age | ± 2σ | Th | U |
| NU19-1-1 | 0.1874 | 0.00408 | 13.47247 | 0.32228 | 0.52144 | 0.01198 | 0.14763 | 0.00374 | 2719 | 36 | 2713 | 22 | 2705 | 50 | 2783 | 66 | 2719 | 36 | 2.99 | 15.77 |
| NU19-1-2 | 0.18596 | 0.00430 | 13.511 | 0.33868 | 0.527 | 0.01238 | 0.1513 | 0.00522 | 2707 | 40 | 2716 | 24 | 2729 | 52 | 2848 | 92 | 2707 | 40 | 1.00 | 7.08 |
| NU19-2-1 | 0.05456 | 0.00392 | 0.44859 | 0.03130 | 0.05963 | 0.00186 | 0.02115 | 0.00166 | 394 | 166 | 376 | 22 | 373 | 12 | 423 | 32 | 373 | 12 | 1.41 | 8.18 |
| NU19-2-2 | 0.05387 | 0.00330 | 0.44863 | 0.02686 | 0.06041 | 0.00174 | 0.02172 | 0.00146 | 366 | 142 | 376 | 18 | 378 | 10 | 434 | 28 | 378 | 10 | 0.89 | 4.79 |
| NU19-4-1 | 0.18358 | 0.00450 | 13.15987 | 0.34396 | 0.51995 | 0.01250 | 0.15221 | 0.00476 | 2685 | 42 | 2691 | 24 | 2699 | 54 | 2864 | 84 | 2685 | 42 | 1.41 | 5.21 |
| NU19-4-2 | 0.17786 | 0.00478 | 12.36166 | 0.34756 | 0.50412 | 0.01252 | 0.13899 | 0.00522 | 2633 | 46 | 2632 | 26 | 2631 | 54 | 2630 | 92 | 2633 | 46 | 1.08 | 3.66 |
| NU19-5-1 | 0.18821 | 0.00414 | 13.686 | 0.33044 | 0.52745 | 0.01216 | 0.14752 | 0.00332 | 2727 | 38 | 2728 | 22 | 2731 | 52 | 2781 | 58 | 2727 | 38 | 21.24 | 25.64 |
| NU19-5-2 | 0.1853 | 0.00402 | 13.35431 | 0.32016 | 0.52273 | 0.01200 | 0.14899 | 0.00328 | 2701 | 36 | 2705 | 22 | 2711 | 50 | 2807 | 58 | 2701 | 36 | 13.80 | 16.20 |
| NU19-6-1 | 0.09321 | 0.00224 | 3.20716 | 0.08314 | 0.24956 | 0.00580 | 0.07522 | 0.00186 | 1492 | 46 | 1459 | 20 | 1436 | 30 | 1466 | 34 | 1492 | 46 | 7.92 | 17.96 |
| NU19-6-2 | 0.09199 | 0.00376 | 3.15892 | 0.10506 | 0.24905 | 0.00592 | 0.07336 | 0.00176 | 1467 | 80 | 1447 | 26 | 1434 | 30 | 1431 | 34 | 1467 | 80 | 7.30 | 17.35 |
| NU19-7-1 | 0.05541 | 0.00330 | 0.44846 | 0.02600 | 0.05871 | 0.00168 | 0.01977 | 0.00132 | 429 | 136 | 376 | 18 | 368 | 10 | 396 | 26 | 368 | 10 | 1.65 | 8.52 |
| NU19-8-1 | 0.091 | 0.00440 | 3.09998 | 0.12876 | 0.24708 | 0.00608 | 0.07287 | 0.00176 | 1447 | 94 | 1433 | 32 | 1423 | 32 | 1422 | 34 | 1447 | 94 | 14.55 | 21.32 |
| NU19-8-2 | 0.08821 | 0.00438 | 2.86252 | 0.12208 | 0.23537 | 0.00594 | 0.06964 | 0.00176 | 1387 | 98 | 1372 | 32 | 1363 | 30 | 1361 | 34 | 1387 | 98 | 27.19 | 35.89 |
| NU19-9-1 | 0.05365 | 0.00324 | 0.43843 | 0.02582 | 0.05928 | 0.00170 | 0.01794 | 0.00126 | 356 | 140 | 369 | 18 | 371 | 10 | 359 | 26 | 371 | 10 | 0.96 | 4.98 |
| NU19-9-2 | 0.05425 | 0.00332 | 0.44206 | 0.02638 | 0.05911 | 0.00170 | 0.01973 | 0.00138 | 381 | 140 | 372 | 18 | 370 | 10 | 395 | 28 | 370 | 10 | 0.95 | 4.88 |
| NU25-01-1 | 0.16994 | 0.00378 | 11.43335 | 0.27810 | 0.48799 | 0.01132 | 0.13956 | 0.00348 | 2557 | 38 | 2559 | 22 | 2562 | 50 | 2641 | 62 | 2557 | 38 | 4.78 | 14.17 |
| NU25-01-2 | 0.17919 | 0.00480 | 12.6053 | 0.35220 | 0.51023 | 0.01262 | 0.14726 | 0.00540 | 2645 | 46 | 2651 | 26 | 2658 | 54 | 2777 | 96 | 2645 | 46 | 2.58 | 8.10 |
| NU25-02-1 | 0.18802 | 0.00494 | 13.97002 | 0.38176 | 0.53891 | 0.01328 | 0.15511 | 0.00836 | 2725 | 44 | 2748 | 26 | 2779 | 56 | 2915 | 146 | 2725 | 44 | 0.77 | 6.28 |
| NU25-02-2 | 0.18751 | 0.00468 | 13.78525 | 0.36256 | 0.53324 | 0.01284 | 0.1872 | 0.00796 | 2720 | 42 | 2735 | 24 | 2755 | 54 | 3468 | 136 | 2720 | 42 | 0.54 | 4.39 |
| NU25-03-1 | 0.18426 | 0.00408 | 13.39282 | 0.31976 | 0.52723 | 0.01196 | 0.14691 | 0.00456 | 2692 | 38 | 2708 | 22 | 2730 | 50 | 2771 | 80 | 2692 | 38 | 1.73 | 16.22 |
| NU25-03-2 | 0.18306 | 0.00402 | 13.31308 | 0.31824 | 0.52749 | 0.01208 | 0.15155 | 0.00458 | 2681 | 38 | 2702 | 22 | 2731 | 50 | 2852 | 80 | 2681 | 38 | 1.26 | 11.34 |
| NU25-04-1 | 0.05399 | 0.00280 | 0.4455 | 0.02264 | 0.05984 | 0.00162 | 0.01927 | 0.00106 | 371 | 120 | 374 | 16 | 375 | 10 | 386 | 22 | 375 | 10 | 2.32 | 10.06 |
| NU25-04-2 | 0.05362 | 0.00318 | 0.4379 | 0.02534 | 0.05924 | 0.00168 | 0.01958 | 0.00120 | 355 | 138 | 369 | 18 | 371 | 10 | 392 | 24 | 371 | 10 | 1.56 | 6.93 |
| NU25-04-3 | 0.05375 | 0.00276 | 0.4519 | 0.02280 | 0.06098 | 0.00164 | 0.01906 | 0.00104 | 361 | 118 | 379 | 16 | 382 | 10 | 382 | 20 | 382 | 10 | 1.57 | 6.73 |
| NU25-05-1 | 0.18683 | 0.00468 | 13.5341 | 0.35642 | 0.52542 | 0.01262 | 0.15956 | 0.00628 | 2714 | 42 | 2718 | 24 | 2722 | 54 | 2992 | 110 | 2714 | 42 | 0.97 | 5.45 |
| NU25-05-2 | 0.18718 | 0.00484 | 13.80431 | 0.37262 | 0.53492 | 0.01296 | 0.14426 | 0.00616 | 2718 | 44 | 2736 | 26 | 2762 | 54 | 2724 | 108 | 2718 | 44 | 0.67 | 3.90 |
| NU25-06-1 | 0.17008 | 0.00448 | 11.0716 | 0.30410 | 0.47217 | 0.01154 | 0.1471 | 0.00668 | 2558 | 46 | 2529 | 26 | 2493 | 50 | 2774 | 118 | 2558 | 46 | 0.69 | 5.60 |
| NU25-06-2 | 0.17987 | 0.00486 | 12.70885 | 0.35788 | 0.51248 | 0.01278 | 0.14734 | 0.00732 | 2652 | 46 | 2658 | 26 | 2667 | 54 | 2778 | 128 | 2652 | 46 | 0.64 | 4.64 |
| NU25-07-1 | 0.05343 | 0.00296 | 0.43665 | 0.02362 | 0.05928 | 0.00164 | 0.02115 | 0.00128 | 347 | 128 | 368 | 16 | 371 | 10 | 423 | 26 | 371 | 10 | 1.08 | 5.95 |
| NU25-07-2 | 0.05311 | 0.00274 | 0.43429 | 0.02198 | 0.05932 | 0.00160 | 0.01972 | 0.00106 | 333 | 120 | 366 | 16 | 371 | 10 | 395 | 22 | 371 | 10 | 2.16 | 10.04 |
| NU25-09-1 | 0.05515 | 0.00316 | 0.44251 | 0.02474 | 0.0582 | 0.00164 | 0.0185 | 0.00120 | 418 | 130 | 372 | 18 | 365 | 10 | 371 | 24 | 365 | 10 | 1.19 | 5.61 |
| NU26-01 | 0.05445 | 0.00404 | 0.4556 | 0.03266 | 0.06069 | 0.00192 | 0.01807 | 0.00160 | 390 | 170 | 381 | 22 | 380 | 12 | 362 | 32 | 380 | 12 | 1.57 | 8.80 |
| NU26-02 | 0.18721 | 0.00424 | 13.4994 | 0.33080 | 0.52302 | 0.01210 | 0.15139 | 0.00398 | 2718 | 38 | 2715 | 24 | 2712 | 52 | 2849 | 70 | 2718 | 38 | 5.36 | 14.90 |
| NU26-03 | 0.05499 | 0.00262 | 0.44744 | 0.02098 | 0.05902 | 0.00154 | 0.01966 | 0.00080 | 412 | 110 | 375 | 14 | 370 | 10 | 394 | 16 | 370 | 10 | 6.33 | 17.23 |
| NU26-04 | 0.09319 | 0.00216 | 3.2823 | 0.08250 | 0.25548 | 0.00588 | 0.08066 | 0.00186 | 1492 | 44 | 1477 | 20 | 1467 | 30 | 1568 | 34 | 1492 | 44 | 18.51 | 34.95 |
| NU26-05 | 0.05383 | 0.00324 | 0.4393 | 0.02572 | 0.0592 | 0.00168 | 0.01829 | 0.00118 | 364 | 138 | 370 | 18 | 371 | 10 | 366 | 24 | 371 | 10 | 2.51 | 11.00 |
| NU26-07 | 0.05499 | 0.00364 | 0.44643 | 0.02692 | 0.05888 | 0.00162 | 0.01837 | 0.00054 | 412 | 152 | 375 | 18 | 369 | 10 | 368 | 10 | 369 | 10 | 2.50 | 11.57 |
| NU26-09 | 0.18735 | 0.00432 | 13.60923 | 0.34040 | 0.52688 | 0.01232 | 0.1547 | 0.00408 | 2719 | 38 | 2723 | 24 | 2728 | 52 | 2907 | 72 | 2719 | 38 | 2.93 | 7.13 |

**Appendix 3A.2. Zircon U-Pb SHRIMP age data for mosaic grains from the Nurbinskaya kimberlitic pipe, Nakyn field, Siberia, Russia**

| Analysis No. | RATIOS | | | | | | | | AGES, Ma (1) | | | | | | CONCENTRATIONS (ppm) | |
|---|---|---|---|---|---|---|---|---|---|---|---|---|---|---|---|---|
| | $^{207}Pb/^{206}Pb$ | ± 2σ | $^{207}Pb/^{235}U$ | ± 2σ | $^{206}Pb/^{238}U$ | ± 2σ | $^{208}Pb/^{232}Th$ | ± 2σ | $^{206}Pb/^{238}U$ | | $^{207}Pb/^{206}Pb$ | | $^{208}Pb/^{232}Th$ | | Th | U |
| **Grain NU-19-03** | | | | | | | | | | | | | | | | |
| 1 (block) | 0.085 | 14 | 0.81 | 15 | 0.0694 | 3 | 0.075 | 19 | 432 | ±14 | 1309 | ±279 | 1455 | ±270 | 2.9 | 19.9 |
| 2 (mix) | 0.077 | 5 | 0.68 | 5 | 0.0644 | 3 | 0.046 | 10 | 402 | ±10 | 1121 | ±95 | 907 | ±87 | 2.9 | 27.2 |
| 3 (block) | 0.05 | 36 | 0.51 | 41 | 0.0735 | 20 | 0.017 | 91 | 457 | ±87 | 206 | ±844 | 338 | ±306 | 4.1 | 26.5 |
| 4 (mix) | 0.058 | 28 | 0.52 | 30 | 0.0656 | 12 | 0.026 | 69 | 409 | ±48 | 522 | ±605 | 528 | ±358 | 3.5 | 27.3 |
| 5 (block) | 0.163 | 15 | 1.56 | 15 | 0.0691 | 4 | 0.18 | 22 | 431 | ±16 | 2489 | ±252 | 3348 | ±690 | 3 | 25.7 |
| 6 (interblock) | 0.059 | 34 | 0.46 | 34 | 0.0567 | 4 | 0.009 | 197 | 356 | ±13 | 573 | ±745 | 180 | ±353 | 4.1 | 25.9 |
| **Grain NU-25-08** | | | | | | | | | | | | | | | | |
| 1 (block) | 0.188 | 22 | 1.9 | 23 | 0.0734 | 7 | 0.435 | 37 | 457 | ±30 | 2722 | ±370 | 7295 | ±2282 | 0.4 | 7.6 |
| 2 (block) | 0.127 | 19 | 1.18 | 21 | 0.0677 | 7 | 0.476 | 39 | 422 | ±27 | 2052 | ±344 | 7869 | ±2527 | 0.3 | 12.4 |
| 3 (block) | 0.093 | 17 | 0.82 | 18 | 0.064 | 5 | 0.295 | 15 | 400 | ±19 | 1492 | ±327 | 5227 | ±702 | 0.3 | 8.9 |
| 4 (inteblock) | 0.015 | 392 | 0.12 | 392 | 0.0565 | 9 | -0.129 | 235 | 354 | ±29 | - | - | -2802 | -7076 | 0.3 | 10.9 |
| 5 (interblock) | 0.042 | 113 | 0.29 | 113 | 0.0501 | 12 | -0.365 | 101 | 315 | ±38 | -250 | ±2848 | -9184 | -11787 | 0.2 | 7.3 |
| **Grain NU-26-08** | | | | | | | | | | | | | | | | |
| 1 (interblock) | 0.039 | 46 | 0.32 | 46 | 0.06 | 4 | 0.01 | 97 | 376 | ±13 | -435 | ±1207 | 206 | ±198 | 6.2 | 23.4 |
| 2 (mix) | 0.077 | 4 | 0.67 | 6 | 0.0626 | 4 | 0.049 | 9 | 391 | ±16 | 1127 | ±89 | 965 | ±87 | 4.1 | 29.2 |
| 3 (block) | 0.073 | 4 | 0.67 | 5 | 0.0663 | 2 | 0.075 | 9 | 414 | ±9 | 1009 | ±83 | 1460 | ±133 | 1.9 | 36.9 |
| 4 (interblock) | 0.089 | 12 | 0.75 | 13 | 0.0615 | 3 | 0.034 | 14 | 385 | ±12 | 1404 | ±237 | 685 | ±94 | 8.3 | 21.7 |

**Comments:**

Errors are 1-sigma; Pbc and Pb* indicate the common and radiogenic portions, respectively.

Error in Standard calibration was 0.39% (not included in above errors but required when comparing data from different mounts).

(1) Common Pb corrected using measured 204Pb.

**Appendix 3A.3. Zircon trace-element data (ppm) for the samples from the Nurbinskaya kimberlitic pipe, Nakyn field, Siberia, Russia**

| Analysis No. | P | Ti | Y | Nb | La | Ce | Pr | Nd | Sm | Eu | Gd | Dy | Ho | Er | Yb | Lu | Hf | Ta | Th | U | Th/U | U/Yb |
|---|---|---|---|---|---|---|---|---|---|---|---|---|---|---|---|---|---|---|---|---|---|---|
| **Mosaic** | | | | | | | | | | | | | | | | | | | | | | |
| **Grain NU-19-03** | | | | | | | | | | | | | | | | | | | | | | |
| interblock_spot1 | 67.1 | 36.2 | 23.2 | 54.4 | 0.01 | 8.55 | 0.11 | 1.16 | 0.60 | 0.25 | 1.38 | 2.53 | 0.78 | 2.95 | 4.88 | 0.83 | 11191 | 52.3 | 6.24 | 45.0 | 0.14 | 9.23 |
| interblock_spot2 | 75.0 | 36.4 | 29.3 | 49.1 | 0.04 | 7.10 | 0.13 | 1.27 | 0.69 | 0.27 | 1.44 | 3.21 | 1.01 | 3.84 | 6.15 | 1.13 | 11423 | 54.1 | 5.77 | 43.0 | 0.13 | 7.00 |
| block_spot1 | 58.1 | 40.8 | 32.3 | 74.8 | 0.03 | 7.41 | 0.10 | 1.01 | 0.59 | 0.22 | 1.39 | 3.55 | 1.13 | 4.50 | 7.45 | 1.20 | 11338 | 66.1 | 5.69 | 43.0 | 0.13 | 5.77 |
| block_spot2 | 58.3 | 38.9 | 56.5 | 75.6 | 0.02 | 4.67 | 0.09 | 0.94 | 0.61 | 0.29 | 1.78 | 6.26 | 2.09 | 8.48 | 13.4 | 2.27 | 11436 | 66.1 | 5.37 | 38.2 | 0.14 | 2.85 |
| interblock_line1 | n/a | n/a | n/a | n/a | 0.05 | 11.1 | 0.17 | 1.80 | 1.20 | 0.49 | 1.73 | 2.49 | 0.65 | 2.27 | 4.81 | 0.59 | 12348 | 65.7 | 7.93 | 80.9 | 0.10 | 16.81 |
| interblock_line2 | n/a | n/a | n/a | n/a | 0.06 | 10.9 | 0.18 | 1.97 | 1.16 | 0.49 | 2.00 | 3.17 | 0.96 | 3.77 | 8.08 | 0.86 | 12246 | 68.1 | 7.17 | 68.6 | 0.10 | 8.49 |
| interblock_line3 | n/a | n/a | n/a | n/a | 0.04 | 10.8 | 0.16 | 1.79 | 1.15 | 0.43 | 1.67 | 2.80 | 0.82 | 3.05 | 6.27 | 0.72 | 12395 | 60.8 | 7.44 | 61.6 | 0.12 | 9.82 |
| interblock_line4 | n/a | n/a | n/a | n/a | 0.04 | 11.7 | 0.16 | 1.92 | 1.15 | 0.51 | 1.64 | 2.44 | 0.64 | 2.35 | 5.05 | 0.59 | 12574 | 63.9 | 5.96 | 85.1 | 0.07 | 16.85 |
| block_line1 | n/a | n/a | n/a | n/a | 0.0514 | 11.05 | 0.172 | 1.8 | 1.2 | 0.486 | 1.73 | 2.49 | 0.65 | 2.27 | 4.81 | 0.59 | 12348 | 65.7 | 7.93 | 80.9 | 0.10 | 16.81 |
| block_line2 | n/a | n/a | n/a | n/a | 0.0521 | 9.27 | 0.163 | 1.71 | 1 | 0.471 | 2.07 | 7.07 | 2.32 | 8.72 | 19.69 | 2.24 | 12335 | 79.6 | 6.1 | 57.3 | 0.11 | 2.91 |
| block_line3 | n/a | n/a | n/a | n/a | 0.0358 | 7.27 | 0.116 | 1.53 | 1 | 0.43 | 2.01 | 6.57 | 2.17 | 8.27 | 18.79 | 2.2 | 12418 | 73.7 | 7.75 | 47.5 | 0.16 | 2.53 |
| block_line4 | n/a | n/a | n/a | n/a | 0.0295 | 8.05 | 0.141 | 1.31 | 1.01 | 0.501 | 2.56 | 8.52 | 2.81 | 10.7 | 24.3 | 2.62 | 12554 | 88.7 | 8.99 | 79.3 | 0.11 | 3.26 |
| **Grain NU-25-08** | | | | | | | | | | | | | | | | | | | | | | |
| interblock_spot1 | 42.8 | 35.8 | 4.82 | 5.36 | 0.01 | 0.70 | 0.00 | 0.03 | 0.06 | 0.04 | 0.20 | 0.44 | 0.10 | 0.27 | 0.25 | 0.04 | 12677 | 4.33 | 0.36 | 11.8 | 0.03 | 46.30 |
| interblock_spot2 | 29.5 | 35.5 | 4.61 | 6.14 | <0 | 0.77 | 0.00 | 0.04 | 0.08 | 0.05 | 0.30 | 0.43 | 0.07 | 0.25 | 0.26 | 0.03 | 12194 | 6.24 | 0.49 | 16.6 | 0.03 | 63.96 |
| block_spot1 | 34.9 | 41.1 | 3.58 | 10.6 | <0 | 0.84 | 0.00 | 0.09 | 0.08 | 0.05 | 0.26 | 0.27 | 0.04 | 0.15 | 0.12 | 0.02 | 11598 | 17.6 | 0.57 | 25.0 | 0.02 | 208.67 |
| block_spot2 | 31.0 | 45.2 | 3.87 | 12.8 | <0 | 0.87 | 0.00 | 0.13 | 0.12 | 0.04 | 0.27 | 0.34 | 0.06 | 0.18 | 0.09 | 0.03 | 11679 | 15.2 | 0.56 | 22.1 | 0.03 | 257.09 |
| interblock_line1 | n/a | n/a | n/a | n/a | <0.01 | 0.80 | 0.01 | 0.22 | 0.25 | 0.10 | 0.50 | 0.65 | 0.13 | 0.37 | 0.44 | 0.06 | 13936 | 6.00 | 0.48 | 12.4 | 0.04 | 28.05 |
| interblock_line2 | n/a | n/a | n/a | n/a | <0.01 | 1.05 | 0.02 | 0.24 | 0.26 | 0.13 | 0.49 | 0.61 | 0.14 | 0.43 | 0.43 | 0.05 | 14256 | 14.1 | 0.60 | 17.9 | 0.03 | 41.72 |
| interblock_line3 | n/a | n/a | n/a | n/a | 0.02 | 0.93 | 0.01 | 0.22 | 0.25 | 0.14 | 0.61 | 0.63 | 0.14 | 0.37 | 0.51 | 0.07 | 14495 | 5.99 | 0.62 | 13.6 | 0.05 | 26.82 |
| block_line1 | n/a | n/a | n/a | n/a | <0.0092 | 0.804 | 0.011 | 0.22 | 0.25 | 0.099 | 0.5 | 0.65 | 0.13 | 0.37 | 0.442 | 0.06 | 13936 | 6 | 0.48 | 12.4 | 0.04 | 28.05 |
| block_line2 | n/a | n/a | n/a | n/a | <0.0070 | 1.05 | 0.016 | 0.24 | 0.26 | 0.126 | 0.49 | 0.61 | 0.14 | 0.43 | 0.43 | 0.05 | 14256 | 14.1 | 0.6 | 17.9 | 0.03 | 41.72 |
| block_line3 | n/a | n/a | n/a | n/a | 0.0214 | 0.931 | 0.013 | 0.22 | 0.25 | 0.137 | 0.61 | 0.63 | 0.14 | 0.37 | 0.507 | 0.07 | 14495 | 5.99 | 0.62 | 13.6 | 0.05 | 26.82 |
| **Grain NU-26-08** | | | | | | | | | | | | | | | | | | | | | | |
| interblock_spot1 | 45.4 | 31.2 | 6.94 | 11.7 | 0.01 | 0.90 | 0.00 | 0.04 | 0.11 | 0.07 | 0.33 | 0.65 | 0.16 | 0.47 | 0.51 | 0.09 | 16182 | 6.59 | 10.1 | 48.2 | 0.21 | 94.40 |
| interblock_spot2 | 44.8 | 30.9 | 9.68 | 13.2 | 0.01 | 0.93 | 0.01 | 0.11 | 0.12 | 0.09 | 0.55 | 1.19 | 0.29 | 0.85 | 1.25 | 0.20 | 15760 | 7.96 | 6.11 | 35.1 | 0.17 | 27.97 |
| block_spot1 | 51.0 | 35.5 | 14.7 | 23.2 | <0 | 1.10 | 0.02 | 0.34 | 0.33 | 0.19 | 0.90 | 1.76 | 0.47 | 1.59 | 2.58 | 0.46 | 14747 | 13.1 | 7.29 | 30.8 | 0.24 | 11.94 |
| block_spot2 | 41.1 | 35.6 | 14.0 | 22.9 | <0 | 1.13 | 0.02 | 0.21 | 0.28 | 0.17 | 1.04 | 1.69 | 0.46 | 1.47 | 2.09 | 0.38 | 15043 | 12.9 | 5.31 | 26.6 | 0.20 | 12.73 |
| interblock_line1 | n/a | n/a | n/a | n/a | 0.01 | 1.29 | 0.03 | 0.25 | 0.39 | 0.19 | 0.86 | 1.41 | 0.30 | 1.02 | 1.79 | 0.20 | 17160 | 9.95 | 8.93 | 53.0 | 0.17 | 29.63 |
| interblock_line2 | n/a | n/a | n/a | n/a | 0.03 | 1.33 | 0.02 | 0.27 | 0.28 | 0.16 | 0.74 | 0.98 | 0.25 | 0.77 | 1.21 | 0.13 | 18007 | 8.96 | 10.7 | 67.4 | 0.16 | 55.68 |
| interblock_line3 | n/a | n/a | n/a | n/a | 0.02 | 1.21 | 0.03 | 0.34 | 0.37 | 0.22 | 1.04 | 1.91 | 0.50 | 1.57 | 2.94 | 0.38 | 17638 | 12.4 | 6.30 | 36.2 | 0.17 | 12.33 |
| interblock_line4 | n/a | n/a | n/a | n/a | <0.01 | 1.21 | 0.02 | 0.25 | 0.26 | 0.17 | 0.67 | 1.22 | 0.32 | 0.89 | 1.65 | 0.21 | 17532 | 9.25 | 6.52 | 50.1 | 0.13 | 30.35 |
| block_line1 | n/a | n/a | n/a | n/a | <0.0073 | 1.616 | 0.041 | 0.53 | 0.63 | 0.293 | 1.3 | 2.27 | 0.6 | 2.03 | 3.93 | 0.49 | 16287 | 16.3 | 9.4 | 35.2 | 0.27 | 8.96 |
| block_line2 | n/a | n/a | n/a | n/a | 0.0233 | 1.862 | 0.039 | 0.4 | 0.55 | 0.264 | 1.52 | 2.66 | 0.71 | 2.24 | 3.54 | 0.39 | 18832 | 10.2 | 28.1 | 55.2 | 0.51 | 15.58 |
| block_line3 | n/a | n/a | n/a | n/a | 0.0087 | 1.17 | 0.038 | 0.48 | 0.69 | 0.38 | 1.89 | 3.74 | 0.94 | 3.05 | 6.42 | 0.81 | 17652 | 17.8 | 8.03 | 29.1 | 0.28 | 4.54 |
| block_line4 | n/a | n/a | n/a | n/a | <0.0068 | 1.278 | 0.029 | 0.33 | 0.45 | 0.272 | 1.17 | 2.45 | 0.66 | 2.38 | 4.84 | 0.6 | 17159 | 15.9 | 7.13 | 40 | 0.18 | 8.26 |
| **Undeformed** | | | | | | | | | | | | | | | | | | | | | | |
| NU-18-01 | 275 | 42.38 | 250.02 | 1.87 | 0.016 | 11.75 | 0.075 | 0.9 | 1.67 | 0.589 | 6.91 | 23.1 | 8.26 | 35.5 | 75.18 | 13.9 | 15272 | 0.13 | 3.73 | 6.67 | 0.56 | 0.09 |
| NU-18-02 | 183 | 24.58 | 387.98 | 1.7 | <0.0084 | 9.08 | 0.063 | 1.16 | 2.14 | 0.856 | 10.7 | 36.5 | 13 | 56.4 | 118 | 21.9 | 16209 | 0.07 | 0.44 | 7.46 | 0.06 | 0.06 |
| NU-18-03 | 213 | 20.37 | 248.85 | 1.78 | <0.0071 | 12.54 | 0.052 | 1.01 | 1.84 | 0.735 | 7.41 | 23.8 | 8.4 | 35.8 | 73.22 | 13.6 | 16896 | 0.09 | 2.8 | 14 | 0.20 | 0.19 |
| NU-18-04 | 86.9 | 14.61 | 75.46 | 4.65 | <0.0066 | 2.247 | 0.03 | 0.71 | 0.97 | 0.775 | 4.01 | 10.2 | 2.77 | 9.41 | 13.73 | 2.15 | 20032 | 2.65 | 5.52 | 15.1 | 0.37 | 1.10 |

| Analysis No. | P | Ti | Y | Nb | La | Ce | Pr | Nd | Sm | Eu | Gd | Dy | Ho | Er | Yb | Lu | Hf | Ta | Th | U | Th/U | U/Yb |
|---|---|---|---|---|---|---|---|---|---|---|---|---|---|---|---|---|---|---|---|---|---|---|
| NU-18-05 | 148 | 7.59 | 66.01 | 4.18 | 0.174 | 15.5 | 0.369 | 4.11 | 3.26 | 1.485 | 6.22 | 9.57 | 2.23 | 6.65 | 8 | 1.2 | 10903 | 1.9 | 19.5 | 32.3 | 0.60 | 4.04 |
| NU-18-06 | 103 | 13.82 | 39.18 | 4.23 | 0.0039 | 1.327 | 0.006 | 0.18 | 0.39 | 0.25 | 1.23 | 4.48 | 1.42 | 4.89 | 8.53 | 1.29 | 19617 | 2.68 | 2.47 | 11.7 | 0.21 | 1.37 |
| NU-18-07 | 247 | 21.33 | 183.4 | 1.72 | 0.0186 | 9.46 | 0.055 | 0.66 | 1.29 | 0.601 | 5.5 | 17.4 | 6.29 | 26.5 | 54.74 | 10.1 | 16226 | 0.09 | 2.06 | 7.01 | 0.29 | 0.13 |
| NU-18-08 | 117 | 15.71 | 52.87 | 5.07 | <0.0065 | 1.697 | 0.008 | 0.25 | 0.48 | 0.326 | 1.74 | 6.01 | 1.79 | 6.85 | 11.98 | 2.03 | 17408 | 3.36 | 3.53 | 15.6 | 0.23 | 1.31 |
| NU-18-09 | 336 | 58.83 | 291.06 | 2.36 | 0.0402 | 15.71 | 0.112 | 1.88 | 2.4 | 0.762 | 8.97 | 27.3 | 9.59 | 40.9 | 85.13 | 15.7 | 14136 | 0.34 | 2.42 | 11.1 | 0.22 | 0.13 |
| NU-25-01 | 256 | 9.76 | 602.17 | 2.35 | <0.0083 | 12.35 | 0.052 | 0.99 | 2.64 | 1.059 | 17.7 | 58 | 20.2 | 83.2 | 155 | 27.8 | 18582 | 0.21 | 4.78 | 14.2 | 0.34 | 0.09 |
| NU-25-02 | 263 | 39.37 | 594.62 | 1.64 | 0.0107 | 11.87 | 0.139 | 2.86 | 5.64 | 2.75 | 25.8 | 66 | 20.9 | 79.9 | 141.5 | 24.5 | 16203 | 0.08 | 0.77 | 6.28 | 0.12 | 0.04 |
| NU-25-03 | 245 | 22.41 | 242.65 | 1.83 | 0.01 | 12.67 | 0.045 | 0.98 | 1.7 | 0.622 | 7.31 | 23.1 | 8.07 | 34.9 | 74.27 | 13.5 | 16894 | 0.11 | 1.73 | 16.2 | 0.11 | 0.22 |
| NU-25-04 | 88.1 | 13.09 | 35.47 | 3.99 | 0.0016 | 1.299 | 0.01 | 0.19 | 0.34 | 0.24 | 1.31 | 3.94 | 1.22 | 4.42 | 7.56 | 1.23 | 19099 | 2.28 | 2.32 | 10.1 | 0.23 | 1.33 |
| NU-25-05 | 305 | 35.18 | 305.03 | 1.75 | <0.0065 | 6.66 | 0.049 | 1.01 | 2.04 | 0.614 | 8.65 | 29.1 | 10.4 | 43.8 | 85.77 | 15.2 | 15826 | 0.09 | 0.97 | 5.45 | 0.18 | 0.06 |
| NU-25-06 | 237 | 29.85 | 223.67 | 1.69 | <0.0126 | 5.84 | 0.031 | 0.88 | 1.35 | 0.634 | 5.83 | 20.6 | 7.47 | 32.9 | 70.72 | 12.9 | 14982 | 0.07 | 0.69 | 5.6 | 0.12 | 0.08 |
| NU-19-01 | 229 | 28.46 | 613.08 | 1.67 | 0.0065 | 13.14 | 0.091 | 1.98 | 4.21 | 1.861 | 21.4 | 64.4 | 21.5 | 87.3 | 160.7 | 28.5 | 16644 | 0.1 | 2.99 | 15.8 | 0.19 | 0.10 |
| NU-19-02 | 84.9 | 10.84 | 13.28 | 4.6 | 0.0042 | 0.966 | 0.006 | 0.05 | 0.05 | 0.061 | 0.36 | 1.07 | 0.35 | 1.43 | 2.93 | 0.53 | 15143 | 3.37 | 1.41 | 8.18 | 0.17 | 2.79 |
| NU-19-04 | 206 | 30.09 | 200.71 | 1.8 | <0.0105 | 7.77 | 0.041 | 0.94 | 1.4 | 0.604 | 5.73 | 18.7 | 6.69 | 28 | 58.04 | 10.7 | 15382 | 0.11 | 1.41 | 5.21 | 0.27 | 0.09 |
| NU-19-05 | 464 | 47.15 | 1147.23 | 2.56 | 0.0494 | 22.05 | 0.253 | 4.3 | 7.78 | 2.242 | 35.4 | 115 | 38.7 | 156 | 289.8 | 51 | 17528 | 0.51 | 21.2 | 25.6 | 0.83 | 0.09 |
| NU-19-07 | 83.4 | 12.5 | 13.91 | 4.28 | 0.0022 | 1.042 | <0.004 | 0.03 | 0.09 | 0.056 | 0.45 | 1.22 | 0.38 | 1.42 | 2.44 | 0.43 | 18090 | 3.04 | 1.65 | 8.52 | 0.19 | 3.49 |
| NU-19-08 | 155 | 5.82 | 53.46 | 3.95 | 0.0585 | 12.43 | 0.231 | 3.15 | 3.28 | 1.52 | 6.05 | 8.48 | 1.84 | 5.24 | 6.17 | 0.84 | 11115 | 1.8 | 27.2 | 35.9 | 0.76 | 5.82 |
| NU-26-01 | 86.7 | 10.18 | 14.98 | 4.57 | <0.0034 | 1.049 | <0.003 | 0.05 | 0.1 | 0.069 | 0.39 | 1.31 | 0.44 | 1.65 | 2.95 | 0.51 | 16813 | 3.55 | 1.57 | 8.8 | 0.18 | 2.98 |
| NU-26-02 | 396 | 46.43 | 573.91 | 2.41 | 0.0524 | 26.16 | 0.207 | 3.14 | 4.65 | 1.224 | 16.9 | 52.6 | 18.5 | 77 | 155.9 | 28.7 | 15554 | 0.32 | 5.36 | 14.9 | 0.36 | 0.10 |
| NU-26-03 | 104 | 14.12 | 85.65 | 4.96 | <0.0051 | 2.316 | 0.041 | 0.9 | 1.39 | 0.814 | 4.48 | 11 | 3.05 | 10.6 | 15.19 | 2.46 | 19209 | 2.85 | 6.33 | 17.2 | 0.37 | 1.13 |
| NU-26-04 | 237 | 6.18 | 91.4 | 3.76 | 0.1033 | 9.45 | 0.178 | 2.32 | 2.9 | 1.559 | 8.03 | 13 | 3.09 | 8.95 | 10.44 | 1.5 | 10678 | 1.58 | 18.5 | 35 | 0.53 | 3.35 |
| NU-26-05 | 93.2 | 13.28 | 38.55 | 3.95 | <0.0096 | 1.347 | 0.012 | 0.19 | 0.3 | 0.239 | 1.32 | 4.43 | 1.22 | 4.82 | 8.22 | 1.42 | 18029 | 2.13 | 2.51 | 11 | 0.23 | 1.34 |
| NU-26-06 | 75.9 | 11.14 | 44.97 | 3.96 | <0.0037 | 1.278 | 0.011 | 0.17 | 0.31 | 0.249 | 1.6 | 4.97 | 1.57 | 5.74 | 10.06 | 1.68 | 17829 | 2.38 | 2.5 | 11.6 | 0.22 | 1.15 |

**Appendix 3A.4. Zircon O-isotope data for mosaic zircons from the Nurbinskaya kimberlitic pipe, Nakyn field, Siberia, Rus**

| Analysis No. | O-ISOTOPES | | | |
|---|---|---|---|---|
| | 18O/16O | Rel. err in % | δ18O | 2σ |
| NU19-1_01 | 0.0020169 | 0.0000002 | 5.84 | 0.23 |
| NU19-1_02 | 0.0020169 | 0.0000002 | 5.86 | 0.23 |
| NU19-1_03 | 0.0020170 | 0.0000002 | 5.89 | 0.22 |
| NU19-1_04 | 0.0020169 | 0.0000002 | 5.84 | 0.23 |
| NU19-1_05 | 0.0020175 | 0.0000003 | 6.12 | 0.26 |
| NU19-1_06 | 0.0020175 | 0.0000003 | 6.13 | 0.25 |
| NU19-1_07 | 0.0020171 | 0.0000003 | 5.95 | 0.26 |
| NU19-1_08 | 0.0020175 | 0.0000002 | 6.15 | 0.23 |
| NU19-1_09 | 0.0020172 | 0.0000002 | 5.99 | 0.25 |
| NU19-1_10 | 0.0020172 | 0.0000003 | 6.00 | 0.27 |
| NU19-1_11 | 0.0020173 | 0.0000002 | 6.03 | 0.25 |
| NU19-1_12 | 0.0020169 | 0.0000002 | 5.84 | 0.23 |
| NU19-2_01 | 0.0020161 | 0.0000003 | 5.44 | 0.27 |
| NU19-2_02 | 0.0020161 | 0.0000003 | 5.45 | 0.26 |
| NU19-2_03 | 0.0020165 | 0.0000003 | 5.65 | 0.28 |
| NU19-2_04 | 0.0020164 | 0.0000003 | 5.57 | 0.27 |
| NU19-2_05 | 0.0020165 | 0.0000003 | 5.62 | 0.25 |
| NU19-2_06 | 0.0020167 | 0.0000003 | 5.73 | 0.27 |
| NU19-2_07 | 0.0020169 | 0.0000003 | 5.84 | 0.28 |
| NU19-2_08 | 0.0020164 | 0.0000003 | 5.56 | 0.28 |
| NU19-2_09 | 0.0020166 | 0.0000002 | 5.68 | 0.24 |
| NU26-1_01 | 0.0020168 | 0.0000003 | 5.80 | 0.26 |
| NU26-1_2 | 0.0020169 | 0.0000003 | 5.81 | 0.29 |
| NU26-1_3 | 0.0020168 | 0.0000003 | 5.76 | 0.27 |
| NU26-1_4 | 0.0020162 | 0.0000003 | 5.47 | 0.27 |
| NU26-1_5 | 0.0020165 | 0.0000003 | 5.61 | 0.32 |
| NU26-1_6 | 0.0020164 | 0.0000003 | 5.59 | 0.28 |
| NU25-1_01 | 0.0020171 | 0.0000003 | 5.92 | 0.26 |
| NU25-1_2 | 0.0020169 | 0.0000003 | 5.81 | 0.26 |
| NU25-1_3 | 0.0020169 | 0.0000003 | 5.84 | 0.28 |
| NU25-1_4 | 0.0020170 | 0.0000003 | 5.88 | 0.27 |
| NU25-1_5 | 0.0020168 | 0.0000003 | 5.78 | 0.28 |

**Appendix 3A.5. Zircon Hf-isotope data for the samples from the Nurbinskaya kimberlitic pipe, Nakyn field, Siberia, Russia**

| Analysis No. | Lu-Hf RATIOS | | | | $Hf_{initial}$ | εHf(T) | ± SE | $T_{DM}$ (Ga) | $T_{DM}^{Crustal}$ (Ga) | U-Pb AGE (Ma) |
|---|---|---|---|---|---|---|---|---|---|---|
| | $^{176}Hf/^{177}Hf$ | 1SE | $^{176}Lu/^{177}Hf$ | $^{176}Yb/^{177}Hf$ | | | | | | |
| **Mosaic** | | | | | | | | | | |
| **Grain NU-19-03** | | | | | | | | | | |
| interblock_line_1 | 0.281674 | 0.000038 | 1.66E-05 | 7.81E-04 | 0.281674 | -31.3 | 1.3 | 2.16 | 3.30 | 360 |
| block_1 | 0.281561 | 0.000034 | 2.21E-05 | 9.24E-04 | 0.281561 | -33.8 | 1.2 | 2.31 | 3.50 | 430 |
| block_2 | 0.281537 | 0.000024 | 1.63E-05 | 8.61E-04 | 0.281537 | -34.6 | 0.9 | 2.34 | 3.56 | 430 |
| **Grain NU-25-08** | | | | | | | | | | |
| block_1 | 0.281556 | 0.000038 | 1.49E-06 | 3.53E-05 | 0.281556 | -34.6 | 1.3 | 2.31 | 3.53 | 400 |
| interblock_line_1 | 0.281597 | 0.000030 | 2.31E-07 | 2.07E-05 | 0.281597 | -34.0 | 1.1 | 2.26 | 3.47 | 360 |
| interblock_line_2 | 0.281596 | 0.000044 | 8.64E-07 | 1.49E-05 | 0.281596 | -34.1 | 1.6 | 2.26 | 3.47 | 360 |
| **Grain NU-26-08** | | | | | | | | | | |
| interblock_1 | 0.281555 | 0.000018 | 1.49E-06 | 5.64E-05 | 0.281555 | -35.3 | 0.6 | 2.32 | 3.55 | 370 |
| interblock_2 | 0.281538 | 0.000038 | 2.50E-06 | 6.50E-05 | 0.281538 | -35.9 | 1.3 | 2.34 | 3.59 | 370 |
| interblock_line_1 | 0.281617 | 0.000026 | 2.73E-06 | 7.73E-05 | 0.281617 | -33.1 | 0.9 | 2.23 | 3.42 | 370 |
| interblock_line_2 | 0.281619 | 0.000016 | 2.83E-06 | 6.78E-05 | 0.281619 | -33.0 | 0.6 | 2.23 | 3.41 | 370 |
| interblock_line_3 | 0.281559 | 0.000026 | 1.41E-06 | 3.61E-05 | 0.281559 | -35.2 | 0.9 | 2.31 | 3.54 | 370 |
| interblock_line_4 | 0.281593 | 0.000028 | 1.70E-06 | 3.84E-05 | 0.281593 | -34.0 | 1.0 | 2.27 | 3.47 | 370 |
| interblock_line_5 | 0.281696 | 0.000023 | 2.61E-06 | 6.66E-05 | 0.281696 | -30.3 | 0.8 | 2.13 | 3.25 | 370 |
| block_line_1 | 0.281558 | 0.000017 | 8.95E-07 | 3.03E-05 | 0.281558 | -34.5 | 0.6 | 2.31 | 3.53 | 400 |
| block_line_2 | 0.281617 | 0.000024 | 4.05E-06 | 1.09E-04 | 0.281617 | -32.4 | 0.9 | 2.23 | 3.40 | 400 |
| block_1 | 0.281642 | 0.000028 | 4.06E-06 | 1.11E-04 | 0.281642 | -31.6 | 1.0 | 2.20 | 3.35 | 400 |
| block_2 | 0.281624 | 0.000021 | 4.86E-06 | 1.35E-04 | 0.281624 | -31.1 | 0.7 | 2.22 | 3.36 | 450 |
| **Grain NU-ZR-C** | | | | | | | | | | |
| interblock_1 | 0.281565 | 0.000009 | 1.96E-06 | 9.48E-05 | 0.28156499 | -34.7 | 0.3 | 2.30 | 3.52 | 380 |
| interblock_2 | 0.281554 | 0.000010 | 1.81E-06 | 7.82E-05 | 0.281554 | -34.2 | 0.4 | 2.32 | 3.52 | 422 |
| block_1 | 0.281591 | 0.000011 | 1.66E-06 | 9.28E-05 | 0.28159099 | -32.9 | 0.4 | 2.27 | 3.44 | 420 |
| block_2 | 0.281550 | 0.000014 | 1.65E-06 | 9.94E-05 | 0.28154999 | -33.8 | 0.5 | 2.32 | 3.52 | 447 |
| block_3 | 0.281573 | 0.000010 | 3.42E-06 | 1.76E-04 | 0.28157297 | -34.0 | 0.4 | 2.29 | 3.50 | 400 |
| **Grain NU-ZR-D** | | | | | | | | | | |
| interblock_1 | 0.281570 | 0.000010 | 1.49E-06 | 7.47E-05 | 0.28156999 | -34.6 | 0.4 | 2.30 | 3.51 | 378 |
| interblock_2 | 0.281552 | 0.000007 | 1.08E-06 | 6.65E-05 | 0.28155199 | -35.3 | 0.2 | 2.32 | 3.55 | 376 |
| interblock_3 | 0.281552 | 0.000011 | 1.81E-06 | 8.56E-05 | 0.28155199 | -35.7 | 0.4 | 2.32 | 3.56 | 358 |
| block_1 | 0.281562 | 0.000010 | 1.65E-06 | 9.00E-05 | 0.28156199 | -34.7 | 0.3 | 2.31 | 3.53 | 385 |
| block_2 | 0.281557 | 0.000011 | 1.69E-06 | 9.43E-05 | 0.28155699 | -34.7 | 0.4 | 2.31 | 3.53 | 393 |
| **Undeformed** | | | | | | | | | | |
| NU-18-06 | 0.282816 | 0.000028 | 1.08E-05 | 5.14E-04 | 0.282816 | 9.26 | 1.0 | 0.60 | 0.76 | 367 |
| NU-19-07 | 0.282812 | 0.000026 | 3.88E-06 | 1.82E-04 | 0.282812 | 9.2 | 0.9 | 0.61 | 0.77 | 370 |
| NU-26-03 | 0.282858 | 0.000023 | 2.02E-05 | 9.99E-04 | 0.282858 | 10.8 | 0.8 | 0.54 | 0.66 | 370 |
| NU-26-05 | 0.282750 | 0.000027 | 1.27E-05 | 5.67E-04 | 0.282750 | 7.0 | 1.0 | 0.69 | 0.91 | 371 |
| NU-26-06 | 0.282765 | 0.000027 | 1.75E-05 | 7.81E-04 | 0.282765 | 7.5 | 1.0 | 0.67 | 0.87 | 371 |
| NU-25-04 | 0.282807 | 0.000033 | 1.06E-05 | 4.99E-04 | 0.282807 | 9.1 | 1.2 | 0.62 | 0.77 | 375 |
| NU-18-08 | 0.282851 | 0.000027 | 1.56E-05 | 7.21E-04 | 0.282851 | 10.7 | 1.0 | 0.55 | 0.67 | 375 |
| NU-18-04 | 0.282894 | 0.000026 | 1.77E-05 | 8.53E-04 | 0.282894 | 12.2 | 0.9 | 0.50 | 0.58 | 375 |
| NU-19-02 | 0.282729 | 0.000021 | 5.14E-06 | 2.47E-04 | 0.282729 | 6.4 | 0.7 | 0.72 | 0.95 | 378 |

| Analysis No. | Lu-Hf RATIOS | | | | | | | | | U-Pb AGE |
|---|---|---|---|---|---|---|---|---|---|---|
| | $^{176}Hf/^{177}Hf$ | 1SE | $^{176}Lu/^{177}Hf$ | $^{176}Yb/^{177}Hf$ | $Hf_{initial}$ | εHf(T) | ± SE | $T_{DM}$ (Ga) | $T_{DM}^{Crustal}$ (Ga) | (Ma) |
| NU-26-01 | 0.282783 | 0.000025 | 5.02E-06 | 2.15E-04 | 0.282783 | 8.4 | 0.9 | 0.65 | 0.82 | 380 |
| MVG126-05-2 | 0.281834 | 0.000008 | 9.93E-06 | 5.13E-04 | 0.281834 | -22.6 | 0.3 | 1.94 | 2.87 | 495 |
| MVG126-05 | 0.281825 | 0.000009 | 1.07E-05 | 5.32E-04 | 0.281825 | -22.8 | 0.3 | 1.95 | 2.89 | 501 |
| MVG126-05-3 | 0.281830 | 0.000005 | 8.57E-06 | 4.35E-04 | 0.281830 | -22.5 | 0.2 | 1.95 | 2.87 | 509 |
| NU-18-05 | 0.281405 | 0.000026 | 1.72E-05 | 8.71E-04 | 0.281405 | -23.2 | 0.9 | 2.52 | 3.43 | 1146 |
| NU-19-08 | 0.281453 | 0.000029 | 1.73E-05 | 8.64E-04 | 0.281453 | -14.7 | 1.0 | 2.45 | 3.13 | 1447 |
| MVG126-02 | 0.281400 | 0.000012 | 1.27E-05 | 6.63E-04 | 0.281400 | -15.7 | 0.4 | 2.52 | 3.23 | 1482 |
| NU-26-04 | 0.281424 | 0.000025 | 1.42E-05 | 7.77E-04 | 0.281424 | -14.7 | 0.9 | 2.49 | 3.17 | 1492 |
| MVG126-04 | 0.281413 | 0.000009 | 1.97E-05 | 1.04E-03 | 0.281412 | -12.1 | 0.3 | 2.51 | 3.11 | 1622 |
| MVG126-08 | 0.281076 | 0.000006 | 1.52E-04 | 6.46E-03 | 0.281069 | -6.6 | 0.2 | 2.96 | 3.37 | 2388 |
| MVG126-10 | 0.281024 | 0.000009 | 9.19E-05 | 3.71E-03 | 0.281019 | -2.6 | 0.3 | 3.03 | 3.31 | 2637 |
| MVG126-07 | 0.281033 | 0.000010 | 1.48E-04 | 6.16E-03 | 0.281026 | -2.2 | 0.3 | 3.02 | 3.29 | 2644 |
| NU-25-01 | 0.281052 | 0.000027 | 2.27E-04 | 1.00E-02 | 0.281041 | -1.6 | 1.0 | 3.00 | 3.26 | 2645 |
| NU-25-06 | 0.280978 | 0.000028 | 2.05E-04 | 9.02E-03 | 0.280968 | -4.0 | 1.0 | 3.10 | 3.42 | 2652 |
| NU-18-03 | 0.280997 | 0.000028 | 1.16E-04 | 4.83E-03 | 0.280991 | -2.4 | 1.0 | 3.07 | 3.34 | 2685 |
| NU-19-04 | 0.281095 | 0.000026 | 1.15E-04 | 5.09E-03 | 0.281089 | 1.0 | 0.9 | 2.94 | 3.12 | 2685 |
| NU-25-03 | 0.281042 | 0.000026 | 1.24E-04 | 5.39E-03 | 0.281036 | -0.7 | 0.9 | 3.01 | 3.24 | 2692 |
| MVG126-01 | 0.281055 | 0.000010 | 2.56E-04 | 1.03E-02 | 0.281042 | -0.4 | 0.4 | 3.00 | 3.22 | 2694 |
| NU-18-01 | 0.281013 | 0.000032 | 1.39E-04 | 5.79E-03 | 0.281006 | -1.6 | 1.1 | 3.05 | 3.30 | 2700 |
| NU-18-02 | 0.281012 | 0.000029 | 2.16E-04 | 8.60E-03 | 0.281001 | -1.4 | 1.0 | 3.05 | 3.30 | 2714 |
| MVG126-03 | 0.281044 | 0.000007 | 9.90E-05 | 3.98E-03 | 0.281039 | -0.1 | 0.2 | 3.00 | 3.21 | 2714 |
| NU-25-05 | 0.281005 | 0.000032 | 1.56E-04 | 6.98E-03 | 0.280997 | -1.5 | 1.1 | 3.06 | 3.30 | 2718 |
| NU-26-02 | 0.281025 | 0.000020 | 1.53E-04 | 6.80E-03 | 0.281017 | -0.7 | 0.7 | 3.03 | 3.26 | 2718 |
| NU-19-01 | 0.281126 | 0.000027 | 2.59E-04 | 1.13E-02 | 0.281113 | 2.7 | 1.0 | 2.91 | 3.04 | 2719 |
| NU-25-02 | 0.281000 | 0.000031 | 2.39E-04 | 1.06E-02 | 0.280988 | -1.7 | 1.1 | 3.07 | 3.32 | 2720 |
| NU-18-09 | 0.281093 | 0.000024 | 1.74E-04 | 6.98E-03 | 0.281084 | 1.7 | 0.9 | 2.94 | 3.11 | 2720 |
| MVG126-09 | 0.281018 | 0.000009 | 2.68E-04 | 1.11E-02 | 0.281004 | -1.2 | 0.3 | 3.05 | 3.29 | 2720 |
| NU-19-05 | 0.281055 | 0.000020 | 4.54E-04 | 2.00E-02 | 0.281031 | 0.0 | 0.7 | 3.02 | 3.22 | 2727 |
| NU-18-07 | 0.281096 | 0.000029 | 9.75E-05 | 3.99E-03 | 0.281091 | 2.1 | 1.0 | 2.93 | 3.08 | 2727 |
| MVG126-06 | 0.281006 | 0.000009 | 1.25E-04 | 5.12E-03 | 0.280999 | -0.8 | 0.3 | 3.05 | 3.28 | 2744 |
| Nurb*-01 | 0.281080 | 0.000007 | 0.000945 | 0.042160 | 0.281040 | -11.7 | 0.3 | 3.02 | 3.55 | 2221 |
| Nurb*-01Rim | 0.281079 | 0.000007 | 0.000926 | 0.039908 | 0.281038 | -9.6 | 0.2 | 3.02 | 3.49 | 2312 |
| Nurb*-02 | 0.281018 | 0.000005 | 0.000246 | 0.010109 | 0.281005 | -2.2 | 0.2 | 3.05 | 3.31 | 2684 |
| Nurb*-02r | 0.281017 | 0.000008 | 0.000249 | 0.010228 | 0.281004 | -2.0 | 0.3 | 3.05 | 3.30 | 2695 |
| Nurb*-03 | 0.281063 | 0.000009 | 0.000155 | 0.006902 | 0.281055 | -2.8 | 0.3 | 2.98 | 3.27 | 2583 |
| Nurb*-03r | 0.281063 | 0.000007 | 0.000134 | 0.005966 | 0.281056 | -0.4 | 0.2 | 2.98 | 3.19 | 2686 |
| Nurb*-10c | 0.280870 | 0.000011 | 0.000061 | 0.003647 | 0.280867 | -12.1 | 0.4 | 3.23 | 3.77 | 2470 |
| Nurb*-10R | 0.280887 | 0.000013 | 0.000071 | 0.004270 | 0.280884 | -14.0 | 0.5 | 3.21 | 3.81 | 2359 |
| Nurb*-11 | 0.280867 | 0.000013 | 0.000067 | 0.003833 | 0.280864 | -14.6 | 0.5 | 3.23 | 3.84 | 2367 |
| Nurb*-11R | 0.280888 | 0.000009 | 0.000031 | 0.001792 | 0.280886 | -10.2 | 0.3 | 3.20 | 3.69 | 2522 |
| Nurb*-12 | 0.281046 | 0.000013 | 0.000200 | 0.009680 | 0.281036 | -1.8 | 0.5 | 3.01 | 3.26 | 2656 |
| Nurb*-21c | 0.281059 | 0.000015 | 0.000149 | 0.007793 | 0.281051 | 0.8 | 0.5 | 2.99 | 3.16 | 2743 |
| Nurb*-21c | 0.281059 | 0.000015 | 0.000149 | 0.007793 | 0.281051 | 0.8 | 0.5 | 2.99 | 3.16 | 2743 |
| Nurb*-21r | 0.281018 | 0.000017 | 0.000121 | 0.006189 | 0.281012 | -1.6 | 0.6 | 3.04 | 3.28 | 2702 |
| Nurb*-23c | 0.281021 | 0.000013 | 0.000130 | 0.006655 | 0.281014 | -1.4 | 0.5 | 3.04 | 3.27 | 2706 |

| Analysis No. | Lu-Hf RATIOS | | | | $Hf_{initial}$ | εHf(T) | ± SE | $T_{DM}$ (Ga) | $T_{DM}^{Crustal}$ (Ga) | U-Pb AGE |
|---|---|---|---|---|---|---|---|---|---|---|
| | $^{176}Hf/^{177}Hf$ | 1SE | $^{176}Lu/^{177}Hf$ | $^{176}Yb/^{177}Hf$ | | | | | | (Ma) |
| Nurb*-23m | 0.281042 | 0.000010 | 0.000224 | 0.011590 | 0.281031 | -1.2 | 0.4 | 3.01 | 3.25 | 2689 |
| Nurb*-23r | 0.281038 | 0.000009 | 0.000178 | 0.009214 | 0.281029 | -1.0 | 0.3 | 3.02 | 3.25 | 2700 |
| Nurb*-26 | 0.281059 | 0.000009 | 0.000243 | 0.010456 | 0.281047 | -1.3 | 0.3 | 2.99 | 3.23 | 2662 |
| Nurb*-26r | 0.281058 | 0.000009 | 0.000218 | 0.009516 | 0.281047 | -0.8 | 0.3 | 2.99 | 3.22 | 2681 |
| Nurb*-27 | 0.281000 | 0.000014 | 0.000121 | 0.005844 | 0.280994 | -2.1 | 0.5 | 3.06 | 3.32 | 2705 |
| Nurb*-31 | 0.281056 | 0.000009 | 0.000198 | 0.010928 | 0.281046 | 0.5 | 0.3 | 2.99 | 3.18 | 2738 |
| Nurb*-31-2 | 0.280992 | 0.000011 | 0.000123 | 0.006345 | 0.280986 | -2.6 | 0.4 | 3.07 | 3.35 | 2696 |
| Nurb*-33c | 0.281052 | 0.000008 | 0.000085 | 0.004419 | 0.281048 | -7.7 | 0.3 | 2.99 | 3.42 | 2382 |
| Nurb*-36c | 0.281070 | 0.000008 | 0.000142 | 0.006260 | 0.281063 | 0.0 | 0.3 | 2.97 | 3.17 | 2694 |
| Nurb*-37c | 0.281056 | 0.000018 | 0.000237 | 0.011320 | 0.281044 | 0.4 | 0.6 | 3.00 | 3.18 | 2739 |
| Nurb*-38c | 0.281154 | 0.000013 | 0.000193 | 0.010276 | 0.281144 | 3.2 | 0.5 | 2.86 | 2.98 | 2706 |
| Nurb*-42c | 0.281066 | 0.000014 | 0.000172 | 0.008871 | 0.281057 | 0.8 | 0.5 | 2.98 | 3.16 | 2733 |
| Nurb*-43c | 0.281045 | 0.000014 | 0.000079 | 0.004278 | 0.281041 | -0.7 | 0.5 | 3.00 | 3.22 | 2695 |
| Nurb*-47c | 0.281069 | 0.000011 | 0.000305 | 0.016817 | 0.281053 | 0.4 | 0.4 | 2.99 | 3.17 | 2723 |
| Nurb*-48-2 | 0.281029 | 0.000012 | 0.000090 | 0.004772 | 0.281024 | 0.1 | 0.4 | 3.02 | 3.22 | 2754 |
| Nurb*-48c | 0.281040 | 0.000012 | 0.000248 | 0.013577 | 0.281027 | -0.2 | 0.4 | 3.02 | 3.22 | 2739 |
| Nurb*-48-r | 0.281048 | 0.000012 | 0.000134 | 0.007036 | 0.281041 | -0.4 | 0.4 | 3.00 | 3.21 | 2707 |
| Nurb*-Zr13c | 0.281079 | 0.000010 | 0.000130 | 0.006454 | 0.281072 | 1.0 | 0.3 | 2.96 | 3.13 | 2721 |
| Nurb*-Zr13r | 0.281052 | 0.000011 | 0.000310 | 0.016661 | 0.281036 | -0.9 | 0.4 | 3.01 | 3.23 | 2692 |
| Nurb*-Zr14 | 0.281066 | 0.000009 | 0.000268 | 0.013346 | 0.281053 | -4.7 | 0.3 | 2.99 | 3.33 | 2501 |
| Nurb*-Zr16 | 0.281043 | 0.000012 | 0.000251 | 0.011111 | 0.281030 | -1.0 | 0.4 | 3.02 | 3.24 | 2699 |
| Nurb*-Zr17 | 0.281570 | 0.000009 | 0.000045 | 0.002609 | 0.281570 | -34.2 | 0.3 | 2.30 | 3.51 | 381 |
| Nurb*-Zr17-1 | 0.281574 | 0.000013 | 0.000037 | 0.002099 | 0.281574 | -33.6 | 0.5 | 2.29 | 3.49 | 399 |
| Nurb*-Zr17-1c | 0.281543 | 0.000013 | 0.000032 | 0.001919 | 0.281543 | -34.5 | 0.5 | 2.33 | 3.55 | 410 |
| Nurb*-Zr17-2 | 0.281581 | 0.000009 | 0.000029 | 0.001626 | 0.281581 | -33.8 | 0.3 | 2.28 | 3.49 | 380 |
| Nurb*-Zr18 | 0.281037 | 0.000011 | 0.000235 | 0.011620 | 0.281025 | -1.3 | 0.4 | 3.02 | 3.26 | 2694 |
| Nurb*-Zr18r | 0.281009 | 0.000008 | 0.000252 | 0.012756 | 0.280996 | -2.3 | 0.3 | 3.06 | 3.32 | 2694 |
| Nurb*-Zr4c | 0.281040 | 0.000010 | 0.000236 | 0.012112 | 0.281028 | -1.4 | 0.4 | 3.02 | 3.26 | 2683 |
| Nurb*-Zr4r | 0.281034 | 0.000008 | 0.000155 | 0.008119 | 0.281026 | -1.2 | 0.3 | 3.02 | 3.25 | 2695 |
| Nurb*-Zr5 | 0.281053 | 0.000010 | 0.000346 | 0.017508 | 0.281037 | -6.2 | 0.4 | 3.01 | 3.39 | 2465 |
| Nurb*-Zr6 | 0.281035 | 0.000006 | 0.000290 | 0.013897 | 0.281020 | -2.1 | 0.2 | 3.03 | 3.29 | 2667 |
| Nurb*-Zr7 | 0.281051 | 0.000008 | 0.000174 | 0.007456 | 0.281042 | -1.4 | 0.3 | 3.00 | 3.24 | 2665 |
| Nurb*-Zr7r | 0.281031 | 0.000009 | 0.000203 | 0.008205 | 0.281021 | -1.7 | 0.3 | 3.03 | 3.27 | 2685 |
| Nurb*-Zr8 | 0.281034 | 0.000009 | 0.000231 | 0.011363 | 0.281022 | -1.2 | 0.3 | 3.03 | 3.26 | 2703 |
| Nurb*-Zr8r | 0.281042 | 0.000008 | 0.000159 | 0.007923 | 0.281034 | -0.8 | 0.3 | 3.01 | 3.23 | 2703 |

*analyzed previously by E. Belousova (unpublished data)

**Appendix 3A.6. Calculated temperature of zircon crystallization using Ti-in-Zirc termometer (Nurbinskaya kimberlitic pipe, Nakyn field, Siberia, Russia)**

| Analysis No. | Ti (ppm) | Calculated temperature | |
|---|---|---|---|
| | | K | °C |
| NU-18-01 | 42.38 | **1159** | **886** |
| NU-18-02 | 24.58 | **1100** | **827** |
| NU-18-03 | 20.37 | **1081** | **807** |
| NU-18-04 | 14.61 | **1048** | **775** |
| NU-18-05 | 7.59 | **990** | **717** |
| NU-18-06 | 13.82 | **1043** | **770** |
| NU-18-07 | 21.33 | **1085** | **812** |
| NU-18-08 | 15.71 | **1055** | **782** |
| NU-18-09 | 58.83 | **1198** | **925** |
| NU-25-01 | 9.76 | **1012** | **739** |
| NU-25-02 | 39.37 | **1151** | **878** |
| NU-25-03 | 22.41 | **1090** | **817** |
| NU-25-04 | 13.09 | **1038** | **765** |
| NU-25-05 | 35.18 | **1138** | **865** |
| NU-25-06 | 29.85 | **1120** | **847** |
| NU-19-01 | 28.46 | **1115** | **842** |
| NU-19-02 | 10.84 | **1021** | **748** |
| NU-19-04 | 30.09 | **1121** | **848** |
| NU-19-05 | 47.15 | **1171** | **898** |
| NU-19-07 | 12.5 | **1034** | **761** |
| NU-19-08 | 5.82 | **969** | **695** |
| NU-26-01 | 10.18 | **1016** | **742** |
| NU-26-02 | 46.43 | **1170** | **896** |
| NU-26-03 | 14.12 | **1045** | **772** |
| NU-26-04 | 6.18 | **973** | **700** |
| NU-26-05 | 13.28 | **1040** | **766** |
| NU-26-06 | 11.14 | **1024** | **750** |

**Appendix 4.1. Zircon U-Pb age data for samples from the Daldyn terrane**

| Analysis No. | RATIOS | | | | | | | | AGES (Ma) | | | | | | | | | | CONCENTRATIONS (ppm) | |
|---|---|---|---|---|---|---|---|---|---|---|---|---|---|---|---|---|---|---|---|---|
| | $^{207}Pb/^{206}Pb$ | ± 2σ | $^{207}Pb/^{235}U$ | ± 2σ | $^{206}Pb/^{238}U$ | ± 2σ | $^{208}Pb/^{232}Th$ | ± 2σ | $^{207}Pb/^{206}Pb$ | ± 2σ | $^{207}Pb/^{235}U$ | ± 2σ | $^{206}Pb/^{238}U$ | ± 2σ | $^{208}Pb/^{232}Th$ | ± 2σ | Used Age | ± 2σ | Th | U |
| **Chomurdakh field, Druzhba pipe** | | | | | | | | | | | | | | | | | | | | |
| 250-4 | 0.04836 | 0.00546 | 0.45299 | 0.04934 | 0.06794 | 0.00258 | 0.01805 | 0.00204 | 117 | 254 | 379 | 34 | 424 | 16 | 362 | 40 | 424 | 16 | 1.34 | 4.69 |
| 250-5 | 0.05468 | 0.00500 | 0.49025 | 0.04310 | 0.06503 | 0.00222 | 0.01806 | 0.00172 | 399 | 210 | 405 | 30 | 406 | 14 | 362 | 34 | 406 | 14 | 2.12 | 7.26 |
| 250-6 | 0.05568 | 0.00486 | 0.50133 | 0.04228 | 0.06531 | 0.00214 | 0.02306 | 0.00206 | 440 | 200 | 413 | 28 | 408 | 12 | 461 | 40 | 408 | 12 | 2.78 | 10.95 |
| 250-7 | 0.06249 | 0.00534 | 0.56991 | 0.04702 | 0.06615 | 0.00214 | 0.02084 | 0.00202 | 691 | 186 | 458 | 30 | 413 | 12 | 417 | 40 | 413 | 12 | 2.12 | 7.89 |
| 250-8 | 0.05139 | 0.00606 | 0.47347 | 0.05436 | 0.06682 | 0.00238 | 0.01729 | 0.00186 | 258 | 274 | 394 | 38 | 417 | 14 | 346 | 36 | 417 | 14 | 1.65 | 5.73 |
| 250-9 | 0.0533 | 0.00444 | 0.48301 | 0.03918 | 0.06573 | 0.00200 | 0.02303 | 0.00154 | 342 | 194 | 400 | 26 | 410 | 12 | 460 | 30 | 410 | 12 | 3.43 | 9.18 |
| **Chomurdakh field, Rassvet pipe** | | | | | | | | | | | | | | | | | | | | |
| MVG120-05 | 0.05417 | 0.01028 | 0.51883 | 0.09506 | 0.06946 | 0.0038 | 0.01839 | 0.00388 | 378 | 434 | 424 | 64 | 433 | 22 | 368 | 78 | 433 | 22 | 1.10 | 4.56 |
| MVG120-06 | 0.05628 | 0.00748 | 0.55969 | 0.07104 | 0.07212 | 0.00322 | 0.0266 | 0.00352 | 463 | 304 | 451 | 46 | 449 | 20 | 531 | 70 | 449 | 20 | 1.21 | 5.09 |
| MVG120-07 | 0.05615 | 0.01322 | 0.59459 | 0.13524 | 0.07681 | 0.00514 | 0.01883 | 0.00582 | 458 | 538 | 474 | 86 | 477 | 30 | 377 | 116 | 477 | 30 | 0.98 | 4.07 |
| MVG120-08 | 0.0564 | 0.01534 | 0.50471 | 0.13106 | 0.06491 | 0.00560 | 0.02422 | 0.00676 | 468 | 612 | 415 | 88 | 405 | 34 | 484 | 134 | 405 | 34 | 1.11 | 4.98 |
| MVG120-09 | 0.05743 | 0.00748 | 0.5621 | 0.06988 | 0.07099 | 0.00304 | 0.02275 | 0.00248 | 508 | 294 | 453 | 46 | 442 | 18 | 455 | 50 | 442 | 18 | 2.81 | 7.05 |
| MVG120-10 | 0.05543 | 0.00710 | 0.53882 | 0.06606 | 0.0705 | 0.00296 | 0.02173 | 0.00238 | 430 | 294 | 438 | 44 | 439 | 18 | 435 | 48 | 439 | 18 | 2.59 | 6.43 |
| MVG120-11 | 0.05584 | 0.00620 | 0.55799 | 0.05904 | 0.07248 | 0.00276 | 0.02281 | 0.00222 | 446 | 254 | 450 | 38 | 451 | 16 | 456 | 44 | 451 | 16 | 2.83 | 7.26 |
| MVG120-12 | 0.05355 | 0.00758 | 0.52712 | 0.07160 | 0.0714 | 0.00316 | 0.01977 | 0.00270 | 352 | 328 | 430 | 48 | 445 | 20 | 396 | 54 | 445 | 20 | 1.58 | 5.42 |
| MVG120-14 | 0.05652 | 0.01082 | 0.59983 | 0.10918 | 0.07698 | 0.00496 | 0.02273 | 0.00534 | 473 | 436 | 477 | 70 | 478 | 30 | 454 | 106 | 478 | 30 | 0.96 | 4.01 |
| MVG120-15 | 0.05632 | 0.00734 | 0.5585 | 0.06936 | 0.07192 | 0.00318 | 0.02089 | 0.00298 | 465 | 298 | 451 | 46 | 448 | 20 | 418 | 58 | 448 | 20 | 1.39 | 5.20 |
| ~~MVG120-04~~ | ~~0.06575~~ | ~~0.00934~~ | ~~0.64068~~ | ~~0.08606~~ | ~~0.07067~~ | ~~0.0036~~ | ~~0.01802~~ | ~~0.0036~~ | ~~798~~ | ~~306~~ | ~~503~~ | ~~54~~ | ~~440~~ | ~~22~~ | ~~361~~ | ~~72~~ | ~~440~~ | ~~22~~ | ~~0.96~~ | ~~4.19~~ |
| ~~MVG120-13~~ | ~~0.05147~~ | ~~0.00876~~ | ~~0.53358~~ | ~~0.08714~~ | ~~0.07519~~ | ~~0.00396~~ | ~~0.02595~~ | ~~0.00366~~ | ~~262~~ | ~~390~~ | ~~434~~ | ~~58~~ | ~~467~~ | ~~24~~ | ~~518~~ | ~~72~~ | ~~467~~ | ~~24~~ | ~~2.06~~ | ~~5.83~~ |
| **Chomurdakh field, Khairgastakh pipe** | | | | | | | | | | | | | | | | | | | | |
| 250-10 | 0.05562 | 0.00630 | 0.49788 | 0.05450 | 0.06493 | 0.00250 | 0.02157 | 0.00222 | 437 | 260 | 410 | 36 | 406 | 16 | 431 | 44 | 406 | 16 | 2.40 | 7.61 |
| 250-11 | 0.05538 | 0.00602 | 0.5192 | 0.05454 | 0.068 | 0.00258 | 0.0214 | 0.00186 | 428 | 248 | 425 | 36 | 424 | 16 | 428 | 36 | 424 | 16 | 3.91 | 9.42 |
| 250-12 | 0.05427 | 0.00342 | 0.50096 | 0.03054 | 0.06696 | 0.00190 | 0.02245 | 0.00140 | 382 | 146 | 412 | 20 | 418 | 12 | 449 | 28 | 418 | 12 | 3.64 | 13.99 |
| 250-13 | 0.05599 | 0.00484 | 0.5343 | 0.04444 | 0.06922 | 0.00242 | 0.02117 | 0.00162 | 452 | 196 | 435 | 30 | 431 | 14 | 423 | 32 | 431 | 14 | 4.90 | 13.08 |
| 250-14 | 0.05358 | 0.00658 | 0.47485 | 0.05616 | 0.06428 | 0.00274 | 0.01865 | 0.00232 | 353 | 284 | 395 | 38 | 402 | 16 | 373 | 46 | 402 | 16 | 1.70 | 6.14 |
| 250-15 | 0.05511 | 0.00532 | 0.4967 | 0.04584 | 0.06538 | 0.00240 | 0.01947 | 0.00200 | 417 | 222 | 409 | 32 | 408 | 14 | 390 | 40 | 408 | 14 | 2.87 | 10.56 |
| 250-16 | 0.05288 | 0.00600 | 0.5078 | 0.05534 | 0.06965 | 0.00284 | 0.02258 | 0.00236 | 324 | 264 | 417 | 38 | 434 | 18 | 451 | 46 | 434 | 18 | 2.21 | 6.95 |
| 250-17 | 0.05655 | 0.00712 | 0.51339 | 0.06224 | 0.06585 | 0.00276 | 0.01998 | 0.00232 | 474 | 286 | 421 | 42 | 411 | 16 | 400 | 46 | 411 | 16 | 2.85 | 8.41 |
| 250-18 | 0.05476 | 0.00598 | 0.50208 | 0.05308 | 0.0665 | 0.00252 | 0.02157 | 0.00196 | 402 | 252 | 413 | 36 | 415 | 16 | 431 | 38 | 415 | 16 | 3.13 | 7.50 |
| 250-19 | 0.05203 | 0.00366 | 0.19851 | 0.01350 | 0.02767 | 0.00082 | 0.00924 | 0.00048 | 287 | 164 | 184 | 12 | 176 | 6 | 186 | 10 | 176 | 6 | 29.42 | 42.78 |
| **Kuranakh field, Malokuonapka pipe** | | | | | | | | | | | | | | | | | | | | |
| MVG073-01 | 0.05071 | 0.00972 | 0.24694 | 0.04572 | 0.03532 | 0.00188 | 0.0076 | 0.00212 | 228 | 438 | 224 | 38 | 224 | 12 | 153 | 42 | 224 | 12 | 2.38 | 11.53 |
| MVG073-03 | 0.05128 | 0.01956 | 0.24749 | 0.09088 | 0.03501 | 0.00374 | 0.01047 | 0.00452 | 253 | 726 | 225 | 74 | 222 | 24 | 211 | 90 | 222 | 24 | 2.17 | 11.53 |
| MVG073-04 | 0.05064 | 0.00630 | 0.24814 | 0.02962 | 0.03554 | 0.00136 | 0.01141 | 0.00124 | 224 | 288 | 225 | 24 | 225 | 8 | 229 | 24 | 225 | 8 | 7.49 | 21.90 |
| MVG073-05 | 0.05071 | 0.01118 | 0.2423 | 0.05172 | 0.03466 | 0.00200 | 0.00973 | 0.00232 | 228 | 496 | 220 | 42 | 220 | 12 | 196 | 46 | 220 | 12 | 2.27 | 10.57 |
| MVG073-06 | 0.05234 | 0.01808 | 0.26533 | 0.08772 | 0.03678 | 0.00382 | 0.01373 | 0.00358 | 300 | 704 | 239 | 70 | 233 | 24 | 276 | 72 | 233 | 24 | 2.47 | 6.83 |
| MVG073-07 | 0.05088 | 0.01214 | 0.23935 | 0.05518 | 0.03412 | 0.00222 | 0.01083 | 0.00208 | 235 | 538 | 218 | 46 | 216 | 14 | 218 | 42 | 216 | 14 | 2.55 | 7.47 |
| MVG073-09 | 0.05061 | 0.01452 | 0.25545 | 0.07022 | 0.03661 | 0.00312 | 0.0095 | 0.00350 | 223 | 594 | 231 | 56 | 232 | 20 | 191 | 70 | 232 | 20 | 1.74 | 8.48 |
| MVG073-10 | 0.05121 | 0.02668 | 0.22493 | 0.11270 | 0.03186 | 0.00472 | 0.01091 | 0.00564 | 250 | 932 | 206 | 94 | 202 | 30 | 219 | 112 | 202 | 30 | 2.22 | 9.95 |
| MVG073-11 | 0.05153 | 0.02228 | 0.25864 | 0.10942 | 0.03641 | 0.00336 | 0.0108 | 0.00452 | 265 | 810 | 234 | 88 | 231 | 20 | 217 | 90 | 231 | 20 | 0.78 | 3.79 |
| MVG074-02 | 0.05078 | 0.01102 | 0.24056 | 0.04998 | 0.03437 | 0.00228 | 0.00894 | 0.00300 | 231 | 488 | 219 | 40 | 218 | 14 | 180 | 60 | 218 | 14 | 1.92 | 9.38 |
| MVG074-03 | 0.05001 | 0.01284 | 0.23394 | 0.05836 | 0.03394 | 0.00214 | 0.00519 | 0.00204 | 195 | 546 | 213 | 48 | 215 | 14 | 105 | 42 | 215 | 14 | 2.19 | 10.13 |

| Analysis No. | RATIOS | | | | | | | | AGES (Ma) | | | | | | | | | | CONCENTRATIONS (ppm) | |
|---|---|---|---|---|---|---|---|---|---|---|---|---|---|---|---|---|---|---|---|---|
| | $^{207}Pb/^{206}Pb$ | ± 2σ | $^{207}Pb/^{235}U$ | ± 2σ | $^{206}Pb/^{238}U$ | ± 2σ | $^{208}Pb/^{232}Th$ | ± 2σ | $^{207}Pb/^{206}Pb$ | ± 2σ | $^{207}Pb/^{235}U$ | ± 2σ | $^{206}Pb/^{238}U$ | ± 2σ | $^{208}Pb/^{232}Th$ | ± 2σ | Used Age | ± 2σ | Th | U |
| MVG074-04 | 0.04914 | 0.01162 | 0.24984 | 0.05664 | 0.03688 | 0.00260 | 0.01111 | 0.00294 | 155 | 506 | 226 | 46 | 233 | 16 | 223 | 58 | 233 | 16 | 1.35 | 6.11 |
| MVG074-05 | 0.04809 | 0.01736 | 0.23315 | 0.08136 | 0.03518 | 0.00338 | 0.01243 | 0.00422 | 104 | 662 | 213 | 66 | 223 | 22 | 250 | 84 | 223 | 22 | 0.62 | 3.35 |
| MVG074-06 | 0.04702 | 0.01078 | 0.21415 | 0.04724 | 0.03304 | 0.00216 | 0.00936 | 0.00252 | 50 | 464 | 197 | 40 | 210 | 14 | 188 | 50 | 210 | 14 | 1.89 | 8.86 |
| MVG074-07 | 0.04795 | 0.02008 | 0.2328 | 0.09604 | 0.03523 | 0.00270 | 0.00904 | 0.00256 | 97 | 732 | 213 | 80 | 223 | 16 | 182 | 52 | 223 | 16 | 2.20 | 6.43 |
| MVG074-08 | 0.04815 | 0.01400 | 0.22771 | 0.06390 | 0.0343 | 0.00272 | 0.00769 | 0.00276 | 107 | 564 | 208 | 52 | 217 | 16 | 155 | 56 | 217 | 16 | 1.47 | 6.57 |
| MVG074-09 | 0.04694 | 0.01560 | 0.2212 | 0.07100 | 0.03419 | 0.00308 | 0.00789 | 0.00348 | 46 | 606 | 203 | 60 | 217 | 20 | 159 | 70 | 217 | 20 | 1.32 | 6.46 |
| MVG074-10 | 0.04706 | 0.00572 | 0.23264 | 0.02730 | 0.03586 | 0.00124 | 0.01095 | 0.00166 | 52 | 268 | 212 | 22 | 227 | 8 | 220 | 34 | 227 | 8 | 5.44 | 29.23 |
| MVG074-11 | 0.04703 | 0.01528 | 0.21433 | 0.06754 | 0.03306 | 0.00272 | 0.012 | 0.00336 | 51 | 590 | 197 | 56 | 210 | 16 | 241 | 68 | 210 | 16 | 1.35 | 6.10 |
| MVG074-12 | 0.04629 | 0.01132 | 0.22822 | 0.05348 | 0.03576 | 0.00262 | 0.00374 | 0.00304 | 13 | 486 | 209 | 44 | 226 | 16 | 75 | 62 | 226 | 16 | 1.25 | 5.64 |
| 250-20 | 0.04995 | 0.00508 | 0.24107 | 0.02380 | 0.035 | 0.00116 | 0.01231 | 0.00138 | 193 | 236 | 219 | 20 | 222 | 8 | 247 | 28 | 222 | 8 | 2.71 | 13.33 |
| 250-22 | 0.04741 | 0.00588 | 0.24173 | 0.02886 | 0.03698 | 0.00156 | 0.01326 | 0.00168 | 70 | 274 | 220 | 24 | 234 | 10 | 266 | 34 | 234 | 10 | 3.77 | 17.09 |
| 250-23 | 0.05036 | 0.00618 | 0.2341 | 0.02780 | 0.03372 | 0.00132 | 0.01202 | 0.00172 | 212 | 282 | 214 | 22 | 214 | 8 | 242 | 34 | 214 | 8 | 2.64 | 16.08 |
| 250-25 | 0.05123 | 0.00722 | 0.23775 | 0.03222 | 0.03366 | 0.00152 | 0.01217 | 0.00206 | 251 | 324 | 217 | 26 | 213 | 10 | 244 | 42 | 213 | 10 | 1.55 | 7.39 |
| 250-26 | 0.05333 | 0.00852 | 0.25441 | 0.03938 | 0.0346 | 0.00164 | 0.01282 | 0.00154 | 343 | 368 | 230 | 32 | 219 | 10 | 257 | 30 | 219 | 10 | 3.48 | 9.70 |
| 250-27 | 0.05071 | 0.00528 | 0.23998 | 0.02442 | 0.03433 | 0.00112 | 0.01244 | 0.00136 | 228 | 244 | 218 | 20 | 218 | 6 | 250 | 28 | 218 | 6 | 2.57 | 12.28 |
| 250-28 | 0.05134 | 0.00686 | 0.24435 | 0.03174 | 0.03452 | 0.00138 | 0.01502 | 0.00184 | 256 | 308 | 222 | 26 | 219 | 8 | 301 | 36 | 219 | 8 | 2.13 | 10.32 |
| 250-29 | 0.0524 | 0.01112 | 0.2461 | 0.05096 | 0.03407 | 0.00184 | 0.01204 | 0.00256 | 303 | 486 | 223 | 42 | 216 | 12 | 242 | 52 | 216 | 12 | 1.37 | 6.38 |
| 250-30 | 0.04944 | 0.00800 | 0.25184 | 0.03918 | 0.03695 | 0.00190 | 0.0104 | 0.00194 | 169 | 368 | 228 | 32 | 234 | 12 | 209 | 38 | 234 | 12 | 1.72 | 8.26 |
| 250-31 | 0.05035 | 0.00568 | 0.24145 | 0.02646 | 0.03479 | 0.00124 | 0.01214 | 0.00104 | 211 | 260 | 220 | 22 | 220 | 8 | 244 | 20 | 220 | 8 | 4.14 | 11.72 |
| 250-32 | 0.0521 | 0.00268 | 0.2488 | 0.01248 | 0.03464 | 0.00088 | 0.01124 | 0.00066 | 290 | 120 | 226 | 10 | 220 | 6 | 226 | 14 | 220 | 6 | 8.36 | 43.21 |
| 250-33 | 0.05234 | 0.00326 | 0.24939 | 0.01510 | 0.03456 | 0.00094 | 0.01201 | 0.00086 | 300 | 146 | 226 | 12 | 219 | 6 | 241 | 18 | 219 | 6 | 5.17 | 28.16 |
| ~~MVG073-08~~ | ~~0.05177~~ | ~~0.01960~~ | ~~0.22295~~ | ~~0.08114~~ | ~~0.03124~~ | ~~0.00338~~ | ~~0.01239~~ | ~~0.00518~~ | ~~275~~ | ~~728~~ | ~~204~~ | ~~68~~ | ~~198~~ | ~~22~~ | ~~249~~ | ~~104~~ | ~~198~~ | ~~22~~ | ~~1.61~~ | ~~8.55~~ |
| ~~MVG074-01~~ | ~~0.04536~~ | ~~0.01412~~ | ~~0.22094~~ | ~~0.06618~~ | ~~0.03534~~ | ~~0.00310~~ | ~~0.00793~~ | ~~0.00326~~ | ~~-1~~ | ~~532~~ | ~~203~~ | ~~56~~ | ~~224~~ | ~~20~~ | ~~160~~ | ~~66~~ | ~~224~~ | ~~20~~ | ~~2.12~~ | ~~10.37~~ |
| ~~250-21~~ | ~~0.03831~~ | ~~0.00582~~ | ~~0.17135~~ | ~~0.02532~~ | ~~0.03244~~ | ~~0.00136~~ | ~~0.0118~~ | ~~0.00144~~ | ~~-390~~ | ~~428~~ | ~~161~~ | ~~22~~ | ~~206~~ | ~~8~~ | ~~237~~ | ~~28~~ | ~~206~~ | ~~8~~ | ~~1.49~~ | ~~6.83~~ |
| ~~250-24~~ | ~~0.03489~~ | ~~0.00842~~ | ~~0.16654~~ | ~~0.03918~~ | ~~0.03462~~ | ~~0.00208~~ | ~~0.00975~~ | ~~0.00286~~ | ~~-78~~ | ~~410~~ | ~~156~~ | ~~34~~ | ~~219~~ | ~~12~~ | ~~196~~ | ~~58~~ | ~~219~~ | ~~12~~ | ~~1.35~~ | ~~6.25~~ |

**Appendix 4.2. Zircon trace-element data (ppm) for the samples from the Daldyn terrane**

| Analysis No. | P | Ti | Y | Nb | La | Ce | Pr | Nd | Sm | Eu | Gd | Dy | Ho | Er | Yb | Lu | Hf | Ta | Th | U | Th/U | Nb/Ta |
|---|---|---|---|---|---|---|---|---|---|---|---|---|---|---|---|---|---|---|---|---|---|---|
| **Chomurdakh field, Rassvet pipe** | | | | | | | | | | | | | | | | | | | | | | |
| MVG120-05 | 96.9 | 13.6 | 22.2 | 2.87 | 0.01 | 1.00 | 0.00 | 0.07 | 0.10 | 0.12 | 0.85 | 2.64 | 0.78 | 2.72 | 3.88 | 0.59 | 21627 | 3.49 | 1.91 | 8.59 | 0.22 | 1.22 |
| MVG120-06 | 93.9 | 12.2 | 23.0 | 3.55 | <0.01 | 0.99 | <0 | 0.15 | 0.05 | 0.11 | 0.86 | 2.68 | 0.78 | 2.86 | 4.10 | 0.61 | 21425 | 3.96 | 1.93 | 8.73 | 0.22 | 1.12 |
| MVG120-07 | 100 | 14.5 | 21.4 | 2.73 | 0.04 | 0.94 | 0.01 | 0.15 | 0.10 | 0.09 | 0.69 | 2.52 | 0.68 | 2.55 | 4.06 | 0.53 | 21934 | 3.10 | 1.82 | 8.08 | 0.23 | 1.14 |
| MVG120-08 | 83.7 | 13.3 | 18.9 | 2.45 | <0 | 0.79 | 0.00 | 0.14 | 0.17 | 0.15 | 0.75 | 2.26 | 0.66 | 2.20 | 3.12 | 0.46 | 21597 | 2.80 | 1.59 | 7.63 | 0.21 | 1.14 |
| MVG120-09 | 87.0 | 24.0 | 73.2 | 3.70 | <0.01 | 1.63 | 0.03 | 0.72 | 1.08 | 0.75 | 4.26 | 10.2 | 2.82 | 9.14 | 12.4 | 1.69 | 21066 | 2.65 | 4.80 | 13.0 | 0.37 | 0.72 |
| MVG120-10 | 77.1 | 25.7 | 63.2 | 3.99 | 0.01 | 1.55 | 0.03 | 0.54 | 1.06 | 0.60 | 3.90 | 9.00 | 2.44 | 7.73 | 10.1 | 1.40 | 22225 | 2.56 | 4.27 | 11.5 | 0.37 | 0.64 |
| MVG120-11 | 88.9 | 29.4 | 69.0 | 4.20 | 0.01 | 1.61 | 0.03 | 0.91 | 1.15 | 0.76 | 4.04 | 9.72 | 2.61 | 8.53 | 11.7 | 1.53 | 21381 | 2.94 | 4.54 | 12.6 | 0.36 | 0.70 |
| MVG120-12 | 99.2 | 14.4 | 28.1 | 5.53 | <0.01 | 1.11 | 0.00 | 0.08 | 0.27 | 0.24 | 1.20 | 3.46 | 0.94 | 3.31 | 4.36 | 0.61 | 21772 | 5.05 | 2.60 | 9.57 | 0.27 | 0.91 |
| MVG120-14 | 96.1 | 12.9 | 21.6 | 3.77 | <0.01 | 0.95 | 0.01 | 0.07 | 0.18 | 0.10 | 0.75 | 2.67 | 0.72 | 2.49 | 3.47 | 0.54 | 22512 | 3.78 | 1.75 | 7.88 | 0.22 | 1.00 |
| MVG120-15 | 98.3 | 15.1 | 25.4 | 4.93 | <0.01 | 1.12 | 0.00 | 0.12 | 0.19 | 0.20 | 1.13 | 3.06 | 0.84 | 2.96 | 4.25 | 0.58 | 21964 | 4.64 | 2.29 | 9.23 | 0.25 | 0.94 |
| **Kuranakh field, Malokuonapka pipe** | | | | | | | | | | | | | | | | | | | | | | |
| MVG073-01 | 112 | 11.6 | 52.8 | 3.94 | | 1.19 | 0.01 | 0.07 | 0.41 | 0.28 | 1.93 | 6.49 | 1.93 | 7.03 | 10.7 | 1.84 | 17638 | 2.99 | 3.12 | 16.4 | 0.19 | 0.76 |
| MVG073-03 | 99.3 | 18.1 | 17.7 | 6.28 | <0 | 1.14 | 0.00 | 0.11 | 0.25 | 0.15 | 0.66 | 2.24 | 0.58 | 1.97 | 2.80 | 0.44 | 18603 | 6.87 | 2.24 | 12.5 | 0.18 | 1.09 |
| MVG073-04 | 80.2 | 9.80 | 135 | 5.66 | <0 | 2.04 | 0.08 | 1.33 | 1.86 | 1.28 | 7.58 | 18.4 | 5.15 | 17.7 | 23.5 | 3.71 | 16505 | 4.62 | 10.5 | 33.0 | 0.32 | 0.82 |
| MVG073-05 | 103 | 9.61 | 60.1 | 4.25 | | 1.05 | 0.00 | 0.15 | 0.29 | 0.30 | 2.08 | 7.07 | 2.21 | 7.90 | 11.2 | 1.92 | 19693 | 3.25 | 3.10 | 15.5 | 0.20 | 0.76 |
| MVG073-06 | 69.9 | 13.0 | 79.2 | 3.68 | | 1.08 | 0.04 | 0.65 | 1.01 | 0.67 | 4.12 | 11.1 | 2.91 | 9.80 | 12.8 | 1.98 | 20240 | 2.21 | 4.39 | 13.2 | 0.33 | 0.60 |
| MVG073-07 | 67.3 | 11.1 | 63.6 | 3.44 | <0 | 1.22 | 0.01 | 0.28 | 0.72 | 0.51 | 3.43 | 9.04 | 2.39 | 7.82 | 9.98 | 1.55 | 21414 | 1.93 | 3.58 | 11.2 | 0.32 | 0.56 |
| MVG073-09 | 53.2 | 10.5 | 33.5 | 3.22 | | 0.94 | <0 | 0.04 | 0.17 | 0.17 | 1.09 | 4.25 | 1.23 | 4.23 | 6.68 | 1.05 | 18938 | 2.16 | 2.18 | 11.4 | 0.19 | 0.67 |
| MVG073-10 | 80.7 | 8.25 | 39.5 | 3.51 | <0 | 0.72 | 0.01 | 0.07 | 0.17 | 0.20 | 1.31 | 4.53 | 1.43 | 5.32 | 7.52 | 1.13 | 20015 | 2.44 | 2.24 | 11.2 | 0.20 | 0.70 |
| MVG073-11 | 63.0 | 10.2 | 13.5 | 3.13 | | 0.55 | 0.00 | 0.01 | 0.04 | 0.03 | 0.28 | 1.33 | 0.41 | 1.43 | 2.13 | 0.33 | 21994 | 2.20 | 1.15 | 6.03 | 0.19 | 0.70 |
| MVG074-02 | 109 | 10.7 | 39.5 | 3.25 | <0 | 0.94 | 0.01 | 0.07 | 0.20 | 0.18 | 1.40 | 4.54 | 1.42 | 4.99 | 7.90 | 1.20 | 20671 | 2.37 | 2.50 | 13.0 | 0.19 | 0.73 |
| MVG074-03 | 112 | 10.7 | 53.6 | 3.88 | <0.01 | 1.06 | 0.00 | 0.09 | 0.27 | 0.27 | 1.67 | 6.72 | 1.98 | 7.30 | 10.7 | 1.69 | 20538 | 3.03 | 3.39 | 17.4 | 0.19 | 0.78 |
| MVG074-04 | 87.7 | 10.3 | 36.6 | 2.79 | <0 | 0.86 | 0.00 | 0.05 | 0.16 | 0.19 | 1.16 | 4.11 | 1.28 | 4.62 | 6.83 | 1.08 | 20958 | 1.79 | 1.95 | 9.44 | 0.21 | 0.64 |
| MVG074-05 | 73.5 | 10.2 | 14.1 | 3.05 | <0 | 0.55 | 0.00 | 0.01 | 0.06 | 0.04 | 0.34 | 1.49 | 0.42 | 1.45 | 2.48 | 0.37 | 23655 | 1.79 | 0.93 | 5.35 | 0.17 | 0.59 |
| MVG074-06 | 96.1 | 10.7 | 42.6 | 3.28 | | 1.00 | 0.00 | 0.12 | 0.26 | 0.21 | 1.49 | 5.09 | 1.52 | 5.52 | 8.16 | 1.31 | 20832 | 2.34 | 2.60 | 13.0 | 0.20 | 0.71 |
| MVG074-07 | 73.2 | 14.5 | 64.9 | 3.00 | <0 | 1.22 | 0.01 | 0.31 | 0.65 | 0.61 | 3.32 | 8.94 | 2.40 | 8.13 | 11.2 | 1.63 | 21700 | 1.64 | 3.45 | 10.8 | 0.32 | 0.55 |
| MVG074-08 | 93.8 | 8.46 | 35.2 | 2.74 | <0 | 0.86 | 0.00 | 0.07 | 0.11 | 0.17 | 1.22 | 4.26 | 1.21 | 4.39 | 6.65 | 1.02 | 20910 | 1.74 | 2.08 | 9.95 | 0.21 | 0.64 |
| MVG074-09 | 91.2 | 11.3 | 33.6 | 3.09 | <0.01 | 0.90 | 0.00 | 0.08 | 0.13 | 0.19 | 1.14 | 4.04 | 1.14 | 4.15 | 6.53 | 0.95 | 21582 | 2.06 | 1.99 | 10.2 | 0.19 | 0.67 |
| MVG074-10 | 61.7 | 7.87 | 118 | 5.16 | <0 | 3.17 | 0.01 | 0.27 | 0.83 | 0.66 | 4.30 | 13.9 | 4.36 | 16.8 | 29.6 | 5.09 | 13863 | 5.29 | 8.18 | 47.0 | 0.17 | 1.03 |
| MVG074-11 | 89.9 | 9.58 | 35.5 | 2.82 | <0 | 0.82 | 0.00 | 0.09 | 0.16 | 0.17 | 1.25 | 4.20 | 1.26 | 4.47 | 6.88 | 1.09 | 21101 | 1.83 | 1.94 | 9.38 | 0.21 | 0.65 |
| MVG074-12 | 82.9 | 12.1 | 32.4 | 2.95 | <0.01 | 0.83 | 0.01 | 0.11 | 0.19 | 0.19 | 1.23 | 3.63 | 1.14 | 4.01 | 6.38 | 0.97 | 21660 | 2.02 | 1.88 | 8.91 | 0.21 | 0.68 |

**Appendix 5.1. Zircon U-Pb age data for samples from the Khapchan terrane**

| Analysis No. | RATIOS | | | | | | | | AGES (Ma) | | | | | | | | | | CONCENTRATIONS (ppm) | |
|---|---|---|---|---|---|---|---|---|---|---|---|---|---|---|---|---|---|---|---|---|
| | $^{207}Pb/^{206}Pb$ | ± 2σ | $^{207}Pb/^{235}U$ | ± 2σ | $^{206}Pb/^{238}U$ | ± 2σ | $^{208}Pb/^{232}Th$ | ± 2σ | $^{207}Pb/^{206}Pb$ | ± 2σ | $^{207}Pb/^{235}U$ | ± 2σ | $^{206}Pb/^{238}U$ | ± 2σ | $^{208}Pb/^{232}Th$ | ± 2σ | Used Age | ± 2σ | Th | U |
| **Ukukit field, Babie Leto pipe** | | | | | | | | | | | | | | | | | | | | |
| 241-02_1 | 0.05522 | 0.00197 | 0.51382 | 0.01842 | 0.06749 | 0.00162 | 0.02054 | 0.00069 | 421 | 78 | 421 | 12 | 421 | 10 | 411 | 14 | 421 | 10 | 8.18 | 25.65 |
| 241-02_2 | 0.05501 | 0.00204 | 0.50990 | 0.01884 | 0.06723 | 0.00162 | 0.02058 | 0.00071 | 413 | 81 | 418 | 13 | 420 | 10 | 412 | 14 | 420 | 10 | 9.68 | 27.83 |
| 241-03_1 | 0.05443 | 0.00468 | 0.50436 | 0.04182 | 0.06721 | 0.00228 | 0.01948 | 0.00170 | 389 | 186 | 415 | 28 | 419 | 14 | 390 | 34 | 419 | 14 | 1.69 | 6.46 |
| 241-03_2 | 0.05295 | 0.00422 | 0.48025 | 0.03700 | 0.06579 | 0.00216 | 0.01864 | 0.00152 | 327 | 176 | 398 | 25 | 411 | 13 | 373 | 30 | 411 | 13 | 2.01 | 8.15 |
| 241-05_1 | 0.05414 | 0.00392 | 0.49912 | 0.03498 | 0.06687 | 0.00209 | 0.01753 | 0.00134 | 377 | 159 | 411 | 24 | 417 | 13 | 351 | 27 | 417 | 13 | 2.15 | 8.27 |
| 241-06_1 | 0.05517 | 0.00169 | 0.50799 | 0.01589 | 0.06678 | 0.00156 | 0.01926 | 0.00057 | 419 | 67 | 417 | 11 | 417 | 9 | 386 | 11 | 417 | 9 | 31.17 | 77.26 |
| 241-08_1 | 0.05573 | 0.00210 | 0.52102 | 0.01954 | 0.06781 | 0.00165 | 0.01987 | 0.00069 | 441 | 82 | 426 | 13 | 423 | 10 | 398 | 14 | 423 | 10 | 8.41 | 22.14 |
| 241-09_1 | 0.05455 | 0.00313 | 0.50448 | 0.02809 | 0.06707 | 0.00186 | 0.01976 | 0.00097 | 394 | 125 | 415 | 19 | 419 | 11 | 395 | 19 | 419 | 11 | 5.13 | 11.33 |
| 242-01_1 | 0.05406 | 0.00406 | 0.48887 | 0.03552 | 0.06559 | 0.00207 | 0.01881 | 0.00134 | 373 | 165 | 404 | 24 | 410 | 13 | 377 | 27 | 410 | 13 | 1.96 | 6.03 |
| 242-02_1 | 0.05325 | 0.00251 | 0.49654 | 0.02300 | 0.06763 | 0.00175 | 0.01938 | 0.00095 | 339 | 105 | 409 | 16 | 422 | 11 | 388 | 19 | 422 | 11 | 4.42 | 16.64 |
| 242-03_1 | 0.05477 | 0.00439 | 0.49646 | 0.03840 | 0.06575 | 0.00218 | 0.01864 | 0.00159 | 403 | 174 | 409 | 26 | 411 | 13 | 373 | 32 | 411 | 13 | 1.38 | 5.12 |
| 242-04_1 | 0.05464 | 0.00361 | 0.49780 | 0.03189 | 0.06607 | 0.00196 | 0.01946 | 0.00109 | 398 | 143 | 410 | 22 | 413 | 12 | 390 | 22 | 413 | 12 | 2.84 | 6.49 |
| 242-05_1 | 0.05515 | 0.00395 | 0.49564 | 0.03434 | 0.06519 | 0.00203 | 0.01889 | 0.00143 | 418 | 155 | 409 | 23 | 407 | 12 | 378 | 28 | 407 | 12 | 1.72 | 6.57 |
| 242-06_1 | 0.05237 | 0.00510 | 0.46649 | 0.04374 | 0.06461 | 0.00238 | 0.01735 | 0.00179 | 301 | 215 | 389 | 30 | 404 | 14 | 348 | 36 | 404 | 14 | 1.41 | 5.29 |
| 242-07_1 | 0.05479 | 0.00137 | 0.50683 | 0.01324 | 0.06710 | 0.00150 | 0.02059 | 0.00055 | 404 | 55 | 416 | 9 | 419 | 9 | 412 | 11 | 419 | 9 | 124.44 | 165.53 |
| MVG273-01 | 0.05374 | 0.00160 | 0.50984 | 0.03934 | 0.06881 | 0.00244 | 0.02151 | 0.00150 | 360 | 68 | 418 | 26 | 429 | 14 | 430 | 30 | 418 | 26 | 120.31 | 131.33 |
| MVG273-02 | 0.05753 | 0.00336 | 0.52178 | 0.02760 | 0.06578 | 0.00162 | 0.02041 | 0.00046 | 512 | 132 | 426 | 18 | 411 | 10 | 408 | 8 | 426 | 18 | 2.65 | 10.50 |
| MVG273-03 | 0.05687 | 0.00520 | 0.52062 | 0.04712 | 0.0664 | 0.00224 | 0.02115 | 0.00216 | 486 | 206 | 426 | 32 | 414 | 14 | 423 | 42 | 426 | 32 | 2.72 | 7.16 |
| MVG273-04 | 0.05627 | 0.00634 | 0.52071 | 0.05482 | 0.06712 | 0.00248 | 0.02201 | 0.00200 | 463 | 256 | 426 | 36 | 419 | 14 | 440 | 40 | 426 | 36 | 6.13 | 15.42 |
| MVG273-05 | 0.05374 | 0.00422 | 0.49067 | 0.03692 | 0.06623 | 0.00176 | 0.02085 | 0.00136 | 360 | 182 | 405 | 26 | 413 | 10 | 417 | 26 | 405 | 26 | 3.95 | 36.18 |
| MVG273-06 | 0.05015 | 0.00278 | 0.46035 | 0.02474 | 0.06659 | 0.00132 | 0.0218 | 0.00168 | 202 | 132 | 385 | 18 | 416 | 8 | 436 | 34 | 385 | 18 | 7.03 | 21.22 |
| MVG273-07 | 0.05627 | 0.00412 | 0.51902 | 0.03596 | 0.0669 | 0.00156 | 0.02082 | 0.00052 | 463 | 166 | 424 | 24 | 417 | 10 | 416 | 10 | 424 | 24 | 3.87 | 9.31 |
| MVG273-08 | 0.05006 | 0.00488 | 0.47127 | 0.04300 | 0.06829 | 0.00212 | 0.0218 | 0.00164 | 198 | 226 | 392 | 30 | 426 | 12 | 436 | 32 | 392 | 30 | 3.95 | 12.13 |
| MVG273-09 | 0.05546 | 0.00660 | 0.50739 | 0.05828 | 0.06636 | 0.00252 | 0.01962 | 0.00238 | 431 | 272 | 417 | 40 | 414 | 16 | 393 | 48 | 417 | 40 | 4.98 | 17.25 |
| MVG273-10 | 0.05968 | 0.00376 | 0.5435 | 0.03398 | 0.06606 | 0.00176 | 0.02087 | 0.00156 | 592 | 140 | 441 | 22 | 412 | 10 | 417 | 30 | 441 | 22 | 3.00 | 11.12 |
| MVG273-11 | 0.05343 | 0.00474 | 0.49513 | 0.04156 | 0.06721 | 0.00196 | 0.02132 | 0.00174 | 347 | 206 | 408 | 28 | 419 | 12 | 426 | 34 | 408 | 28 | 2.29 | 8.84 |
| MVG273-12 | 0.05195 | 0.00594 | 0.47877 | 0.05168 | 0.06685 | 0.00226 | 0.02135 | 0.00218 | 283 | 268 | 397 | 36 | 417 | 14 | 427 | 44 | 397 | 36 | 4.08 | 14.52 |
| MVG273-13 | 0.05639 | 0.00444 | 0.51802 | 0.03944 | 0.06663 | 0.00192 | 0.02087 | 0.00178 | 468 | 178 | 424 | 26 | 416 | 12 | 417 | 36 | 424 | 26 | 8.62 | 20.95 |
| MVG273-14 | 0.05512 | 0.00360 | 0.50969 | 0.03180 | 0.06708 | 0.00164 | 0.02173 | 0.00128 | 417 | 150 | 418 | 22 | 419 | 10 | 435 | 26 | 418 | 22 | 7.49 | 23.75 |
| MVG273-15 | 0.05541 | 0.00330 | 0.51335 | 0.02914 | 0.0672 | 0.00148 | 0.02101 | 0.00124 | 429 | 136 | 421 | 20 | 419 | 8 | 420 | 24 | 421 | 20 | 6.69 | 16.81 |
| MVG273-16 | 0.0625 | 0.00382 | 0.57127 | 0.03384 | 0.0663 | 0.00168 | 0.01634 | 0.00134 | 691 | 134 | 459 | 22 | 414 | 10 | 328 | 26 | 459 | 22 | 6.27 | 20.26 |
| MVG273-17 | 0.05442 | 0.00352 | 0.50221 | 0.03126 | 0.06694 | 0.00158 | 0.02003 | 0.00134 | 388 | 148 | 413 | 22 | 418 | 10 | 401 | 26 | 413 | 22 | 1.51 | 5.25 |
| ~~241-01_1~~ | ~~0.64146~~ | ~~0.02830~~ | ~~21.70225~~ | ~~0.80971~~ | ~~0.24541~~ | ~~0.00961~~ | ~~0.08898~~ | ~~0.00272~~ | ~~4605~~ | ~~63~~ | ~~3171~~ | ~~36~~ | ~~1415~~ | ~~50~~ | ~~1723~~ | ~~50~~ | | | ~~11.96~~ | ~~2.40~~ |
| ~~241-01_2~~ | ~~0.65188~~ | ~~0.01979~~ | ~~23.83177~~ | ~~0.67239~~ | ~~0.26516~~ | ~~0.00766~~ | ~~0.09975~~ | ~~0.00233~~ | ~~4628~~ | ~~44~~ | ~~3262~~ | ~~28~~ | ~~1516~~ | ~~39~~ | ~~1922~~ | ~~43~~ | | | ~~10.39~~ | ~~2.00~~ |
| **Ogoner-Yuryakh field, Baltiiskaya pipe** | | | | | | | | | | | | | | | | | | | | |
| BAL-1 | 0.11439 | 0.00324 | 5.47909 | 0.15724 | 0.34741 | 0.00788 | 0.11319 | 0.00508 | 1870 | 52 | 1897 | 24 | 1922 | 38 | 2167 | 92 | 1870 | 52 | 108.18 | 543.67 |
| BAL-12 | 0.05178 | 0.00258 | 0.32517 | 0.01582 | 0.04555 | 0.00118 | 0.01477 | 0.00084 | 276 | 116 | 286 | 12 | 287 | 8 | 296 | 16 | 287 | 8 | 404.73 | 279.96 |
| BAL-13 | 0.12593 | 0.00430 | 6.4249 | 0.21982 | 0.37007 | 0.00884 | 0.10914 | 0.00654 | 2042 | 62 | 2036 | 30 | 2030 | 42 | 2094 | 120 | 2042 | 62 | 360.40 | 790.91 |
| BAL-14 | 0.15061 | 0.00560 | 9.32484 | 0.34586 | 0.44904 | 0.01112 | 0.14472 | 0.00952 | 2353 | 66 | 2370 | 34 | 2391 | 50 | 2732 | 168 | 2353 | 66 | 284.54 | 331.54 |
| BAL-18 | 0.05411 | 0.00234 | 0.34598 | 0.01472 | 0.04637 | 0.00116 | 0.01488 | 0.00096 | 376 | 100 | 302 | 12 | 292 | 8 | 299 | 20 | 292 | 8 | 502.10 | 591.52 |
| BAL-2 | 0.05359 | 0.00230 | 0.3377 | 0.01424 | 0.0457 | 0.00114 | 0.01479 | 0.00070 | 354 | 100 | 295 | 10 | 288 | 8 | 297 | 14 | 288 | 8 | 254.87 | 365.37 |

| Analysis No. | RATIOS | | | | | | | | AGES (Ma) | | | | | | | | | | CONCENTRATIONS (ppm) | |
|---|---|---|---|---|---|---|---|---|---|---|---|---|---|---|---|---|---|---|---|---|
| | $^{207}Pb/^{206}Pb$ | ± 2σ | $^{207}Pb/^{235}U$ | ± 2σ | $^{206}Pb/^{238}U$ | ± 2σ | $^{208}Pb/^{232}Th$ | ± 2σ | $^{207}Pb/^{206}Pb$ | ± 2σ | $^{207}Pb/^{235}U$ | ± 2σ | $^{206}Pb/^{238}U$ | ± 2σ | $^{208}Pb/^{232}Th$ | ± 2σ | Used Age | ± 2σ | Th | U |
| BAL-3 | 0.11475 | 0.00586 | 5.2115 | 0.25802 | 0.32942 | 0.00988 | 0.09373 | 0.00702 | 1876 | 94 | 1854 | 42 | 1836 | 48 | 1811 | 130 | 1876 | 94 | 50.09 | 68.48 |
| BAL-5 | 0.0502 | 0.00324 | 0.31796 | 0.01980 | 0.04594 | 0.00132 | 0.01443 | 0.00076 | 204 | 154 | 280 | 16 | 290 | 8 | 290 | 16 | 290 | 8 | 180.48 | 126.85 |
| BAL-7 | 0.17356 | 0.00556 | 11.51557 | 0.36764 | 0.48124 | 0.01136 | 0.13777 | 0.00720 | 2592 | 54 | 2566 | 30 | 2533 | 50 | 2609 | 128 | 2592 | 54 | 152.16 | 151.41 |
| BAL-9 | 0.11532 | 0.00410 | 5.3669 | 0.19198 | 0.33749 | 0.00836 | 0.10051 | 0.00606 | 1885 | 66 | 1880 | 30 | 1875 | 40 | 1936 | 112 | 1885 | 66 | 271.15 | 310.77 |
| ~~BAL-15~~ | ~~0.30764~~ | ~~0.01016~~ | ~~25.57295~~ | ~~0.85392~~ | ~~0.6029~~ | ~~0.01440~~ | ~~0.13425~~ | ~~0.00782~~ | ~~3509~~ | ~~52~~ | ~~3330~~ | ~~32~~ | ~~3042~~ | ~~58~~ | ~~2546~~ | ~~140~~ | | | ~~414.27~~ | ~~712.64~~ |
| ~~BAL-8~~ | ~~0.07632~~ | ~~0.00290~~ | ~~0.85478~~ | ~~0.03200~~ | ~~0.08123~~ | ~~0.00200~~ | ~~0.0379~~ | ~~0.00202~~ | ~~1103~~ | ~~78~~ | ~~627~~ | ~~18~~ | ~~503~~ | ~~12~~ | ~~752~~ | ~~40~~ | | | ~~121.36~~ | ~~294.56~~ |
| **Ogoner-Yuryakh field, Aerogeological pipe** | | | | | | | | | | | | | | | | | | | | |
| ARG2A-06 | 0.04527 | 0.00744 | 0.2237 | 0.03570 | 0.03584 | 0.00166 | 0.01262 | 0.00090 | -6 | 356 | 205 | 30 | 227 | 10 | 253 | 18 | 227 | 10 | 31.83 | 27.72 |
| ARG2A-07 | 0.15419 | 0.00442 | 8.52535 | 0.24492 | 0.40102 | 0.00892 | 0.11406 | 0.00516 | 2393 | 50 | 2289 | 26 | 2174 | 42 | 2183 | 94 | 2393 | 50 | 112.79 | 479.35 |
| ARG2A-12 | 0.05139 | 0.00550 | 0.3335 | 0.03442 | 0.04706 | 0.00132 | 0.01481 | 0.00040 | 259 | 250 | 292 | 26 | 296 | 8 | 297 | 8 | 296 | 8 | 309.12 | 501.63 |
| ARG2A-16 | 0.05058 | 0.00746 | 0.26889 | 0.03806 | 0.03856 | 0.00190 | 0.01207 | 0.00100 | 222 | 338 | 242 | 30 | 244 | 12 | 243 | 20 | 244 | 12 | 88.81 | 56.04 |
| ARG2A-18 | 0.05343 | 0.00256 | 0.36952 | 0.01722 | 0.05017 | 0.00128 | 0.01609 | 0.00094 | 347 | 110 | 319 | 12 | 316 | 8 | 323 | 18 | 316 | 8 | 233.07 | 375.36 |
| ARG2A-22 | 0.10809 | 0.00648 | 3.76194 | 0.20234 | 0.25242 | 0.00670 | 0.07312 | 0.00200 | 1767 | 112 | 1585 | 44 | 1451 | 34 | 1426 | 38 | 1767 | 112 | 105.93 | 241.17 |
| ARG2A-22R | 0.11374 | 0.00398 | 4.56575 | 0.15778 | 0.29117 | 0.00702 | 0.08712 | 0.00458 | 1860 | 64 | 1743 | 28 | 1647 | 36 | 1688 | 86 | 1860 | 64 | 47.18 | 90.39 |
| ARG2A-24 | 0.05785 | 0.00272 | 0.64134 | 0.02924 | 0.08041 | 0.00202 | 0.02507 | 0.00148 | 524 | 106 | 503 | 18 | 499 | 12 | 500 | 30 | 499 | 12 | 125.56 | 186.65 |
| ARG2A-28 | 0.20036 | 0.00724 | 15.17726 | 0.54486 | 0.54945 | 0.01320 | 0.15023 | 0.00972 | 2829 | 60 | 2826 | 34 | 2823 | 54 | 2829 | 170 | 2829 | 60 | 349.63 | 670.04 |
| ARG2A-29 | 0.16038 | 0.00544 | 10.08809 | 0.33742 | 0.45622 | 0.01070 | 0.13539 | 0.00754 | 2460 | 58 | 2443 | 30 | 2423 | 48 | 2566 | 134 | 2460 | 58 | 68.76 | 116.28 |
| ARG2A-33 | 0.0512 | 0.00252 | 0.33316 | 0.01600 | 0.0472 | 0.00120 | 0.01466 | 0.00092 | 250 | 116 | 292 | 12 | 297 | 8 | 294 | 18 | 297 | 8 | 381.05 | 367.48 |
| ARG2A-43 | 0.05494 | 0.00434 | 0.35267 | 0.02674 | 0.04656 | 0.00150 | 0.01541 | 0.00114 | 410 | 182 | 307 | 20 | 293 | 10 | 309 | 22 | 293 | 10 | 92.69 | 90.44 |
| ~~ARG2A-01~~ | ~~0.05573~~ | ~~0.00522~~ | ~~0.31364~~ | ~~0.02814~~ | ~~0.04082~~ | ~~0.00146~~ | ~~0.01245~~ | ~~0.00092~~ | ~~442~~ | ~~214~~ | ~~277~~ | ~~22~~ | ~~258~~ | ~~10~~ | ~~250~~ | ~~18~~ | ~~258~~ | ~~10~~ | ~~44.80~~ | ~~71.56~~ |
| ~~ARG2A-04~~ | ~~0.05542~~ | ~~0.00234~~ | ~~0.34565~~ | ~~0.01418~~ | ~~0.04524~~ | ~~0.00108~~ | ~~0.01456~~ | ~~0.00064~~ | ~~429~~ | ~~96~~ | ~~301~~ | ~~10~~ | ~~285~~ | ~~6~~ | ~~292~~ | ~~12~~ | ~~285~~ | ~~6~~ | ~~554.31~~ | ~~397.77~~ |
| ~~ARG2A-44~~ | ~~0.16639~~ | ~~0.01276~~ | ~~9.20772~~ | ~~0.64856~~ | ~~0.40134~~ | ~~0.01216~~ | ~~0.1114~~ | ~~0.00350~~ | ~~2522~~ | ~~132~~ | ~~2359~~ | ~~64~~ | ~~2175~~ | ~~56~~ | ~~2135~~ | ~~64~~ | ~~2522~~ | ~~132~~ | ~~491.35~~ | ~~847.43~~ |

**Appendix 5.2. Zircon trace-element data (ppm) for the samples from the Khapchan terrane**

| Analysis No. | P | Ca | Ti | Y | Nb | La | Ce | Pr | Nd | Sm | Eu | Gd | Dy | Ho | Er | Yb | Lu | Hf | Ta | Th | U | Th/U | Nb/Ta | Total REE | U-Pb age |
|---|---|---|---|---|---|---|---|---|---|---|---|---|---|---|---|---|---|---|---|---|---|---|---|---|---|
| **Ogoner-Yuryakh field, Baltiiskaya pipe** | | | | | | | | | | | | | | | | | | | | | | | | | |
| BAL-1 | 147.87 | 647.34 | 27.33 | 397 | 1.87 | 5.13 | 22.4 | 2.81 | 13.23 | 4.45 | 1.34 | 10.4 | 37.3 | 13.54 | 61.9 | 133.2 | 23.2 | 11290 | 1.07 | 81.2 | 424.4 | 0.19 | 0.57 | 328.92 | 1870 |
| BAL-2 | 217.22 | 181.77 | 9.51 | 929 | 3.29 | 1.88 | 28.91 | 0.66 | 4.58 | 4.96 | 0.68 | 19.8 | 79.5 | 29.46 | 137.5 | 310.6 | 55.9 | 8885 | 1.12 | 172.8 | 256.2 | 0.67 | 0.34 | 674.48 | 288 |
| BAL-3 | 1053.6 | 2554.6 | 37.57 | 737 | 1.659 | 5.84 | 20.12 | 3.07 | 16.7 | 7.29 | 0.96 | 21.7 | 72.7 | 25.97 | 109.4 | 213.3 | 37.7 | 7482 | 0.59 | 35.4 | 51.5 | 0.69 | 0.36 | 534.72 | 1876 |
| BAL-5 | 195 | 55.37 | 8.82 | 909 | 1.826 | 0.02 | 22 | 0.27 | 4.18 | 5.99 | 1.17 | 24.2 | 82.2 | 30 | 134.3 | 276.0 | 48.9 | 8847 | 0.82 | 133.9 | 97.6 | 1.37 | 0.45 | 629.11 | 290 |
| BAL-7 | 185.44 | 83.13 | 33.54 | 465 | 1.437 | 0.21 | 26.71 | 0.14 | 1.901 | 3.22 | 0.85 | 12.8 | 42.2 | 14.64 | 67.0 | 146.4 | 27.3 | 9106 | 0.48 | 111.7 | 116.0 | 0.96 | 0.33 | 343.36 | 2592 |
| BAL-9 | 145.37 | 255.84 | 222.9 | 489 | 6.71 | 1.20 | 15.61 | 0.45 | 2.85 | 2.98 | 0.30 | 11.5 | 45.8 | 16.59 | 72.8 | 151.9 | 26.3 | 10284 | 1.91 | 181.2 | 211.4 | 0.86 | 0.29 | 348.25 | 1885 |
| BAL-12 | 1055.1 | 2345.3 | 6.8 | 2308 | 3.64 | 9.28 | 76.77 | 3.59 | 22.7 | 16.57 | 4.72 | 66.3 | 225.4 | 79.13 | 341.2 | 648.2 | 112.4 | 8079 | 0.95 | 298.4 | 214.5 | 1.39 | 0.26 | 1606.14 | 287 |
| BAL-13 | 468.13 | 1125.9 | 54.1 | 2301 | 6.99 | 5.12 | 38.01 | 3.77 | 25.34 | 13.56 | 3.46 | 50.4 | 209.8 | 80.85 | 366.6 | 709.8 | 124.9 | 9554 | 1.72 | 258.1 | 603.4 | 0.43 | 0.25 | 1631.68 | 2042 |
| BAL-14 | 455.98 | 252.65 | 269.51 | 2116 | 14.37 | 378.38 | 282.87 | 111.82 | 383.82 | 75.83 | 7.40 | 90.4 | 241.8 | 75.13 | 293.1 | 463.0 | 71.0 | 8805 | 1.96 | 222.0 | 269.7 | 0.82 | 0.14 | 2474.45 | 2353 |
| BAL-18 | 1915.9 | 4690.5 | 4.89 | 1046 | 5.31 | 21.79 | 92.06 | 6.77 | 28.86 | 10.08 | 2.24 | 27.5 | 90.1 | 33.33 | 157.5 | 384.9 | 73.1 | 9646 | 2.06 | 372.5 | 455.1 | 0.82 | 0.39 | 928.25 | 292 |
| **Ogoner-Yuryakh field, Aerogeological pipe** | | | | | | | | | | | | | | | | | | | | | | | | | |
| ARG2A-06 | 169 | <52.1 | 24.7 | 486 | 1.61 | <0.01 | 25.0 | 0.10 | 1.92 | 3.53 | 1.05 | 13.7 | 49.0 | 17.2 | 73.6 | 164.7 | 29.4 | 7237 | 0.47 | 23.5 | 21.4 | 1.10 | 0.29 | 379.13 | 227 |
| ARG2A-07 | 74.8 | 46.6 | 9.22 | 137 | 0.90 | 0.03 | 2.65 | 0.07 | 1.14 | 2.47 | 0.27 | 10.5 | 18.5 | 4.58 | 14.8 | 21.5 | 3.5 | 11312 | 0.42 | 76.5 | 335.8 | 0.23 | 0.47 | 79.97 | 2393 |
| ARG2A-12 | 101 | <44.3 | 9.27 | 1835 | 2.52 | 0.11 | 7.03 | 0.37 | 5.77 | 10.8 | 0.70 | 48.4 | 183.7 | 64.6 | 271.1 | 541.6 | 85.7 | 6803 | 0.70 | 183.7 | 310.9 | 0.59 | 0.28 | 1219.95 | 296 |
| ARG2A-16 | 192 | 55.4 | 9.23 | 1609 | 1.87 | 0.01 | 20.5 | 0.19 | 3.79 | 9.83 | 2.57 | 51.1 | 179.2 | 60.0 | 232.2 | 408.3 | 61.2 | 9055 | 0.68 | 55.0 | 35.9 | 1.53 | 0.36 | 1028.97 | 244 |
| ARG2A-18 | 599 | 1284 | 4.34 | 741 | 2.56 | 4.41 | 39.7 | 1.19 | 6.51 | 4.46 | 1.66 | 17.4 | 63.2 | 23.6 | 106.3 | 262.7 | 47.3 | 9345 | 0.91 | 149.7 | 257.9 | 0.58 | 0.36 | 578.42 | 316 |
| ARG2A-22 | 201 | <50.1 | 5.58 | 667 | 3.04 | 0.06 | 9.39 | 0.14 | 1.69 | 3.03 | 0.27 | 15.1 | 63.2 | 23.6 | 102.5 | 212.1 | 36.5 | 9653 | 0.96 | 39.0 | 75.3 | 0.52 | 0.32 | 467.63 | 1767 |
| ARG2A-22R | 184 | <52 | 7.43 | 635 | 2.98 | 0.02 | 9.01 | 0.08 | 1.48 | 2.64 | 0.23 | 14.0 | 59.5 | 22.8 | 97.2 | 203.3 | 34.5 | 9693 | 0.92 | 33.5 | 63.6 | 0.53 | 0.31 | 444.78 | 1860 |
| ARG2A-24 | 857 | <47.7 | 8.28 | 2242 | 1.95 | 0.02 | 6.58 | 0.07 | 1.44 | 4.35 | 0.16 | 31.0 | 191.3 | 76.6 | 350.3 | 734.9 | 123.7 | 10624 | 0.80 | 98.9 | 148.6 | 0.67 | 0.41 | 1520.48 | 499 |
| ARG2A-28 | 385 | <39.6 | 7.43 | 2156 | 2.53 | 0.05 | 18.5 | 0.18 | 3.41 | 8.02 | 2.88 | 55.8 | 210.9 | 73.1 | 301.8 | 623.7 | 101.8 | 10062 | 0.86 | 223.4 | 440.6 | 0.51 | 0.34 | 1400.06 | 2829 |
| ARG2A-29 | 1471 | 3795 | 20.8 | 459 | 1.72 | 2.91 | 14.1 | 1.44 | 9.22 | 4.63 | 0.43 | 12.9 | 43.1 | 15.8 | 69.0 | 147.2 | 25.8 | 9358 | 0.65 | 53.1 | 93.7 | 0.57 | 0.38 | 346.55 | 2460 |
| ARG2A-33 | 283 | <48.8 | 4.62 | 1906 | 3.14 | 0.06 | 35.6 | 0.49 | 8.10 | 12.5 | 4.82 | 51.5 | 184.8 | 66.2 | 284.4 | 614.7 | 105.8 | 7962 | 0.97 | 248.1 | 258.0 | 0.96 | 0.31 | 1369.03 | 297 |
| ARG2A-43 | 1437 | 3099 | 9.77 | 911 | 2.35 | 25.33 | 77.3 | 6.90 | 31.5 | 8.94 | 1.68 | 20.7 | 79.9 | 31.0 | 143.1 | 342.3 | 61.7 | 8107 | 0.63 | 74.4 | 73.9 | 1.01 | 0.27 | 830.29 | 293 |

**Appendix 5.3. Zircon Hf-isotope data for the samples from the Khapchan terrane**

| Analysis No. | Lu-Hf RATIOS | | | | $Hf_{initial}$ | εHf(T) | ± SE | $T_{DM}$ (Ga) | $T_{DM}^{Crustal}$ (Ga) | U-Pb AGE |
|---|---|---|---|---|---|---|---|---|---|---|
| | $^{176}Hf/^{177}Hf$ | 1SE | $^{176}Lu/^{177}Hf$ | $^{176}Yb/^{177}Hf$ | | | | | | (Ma) |
| **Ogoner-Yuryakh field, Baltiiskaya pipe** | | | | | | | | | | |
| BAL-12 | 0.282165 | 0.000027 | 0.001159 | 0.029804 | 0.282159 | -15.8 | 1.0 | 1.54 | 2.28 | 287 |
| BAL-02 | 0.282451 | 0.000028 | 0.000966 | 0.025109 | 0.282446 | -5.6 | 1.0 | 1.13 | 1.64 | 288 |
| BAL-05 | 0.282132 | 0.000016 | 0.000643 | 0.017460 | 0.282129 | -16.8 | 0.6 | 1.56 | 2.35 | 290 |
| BAL-18 | 0.282027 | 0.000020 | 0.000995 | 0.024575 | 0.282022 | -20.5 | 0.7 | 1.73 | 2.58 | 292 |
| BAL-01 | 0.281527 | 0.000028 | 0.000498 | 0.014001 | 0.281509 | -3.0 | 1.0 | 2.38 | 2.73 | 1870 |
| BAL-03 | 0.28177 | 0.000022 | 0.000944 | 0.025911 | 0.281736 | 5.2 | 0.8 | 2.08 | 2.21 | 1876 |
| BAL-09 | 0.281457 | 0.000029 | 0.000390 | 0.010383 | 0.281443 | -5.0 | 1.0 | 2.47 | 2.87 | 1885 |
| BAL-13 | 0.281831 | 0.000026 | 0.002070 | 0.055845 | 0.281751 | 9.6 | 0.9 | 2.05 | 2.06 | 2042 |
| BAL-14 | 0.281342 | 0.000024 | 0.001715 | 0.052176 | 0.281265 | -0.4 | 0.9 | 2.72 | 2.95 | 2353 |
| BAL-07 | 0.281115 | 0.000020 | 0.000612 | 0.015596 | 0.281085 | -1.3 | 0.7 | 2.95 | 3.19 | 2592 |
| **Ogoner-Yuryakh field, Aerogeological pipe** | | | | | | | | | | |
| ARG2A-16 | 0.282479 | 0.000022 | 0.000732 | 0.021202 | 0.282476 | -5.5 | 0.8 | 1.09 | 1.60 | 244 |
| ARG2A-43 | 0.282608 | 0.000029 | 0.001133 | 0.029400 | 0.282602 | 0.0 | 1.0 | 0.92 | 1.29 | 293 |
| ARG2A-12 | 0.282509 | 0.000049 | 0.000985 | 0.028184 | 0.282504 | -3.4 | 1.7 | 1.05 | 1.51 | 296 |
| ARG2A-33 | 0.282119 | 0.000022 | 0.001620 | 0.043090 | 0.282110 | -17.3 | 0.8 | 1.62 | 2.38 | 297 |
| ARG2A-18 | 0.282367 | 0.000027 | 0.000692 | 0.018023 | 0.282363 | -7.9 | 1.0 | 1.24 | 1.81 | 316 |
| ARG2A-24 | 0.282518 | 0.000022 | 0.001984 | 0.056375 | 0.282499 | 1.0 | 0.8 | 1.07 | 1.39 | 499 |
| ARG2A-22R | 0.281653 | 0.000026 | 0.000655 | 0.018583 | 0.281630 | 1.1 | 0.9 | 2.22 | 2.47 | 1860 |
| ARG2A-07 | 0.281206 | 0.000030 | 0.000095 | 0.002731 | 0.281202 | -1.8 | 1.1 | 2.79 | 3.07 | 2393 |
| ARG2A-29 | 0.281238 | 0.000036 | 0.000628 | 0.017154 | 0.281209 | 0.0 | 1.3 | 2.78 | 3.01 | 2460 |
| ARG2A-28 | 0.281207 | 0.000021 | 0.001186 | 0.031736 | 0.281143 | 6.3 | 0.7 | 2.87 | 2.89 | 2829 |

**Appendix 6.1. Zircon U-Pb age data for samples from the Birekta terrane**

| Analysis No. | RATIOS | | | | | | | | AGES (Ma) | | | | | | | | | | CONCENTRATIONS (ppm) | |
|---|---|---|---|---|---|---|---|---|---|---|---|---|---|---|---|---|---|---|---|---|
| | $^{207}Pb/^{206}Pb$ | ± 2σ | $^{207}Pb/^{235}U$ | ± 2σ | $^{206}Pb/^{238}U$ | ± 2σ | $^{208}Pb/^{232}Th$ | ± 2σ | $^{207}Pb/^{206}Pb$ | ± 2σ | $^{207}Pb/^{235}U$ | ± 2σ | $^{206}Pb/^{238}U$ | ± 2σ | $^{208}Pb/^{232}Th$ | ± 2σ | Used Age | ± 2σ | Th | U |
| **Merchemdenskoe field, Vostok-6 pipe** | | | | | | | | | | | | | | | | | | | | |
| 121-06_1 | 0.05457 | 0.00756 | 0.48185 | 0.06527 | 0.06405 | 0.00244 | 0.01888 | 0.00230 | 394 | 297 | 399 | 45 | 400 | 15 | 378 | 46 | 400 | 15 | 2.44 | 7.08 |
| 121-06_2 | 0.04941 | 0.00854 | 0.44695 | 0.07461 | 0.06562 | 0.00345 | 0.02087 | 0.00288 | 167 | 381 | 375 | 52 | 410 | 21 | 418 | 57 | 410 | 21 | 2.52 | 7.05 |
| 121-06_3 | 0.05489 | 0.00709 | 0.49244 | 0.06181 | 0.06507 | 0.00255 | 0.01944 | 0.00192 | 408 | 277 | 407 | 42 | 406 | 15 | 389 | 38 | 406 | 15 | 2.65 | 7.68 |
| 121-06_4 | 0.05126 | 0.00714 | 0.46662 | 0.06250 | 0.06603 | 0.00308 | 0.01728 | 0.00224 | 253 | 306 | 389 | 43 | 412 | 19 | 346 | 44 | 412 | 19 | 2.88 | 8.45 |
| 121-06_5 | 0.05485 | 0.00679 | 0.49378 | 0.05960 | 0.06530 | 0.00240 | 0.01955 | 0.00174 | 406 | 265 | 408 | 41 | 408 | 15 | 391 | 34 | 408 | 15 | 2.77 | 7.81 |
| 121-06_6 | 0.05818 | 0.00885 | 0.51245 | 0.07537 | 0.06389 | 0.00300 | 0.01846 | 0.00224 | 536 | 318 | 420 | 51 | 399 | 18 | 370 | 44 | 399 | 18 | 3.14 | 9.23 |
| 121-06_7 | 0.05514 | 0.00731 | 0.49409 | 0.06395 | 0.06500 | 0.00247 | 0.02087 | 0.00212 | 418 | 284 | 408 | 43 | 406 | 15 | 418 | 42 | 406 | 15 | 2.68 | 7.58 |
| 121-06_8 | 0.05486 | 0.00746 | 0.49301 | 0.06540 | 0.06519 | 0.00254 | 0.01467 | 0.00166 | 406 | 291 | 407 | 44 | 407 | 15 | 294 | 33 | 407 | 15 | 2.53 | 7.15 |
| 121-06_9 | 0.05460 | 0.00651 | 0.48402 | 0.05552 | 0.06430 | 0.00263 | 0.02314 | 0.00231 | 396 | 256 | 401 | 38 | 402 | 16 | 462 | 46 | 402 | 16 | 2.90 | 8.01 |
| 121-06_10 | 0.05081 | 0.01035 | 0.47208 | 0.09374 | 0.06740 | 0.00354 | 0.02019 | 0.00353 | 232 | 438 | 393 | 65 | 420 | 21 | 404 | 70 | 420 | 21 | 2.18 | 6.02 |
| **Merchemdenskoe field, Operatorskaya pipe** | | | | | | | | | | | | | | | | | | | | |
| OPER-1 | 0.20088 | 0.00700 | 15.21004 | 0.53370 | 0.54932 | 0.01374 | 0.15206 | 0.00908 | 2833 | 58 | 2828 | 34 | 2822 | 58 | 2861 | 160 | 2833 | 58 | 192.00 | 293.38 |
| OPER-11 | 0.18811 | 0.00578 | 13.77154 | 0.42578 | 0.53105 | 0.01246 | 0.14737 | 0.00722 | 2726 | 52 | 2734 | 30 | 2746 | 52 | 2779 | 128 | 2726 | 52 | 222.80 | 171.95 |
| OPER-12 | 0.18643 | 0.00566 | 13.40564 | 0.41006 | 0.52158 | 0.01204 | 0.14468 | 0.00720 | 2711 | 52 | 2709 | 28 | 2706 | 52 | 2731 | 128 | 2711 | 52 | 364.65 | 550.23 |
| OPER-14 | 0.20052 | 0.00742 | 14.7181 | 0.54146 | 0.53244 | 0.01316 | 0.07865 | 0.00520 | 2830 | 62 | 2797 | 34 | 2752 | 56 | 1530 | 98 | 2830 | 62 | 267.48 | 319.15 |
| OPER-15 | 0.23085 | 0.00732 | 18.99799 | 0.60590 | 0.59697 | 0.01400 | 0.1687 | 0.00894 | 3058 | 52 | 3042 | 30 | 3018 | 56 | 3151 | 154 | 3058 | 52 | 573.11 | 313.23 |
| OPER-16 | 0.12216 | 0.00482 | 5.84023 | 0.22860 | 0.3468 | 0.00882 | 0.09097 | 0.00650 | 1988 | 72 | 1952 | 34 | 1919 | 42 | 1760 | 120 | 1988 | 72 | 71.11 | 292.38 |
| OPER-19 | 0.12624 | 0.00438 | 6.48136 | 0.22408 | 0.37245 | 0.00892 | 0.11623 | 0.00722 | 2046 | 62 | 2043 | 30 | 2041 | 42 | 2222 | 130 | 2046 | 62 | 33.13 | 272.48 |
| OPER-2 | 0.11961 | 0.00372 | 5.81776 | 0.18172 | 0.35279 | 0.00840 | 0.10219 | 0.00452 | 1950 | 56 | 1949 | 28 | 1948 | 40 | 1967 | 82 | 1950 | 56 | 125.12 | 117.75 |
| OPER-20 | 0.18918 | 0.00654 | 13.77217 | 0.47384 | 0.52811 | 0.01258 | 0.14846 | 0.00894 | 2735 | 58 | 2734 | 32 | 2733 | 54 | 2798 | 158 | 2735 | 58 | 193.07 | 377.49 |
| OPER-21C | 0.18784 | 0.00970 | 13.0077 | 0.65712 | 0.50234 | 0.01440 | 0.15264 | 0.01504 | 2723 | 88 | 2680 | 48 | 2624 | 62 | 2871 | 264 | 2723 | 88 | 115.50 | 256.00 |
| OPER-22 | 0.12771 | 0.00532 | 6.59979 | 0.26916 | 0.37492 | 0.00938 | 0.10867 | 0.00832 | 2067 | 76 | 2059 | 36 | 2053 | 44 | 2085 | 152 | 2067 | 76 | 131.28 | 403.05 |
| OPER-3 | 0.12094 | 0.00374 | 5.88588 | 0.18302 | 0.353 | 0.00838 | 0.10394 | 0.00460 | 1970 | 56 | 1959 | 26 | 1949 | 40 | 1999 | 84 | 1970 | 56 | 163.35 | 128.31 |
| OPER-4 | 0.18703 | 0.00546 | 13.56607 | 0.40086 | 0.52614 | 0.01228 | 0.14504 | 0.00646 | 2716 | 50 | 2720 | 28 | 2725 | 52 | 2738 | 114 | 2716 | 50 | 192.76 | 151.91 |
| OPER-6 | 0.18708 | 0.00652 | 13.49103 | 0.46516 | 0.52308 | 0.01372 | 0.14464 | 0.00698 | 2717 | 58 | 2715 | 32 | 2712 | 58 | 2730 | 124 | 2717 | 58 | 39.65 | 29.61 |
| OPER-9 | 0.18698 | 0.00554 | 13.5605 | 0.40586 | 0.52606 | 0.01220 | 0.14504 | 0.00680 | 2716 | 50 | 2720 | 28 | 2725 | 52 | 2738 | 120 | 2716 | 50 | 222.75 | 244.04 |
| ~~OPER-10~~ | ~~0.21707~~ | ~~0.00646~~ | ~~9.48961~~ | ~~0.28498~~ | ~~0.3171~~ | ~~0.00732~~ | ~~0.04516~~ | ~~0.00218~~ | ~~2959~~ | ~~50~~ | ~~2387~~ | ~~28~~ | ~~1776~~ | ~~36~~ | ~~893~~ | ~~42~~ | ~~2959~~ | ~~50~~ | ~~481.88~~ | ~~528.59~~ |
| ~~OPER-13~~ | ~~0.19943~~ | ~~0.00652~~ | ~~11.37194~~ | ~~0.37114~~ | ~~0.41365~~ | ~~0.00980~~ | ~~0.08972~~ | ~~0.00492~~ | ~~2822~~ | ~~54~~ | ~~2554~~ | ~~30~~ | ~~2232~~ | ~~44~~ | ~~1737~~ | ~~92~~ | ~~2822~~ | ~~54~~ | ~~298.43~~ | ~~264.99~~ |
| ~~OPER-17~~ | ~~0.18791~~ | ~~0.00616~~ | ~~7.8814~~ | ~~0.25872~~ | ~~0.30426~~ | ~~0.00716~~ | ~~0.02507~~ | ~~0.00140~~ | ~~2724~~ | ~~56~~ | ~~2218~~ | ~~30~~ | ~~1712~~ | ~~36~~ | ~~500~~ | ~~28~~ | ~~2724~~ | ~~56~~ | ~~1620.68~~ | ~~661.12~~ |
| ~~OPER-18~~ | ~~0.16117~~ | ~~0.00630~~ | ~~9.25497~~ | ~~0.35998~~ | ~~0.41656~~ | ~~0.01064~~ | ~~0.08681~~ | ~~0.00600~~ | ~~2468~~ | ~~68~~ | ~~2364~~ | ~~36~~ | ~~2245~~ | ~~48~~ | ~~1683~~ | ~~112~~ | ~~2468~~ | ~~68~~ | ~~286.71~~ | ~~263.93~~ |
| ~~OPER-21R~~ | ~~0.18776~~ | ~~0.00870~~ | ~~9.47569~~ | ~~0.43014~~ | ~~0.36613~~ | ~~0.01032~~ | ~~0.06279~~ | ~~0.00504~~ | ~~2723~~ | ~~78~~ | ~~2385~~ | ~~42~~ | ~~2011~~ | ~~48~~ | ~~1231~~ | ~~96~~ | ~~2723~~ | ~~78~~ | ~~256.95~~ | ~~103.00~~ |
| ~~OPER-8~~ | ~~0.18787~~ | ~~0.00546~~ | ~~11.56394~~ | ~~0.34228~~ | ~~0.44646~~ | ~~0.01042~~ | ~~0.10171~~ | ~~0.00462~~ | ~~2724~~ | ~~48~~ | ~~2570~~ | ~~28~~ | ~~2379~~ | ~~46~~ | ~~1958~~ | ~~84~~ | ~~2724~~ | ~~48~~ | ~~305.44~~ | ~~283.87~~ |
| **Kuoika field, Khrizolit pipe** | | | | | | | | | | | | | | | | | | | | |
| 121-Khr_1 | 0.04991 | 0.00408 | 0.16832 | 0.01325 | 0.02446 | 0.00077 | 0.00754 | 0.00049 | 191 | 185 | 158 | 12 | 156 | 5 | 152 | 10 | 156 | 5 | 27.26 | 60.40 |
| 121-Khr_2 | 0.04852 | 0.00328 | 0.16611 | 0.01091 | 0.02483 | 0.00066 | 0.00758 | 0.00038 | 125 | 156 | 156 | 10 | 158 | 4 | 153 | 8 | 158 | 4 | 25.90 | 54.92 |
| 121-Khr_3 | 0.04767 | 0.00374 | 0.16612 | 0.01266 | 0.02528 | 0.00072 | 0.00795 | 0.00045 | 82 | 183 | 156 | 11 | 161 | 5 | 160 | 9 | 161 | 5 | 18.93 | 44.67 |
| 121-Khr_4 | 0.04953 | 0.00398 | 0.16557 | 0.01280 | 0.02425 | 0.00075 | 0.00761 | 0.00049 | 173 | 182 | 156 | 11 | 154 | 5 | 153 | 10 | 154 | 5 | 26.24 | 57.09 |
| 121-Khr_5 | 0.04951 | 0.00433 | 0.16548 | 0.01393 | 0.02424 | 0.00079 | 0.00837 | 0.00057 | 172 | 198 | 156 | 12 | 154 | 5 | 168 | 12 | 154 | 5 | 13.54 | 34.21 |
| 121-Khr_6 | 0.05040 | 0.00470 | 0.17136 | 0.01544 | 0.02466 | 0.00081 | 0.00772 | 0.00060 | 214 | 209 | 161 | 13 | 157 | 5 | 156 | 12 | 157 | 5 | 17.47 | 44.08 |

| Analysis No. | RATIOS | | | | | | | | AGES (Ma) | | | | | | | | | | CONCENTRATIONS (ppm) | |
|---|---|---|---|---|---|---|---|---|---|---|---|---|---|---|---|---|---|---|---|---|
| | $^{207}Pb/^{206}Pb$ | ± 2σ | $^{207}Pb/^{235}U$ | ± 2σ | $^{206}Pb/^{238}U$ | ± 2σ | $^{208}Pb/^{232}Th$ | ± 2σ | $^{207}Pb/^{206}Pb$ | ± 2σ | $^{207}Pb/^{235}U$ | ± 2σ | $^{206}Pb/^{238}U$ | ± 2σ | $^{208}Pb/^{232}Th$ | ± 2σ | Used Age | ± 2σ | Th | U |
| 121-Khr_7 | 0.05239 | 0.00464 | 0.17770 | 0.01521 | 0.02460 | 0.00079 | 0.00745 | 0.00059 | 303 | 195 | 166 | 13 | 157 | 5 | 150 | 12 | 157 | 5 | 15.55 | 41.46 |
| 121-Khr_8 | 0.04625 | 0.00395 | 0.16072 | 0.01325 | 0.02521 | 0.00079 | 0.00769 | 0.00055 | 11 | 199 | 151 | 12 | 161 | 5 | 155 | 11 | 161 | 5 | 14.87 | 38.23 |
| 121-Khr_9 | 0.04936 | 0.00433 | 0.16716 | 0.01425 | 0.02457 | 0.00074 | 0.00800 | 0.00059 | 165 | 199 | 157 | 12 | 156 | 5 | 161 | 12 | 156 | 5 | 12.23 | 32.75 |
| ~~121-Khr_10~~ | ~~0.04416~~ | ~~0.00351~~ | ~~0.15264~~ | ~~0.01171~~ | ~~0.02507~~ | ~~0.00074~~ | ~~0.00808~~ | ~~0.00048~~ | ~~0~~ | ~~0~~ | ~~144~~ | ~~10~~ | ~~160~~ | ~~5~~ | ~~163~~ | ~~10~~ | ~~160~~ | ~~5~~ | ~~19.99~~ | ~~45.36~~ |
| **Kuoika field, Pyatnitsa pipe** | | | | | | | | | | | | | | | | | | | | |
| 121-Ptn_1 | 0.04896 | 0.01496 | 0.14726 | 0.04344 | 0.02182 | 0.00184 | 0.00553 | 0.00159 | 146 | 646 | 140 | 38 | 139 | 12 | 112 | 32 | 139 | 12 | 3.07 | 9.82 |
| 121-Ptn_2 | 0.04937 | 0.00473 | 0.15702 | 0.01445 | 0.02307 | 0.00080 | 0.00758 | 0.00059 | 166 | 216 | 148 | 13 | 147 | 5 | 153 | 12 | 147 | 5 | 13.64 | 36.26 |
| 121-Ptn_3 | 0.04906 | 0.00341 | 0.15858 | 0.01065 | 0.02344 | 0.00067 | 0.00778 | 0.00040 | 151 | 159 | 150 | 9 | 149 | 4 | 157 | 8 | 149 | 4 | 29.10 | 60.54 |
| 121-Ptn_4 | 0.04964 | 0.00375 | 0.15661 | 0.01150 | 0.02288 | 0.00065 | 0.00694 | 0.00038 | 178 | 172 | 148 | 10 | 146 | 4 | 140 | 8 | 146 | 4 | 25.63 | 56.28 |
| 121-Ptn_5 | 0.04908 | 0.00318 | 0.15942 | 0.00997 | 0.02356 | 0.00066 | 0.00745 | 0.00036 | 152 | 148 | 150 | 9 | 150 | 4 | 150 | 7 | 150 | 4 | 45.03 | 78.76 |
| 121-Ptn_6 | 0.04863 | 0.00328 | 0.15623 | 0.01018 | 0.02330 | 0.00066 | 0.00722 | 0.00038 | 130 | 155 | 147 | 9 | 149 | 4 | 145 | 8 | 149 | 4 | 31.50 | 62.73 |
| 121-Ptn_7 | 0.04836 | 0.00414 | 0.15570 | 0.01291 | 0.02335 | 0.00071 | 0.00734 | 0.00046 | 117 | 196 | 147 | 11 | 149 | 4 | 148 | 9 | 149 | 4 | 26.69 | 55.30 |
| 121-Ptn_8 | 0.04882 | 0.00386 | 0.15886 | 0.01219 | 0.02360 | 0.00068 | 0.00794 | 0.00044 | 139 | 180 | 150 | 11 | 150 | 4 | 160 | 9 | 150 | 4 | 20.37 | 46.39 |
| 121-Ptn_9 | 0.04854 | 0.00754 | 0.16106 | 0.02417 | 0.02407 | 0.00110 | 0.00736 | 0.00098 | 126 | 347 | 152 | 21 | 153 | 7 | 148 | 20 | 153 | 7 | 10.09 | 25.50 |
| 121-Ptn_10 | 0.04862 | 0.02126 | 0.14488 | 0.06257 | 0.02162 | 0.00158 | 0.00819 | 0.00298 | 130 | 894 | 137 | 55 | 138 | 10 | 165 | 60 | 138 | 10 | 1.41 | 5.82 |
| 121-Ptn_11 | 0.04924 | 0.01566 | 0.14846 | 0.04656 | 0.02187 | 0.00126 | 0.00735 | 0.00241 | 159 | 669 | 141 | 41 | 140 | 8 | 148 | 48 | 140 | 8 | 1.69 | 7.18 |
| **Kuoika field, Ruslovaya pipe** | | | | | | | | | | | | | | | | | | | | |
| 121-Rusl_01 | 0.04863 | 0.00478 | 0.15446 | 0.01463 | 0.02304 | 0.00080 | 0.00743 | 0.00041 | 130 | 224 | 146 | 13 | 147 | 5 | 150 | 8 | 147 | 5 | 28.15 | 31.93 |
| 121-Rusl_02 | 0.04872 | 0.00661 | 0.15071 | 0.01964 | 0.02244 | 0.00100 | 0.00718 | 0.00053 | 134 | 304 | 143 | 17 | 143 | 6 | 145 | 11 | 143 | 6 | 21.93 | 25.02 |
| 121-Rusl_03 | 0.04849 | 0.00465 | 0.15222 | 0.01400 | 0.02277 | 0.00079 | 0.00732 | 0.00042 | 123 | 218 | 144 | 12 | 145 | 5 | 148 | 8 | 145 | 5 | 17.61 | 22.43 |
| 121-Rusl_04 | 0.04848 | 0.00500 | 0.15237 | 0.01510 | 0.02280 | 0.00082 | 0.00733 | 0.00049 | 123 | 234 | 144 | 13 | 145 | 5 | 148 | 10 | 145 | 5 | 18.49 | 29.56 |
| 121-Rusl_05 | 0.04926 | 0.00675 | 0.15231 | 0.02008 | 0.02243 | 0.00100 | 0.00741 | 0.00065 | 160 | 306 | 144 | 18 | 143 | 6 | 149 | 13 | 143 | 6 | 13.56 | 26.19 |
| 121-Rusl_06 | 0.04682 | 0.00714 | 0.14830 | 0.02176 | 0.02297 | 0.00111 | 0.00754 | 0.00064 | 40 | 346 | 140 | 19 | 146 | 7 | 152 | 13 | 146 | 7 | 19.52 | 25.64 |
| 121-Rusl_07 | 0.04989 | 0.00798 | 0.15535 | 0.02414 | 0.02259 | 0.00100 | 0.00728 | 0.00050 | 190 | 352 | 147 | 21 | 144 | 6 | 147 | 10 | 144 | 6 | 20.96 | 19.82 |
| 121-Rusl_08 | 0.04909 | 0.00742 | 0.15709 | 0.02325 | 0.02321 | 0.00088 | 0.00755 | 0.00044 | 152 | 336 | 148 | 20 | 148 | 6 | 152 | 9 | 148 | 6 | 17.65 | 17.14 |
| 121-Rusl_09 | 0.04843 | 0.00832 | 0.15306 | 0.02528 | 0.02292 | 0.00122 | 0.00735 | 0.00067 | 120 | 382 | 145 | 22 | 146 | 8 | 148 | 14 | 146 | 8 | 19.29 | 20.60 |
| 121-Rusl_10 | 0.04327 | 0.00861 | 0.14272 | 0.02739 | 0.02393 | 0.00140 | 0.00705 | 0.00074 | 0 | 155 | 136 | 24 | 152 | 9 | 142 | 15 | 152 | 9 | 17.76 | 17.23 |
| 427-10 | 0.14953 | 0.01184 | 8.76225 | 0.63674 | 0.425 | 0.01334 | 0.11919 | 0.00366 | 2341 | 138 | 2314 | 66 | 2283 | 60 | 2276 | 66 | 2341 | 138 | 33.71 | 33.45 |
| 427-11 | 0.05904 | 0.00478 | 0.67338 | 0.05172 | 0.08273 | 0.00214 | 0.0256 | 0.00066 | 568 | 180 | 523 | 32 | 512 | 12 | 511 | 14 | 512 | 12 | 257.26 | 606.53 |
| 427-12 | 0.12012 | 0.00412 | 5.64632 | 0.19654 | 0.34099 | 0.00840 | 0.09804 | 0.00572 | 1958 | 62 | 1923 | 30 | 1891 | 40 | 1890 | 106 | 1958 | 62 | 209.41 | 191.10 |
| 427-13 | 0.06077 | 0.00330 | 0.72755 | 0.03842 | 0.08685 | 0.00244 | 0.02673 | 0.00136 | 631 | 120 | 555 | 22 | 537 | 14 | 533 | 26 | 537 | 14 | 51.91 | 78.37 |
| 427-15 | 0.15826 | 0.00860 | 9.32164 | 0.43280 | 0.4272 | 0.01202 | 0.11915 | 0.00344 | 2437 | 94 | 2370 | 42 | 2293 | 54 | 2275 | 62 | 2437 | 94 | 57.20 | 107.89 |
| 427-15R | 0.16517 | 0.00492 | 10.40193 | 0.31712 | 0.45683 | 0.01114 | 0.12783 | 0.00548 | 2509 | 52 | 2471 | 28 | 2426 | 50 | 2431 | 98 | 2509 | 52 | 65.03 | 69.96 |
| 427-16 | 0.05439 | 0.00436 | 0.45885 | 0.03550 | 0.06119 | 0.00204 | 0.01835 | 0.00130 | 387 | 184 | 383 | 24 | 383 | 12 | 368 | 26 | 383 | 12 | 136.79 | 122.78 |
| 427-19 | 0.05247 | 0.00332 | 0.34294 | 0.02106 | 0.0474 | 0.00138 | 0.0154 | 0.00094 | 306 | 148 | 299 | 16 | 299 | 8 | 309 | 18 | 299 | 8 | 395.69 | 246.74 |
| 427-20 | 0.05713 | 0.00408 | 0.68064 | 0.04544 | 0.08641 | 0.00216 | 0.02684 | 0.00066 | 497 | 160 | 527 | 28 | 534 | 12 | 535 | 12 | 534 | 12 | 167.96 | 350.79 |
| 427-21 | 0.05801 | 0.00312 | 0.67572 | 0.03566 | 0.0845 | 0.00238 | 0.02711 | 0.00194 | 530 | 120 | 524 | 22 | 523 | 14 | 541 | 38 | 523 | 14 | 90.36 | 248.06 |
| 427-23 | 0.06048 | 0.00272 | 0.72194 | 0.03192 | 0.08659 | 0.00226 | 0.02735 | 0.00136 | 621 | 100 | 552 | 18 | 535 | 14 | 545 | 26 | 535 | 14 | 78.92 | 115.30 |
| 427-25 | 0.05802 | 0.00278 | 0.69224 | 0.03264 | 0.08656 | 0.00230 | 0.02756 | 0.00142 | 531 | 108 | 534 | 20 | 535 | 14 | 550 | 28 | 535 | 14 | 65.51 | 99.49 |
| 427-29 | 0.05769 | 0.00234 | 0.69519 | 0.02810 | 0.08742 | 0.00220 | 0.02708 | 0.00138 | 518 | 92 | 536 | 16 | 540 | 14 | 540 | 28 | 540 | 14 | 86.04 | 168.42 |
| 427-29R | 0.06071 | 0.00266 | 0.72743 | 0.03138 | 0.08692 | 0.00224 | 0.02711 | 0.00142 | 629 | 96 | 555 | 18 | 537 | 14 | 541 | 28 | 537 | 14 | 69.75 | 127.27 |
| 427-31 | 0.06284 | 0.00278 | 0.74966 | 0.03262 | 0.08655 | 0.00224 | 0.02807 | 0.00152 | 703 | 96 | 568 | 18 | 535 | 14 | 560 | 30 | 535 | 14 | 97.12 | 134.66 |

| Analysis No. | RATIOS | | | | | | | | AGES (Ma) | | | | | | | | | | CONCENTRATIONS (ppm) | |
|---|---|---|---|---|---|---|---|---|---|---|---|---|---|---|---|---|---|---|---|---|
| | $^{207}Pb/^{206}Pb$ | ± 2σ | $^{207}Pb/^{235}U$ | ± 2σ | $^{206}Pb/^{238}U$ | ± 2σ | $^{208}Pb/^{232}Th$ | ± 2σ | $^{207}Pb/^{206}Pb$ | ± 2σ | $^{207}Pb/^{235}U$ | ± 2σ | $^{206}Pb/^{238}U$ | ± 2σ | $^{208}Pb/^{232}Th$ | ± 2σ | Used Age | ± 2σ | Th | U |
| 427-33C | 0.05197 | 0.00322 | 0.34801 | 0.02110 | 0.04857 | 0.00146 | 0.01562 | 0.00144 | 284 | 146 | 303 | 16 | 306 | 8 | 313 | 28 | 306 | 8 | 255.05 | 644.74 |
| 427-34R | 0.06183 | 0.00328 | 0.75183 | 0.03906 | 0.0882 | 0.00250 | 0.02916 | 0.00210 | 668 | 116 | 569 | 22 | 545 | 14 | 581 | 42 | 545 | 14 | 94.70 | 177.42 |
| 427-35 | 0.11487 | 0.00410 | 5.19956 | 0.18626 | 0.32842 | 0.00822 | 0.10064 | 0.00578 | 1878 | 66 | 1853 | 30 | 1831 | 40 | 1938 | 106 | 1878 | 66 | 48.53 | 81.86 |
| 427-37 | 0.05879 | 0.00468 | 0.73863 | 0.05670 | 0.09113 | 0.00318 | 0.02817 | 0.00264 | 559 | 178 | 562 | 34 | 562 | 18 | 562 | 52 | 562 | 18 | 77.35 | 108.09 |
| 427-38 | 0.0518 | 0.00284 | 0.3271 | 0.01752 | 0.04581 | 0.00126 | 0.01513 | 0.00098 | 277 | 128 | 287 | 14 | 289 | 8 | 304 | 20 | 289 | 8 | 236.09 | 211.49 |
| 427-39 | 0.06015 | 0.00270 | 0.73696 | 0.03278 | 0.08887 | 0.00236 | 0.02786 | 0.00136 | 609 | 100 | 561 | 20 | 549 | 14 | 555 | 26 | 549 | 14 | 95.11 | 155.36 |
| 427-3C | 0.0518 | 0.00188 | 0.32979 | 0.01196 | 0.04619 | 0.00110 | 0.01487 | 0.00066 | 277 | 86 | 289 | 10 | 291 | 6 | 298 | 14 | 291 | 6 | 503.47 | 480.79 |
| 427-41 | 0.11506 | 0.00314 | 5.21929 | 0.14918 | 0.32908 | 0.00768 | 0.09888 | 0.00414 | 1881 | 50 | 1856 | 24 | 1834 | 38 | 1906 | 76 | 1881 | 50 | 262.80 | 449.69 |
| 427-42 | 0.06112 | 0.00494 | 0.71352 | 0.05410 | 0.08467 | 0.00240 | 0.02609 | 0.00074 | 643 | 178 | 547 | 32 | 524 | 14 | 521 | 14 | 524 | 14 | 45.56 | 92.23 |
| 427-43 | 0.07113 | 0.00250 | 1.52107 | 0.05402 | 0.15511 | 0.00384 | 0.04833 | 0.00212 | 961 | 74 | 939 | 22 | 930 | 22 | 954 | 40 | 930 | 22 | 162.65 | 139.64 |
| 427-45 | 0.05864 | 0.00260 | 0.70523 | 0.03074 | 0.08724 | 0.00226 | 0.02867 | 0.00160 | 554 | 98 | 542 | 18 | 539 | 14 | 571 | 32 | 539 | 14 | 139.67 | 229.92 |
| 427-49 | 0.05883 | 0.00244 | 0.71529 | 0.02946 | 0.08821 | 0.00224 | 0.02804 | 0.00134 | 561 | 92 | 548 | 18 | 545 | 14 | 559 | 26 | 545 | 14 | 98.92 | 152.21 |
| 427-50 | 0.0502 | 0.00318 | 0.28564 | 0.01760 | 0.04128 | 0.00120 | 0.01342 | 0.00068 | 204 | 150 | 255 | 14 | 261 | 8 | 269 | 14 | 261 | 8 | 154.94 | 114.32 |
| 427-52 | 0.06305 | 0.00322 | 0.73339 | 0.03658 | 0.08437 | 0.00234 | 0.02721 | 0.00146 | 710 | 112 | 559 | 22 | 522 | 14 | 543 | 28 | 522 | 14 | 57.95 | 87.89 |
| 427-53 | 0.10965 | 0.00510 | 4.72455 | 0.18640 | 0.31249 | 0.00772 | 0.09039 | 0.00240 | 1794 | 86 | 1772 | 34 | 1753 | 38 | 1749 | 44 | 1794 | 86 | 46.91 | 261.97 |
| 427-56 | 0.05523 | 0.00354 | 0.53853 | 0.03166 | 0.07071 | 0.00180 | 0.02205 | 0.00058 | 422 | 146 | 437 | 20 | 440 | 10 | 441 | 12 | 440 | 10 | 126.22 | 457.36 |
| 427-58 | 0.05843 | 0.00220 | 0.73736 | 0.02772 | 0.09153 | 0.00228 | 0.02957 | 0.00158 | 546 | 84 | 561 | 16 | 565 | 14 | 589 | 32 | 565 | 14 | 188.41 | 317.04 |
| 427-6 | 0.11334 | 0.00384 | 5.09603 | 0.17406 | 0.32617 | 0.00794 | 0.09409 | 0.00552 | 1854 | 62 | 1835 | 28 | 1820 | 38 | 1818 | 102 | 1854 | 62 | 132.16 | 481.40 |
| 427-64 | 0.05232 | 0.00220 | 0.32958 | 0.01374 | 0.04569 | 0.00116 | 0.01507 | 0.00078 | 299 | 98 | 289 | 10 | 288 | 8 | 302 | 16 | 288 | 8 | 412.35 | 364.71 |
| 427-67 | 0.05401 | 0.00396 | 0.33365 | 0.02362 | 0.04481 | 0.00142 | 0.01363 | 0.00090 | 371 | 170 | 292 | 18 | 283 | 8 | 274 | 18 | 283 | 8 | 208.59 | 109.32 |
| 427-7 | 0.05735 | 0.00258 | 0.69831 | 0.03110 | 0.08834 | 0.00234 | 0.02636 | 0.00164 | 505 | 102 | 538 | 18 | 546 | 14 | 526 | 32 | 546 | 14 | 101.20 | 243.01 |
| 427-71 | 0.05847 | 0.00250 | 0.68869 | 0.02912 | 0.08544 | 0.00220 | 0.02716 | 0.00152 | 547 | 96 | 532 | 18 | 529 | 14 | 542 | 30 | 529 | 14 | 113.00 | 176.78 |
| 427-73 | 0.16764 | 0.00880 | 10.37617 | 0.46932 | 0.4489 | 0.01190 | 0.12451 | 0.00364 | 2534 | 90 | 2469 | 42 | 2390 | 52 | 2372 | 66 | 2534 | 90 | 35.33 | 654.41 |
| 427-73R | 0.15763 | 0.00790 | 8.95628 | 0.38208 | 0.41209 | 0.01088 | 0.11498 | 0.00326 | 2430 | 88 | 2334 | 38 | 2224 | 50 | 2200 | 60 | 2430 | 88 | 137.40 | 1391.74 |
| 427-77 | 0.06402 | 0.00284 | 0.77392 | 0.03410 | 0.08769 | 0.00234 | 0.0273 | 0.00190 | 742 | 96 | 582 | 20 | 542 | 14 | 544 | 38 | 542 | 14 | 136.97 | 332.89 |
| 427-78 | 0.05895 | 0.00238 | 0.70906 | 0.02878 | 0.08723 | 0.00226 | 0.02518 | 0.00166 | 565 | 90 | 544 | 18 | 539 | 14 | 503 | 32 | 539 | 14 | 248.35 | 493.99 |
| 427-8 | 0.05394 | 0.00376 | 0.32916 | 0.02230 | 0.04427 | 0.00138 | 0.01338 | 0.00092 | 369 | 160 | 289 | 18 | 279 | 8 | 269 | 18 | 279 | 8 | 187.82 | 154.91 |
| 427-9 | 0.16129 | 0.00574 | 9.75857 | 0.34778 | 0.43893 | 0.01086 | 0.12725 | 0.00756 | 2469 | 62 | 2412 | 32 | 2346 | 48 | 2421 | 136 | 2469 | 62 | 210.06 | 130.71 |
| 427-9R | 0.16049 | 0.00632 | 9.77324 | 0.38124 | 0.44177 | 0.01144 | 0.12912 | 0.00854 | 2461 | 68 | 2414 | 36 | 2359 | 52 | 2455 | 152 | 2461 | 68 | 114.07 | 85.14 |
| ~~427-26~~ | ~~0.11085~~ | ~~0.00518~~ | ~~3.9705~~ | ~~0.18094~~ | ~~0.25986~~ | ~~0.00720~~ | ~~0.07908~~ | ~~0.00582~~ | ~~1813~~ | ~~86~~ | ~~1628~~ | ~~36~~ | ~~1489~~ | ~~36~~ | ~~1538~~ | ~~110~~ | ~~1813~~ | ~~86~~ | ~~84.00~~ | ~~108.11~~ |
| ~~427-30~~ | ~~0.0745~~ | ~~0.00334~~ | ~~1.31306~~ | ~~0.05794~~ | ~~0.12789~~ | ~~0.00340~~ | ~~0.04392~~ | ~~0.00314~~ | ~~1055~~ | ~~92~~ | ~~851~~ | ~~26~~ | ~~776~~ | ~~20~~ | ~~869~~ | ~~60~~ | ~~776~~ | ~~20~~ | ~~358.91~~ | ~~334.08~~ |
| ~~427-34C~~ | ~~0.09513~~ | ~~0.01234~~ | ~~1.24691~~ | ~~0.15158~~ | ~~0.09517~~ | ~~0.00528~~ | ~~0.04135~~ | ~~0.00596~~ | ~~1531~~ | ~~252~~ | ~~822~~ | ~~68~~ | ~~586~~ | ~~32~~ | ~~819~~ | ~~116~~ | ~~1531~~ | ~~252~~ | ~~42.46~~ | ~~40.81~~ |
| ~~427-4~~ | ~~0.08942~~ | ~~0.00306~~ | ~~1.15955~~ | ~~0.03966~~ | ~~0.09407~~ | ~~0.00230~~ | ~~0.04059~~ | ~~0.00190~~ | ~~1413~~ | ~~66~~ | ~~782~~ | ~~18~~ | ~~580~~ | ~~14~~ | ~~804~~ | ~~36~~ | ~~1413~~ | ~~66~~ | ~~136.53~~ | ~~227.02~~ |
| ~~427-5~~ | ~~0.05051~~ | ~~0.00206~~ | ~~0.16464~~ | ~~0.00662~~ | ~~0.02365~~ | ~~0.00058~~ | ~~0.00749~~ | ~~0.00036~~ | ~~219~~ | ~~96~~ | ~~155~~ | ~~6~~ | ~~151~~ | ~~4~~ | ~~151~~ | ~~8~~ | ~~151~~ | ~~4~~ | ~~1363.38~~ | ~~710.76~~ |
| **Kuoika field, Olivinovaya pipe** | | | | | | | | | | | | | | | | | | | | |
| 7-57_1 | 0.05145 | 0.00418 | 0.15683 | 0.01220 | 0.02214 | 0.00072 | 0.0072 | 0.00072 | 261 | 192 | 148 | 10 | 141 | 4 | 145 | 14 | 141 | 4 | 42.36 | 248.99 |
| 7-57_10 | 0.05692 | 0.00188 | 0.45401 | 0.01482 | 0.05786 | 0.00130 | 0.01815 | 0.00072 | 488 | 74 | 380 | 10 | 363 | 8 | 364 | 14 | 363 | 8 | 335.07 | 418.37 |
| 7-57_11 | 0.10675 | 0.00460 | 3.67809 | 0.13374 | 0.2499 | 0.00578 | 0.07249 | 0.00176 | 1745 | 80 | 1567 | 30 | 1438 | 30 | 1414 | 34 | 1745 | 80 | 57.51 | 141.58 |
| 7-57_12 | 0.05841 | 0.00300 | 0.5967 | 0.02978 | 0.07413 | 0.00198 | 0.02317 | 0.00146 | 545 | 114 | 475 | 18 | 461 | 12 | 463 | 28 | 461 | 12 | 97.18 | 181.15 |
| 7-57_13 | 0.05599 | 0.00372 | 0.57546 | 0.03580 | 0.07455 | 0.00176 | 0.02321 | 0.00054 | 452 | 152 | 462 | 24 | 463 | 10 | 464 | 10 | 463 | 10 | 241.18 | 347.93 |
| 7-57_14 | 0.05742 | 0.00340 | 0.61238 | 0.03268 | 0.07734 | 0.00196 | 0.02401 | 0.00066 | 508 | 134 | 485 | 20 | 480 | 12 | 480 | 14 | 480 | 12 | 65.01 | 273.59 |
| 7-57_15 | 0.06073 | 0.00188 | 0.811 | 0.02510 | 0.09687 | 0.00218 | 0.02973 | 0.00126 | 630 | 68 | 603 | 14 | 596 | 12 | 592 | 24 | 596 | 12 | 184.99 | 385.99 |

| Analysis No. | RATIOS | | | | | | | | AGES (Ma) | | | | | | | | | | CONCENTRATIONS (ppm) | |
|---|---|---|---|---|---|---|---|---|---|---|---|---|---|---|---|---|---|---|---|---|
| | $^{207}Pb/^{206}Pb$ | ± 2σ | $^{207}Pb/^{235}U$ | ± 2σ | $^{206}Pb/^{238}U$ | ± 2σ | $^{208}Pb/^{232}Th$ | ± 2σ | $^{207}Pb/^{206}Pb$ | ± 2σ | $^{207}Pb/^{235}U$ | ± 2σ | $^{206}Pb/^{238}U$ | ± 2σ | $^{208}Pb/^{232}Th$ | ± 2σ | Used Age | ± 2σ | Th | U |
| 7-57_16 | 0.05553 | 0.00262 | 0.34358 | 0.01594 | 0.04488 | 0.00116 | 0.01294 | 0.00074 | 434 | 108 | 300 | 12 | 283 | 8 | 260 | 14 | 283 | 8 | 944.12 | 345.73 |
| 7-57_17 | 0.05191 | 0.00298 | 0.2963 | 0.01666 | 0.04142 | 0.00116 | 0.01402 | 0.00106 | 281 | 134 | 264 | 14 | 262 | 8 | 281 | 22 | 262 | 8 | 142.74 | 377.19 |
| 7-57_18 | 0.115 | 0.00432 | 4.92965 | 0.18664 | 0.31095 | 0.00782 | 0.0881 | 0.00556 | 1880 | 70 | 1807 | 32 | 1745 | 38 | 1707 | 104 | 1880 | 70 | 62.53 | 129.40 |
| 7-57_19 | 0.05839 | 0.00202 | 0.41074 | 0.01416 | 0.05102 | 0.00118 | 0.01636 | 0.00078 | 544 | 78 | 349 | 10 | 321 | 8 | 328 | 16 | 321 | 8 | 210.63 | 469.16 |
| 7-57_20 | 0.05377 | 0.00310 | 0.36632 | 0.02104 | 0.04941 | 0.00144 | 0.01536 | 0.00148 | 361 | 134 | 317 | 16 | 311 | 8 | 308 | 30 | 311 | 8 | 655.71 | 989.46 |
| 7-57_21 | 0.06094 | 0.00378 | 0.63752 | 0.03830 | 0.07584 | 0.00234 | 0.02849 | 0.00208 | 637 | 136 | 501 | 24 | 471 | 14 | 568 | 40 | 471 | 14 | 153.79 | 271.99 |
| 7-57_3 | 0.05747 | 0.00226 | 0.45393 | 0.01742 | 0.05731 | 0.00136 | 0.01837 | 0.00080 | 510 | 88 | 380 | 12 | 359 | 8 | 368 | 16 | 359 | 8 | 143.42 | 302.40 |
| 7-57_30 | 0.0551 | 0.00390 | 0.32723 | 0.02128 | 0.04307 | 0.00122 | 0.01344 | 0.00044 | 416 | 162 | 287 | 16 | 272 | 8 | 270 | 8 | 272 | 8 | 68.88 | 494.38 |
| 7-57_32 | 0.05586 | 0.00188 | 0.63043 | 0.02086 | 0.08186 | 0.00186 | 0.02554 | 0.00100 | 447 | 76 | 496 | 12 | 507 | 12 | 510 | 20 | 507 | 12 | 106.43 | 258.79 |
| 7-57_33 | 0.11325 | 0.00300 | 4.79659 | 0.12816 | 0.30715 | 0.00684 | 0.08949 | 0.00306 | 1852 | 48 | 1784 | 22 | 1727 | 34 | 1732 | 56 | 1852 | 48 | 93.87 | 163.91 |
| 7-57_4 | 0.05695 | 0.00194 | 0.59541 | 0.02000 | 0.07584 | 0.00172 | 0.02374 | 0.00090 | 490 | 76 | 474 | 12 | 471 | 10 | 474 | 18 | 471 | 10 | 207.20 | 290.36 |
| 7-57_41 | 0.17285 | 0.00696 | 11.39528 | 0.44374 | 0.4782 | 0.01156 | 0.15406 | 0.01130 | 2585 | 68 | 2556 | 36 | 2519 | 50 | 2896 | 198 | 2585 | 68 | 133.54 | 477.56 |
| 7-57_42 | 0.05822 | 0.00326 | 0.42521 | 0.02286 | 0.05295 | 0.00142 | 0.01694 | 0.00118 | 538 | 126 | 360 | 16 | 333 | 8 | 340 | 24 | 333 | 8 | 276.12 | 306.56 |
| 7-57_43 | 0.13033 | 0.00454 | 6.33793 | 0.21646 | 0.3529 | 0.00840 | 0.10342 | 0.00558 | 2102 | 62 | 2024 | 30 | 1948 | 40 | 1989 | 102 | 2102 | 62 | 87.44 | 117.23 |
| 7-57_46 | 0.11296 | 0.00376 | 5.1194 | 0.16884 | 0.32877 | 0.00784 | 0.0976 | 0.00466 | 1848 | 62 | 1839 | 28 | 1832 | 38 | 1882 | 86 | 1848 | 62 | 185.44 | 102.50 |
| 7-57_5 | 0.11983 | 0.00390 | 5.47332 | 0.17346 | 0.3312 | 0.00724 | 0.09873 | 0.00502 | 1954 | 60 | 1896 | 28 | 1844 | 36 | 1903 | 92 | 1954 | 60 | 350.69 | 311.26 |
| 7-57_53 | 0.0556 | 0.00226 | 0.35073 | 0.01386 | 0.04577 | 0.00110 | 0.01372 | 0.00070 | 436 | 92 | 305 | 10 | 288 | 6 | 275 | 14 | 288 | 6 | 1066.48 | 463.23 |
| 7-57_54 | 0.11323 | 0.00532 | 5.07818 | 0.23134 | 0.32522 | 0.00914 | 0.08539 | 0.00596 | 1852 | 86 | 1832 | 38 | 1815 | 44 | 1656 | 110 | 1852 | 86 | 76.20 | 59.71 |
| 7-57_57 | 0.05736 | 0.00958 | 0.36406 | 0.05964 | 0.04603 | 0.00146 | 0.01429 | 0.00042 | 505 | 380 | 315 | 44 | 290 | 8 | 287 | 8 | 290 | 8 | 848.24 | 771.00 |
| 7-57_6 | 0.10814 | 0.00466 | 4.23819 | 0.15436 | 0.28425 | 0.00656 | 0.08234 | 0.00198 | 1768 | 80 | 1681 | 30 | 1613 | 32 | 1599 | 38 | 1768 | 80 | 60.85 | 126.21 |
| 7-57_64 | 0.18354 | 0.00536 | 12.78248 | 0.37048 | 0.50518 | 0.01122 | 0.1505 | 0.00678 | 2685 | 50 | 2664 | 28 | 2636 | 48 | 2834 | 120 | 2685 | 50 | 367.80 | 278.49 |
| 7-57_68 | 0.055 | 0.00220 | 0.3708 | 0.01454 | 0.04891 | 0.00118 | 0.01564 | 0.00082 | 412 | 92 | 320 | 10 | 308 | 8 | 314 | 16 | 308 | 8 | 168.67 | 305.62 |
| 7-57_7 | 0.11195 | 0.00310 | 4.70828 | 0.13080 | 0.3051 | 0.00666 | 0.08788 | 0.00362 | 1831 | 52 | 1769 | 24 | 1717 | 32 | 1702 | 68 | 1831 | 52 | 143.76 | 517.99 |
| 7-57_8 | 0.16395 | 0.00592 | 8.89743 | 0.25348 | 0.39359 | 0.00874 | 0.1094 | 0.00256 | 2497 | 62 | 2328 | 26 | 2139 | 40 | 2098 | 46 | 2497 | 62 | 148.06 | 784.29 |
| ~~7-57_2~~ | ~~0.11254~~ | ~~0.00412~~ | ~~3.84075~~ | ~~0.13862~~ | ~~0.24786~~ | ~~0.00616~~ | ~~0.07421~~ | ~~0.00410~~ | ~~1841~~ | ~~68~~ | ~~1601~~ | ~~30~~ | ~~1427~~ | ~~32~~ | ~~1447~~ | ~~78~~ | ~~1841~~ | ~~68~~ | ~~124.41~~ | ~~186.02~~ |
| ~~7-57_28~~ | ~~0.10858~~ | ~~0.00420~~ | ~~3.25033~~ | ~~0.10216~~ | ~~0.2171~~ | ~~0.00490~~ | ~~0.06286~~ | ~~0.00148~~ | ~~1776~~ | ~~72~~ | ~~1469~~ | ~~24~~ | ~~1267~~ | ~~26~~ | ~~1232~~ | ~~28~~ | ~~1776~~ | ~~72~~ | ~~321.46~~ | ~~817.73~~ |
| ~~7-57_65~~ | ~~0.07611~~ | ~~0.00462~~ | ~~0.57868~~ | ~~0.03364~~ | ~~0.05516~~ | ~~0.00166~~ | ~~0.01634~~ | ~~0.00118~~ | ~~1098~~ | ~~124~~ | ~~464~~ | ~~22~~ | ~~346~~ | ~~10~~ | ~~328~~ | ~~24~~ | ~~1098~~ | ~~124~~ | ~~227.70~~ | ~~154.49~~ |
| ~~7-57_9~~ | ~~0.08748~~ | ~~0.00430~~ | ~~1.44332~~ | ~~0.06774~~ | ~~0.11966~~ | ~~0.00322~~ | ~~0.03066~~ | ~~0.00164~~ | ~~1371~~ | ~~96~~ | ~~907~~ | ~~28~~ | ~~729~~ | ~~18~~ | ~~610~~ | ~~32~~ | ~~1371~~ | ~~96~~ | ~~43.16~~ | ~~49.91~~ |
| **Kuoika field, Vtorogodnitsa pipe** | | | | | | | | | | | | | | | | | | | | |
| 75-1_1 | 0.11629 | 0.00362 | 5.88354 | 0.18570 | 0.36699 | 0.00900 | 0.10848 | 0.00462 | 1900 | 58 | 1959 | 28 | 2015 | 42 | 2082 | 84 | 1900 | 58 | 32.39 | 56.36 |
| 75-1_10 | 0.1055 | 0.00310 | 4.26257 | 0.12340 | 0.29307 | 0.00652 | 0.0898 | 0.00386 | 1723 | 56 | 1686 | 24 | 1657 | 32 | 1738 | 72 | 1723 | 56 | 170.55 | 194.86 |
| 75-1_11 | 0.11587 | 0.00346 | 5.08368 | 0.15196 | 0.31834 | 0.00740 | 0.09195 | 0.00398 | 1893 | 54 | 1833 | 26 | 1782 | 36 | 1778 | 74 | 1893 | 54 | 137.47 | 153.00 |
| 75-1_12 | 0.12365 | 0.00398 | 5.95335 | 0.19000 | 0.34932 | 0.00826 | 0.10055 | 0.00496 | 2010 | 58 | 1969 | 28 | 1931 | 40 | 1937 | 92 | 2010 | 58 | 107.07 | 139.84 |
| 75-1_13 | 0.05299 | 0.00322 | 0.38077 | 0.02234 | 0.05213 | 0.00150 | 0.01659 | 0.00090 | 328 | 142 | 328 | 16 | 328 | 10 | 333 | 18 | 328 | 10 | 128.03 | 112.77 |
| 75-1_15C | 0.05102 | 0.00162 | 0.29166 | 0.00914 | 0.04147 | 0.00094 | 0.01311 | 0.00056 | 242 | 74 | 260 | 8 | 262 | 6 | 263 | 12 | 262 | 6 | 808.09 | 946.77 |
| 75-1_15R | 0.05124 | 0.00186 | 0.27583 | 0.00984 | 0.03905 | 0.00092 | 0.01302 | 0.00064 | 252 | 86 | 247 | 8 | 247 | 6 | 261 | 12 | 247 | 6 | 441.99 | 662.28 |
| 75-1_18 | 0.06027 | 0.00226 | 0.58148 | 0.02070 | 0.06997 | 0.00158 | 0.01868 | 0.00104 | 613 | 82 | 465 | 14 | 436 | 10 | 374 | 20 | 436 | 10 | 1261.65 | 1069.28 |
| 75-1_20 | 0.16571 | 0.00636 | 8.96082 | 0.28422 | 0.39219 | 0.00850 | 0.1089 | 0.00254 | 2515 | 66 | 2334 | 28 | 2133 | 40 | 2089 | 46 | 2515 | 66 | 59.73 | 315.54 |
| 75-1_20R | 0.17764 | 0.00806 | 9.56993 | 0.40516 | 0.39063 | 0.00984 | 0.11076 | 0.00890 | 2631 | 78 | 2394 | 38 | 2126 | 46 | 2123 | 162 | 2631 | 78 | 62.03 | 137.42 |
| 75-1_24 | 0.1123 | 0.00422 | 5.13729 | 0.18234 | 0.33177 | 0.00774 | 0.09767 | 0.00616 | 1837 | 70 | 1842 | 30 | 1847 | 38 | 1884 | 114 | 1837 | 70 | 50.04 | 96.80 |
| 75-1_27 | 0.05964 | 0.00358 | 0.62156 | 0.03564 | 0.07562 | 0.00210 | 0.02754 | 0.00166 | 591 | 134 | 491 | 22 | 470 | 12 | 549 | 32 | 470 | 12 | 3.64 | 54.04 |
| 75-1_28 | 0.0529 | 0.00312 | 0.35561 | 0.02024 | 0.04875 | 0.00134 | 0.01847 | 0.00094 | 325 | 138 | 309 | 16 | 307 | 8 | 370 | 18 | 307 | 8 | 11.72 | 99.31 |

| Analysis No. | RATIOS | | | | | | | | AGES (Ma) | | | | | | | | | | CONCENTRATIONS (ppm) | |
|---|---|---|---|---|---|---|---|---|---|---|---|---|---|---|---|---|---|---|---|---|
| | $^{207}Pb/^{206}Pb$ | ± 2σ | $^{207}Pb/^{235}U$ | ± 2σ | $^{206}Pb/^{238}U$ | ± 2σ | $^{208}Pb/^{232}Th$ | ± 2σ | $^{207}Pb/^{206}Pb$ | ± 2σ | $^{207}Pb/^{235}U$ | ± 2σ | $^{206}Pb/^{238}U$ | ± 2σ | $^{208}Pb/^{232}Th$ | ± 2σ | Used Age | ± 2σ | Th | U |
| 75-1_29 | 0.05366 | 0.00260 | 0.33105 | 0.01552 | 0.04478 | 0.00114 | 0.01664 | 0.00096 | 357 | 112 | 290 | 12 | 282 | 8 | 334 | 20 | 282 | 8 | 63.76 | 494.55 |
| 75-1_2C | 0.04949 | 0.00250 | 0.15857 | 0.00792 | 0.02324 | 0.00062 | 0.00725 | 0.00034 | 171 | 120 | 149 | 6 | 148 | 4 | 146 | 6 | 148 | 4 | 1089.82 | 407.14 |
| 75-1_2R | 0.05067 | 0.00312 | 0.17245 | 0.01034 | 0.02469 | 0.00074 | 0.00862 | 0.00050 | 226 | 146 | 162 | 8 | 157 | 4 | 173 | 10 | 157 | 4 | 372.53 | 325.79 |
| 75-1_3 | 0.05831 | 0.00568 | 0.30212 | 0.02826 | 0.03759 | 0.00150 | 0.01324 | 0.00114 | 541 | 218 | 268 | 22 | 238 | 10 | 266 | 22 | 238 | 10 | 209.83 | 144.64 |
| 75-1_31 | 0.06269 | 0.00380 | 0.64865 | 0.03732 | 0.07508 | 0.00210 | 0.02598 | 0.00182 | 698 | 132 | 508 | 22 | 467 | 12 | 518 | 36 | 467 | 12 | 22.63 | 161.07 |
| 75-1_32 | 0.11306 | 0.00648 | 4.79778 | 0.24638 | 0.30778 | 0.00782 | 0.08875 | 0.00232 | 1849 | 106 | 1785 | 44 | 1730 | 38 | 1719 | 44 | 1849 | 106 | 21.09 | 182.96 |
| 75-1_33 | 0.11643 | 0.00386 | 5.35573 | 0.17116 | 0.33374 | 0.00742 | 0.10669 | 0.00502 | 1902 | 60 | 1878 | 28 | 1856 | 36 | 2049 | 92 | 1902 | 60 | 15.63 | 177.88 |
| 75-1_34 | 0.05506 | 0.00276 | 0.30257 | 0.01436 | 0.03985 | 0.00098 | 0.01379 | 0.00084 | 415 | 114 | 268 | 12 | 252 | 6 | 277 | 16 | 252 | 6 | 52.30 | 388.77 |
| 75-1_35 | 0.10432 | 0.00542 | 3.9996 | 0.18500 | 0.27806 | 0.00654 | 0.08084 | 0.00198 | 1702 | 98 | 1634 | 38 | 1582 | 34 | 1571 | 36 | 1702 | 98 | 15.20 | 132.31 |
| 75-1_36 | 0.11519 | 0.00386 | 5.1383 | 0.16494 | 0.32359 | 0.00714 | 0.10052 | 0.00474 | 1883 | 62 | 1842 | 28 | 1807 | 34 | 1936 | 88 | 1883 | 62 | 16.07 | 200.82 |
| 75-1_4C | 0.15739 | 0.00518 | 10.03262 | 0.33190 | 0.46238 | 0.01132 | 0.13127 | 0.00696 | 2428 | 58 | 2438 | 30 | 2450 | 50 | 2493 | 124 | 2428 | 58 | 128.37 | 105.15 |
| 75-1_4R | 0.15375 | 0.00492 | 9.20162 | 0.29928 | 0.4341 | 0.01074 | 0.12551 | 0.00650 | 2388 | 56 | 2358 | 30 | 2324 | 48 | 2390 | 116 | 2388 | 56 | 66.21 | 88.95 |
| 75-1_5CR | 0.19725 | 0.00802 | 14.30577 | 0.58590 | 0.5261 | 0.01432 | 0.15394 | 0.01184 | 2804 | 68 | 2770 | 38 | 2725 | 60 | 2894 | 208 | 2804 | 68 | 174.02 | 330.15 |
| 75-1_5R | 0.11706 | 0.00516 | 5.12134 | 0.19184 | 0.3173 | 0.00738 | 0.09118 | 0.00236 | 1912 | 80 | 1840 | 32 | 1777 | 36 | 1764 | 44 | 1912 | 80 | 21.00 | 292.60 |
| 75-1_7 | 0.11438 | 0.00352 | 5.13702 | 0.16028 | 0.32574 | 0.00766 | 0.07706 | 0.00400 | 1870 | 56 | 1842 | 26 | 1818 | 38 | 1500 | 76 | 1870 | 56 | 255.64 | 460.39 |
| 75-1_9C | 0.05159 | 0.00490 | 0.27086 | 0.02464 | 0.0381 | 0.00138 | 0.01256 | 0.00092 | 267 | 222 | 243 | 20 | 241 | 8 | 252 | 18 | 241 | 8 | 133.09 | 133.93 |
| 75-1_9R | 0.05486 | 0.00290 | 0.30664 | 0.01566 | 0.04056 | 0.00110 | 0.01358 | 0.00078 | 407 | 122 | 272 | 12 | 256 | 6 | 273 | 16 | 256 | 6 | 329.93 | 377.95 |
| ~~75-1_14~~ | ~~0.05245~~ | ~~0.00592~~ | ~~0.33312~~ | ~~0.03656~~ | ~~0.04606~~ | ~~0.00124~~ | ~~0.01445~~ | ~~0.00036~~ | ~~305~~ | ~~264~~ | ~~292~~ | ~~28~~ | ~~290~~ | ~~8~~ | ~~290~~ | ~~8~~ | ~~290~~ | ~~8~~ | ~~234.15~~ | ~~283.87~~ |
| ~~75-1_16~~ | ~~0.08528~~ | ~~0.00838~~ | ~~2.25306~~ | ~~0.21040~~ | ~~0.19161~~ | ~~0.00580~~ | ~~0.0569~~ | ~~0.00188~~ | ~~1322~~ | ~~196~~ | ~~1198~~ | ~~66~~ | ~~1130~~ | ~~32~~ | ~~1119~~ | ~~36~~ | ~~1130~~ | ~~32~~ | ~~27.66~~ | ~~60.52~~ |
| ~~75-1_17~~ | ~~0.16119~~ | ~~0.00544~~ | ~~7.58429~~ | ~~0.24502~~ | ~~0.34122~~ | ~~0.00760~~ | ~~0.08991~~ | ~~0.00490~~ | ~~2468~~ | ~~58~~ | ~~2183~~ | ~~28~~ | ~~1893~~ | ~~36~~ | ~~1740~~ | ~~90~~ | ~~2468~~ | ~~58~~ | ~~465.53~~ | ~~856.36~~ |
| ~~75-1_19~~ | ~~0.10784~~ | ~~0.00554~~ | ~~3.68443~~ | ~~0.16754~~ | ~~0.2478~~ | ~~0.00594~~ | ~~0.0718~~ | ~~0.00178~~ | ~~1763~~ | ~~96~~ | ~~1568~~ | ~~36~~ | ~~1427~~ | ~~30~~ | ~~1402~~ | ~~34~~ | ~~1763~~ | ~~96~~ | ~~55.62~~ | ~~115.33~~ |
| ~~75-1_21C~~ | ~~0.08262~~ | ~~0.00546~~ | ~~0.64269~~ | ~~0.03960~~ | ~~0.05642~~ | ~~0.00172~~ | ~~0.01827~~ | ~~0.00150~~ | ~~1260~~ | ~~132~~ | ~~504~~ | ~~24~~ | ~~354~~ | ~~10~~ | ~~366~~ | ~~30~~ | ~~354~~ | ~~10~~ | ~~79.11~~ | ~~103.10~~ |
| ~~75-1_21R~~ | ~~0.06694~~ | ~~0.00342~~ | ~~0.4338~~ | ~~0.02112~~ | ~~0.04699~~ | ~~0.00124~~ | ~~0.01377~~ | ~~0.00098~~ | ~~836~~ | ~~108~~ | ~~366~~ | ~~14~~ | ~~296~~ | ~~8~~ | ~~276~~ | ~~20~~ | ~~296~~ | ~~8~~ | ~~201.32~~ | ~~319.78~~ |
| ~~75-1_22~~ | ~~0.11573~~ | ~~0.00528~~ | ~~4.303~~ | ~~0.18540~~ | ~~0.26965~~ | ~~0.00694~~ | ~~0.08397~~ | ~~0.00664~~ | ~~1891~~ | ~~84~~ | ~~1694~~ | ~~36~~ | ~~1539~~ | ~~36~~ | ~~1630~~ | ~~124~~ | ~~1891~~ | ~~84~~ | ~~47.54~~ | ~~114.91~~ |
| ~~75-1_23~~ | ~~0.06721~~ | ~~0.01158~~ | ~~0.6817~~ | ~~0.11064~~ | ~~0.07355~~ | ~~0.00466~~ | ~~0.02546~~ | ~~0.00426~~ | ~~844~~ | ~~372~~ | ~~528~~ | ~~66~~ | ~~458~~ | ~~28~~ | ~~508~~ | ~~84~~ | ~~458~~ | ~~28~~ | ~~6.55~~ | ~~15.33~~ |
| ~~75-1_25~~ | ~~0.06766~~ | ~~0.03018~~ | ~~0.21753~~ | ~~0.09624~~ | ~~0.02332~~ | ~~0.00132~~ | ~~0.0071~~ | ~~0.00026~~ | ~~858~~ | ~~964~~ | ~~200~~ | ~~80~~ | ~~149~~ | ~~8~~ | ~~143~~ | ~~6~~ | ~~149~~ | ~~8~~ | ~~406.48~~ | ~~115.88~~ |
| ~~75-1_26~~ | ~~0.09341~~ | ~~0.00372~~ | ~~0.33557~~ | ~~0.01268~~ | ~~0.02606~~ | ~~0.00064~~ | ~~0.01598~~ | ~~0.00062~~ | ~~1496~~ | ~~78~~ | ~~294~~ | ~~10~~ | ~~166~~ | ~~4~~ | ~~320~~ | ~~12~~ | ~~166~~ | ~~4~~ | ~~23.83~~ | ~~213.66~~ |
| ~~75-1_30~~ | ~~0.08268~~ | ~~0.00306~~ | ~~0.93543~~ | ~~0.03298~~ | ~~0.08207~~ | ~~0.00186~~ | ~~0.03394~~ | ~~0.00162~~ | ~~1262~~ | ~~74~~ | ~~670~~ | ~~18~~ | ~~508~~ | ~~12~~ | ~~675~~ | ~~32~~ | ~~508~~ | ~~12~~ | ~~53.67~~ | ~~303.26~~ |
| ~~75-1_39~~ | ~~0.09031~~ | ~~0.02062~~ | ~~0.53104~~ | ~~0.11960~~ | ~~0.04265~~ | ~~0.00162~~ | ~~0.01259~~ | ~~0.00056~~ | ~~1432~~ | ~~456~~ | ~~433~~ | ~~80~~ | ~~269~~ | ~~10~~ | ~~253~~ | ~~12~~ | ~~269~~ | ~~10~~ | ~~222.99~~ | ~~1098.92~~ |
| ~~75-1_6~~ | ~~0.1118~~ | ~~0.00598~~ | ~~1.04085~~ | ~~0.05282~~ | ~~0.06753~~ | ~~0.00200~~ | ~~0.01442~~ | ~~0.00106~~ | ~~1829~~ | ~~100~~ | ~~724~~ | ~~26~~ | ~~421~~ | ~~12~~ | ~~289~~ | ~~22~~ | ~~1829~~ | ~~100~~ | ~~292.61~~ | ~~104.00~~ |
| ~~75-1_8~~ | ~~0.05982~~ | ~~0.01064~~ | ~~0.6418~~ | ~~0.11250~~ | ~~0.07782~~ | ~~0.00238~~ | ~~0.02404~~ | ~~0.00068~~ | ~~597~~ | ~~400~~ | ~~503~~ | ~~70~~ | ~~483~~ | ~~14~~ | ~~480~~ | ~~14~~ | ~~483~~ | ~~14~~ | ~~268.88~~ | ~~223.66~~ |

**Appendix 6.2. Zircon trace-element data (ppm) for the samples from the Birekta terrane**

| Analysis No. | P | Ca | Ti | Y | Nb | La | Ce | Pr | Nd | Sm | Eu | Gd | Dy | Ho | Er | Yb | Lu | Hf | Ta | Th | U | Th/U | Nb/Ta | Total REE | U-Pb age |
|---|---|---|---|---|---|---|---|---|---|---|---|---|---|---|---|---|---|---|---|---|---|---|---|---|---|
| **Merchemdenskoe field, Operatorskaya pipe** | | | | | | | | | | | | | | | | | | | | | | | | | |
| OPER-1 | 116.7 | <40.99 | 6.5 | 551.9 | 1.03 | 0.00 | 11.86 | 0.03 | 0.63 | 1.57 | 0.25 | 9.95 | 44.6 | 17.4 | 82.5 | 177.6 | 32.6 | 10489 | 0.51 | 92.18 | 136.17 | 0.68 | 0.50 | 378.85 | 2833 |
| OPER-2 | 103.8 | 53.5 | 10.7 | 210.8 | 0.88 | <0.0084 | 14.54 | 0.11 | 1.87 | 2.87 | 0.91 | 10.04 | 23.0 | 7.1 | 27.8 | 50.0 | 8.9 | 8800 | 0.28 | 88.71 | 87.01 | 1.02 | 0.32 | 147.21 | 1950 |
| OPER-3 | 193.8 | <39.02 | 16.8 | 402.9 | 1.15 | 0.04 | 21.67 | 0.33 | 5.31 | 5.85 | 2.03 | 18.43 | 42.1 | 13.2 | 54.1 | 94.2 | 16.4 | 7392.1 | 0.23 | 115.69 | 94.74 | 1.22 | 0.20 | 273.54 | 1970 |
| OPER-4 | 193.7 | 62.0 | 4.3 | 1583.0 | 1.02 | 0.03 | 17.66 | 0.38 | 5.82 | 9.39 | 2.02 | 43.87 | 154.9 | 54.4 | 232.3 | 416.0 | 71.3 | 8760.6 | 0.36 | 138.33 | 113.99 | 1.21 | 0.35 | 1008.09 | 2716 |
| OPER-6 | 170.0 | <41.87 | 29.1 | 371.6 | 1.63 | 0.02 | 26.08 | 0.31 | 4.34 | 6.00 | 1.86 | 19.15 | 44.8 | 13.0 | 47.8 | 77.1 | 12.6 | 7361.3 | 0.40 | 28.26 | 22.01 | 1.28 | 0.25 | 253.11 | 2717 |
| OPER-9 | 2087.0 | 6291.9 | 5.1 | 502.0 | 0.68 | 5.51 | 35.66 | 3.11 | 18.17 | 7.89 | 1.95 | 18.06 | 46.8 | 16.2 | 73.6 | 173.8 | 34.1 | 10139 | 0.24 | 165.17 | 188.91 | 0.87 | 0.35 | 434.90 | 2716 |
| OPER-11 | 285.7 | 315.4 | 7.7 | 493.2 | 2.17 | 2.16 | 40.14 | 0.83 | 4.92 | 3.73 | 0.67 | 14.79 | 47.5 | 16.0 | 69.3 | 137.0 | 24.5 | 9771.2 | 0.71 | 152.11 | 122.62 | 1.24 | 0.33 | 361.45 | 2726 |
| OPER-12 | 100.7 | <39.81 | 3.5 | 500.9 | 1.83 | 0.03 | 19.12 | 0.05 | 0.87 | 1.73 | 0.53 | 9.45 | 38.9 | 15.4 | 76.9 | 206.5 | 42.4 | 11101 | 1.20 | 247.38 | 390.80 | 0.63 | 0.66 | 411.79 | 2711 |
| OPER-14 | 793.2 | 1041.7 | 31.9 | 855.7 | 1.40 | 25.44 | 72.03 | 8.24 | 37.70 | 16.78 | 9.02 | 71.24 | 113.6 | 29.6 | 114.5 | 218.9 | 39.9 | 10047 | 0.46 | 175.99 | 238.06 | 0.74 | 0.33 | 756.95 | 2830 |
| OPER-15 | 269.2 | <37.90 | 6.6 | 1462.2 | 2.12 | 0.48 | 59.58 | 1.92 | 22.80 | 25.32 | 9.31 | 72.36 | 163.0 | 49.1 | 195.9 | 362.6 | 64.4 | 7842.8 | 0.53 | 395.27 | 225.35 | 1.75 | 0.25 | 1026.86 | 3058 |
| OPER-16 | 304.9 | 683.6 | 160.5 | 1020.6 | 2.59 | 1.28 | 15.02 | 2.01 | 14.42 | 11.78 | 4.07 | 38.87 | 110.2 | 35.0 | 143.1 | 263.5 | 45.3 | 10348 | 0.81 | 53.99 | 202.03 | 0.27 | 0.31 | 684.43 | 1988 |
| OPER-19 | 478.7 | 83.5 | 2.8 | 1259.7 | 1.87 | 0.23 | 13.70 | 0.64 | 7.29 | 10.01 | 0.84 | 35.37 | 122.4 | 40.3 | 179.2 | 451.0 | 86.5 | 11016 | 0.66 | 23.97 | 195.41 | 0.12 | 0.35 | 947.57 | 2046 |
| OPER-20 | 62.9 | <39.92 | 2.3 | 204.5 | 0.67 | <0.0047 | 12.92 | 0.02 | 0.40 | 0.70 | 0.19 | 3.40 | 14.2 | 6.2 | 32.3 | 97.1 | 21.3 | 11250 | 0.34 | 132.15 | 269.43 | 0.49 | 0.52 | 188.64 | 2735 |
| OPER-21C | 149.8 | <37.51 | 5.6 | 453.4 | 1.72 | 0.00 | 19.41 | 0.03 | 0.69 | 1.64 | 0.30 | 8.68 | 36.7 | 14.1 | 67.7 | 159.6 | 30.6 | 10332 | 0.55 | 73.07 | 79.83 | 0.92 | 0.32 | 339.49 | 2723 |
| OPER-22 | 183.3 | 152.7 | 12.3 | 888.1 | 2.54 | 1.82 | 26.40 | 2.26 | 21.25 | 22.76 | 8.72 | 63.45 | 111.3 | 28.9 | 101.6 | 158.1 | 26.6 | 6506.3 | 0.44 | 106.76 | 306.83 | 0.35 | 0.17 | 573.22 | 2067 |
| **Kuoika field, Ruslovaya pipe** | | | | | | | | | | | | | | | | | | | | | | | | | |
| 427-13 | 312.1 | | 34.1 | 1217.4 | 2.18 | 0.08 | 4.63 | 0.22 | 3.16 | 5.87 | 1.49 | 32.49 | 120.1 | 41.7 | 179.6 | 305.4 | 57.8 | 15184 | 0.79 | 71.04 | 115.25 | 0.62 | 0.36 | 752.45 | 537 |
| 427-15 | 255.3 | | 30.8 | 735.9 | 3.68 | 0.21 | 15.62 | 0.25 | 2.12 | 3.21 | 0.48 | 16.08 | 63.2 | 24.0 | 110.9 | 215.2 | 42.0 | 17931 | 1.28 | 55.33 | 97.00 | 0.57 | 0.35 | 493.28 | 2437 |
| 427-15R | 476.0 | | 18.4 | 1255.3 | 4.97 | 0.04 | 20.04 | 0.25 | 3.11 | 5.81 | 0.84 | 30.80 | 114.5 | 42.4 | 186.2 | 341.6 | 65.3 | 16785 | 1.41 | 86.07 | 97.86 | 0.88 | 0.28 | 810.82 | 2509 |
| 427-16 | 472.3 | | 21.5 | 2451.0 | 2.72 | 0.30 | 42.58 | 0.65 | 8.34 | 12.98 | 5.06 | 65.65 | 224.5 | 82.4 | 364.7 | 692.9 | 138.5 | 15675 | 0.80 | 197.83 | 189.69 | 1.04 | 0.30 | 1638.43 | 383 |
| 427-19 | 807.9 | 439.8 | 12.2 | 4356.3 | 9.69 | 5.37 | 141.43 | 2.60 | 21.74 | 23.31 | 6.57 | 96.44 | 373.7 | 139.6 | 649.1 | 1288.8 | 252.8 | 16980 | 2.04 | 586.44 | 389.13 | 1.51 | 0.21 | 3001.47 | 299 |
| 427-21 | 300.6 | 158.7 | 10.1 | 1825.7 | 49.40 | 5.48 | 38.26 | 2.67 | 13.11 | 8.92 | 1.00 | 42.94 | 182.7 | 65.4 | 273.5 | 410.4 | 68.9 | 19181 | 13.96 | 92.00 | 254.73 | 0.36 | 0.28 | 1113.28 | 523 |
| 427-29 | 285.7 | | 10.8 | 1829.6 | 43.46 | 0.22 | 38.81 | 0.17 | 3.07 | 7.84 | 0.56 | 44.46 | 185.3 | 64.9 | 270.0 | 425.3 | 74.0 | 19546 | 12.89 | 123.29 | 257.13 | 0.48 | 0.30 | 1114.69 | 540 |
| 427-29R | 304.8 | | 12.3 | 1746.1 | 34.76 | | 38.00 | 0.16 | 3.12 | 8.34 | 0.62 | 45.75 | 178.0 | 62.2 | 258.9 | 400.8 | 69.0 | 18812 | 10.02 | 99.59 | 193.63 | 0.51 | 0.29 | 1064.78 | 537 |
| 427-31 | 239.9 | | 13.8 | 2167.3 | 40.64 | 0.44 | 72.11 | 0.49 | 7.47 | 13.48 | 1.98 | 65.13 | 229.4 | 76.9 | 314.8 | 493.8 | 87.2 | 16392 | 10.31 | 135.46 | 200.18 | 0.68 | 0.25 | 1363.21 | 535 |
| 427-35 | 256.1 | | 95.3 | 664.7 | 4.45 | 0.82 | 19.91 | 0.43 | 3.26 | 3.74 | 0.63 | 17.06 | 61.1 | 21.6 | 97.1 | 189.5 | 36.9 | 17512 | 1.08 | 66.86 | 120.21 | 0.56 | 0.24 | 452.09 | 1878 |
| 427-37 | 336.9 | | 33.5 | 2470.7 | 8.62 | 0.16 | 13.40 | 0.65 | 11.38 | 20.35 | 3.76 | 94.36 | 286.1 | 91.2 | 352.6 | 526.3 | 91.2 | 16834 | 2.41 | 81.40 | 120.03 | 0.68 | 0.28 | 1491.44 | 562 |
| 427-38 | 336.7 | 214.3 | 21.3 | 1927.1 | 4.30 | 0.81 | 56.94 | 0.42 | 4.85 | 6.12 | 2.05 | 34.72 | 152.0 | 60.5 | 298.2 | 641.8 | 131.7 | 14666 | 1.06 | 314.38 | 300.48 | 1.05 | 0.25 | 1390.02 | 289 |
| 427-41 | 349.2 | | 32.1 | 2994.4 | 3.29 | 0.87 | 24.64 | 2.31 | 28.35 | 31.04 | 1.76 | 111.08 | 305.3 | 100.1 | 408.3 | 636.7 | 115.3 | 16114 | 1.66 | 355.32 | 642.98 | 0.55 | 0.50 | 1765.74 | 1881 |
| 427-42 | 239.7 | | 624.6 | 1449.1 | 21.69 | 2.93 | 23.03 | 1.10 | 8.68 | 7.64 | 1.36 | 40.50 | 150.7 | 51.8 | 211.0 | 325.2 | 57.6 | 16067 | 5.64 | 61.05 | 130.14 | 0.47 | 0.26 | 881.55 | 524 |
| 427-43 | 280.1 | | 20.0 | 1519.7 | 1.75 | 0.09 | 29.75 | 0.25 | 4.97 | 8.27 | 2.00 | 37.59 | 134.8 | 49.2 | 220.9 | 426.9 | 84.1 | 18707 | 0.77 | 227.94 | 206.15 | 1.11 | 0.44 | 998.84 | 930 |
| 427-49 | 236.2 | | 19.9 | 2356.4 | 1.32 | 0.25 | 8.62 | 0.76 | 10.54 | 16.98 | 3.78 | 75.50 | 246.3 | 82.6 | 339.2 | 527.1 | 95.7 | 16593 | 0.62 | 141.75 | 230.84 | 0.61 | 0.47 | 1407.17 | 545 |
| 427-50 | 409.1 | | 20.6 | 1870.7 | 4.81 | 0.01 | 87.67 | 0.25 | 5.16 | 8.73 | 1.54 | 40.86 | 163.3 | 62.1 | 292.6 | 599.9 | 123.9 | 15203 | 1.44 | 219.77 | 171.63 | 1.28 | 0.30 | 1385.98 | 261 |
| 427-53 | 371.0 | 469.3 | 14.8 | 764.0 | 5.52 | 7.05 | 24.05 | 2.22 | 10.08 | 4.03 | 0.30 | 14.42 | 60.8 | 24.4 | 122.6 | 293.4 | 64.2 | 18248 | 2.37 | 85.17 | 367.52 | 0.23 | 0.43 | 627.51 | 1794 |
| 427-56 | 335.8 | | 14.7 | 1759.7 | 4.50 | 0.42 | 6.94 | 0.13 | 2.32 | 4.46 | 0.95 | 29.12 | 133.8 | 53.5 | 260.1 | 562.3 | 119.5 | 17314 | 1.43 | 171.45 | 657.17 | 0.26 | 0.32 | 1173.55 | 440 |
| 427-58 | 297.5 | | 13.9 | 3704.4 | 85.80 | 0.36 | 57.03 | 0.76 | 9.65 | 16.66 | 2.21 | 92.02 | 384.3 | 131.0 | 533.7 | 763.4 | 125.0 | 16609 | 19.97 | 287.61 | 512.14 | 0.56 | 0.23 | 2116.16 | 565 |
| 427-64 | 567.4 | 435.7 | 13.5 | 3080.5 | 5.93 | 5.64 | 104.94 | 2.39 | 15.37 | 15.56 | 3.86 | 67.69 | 258.0 | 98.3 | 460.5 | 927.2 | 187.8 | 15334 | 1.54 | 573.06 | 537.24 | 1.07 | 0.26 | 2147.22 | 288 |
| 427-67 | 447.9 | | 28.6 | 2752.1 | 5.54 | 0.17 | 90.44 | 0.54 | 7.13 | 11.90 | 3.09 | 56.76 | 229.3 | 87.9 | 416.7 | 855.1 | 171.1 | 15112 | 1.22 | 343.29 | 190.27 | 1.80 | 0.22 | 1930.12 | 283 |
| 427-73 | 503.0 | 122.9 | 14.5 | 1014.0 | 1.85 | 1.47 | 10.58 | 1.32 | 8.33 | 5.92 | 1.69 | 22.87 | 92.5 | 32.0 | 144.0 | 284.5 | 54.9 | 25967 | 0.59 | 42.55 | 833.34 | 0.05 | 0.32 | 660.13 | 2534 |
| 427-73R | 559.9 | 148.1 | 10.3 | 1442.6 | 2.32 | 1.70 | 13.62 | 1.72 | 11.02 | 8.69 | 1.96 | 28.46 | 121.2 | 44.9 | 215.3 | 483.4 | 93.2 | 22857 | 2.17 | 138.25 | ###### | 0.09 | 0.94 | 1025.12 | 2430 |
| 427-77 | 288.6 | | 14.0 | 1736.7 | 1.19 | 0.10 | 10.40 | 0.24 | 3.37 | 6.40 | 1.96 | 27.46 | 124.3 | 52.8 | 284.2 | 717.4 | 166.1 | 17712 | 0.44 | 166.73 | 432.24 | 0.39 | 0.37 | 1394.71 | 542 |
| **Kuoika field, Olivinovaya pipe** | | | | | | | | | | | | | | | | | | | | | | | | 0.00 | |
| 7-57_1 | 236.9 | 317.4 | 12.9 | 568.5 | 2.19 | 0.34 | 18.13 | 0.56 | 8.30 | 9.41 | 4.61 | 27.57 | 60.5 | 18.5 | 80.5 | 213.2 | 35.9 | 19431 | 0.71 | 48.10 | 231.43 | 0.21 | 0.32 | 477.53 | 141 |
| 7-57_4 | 646.7 | 74.5 | 22.1 | 7278.1 | 2.93 | 0.35 | 14.89 | 0.71 | 11.32 | 22.62 | 4.83 | 151.64 | 682.2 | 248.9 | 1088.7 | 2230.7 | 332.0 | 15549 | 1.31 | 260.44 | 372.28 | 0.70 | 0.45 | 4788.88 | 471 |
| 7-57_10 | 337.4 | 159.8 | 20.3 | 1728.4 | 5.01 | 0.96 | 58.76 | 0.86 | 7.61 | 9.47 | 3.26 | 39.88 | 151.4 | 56.0 | 262.8 | 685.3 | 112.4 | 20365 | 2.03 | 431.52 | 555.74 | 0.78 | 0.41 | 1388.69 | 363 |
| 7-57_11 | 199.2 | 63.6 | 254.5 | 451.8 | 3.76 | 0.16 | 12.92 | 0.26 | 3.42 | 4.13 | 0.92 | 14.80 | 44.1 | 14.8 | 62.3 | 140.0 | 21.8 | 18811 | 1.54 | 73.72 | 197.10 | 0.37 | 0.41 | 319.47 | 1745 |

| Analysis No. | P | Ca | Ti | Y | Nb | La | Ce | Pr | Nd | Sm | Eu | Gd | Dy | Ho | Er | Yb | Lu | Hf | Ta | Th | U | Th/U | Nb/Ta | Total REE | U-Pb age |
|---|---|---|---|---|---|---|---|---|---|---|---|---|---|---|---|---|---|---|---|---|---|---|---|---|---|
| 7-57_12 | 309.9 | 91.1 | 29.4 | 2269.7 | 2.26 | 0.36 | 29.20 | 0.84 | 13.08 | 15.77 | 4.71 | 64.08 | 215.3 | 75.1 | 323.9 | 751.6 | 118.1 | 14495 | 0.85 | 125.12 | 238.33 | 0.52 | 0.38 | 1611.93 | 461 |
| 7-57_13 | 164.1 | | 8.4 | 1167.4 | 1.87 | 0.05 | 32.92 | 0.37 | 5.29 | 7.49 | 3.32 | 27.70 | 101.6 | 36.8 | 173.7 | 492.3 | 82.8 | 15431 | 1.11 | 307.12 | 452.95 | 0.68 | 0.59 | 964.21 | 463 |
| 7-57_14 | 167.6 | 55.0 | 21.7 | 733.9 | 1.43 | 0.24 | 13.18 | 0.28 | 3.07 | 4.07 | 1.41 | 14.96 | 59.6 | 22.2 | 109.7 | 331.4 | 58.2 | 15573 | 0.50 | 92.01 | 394.51 | 0.23 | 0.35 | 618.25 | 480 |
| 7-57_15 | 529.0 | | 23.9 | 2702.3 | 3.64 | 0.05 | 18.77 | 0.36 | 5.39 | 9.61 | 4.15 | 50.56 | 224.2 | 86.4 | 413.2 | 1092.3 | 187.0 | 14951 | 1.51 | 255.79 | 546.71 | 0.47 | 0.41 | 2092.07 | 596 |
| 7-57_16 | 787.5 | 201.3 | 23.3 | 7358.4 | 8.37 | 1.02 | 222.09 | 3.84 | 61.13 | 75.53 | 28.94 | 238.59 | 724.9 | 241.5 | 1048.0 | 2524.2 | 400.1 | 12785 | 1.29 | ###### | 462.85 | 2.75 | 0.15 | 5569.73 | 283 |
| 7-57_17 | 347.4 | 57.9 | 21.2 | 5708.0 | 13.42 | 3.36 | 36.97 | 2.00 | 22.88 | 31.60 | 1.75 | 152.51 | 589.3 | 211.8 | 880.3 | 1649.5 | 234.2 | 12206 | 4.07 | 194.59 | 529.68 | 0.37 | 0.30 | 3816.21 | 262 |
| 7-57_18 | 365.9 | 246.4 | 37.0 | 1197.0 | 5.33 | 3.06 | 15.26 | 1.07 | 8.30 | 6.69 | 0.56 | 28.93 | 115.5 | 41.8 | 185.6 | 416.7 | 64.0 | 16761 | 1.97 | 70.12 | 148.02 | 0.47 | 0.37 | 887.41 | 1880 |
| 7-57_19 | 1131.8 | 978.4 | 15.7 | 2272.8 | 5.98 | 4.90 | 35.35 | 2.61 | 15.76 | 10.14 | 1.94 | 41.69 | 199.8 | 77.0 | 362.3 | 860.5 | 134.9 | 21085 | 3.34 | 293.67 | 676.56 | 0.43 | 0.56 | 1746.95 | 321 |
| 7-57_21 | 382.3 | 343.4 | 44.9 | 1117.3 | 4.04 | 2.28 | 48.50 | 2.10 | 12.77 | 10.78 | 3.81 | 27.21 | 98.8 | 36.6 | 171.0 | 514.6 | 84.7 | 18341 | 1.52 | 249.93 | 438.20 | 0.57 | 0.38 | 1013.19 | 471 |
| 7-57_30 | 146.7 | 302.1 | 30.9 | 504.1 | 3.31 | 0.15 | 13.20 | 0.09 | 0.84 | 1.56 | 0.57 | 9.08 | 40.9 | 16.0 | 81.5 | 279.5 | 50.0 | 24160 | 1.53 | 111.26 | 722.45 | 0.15 | 0.46 | 493.40 | 272 |
| 7-57_32 | 11.5 | | 1.8 | 268.9 | 1.25 | 0.01 | 1.31 | 0.03 | 0.16 | 0.38 | 0.37 | 3.12 | 23.4 | 9.2 | 50.5 | 151.6 | 23.7 | 13413 | 0.69 | 157.07 | 399.15 | 0.39 | 0.55 | 263.71 | 507 |
| 7-57_33 | 325.5 | | 32.5 | 1775.4 | 6.78 | 0.07 | 14.54 | 0.36 | 6.09 | 10.54 | 0.70 | 45.61 | 175.1 | 62.7 | 272.1 | 582.1 | 87.9 | 17097 | 2.60 | 142.22 | 255.18 | 0.56 | 0.38 | 1257.73 | 1852 |
| 7-57_41 | 350.6 | 79.9 | 32.2 | 1184.1 | 13.44 | 1.21 | 34.95 | 0.23 | 2.04 | 5.48 | 2.49 | 27.25 | 91.9 | 32.9 | 151.8 | 405.0 | 72.6 | 18380 | 7.93 | 208.01 | 748.26 | 0.28 | 0.59 | 827.91 | 2585 |
| 7-57_42 | 67.9 | | 12.9 | 1521.3 | 20.17 | 0.32 | 125.66 | 0.27 | 2.78 | 4.24 | 1.83 | 21.45 | 105.3 | 44.6 | 232.8 | 659.8 | 108.6 | 19678 | 8.74 | 388.24 | 457.51 | 0.85 | 0.43 | 1307.74 | 333 |
| 7-57_46 | 337.9 | 61.9 | 91.1 | 650.2 | 4.55 | 0.50 | 37.52 | 0.28 | 3.34 | 5.03 | 0.70 | 17.82 | 64.7 | 21.5 | 90.4 | 196.8 | 30.7 | 19079 | 1.92 | 296.17 | 163.73 | 1.81 | 0.42 | 469.13 | 1848 |
| 7-57_5 | 312.4 | | 20.7 | 1448.6 | 4.49 | 0.07 | 75.03 | 0.62 | 10.85 | 17.03 | 4.14 | 51.75 | 139.6 | 45.7 | 196.7 | 454.8 | 73.3 | 20668 | 1.61 | 479.24 | 437.73 | 1.09 | 0.36 | 1069.59 | 1954 |
| 7-57_54 | 841.9 | 91.9 | 322.0 | 2782.1 | 6.60 | 7.26 | 69.38 | 2.50 | 18.87 | 20.24 | 5.52 | 81.28 | 282.3 | 96.9 | 413.2 | 884.9 | 136.7 | 16137 | 2.49 | 138.45 | 135.51 | 1.02 | 0.38 | 2019.10 | 1852 |
| 7-57_7 | 289.3 | 218.9 | 246.3 | 1172.4 | 11.98 | 1.27 | 17.37 | 0.73 | 5.19 | 5.83 | 0.91 | 23.77 | 104.9 | 39.1 | 183.3 | 477.4 | 75.4 | 20072 | 6.48 | 173.98 | 645.99 | 0.27 | 0.54 | 935.14 | 1831 |
| 7-57_8 | 286.7 | 171.8 | 190.6 | 270.1 | 2.12 | 0.86 | 5.88 | 0.58 | 8.71 | 22.72 | 0.26 | 72.21 | 63.8 | 9.0 | 17.1 | 17.3 | 1.8 | 22695 | 0.23 | 155.36 | 885.08 | 0.18 | 0.11 | 220.22 | 2497 |
| **Kuoika field, Vtorogodnitsa pipe** | | | | | | | | | | | | | | | | | | | | | | | | | |
| 75-1_1 | 103.2 | | 9.6 | 297.7 | 1.84 | 0.01 | 4.61 | 0.05 | 1.01 | 1.73 | 0.13 | 7.92 | 26.8 | 9.7 | 42.3 | 83.3 | 15.5 | 9440.7 | 0.47 | 23.53 | 43.78 | 0.54 | 0.26 | 193.03 | 1900 |
| 75-1_2R | 78.5 | | 6.0 | 904.5 | 2.84 | 0.07 | 50.43 | 0.31 | 4.88 | 6.23 | 2.00 | 24.06 | 75.3 | 27.3 | 127.2 | 300.3 | 56.1 | 9454.7 | 0.61 | 274.66 | 233.03 | 1.18 | 0.22 | 674.33 | 148 |
| 75-1_4C | 124.2 | | 8.9 | 430.1 | 2.47 | 0.02 | 16.57 | 0.08 | 1.17 | 2.17 | 0.56 | 9.75 | 38.7 | 14.3 | 66.2 | 148.3 | 28.0 | 9750.1 | 1.05 | 83.22 | 112.32 | 0.74 | 0.42 | 325.68 | 2428 |
| 75-1_4R | 97.9 | | 8.7 | 272.5 | 2.01 | 0.04 | 12.74 | 0.03 | 0.50 | 0.88 | 0.28 | 4.93 | 21.5 | 8.6 | 42.2 | 103.3 | 20.4 | 10221 | 1.04 | 51.29 | 79.16 | 0.65 | 0.52 | 215.34 | 2388 |
| 75-1_5CR | 208.9 | 40.5 | 300.4 | 1149.0 | 3.50 | 0.13 | 12.24 | 0.15 | 2.06 | 3.09 | 1.04 | 19.71 | 89.7 | 36.4 | 179.7 | 429.1 | 81.4 | 8313.4 | 0.73 | 134.48 | 261.17 | 0.51 | 0.21 | 854.77 | 2804 |
| 75-1_5R | 67.9 | | 7.1 | 198.3 | 1.42 | 0.04 | 3.36 | 0.04 | 0.18 | 0.43 | 0.20 | 2.98 | 15.5 | 6.1 | 30.8 | 84.6 | 15.2 | 12143 | 0.96 | 31.13 | 217.02 | 0.14 | 0.68 | 159.47 | 1912 |
| 75-1_7 | 238.6 | 39.8 | 15.8 | 1191.9 | 26.77 | 0.59 | 17.35 | 0.38 | 2.27 | 3.39 | 0.32 | 18.05 | 93.5 | 38.0 | 194.6 | 470.0 | 82.5 | 11257 | 10.43 | 423.65 | 512.12 | 0.83 | 0.39 | 920.90 | 1870 |
| 75-1_9C | 200.4 | 39.5 | 35.7 | 476.8 | 1.59 | 0.46 | 15.67 | 0.21 | 1.87 | 2.59 | 0.46 | 11.56 | 41.1 | 14.6 | 68.7 | 145.3 | 28.7 | 9201.6 | 0.48 | 126.17 | 131.84 | 0.96 | 0.30 | 331.14 | 241 |
| 75-1_10 | 323.6 | 123.0 | 12.9 | 760.0 | 2.34 | 1.38 | 11.42 | 0.38 | 2.38 | 2.65 | 0.12 | 14.14 | 67.1 | 25.5 | 117.7 | 240.6 | 41.5 | 11413 | 0.97 | 121.68 | 143.83 | 0.85 | 0.42 | 524.89 | 1723 |
| 75-1_11 | 101.4 | | 4.4 | 243.7 | 2.07 | 0.32 | 58.23 | 0.75 | 8.91 | 7.14 | 1.62 | 14.36 | 26.5 | 8.3 | 35.8 | 74.7 | 13.8 | 9004.1 | 0.62 | 81.38 | 92.15 | 0.88 | 0.30 | 250.39 | 1893 |
| 75-1_12 | 121.8 | | 7.0 | 334.0 | 1.94 | 0.02 | 9.00 | 0.05 | 0.78 | 1.36 | 0.09 | 7.45 | 29.7 | 11.1 | 50.4 | 104.0 | 18.8 | 10902 | 0.63 | 79.73 | 105.85 | 0.75 | 0.33 | 232.74 | 2010 |
| 75-1_13 | 204.7 | 67.8 | 11.2 | 735.9 | 3.55 | 0.53 | 32.24 | 0.28 | 2.34 | 3.58 | 0.93 | 15.92 | 63.8 | 24.1 | 112.5 | 244.1 | 46.6 | 8803.2 | 0.98 | 95.22 | 99.90 | 0.95 | 0.28 | 546.91 | 328 |
| 75-1_15C | 492.3 | 33.0 | 5.6 | 1813.5 | 15.80 | 10.50 | 53.45 | 3.12 | 12.71 | 6.47 | 0.79 | 31.45 | 155.0 | 60.1 | 280.0 | 574.5 | 101.6 | 12294 | 4.53 | 574.53 | 686.21 | 0.84 | 0.29 | 1289.60 | 262 |
| 75-1_15R | 423.4 | | 3.5 | 1403.5 | 9.69 | 1.56 | 22.60 | 0.58 | 2.61 | 3.25 | 0.34 | 22.83 | 117.6 | 46.5 | 217.0 | 462.8 | 83.1 | 12645 | 3.08 | 304.96 | 463.12 | 0.66 | 0.32 | 980.69 | 247 |
| 75-1_27 | 578.8 | 392.8 | 32.1 | 1620.5 | 2.46 | 1.16 | 17.15 | 0.67 | 5.48 | 7.81 | 1.42 | 37.51 | 153.2 | 56.1 | 248.7 | 564.7 | 89.3 | 14208 | 0.95 | 33.51 | 87.49 | 0.38 | 0.39 | 1183.25 | 470 |
| 75-1_28 | 576.3 | 649.2 | 53.7 | 1697.4 | 2.97 | 4.00 | 21.39 | 1.60 | 11.91 | 11.27 | 2.68 | 47.94 | 166.4 | 58.6 | 257.6 | 572.2 | 92.6 | 13859 | 0.90 | 102.33 | 149.33 | 0.69 | 0.30 | 1248.21 | 307 |
| 75-1_29 | 718.9 | 590.5 | 14.4 | 3587.0 | 3.33 | 4.35 | 42.85 | 2.30 | 18.99 | 22.26 | 4.87 | 95.10 | 345.6 | 121.7 | 531.0 | 1195.6 | 185.5 | 14676 | 1.33 | 449.58 | 635.67 | 0.71 | 0.40 | 2570.13 | 282 |
| 75-1_32 | 242.4 | | 21.9 | 1157.0 | 5.66 | 0.39 | 41.12 | 0.31 | 2.90 | 4.79 | 1.34 | 22.49 | 94.8 | 36.4 | 177.5 | 504.0 | 85.6 | 17366 | 1.88 | 196.46 | 268.90 | 0.73 | 0.33 | 971.59 | 1849 |
| 75-1_33 | 381.5 | | 36.3 | 1650.5 | 10.15 | 0.76 | 15.15 | 0.41 | 4.96 | 7.85 | 0.56 | 37.61 | 157.2 | 56.5 | 252.5 | 560.1 | 86.8 | 18636 | 3.88 | 136.28 | 269.27 | 0.51 | 0.38 | 1180.25 | 1902 |
| 75-1_35 | 546.3 | 229.9 | 58.9 | 1968.4 | 2.89 | 1.50 | 13.25 | 1.13 | 9.95 | 13.52 | 2.66 | 56.41 | 201.5 | 69.0 | 293.7 | 632.2 | 93.1 | 15436 | 1.21 | 115.26 | 174.78 | 0.66 | 0.42 | 1387.92 | 1702 |
| 75-1_36 | 328.6 | 135.3 | 33.6 | 1372.3 | 17.04 | 0.41 | 20.09 | 0.25 | 2.65 | 4.57 | 0.28 | 25.99 | 125.0 | 47.0 | 217.4 | 501.4 | 77.8 | 18915 | 6.20 | 150.35 | 321.65 | 0.47 | 0.36 | 1022.79 | 1883 |
| 75-1_18 | 532.4 | 973.1 | 64.3 | 1183.9 | 9.76 | 5.52 | 72.25 | 2.09 | 11.29 | 6.28 | 1.98 | 19.24 | 85.1 | 33.7 | 177.2 | 488.5 | 101.7 | 10977 | 2.56 | 673.72 | 590.96 | 1.14 | 0.26 | 1004.78 | 436 |
| 75-1_20 | 141.2 | | 25.6 | 513.0 | 3.12 | 0.04 | 5.23 | 0.04 | 0.46 | 0.80 | 0.15 | 5.69 | 35.2 | 15.6 | 85.8 | 238.1 | 48.9 | 12061 | 4.34 | 60.41 | 326.94 | 0.18 | 1.39 | 435.97 | 2515 |
| 75-1_20R | 200.1 | 69.3 | 23.5 | 1060.1 | 3.21 | 0.16 | 7.13 | 0.17 | 2.09 | 3.64 | 0.61 | 21.27 | 94.3 | 36.2 | 166.8 | 350.0 | 64.9 | 10405 | 1.81 | 67.14 | 207.94 | 0.32 | 0.56 | 747.18 | 2631 |
| 75-1_24 | 203.1 | 53.0 | 23.5 | 814.2 | 1.42 | 0.40 | 5.08 | 0.41 | 3.36 | 4.70 | 0.80 | 19.74 | 77.4 | 28.0 | 123.9 | 237.7 | 42.7 | 8992.7 | 0.53 | 46.06 | 92.86 | 0.50 | 0.37 | 544.16 | 1837 |

**Appendix 6.3. Zircon Hf-isotope data for the samples from the Birekta terrane**

| Analysis No. | Lu-Hf RATIOS | | | | $Hf_{initial}$ | εHf(T) | ± SE | $T_{DM}$ (Ga) | $T_{DM}^{Crustal}$ (Ga) | U-Pb AGE | Oxygen | |
|---|---|---|---|---|---|---|---|---|---|---|---|---|
| | $^{176}Hf/^{177}Hf$ | 1SE | $^{176}Lu/^{177}Hf$ | $^{176}Yb/^{177}Hf$ | | | | | | (Ma) | $\delta^{18}O$ | 2σ |
| **Merchemdenskoe field, Operatorskaya pipe** | | | | | | | | | | | | |
| OPER-14 | 0.281034 | 0.000015 | 0.000379 | 0.011189 | 0.281013 | 1.8 | 0.5 | 3.04 | 3.19 | 2830 | - | - |
| OPER-15 | 0.280915 | 0.000018 | 0.000990 | 0.030348 | 0.280857 | 1.6 | 0.6 | 3.25 | 3.38 | 3058 | - | - |
| OPER-16 | 0.281667 | 0.000015 | 0.000977 | 0.031199 | 0.281630 | 4.1 | 0.5 | 2.22 | 2.38 | 1988 | - | - |
| OPER-17 | 0.280945 | 0.000020 | 0.000421 | 0.011202 | 0.280923 | -3.9 | 0.7 | 3.16 | 3.47 | 2724 | - | - |
| OPER-18 | 0.281258 | 0.000021 | 0.001202 | 0.031879 | 0.281201 | 0.0 | 0.7 | 2.80 | 3.02 | 2468 | - | - |
| OPER-19 | 0.281555 | 0.000016 | 0.000943 | 0.025544 | 0.281518 | 1.4 | 0.6 | 2.37 | 2.59 | 2046 | - | - |
| OPER-20 | 0.280918 | 0.000020 | 0.000359 | 0.009698 | 0.280899 | -4.5 | 0.7 | 3.19 | 3.51 | 2735 | - | - |
| OPER-21 | 0.280902 | 0.000018 | 0.000776 | 0.028560 | 0.280862 | -6.2 | 0.6 | 3.25 | 3.61 | 2723 | - | - |
| OPER-22 | 0.281606 | 0.000026 | 0.000481 | 0.016106 | 0.281587 | 4.4 | 0.9 | 2.28 | 2.42 | 2067 | - | - |
| **Kuoika field, Ruslovaya pipe** | | | | | | | | | | | | |
| 427-10 | 0.281015 | 0.000010 | 0.000558 | 0.018792 | 0.280990 | -10.5 | 0.4 | 3.08 | 3.48 | 2341 | 4.95 | 0.62 |
| 427-11 | 0.282619 | 0.000007 | 0.001344 | 0.053968 | 0.282606 | 5.1 | 0.3 | 0.91 | 1.09 | 512 | - | - |
| 427-12 | 0.281161 | 0.000013 | 0.000168 | 0.006170 | 0.281155 | -13.5 | 0.5 | 2.85 | 3.35 | 1958 | - | - |
| 427-13 | 0.282662 | 0.000012 | 0.000664 | 0.023755 | 0.282655 | 7.4 | 0.4 | 0.83 | 0.98 | 537 | 8.30 | 0.64 |
| 427-15 | 0.28113 | 0.000010 | 0.000597 | 0.020112 | 0.281101 | -2.6 | 0.4 | 2.93 | 3.16 | 2509 | 5.40 | 0.61 |
| 427-16 | 0.282767 | 0.000011 | 0.001592 | 0.052587 | 0.282756 | 7.5 | 0.4 | 0.70 | 0.85 | 383 | - | - |
| 427-19 | 0.282095 | 0.000011 | 0.001871 | 0.059728 | 0.282085 | -18.1 | 0.4 | 1.67 | 2.27 | 299 | 4.56 | 0.59 |
| 427-20 | 0.282607 | 0.000010 | 0.000885 | 0.033530 | 0.282598 | 5.3 | 0.3 | 0.91 | 1.10 | 534 | 7.30 | 0.61 |
| 427-21 | 0.282652 | 0.000013 | 0.000488 | 0.018535 | 0.282647 | 6.8 | 0.5 | 0.84 | 1.00 | 523 | - | - |
| 427-23 | 0.282612 | 0.000025 | 0.000612 | 0.022299 | 0.282606 | 5.6 | 0.9 | 0.90 | 1.08 | 535 | - | - |
| 427-25 | 0.282639 | 0.000012 | 0.000690 | 0.025965 | 0.282632 | 6.5 | 0.4 | 0.86 | 1.03 | 535 | - | - |
| 427-29c | - | - | - | - | - | - | - | - | - | | 8.24 | 0.60 |
| 427-29r | - | - | - | - | - | - | - | - | - | | 7.68 | 0.61 |
| 427-3 | 0.28286 | 0.000022 | 0.002242 | 0.088914 | 0.282848 | 8.7 | 0.8 | 0.58 | 0.70 | 291 | - | - |
| 427-33 | 0.281765 | 0.000012 | 0.000520 | 0.017273 | 0.281762 | -29.4 | 0.4 | 2.06 | 2.92 | 306 | 6.65 | 0.61 |
| 427-35 | 0.281321 | 0.000009 | 0.000371 | 0.012495 | 0.281308 | -9.9 | 0.3 | 2.65 | 3.08 | 1878 | 5.89 | 0.60 |
| 427-38 | 0.282698 | 0.000011 | 0.001681 | 0.054677 | 0.282689 | 3.0 | 0.4 | 0.80 | 1.03 | 289 | 4.02 | 0.59 |
| 427-39 | 0.282621 | 0.000011 | 0.000569 | 0.021745 | 0.282615 | 6.2 | 0.4 | 0.88 | 1.05 | 549 | 7.60 | 0.61 |
| 427-41 | 0.2815 | 0.000011 | 0.001002 | 0.035142 | 0.281464 | -4.3 | 0.4 | 2.45 | 2.75 | 1881 | 5.97 | 0.61 |
| 427-42 | 0.282553 | 0.000013 | 0.000488 | 0.019163 | 0.282548 | 3.3 | 0.5 | 0.98 | 1.21 | 524 | 7.48 | 0.61 |
| 427-43 | 0.282332 | 0.000010 | 0.000745 | 0.024927 | 0.282319 | 4.3 | 0.3 | 1.29 | 1.48 | 930 | 7.30 | 0.61 |
| 427-45 | - | - | - | - | - | - | - | - | - | | 6.72 | 0.60 |
| 427-49 | - | - | - | - | - | - | - | - | - | | 8.04 | 0.61 |
| 427-5 | 0.282921 | 0.000014 | 0.000044 | 0.001899 | 0.282921 | 8.2 | 0.5 | 0.46 | 0.62 | 151 | - | - |
| 427-50 | 0.282228 | 0.000014 | 0.001290 | 0.041030 | 0.282222 | -14.1 | 0.5 | 1.46 | 2.01 | 261 | 5.00 | 0.61 |

| Analysis No. | Lu-Hf RATIOS | | | | $Hf_{initial}$ | εHf(T) | ± SE | $T_{DM}$ (Ga) | $T_{DM}^{Crustal}$ (Ga) | U-Pb AGE | Oxygen | |
|---|---|---|---|---|---|---|---|---|---|---|---|---|
| | $^{176}Hf/^{177}Hf$ | 1SE | $^{176}Lu/^{177}Hf$ | $^{176}Yb/^{177}Hf$ | | | | | | (Ma) | $\delta^{18}O$ | 2σ |
| 427-52 | 0.282602 | 0.000013 | 0.001095 | 0.041466 | 0.282591 | 4.8 | 0.5 | 0.92 | 1.12 | 522 | 8.13 | 0.61 |
| 427-53 | 0.281654 | 0.000013 | 0.000529 | 0.018525 | 0.281636 | -0.2 | 0.5 | 2.21 | 2.44 | 1794 | 5.72 | 0.60 |
| 427-56 | 0.282735 | 0.000010 | 0.000996 | 0.031453 | 0.282727 | 7.7 | 0.3 | 0.73 | 0.88 | 440 | 9.27 | 0.62 |
| 427-58 | 0.282587 | 0.000006 | 0.000482 | 0.017950 | 0.282582 | 5.4 | 0.2 | 0.93 | 1.12 | 565 | 8.15 | 0.61 |
| 427-6 | 0.281402 | 0.000011 | 0.000116 | 0.003673 | 0.281398 | -7.3 | 0.4 | 2.53 | 2.90 | 1854 | - | - |
| 427-64 | 0.282547 | 0.000009 | 0.001046 | 0.032905 | 0.282541 | -2.2 | 0.3 | 1.00 | 1.34 | 288 | 5.86 | 0.60 |
| 427-67 | 0.282636 | 0.000012 | 0.001529 | 0.049782 | 0.282628 | 0.7 | 0.4 | 0.89 | 1.16 | 283 | 5.85 | 0.61 |
| 427-7 | 0.282606 | 0.000011 | 0.000686 | 0.021570 | 0.282599 | 5.6 | 0.4 | 0.91 | 1.09 | 546 | - | - |
| 427-71 | 0.282619 | 0.000009 | 0.000747 | 0.029060 | 0.282612 | 5.7 | 0.3 | 0.89 | 1.07 | 529 | 7.61 | 0.60 |
| 427-73 | 0.281204 | 0.000008 | 0.000469 | 0.018550 | 0.281181 | 1.0 | 0.3 | 2.82 | 2.97 | 2543 | 6.57 | 0.61 |
| 427-77 | 0.282891 | 0.000008 | 0.000890 | 0.024754 | 0.282882 | 15.5 | 0.3 | 0.51 | 0.50 | 542 | 4.92 | 0.60 |
| 427-78 | 0.282612 | 0.000007 | 0.001285 | 0.050047 | 0.282599 | 5.4 | 0.2 | 0.91 | 1.09 | 539 | 6.39 | 0.59 |
| 427-8 | 0.282086 | 0.000008 | 0.000821 | 0.026791 | 0.282082 | -18.7 | 0.3 | 1.64 | 2.29 | 279 | - | - |
| 427-9 | 0.281069 | 0.000011 | 0.000339 | 0.011455 | 0.281053 | -5.3 | 0.4 | 2.99 | 3.28 | 2469 | - | - |
| **Kuoika field, Olivinovaya pipe** | | | | | | | | | | | | |
| 7-57-1 | 0.282058 | 0.000011 | 0.000145 | 0.003469 | 0.282058 | -22.5 | 0.4 | 1.65 | 2.40 | 144 | - | - |
| 7-57-10 | 0.282743 | 0.000008 | 0.000606 | 0.017651 | 0.282739 | 6.4 | 0.3 | 0.71 | 0.89 | 363 | 7.47 | 0.60 |
| 7-57-11 | 0.281188 | 0.000019 | 0.000148 | 0.004840 | 0.281183 | -17.4 | 0.7 | 2.82 | 3.40 | 1745 | 5.75 | 0.60 |
| 7-57-12 | 0.282707 | 0.000015 | 0.001385 | 0.045906 | 0.282695 | 7.1 | 0.5 | 0.78 | 0.93 | 461 | 6.84 | 0.63 |
| 7-57-13 | 0.28253 | 0.000014 | 0.000856 | 0.025509 | 0.282523 | 1.0 | 0.5 | 1.02 | 1.29 | 463 | 7.14 | 0.60 |
| 7-57-14 | 0.282719 | 0.000012 | 0.000896 | 0.027395 | 0.282711 | 8.1 | 0.4 | 0.75 | 0.89 | 480 | 8.54 | 0.60 |
| 7-57-15 | 0.282666 | 0.000014 | 0.002050 | 0.062276 | 0.282643 | 8.3 | 0.5 | 0.85 | 0.97 | 596 | 7.95 | 0.61 |
| 7-57-16 | 0.282249 | 0.000013 | 0.003835 | 0.123050 | 0.282229 | -13.4 | 0.5 | 1.53 | 1.98 | 283 | 4.96 | 0.60 |
| 7-57-17 | 0.282963 | 0.000016 | 0.001948 | 0.065098 | 0.282953 | 11.8 | 0.6 | 0.42 | 0.49 | 262 | - | - |
| 7-57-18 | 0.281631 | 0.000012 | 0.000432 | 0.014035 | 0.281616 | 1.1 | 0.4 | 2.24 | 2.44 | 1880 | 5.31 | 0.61 |
| 7-57-19 | 0.282857 | 0.000013 | 0.001069 | 0.036697 | 0.282851 | 9.5 | 0.5 | 0.56 | 0.68 | 321 | - | - |
| 7-57-20 | 0.282551 | 0.000010 | 0.001061 | 0.034107 | 0.282545 | -1.6 | 0.4 | 0.99 | 1.32 | 311 | 7.33 | 0.60 |
| 7-57-21 | 0.282509 | 0.000014 | 0.002651 | 0.087450 | 0.282486 | -0.1 | 0.5 | 1.10 | 1.36 | 471 | 8.32 | 0.62 |
| 7-57-3 | 0.28259 | 0.000010 | 0.000690 | 0.022555 | 0.282585 | 0.9 | 0.4 | 0.93 | 1.21 | 359 | - | - |
| 7-57-30 | 0.282028 | 0.000014 | 0.000695 | 0.021233 | 0.282024 | -20.9 | 0.5 | 1.71 | 2.41 | 272 | 4.39 | 0.60 |
| 7-57-32 | 0.282702 | 0.000013 | 0.000212 | 0.007047 | 0.282700 | 8.3 | 0.5 | 0.76 | 0.90 | 507 | 5.08 | 0.62 |
| 7-57-33 | 0.281537 | 0.000012 | 0.000399 | 0.012893 | 0.281523 | -2.9 | 0.4 | 2.36 | 2.65 | 1852 | 5.06 | 0.61 |
| 7-57-4 | 0.282754 | 0.000008 | 0.002617 | 0.088856 | 0.282731 | 8.6 | 0.3 | 0.74 | 0.85 | 471 | - | - |
| 7-57-41 | 0.281061 | 0.000012 | 0.000458 | 0.015426 | 0.281038 | -3.1 | 0.4 | 3.01 | 3.25 | 2585 | - | - |
| 7-57-42 | 0.282207 | 0.000013 | 0.000003 | 0.000075 | 0.282207 | -13.0 | 0.5 | 1.44 | 2.01 | 333 | 6.03 | 0.60 |
| 7-57-43 | 0.281143 | 0.000011 | 0.000531 | 0.014652 | 0.281122 | -11.4 | 0.4 | 2.90 | 3.34 | 2102 | 6.24 | 0.61 |
| 7-57-5 | 0.281307 | 0.000011 | 0.000525 | 0.015938 | 0.281288 | -8.9 | 0.4 | 2.68 | 3.08 | 1954 | - | - |
| 7-57-53 | 0.282467 | 0.000012 | 0.001696 | 0.048871 | 0.282458 | -5.2 | 0.4 | 1.13 | 1.51 | 288 | 7.10 | 0.61 |

| Analysis No. | Lu-Hf RATIOS | | | | $Hf_{initial}$ | εHf(T) | ± SE | $T_{DM}$ (Ga) | $T_{DM}^{Crustal}$ (Ga) | U-Pb AGE | Oxygen | |
|---|---|---|---|---|---|---|---|---|---|---|---|---|
| | $^{176}Hf/^{177}Hf$ | 1SE | $^{176}Lu/^{177}Hf$ | $^{176}Yb/^{177}Hf$ | | | | | | (Ma) | $\delta^{18}O$ | 2σ |
| 7-57-54 | 0.281708 | 0.000016 | 0.001101 | 0.036477 | 0.281669 | 2.3 | 0.6 | 2.17 | 2.34 | 1852 | - | - |
| 7-57-57 | 0.282741 | 0.000018 | 0.001474 | 0.048832 | 0.282733 | 4.6 | 0.6 | 0.73 | 0.94 | 290 | 6.22 | 0.60 |
| 7-57-6 | 0.281657 | 0.000010 | 0.000627 | 0.019724 | 0.281636 | -0.8 | 0.4 | 2.21 | 2.46 | 1768 | - | - |
| 7-57-64 | 0.281157 | 0.000019 | 0.000772 | 0.024198 | 0.281117 | 2.1 | 0.7 | 2.90 | 3.03 | 2685 | 6.04 | 0.68 |
| 7-57-68 | 0.282668 | 0.000020 | 0.002531 | 0.079901 | 0.282653 | 2.2 | 0.7 | 0.86 | 1.10 | 308 | 5.09 | 0.61 |
| 7-57-7 | 0.281609 | 0.000008 | 0.000589 | 0.018039 | 0.281589 | -1.0 | 0.3 | 2.28 | 2.52 | 1831 | - | - |
| 7-57-8 | 0.281138 | 0.000009 | 0.000014 | 0.000725 | 0.281137 | -1.6 | 0.3 | 2.87 | 3.09 | 2497 | 6.22 | 0.60 |
| **Kuoika field, Vtorogodnitsa pipe** | | | | | | | | | | | | |
| 7-75-01 | 0.281599 | 0.000009 | 0.000455 | 0.014329 | 0.281583 | 0.3 | 0.3 | 2.28 | 2.49 | 1900 | 6.64 | 0.60 |
| 7-75-02 | 0.282274 | 0.000009 | 0.000777 | 0.022852 | 0.282272 | -14.7 | 0.3 | 1.37 | 1.96 | 157 | 4.75 | 0.61 |
| 7-75-03 | 0.282172 | 0.000009 | 0.001102 | 0.034953 | 0.282167 | -16.6 | 0.3 | 1.53 | 2.13 | 238 | 3.95 | 0.62 |
| 7-75-04c | 0.280723 | 0.000009 | 0.000585 | 0.019069 | 0.280696 | -18.9 | 0.3 | 3.47 | 4.04 | 2428 | 5.69 | 0.60 |
| 7-75-04r | - | - | - | - | - | - | - | - | - | | 5.84 | 0.60 |
| 7-75-05c | 0.281087 | 0.000017 | 0.001528 | 0.043560 | 0.281005 | 0.8 | 0.6 | 3.06 | 3.19 | 2804 | 5.26 | 0.60 |
| 7-75-05r | 0.281721 | 0.000039 | 0.000373 | 0.010551 | 0.281707 | 5.1 | 1.4 | 2.11 | 2.23 | 1912 | 6.26 | 0.60 |
| 7-75-07 | 0.281817 | 0.000034 | 0.001109 | 0.033323 | 0.281778 | 6.6 | 1.2 | 2.02 | 2.10 | 1870 | 4.34 | 0.73 |
| 7-75-08 | - | - | - | - | - | - | - | - | - | | 6.06 | 0.61 |
| 7-75-09 | 0.282079 | 0.000010 | 0.000449 | 0.014117 | 0.282077 | -19.4 | 0.4 | 1.63 | 2.31 | 256 | 4.97 | 0.60 |
| 7-75-10 | 0.281538 | 0.000009 | 0.000533 | 0.017803 | 0.281521 | -5.9 | 0.3 | 2.37 | 2.72 | 1723 | 7.44 | 0.61 |
| 7-75-11 | - | - | - | - | - | - | - | - | - | | 5.88 | 0.61 |
| 7-75-12 | 0.281194 | 0.000009 | 0.000240 | 0.007811 | 0.281185 | -11.3 | 0.3 | 2.81 | 3.26 | 2010 | - | - |
| 7-75-13 | 0.282077 | 0.000013 | 0.001336 | 0.043301 | 0.282069 | -18.0 | 0.5 | 1.67 | 2.29 | 328 | 5.68 | 0.60 |
| 7-75-15 | 0.282119 | 0.000009 | 0.001274 | 0.041635 | 0.282113 | -17.9 | 0.3 | 1.61 | 2.23 | 264 | 5.41 | 0.61 |
| 7-75-18 | 0.282359 | 0.000012 | 0.001535 | 0.045046 | 0.282346 | -5.8 | 0.4 | 1.28 | 1.67 | 436 | 5.35 | 0.60 |
| 7-75-20 | 0.281048 | 0.000018 | 0.001000 | 0.031052 | 0.280998 | -3.5 | 0.6 | 3.07 | 3.31 | 2631 | 5.86 | 0.62 |
| 7-75-21 | 0.282603 | 0.000013 | 0.000935 | 0.027942 | 0.282598 | 0.0 | 0.5 | 0.92 | 1.22 | 296 | - | - |
| 7-75-23 | 0.282597 | 0.000008 | 0.000669 | 0.020146 | 0.282591 | 3.3 | 0.3 | 0.92 | 1.15 | 458 | - | - |
| 7-75-27 | 0.282738 | 0.000012 | 0.001330 | 0.042291 | 0.282726 | 8.4 | 0.4 | 0.74 | 0.86 | 470 | - | - |
| 7-75-28 | 0.282675 | 0.000015 | 0.000822 | 0.025107 | 0.282670 | 2.8 | 0.5 | 0.81 | 1.06 | 307 | - | - |
| 7-75-29 | 0.282595 | 0.000014 | 0.002065 | 0.068565 | 0.282584 | -0.8 | 0.5 | 0.96 | 1.25 | 282 | - | - |
| 7-75-31 | 0.282564 | 0.000012 | 0.000518 | 0.019263 | 0.282559 | 2.4 | 0.4 | 0.96 | 1.21 | 467 | - | - |
| 7-75-32 | 0.281502 | 0.000011 | 0.001368 | 0.040647 | 0.281454 | -5.4 | 0.4 | 2.47 | 2.79 | 1849 | - | - |
| 7-75-33 | 0.281592 | 0.000010 | 0.000637 | 0.021172 | 0.281569 | -0.1 | 0.4 | 2.30 | 2.52 | 1902 | - | - |
| 7-75-34 | 0.282133 | 0.000008 | 0.000722 | 0.023635 | 0.282130 | -17.6 | 0.3 | 1.57 | 2.20 | 252 | - | - |
| 7-75-36 | 0.281575 | 0.000009 | 0.000633 | 0.020789 | 0.281555 | -5.2 | 0.3 | 2.33 | 2.66 | 1702 | - | - |